SEISMIC STRATIGRAPHIC SEQUENCE ANALYSIS OF A PART OF THE NIGER DELTA

by

Timothy Effiong Okon
BSc, MSc, DIC

November, 1988

A thesis submitted for the degree of
Doctor of Philosophy of the University of London
and for the
Diploma of Membership of the Imperial College

Department of Geology
(Petroleum Geophysics Section)
Royal School of Mines
Imperial College
London SW7 2BP

To my Father:

This mattoid is as chastened, as he who has peered

Through, all the abstinence and quiet interlocution;

Through battened faith and the waiting; that this pleated

Song may yet prove worthy of a prodigal's absolution,

And mend familial labyrinths, so arcanely sheared.....

FACING THE GAVEL

Still replete with *angst*, still blithe. One ploughs
Stone. Nomadic this garb, goaded by the twin trades
That I'm sworn. Each pathetic; craft of soughts. Cursed
With yearning; lithe with fright. Bane of such escapades,
Fabricated with vain ubiquitous theses; and furtive

As some, hewers of words would. Levitating, embellished
By the stoned virtuosity of these drab archaic walls,
Rigidly imperial, as this stoic science I claim to uphold.
Perpetuity scours truth's rusty barrel, that enthrals
An army of partisans, in tainted pusillanimous bravado,

Aching to raise beleaguered flags of discovery within
The enigma of fables; and lend light or retrace
The entrails of geologic passage, for a crown of fleece,
To a vulture's bald persistance. For we enter her embrace
Through archaic gates; legend-emboldened plaques of honour;

A roll call of Nobellian men to cleave one's lethargy
With awe; that hallowed sense of liturgic stupor pealing
Like sunday bells. And dare I crave those unsullied rites
Of passage for the mural-crown; sail hope's keeling
Vessels with the Dunkirk spirit, for new beginnings;

Dare I, (a novice, surmise some synthesis from truth's sippets;
A dog, wag tailess; mere bark than bite; dream than intent;)
Say, I've carved my niche on a pilgrim's Ka'aba, amongst apparitions
Of haunting legends, as will the brash nubiles to come. For content
Is he whose eulogy beggars mention; even as mere footnote

In vast chronologies, hived from these fields; long ploughed
And still, re-ploughed; by those fettered with the disposition
To meticulous dexterity. Yet with lassitude, I face the raised gavel
Before it's fall, twin egoed as scientist and poet, such proposition
That coined this treatise, twitching at you, my executioner, my sage.

LONDON; JULY, 1988.

ACKNOWLEDGEMENTS

This research project was sponsored at the behest of the recommendation by Mr. C. J. Burnett, who believed it possible; and sustained under the auspices of Messrs. M. A. Minai; A. K. Koch; S. A. Oladunni; J. R. Gaca; W. Frost; and O. A. Sawyerr. To them, my sincerest appreciation.

Acknowledgements and profound gratitude are also due to the following:

- my supervisor, Mr. Ian Williamson for helpful suggestions and proof-reading the many drafts;
- Professor Stoneley, the head of section and Dr. R. C. Selley, head of department;
- Brian Hallet and Steve Shore for help with the drafting;
- Gill Davies for help with typing and for generosity of spirit in suffering (gladly?) the endless streams of my pleated poetry and the burden of wieldy windmill-tilting doggerels and repartee;
- my colleagues, both at school and work (too numerous for individual citations; but who surely, most deservedly know themselves) for their companionship and support;
- Charles, Rachel and family, whose home was always welcoming;
- the Readheads and the Church in Werrington - such is the fellowship they have accorded this passionate rambler.

VOLUME ONE — TEXT

INDEX OF CONTENTS

DEDICATION
ACKNOWLEDGEMENTS
LIST OF FIGURES
LIST OF ENCLOSURES
ABSTRACT

CHAPTER ONE

INTRODUCTION *023*

1.1 Area of study..... 024
1.2 The data base.....024
1.3 Thesis structure.....025
1.4 Previous work and problem definition.....026
1.5 Objective of study.....028
1.6 Notation and abbreviations.....029
1.7 Method and Approach adopted.....030
1.8 Data preparation and manipulation 038
1.9 Interpretation flow chart..... 041

CHAPTER TWO

STRATIGRAPHIC VELOCITY REVIEW.....*042*

2.1 Outline.....043
2.2 Stratigraphic Velocity Interpretation 043
2.3 Stratigraphic Anomalies 045
2.3.1 Seismic resolution and anomalies 047
2.4 Errors in Velocity Estimation 049
2.4.1 Errors in rms velocity 052
2.4.2 Error Estimation in V^2_{rms} 054
2.4.3 Errors in V_{int} Estimation.....056
2.5 Coefficient of heterogeneity 059
2.6 Litho-velocity relationships.....061
2.6.1 Application to study area 064

2.7 Summary 065
2.8 Sample table of computed interval velocities 067

CHAPTER THREE

REVIEW OF STRUCTURE AND STRATIGRAPHY 068

3.1 Regional and geologic setting 069
3.2 Stratigraphy and structure 071
3.2.1 Stratigraphic framework. 071
3.2.2 Structural framework. 076
3.2.3 Structure at the TIBU level 079
3.2.4 Structure at the BQI level 080
3.2.5 Structure at the QUA5 level 083
3.3 Summary 083

CHAPTER FOUR

SEISMIC STRATIGRAPHIC SEQUENCE ANALYSIS 085

4.1 Review 086
4.1.1 Unconformity types 087
4.1.2 Definition and delineation of mapped horizons 088
4.2 System tracts 096
4.3 Summary 098

CHAPTER FIVE

TERTIARY SEA LEVEL CHANGES 100

5.1 Review 101
5.2 Sequence Correlation 106
5.3 Summary 108

CHAPTER SIX

BIAFRA SEQUENCE AND FACIES ANALYSIS.....110

6.1 Outline.....111
6.2 The Older Biafra Sequences.....113
6.3 The Lower Intra-Biafra Rubble.....115
6.4 SEQ. BS2.....116
6.5 The Upper Intra Biafra Rubble.....116
6.6 SEQ. BS4.....118
6.7 Biafra Litho-velocity analysis.....119
6.8 Summary.....121
6.9 Biafra seismic facies tables.....123

CHAPTER SEVEN

RUBBLE BED SEQUENCE AND FACIES ANALYSIS.....129

7.1 General.....130
7.2 Facies distribution of Rubble Beds.....132
7.2.1 Chaotic facies.....133
7.2.2 Proximal Onlap facies.....133
7.2.3 Mounded Onlap facies.....133
7.2.4 Distal Onlap facies.....134
7.2.5 Prograding facies.....134
7.3 Emplacement of the Rubble Beds.....134
7.3.1 The Depositional model.....135
7.3.2 Tectonic effects and sea level changes.....136
7.3.3 Canyon development.....137
7.4 Sequence interval velocity analysis.....138
7.5 Summary.....140

CHAPTER EIGHT

QUA IBOE SEQUENCE AND FACIES ANALYSIS.....142

8.1 Outline and Classification.....143
8.2 The Lower Qua Iboe sequences.....145

8.2.1 SEQ.QS1 145
8.2.2 SEQ.QS2 146
8.2.3 SEQ.QS3 146
8.2.4 The Intra Qua Iboe "sand" package 148
8.2.5 The depositional model 150
8.2.6 Mechanisms of emplacement 150
8.2.7 The proximal facies 152
8.2.8 Mounded hummocky facies 154
8.2.9 Mounded fan complex facies 156
8.2.10 Onlapping fill facies 157
8.2.11 Sheet facies 158
8.3 Sequence velocity analysis 160
8.4 The Upper sequences 162
8.4.1 SEQ.QS4 163
8.4.2 SEQ.QS5 164
8.4.3 SEQ.QS6 165
8.4.4 SEQ.QS7 166
8.4.5 SEQ.QS8 167
8.4.6 SEQ.QS9 167
8.5 Origin of the Qua Iboe 169
8.6 Summary 170

CHAPTER NINE

SYNOPSIS *173*

9.1 General 174
9.2 The pre-Qua Iboe slope setting 174
9.3 The Qua Iboe slope setting 176
9.3.1 Primary controls on deep sea sedimentation 176
9.3.2 Review of classical models of deep sea clastic sedimentation 178
9.3.3 The delta-slope-submarine fan model 180
9.3.4 Analogy between the Qua Iboe Embayment and the Hackberry Embayment 184
9.3.5 The Upper Qua Iboe 187

CHAPTER TEN

CONCLUSIONS AND RECOMMENDATIONS *191*

10.1 Conclusions 192
10.2 Recommendations 196

BIBLIOGRAPHY AND REFERENCES *198*

APPENDICES *221*

LIST OF FIGURES

FIGURE	TITLE	PAGE
1.1	Seismic data base and coverage map	.....
1.2	Field recording and processing parameters	.....
1.3a	Typical roll-over structure	.....
1.3b	Stratigraphic play in slope channel fill	.....
1.3c	Truncation trap over paralic sequences	.....
1.4a	Terminology used in sequence boundary delineation	.....
1.4b	Schematic diagram of sequence types	.....
1.5	Typical GMA synthetic seismogram display	.....
1.6	Stratigraphic sequences and sea level changes	.....
1.7a	Reflection configurations and facies terminology	.....
1.7b	External geometry of some seismic facies	.....
1.7c	Parallel/divergent seismic types and modifications	.....
1.7d	Progradational facies types	.....
1.7e	Mounded and drape facies types	.....
1.7f	Onlap and fill seismic facies types	.....
1.8a	Velsect data analysis	.....
1.8b	V_{int} presentation using GEM	.....
1.8c	Flow diagram of velocity interpretation	.....
1.8d	Polynomial fit of a stacking velocity curve	.....
1.8e	Modified flow diagram	.....
1.9a	Flow chart for CPS1 mapping package	.....
1.9b&c	CPS1 display listings	.....
		.....
2.1	A depositional mound	.....
2.2a	Anomaly at the foot of the progradational toe	.....
2.2b	Anomaly due to slump on progradational slope	.....
2.2c	Anomaly with a predominant axis or trend	.....
2.2d	The chaotic and disruptive facies anomaly	.....
2.2e	Rubble Bed type anomaly	.....
2.2f	Anomaly with parallel reflectors	.....
2.2g	Stratigraphic anomaly distribution map (Rubble Beds)	.....
2.2h	Stratigraphic anomaly distribution map(Qua Iboe)	.....
2.3a	Horizontal resolution; the Fresnel zone	.....
2.3b	Nomogram for deriving horizontal resolution	.....
2.3c	Model of sand body size and relationship to resolution	.....

2.3d	Stratigraphic anomaly; line 82-349	.....
2.4a	The CDP method as a focussing device	.....
2.4b	Log-Log plot of interval velocity error	.....
2.4c	Error in $V_{int} versus V_{rms}$	.....
2.5a	Qua Iboe Litho-velocity chart	.....
2.5b	A simplified error analysis model	.....
3.1	Regional tectonic framework during the Cenozoic	.....
3.2	Tectonic setting of the eastward extension of the delta	.....
	and it's relationship with the Rio del Rey basin	.....
3.3a	The zone of shale diapirs, S.E. Niger Delta	.....
3.3b	Schematic section across the zone of shale diapirs	.....
3.4a	Hypothetical section showing the sedimentary bulge	.....
3.4b	Regional seismic section across the delta(west)	.....
3.4c	Regional seismic section across the delta(east)	.....
3.5	Canyon incision of the Niger continental slope	.....
3.6a	Stratigraphic evolution of the Niger Delta	.....
3.6b	Major formation units of the study area	.....
3.7	Seismic Line 82-251	.....
3.8	Seismic Line 82-279	.....
3.9	Development of the eastern delta	.....
3.10a	Akata shale formation type section	.....
3.10b	Biafra member type section	.....
3.10c	Rubble Bed member type section	.....
3.10d	Qua Iboe member type section	.....
3.10e	D-1 type section	.....
3.10f	Benin formation type section	.....
3.11a	The Stratigraphic column	.....
3.11b	Seismic Line 82-149	.....
3.11c	Seismic line 82-231	.....
3.11d	Seismic line 82-377	.....
3.12	Regional cross-section Evamy *et al.*(1978)	.....
3.13a	Megaunits and associated synsedimentary faults	.....
3.13b	Development of simple and complex growth faults	.....
3.14a,b,c	Structures at the TIBU, BQI and QUA5 levels	.....
3.15a	Terracing at the BQI level(line 82-163)	.....
3.15b	Erosional anticline at the BRB level(line 82-110)	.....
3.15c	Erosional anticline at the TIBU level(line 82-190a)	.....
3.16	Rollover anticline (shale mass supported)Line 82-106	.....

3.17	Rollover anticline with landward dips	.....
3.18	Rollover anticline with seaward dips	.....
3.19a	Shale mass structure flank	.....
3.19b	Shale diapir; line A-23	.....
3.20	Shale mass structure crestal	.....
3.21	Structure at the southeastern block	.....
3.22	Annealment type structure	.....
3.23	Structure at the Qua4 level	.....
4.1a	Depositional processes and unconformity types	.....
4.1b,c	System tracts	.....
4.2	Canyons and their relationship to shelf(line 259)	.....
4.3a	Seismic line 82-66 (the older sequences)	.....
4.3b	Seismic line 82-88a	.....
4.3c	Synthetic seismogram fit for older sequences	.....
4.4a	Line 82-212a	.....
4.4b	Synthetic seismogram fit for LBIBR	.....
4.5a	Line 82-393a	.....
4.5b	Line 82-393	.....
4.6a	Line 82-381	.....
4.6b	Line 82-301	.....
4.7a	Line 82-353	.....
4.7b	Line 82-180	.....
4.7c	Synthetic seismogram fit for TIBU	.....
4.8	Line 82-107(BIBBEN horizon)	.....
4.9a	Line 82-142(Rubble canyon)	.....
4.9b	Line 82-88a(Intra Rubble unconformities)	.....
4.9c	Synthetic seismogram fit for BRB	.....
4.10a	Line 82-261	.....
4.10b	Line 82-285	.....
4.10c	Line 82-106	.....
4.10d,e	Synthetic seismogram fit for BQI	.....
4.11a	Intra Qua Horizon definition	.....
4.11b	Qua Iboe progradation and the turbidite toe	.....
4.11c	Line 82-203	.....
4.11d	Qua3; line 82-361	.....
4.11e	Condensed sections	.....
4.12	The Pleistocene canyon	.....
4.13a	Line 82-269; system tracts of the study area	.....

4.13b,c	Lower system tracts in different tectonic settings	.....
4.13d	Line 82-251	.....
4.13e	Line 82-391	.....
5.1a,b	The Haq *et al.*(1987) and the Vail *et al.*(1977) curves	
5.2a,b,c	The eustatic curves from 1977 to 1987	.....
5.3a,b	Correlation of coastal onlap curves	.....
5.4	Correlation of the Moore *et al.* and Haq *et al.* curves	.....
5.5	Late Neogene Oxygen-18 curves	.....
5.6a	Comparison of Vail's curve to the Oxygen-18 curve	.....
5.6b	Model of turbidite deposition during sea level change	.....
5.7a,b	Chronostratigraphic chart line 82-197	.....
5.8a,b	Chronostratigraphic chart line 82-259	.....
5.9a,b	Chronostratigraphic chart line 82-373	.....
5.10a,b,c,d,e	Sequence correlation summary	.....
5.11a,b,c	Mobility diagrams	.....
5.12a,b&c	Lines 82-197, 82-259, and 82-373	.....
6.1a,b&c	Biafra structural and stratigraphic evolution	.....
6.2	Representative seismic facies types	.....
6.3a&b	Lines 82-183 & 82-86	.....
6.4	Map showing the limit of truncation of BIBBEN	.....
6.5	Line 82-66	.....
6.6	Line 82-211	.....
6.7a,b,c	Characteristic log response of the Older sequences	.....
6.8a	Composte facies distribution map of older sequences	.....
6.8b&c	Paleoenvironment curves for the Older sequences	.....
6.9	Facies distribution map of LIBR	.....
6.10a&b	The Lower Intra Biafra Rubble	.....
6.11a	Facies distribution of SEQ.BS2	.....
6.11b&c	lines 82-339 and 82-220a	.....
6.12a	Line 82-283	.....
6.12b	Line 82-106	.....
6.12c	Line 82-339	.....
6.12d	Line 82-377	.....
6.13a	Facies distribution of UIBR	.....
6.13b	Paleoenvironment curve for UIBR	.....
6.14a&b	High amplitude anomalies in UIBR	.....
6.15	Line 82-132a; SEQ.BS4	.....

6.16a	Facies distribution for SEQ.BS4	.....
6.16b	Paleoenvironment curve for SEQ.BS4	.....
6.17a	Sand percentage map of the Biafra	.....
6.17b	Interval velocity map of the Biafra	.....
6.18	Juxtaposition of the av. int. vel. map and sand % map	.....
6.19a	Litho-velocity chart for Biafra	.....
6.19b	Upper Intra Biafra Rubble velocity analysis	.....
6.20	A composite map of the delta front for Biafra sequences	.....
7.1a	Line 82-106; BRB as a PGM feature	.....
7.2	Line 82-142	.....
7.3a	Unit 1 Rubble; Line 82-287	.....
7.3b&c	Unit 2 Rubble(82-387; 82-142)	.....
7.4	Distribution of Unit 1 Rubble	.....
7.5	Distribution of Unit 2 Rubble	.....
7.6	Seismic facies of the Rubble Beds	.....
7.7	Facies distribution of the Rubble Beds	.....
7.8a	Line 82-118; the chaotic facies	.....
7.8b	Line 82-253; the proximal facies	.....
7.8c	Line 82-197; mounded proximal facies	.....
7.8d	Line 82-291; mounded onlap facies	.....
7.8e	Line 82-168a; the distal facies	.....
7.8f	Line 82-216a; the prograding facies	.....
7.9a	Rubble Bed depositional model	.....
7.9b	Mechanisms for Rubble Bed formation	.....
7.10a	Rockfall	.....
7.10b	Development of channel system(82-251)	.....
7.11a	The western Rubble Bed canyon (line 82-142)	.....
7.11b	The eastern canyon	.....
7.11c	The eastern canyon (line 82-337)	.....
7.12	Distribution of Stratigraphic anomalies	.....
7.13	Litho-velocity chart for the Rubble Beds	.....
7.14	Distribution of sand build-ups based on velcity	.....
7.15a&b	The northern anomalies	.....
7.15c	The southeastern anomaly	.....
8.1	Qua Iboe shale limit	.....
8.2a&b	Lines 82-279 and line 82-185	.....
8.3	Composite of shelf breaks	.....

8.4	Representative facies types	.....
8.5a	Structural map of Horizon QUA2	.....
8.5b	Isochron map of QS1	.....
8.5c	Facies distribution map QS1	.....
8.6a&b	Lines 82-201 and 82-409	.....
8.6c	Facies distribution map of QS2	.....
8.6d	Composite anomaly map of QS1 and QS2	.....
8.7a	Line 82-229	.....
8.7b	Distribution map of seismic mounds	.....
8.7c	Line 82-231	.....
8.7d	The prograding terrace, line 82-271	.....
8.8a	Structure map of QUA4	.....
8.8b	Facies distribution map of QS3	.....
8.8c	Line 82-212a	.....
8.9	The Lower Qua Iboe depositional model	.....
8.10a	Paleodepth estimation from progradation	.....
8.10b	Environmental depth zones	.....
8.10c	Process continuum in deep sea sedimentation	.....
8.10d&e	Seismic evidence of slumping (line 82-251)	.....
8.11	Seismic indicators of Turbidite sequences	.....
8.12a	Line 82-154s	.....
8.12b	Line 82-146b	.....
8.12c	Line 82-251	.....
8.12d	Line 82-267	.....
8.13a	Proximal facies illustration(82-114)	.....
8.13b	Mounded proximal facies	.....
8.13c	Line 82-291	.....
8.13d	Proximal onlap(line 82-409)	.....
8.13e	Proximal Uplap(line 82-353)	.....
8.14	Formation of seismic mounds(model)	.....
8.15	Composite of the distribution of seimic mounds	.....
8.16a	Build-up of the central anomaly	.....
8.16b	Build-up of the southwest anomaly	.....
8.16c	Build up of the northwest anomaly	.....
8.16d	The centre-west anomaly	.....
8.16e	The centre-east(1&2)	.....
8.16f	The eastern anomaly	.....
8.17	Line 82-142	.....
8.18a	Mounded fan complex facies(line 82-182a)	.....

8.18b	Depositional model of stacked channels	.....
8.19a	Line 82-174	.....
8.19b	Line 82-185	.....
8.20	Line 82-154b	.....
8.21a	Sheet facies: line 82-349	.....
8.21b	Line 82-106	.....
8.22	Line 82-220a	.....
8.23	Sigmoidal facies: line 82-369	.....
8.24	Oblique facies: line 82-429	.....
8.25a	Litho-Velocity chart	.....
8.25b	Interval velocity map	.....
8.26a	Interpreted litho-vel chart	.....
8.26b	Sandiness map	.....
8.26c	Coefficient of heterogeneity map	.....
8.27a	Facies distribution map QS4	.....
8.27b	Line 82-86	.....
8.28a	Line 82-215	.....
8.28b	Line 82-289	.....
8.29a	Line 82-345	.....
8.29b	Line 82-169	.....
8.29c	Facies distribution map of QS5	.....
8.29d	Line 82-385	.....
8.30	Facies distribution of QS7	.....
8.31	Line 82-341	.....
8.32a&b	The chaotic facies	.....
8.33	Coastal onlap on line 82-369	.....
8.34a&b	The Pleistocene canyon	.....
8.35	Extent of the canyon	.....
8.36	Line 82-223	.....
9.1	Turbidites and sea level changes	.....
9.2a&b	Three end-member fan classification	.....
9.3a&b	Comparison of modern and ancient fans	.....
9.4a	The Mississippi submarine fan model	.....
9.4b	The Submarine ramp model	.....
9.4c	Facies comparison, ramp model versus ancient model	.....
9.4d	The shelf-Slope model	.....
9.5a	The Lower Qua Iboe fan model	.....
9.5b	Map of seismic mounds	.....

9.6	Seismic criteria for fan recognition	.....
9.7	Relationship between fan width and valley size	.....
9.8a&b	The northern feeder canyon	.....
9.8c	Seismic example of a turbidite fan	.....
9.9a&b	Slope models	.....
9.10	The Texas-Louisiana slope	.....
9.11	The Hackberry Embayment	.....
9.12a&b	Stratigraphic setting of Hackberry onlap slope system	.....
9.13	Depositional overview of the Hackberry slope system	.....
9.14	Depositional setting of the Hackberry	.....
9.15	Canyon fills of the Niger Delta	.....
9.16	Canyon fills of the Gulf coast	.....
9.17	The submerged shelf margin	.....
9.18	Shelf margin deltas during lowstand of sea level	.....
9.19	Progradation and eustatic sea level changes	.....

LIST OF ENCLOSURES

ENCLOSURE	TITLE	PAGE
1	LBIBR Seismic Two Way Time Map	 xxx
2a	LIBU Seismic Two Way Time Map	 xxx
2b	LIBU Isometric Projection Map	 xxx
3	LIBR Isochron	 xxx
4	BIBR Seismic Two Way Time Map	 xxx
5a	TIBU Seismic Two Way Time Map	 xxx
5b	TIBU Isometric Projection Map	 xxx
6	UIBR Isochron	 xxx
7a	BRB Seismic Two Way Time Map	 xxx
7b	BRB Isometric Projection Map	 xxx
8a	BQI Seismic Two Way Time Map	 xxx
8b	BQI Isometric Projection Map	 xxx
9	Rubble Beds Isochron Map	 xxx
10a	QUA3 Two Way Time Map	 xxx
10b	Isochron of IQI-QUA3	 xxx
11a	QUA4.2 Seismic Two Way Time map	 xxx
11b	Isochron of the Qua Iboe	 xxx
11c	QUA5 Seismic Two Way Time map	 xxx
11d	QUA6 Seismic Two Way Time map	 xxx
11e	QUA7 Seismic Two Way Time map	 xxx
12	Chronostratigraphic charts	.....
13	Build up of the Qua Iboe embayment	.....

LIST OF ENCLOSURES

ENCLOSURE	TITLE	PAGE
1	LBIBR Seismic Two Way Time Map	 xxx
2a	LIBU Seismic Two Way Time Map	 xxx
2b	LIBU Isometric Projection Map	 xxx
3	LIBR Isochron	 xxx
4a	BIBR Seismic Two Way Time Map	 xxx
4b	BIBR Isometric Projection Map	 xxx
5a	TIBU Seismic Two Way Time Map	 xxx
5b	TIBU Isometric Projection Map	 xxx
6	UIBR Isochron	 xxx
7a	BRB Seismic Two Way Time Map	 xxx
7b	BRB Isometric Projection Map	 xxx
8a	BQI Seismic Two Way Time Map	 xxx
8b	BQI Isometric Projection Map	 xxx
9a	Rubble Beds Isochron Map	 xxx
10a	QUA3 Two Way Time Map	 xxx
10b	Isochron of IQI-QUA3	 xxx
11a	QUA4.2 Seismic Two Way Time map	 xxx
11b	Isochron of the Qua Iboe	 xxx
11c	QUA5 Seismic Two Way Time map	 xxx
11d	QUA6 Seismic Two Way Time map	 xxx
11e	QUA7 Seismic Two Way Time map	 xxx
12	Chronostratigraphic charts	.....
13	Build up of the Qua Iboe embayment	.....

ABSTRACT

Seismic stratigraphic sequence analysis of a part of the Tertiary Niger Delta has been undertaken, in the light of the increasing paucity of large structural plays, to examine the distribution of sedimentary sequences and sequence bounding unconformities. In addition, the relationship between seismically derived interval velocity and sand development within specified sequences has been studied.

This analysis reveals a complex distribution of 18 sedimentary sequences spanning Miocene to Holocene, reflecting the effect of sea level changes and a varied tectonic history. Within the Miocene, five prominent angular unconformities, with important implications for structural trap development and thus hydrocarbon exploration, have been identified namely:

- Lower Intra Biafra Unconformity .....LIBU.
- Base Intra Biafra Rubble .....BIBR.
- Top Intra Biafra Unconformity.....TIBU.
- Base Rubble Beds.....BRB.
- Base Qua Iboe Unconformity.....BQI.

Similarly, in the Pliocene and Pleistocene, five unconformities with varying hiatus are evident. These are:

- Lower Qua Iboe 1.....QUA_3.
- Lower Qua Iboe 2.....QUA_4.
- Upper Qua Iboe 1.....$QUA_{4.2}$.
- Upper Qua Iboe 2.....QUA_7.
- Late Pleistocene Unconformity.....Pu.

Seismic stratigraphic anomalies (seismic mounds) were defined for the study area in respect of sequences interpreted to have been formed during lowstand of sea level such as the **Lower Intra Biafra Rubble(LIBR), Upper Intra Biafra Rubble(UIBR), and Rubble Beds**, and the **Lower Qua Iboe sequences** which correspond to a Pliocene highstand, and are interpreted as turbidites.

The Intra Biafra Rubble and Rubble Beds systems were deposited in a destructive onlap slope setting characterized by structural deformation; while the Qua Iboe is generally associated with a constructive slope setting. Consequently, a **delta slope submarine fan** depositional model is proposed for the Lower Qua Iboe while a **normal clastic slope apron** model is characteristic of the Upper Qua Iboe.

Examination of seismic interval velocities of these sequences reveals the existence of broad correlation of sand development with increasing values of corrected interval velocities. This observation confirms that, under appropriate constraints, seismic interval velocity may be used as a predictive tool for sand development in the Tertiary Niger Delta.

However, sand percentage estimation is tenuous because the separation between the end-member lithologies at the depth of interest is small in magnitude and because of the sometimes significant error margin in interval velocity estimation from seismic data.

From the analysis of sequence interval velocities in this area, the necessary prerequisite for better resolution of sand trends within seismic stratigraphic anomalies include the following:

- More closely spaced velocity analysis points, than the 1.5km spacing along seismic profiles utilized for this study. A 400metre spacing or less is recommended in line with the dense seismic profile grid of 400metres square in most areas.

- Unambiguous sequence boundaries for sequence-keyed interval velocity derivation and sequence interval of more than 1000ft(300m) to minimise errors.

It is observed, as a consequence, that reliable seismic interval velocity values may be obtained through better subsurface sampling of the anomaly. This technique represents a cost effective preliminary method of evaluating stratigraphic plays in comparison to 3-dimensional survey over such anomalies.

CHAPTER ONE

INTRODUCTION

1.1 Area of study. 024
1.2 The data base. 024
1.3 Thesis structure. 025
1.4 Previous work and problem definition. 026
1.5 Objective of study. 028
1.6 Notation and abbreviations. 029
1.7 Method and Approach adopted. 030
1.8 Data preparation and manipulation 038
1.9 Interpretation flow chart. 041

1.1 AREA OF STUDY

The area under consideration forms a part of the Niger Delta presently being explored under prospecting and mining licenses. For reasons of confidentiality, the exact location cannot be disclosed and an arbitrary grid commencing from 0,0 cordinates at the bottom left hand corner was set for a study area measuring 110km east-west by 66km north-south. This notwithstanding, the project is discussed within the context of a microcosm of the Niger Delta complex and the related Rio Del Rey basin of Cameroun to the east.

1.2 THE DATA BASE

Over 9000km of 36-fold seismic data, shot in 1982 by **Sefel** was utilized in the study, all of which were the same vintage(Fig.1.1). Odd number lines indicate North-South traverses while even number lines are East-West. Coverage grid varied from 0.16 sq.km to the west and 0.32sq.km to the east.(i.e. profile spacing of 400 by 400 metres increasing to 400 by 800 metres in the east and 1600 by 1600 metres in the south central areas of the acreage). The consistent data vintage allowed for comparative seismic reflection character analysis and minimal data shifts and misties.

Field recording and processing parameters applied to the data are given in Fig.1.2. Because compression was recorded as negative on tape, and the sections displayed with normal polarity (i.e. positive number gives black peak), a positive reflection coefficient appears as *white* on the seismic section.

A standard processing sequence was followed consisting of predictive deconvolution before and after stack, trace amplitude equalization before and after migration with velocity analysis every 1.5km using Constant Velocity Stacks(CVS). The seismic display scale used in interpretation was 1:11811 (horizontal) and 1sec/9.525cm (vertical). Seismic lines used as examples in the report were mainly scaled down versions having horizontal scales of 1:50,000 and vertical scales of 1sec/5cm except where indicated. Each shot point interval corresponds to 25metres.

Seismic interpretation was carried out on time sections for reasons consistent with normal seismic interpretation procedures* after faults might have been picked

* Migrated seismic sections often give misties between dip and strike lines with dipping reflectors such as the Biafra in the study area

using migrated sections. For identification of the stratigraphic anomalies however, migrated sections were used to minimise the possible effects of noise and diffractions affecting the geometric expression of the seismic mounds. All the seismic examples used as figures in the study are migrated sections.

In general seismic data quality may be considered very good, if the non-collapse of diffractions along fault planes due perhaps to unreliable migration velocities and the poor data often associated with the presence of gas charged sediments and shale mass development are discounted. Minor misties due to strong dips in deeper Biafra sections were corrected accordingly.

Permission for the use of a limited number of wells was granted by the owners of the data and are listed in Appendix 4. This included some check shot surveys for well to seismic section correlation.

1.3 THESIS STRUCTURE

The results of this study are presented in the following format:

- **Volume One —— Text**
- **Volume Two —— Figures**
- **Volume Three — Enclosures**

Chapter One:

This chapter consists of a general introduction of the area and aims of study along with a preliminary examination of the various themes considered in the main body of the thesis.

Chapter Two:

Consideration is given here to the concept of stratigraphic velocity interpretation and stratigraphic anomalies are defined and explained. Errors associated with the use of seismically derived interval velocities are discussed and quantified. A preliminary discussion of Litho-velocity relationships is also undertaken.

Chapter Three:

The typical structures and stratigraphic framework of the Niger Delta is enunciated. A localized stratigraphic column for the study area is proposed. Structural development at three levels from the Miocene to the Pliocene is also considered.

Chapter Four:

This chapter deals with the preliminary aspects of sequence analysis by defining unconformity types and outlining the varoius sequence bounding unconformities identified in the study. These are correlated with synthetic seismograms and well log signatures.

Chapter Five:

Tertiary sea level changes and their effect on the depositional styles in the study area are scrutinized.

Chapters Six, Seven, & Eight:

These chapters have been devoted to seismic sequence, facies and interval velocity analysis of the Biafra, Rubble and Qua Iboe members (as previously defined) respectively.

Chapter Nine:

Sums up analysis of the study area, discusses the various depositional models and relates the area to the Gulf Coast(U.S.A).

Chapter Ten:

Conclusions and recommendations. Further work.

References and Bibliography

Appendices

1.4 PREVIOUS WORK AND PROBLEM DEFINITION

As an actively explored area, the study acreage has undergone significant scrutiny in terms of its hydrocarbon potential. Previous work published, have been

about the general geology, and hydrocarbon province of the Niger Delta, mainly by Shell-BP and Gulf Nigeria geologists(Short and Stauble, 1967; Frankl and Cordry, 1967; Merki, 1972; Weber, 1971; Weber and Daukoru, 1975; and Evamy *et al.*, 1978). Other work include stratigraphic and unconformity traps(Orife and Avbovbo, 1982), canyon fills(Petters, 1984) and the comprehensive *Petroleum Geology of Nigeria*(Whiteman, 1982). Apart from these, there has been little published material directly concerning the seismic stratigraphy of the Niger Delta.

The relatively recent topic of seismic stratigraphy led to two limited in-house reviews of the Niger Delta basin, in view of the new concepts in 1978 (concerning the "Rubble Beds") and in 1982/83 (concerning the Qua Iboe)*. The latter was carried out by the author using the newly acquired 1982 seismic data base. This project is however the first attempt at using this data base to discuss the seismic stratigraphy of the myriads of stratigraphic sequences evident in this study area.

In general, exploration strategy in the Niger Delta (the study area being no exception) has mainly been concentrated on the following objectives:

- The drilling of rollover structures within the Agbada formation, mostly of the type shown in Fig.1.3a(Weber and Daukoru, 1975).
- A few stratigraphic plays in slope channel fills and turbidite fan sands as shown in the Egbeme field(Weber and Daukoru, 1975). See Fig.1.3b.
- And truncation traps where "gully fills"** cut the paralic sequences beneath (see Fig.1:3c).***

Exhaustion of large scale structures has made it imperative to look at possible stratigraphic plays within recognizable sequences. Sequence outline, definition and evaluation belong to the realm of seismic stratigraphy. Relating these to a regional concept of sea level changes in a passive Atlantic-type margin enables evaluation of the distribution of different clastic types within such basins.

---

* See Section 3.2 for definition of "Rubble" and Qua Iboe. The Qua Iboe is spelt *Kwa Ibo* in some literature, but the spelling used in this report is the current standard usage.

** A term for abandoned and filled river gullies that are supposed to have cut into the underlying Agbada formation(Weber and Daukoru, 1975).

*** For guidance, a summary of the main lithostratigraphic units in the Niger Delta is shown in Fig.1.3d

Incorporating within the above stated framework stratigraphic velocity interpretation through examining the distribution of interval velocities within the respective sequences is the appropriate recourse for qualifying clastic potential and distribution.

Inferring clastic-type distribution using the combined tools of seismic stratigraphy and stratigraphic velocity interpretation is attempted here, since distinct seismic facies within sequences imply variable lateral lithologies. Interval velocity analysis (within certain constraints which are discussed in Chapter 2) offers a quantitative interpretation of seismic facies distribution using the adequate statistical data base provided by wells in the study area. The problem therefore, in this study, is to outline within the sequences mapped, stratigraphic anomalies and quantify the relationships between lithology and interval velocities within the depositional framework defined by seismic stratigraphy.

1.5 OBJECTIVES OF STUDY

Stated below, is an enunciation of the objectives of this study which include:

1. The interpretation and mapping of sequence and facies boundaries within a section of the Niger Delta system. Relating these to relative changes of sea level and the regional setting of the Delta as a passive Atlantic-type margin.

2. The development of a depositional framework and tectonic depositional models for the respective sequences identified through the analysis of seismic facies, the observed stratigraphic and geographic distribution of clastic reservoir facies and consequently obtain an environmental interpretation.

3. Comparing the afore-mentioned depositional framework and models with similar deltaic provinces such as the Gulf coast.

4. The examination of the relationship between interval velocities and lithologic variation. To see whether litho-velocity results are consistent with the depositional models described from facies distribution.

5. In this regard, the aim is to develop an integrated seismic stratigraphic approach to the identification and quantification of prospective stratigraphic anomalies through comparisons of interval velocities within de-

lineated sequences and thereby predicting quantitatively sand development.

Although the aim was not to undertake detailed analysis of the structural framework of the area, structural maps and isochrons of the various depositional sequences are presented in this report. No time-depth conversions were therefore undertaken for the time maps because of the regional nature of the study involving the stratigraphy rather than structure, and the fact that within major growth fault couples, average velocity function only minimally varies. Well velocities were however used in litho-velocity analysis as appropriate. The main thrust of this research has been in isolating and analysing stratigraphic anomalies within an outlined stratigraphic setting.

Such objectives as outlined above, must as of necessity be multi-disciplinary incorporating relevant aspects of geology and geophysics. This report is a product of the combination of such tools as are available to the petroleum explorationists towards the paramount objective of predicting the presence of hydrocarbon reservoirs.

1.6 NOTATION AND ABBREVIATIONS

The notation and abbreviations given below have been used throughout the text and particularly in chapter two where corrections for stacking velocity errors are discussed. Their meanings are valid except where superseded by subsequent redefinition within the derived equations.

V_{int} = Interval velocity

V_a = Average velocity

V_{rms} = Root mean square velocity

V_{nmo} = Normal move out velocity

V_{st} = Stacking velocity

V_{a_n} = Average velocity to the nth layer

V_{rms_n} = Root mean square vel. to the nth layer

$V_{(t)}$ = Instantaneous velocity

$Z =$ Depth

$T_g =$ Absolute geologic age in years

$t =$ Seismic two-way travel time

$sT =$ sonic log time

$g =$ Coefficient of heterogeneity

$\rho =$ Formation density.

LBIBR- Lower Base Intra Biafra Rubble.

LIBU- Lower Intra Biafra Unconformity.

BIBR- Base Intra Biafra Rubble.

TIBU- Top Intra Biafra Unconformity.

BIBBEN- Base Intra Biafra Benin sands.

BRB- Base Rubble Beds

BQI- Base Qua Iboe.

TIQI- Top Intra Qua Iboe

QUA3 etc- Intra Qua Iboe horizon 3 etc

Pu- Pleistocene Unconformity

1.7 METHOD AND APPROACH ADOPTED

The basic techniques used in this analysis are those elucidated by the Vail *et al.* classic(Vail *et al.*, 1977) which outlines a multi-step approach namely:

A. Seismic sequence analysis;

B. Correlation to relative sea level changes; and

C. Seismic facies analysis.

The above methods constitute an intergrated approach to inferring stratigraphy from seismic data and are highlighted in a flow chart at the end of this chapter (see Fig.1.4a).

A. Seismic Sequence Analysis:

A seismic sequence corresponds to a depositional sequence seismically expressed by a gamut of seismic reflection patterns, formed as a result of the interaction between rates of eustacy, subsidence and sediment supply and is bounded by unconformities and their correlative conformities.

Seismic sequence analysis, therefore, involves the recognition and delineation of sequence bounding unconformities and interpretation of the processes and environmental associations. Seismic sequences as defined and illustrated are attached(see Fig.1.4b & c). These are detailed in Chapter 4.

This analysis however incorporates the following:

- Establishing well seismic ties using sonic logs as input into synthetic seismogram routines, thus predicting the effect of stratigraphy on seismic records.
- Examining whether there is a unique relationship between interval velocity (as determined by fitting a regression curve to the stacking velocities and using Dix's equation to compute velocities over sequence intervals) and clastic composition of the sequence intervals.
- Relating, where possible, characteristic log motifs to the environmental interpretation of the sequences.

Most of the wells were however drilled before the advent of Vertical Seismic Profile(VSP) imaging which could have been a better tool in describing the subsurface around any study well. A commercially available one-dimensional synthetic seismogram package by Geophysical Modelling Application (GMA) of Canada was used. A typical presentation is shown in Fig.1.5. The basic theory behind the synthetic seismogram assumes that a restricted segment of the earth may be represented as being horizontally layered which on propagation of a plane wave consists of partial reflections of the plane wave from each of the planar boundaries.

The equation of the one-dimensional synthetic seimogram(Peterson *et al.*, 1955) is given as:

$$S_{(t)} = r_{(t)} * b_{(t)} + n_{(t)}$$

where $n_{(t)}$ is noise; $r_{(t)}$ is the reflectivity function defined as

$$r_{(t)} = \frac{1}{2dt}(dln\rho_{(t)})V_{(t)};$$

with $\rho_{(t)}$ as the density at time t and $V_{(t)}$ the instantaneous velocity.

$b_{(t)}$ is the attenuated shot pulse defined as

$$b_{(t)} = f_{(t)} * e_{(t)};$$

and $f_{(t)}$ is the shot pulse while $e_{(t)}$ is the filtering external to the earth which includes the combined effect of all instruments plus geophone coupling.

In a sampled form, the reflectivity function $R_{(t_i)}$ (the instantaneous reflection coeficient) may be represented as:

$$R_{(t_i)} = \frac{\rho_{(t_i)}V_{(t_i)} - \rho_{(t_{i-1})}V_{(t_{i-1})}}{\rho_{(t_i)}V_{(t_i)} + \rho_{(t_{i-1})}V_{(t_{i-1})}}.$$

R_T, the reflectivity series becomes

$$R_{(T)} = R_{(t_i)}d_{(t-1,t)}.$$

In order to adequately represent the continuous velocity log(sonic) a sample interval of 0.5msecs was used. This differs from the processing sample interval of 4msecs and was carried out to ensure better detailing of possible features in the synthetic seismogram *vis a vis* the field records. Where applicable the synthetic seismogram is matched with the respective sequence boundaries.

After several forward modelling trials a Ricker assymmetric wavelet of 20msecs duration and peak frequency of 39Hz* was chosen.

---

* The peak frequency is defined as the frequency component with the largest Fourier amplitude spectrum. The chosen frequency, 39Hz, is regarded as the optimum frequency consistent with the zone of investigation in the study area. See Section 2.3.1 for discussion of seismic resolution.

Most source wavelets in exploration are minimum-phase except where vibroseis data is involved. Ideally, the desired wavelet would be zero-phase for good resolution. This is an essential requirement for peak-trough times to be valid measurements for estimating bed thicknesses which could be used in defining reservior dimensions. This was attempted using an Orsmby wavelet with terminal frequencies of 5 10 50 55 (Ormsby wavelet is an approximation of the *Sinc wavelet*) with a fair result. The minimum phase wavelet was chosen for event matching purposes because it is likely to bear closest resemblance to the field source.

In most cases a reasonable match with the field records was obtained (considering that density variations and noise were not taken into account)**.

Dipmeter logs were used to aid the identification of "Rubble"- reworked sediments dumped at the flank of structural highs especially the Rubble Beds and the Intra Biafra Rubble, but in most cases seismic facies differentiation was sufficient in defining their occurrence.

B. Relative Sea level changes:

Post-Vail *et al.*(1977) thinking, largely validates the effect of sea level change as a primer for the widespread distribution of certain types of depositional sequences at particular periods in the geologic record.

Sequences can be related to changes of sea level by determining age and distribution of coastal and marine onlap, comparing regional curves to a "global curve" to understand local tectonic events, and determining eustatic changes of sea level by analysis of subsidence rate and uplift. (See Fig.1.6; line 82-216a for example.) Vail's Tertiary sea level curve was used extensively and modified to take account of the unconformities evident in the study area. The relationship between sea level change and development of seismic sequences is reviewed in Chapter 5. Recent criticisms of the concept of a global curve are also discussed.

C. Seismic Facies Analysis and Stratigraphic Velocity Interpretation

This involves analysing the internal seismic architecture of sequences and other intrinsic attributes such as amplitude, frequency and interval velocity to infer depositional environment and lithologic relationships.

** See Section 4.1.2 for synthetic ties with delineated sequence boundaries.

Once again, the basic reference in use is from Mitchum *et al.*(1977) in respect of the relevant terminology(see Fig.1.7a) and Sangree and Widmeir(1977), as modified by Brown and Fisher(1980), with regards to environmental facies interpretation. The four principal types of seismic reflection configurations which give rise to seismic facies associations are:

- parallel/divergent;
- progradational;
- mounded/drape; and
- onlap/fills.

External geometry of some of the facies and schematic displays showing the various combinations of reflection configuration are given in Figs.1.7b, c, d, e, and f. The next stage is the derivation of Velocity-Lithology calibration curves for different seismic facies units or stratigraphic anomalies through the calculation of closely spaced interval velocities. The calibration curves may then be used to predict and map lithology.

It is important to state briefly the methods commonly used in velocity derivation from seismic data. These are:

1. Velocity determination from seismic amplitudes.
2. The normal move out relation.

The former is often referred to as *trace inversion modelling* involving the assumption that the earth's reflectivity function may be derived from a noise free seismic trace, and the notion that amplitude is proportional to the reflection coefficient. This may be mathematically represented as given below * :

$$\Delta(log\rho V) = 2R = KA \tag{1.6.1}$$

where ρ is density, V is instantaneous velocity, R is reflection coefficient, K a constant of proportionality between amplitude and reflection coefficient, and A

* Equation 1.6.1 is another form of the original Peterson *et al.*(1955) equation given earlier.

amplitude. Density is either assumed to be constant or a function of velocity through the empirically derived relation(Gardner *et al.*, 1974):

$$\rho=0.23V^{0.25}$$

where V is the instantaneous velocity in ft/sec and ρ the density in gm/cm^3.

Instantaneous velocity is then displayed in an appropriate colour code(see Lavergne and Wilson(1977), and Lindseth(1976)).

The latter is based on the velocity information inherent in moveout curves and is considered an appropriate method with regards to the data base provided. This is discussed below.

Abrupt lateral changes in subsurface lithology are known to distort stacking velocities as determined from reflections at depth below them. In the same vein, zones of greater porosity are likely to have a slower stacking velocity as picked from velocity analysis for reflectors below such zones, compared with similar sections of lower porosity within the same stratigraphic interval*. It is therefore possible to delineate zones by investigating stacking velocities to a horizon immediately below such intervals. The magnitude of stacking velocities thus relates indirectly to the lithology. Such delineated zones are referred to in this text as **Stratigraphic Anomalies**. This is considered in Section 2:3.1

For stratigraphic velocity analysis, the following steps were utilized:

1. Generate a velocity section from CDP data over the entire seismic profile.
2. Incorporate the relevant horizon picks from seismic interpretation
3. Compute interval velocity using Dix's equation.

Because of the great expense involved this was done over the central anomaly only, and on lines 82-148, 82-142, 82-138, 82-136 and 1839. For example, see Figs.1.8a, b. The flow diagram is shown in Fig.1.8c.

---

* Porosity is linearly related to transit time as may be seen in the Wyllie time average equation i.e. $\Delta sT = \phi\Delta sT_f + (1-\phi)\Delta sT_{ma}$. See Section 1.6 for the meaning of symbols.

In the absence of velocity sections, stacking velocities are computed for specified horizons across the line of seismic profile (by a polynomial regression fit of stacking velocities at velocity analysis points and interpolation to the mapped reflector seismic times). See Fig.1.8d. In such a case, the flow diagram as accordingly modified is shown in Fig.1.8e.

Velocities obtained are plotted separately for each reflection according to the analysis locations.

By overlaying the derived stacking velocity of the shallower horizon and the deeper horizon across the line of seismic profile, crossover zones may be identified and may be attributed to local lithology changes.

The essence of litho-velocity analysis is to establish a relationship between lithology and seismic interval velocity, then use the derived relationship to predict lithology from interval velocity. This is applied here within a single depositional system and stratigraphic interval. The stratigraphic and geographic extent over which a particular relationship [calibration curve] remains valid is dependent on the geological setting of the area and the vertical and lateral continuity of the velocity curve for a given lithology.

To calculate a calibration curve, sonic logs are utilized in finding the average interval velocity and cross plotted with seismic interval velocity for the same stratigraphic interval or zone to find out the degree of variance between the two.

Success is therefore dependent on geologic continuity and on plot separation of the calibration curves representative of specific lithologies (end-members). Construction of the curves consists of plotting depth and interval travel time from sonic logs for the various end-member lithologies.

All available data were utilized for the analysis* because sample selection must reflect the need for a rigorous and robust statistical base. Plotting of velocity-depth pairs showing best least squares fit shale and sand lines; and the sand-shale transition line is the consequence.

Generation of litho-vel maps and cross sections based on an appropriate time and velocity file is the next step. The velocity file was set up using stacking velocities displayed on the seimic sections.

---

* Exceptions were in respect of seismic interval velocities derived from faulted, disturbed or near surface anomaly zones

V_{int} is then calculated using Dix's equation and litho-vel values for each set of stacking velocities. Posting and contouring of the values on a base map produces a litho-vel map for sand trend analysis. Each litho-vel map is normalised for its own stratigraphic interval**.

Four of such intervals are of interest in this study namely:

1. The Lower Intra Biafra Rubble(LIBR).
2. The Upper Intra Biafra Rubble(UIBR).
3. The Rubble Beds.
4. The Lower Qua Iboe sequences.

The intervals mentioned above all conform to the important criteria of:

- low reflector dips for Dix's equation to be valid; and
- are bounded by prominent reflectors consistent or near consistent regionally.

Depth maps were not prepared for the following reasons:

1. The largely regional nature of the study.
2. Restrictions placed on the use of velocity data for some wells.

However, time structural maps in practice, wholly depict the structural configuration at the corresponding depths in the study area as is to be expected in a classic sand-shale series with no evidence of salt or carbonate sequences.

Moreover this study is mainly concerned with the stratigraphic sequences; their seismic facies and relationship to sea level changes; stratigraphic anomalies and interval velocity analysis of such anomalies.

** This is to confine the computed interval velocity interpretation to rocks within the same geologic age group. At a given depth, interval velocity is known to show a significant statistical increase with increasing geologic age(Faust, 1951). See Section 2.6; Litho-Velocity relationships.

1.8 DATA PREPARATION AND MANIPULATION.

Data preparation broadly involved three operations:

- Interpretation of seismic profiles and tieing into well logs through synthetic seismograms where possible.
- Digitizing the seismic data base and interpreted seismic sections using CPS-1 digitizing and mapping software; and
- The setting up of a data matrix using a Hewlett Packard software package which allows for user input of data, data editing, tranformation, storing, listing and computation. A data base was created by transferring stacking velocities into spread-sheet files for plotting, sorting and interval velocity manipulation. Input data were mainly well-log end member velocities and stacking velocities as derived from the seismic data.

Input data for interval velocity analysis are provided in the Appendix.

1.8.1 THE CPS-1 MAPPING SOFTWARE

The CPS-1 program as configured on the Vax 11/780 consists of a digitizing software and a contouring program which constitutes the main body of the package. The digitizing software comes with several options for digitizing the following:

- Spot height map(DIGISPOT),
- Seismic profiles(DEVNT; x,t),
- Seismic profile base map(DIGIMAP; x,y),
- Faults(DIGIFLT), and
- Contour digitizing(DIGICONT)

An available file merging facility(MASH) enables one to output x,y,t data with format(3(1X,E14.8)) from inputs of x,y (from DIGIMAP) and x,t (from DEVNT). The x,y,t data forms the input into the CPS-1 contouring package proper. A flow chart showing the inputs into the CPS-1 package is given in Fig.1.9a. Sample display listings of the digitizing options are also shown in Figs.1.9b&c.

All contouring jobs are submitted by batch mode through a series of verb card statements residing in a job file as shown below.

```
$VC JOB=1 $END

READ, GRID, SCALE, SAVE AND CONTOUR BQI DATA

$VC AOI=1, XMIN=0., XMAX=109750., XINC=2000., YMIN=0.,YMAX=
    65360., YINC=2000. $END

$VC MGRD=1,SLM=12000.,IFMT=-4,LUN=24,NCP=9962 $END

(3(1X,E14.8))

$VC SCLE=1,ZIDA=1,ZIDC=2,MODE=1,SFAC=-1.0 $END

$VC SAVE=1,LUN=26,FILE=1,ZIDA=2 $END

$VC DSPL=1,DEL=.05,XSCL=2540.0,ISMB=0,NCH=48,ZIDA=2 $END

BQI STRUCTURE TIME MAP

$VC STOP=1 $END
```

Program ease of use and efficiency was hampered by the following:

- The batch mode of input for program execution making errors in the verb card sequence not easily detectable until the program has run.
- The slow grinding nature of the program itself; requiring a lot of CPU time es pecially for gridding, fault incorporation and projection.
- The complicated file assignment structure of the program leading to inefficient use of storage space especially in operations involving the manipulation of more than one set of gridded x,y,t data such as in isochron map generation.

CPU time proved the limiting factor to the programs effective usage in including fault patterns on the structure maps. Consequently because of the large data sets in use*, allocated CPU time according to the priority level was often exceeded during fault incorporation. Thus structure maps are plotted without faults but

* For the BQI 9962 control points were gridded for contouring an area of approximately 5,500 sq.km.

with faults patterns juxtaposed using overlays. (See time structural maps in the Enclosures.)

Isochrons for the Rubble Bed and Intra Qua Iboe sequences were manually smoothed to remove the effects of minor faults. Only major structure building growth faults are shown on such maps.

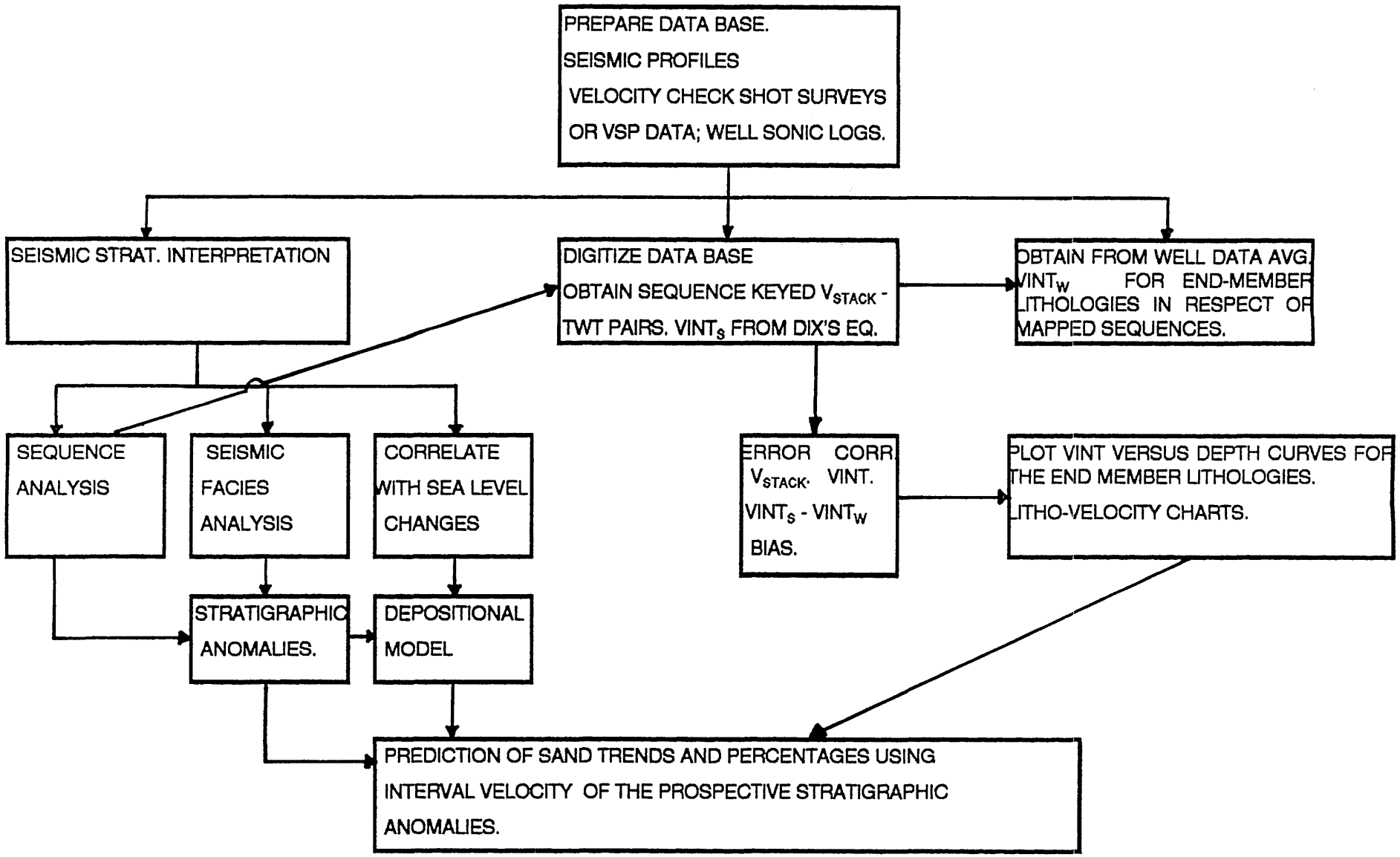

1.9 INTERPRETATION FLOW CHART

CHAPTER TWO

STRATIGRAPHIC VELOCITY REVIEW

2.1 Outline 043
2.2 Stratigraphic Velocity Interpretation 043
2.3 Stratigraphic Anomalies 045
2.3.1 Seismic resolution and anomalies 047
2.4 Errors in Velocity Estimation 049
2.4.1 Errors in rms velocity 053
2.4.2 Error estimation in V_{rms}^2 054
2.4.3 Errors in V_{int} estimation 056
2.5 Coefficient of heterogeneity 059
2.6 Litho-velocity relationships 061
2.6.1 Application to study area 064
2.7 Summary 065
2.8 Sample table of computed interval velocities 067

2.1 OUTLINE

As the flow diagram in the previous chapter suggests, seismic sequence analysis naturally leads to attempts to qualify seismic facies associations within such sequences with the spatial distribution of the velocity function. Stratigraphic velocity interpretation is such an attempt.

First, sequences are delineated and correlated with sea level changes. Seismic facies analysis is used to infer process and environment of deposition. Stratigraphic anomalies are thus identified and analysed using seismic velocities for quantitative estimation of clastic type and distribution.

This chapter considers the theoretical aspects of stacking velocity error estimation, stacking interval velocity error estimation, velocity-depth and velocity/lithology relationships. It further outlines their applications to the delineation and evaluation of seismic stratigraphic anomalies.

2.2 STRATIGRAPHIC VELOCITY INTERPRETATION

Beyond seismic sequence analysis and seismic facies recognition, velocity analysis offers an indirect way of quantifying estimates of the extent of reservoir rock within the seismic environment. The use of interval velocity derived from seismic data to infer lithology enables this assessment in areas of little well control. Listed below is an outline of the technique which involves the following:

1. Derivation of velocity corridors and reservoir sand versus total sand relationships for the appropriately selected wells within the time stratigraphic seismic sequence and facies framework.

2. Construction of Litho-Velocity calibration curves for as many different sequences and facies units as necessary.

3. Calculation of closely spaced seismic interval velocities.

4. Application of calibration curves to predict and map lithology.

This Litho-Velocity technique is referred to by Peikert(1985) as stratigraphic velocity interpretation and relies on interval velocities derived from stacking velocities (V_{nmo}- using Dix's equation) being intrinsically unique comparable with velocity derived from sonic logs. As discussed under method and approach, the analysis entailed following:

a. The use of wells to obtain Litho-Velocity data.

b. V_{int} versus depth curves for each sequence and each lithologic unit within the sequence*.

c. Application of the curves to the seismic velocity data to remove the effect of present day depth on velocity(decompaction).

d. Application of the variations in the residual velocity as a function of lithologic variations, within the context of seismic facies units.

The separation of lithologies on the basis of velocity and the derivation of Litho-Velocity curves are dependent on a reliable data base. However, the use of V_{int} derived from stacking velocities has some limitations, namely:

1. Velocity analysis (V_{nmo}) in the study area was carried out every 1.5 km. This lateral spacing of velocity points imposes a horizontal resolution of stratigraphic anomalies of over 1.5km for the influence of lithology on velocity to be evident. Since the premise is to observe real and small scale variations in intra sequence V_{int}, lateral smoothing of derived velocities cannot be considered, though two dimensional interval velocity ties have been performed.

2. The rounding off of stacking velocities used during data processing creates subtle inaccuracies which may be significant in V_{int} computation. Errors, thus have to be estimated.

3. V_{int} may be subject to random noise, ray path distortions mainly affecting V_{nmo} etc.(Blackburn, 1980), and velocity anisotropy(Banik, 1984). The ability to resolve a unique V_{nmo} for the top and base of the seismic sequence (a function of the seismic band width and the time difference between sequence boundaries) is suspect and sequence boundaries are not always marked by prominent and continuous seismic reflections. Thus V_{int} values from such estimates may have less stratigraphic resolution (Peikert, 1985).

---

* The relationship between velocity and depth was examined by Faust(1951), and Acheson(1959, 1963 and 1981).

4. Discrepancies which exist between V_{nmo} derived velocities and well velocities (Levin 1978, 1979, 1980), as well as observed differences between check shot survey velocities and sonic velocities (Stewart *et al.*, 1984).

5. Also, over thick sequences, interval velocity becomes a mean value of more elementary layers within the sequence. The choice of intervals is therefore important. In this study such intervals are characterized by unambiguous boundaries with reasonably consistent reflectors showing significant acoustic impedance contrasts.

A unique V_{nmo} for a specified seismic horizon was obtained by fitting polynomials of varying degrees to the stacking velocity data and picking an appropriately assumed stacking velocity for the specified horizon two way time. This undeniably introduces errors in stacking velocity estimation. However most of the initial stacking velocity picks were close to the major sequence boundaries. An example is given in Fig.1.8d. The velocity analysis is over the central anomaly on line 82-142. The interval is the Lower Qua Iboe sequence. Computed V_{nmo} for the top and base of the interval is as shown. Interval velocity is derived using Dix's equation and errors estimated.

A general treatment of errors is given under error estimation*. This estimation is necessary in order to test the validity and sensitivity of the use of interval velocities derived from normal move out correction on seismic sections.

2.3 STRATIGRAPHIC ANOMALIES

A seismic stratigraphic anomaly is defined here as a stratigraphic feature with clearly ascertainable boundaries, characterized by distinct seismic facies in general and unique stratal relationship within a seismic sequence. This distinction may be conveyed by the following:

a. Reflection discontinuities and reflection strength (in which case a high amplitude anomaly may be stratigraphic if it is not associated with a structure). Such frequent amplitude changes often suggest a variable lithology.

b. Unique reflection termination patterns that emphasize the distinct seismic facies.

---

* See Section 2.4

c. Reflection geometry that suggests depositional processes such as thickening isochron over the anomaly due to differential compaction and the systematic correlation of such features within a valid depositional framework.

It is difficult to define exclusively what this variance from the expected should be. However, in the study area, these anomalies are invariably seismic mounds or features of similar geometric expression (lensoidal) primarily defined by their seismic facies and not necesarily by a structural closure. In other words a purely depositional feature.

Consequently where a depostional mound exists(See Fig.2.1), caused by say channel sand enveloped by shale, this may be expressed as a seismic mound which, depending on the percentage distribution of coarse to fine clastics, may have high velocity anomaly characteristics. Although not all stratigraphic anomalies may be expected to be high velocity anomalies, a high interval velocity anomaly coincidental with a stratigraphic anomaly has important implications for exploration within the study area. By the same corollary, a low velocity anomaly may suggest a lack of reservoir rock, as long as the following provisos are valid:

a. we are within a clastic depostional setting;

b. no gas-charged shallow sediments are associated with the anomaly; and

c. high-pressure shales(such as may be found within the Akata formation) are not present.

This investigation reveals that three types of anomalies are prevalent by virtue of the definition above:

- Anomalies that occur at the foot of the progradational toe. These are mainly small scale features with "micro-fan wedge geometry" that are found off the progradational slope(See Fig. 2.2a; line 82-263) and are distinct from mounds often evident on strike sections of a prograding wedge. Anomalies of this type include slump features on the progradational slope(See Fig.2.2b; line 82-263).

- Anomalies showing mounded seismic facies with a predominant axis or trend. These of course are channel associated and commonly occur within the Lower Qua Iboe sequences (See Fig. 2.2c; line 82-257).

- Anomalies characterized by chaotic and disrupted seismic facies as distinct from mounds with hummocky facies(Fig.2.2d; line 82-178); and those particularly within the "Rubble Beds" which show offlapping reflection patterns(See Fig. 2.2e; line 82-212a).

Other variants to the aforementioned exist, e.g. anomalies characterised by high amplitude parallel reflectors within a generally subdued amplitude medium showing onlap to the base below and apparent truncation above. See Horizon Qua2 on line 82-106(Fig.2.2f). By outlining such features, it is possible to observe and quantify the modifying influence of these anomalies on spatial interval velocity trends.

Facies differentiation and therefore anomaly characterization within the sequences mapped is more pronounced within the Rubble Beds and the Qua Iboe than other sequences. This is perhaps, largely as a result of the greater depth of burial of the Intra Biafra Rubble systems, and the generally lower frequencies encountered at greater seismic depths, requiring larger stratigraphic features to register an anomaly(see seismic resolution of anomalies below).

Detailed examination of these anomalies is therefore restricted to the Rubble Bed and Qua Iboe members although interval velocities of the Intra Biafra Rubble system are discussed. The distribution of the anomalies within the Rubble and Qua Iboe are shown in Figs.2.2g and 2.2h respectively. For the Rubble Beds, two **northern anomalies** and a **south eastern anomaly** have been identified. The lower sequences of the Qua Iboe show three main trends namely:

- in the central area(**the central anomaly**),
- to the east(**the eastern anomaly**), and
- and in the west(**the western anomaly**).

Minor anomalies are evenly distributed over the study area, especially at the toe of Qua Iboe progradation*. Stratigraphic anomalies are considered in detail under sequence analysis of the respective members of the Agbada formation.

2.3.1 SEISMIC RESOLUTION AND ANOMALIES

* Qua Iboe is a prograding shale prone member of the Agbada formation in the acreage. Definition, geologic setting and type sections are discussed in Section 3.1

The ability to resolve a unique reflector within a seismic sequence is dependent on the resolution of the seismic system. Discussions on temporal(vertical) and spatial(horizontal) resolution have been pioneered by various workers including Kallweit and Wood(1982), Koefed(1981), Meckel and Nath(1977), Sheriff(1977, 1980, 1985), Widess(1973, 1980), Schoenberger(1974) and Ricker(1953).

Kallweit and Wood(1982), give the temporal resolution T_R as

$$T_R = \frac{1}{3.0 f_p} \tag{2.3.1}$$

where f_p is the peak frequency* related to a peak wavelength and defined as the frequency component having the largest value in the Fourier amplitude spectrum.

In a similar vein, the tuning thickness** $\frac{b}{2}$ may be expressed by the equation below:

$$\frac{b}{2} = \frac{1}{2.6 f_p} \tag{2.3.2}$$

where b is the wavelet breadth time. Predominant frequency (the reciprocal of the wavelet's breadth time) $\bar{f}_p$ becomes

$$\bar{f}_p = \frac{1}{b} = 1.3 f_p. \tag{2.3.3}$$

Temporal resolution is thus

$$T_R = \frac{1}{2.3 \bar{f}_p}, \tag{2.3.4}$$

and tuning thickness

---

* The term peak frequency is used in conjunction with the Ricker wavelet and is different from *terminal frequency* which is the maximum or minimum frequency for band limited transients such as *Sinc wavelets.*

** This is relevant when considering the tuned high amplitude reflectors of the Intra Qua Iboe sheet facies caused by thin sand bodies in Chapter 8.

$$\frac{b}{2} = \frac{1}{2\bar{f}_p}. \tag{2.3.5}$$

At subsea depths of about 5000 feet(1524m; our zone of interest with respect to the Intra Qua Iboe) , interval velocity of 8000ft/sec and dominant frequency of 39Hz, the vertical resolution approximates 44ft(13.4m) and tuning thickness 50ft(15.2m).

On the other hand, reflections are deemed to be a summation of responses from an area called the **Fresnel zone**(See Fig.2.3a). The limit of this zone is regarded as the limit of spatial resolution and it is dependent on distance from source, effective velocity, and the frequency composition of a wavelet(Meckel and Nath, 1977).

Neidell and Poggiagliomi(1977), give the mathematical relationship derived from the geometry of the Fresnel zone and empirical weighting as

$$R_1 \approx \frac{V}{4}\sqrt{\frac{t}{\bar{f}_p}} \tag{2.3.6}$$

where R_1 is the radius of the first Fresnel zone as shown in Fig.2.3a and t, two way travel time. A nomogram (after Sheriff, 1980) for determining the size of the Fresnel zone is shown in Fig.2.3b. Fig.2.3c shows model response for different size sand bodies illustrating the significance of the Fresnel zone.

Using the same values as in the vertical resolution example above, the lateral resolution for an anomaly caused by a sand body is 75ft(23m). For the purposes of this study however, the size of the anomaly must exceed at least twice the velocity analysis spacing(1.5km) to avoid spatial aliasing. Thus several small seismic mounds although anomalous have been mentioned but not analysed because they were not large enough to be sampled laterally by successive stacking velocities(Fig.2.3d, line 82-345).

2.4 ERRORS IN VELOCITY ESTIMATION

In general, stacking velocity or V_{nmo} is often approximated as V_{rms}. Methods for estimating this velocity include the following (see Sheriff and Geldart(1983):

- The $X^2 - T^2$ method which involves the solving of the relation

$$T^2 = T_0^2 + \frac{X^2}{V_s^2}.$$

- The $T - \Delta T$ method based on the equation below

$$V_{st} = \frac{X}{(2T_0 \Delta T_n)^{\frac{1}{2}}}.$$

- Best-fit methods which are based either on fitting a hyperbola to coherent events or finding which stacking velocity best stacks a reflector*.

The relationship between the different velocities discussed above and below is given thus:

$$V_{nmo} \geq V_{rms} \geq V_a$$

where V_{rms} is the root mean square velocity and V_a is the average or mean velocity obtained from sonic logs or check shot surveys.

$$V_a = \frac{1}{T} \int_0^T V_{(t)} dt \tag{2.4.1}$$

where $V_{(t)}$ is the instantaneous velocity.

$$\begin{aligned} V_{rms}^2 &= \frac{1}{T} \int_0^T V_{(t)}^2 dt \\ V_{rms} &= \sqrt{\left[\frac{1}{T} \int_0^T V_{(t)}^2 dt\right]} \end{aligned} \tag{2.4.2}$$

---

* The latter of the two best-fit methods was used in respect of this seismic data, and is referred to as Constant Velocity Stacks in Fig.1.2.

Dix, 1955 showed that;

$$V_{int} = \sqrt{\frac{\sum_{i=1}^{i=n} V_i^2 t_i}{\sum_{i=1}^{i=n} t_i}} \tag{2.4.3}$$

- assuming small source to geophone distance compared to depth of investigation and dips of less than 5^0 . The basis for our velocity analysis is the approximation $V_{nmo} \approx V_{rms}$. The difference between V_{rms} and V_{nmo} is known to increase with the heterogeneity of the subsurface (a factor that reflects the different ray paths). This difference can largely be ignored (Al-Chalabi, 1979). However, techniques used in velocity estimation are prone to errors. For the purposes of this study, the associated errors are categorized as given below:

a. Errors due to anisotropy(see Banik, 1984).

b. Errors in the root mean square velocity due to a time error E_t in ΔT, the measure of normal move out(Shugart, 1969).

c. Errors in the estimation of interval velocity from seismically measured root-mean-square velocity due to dip, interface curvature and velocity gradients.

Errors due to anisotropy become significant when we are dealing with more compacted units; when large offset angle data is in use and in respect of shallow reflection mapping. Otherwise this is negligible as is the case in the study area where none of the above is thought to be applicable. However, anisotropy may be represented by the equations given below.

$$V_h = AV_v$$

where V_h is the horizontal velocity, V_v the vertical velocity and A, the anisotropy factor which when incorporated into the move out equation, gives:

$$T^2 = T_0^2 + \frac{X^2}{A^2 V_{rms}^2} \tag{2.4.4}$$

Errors itemized in (b) and (c) are important and are reviewed further.

Dix's equation given by

$$V_{ij}^2 = \frac{V_j^2 T_j - V_i^2 T_i}{T_j - T_i}$$

may be represented as a partial diffential of the square of velocity;

$$V_{int}^2 = \frac{\delta V_t^2}{\delta t} t$$

and for a dipping reflector

$$V_{int}^2 = \frac{\delta (V_t \cos\theta)^2}{\delta t} t.$$

Evaluating the partial differentials results in the following:

$$V_{int}^2 = 2V_t \frac{\delta V}{\delta t} t + V_t^2$$

and for a dipping reflection

$$V_{int}^2 = 2V_t cos\theta \frac{\delta V_t \cos\theta}{\delta t} t + (V_t \cos\theta)^2$$

V_{int} is therefore dip-dependent . In the common case, where the measured stacking velocity V_{st} which is often assumed to be V_{rms} is over a reflector with dip θ, the correction required to obtain a more accurate V_{nmo} is given below:

$$V_{nmo} = \frac{V_{rms}}{\cos\theta}.$$

Dip correction to V_{rms} was applied accordingly in respect of the following reflectors:

- Base Rubble Beds(BRB),

- Top Intra Biafra Unconformity(TIBU),
- Base Intra Biafra Rubble(BIBR), and
- Lower Base Intra Biafra Rubble(LBIBR).

2.4.1 ERRORS IN RMS VELOCITY

The accuracy of V_{rms} measurements are affected by the following parameters (Al-Chalabi, 1979):

- Recording fold of the survey. Accuracy is dependent on $\sqrt{N}$ where N is number of samples.
- Signal to noise ratio S/N.
- Frequency bandwidth.
- Spread length X.

The relationship between root-mean-square error and travel time for different signal to noise ratios is displayed in Fig.2.4a and it is observed that velocity accuracy with increased travel time decreases past 2 seconds because the moveout is getting smaller; at the same time, the shallow events have increased velocity error because the far traces are muted(Schneider, 1971).

For the study area, the zone of interest lies between 1.4 and 2 secs which, superimposed on the chart in Fig.2.4a, gives a worse case error percent when signal to noise ratio is 2 of between 3 to 4%. The best case with signal to noise ratio of 8 shows an error percent of about 1%.

With respect to spread length, errors in V_{rms} may be estimated using the normal moveout equation as applied to a simple horizontal layer model, and approximating the normal move out equation by truncating the higher order terms resulting in the following:

$$T^2 = T_0^2 + \frac{X^2}{V_{st}^2} \tag{2.4.5}$$

Manipulating the equation above yields

$$V_{st} = \sqrt{\frac{X^2}{T^2 - T_0^2}}$$
$$= \sqrt{\frac{X^2}{2T_0\Delta T + \Delta T^2}} \qquad (2.4.5a)$$

when $T - T_0 = \Delta T$.

Errors in stacking velocities would therefore be dependent on time, and distance and indirectly on velocity. If E_{st} is defined as the error in stacking velocity caused by an error E_t at time T_0 then for a minimum E_{st} when E_t is positive;

$$V_{st} + E_{st} = \sqrt{\frac{X^2}{T^2 - (T_0 + E_{(t)})^2}} \qquad (2.4.6a)$$

Expanding and retaining lower order terms gives the following relation:

$$E_{st} \approx \frac{X}{T^3} T_0 E_t \qquad (2.4.6b)$$

where X is the far trace distance and T its reflection time; and

T_0 is the reflection time at X=0.

2.4.2 ERROR ESTIMATION IN V^2_{rms}.

If V^2_{rms} has a variation due to an error in defining the moveout curve by E_T at distance X and

$$V^2_{rms} = \frac{X^2}{\Delta T^2 + 2T_0\Delta T}$$

where X is the offset distance,

$\Delta T = T - T_0$,

T the reflection time at X, and

T_0 is the reflection time at $X = 0$.

$$\Delta V_{rms}^2 = V_{rms}^2 - \hat{V}_{rms}^2$$

where $\hat{V}_{rms}^2$ is the rms velocity squared obtained by assuming a normal move-out increment at X of $\Delta T + E_T$. The variation of ΔV_{rms}^2 takes the form of

$$\begin{aligned}\Delta V_{rms}^2 &= \frac{X^2}{T^2 + 2T_0\Delta T} \\ &\quad - \frac{X^2}{\Delta T^2 + 2T_0\Delta T + 2T_0E_T + 2E_T\Delta T + E_T^2} \\ &= \frac{X^2}{(\Delta T^2) + 2T_0\Delta T}\left\{1 - \frac{1}{1 + \frac{(2T_0E_T + 2E_T\Delta T + E_T^2)}{(T^2 + 2T_0\Delta T)}}\right\}\end{aligned}$$

Using Taylor's series expansion the bracket terms as indicated become convergent; thus retaining only the first two terms results in the following relation:

$$\Delta V_{rms}^2 \doteq \frac{V_{rms}^4(2T_0 + 2\Delta T)E_T + E_T^2}{X^2} \tag{2.4.7}$$

Since the error associated with two way travel time T at X is small, then $E_T^2 \Rightarrow 0$ and $(2T_0 + 2\Delta T)E_T \gg E_T^2$ over the range of velocities and times commonly encountered in seismic exploration. The equation above may be simplified to the following:

$$\Delta V_{rms}^2 \doteq \frac{V_{rms}^4(2E_T T)}{X^2} \tag{2.4.8}$$

or

$$\Delta V_{rms}^2 \propto \frac{V_{rms}^4 T}{X^2}$$

where $2E_T$ is a constant of proportionality. If E_T is 0.001 secs independent of distance, then errors may be predicted. These estimated errors are then input into the Dix's equation to compute errors in the interval velocities derived for a particular seismic sequence mapped.

From the relationship established above, a relative error in V_{rms} may be derived. The relative error in V_{rms} is defined as $\frac{\Delta V_{rms}}{V_{rms}}$.

But,

$$\Delta V_{rms} = \sqrt{V_{rms}^2 + \Delta V_{rms}^2} - V_{rms}.$$

Therefore,

$$\frac{\Delta V_{rms}}{V_{rms}} = \frac{\sqrt{V_{rms}^2 + \Delta V_{rms}^2} - V_{rms}}{V_{rms}}.$$

Substituting the previously derived equation for ΔV_{rms}^2which is equation 2.4.8 given below

$$\Delta V_{rms}^2 \doteq \frac{V_{rms}^4}{X^2} 2E_T T$$

yields the following as relative error:

$$\frac{\Delta V_{rms}}{V_{rms}} = \sqrt{1 + \frac{2E_T V_{rms}^2 T}{X^2}} - 1$$

Using Taylors series expansion of the right hand side of the above equation as $\frac{2E_T V_{rms}^2 T}{X^2} \ll 1$ the following is obtained:

$$\frac{\Delta V_{rms}}{V_{rms}} \doteq E_T \frac{V_{rms}^2 T}{X^2} \tag{2.4.9}$$

The above equation is important as it gives relative velocity error as a function of variables involved in velocity estimation namely: V_{rms}, Time T, Distance X, and E_t which is a constant. These estimated errors are then used as inputs in the estimation of interval velocity errors.

2.4.3 ERRORS IN INTERVAL VELOCITY ESTIMATION

Errors in interval velocity estimation are dependent on errors in V_{rms} since most techniques for interval velocity calculation are indirect using Dix's equation. Two methods are considered here.

The first is by Hajnal and Sereda(1981), who derive an uncertainty equation for error estimation based on Taylor's series expansion techniques(treated in standard texts). The equation is given as:

$$
\begin{aligned}
\Delta V_{I,n} \doteq \Delta v_n & \left[\left(\frac{1}{ac}\right)^{1/2} v_n T_n\right] \\
& + \Delta v_{n-1}\left[-\left(\frac{1}{ac}\right)^{1/2} v_{n-1} T_{n-1}\right] \\
& + \Delta T_n\left[-1/2\left(\frac{b^2}{a^3 c}\right)^{1/2} T_{n-1}\right] \\
& + \Delta T_{n-1}\left[1/2\left(\frac{b^2}{a^3 c}\right)^{1/2} T_n\right]
\end{aligned}
$$

where

$$
\begin{aligned}
\Delta V_{I,n} &= \textit{Interval velocity error} \\
\Delta v_n, \Delta v_{n-1} &= \textit{rms velocity error} \\
\Delta T_n, \Delta T_{n-1} &= \textit{normal incidence time errors} \\
a &= T_n - T_{n-1} \\
b &= v_n^2 - v_{n-1}^2 \\
c &= v_n^2 T_n - v_{n-1}^2 T_{n-1}
\end{aligned}
$$

Calculating a possible maximum error by assuming the absolute values of the terms on the right hand side of the equation above, and upon simplification gives:

$$
\begin{aligned}
\Delta V_{I,n} \doteq \left(\frac{1}{ac}\right)^{1/2} & [v_n T_n |\Delta v_n| \\
& + v_{n-1} T_{n-1} |\Delta v_{n-1}|] \\
& + \frac{1}{2}\left(\frac{b^2}{a^3 c}\right)^{1/2} [T_n |\Delta T_{n-1}| + T_{n-1} |\Delta T_n|]
\end{aligned}
$$

Evidently, *the uncertainty in calculated interval velocity consists of two parts; the first depending on the uncertainty in the rms velocity estimate and the second on errors in normal incidence time estimates.*

Further simplification may be made by assuming the following:

1. A comparatively thin interval compared to depth i.e. $T_{n-1} \gg a$
2. A relatively small velocity contrast for the said interval; thus $v_n = v_{n-1}$; $b = v_n^2 - v_{n-1}^2 \doteq 0$; $c = v_n^2 T_n - v_{n-1}^2 T_{n-1} \doteq v_n^2 a$.
3. A constant error in rms velocity.

These simplifications lead to the equation below:

$$\Delta V_{I,n} \doteq \frac{2T_{n-1}}{a} \Delta v_{n-1} \tag{2.4.10}$$

Thus the uncertainty increases with the reflection time to the top of layer and is inversely proportional to the interval travel time of the layer(see Fig.2.4b). The equation above may be rearranged in terms of dimensionless parameters in a logarithmic form given by:

$$ln(\Delta V_{I,n}/\Delta v_{n-1}) \doteq ln2 - ln(a/T_{n-1}) \tag{2.4.11}$$

A logarithmic plot of the error ratio of interval and rms velocities versus the time thickness to depth ratio for the study area approximates a straight line as might be expected(See Fig.2.4b).

What may be deduced from the equation above is that an error magnification occurs as the interval velocity is taken from either deeper zones or thin zones. This also implies that larger depth intervals must be taken with deeper zones to ensure the same accuracy(Fig.2.4c).

Such an error magnification has also been discussed by McQuillin, McEnvoy & Steele(1984), where an equation relating the standard error in the interval velocity σ_{int} with the standard error in rms velocity σ_{rms} is given as:

$$\sigma_{int} \doteq \frac{1.4\sigma_{rms} D}{h},$$

where h is interval thickness, and D is average depth.

The following observations may however be made in respect of the study area. Interval velocity errors due to interval travel times of about .3 secs for the Intra

Qua Iboe and a 3% error in V_{rms} results in about 20% error in V_{int}. Errors in rms velocity therefore appears to be the most significant contributor to possible errors in V_{int} estimation. Such a result is unacceptable in respect of lithology estimation. This handicap is discussed further at the end of this chapter under summary, after litho-velocity relationships have been discussed.

The second method of interval velocity error estimation involves ignoring normal incidence time errors and deriving a relation based on errors in the rms velocities to the top and base of the interval. Employing Dix's equation

$$V_{I,n}^2 = \frac{v_n^2 T_n - v_{n-1}^2 T_{n-1}}{T_n - T_{n-1}},$$

error in interval velocity due to error in the rms velocities may be represented by the following:

$$(V_{I,n} + \Delta V_{I,n})^2 = \frac{(v_n + \Delta v_n)^2 T_n - (v_{n-1} + \Delta v_{n-1})^2 T_{n-1}}{(T_n - T_{n-1})}.$$

This may be simplified by algebraic manipulation and ignoring error squared terms produces the result below.

$$\Delta V_{I,n} = \frac{v_n \Delta v_n T_n - v_{n-1} \Delta v_{n-1} T_{n-1}}{V_{I,n}(T_n - T_{n-1})} \tag{2.4.12}$$

Maximum error in $\Delta V_{I,n}$ therefore occurs, if Δv_{n-1} is negative. The above equation may be written in the form

$$\Delta v_n = P \Delta v_{n-1} + Q \Delta V_{I,n}, \tag{2.4.13}$$

where

$$P = \frac{\Delta v_{n-1} T_{n-1}}{\Delta v_n T_n};$$

and

$$Q = \frac{\Delta V_{I,n}(T_n - T_{n-1})}{\Delta v_n T_n}.$$

Equation 2.4.13 gives a family of straight lines for differing values of $\Delta V_{I,n}$(See Fig.2.4d).

2.5 COEFFICIENT OF HETEROGENEITY

THE $V_{rms}^2 - V_a^2$ RELATIONSHIP.

Another consideration in the indirect evaluation of stratigraphic anomalies is the relationship $V_{rms}^2 - V_a^2$. Al-Chalabi(1974), notes the significance of the derivation of $V_{rms}^2 - V_a^2$, i.e. the difference between the square of the root mean square velocity and the square of the mean velocity(average) is the variance of the set of interval velocities V_{int}.

This increases with the heterogeneity and thus the significance in facies analysis. The coefficient of heterogeneity g is given as

$$g = \frac{V_{rms}^2 - V_a^2}{V_a^2} \tag{2.5.1}$$

In terms of seismic time, depth and thickness of the various layers, the coefficient of heterogeneity as given by Al-Chalabi(1974) is expressed as:

$$g = \frac{1}{Z^2} \sum_{i=1}^{n-1} h_i \sum_{k=1}^{n} h_k \frac{(V_i - V_k)^2}{V_i V_k} \tag{2.5.2}$$

where g is non negative and gives a measure of the heterogeneity of the sediments above the reflector k(kth layer), Z is depth and h is seismic time. Data from a sonic log corrected by check shot survey allows for the calculation of values g as a function of depth Z. The sequence of values of g constitute the "curve of heterogeneity". Comparison of these curves of heterogeneity for wells passing through a "similar" series of strata may be used as indicators of facies change.

A map of heterogeneity for different stratigraphic levels is the natural consequence. Within the basin, these could be used as guides for conversion of velocities derived from analysis(considered here as approximating values of V_{rms}) into values of mean vertical velocity V_a for a general Time- Depth conversion.

The coefficient of heterogeneity map for the Base Qua Iboe level as it relates to the Stratigraphic anomalies is discussed in Chapter 8.

For a heterogenous sand-shale series, and for a given time interval, the difference $V_{rms} - V_a$ depends on:

- The percentage of sand in the interval; the greater this is the larger the difference $[V_{rms} - V_a]$.

Between 0% to 50% sand $[V_{rms} - V_a]$ tends to increase; between 50% sand and 100% sand the effects tend to cancel out (Cordier, 1985).

2.6 LITHO-VELOCITY RELATIONSHIPS

The empirical relationship between V_{int}, depth and geologic age (Faust, 1951) is shown below:

$$V_p = 125.3(ZT_g)^{\frac{1}{6}} \tag{2.6.1}$$

where V_p is the compressional wave(p) velocity in ft/sec, Z is depth and T_g is geologic time in years. The result is a series of lines known as Faust's lines when interval velocities are plotted against mean depth.

Acheson(1959), however, proposed an empirical formula different from that above which claims more consistency than Faust's with n varying between 0.83 and 1 as shown below.

$$t_z = aZ^n + b, \tag{2.6.2}$$

where t_z is the seismic time at depth Z and a and b are constants.

V_z, the velocity at depth Z is thus given as:

$$V_z = CZ^{1-n}. \tag{2.6.3}$$

It suffices that n increases as the section is more compact(maximum n =1); and is also independent of lithology and age; but related to depositonal history. a indicates gross lithology and is independent of time.

Acheson's equations basically show what he refers to as "secular variations" of velocity, i.e. velocity changes as a, C and n corresponding to major changes in lithology, pressure or compaction. Intra-formational velocity fluctuations caused by variations in grain size, porosity etc. are not indicated. Such variations are however where the main interest of this research lies.

The following basic assertions are made:

- For a given geologic age, interval velocity increases as depth increases and at a given depth the velocity increases with geologic age.
- For a sand/shale series such as the study area with fluid filled porosity, velocity also becomes dependent on porosity[and the shape of the pores]. Thus interval velocity increases with increase in sand percentage
- Depth and sand percentage within sequences of the same geologic age are the dominating factors affecting interval velocity.

Two schools of thought have persisted as to the behaviour of the velocity function in a sand/shale series. They are the logarithmic(Faust, 1951) and the semi-logarithmic(Pirson, 1977) relationship.

The logarithmic relationship is of the form:

$$V_z = KZ^n \tag{2.6.4a}$$

$$\frac{dZ}{dt} = KZ^n$$

$$Z = \sqrt[1-n]{(1-n)Kt}. \tag{2.6.4b}$$

$$\begin{aligned} V_a &= K(1-n)Z^n \\ &= (1-n)V_z \end{aligned} \tag{2.6.4c}$$

where V_z is velocity at depth Z and K is a constant called the "compaction factor". This power-law relationship appears to be valid with regards to the Qua Iboe. See Fig. 2.5a.

Pirson(1977), shows a semi-logarithmic relationship of the form

$$V_z = V_0 e^{KZ} \tag{2.6.5a}$$

The semi-log relationship between interval velocity and depth when plotted gives the theoretical velocity of sand-shale sequence called the "average velocity

function". Deviations from this curve indicate deviations from the mean lithologic composition. The function is obtained by the calculation of a "regression line" called the "compaction line". The equation of the regression line is may be used to interpret shaliness.

Equation 2.6.5 may be rewritten as given below.

$$V_{int} = V_0 e^{KZ} \tag{2.6.5b}$$

where V_0 and K are constants, Z is depth and V_{int} is interval velocity. Since velocity is $\frac{dZ}{dt}$, the equation for normal compaction in a sand-shale sequence becomes:

$$\begin{aligned} \frac{dZ}{dt} &= V_0 e^{KZ} \\ dZ &= V_0 e^{KZ} dt \\ Z &= \frac{1}{K} ln \frac{1}{1 - V_0 K t} \end{aligned} \quad . \tag{2.6.6a}$$

By replacing Z with its value in equation 2.6.5b, V_{int} becomes:

$$V_{int} = \frac{V_0}{1 - V_0 K t}. \tag{2.6.6b}$$

Average velocity may then be derived from the previously established relation:

$$\begin{aligned} V_a &= \frac{1}{T} \int_0^T V_{(t)} dt \\ &= \frac{1}{T} \int_0^T \frac{V_0}{(1 - V_0 K t)} dt \\ V_a &= \frac{1}{KT} ln \frac{1}{(1 - V_0 K t)} \end{aligned} \tag{2.6.7}$$

Similarly;

$$
\begin{aligned}
V_{rms}^2 &= \frac{1}{T}\int_0^T V_{(t)}^2 dt \\
&= \frac{1}{T}\int_0^T \frac{V_0^2}{(1-V_0KT)^2} \\
&= \frac{V_0^2}{1-V_0KT}
\end{aligned}
\tag{2.6.8}
$$

Over a limited interval such as the sequences mapped in this area, a linear approximation of the relationship between velocity and depth is appropriate. Thus,

$$
\begin{aligned}
V_z &= V_0 + KZ \\
t &= \frac{2}{K} ln(\frac{V_0}{K} + Z). \\
V_a &= \frac{KZ}{ln(\frac{V_0}{K} + Z)}.
\end{aligned}
\tag{2.6.9a, b, c}
$$

where t is the two-way travel time to depth Z.

V_0 and K can be statistically determined from bore hole measurements of velocity versus depth for both sands and shale.

These formulae constitute the basic theoretical framework used to infer sand prone and shale areas within a clastic environment such as the Niger Delta and provide a rigorous treatment of velocity variation as a function of lithology. They are utilized in the relevant sections of this thesis.

2.6.1 APPLICATION TO STUDY AREA

Interval velocity for the seismic sequence of interest, may be thought of as a function of V_{int} of the component end-member lithologies. i.e. the proportions in which these lithologies are present in the interval. In practice, seismic interval velocity V_{int_s} shows a positive variation from well derived interval velocity V_{int_w}. This positive bias averages about 4% for the Intra Qua Iboe and Rubble Bed intervals and a correction is applied to the seimic interval velocity before lithology

estimation is undertaken*. The mismatch of V_{int_s} and V_{int_w} is due to the fact that both methods measure different physical parameters(see Stewart *et al.*, 1980).

A sample table illustrating the input values, error corrections applied in respect of line 82-142 over the western and central anomalies is shown at the end of this chapter. Using the linear law (equation 2.6.9a) decompacted velocities may be compared.

Seismically derived velocities which show variance from the expected shale velocities at a depth may be interpreted as due to the following:

- abnormally over-pressured shale, if the velocity is less; or
- if more, then the likely causes could be in the case of the study area, the presence of sand within the sequence or tectonic uplift. In the latter case, higher than expected Biafra velocities within shale** immmediately overlying prominent unconformities such as TIBU and LIBU in the northwestern and northeastern parts of the study area, were interpreted as due to tectonic uplift and are utilized as the basis for the construction of mobility diagrams(burial history curves).

The sequence intervals considered here are young and immature, varying in age between 3.5 to 15 million years and this has implications for the degree of compaction of the sediments and the separation of end-member lithologies on litho-velocity plots.

Well velocity data over the central anomaly along with interpreted sequence boundaries are discussed in Chapter 8. Application of the well derived curves to the seismic interval velocity data results in a map of sand/shale distribution for the interval of interest. The shale field boundary corresponds to the highest decompacted shale velocity, while the sand field is the lowest decompacted sand velocity using the appropriate equations discussed earlier.

---

* For the Rubble Beds, few of the wells provided tested the complete Rubble interval.

** These shale units are referred to later in the text as transgressive shale often forming part of a transgressive system tract. They also provide cap-rock for hydrocarbon traps.

2.7 SUMMARY

The pitfalls in the use of interval velocities computed from stacking velocities for sand percentage estimation are due to errors inherent in the estimated V_{rms}. Errors in stacking velocity estimates are often compounded into errors in interval velocity. The interval velocity error is proportional to the reflection time to the top of the layer and inversely proportional to the interval travel time of the layer. This is best illustrated in Fig.2.5b where a graph of V_{int} error versus V_{rms} error shows an error magnification in V_{int} of *5 times* V_{rms} error.

A 10% maximum velocity separation between the shale line curve and the sand line is more than likely to be obliterated by errors in V_{int} estimation(see Fig.2.6a). Attempts at sand percentage estimation using stacking velocities must therefore be fruitless. Instead, in general, we infer instead sand prone seismic facies with associated velocity anomalies from which the phrase the "Intra Qua Iboe sand package" is coined.

Banttari(1976), quoted in Hilterman(1981), used the sand-shale ratio method to quantify errors involved in estimating sand percentage. The error analysis model shown in Fig.2.5c is based on component velocity variation of sands and shale within a stratigraphic interval and conclusions drawn are similar and include the following:

- Intervals containing more than 3% of limestone must be excluded from sand percentage calculations; and
- stratigraphic intervals of more than 3000ft must be considered.

Maximum sand percentage for this Intra Qua Iboe interval of interest appears to be only 30%. This is apparently within the limits for which increasing sand percentage leads to higher coefficient of heterogeneity values(see Section 2.5).

However, V_{int} computed for the stratigraphic anomalies and Rubble Bed sequences, are compared within their respective stratigraphic framework. This comparison is qualitative and not quantitative. Before such a comparison, computed interval velocities have to be 'decompacted'.

Over a comparatively small interval(about 1000ft(300m)) such as characterizes the Intra Qua Iboe, the velocity-depth function may be approximated by a linear relationship of the form:

$$V_{int} = V_0 + KZ \tag{2.6.10}$$

where K is the compaction factor derived from the gradient of the straight line with dimensions of sec^{-1} and a value (in the case of the Qua Iboe) of 0.48. The decompacted velocities V_0 are then compared.

SAMPLE TABLE OF COMPUTED INTERVAL VELOCITIES

LINE 82-142

Shot Point	V_n m/sec	V_{n-1} m/sec.	T_n millisec.	T_{n-1} millisec.	$V_{I,n}$ m/sec.	ΔV_{n-1} m/sec.	$\Delta V_{I,n}$ m/sec.	V_{Int_c} m/sec.	Depth ft.
1092	2290	2000	1900	1500	3148	17·2	170	2978	5966
1012	2300	2100	1900	1530	3056	19·9	165	2891	6030
972	2300	2077	1950	1630	3200	20·1	198	3002	6360
932	2270	2142	1950	1640	2851	22·1	214	2637	6390
280	2100	2000	1710	1400	2500	16·5	149	2351	
100	2100	2000	1700	1430	2565	16·7	177	2388	

CHAPTER THREE

REVIEW OF STRUCTURE AND STRATIGRAPHY

3.1 Regional and geologic setting.....xxx

3.2 Stratigraphic and structural framework.....xxx

3.2.1 Stratigraphic framework. xxx

3.2.2 Structural framework. xxx

3.2.3 Structure at the TIBU level xxx

3.2.4 Structure at the BQI level.....xxx

3.2.5 Structure at the QUA5 level xxx

3.1 REGIONAL AND GEOLOGIC SETTING

A structural composite of the regional tectonic framework of the Niger Delta during the Cenozoic is shown in Fig.3.1. The setting of the Niger Delta was shaped by several important structural elements which include the **Benin Hinge zone** to the west(derived from the Chain Fracture zone originating from the split-up of the Atlantic), the **Onitsha High, the Abakaliki High and the Oban Massif** to the east.

The build up of the delta from Eocene to Pleistocene revealed in Fig.3.1, indicates that by late Miocene, the delta approximated the present day shoreline, and by Pleistocene, sediment growth was well into the present day offshore. The study area although not shown is offshore. This sustained sedimentary input is characteristic of the depositional picture depicted throughout the Tertiary. The shoreline positions of these deltaic regimes, at certain geologic time intervals, arguably bear great significance for correlation to "global" events such as sea level changes. The position of the late Miocene shoreline for example means that during the late Miocene lowstand, this area would have been the exposed shelf that fed sediments into an embayment(palaeobasin) to the south.

The Niger Delta basin extends eastward offshore into the **Rio del Rey** basin of Cameroun, bounded to the east by the **Cameroun- Annobon volcanic axis** which is part of the **Fernando Po-Ascension Fracture Zone** extending into the Atlantic(See Fig.3.2). The Miocene volcanicity along this axis is thought to have affected the eastern part of the Niger delta leading to uplift and provided a ridge against which shale diapirism was later prolific* (Fig.3.3). The influence exerted by Tertiary tectonism in the eastern part of the delta on the seismic stratigraphy of the study area is of primary significance and is considered later.

However, the relationship between the delta and the continental margin is that of a large sedimentary bulge (comprising the megasequences; **Akata, Agbada and Benin** formations) caused by progradation and loading (aggradation).

---

* See Whiteman(1982) for possible reasons as regards the strong diapirism offshore compared to onshore. These include the Akata being older to the north and diapirism being a feature of the less de-watered younger Akata offshore; the basement high underlying the present coastline and the diapiric zone acting as barriers to the up-dip water migration of shales further south; and the shale type of the Akata formation changing from low montmorillonite in pre-Miocene time to high montmorillonite in post-Oligocene.

Fig.3.4a. Based on this and other proprietary seismic data (Fig.3.4b and c) the present continental shelf ranges from 50-80km(31-50miles) wide with the shelf edge occurring at between 100-200m (328-656ft)water depth. The continental slope (with steeper average gradient of 1.6, extends to about 2000-3000m(6560-9840ft) water depth into the continental rise and abyssal plain at water depths of over 4500m(15,000ft).

Allen (1964, 1965) shows that modern deltaic sedimentation is limited to the inner shelf with prodelta sediments reaching only as deep as 40m, the outer shelf being presently an area of little deposition. The continental slope on the other hand is incised by four canyons: **Avon, Mahin, Niger, and Calabar**(Burke, 1972 and Gorini, 1981)*. In the Niger Delta, the origins of the canyons are thought to be erosion of the continental slope by mass movement (slump, sliding and debris flow) generated in response to failure of unstable sediments and to erosion and back-cutting by turbidity currents during lowstands of sea level(Fig.3.5).

If the presence of these canyons is anything to go by, then we can infer the possible occurrence of similar features in the older sedimentary sequences. These have been identified and examined further on in the text.

In water depths deeper than 1000m(3280ft), erosional canyons are no longer evident in the modern day Niger Delta complex. Instead submarine levees and channels predominate and are therefore indicative of deeper depths of deposition in this area. Such a relationship between shelf, shelf edge and margin is crucial in interpreting environment (and depth) of deposition of the various seismic facies analysed later. The assumption** is that, essentially, the native characteristics of the Niger Delta margin has remained largely unchanged from the Tertiary to the Present.

The structural features are similar to the unstable progradational clastic margin of the Gulf Coast (Winker, 1983) induced by down slope mass movement and may be classified into:

---

* Also see Shepard(1981) for review of the origins of canyons.

** The major phase of thermal and isostatic subsidence is thought have terminated in early Tertiary with the formation of the proto-Niger Delta basin(see Fig.3.6). Greater prominence for local and near regional events such as fluctuating sediment accumulation rates and subsidence, shale tectonism and long shore drift were thus the consequence. It may also be noted that these events may in combination overshadow global changes in sea level especially in a deep water area.

(a) an upper extensional regime characterized by growth faulting (Winker, 1982; Galloway, 1986) and

(b) a lower thrust regime (or toe) of a mega-landslide (the shortening domain).

The structural and stratigraphic features now evident implies that during much of the Tertiary, the study area was confined to the upper extensional regime.

3.2 STRATIGRAPHY AND STRUCTURE

3.2.1 STRATIGRAPHIC FRAMEWORK

Fig.3.6 shows the growth of the Tertiary Niger Delta complex from the Gulf of Guinea. Through the use of palynological zonal markers(Evamy *et al.*, 1978), growth of the delta complex is depicted from the Paleocene to Present, as forming by a series of coalescing (overlapping) depocentres in the west and rapid advance of the delta front. Growth was accelerated in the eastern part by the development of an additional source, namely the Cameroun Swell or Uplift (Whiteman, 1982).

Translated into the study area, this growth is represented by a main depocentre trending in a NW-SE direction during the Pliocene consisting of the main stratigraphic sequences as can be shown on lines 82-251 and 82-279 (See Figs. 3:7 and 3:8) and is consistent with the transportation trends of the Qua Iboe and Cross River systems respectively (see Fig.3.5) which fed Burke's (1972) "Cross River Delta" during Miocene-Pliocene times(Fig.3.9). The build up of the depocentre within the study area is discussed in detail under Upper Qua Iboe analysis. Isochrons of the progradational units confirm the NW-SE trend. Burke's (1972) assertion that canyons may develop at the delta nose is confirmed by the presence of submarine canyons on lines 82-251 (the central canyon system) and line 82-279 (the Pleistocene canyon).

Three principal formations are recognised namely:

- The holomarine Lower Miocene to Oligocene **Akata shale** formation, which is overlain by the marine/paralic interbedded sands and shales of the Miocene to Pliocene **Agbada** formation topped by the non-marine/paralic Pliocene to Recent **Benin** formation.

- The **Agbada** formation which is of great importance in terms of hydrocarbon traps is further subdivided into **Biafra, Rubble and Qua Iboe members.**

Petrophysical characteristics of type sections with Intra and Inter formational relationship are shown in Figs.3.10a,b,c,d,e. Specific log response curves for these litho-stratigraphic units and their relationship to the respective seismic facies evident is discussed later under seismic sequence analysis of the **Biafra, Rubble and Qua Iboe members.**

A generalised stratigraphic column for the study area is given in Fig.3.11a showing the vertical succession of lithologies. The major litho-stratigraphic units become increasingly shalier southwards and merge into the Akata shale formation*. The Biafra may occur as thick continental/fluviatile sediments to the north which progrades into delta plain and delta front deposits and further south becomes prodelta deposits shaling out into Akata (see line 82-149; Fig.3.11b).

Accordingly, the stratigraphic column envisages a situation whereby the Qua Iboe shale actually rests on the Akata formation. Although this is not evident in the study area (except in areas of shale diapirism to the southeast), this shaling-out is responsible for the lack of major reservoirs in the Rio del Rey basin to the east. Increasing shaliness and plasticity of the Akata shales are contributory factors in the formation of the zone of shale diapirs(Fig.3.3 refers)**.

The stratigraphic column derived here, differs substantially from those so far published (Whiteman, 1982) by virtue of the subdivision of the Agbada formation in terms of regional unconformities related to sea level changes(discussed in Chapter 4). Two type seismic sections, 82-231, to the west and 82-377 to the east reinforce this (Fig. 3:11c and d).

From the stratigraphic column, the Biafra is essentially Early to Late Miocene in age over the study area, while the Rubble Beds are predominantly Late Miocene. The Qua Iboe Member including the D-1 sequences are regarded as Pliocene with each progradational sequence set baselapping the previous prograding set. The Benin formation is Pleistocene to Recent, deposition of which appears to have been interrupted by the Pleistocene canyon fill sediments.

---

* An exception would be "Rubble" sequences which are formed from reworking of Biafra sediments; and coarse clastics of these sequences are known to exist further south.

** The relative position of the sequences are discussed and mention made of their bounding unconformities, details of which are examined in Chapter 5.

The Biafra, as the lowermost sequence analysed seismically is subdivided into Lower, Middle, and Upper Biafra, separated by prominent unconformities accordingly. Beneath each angular unconformity, there are certain seismically distinct sequences referred to in this study as "Rubble". These sequences are regarded as products of eroded and reworked sediments. The Lower Intra Biafra Unconformity(LIBU) overlies such a sequence i.e. the Lower Intra Biafra Rubble (LIBR). Similarly, the Top Intra Biafra Unconformity (TIBU) is underlain in some areas by the Upper Intra Biafra Rubble (UIBR) sequence.

Above the Biafra, in most parts of the acreage, the Rubble Bed member onlaps Biafra 'highs'. These are also eroded and reworked sediments, the base of which is a seismic marker, the **Base Rubble Beds (BRB)**. Note that the distinction between the **"Rubble Beds"** and the **"Intra Biafra Rubble Beds"** is essentially in terms of geologic age. The former occurs *above* the **"Biafra"** while the latter occurs *within* the Biafra member. Both are however genetically related and interpreted as having been formed from the erosion of local "Biafra Highs".

Overlying the Biafra, or the "Rubble Beds" when Rubble Beds are present, is the **Qua Iboe member**, which is predominantly prograding shale and acts as cap-rock in respect of **"Base Qua Iboe unconformity plays"**. When intercalations of sands are present, the Qua Iboe forms what is referred to in the study as **"Stratigraphic Anomalies"**, which are potential reservoir rocks enveloped by shale. Sequence boundaries shown in the stratigraphic column define progradational sets within the deltaic building block. Thus $Q_2Q_3, Q_3Q_4, Q_4Q_{4.2}, Q_{4.2}Q_5, Q_5Q_6, and\ \ Q_6Q_7$ are progradational sequence sets becoming increasing younger from $Q_2Q_3 - Q_6Q_7$.

The origin of the Qua Iboe is often explained by canyon fill hypothesis(Burke, 1972) or by the river gully hypothesis(Weber and Daukorou, 1975). These hypotheses, do not however, adequately account for the features discussed later in the text. These include:

- the presence of erosional anticlines (Palaeo- geomorphological (PGM) features), and
- slope dependent, mass movement emplaced seismic facies along with evidence of the Qua Iboe as a transgressive deposit.

The Qua Iboe grades vertically upward into the transitional shallow marine D-1 [named after the type section from well MD-1 (see Fig.3.10e)], which is overlain by the continental Benin formation.

Because of the foregoing, the stratigraphic interval between the **Base Qua Iboe unconformity** (BQI) and the **Pleistocene** unconformity represents a megasequence defined at the base and top by transgressive sands. The interval commenced with the deposition of deep water slope related turbidites of the Qua Iboe and ended with continental sands of the Benin formation. Thus, the megasequence is characterized by a general upward shallowing due to deltaic build-up to the south interrupted by major sea level changes(Vail *et al.*'s third cycles). The unconformities mark major eustatic lowstands of sea level.

In the study area, 18 sequences have been identified commencing from the Biafra to the Benin lithostratigraphic units i.e. from the oldest to the youngest. All of the sequences are bounded by unconformities, most of which are regional. The nomenclature of the sequences is in accordance with the formations discussed above. These are listed below.

3.2.1.1 SEQUENCES MAPPED

SEQUENCE	UNCONF./CORR. CONF.	AGE
OBS1	Top- TOP INTRA BIAF. CYCLE 1 Base-BASE INTRA BIAF. CYCLE 1	**E.M.MIO**
OBS2	Top- TOP INTRA BIAF. CYCLE 2 Base- TOP INTRA BIAF. CYCLE 1	**E.M.MIO**
OBS3	Top- TOP INTRA BIAF. CYCLE 3 Base- TOP INTRA BIAF. CYCLE 2	**M.M.MIO**
OBS4	Top- BASE QUA IBOE Base- TOP INTRA BIAF. CYCLE 3(BIBBEN)	**M.M.MIO**
BS1 **(LIBR)**	Top- LOWER INTRA BIAF. UNCONF.(LIBU) Base- L. BASE INTRA BIAF. RUBBLE(LBIBR)	**L.M.MIO**
BS2	Top- BASE INTRA BIAF. RUBBLE(BIBR) Base- LOWER INTRA BIAF. UNCONF.(LIBU)	**L.M.MIO**
BS3 **(UIBR)**	Top- TOP INTRA BIAF. UNCONF.(TIBU) Base- BASE INTRA BIAF. RUBBLE(BIBR)	**E.L.MIO**

BS4	Top- BASE RUBBLE BEDS(BRB) Base- TOP INTRA BIAF. UNCONF.(TIBU)	**M.L.MIO**
BS5 **(RUBBLE)**	Top- BASE QUA IBOE(BQI) Base-BASE RUBBLE BEDS(BRB)	**L.MIO.**
QS1	Top- INTRA QUA IBOE QUA2 Base- BASE QUA IBOE(BQI)	**E.PLI.**
QS2	Top- INTRA QUA IBOE QUA3($TIQI_3$) Base- INTRA QUA IBOE QUA2	**E.PLI.**
QS3	Top- INTRA QUA IBOE QUA3($TIQI_4$) Base- INTRA QUA IBOE QUA3($TIQI_3$)	**E.PLI.**
QS4	Top- INTRA QUA IBOE QUA4.2($TIQI_{4.2}$) Base- INTRA QUA IBOE QUA4($TIQI_4$)	**L.PLI.**
QS5	Top- INTRA QUA IBOE QUA5($TIQI_5$) Base- INTRA QUA IBOE QUA4.2	**L.PLI.**
QS6	Top- INTRA QUA IBOE QUA6 Base- INTRA QUA IBOE QUA5	**E.PLE.**
QS7	Top- INTRA QUA IBOE QUA7 Base- INTRA QUA IBOE QUA6	**L.PLE.**
QS8	Top- PLEISTOCENE UNCONFORMITY(Pu) Base- INTRA QUA IBOE QUA7	**L.PLE.**
QS9	Top- QUA10 PLEISTOCENE UNCONFORMITY(Pu)	**REC**

OBS1 to OBS4 are older Biafra sequences which occur to the northwest of Fault-3. Their bounding unconformities are characterized by toplap or downlap. Erosional truncation is not evident. They are not correlatable to Biafra sequences to the south. Biafra sequences BS1 to BS4 which occur to the south of Fault-3 may have been largely eroded to the northwest but partly eroded to the northeast and are attributed to tectonic uplift at various times during the Miocene. These

and other aspects of structure are considered in the next section under structural framework.

Of the Intra Qua Iboe horizons mapped, $QUA2$ is limited to the west of the study area. $QUA4$ marks the base of the paralic D-1 to the north. $QUA5$ is the base of coastal onlap to the north and becomes $TIQI_5$ to the southeast. Similarly, QUA7 correlates to the top of a canyon fill to the southeast.

Seismic lines 82-197, 82-259 and 82-373 are regional examples spread across the study area. Seismic, chronostratigraphic and burial history* interpretation of these lines are shown in Figs.5.7, 5.8, 5.9. Detailed analysis of these seismic lines may be found in Section 5.2 along with correlation to the eustatic curve, summary of which in given in Figs.5.10a,b,c&d. In the mean time, the table above would suffice.

3.2.2 STRUCTURAL FRAMEWORK

The structural evolution is, as a consequence of the offlapping style, dominated by growth faulting, anti-thetic and counter-regional faults, shale diapirism and perhaps more importantly, regional tectonism(see Figs. 3.12 and 3.13). A pattern of parallel and near-parallel seaward dipping arcuate faults setting up dynamic and annealment type traps and their anti-thetic components emerges at the Top Intra Biafra Unconformity (TIBU), Base Qua Iboe(BQI), and Qua5 levels(see Figs. 3.14a, b, c). The pattern is a microcosm of the picture depicted by Evamy *et al.*(1978). These are considered in detail under Sections 3.2.3, 3.2.4 and 3.2.5.

These faults have been aptly named according to whether they are major growth faults, anti-thetic or smaller growth faults that occur off the majors. Thus Fault-1, Fault-2, Fault-3, and Fault-4 are major contemporaneous growth faults or *Major Structure Building faults(MSB)* while faults such as Fault-4-2a and F-4-1s are anti-thetic and *Structure Building growth faults(SB)* respectively. The major faults appear to have commenced development in early Miocene and are active to present.

---

* Burial history curves or mobility diagrams are only approximate as absolute age determination (van Hinte's geohistory analysis etc) was not undertaken. Shale interval velocities at unconformities were plotted on a velocity-depth chart and extrapolated to a previously determined statistical least squares fit line for the expected depth of occurrence of such velocities.

Fault-3 has the added significance of being a basin enclosing fault as can be seen in its noticeably more arcuate pattern than Faults 1 and 2 to the north. The palaeobasin so defined, appears to have been affected by regional tectonism leading to the formation of anticlinal closures (see Fig.3.14a,b&c).

Within the study area, four major near-parallel arcuate growth faults are evident representing important phases in the depositional regime. Their origin, whether as slump faults resulting from density contrasts and gravity instability (Curtis, 1970) or faults at the toe of the advancing slope on the flanks of a shale ridge (Merki, 1972) is not discussed here. However, the classification terminology of fault and structural trap types as proposed by Evamy *et al.*(1978) is used extensively in the study. Typical structural traps include:

1a. Simple erosional anticline(Palaeo-Geomorphological features). These are characterized by significant vertical closure, sometimes over 1000ft and may also display terracing as can be seen on line 82-163(Fig.3.15a). These structures are referred to in the text as PGM features or in a more descriptive sense, *erosional cuestas*, impling subaerial exposure and erosion. They commonly occur at the Base Qua Iboe unconformity level in areas north of the palaeobasin boundary(Fault-3); the major structures trending NE-SW, although in the southeast, a series of such structures trending NW-SE with several re-entrants are to be found. Similarly at the Base Rubble Bed level, few such anticlines exist. In particular, to the east of the study area as shown on line 82-110(Fig.3.15b). The only simple erosional anticline at the TIBU level is evident on line 82-190a(Fig.3.15c).

1b. Simple rollover anticline ((shale mass supported). These are typified by structural 'highs' raised by shale movements of a limited scale as opposed to structures formed due to diapirism. They occur mainly in the region south of the palaeobasin boundary, Fault-3 and are widespread at the LIBU, TIBU and BQI levels. Examples include line 82-106(Fig.3.16).

2a. Rollover structure with landward dips(and Rubble Bed onlap). See Fig.3.17. They occur mainly within the palaeobasin defined by Fault-3 and within a growth fault couple. Rollover in this case is as a consequence of Rubble Bed deposition resulting in the reactivation of faulting and tilting of Biafra blocks on the plastic Akata shale beneath.

2b. Rollover structure with seaward dips (Fig.3.18). This is similar to the type discussed above with landward dips except that they are not common and generally do not show Rubble Bed onlap.

3a. Shale mass structure flank (Fig.3.19a) Line 82-180 shows this type of structure at the TIBU level. Similarly at the BQI and LIBU levels structures that form at the flank of shale masses or shale diapir as is the case of line A-23(Fig.3.19b) are common place. However these are restricted to the southeastern parts of the acreage.

3b. Shale mass structure crestal(Fig.3.20). These structures are tilted blocks with structural trap dependent on the crestal faulting often associated with shale tectonics. The structures are few and are seldom tested for fear of shaling-out of prospective reservoirs and the possibility of encountering high pressure Akata shale.

These structural styles are the culmination of at least 3 important tectonic events during the Miocene, all of which are related to the Miocene volcanicity of the **Cameroun-Annobon volcanic axis.**

The oldest episode noticeable in the study area, and also coincidental with the LIBU, appears to have occurred during **Late Mid-Miocene (i.e. Serravallian?).*** Uplift appears to have been pronounced in the southeast with truncation at the LIBU where it is closest to the volcanic axis and also to the northeast where a well developed **Lower Intra Biafra Rubble system** is evident. This is the **Late Mid-Miocene episode.**

The aforementioned episode appears to have been followed by one coincidental with TIBU corresponding to an Early Late-Miocene tectonism which was characterized also by uplift, block rotation and erosion across much of the study area. The duration of this episode (much longer than the previous) is significant as is its association with two Rubble Bed regimes that constitute the **Upper Intra Biafra Rubble.** This episode is referred to as the **Early Late-Miocene episode(or Early Tortonian).**

A final phase of tectonic activity occurred in the **Late Miocene** and is largely associated with **Rubble Bed** deposition and the BQI. The increasing duration of these tectonic phases is represented by the extent and thickness of the Intra Biafra Rubble systems culminating with the considerable sediment removal characterizing the BQI.

---

* Ages of sequences and attributable tectonic events are approximate; they are estimated from correlation with sea level changes and coastal onlap, based on the Haq *et al.*(1987) curve.

Pliocene was largely quiet tectonics-wise except for the initial rather rapid subsidence leading to the deposition of the Qua Iboe and syn-sedimentary faulting as a consequence of sustained sediment input mainly resulting in the reactivation of previous faults.

This interplay between structure and stratigraphy is for the most part responsible for the prolific nature of hydrocarbon occurrence and the seismic facies evidently a function of structural and stratigraphic setting which relates to depth of deposition. Deep water deposits (the Intra Qua Iboe) were particularly influenced by the paleotopography of the Base Qua Iboe structures.

Within the context of a passive margin, cyclicity of transgressive - regressive sedimentation is common place, broken by eustatic sea level changes and regional tectonism. This cyclicity in sedimentation patterns is important because they contribute to the knowledge of the environmental history, the cycles carry time information and may be used along with palaeontology as absolute time determinants.

Because of growth faulting and tectonic rotation, analysis and classification of these cycles are confined within major growth fault couples. Regional unconformities such as TIBU and BQI however are very extensive. Structural development at these unconformities and at the Qua5 level is considered next.

3.2.3 STRUCTURE AT THE TIBU LEVEL

Structural development at the TIBU level was greatly affected by regional and shale tectonics. Of the four regional arcuate faults mentioned earlier, Fault-2, Fault-3 and Fault-4 are evident at this level. The main structural elements can be subdivided according to the different structural traps previously defined, namely:

- fault dependent closures,
- shale mass supported rollover anticlines,
- and occassionally, simple erosional anticlines.

The northernmost down-to-the-south growth fault, Fault-2, is evident to the NE only(Fig.3.14a), because the TIBU level is interpreted as having been removed by the subsequent BQI unconformity in areas to the northwest. The structures associated with this fault are all dependent on it for closure on the upthrown side.

Structural development within growth fault couples Faults-2&3 are mainly fault dependent rollover structures with onlap of the Upper Intra Biafra Rubble. Intra Biafra canyons are not uncommon at this level.

Between Faults-3&4, Upper Intra Biafra Rubble deposition by the erosion of "upland" areas into the palaeobasin hinge or margin defined by Fault-3 led to the tilting of Biafra beds and truncation at the TIBU level. The results of this are simple erosional anticlines sometimes but not always fault-dependent for closure. Of these LL, NN, and OO are the most significant. Other structural types evident include shale mass supported rollover anticlines(VV; partly fault dependent).

Further south, the south eastern block shows erosional anticlines some of which are fault dependent(Fig.3.21). However, Upper Intra Biafra Rubble deposition is not prolific. In general structure to the south consists of a north-south trending ridge at the centre of the study acreage, an embayment eastwards of this and another north-south trending ridge defining the western boundary of the southeastern block.

3.2.4 STRUCTURE AT THE BQI LEVEL

The fault pattern at the BQI level is shown in Fig.3.14b. This consists of the four major arcuate faults, Fault-1, Fault-2, Fault-3, & Fault-4 and regional antithetic components such as Fault-5, Fault-7, Fault-6-1, and Fault-6. In between these major arcuate faults, are eastward-dipping faults thought to have formed at the instance of long shore drift from west to the east*. All the aforementioned faults, define to a large extent the major structural elements at the BQI level.

Regional growth Fault-4 is separated by an anti-thetic Fault-4-1a and both segments enclose their respective intra-slope sub-basins limited to the south by Faults-6 and 7-1 respectively. Separating the Intra-slope basins, is a north-south trending Akata shale ridge inducing structures at both the TIBU and BQI levels. Faulting being contemporaneous with sedimentation is revealed by the fact that, most structures formed are fault dependent rollovers, or subaerially exposed erosional anticlines at the Base Qua Iboe unconformity. Undoubtedly, this subaerial

* Note that the Late Miocene shelf approximated the present day shore line(see Fig.3.6) and long shore drift would have led to the funnelling of sediments from west to east and the formation of synsedimentary faults. Burke(1972), also ascribes to long shore drift the role of funnelling sediments into the Avon, Mahin, Niger and Calabar canyons(Fig.3.5).

exposure is manifestly limited to areas to the north and southeast defining the boundaries of a palaeobasin that is considered in later sections of the study.

Structures formed may be grouped according to growth fault couples as certain structural types appear to predominate within specific growth fault couples. At the BQI level, these are:

- shale mass supported simple rollover structures; or
- simple erosional anticlines; or
- rollover fault dependent structures with or without Rubble Bed onlap and with or without landward dips.

Faults-1&2-

The structures BB and CC-1 are fault dependent closures on the upthrown side of Fault-2. To the northeast, the set of structures referred to as DD are mostly erosional anticlines, but some are closure dependent on the upthrown side of Fault-2.

Faults-2&3-

Most of the structures within this couple are erosional anticlines (Palaeo-Geomorphological features (PGM)). These are, AA, FF, GG and RR amongst others. Vertical closure is often very significant, over .25secs (about 300m(1000ft)) in the case of the 'FF' structure, indicating considerable sediment removal. EE structure to the west, is a fault dependent rollover anticline which is east-west trending; whilst JJ is a simple erosional anticline(PGM feature) also fault dependent to the west. Others like the KK and II structures are shale mass supported rollover anticlines more akin to those found within the Fault-3&4 growth fault couple. In all, the tally for PGM features is higher within this growth fault couple than all the others and may be explained by the fact that this zone is the outer fringe of the palaeobasin defined by Fault-3 and also that Fault-2 marks the approximate northern limits of the Qua Iboe shale as outlined in Chapter 8. Where the Qua Iboe is no longer present, the PGM features are absent likewise.

Faults-3&4-

Shale mass supported rollover anticlines dominate this growth fault couple such as LL, NN, OO, and VV. Where this is not so, the structures are fault dependent rollover structures with Rubble Bed onlap such as UU, simple erosional anticline, fault dependent to the south and west, UU-S, and a Rubble Bed formed simple erosional anticline MM.

Faults-4& Anti-thetic Fault-6-1-

Further south of the major contemporaneous growth faults, regional antithetic fault systems become prominent as compensational north-dipping faults in response to the south dipping growth faults discussed above. One of such is Fault-6-1a to the southeast of the study area. Fault-6 along with the eastern extension of Fault-4, enclose what at the BQI level is an en-echelon of simple erosional anticlines (PGM features) such as TT, TT-N, TT-S and fault dependent rollover structures such as TT-E(with Rubble Bed onlap) and TT-W(with Rubble Bed onlap). This southeastern area is referred to in the subsequent text as the southeastern block alluding to the fact that for these structures to have been subaerially exposed, it may have been uplifted *.

South of Fault-5; and Fault-7-

Most of the structures are fault dependent in respect of these antithetic faults. East of Fault-7, the north-south trending fault dependent closure is the most prominent feature. Very little rollover is evident in this case other than Rubble Bed onlap.

On the whole, the structural configuration at the BQI level is varied. Although the main arcuate faults defined most of the important structural elements, and give clue to the main direction of sediment input(in this case NW to SE), other faults such as the down to the east Fault-1s, Fault-2s, Fault-3s and Fault-4-1s indicate that longshore drift from west to east played an important part in generating contemporaneous faults within the major growth couples. The palaeo-basin defined by Fault-3 is singularly the most important palaeo-slope basin in the study area for reasons of its being a turbidite basin during the Pliocene.

---

* The southeastern block at the TIBU level also shows pronounced angular unconformity implying that tectonic instability reinforced the effect of sea level lowstand.

3.2.5 STRUCTURE AT THE QUA5 LEVEL

At the QUA5 level, only the major south dipping arcuate faults are evident, and these migrate northwards with shallowing depth and younger sediments. Within the study area, the principal growth faults are Fault-3 and Fault-4(see Fig.3.14c). Antithetic Fault-5, Fault-7, and Fault-6 are also present.

Fault-4 dies out to the east as does Fault-3. Most of the structural features are fault dependent rollover anticlines. Fig.3.22 shows an example of such a structure which we refer to here as an annealment type trap on the down thrown side of the fault. At the QUA4 level this structure does not exist(see Fig.3.23). The Qua5 level with respect to Fault-4, is the level at which reactivation of Fault-4 commenced due to increased sediment input.

Most of the structures formed are broad rollover anticlines such as, for example, the oblong NE-SW trending anticline to the northwest of the study area and north of Fault-3; a similarly trending rollover immediately south of Fault-3; and other smaller rollovers as evident in Fig.3.14c. In the southeast block, an Intra Qua Iboe "gully" system trending NE-SW cuts through the QUA5 level(see Fig.3.22).

3.3 SUMMARY

The stratigraphy of the study area consists of 3 main litho-stratigraphic units namely; the marine **Akata shale**; the paralic **Agbada formation** and the non-marine **Benin formation**. The Agbada formation is further subdivided into **the Biafra , the Rubble Beds** and **the Qua Iboe** members.

The Biafra is mostly Early to Late Miocene in age; the Rubble Beds Late Miocene and the Qua Iboe, Pliocene. 18 sequences bounded by unconformities and/or their correlative conformities have been outlined mostly within the Biafra, Rubble Beds and the Qua Iboe and 3 chronostratigraphic sections prepared covering the western, central and eastern parts of the study area.

Structural development appears to have been dominated by growth faulting regional and shale tectonism (to the southeast) during the Miocene. A palaeobasin largely defined by Fault-3 was formed in Early Miocene and appears to have persisted throughout Pliocene. This combined with the episodic regional tectonism and sea level changes account for the presence of Rubble Bed systems in only this part of the Delta.

Three such tectonic phases have been identified:

- the **Late Mid-Miocene episode(Serravallian?)**;
- the **Early Late Miocene episode(Early Tortorian?)**; and
- the **Late Miocene episode(Late Tortonian/Messinian)**.

All three tectonic phases are coincidental with prominent unconformities such as the LIBU, TIBU and BQI with their **Lower Intra Biafra Rubble; Upper Intra Biafra Rubble and Rubble Beds** respectively.

Typical structural traps include the following:

- Simple erosional anticline(or Palaeo-Geomorphological features),
- Simple rollover anticline(shale mass supported),
- Rollover structure with landward dips and Rubble Bed onlap,
- Rollover structure with seaward dips,
- Shale mass structure- flank,
- Shale mass structure- crestal.

Pliocene was largely characterized by subsidence and sustained sediment input into the basin. Reactivation of growth faults and progradation was typical.

CHAPTER FOUR

SEISMIC STRATIGRAPHIC SEQUENCE ANALYSIS

4.1 Review xxx

4.1.1 Unconformity types xxx

4.1.2 Definition and delineation of mapped horizons xxx

4.2 System tracts xxx

4.3 Summary xxx

4.1 REVIEW

Seismic sequence analysis has brought with it a plethora of jargon utilized in the description of stratigraphic intervals. The self explanatory terminologies used in the accompanying text are shown in Figs.4.1a,b & c, and are based on Galloway *et al.*(1979), and Mitchum *et al.*(1977).

While Fig.4.1a defines unconformity types and sedimentary processes that result in certain depositional units, Figs. 4.1b & c, are schematic sections showing the likely distribution of depositional systems which Vail refers to as system tracts, in a hypothetical continental margin. Seismic examples of these system tracts as displayed in the study area are analysed in the following text.

4.1.1 UNCONFORMITY TYPES

An important tenet in seismic stratigraphic analysis is sequence and facies boundary recognition. Both boundary types delimit temporally or spatially the extent of geologic environments and processes. A boundary defined by a continuous reflector is in effect an isochronous surface and, by implication, represents events occurring at the same time. This surface does not necessarily separate facies.

In general, unconformities are formed by tectonic, eustatic and sedimentary processes in subaerial as well as submarine environments. Each of these processes may be the sole contributor to the formation of an unconformity or may be in combination with the others along a particular sequence boundary as will be seen in the unconformities mapped in the study area.

Apart from the classification of unconformities into **non-conformity, angular unconformity and disconformity***, Vail *et al.*(1984) proposes a scheme based on the stratal relationships at sequence boundaries which is related below to the sequence boundaries mapped.

Vail's TYPE 1 unconformity is typified by both subaerial and subaqueous erosion (canyon cutting) and are formed when eustatic sea level fall exceeds the rate of subsidence at the depositional shore line. Canyon cutting is particularly significant as regards the BQI and the BRB and to lesser extent, the TIBU, the BIBR and Intra Qua Iboe "Gully" system . Canyons, where they occur, are indicators of the position of the shelf and by implication, the slope(see Fig.4.2).

* see also Dunbar and Rodgers(1957), and Krumbein and Sloss(1963).

The BQI, TIBU, and LIBU are attributed in this study to be truncation unconformities caused by coinciding sea level fall with tectonic uplift. The BRB and BIBR are more as a result of submarine erosion than subaerial exposure due to tectonic uplift. Regional unconformities may also be due to sea level changes without accompanying tectonic tilting(Riba, 1976; Miall, 1978; and Vail *et al.*, 1984).

Whether the postulated tectonic episodes(see Chapter 3) are related to globally synchronous episodes of tectonic uplift (Sloss, 1984) is not clear. One such prediction in the late Tertiary (Schwan, 1980), 10-9 Ma(late Miocene) is close to the episodes associated in this study with the TIBU and BQI respectively, though Miall(1984), suggests that most of the 'global tectonic' events defined by Schwan(1980), correlate to periods of rising sea level.

Although there may be no apparent relationship between the severity of structural discordance at an unconformity and it's geographical extent, regional importance, or the magnitude of its associated temporal break, the BQI in relation to the TIBU and LIBU, all of which are TYPE 1 sequence boundaries in this area, appears to be the most significant especially in terms of hydrocarbon trapping potential.

On the other hand, Vail's TYPE 2 unconformity is represented by the broad progradational fronts defined by horizons $Q_1 - Q_9$ (except Q_3, Q_4& $Q_{4.2}$ where significant submarine erosion by turbidity currents, mass movement etc are thought to be responsible for this type of unconformity referred to by Shanmugam(1987) as 'sharp and clean' or 'marine swept' sequence boundaries)* and Intra-Biafra horizons such as $B_4, \& B_5$.

These are associated only with subaerial exposure where the underlying slope deposits of the Qua Iboe toplap against the D-1 shelf system. The toplap indicates sedimentary by-pass. TYPE 2 is thought to occur when the rate of eustatic fall is less than the rate of subsidence at the depositional shoreline break.

Occassionally significant sediment removal from the shelf areas result in deposition of coarse clastics at the foot of slope (noted here as Upper Qua Iboe seismic mounds). This deposition is small-scale, though occurs clearly as a result of sea level fluctuations resulting in marine hiatus prevalent at the base D-1.

* See Fig.4.2. Note the prominent reflectors Q_3 & $Q_{4.2}$.

In this study, a major sequence boundary corresponds to Vail's type 1 unconformity, whilst a minor sequence boundary would correspond to type 2. Major sequence boundaries are listed agewise, starting from the oldest to the youngest below:

Lower Base Intra Biafra Rubble—LBIBR or Horizon B_0

Lower Intra Biafra Unconformity—LIBU or Horizon B_1

Base Intra Biafra Rubble———BIBR or Horizon B_2

Top Intra Biafra unconformity——TIBU or Horizon B_3

Base Rubble Beds————-BRB

Base Qua Iboe————-BQI

Top Intra Qua Iboe————TIQI or $Q_3, Q_4, Q_{4.2}, Q_5$

(These are downlap surfaces)

Pleistocene Unconformity———Pu

These are distinct from the minor boundaries such as:

Intra Biafra Horizons ———$OB_1, OB_2, OB_3, BIBBEN, B_4, B_5, B_6$

Qua Iboe prograding fronts——Qua2-Qua9(except those listed above)

4.1.2 DEFINITION AND DELINEATION OF MAPPED HORIZONS

(a) THE OLDER BIAFRA HORIZONS($OB_1, OB_2 \& OB_3$)-

These horizons mark the top of paralic units beneath which are the subdued amplitude facies that are characteristic of continental sediments. Three such cycles are evident in the northwest of the study area and are bounded by horizons $OB_1, OB_2, and\ OB_3$. The fourth cycle is often partially eroded and is defined at the base by the horizon BIBBEN. These horizons are basically subtly toplapped from beneath or baselapped from above(see Fig.4.3a; line 82-66). It has not been possible to carry these horizons to the northeast where two prograding cycles are evident beneath the LBIBR(see Fig.4.3b; line 82-88a).

A synthetic seismogram fit of the horizons is shown in Fig.4.3c over line 82-183.

(b) LOWER BASE INTRA BIAFRA RUBBLE (LBIBR) B_0-

The Lower Base Intra Biafra unconformity is a low frequency, high amplitude event that defines the base of the lowermost subdued amplitude zone within the Biafra, mapped in this project, and the top of a paralic (parallel to divergent seismic facies) sequence that may be recognized on line 82-212a in Fig.4:4a. The subdued or acoustically transparent seismic facies of the sequence above is characteristic of **Rubble** or reworked sediments. Horizon B_0 may be an erosional surface as evident on line 82-212a(in the southeast) with sediments baselapping from above.

Few wells have penetrated this level as it has never been regarded as an objective or prospective level. Rarely, when this occurs it has been over the structural high points where there may have been a possible shaling-out of the Biafra by Akata shale. A synthetic seismogram that correlates the reflection to well data is shown in Fig.4.4b.

(c) LOWER INTRA BIAFRA UNCONFORMITY(LIBU) B_1-

Unlike the LBIBR, this horizon commonly occurs as a high amplitude, high frequency reflector defining a major unconformity of the Biafra at the base of a paralic sequence. It is recognized by erosional truncation in the southeast, where the Lower Intra Biafra Rubble(LIBR) is wedged out over the crest of structure; but appears conformable over the LIBR(see Fig.4.5a ; line 82-393a). This angularity is sometimes associated with shale tectonics. The likely cause, is upwarping of a depositional shale mass(not diapir as there is often no piercement evident) with subsequent erosion resulting in prominent truncation at the flanks.

Depending on the presence or otherwise of the "Lower Intra Biafra Rubble" the LIBU may be toplapped from beneath, baselapped from above by a swath of downlapping events or show conformable relationships in the presence of the Lower Intra Biafra Rubble beneath (in which case it's the top of the subdued amplitude expressed by the "Rubble" that is the pick).

To the NE, the boundary relationship is one of subtler truncation and association with high amplitude anomalies(Fig.4.5b ; line 82-393). A toplapping relationship appears to persist to the west within the paleobasin although whether the horizon mapped is the LIBU is arguable because of the generally thinner section of Biafra due to shaling-out by the Akata shale.

A synthetic seismogram match of this horizon is shown in Fig.4.4c , over line 82-385. Well DD-S-1 shows the LIBU tie.

(d) BASE INTRA BIAFRA RUBBLE(BIBR) B_2-

This is characterized by a prominent reflector pair onlapped by a low amplitude (acoustically transparent) seismic sequence (the Upper Intra Biafra Rubble) and show erosional truncation or sedimentary by-pass (Toplap) of the Biafra beneath.

The seismic attribute of this sequence boundary varies in a N-S manner. This variation is illustrated by line 82-381 as shown in Fig.4.6a. It occurs as both an erosional canyon, and (unlike the Lower Base Intra Biafra Rubble is not very pronounced in the northeast because of the general lack of the Upper Intra Biafra Rubble in this area) a surface of onlap southwards. This surface truncates against the TIBU in the southeastern block.

To the west, this base appears to be less erosional and more conformable with the Biafra below(see line 82-301; Fig.4.6b).

(e) TOP INTRA BIAFRA UNCONFORMITY (TIBU) B_3-

This horizon is often characterized by a continuous reflector pair with high amplitude and low frequency. Reflector continuity however, diminishes where there is angular truncation and/or the presence of Biafra Rubble. The top of the reflector pair onlaps unto structural "highs" (see line 82-353; Fig.4.7a). Much like the LIBU preceding it, angularity may have been caused by upwarping of a depositional shale mass coupled with erosion resulting in prominent truncation at the flanks(e.g. line 82-180; Fig.4.7b).

In a similar vein to the LIBU, truncation is prevalent in the southeastern block, where the Upper Intra Biafra Rubble(UIBR) is not present leading to the

formation of simple erosional anticlines.* The UIBR onlaps to the northeast and southeast against these "highs".

Immediately above this unconformity, is a "high velocity shale" unit. This unique shale in fact defines the nature of the TIBU reflector i.e. high amplitude but low frequency. This is revealed in synthetic seismograms in the northeast(Fig.4.4c; Itut); and the central areas. In the southeast, this high interval velocity is not evident(Fig.4.7c). A possible explanation is that the shale over the unconformity becomes increasingly younger southwards and therefore less compacted, with a lower interval velocity as the consequence.

Paleontological zonation, although not undertaken by the author for the study area, is known to have revealed a unique faunal assemblage associated with this shale aptly called Faunal zone III shale. The shale thickness is known to vary from about 1000ft in the north to about 500ft in the southeast. Its importance lies in the provision of significant cap-rock for possible hydrocarbon plays.

(f) BASE INTRA BIAFRA "BENIN"(BIBBEN)-

This horizon is a high-amplitude, high-frequency reflector that occurs at the base of a generally subdued amplitude seismic facies of the Biafra, immediately below the Base Qua Iboe unconformity. It occurs to the northwest of the study area where the Qua Iboe shale thins progressively northwestwards. The subdued amplitude seismic facies overlying the reflector is characteristic of the Benin formation. The reflector is truncated to the south at the Base Qua Iboe which encloses the subdued amplitude facies as a southward thinning onlap wedge. Line 82-107(Fig.4.8) is a north-south line showing the BIBBEN being largely truncated to the south. The manner in which the Qua Iboe shale thins into a prograding onlap wedge to the north is also worthy of mention here.** The contact between Qua Iboe and the continental sands is less pronounced westward until the Qua Iboe becomes a thin veneer. For synthetic seismogram fit at this level see Fig.4.3c.

---

* See structure at the TIBU level; Section 3.2.3.

** The argument in favour of a canyon-fill origin for the Qua Iboe is best supported by the nature of BQI unconformity at the western limit of Qua Iboe shale. Other opposing arguments are considered in Chapter 8.

(g) THE BASE RUBBLE BEDS (BRB)-

This pick marks the sharp transition between an often parallel to divergent seismic facies within the Biafra, to the chaotic to mounded subdued amplitude facies of the Rubble Beds and defines the vertical limit (or temporal) of eroded and reworked Biafra sediments. It may be an erosional(channel associated) or an onlap unconformity surface. See line 82-142 in Fig.4.9a.

As an unconformity surface, the BRB pick takes cognisance of the following:

(i) The presence of different generations (seismic facies) of reworked material suggesting significant age differentials.

(ii) The development of Intra Rubble channel systems and thus Intra Rubble unconformities. This may offset recognition of the Base Rubble which may be below a distal Rubble Bed facies with continuity of reflectors similar to the Biafra as can be seen along line 82-86 of Fig.4.9b.

Where this seismic pick is difficult to ascertain, the transition to higher velocity of shales within the Rubble Beds is often a reliable marker when a well is available. It is also possible to use the dipmeter log, in which case the boundary showing a sharp contrast between the usually consistently-dipping Biafra and the scatter associated with Rubble Beds may be used.

A synthetic seismogram of a well that tested the Base Rubble Beds(BRB) as a shale filled erosional channel is shown in Fig.4.9c. Seismic tie is established where the interval velocity increases sharply.

(h) BASE QUA IBOE(BQI)-

The erosional unconformity characterized by truncating Biafra beds is also known to be conformable where Rubble Beds are present. Its seismic expression is often clear, due to high amplitude anomaly association.

Difficulties arise where:

- the Qua Iboe thins to the northwest, in which case the BQI level becomes Top Agbada with the Benin formation directly overlying the Agbada(line 82-67, Fig.4.8b); and

- where basal transgressive sands commonly baselap in the central area as illustrated in Fig.4.10a.

Poor differentiation between the Intra Qua Iboe and the Rubble Beds often occurs as a result of the non-development of the characteristic reflector pair at the BQI level in some Rubble Bed areas. Line 82-285 (Fig.4:10b) shows the basis for the respective picks of BRB and BQI.

The top of the Rubble Beds(at the flanks of BQI highs) are often associated with two or three low to high frequency reflection cycles especially in areas north of Fault-4. These reflector pairs or triplets essentially onlap the Biafra highs. They mask the easy identification of the BQI. These are Basal Transgressive Sands and represent the transition from the general Lowstand of Late Miocene to Pliocene Highstand. The patchy nature of the reflectors described here as Basal trangressive sands represent the sand/shale content of the clastics deposited. Thinner, shalier clastics would result in more continuous reflector pairs or triplets with higher frequency indicating probable tuning when critical resolution thickness is approached.

The major factors which affect transgressive sand deposition and preservation are the relative rate of sea level rise and the topography over which the sea is transgressing. The basal clastic unit forms as an erosional lag left behind in the wake of transgression. Thus they occur in areas closest to the main sedimentary chute i.e. the central zone of the study area, where the presence of Rubble Beds are also a prerequisite.

The lateral changes in acoustic patterns from a weak single reflector cycle at the crest of a structure to several weak to strong cycles at the flank is common. These changes can be seen along line 82-106, S.P. 2050- 2250(Fig.4.10c). East of this trend, the BQI is represented by a prominent reflector and the Lower Qua Iboe shows characteristics of ponded turbidites- parallel continuous reflectors as may be seen on line 82-349.

For the present discourse, the BQI is mapped beneath these trangressive sands (occur as erratic disruptive reflection patterns) which are related to rapid sea-level rise at the end of Rubble Bed deposition. The implications of these basal trangressive sands are considered under Lower Qua Iboe sequence analysis.

Synthetic seismogram ties of the BQI over a truncation; over Rubble Beds and involving basal transgressive sands are shown in Figs.4.10d & e. In each case, a marked increase in interval velocity at the sharp transition from Qua Iboe to Biafra/Rubble Beds is evident.

(i) THE INTRA QUA IBOE HORIZONS-

Fig.4.11a is a schematic diagram showing how the Intra Qua Iboe horizons are defined and mapped. In a prograding suite of deltaic origin, three distinct "facies"* associations are evident. This consists of the PRODELTA overlain by a prograding DELTA FRONT which in turn is overlapped by the DELTA TOP facies. At the toe of the prodelta, turbidites may develop. The relationship is illustrated line 82-245 in Fig.4:11b.

Each Qua Iboe sequence is, thus, a progradational composite set that is comprised of sequence boundaries which, at the toe of progradation, is referred to as the Top Intra Qua Iboe(TIQI). Horizon QUA_5 for example commences within the D-1, through the Upper Qua Iboe, and further south, becomes the $TIQI_5$ downlapped by a younger Upper Qua Iboe.

The oldest Intra Qua Iboe horizon delineated is QUA_2, which is the top of a hummocky facies or sometimes onlapping fill facies within the growth faults 3&4; occurring mainly to the west of the acreage(see Fig.4.11c; line 82-203).

The most prominent of the Intra Qua Iboe horizons is QUA_3, which is most pronounced south of Fault-3 within the paleobasin defined by the same fault. It is baselapped by the Upper Qua Iboe above and thus is a ***downlap surface***, especially westwards. To the east, QUA_3 maps the top of a sheet drape facies or is the top of a ponded onlapping fill facies(Fig.4.11d; line 82-361).

QUA_4 horizon defines a toplapped surface(due to sedimentary by-pass) north of Fault-3, the top of an amplitude anomaly to the south which is similarly toplapped from beneath(see Fig.4.11c), and becomes the Top Intra Qua Iboe further south. To the east, it is essentially the top of a sigmoidal progradation which becomes sheet facies to the south.

QUA_5 horizon approximates the top of the D-1 west of the acreage, marking the transition from the continental Benin sands to a paralic sequence and the Top Qua Iboe. South of Fault-4, QUA_5 becomes the top of an onlapping fill facies and top sheet facies further on. In the east, the relationship is similar to QUA_4, i.e. top of a sigmoidal prograding sequence, which, further south, becomes top sheet facies.

QUA_6, QUA_7, QUA_8, and QUA_9 are all Intra Qua Iboe horizons within the D-1 paralic sequences increasing younger in age to the south. QUA_7 becomes the

* Facies here does not necessarily denote seismic facies.

top of the new transition between the Benin sands and the Qua Iboe(see Fig.4.11c). In the east, it is also near top Intra Qua Iboe "gully" system.

From the above, it may be observed that thinning clinoform reflection patterns above the TIQI and build of the prograding front result in a gradual thickening of the turbidite toe. As a result, new turbidity deposits accumulate basinward(This is a function of sediment supply and eustatic sea-level change). A thickening turbidite toe obviously confers time-transgressive characteristics on the Top Intra Qua Iboe(TIQI) which is significant in terms of facies associations and stratigraphic plays within the Qua Iboe. This is considered under Qua Iboe analysis.

TOP INTRA QUA IBOE(TIQI)-

This horizon is identified by the downlap of clinoform reflectors of the Upper Qua Iboe from above. It marks the change from the end of "transgression" to the start of "regression" as the rate of eustatic rise decreases and sediments begin to prograde out over the old starved surface. The downlap represents deep marine clinoform toes developed as progradation progresses seaward.

The TIQI as an unconformity, represents starved sections of a prograding front in considerably deeper water and occur basinward of Vail's *condensed sections.* Condensed sections are thin marine stratigraphic intervals characterized by slow depositional rates(see the illustration in Fig.4.11e). In vertically deepening upward sections, condensed sections commonly mark the greatest paleodepth.

The limit of the shelf edge through geologic time is the consequence of such an analysis. Especially in the Upper Qua Iboe where each prograding arm or front defines the shelf, slope and basin.

Sequence boundaries within the "Qua Iboe" ($Q_3 - Q_9$) are defined solely by toplapping relationships and coastal onlap landward.

(j) THE PLEISTOCENE UNCONFORMITY-

The Pleistocene unconformity (Pu) maps the floor of the Pleistocene canyon in the south of the study area. The top of the resulting canyon fill to which Pu is truncated against is horizon Q_{11}. This is not carried extensively as it is affected by shallow seismic noise trains and the mute curve applied during processing. A typical example may be seen in Fig.4.12.

These seismic sequence bounding unconformities mapped define in a temporal sense, depositional sequences developed as a result of a combination sedimentary processes recognized in the reflection patterns displayed on seismic sections.

4.2 SYSTEM TRACTS

Having defined and delineated sequence bounding unconformities in the study area, it is worthwhile to discuss at this juncture, the depositional units they enclose. System tracts is a term defining the position of depositional systems within sequences coined from Brown and Fisher(1977) and applied by Vail *et al.*(1988) to depositional systems deposited during specific increments of the eustatic curve.

The four common system tracts are evident in the study area. These are:

a. Lowstand System Tracts(LST);

b. Transgressive System Tracts(TST);

c. Shelf Margin System Tracts(SMST); and

d. Highstand System Tracts(HST).

Definition of the above terms can be found in Fig.4.1a. The vertical succession and seismic expression of the system tracts *vis-a-vis* the study area are shown in Figs.4.13a(line 82-269) and 4.13b,c&d.

The use of two of these terms in this study namely; LST and HST involved the modification of Vail's terminology to avoid the suggestion that all LSTs are formed from sea level lowstand(most are). Thus the LST is referred to as the Lower System Tract, while the HST is called the Higher System Tract.

The three Rubble sequences highlighted in Fig.4.13a are namely:

- SEQ.$BS1$ (the Lower Intra Biafra Rubble),
- SEQ.$BS3$(the Upper Intra Biafra Rubble),
- and the Rubble Beds.

The Rubble sequences, mentioned above, constitute lower system tracts. Each of them is capped by transgressive system tracts. In addition, basal transgressive sands as highlighted above the BQI in Fig.4.13a may occur.

The Qua Iboe, both its lower and upper units, separated by a downlap surface is part of a Lower System Tract which is wedge against the D-1. The D-1 on the other hand comprises Higher, Trangressive and Shelf margin system tracts.

The Lower System Tracts are however of special significance because the stratigraphic anomalies discussed in Chapter 2 are mostly present within such system tracts. Figs.4.13b&c show schematic sections of lower system tracts in two different tectonic settings, namely the shelf and growth fault settings, which are both fully represented in the study area. The accompanying seismic examples on line 82-127 for shelf setting and 82-377 for growth fault setting, highlight the significance.

Subdivision of the Lower System Tracts for a basin with a definitive shelf break into lowstand wedge, slope fan and basin floor fan variants as shown in Vail's schematic diagram (Fig.4.1b.) is discussed below.

THE LOWSTAND WEDGE

According to Vail(1988), this is characterized by incised valley fills in the shelf and commonly onlaps the sequence boundary. While on the slope, progradational fill with wedge geometry overlying and downlapping onto the basin floor fan or the slope fan. (See Fig 4.1b).

This is almost an exact description of the Qua Iboe which is composed of progradational(line 82-251; Fig.4.13b) and aggradational sets(line 82-391; Fig.4.13c) onlapping onto the BQI in the northwest, where it appears to have been fed from cut channels. Offlapping patterns in the slope proper commonly occur and at the toe of slope, slope fans of the Lower Qua Iboe develop.

Other terms have been used to describe such depositional systems among which the onlap slope system is well known(Brown and Fisher, 1980). In the accompanying text, the term onlap slope wedge is preferred and used accordingly.

SLOPE FANS

Slope fans, as the name implies, are often found in the middle of slopes, and consist mainly of turbiditic and debris flow deposits. The likely conditions for their formation are:

- a gradual rise of relative sea level,
- continued subaerial exposure of the shelf areas, and
- slumping, mass flow and development of prograding lowstand deltas.

In the study area, the proliferation of stratigraphic anomalies (seismic mounds) particularly in the Lower Qua Iboe is perhaps the best indication of this.

BASIN FLOOR FANS

Basin floor fans*, occur at the foot of the slope(or lower slope) and are mainly characterized by deposition of submarine fans the top of which is often downlapped from above. Submarine erosion is thought to be prevalent; so is slumping and the deposition of thin-bedded suspension derived shales(sometimes referred to as hemipelagic shale). Its base is often a TYPE 1 sequence boundary(Vail *et al.*, 1988) which in the case of the study area is BQI.

The above analysis of first sequence boundaries mapped and preliminary discussion of the types of sequences associated with the study area, show a varied and widespread stratigraphic facies pattern distribution and naturally lead to the examination of the role of sea level changes. Tertiary sea level changes and sequence correlation for this area are discussed in the next chapter.

4.3 SUMMARY

Outline of the sequence stratigraphy and unconformity types in the study area reveals a complex relationship between the sequences and their bounding unconformities. Tectonic influence is almost certainly associated with the erosional truncation of such TYPE 1 unconformities as LIBU, TIBU and BQI engendered

* May be compared to the mounded fan complex facies of the Lower Qua Iboe sequences discussed in Chapter 8.

by subaerial exposure. On the other hand, BIBR and BRB are more a result of submarine erosion than subaerial exposure due to tectonic uplift. Vail's TYPE 2 unconformities dominate the Intra Qua Iboe horizons. The significance of these unconformities in the case of the study area, are that:

a. they mark upper boundaries of zones of increasing porosity(e.g. BQI and TIBU);

b. they may act as hydrocarbon traps(e.g. BQI and TIBU);

c. they could provide avenues for migration; and

d. they may prove useful in the prediction of deep sea turbidites facies (see Shanmugam, 1980).

Mapped horizons were delineated using synthetic seismograms. This helps to clarify where wells are available, the basis for such picks. Of particular interest are the Intra Qua Iboe horizons within the Pliocene defining progradational composite sets each consisting of the delta plain, delta front, prodelta and basin plain turbidites.

The four system tracts* (Vail, 1988):

- *Lower System Tracts(LST)*,
- *Shelf Margin System Tract(SMST)*,
- *Transgressive System Tracts(TST)*, and
- *Higher System Tracts(HST)*

are represented in the acreage. Seismic expression of the different system tracts are shown in Figs.4.13a,b,c,d.

The LST is important in this area because most of the stratigraphic anomalies and the Rubble system(LIBR, UIBR, and Rubble Beds)occur within this system tract. Variants of this system tract include the *Onlap slope wedge* which the Lower Qua Iboe, in general, correlates to; *Slope fans* which are correlatable to seismic mounds formed by slumping; and the *Basin floor fan* to which the *Mounded fan complex facies* discussed in Chapter 8 may be attributed.

---

* System tracts define the position of depositional systems within a delineated seismic sequence.

CHAPTER FIVE

TERTIARY SEA LEVEL CHANGES

5.1 Review.....101
5.2 Sequence Correlation.....106
5.3 Summary 108

5:1 REVIEW

The factors that control the distribution of stratigraphic sequences and the variation of their stratal patterns have been attributed to tectonic subsidence, eustatic sea level changes, sediment supply volume and climate.

Over the years, two schools of thought have persisted concerning tectonic and/or eustatic control of stratigraphic sequence distribution.

One such school of thought, holds the view that stratigraphic sequence distribution is controlled by tectonic activity. The other, maintains that sequence distribution may be solely influenced by eustacy.

Advocates of tectonic control include:

- Pitman(1978; 1979), who using variations in the volume of the mid-oceanic ridges(spreading rate changes: slower rate and lower volume), show its effects on second order sea level changes, which in turn affect the distribution of stratigraphic sequences; and

- Sloss & Speed(1974) and Watts(1981; 1982), both of whom suggest tectonic rather than eustatic control as responsible for progressively younger coastal onlap in Atlantic-type margins.

The lack of an adequate mechanism to suggest tectonic control at the scale indicated by Sloss and Speed had previously been highlighted.

Backstripping studies of the U.S. Atlantic margin (Watts and Thorne, 1984) however show that the main factors affecting the subsidence of rifted sedimentary basins are thermal contraction and sedimentary loading, with compaction, paleobathymetry, erosion and global sea level changes only having minimal effects. Their model provides an alternative to eustacy in explaining the long-term trend in sea level changes (Supercycles of Vail *et al.*(1977)).

The importance of global eustacy however, has been articulated using seismic stratigraphic techniques such as the disposition of coastal onlap on the margins(Vail *et al.*, 1977) and other correlation techniques(Hallam, 1981). The Haq *et al.* 1987 curve is shown in Fig.5.1a while the Vail *et al.*(1977) are shown in Fig.5.1b.

The higher order cycles of Vail are attributed to glacial cycles superimposed upon the long-term sea level changes of Pitman(1978)*.

The coastal onlap curve(Vail *et al.*, 1977) has been criticized for the following reasons:

1. The equation of coastal onlap with relative sea level changes** .
2. The instantaneous sea level falls. These have since been smoothed out and large sea level changes moderated(Vail and Todd, 1981; Vail *et al.*, 1984 and Haq *et al.*, 1987).
3. The arbitrary assumption that sea level had not been much below present levels before the outset of major glaciation.

Some of the criticisms centre on the applicability of the technique to cases where large water depth changes occur across a basin (Watts and Thorne, 1984) and the lack of local and regional subsidence corrections which affect the magnitude of sea level change estimates (Watts, 1982). Others include the implied assumption that the sea level drop was in excess of subsidence (Pitman, 1983), the global correlativity of the curve(often referred to as the "global synchroneity" problem) with those of other basins with different tectonic styles (Brown and Fisher, 1980; Morner, 1981), the rarity of downward shift in coastal onlap and the application to marine onlap (Brown and Fisher, 1980).***

Parkinson and Summerhayes(1985), argue that while these sequences develop in response to relative sea level changes, the relative shifts may not be due to global fluctuations of eustatic sea level. They propose a mechanism for producing synchronous relative sea level changes in widely separated and geologically independent basins without short period fluctuations of 100,000 years in the global sea level curve.

---

* Pitman's long term sea level change curve has since been modified by Kominz(1984) and Kerr(1984) using improved time scales and shows a maximum possible height of sea level at about 365m and a minimum of 45m. Large errors were however noted.

** A relative change in sea level is the combined or net effect of subsidence and eustatic change in sea level. For summary of the causes of world-wide sea level change(Donovan and Jones, 1979), see Appendix 2.

*** See Appendix 3 for a review of the global synchroneity controversy.

In Figs.5.2a, b & c, the metamorphosis of Vail's sea level curves from 1977 to 1987 is shown with specific emphasis on the Tertiary. The corresponding relative coastal onlap curves are also correlated in Figs.5.3a&b. The underlying relationship between the short term curves remains the same. However, the amplitudes and frequency(timing) of change appear to vary considerably. The latest curve(Haq *et al.*, 1987), is the most detailed so far.

Whereas the 1977 curve(see Fig.5.2c) shows a sharp asymetric signature, the 1979 curve (see Fig.5.2b) merely rounded these off. In comparison, the latest curve(see Fig.5.2a) shows more third order cycles during the late Oligocene fall(3 more intermittent peaks and lows on the eustatic curve), 11 third order cycles (21 peaks and lows on the eustatic curve) during the Miocene as against 10 on the 1979 curve(Fig.5.2b) and 8 on the 1977 curve(Fig.5.2c).

This refinement and modification is in line with more conservative estimates of Tertiary sea level change by other workers with a generally less optimistic estimate of the magnitude of change. The new curve also separates coastal onlap from relative change of sea level. Taking the Miocene for example, it may be seen in Fig.5.3a that there is less cyclicity of third order cycles in relation to coastal onlap. The eustatic peaks and lows correlate to the different system tracts.

These criticisms not withstanding, broad support for Vail's eustatic sea level curve has now emerged from different sources applying different techniques, some of which include the use of the downward tilt of sediment beds to estimate crustal subsidence due to crustal cooling and weight of sediments(Moore *et al.*, 1987), and the Oxygen-18 isotope record which is thought to reflect ice-volume changes driving fluctuations in sea level(Fairbanks and Matthews, 1978; Miller and Fairbanks, 1984; and Matthews, 1984). These are discussed below:

- While the latest curve(Haq *et al.*, 1987) derives estimates of crustal subsidence from the long term sea level curve of Pitman(1978)(with improved time scales), Moore *et al.* (reported by Kerr, 1987) used the downward tilt of sediment beds in their estimates. Fig.5.4 shows the result of the correlation of the latest curve to that of Moore *et al.* Both indicate good agreement in terms of amplitude of short term events as determined in the Baltimore canyon area of the U.S. Atlantic shelf. However, exception to the good tie is in the late Oligocene sea level fall, where Moore's estimate is about half of the original (Vail *et al.*, 1977) estimate of 160 metres.

- The marine oxygen isotope record, (O^{18}/O^{16} ratio) is now known to directly reflect ice-volume changes on the continents at least during the Quaternary. The O^{18} signal is used as a record of continental ice volume. The Quaternary fluctuations are thought to be up to -180m (Prell, 1982).

  Evidence also now points to the existence of glacial climatic fluctuations from the Oligocene(Miller and Fairbanks, 1984). Fig.5.5 shows the oxygen-18 curve for late Neogene based on studies in the pelagic and hemipelagic deep-sea sediments which best reveal the timing and intensity of glacio-eustatic sea-level fluctuations. The curve indicates the onset of extensive continental glaciation at about late Pliocene (2.4 Million years) and thus larger fluctuations of sea-level. It must be noted that glacial maxima indicates lowstand while inter glacial maxima show highstand.

  Beginning from late Quaternary(.8 Million years) glacial and interglacial cycles of 0.1 Myrs periods are noted. Fairbank and Matthews(1978), calibrated the oxygen-18 signal as a function of changing elevation of sea level -estimated at -0.11%/metre. Matthews(1984) and Imbrie(1985) applied the late Quaternary dynamic model to post-Eocene deep-sea oxygen-18 record. This extension into early Tertiary is less exact compared to the Quaternary estimates. Fig.5.6a, shows the comparison of the sea level curve based on oxygen-18 ice volume estimates to that of Vail *et al.*(1977).

Vail's curve shows major transgressions and regressions of 1 Myr frequency and duration. When the 0.1 Myrs frequency curve is smoothed into a 1 Myrs period curve, there appears to be good agreement in terms of timing of major eustatic events between the two. The magnitude of sea level changes however differ widely and Vail's estimates have been refined and scaled down considerably.

There is still scepticism as regards the existence of ice ages earlier than 50million years ago, when short term Vail cyles with a similar amplitude as those in the Oligocene to Recent occur as early as 150 million years ago. An alternative mechanism proposed by Karner, (1988?) suggests that the Vail cycles are due to the bending of the weakened crust of sedimentary basins by changes in the stress of the tectonic plates in which the basins are embedded, implying that Vail's curves are regional and not global.

The above discussion on the oxygen-18 curve therefore underpins the increasing support for the global nature of relative sea level changes in the Tertiary the effects of which have been modified by regional and local tectonic factors. Thus it

is clear that sea level changes could have imprinted itself on the continental shelf of the Niger delta. Depending on the rates of subsidence this could have resulted in subaerial exposure and thus erosion. The margin in question was particularly suited for the following reasons:

(1). Broad, relatively smooth and uniform morphology of the shelf as evident today.

(2). Abundant sediment supply during the Tertiary and thus rapid subsidence rates which result in the intercalation of marine deposits over continental deposits. Given a subsidence rate of 5cm/1000yrs typical of passive margins (Emery and Uchupi, 1972), a 50m (164ft) drop in sea level causing an unconformity at the shelf could within 1 Myrs be submerged and overlain by deep marine deposits. (The analogy of the lower Qua Iboe sequence overlying the Base Qua Iboe unconformity is elaborated upon later in the report).

(3). Long shore drift was particularly active (Burke, 1972). Thus, movement of sediments along the shelf and into canyons for the deeper basinal environments were plausible.

(4). The depositional patterns expressed in the study area show increasing complexity that may not be wholly explained by thermal contraction and sedimentary loading. In fact, this complexity may be due to the following:

- The major phase of thermal and isostatic subsidence terminating in early Tertiary, resulting in greater prominence of local events such as fluctuations in subsidence and sediment accumulation rates, changing flow patterns of long shore currents or probably streams.

- The effects of glacio-eustatic sea level changes as expressed in the number of regional unconformities such as the LBIBR, LIBU, BIBR, TIBU, BRB, BQI and Pu*.

Global eustatic lowstands are important for aiding the transport of coarse clastics to deep water and redistribution of the sediments through bottom currents (see Fig.5.6b). Although Pitman (1978) contends that eustatic sea level changes are of insufficient rates to drop sea level below a shelf edge in a basin undergoing "normal" rates of subsidence, curves based on oxygen-18 show that sea level lowering to about -150m is probable.

* Shorthand for the mapped horizons previously defined in Chapter 4.

Evidence for the interplay of eustatic sea level and the stratigraphy in the study area include:

a. The presence of Rubble Beds(eroded and reworked sediments dumped on the flanks of structural highs) which indicate sea level lowstands. They are also marine onlapping units.

b. The architecture of some unconformities (namely BQI, TIBU, BRB and Pu) indicate relict erosional anticlines (Paleo-geomorphological features, PGM) which were subaerially exposed(see Fig.3.15a).

c. Alternating cycles of onlap and offlap as indicators of these eustatic fluctuations. This is examined in detail with regard to the Qua Iboe, as not all marine onlap may be attributed to sea level lowstands.

The degree to which the stratigraphy reflects Vail's sea level curve is analysed and the variations due to the locality modelled.

5.2 SEQUENCE CORRELATION

Derivation of an appropriate sea level curve for the area and/or correlation to the Vail curve hinges on the availability of relevant data sets. This is only partially fulfilled in the case of the study area. The information required are three-fold namely:

1. A regional grid of seismic sections adequately showing the shelf edge and a complete section of coastal onlap with available well information incorporated.

2. A structurally undeformed stratigraphic sequence or, in the absence of this, minimal deformation.

3. Availability of biostratigraphic information- mainly planktonic foraminefera and palynological data necessary for biozonation. Also in turn, absolute age and environment of deposition determination. Quantitative techniques in geohistory analysis are discussed by van Hinte(1978).

On the first score, the study area has an adequate seismic data base. Unfortunately, these seismic profiles were shot over the main areas of hydrocarbon interest and not necessarily over the region of the shelf showing a complete section of coastal onlap.

Secondly, structural deformation has been very considerable as described in Chapter 3 under structural framework. Shale and regional tectonism in particular, and contemporaneous growth faulting (which is often accompanied by lithologic changes across such faults that make correlation difficult) have shaped the continental shelf and slope, leading to tilting, uplift and erosion of sediments throughout Tertiary.

With respect to the third requirement, biostratigraphic information has been scanty and in this actively explored, and prolific acreage, it has been largely ignored. No attempt at identifying biozones was carried out as this is largely outside the scope of this research apart from the fact that the accuracy of Cenozoic biozonation is notoriously tenuous(Poag and Schlee, 1984). In the two instances where this information has been available, they have been incorporated into the study as stated below:

- The Faunal Zone III shale- a transgressive sometimes high velocity shale immediately above the Top Intra Biafra Unconformity(TIBU).
- And the Top Intra Qua Iboe(QUA3) marker which, although seismically defined, also corresponds to the top of a zone characterized by a foraminefera *Textularia sp.1.*

In view of the above, a reliable coastal onlap curve could not be constructed with any certainty and, in any case, the major unconformities such as the BQI, TIBU, and LIBU do not show a corresponding coastal onlap because of subaerial exposure and erosion leading to the formation of marine onlap in the form of the "Rubble" sediments. Determination of an eustatic sea level curve was also not attempted, as the latest curve will suffice. Sequence correlation here is therefore the matching of the ages of the sequence bounding unconformities and their correlative conformities with short-term shifts of sea level on the Haq *et al.*(1987) curve.

The correlated sequences are grouped according to their formational units i.e. **the Biafra, the Rubble and the Qua Iboe**. Three regional seismic lines (82-197, 82-259 and 82-373) representing the western, central and eastern parts of the study area were used in correlation.

- First, chronostratigraphic charts were derived for each line and the various stratigraphic hiatuses and unconformities identified (see Enclosures 12a,b&c). The various sequences were then correlated to the Haq *et al.*(1987) curve. Broadly, good correlation exists between the sequences

mapped, their postulated system tracts and sea level change, except for an Early Pleistocene lowstand recognized in the study area by a canyon system referred to as the Intra Qua Iboe "gully" system, the top of which is Horizon QUA7. Results of this correlation are summarized in Figs.5.10a,b,c,d&e. All the major unconformities correlate to sea level lowstands. Build up of the delta during highstands, led to the trapping of sediments on the shelf and the development of prodelta in the palaeobasin.

- Secondly mobility diagrams at strategic points on the seismic lines chosen above were undertaken to highlight tectonic movements during the Miocene. Results may be seen in Figs.5.11a,b,&c.

- Thirdly, back-stripping studies along the same seismic sections were also undertaken to illustrate the evolution of the study area(Fig.5.12a,b,&c).

Variation between sequence types across the study area is evident, beginning from the older Biafra sequences to the Qua Iboe. In the Miocene, the southeastern block appears to have been the most tectonically active with tilted fault blocks characteristic(discussed in chapter 3, line 82-373); the central part was dominated by the north-south trending shale ridge system to the south(line 82-259); and the north west by Intra Biafra growth faulting(line 82-197).

On the whole, the delta that fed sediments to the western parts of the basin is different from that in the east, both in terms orientation and the efficacy of sediment input. The explanation for this variance may be seen in Chapter 9, but highlights include the fact that sedimentation in the western parts of the study area appears to have been fed by shelf margin deltas while to the east, a submerged shelf was typical. Evidence comes from the following:

- The less pronounced dips of progradation characteristic of the east. The reflection clinoforms generally tend to be sigmoidal.

- The scarcity of seismic mounds to the east except in the southeast corner in Early Pleistocene where oblique progradation appears to have commenced.

Individual sequence and facies analysis is considered in detail in Chapters 6 (Biafra), Chapter 7 (Rubble Beds) and Chapter 8(Qua Iboe).

5.3 SUMMARY

Broad consensus now widely supports the sea level and relative coastal onlap curves of Vail *et al.*, especially in the Tertiary. The 1987 version of this curve has been applied to the study area and the stratigraphic sequences evident, indicate the imprint of eustatic sea level changes on the margin.

Chronostratigraphic sections for seismic lines 82-197, 82-259, and 82-373 representing the western, central and eastern parts of the study area are shown in Enclosure 12 and reveal a varied succession of system tracts reflecting primarily the effect of sea level changes and the varied impact of local and regional tectonism in certain parts of the acreage.

A summary of the regional sequence correlation is shown in Figs.5.10a,b,c&d. Correlation with the Haq *et al.*(1987) curve is good. However a significant discrepancy occurs in the early Pleistocene represented by a lowstand canyon system (The Intra Qua Iboe "gully") in the study area. This lowstand is not apparent in the Haq *et al.*(1987).

All the major unconformities are associated with eustatic lowstand on the curve. Variation between the western and eastern parts of the acreage is noted from the mobility diagrams in Figs.5.11a,b&c and from backstripping studies illustrated in Fig.5.12a,b& c. The eastern part of the acreage is thought to have been more active tectonically.

CHAPTER SIX

BIAFRA SEQUENCE AND FACIES ANALYSIS.....110

6.1 Outline.....111
6.2 The Older Biafra Sequences.....113
6.3 The Lower Intra Biafra Rubble(LIBR).....115
6.4 SEQ. BS2.....116
6.5 The Upper Intra Biafra Rubble(UIBR).....116
6.6 SEQ. BS4.....118
6.7 Biafra Litho-Velocity analysis.....119
6.8 Summary.....121
6.9 Biafra seismic facies tables.....124

6.1 OUTLINE

Evidence from the chronostratigraphic sections in Enclosure 12 suggests that the Biafra underwent significant structural deformation during the Miocene. This is very much in line with the structural framework summarized in Chapter 3.2. Sequence and facies analysis of the Biafra requires the determination of the structural history of the area and the following is a resumé of Biafra development.

The structural and stratigraphic evolution of Biafra through Miocene to Recent is shown in Figs.6.1a,b&c. In conjunction with the chronostratigraphic sections in Enclosure 12, and the mobility diagrams(Figs.5.11a,b,&c), evidence of a well developed Biafra section by Mid-Miocene can be shown. This well developed Biafra formed to the north of the already emplaced palaeobasin, while within the palaeobasin, prodelta sediments and Akata shale were dominant.

The **Late Mid-Miocene tectonism** resulted in uplift to the southeast, east-central and northwestern parts of the acreage coupled with sea level drop and subsequently leading to **Lower Intra Biafra Rubble** deposition. Evidence, in respect of the above, can be seen in the major relict Intra Biafra faults on lines 82-197 and 82-373 in Enclosure 12 and the thinning or absence of sequences in areas of possible tectonic uplift on back-stripped sections.

Sedimentation was soon disrupted by the **Early Late Miocene tectonism.** Uplift in the southeast, northeast and north-central* and northwest are evident, with the **Upper Intra Biafra Rubble** largely confined within the well developed palaeobasin. A subsequent **Late Miocene** drop in sea level in conjunction with the final phase of regional tectonism led to the formation of the Rubble beds. Sequences identified within the Biafra are given below:

SEQUENCE	UNCONF./CORR. CONF.	AGE
OBS1	Top- TOP INTRA BIAF. CYCLE 1 Base-BASE INTRA BIAF. CYCLE 1	E.M.MIO
OBS2	Top- TOP INTRA BIAF. CYCLE 2 Base- TOP INTRA BIAF. CYCLE 1	E.M.MIO

* see line 82-293; Fig.6.1d for evidence of uplift within the palaeobasin, which appears to have persisted during Late Miocene

6.2 THE OLDER BIAFRA SEQUENCES

The Older Biafra may be broadly divided into four fluvio-deltaic cycles in the northwest(sequence OBS1, OBS2, OBS3, and OBS4; (see Fig. 6.3a; line 82-183)) or two deltaic cycles as evident in the northeast(see Fig.6.3b; line 82-86). These sequences appear to be vertically stacked and with regard to the northwest show similar thicknesses of about 300 msecs.

The sequences to the northwest, in general, thicken west and southwestwards, as can be seen on line 82-67 in Fig.6.3c. Sequence correlation indicates a geologic age of **Early to Middle Mid-Miocene** *. The predominant system tract to the northwest is Higher System Tract(HST), corresponding to the third order cycle 2.4 on the Haq *et al.*(1987) eustatic curve(see line 82-197 in Enclosure 12).

This higher system tract is followed by a shallowing lower system tract. In this respect, the northwest area shows good correlation with the eustatic curve. Of these four sequences, OBS4 is largely truncated against the BQI. The limit of truncation of the sequence base (BIBBEN) is shown in Fig.6.4.

Each cycle is characterised by *toplap and downlap* relationships. SEQ.OB3 is the most prominent with truncation evident. These sequences have been correlated to line 82-66 (Fig.6.5) and line 82-211 (Fig.6.6).

On line 82-66, considerable faulting close to Fault-3 masks sequence boundary definition. Furthermore, detachment of Biafra section and Rubble Bed development at the fringes of Fault-3 (palaeobasin boundary), also means that the younger sequences such as SEQ.OBS3 and SEQ.OBS2 truncate against the Rubble Bed section. Correlation across Fault-3 is tenuous, due to the shaling-out of these sequences into Akata shale in the palaeobasin. The early stages of the formation of the palaeobasin is also self evident on line 82-66.

At least two sequences in the northeast make up the episode characterized by deltaic cycles. Progradation appears to be mainly to the south and south west. Facies associations show familiar trends of *delta front-prodelta-deep marine.* Sequence boundaries are commonly defined by toplap with high amplitude anomalies associated with the updip portions of prograding fronts.

---

* See Fig.3.12 for a generalized cross-section of the delta. The Older sequences here correspond to the Mid-Miocene which is shown as shaling out to the south before reaching the present day shelf break.

OBS3	Top- TOP INTRA BIAF. CYCLE 3 Base- TOP INTRA BIAF. CYCLE 2	**M.M.MIO**
OBS4	Top- BASE QUA IBOE Base- TOP INTRA BIAF. CYCLE 3(BIBBEN)	**M.M.MIO**
BS1 (LIBR)	Top- LOWER INTRA BIAF. UNCONF.(LIBU) Base- L. BASE INTRA BIAF. RUBBLE(LBIBR)	**L.M.MIO**
BS2	Top- BASE INTRA BIAF. RUBBLE(BIBR) Base- LOWER INTRA BIAF. UNCONF.(LIBU)	**L.M.MIO**
BS3 (UIBR)	Top- TOP INTRA BIAF. UNCONF.(TIBU) Base- BASE INTRA BIAF. RUBBLE(BIBR)	**E.L.MIO**
BS4	Top- BASE RUBBLE BEDS(BRB) Base- TOP INTRA BIAF. UNCONF.(TIBU)	**M.L.MIO**
BS5 (RUBBLE)	Top- BASE QUA IBOE(BQI) Base-BASE RUBBLE BEDS(BRB)	**L.MIO.**

Because of this complexity and difficulties in correlating across major sequence building growth faults, Biafra sequence and facies analysis is divided into two provinces namely:

- areas to the northwest and northeast of Fault-3; and
- areas to the northeast and the south.

Sequences dominating the northwest province have been referred to as the Older Biafra sequences while those to the south and northeast are BS1, BS2, BS3 and BS4. These also include sequences that occur beneath the LBIBR to the northeast. They are examined next.

Representative seismic facies types within the Biafra are shown in Fig.6.2., along with likely environmental interpretation. Such interpretation is only meaningful when done in conjunction with the depositional setting of the seismic facies. A summary of the facies and environmental interpretation is tabulated at the end of this chapter.

Based on seismic expression, three distinct seismic facies types are often associated within each cycle grading vertically and laterally. See the representative facies descriptions and their reflection character types in Fig.6.2.

1. DELTA PLAIN/DELTA FRONT FACIES:

   The reflections here are parallel to divergent. Reflection continuity is characteristic probably representing distributary mouth bars. The characteristic log response of this seismic facies is given in Fig.6.7a.

2. CONTINENTAL FACIES/SUBDUED AMPLITUDE SEISMIC FACIES:

   A fluvial section characterized by discontinuous variable amplitude events reflecting perhaps the complex morphology of the alluvial plain with extensive coalescing and reworking. See Fig 6.7b for characteristic log response.

3. PRODELTA FACIES/SUBDUED TO SUBTLY PARALLEL SEISMIC FACIES:

   Commonly a sudued amplitude reflection free sequence with subtle progradation and may be locally chaotic. Line 82-86 in Fig.6.3b shows the Upper units of this facies toplap the delta front facies. Typical log response is shown in Fig.6.7c.

Fig.6.3c, shows a classic display of the vertical stacking of the component seismic facies outlined above. Commencing from beneath the BQI, the *subdued amplitude facies of the non-marine clastics*, overlies the *parallel seimic facies* of the Delta plain. The Delta plain in turn drapes over the Delta front tending towards Prodelta. The Delta front is repeated again over Prodelta and possibly turbidites.

To the northeast, the vertical succession of sequences is given below.

(a) Two deltaic cycles overlain by

(b) The Intra Biafra Rubble(with two units - an onlapping lower facies and an upper offlapping facies.

(c) An Offlapping sequence

(d) A slope front fill facies/onlapping facies and

(e) A parallel/divergent seismic facies (delta plain facies.)

A generalized facies distribution map is shown in Fig.6.8a.

The central part of the study area does not show these older sequences largely as a result of shaling out of the Biafra section within the palaeobasin defined by Fault-3; and also because line 82-259 does not extend further north over these sequences. To the northeast, the older sequences are essentially shelf-margin system tract. Paleoenvironment curves for the Older sequences are shown in Figs.6.8b & c.

From the facies distribution map, we infer that predominant sediment movement direction in the east, was from the NE to SW and in the northwest, from the NW to SE. The obvious implication of this, is that two "deltas" fed sediments into the acreage; one in the northeast and the other mainly in the north-central and the northwest regions.*

6.3 THE LOWER INTRA BIAFRA RUBBLE(LIBR)

As the lowest onlapping Intra Biafra Rubble system mapped, the LIBR is largely affected by shale tectonism. Thus over much of the study area, it has either been eroded by a subsequent regional tectonic episode described earlier, or shaled out within the palaeobasin. Structural map of the sequence base (LBIBR) is shown in Enclosure 1. The top of the sequence is shown in Enclosure 2a.

This subaerial sediment removal may be seen on line 82-197, where a significant stratigraphic hiatus covering much of the Mid and Late Miocene is evident. On the aforementioned line, from shot points 100 to 500, inference may be made that a succession of tectonic uplifts culminating in the BQI erosional anticlines could have been responsible for the absence of LIBU. It is apparent that any equivalent Lower Intra Biafra Unconformity would have been eroded during the Late Miocene lowstand.

The Lower Intra Biafra Rubble(LIBR), correlates to the third order cycle 2.6 on the eustatic curve. In the central area, the chronostratigraphic section of line 82-259 shows what may be a thinner Lower Intra Biafra Rubble and to the northeast and southeast lowstand system tracks dominate with a vertical succession of system tracts from Lower to Transgressive to Higher. Good correlation with the Haq *et al.*(1987) curve is apparent with the Lower Intra Biafra Unconformity capping the sequence.

---

* Additional source of sediments was the uplifted southeastern block.

It appears to be well developed only in the northeast and southeast. Thicknesses vary considerably. However, maximum thickness of about 400 msecs occurs to the northeast, on the downthrownside of antithetic Fault-2A.

Facies distribution is shown in Fig.6.9. Although the predominant facies geometry is onlap fill, variation in seismic attributes can be seen. This takes the form of differentiation into upper and lower units in the northeast. A typical example is on line 82-381 in Fig.6.10a. The lower unit in this case is essentially onlapping and is associated with a high amplitude anomaly. On the other hand, the upper unit progrades northwards, baselapping the lower unit below. In the southeast, erosional truncation at the base and top of this sequence is typical (see Fig.6.10b; line 82-393a).

Subdued amplitude facies appears to be typical within this basinal marine onlap. Whether this may be interpreted as an indication of good sand development is not clear, as only one well has tested this sequence. It is likely though, as with most lower system tracts caused by lowering of sea level, that this Rubble system may be promising in terms of reservoir development.

Few stratigraphic anomalies(see Fig.6.10c) have been noticed within the LIBR. This is in addition to the presence of high amplitude anomalies. The high amplitude anomaly at least, is an indication of possible good sand development.

6.4 SEQ. BS2

This sequence is largely undifferentiated Biafra and is correlated to cycle 2.6 on the eustatic curve.

It is noticeably thin in the northeast and the western part of the palaeobasin due perhaps to erosion of Early Late Miocene that resulted in the Top Intra Biafra unconformity. A thicker section of SEQ.BS2 is found in the southeast as can be seen in the isochron (Fig.6.11a). The predominant facies appears to be a variable amplitude (highly continuous) seismic character which is interpreted as prodelta facies.

6.5 THE UPPER INTRA BIAFRA RUBBLE(UIBR)

The Upper Intra Biafra Rubble system is considerably widespread. As usual, it is attributed to a lowstand of sea level. On the eustatic curve, this sequence

corresponds to third order cycle 3.1. Chronostratigraphic section in the central area (line 82-259), reveals a significant hiatus at the erosional unconformity. To the northeast and southeast(line 82-373), similar hiatus are evident confirming the role of tectonic uplift coupled with sea level fall as the inducement for Rubble generation. The common vertical succession of system tracts is Lower system tract capped by a trangressive unit. Enclosures 4a & 5a show the structural maps of the base(BIBR) and top of this sequence (TIBU).

Prominent truncation at the top(TIBU) is characteristic. The Biafra Rubble, as the name implies, represents eroded and reworked material dumped mostly on the flanks of highs. Facies association is essentially onlap although differentiation into offlapping and slope front fill varieties have been identified.

DEVELOPMENT OF THE RUBBLE

The Intra Biafra Rubble episode may be attributed to the **Early Late Miocene lowstand.** A NE-SW trending canyon system is associated with the Rubble to the northeast (Fig. 6.10a; line 82-381). The canyon broadens southwards into the "embayment proper" and can be identified by its predominantly chaotic facies and erosional base. The northern limit of the canyon is also indicative of the position of the shelf vis a vis the slope. The NE-SW axis of the canyon is perpendicular to the shelf break; an attribute that is consistent with all other canyons in the study area.

The canyon is evidence of an exposed shelf imprinted upon by sea level change. Apart from the canyon, very limited Rubble may be seen to the northeast except to the south, where the characteristic onlap is prevalent. So also is the effect of tectonic control in conjunction with sea level change which is asserted by the accentuated angularity of the Top Intra Biafra unconformity in the central and southeastern parts of the acreage. Once again the dominant cause* of Rubble formation is the volcanicity along the Cameroun-Annobon volcanic axis coincidental with Early Late Miocene sea level change(see Fig.3.2).

Shale mass movement due to the deposition of Rubble, induced onlap and indigenous bottom currents moved sediments downslope, in areas to the south and west. Subaqueous erosion was therefore prevalent in these areas.

---

* Tectonism and sea level change as causal events in the formation of Rubble material are considered in Chapter 7. The cumulative effects of Miocene instability and sea level fall are thought to have formed the Rubble Beds.

FACIES DISTRIBUTION

The UIBR is wedged against local 'highs' in the northeast, east-central, south-east and against shale mass induced rollovers within the palaeobasin.

The Upper Intra Biafra Rubble shows a variety of seismic units. Line 82-283(Fig.6.12a) illustrates a lower unit with subdued/chaotic facies. Above it, there is an upper unit with increasing continuity of seismic reflectors. Line 82-106(Fig.6.12b) shows a similar differentiation within the central area. However, in the north-east areas, the Intra Biafra Rubble system occurs as a chaotic onlapping fill facies with extensive erosion of the base(BIBR). See line 82-339, Fig.6.12c.

This differentiation, which occurs sometimes as alternating cycles of onlap and offlap, suggest a deep water association relating deposition to eustatic changes of sea level.

The Intra Biafra Rubble appears to be restricted by the palaeobasin boundary (Fault-3) except to the northeast (related to canyon development). The chaotic onlap fill, oblique progradational and distal onlap facies predominate in the east. The chaotic facies in general, commonly show an eroded base indicating extensive scouring (see line 82-377; Fig.6.12d for truncation at the Base Intra Biafra Rubble (BIBR) of underlying Biafra beds). A cursory look at thicknesses of the Upper Intra Biafra Rubble compared to the Rubble beds reveal both to be similar at least in the central part of the study area, near the palaeobasin margin.

Facies distribution is shown in Fig.6.13a. In the central region, facies types are mainly distal onlap and slope front fill. The subsequent gradual rise of sea level is reflected in the definition of the TIBU by the absence of basal transgressive sands as compared with the BQI.

Although stratigraphic anomalies(as defined in chapter 2) are not evident within this particular Rubble system, high amplitude anomalies occurring at the flanks Intra Biafra 'highs' exist(Fig.6.13b, line 82-353 and 6.13c; line 82-158). The presence of significant sand development, even in provinces commonly regarded as predominantly shaly Biafra in the southeastern block, is thus probable.

6.6 SEQ. BS4

Lowstand appears to have been followed by highstand represented in this area by marine sand-shale sequences. A massive shale unit (about 1000feet) acts as a

cap rock for unconformity plays across the acreage. This is the transgressive system tract caused by a gradual rise of sea level. Sequence B3-B4 and B4-B5 consists of parallel divergent reflectors, offlapping prodelta patterns in the northeast.

The respective facies become increasingly deep water to the south. The highstand episode was interrupted by the **Late Miocene Lowstand** responsible for the formation of the Rubble Bed member.

In the central parts of the acreage, this sequence is comparatively thin. It correlates to highstand of sea level that accompanied lowstand of the Upper Intra Biafra Rubble. At cycle 3.2 on the third order curve, this sequence is generally higher system tract.

SEQ.B3-B4 - Repetition of the Delta plain facies.

SEQ.B4-B5 - Often eroded by the effect of Rubble beds but appears to be an extension of the delta plain facies.

For example, above TIBU, (i.e. above the Intra Biafra Rubble system), delta plain facies types predominate (parallel to divergent reflectors) in the central area(see line 82-261), while to the east (line 82-132a, Fig. 6.15), distal delta front facies merges at the base of slope into onlapping fill facies.

On line 82-132a, two prominent deltaic cycles are evident. These consists of prodelta sediments prograding southeastwards into basin plain turbidites(interpreted mainly because of the parallel bedding that appears to have been ponded).

Facies distribution map of this sequence is shown in Fig.6.16a. The paleoenvironment curve for the southeastern block, highlighting the relationship between SEQ.BS4 and other sequences is shown in Fig.6.16b

6.7 BIAFRA LITHO-VELOCITY ANALYSIS

The absence of stratigraphic anomalies(seismic mounds) as defined in Chapter 2, within the Biafra cannot be simply explained as due to compaction of the Intra Biafra Rubble sediments because of their slightly older age. What is more plausible is that channel-levee systems that are characteristic of the Rubble beds and Qua Iboe do not occur within the Biafra because most of the Biafra channels are erosional.

Although, the Intra Biafra canyon system has been identified in the northeast, associated with the Upper Intra Biafra Rubble system, the seismic facies evident, do not include seismic mounds. With this in mind, two approaches were adopted in the analysis of Biafra Interval velocity namely:

1. analysis of the Biafra as a unit* in terms of interval velocity, sand percentage and depth in order to develop litho-velocity curves for the Biafra; and

2. analysis of the seismic interval velocity of the sequences, especially the Intra Biafra Rubble system. These are discussed next.

Fig.6.17a, is a sand percentage map of the Biafra based on selected well data. The map shows the predominance of higher sand percentages** in area to the north, northeast, northwest and west of the palaeobasin. These are areas where the older sequences have been mapped. On the other hand, to the south, a zone of shaled out Biafra is often presumed.

A comparison between the sand percentage map, and the average interval velocity map which is Fig.6.17b, shows broad correspondence between the two. In Fig.6.18, juxtaposition of both maps confirms the general trend of higher interval velocities with increasing sand percentage in the northern parts mentioned above. This may be a confirmation of the fact that these sequences are older, or that the higher interval velocities are due to higher sand percentage. Neither of the two plausible explanations deal with the role of the Intra Biafra Rubble system in the overall interval velocity picture. That is discussed later.

A litho-velocity curve derived from well data is shown in Fig.6.19a. The relationship between interval velocity and depth for the end-member lithologies depicted in Fig.6.19 show this to be very erratic. The separation between the two is narrow (about 600-700ft/sec) at the crucial depths of between 6000ft and 7500ft. This represents about 10% variation which could easily be obliterated by inaccuracies in the seismic interval velocity estimation technique at such depths. Derivation of sand percentage values from seismic interval velocities using the curve is therefore tenuous. The above result was based on data from all of Biafra

* Albeit, a large and diverse unit as already depicted earlier.

** Sand percentage calculations are invariable based on the total depth penetrated by the well, which in most cases depends on the target of the objective in the first place. These are often the BQI with the secondary objective, upside potential in the Biafra.

irrespective of sequences as identified from this study. Litho-velocity analysis using only sequence specified data is shown in Fig.6.19b in respect of the Upper Intra Biafra Rubble.

The result shows that the litho-velocity curve, approximates a power relationship between velocity and depth. It also confirms the fact that sands within this Rubble sequence are the main contributors to the above average sand percentage evident within the palaeobasin. Seismic interval velocity, computed and corrected as per the techniques outlined in Chapter 2 show the sand prone nature of the Upper Intra Biafra Rubble system. The cluster of points on the estimated sand line of the litho-velocity chart is evident. A map of the results is shown in Fig.6.19c. A similar result was obtained for the Lower Intra Biafra Rubble although, the accuracy of the seismic interval velocity estimates over such depths may cast some doubt in respect of the LIBR.

What this means in effect is, that irrespective of the part of the acreage, where the Intra Biafra Rubble system is evident, good sand development may be probable within such a Rubble system.

6.8 SUMMARY

The imprint of sea level changes on the Niger delta margin is validated by the correlation of sequences within the Biafra to the Tertiary eustatic curve of Haq *et al.*, (1987). The Biafra has been classified into:

- Pre-Lower Intra Biafra Rubble(The Older Sequences);
- Lower Intra Biafra Rubble(LIBR);
- Post Lower Intra Biafra Rubble(SEQ.BS2);
- Upper Intra Biafra Rubble(UIBR); and
- Post Upper Intra Biafra Rubble(SEQ.BS4).

Both Intra Biafra Rubble systems are attributed to sea level lowstands coincidental with the regional tectonism along the Cameroun-Annobon volcanic axis. A summary of the sequence correlation to the eustatic curve is shown in Fig.5.10. The other sequences appear to correlate to either rising sea level or stillstand.

Based on backstripping studies and the distribution of seismic facies, the tectonic influence exerted throughout Miocene appears to have varied in emphasis

according to the locality. Thus, the LIBR system is wedged against the positive structural element that persisted in the Mid-Miocene(see facies distribution map of the LIBR, Fig.6.9). Onlap from the north(the LIBR prograding to the north), west and southeast is interpreted.

On the other hand, the UIBR system is largely confined to the palaeobasin, and absent in the northeast(except for the canyon) and southeast. Tectonic influence is revealed by truncation of underlying beds.

Facies differentiation into offlap/onlap units, is noted in the northeast with respect to the LIBR; and slope front fill/distal onlap to the west; distal onlap/offlap to the south in respect of the UIBR, where chaotic onlap in the east (due to scouring of the base of canyons) differentiates westward into a lower onlapping unit/slope front fill facies and an upper offlapping facies unit. (line 82-106, Fig.6.12b).

It may be deduced that significant clastic contribution came from the east as well as north of the acreage. Thus the general southwesterly drift of the megadeltas of the Older sequences to the east; and southeastern progradation of the Older sequences of the northwest.

SEQ.BS4 however shows progradation to the east in the eastern part of the study area, and westwards in the western part of the study separated by the north-south trending south-central ridge system, that bifurcates the palaeobasin.

Shifting of depocentres was common place and since maximum subsidence corresponds to the centre of the applied load which is generally at the upper slope or shelf break, ancient shelf margins may be determined. A composite map delineating the maximum push of delta front sands into deeper water is shown in Fig.6.20.

The vertical stack of high amplitude anomalies on line 82-377 (Fig.6.12d), are sand-build ups at the updip portions of these prograding units.

Similarities between the Intra Biafra Rubble and the Rubble Bed member(discussed later) include Intra Rubble unconformities. Line 82-377 shows differentiation between offlapping unit downlapping and onlapping unit.

However, an important difference is the absence of relict type structures associated with subaerial exposure during such lowstands of sea level, an indication perhaps of the lesser effect of sea level fall than in Late Miocene. See Fig.5.10.

Biafra litho-velocity analysis shows:

- that a power relationship exist between the velocity and depth within the Biafra;
- that the Intra Biafra Rubble system is the main contributor of the 'above-average' sand percentage evident within the palaeobasin;
- that the paucity of stratigraphic anomalies within these Rubble systems is due to the fact that channel-levee systems are not characteristic of the Intra Biafra Rubble as is often the case in Rubble Beds(Chapter 7) and Qua Iboe(Chapter 8);
- that irrespective of the part of the acreage, the presence of the Intra Biafra Rubble system is a good indication of sand development.

A list of facies units identified within the Biafra is given below:

SLOPE FRONT FILL FACIES

DELTA PLAIN/DELTA FRONT FACIES

DISTAL ONLAPPING FILL FACIES

CHAOTIC ONLAPPING FILL FACIES

OBLIQUE PROGRADATIONAL FACIES

PRODELTA FACIES.

Description of the various facies units is given in the accompanying tables.

BIAFRA SEISMIC FACIES ANALYSIS

SEQUENCE/AGE	EXTERNAL FEATURES	INTERNAL FEATURES	FACIES AND INTERPRETATION
SEQ.OBS1/E.M.MIO.	Mostly conformable at the top or gentle toplap. Baselap at base.	Variable amplitude. Cycle breadth decreases downdip as bed thins. Higher amplitude associated with the top delta plain deposits. Lower or subdued amplitude section beneath corresponds to continental fluvial sands. In either case reflections are only gently prograding but mostly parallel.	These are fluvial deposits intercalated with delta plain or paralic sediments which constitute one depositional cycle. High terrigenous influx results in non-marine coastal aggradation and regression. Low terrigenous influx during transgression results in the paralic sediments of the delta plain. The older Biafra sequences in general constitute *Higher system tracts* formed as a result of sea level highstand.
SEQ.OBS2/E.M.MIO.	External features are similar to those above.	Internal features show greater differentiation between the parallel to divergent seismic facies of the delta plain superimposed on the subdued amplitude facies of the non-marine clastics.	Facies interpretation and depositional environment are same as above.

BIAFRA SEISMIC FACIES ANALYSIS

SEQUENCE/AGE	EXTERNAL FEATURES	INTERNAL FEATURES	FACIES AND INTERPRETATION
SEQ.OBS3/M.M.MIO.	External features of this sequence although similar to those in OBS1, show a thicker paralic section. The top of this sequence is sometimes toplapped as prominently as the base is baselapped.	Seismic amplitudes are vary as those in OBS1 but are stronger. High amplitude anomalies are common.	Facies interpretation is consistent with OBS1 and OBS2 except for more pronounced progradational dips commonly associated with this sequence.
SEQ.OBS4/M.M.MIO.	The top is sometimes conformable, but also truncated at the BQI. The base is often toplapped from beneath or conformable. The sequence occurs as an onlapping wedge due BQI erosion and is truncated by the BQI basinward.	Variable amplitude but mostly subdued with very little continuity. Mostly reflection free landward, but continuity increases basinward where it joins the delta plain facies.	These continental and fluvial facies occur as massive sheets of sand or may be wedge shaped. They are found to the northwest of the study area limited to the north by the Qua Iboe shale limit(Fig.8.1).
SEQ.OBS/M.MIO.	The external geometry is that of two prograding cones juxtaposed one over the other. The top is the LBIBR unconformity. Toplap and baselap characterize boundary relationships for the top and base respectively.	The internal configuration features high amplitude reflectors (mostly divergent), prograding basinward. At the toe of progradation is subdued amplitude facies or prodelta.	This is a shelf margin system tract. The shelf facies merges downdip with the prodelta facies.

BIAFRA SEISMIC FACIES ANAYSIS

SEQUENCE/AGE	EXTERNAL FEATURES	INTERNAL FEATURES	FACIES AND INTERPRETATION
LIBR/L.M.MIO.	Commonly shows toplap at the upper boundary or erosional truncation and baselap at the lower boundary. Occurs mainly as onlap wedges.	Seismic amplitude is sometimes variable but mostly subdued. It may be disruptive when associated with channels. High amplitude anomalies may be present.	LIBR(Lower Intra Biafra Rubble) consists mainly of onlapping fill or slope front fill facies. Subdivision into a lower onlapping and upper offlapping units is common in the northeast. They are eroded and reworked sediments found on the flanks of Biafra 'highs'. They are regarded as Lowstand system tracts.
SEQ.BS2/L.M.MIO.	Occurs as sheet-like to wedge shaped sequence within the palaeobasin to the west. Tabular on shelf. Concordant at the top but the base may be toplapped from beneath. To the southeast, occurs as a massive sequence alternating with shelf(parallel and tabular) and subdued amplitude prodelta	Mainly consists of parallel to divergent reflectors(high amplitude high continuity and high frequency) or subdued amplitude clinoforms beneath the parallel to divergent reflectors.	Paralic delta plain facies dominate to the west. Shelf facies alternating with prodelta sediments are characteristic of the east. They are mainly Transgressive and Higher system tracts. Deltaic progradation appears to have been SW to NE and SE to NE.

BIAFRA SEISMIC FACIES ANAYSIS

SEQUENCE/AGE	EXTERNAL FEATURES	INTERNAL FEATURES	FACIES AND INTERPRETATION
UIBR/E.L.MIO.	Configured as a channel fill. The top may be concordant but the base shows erosional truncation.	Mainly subdued amplitude disrupted seismic reflectors.	This is the chaotic facies of the Upper Intra Biafra Rubble(UIBR). They occur in eroded canyons on the Biafra shelf formed from lowstand of sea level and filled by a subsequent highstand. Two main canyons trending NE - SW empty into the palaeobasin. The shale in-filling is transgressive system tract even though the canyons were formed during lowstand.
UIBR/E.L.MIO.	The UIBR has an onlap slope wedge configuration. It may be concordant at the top or show subtle erosional truncation. The base is often onlapped.	Sometimes characterized by obliquely offlapping reflection with variable amplitude along depositional dip in the upper portions. Moderate continuity and subdued amplitude reflectors are typical in the lower portion.	The UIBR may be subdivided into two units to the west of the palaeobasin. Typically, the upper unit is the slope front fill facies, while the lower unit is the distal facies. They are turbidites deposited during sea level lowstand and therefore are Lower system tracts. Typically sand prone in the central parts of the palaeobasin. Appears to have been deposited from the NE to SW and south to north.

BIAFRA SEISMIC FACIES ANALYSIS

SEQUENCE/AGE	EXTERNAL FEATURES	INTERVAL FEATURES	FACIES AND INTERPRETATION
SEQ.BS4/M.L.MIO.	Sheet-like to wedge shaped. Tabular on the shelf. Rarely concordant at the top due to the erosional Base Rubble Beds(BRB). Base may be conformable or also truncated from beneath by slope clinoforms of the UIBR.	Parallel to slightly divergent. High continuity with prominent reflectors. High frequency common.	These are delta plain and delta front sediments, commonly paralic with alternating sands and shales. They are the principal reservoirs for truncating Biafra at the BQI unconformity. They are interpreted as higher system tracts and are dominant in the central, western and northeastern parts of the study area.
SAME AS ABOVE	Prograding clinoforms are typical of the sequence. The top is truncated by BRB and the base is concordant or shows baselapped.	Sigmoidal progradation is typical with moderate to subdued amplitude reflections. Higher amplitudes occur at the turbidite toe which has characteristics of sheet facies (high amplitude may be due to seismic tuning).	This is the prodelta facies deposited in deeper water. The sequence is mostly shaly (characterized by sigmoidal clinoforms) but the turbidite toe has never been tested. Type section occurs to the east where two prodelta cycles are recognized(line 82-132a; Fig.6.15). The thinned clinoform patterns and tuned turbidite toe represent *condensed sections*, and form part of the interpreted Higher system tract.

CHAPTER SEVEN

RUBBLE BED MEMBER SEQUENCE AND FACIES ANALYSIS

7.1 General 130
7.2 Facies distribution of Rubble Beds 132
7.2.1 Chaotic facies 133
7.2.2 Proximal Onlap facies 133
7.2.3 Mounded Onlap facies 133
7.2.4 Distal Onlap facies 134
7.2.5 Offlapping facies 134
7.3 Emplacement of the Rubble Beds 134
7.3.1 The Development model 135
7.3.2 Tectonic effects and sea level changes 136
7.3.3 Canyon development 137
7.4 Sequence velocity analysis 138
7.5 Summary 140

7.1 GENERAL

The Rubble Beds occur as low amplitude, discordant seismic events that onlap Biafra "highs" which may be 'PGM' features (line 82-108; Fig.7.1a) or tilted fault blocks with Rubble onlap on both sides of the fault(line 82-142; Fig.7.2). They consist essentially of eroded and broken rock material from Biafra Beds and are elaborate and extensive with northern limits approximating the boundary of the palaeobasin (bounded by Fault-3 where they form a thick wedge at the basin hinge), though it extends beyond this in the northeast. The Rubble Beds are sandwiched between Biafra sequence BS4 and the Qua Iboe sequence QS1 as shown below.

SEQUENCE	UNCONF./CORR. CONF.	AGE
BS4	Top- BASE RUBBLE BEDS(BRB) Base- TOP INTRA BIAF. UNCONF.(TIBU)	M.L.MIO
BS5 (RUBBLE)	Top- BASE QUA IBOE(BQI) Base-BASE RUBBLE BEDS(BRB)	L.MIO.
QS1	Top- INTRA QUA IBOE QUA2 Base- BASE QUA IBOE(BQI)	E.PLI.

Isochron of the Rubble Beds reveal that the thickest sections occur to the northwest near the palaeo-basin boundary, and also to the southwest, east central and to the south. It pinches against structurally positive elements such as the central high, the north-south trending ridge to the south and the southeastern block. See Encl.9.

A cursory look at the distribution of the thickest sections of Rubble (i.e. areas of 200msecs and above), shows that these are closest to where considerable removal of the adjacent Biafra is the norm. This is true of the northwest where PGM features to the north of Fault-3 have particularly high vertical closures and the southeastern block which fed the east central area with Rubble(see isometric projection of Rubble isochron Encl.9b).

The evolution of the palaeobasin appears to have been in consert with deposition throughout the Miocene as it manifestly delimits most of the Rubble so

far discussed (namely the Upper Intra Biafra Rubble (UIBR) and the Lower Intra Biafra Rubble(LIBR)) within its confines.*

Notwithstanding their being differentiated into respective seismic facies, two broad genetic derivatives within the Rubble may be established namely:

(a) A lower Rubble unit (UNIT 1) essentially onlapping varying from chaotic onlap to distal onlapping fill facies(line 82-287; Fig.7.3a).

(b) An upper unit(UNIT 2) variable from mounded onlap to offlapping fill facies(see lines 82-387 and 82-142, Figs.7.3b and 7.3c respectively).

Segregation into a lower and upper units is common place in the central, eastern and southeastern parts of the study area. Alternating cycles of onlap and offlap are indicators of eustatic control of deposition although progradation may indicate the extent of paleotopographic control on seismic facies relationships and sustained sediment input. Fig.7.4 and 7.5 show the extent of each unit.

Evidence of eustatic control on Rubble Bed deposition stems from differentiation into lower and upper units as discussed earlier. The eustatic curve in Haq *et al.*, (1987), shows a Late Miocene drop of four cycles of fall, the latter two (cycles 3.3 and 3.4) of which may be correlated to the occurrence of Rubble Beds. The consequence of rapid fall is a Type 1 unconformity and another fall results in the superposition of another Type 1 unconformity within the Rubble Beds. It follows therefore, that the Intra Rubble unconformities evident in areas close to the palaeo-basin boundary (Fault-3) such as may be seen on line 82-86 (Fig.4.9b), are in response to these sea level change signatures.

Although the base of Rubble Beds is generally an onlapped unconformity, channel associated Rubble have been identified often with erosional gorges of considerable width and depth. Rubble Bed differentiation may thus be manifested as Intra Rubble unconformities caused by numerous active channels prevalent during sea level lowstand. For example, the chaotic facies is often associated with scouring at the base. Line 82-86 (Fig.4.9b) illustrates proximal type Rubble with high reflection amplitudes, distal types with lower amplitudes and more continuous reflectors and channel associated Rubble with a broad Rubble Bed onlap. The Rubble Beds is therefore not a sequence of continuous uninterrupted deposition.

---

* Exception may be made of the LIBR which occurs north of Fault-3 in the northeast but onlaps onto a 'high' on the down thrownside of Fault-2-1s.(see line 82-377; Fig.6.12d)

Helms(1978), first pointed out the different seismic facies expressed within the Rubble Beds. Their distribution in the study area has been modified using a much improved data base. These seismic facies are listed in Fig.7.6 and below.

- **Chaotic fill facies**
- **Mounded onlapping fill facies**
- **Proximal onlapping fill facies**
- **Distal onlapping fill facies**
- **Prograding facies**

The distribution of the different seismic facies units associated with Rubble Beds is shown in Fig.7.7, superimposed over the fault pattern at the BQI level, and is discussed in Section 7.2.

7.2 FACIES DISTRIBUTION OF RUBBLE BEDS

Facies distribution as revealed in Fig.7.7 consists of the **proximal onlap facies** largely confined to the palaeobasin boundary to the northwest; the **mounded onlap facies** scattered in the north central, east and far eastern parts of the study area. Others like the **distal onlap facies** are present to the southwest, south central and far southeastern parts. The **chaotic facies** is concentrated in the northeast, mostly associated with erosional gorges; while the **offlapping facies** is present in the southeast.

Sand percentages are difficult to compute for the Rubble Beds because almost no wells would have tested a complete section, unlike the Qua Iboe. This is because they flank BQI 'highs' which are often the primary objectives. Also the concept of a stratigraphic anomaly play within the Rubble has been largely ignored. However, analysis of the seismic facies, along with interval velocity inputs as to the sandiness etc. of anomaly features is undertaken in Section 7.4.

7.2.1 THE CHAOTIC FILL FACIES

The Chaotic fill facies as the name implies, is characterized by disrupted seismic reflections commonly occurring with an erosional gorge at the base to the northeast of the acreage, at the margin of the palaeobasin. Line 82-118, Fig.7.8a is a typical example. Although onlap is evident no preferred orientation of reflectors can be seen. The erosional gorge is shown on shot points 2350 to 2500; and trends southwestwards from the palaeobasin hinge. Sometimes subdued amplitudes dominate with an erosional base illustrating perhaps a monotonous lithology.

The likely environment of deposition inferred from this facies type is one consistent with gravity, mass transport and high energy turbidity current sediments. The proximity to the source(i.e. the eroded shelf north of the palaeobasin) means that this facies could be sand-prone although poorly segregated deposits.

7.2.2 THE PROXIMAL ONLAP FACIES

The proximal facies is primarily characterized by subdued amplitude reflectors grading upward into more continuous patterns. They occur mainly at the margins of the palaeobasin to the northwest. The distinction between this facies and chaotic facies is that there is no erosional gorge formed at the base though occasionally, mounding is evident. Line 82-253(Fig.7.8b), shows a typical example without mounding, while line 82-197(Fig.7.8c), shows the facies with mounding at the base.

They are thought to have been deposited by moderately high velocity turbidity currents. Where these sediments have been rapidly deposited, mounding is the resultant feature but these are often not concentrated in a particular locality as is the case where we have the mounded onlap facies.

7.2.3 THE MOUNDED ONLAP FACIES

This seismic facies largely shows irregular reflection patterns, hummocky and sometimes wavy. The facies type commonly occurs in the central, eastern and far eastern parts of the study acreage, and along with the proximal and distal onlap facies, make up the bulk of the Rubble Beds in the study area.

A typical example is shown on line 82-291(Fig.7.8d). Within the Rubble, mounding can be regarded as a good indication of sand build-up and intercalation with shale.*

Because of the mounding, environment of deposition is thought to be high velocity turbidity currents rapidly dumping coarse as well as fine grained clastics within the palaeobasin.

7.2.4 THE DISTAL ONLAP FACIES

The distal facies consists of generally more subdued amplitude configuration with higher continuity of reflectors than the proximal facies. As the name implies, it occurs largely to the south of the study area. All the canyon associated Rubble Beds tend to feed the distal facies. Typical seismic example is shown on line 82-168a(Fig.7.8e). Distal onlap is shown on both sides of the fault.

They occur as a result of relatively slower turbidity currents especially in the lower energy environment located further south from source area as compared to the proximal facies. Consequently, the distal facies is most likely to be shalier than the others.

7.2.5 THE PROGRADING FACIES

This facies type occurs mainly in the southeast of the acreage and is predominantly characterized by oflapping high amplitude reflection patterns within an onlap wedge onto a BQI high. It grades into the mounded facies basinward. Line 82-216a(Fig.7.8f) is shown as example.

Relatively high velocity turbidity current deposits are inferred forming a stratigraphic anomaly that is considered later in Section 7.4.

7.3 EMPLACEMENT OF THE RUBBLE BEDS

Rubble deposition is directly attributable to the late Miocene sea level drop. Erosion as a consequence of this sea level drop may be quantified by the extent of

---

* This mounded indication of sand build-up is also confirmed in the Qua Iboe. The example shown on Fig.7.8d is chosen from an area considered to be the main sedimentary thalweg to the south.

removal of underlying Biafra sediments represented by the vertical closure of relict structures bordering Fault-3. Removal in excess of 2500ft of Biafra top cover is common place.

The extent of the role of sea level change in modelling the paleoenvironment is controversial (discussed earlier under Tertiary sea level changes), especially in this case, as Rubble Beds are not known to exist in all areas of the Niger Delta complex and may therefore, not be entirely attributable to sea level lowering.

It is however, incontrovertible, that the effect of sea level lowering is to enhance the deposition of terrigenous sediments by turbidity currents. Increased sedimentation rates of up to 1000cm/1000yrs have been documented by Bouma *et al.*(1985) of the Wisconsian lowstand. Such increased sedimentation would also be enhanced by the effect of long shore drift prevalent on the continental shelf of the Niger Delta (Burke, 1972). Massive deposition would then result in isostatic adjustment. The resultant tectonism is responsible for the prominent angularity of the Base Qua Iboe unconformity.

7.3.1 THE DEPOSITIONAL MODEL

The proposed model for the deposition of Rubble Beds is derived from analysis of the distribution of the different facies discussed above, and incorporates the following(Fig.7.9a):

1. Subaerial exposure of areas north of Fault-3 resulting in relict erosional anticlines and dumping of eroded sediments into thick sedimentary wedges down flank, and subaqueous movement of the sediments downslope into distal facies associations. Thus, the northwestern, northern, northeastern and east central parts of the study area were subaerially exposed forming an arc bounding the central, south central and south eastern parts into an embayment.

2. Rubble Bed deposition then leads to renewed dynamism along major fault planes (considering the high rates of sedimentation referred to earlier) resulting in block rotation and sliding along the Biafra and Akata shale boundary. As will be seen later, this in turn led to canyon development.

7.3.2 TECTONIC EFFECTS AND SEA LEVEL CHANGES

Earlier in the text, under Structural framework* three tectonic episodes were postulated, all of which are coincidental with either the Intra Biafra Rubble systems(LIBR and UIBR), or the Rubble Beds respectively. The Late Miocene regional tectonic episode is of relevance to the Rubble Beds.

It is self evident, from the severity of the truncation and the features associated with structures at the BQI unconformity that a measure of tectonic control was exerted during Rubble Bed deposition. The possible mechanisms responsible may include the following:

- Regional tectonic uplift related to Miocene activity in the Cameroun-Fernando Po volcanic axis** of which subsequent downwarping, left the area in deep water.

- Isostatic adjustment in response to sea level lowering or uplift. The magnitude of sea level change required for such an isostatic adjustment (in excess of 3000ft in some areas), far exceeds estimates derived from the Haq *et al.*(1987) curve.

- Uplift related to local shale diapirism. There is no evidence of shale tectonism to the north of the palaeobasin(Fault-3) even though the simple erosional cuestas*** prevalent are indicative of subaerial exposure at the BQI level. Shale tectonism is common only within the palaeobasin and to the southeast

- Compressional uplift related to differential loading along major growth fault systems. Such a differential loading would have been caused by the deposition of Rubble Beds on the downthrown sides of major growth faults, with erosion of the upland areas prompted by sea level fall since deposition induced subsidence would have been greater under lowstand due to high sedimentation rates from terrigenous influx than highstand. The schematic diagram in Fig.7.9b illustrates the various mechanisms discussed above.

---

* See Section 3.2.2

** Machen(1970), describes this volcanic activity and geothermal gradient studies in Avbovbo(1980), also confirm high geothermal gradients for the eastern delta offshore, which may be explained by Miocene volcanicity.

*** see Structures at the BQI level; Fig 3.14b

Based on the above, this study contends that sea level lowering in association with regional tectonism was the prompter for Rubble development and deposition into a palaeobasin already defined by a Late Miocene regional tectonic event. Isostatic adjustment due to massive Rubble deposits, also exerted local tectonic control on sedimentation but to a lesser extent. Lines 82-142, 82-158, 82-174 and 82-186 (regional east-west lines) traverse this possible embayment showing local tectonic elements (such as horst blocks), within the embayment, all of which are draped by different regimes of Rubble Beds (See enclosure 12).

This regional tectonism may also explain the mechanism of the subsequent downwarp of the basin in Pliocene during the deposition of the Qua Iboe shale and its equivalent in the Camerouns(called the Bonito Shale), which characteristically drape over relict erosional anticlines, in much the same way as discussed for the study area.

Uplift due to shale diapirism is local in extent and appears to be a mechanism more influential with respect to the Top Intra Biafra unconformity (TIBU). See line 82- 110(Fig.3.10b). The late Miocene drop of about 150metres could have generated enough sedimentation to cause considerable subsidence within the embayment, with a subsequent Pliocene highstand resulting in deep water deposition of the Qua Iboe. This embayment hypothesis is discussed in detail, in relation to the Intra Biafra Rubble system and Rubble Beds, and the Qua Iboe shale in Chapter 9.

7.3.3 CANYON DEVELOPMENT

The mechanism for the development of the canyon system is given below:

- *The detachment of Biafra section often as a tensional depression associated with a weak zone (glide plane) such as Intra Biafra fault planes.*
- *Accretion and scouring of the Biafra Base often by bottom undercutting accelerating slumping etc; sweeping down of debris by submarine currents resulting in the deepening of the pathway.*

This fits the mass gravity transport model of Kruit *et al.*(1975), which outlines the process of **rockfall, sliding and slumping, sediment gravity flow and turbidity current flow** (Figs. 7:10a, b). Line 82-251(Fig.7.10b) illustrates the central canyon system.

Within the study area, three main canyons, all south trending (see Fig.7:2) appear to head on the slope beyond the shelf break. These are **the western, central and eastern canyons** *.

Structural similarity between the central and eastern canyons is evident in the antithetic fault system that occurs just north of the respective canyons. These suggest that a raised block must have been in existence in these areas with the subsequent detachment of Biafra section leading to the formation of the canyons.

The western canyon is shown on line 82-142 (Fig.7.11a) and occurs at the southwestern corner of the acreage. The eastern canyon is shown in Fig.7.11b. Channelization in the eastern canyon occurs along a NNW-SSE direction beginning at about the mid-section of the TT-N structure. The Rubble Beds associated with the eastern channel show a disruptive character with generally subdued amplitudes. Further south the canyon is obscured by shale tectonics(line 82-337; Fig.7.11c).

In all cases, the channel systems feed the distal facies of the Rubble Beds. The significance of these canyons appears to be that in the Pliocene, they formed the main axis for coarse clastic sedimentation fed by turbidity currents.

7.4 SEQUENCE INTERVAL VELOCITY ANALYSIS

The distribution of stratigraphic anomalies within the Rubble is shown in Fig.7.12. The most important of these occur close to the palaeobasin margin and in the southeastern corner of the acreage. These are referred to as the **northern anomalies** and the **southeastern anomaly**. In general these anomalies occur within the proximal, mounded onlap and prograding facies as previously outlined.

Using the techniques discussed in Chapter 2, interval velocities were evaluated over the Rubble Beds and plotted on the Litho-Velocity curve previously derived for the Rubble Beds(Fig.7.13).

Due to their unconsolidated nature (thus the acronym "Rubble") they consistently show lower interval velocities compared to the Biafra member of equivalent

* For this study, a distinction is made between Rubble Bed canyons that have the entire Rubble Bed section as part of the channel and Intra Rubble canyons in which the channel associated chaotic facies is Unit 2 Rubble within an older Unit 1 Rubble unit (see Fig.4.9b).

depth and in some cases, significantly less than the "lower Qua Iboe Unit" above (Okon, 1983).

As expected the litho-velocity curve for the Rubble Beds shows a logarithmic (power-law) relation between velocity and depth for the end-member lithologies. Comparison between the seismic interval velocity and the litho-velocity curve, yields the sand/shale map of the Rubble Beds (Fig.7.14). As usual, the sand contour represents the lowest value of interval velocity for sand.

Fig.7.14 shows that the distribution of sand packages correlates with the high amplitude mounded facies. The mounded seismic facies is therefore synonymous with greater sand content in the package, and has the best potential for reservoir development.

Of the various anomalies considered, the northern anomaly and the southeastern anomaly are the most significant because of their association with structure.

The northern anomaly is best shown on line 82-271(Fig.7.15a) capped by a high amplitude anomaly. An abrupt facies change with the surrounding Rubble Beds is also evident. Association with Fault-3 at the palaeobasin boundary is an added guarantee of possible hydrocarbon migration into the rollover structure induced by the same fault. Interval velocities for this anomaly show a drop over the high amplitude. This is attributed here to the possible presence of gas. Similar decompacted velocities have been obtained within Rubble Beds with proven gas reservoirs in the east of the study area. Where the seismic stratigraphic anomaly exists without the high amplitude cap, higher interval velocities are evident.

The implications for the exploration potential of this anomaly is two-fold.

1. The northern anomaly occurs within the same trend as the NW-SE trending canyon system and was probably fed by the northern canyon emptying into the palaeobasin bounded by Fault-3. Good sand development is thus, likely to be assured.

2. The anomaly (UNIT 1 Rubble) which is also coincidental with the central anomaly of the Lower Qua Iboe discussed later, is dependent for seal on the Intra Rubble canyon system(UNIT 2 Rubble) shown in Fig.4.9b (line 82-88a) indicating the important influence of eustatic changes of sea level on the depositional sequences mapped.

The southeastern anomaly(line 82-216a; Fig.7.15b) consists of several mound 'pockets' within an onlapping Rubble Bed wedge. It occurs in an area that hitherto

has been regarded as shaly based on wells mainly drilled on shale mass supported structures. It does not clearly show the two-unit differentiation though Unit 1 appears to be a veneer sediment and thus it is classified UNIT 2. The following features are of particular importance with respect to this anomaly:

- The presence of high amplitude anomalies associated with the mounds with no apparent drop in interval velocity to suggest a gas play.
- The occurrence of stratigraphic anomalies on both sides of a fault - which may be a probable pathway for migration with the guarantee of structural trap development.

7.5 SUMMARY

1. Rubble deposition is correlatable to the Late Miocene sea level fall(cycles 3.3 and 3.4). A maximum drop of about 150metres in each of these cycles is postulated.

2. Subaerial exposure of outland areas resulted in downflank deposition into the "Qua Iboe embayment" and the subsequent subaqueous mass movement of sediments within the palaeobasin.

3. Sea level drop is clearly the prompter for the generation of Rubble material coincidental with the Miocene volcanic activity of the Cameroun- Fernando Po axis. The effect of this regional tectonic activity was to emphasize angularity of the unconformity (BQI) and enhance shale diapirism. (Note the zone of shale diapirs in Fig.3.3). Within the embayment the regional tectonism of the Cameroun-Fernando Po volcanic activity is reflected by N-S trending horst blocks (see Enclosure 13), most of which are draped by first and second generation Rubble Beds indicating that subaerial exposure was not common place within the embayment. The embayment persisted and even became more extensive during the Pliocene highstand. Thus the Qua Iboe shale formed as a distal deeper water "facies" of a prograding series of sequences the landward equivalent of which is the continental Benin formation.

4. Rubble Beds differentiate broadly into lower, upper and channel associated units, an indication of sea level fall accompanied by a faster rate of fall. See Fig.5.10. The lower Rubble unit (UNIT 1) appears to be essentially mass movement emplaced showing chaotic onlap and/or subdued amplitudes - reflection free characteristics. The upper unit shows more prominent reflectors

which may, or may not, be ponded and offlapping (mainly oblique) patterns where there is topographic control/sustained sediment input due to sharper sea level fall. For example, the southeast of the study area.

5. Progradation within the upper unit suggests deeper water environment of deposition probably upper bathyal (i.e. more than 600ft of water) in an area close to the Cameroun-Fernando Po tectonic regime. The alternating cycle of onlap and offlap is clearly indicative of eustatic control. See line 82-212a, Fig.1.6a.

6. Of the seismic facies recognised some are more sand prone than others. Proximal, chaotic and mounded onlap are prime candidates for reservoir rock. The distal facies are more shale prone. Analysis of interval velocity within the Rubble confirm the correspondence of sand development with the mounded seismic facies. The most prospective of these are within the northern anomalies where the mounded facies is also associated with an amplitude anomaly in a structural closure and the southeast anomaly which consists of seismic mounds with corresponding high amplitude anomaly within an onlap wedge.

CHAPTER EIGHT

QUA IBOE SEQUENCE AND FACIES ANALYSIS *142*

8.1 Outline and Classification 143
8.2 The Lower Qua Iboe sequences 145
8.2.1 SEQ.QS1 145
8.2.2 SEQ.QS2 146
8.2.3 SEQ.QS3 147
8.2.4 The Intra Qua Iboe "sand" package 148
8.2.5 The depositional model 150
8.2.6 Mechanisms of emplacement 150
8.2.7 The proximal facies 152
8.2.8 Mounded hummocky facies 154
8.2.9 Mounded fan complex facies 156
8.2.10 Onlapping fill facies 157
8.2.11 Sheet facies 158
8.3 Sequence interval velocity analysis 160
8.4 The Upper sequences 162
8.4.1 SEQ.QS4 163
8.4.2 SEQ.QS5 164
8.4.3 SEQ.QS6 165
8.4.4 SEQ.QS7 166
8.4.5 SEQ.QS8 167
8.4.6 SEQ.QS9 167
8.5 Origin of the Qua Iboe 169
8.6 Summary 170

8.1 OUTLINE AND CLASSIFICATION

The Qua Iboe member occurs as a transgressive deposit massively overlying truncated Biafra and/or Rubble Bed sections (see stratigraphic column Fig.3.11a). It consists mainly of shale but significant sand development have been identified in the lower sections and the transitional zones to the Benin formation above.

Fig.8.1 shows its lateral extent, with a western boundary trending NE-SW in the study area. The eastern limit occurs east of the acreage. The Qua Iboe is thought to be equivalent to the Bonito shale of the Rio del rey basin in western Cameroun. It acts as cap rock unconformably overlying the Biafra below providing the principal trapping mechanism for hydrocarbons in the study area.

Based on seismic analysis, the Qua Iboe may be divided broadly into composite progradational sets which define a seismic sequence. Each progradational set consists of:

- a **Lower unit**(bottomset) representing the toe of progradation(only gently prograding if at all);
- an **Upper unit**(foreset) which is the prograding arm of the set; and
- a **paralic unit**(topset) at the top(D-1) representing the shelf.

Sequences of the Qua Iboe and Benin formation mapped are shown below.

SEQUENCE	UNCONF./CORR. CONF.	AGE
QS1	Top- INTRA QUA IBOE QUA2 Base- BASE QUA IBOE(BQI)	E.PLI.
QS2	Top- INTRA QUA IBOE QUA3($TIQI_3$) Base- INTRA QUA IBOE QUA2	E.PLI.
QS3	Top- INTRA QUA IBOE QUA3($TIQI_4$) Base- INTRA QUA IBOE QUA3($TIQI_3$)	E.PLI.
QS4	Top- INTRA QUA IBOE QUA4.2($TIQI_{4.2}$) Base- INTRA QUA IBOE QUA4($TIQI_4$)	L.PLI.
QS5	Top- INTRA QUA IBOE QUA5	L.PLI.

	Base- INTRA QUA IBOE QUA4.2	
QS6	Top- INTRA QUA IBOE QUA6 Base- INTRA QUA IBOE QUA5	**E.PLE.**
QS7	Top- INTRA BENIN QUA7 Base- INTRA QUA IBOE QUA6	**E.PLE.**
QS8	Top- PLEISTOCENE UNCONFORMITY(Pu) Base- INTRA QUA IBOE QUA7	**L.PLE.**
QS9	Top- QUA10 Base- PLEISTOCENE UNCONFORMITY(Pu)	**Rc**

Line 82-279(Fig.8.2a) and Line 82-185(Fig.8.2b) are used as basis for the classification. Reference may also be made to the chronostratigrahic charts in Enclosure 12. The progradational composite sets listed above are pronounced south of the palaeobasin hinge line (Fault-3).

Sequences QS1, QS2 and QS3 make up the **Lower Qua Iboe sequences.** Sequences QS1 and QS2 together form the Intra Qua "Sand" package or Lower Qua Iboe 1. QS3 constitutes the Lower Qua Iboe 2. Sequences QS4, QS5, QS6, and QS7, are referred to as **Upper Qua Iboe sequences.**

This subdivision is necessary because, Lower Qua Iboe sequences appear to be the most sand prone, and for the purposes of interval velocity analysis are grouped together for sequence velocity interpretation later. Detailed analysis of individual sequences are given under the appropriate sub-headings in this chapter.

Progradation was from the NW to SE, with each sequence having a shelf break, slope and basin. A composite of the shelf breaks through Pliocene with respect to the different sequences is shown in Fig.8.3. Although, the general direction of deltaic build-up appears to be the same for most parts of the study area, the prominence of sigmoidal progradation in the northeast and east as against thicker oblique progradation tending towards sigmoid in the central parts of the study area, suggests that two main deltas might have been active during Pliocene. The southward swing of the shelf breaks in the northeast and the east may also be a pointer to this.

Each sequence is analysed for its boundary relationships and seismic facies. The common seismic facies types associated with the Qua Iboe sequences and their lithologic and environmental interpretation are shown in Fig.8.4. Within the interpreted depositional framework, individual seismic facies subunits of the sequences mapped combine together to form aggregate facies units defined in relation to their depositional setting. Thus, the proximal facies of the combined Lower Qua Iboe 1 sequences is defined by its proximity to sediment source. For the purposes of correlation, our basic reference is the interpretation on the eustatic curve shown in Figs.5.10a,b,c,d.

8.2 THE LOWER QUA IBOE SEQUENCES

8.2.1 SEQ.QS1

This is the lowermost Qua Iboe sequence mapped, whose base is the BQI unconformity. It is defined at its top by a minor unconformity QUA_2 in the western part of the palaeobasin and poorly defined to the east. In the eastern half of the study acreage, this sequence is largely undifferentiated occurring as sheet drape over the BQI.

It correlates with the **Early Pliocene highstand**(cycle 3.4) of approximately 100metres on the eustatic curve. Horizon QUA_2 represents the point on the eustatic curve where the sea level begins to drop. Structure and the isochron maps are shown in figs.8.5a & b. Facies distribution is shown in Fig.8.5c. The main seismic facies units within this sequence are:

- subdued amplitude drape facies, predominantly found to the north of the palaeobasin, to the east and south;
- drape onlap and high amplitude onlap usually associated with PGM features to the north of the palaeobasin(often consisting of ponded turbidites);
- sheet facies commonly occurring in the palaeobasin; and
- mounded hummocky facies present in small and moderately sized pockets within the palaeobasin. They form stratigraphic anomalies such as the **southwest, northwest, and the central anomalies**(see facies map, Fig.8.5c).

Because of the preponderance of sheet drape facies(bottomset beds) within this sequence, inference may be drawn that the palaeobasin was further from the possible source of sediments. Especially in view of the rapid sea level rise postulated by the eustatic curve, in the aftermath of the Late Miocene sea level falls. The exception occurs over central anomaly, where a conduit for funnelling coarse clastics had been established since Late Miocene during Rubble Beds deposition, where basal transgressive sands are prevalent(see Fig.8.5c).

8.2.2 SEQ.QS2

Sequence QS2 is associated with sequence QS1 and in most areas to the east of the acreage is undifferentiated from the sequence below. The top of the sequence is Qua3, an unconformity corresponding to the sharp fall in sea level at the commencement of cycle 3.6 on the eustatic curve. The sequence itself, correlates with cycle 3.5. Build-up of the western and eastern deltas southward may be seen in the increasing prominence of oblique progradation to the north of the palaeobasin(see line 82-201, Fig.8.6a; and line 82-409, Fig.8.6b respectively). The oblique progradation tends towards a slope front fill facies at the palaeobasin margin forming "*uplap*"(a Brown & Fisher, 1980 term). As the sequence below, it thickens close to the palaeobasin boundary.

The structural map of the sequence top(Qua3) is shown in Encl.10a. Isochron of sequence QS1 and QS2 combined is given in Encl.10b. Seismic facies distribution may be seen in Fig.8.6c. The dominant facies include the following:

- onlapping fill facies to the south and east;
- sheet and sheet drape facies to the west, northeast and southeast;
- oblique progradation to the north of the palaeobasin; and
- mounded hummocky facies, part of the central anomaly.

Stratigraphic anomalies formed by the mounded hummocky facies in this sequence include, the **southwest anomaly** and the **centre-west anomaly** (see the composite anomaly map, Fig.8.6d).

8.2.3 SEQ.QS3

Sequence QS3 correlates with rising sea level on the eustatic cycle after the lowstand of cycle 3.6. This lowstand is inferred in the acreage by the presence of prominent and discreet mounds largely of a circular geometry and not directional. They occur downdip of clinoform patterns(at the foot of progradation) and appear to fit the Vail *et al.*(1988) model of basin floor fans within a Lower system tract(see Fig. 8.7a; line 82-229).

These seismic mounds within the palaeobasin form trends that parallel the palaeobasin boundary. Fig.8.7b shows the distribution of these mounds which are named according to the composite set within which they developed. Thus, MQ1Q2 refers to a mound within the Q1Q2 seismic stratigraphic sequence. Two such trends, MQ3Q4(1) and MQ3Q4(2) occur north of growth fault-4 and its anti-thetic components.

Obviously, fault development obscures their recognition, but where they occur at the downthrown sides of post upper Qua Iboe growth faults within a rollover structure or on upthrown sides, potential trap formation is the consequence(see line 82-231, Fig.8.7c).

The top of sequence(Qua4) is dominanted by toplapping relationships to the north of the palaeobasin and the northern parts of the palaeobasin; the base(Qua3), is characterized by baselap. For the first time, the shelf edge had moved to within the palaeobasin basin proper(see Fig.8.7d) due to sustained progradation in the central parts of the palaeobasin. A prograding "terrace" showing the characteristic oblique seismic facies(line 82-271, Fig.8.7d) with the clinoforms consisting mainly of high amplitude reflectors*.

Structural time map of Qua4 is shown in Fig.8.8a. Isochron of this sequence shows considerable thinning to the south. The main depocentre remained the central and northwestern parts of the palaeobasin. To the northeast and east, progradation was gentle, and sequences in general are thinner.

Facies distribution is shown in Fig.8.8b. The dominant seismic facies include the following:

- offlapping(oblique) facies which dominate north of the palaeobasin, the north-central parts of the palaeobasin and the southeastern corner of the

* The implications of this type of shelf-slope are discussed in Chapter 9.

acreage where this is **parallel oblique** distinguished from the sigmoidal facies by it's greater dip and sharp termination of clinoform patterns within the generally thin SEQ.QS3(less than 100ms on line 82-212A, Fig.8.8c);

- offlapping(sigmoid) facies, common to the southwest, northeast and east;
- onlapping fill facies in the south-central parts; and
- mounded hummocky facies of the **central, centre-east and eastern anomalies.** The facies distribution also shows the discrete seismic mounds mentioned earlier.

8.2.4 INTRA QUA IBOE "SAND" PACKAGE

As stated previously, QS1 and QS2 are grouped together and referred to as the Intra Qua Iboe "sand" package. The reasons for this include the unique seismic facies association of the package, the presence of well developed seismic mounds that point to good sand development. This sequence was also the subject of litho-velocity analysis for the above reasons and also those mentioned in Chapter 2 under stratigraphic velocity interpretation.

Before a meaningful velocity-lithology relationship may be derived, the depositional framework has to be determined. The following are the characteristics of the package and the proposed depositional model for subsequent input into the analysis of interval velocities over the Lower Qua Iboe sequences.

The Intra Qua Iboe sand package is defined by the following:

1. A high amplitude, sometimes hummocky, continuous to discontinuous set of seismic events usually but not always having it's top defined by downlapping of the sequence above. In general the higher amplitude of reflectors within the sequence distinguish it from the upper Qua Iboe sequence.

2. A higher than normal sand percentage within a shaly Qua Iboe which is seismically mappable; thus the term sand package.

3. An unconformable or conformable top which coincides with the paleomarker *Textularia sp. 1*, representing the top of a deep water sequence(Gibson and Guerra, 1982), commonly but not always marked by

a sand body. It can also be picked from electrical logs due to it's higher resistivity responses. Seismically this top is concordant and sometimes disconcordant when the upper sequence downlaps the sand package.

4. This depositional sequence is limited to the north by the basin hinge line which is approximated by fault-3(compares with the limit of the Rubble beds). Though in areas north of the palaeobasin boundary where slope development are evident, ponding of sediments on the downthrown sides of growth faults onlap erosional anticlines (see line 82-409; Fig.8.6b).

The lower Qua Iboe sequence therefore occurs as a function of the basin slope and palaeo-topography and is time transgressive; older in the north and progressively younger southward.

Seven seismic facies associations have been recognised:

1. Mounded hummocky facies.

2. Mounded fan complex facies.

3. Onlapping fill facies -
   - Mounded onlap
   - Proximal onlap
   - Distal onlap

4. Sheet facies-
   - Proximal sheet
   - Distal sheet
   - Drape sheet

5. Proximal/slope front fill facies.

6. Sigmoidal facies.

7. Oblique facies.

Genetically all of the above constitute 3-dimensional assemblages of facies units related by depositional processes and environments. The palaeobasin consists of several intra-slope sub-basins.

8.2.5 THE DEPOSITIONAL MODEL

Facies distribution of the Intra Qua Iboe "sand" package is a reflection of basin slope, basin topography and proximity to source.

A depositional model(Fig.8.9) is proposed which shows a largely undifferentiated Qua Iboe shale in the upland area north of the palaeobasin boundary(except where it drapes over erosional anticlines or onlaps such "buried hills") . Within the palaeobasin, the proximal facies dominates the margins of the basin by virtue of it's nearness to the source, characterized by rapidly deposited and unsorted sediments. The mounded, chaotic facies is along a NW-SE trend superimposed over the central Rubble bed channel system. This facies opens into the mounded fan complex facies. The sheet facies predominate in the east and flank the mounded facies in some areas. The onlapping fill facies onlaps BQI highs. Variation within facies associations outlined above exist. For example, mounded onlap, proximal etc(note that seismic character and geometry define a seismic facies unit).

8.2.6 MECHANISM OF EMPLACEMENT.

In a progradational system, where clinoform reflection surfaces represent depositional slopes, paleodepth estimates may be obtained by measuring the vertical relief between shelf- margin(slope break) and base of slope(Fig.8.10a).

Using lines 82-267 and 82-279, estimates of the depth of progradation averages about 220msec for a "prograding terrace" type slope. With an average interval velocity of 7500ft/sec, estimate of the pseudo-depth amounts to 825ft. The real depth is estimated by dividing the pseudo-depth by a compaction factor(.48). Depths of approximately 1600ft mean that the environment of deposition of the Intra Qua Iboe " sand" package is **upper bathyal**(Fig.8.10b). Evidence from biostratigraphy suggest a deepwater environment for the lower Qua Iboe sequence(Gibson and Guerra, 1983).

Deep sea sedimentation is primarily controlled by sediment supply, tectonics and sea level fluctuations. Tectonic control is often exerted when depositional rates are less than subsidence rates. The dominant process involved in deep sea sedimentation is mass gravity transport and normal bottom currents(or indigenous bottom currents). Stow(1985), summarises the process continuum involved in deep sea sedimentation in Fig.8.10c.

Rockfall and accompanying processes have been discussed under Rubble Bed formation including seismic examples of initiation at the boundary of the palaeobasin as defined. A mechanism for the emplacement of the lower Qua Iboe invariable involves slumping. The following observations may be made:

- Slumping of shallow marine sdiments from the upland areas into the palaeobasin. Slumping of delta front sands so typical of shelf margin deltas results in displacement of significant clastics down slope. Because of gravity flow, coarse clastics are deposited initially and preferentially into bathymetric lows. Thus deposition of the lower Qua Iboe along the axis of the central Rubble Bed channel(see model; Fig.8.9).

- Seismic evidence for slumping as a mechanism for the deposition of the lower Qua Iboe is shown in figs.8.10d&e. Attached is the model of Dott(1963). Progressive slumping occurs even on gentle slopes(Lewis, 1971 and Robert, 1972) and could be from the same formation or from older rocks. Lewis(1971) also argues that a large slump on a slope typically has at it's head characteristic tensional structures such as faults, slump scars and bed deficiency. The main body of the slump mass may be relatively undisturbed. This fact is also reflected on line 82-251(Fig.8.10e).

- Palaeobathymetric control of deposition is a reflection of sediment gravity flow materials in the fluid medium of the palaeobasin. Turbidity currents* then remodel the depositional topography accordingly. Thus the sheet facies occurs in areas of low energy turbidity currents, away from the main sedimentary chute and areas of ponding of sediments; mounded hummocky facies along erosional channels and drape sheet and onlap over bathymetric highs(see Emplacement model, Fig.8.9). A hydrodynamic interpretation of each of the seismic facies is elaborated upon under their respective seismic facies analysis later.

- The style of association of these depositional sequences within the Qua Iboe is in the classical pattern of delta fed turbidites. Berg(1982), based on Sangree and Widmier(1977) compiled characteristic seismic indicators of turbidite sequences(Fig.8.11).

The essential elements of such systems include the following:

---

* Stow(1985), classifies turbidity currents into high and low density. The seismic facies displayed by turbidity current deposits are a reflection of these.

(a) Evidence of channelling (Trough or canyon)

(b) Mounding along strike and dip of such sequences

(c) Clinoform reflection patterns
    (i.) Thinning clinoform reflection patterns
    (ii.) Underlying seismic facies interval onlapping and offlapping a depositional slope.

The seismic examples are shown in figs. 8:12a, b, c, d. Note that the central channel system feeds the mounded fan complex facies as is expected of most delta-fed fans (Moore and Fullman, 1975). The channel cuts into underlying rocks. Build-up of the stratigrahic anomalies within the Lower Qua Iboe sequences southward is considered under the dominant facies of such anomalies(**mounded hummocky facies**).

8.2.7 THE PROXIMAL FACIES

The seismic character that constitutes the proximal facies is varied. The presence of high amplitude reflectors within a subdued amplitude medium is however common and the ensuring seismic facies may be defined by the "proximity" to sediment source. Rudimentary progradation (offlap- mainly oblique may be inferred despite the ponding into the basin.

Where slumping and debris flow material constitute the facies, mounded high amplitude reflectors within a subdued medium is typical. Thus the *mounded proximal facies*(line 82- 114; Fig. 8.13a). Slumping and erosion resulting in downdip sediment movement and turbidity flow into a confined space forms the **proximal onlap facies** as the consequence(see line 82-409, Fig.8.6b).

MOUNDED PROXIMAL FACIES - Non continuous high amplitude seismic unit mainly hummocky. Variable energy deposits due to rapid sedimentation of slump material poorly sorted into the palaeo- basin margins(Fig.8.13b).

PROXIMAL ONLAP - Ponding of turbidites in a confined space onlapping unto BQI highs. They are essentially high energy deposits characterized by near parallel continuous events indicating sand/shale intercalations or tuning(Fig.8.13c).

SUBDUED ONLAP- The shalier variety of proximal onlap essentially low energy mud and debris flow deposits ponded in an Intra slope basin.

PROXIMAL"UPLAP" - Brown and Fisher, 1977 terminology. (SIMILAR TO SLOPE FRONT FILL) It is used here to refer to slope break points indicating dip contrast engendering turbidity current deposits. Often associated with subsiding slope. It onlaps relict BQI structures and occurs mainly on their seaward facing margins. There is close similarity to proximal onlap with medium amplitude, continuous reflectors except that it merges upward into the oblique progradational facies(lines 82-171, Fig.8.14c and 82-211, Fig.8.13d). Probably caused by highstand during which lowstand fans (small scale) and other sediments of the outer shelf and upper slope are deposited. Uplap in this case occurs as wedges deposited along the margins of the palaeobasin. Aggradational sedimentary patterns are typical.

The proximal facies is therefore broadly indicative of rapid, mass slumping of sediments commonly unsorted with sand development varying from good to poor depending on source. Because this facies is prevalent along the low lying margins of the palaeobasin, very few wells have tested it. An example is NB-1. Along these margins, the Intra Qua Iboe sand package (defined by a prominent reflector (line 82- 353, Fig.8.13e) "uplaps" along a prograding arm north of fault-3 and merges with the Oblique progradational part of the Lower Qua Iboe.

In many respects the proximal facies of the lower Qua Iboe is similar to that of the Rubble beds considering that similar processes may have prevailed along these margins, although the proximal onlap of the Rubble beds which is due to lowstand (important for aiding coarse clastic transport to deepwater, Vail(1977) is coarser. A table showing well statistics is attached.

WELL	NB-1
I.Q.I.	1410ft
NET SAND	205ft
SAND %	14.5
TH. CL. SAND	58ft(BASE)
SAND ϕ; %	30%
INT. VEL.(SONIC)	
INT. VEL.(SEISMIC)	

8.2.8 THE MOUNDED, HUMMOCKY FACIES

This facies unit is characterized by a mounded reflection configuration that vary laterally on both sides into parallel subdued reflector patterns. It predominates along the central Rubble Bed channel system in a NW to SE axis(Fig.8.9). The mounded external form coupled with the internal hummocky reflection pattern is thought to be caused by compaction which tends to accentuate elongate shapes of channel sands within a shale medium. (See Pettijohn *et al.*(1972); Fig. 8.14). Thus individual sand bodies tend to be lenticular.

The sometimes chaotic character (emphasized by diffractions)is suggestive of high depositional energy associated with sand prone deposits which show increasing irregularity of reflection pattern. The base of the mounds are commonly erosional. The facies unit becomes increasingly higher amplitude, low continuity (interpreted as channel associated) to the NW flanked by lower amplitude, higher continuity seismic character (interpreted as over-bank deposits).

Seismic mounds occur extensively within the lower Qua Iboe and also above (less frequently). A distribution map of stratigraphic anomalies is shown in Fig.8.15 and gives the best indication of likely sand development.

The anomalies are:

- the central anomaly(Fig.8.16a)
- the southwest anomaly(Fig.8.16b)
- the northwest anomaly(Fig.8.16c)

- the centre-west anomaly(Fig.8.16d)
- the centre-east(1&2) anomalies(Fig.8.16e) and
- the eastern anomaly(Fig.8.16f).

Build up of these anomalies is shown in the respective figures listed above. Five wells within the central anomaly system have tested this facies. Well statistics are provided below in the following table.

WELLS	CA-1	CA-2	CA-3	CA-7	CA-8
I.Q.I.	1106ft	1843ft	1611ft	1077ft	1604ft
NET SAND	160ft	438ft	572ft	133ft	291ft
SAND %	16.3	24	35.5	12.4	18
TH. CL. SAND	35ft(BASE)	92ft(BASE)	80ft(BASE)	25ft(BASE)	66ft(BASE)
SANDϕ; %	26	28	26	27	30
V_{int}SONIC					
V_{int}SEISMIC					

The following deductions may also be made:

1. The sands are channel lag and overbank deposits with erosional base and lateral variability. Continuity along strike is evident.
2. The morphology of the hummocky facies subunits suggest that they are modified depositional channel systems*.
3. Two main sand regimes wholly enveloped by Qua Iboe shale are evident. Sand occurences could be in many intervals with thick sections(Fig.8.17).
4. Mounded seismic facies appear to follow bathymetric lows especially Rubble bed channel systems. This supports the notion that the channels

* Normark(1978), classifies fan valley types into erosional or depositional systems. The depositional types show little eroded base. In general it may be said that within the Qua Iboe most of the channels were depositional compared to the Rubble Beds where erosional channels are common place. This is attributable to the effects of eustatic sea level changes and is considered fully in Chapter 9.

remained active as conduits for Intra Qua Iboe sands. Downslope mass transport and density underflow tend to deposit coarsest sediments at the bottom of the depositional sequence(Galloway and Hobday, 1983). The same is true of the central anomaly as the table above shows.

5. Average sand percentage of over 21% and average porosity of about 28% have been observed.

6. Mounding is an important indicator of Intra Qua Iboe sand development, the chaotic seismic pattern caused by diffractions at the edges of switching feeder channels. Mounding is thus a tool for evaluating prospectivity of stratigraphic plays.

7. The mounded, hummocky facies is the most prospective of all the lower Qua Iboe facies units.

8.2.9 THE MOUNDED FAN COMPLEX FACIES

Where the central Rubble bed channel opens into the distal facies(of the Rubble beds) the mounded, hummocky facies assumes the morphology of a mounded fan complex. The fan complex facies is characterized by mounded reflection configuration at the top of the sequence over a more continuous, parallel base. It differs from the mounded chaotic facies by having a higher width to depth ratio and the parallel to continuous base with the upper mounds downlapping it. Line 82-182A(Fig.8.18a), used as a typical example shows a series of undulatory mounds (wavy top) coalescing into a broad complex about 6km wide. The small mounds may reflect sub-channels branching off from the main feeder channels of the mounded hummocky facies.

As discussed earlier, mounding is often as a result of compaction. MacPherson(1978), shows a hypothetical model for turbidite fan development(Fig.8.18b). Fan development often occurs in episodes (perhaps as controlled by eustatic sea level changes-considered later) which are superimposed one over the other resulting in the morphology evident on line 82-174 in Fig.8.19a. The lateral margins of the fan complex is flat hinged (ponded) indicating distibution of sheet sand overspills from the sub-channels.

Three broad subunits may be mapped within the fan complex. Unit A is a subdued amplitude sub-facies, Unit B, the western sub- channel lobe and Unit C, a central sub-channel lobe. Faulting along a shale ridge provides the eastern limit

to the fan complex facies. In fact these subunits represent the various sequences that make up the Lower Qua Iboe namely:

- Unit A (SEQ.QS1)
- Unit B (SEQ.QS2)
- Unit C (SEQ.QS3).

Another example is the northwest anomaly (Fig.8.19b), showing a wavy top within SEQ.QS1.

The facies is interpreted as suggesting variable energy deposits and appear to be cyclic piles of sediments fed through upslope submarine troughs by gravity transport processes. Three wells are used as examples,and like the mounded, hummocky facies the sands are channel cuts which may be genetically similar but not correlatable to each other. Sand thicknesses vary accordingly within the proximal, mid and distal parts of the fan complex but areas a rule smaller than those of the channel system that fed the fan because coarser sediments are deposited first. Average sand percentage is 14% while average sand porosity stands at 30%. See table below.

WELLS	SCA-1	SCA-2	SCA-3
I.Q.I.INTERVAL	1255ft	1220ft	1235
NET SAND	175ft	146ft	222ft
SAND%	14	12	18
TH. CL. SAND	36ft(BASE)	55ft(BASE)	55ft(BASE)
SANDϕ;%	29.8	30	30
V_{int}(SONIC)			
V_{int}(SEISMIC)			

8.2.10 THE ONLAPPING FILL FACIES

This facies unit is characterized by high amplitude, moderately continuous reflectors which appear to thin (or are convergent) over local highs. It predominantly occurs where heaving Akata shale mass ridges create a slope system inducing marine onlap(line 82-174, Fig.8.19a). Onlap also occurs over non-shale induced

structural highs such as "relict anticlines". They are mainly low to moderate energy deposits though occassional high energy sand rich turbidity deposits occur leading to mounded onlap. (see line 82-154B; Fig.8:20). Well statistics reveal that sand occurences are in onlapping stringers,thin and shaly over the associated structural high. These may be few or several intervals increasing down slope. Sand percentages similarly vary from a low of less than 5% on the structure to over 15% down slope. However, further into the basin,where the facies assumes sheet characteristics and sand percentages revert to those of the sheet facies i.e. under 10%. Sand correlation is possible with a fair amount of certainty. See table below.

WELLS	SSCA-5	EA-3	SSCA-6	SSCA-1	SSCA-2	SSCA-3	SSCA-4
I.Q.I.	714ft	1151ft	1045ft	656ft	728ft	1100ft	824ft
NET SAND	120ft	98.5ft	105ft	27ft	26ft	132ft	
SAND%	17	8.6	10	4	3.5	12	
TH. CL. SAND	25ft(TOP)	30ft(BASE)	18ft(TOP)	7ft(BASE)	4ft	32ft(BASE)	
SANDϕ;%	29	31	25	26		30	
V_{int}(SONIC)							
V_{int}(SEISMIC)							

8.2.11 THE SHEET FACIES

This facies unit is characterized by parallel, continuous, moderate to high amplitude reflectors. As the name implies, it has a sheet-like external form, tabular with high **width to thickness ratio**- evidence of sedimentation on low depositional gradients.

The parallel attributes of reflectors seem to suggest finer grained sediments with a uniform sand stringer system. They are regarded as low energy thin bedded turbidites distributed by indigenous bottom currents. Seismic tuning due to thin beds is thought to be responsible for the associated high amplitudes. The thin beds do not suggest distal or basin plain turbidites as they may occur in basin margin areas such as the fault-3 boundary area(see line 82-349, Fig.8.21a). This facies is indication of restricted sediment supply as they occur mainly flanking the NW-SE progradational sediment chute (see line 82- 251, Fig.8.10e) in the central

region of the study area. Lines 82-353(Fig.8.13d) and 82-106(Fig.8.21b) are used as type sections.

Where reflectors are absent or have low amplitudes the **sheet drape or subdued amplitude facies** result.

> SHEET DRAPE/BLANKET FACIES- They are characterized by low amplitude reflectors which are parallel and drape over underlying topography. They occur as massive low energy hemipelagic mud blankets with the typical high width to thickness ratio. These mud blankets are often associated with sandstone packages deposited in deepwater environments, usually overlying or separating the different packages(Walker, 1978). The higher amplitude variety is referred to as the sheet facies. The significance of the sheet drape facies lies in it's function as cap rock to prospective reservoirs within the lower Qua Iboe sequence (i.e. Intra Qua Iboe "sand" package).

These occur mainly within SEQ.QS1 and SEQ.QS2 of the lower Qua Iboe sequence draping over BQI highs. In such a case sand percentage is often nil and they may be regarded as hemipelagic drape. The sheet facies may be evident within any of the units that make up the lower Qua Iboe sequence where the tripatite subdivision is valid. For example, line 82- 220A(Fig.8.22b) where an offlapping facies (oblique) within SEQ.QS3 separates QS1 and QS2 sheet drape from SEQ.QS5 sheet facies respectively. Examples of wells that tested the sheet facies are given overleaf. Sands present in the sheet facies are generally less than 40ft in thickness. See table below.

WELLS	CA-4	CA-5	CA-6	CA-9	CA-10	CA-11
I.Q.I.	1286ft	1366ft	1064ft	1336ft	1220ft	1066ft
NET SAND	56ft	80ft	132ft	110ft	228ft	88ft
SAND%	4.4	6	12.5	8.3	18.6	8
TH. CL. SAND	22ft(BASE)	20ft(BASE)	42ft(MID)	20ft(BASE)	45ft(BASE)	22ft(BASE)
SANDϕ; %	28	29	28	28	25	28
V_{int}(SONIC)						
V_{int}(SEISMIC)						

Other seismic facies evident within the lower Qua Iboe are sigmoidal facies which occur in the eastern part of the acreage(see line 82-365, Fig.8.23).

SIGMOIDAL FACIES- The sigmoidal configuration is the predominant offlapping facies of the Qua Iboe, though sometimes associated in a complex oblique-sigmoidal set up. (see Fig.8.10e,line 82- 251). The sigmoid pattern indicate a generally shalier prodational facies than the oblique. Progradation often commences as oblique and becomes sigmoidal as finer grained clastic deposition increases seaward. The sigmoid configuration is particularly typical of areas to the east which flank the main progradational trend except in the northeastern corner of the study(see line 82-429, Fig.8.24). Thus progradation is less pronounced compared to the aggradation as a consequence of which the gently dipping sigmoidal character predominates.

The SLOPE FRONT FILL FACIES bears some similarity to the onlapping fill facies(see Sangree and Widmier,1979) and has been merged together in this report. Where the sigmoidal facies dominates in the east of the study area, the boundary between the lower Qua Iboe sequence and the upper sequence becomes tenuous since the TIQI is progradational in these parts.

8.3 SEQUENCE INTERVAL VELOCITY ANALYSIS

The Litho-Velocity chart for the Qua Iboe is shown in Fig.8.25a, and is derived from wells in the study area. The best fit sand line shows a power relation between velocity and depth, as does the shale line. As expected, the oil sands show a lower interval velocity when compared with wet sands. Thus the separation between oil sand interval velocities and shale interval velocities are even narrower than those between wet sand and shale.

Analysing the litho-velocity chart, important curve crossover points may be noted:

1. The interval velocities of wet sands exceed those of the interbedded or "*higher velocity shales*" at depths deeper than 4600 feet. At depths shallower than this crossover point, the relationship appears to be reversed.

2. At depths deeper than 5600 feet, the interval velocities of oil is expectedly higher than the interbedded shale. Similarly, the reverse applies at shallower depths.

Using the composite facies map and the depositional model derived from it, the relationship between sand development and the seismic interval velocity is as given below:

- In general, there appears to be correlation of higher interval velocities with increasing sandiness as represented by the mounded hummocky facies.

- When the corrected seismic interval velocities for specific seismic facies units are plotted on the Litho-Velocity chart, the mounded hummocky facies(the mounded fan complex facies is included in this) is clustered closest to the sand line. The sheet drape facies is clustered closest to the shale line. The onlapping fill facies appeared to be scattered across the velocity-depth cone signifying the wide variation within this facies unit. Similarly, the proximal facies showed such a wide scatter(Fig.8.26a).

- A map of sandiness(Fig.8.26b) based on this however shows in general an optimistic estimate of the sand trends in respect of the central anomaly and a pessimistic estimate concerning the centre-west anomaly. This in part is due to the presence of gas sands in the centre-west anomaly.

- From the above results, it may be deduced that the centre-east anomalies are likely to be sand prone. However, calculating a sand percentage for the anomaly is virtually impossible as the separation between the sand line and the shale line on the Litho-Velocity chart is not very wide. The same optimism may be deduced in respect of the eastern anomaly.

- Differentiation between oil bearing and water bearing sands based on the interval velocity data discussed above is very tenuous. This is because of poor separation between the interval velocities of oil bearing and water bearing sands at equivalent depths (when the positive bias of seismic velocities and other corrections are removed) on the one hand, and the even poorer separation between the oil bearing sands and the interbedded shales at equivalent depths on the other hand.

- A map of g(the coefficient of heterogeneity) at the BQI level over the anomalies and other areas where well data is available, shows broad

correspondence with the expected results i.e. higher values of g were obtained for areas where the seismic facies predicts good sand development. The map(Fig.8.26c) shows a contour "nose" over the central and other anomalies. The severity of the divergence is an indication of sandiness of the Intra Qua Iboe sand package. It may also be noted from the well data, that the maximum sand percentage within the Intra Qua Iboe "sand" package so far tested is 36%. This corresponds to the zone of highest seismic interval velocity and the map of heterogeneity shows $(V_{rms} - V_a)$ increases with increasing sand percentage as previously considered in Chapter 2.

Several reasons may be adduced as to why the central anomaly is the most extensive in the study area. Based on the analysis of interval velocity and seismic facies interpretation, the following may be plausible explanations:

1. The presence of a prominent central Rubble Bed canyon system in this part of the palaeobasin. Intra Qua Iboe sand package was deposited along bathymetric lows and this canyon system served as a conduit for gravity flow sediments and other sediments formed from turbiditic flow.

2. The central region of the palaeobasin was the main depocentre for deltaic build-up. Thus the prominent southeastward progradation from SEQ.QS1 north of the palaeobasin to SEQ.QS3 with oblique clinoform patterns and terrace type shelf breaks within the palaeobasin which is evident. These provided the sediments for deposition at the toe of progradation. The oblique clinoforms are caused by higher depositional energy than sigmoid.

3. The rate of sedimentation exceeded the rate of subsidence in these areas and not much dispersal of coarse clastics took place, these sediments having been trapped in intra slope bathymetric lows.

8.4 THE UPPER SEQUENCES

The Upper Qua Iboe sequences consists of SEQ.QS4, SEQ.QS5, SEQ.QS6 and SEQ.QS7. This term may itself be regarded as a misnomer, because most of the aforementioned sequences in the northern parts of the palaeobasin are made

up of shelfal sediments of the D-1 which prograde southwards into the slope type Qua Iboe shale.

Although SEQ.QS8 is treated in this section, it mainly consists of non-marine clastics (the Benin formation) in the study area but is likely, further south to grade into Qua Iboe type sediments. As will be seen later, the slope type facies within these sequences are regarded here as generally shaly even though some seismic mounds have been identified.

8.4.1 SEQ.QS4

SEQ.QS4 is classified higher system tract, deposited mainly during a stillstand of sea level that may be correlated to latter part of cycle 3.6 on the eustatic curve. Sustained sediment input into the Qua Iboe embayment was characteristic of the period. This sequence marks the commencement of the Upper Qua Iboe sequences in Late Pliocene.

The top of the sequence is horizon Qua4.2 which shows marked truncation that is consistent with the subsequent lowstand indicated on the eustatic curve. The base(Qua4) is largely baselapped from within the sequence. The sequence appears to have been deposited mainly in a slope-basin setting. Horizon Qua4.2 occurs as a truncating surface to the north, becoming top of a sigmoidal facies southwards, and sheet and onlapping fill facies to the southeast and south. The sequence thins considerably southwards. Facies distribution is given in Fig.8.27a. The predominant seismic facies are given below:

- sigmoidal facies;
- sheet facies; and
- onlapping fill facies.

Only one seismic anomaly is apparent within this sequence and this occurs in the east. On east-west seismic profiles, large scale seismic mounds are evident within this sequence. These differ from the stratigraphic anomalies defined in Chapter 2. They are formed from prograding clino- form slope lobes which are mounded in shape along strike or the transverse (in this case E-W) direction commonly enhanced by local erosion. An example may be seen on line 82-86(Fig.8.27b) where several such lobes, prograding into the palaeobasin indicate a multiple sediment dispersal pattern.

The stratigraphic hiatus at the top of the sequence was accompanied by the reactivation growth faulting in shelfal areas.

8.4.2 SEQ.QS5

The prominent Late Pliocene lowstand on the eustatic curve(the early part of cycle 3.7) is represented by the erosional truncation characteristic of the base of this sequence. The top of the sequence is horizon Qua5 which marks the transition from the paralic D-1 to the non-marine clastics of the Benin formation in the northern parts of the palaeobasin.

Beginning with this sequence, correlation divergence from the eustatic curve becomes apparent although the underlying trends remain. The stratigraphic hiatus predicted by the curve is present.

Beyond Qua5, the Early Pleistocene lowstand is evident in the progradation of the shelf over the interpreted slope of SEQ.QS5. Line 82-215 in Fig.8.28a, shows this interplay of shelf and slope as a consequence of sea level changes. This occurs in the western part of the acreage. The top of SEQ.QS5(Qua5) also shows discordance and is correlated to a lowstand in the central area(see Fig.8.28b; line 82-289).

This sequence also marks the commencement of intensive shelf building with the development of the D-1 type sections. In sensu-stricto, the D-1 is a shallow marine variety (facies) of the deepwater Qua Iboe occuring only where the Qua Iboe shale is present. The limit of the Qua Iboe is therefore the limit of the D-1. It derives it's name from the first well, MD-1, to have been interpreted as showing the transitional facies. As stated previously, each Qua Iboe progradational composite set consists of the D-1 as its *topset.*

The reflection configuration is typically parallel to shingled. This represents progradation into shallow water. The shingled configuration is due to strand- line sands. Strong amplitudes often mark the top of the D-1 sands due to significant acoustic impedance contrasts. They are delta plain shallow marine paralic deposits characterized by intercalating shales that separate and seal the sands. Lines 82-345(Fig.8.29a) and 82-169(Fig.8.29b) are shown as examples.

Sequence QS5 is considerably thinner than previous sequences. No isochrons were therefore made. Facies distribution map is shown in Fig.8.29c. The dominant seismic facies are:

- parallel/divergent representing the shelf in the northern parts of the palaeobasin(north of the palaeobasin subdued amplitude facies interpreted as non-marine clastics are prevalent); and

- sigmoidal facies to the south which tend towards onlapping fill and to the east.

Although seismic stratigraphic anomalies are absent within this sequence, in the eastern part of the acreage, vertical stacking of high amplitude anomalies are evident within the Upper sequences in general. These represent good sand development at the updip portions of sigmoid progradation(see Fig.8.29d, line 82-385).

8.4.3 SEQ.QS6

SEQ.QS6 is a continuation of QS5 with the paleoshelf edge prograding significantly southwards. In the western part of the palaeobasin, this is indicated by the parallel/divergent seismic facies of the D-1 overlying a subdued amplitude prograding facies of the slope(see line 82-215, Fig.8.28a). This is an indication of gradually lowering sea level evidently buttressed by the toplap associated with the top of the sequence Qua6. This lowstand correlates to the Early Pleistocene Lowstand.

In the south-central areas, Qua6 shows truncation and is associated with slumping from the slope leading to two prominent mounds within the sequence. This seismic mound differs from those of the lower Qua Iboe. The former is formed as a result of upper slope instability, while the latter are mostly channel fed. The mounded features are however not all continuous along their respective trends. For example on line 82-289(Fig.8.28b), only MQ2Q3 and MQ5Q6 are evident. This is interpreted to suggest that slump development was episodic and controlled by the steepness of the clinoform surface as well as by sea level changes.

The dominant seismic facies is sigmoidal to the east, parallel/divergent to the west of the palaeobasin and subdued amplitude non-marine clastics to the north.

The updip portions of prograding composite sets where the clinoform *foresets* toplaps the *topset*, is often characterized by sand build-up. This is represented in the eastern part of the study area by high amplitude anomalies (HCIs). They may occur as vertically stacked units when there is relative *stillstand* (rate of

sedimentation equals the rate of subsidence) and thus aggradation or as a step-wise build-up of anomalies (en-echelon) landward (see line 82-349, Fig.8.21a and 82-385, Fig.8.29d) in cases of relative *highstand* or when the rate of subsidence is more than the sedimentation rate. Similarly intermittent *lowstand* results in a step-wise build-up seaward(line 82-279, Fig.8.2a).

8.4.4 SEQ.QS7

This sequence is characterized largely by non-marine clastics to the north and west, and parallel/divergent seismic facies indicative of shelf deposition in the southern parts of the acreage. To the east, the sequence appears to have been interrupted by a channel system essentially showing a chaotic facies. The top of QS7 is horizon Qua7 which corresponds to the a lowstand of sea level on the eustatic curve. The stratigraphic hiatus associated with Qua7 appears to be pronounced in the southeast of the acreage where oblique progradation is typical of this sequence with the top of sequence showing truncation.

The occurrence of this oblique seismic clinoforms within this sequence is important for the following reasons:

- It marks the commencement of out-built shelf break in an area where this was hitherto not the case.
- It indicates that the rate of sedimentation exceeded the rate of subsidence.
- And more importantly it is a clue to the probability of seismic mounds forming to the south of this progradation as is evident in SEQ.QS3 with the prograded "terrace".

Facies distribution is shown in Fig.8.30. Summary of the seismic facies and the typical seismic profiles describing them are given below.

OBLIQUE FACIES- The seismic configuration of this facies is typically that of clinoform reflection patterns which toplap the D-1 seimic sequence and downlap the Intra Qua Iboe "sand"package(line 82-341, Fig.8.31).

They are considered low energy deposits with high depositional energy in updip portions, each prograding arm becoming shalier downdip. Oblique progradation trends southward into the sigmoidal characteristics. Sand percentages within the facies is almost nil except updip where the toplap relation with the D-1 exists. Discrete sand systems (mounds) however

occur especially at the basal contact with the lower Qua Iboe sequence (Fig.8.31, line 82-341). These may be the result of slumping off the prograding slope especially during lowstand. Critical slope dips of about 3-4 degrees have been estimated.

THE CHAOTIC FACIES- These appear as seismic disruptions within the Qua Iboe depositional sequence, often cutting into bedding planes of both the upper and lower Qua Iboe sequences. The chaotic characteristics is suggestive of submarine gully fills. It occurs within the study area as a NE to SW trending system in the southeastern corner of the acreage. They appear to consist of slump and debris flow deposits formed by shelf edge collapse or from crests of intra slope highs. The cut and fill shelf in these areas appear to be younger than both the upper and the lower Qua Iboe sequences, though pre-D-1 sand development is poor as evident on line 82-353, Fig.8.32a, b used here as examples.

8.4.5 SEQ.QS8

This sequence is made up of non-marine clastics of the Benin formation. The top is the Late Pleistocene unconformity corresponding to a lowstand of sea level on the eustatic curve. The unconformity is largely limited to the south-central and northeastern parts of the study area. In both cases this unconformity forms the floor of a canyon filled with sediments(mainly shale) of SEQ.QS9. To the south and east

Horizon Q8 corresponds to the topmost section of the D-1 mapped over the study area(no doubt further south other younger top D- 1's may be expected as the delta progrades). Horizon Q8 also marks the commencement of relative sea level fall noted by the coastal onlap of continental Benin formation (see line 82-369, Fig.8.33). The Benin formation is interrupted by the pleistocene unconformity discussed next.

8.4.6 SEQ.QS9

The Late Pleistocene lowstand is imprinted on the shelf in the form of a canyon, the base of which is an unconformity with an irregular surface suggesting scouring. The subsequent rise in sea level led to the filling of these canyons. Two prominent canyons of this age are evident within the study area:

1. the south-central, and

2. the northeastern Pleistocene canyons.

Although sediments are unconsolidated several reflection patterns are evident including *offlap, sheet and chaotic* indicating probable relationship to submarine slumping(Fig.8.34a,b; lines 82-281, 82-186). This wedge is interpreted as a submarine canyon the extent of which is shown in Fig.8.35.

Whittaker(1974) and Shephard (1981) have examined the nat- ure and origins respectively of ancient submarine canyon systems. Characteristics of submarine canyons as published in both accounts are used below as basis for comparison between the Pleistocene canyon indicated by Fig.8.35 and to dispute the concept of a so called Qua Iboe canyon fill.

SCALE OF EXCAVATION

The south-central Pleistocene canyon has a width of about 6.5km and maximum thickness of 600ft (within the study area). These measurements are consistent with the dimensions summarized by Whittaker(1974) in respect of canyon fills in the U.S. Gulf coast. With width in excess of 100km, and maximum thickness of over 3600ft, the Qua Iboe is much larger than common canyon fills and would require a mechanism beyond mere sea level lowering and the incision of fluvial channels on the continental shelf for its development. Such mechanism may include turbidity current and/or subsidence during development. These are examined in detail in Chapter 9 in the comparison between the proposed Qua Iboe embayment and the Hackberry embayment of the Gulf coast.

ACTIVE GROWTH FAULT ASSOCIATION

The South central Pleistocene canyon does not appear to be asociated with a fault valley which could have been modified by marine erosion. However within the Rubble bed member, 3 canyons, the western, central and eastern canyons* are related to the detachment of underlying rock from a shear plane such as relict intra Biafra faults and submarine erosion thereafter.

* The development of Rubble Bed channels through detachment of underlying Biafra section usually along relict fault planes is discussed in Chapter 7.

HIGHLY SERRATE LOG PATTERNS

Lock and Kurth(1981), and Ewing and Reed(1984), suggest highly serrate log patterns as typical of the canyon fill. Wells that have the Intra Qua Iboe gully system confirm this at the top of the canyon fill. However, the Pleistocene canyon is essentially shale-filled.

CAPPING BY PROGRADING SEQUENCES

Evidence of overlapping prograding facies sequence is typical of both the Pleistocene canyon and the Intra Qua Iboe gully especially at the top where D-1 type reflection character is evident, indicating a resumption of shallow water shelf and shore face deposition.

8.5 ORIGIN OF THE QUA IBOE

From the foregoing, it is perhaps pertinent to discuss the question of the origin of Qua Iboe shale. The origin is of course, widely disputed, though Qua Iboe has been compared with other clay sequences such as Afam clay member (Short and Stauble, 1967) and Opuoma clay member (Orife and Avbovbo, 1982 and Petters, 1984). Two hypothesis have been proposed:

a. the submarine canyon fill hypothesis, which considers the sediments as upper canyon deposits filled by long shore drift(Burke, 1972); and

b. the initial river valley transgression hypothesis(Weber and Daukoru, 1975).

Based on this seismic sequence analysis however, the canyon-fill and gully-fill hypotheses, do not appear to adequately explain the suite of seismic facies displayed by the Qua Iboe and described under seismic facies analysis. (See Whiteman, 1982 for details of the origins of the Qua Iboe).

The following evidence from seismic stratigraphic analysis would suggest an origin contrary to those postulated above:

1. Progradation within the upper Qua Iboe shows a transition from oblique seismic facies to sigmoidal facies from north to south, downlapping a lower sequence which shows slope dependent seismic. Features include hemipelagic drape over erosional aniclines proximal onlap facies typical of

turbidity current deposits (ponding of sediments between highs - highly continuous seismic reflections.

2. The buried hill topography (relict anticlines) of the BQI in some parts of the acreage reflects subaerial exposure of the shelf and sediment removal according of the least resistant rock. This differs from the cut and fill configuration of most canyons. In fact an Intra Qua Iboe gully system with chaotic type deposits is evident within the broad Qua Iboe system; and canyon systems at the BQI which have been mapped are limited in width (no more than 5km).

3. Within a composite progradational set (defined earlier) lateral facies changes from non-marine, shelf related marine and slope facies are evident. This represents a basinal rather than canyon type fill. Clearly the Qua Iboe is a distal marine variant confined within an existing embayment with it's non- marine equivalent, Benin formation occuring to the north of the embayment. Line 82-223, Fig.8.36 is used as an example. An analogy with the Hackberry embayment of the U.S. Gulf coast is considered later.

8.6 SUMMARY

The Qua Iboe is a transgressive Pliocene deposit massively overlying truncated Biafra and/or Rubble Beds, characterized by mainly slope and basinal type facies prograding onto the paleoslope. Each composite progradational set consists of a lower unit(the bottomset beds), an upper unit(the foreset beds) and a topset referred to as D-1.

The Qua Iboe has been classified into the sequences listed below, which are related to the imprint of eustatic sea level changes on the Niger Delta margin.

SEQUENCE	UNCONF./CORR. CONF.	AGE
QS1	Top- INTRA QUA IBOE QUA2 Base- BASE QUA IBOE(BQI)	E.PLI.
QS2	Top- INTRA QUA IBOE QUA3($TIQI_3$) Base- INTRA QUA IBOE QUA2	E.PLI.

QS3	Top- INTRA QUA IBOE QUA3($TIQI_4$) Base- INTRA QUA IBOE QUA3($TIQI_3$)	**E.PLI.**
QS4	Top- INTRA QUA IBOE QUA4.2($TIQI_{4.2}$) Base- INTRA QUA IBOE QUA4($TIQI_4$)	**L.PLI.**
QS5	Top- INTRA QUA IBOE QUA5 Base- INTRA QUA IBOE QUA4.2	**L.PLI.**
QS6	Top- INTRA QUA IBOE QUA6 Base- INTRA QUA IBOE QUA5	**E.PLE.**
QS7	Top- INTRA BENIN QUA7 Base- INTRA QUA IBOE QUA6	**E.PLE.**
QS8	Top- PLEISTOCENE UNCONFORMITY(Pu) Base- INTRA QUA IBOE QUA7	**L.PLE.**
QS9	Top- QUA10 Base- PLEISTOCENE UNCONFORMITY(Pu)	**Rec**

The basis for this correlation is the eustatic curve of Haq *et al.*(1987). Although broad correspondence has been established between this curve and the sequences interpreted on the Niger Delta margin, variation in Late Pliocene is also evident.

Based on this analysis, **five cycles** of low and highstands have been deduced from the Pliocene to Recent. Sequences QS1, QS2 and QS3 are the referred to as the Lower Qua Iboe sequences. From the seismic facies of these, snad trends have been postulated. These occur as stratigraphic anomalies.

The distribution of these anomalies is shown in Fig.8.15. The anomalies include the following:

- the central anomaly(Fig.8.16a)
- the southwest anomaly(Fig.8.16b)
- the northwest anomaly(Fig.8.16c)
- the centre-west anomaly(Fig.8.16d)

- the centre-east(1&2) anomalies(Fig.8.16e) and
- the eastern anomaly(Fig.8.16f).

Of these, the central anomaly is the most extensive occurring in the main pathway for both delta building and channel development. Thus the sand prone nature of this NW-SE trending feature. Deposition of coarse clastics essentially followed bathymetric lows.

Evaluation of the Lower Qua Iboe using seismic interval velocities confirm that the mounded hummocky facies is the most prospective facies. Plots of the seismic interval velocity for the facies clustered around the sand line on the Litho-Velocity chart, while the onlapping and proximal facies showed a wide scatter. The sheet drape facies generally plotted close to the shale line. Although in general, dominant lithologies may be determined by this method, reliable sand percentage estimation is not possible because of the relatively small separation between sands and shales at the depth of interest.

The Upper Qua Iboe sequences in general showed less stratigraphic anomalies and the dominant seismic slope facies seems to be sigmoidal facies. However, the stacking of high amplitude anomalies at the updip portions of the sigmoidal progradation was common, especially to the east of the study area.

The toplapping relationship between slope and shelf enables the identification of paleoshelf edges. The exact position of the shelf edge (margin) may be obscured by growth faulting. Map of the shelf breaks for some of the composite progradational sets is shown in Fig.8.3. Evidence that the basin has been filled by offlapping depocentres migrating basinward and the timing of maximum activity of growth faults becoming progressively later can be seen in the area.

Early and Late Pleistocene canyons have been identified in the study area.

CHAPTER NINE

SYNOPSIS *173*

9.1 General 174
9.2 The pre-Qua Iboe slope setting 174
9.3 The Qua Iboe slope setting 176
9.3.1 Primary controls on deep sea sedimentation 176
9.3.2 Classical models of deep sea clastic sedimentation 178
9.3.3 The delta-slope-submarine fan model 180
9.3.4 Comparison between the Qua Iboe Embayment and the Hackberry Embayment 184
9.3.5 The Upper Qua Iboe 187

9.1 GENERAL

Enclosure 13 is an illustration of the development of the palaeobasin consisting of a series of E-W seismic profiles across the basin from north to south. From the stratigraphic sequence analysis carried out in the preceeding chapters, the evolution of the basin falls into two broad categories namely:

1. the **pre-Qua Iboe slope setting**, and
2. the **Qua Iboe slope setting.**

The pre-Qua Iboe slope setting was largely dominated by structural deformation, and the development of Rubble systems as was characteristic of the Miocene in this area. The Qua Iboe slope setting on the other hand was characterized by sustained progradation into the basin without significant tectonism other than subsidence, coupled with the development of turbidites during the Pliocene.

In both of the above, the underlying control that separated these features from the classic Niger Delta depicted in most available literature, was the embayment, unique in many respects to this study area. This embayment is largely defined by the palaeobasin referred to numerous times in the preceeding text but not exclusively so. This is especially true of the northeast though the southern and eastern extension of the embayment is also not known. The attributes of this embayment in part defined by sea level changes and tectonism through geologic time, may be grouped under a framework of shelf and slope systems.

This chapter in addition, attempts a summation of the data analysed and presented in this report, with a regional perspective in mind, and underscores the comparative styles of Atlantic-type margins, by comparing the study area with the U.S. Gulf coast.

9.2 THE PRE-QUA IBOE SLOPE SETTING

Brown and Fisher(1980), recognized from seismic data, two principal types of slope systems(excluding structurally active basins):

1. **constructive slopes** characterized either by offlap(when rate of deposition is more than rate of subsidence) or *Uplap*(superposed or onlap fill); and

2. **destructive slopes** where marine onlap dominates when rate of deposition is less than rate of subsidence.

Within the above context, the model for the pre-Qua Iboe slope fits the latter(i.e. destructive slopes). Prominent lowstands of sea level during the Miocene, even without the associated tectonism, could have resulted in erosion of the shelf and the formation of marine onlap. In the event, the structural deformation merely enhanced the development of **onlap slope wedges** such as the Lower Intra Biafra Rubble(LIBR), Upper Intra Biafra Rubble(UIBR), and Rubble Beds.

Enclosure 13 depicts the evolution of this embayment, and highlights the constituent structural elements(such as the southeastern block, the south central ridge system, the northwest and northeast tilted fault blocks, and the Rubble Bed canyon systems) reactivated during the three previously outlined tectonic episodes namely:

- the Late Mid. Miocene episode, associated with the Lower Intra Biafra Rubble(LIBR),
- the Early Late Miocene episode associated with the Upper Intra Biafra Rubble(UIBR), and
- the Late Miocene episode which led to the formation of the Rubble Bed member.

The outline of the embayment is shown with the intra slope basins highlighted. The extent of the three onlap slope wedges during the Miocene largely delimit the embayment. Thus the presence of LIBR in the northeast (line 82-88a) of the palaeobasin and also in the southeast(line 82-186), suggests that the Mid-Miocene embayment was considerably larger than the subsequent embayments. On the other hand, UIBR is echoed by the Rubble Beds and limited to the palaeobasin. Both form a thick wedge of approximately the same thickness at this margin.

Also, to be noted, is the shale diapir on line 82-186. This is the commencement of the zone of shale diapirs and shows the piercement of the Qua Iboe the timing of which may be late or post-Pliocene.

The fact that this embayment persisted into the Pliocene is reflected in the presence of the basinal Qua Iboe shale, albeit, with the **destructive onlap slope** characteristic of the embayment changing (in the absence of the Miocene tectonism caused by volcanicity of the Cameroun-Annobon axis) to a **constructive slope** during the Pliocene.

9.3 THE QUA IBOE SLOPE SETTING

Qua Iboe deposition may be viewed within the context of a Delta-slope-submarine fan model. In the preceeding chapters, the Qua Iboe has been shown to be a deep marine wedge grading upward from upper bathyal(Lower Qua Iboe) to inner neritic (D-1) environments. The tripatite subdivision into Lower, Upper and D-1 units has earlier been discussed.

The morphology of the Lower Qua Iboe sequences begets comparison with submarine fan models. The term submarine fan is used liberally to indicate bodies that contain deep water sands(Bouma, 1988) and for that reason is applicable to the Lower Qua Iboe sequences.

Factors affecting fan development on passive margins as adopted from Shanmugam *et al.*(1985) is given in the table below:

FACTOR	PASSIVE MARGIN
Eustatic influence	High
Tectonic influence	Low
Shelf width	Wide
Shelf exposure/Sed. Supply	Large
Sediment transport	Long distance
Fan sediment	Mud rich
Modern example	Amazon

The "high" eustatic influence, wide shelf width, and large sediment supply (listed above) are reflected in the distribution of the Qua Iboe seismic facies discussed in Chapter 8. The controlling factors for the deposition of such sequences are considered next.

9.3.1 PRIMARY CONTROLS OF DEEP SEA SEDIMENTATION

Stow *et al.*(1985), propose three primary controls on fan development and deep sea sedimentation (all of which are inter-related) namely:

(a) Sediment-type and supply:

In this case, active delta distributaries fed large and rapid sediment supply to the shelf; the availability of material is thought to have been aided by the significant shelf width(more than 10km) and sea level.

(b) Tectonic setting and activity:

In a passive margin like the Niger Delta, tectonic parameters that determine fan type include size and internal geometry of the basin(i.e. the palaeobasin) including basin gradient. Gradient and sediment supply mechanism(delta fed progradation) are important as they may cause slope instability triggering large slumps that develop into debris flow and turbidity currents. However, sea level change remains the primary prompter for deep sea sedimentation (Moiola and Shanmugam, 1984). It is clear that in the study area, build-up of the delta, in concert with sea level changes provided the large supply of unconsolidated sediments required to generate major turbidity currents that form fans and other deep sea sediments. These are seldom initiated by tectonic uplift alone.

(c) Sea level changes:

The effects of these have been considered in Chapter five. Relative **highstand** results in sediments being trapped along a broad shelf. Thus, the paralic sequence defined by the D-1. **Lowstand** results in a narrower shelf and more direct funnelling of sediments into the deep basin. Within the Lower Qua Iboe alternating cycles of offlap and onlap (or condensed section) are common indicators of such changes. Progradation, rejuvenation and channel incision are akin to lowstand and regradational sequences while channel and lobe abandonment relate to highstand. Shanmugam and Moiola(1982), show a correlation between turbidites and sea level changes through geologic time(see Fig.9.1), though Nardin(1983), argues in the case of the California borderlands that it's the transition from low to highstand that results in massive terrigenous influx.

The variables associated with low and highstand are shown in the accompanying table. The purpose of this summation is however, to examine whether seismic association and distribution within the Qua Iboe may be fitted into a general framework of either a **slope wedge model** consisting mainly of widespread channel and overbank deposits with possible fan development further south or a **submarine fan lobe model.**

VARIABLES ASSOCIATED WITH SEA LEVEL CHANGES(Moiola and Shanmugham, 1984)

VARIABLES	LOW SEA LEVEL	HIGH SEA LEVEL
Episodes	Regressive	Transgressive
Volume of exposed land	Large	Small
Erosion of land and shelf	High	Low
Turbidity currents	Important	Unimportant
Oceanic thermal Gradients	High	Low
Contour currents	Vigorous(high energy)	Sluggish(low energy)
Shelf deposition	Minor	Major
Slope deposition	Slumps and Canyon fills	Hemipelagic mud
Basin deposition	Turbidite sand	Hemipelagic mud
Sedimentation rate	High	Low
Coastal Upwelling	Local	Global
Carbon 13 isotope	Light	Heavy
Possibility of glaciation	Mod./High	Low/Absent
Spreading rate	Low	High
Potential reservoir	Submarine Fan turbidites	Carbonate/Deltaic deposits

A review of the classical fan models is given below.

9.3.2 CLASSICAL MODELS OF DEEP SEA CLASTIC SEDIMENTATION

Stow *et al.*(1985), based on variations in sediment type and in the nature and rate of supply in modern fans, propose a two end-member submarine fan type classification (**elongate and radial**) and a third non-fan end-member, the **slope apron**(or debris apron system; i.e. non submarine canyon fed system but turbidite related system). This may be seen in Fig.9.2a&b.

Classical fan models have been reviewed extensively in literature (with a suite of differing nomenclature as the consequence) along the lines established by Normark(1970, 1974 and 1978), for modern fans and Mutti and Ricci Lucchi's (1972) ancient fan models. A comparison between the two is shown in Fig.9.3a&b.

Normark's model (based on studies of the California continental margin) consists of lower, middle and upper divisions. In this model the upper fan consists mainly of a leveed channel* system immediately below a feeder canyon; the middle fan(supra fan) has numerous channelized deposits (since modified by Walker(1978), showing a series of lobes at the terminus of branching or braiding channels) and a lower fan with minimal sands.

Mutti and Ricci Lucchi's(1972) initial model of the ancient fan showed the distribution of fan lobes in the lower fan though a model(Mutti and Ricci Lucchi, 1975) indicates lobe detachment from their feeder channels as a result of sediment by-passing. Both models discussed above are based on active margins. Other models based on passive margins include the following:

- Mississippi fan model(Fig.9.4a), characterized by distinct depositional units referred to as fanlobes which are channel-overbank complexes deposited during specific increments of sea level; such fanlobes do not normally stack vertically but onlap each other(Bouma, 1988).

- Submarine Ramp model(Fig.9.4b) of Heller and Dickinson(1985) which lacks a primary slope channel or canyon that acts as a conduit for moving sediments to the basin. This model requires:

  a. rapid sedimentation(more than 250m/m.y.) commonly found in a sandy deltaic system that has prograded to the shelf break of a narrow marine shelf; and

  b. a prodelta slope (mud-rich) which forms part of the slope of the receiving basin.

  The model also shows proximal (sand-rich), distal (less sandy) and basin plain (fringe fan deposits) facies subdivisions, but without the channelized sub-environments characteristic of the classical inner and middle fans. This may be attributed to the absence of a feeder canyon(Fig.9.4c). A modification of this model is the Shelf-Slope model(Fig.9.4d) of Surlyk(1987) which emphasizes tectonic control rather than sea level change.

---

* Note that the channels are identified by their convex upward mounded geometry which are different from the mounds associated with slumping off the prograding clinoforms in the upper Qua Iboe that are mainly localized and of a smaller scale. They also occur above the TIQI and have been discussed under the Lower Qua Iboe sequences.

Fan models are discussed in detail in Bouma *et al.*(1985), and Bouma(1988).

An examination of the respective fan models in Figs.9.3 and 9.4 compared to the Lower Qua Iboe model(Fig.9.5a) and map of the mounded seismic facies (channel and overbank facies indicator; Fig.9.5b) reveals the lack of fit with the classical fan lobe framework. The mounded seismic facies system does not appear to converge landward in the northern canyon area. Instead a few channel-levee sytems occur although the dominant system is the central anomaly associated with the Rubble Bed channel system as are other mounded hummocky facies which occur separately.

However, the central mounded system becomes laterally extensive to the south (mounded fan complex facies) developing a micro-fan geometry. Although seismic criteria for the recognition of fans(Mitchum(1985), Fig.9.6) appear to have been met, it is not certain whether the size criterion (Normark(1978), Fig.9.7) has been met, because the extent of the embayment to the east is not clear. The mounded fan complex facies is not laterally extensive (less than 15km). Notwithstanding, small fans develop especially in an enclosed palaeobasin with episodic sediment supply and Normark(1978), suggests that fan size itself is not important in determining geomorphic characteristics of a submarine fan.

Despite this, the depositional setting of the Lower Qua Iboe, the depth of emplacement of the sediments and the seismic facies, suggest a model consistent with a Delta-Slope-Submarine fan system. This is discussed below.

9.3.3 THE DELTA SLOPE SUBMARINE FAN MODEL

If the Lower Qua Iboe sequences are taken on a regional scale, the picture that emerges is that of an embayment largely filled by a mega-turbidite fan(Encl.13).

Lines 82-66, 82-88a, 82-106, 82-142, 82-158, 82-174, and 82-186 (all E-W lines) show the build up of the Lower Qua Iboe sequences southward. Several channel systems are evident in the middle segment bounded by Fault-3 and Fault-4 namely the western, west- central (line 82-142), east-central (line 82-158) and an eastern system (line 82-174). More often than not, these channels are juxtaposed over Rubble Bed canyons. The seismic geometry above the canyons give an indication of the axis of sediment movement and deposition during the Pliocene highstand.

The important characteristics that are evident include features which are present in the Normark(1978), Mutti and Ricci Lucchi(1972, 1978), Mississippi

fanlobes (Bouma, 1985) and Heller and Dickinson(1985) models. These are given below.

- A NW-SE trending feeder canyon has been identified to the north of the study area. This forms part of the same trend as the central anomaly which is the southern extension of this channel system(Fig.9.8a&b). This fits the Mississippi fanlobe model as the central anomaly is the predominant channel levee system in the study area.

- There is no evidence to suggest the convergence of the other mounded seismic features which make up the southwest, northwest and eastern anomalies at the feeder channel; nor is there evidence of feeder canyons to the north of the palaeobasin supporting the mounded hummocky facies of the eastern, southwest and northwest anomalies. Although these anomalies are often associated with bathymetric lows formed where an underlying Rubble Bed canyon exist. Thus these anomalies may actually be detached fanlobes and would fit the model of Heller and Dickinson(1985) along with the fact that the fans are delta-fed. The high sedimentation rate for the Niger Delta, and the mud-rich prodelta slope which is also the slope of the palaeobasin are also additional factors.

- Similarly, the presence of sand-rich proximal turbidites and fine grained distal turbidites(sheet facies) laterally juxtaposed within the study area may be a pointer to the radial shape of the submarine fan. The data base so far does not afford an overall picture of a radial fan. Stow(1985) however, has indicated that such a juxtaposition is possible because of the radial geometry of some fans.

- The proximal facies of the Lower Qua Iboe"sand" package occur at the margin of the palaeobasin banking-up(uplap of Brown and Fisher(1980)) against the prograding delta slope(see Fig.9.8c). These are formed from high density turbidity currents which are channelled locally at the base of slope but may also be dominantly sheet flows spreading out onto the ramp surface. Low energy turbidity currents form subdued sheet facies.

- The central channel system is the most prominent seismically. This may be due to the focussing effect of the central channel across the upper slope and changes in gradient for localization within the slope. The channels become aggradational due to the relative rise of sea level. Well data given earlier confirm the presence of stacked sand bodies in the central core area. Interspaced between the channels are turbidites characterized by

more continuous reflectors and less hummocky character due to ponding and palaeotopographic control.

For a delta-fed system, fans tend to lack high relief depositional bulges i.e. supra fans. Enhanced overbank deposition produces relatively straight leveed channels that grow rapidly downdip. Delta fed fans are thus characterized by long distance transport(Nardin, 1983).

Lower Qua Iboe development was therefore not a simple process but involved episodic growth of spatially variable seimic facies some of which may not be synchronous in space and time. Evidence derived from alternating cycles of onlap and offlap buttress the view of high frequency sea level variation in the Pliocene.

Episodes of marine transgression and highstand of sea level cause significant destructive modification of deep sea deposits with redistribution of outer shelf and upper slope sediments. The result is evident in the distribution of Proximal, Mounded Proximal, Distal, Onlapping fill and Slope front fill seismic facies of the lower Qua Iboe sequence. As expected the Lower Qua Iboe overlies a major sequence boundary [BQI] when sea level fell to a point below the shelf margin.

The considered view point is one which would regard the Lower Qua Iboe sequence as part of a **constructive slope** system filled by onlapping turbidity current channel and overbank deposits in bathymetrically low areas.

Thus the preferred model is therefore a **Composite of the passive margin models of the submarine fan** considered earlier. arranged within the basin. The onlap slope model of the Lower Qua Iboe is overlain by the offlap/submarine apron slope of the Upper Qua Iboe. Both constitute the **Constructive type slope** of Brown and Fisher(1980), (Fig.9.9a, b) overlying the **destructive type slope** prevalent during the late Miocene lowstand that resulted in Rubble Bed formation.

The Qua Iboe slope wedge is analogous to the Hackberry member of the Frio formation of the Texas-Louisiana slope, Gulf of Mexico(Fig.9:10). The framework and facies of this continental slope have been discussed extensively by Sangree *et al.*(1978), Woodbury *et al.*(1978), Amery(1978), Moore *et al.*(1978), Sidney *et al.*(1978), Caughey(1981), Galloway and Hobday(1983), and Winker and Edwards(1983).

An analogy between the two provinces is entirely appropriate for the following reasons:

- The sustained and prolific sedimentary input which progrades into a deep basin, and like most Atlantic type margins show the imprint of sea level variations.

- The intermitent diapiric deformation sometimes contemporaneous with sedimentation(shale tectonics and in the case of the Gulf coast salt tectonics as well). Similar structural styles have been documented.

- The hydrocarbon play of the reservoirs in the Lower Hackberry is almost a replica of the hydrocarbon setting of the Lower Qua Iboe.

Although, seismic data for the Oligocene Hackberry area has not been published, the morphology of the Lower Hackberry turbidite reservoirs have been described(see Berg and Powers(1980)). A comparison between the Hackberry embayment and the Qua Iboe embayment shows important similarities and contrasts. These are tabulated below. The important focus of such a comparison is in the reinforcement of the characteristic style of turbidites in passive margins. Thus, this comparison would apply in similar circumstances, to all passive margins where the following criteria are met:

- broad shelf with a relatively smooth morphology;

- a tectonic setting that is characterized by enclosed slope basins;

- sustained sediment input into the basin by deltaic progradation alone or in combination with longshore drift; and

- eustatic sea level changes.

9.3.4 COMPARISON OF HACKBERRY AND QUA IBOE EMBAYMENTS

HACKBERRY EMBAYMENT	QUA IBOE EMBAYMENT
LOCATION: The Hackberry member of the Frio formation is considered to be deep water marine deposits, extending from the eastern flank of the *Houston Delta system* along a strike into western Louisiana. It is bounded to the north by the Hartburg flexure(see Fig.9.11) and thickens seaward(Berg and Powers, 1980).	This is equally a deep water marine wedge extending from the eastern flank of the contemporary Niger delta into the Cameroun sector of the continental margin where it is often referred to as the *Bonito shale*
STRATIGRAPHIC SETTING: Stratigraphically it occurs within the Oligocene *Middle Frio* transgressive shelf system. Its base is a prominent unconformity characterized by extensive erosional truncation(Figs.9.12a & b). It is capped by a prograding barrier strand plain system and grades upwards into *Upper Frio* sediments of shallow water origin.	The stratigraphic setting is within the paralic *Agbada formation* which is Miocene to Pliocene in age in the study area(Fig.3.11a), bounded by the Base Qua Iboe unconformity below and the transgressive D-1 sequence indicative of shelf facies above.
CLASSIFICATION: The Hackberry member of the Frio formation may be subdivided into a Lower sand rich sequence and an upper mainly shaly sequence. There are indications in literature that the upper unit progrades.	Similar subdivision is possible. The Lower Qua Iboe is commonly the sand rich part of the Qua Iboe. The upper parts are predominantly prograding. About six prograding episodes, each capped by the D-1 are evident.
FACIES: Onlapping and retrograding submarine channel and fan sequence are characteristic. Log patterns show deposition within a highly channelled submarine fan system. The sand bodies are lenticular, and occur in dip aligned bands. Flanking channels are overbank or levee deposits. They may include turbidites formed by spillover from large channelized flows and are the facies poorest in sand. For example, the sheet facies of the lower Qua Iboe. Axes prone to higher sand percentages follow the channels(Fig.9.13)	Facies analysis shows similar characteristics. The wells within the central anomaly show the presence of channel aligned sand bodies juxtaposed over Rubble Bed channels. (see tables provided under the respective seismic facies discussions). Within the mounded, hummocky facies, steady up-section decrease in average thickness of channel sandstone. The depth of scour decreases with time.

HACKBERRY EMBAYMENT	QUA IBOE EMBAYMENT
BASIN TOPOGRAPHY: The Lower Hackberry was deposited upon a highly channelled surface. The topography of the unconformity upon which lies the Hackberry has been greatly influenced by salt tectonics.	Base Qua Iboe topography although dominated by the paleo-basin bounded by Fault-3, was likewise affected by shale tectonics especially to the south.
PLAYS: Updip plays have been reported at the contact between the barrier strand plain *Frio* and the Upper Hackberry. Also deep water sands may occur within the Upper Hackberry, especially in the middle. See Ewing and Reed(1985).	Similar plays at the updip portions of the offlapping seismic patterns and high amplitude anomalies within the D-1 sequence which caps the upper Qua Iboe are evident. Deep-water sands within the Upper Qua Iboe are related to slumps, off the slope of progradation. These occur as mounded features described earlier in the text.
ORIGIN: Coarse clastics occur within the Hackberry embayment along with other turbidite infill sediments of the Gulf coast. Berg(1981), discusses the variety of depositional setting of the Gulf coast from Paleocene to Miocene. These are shown in Fig.9.14; ranging from *Constructional channel sandstones, submarine canyons, unstable slope depositon, unstable fans, structurally controlled deposition.* The Hackberry member of the Frio formation consists of turbidite channel sands within basinal shale. Comparisons have been drawn between it(the hackberry member) and the mainly shale infilled *Yoakum canyon* of the *Lower Wilcox*, on the basis of their occurrence on the same shelf/slope system. The extensive nature of the Hackberry (over 120 miles across) as compared to the Yoakum which is mainly a shale infill of limited areal extent which acts as a cap rock trapping truncated Lower Wilcox reservoirs, makes this comparison tenuous(Fig.9.16)	The Qua Iboe embayment is similarly disposed in relation the continental shelf and slope of the Niger delta. Other deep water deposits have been reported by Burke(1972), and Weber & Daukoru (1975). The proposed origin of these, namely: *canyon fill and gully fill hypothesis* have been used to explain the occurence of the *Afam clay member, and the Opuama shale member.* Similarly, this interpretation does not however regard the Qua Iboe as a canyon or gully fill because of the lack of a cut and fill pattern often associated with canyon fills and is evident in the Opuama shale member. (See Orife and Avbovbo, 1982 and Peters, 1984; Fig.9.15). The Opuama with it's upper channel axial slope of 11 (Petters, 1984) fits Shepherds (1981) classification of canyon types and similar to the Yoakum shale channel acts a trapping mechanism for underlying truncated beds in this case the Biafra beneath.

HACKBERRY EMBAYMENT	QUA IBOE EMBAYMENT
ORIGIN Cont'd: Ewing and Reed(1985) suggest that the Hackberry member was deposited from basin infilling created by normal subsidence under conditions of sediment bypassing leading to the creation of a retreating shelf/slope boundary and feeding an onlapping submarine fan complex. It is from these few channels that the embayment formed offshore of major sediment sources such as the Houston delta system. The could have been similar to the Pleistocene Mississippi canyon. The channels then captured most of the fine-grained sediment supply preventing maintenance of the shelf margin and fostering the cutting of lesser canyons along the retreating shelf edge. Log patterns appear to indicate channel and suprafan deposition, though limited size and time span onlap depositional architecture is typical. The embayment deposits have been attributed to the *Late Oligocene sea level lowstand* (See Fig. 9.17). Except for the apparent absence of the equivalent of the Rubble Beds(no reference in the literature has been made in respect of such reworked sediments) broad correspondence exists between the Hackberry and the Qua Iboe as the above comparison indicates.	The embayment may have formed as a consequence of the regional tectonism which largely defined the palaeobasin. Subsidence due to a sustained sediment supply was probable. Their long term persistence may have been aided by convergent long shore drift (Burke, 1972) and the tectonic hinge axis called the *Cameroun- Fernando Po volcanic line* which defined the eastern limits of the embayment and was one of the sources of sediments. The log patterns in the Lower Qua Iboe also indicate channel and suprafan deposits(Fig.9.18), though the time span and size do not match the mega scale of such modern day fans as the Mississippi, the Indus and the Amazon. However, the suite of seismic facies associated with the Lower Qua Iboe and the calculated depth of emplacement indicate a deep marine origin. The Lower Qua Iboe broadly correlates with the E. Pliocene highstand. Minor episodes of Lowstand are observed in the different seismic facies displayed. The scenerio is that of a rapid rise in sea level after the Late Miocene lowstand accompanied by a lowering of sea level with the attendant clastic influx as evident in subunits Q_3Q_4,& $Q_4Q_{4.2}$ as seismic mounds within the Lower Qua Iboe.

9.3.5 THE UPPER QUA IBOE

A model for the Upper Qua Iboe is best represented by the **submarine slope apron system** of Stow(1985). In this case a **normal clastic slope apron**(Fig.9.2b). Accordingly, these slope types may be **constructive** (i.e. relatively smooth convex- concave profile built upwards and outwards by slope progradation) or **destructive** (with erosion, slumping and sliding *etc.* on the face of the slope causing steeper and more irregular profile to be developed ; see Stow(1985). The former is lower energy whilst the latter is higher energy. Both cases are reflected in the upper Qua Iboe and are considered later.

Facies distribution within the progradational episodes are irregular but dominated by fine grained sediments.The main corresponding seismic facies are Oblique offlap facies tending towards Sigmoid which downslope assumes the sheet drape facies. Layered turbidite sequences are also common place with well displayed bedding sometimes lapping unto highs.

The chaotic facies of the Upper Qua Iboe corresponds to chaotic tongues consisting of slump and debris flow deposits. They often occur in cut and fill type situations. The Upper Qua Iboe model shows a multiple sediment source feeding directly across a non-channelized or "straight" gullied slope, long lived point source sediment dispersal pattern that is apparent for the Lower Qua Iboe in the central portion of the study area is generally absent except for the Early and Late Pleistocene canyons evident to the east and south of the study area.

Thus, apart from the episodic nature of Qua Iboe deposition, lateral facies association suggest a central area of intense shelf margin delta development and progradation and the eastern area of a submerged shelf system. See Fig.9:17(unstable shelf margin model).

The Quaternary continental slope of the North central Gulf of Mexico, described by Lehner(1969), Sangree *et al.*(1978) and Woodbury *et al.*(1978) is an analogous slope apron. Like the Gulf coast continental slope, Upper Qua Iboe shows complex morphology (intersparsed by shale diapirs and intra slope basins) complicated by growth fault modified shelf edges.

In considering the Upper Qua Iboe as an unstable margin system, the shelf break plays an important role in sediment control and distribution and Qua Iboe analysis is essentially shelf margin analysis. The distribution, geometry and intrinsic characteristics of the clinoform reflection patterns reveal positions of relict shelf edges (although this may be obscured by syndepositional gravity tectonics).

A map of the paleo shelf edges is given in Fig.8.3 and the criteria for recognising ancient shelf margins is given in the accompaning table.

Consequently, shelf margin migration is useful as an indicator of the long term balance between sediments supply and subsidence because it is less sensitive than the shore line to short term perturbations in sea level[Winker, 1981]. It is also known that the deltaic sedimentation and syndepositional structural growth near the shelf edge[lowstand deltas] are considerably different than on the inner to middle shelf. Evidence for this stems from clinoform stratification being steeper on the margins than the inner shelf(see Fig.9.18).

A rapid rate of subsidence which is responsible for steeper clinoform patterns may be attributable to several causes:

1. Flexural depression of the crust due to sedimentary loading on an elastic [or visco elastic] lithosphere by the prograding depocentre[Walcott, 1972]. Maximum subsidence corresponds to the centre of the applied load which generally occurs at the upper slope or shelf break [Woodbury*et al.*(1973); Stuart and Caughey(1977)].

2. Rapid extension of the shelf margin due to listric faulting which causes a net regional thinning of sedimentary section above the decoullement zone.

3. The amplification mechanism i.e. compaction of the thick section of recent sediments.

As discussed earlier, progradation commences as oblique and becomes sigmoidal to the south. This reflects the shalier facies basinward and the enhanced role of margin subsidence especially in relation to Fault-3, the boundary of the palaeobasin.

The seismic expression of the geometry of the identified shelf edges units may be considered as a function of the sedimentation rates and shelf energy field(Field *et al.*, 1983). Three main types are evident in the study area:

a) The prograded shelf

b) The up-built and out-built shelf and

c) The cut and fill type shelf.

Horizons Qua2 to Qua7 represent the phases of deposition and non deposition. The effects of eustatic changes are therefore superimposed on those produced by almost continuous subsidence of the shelf. On line 82-279 (Fig.8.2a), the cycle of deposition between peaks of stillstand on the shelf occur in thicknesses of less than 100ms.

Progradation on the shelf requires a balance between sediment input and the available hydrodynamic energy that transports and redistributes the sediment. Any change in this may result in a change in the dominant facies. The presence of the various types suggest that progradation was episodic.

Mougenot *et al.*(1983), have modelled the effects of different hydrodynamic conditions, tilting and subsidence of the margin and eustatic sea level on progradation[see Fig.9.19]. Assuming shelf erosion during lowstand was not intense, the thickness of the horizontal layer deposited during highstand serves as a base to estimate the amount of subsidence that occur during the event and the previous lowstand. Between Qua2 and Qua7, a subsidence within the palaeobasin of about 5000ft has been estimated(compaction has not been considered).

The following observations may be made with respect to the Upper Qua Iboe:

1. That the predominant progradational facies was sigmoid. This is due to rapid subsidence and the fact that the margin is a young one. Oblique progradation is restricted to areas north of Fault-3 due to slower subsidence rates in these areas.

2. That the shelf break is significantly prograding only where the shelf forms on a slightly inclined slope. Thus upper Qua Iboe offlap is minimal in the western area of the acreage but pronounced in the central portion. Likewise Upper Qua Iboe offlap is less prominent to the east except, the southeast portion. The corollary is that the D-1 is thickest where the upper Qua Iboe thins significantly.

3. Shelf edge failures often result in evacuation scars that are later infilled. The chaotic facies of the Intra Qua Iboe gully system in the southeast of the acreage is an example. Its infilled sediments are often called accretion units. Note the convex upward top accompanied by toplap and a concave upward base (see line 82-353). They may be referred to as cut and fill deposits.

4. Slumps are identified as upper Qua Iboe "mounds". Slumps feeding the submarine slope apron are small, locally clustered and intermittently active. Critical slope dip that would result in these mounds is about 5 degrees.

5. During eustatic lowering of sea level, increased sediment transport and erosion[or non depositon] ensued on the continental shelf. A drop of about 200m means the shore line could have approached or reached the shelf break in this area resulting in increased deposition on the slope and rise. In contrast, during highstands, the coast is located near a position occupied prior to regression, prograding conditions at and near the shelf break is re-established. It appears that eustastic rise was fast to reinstate the shelf break depth H after erosion at lowstand.

6. Discontinuities as a result of these oscillations were identified and mapped as Qua2 to Qua7. The alternation of well stratified clinoforms with acoustically dead or transparent clinoforms common with the Lower Qua Iboe sequences, is less pronounced in the Upper Qua Iboe. Each sigmoidal unit consists of a generally horizontal and well stratified upper layer and gently dipping slope at the the tail end of which is a deeper acoustically dead or transparent talus deposit. The near horizontal series represent the shelf facies. Deposition occurs as follows:

[i] Accumulation on the outer shelf of a well stratified horizontal layer which progrades only slightly.

[ii] Non-deposition on the outer shelf and rapid progradation of the break.

[iii] Erosion or non-deposition on the shelf without evidence of contemporaneous progradation on the shelf but on the slope. Phases 1 and 2 are due to **highstand**; Phase 3 correlates with **lowstand**.

CHAPTER TEN

CONCLUSIONS AND RECOMMENDATIONS

10.1 Conclusions.....192
10.2 Recommendations.....196

10.1 CONCLUSIONS

1. Seismic stratigraphic sequence analysis of a part of the Niger Delta reveals a complex distribution of depositional sequences. In total, 18 Miocene to Pleistocene sequences have been identified and mapped. They have also been correlated to the eustatic sea level curve of Haq *et al.*(1987). A sequence summary is given on pages 67 and 68; correlation to the eustatic sea level curve is shown in Fig.5.10. The major unconformities are attributed to sea level lowstand and include the following:

   - the Lower Intra Biafra Unconformity(LIBU),
   - the Base Intra Biafra Rubble(BIBR),
   - the Top Intra Biafra Unconformity(TIBU),
   - the Base Rubble Beds(BRB), and
   - the Base Qua Iboe unconformity(BQI), all of which are Miocene.

   Others include

   - Intra Qua Iboe QUA3,
   - Intra Qua Iboe QUA4,
   - Intra Qua Iboe QUA4.2,
   - Intra Qua Iboe QUA7, and
   - Late Pleistocene unconformity(Pu).

2. Using systematic and integrated techniques involving seismic sequence interpretation and sequence interval velocity correlation, analysis of the three megasequences that make up the Agbada formation, the **Biafra, Rubble Bed and Qua Iboe members** has been undertaken. Possible depositional source, areal extent of seismic facies units and zones of best sand development fitted into an overall depositional model and framework is the consequence. An important feature of the model is the palaeobasin bounded by Fault-3, formed within a larger embayment defined largely as a result of Miocene tectonism. In general each member of the Agbada formation is accordingly subdivided into groupings reflecting the interpreted effects of regional tectonism and/or sea level changes as follows:

- The **Biafra** may be subdivided into lower, middle and upper; separated by Intra Biafra Rubble systems(see Fig.3.11a; the stratigraphic column) such as the Lower Intra Biafra Rubble(LIBR) and the Upper Intra Biafra Rubble(UIBR). The former corresponds to the Late Mid-Miocene sea level lowstand(cycle 2.6 on the eustatic curve) coincidental with Miocene tectonism along the Cameroun-Annobon axis, while the latter is associated with Early Late Miocene lowstand(cycle 3.1). The intervening sequences mainly consist of delta plain, delta front and prodelta sediments mostly progradational.

  This is contrary to the notion of the Biafra as a wholly paralic member of the Agbada formation as found in standard Niger Delta literature. Thus, by establishing a relationship between the sequences, eustatic sea level changes and tectonism, we refer to the Intra Biafra Rubble sequences(LIBR and UIBR) as Lower system tracts sandwiched between Higher or Shelf-Margin system tracts of SEQ.BS2 and SEQ.BS4. LIBR and UIBR thicken in general at the margins of the palaeobasin. Their formation as **onlap slope wedges** coupled with the afore-mentioned tectonism, means that the predominant slope style in the Miocene was a **destructive type slope.**

  The dominant seismic facies within the Intra Biafra Rubble system are **slope front fill facies, distal facies, onlapping fill facies, chaotic and offlapping fill facies.**

  Few stratigraphic anomalies are present within the Intra Biafra Rubble system although high amplitude anomalies are evident, mostly occurring at the flank of truncating Biafra beds. Two of these high amplitude anomalies are recommended overleaf for exploratory drilling.

  Biafra Litho-velocity analysis shows that a logarithmic(or power-law) relationship exists between velocity and depth for the respective end-member lithologies. The Intra Biafra Rubble system, is the main contributor of the 'above-average' sand percentage evident within the palaeobasin.

  The absence of stratigraphic anomalies within the Intra Biafra Rubble is due to the fact that channel-levee systems are not characteristic of the Intra Biafra Rubble as are often the case in the Rubble Beds(Chapter 7) and Qua Iboe(Chapter 8).

Irrespective of the part of the acreage, the presence of the Intra Biafra Rubble system is a good indication of sand development except within the Intra Biafra canyon(UIBR) where shale in-filling may be expected.

- The **Rubble Beds** occur as onlapping reworked Biafra sediments, attributable to the last two drops in sea level in the Late Miocene(cycle 3.3 and 3.4 on the eustatic curve), forming two units separated by an Intra Rubble unconformity. Possible mechanisms for the Late Miocene tectonism responsible for the formation of Rubble Beds include regional tectonic uplift; isostatic adjustment in response to sea level lowering or uplift; uplift related to local shale diapirism and compressional uplift due to differential loading along major growth fault systems. The presence of deep water Qua Iboe deposits (upper bathyal) overlying subaerially exposed Biafra beds is an important indication of a regional mechanism responsible for the uplift and subsequent subsidence in conjunction with sea level changes.

  Five seismic facies associations have been identified namely: **Mounded onlap, proximal onlap, chaotic onlap, distal onlap and prograding facies.** The chaotic facies is associated with Rubble Bed canyon development. 3 canyons are evident in the study area; the western, central and eastern canyons. The canyon systems generally N-S trending, feed the distal facies of the Rubble Beds to the south.

  The litho-velocity chart for the Rubble Beds shows a logarithmic(or power-law) relationship between velocity and depth for the end-member lithologies. The scatter plot on the litho-vel chart shows that the proximal, mounded and prograding facies plot closest to the sand line. Based on interval velocity studies, sand distribution correlates with the high amplitude mounded onlap facies. The mounded onlap facies is therefore synonymous with greater sand content and has the best potential for reservoir development. Of the various stratigraphic anomalies considered, the **northern and southeastern anomalies** are the most prospective because of their association with either high amplitude anomalies or structure or both.

  Rubble Beds occur as **onlap slope wedges** formed from tectonic uplift of the Biafra and erosion causing a **destructive type slope.**

- The **Qua Iboe** occurs as a transgressive Pliocene deposit massively overlying truncated Biafra and/or Rubble Beds. It is characterized by mainly slope and basinal type facies prograding onto the paleoshelf. Eight sequences within the Qua Iboe, D-1 and Benin formation have been mapped. Each sequence consists of at least a composite progradational set made up of a lower unit of bottomset beds, an upper unit of foreset beds and a topset D-1. Five cycles of low and highstand from the Pliocene to Recent correlate to these sequences. QS1, QS2 and QS3 make up the Lower Qua Iboe sequences and are the most sand prone and therefore prospective section of the Qua Iboe. This report correlates these to the latter part of cycle 3.4, and cycles 3.5 and 3.6 on the eustatic curve. The alternating cycles of low and highstand is represented by alternating well stratified clinoforms (on dip seismic profiles) during lowstand and a variable or acoustically dead clinoforms in highstand.

  Facies distribution within the Lower sequences shows elongate patterns of the mounded hummocky facies in the western, central and eastern areas. These are stratigraphic anomalies. Other seismic facies include the sheet, onlapping fill, proximal, and mounded fan complex facies.

  Seven stratigraphic anomalies within the Lower Qua sequences are generally indicative of channel-levee systems, most of which appear to be underlain by Rubble Bed canyons which might have remained conduits for sediments in the Pliocene. Of these, the central anomaly is the most prominent occurring at the southern extension of a northern feeder canyon. This is the main pathway for both delta building and channel development.

  From the distribution of these anomalies and the regional depositional setting of the Lower Qua Iboe sequences, a **delta-slope-submarine fan model** is described for the area. Although the preferred model does not fit the classical models of fan development, it appears to be a combination of the **Mississippi fanlobe model** of Bouma *et al.*(1985) and the delta-fed **submarine ramp model** of Heller and Dickinson(1985). The composite model indicates that Lower Qua Iboe slope setting was of a **constructive type**.

  Sequence interval velocity analysis for the Lower Qua Iboe shows broad correspondence between the stratigraphic anomalies and good sand development. The Qua Iboe litho-velocity chart shows a greater cluster of

mounded hummocky facies velocities close to the sand line. The onlapping fill and proximal facies showed a wider scatter on the chart but was generally closer to the sand line when mounded. The sheet facies plots closer to the shale line. In the order of sand potential, the mounded hummocky facies is first follow by mounded fan complex, proximal mounded onlap and sheet facies. Although sand potential may be determined using this method, differentiation between oil-bearing and water-bearing sands based on their respective interval velocities is not possible because of the poor separation between the two curves on the litho-velocity chart.

The Upper Qua Iboe sequences on the other hand are made up of finer grained clastics in general than the Lower Qua Iboe. The dominant seismic facies is sigmoidal facies. Few stratigraphic anomalies have been mapped within these sequences. It best fits the **normal clastic slope apron** of Stow(1985).

For reasons that include the distribution of seismic facies within the Lower and Upper Qua Iboe, which indicate its slope and basinal setting, its wide extent and prograding paleoshelf edges southward, the Qua Iboe cannot be regarded as a canyon fill. Moreover, an Intra Qua Iboe "gully" system has been identified related to an Early Pleistocene lowering of sea level.

Pleistocene was characterized by canyon development with the formation of the Intra Qua Iboe "gully" system in Early Pleistocene and the Late Pleistocene canyon to the south. This gives an indication of possible fan development to the south of the study area.

10.2 RECOMMENDATIONS

1. Although the aims of the project did not include evaluation of the petroleum prospectivity of the study area in terms structure and stratigraphy, seismic stratigraphic analysis and Litho-velocity analysis of the sequences identified has led to the identification of prospective plays. These are structural as well as stratigraphic and are listed below:

   - The high amplitude anomalies within the Upper Intra Biafra Rubble(UIBR) shown in Figs.6.13b&c. Structures at the LIBU level in the southeast (line 82-216a; Fig.2.)

- The northern and southeastern anomalies within the Rubble Beds which show a mounded hummocky seismic character and plot close to the sand line on the litho-velocity chart. They are also associated with faulting and structure which should guarantee migration path and trap development.

- The Base Qua Iboe structure on the upthrown side of Fault-6.

- The eastern, southwest, northwest, centre-east(2) anomalies of the Lower Qua Iboe.

- The high amplitude anomalies of the Upper sequences vertically stacked in the eastern part of the acreage and to the west(see Fig.8.2).

2. In order to evaluate these plays, especially those that have been identified as stratigraphic anomalies, closely spaced, sequence-keyed velocity analysis is recommended for a reliable derivation of interval velocity and computation of the degree of sandiness of the anomaly(reservoir potential). Velocity analysis spacing of 400metres or less is recommended in line with the present seismic profile grid of approximately $1600m^2$ in the areas of interest. This may prove more cost effective even in the case of an existing field, than 3-dimensional seismic shooting over a stratigraphic play.

3. A seismic acquisition program along the strike and dip of the northern canyon, to investigate upper fan deposits that are likely to occur in respect of the Lower Qua Iboe is recommended.

4. Further work in this area is recommended to include updating the velocity-depth data as more wells and higher quality seismic data become available, for a more precise definition of the litho-velocity relationship. This should be undertaken in respect of the Intra Biafra Rubble system, Rubble Beds and the Qua Iboe. Ray trace modelling of the identified stratigraphic anomalies is also recommended.

REFERENCES AND BIBLIOGRAPHY

** NOTES ON ABBREVIATIONS

AAPG- American Association of Petroleum Geologists
SEG- Society of Exploration Geophysicists
SEPM- Society of Economic Palaeontologists and Mineralogists

ACHESON, C.H., 1963: Time-Depth Velocity-Depth Relations in Western Canada. GEOPHYSICS, VOL. 28, NO. 5, p. 894-909.

ACHESON, C.H., 1981: Time-Depth and Velocity-Depth Relations In Sedimentary Basins. A Study Based on Current Investigation in the Arctic Islands and on Interpretation of experience elsewhere. GEOPHYSICS, V. 46, No. 5.

AL-CHALABI, M., 1973: Series Approximations in Velocity and Travel time Computations: GEOPHYSICS, V.21, p. 783-795.

———, 1974: Analysis of Stacking, RMS, Average and Interval Velocity: GEOPHYSICAL PROSP., V. 22, p. 458-475.

————-, 1979: Velocity Determination from Seismic Reflection Data: in DEVELOPMENTS IN GEOPHYSICAL EXPLORATION METHODS, VOL. 1; ED. A.A. FITCH. APPLIED SCIENCE PUBLISHERS LTD. p.1-68.

ALLEN, J.R.L., 1964: The Nigerian Continental Margin: Bottom Sediments Submarine morphology and Geological Evolution: MARINE GEOLOGY, v. 1, P. 289-332.

———, 1965: Late Quaternary Niger Delta, and adjacent Areas: Sedimentary Environments and Lithofacies: AAPG Bull., V. 49, p. 547-600.

AMERY, G.B., 1978: Structure of Continental Slope, Northern Gulf of Mexico. AAPG STUDIES IN GEOLOGY No. 7

ANSTEY, N.A., 1977: Seismic Interpretation: The Physical aspects. IHRDC Publications. Boston.

AVBOVBO, A. A., 1978: Geothermal gradients in the southern Nigeria Basin. BULL. CAN. PETROL. GEOL. Vol. 26 no. 2.

AYNARD, C., 1961: Variation of velocities with age and lithology. GEOPHYSICAL PROSP., V. 9, No.1.

BANIK, N.C., 1984: Velocity Anisotropy of Shales and Depth Estimation in the North Sea. GEOPHYSICS, Vo. 49, p.

BARNES, N.E. & NORMARK, W.R., 1985: Diagnostic Parameters for comparing Modern Submarine fans and Ancient Turbidite Systems. In BOUMA *ET AL.* SUBMARINE FANS AND RELATED TURBIDITE SYSTEMS. SPRINGER VERLAG.

BEARD, *ET AL.*, 1982: Quaternary Chronology, Paleoclimate, depositional sequences and eustatic cycles: AAPG BULL., V. 66, p. 158-169.

BENSON, P.H., 1971: Geology of the Oligocene Hackberry Trend. TRANS. GULF COAST ASSOC. GEOL. SOCS., V. 21, p. 1-14.

BERG, O.R., 1982: Seismic Detection and Evaluation of Delta and Turbidite Sequences; their Application to Exploration of the Subtle Trap. AAPG Mem. 32, p. 57-75.

BERG, R.R., 1981: Deep-water Reservoir Sandstones of the Texas Gulf Coast: TRANS. GULF COAST ASSOC. GEOL. SOCS., V. 31, p. 31-40.

———, 1986: Slumped, Delta-front Reservoir Sandstone in the Eocene Yegua Formation, East Sour Lake field, S.E. Texas. TRANS. GULF COAST ASSOC. GEOL. SOCS., V. 36, P.401-407.

——— & POWERS, B.K., 1980: Morphology of Turbidite Channel Reservoirs, Lower Hackberry (Oligocene), SE Texas: TRANSACTIONS; GULF COAST ASSOC. GEOL. SOCS., V. 30, p. 41-48.

BIEL, R. & BUCK, G.H., 1978: Paleostructural Mapping in Bathyal Environments: TRANS. GULF COAST ASSOC. GEOL. SOCS., V. 28, p. 49-63.

BLACKBURN, G., 1980: Errors in Stacking Velocity - True Velocity Conversion over Complex Geological Situations. GEOPHYSICS V. 45, No. 10.

BOTT, M.H.P., 1979: Subsidence Mechanisms at Passive Continental Margins: AAPG Mem. 29, p. 319-327.

BOUMA, A.H., 1981: Depositional Sequences in Clastic Continental Slope Deposits, Gulf of Mexico: GEO-MARINE LETTERS, V. 1, p. 115-121.

———, 1982: Intraslope basins in NW Gulf of Mexico: Key to ancient submarine canyons and fans, IN WATKINS & DRAKE (Eds.), GEOLOGIC EVOLUTION OF CONTINENTAL MARGINS: AAPG MEM. 34 p. 567-581.

———, *ET AL.*, 1981: Seismic Stratigraphic Characteristics of the Upper Louisiana Continental Slope: An Area East of Green Canyon: PROC.; OFFSHORE TECHNOLOGY CONFERENCE, PAPER 4098, HOUSTON, TX. p. 283-291.

———, *ET AL.*, 1978: Intraslope basin in NW Gulf of Mexico: In AAPG STUDIES IN GEOLOGY, No. 7, p. 289-302.

———, *ET AL.* (Eds.), 1985: Submarine Fans and Related Turbidite Systems: Frontiers in Sedimentary Geology, SPRINGER-VERLAG.

BOUMA, A.H., & COLEMAN, J.M., 1986: Interslope Basin Deposits and Potential Relation to the Continental Shelf, Northern Gulf of Mexico. TRANS. GULF COAST ASSOC. OF GEOL. SOCS., V. 36, p. 419-428.

BOUMA, A. H., 1988: Submarine Fans: Diagnostic Criteria for exploration. J.A.P.E.C. Course notes No. 78.

BROECKER, W.S. & VAN DONK, J., 1970: Insolation changes, Ice Volumes and the O_{18} record in Deep-sea Cores: REVIEWS OF GEOPHYSICS AND SPACE PHYSICS, V. 8, p. 169-198.

BROWN, L.F. Jr. & FISHER, W.L., 1977: Seismic Stratigraphic Interpretation of Depositional System: Examples from Brazilian Rift and Pull-apart basins. IN SEISMIC STRATIGRAPHY C.E. PAYTON (ED.) AAPG MEM. 26 p.

——— & ———, 1980: Seismic Stratigraphy. AAPG Course Notes. NO. 16.

BRUCE, C.H., 1973: Pressured shales and related sediment Deformation: Mechanism for Development of Regional Contemporaneous (or growth) faults. AAPG BULL. V. 57, p. 898-886.

BURKE, K.C.B., 1972: Longshore drift, Submarine canyons, and Submarine fans: AAPG BULL., V. 56, p. 1975-1983.

———, *ET AL.*, 1971. The Opening of the Gulf of Guinea and the Geological history of the Benue Depression and Niger Delta: NATURE PHYS. SCI., V. 233, p. 51-55.

BUSCH, D.A., 1971. Genetic Units in Delta Prospecting. AAPG BULL., V. 55, No. 8, p.

BUSCH, D.A., 1975. Influence of Growth Faulting on Sedimentation and Prospect Evaluation. AAPG BULL., V. 59, p. 217-230.

CARTER, R.M., 1975. A Discussion and Classification of Subaqueous mass-transport with Particular Application to Grain-flow, Slurry-flow and Fluxo- turbidites: EARTH & SCIENCE REVIEW, 11, p.145-177.

CASNEDI, R., 1983. Hydrocarbon-bearing Submarine Fan System of Cellino Formation, Central Italy. AAPG BULL., V. 67, p. 359-370.

CAUGHEY, C.A., 1981. Deltaic and Slope deposits in the Planulina trend (Basal Miocene) S.W. Louisiana. In Gulf Coast Section, SEPM 2nd ANN. RES. CONFERENCE. ABST. P. 20-21.

CAUGHEY, C.A. & AMES. C.A. Jr., 1976. Pleistocene Stratigraphy and Depositional History, N.W. Gulf of Mexico. GEOL. SOC. AMERICA ABST. WITH PROGRAMS, V. 8, no. 1, P. 11-12.

——— & STUART, C.J., 1976. Where the Potential is in the Deep Gulf of Mexico. WORLD OIL, V. 183, No. 1, P. 67-72.

COLEMAN, J.M., 1982. Deltas, Processes of Deposition and Models for Exploration. I.H.R.D.C., BOSTON, 124 p.

——— & GARRISON, L.E., 1977. Geological Aspects of Marine slope Instability, N.W. Gulf of Mexico: MARINE GEOTECHNOLOGY, V. 2, p. 9-43.

COLEMAN, J.M. & PRIOR, D.B., 1980. Deltaic Sand Bodies: AAPG CONTINUING EDUCATION COURSE NOTES, No.15, p.171.

——— *ET AL.*, 1983. Deltaic influences on shelf- edge. Instability processes, IN STANLEY & MOORE, EDS, THE SHELF BREAK, CRITICAL INTERFACE ON CONTINENTAL MARGINS: SEPM. SP. PUBL., No. 33, p. 121- 137.

COOK, H.E., 1979. Ancient Continental Slopes and their value in Understanding Modern Slope Development. SEPM SP. PUBL., No. 27, p. 287-306.

CORDIER, J.P., 1985. Velocities in Reflection Seismology. D. REIDEL PUBL. CO., 197 P.

CRANS, ET. AL., 1980. On the Theory of Growth Faulting: A Geomechanical Delta Model Based on Gravity Sliding: JOURNAL OF PET. GEOL. V. 2, P. 256-307.

CURTIS, D.M., 1970. Miocene Deltaic Sedimentation, Louisiana Gulf Coast in MORGAN, J.P., ED. DELTAIC SEDIMENTATION, MODERN AND ANCIENT SEPM. SP. PUBL. 15, p. 293-308.

——— & PICOU, E.B., 1980. Gulf Coast Cenozoic; A Model for the Application of Stratigraphic Concepts to Exploration on Passive Margins. CANADIAN SOC. PET GEOL. MEM. 6, P. 243-268.

DAILLY, G.C., 1976. A Possible Mechanism Relating Progradation, Growth Faulting, Clay Diapirism and Overthrusting in a Regressive Sequence of Sediments. CANADIAN PET. GEOL. BULL., V. 37, p. 92-116

DAMUTH, J.E., 1977. Late Quaternary Sedimentation in the Western Equatorial Atlantic: GEOL. SOC. AMER.BULL. V. 88, p. 695-710.

——— *ET AL.*, 1983. Distributary channel Meandering and Bifurcation Patterns on Amazon Deep-sea Fan as Fan as Revealed by Long-Range Side-Scan Sonar (GLORIA); GEOLOGY, V. 11, p. 94-98.

DELTEIL, *ET AL.*, 1974. Continental Margin in the Northern part of the Gulf of Guinea: in C.A. BURKE & C.L. DRAKE (Eds)., THE GEOLOGY OF CONTINENTAL MARGINS, SPRINGER VERLAG, NEW YORK, p. 297-311.

DIETZ, R.S., 1963. Collapsing Continental Rises: An Actualistic Concept of Geosynclines and Mountain Building: JOURNAL OF GEOL., V. 71, p. 314-333.

DINGLE, R.V., 1980. Large Allochthonous Sediment Masses and their role in the Construction of the Continental Slope and Rise off South-western Africa: MARINE GEOLOGY, V. 37, p. 333-354.

DIX, C.H., 1955. Seismic Velocities from Surface Measurements, GEOPHYS. V. 20, p. 68-86.

DONOVAN, D.T. 7 JONES, E.J.W., 1979: Causes of World-Wide changes in sea level. JOURNAL GEOL SOC. LONDON Vol. 136, p. 187-192.

DUNBAR, C.O. & RODGERS, J., 1957: Principles of Stratigraphy. New York: Wiley, 356 p.

EDWARDS, M.B., 1981. Upper Wilcox Rosita Delta System of of south Texas: Growth-Faulted Shelf Edge Deltas. AAPG BULL., V. 65, p. 54-73.

EMBLEY, R.W. & JACOBI, R.D., 1977. Distribution and Morphology of Large Sediment Slides and Slumps on Atlantic Continental Margins: MARINE GEOTECHNOLOGY, V. 2, p. 205-228.

EMERY, K.O. *ET AL.*, 1975. Continental Margin off W. Africa: Angola to Sierra Leone: AAPG BULL., V. 59, p. 2209-2265.

EMERY, K.O. 1977. Stratigraphy and Structure of Pull- apart Margins in Geology of Continental Margins: AAPG CONTINUING EDUCATION COURSE 5, P. B1-B20.

EVAMY *ET AL.*, 1978. Hydrocarbon Habitat of Tertiary Niger Delta: AAPG BULL., V. 62, p. 1-39.

EWING, T.E. & REED, R.S., 1984. Depositional Systems and Structural Controls of Hackberry Sandstone Reservoirs in S.E. Texas:

THE UNIV. TEXAS. BUREAU ECON. GEOL. GEOLOGICAL CIRCULAR, 84-7, 48 p.

——— & ———, 1985. Depositional History Gives Clue to Hackberry Production: WORLD OIL, V. 200, No. 2, pp. 47-52.

FAIRBANKS, R.G. & MATTEWS, R.K., 1978. The Marine Oxygen Isotope Record in Pleistocene Coral, Barbados, West Indies: QUATERNARY RESEARCH, V. 10, p.181-196.

FAUST, L.Y., 1951. Seismic Velocity as a function of Depth and Geologic time: GEOPHYSICS, V. 16, p. 192-206.

FIELD, *ET AL.*, 1983. Seismic facies of Shelf Edge Deposits U.S. Pacific Continental Margin. In SEPM SP. PUBL., No. 33, p.

FISHER, W.L. & McGOWEN, J.H., 1967. Depositional Systems in the Wilcox Group of Texas and their relationship to Occurrence of Oil and Gas: TRANS. GULF COAST ASSOC. GEOL. SOCS., V. 17, p. 105-125.

FISHER, W.L., *ET AL.*, 1969. Delta Systems in the Exploration for Oil and Gas: A Research Colliguium: UNIV. TEXAS, AUSTIN, BUR. ECON. GEOL., 78 p.

FRANKL E.J. & CORDRY, E.A., 1967: The Niger Delta Oil Province: Recent Developments onshore and Offshore. PROC. SEVENTH WORLD PETROL. CONG., p. 195-209.

FRAZIER, D.E., 1974. Depositional Episodes: Their Relationship to the Quaternary Stratigraphic Framework in the N.W. portion of the Gulf Basin: TEXAS UNIVERSITY BUREAU OF ECON. GEOL. CIRCULAR 741, 28 p.

GALLOWAY, W.E., 1985. Submarine Canyon System in the Frio Formation of S. Texas. TRANS. GULF COAST ASSOC. GEOL. SOCS., V. 35, p. 75-84.

———, 1986. Growth Faults and Fault-Related Structures of Prograding Terrigenous Clastic Continental Margins. TRANS. GULF COAST ASSOC. GEOL. SOCS., V. 36, p. 121-128.

——— & HOBDAY, D.K., 1983. Terrigenous Clastic Depositional Systems. SPRINGER VERLAG, 416 p. New York.

GALLOWAY, W.E. *ET AL.*, 1979: Depositional and groundwater flow systems in the exploration for Uranium; a research colloqium. UNIV. TEXAS AUSTIN; BUREAU OF ECON. GEOL. 267p.

GARDNER, G.H.F. *ET AL.*, 1974. Formation Velocity and Density. The diagnostic Basics for Stratigraphic Traps. GEOPHYSICS, V. 39 No. 6, p. 770-780.

GIBBS, R.J., 1981. Sites of River-Derived Sedimentation in the Ocean: GEOLOGY, V.9, p. 77-80.

GIRARD, O.W., 1979. Petroleum Geology of the Niger Delta, REPORT ON THE PETROLEUM RESOURCES OF THE FEDERAL REPUBLIC OF NIGERIA. U.S. ENERGY DEPT., p B1-B29.

GORINI, M.A., 1981. The Tectonic Fabric of the Equatorial Atlantic and Adjoining Continental Margins: Gulf of Guinea to N.E. Brazil: In CHAVES, H.A.F. (EDS), STRUCTURE AND TECTONICS OF THE BRAZILIAN CONTINENTAL MARGIN AND ITS IMPLICATIONS FOR SEDIMENTARY PROCESSES AND HYDROCARBON POTENTIAL, PROJ. SERIES REMAC, V.9, P. 11-116.

GRAHAM, S.A. & BACKMAN, S.B., 1983. Structural controls on Submarine fan geometry and internal architecture; Upper La Jolla fan system offshore S. California. AAPG BULL., V. 67, p. 83-96.

GRALKA *ET AL.*, 1980. Prediction of reservoir sand in immature areas from seismic stratigraphic analysis of interval velocity, in The Sedimentation of the N. Sea Reservoir Rocks, a Symposium in Geilo, Norway: Oslo, Norwegian Petroleum Soc. V. 1-9.

GROW, J.A. *ET AL.*, 1979. Multichannel Seismic Depth sections and interval velocities over outer continental shelf and upper continental slope between Cape Hatteras and Cape Cod: in Watkins, J.S. et al (Eds.), Geological and geophysical investigations of Continental Margins. AAPG Mem. 29, p. 65-83.

GUERRA, R.T., 1983. Stratigraphic Correlations, Offshore Nigeria. Proprietary report.

GUERRA, R.T. & GIBSON, L.B., 1982. Biostratigraphy, ecology and correlations offshore Nigeria. PROPRIETARY REPORT.

HAJNAL & SEREDA, I.T., 1981: Maximum uncertainty of interval velocity estimates. GEOPHYSICS VOL. 46 no 11; p.1543 - 1547.

HALLAM, A., 1978: [illegible]

HALLAM, A., 1981. A Revised Sea-level curve for the Early Jurassic: JOURNAL OF THE GEOL. SOC. LONDON, V. 138, p. 735-743.

HANCOCK, J.M. & KAUFMAN, E.G., 1979. The Great Transgression of the Late Cretaceous: JOURNAL GEOL. SOC. LONDON, V. 136, p. 175-186.

HAQ, *ET AL.*, 1987: Chronology of Fluctuating Sea Levels since the Triassic. SCIENCE, VOL. 235. p.1156 - 1166.

HARDENBOL, VAIL, & FERRER, 1981. Interpreting Paleoenvironments, Subsidence History, and Sea-level changes of Passive Margins from Seismic and Biostratigraphy: 26th INTERNATIONAL GEOLOGICAL CONGRESS, PARIS, COLLOQ. C3, GEOLOGY OF CONT. MARGINS; OCEAN. ACTA, SUPPL. V. 4, p. 33-44.

HARRISON, C.G.A. *ET AL.*, 1981. Sea-level variations, Global Sedimentation Rates and the Hyposographic Curve: EARTH AND PLANETARY SCIENCE LETTERS, V. 54, p. p. 1-16.

HAYS, J.D. & PITMAN, W.C. III, 1973. Lithospheric Plate Motion, Sea-Level Changes and Climatic and Ecological Consequences: NATURE, V. 246, p.18-22.

HELLER, P.L. *ET AL.*, 1982. Episodic Post-rift Subsidence of the U.S. Atlantic Continental Margin: GEOL. SOC. AMER. BULL., V. 93, p. 379-390.

HELLER, P.L., & DICKINSON, W.R., 1985: Submarine ramp facies model for delta-fed, sand-rich turbidite systems. A.A.P.G. Bull., v.69, p.960-976.

HELMS, R.B., 1978. A Seismic Stratigraphic Analysis and Prospectivity assessment of Rubble Beds. PROPRIETARY REPORT.

HILTERMAN, F.J., 1981. Seismic Velocities; An Updated approach for the interpreter. in AAPG-SEG STRATIGRAPHIC INTERPRETATION OF SEISMIC DATA SCHOOL, LONDON 1981.

HOUBOLT, J.J.H.C., 1973. The Deep-Sea Canyons in the Gulf of Guinea near Fernando Poo: VERHANDELINGEN KONINKLIJK NEDERLANDS GEOLOGISCH MIJNBOUWKUNDIG GENOOT SCHAP, V. 30, p. 7-18.

HOWELL, D.G. & NORMARK, W.R., 1982. Sedimentology of Submarine Fans, in P.A. SCHOLLE & d. SPEARING, EDS, SANDSTONE DEPOSITIONAL ENVIRONMENTS.AAPG MEM. 31, p. 365-404.

HOYT, W.V., 1959. Erosional Channel in the Middle Wilcox near Yoakum, Lavaca County, Texas: TRANS. GULF COAST ASSOC. GEOLOGICAL SOCS., V. 9, p. 41-50.

HSU, K.J., 1977. Studies of Venture Field, California. Facies Geometry and Genesis of Lower Pliocene Turbidites. AAPG BULL.,V. 61, p. 137-191.

HUBRAL, P., 1975. Locating a Diffractor below Plane Layers of Constant Interval Velocity and Varying Dip. GEOPHY. PROSP., V. 23, p. 313-322.

HUBRAL, P., 1976. Some Remarks on Computing Travel Times in Plane Layered Media. GEOPHY. PROSP., V.24, p. 719-724.

——— & KREY, T., 1980. Interval Velocities from Seismic Reflection Time Measurements. SEG Publ.

HUCKABAY, W.A.1985. Seismic Stratigraphy of the Winedale Prospect. Updip Wilcox Trend - Onshore Texas Gulf Coast. TRANS. GULF COAST ASSOC. GEOL. SOCS., V. 35, p. 125-142.

IMBRIE, J., 1985. A Theoretical Framework for the Pleistocene Ice Ages: J. GEOL. SOC. LONDON, V. 142, p. 417-432.

KALLWEIT, R.S., & WOOD, L.C., 1982: The limits of resolution of zero-phase wavelets. GEOPHYSICS, V. 47, p. 1035-1046.

KEELING, G. & STANLEY, D.J., 1976. Sedimentation in Canyon, Slope and Base of Slope Environments. STANLEY & SWIFT (EDS.) MARINE SEDIMENT TRANSPORT AND ENVIRONMENT MANAGEMENT. NEW YORK, WILEY, p. 378-435.

KERR, R.A., 1980. Changing Global Sea-level as a Geologic Index. SCIENCE, V. 209, p. 483-486.

KERR, R.A., 1987: Refining and Defending the Vail Sea Level Curve. SCIENCE, V. 235; p.1141 - 1142.

———, 1984. Sea floor spreading is not variable: SCIENCE, V. 223, p. 472-473.

KOEFED, O., 1981: Aspects of vertical seismic resolution. GEOPHYSICAL PROSPECTING, V. 29, p.21-30.

KOMINZ, M.A., 1984: Oceanic Ridge Volumes and Sea-Level Change - An Error Analysis. In AAPG MEM. 36, Ed. J. SCHLEE, p. 109-127.

KOSTERS, E.C., 1985. Deeply Buried Tertiary Sand Bodies in the Northern Gulf of Mexico: Examples from the Lower Hackberry and Houma Embayments. TRANS. GULF COAST ASSOC. GEOLOGICAL SOCS., V. 35, p. 161-170.

KRUIT *ET AL.*, 1975: Une excursion aux cones d'alluvions en eau profonde d'age Tertiare pres de San Sebastian (province de Guipuzcoa, Espagne). 9th International Sedimentological Congress, Nice, 1975. Excursion 23, pp. 75

KRUMBEIN, W.C. & SLOSS, L.L., 1963: Stratigraphy and Sedimentation: W.H. Freeman and company, 660 p.

LEVIE, D.S. Jr., 1985. Interdomal Sediment Ponding: A new Lower Hackberry Play

LEVIN, F.K., 1971. Apparent velocity from dipping interface reflections. GEOPHYSICS, V. 36, p.510- 516.

———, 1978. The reflection, refraction and diffraction of waves in media with elliptical velocity dependance. GEOPHYSICS, V. 43, p.528-537.

———, 1979. Seismic velocities in transversely isotropic media, Part I. GEOPHYSICS, V. 44, No.5.

———, 1980. Part II, GEOPHYSICS, V. 45, No. 1,

LEWIS, K.B., 1971. Slumping on a Continental Slope inclined at 1 - 4 : SEDIMENTOLOGY, V. 16, p. 97-110.

LINDSETH, R.O., 1974. Seislog Process uses Seismic Reflection Traces, IN OIL AND GAS JOURNAL, V. 43, p. 67-71.

———, 1979. Synthetic Sonic logs. A process for stratigraphic interpretation. GEOPHYSICS, V.44, No.1.

LOWE, D.R., 1979. Sediment gravity flows: Their classification and some problems of its application to natural flows and deposits: in SEPM SP. PUBL. No. 27.

LOWRIE, A., 1985. Seismic Stratigraphy, Pleistocene Climate and Tertiary Sea level changes (ABS.): AAPG BULL., V. 69, p. 281.

LOWRIE, A., 1986. Model for Fine-Scale Movements Associated with Climate and Sea-level Changes along Louisiana Shelf-Break Grow th Faults. TRANS. GULF COAST ASSOC. GEOL. SOCS., V. 36, p. 497-509.

——— & McDANIEL-LOWRIE, M.L., 1985. Application of Pleistocene Climate Models to Gulf Coast Stratigraphy. TRANS. GULF COAST ASSOC. GEOL. SOCS., V. 35, p. 201-208.

LYNN, W.S. & CLAERBOUT, J.F., 1982. Velocity Estimation in Laterally Varying Media. GEOPHYSICS, V. 47, No. 6, p. 884-897.

MACHEN, E., 1970: Mesozoic evaporite belts of Africa. Hess. Landesamt Bodenforsch., Abh., no. 56; p. 97 - 111.

MACPHERSON, B.A., 1978. Sedimentation and Trapping Mechanism in Upper Miocene Stevens and Older Turbidite fans of S.E. San

Joaquim Valley, California. AAPG BULL., V. 62, p. 2243-2274.

McMASTER, R.L. *ET AL.*, 1970. Magnetic and Seismic Reflection Studies on Continental Shelf off Portuguese Guinea, Guinea and Sierra Leone, West Africa. AAPG BULL., V. 54, p. 158-167.

———, 1970. Continental Shelf Geomorphic features off Portuguese Guinea, Guinea, and Sierre Leone (W. Africa). MARINE GEOLOGY, V. 9, p. 203-213.

MANDL, G. & CRANS, W., 1981. Gravitational Sliding in Deltas. In THRUST & NAPPE TECTONICS. GEOL. SOC. LONDON, p. 41-54.

MASCLE, J., *ET AL.*, 1973. Diapiric Structures off the Niger Delta. AAPG BULL., V. 57, p. 2672-2678.

MALLOY, R.J., 1968. Depositional "Anticlines" versus "Reverse Drag": TRANS. GULF COAST ASSOC. GEOL. SOCS., V. 18, p. 114-123.

MATTHEWS, R.K., 1985. Oxygen Isotope Record of Ice-Volume History. 100 million years of Glacio-eustatic sea-level fluctuation. In AAPG MEM. 36, Ed. J. Schlee.

MATTHEWS, R.K. and POORE, R.Z., 1980. Tertiary oxygen 18 record and flacio-eustatic sea-level fluctuations: GEOLOGY, V. 8, p. 501-504.

———, 1974. Dynamic Stratigraphy: PRENTICE-HALL INC., 370 p.

MAY, J.A. *ET AL.*, 1983. Role of submarine canyons on shelf break erosion and sedimentation; modern and ancient examples in SEPM SP. PUBL. No. 33, p. 315-332.

McCULLOH, R.P. & EVERSULL, L.G., 1986. Shale-filled Channel System in the Wilcox Group (Paleocene-Eocene) N.E. South Louisiana. TRANS. GULF COAST ASSOC. GEOL. SOCS., V. 36, p. 213-218.

McGEE, N., 1979. Offshore Nigeria, Report on seismic stratigraphy study. PROPRIETARY REPORT. 17 p.

MECKEL, L.D., Jr. & NATH, A.K., 1977. Geological considerations for stratigraphic modelling and interpretation. In MEMOIR 26, AAPG, p. 417-438.

MERKI, P., 1972: Structural geology of the Cenozoic Niger Delta. In AFRICAN GEOLOGY (T.F.J. DESSAUVAGIE and A.J. WHITEMAN Eds.), IBADAN UNIVERSITY PRESS. p.635-646.

MIALL, A.D. ED, 1980. Facts and Principles of World Petroleum Occurrence. CANADIAN SOCIETY OF PETROL. GEOL. MEM. 6, 1003 p.

MIALL, A.D., 1984: Principles of sedimentary basin analysis. NEW YORK. SPRINGLER-VERLAG 490p.

MIALL, A.D., 1986. Eustatic sea level changes interpreted from seismic stratigraphy: a critique of the methodology with particular reference to the North sea Jurassic record. A.A.P.G. Bull., v.70, p.131-137.

MIDDLETON, G.V. and HAMPTON, M.A., 1976. Subaqueous sediment transport and deposition by sediment gravity flows, IN STANLEY, D.J. and SWIFT, D.J.P., Eds., Marine Sediment Transport and Environmental Management: New York, Wiley, p. 197-218.

MILLER, K.G. & FAIRBANKS, R.G., 1985. Cenozoic 18 record of climate and sea level: SOUTH AFRICAN JOURN. SCI., V.81, p. 248-249.

MILLER, K.G. *ET AL.*, 1985. Oligocene glacio-eustacy and erosion on the margins of the North Atlantic. GEOLOGY, V. 13, p. 10-13.

MITCHUM, R.M. Jr., 1977. Seismic Stratigraphy and global changes of sea-level, Part II: Glossary of terms used in seismic stratigraphy. In AAPG Mem. 26. C.E. Payton. Ed. p. 205-212.

MITCHUM, R.M. Jr., 1978. Seismic Stratigraphic investigation of West Florida Slope, Gulf of Mexico. In AAPG STUDIES IN GEOLOGY NO. 7 p.

MITCHUM, R.M. Jr., 1985. Seismic Stratigraphic expression of Submarine fans in AAPG MEM. 39, Eds. O.R. Berg & D.G. Woolverton, p. 117-136.

——— & Vail, P.R., 1977. Seismic Stratigraphy and global changes of sea-level, Part 7; Seismic Stratigraphic interpretation procedure. In AAPG MEM, 26, p. 135-145.

MITCHUM, R.M. Jr., VAIL, P.R. & THOMPSON, S. III, 1977a. Seismic Stratigraphy and global changes of sea-level - Part 2: the depositional sequence as a basic unit for stratigraphic analysis. AAPG MEM. 26, p. 53-62.

MITCHUM, R.M. Jr., VAIL, P.R. & SANGREE, J.B., 1977b. Seismic stratigraphy and global changes of sea-level Part 6: Stratigraphic interpretation of seismic reflection patterns in depositional sequences: AAPG MEM. 26, p. 117-134.

MOIOLA, R.J. & SHANMUGAM, G., 1980: Submarine fan sedimentation, Ouachita Mts, Arkansas and Oklahoma.

MOORE G.T. & FULLMAN, T.J. 1975: Submarine channel systems and their potential for petroleum localization. In DELTAS, MODELS FOR EXPLORATION. HOUSTON GEOL. SOC. p. 165 - 189.

MOORE, G.T. *ET AL.*, 1978. Mississippi fan, Gulf of Mexico - Physiography, stratigraphy and sedimentation patterns. In AAPG STUDIES IN GEOLOGY NO. 7, p. 155-191.

MOORE *ET AL.*, 1987: in press.

MORNER, N.A., 1976. Eustacy and geoid changes: JOURNAL OF GEOL., V. 84, p. 123-151.

MORNER, N.A. Ed., 1980. Earth rheology, isostasy and eustacy: Chichester, John Wiley & Sons, 599 p.

MOUGENOT, D. *ET AL.*, 1983. Prograding shelf break types on passive continental margins. IN SEPM SPECIAL PUBL., NO. 33, p. 61-77.

MUTTI, E., 1974. Examples of ancient deep-sea fan deposits from circim - Mediterranean geosynclines R.H. Dott, Jr. and R.H. Shower, Eds., SEPM SP. PUBL., NO. 19, p. 92-105.

MUTTI, E. & RUCCI-LUCCHI, F., 1972. Turbidites of the Northern Appennines: Introduction to Facies Analysis: INTERNATIONAL GEOL. REVIEW, V. 20, p. 125-166.

MUTTI, E. & RUCCI-LUCCHI, F., 1975. Turbidite facies and facies Associations from selected formations of the northern Apennines. Field Trip Guide Book A-11. INTERNATIONAL SEDIMENTOLOGICAL CONGRESS IX. Nice, p. 31-36.

NARDIN, T.R., 1983. Late Quaternary depositional systems and sea-level change - Santa Monica and San Pedro Basins, California continental borderland: AAPG BULL., V. 67, P. 1104-1124.

NARDIN, T.R. *ET AL.*, 1979. A review of mass movement processes, sediment and acoustic characteristics and contrasts in slope and base of slope systems versus canyon-fan basin floor systems. IN SEPM SP. PUBL. NO. 27, p. 61-73.

NARDIN, T.R. *ET AL.*, 1979. Santa Cruz Basin, California Borderland: Dominance of Slope Prrocesses in Basin Sedimentation. IN SEPM SP. PUBL. NO. 27 p.

NEIDELL, N.S. & POGGIAGLIOLMI, E., 1977: Stratigraphic modelling and interpretation. A.A.P.G. MEM. 26, p.389-416.

NELSON, H. & KULM, L.D., 1973. submarine fans and channels. In Middleton & Bouma, Eds., Turbidites and Deep Sea Sedimentation. SEPM SHORT COURSE NOTES. p. 39-78.

NELSON, H. & NILSON, T.H., 1974. Depositional trends of modern and ancient deep-sea fans. In SEPM SP. PUBL., NO. 19, p. 69-91.

NORMARK, W.R., 1970. Growth patterns of deep-sea fans. AAPG BULL., V. 54, p. 2170-2195.

———, 1974. Submarine canyons and fan valleys; factors affecting growth patterns of deep-sea fans In SEPM SP. PUBL., NO. 19, p. 56-68.

NORMARK, W.R., 1978. Fan Valleys, channels and depositional lobes on modern submarine fans, characters for recognition of sandy turbidite environments. AAPG BULL., V. 62, p. 912-931.

OKON, T.E., 1983. Regional seismic stratigraphic analysis Offshore Nigeria. PROPRIETARY REPORT.

ORIFE, J.M. & AVBOVBO, A.A., 1982. Stratigraphic and Unconformity Traps in the Niger Delta. IN AAPG MEM. 32, p. 251-265.

PARKINSON, N. & SUMMERHAYES, C., 1985. Synchronous global sequence boundaries. AAPG BULL., V. 69, p. 685-687.

PAYTON, C.E., 1977. Seismic stratigraphy: Applications to Hydrocarbon Exploration. AAPG MEM. 26

PEIKERT, E.W., 1985. Stratigraphic Velocity Interpretation: Alaska. National Petroleum Reserve. In AAPG MEM. 39, p. 209-224.

PETTERS, S.W., 1984. An Ancient Submarine Canyon in the Oligocene - Miocene of the Western Niger Delta: SEDIMENTOLOGY, V. 31, p. 805-810.

PIPER, D.J.W. & NORMARK, W.R., 1983. Turbidite Depositional Patterns and Flow characteristics, Navy Fan California Borderland: SEDIMENTOLOGY, V. 30, p. 681-694.

PIPER, D.J.W. *ET AL.*, 1976. The Rio Dell Formation: A Pli-Pleistocene Basin Slope Deposit in N. California: SEDIMENTOLOGY, V. 23, p. 309-328.

PIRSON, S.J., 1977: Geological well log analysis. GULF PUBLISHING, HOUSTON.

PITMAN, W.C. III, 1978. Relationship Between Eustasy and Stratigraphic Sequences of Passive Margins: GEOL. SOC. AMER. BULL., V. 89, p. 1389-1403.

———, 1979. The Effect of Eustatic Sea Level Changes On Stratigraphic Sequences at Atlantic Margins. AAPG MEM. 29, p. 453-460.

——— & GOLOUCHENKO, X., 1983. The Effect of sea level change on the shelf edge and slope of Passive Margins. IN SEPM SP. PUBL., No. 33, p. 41-58.

POAG, C.W. & SCHLEE, J.S., 1984. Depositional sequences and stratigraphic gaps on submerged U.S. Atlantic Margin. In AAPG MEM. 36, p. 165-182.

PRELL, W.L., 1982. Oxygen and Carbon Isotope Stratigraphy for the Quaternary of HOLE 502B: Evidence for two Modes of Isotopic Variability, In W.L. PRELL ET AL.,INITIAL REPORTS OF THE DEEP SEA DRILLING PROJECT, 68: WASHINGTON D.C., U.S. GOVT. PRINTING OFFICE p. 455-464.

READING, H.G. (ED.), 1985. Sedimentary Environments and Facies. 2nd Edition. NEW YORK, ELSEVIER.

RICKER, N., 1953: Wavelet contraction, wavelet expansion and the control of seismic resolution. GEOPHYSICS, V. 18, p.769-792.

ROBERTS, H.H. *ET AL.*, 1986. Distal Shelf and Upper Slope Sediments Deposited During Rise Sea Level, North Central Gulf of Mexico. TRANS. GULF COAST ASSOC. GEOL. SOCS., V. 36, p. 541-551.

RODINE, P.A. & JOHNSON, A.M., 1976. The Ability of Debris Heavily freighten with coarse clastic material flow on gentle slopes: SEDIMENTOLOGY, V. 23, p. 213-234.

SALES, J.K., 1985. Tectonic Controls on Sedimentation: PROPRIETARY REPORT.

SANGREE, J.B. & WIDMIER, J.M., 1977. Seismic Interpretation of clastic facies. In AAPG MEM. 26, P. 165-184.

——— & ———, 1979. Interpretation of depositional facies from seismic data. GEOPHYSICS, V. 44, No. 2, p. 131-160.

SANGREE *ET AL.*, 1978. Recognition of Continental-slope seismic facies, offshore Texas - Louisiana. IN AAPG STUDIES IN GEOLOGY, No. 7, p. 87-116.

SCHLEE, J.S., 1980. Seismic stratigraphy of the Baltimore Canyon trough. AAPG BULL., V. 65, p. 26-53.

SCHLEE, J.S. & FRITSCH, 1982. Seismic stratigraphy of the Georges Bank complex, offshore New England: AAPG MEM. 34, p. 223-251.

SCHLEE, J.S. *ET AL.*, 1979. Structure of the Continental Slope of the Eastern United States. In GEOLOGY OF CONTINENTAL SLOPES. SEPM SP. PUBL., NO. 27, p. 95-118.

SCHOENBERGER, M., 1974. Resolution comparison of minimum phase and zero phase signals: GEOPHYSICS, V. 39, p.826-833.

SCHWAN, W., 1980: Geodynamic peaks in Alpinotype orogenies and changes in ocean-floor spreading during Late Jurassic to Late Tertiary time. A.A.P.G. BULL. 64:359-373.

SCHRANM, M.W., Jr. *ET AL.*, 1977. Practical Stratigraphic Modelling and Interpretation. In AAPG MEM. 26, p. 477-502.

SEIGLIE, G.A. & BAKER, M.B., 1984. Relative sea-level changes during the Middle and Late Cretaceous from Zaire to Cameroun (Central W. Africa). In AAPG MEM. 36, p. 81-88.

SEIBOLD, E. and HINZ, K., 1974. Continental slope construction and destruction, West Africa, In BURK, C.A. & DRAKE, C.L. Eds., Geology of the Continental margins: Berlin, Springer-Verlag p.179- 198.

SHACKLETON, N.J. and OPDYKE, N.D., 1976. Oyxgen isotope and paleomagnetic stratigraphy of Pacific core V.28- 239, Late Pliocene to Latest Pleistocene. In Cline and Hars (Eds.) Investigations of Late Quaternary Paleoceanography and paleoclimatology. GEOL. SOC. AMER. MEM. 145, p. 147-163.

——— *ET AL.*, 1984. Oxygen-isotope calibration of the onset of ice-rafting and history of glaciation in the North Atlantic region: NATURE, V. 307, p. 620-623.

SHANMUGAM, G. & MOIOLA, R.J., 1982. Eustatic Control of turbidites and winnowed turbidites: GEOLOGY, V. 10 p. 231-235.

—— & ——, 1982. Prediction of deep-sea reservoir facies in TRANS. GULF COAST ASSOC. GEOL. SOCS., V. 32, p. 275-281.

—— & ——, 1985. Submarine Fan Models: Problems and Solutions. In Submarine Fans and Related Turbidite Systems (Frontiers in Sedimentary Geol.) Eds. Bouma et al. SPRINGER VERLAG., p. 29- 33

SHANMUGAM, G., MOIOLA, R.J., & DAMUTH, J.E., 1985. Eustatic control of submarine fan development. In SUBMARINE FANS AND RELATED TURBIDITE SYSTEMS. Eds. Bouma et al., Springer Verlag, p. 23-28.

SHEPHARD, F.P., 1981. Submarine canyons: Multiple causes and long time persistence: AAPG BULL., V. 65, p.1062- 1077.

SHERIFF, R.E., 1976. Inferring Stratigraphy from seismic data. AAPG BULL., V. 60, p. 528-542.

———, 1977. Limitations on resolution of seismic reflections and geologic detail derivable from them. AAPG MEM. 26, p.3-14.

——— , 1985. Aspects of Seismic Resolution in AAPG MEM. 39, p. 1-12.

SHORT, K.C. & STAUBLE, A.J., 1967. Outline of the Geology of Niger Delta: AAPG BULL., V. 51, p. 761-779.

SIDNER, B.R. *ET AL.*, 1978. Late Pleistocene Geologic History of Texas Outer Continental Shelf and Upper Con tinental Slope. In AAPG STUDIES IN GEOL., NO. 7, p. 243-266.

SLATT, R.M., 1986. Exploration Models for Submarine Slope Sandstones. TRANS. GULF COAST ASSOC. GEOL. SOCS., V. 36, p. 295-304

SLOSS, L.L., 1984. Comparative Anatomy of Cratonic Unconformities in AAPG MEM. 36, p. 1-6.

SLOSS, L.L. & SPEED, R.C., 1974. Relationships of Cratonic and Continental Margin tectonics Episodes in SEPM SP. PUBL., No. 22, p. 98-119.

STANLEY, D.J. & KELLING, G. (EDS.) 1978. Sedimentation in Submarine Canyons, fans and Trenches: DOWDEN, HUTCHINSON & ROSS INC.

STANLEY, & UNRUG, R., 1972. Submarine Channel Deposits, Fluxoturbidites and other Indicators of Slope and Base of Slope Environments. IN SEPM SP. PUBL. NO. 16, p. 287-340.

STECKLER, M.S. & WATTS, A.B., 1981. Subsidence History and Tectonic Evolution of Atlantic-type margins. IN DYNAMICS OF PASSIVE MARGINS GEODYNAMIC SERIES, V.6 AMERICAN GEOPHY. UNION, p. 184-196.

STOW, D.A.V., 1985. Deep-sea Clastic Review - Where are we and where are we going. GEOL. SOC. LOND. SP. PUBL.

—— *ET AL.*, 1985. Sedimentation, Tectonic and Sea- level controls. In SUBMARINE FANS AND RELATED TURBIDITE SYSTEMS. ED. Bouma et al. Springer verlag.

STUART, C.J. and CAUGHEY, C.A., 1977. Seismic facies and sedimentology of Terrigenous Pleistocene deposits in N.W. & Central Gulf of Mexico. In AAPG MEM. 26, p . 2345-2375

SURLYK, F., 1987: Slope and Deep Shelf Gully sandstones, Upper Jurassic, East Greenland. AAPG BULL. 71(4), p. 464-475.

SUTER, J.R. & BERRYHILL, H.L., Jr., 1985. Late Quaternary Shelf margin deltas, NW Gulf of Mexico. AAPG BULL., V. 69, p. 77-91.

———, —— & PENLAND, S., 1985. Environ ments of Sand Deposition, S.W. Louisiana Continental Shelf.TRANS. GULF COAST ASSOC. GEOL. SOCS., V. 35, p. 495-504

TANER, M.T. & SHERIFF, R.E., 1977. Application of amplitude frequency and other attributes to stratigraphic and hydrocarbon determination. IN AAPG MEM. 26, p. 301-328.

TEGLAND, E.R., 1970. Sand-shale ratio determination from seismic interval velocity: 23rd Annual Midwestern Region. Mtg. SEG and AAPG, Dallas March 8.

TUCHOLKE, B.E. & EMBLEY, R.W., 1984. Cenozoic Regional erosion of the abyssal sea floor off South Africa. IN AAPG MEM. 36, p. 145-164.

VAIL, P.R. & HARDENBOL, J., 1979. Sea level changes during the Tertiary, OCEANUS, V. 22, P. 71-79.

—— & TODD, R.G., 1981. Northern North Sea Jurassic unconformities, chronostratigraphy, and sea level changes from seismic stratigraphic, in L.V. Illing and G.D. Hudson, Eds., PETROLEUM GEOLOGY OF THE CONTINENTAL SHELF OF NORTHWEST EUROPE: London, Institute of Petroleum, p. 216-235.

——, HARDENBOL, J. & TODD, R.G., 1981. Jurassic unconformities, chronostratigraphy, and sea-level changes from seismic and biostratigraphy: Beiijing, china, Proceedings of the Joint Meeting of the China Geophysical Society and the Society of Exploration Geophysicists.

VAIL, P.R. HARDENBOL, J. & TODD, R.G., 1982. Jurassic unconformities and global sea-level changes from seismic and biostratigraphy: HOUSTON GEOLOGICAL SOCIETY BULL., p. 3-4 (Abs.).

——,——, & ——, 1984. Jurassic unconformities, chronostratigraphy, and sea-level changes from seismic stratigraphy and biostratigraphy,in J.S. Schlee Ed., Interregional unconformities and hydrocarbon accumulation: AAPG MEMOIR 36, p. 129-144.

———, *ET AL.*, 1977. Seismic stratigraphy and global changes of sea level, in C.E. Payton ed., Seismic stratigraphy - applications to hydrocarbon exploration: AAPG MEMOIR 26, p. 49-212.

WALCOTT, R.I., 1972: Gravity, flexure and the growth of sedimentary basins at a continental edge. GEOL. SOC. AMER. BULL. 83, p.1845-1848.

WALKER, R.G., 1978. Deep-water sandstone facies and ancient submarine fans - models for exploration for stratigraphic traps: AAPG BULL., V. 62, p. 932-966.

——, 1980. Exploration of turbidites and other deep water sandstones. AAPG Fall Education Conference, Houston, Texas, p. 1-72.

———, 1980. Modern and ancient submarine fans. AAPG BULL., V. 64, p. 1101-1108.

WATKINS, D.J. and KRAFT, L.M., Jr., 1978. Stability of continental shelf and slope off Louisiana and Texas: Geotechnical aspects. In AAPG STUDIES IN GEOLOGY NO. 7, p. 267-286.

WATTS, A.B., 1982. Tectonic Subsidence, Flexure and global changes of sea level. NATURE, V. 297, p. 469-474.

——— & STECKLER, M.S., 1981. Subsidence and tectonics of Atlantic-type continental margins. In Proceedings of the 26th International Geological Congress: OCEANOLOGICA ACTA, p. 143-153.

——— *ET AL.*, 1982. Lithospheric flexure and the evolution of sedimentary basins. PHILOSOPHICAL TRANSACTIONS OF THE ROYAL SOCIETY OF LONDON, SERIES A, V. 305, p. 249-281.

——— & THORNE, J. 1984: Tectonics, global changes in sea level and their relationship to stratigraphic sequences at the U.S. Atlantic margin: Marine and Petrol. Geol. Vol. 1, no 4. p. 319 - 339.

WEBB, G.W., 1981. Stevens and earlier Miocene turbidite sandstones, S. San Joaquim Valley, California. AAPG BULL., V. 65, p. 438-465.

WEBER, K.J., 1971: Sedimentological aspects of oilfields in the Niger Delta. GEOL. EN MINBOUW. 50(3), 559-576.

——— & E. DAUKORU, 1975: Petroleum geology of the Niger Delta. NINTH WORLD PETROLEUM CONGRESS 2, 209-221.

WESSER, O.E., 1978. Oil Trapping Characteristics of Turbidites. In AAPG STUDIES IN GEOLOGY, No.7, p. 227-242.

WHITAKER, J.H. mcD, 1974. Ancient Submarine Canyons and fan valleys.In MODERN AND ANCIENT GEOSYNCLINAL SEDIMENTATION EDS. DOTT & SHAVER. SEPM SP. PUBL. NO. 19, p. 106-125.

WHITEMAN, A., 1982: Nigeria: Its Petroleum Geology, Resources, and Potential: GRAHAM AND TROTMAN, LONDON, VOLS. 1 & 2, 394 p.

WIDESS, 1973: How thin is a thin bed?. GEOPHYSICS, V. 38, p.1176-1180.

——, 1980: Generalized resolving power and system optimization. 50th Annual Int. SEG Meeting, November 19, Houston.

WILLIAMS, D.F. & TRAINOR, D., 1986 Application of Isotope Chronostratigraphy in the N. Gulf of Mexico. In TRANS. GULF COAST ASSOC. GEOL. SOCS., V. 36, p. 589-600.

WINKER, C.D., 1982. Cenozoic Shelf margins, N.W. Gulf of Mexico. TRAN. GULF COAST ASSOC. GEOL. SOCS., V. 32, p. 427-448.

——— & EDWARDS, M.B., 1983. Unstable progradational clastic shelf margins. In SEPM SP. PUBL., No.33, p. 139-157.

WOODBURY, H.O. *ET AL.*, 1973. Pliocene and Pleistocene Depocentres. Outer Continental Shelf, Louisiana and Texas: AAPG BULL., V. 59, p. 2438-2439.

———, *ET AL.*, 1978. Gulf of Mexico Continental Slope Sediments and Sedimentation. In AAPG STUDIES IN GEOL., No. 7, p. 117-138.

APPENDICES

APPENDIX 1.

A.1 THE SYNTHETIC SEISMOGRAM

Peterson, et al, 1955, first proposed a linear filter model of the reflection process whose output they called the synthetic seimogram.

b(t) REFLECTIVITY FUNCTION s(t)

The earth is treated as a filter whose impulse response function is a set of reflection coefficients properly spaced in time. b(t) is the input shot pulse and the out is the synthetic seismogram s(t) which is the convolution of the reflectivity with the shot pulse.

$$s_{(t)} = \sum_k R_{(t-T_k)} \times b$$

For a continuous velocity log, the summation in the limit of the layer approaching zero becomes the convolution integral

$$s_{(t)} = R_{(T)} * b_{(t-T)} dT$$

Peterson also proposed a logarithmic approximation to the reflection coefficient for small density variations using the reflection coefficient formula at an interface:

$$\begin{aligned} R_s &= \frac{V_d - V_s}{V_d + V_s} \\ &= \frac{\Delta v}{2V_s + \Delta v} \\ &\approx \frac{1}{2}\frac{\Delta v}{V_s} \\ &\approx \frac{\Delta \, log \, V_s}{2} \end{aligned}$$

This approximation is valid for reflection coefficients of less than 0.3. When density variations are considered,

$$R_s \doteq \frac{\Delta log \, \rho V_s}{2}$$

If density is related to the velocity by a general expression of the form

$$\rho = kv^m$$

where k and m are constants

$$\rho v = kv^{m+1}$$

Then the reflection coefficient may be given by

$$R = \frac{(m+1)}{2} \Delta log\, V$$

The reflection coefficient being proportional to the change in the logarithm of velocity. The logarithm of velocity as a function of time is sometimes called the velocity function, $log\, v_{(t)}$. The derivative of the velocity function is the expression of the reflectivity function, $r_{(t)}$.

Thus

$$r_{(t)} = \frac{1}{2}\frac{d}{dt} log\, v_{(t)}.$$

This is essentially a one-dimensional treatment of wave theory.

APPENDIX 2.

Two types of sea level changes are possible;

1. EUSTATIC SEA LEVEL CHANGES- World-wide sea level variation that affect the oceans. In Tertiary, this is often attributable to climatic changes that result in ice caps.

2. EPEIROGENIC SEA LEVEL CHANGES- Changes in sea level caused by vertical tectonic movements of the crust,due mostly to isostatic adjustments (mainly uplift) in response to the relief of ice-caps or thermal expansion and contraction.

A relative change of sea level is the NET change due to a combination of eustatic and tectonic controls. Evidence from seismic sequence analysis suggest eustatic control as the primary cause of sequence differentiation on the margin.

Donovan and Jones (1979) summarizes the causes of world-wide sea level changes thus:

CAUSES	AMOUNT	RATE
Changes in the volume of land ice.	150m	1cm/yr
Changes in the volume of ocean ridges.	300m	1cm/1000yrs
Sediment accumulation.	?	1cm/1000yrs
Dessication of isolated ocean basins	15m	1cm/yr

APPENDIX 3

Eustatic sea level changes/ Synchronous global sequence boundaries

Deductions from the correlation of sequence boundaries around the world by Vail *et al.*(1977), Vail and Hardenbol(1979), Vail and Todd(1981) and Hardenbol *et al.*(1981) seem to suggest that sequences develop in response to relative changes in sea level and that changes are related to global fluctuations of eustatic sea level.

Criticisms of this global linkage among other things stem from the lack of polar ice at certain periods in the geologic record and the apparent lack of adequate mechanism for producing the so called third order sequences by high amplitude changes in sea level with a period of 1-10 M.yrs. (Parkinson and Summerhayes(1985)

Pitman(1978), discussing the possible causes of change of sea level, considers the effects of continuing differentiation of lithosphere, sediment build and the removal, crest shortening and thermal welts and changes in the volume of the mid-oceanic ridge systems. He concluded thus, that trangressive or regressive events recorded at numerous subsiding basins, may not be indicative of eustatic sea level rise or fall, but may be caused by changes in the *rate of sea level change.*

Pitman's theoretical curve has since been modified by Kerr(1984); Kominz(1984) although there is general agreement as to the consistent fall of sea level from the Cretaceous to the present(about 350 metres cumulative), with rates of fall depending on differing rates of new crust formation.

Pitman's model hypothesizes that rates of change of sea level except those due to glacial fluctuations and catastrophies, are always less than the rate of subsidence at the shelf edge of Atlantic-type margins. This differs from the Vail *et al.* model which implies eustatic rates being consistently greater than basin subsidence.

Pitman *et al.*(1983) summs up the debate about the effect of sea level change on the shelf break as follows:

1. That except during major glacial episodes sustained sea level change may not exceed 1cm/1000years. Thus, if a shelf edge lies well landward of the ocean-continent boundary, the subsidence rate may be less than 1cm/1000 years and the shoreline may regress beyond the shelf edge.(Note: subsidence is maximum at the ocean-continent boundary

and zero at the continental margin hinge zone). However if the shelf has prograded out to the ocean-continent boundary, the shoreline may not out over the shelf.

2. That the extent and volume of present day ice sheets suggest a maximum drop of 50 metres in sea level in an episode, and no indications of a larger glaciation exist during the Mesozoic and Cenozoic up to mid-Miocene.

3. For shoreline to migrate over the shelf edge, the rate of sea level fall should be greater than the rate of subsidence at the shelf edge and the magnitude of sea level fall must be sufficient to drop sea level down the shelf edge.

4. For shoreline to remain on the subsiding part of the platform, sea level must be falling and if at a constant rate, then this is *still stand* as against the notion of unchanging sea level.

5. If changes in sea level are synchronous worldwide, they cause non-synchronous transgressive and regressive events on various margins depending on local subsidence rates and basin geometry.

6. Based on Vail *et al.*(1977) and Pitman(1978) sea level lowering of 350 metres since Late Cretaceous, (an average of 0.5cm/1000 years) may be deduced. Thus the olders margins such as Eastern North America, and west Africa would have had coastlines close to the shelf edge and the Mio-Oligocene lowstand (drop of 3 metres) due to glaciation in the Antarctic may have been sufficient to displace the coastline to the shelf edge leading to sub-aerial exposure and erosion. (See main body of report)

Parkinson and Summerhayes(1985), however, propose a mechanism for producing synchronous relative sea level changes in widely separated and geologically independent basins without producing changes in all basins and without requiring short-period fluctuations in the global sea level curve. They argue that the same mechanism can produce non-synchronous but related shoreline shifts in separate basins while the rate of fall of sea level change remains constant. This mechanism is highlighted in fig.A.1 and entails the critical interplay of rate of fall of sea level(R), with rate of subsidence(S) in three hypothetical basins A, B, C. The regressive events T' and T" are a function of the tectonic histories of basins B and C and not sea level change. The only link between B and C are subsidence rates and they could be wide apart geographically.

They conclude that global events do not have to occur in the coastal onlap curves as Vail's own curves show variations and that each basin can be expected to have its own onlap curve with some events of global and others of local significance.

Although the notion of expressing the eustatic factor by a globally valid curve still remains tenuous, the new fine-tuned curve by Haq *et al.*(1987) has found many supporters. Discrepancies often noticed do not appear to constitute complete departure though, other workers noted wide disagreements with the previous curves. (See Morner(1981); Carter(1985); Miller, Mountain & Tucholke(1985); and Olson, Miller & Ungrady(1980); especially concerning the cenozoic.)

APPENDIX 4

Raw data as obtained on every well.

Depth intervals (FT-SS)	Data points (FT-SS)	Sand %	Average interval velocity (FT/SEC)
1. DD-S-1 1 (BQI = -3589'SS)			
3589 – 4089	3839	90.00	8169
4089 – 4589	4339	49.40	8130
4581 – 5089	4839	68.00	8711
5089 – 5589	5339	63.40	8879
5589 – 6089	5839	61.00	9259
6089 – 6589	6339	62.00	9615
6589 – 7089	6839	55.20	9756
7089 – 7589	7339	43.60	10246
7589 – 7999	7794	30.60	9832
Average		54.64	9254
2. EE-1 (BQI = -3609'SS)			
3609 – 4129	3869	96.00	8012
4129 – 4629	4379	77.00	8183
4629 – 5129	4879	79.80	8418
5129 – 5629	5379	53.00	8681
5629 – 6129	5879	62.60	9259
6129 – 6629	6379	6.00	9025
6629 – 7129	6879	27.40	9157
7129 – 7629	7379	36.80	9804
7629 – 8129	7879	70.60	10352
8129 – 8629	8379	58.40	10869
8629 – 9129	8879	40.80	11494
Average		55.31	9389
3. KK-12 (BQI = -5298'SS)			
5298 – 5675	5487	33.15	8568

Depth intervals (FT-SS)	Data points (FT-SS)	Sand %	Average interval velocity (FT/SEC)
4. EE-3A (BQI = -3689'SS)			
3694 – 4159	3927	78.00	7869
4159 – 4631	4395	75.40	8091
4631 – 5100	4866	54.40	8224
5100 – 5573	5336	48.50	8591
5573 – 6053	5836	48.40	8913
6053 – 6543	6336	5.00	8977
6543 – 7038	6836	30.40	8960
7038 – 7537	7336	53.80	9804
7537 – 8036	7836	64.80	10482
8036 – 8406	8336	54.86	10663
Average		51.79	9057
5. EE-15 (BQI = -4807'SS)			
4807 – 5321	5064	79.96	8727
5321 – 5821	5571	72.60	9009
5821 – 6321	6071	66.60	9174
6321 – 6821	6571	27.20	9276
6821 – 7321	7071	60.00	9766
7321 – 7821	7571	31.80	9615
Average		57.80	9261
6. LL-1 (BQI = -6049'SS)			
6049 – 6549	6299	66.60	9615
6549 – 7049	6799	52.00	8651
7049 – 7549	7299	29.60	9690
7549 – 8049	7799	00.00	9470
8049 – 8449	8299	11.75	9009
Average		31.52	9288

Depth intervals (FT-SS)	Data points (FT-SS)	Sand %	Average interval velocity (FT/SEC)
7. LL-2 (BQI = -5251'SS)			
5251 – 5721	5486	82.98	8393
5721 – 6221	5971	68.40	9398
6221 – 6721	6471	74.40	10081
6721 – 7121	6971	33.25	10101
Average		67.26	9493
8. EE-W-1 (BQI = -3568'SS)			
3568 – 4073	3818	84.55	7757
4073 – 4573	4323	85.20	8039
4573 – 5073	4823	59.20	7987
5073 – 5573	5323	45.00	7949
5573 – 6073	5823	49.80	8803
6073 – 6573	6323	21.40	8818
6573 – 7073	6823	23.78	9107
7073 – 7573	7323	43.00	9434
7573 – 8073	7823	60.20	9709
8073 – 8573	8323	48.80	10204
8573 – 9073	8873	63.80	10941
9073 – 9573	9373	9.00	10683
Average		49.48	9119
9. OO-1 (BQI = -5066'SS)			
5066 – 5517	5292	49.61	8665
5517 – 6017	5767	35.60	9434
6017 – 6517	6267	2.00	5772
6517 – 7017	6767	57.40	10101
7017 – 7359	7267	42.57	9402
Average		37.44	9275
10. UU-19D (BQI = -5296'SS)			
5296 – 5721	5509	63.53	9259

Depth intervals (FT-SS)	Data points (FT-SS)	Sand %	Average interval velocity (FT/SEC)
11. OO-2 (BQI = -4416'SS)			
4416 – 4923	4670	28.79	6898
4923 – 5423	5173	18.60	8224
5423 – 5923	5673	14.00	7463
5923 – 6423	6173	2.60	6906
Average		15.99	7389
12. NN-3A (BQI = -5571'SS)			
5580 – 6071	5826	47.40	9093
6071 – 6571	6321	36.60	9728
6571 – 7071	6821	33.00	9823
7017 – 7571	7321	52.60	10225
7571 – 8071	7821	31.60	10460
8071 – 8571	8321	29.12	10309
Average		33.38	9768
13. NN-4B (BQI = -5895'SS)			
5895 – 6395	6145	41.00	9293
6395 – 6751	6573	27.81	8812
Average		33.11	9053
14. CC-7B (BQI = -4951'SS)			
4951 – 5421	5186	65.85	9362
5421 – 5921	5671	62.20	9416
5921 – 6421	6171	55.80	9708
6421 – 6921	6671	58.40	10163
6921 – 7421	7171	53.00	10309
7421 – 8421	8171	43.38	7692
Average		50.10	9593

Depth intervals (FT-SS)	Data points (FT-SS)	Sand %	Average interval velocity (FT/SEC)
15.	AA-S-1	(BQI = -3172'SS)	
3172 – 3671	3422	51.10	6997
3671 – 4171	3921	60.20	7634
4171 – 4671	4421	60.80	7645
4671 – 5171	4921	60.00	7645
5171 – 6171	5921	16.80	8333
6171 – 6671	6421	49.60	9159
6671 – 7171	6921	20.00	9124
7171 – 7671	7421	27.60	9294
7671 – 8171	7921	32.80	10000
8171 – 8671	8421	26.00	9881
Average		32.82	8600
16.	CC-N-7B	(BQI = -2846'SS)	
2846 – 3323	3085	89.09	7067
3323 – 3823	3573	88.20	7564
3823 – 4323	4073	85.00	8065
4323 – 4823	4573	71.60	8306
4823 – 5323	5073	64.60	8460
5323 – 5823	5573	55.80	8772
5823 – 6323	6073	55.40	8961
6323 – 6823	6573	10.00	9823
6823 – 7323	7073	43.00	9507
7323 – 7823	7573	61.80	10162
7823 – 8323	8073	22.80	10000
8323 – 8823	8573	41.00	10267
8823 – 9318	9071	7.27	10526
Average		53.50	9037

Depth intervals (FT-SS)	Data points (FT-SS)	Sand %	Average interval velocity (FT/SEC)
17. FF-1 (BQI = -4538'SS)			
4538 – 5034	4786	84.28	8039
5034 – 5534	5284	82.40	8389
5534 – 6034	5784	60.00	8726
6034 – 6534	6284	25.40	8862
6534 – 6984	6759	12.22	9346
Average		55.34	8672
18. FF-4 (BQI = -3654'SS)			
3654 – 4134	3894	89.17	7779
4134 – 4634	4384	74.40	8052
4634 – 5134	4884	72.60	8143
5134 – 5634	5384	76.20	8446
5634 – 6134	5884	72.60	8711
6134 – 6634	6384	27.60	8834
6634 – 7134	6884	60.00	9597
7134 – 7634	7384	20.20	9560
7634 – 8134	7884	45.00	10142
8134 – 8484	8309	15.15	10174
Average		54.99	8943
19. PP-1 (BQI = -5039'SS)			
5039 – 5529	5284	78.04	9074
5529 – 6029	5779	62.00	9615
6029 – 6529	6279	41.00	9921
6529 – 7029	6779	35.00	9785
Average		51.00	9599
20. KK-16 (BQI = -5723'SS)			
5721 – 6221	5971	42.20	4294
6221 – 6631	6426	34.40	9263
Average		38.30	9279

Depth intervals (FT-SS)	Data points (FT-SS)	Sand %	Average interval velocity (FT/SEC)
21.	PP-2	(BQI = -3856'SS)	
3856 – 4357	4106	64.27	7877
4357 – 4857	4607	56.80	8446
4857 – 5357	5107	40.60	8532
5357 – 5857	5607	16.40	8711
5857 – 6357	6107	63.00	9804
6357 – 6980	6669	63.03	11369
Average		49.02	9123
22.	DD-N-1	(BQI = -3440'SS)	
3440 – 3947	3694	92.89	8311
3947 – 4447	4197	52.00	8026
4447 – 4947	4697	71.80	8561
4947 – 5447	5197	70.60	9259
5447 – 5947	5697	69.40	9259
5947 – 6447	6197	78.40	9823
6447 – 6947	6697	37.80	9728
6947 – 7447	7697	7.40	9921
Average		56.29	9188
23.	VV-2	(BQI = -5599'SS)	
5599 – 6099	5849	13.40	8389
24.	JJ-N-3	(BQI = -4685'SS)	
4685 – 5138	4912	28.16	8263
5138 – 5600	5399	44.60	8210
5600 – 6063	5832	42.60	8711
6063 – 6532	6298	5.00	8771
6532 – 7009	6770	45.00	9208
7009 – 7485	7249	15.82	9227

Depth intervals (FT-SS)	Data points (FT-SS)	Sand %	Average interval velocity (FT/SEC)
25. JJ-N-4 (BQI = -4226'SS)			
4226 – 4723	4475	37.02	8569
4723 – 5223	4973	52.60	7599
5223 – 5723	5473	40.20	8432
5723 – 6223	5973	32.00	8726
6223 – 6723	6473	8.80	8834
6723 – 7223	6973	27.40	8475
Average		33.00	8439
26. JJ 4 (BQI = -5600'SS)			
5600 – 6084	5842	61.98	8374
6084 – 6584	6334	33.00	8850
6584 – 7084	6834	47.00	9766
7084 – 8084	7834	3.00	9766
8084 – 8584	8334	13.00	9677
8584 – 9084	8834	17.00	8489
Average		28.45	9275
27. ATA 4 (BQI = -2794'SS)			
2794 – 3300	3047	91.49	7319
3300 – 3800	3550	90.40	7886
3800 – 4300	4050	78.80	8013
4300 – 4800	4550	69.40	8319
4800 – 5300	5050	74.20	8562
5300 – 5800	5550	60.80	9025
5800 – 6300	6050	41.50	9488
6800 – 7300	7050	44.40	9842
7300 – 7800	7550	80.20	10373
7800 – 7954	7877	78.09	10857
Average		69.39	8990

Depth intervals (FT-SS)	Data points (FT-SS)	Sand %	Average interval velocity (FT/SEC)
28. ATA 1 (BQI = -2619'SS)			
2619 – 3149	2884	88.87	6235
3149 – 3649	3399	73.00	6983
3649 – 4149	3899	64.40	7764
4149 – 4649	4399	55.20	7716
4649 – 5149	4899	59.00	8183
5149 – 5649	5399	58.00	8475
5649 – 6149	5899	58.00	8993
6149 – 6649	6399	60.00	9434
6649 – 7149	6899	48.60	9542
7149 – 7649	7399	45.00	9843
7649 – 8149	7899	16.00	9541
8149 – 8649	8399	55.00	10417
8649 – 9149	8899	19.00	10593
9149 – 9749	9449	31.48	10714
Average		52.93	8888
29. SS-N-1 (BQI = -5771'SS)			
5771 – 6273	6022	18.13	8655
6273 – 6773	6523	6.00	9174
AKATA (BQI = -6773'SS)			
6773 – 7273	7023	0.00	7022
7273 – 7673	7473	0.00	6838
Average		12.07	7922
30. SS-6			
5561 – 5921	5741	24.44	8571
31. RR-1			
3855 – 4365	4110	50.00	8044
4365 – 4865	4615	15.00	8726
Average		69.39	8990

Depth intervals (FT-SS)	Data points (FT-SS)	Sand %	Average interval velocity (FT/SEC)
32. TT-N-2 (BQI = -6231'SS)			
6231 – 6721	6476	11.63	9007
6721 – 7221	6971	4.60	9671
7221 – 7721	7471	0.00	9071
7721 – 8221	7971	37.00	9690
Average		13.30	9365

Depth intervals (FT-SS)	Data points (FT-SS)	Sand %
33. LL-7 (BQI = -5264'SS)		
5264 – 5771	5518	66.27
5771 – 6271	6021	63.40
6271 – 6771	6521	59.60
6771 – 7171	7021	53.00
Average		60.57
34. 1 (BQI = -4790'SS)		
4790 – 5298	5044	62.99
5298 – 5798	5548	54.00
5798 – 5948	5873	23.33
Average		46.33
35. M-D 1 (BQI = -5891'SS)		
5891 – 6400	6146	65.22
6400 – 6900	6650	72.00
6900 – 7400	7150	31.80
7400 – 7900	7650	51.20
7900 – 8400	8150	31.00
8400 – 8900	8650	56.80
8900 – 9400	9150	47.80
9400 – 9900	9650	11.00
Average		45.85

Depth intervals (FT-SS)	Data points (FT-SS)	Sand %
36. CC 2^A (BQI = -4640'SS)		
4640 – 5140	4890	56.20
5140 – 5640	5390	40.80
5640 – 6140	5890	68.40
6140 – 6640	6390	51.60
6640 – 7140	6890	55.40
7140 – 7640	7390	52.00
7640 – 8140	7890	29.00
8140 – 8640	8390	37.60
8640 – 9140	8890	28.40
9140 – 9640	9390	48.60
Average		46.80
37. BB-N-1 (BQI = -4748'SS)		
4748 – 5248	4998	62.20
5248 – 5748	5498	60.60
5748 – 6248	5998	29.60
6248 – 6748	6498	22.40
6748 – 7248	6998	4.00
7248 – 7748	7498	57.60
Average		30.40
38. QQ-EE-1 (BQI = -5011'SS)		
5011 – 5434	5223	86
5434 – 5934	5684	32
5934 – 6434	6184	38
6434 – 6934	6684	27
Average		46

Depth intervals (FT-SS)	Data points (FT-SS)	Sand %
39. NB-1 (BQI = -5270'SS)		
5270 – 5749	5510	29
5749 – 6249	5999	50
6249 – 6749	6499	29
6749 – 7249	6999	51
7249 – 7749	7499	81
7749 – 8249	7999	76
Average		53
40. FF-EE-1 (BQI = -4538'SS)		
4538 – 5034	4786	84.27
5034 – 5534	5284	82.40
5534 – 6034	5784	72.40
6034 – 6534	6284	25.40
6534 – 6984	6759	12.22
Average		53.34

Data from zones with 100% sand.

S/No	Wells	Depth intervals (FT-SS)	Data points (FT-SS)	Ave. Int. Velocity (FT/SEC)
1	ATAKTAK 1	5243 – 5323	5283	8696
2	ATAKTAK 1	6833 – 6883	6858	9259
3	AA-S-1	3841 – 3981	3911	7777
4	PP-2	4067 – 4262	4165	8125
5	PP-2	6342 – 6397	6370	12222
6	PP-2	5841 – 5951	5896	9243
7	LL-1	6537 – 6649	6593	10182
8	JJ-N-4	5796 – 5892	5844	9143
9	JJ-N-4	5013 – 5223	5118	8140
10	JJ-N-4	6153 – 6223	6188	8861
11	JJ-N-3	5491 – 5546	5519	8088
12	KK-12	5531 – 5576	5554	8824
13	FF-4	3899 – 4004	3952	7955
14	FF-4	5394 – 5484	5439	8036
15	DD-N-1	3440 – 3832	3636	8218
16	DD-N-1	6257 – 6447	6352	9948
17	EE-W-1	3713 – 3838	3777	7764
18	EE-W-1	6809 – 6928	6869	9297
19	EE-W-1	8508 – 8743	8627	10587
20	EE-3[A]	7626 – 7761	7694	9712
21	EE-3[A]	8273 – 8463	8368	10382
22	EE-4[B]	6256 – 6321	6289	9286
23	CC-7[B]	8031 – 8111	8071	10811
24	M-D 1	6028 – 6103	6066	10135

Int. Vel. Distribution for 100% Sand
From 6250 — 6750'SS

S/No	Wells	Depth intervals (FT-SS)	Ave. Int. Velocity (FT/SEC)
1	FIOM 1	6598 – 6661	9259
2	LL-1	6569 – 6649	9804
3	NN 4B	6259 – 6321	9346
4	ATA 5	6744 – 6819	9804
5	ATA 1	6319 – 6393	10101
6	PP 2	6341 – 6397	12121
7	PP 2	6467 – 6552	12500
8	PP 2	6562 – 6617	12195
9	DD 1	6369 – 6423	9346
10	DD 1	6529 – 6589	9804
11	DD 1	6711 – 6749	10000
12	LL 2	6351 – 6401	9804
13	JJ 4	6634 – 6674	9524
14	NN 3^A	6371 – 6421	9708
15	NN 3^A	6591 – 6629	10000
16	NN 3^A	6718 – 6818	10000
17	CC 7^B	6275 – 6316	9804
18	CC 7^B	6551 – 6610	9804
19	CC 7^B	6673 – 6716	10000
20	M-D 1	6428 – 6302	10000
21	M-D 1	6428 – 6468	9804
22	M-D 1	6588 – 6628	9804
23	OO 1	6639 –6689	1111
24	DD-E 1	6317 – 6447	10000
25	DD-E 1	6517 – 6637	10101
26	FF 4	6394 – 6454	9804

Int. Vel. Distribution for 100% Shale
From 6250 — 6750'SS

S/No	Wells	Depth intervals (FT-SS)	Interval Velocity (FT/SEC)
1	FIOM 1	6321 – 6401	8929
2	FIOM 1	6521 – 6591	9524
3	FIOM 1	6711 – 6771	9259
4	LL 1	6349 – 6409	10524
5	LL 1	6649 – 6759	10000
6	NN 4B	6321 – 6371	8772
7	ATA 1	6253 – 6319	9259
8	ATA 1	6699 – 6729	8696
9	PP 2	6685 – 6737	9900
10	DD 1	6469 – 6529	9708
11	DD 1	6619 – 6669	9804
12	ATAKTAK 1	6463 – 6673	8696
13	JJ 4	6444 – 6502	9708
14	JJ 4	6219 – 6369	8403
15	JJ 3	6461 – 6561	8547
16	JJ 3	6641 – 6561	9091
17	EE 3^A	6271 – 6371	9091
18	EE 3^A	6441 – 6491	8547
19	NN 3^A	6448 – 6521	9615
20	NN 3^A	6629 – 6679	9804
21	M-D 1	6302 – 6383	9259
22	EE 1	6329 – 6529	9259
23	NSIMBO 1	6648 – 6748	8772
24	OO 1	6459 – 6529	9346
25	EE 15	6471 – 6521	9091
26	EE 15	6581 – 6651	9615

	Wells	Depth intervals	Interval Velocity
S/No		(FT-SS)	(FT/SEC)
27	FF 1	6350 – 6400	8696
28	FF 1	6550 – 6620	9091
29	DD-E	6447 – 6517	9259
30	DD-E	6697 – 6797	9615
31	EE-W 1	6323 – 6423	9091
32	JJ 4	6505 – 6563	8929
33	FF 4	6314 – 6394	8929
34	FF 4	6534 – 6634	9259

List of selected wells

S/No	Wells	Average sand %	Average Interval Velocity (FT/SEC)
1	DD 1	55	9254
2	EE 1	55	9389
3	EE 3^A	51	9059
4	EE 15	58	9261
5	LL 2	67	10124
6	EE W-1	49	9119
7	OO 1	37	9275
8	EE 4	16	7389
9	NN 3^A	38	9768
10	NN 3^B	33	9553
11	ATA 1	53	8888
12	ATA 5	69	8990
13	CC 7^B	50	9593
14	LL 1	32	9288
15	FIOM 1	33	8600
16	ATAKTAK 1	54	9037
17	FF 1	55	8672
18	FF 4	55	8943
19	PP 1	51	9599
20	PP 2	49	9123
21	DD-E	56	9188
22	KK 12	33	8568

	Wells	Average sand	Average Interval Velocity
S/No		%	(FT/SEC)
23	VV 2	13	8389
24	JJ 3	29	8732
25	JJ 4	33	8439
26	JJ 4	28	9275
27	UU 19D	64	9259
28	LL 7	61	–
29	M-D 1	46	–
30	CC 2[A]	47	–
31	UU 1	46	–
32	SS W1	12	7922
33	SS 6	24	8571
34	RR 1	33	8385
35	TT-N 2	13	9565
36	NSIMBO 1	57	–
37	QQ EAST 1	46	–
38	NB 1	53 –	
39	FF EE 1	53 –	

Data from zones with 100% shale.

S/No	Wells	Depth intervals (FT-SS)	Data points (FT-SS)	Ave. Int. Velocity (FT/SEC)
1	ATAKTAK 1	6463 – 6673	6568	8750
2	FIOM 1	3266 – 3466	3366	6601
3	FIOM 1	5401 – 5571	5486	8333
4	FIOM 1	5766 – 6091	5929	8105
5	PP 2	5082 – 5322	5202	8481
6	PP 2	5357 – 5607	5482	8722
7	LL 2	5951 – 6083	6017	9296
8	LL 1	6649 – 6759	6704	9909
9	JJ 4	7181 – 6723	6568	8732
10	JJ 4	6413 – 6723	6568	8732
11	JJ 4	5723 – 5913	5818	8597
12	JJ 3	4521 – 4881 (QI)	4701	7912
13	KK 12	5321 – 5456	5389	7988
14	KK 12	5675 – 5821 (AK)	5748	7487
15	FF 4	6199 – 6404	6302	8613
16	DD-E 1	2940 – 3440 (QI)	3190	6281
17	DD-E 1	4327 – 4547	4437	7432
18	DD-E 1	7572 – 7847	7710	9167
19	EE W-1	3265 – 3568 (QI)	3417	7030
20	EE W-1	6223 – 6723	6473	8726
21	EE W-1	8923 – 9423	9173	10730

Data from zones with 100% shale.

	Wells	Depth intervals	Data points	Ave. Int. Velocity
S/No		(FT-SS)	(FT-SS)	(FT/SEC)
22	EE 3^A	6446 – 6771	6609	8953
23	EE 3^A	7371 – 7556	7464	10109
24	NN 4^B	5321 – 5821 (QI)	5571	7936
25	NN 4^B	6321 – 6621	6471	8596
26	IDIO 7^B	8621 – 8770 (AK)	8696	7979
27	IDIO 7^B	8931 – 9421 (AK)	9176	7679
28	SS-N-1	6773 – 7273 (AK)	7023	7022
29	SS-N-1	7273 – 7673 (AK)	7473	6838

APPENDIX 5

A SELECTION OF RUBBLE BEDS INTERVAL VELOCITY DATA

LINE 82-208A

SHOT POINT	INT. VEL M/SEC
898	2365
958	2362
1018	2475
1088	2170
1138	2544
1198	2400
1258	2415

LINE 82-212A

SHOT POINTS	INT. VEL. M/SEC
926	2408
986	2438
1046	2420
1106	2300
1166	2630
1226	2567
1286	2450
1346	2240

LINE 82-216A

SHOT POINTS	INT. VEL. M/SEC
896	2325
956	2296
1016	2587
1076	2300
1136	2476
1196	2150
1256	2380
1376	2066
1436	2045

LINE 82-220A

SHOT POINT	INT. VEL. M/SEC
918	2280
978	2362
1038	2467
1098	2397
1158	2258
1218	2223
1278	2310
1338	2500
1398	2206
1458	2250

LINE 82-224A

SHOTPOINT	INT. VEL. M/SEC
1177	2275
1237	2295
1297	2487
1417	2205
1477	2216
1536	2400

LIST OF FIGURES

FIGURE	TITLE	PAGE
1.1	Seismic data base and coverage map	.....
1.2	Field recording and processing parameters	.....
1.3a	Typical roll-over structure	.....
1.3b	Stratigraphic play in slope channel fill	.....
1.3c	Truncation trap over paralic sequences	.....
1.4a	Terminology used in sequence boundary delineation	.....
1.4b	Schematic diagram of sequence types	.....
1.5	Typical GMA synthetic seismogram display	.....
1.6	Stratigraphic sequences and sea level changes	.....
1.7a	Reflection configurations and facies terminology	.....
1.7b	External geometry of some seismic facies	.....
1.7c	Parallel/divergent seismic types and modifications	.....
1.7d	Progradational facies types	.....
1.7e	Mounded and drape facies types	.....
1.7f	Onlap and fill seismic facies types	.....
1.8a	Velsect data analysis	.....
1.8b	V_{int} presentation using GEM	.....
1.8c	Flow diagram of velocity interpretation	.....
1.8d	Polynomial fit of a stacking velocity curve	.....
1.8e	Modified flow diagram	.....
1.9a	Flow chart for CPS1 mapping package	.....
1.9b&c	CPS1 display listings	.....
		.....
2.1	A depositional mound	.....
2.2a	Anomaly at the foot of the progradational toe	.....
2.2b	Anomaly due to slump on progradational slope	.....
2.2c	Anomaly with a predominant axis or trend	.....
2.2d	The chaotic and disruptive facies anomaly	.....
2.2e	Rubble Bed type anomaly	.....
2.2f	Anomaly with parallel reflectors	.....
2.2g	Stratigraphic anomaly distribution map (Rubble Beds)	.....
2.2h	Stratigraphic anomaly distribution map(Qua Iboe)	.....
2.3a	Horizontal resolution; the Fresnel zone	.....
2.3b	Nomogram for deriving horizontal resolution	.....
2.3c	Model of sand body size and relationship to resolution	.....

2.3d	Stratigraphic anomaly; line 82-349	.....
2.4a	The CDP method as a focussing device	.....
2.4b	Log-Log plot of interval velocity error	.....
2.4c	Error in $V_{int} versus V_{rms}$	.....
2.5a	Qua Iboe Litho-velocity chart	.....
2.5b	A simplified error analysis model	.....
3.1	Regional tectonic framework during the Cenozoic	.....
3.2	Tectonic setting of the eastward extension of the delta	.....
	and it's relationship with the Rio del Rey basin	.....
3.3a	The zone of shale diapirs, S.E. Niger Delta	.....
3.3b	Schematic section across the zone of shale diapirs	.....
3.4a	Hypothetical section showing the sedimentary bulge	.....
3.4b	Regional seismic section across the delta(west)	.....
3.4c	Regional seismic section across the delta(east)	.....
3.5	Canyon incision of the Niger continental slope	.....
3.6a	Stratigraphic evolution of the Niger Delta	.....
3.6b	Major formation units of the study area	.....
3.7	Seismic Line 82-251	.....
3.8	Seismic Line 82-279	.....
3.9	Development of the eastern delta	.....
3.10a	Akata shale formation type section	.....
3.10b	Biafra member type section	.....
3.10c	Rubble Bed member type section	.....
3.10d	Qua Iboe member type section	.....
3.10e	D-1 type section	.....
3.10f	Benin formation type section	.....
3.11a	The Stratigraphic column	.....
3.11b	Seismic Line 82-149	.....
3.11c	Seismic line 82-231	.....
3.11d	Seismic line 82-377	.....
3.12	Regional cross-section Evamy *et al.*(1978)	.....
3.13a	Megaunits and associated synsedimentary faults	.....
3.13b	Development of simple and complex growth faults	.....
3.14a,b,c	Structures at the TIBU, BQI and QUA5 levels	.....
3.15a	Terracing at the BQI level(line 82-163)	.....
3.15b	Erosional anticline at the BRB level(line 82-110)	.....
3.15c	Erosional anticline at the TIBU level(line 82-190a)	.....
3.16	Rollover anticline (shale mass supported)Line 82-106	.....

3.17	Rollover anticline with landward dips	.....
3.18	Rollover anticline with seaward dips	.....
3.19a	Shale mass structure flank	.....
3.19b	Shale diapir; line A-23	.....
3.20	Shale mass structure crestal	.....
3.21	Structure at the southeastern block	.....
3.22	Annealment type structure	.....
3.23	Structure at the Qua4 level	.....
4.1a	Depositional processes and unconformity types	.....
4.1b,c	System tracts	.....
4.2	Canyons and their relationship to shelf(line 259)	.....
4.3a	Seismic line 82-66 (the older sequences)	.....
4.3b	Seismic line 82-88a	.....
4.3c	Synthetic seismogram fit for older sequences	.....
4.4a	Line 82-212a	.....
4.4b	Synthetic seismogram fit for LBIBR	.....
4.5a	Line 82-393a	.....
4.5b	Line 82-393	.....
4.6a	Line 82-381	.....
4.6b	Line 82-301	.....
4.7a	Line 82-353	.....
4.7b	Line 82-180	.....
4.7c	Synthetic seismogram fit for TIBU	.....
4.8a	Line 82-107(BIBBEN horizon)	.....
4.8b	Line 82-133(thinning BIBBEN)	.....
4.9a	Line 82-142(Rubble canyon)	.....
4.9b	Line 82-88a(Intra Rubble unconformities)	.....
4.9c	Synthetic seismogram fit for BRB	.....
4.10a	Line 82-261	.....
4.10b	Line 82-285	.....
4.10c	Line 82-106	.....
4.10d,e	Synthetic seismogram fit for BQI	.....
4.11a	Intra Qua Horizon definition	.....
4.11b	Qua Iboe progradation and the turbidite toe	.....
4.11c	Line 82-203	.....
4.11d	Qua3; line 82-361	.....
4.11e	Condensed sections	.....
4.12	The Pleistocene canyon	.....

4.13a	Line 82-269; system tracts of the study area	.....
4.13b,c	Lower system tracts in different tectonic settings	.....
4.13d	Line 82-251	.....
4.13e	Line 82-391	.....
5.1a,b	The Haq *et al.*(1987) and the Vail *et al.*(1977) curves	
5.2a,b,c	The eustatic curves from 1977 to 1987	.....
5.3a,b	Correlation of coastal onlap curves	.....
5.4	Correlation of the Moore *et al.* and Haq *et al.* curves	.....
5.5	Late Neogene Oxygen-18 curves	.....
5.6a	Comparison of Vail's curve to the Oxygen-18 curve	.....
5.6b	Model of turbidite deposition during sea level change	.....
5.7a,b	Chronostratigraphic chart line 82-197	.....
5.8a,b	Chronostratigraphic chart line 82-259	.....
5.9a,b	Chronostratigraphic chart line 82-373	.....
5.10a,b,c,d,e	Sequence correlation summary	.....
5.11a,b,c	Mobility diagrams	.....
5.12a,b&c	Lines 82-197, 82-259, and 82-373	.....
6.1a,b&c	Biafra structural and stratigraphic evolution	.....
6.2	Representative seismic facies types	.....
6.3a&b	Lines 82-183 & 82-86	.....
6.4	Map showing the limit of truncation of BIBBEN	.....
6.5	Line 82-66	.....
6.6	Line 82-211	.....
6.7a,b,c	Characteristic log response of the Older sequences	.....
6.8a	Composte facies distribution map of older sequences	.....
6.8b&c	Paleoenvironment curves for the Older sequences	.....
6.9	Facies distribution map of LIBR	.....
6.10a&b	The Lower Intra Biafra Rubble	.....
6.11a	Facies distribution of SEQ.BS2	.....
6.11b&c	lines 82-339 and 82-220a	.....
6.12a	Line 82-283	.....
6.12b	Line 82-106	.....
6.12c	Line 82-339	.....
6.12d	Line 82-377	.....
6.13a	Facies distribution of UIBR	.....
6.13b	Paleoenvironment curve for UIBR	.....
6.14a&b	High amplitude anomalies in UIBR	.....

6.15	Line 82-132a; SEQ.BS4	.....
6.16a	Facies distribution for SEQ.BS4	.....
6.16b	Paleoenvironment curve for SEQ.BS4	.....
6.17a	Sand percentage map of the Biafra	.....
6.17b	Interval velocity map of the Biafra	.....
6.18	Juxtaposition of the av. int. vel. map and sand % map	.....
6.19a	Litho-velocity chart for Biafra	.....
6.19b	Upper Intra Biafra Rubble velocity analysis	.....
6.20	A composite map of the delta front for Biafra sequences	.....
7.1a	Line 82-106; BRB as a PGM feature	.....
7.2	Line 82-142	.....
7.3a	Unit 1 Rubble; Line 82-287	.....
7.3b&c	Unit 2 Rubble(82-387)	.....
7.4	Distribution of Unit 1 Rubble	.....
7.5	Distribution of Unit 2 Rubble	.....
7.6	Seismic facies of the Rubble Beds	.....
7.7	Facies distribution of the Rubble Beds	.....
7.8a	Line 82-118; the chaotic facies	.....
7.8b	Line 82-253; the proximal facies	.....
7.8c	Line 82-197; mounded proximal facies	.....
7.8d	Line 82-291; mounded onlap facies	.....
7.8e	Line 82-168a; the distal facies	.....
7.8f	Line 82-216a; the prograding facies	.....
7.9a	Rubble Bed depositional model	.....
7.9b	Mechanisms for Rubble Bed formation	.....
7.10a	Rockfall	.....
7.10b	Development of channel system(82-251)	.....
7.11a	The western Rubble Bed canyon (line 82-142)	.....
7.11b	The eastern canyon	.....
7.11c	The eastern canyon (line 82-337)	.....
7.12	Distribution of Stratigraphic anomalies	.....
7.13	Litho-velocity chart for the Rubble Beds	.....
7.14	Distribution of sand build-ups based on velcity	.....
7.15a&b	The northern anomalies	.....
7.15c	The southeastern anomaly	.....
8.1	Qua Iboe shale limit	.....
8.2a&b	Lines 82-279 and line 82-185	.....

8.3	Composite of shelf breaks	.....
8.4	Representative facies types	.....
8.5a	Structural map of Horizon QUA2	.....
8.5b	Isochron map of QS1	.....
8.5c	Facies distribution map QS1	.....
8.6a&b	Lines 82-201 and 82-409	.....
8.6c	Facies distribution map of QS2	.....
8.6d	Composite anomaly map of QS1 and QS2	.....
8.7a	Line 82-229	.....
8.7b	Distribution map of seismic mounds	.....
8.7c	Line 82-231	.....
8.7d	The prograding terrace, line 82-271	.....
8.8a	Structure map of QUA4	.....
8.8b	Facies distribution map of QS3	.....
8.8c	Line 82-212a	.....
8.9	The Lower Qua Iboe depositional model	.....
8.10a	Paleodepth estimation from progradation	.....
8.10b	Environmental depth zones	.....
8.10c	Process continuum in deep sea sedimentation	.....
8.10d&e	Seismic evidence of slumping (line 82-251)	.....
8.11	Seismic indicators of Turbidite sequences	.....
8.12a	Line 82-154s	.....
8.12b	Line 82-146b	.....
8.12c	Line 82-251	.....
8.12d	Line 82-267	.....
8.13a	Proximal facies illustration(82-114)	.....
8.13b	Mounded proximal facies	.....
8.13c	Line 82-291	.....
8.13d	Proximal onlap(line 82-409)	.....
8.13e	Proximal Uplap(line 82-353)	.....
8.14	Formation of seismic mounds(model)	.....
8.15	Composite of the distribution of seimic mounds	.....
8.16a	Build-up of the central anomaly	.....
8.16b	Build-up of the southwest anomaly	.....
8.16c	Build up of the northwest anomaly	.....
8.16d	The centre-west anomaly	.....
8.16e	The centre-east(1&2)	.....
8.16f	The eastern anomaly	.....
8.17	Line 82-142	.....

8.18a	Mounded fan complex facies(line 82-182a)	.....
8.18b	Depositional model of stacked channels	.....
8.19a	Line 82-174	.....
8.19b	Line 82-185	.....
8.20	Line 82-154b	.....
8.21a	Sheet facies: line 82-349	.....
8.21b	Line 82-106	.....
8.22	Line 82-220a	.....
8.23	Sigmoidal facies: line 82-369	.....
8.24	Oblique facies: line 82-429	.....
8.25a	Litho-Velocity chart	.....
8.25b	Interval velocity map	.....
8.26a	Interpreted litho-vel chart	.....
8.26b	Sandiness map	.....
8.26c	Coefficient of heterogeneity map	.....
8.27a	Facies distribution map QS4	.....
8.27b	Line 82-86	.....
8.28a	Line 82-215	.....
8.28b	Line 82-289	.....
8.29a	Line 82-345	.....
8.29b	Line 82-169	.....
8.29c	Facies distribution map of QS5	.....
8.29d	Line 82-385	.....
8.30	Facies distribution of QS7	.....
8.31	Line 82-341	.....
8.32a&b	The chaotic facies	.....
8.33	Coastal onlap on line 82-369	.....
8.34a&b	The Pleistocene canyon	.....
8.35	Extent of the canyon	.....
8.36	Line 82-223	.....
9.1	Turbidites and sea level changes	.....
9.2a&b	Three end-member fan classification	.....
9.3a&b	Comparison of modern and ancient fans	.....
9.4a	The Mississippi submarine fan model	.....
9.4b	The Submarine ramp model	.....
9.4c	Facies comparison, ramp model versus ancient model	.....
9.4d	The shelf-Slope model	.....
9.5a	The Lower Qua Iboe fan model	.....

9.5b	Map of seismic mounds	.....
9.6	Seismic criteria for fan recognition	.....
9.7	Relationship between fan width and valley size	.....
9.8a&b	The northern feeder canyon	.....
9.8c	Seismic example of a turbidite fan	.....
9.9a&b	Slope models	.....
9.10	The Texas-Louisiana slope	.....
9.11	The Hackberry Embayment	.....
9.12a&b	Stratigraphic setting of Hackberry onlap slope system	.....
9.13	Depositional overview of the Hackberry slope system	.....
9.14	Depositional setting of the Hackberry	.....
9.15	Canyon fills of the Niger Delta	.....
9.16	Canyon fills of the Gulf coast	.....
9.17	The submerged shelf margin	.....
9.18	Shelf margin deltas during lowstand of sea level	.....
9.19	Progradation and eustatic sea level changes	.....

CHAPTER ONE

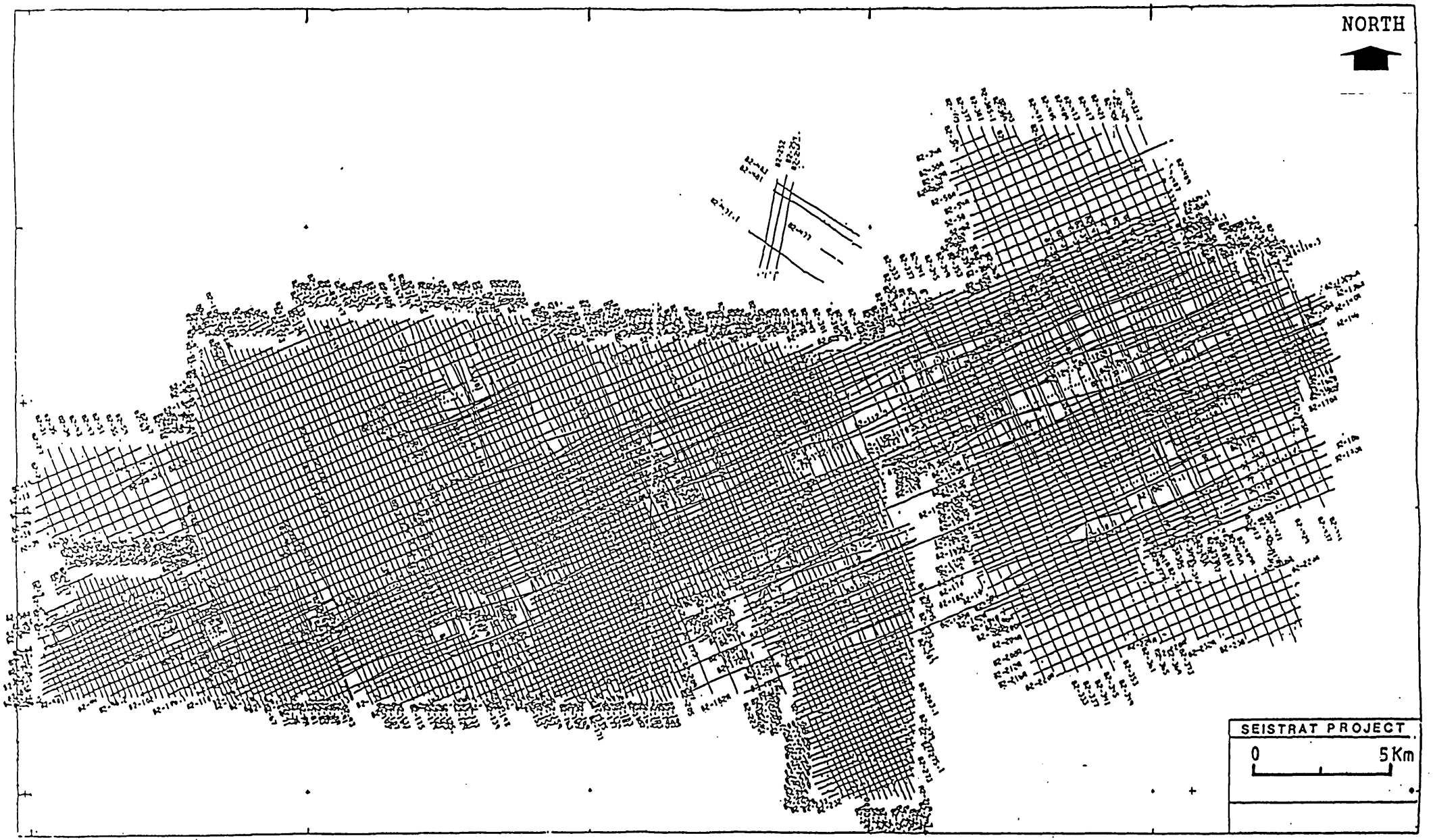

Fig.1.1 Seismic data base and coverage map.

SEFEL GEOPHYSICAL
SEISMIC DATA PROCESSING
LONDON ENGLAND

DATE PROCESSED JULY 1982
REEL NUMBER
CONTRACT NUMBER 840

FIELD RECORDING

RECORDED BY M.V. HANS EGEDE
DATE 13TH APRIL 1982 SYSTEM LITTON 888
FORMAT SEG C 1600 B.P.I. GAIN I.F.P.

ENERGY SOURCE

TYPE BOLT. PAR AIR GUN
ARRAY 1X8. 1X6 DEPTH 7M

STREAMER

LENGTH 1800M NO. TRACES 72
DEPTH 10M AVERAGE GROUP INTERVAL 25M
ARRAY 16 GEOPH/TR OVER 25M

PARAMETERS

RECORDING FOLD 36 S.P. SPACING 25M
SAMPLE INTERVAL 2MS RECORD LENGTH 4 SEC
RECORDING FILTER LO-6HZ. 18DB/OCT. HI-125HZ 72DB/OCT.

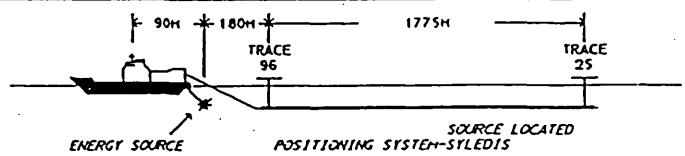

DIGITAL PROCESSING

SEQ	PROCESS	PARAMETERS
1	DEMULTIPLEX	SUB-SAMPLE 2TO4MS ANTI-ALIAS FILTER APPLIED
2	CDP SORT	36 FOLD
3	DEPHASE	INSTRUMENT FILTER RESPONSE COMPENSATION
4	GAIN RECOVERY	APPLING INVERSE AMPLITUDE DECAY CURVES
5	DECONVOLUTION	SEE BELOW
6	VELOCITY ANALYSIS	CVS EVERY 1.5 KM
7	NMO REMOVAL + MUTE	NMO CORRECTION AND STRETCH REMOVAL
8	HORIZONTAL STACK	
9	DECONVOLUTION	SEE BELOW
10	FILTER	BROAD PASS BAND FILTER (6-60HZ)
11	EQUALISATION	500MS WINDOWS 50% OVERLAP
12	MIGRATION	WAVE EQUATION MIGRATION
13	TV FILTER	SEE BELOW
14	EQUALISATION	WHOLE TRACE EQUALISATION
15	STATICS + DISPLAY	GUN AND CABLE DEPTH CORRECTIONS

ADDITIONAL PARAMETERS

DECON	* OPERATOR LENGTH	PREDICTIVE GAP	DERIVATION WINDOWS	APPLICATION WINDOWS
SEQ 5	200	24	N.T. 0-3000 MS	WHOLE TRACE
			F.T. 1700-4700 MS	WHOLE TRACE
SEQ 9	200	20	600-3600 MS	WHOLE TRACE

APPLICATION TIMES

FILTER	CUT OFF POINT	100% PASS POINT	100% PASS POINT	CUT OFF POINT	APPLICATION TIMES FOR SHOTPOINTS SPECIFIED		
SEQ13	7	10	55	65	700MS OVERLAP		
	6	10	45	55	1500MS		
	5	10	35	45	2800MS		
	5	10	30	40	3500MS		
					EOD		

ALL TIMES IN MILLISECONDS ALL FREQUENCIES IN HERTZ
FILTERS INTERPOLATED LINEARLY BETWEEN APPLICATION TIMES
APPLICATION TIMES INTERPOLATED LINEARLY BETWEEN SHOTPOINTS
*OPERATOR LENGTH GIVEN IS ACTIVE LENGTH ADD GAP FOR TOTAL LENGTH

SAMPLE RATE: 4MS: DATUM CORRECTION: 12MS TO MSL

SCALES: HORIZONTAL 1:11811 VERTICAL 3.75IN/SEC

RECORDING POLARITY: COMPRESSION RECORDED AS NEG ON TAPE

PROCESSING POLARITY: POSITIVE NO. GIVES BLACK PEAK

Fig.1.2 Field recording and processing parameters.

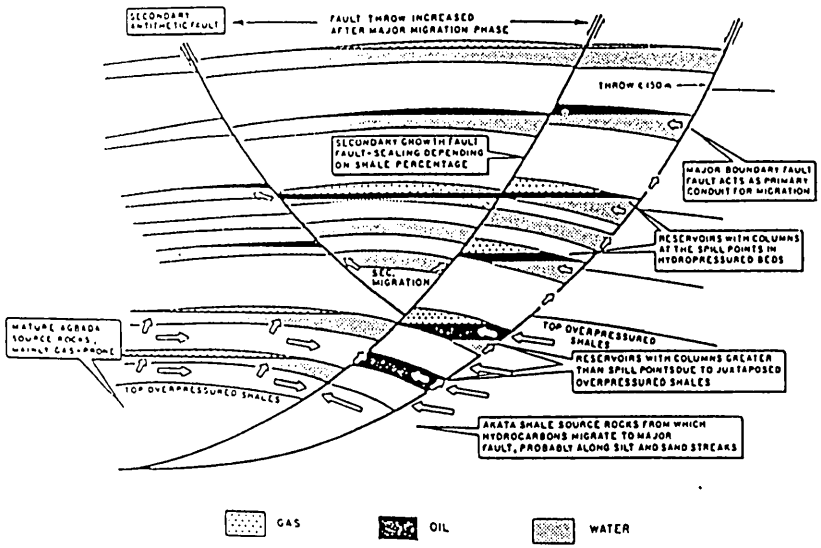

Fig.1.3a Typical roll-over structure.

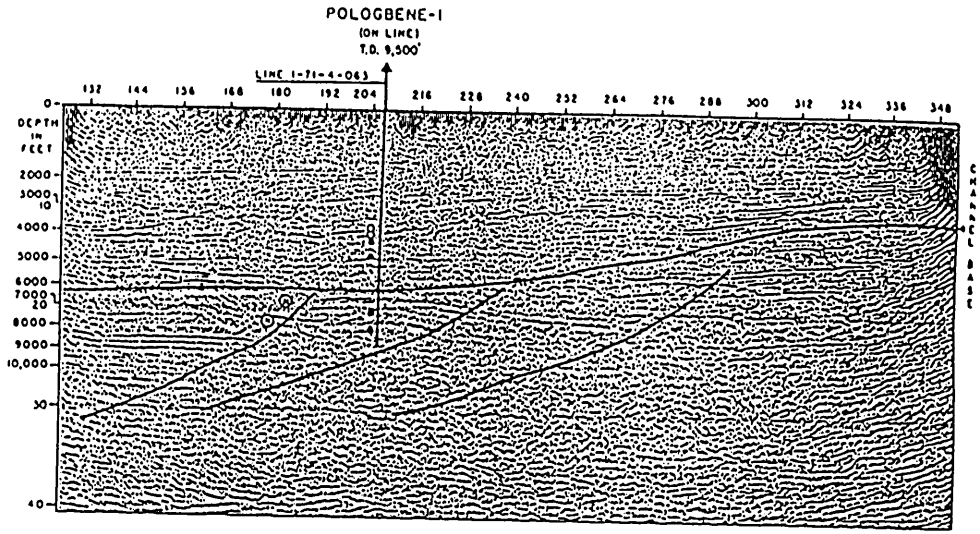

Fig.1.3b Stratigraphic play in slope channel fill.

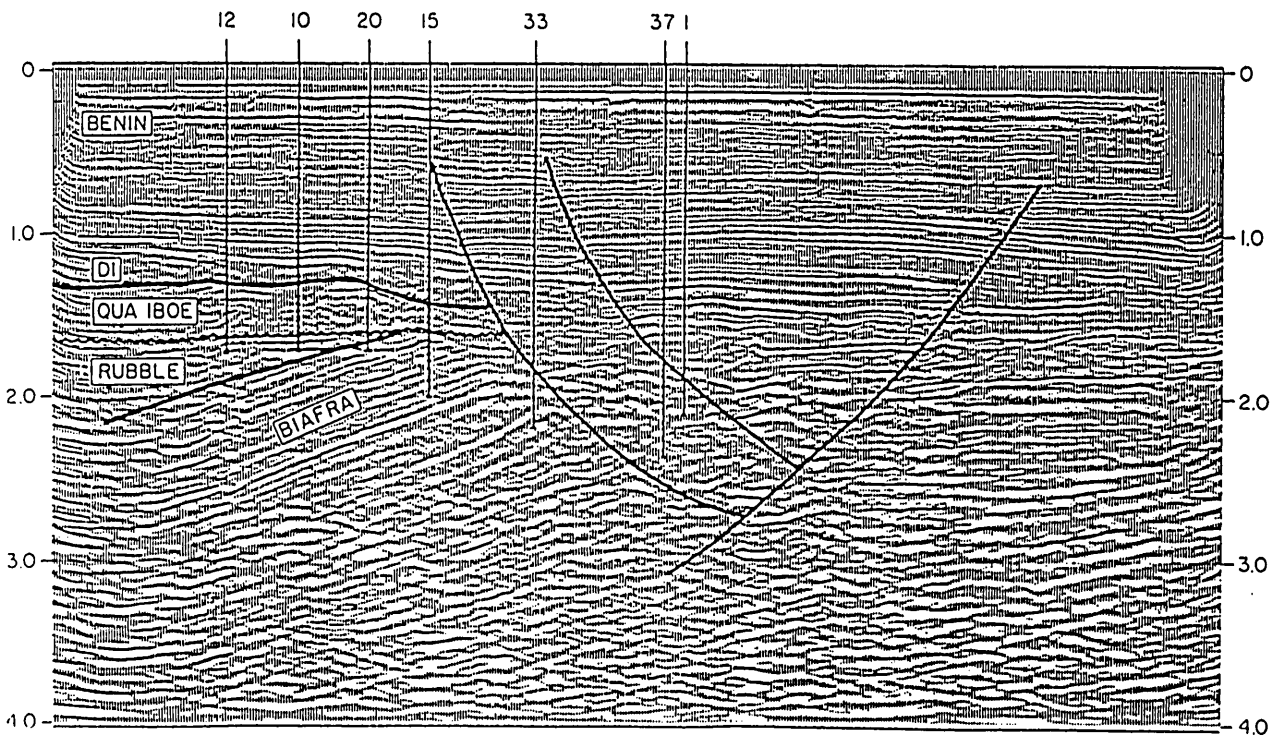

Fig.1.3c Truncation trap over paralic sequences.

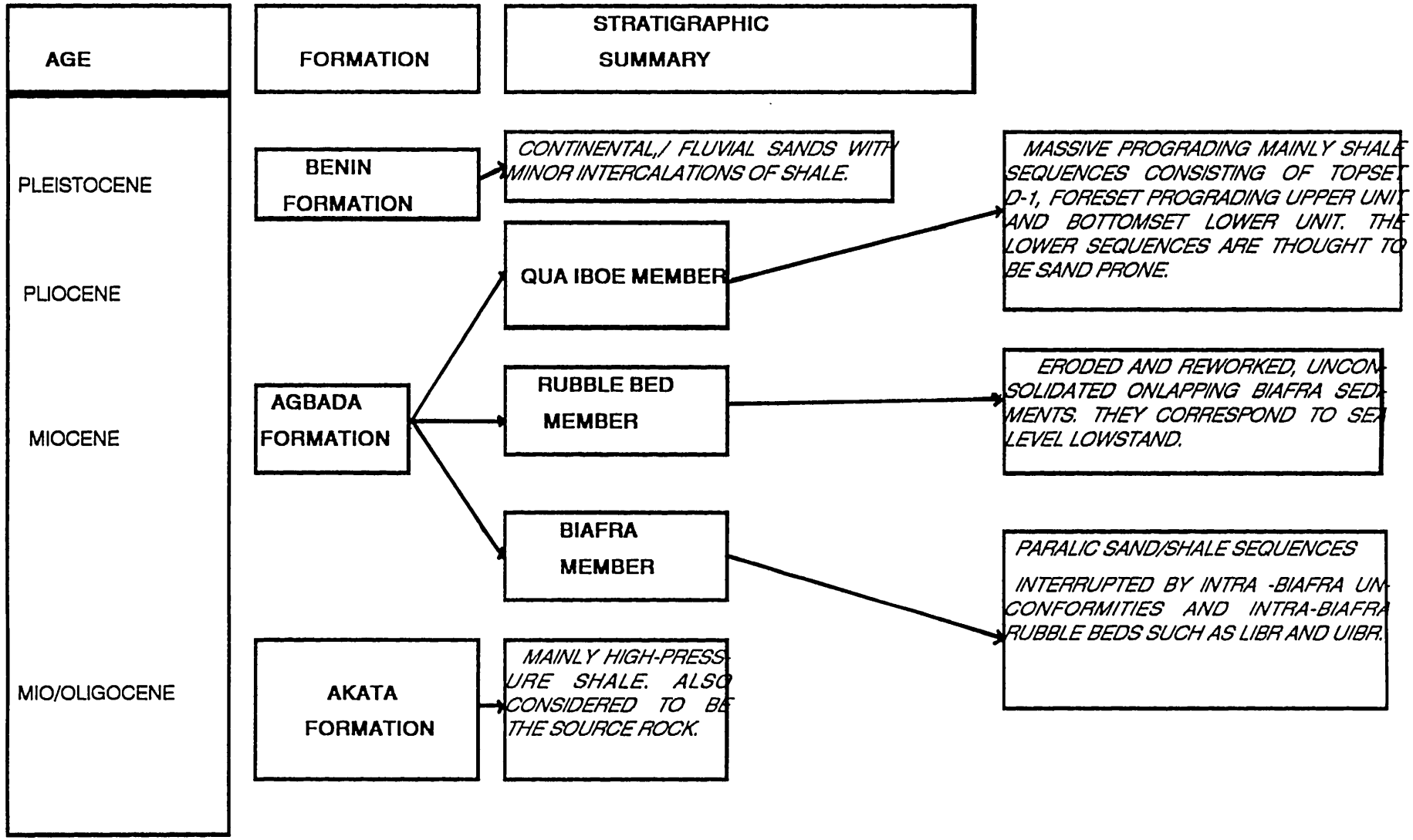

FIG.1.3d Litho-stratigraphic units of the study area.

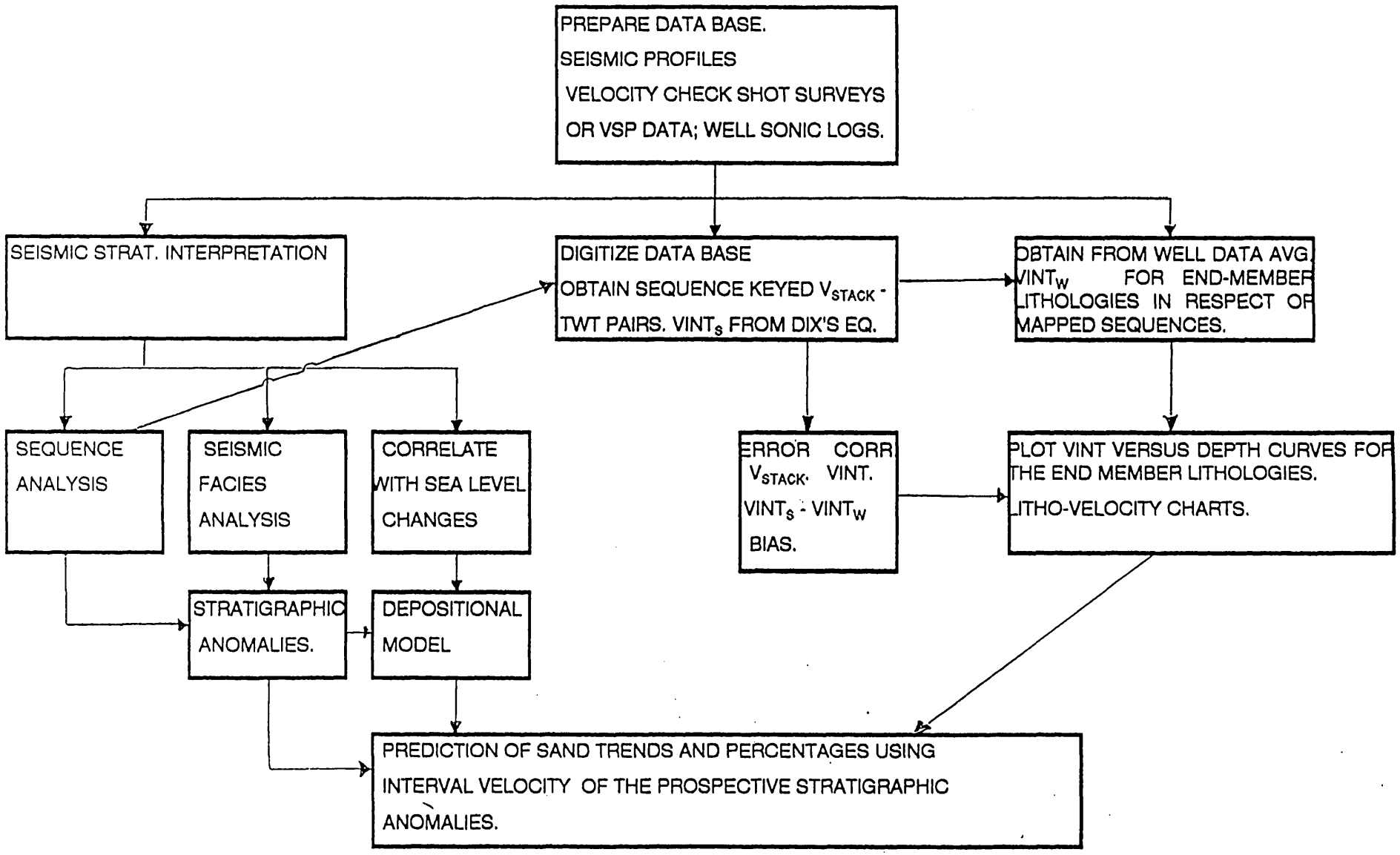

Fig.1.4a Flow diagram showing the methodology used.

SEISMIC SEQUENCE ANALYSIS. GLOSSARY OF TERMS (AFTER VAIL, 1988)

SEISMIC SEQUENCE

A seismic sequence corresponds to a depositional sequence seismically expressed by a gamut of seismic reflection patterns, formed as a result of the interaction between rates of eustacy, subsidence and sediment supply and is bounded by unconformities and their correlative conformities. They may be divided into TYPE 1 and TYPE 2 unconformities respectively.

TYPE 1 UNCONFORMITY:

Formed through subaerial exposure and concurrent subaerial erosion; and associated with basinward shift in coastal onlap and onlap over lying strata. i.e. R_F IS MORE THAN R_S AT DEP. SHORE LINE.

SYSTEM TRACTS: defined by their position within the sequence and are a linkage of contemporaneous depositional systems.

TYPE 2 UNCONFORMITY:

is marked by subaerial exposure but shows no subaerial erosion associated with canyon cutting.

R_F IS LESS THAN R_S AT THE DEP. SHORE LINE.

PARASEQUENCE: a relatively conformable succession of genetically related beds bounded by marine flooding surfaces (MFS).

SYSTEM TRACTS OF TYPE 1 SEQUENCES:

1. LOWSTAND S.T.
2. TRANSGRESSIVE S.T.
3. HIGHSTAND S.T.

Lowstand s.t. is the lowermost s.t. and in a basin with a shelf break may be subdivided into:

a. Basin-floor fan

b. Slope fan

c. Lowstand wedge.

Highstand s.t. is an upper s.t. occuring commonly on the shelf in both type 1 and type 2 sequences.

*****NOTE***

In the accompanying text, the terms LOWSTAND S.T. and HIGHSTAND S.T. have been substituted with LOWER S.T. & HIGHER S.T. respectively. This is because the terms lowstand and highstand by definition do not imply a unique period of time or position on a cycle of eustatic or relative sea level change. (Vail, 1988).

Figures overleaf show the schematic diagrams of the sequence types in this study.

SYSTEM TRACTS OF TYPE 2 SEQUENCES:

1. SHELF MARGIN S.T.
2. TRANSGRESSIVE S.T.
3. HIGHSTAND S.T.

Shelf margin s.t. is the lowermost s.t. associated with type 2 sequence boundary, commonly progradational and /or aggradational, the top of which is a transgressive surface.

Transgressive s.t. is considered the middle s.t. the top of which is a downlap surface.

Fig.1.4b Sequence boundary definitions and glossary of terms (after Vail, 1988).

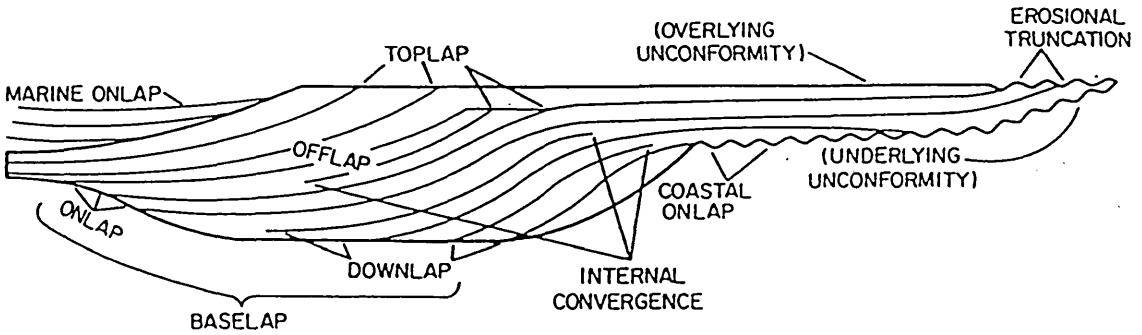

SEQUENCE STRATIGRAPHY
BLOCK DIAGRAM
SHOWING SEQUENCES, SYSTEMS TRACTS AND LITHOFACIES

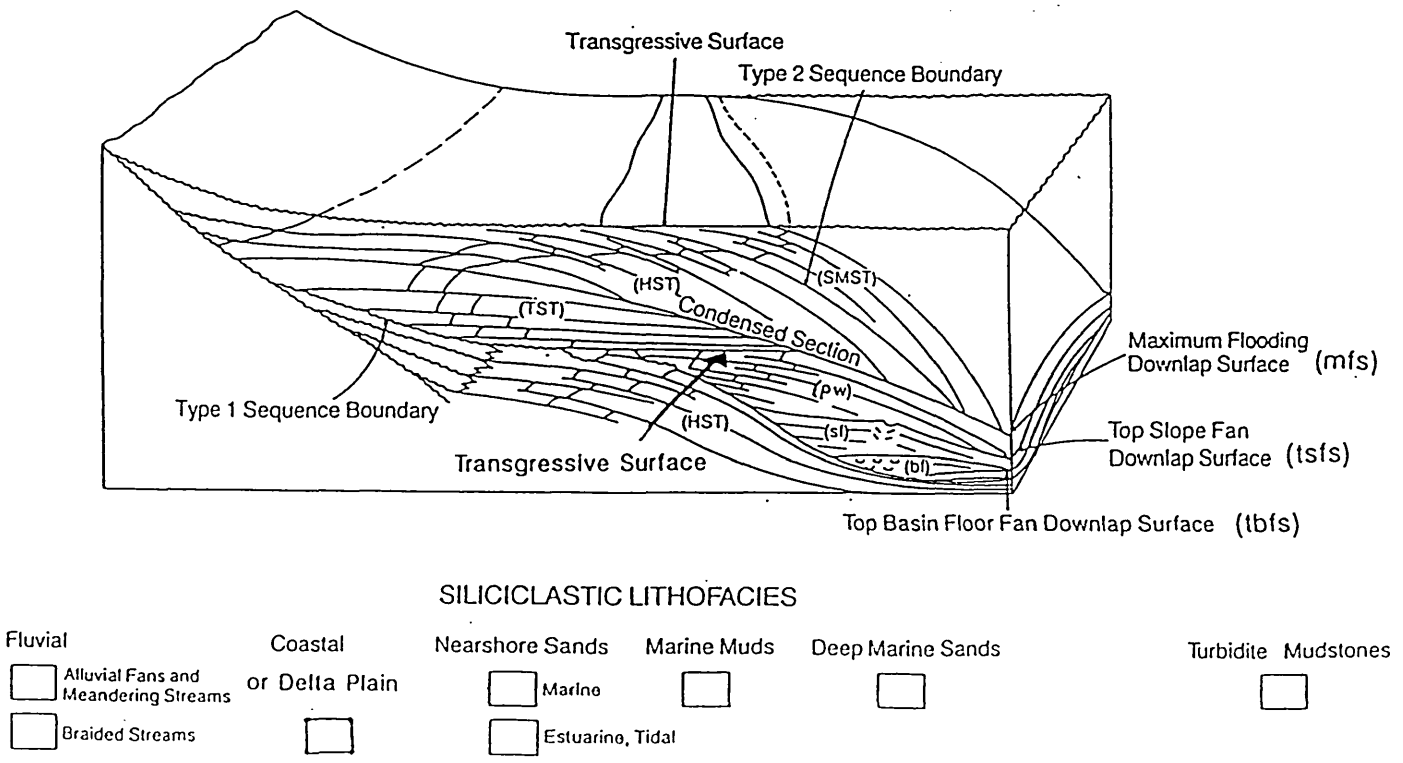

Fig.1.4c Schematic diagram of sequence types.

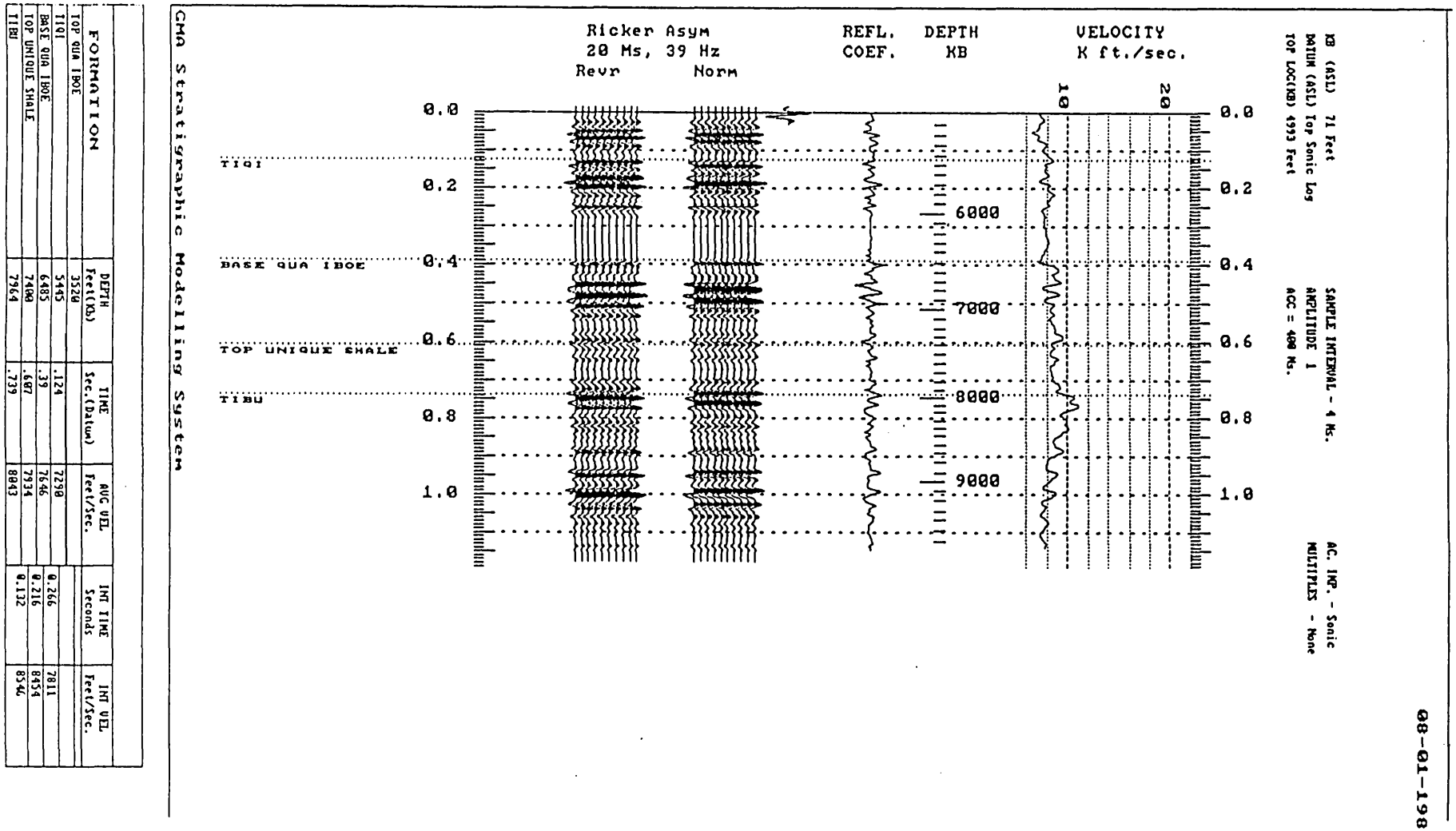

FORMATION	DEPTH Feet(KB)	TIME Sec.(Datum)	AVG VEL Feet/Sec.	INT TIME Seconds	INT VEL Feet/Sec.
TOP QUA IBOE	3520		7298		
TIQI	5445	.124		0.266	7811
BASE QUA IBOE	6485	.39	7646	0.216	8454
TOP UNIQUE SHALE	7400	.607	7934	0.132	8546
TIBU	7964	.739	8043		

Fig.1.5 Typical GMA synthetic seismogram presentation.

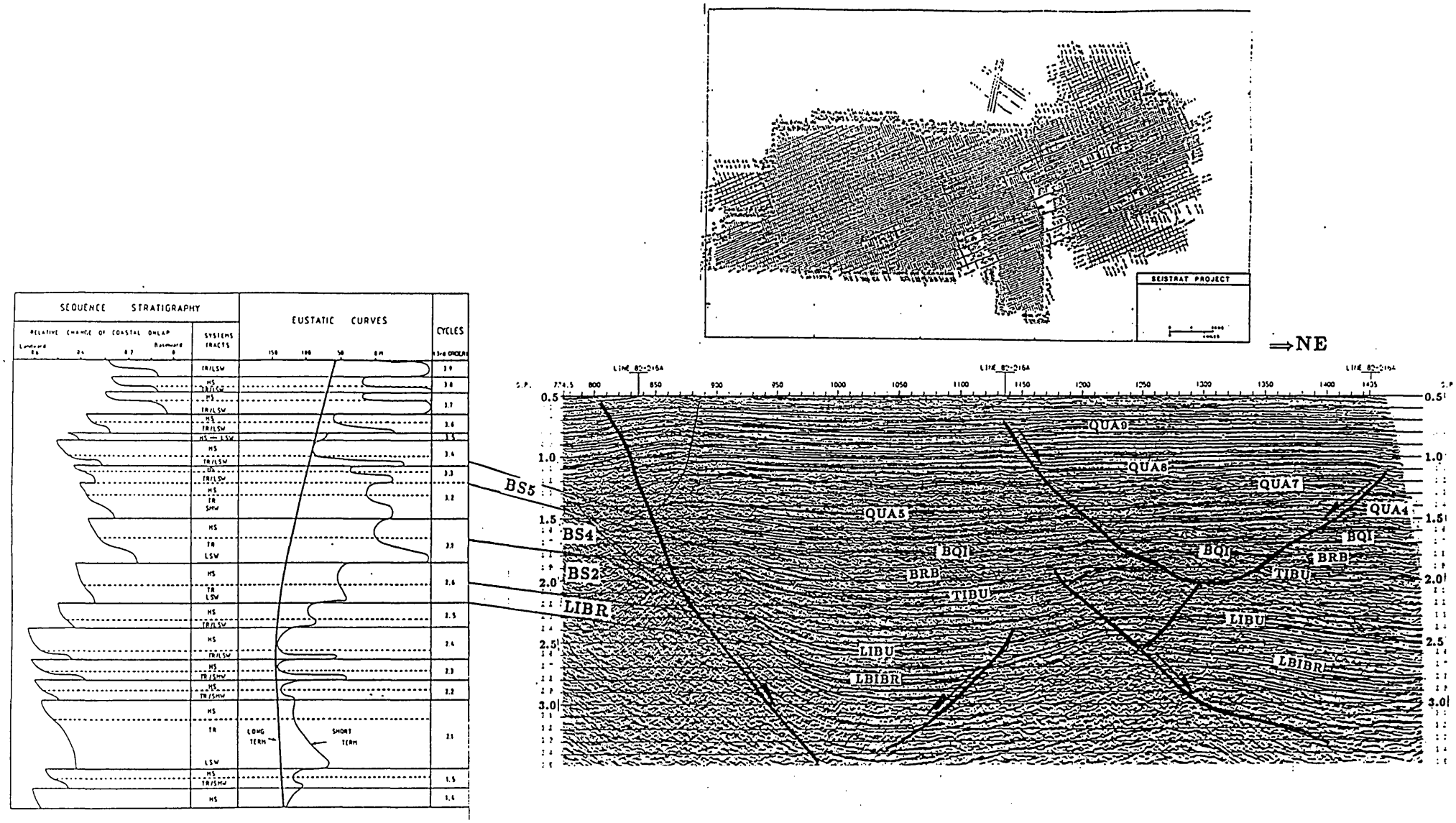

Fig.1.6 Seismic line 82-216a showing the correlation of stratigraphic sequences mapped with sea level change using the Haq *et al.*(1987) curve.

REFLECTION TERMINATIONS (AT SEQUENCE BOUNDARIES)	REFLECTION CONFIGURATIONS (WITHIN SEQUENCES)		EXTERNAL FORMS (OF SEQUENCES AND SEISMIC FACIES UNITS)
LAPOUT	PRINCIPAL STRATAL CONFIGURATION		
BASELAP	PARALLEL		SHEET
ONLAP	SUBPARALLEL		SHEET DRAPE
DOWNLAP	DIVERGENT		WEDGE
TOPLAP	PROGRADING CLINOFORMS		BANK
TRUNCATION	SIGMOID		LENS
EROSIONAL	OBLIQUE		MOUND
STRUCTURAL	COMPLEX SIGMOID-OBLIQUE		FILL
CONCORDANCE	SHINGLED		
(NO TERMINATION)	HUMMOCKY CLINOFORM		
	CHAOTIC		
	REFLECTION-FREE		
	MODIFYING TERMS		
	EVEN	HUMMOCKY	
	WAVY	LENTICULAR	
	REGULAR	DISRUPTED	
	IRREGULAR	CONTORTED	
	UNIFORM		
	VARIABLE		

Fig.1.7a Reflection configurations and facies terminology.

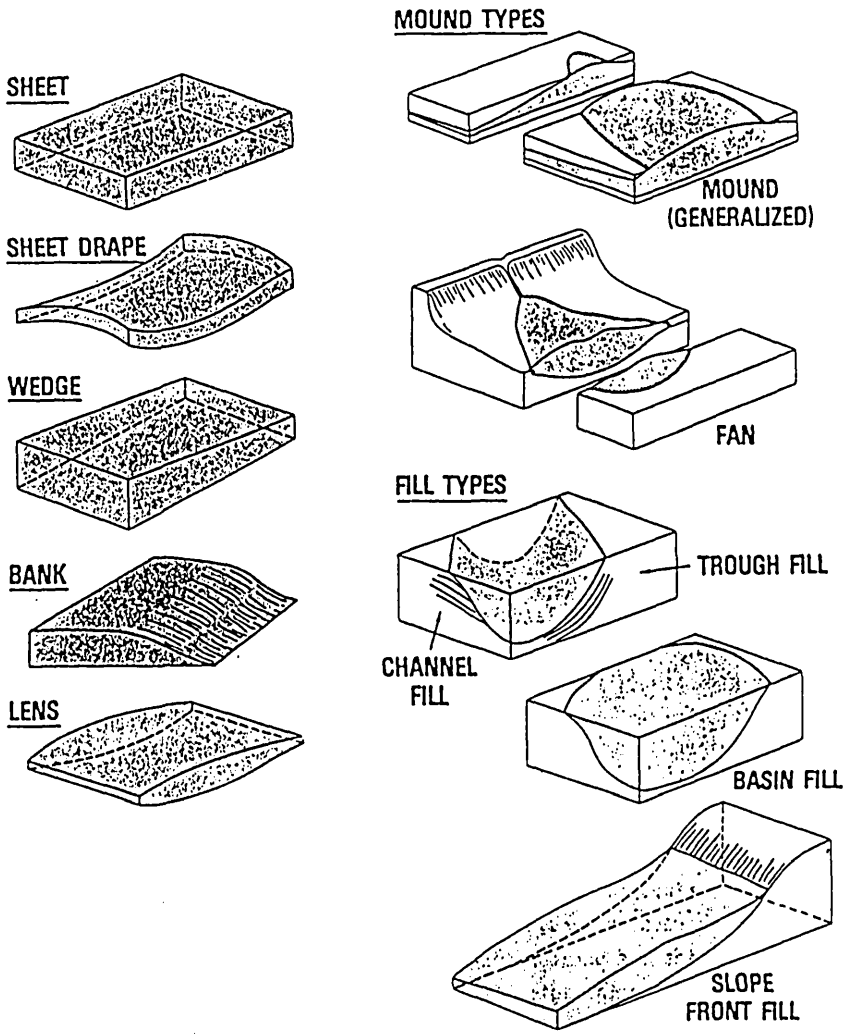

Fig.1.7b External geometry of some seismic facies.

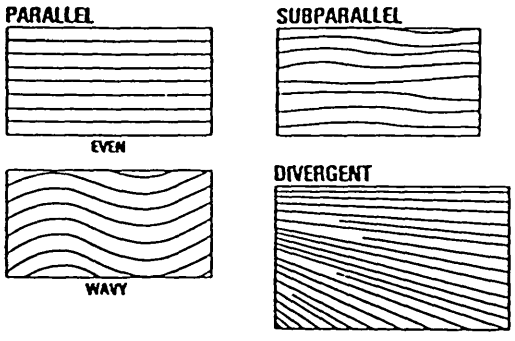

Parallel, subparallel and divergent seismic reflection configurations. From Mitchum et al. (1977).

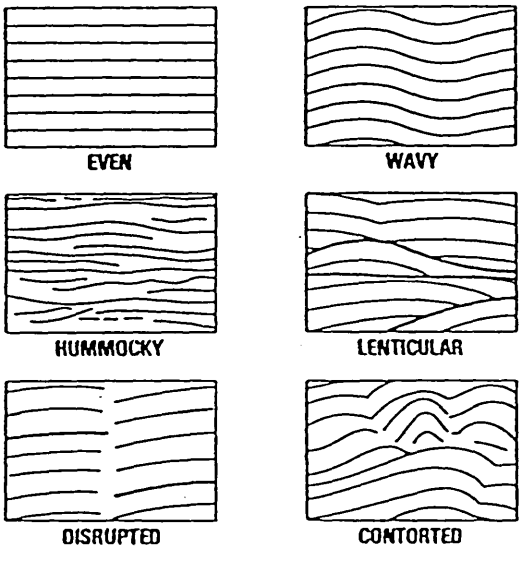

Some modifying seismic reflection configurations. From Mitchum et al. (1977).

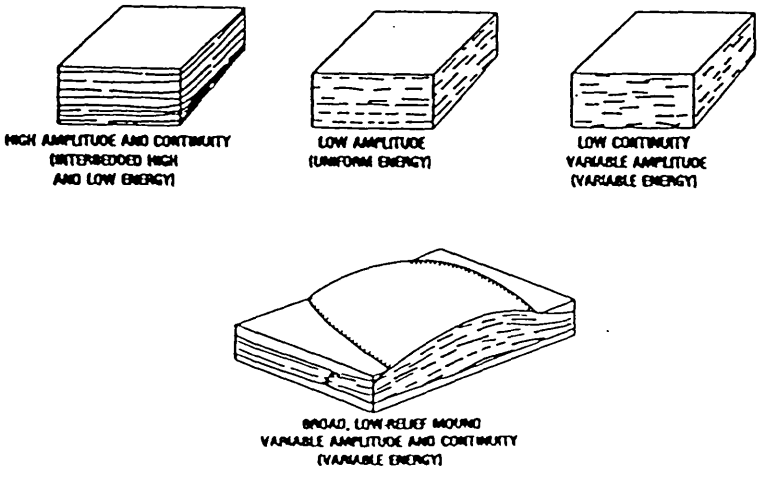

Fig.1.7c Parallel/divergent seismic seismic facies.

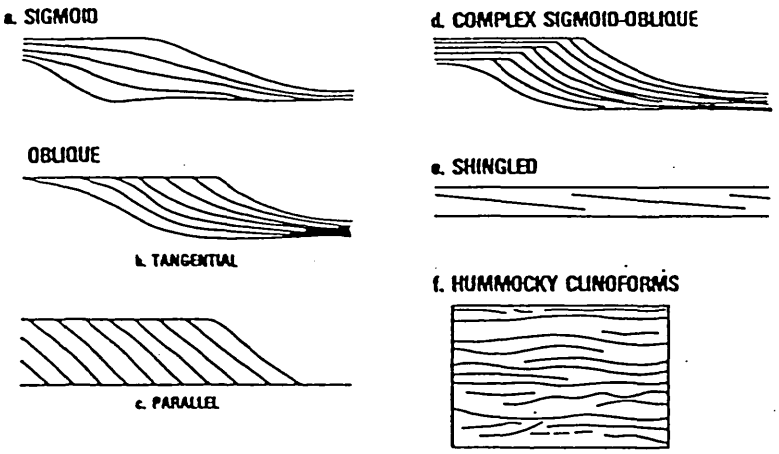

Progradational seismic reflection patterns. From Mit chum et al. (1977).

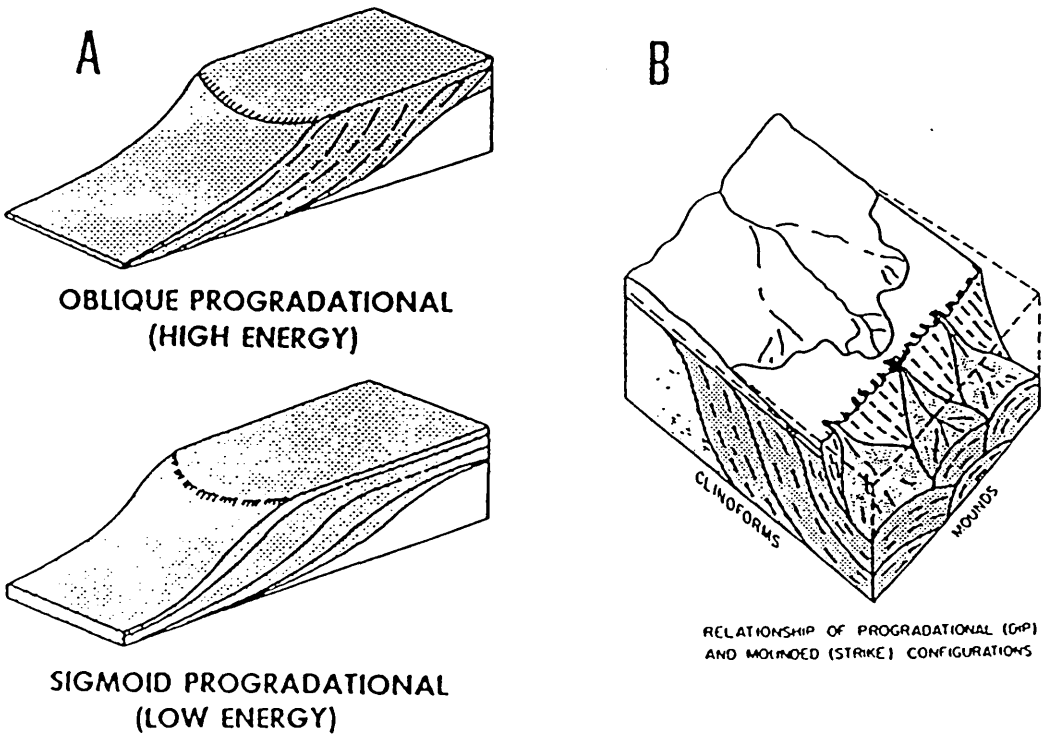

Fig.1.7d Progradational facies types.

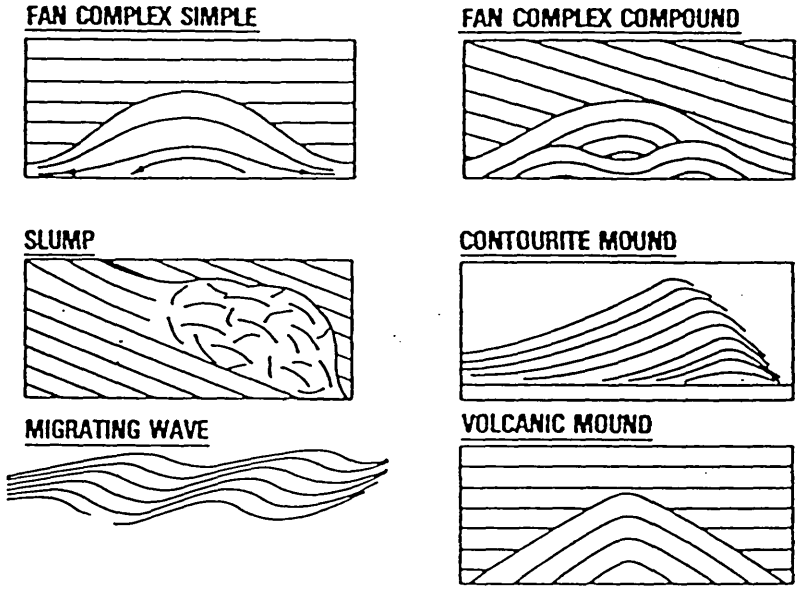

Clastic mounded seismic facies configurations. From Mitchum et al. (1977).

Fig.1.7e Mounded and drape facies types.

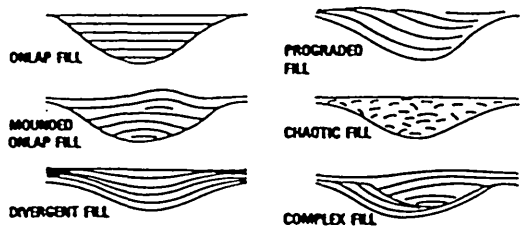

Figure 41. Fill seismic facies configurations. From Mitchum et al. (1977).

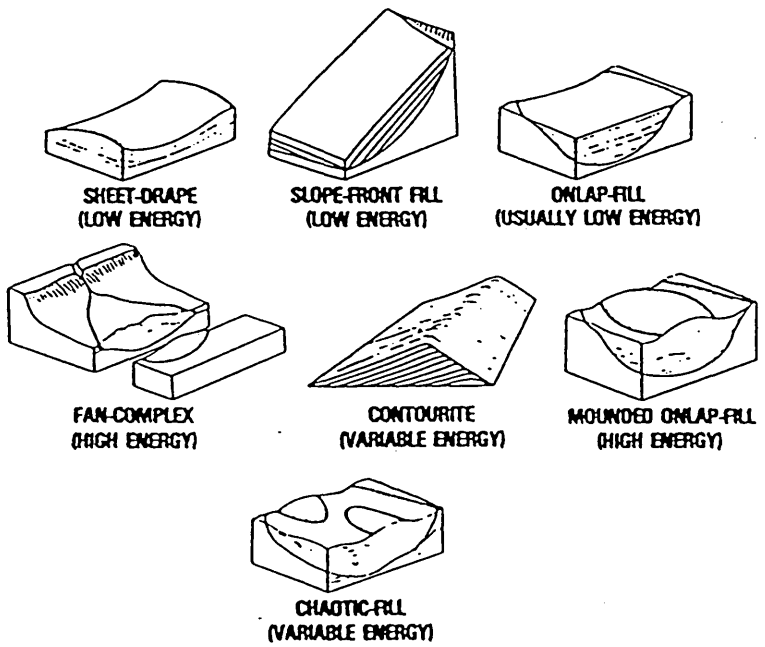

Fig.1.7f Onlap and fill seismic facies types.

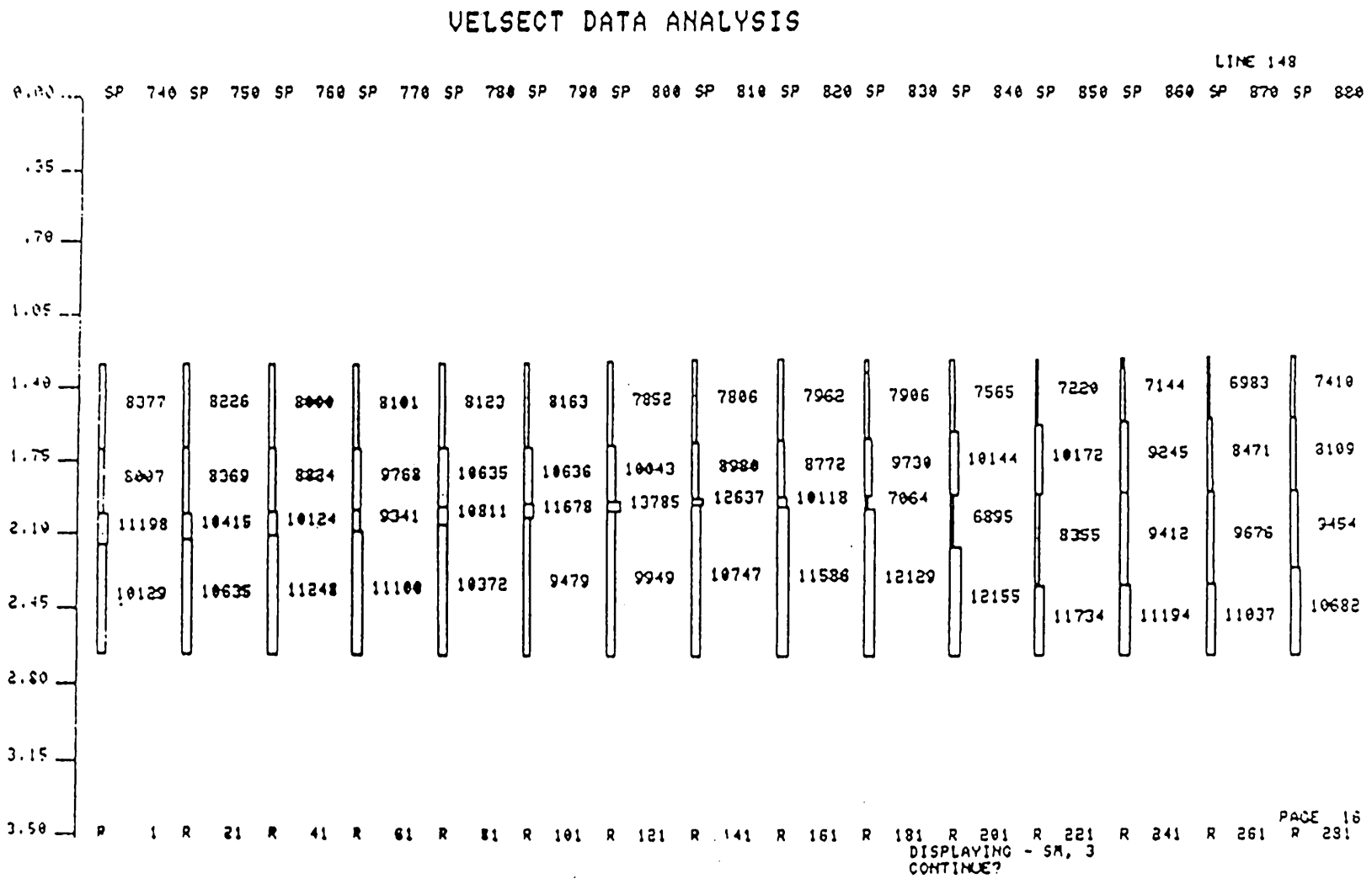

Fig.1.8a Velsect data analysis.

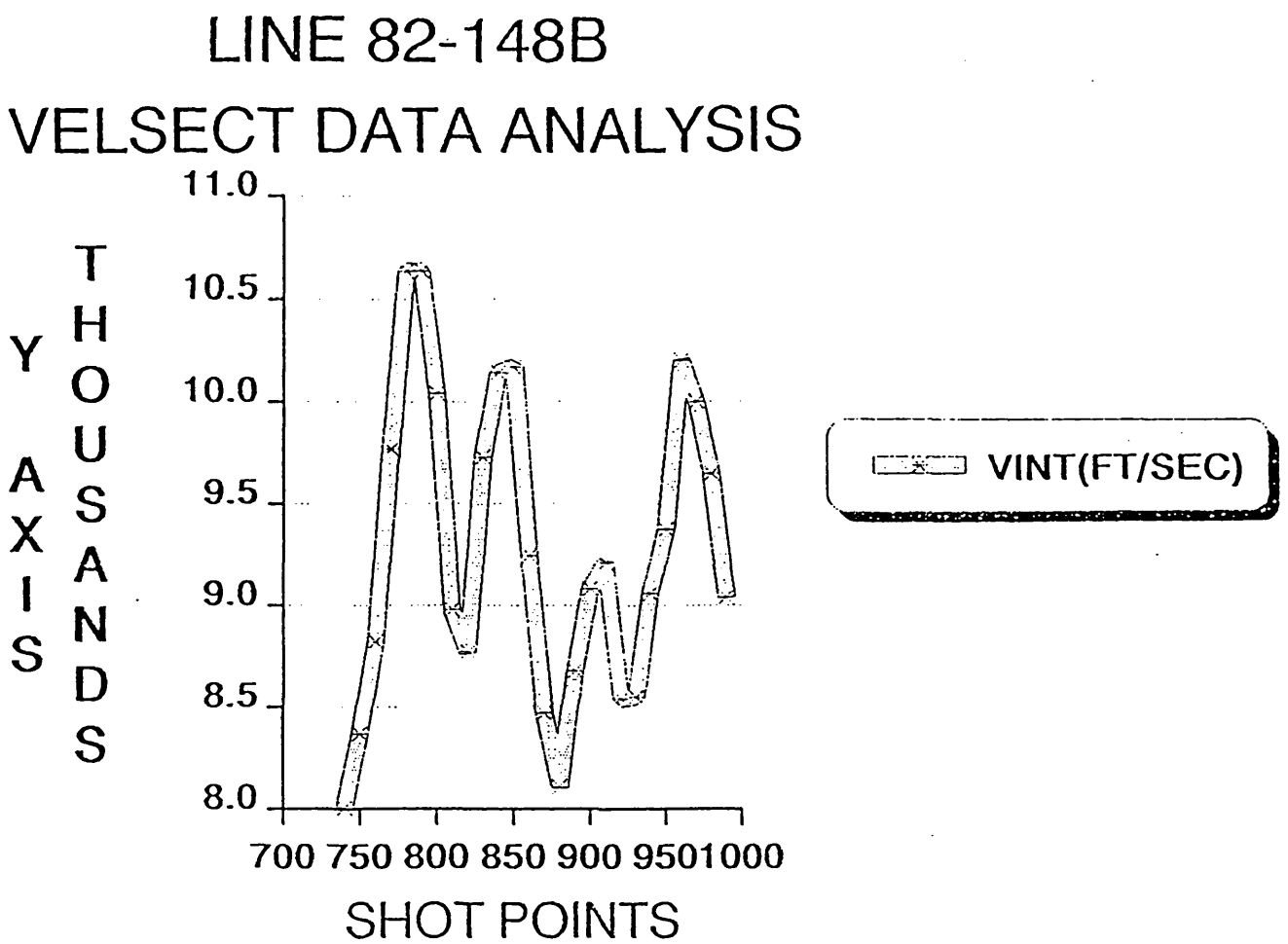

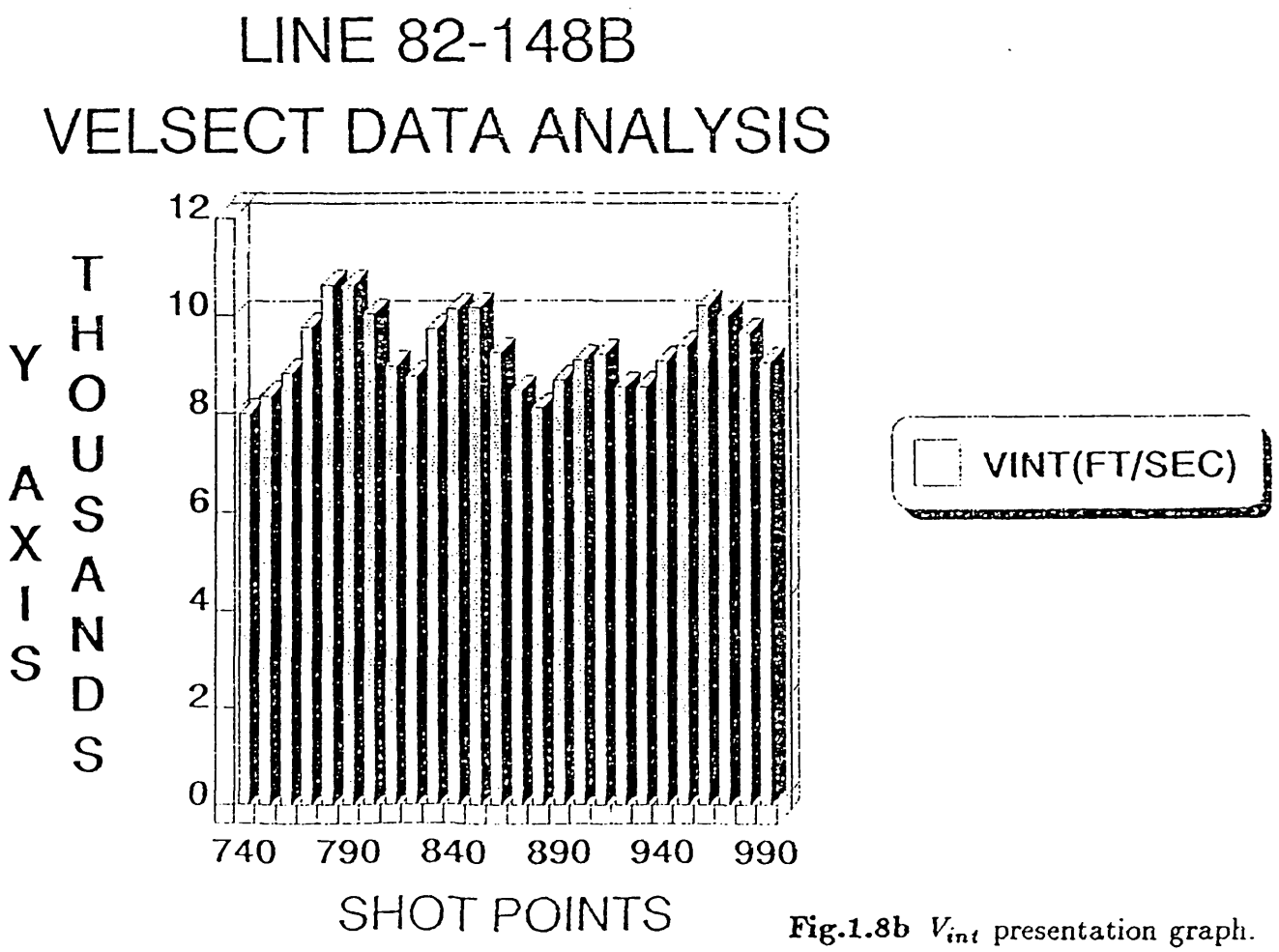

Fig.1.8b V_{int} presentation graph.

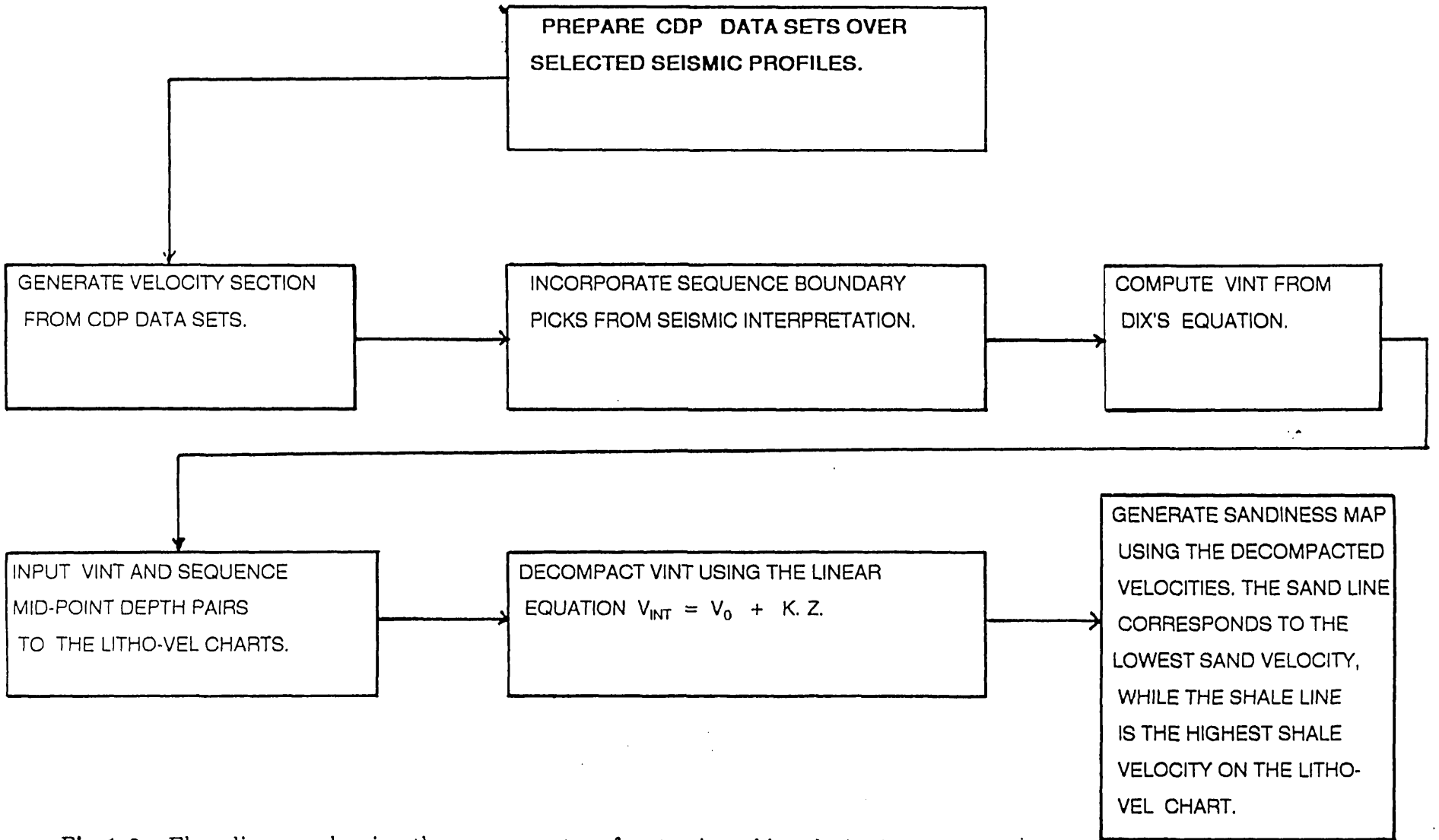

Fig.1.8c Flow diagram showing the sequence steps for stratigraphic velocity interpretation.

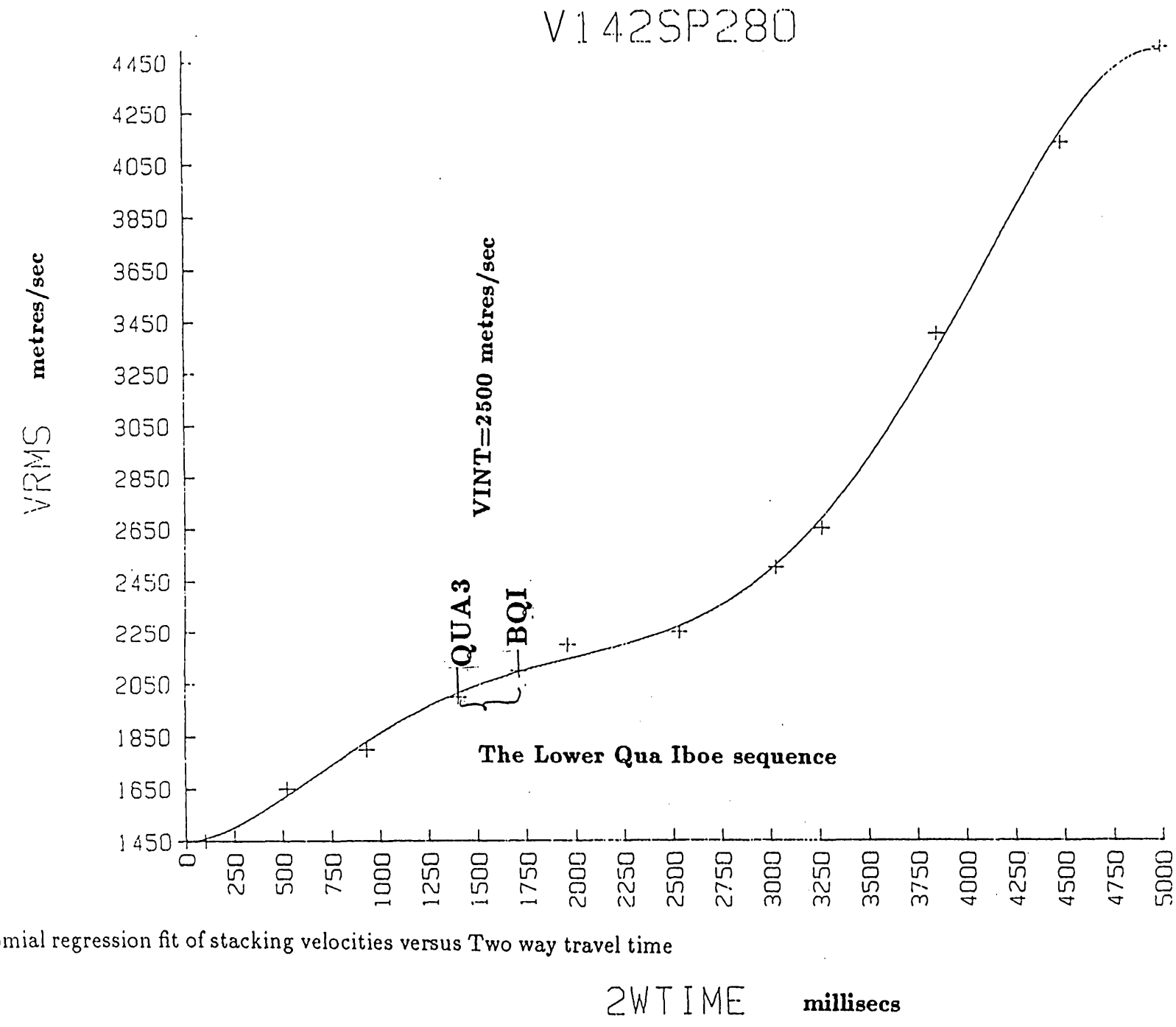

Fig.1.8d Polynomial regression fit of stacking velocities versus Two way travel time

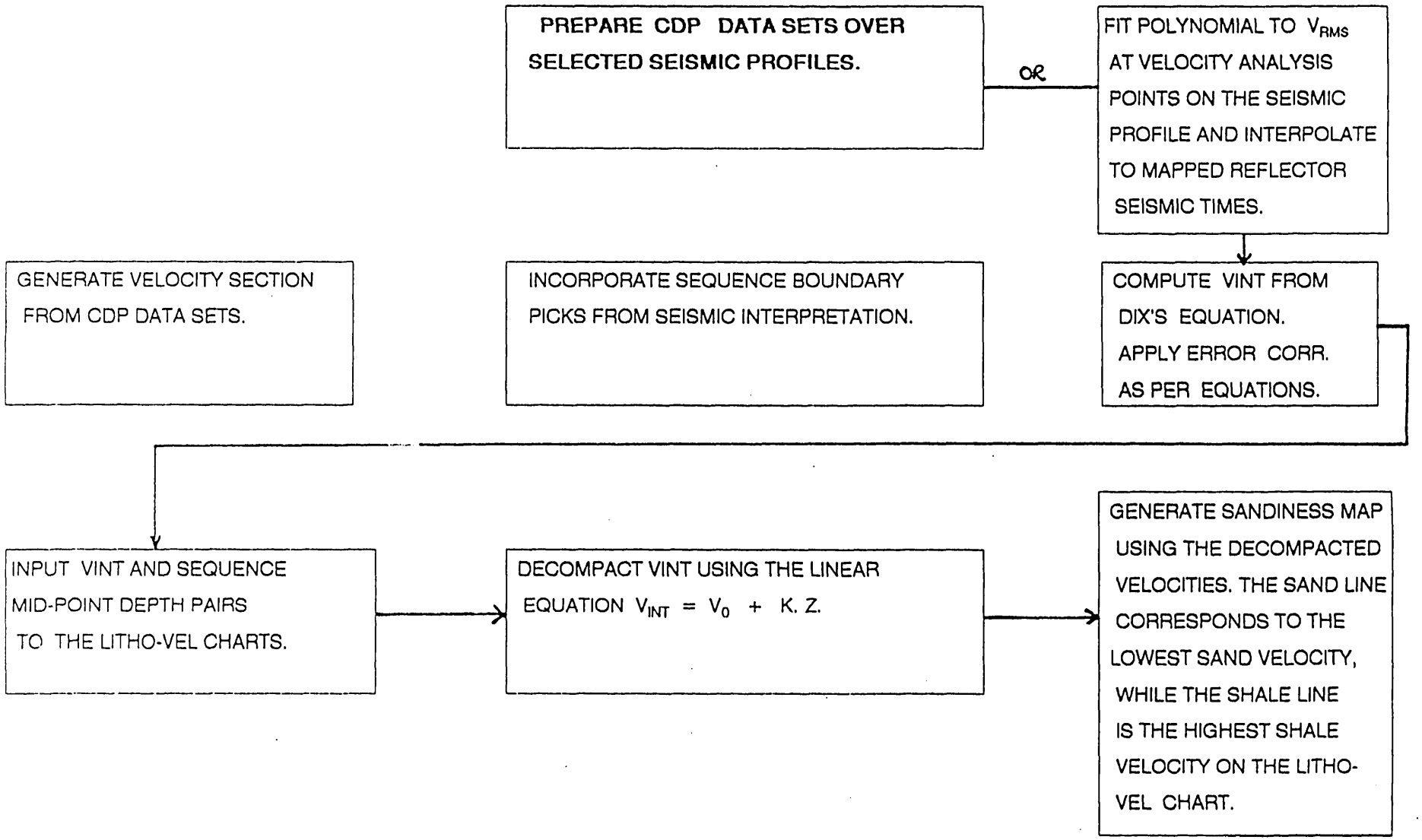

Fig.1.8e Modified flow diagram showing the sequence steps of stratigraphic velocity interpretation.

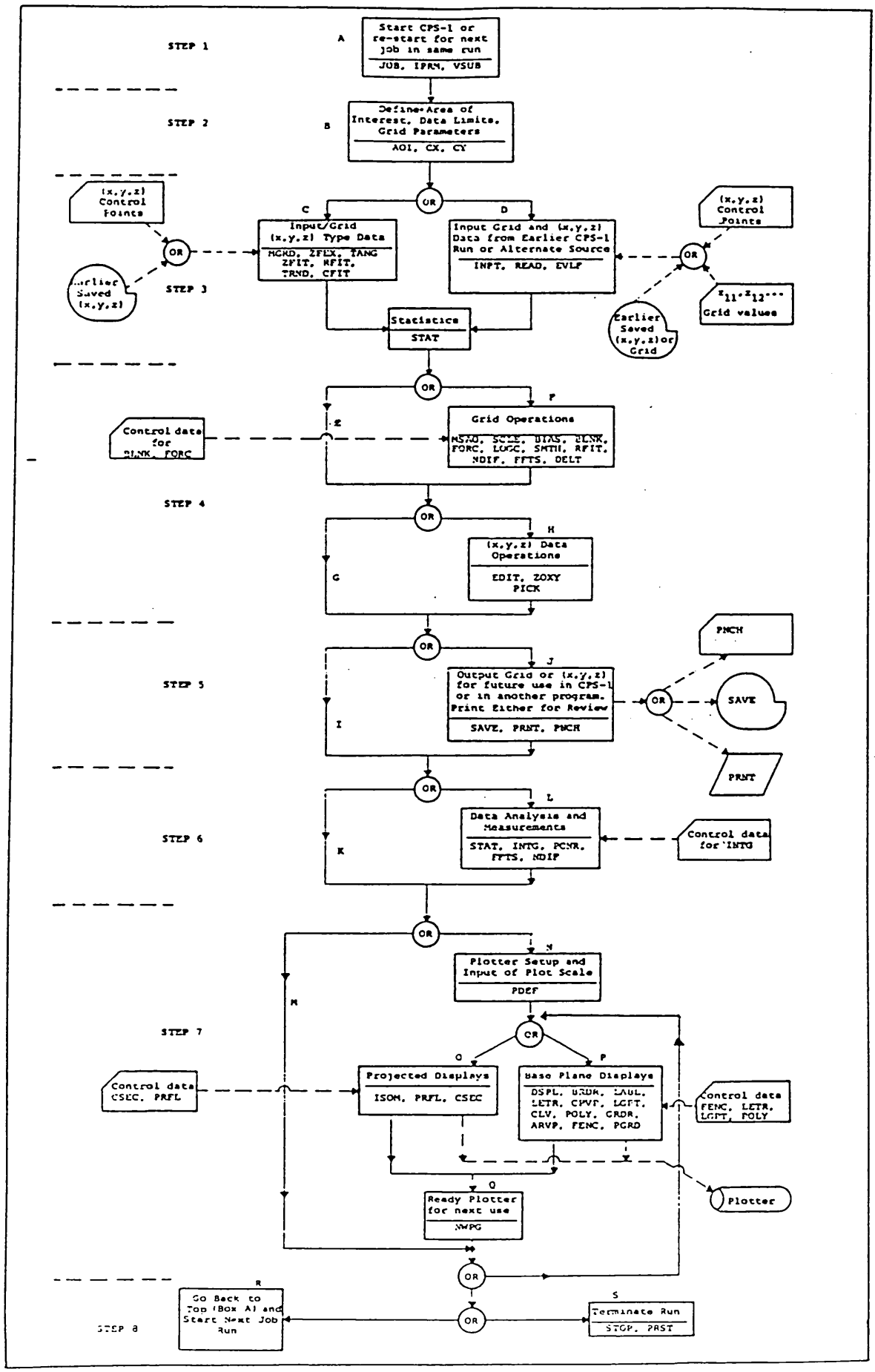

Logic Diagram for the Recommended CPS-1 Verb Program

Fig.1.9a Flow diagram showing the CPS-1 mapping software algorithm structure.

```
                    CPS-1 DIGITISING PACKAGE
                    ========================
Version PEH 1.02
                              Options

1. Digitise map of seismic lines. ( DIGIMAP )

2. Digitise seismic events/horizons. ( DEVNT )

3. Digitise fault polygons from map. ( DIGIFLT )

4. Generate CPS-1 files from map and event files. ( MASH )

5. Digitise a contour map. ( DIGICONT )

6. Digitise a spot height map. ( DIGISPOT )

7. Help.

8. Exit.

                              Option >
```

```
          MASH MAP AND SEISMIC HORIZON FILE GENERATOR

     1. Get a map file.

     2. Get one or more horizon/event files.

     3. Define the event to be used.

     4. Review the map file.

     5. Review a horizon/event file.

     6. Generate the output file.

     7. Help.

     8. Exit from the programme.

Option >
```

Fig.1.9b&c CPS-1 display listing.

LIST OF FIGURES

FIGURE	TITLE	PAGE
1.1	Seismic data base and coverage map	.....
1.2	Field recording and processing parameters	.....
1.3a	Typical roll-over structure	.....
1.3b	Stratigraphic play in slope channel fill	.....
1.3c	Truncation trap over paralic sequences	.....
1.4a	Terminology used in sequence boundary delineation	.....
1.4b	Schematic diagram of sequence types	.....
1.5	Typical GMA synthetic seismogram display	.....
1.6	Stratigraphic sequences and sea level changes	.....
1.7a	Reflection configurations and facies terminology	.....
1.7b	External geometry of some seismic facies	.....
1.7c	Parallel/divergent seismic types and modifications	.....
1.7d	Progradational facies types	.....
1.7e	Mounded and drape facies types	.....
1.7f	Onlap and fill seismic facies types	.....
1.8a	Velsect data analysis	.....
1.8b	V_{int} presentation using GEM	.....
1.8c	Flow diagram of velocity interpretation	.....
1.8d	Polynomial fit of a stacking velocity curve	.....
1.8e	Modified flow diagram	.....
1.9a	Flow chart for CPS1 mapping package	.....
1.9b&c	CPS1 display listings	.....
		.....
2.1	A depositional mound	.....
2.2a	Anomaly at the foot of the progradational toe	.....
2.2b	Anomaly due to slump on progradational slope	.....
2.2c	Anomaly with a predominant axis or trend	.....
2.2d	The chaotic and disruptive facies anomaly	.....
2.2e	Rubble Bed type anomaly	.....
2.2f	Anomaly with parallel reflectors	.....
2.2g	Stratigraphic anomaly distribution map (Rubble Beds)	.....
2.2h	Stratigraphic anomaly distribution map(Qua Iboe)	.....
2.3a	Horizontal resolution; the Fresnel zone	.....
2.3b	Nomogram for deriving horizontal resolution	.....
2.3c	Model of sand body size and relationship to resolution	.....

2.3d	Stratigraphic anomaly; line 82-349	.....
2.4a	The CDP method as a focussing device	.....
2.4b	Log-Log plot of interval velocity error	.....
2.4c	Error in $V_{int} versus V_{rms}$	.....
2.5a	Qua Iboe Litho-velocity chart	.....
2.5b	A simplified error analysis model	.....
3.1	Regional tectonic framework during the Cenozoic	.....
3.2	Tectonic setting of the eastward extension of the delta	.....
	and it's relationship with the Rio del Rey basin	.....
3.3a	The zone of shale diapirs, S.E. Niger Delta	.....
3.3b	Schematic section across the zone of shale diapirs	.....
3.4a	Hypothetical section showing the sedimentary bulge	.....
3.4b	Regional seismic section across the delta(west)	.....
3.4c	Regional seismic section across the delta(east)	.....
3.5	Canyon incision of the Niger continental slope	.....
3.6a	Stratigraphic evolution of the Niger Delta	.....
3.6b	Major formation units of the study area	.....
3.7	Seismic Line 82-251	.....
3.8	Seismic Line 82-279	.....
3.9	Development of the eastern delta	.....
3.10a	Akata shale formation type section	.....
3.10b	Biafra member type section	.....
3.10c	Rubble Bed member type section	.....
3.10d	Qua Iboe member type section	.....
3.10e	D-1 type section	.....
3.10f	Benin formation type section	.....
3.11a	The Stratigraphic column	.....
3.11b	Seismic Line 82-149	.....
3.11c	Seismic line 82-231	.....
3.11d	Seismic line 82-377	.....
3.12	Regional cross-section Evamy *et al.*(1978)	.....
3.13a	Megaunits and associated synsedimentary faults	.....
3.13b	Development of simple and complex growth faults	.....
3.14a,b,c	Structures at the TIBU, BQI and QUA5 levels	.....
3.15a	Terracing at the BQI level(line 82-163)	.....
3.15b	Erosional anticline at the BRB level(line 82-110)	.....
3.15c	Erosional anticline at the TIBU level(line 82-190a)	.....
3.16	Rollover anticline (shale mass supported)Line 82-106	.....

3.17	Rollover anticline with landward dips	.....
3.18	Rollover anticline with seaward dips	.....
3.19a	Shale mass structure flank	.....
3.19b	Shale diapir; line A-23	.....
3.20	Shale mass structure crestal	.....
3.21	Structure at the southeastern block	.....
3.22	Annealment type structure	.....
3.23	Structure at the Qua4 level	.....
4.1a	Depositional processes and unconformity types	.....
4.1b,c	System tracts	.....
4.2	Canyons and their relationship to shelf(line 259)	.....
4.3a	Seismic line 82-66 (the older sequences)	.....
4.3b	Seismic line 82-88a	.....
4.3c	Synthetic seismogram fit for older sequences	.....
4.4a	Line 82-212a	.....
4.4b	Synthetic seismogram fit for LBIBR	.....
4.5a	Line 82-393a	.....
4.5b	Line 82-393	.....
4.6a	Line 82-381	.....
4.6b	Line 82-301	.....
4.7a	Line 82-353	.....
4.7b	Line 82-180	.....
4.7c	Synthetic seismogram fit for TIBU	.....
4.8a	Line 82-107(BIBBEN horizon)	.....
4.8b	Line 82-133(thinning BIBBEN)	.....
4.9a	Line 82-142(Rubble canyon)	.....
4.9b	Line 82-88a(Intra Rubble unconformities)	.....
4.9c	Synthetic seismogram fit for BRB	.....
4.10a	Line 82-261	.....
4.10b	Line 82-285	.....
4.10c	Line 82-106	.....
4.10d,e	Synthetic seismogram fit for BQI	.....
4.11a	Intra Qua Horizon definition	.....
4.11b	Qua Iboe progradation and the turbidite toe	.....
4.11c	Line 82-203	.....
4.11d	Qua3; line 82-361	.....
4.11e	Condensed sections	.....
4.12	The Pleistocene canyon	.....

4.13a	Line 82-269; system tracts of the study area	.....
4.13b,c	Lower system tracts in different tectonic settings	.....
4.13d	Line 82-251	.....
4.13e	Line 82-391	.....
5.1a,b	The Haq *et al.*(1987) and the Vail *et al.*(1977) curves	
5.2a,b,c	The eustatic curves from 1977 to 1987	.....
5.3a,b	Correlation of coastal onlap curves	.....
5.4	Correlation of the Moore *et al.* and Haq *et al.* curves	.....
5.5	Late Neogene Oxygen-18 curves	.....
5.6a	Comparison of Vail's curve to the Oxygen-18 curve	.....
5.6b	Model of turbidite deposition during sea level change	.....
5.7a,b	Chronostratigraphic chart line 82-197	.....
5.8a,b	Chronostratigraphic chart line 82-259	.....
5.9a,b	Chronostratigraphic chart line 82-373	.....
5.10a,b,c,d,e	Sequence correlation summary	.....
5.11a,b,c	Mobility diagrams	.....
5.12a,b&c	Lines 82-197, 82-259, and 82-373	.....
6.1a,b&c	Biafra structural and stratigraphic evolution	.....
6.2	Representative seismic facies types	.....
6.3a&b	Lines 82-183 & 82-86	.....
6.4	Map showing the limit of truncation of BIBBEN	.....
6.5	Line 82-66	.....
6.6	Line 82-211	.....
6.7a,b,c	Characteristic log response of the Older sequences	.....
6.8a	Composte facies distribution map of older sequences	.....
6.8b&c	Paleoenvironment curves for the Older sequences	.....
6.9	Facies distribution map of LIBR	.....
6.10a&b	The Lower Intra Biafra Rubble	.....
6.11a	Facies distribution of SEQ.BS2	.....
6.11b&c	lines 82-339 and 82-220a	.....
6.12a	Line 82-283	.....
6.12b	Line 82-106	.....
6.12c	Line 82-339	.....
6.12d	Line 82-377	.....
6.13a	Facies distribution of UIBR	.....
6.13b	Paleoenvironment curve for UIBR	.....
6.14a&b	High amplitude anomalies in UIBR	.....

6.15	Line 82-132a; SEQ.BS4	.....
6.16a	Facies distribution for SEQ.BS4	.....
6.16b	Paleoenvironment curve for SEQ.BS4	.....
6.17a	Sand percentage map of the Biafra	.....
6.17b	Interval velocity map of the Biafra	.....
6.18	Juxtaposition of the av. int. vel. map and sand % map	.....
6.19a	Litho-velocity chart for Biafra	.....
6.19b	Upper Intra Biafra Rubble velocity analysis	.....
6.20	A composite map of the delta front for Biafra sequences	.....
7.1a	Line 82-106; BRB as a PGM feature	.....
7.2	Line 82-142	.....
7.3a	Unit 1 Rubble; Line 82-287	.....
7.3b&c	Unit 2 Rubble(82-387)	.....
7.4	Distribution of Unit 1 Rubble	.....
7.5	Distribution of Unit 2 Rubble	.....
7.6	Seismic facies of the Rubble Beds	.....
7.7	Facies distribution of the Rubble Beds	.....
7.8a	Line 82-118; the chaotic facies	.....
7.8b	Line 82-253; the proximal facies	.....
7.8c	Line 82-197; mounded proximal facies	.....
7.8d	Line 82-291; mounded onlap facies	.....
7.8e	Line 82-168a; the distal facies	.....
7.8f	Line 82-216a; the prograding facies	.....
7.9a	Rubble Bed depositional model	.....
7.9b	Mechanisms for Rubble Bed formation	.....
7.10a	Rockfall	.....
7.10b	Development of channel system(82-251)	.....
7.11a	The western Rubble Bed canyon (line 82-142)	.....
7.11b	The eastern canyon	.....
7.11c	The eastern canyon (line 82-337)	.....
7.12	Distribution of Stratigraphic anomalies	.....
7.13	Litho-velocity chart for the Rubble Beds	.....
7.14	Distribution of sand build-ups based on velcity	.....
7.15a&b	The northern anomalies	.....
7.15c	The southeastern anomaly	.....
8.1	Qua Iboe shale limit	.....
8.2a&b	Lines 82-279 and line 82-185	.....

8.3	Composite of shelf breaks	.....
8.4	Representative facies types	.....
8.5a	Structural map of Horizon QUA2	.....
8.5b	Isochron map of QS1	.....
8.5c	Facies distribution map QS1	.....
8.6a&b	Lines 82-201 and 82-409	.....
8.6c	Facies distribution map of QS2	.....
8.6d	Composite anomaly map of QS1 and QS2	.....
8.7a	Line 82-229	.....
8.7b	Distribution map of seismic mounds	.....
8.7c	Line 82-231	.....
8.7d	The prograding terrace, line 82-271	.....
8.8a	Structure map of QUA4	.....
8.8b	Facies distribution map of QS3	.....
8.8c	Line 82-212a	.....
8.9	The Lower Qua Iboe depositional model	.....
8.10a	Paleodepth estimation from progradation	.....
8.10b	Environmental depth zones	.....
8.10c	Process continuum in deep sea sedimentation	.....
8.10d&e	Seismic evidence of slumping (line 82-251)	.....
8.11	Seismic indicators of Turbidite sequences	.....
8.12a	Line 82-154s	.....
8.12b	Line 82-146b	.....
8.12c	Line 82-251	.....
8.12d	Line 82-267	.....
8.13a	Proximal facies illustration(82-114)	.....
8.13b	Mounded proximal facies	.....
8.13c	Line 82-291	.....
8.13d	Proximal onlap(line 82-409)	.....
8.13e	Proximal Uplap(line 82-353)	.....
8.14	Formation of seismic mounds(model)	.....
8.15	Composite of the distribution of seimic mounds	.....
8.16a	Build-up of the central anomaly	.....
8.16b	Build-up of the southwest anomaly	.....
8.16c	Build up of the northwest anomaly	.....
8.16d	The centre-west anomaly	.....
8.16e	The centre-east(1&2)	.....
8.16f	The eastern anomaly	.....
8.17	Line 82-142	.....

8.18a	Mounded fan complex facies(line 82-182a)	.....
8.18b	Depositional model of stacked channels	.....
8.19a	Line 82-174	.....
8.19b	Line 82-185	.....
8.20	Line 82-154b	.....
8.21a	Sheet facies: line 82-349	.....
8.21b	Line 82-106	.....
8.22	Line 82-220a	.....
8.23	Sigmoidal facies: line 82-369	.....
8.24	Oblique facies: line 82-429	.....
8.25a	Litho-Velocity chart	.....
8.25b	Interval velocity map	.....
8.26a	Interpreted litho-vel chart	.....
8.26b	Sandiness map	.....
8.26c	Coefficient of heterogeneity map	.....
8.27a	Facies distribution map QS4	.....
8.27b	Line 82-86	.....
8.28a	Line 82-215	.....
8.28b	Line 82-289	.....
8.29a	Line 82-345	.....
8.29b	Line 82-169	.....
8.29c	Facies distribution map of QS5	.....
8.29d	Line 82-385	.....
8.30	Facies distribution of QS7	.....
8.31	Line 82-341	.....
8.32a&b	The chaotic facies	.....
8.33	Coastal onlap on line 82-369	.....
8.34a&b	The Pleistocene canyon	.....
8.35	Extent of the canyon	.....
8.36	Line 82-223	.....
9.1	Turbidites and sea level changes	.....
9.2a&b	Three end-member fan classification	.....
9.3a&b	Comparison of modern and ancient fans	.....
9.4a	The Mississippi submarine fan model	.....
9.4b	The Submarine ramp model	.....
9.4c	Facies comparison, ramp model versus ancient model	.....
9.4d	The shelf-Slope model	.....
9.5a	The Lower Qua Iboe fan model	.....

9.5b	Map of seismic mounds	.....
9.6	Seismic criteria for fan recognition	.....
9.7	Relationship between fan width and valley size	.....
9.8a&b	The northern feeder canyon	.....
9.8c	Seismic example of a turbidite fan	.....
9.9a&b	Slope models	.....
9.10	The Texas-Louisiana slope	.....
9.11	The Hackberry Embayment	.....
9.12a&b	Stratigraphic setting of Hackberry onlap slope system	.....
9.13	Depositional overview of the Hackberry slope system	.....
9.14	Depositional setting of the Hackberry	.....
9.15	Canyon fills of the Niger Delta	.....
9.16	Canyon fills of the Gulf coast	.....
9.17	The submerged shelf margin	.....
9.18	Shelf margin deltas during lowstand of sea level	.....
9.19	Progradation and eustatic sea level changes	.....

CHAPTER ONE

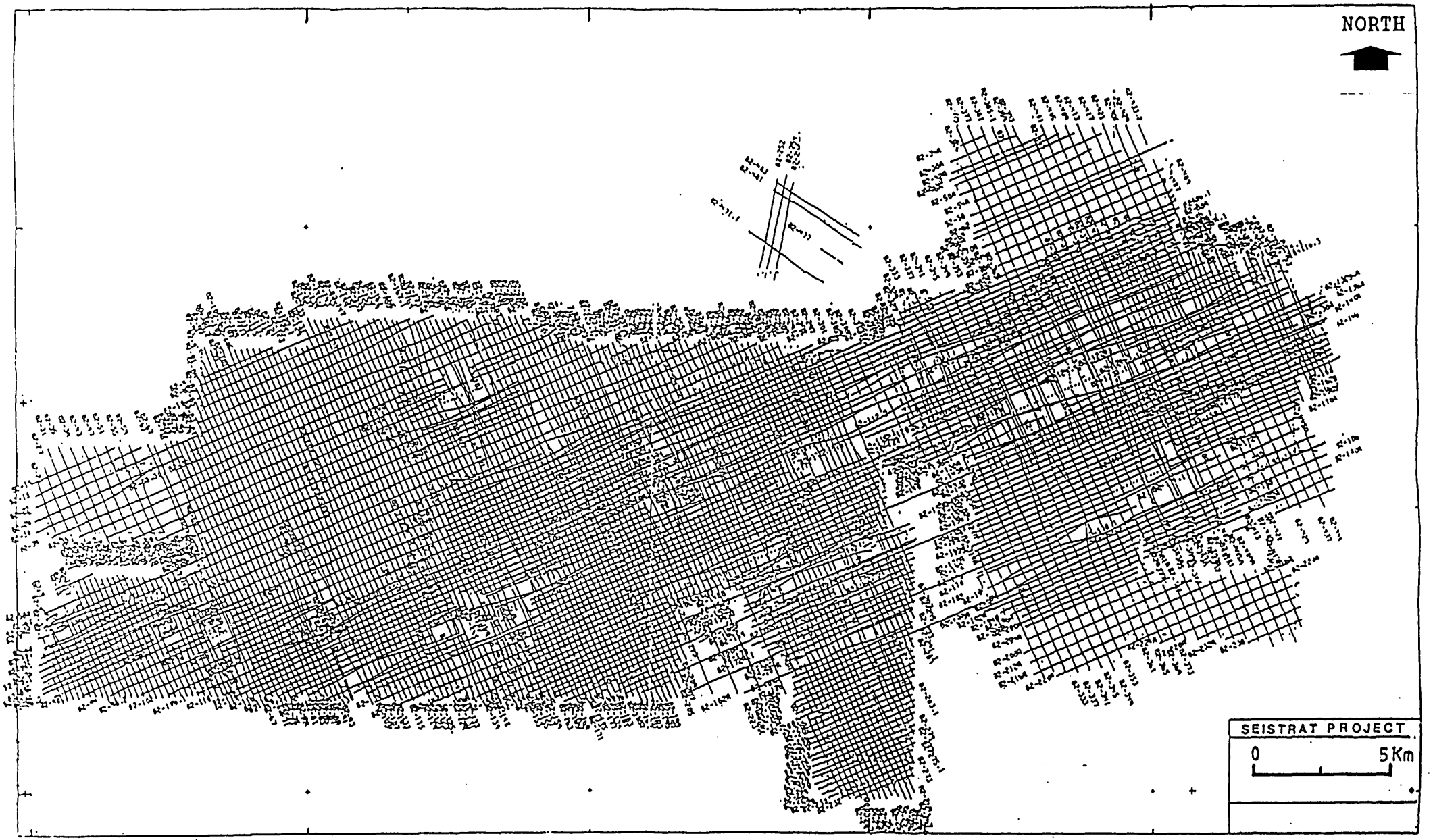

Fig.1.1 Seismic data base and coverage map.

SEFEL GEOPHYSICAL
SEISMIC DATA PROCESSING
LONDON ENGLAND

DATE PROCESSED JULY 1982
REEL NUMBER
CONTRACT NUMBER 840

FIELD RECORDING

RECORDED BY M.V. HANS EGEDE
DATE 13TH APRIL 1982 SYSTEM LITTON 888
FORMAT SEG C 1600 B.P.I. GAIN I.F.P.

ENERGY SOURCE

TYPE BOLT. PAR AIR GUN
ARRAY 1X8. 1X6 DEPTH 7M

STREAMER

LENGTH 1800M NO. TRACES 72
DEPTH 10M AVERAGE GROUP INTERVAL 25M
ARRAY 16 GEOPH/TR OVER 25M

PARAMETERS

RECORDING FOLD 36 S.P. SPACING 25M
SAMPLE INTERVAL 2MS RECORD LENGTH 4 SEC
RECORDING FILTER LO-6HZ. 18DB/OCT. HI-125HZ 72DB/OCT.

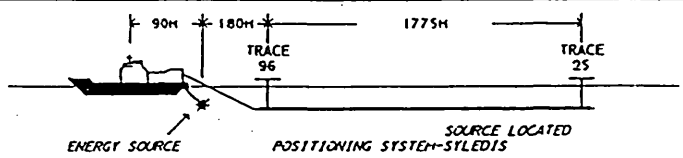

DIGITAL PROCESSING

SEQ	PROCESS	PARAMETERS
1	DEMULTIPLEX	SUB-SAMPLE 2TO4MS ANTI-ALIAS FILTER APPLIED
2	CDP SORT	36 FOLD
3	DEPHASE	INSTRUMENT FILTER RESPONSE COMPENSATION
4	GAIN RECOVERY	APPLING INVERSE AMPLITUDE DECAY CURVES
5	DECONVOLUTION	SEE BELOW
6	VELOCITY ANALYSIS	CVS EVERY 1.5 KM
7	NMO REMOVAL + MUTE	NMO CORRECTION AND STRETCH REMOVAL
8	HORIZONTAL STACK	
9	DECONVOLUTION	SEE BELOW
10	FILTER	BROAD PASS BAND FILTER (6-60HZ)
11	EQUALISATION	500MS WINDOWS 50% OVERLAP
12	MIGRATION	WAVE EQUATION MIGRATION
13	TV FILTER	SEE BELOW
14	EQUALISATION	WHOLE TRACE EQUALISATION
15	STATICS + DISPLAY	GUN AND CABLE DEPTH CORRECTIONS

ADDITIONAL PARAMETERS

DECON	* OPERATOR LENGTH	PREDICTIVE GAP	DERIVATION WINDOWS	APPLICATION WINDOWS
SEQ 5	200	24	N.T. 0-3000 MS	WHOLE TRACE
			F.T. 1700-4700 MS	WHOLE TRACE
SEQ 9	200	20	600-3600 MS	WHOLE TRACE

APPLICATION TIMES

FILTER	CUT OFF POINT	100% PASS POINT	100% PASS POINT	CUT OFF POINT	APPLICATION TIMES FOR SHOTPOINTS SPECIFIED		
					700MS OVERLAP		
SEQ13	7	10	55	65	1500MS		
	6	10	45	55	2800MS		
	5	10	35	45	3500MS		
	5	10	30	40	EOD		

ALL TIMES IN MILLISECONDS ALL FREQUENCIES IN HERTZ
FILTERS INTERPOLATED LINEARLY BETWEEN APPLICATION TIMES
APPLICATION TIMES INTERPOLATED LINEARLY BETWEEN SHOTPOINTS
*OPERATOR LENGTH GIVEN IS ACTIVE LENGTH ADD GAP FOR TOTAL LENGTH

SAMPLE RATE: 4MS: DATUM CORRECTION: 12MS TO MSL

SCALES: HORIZONTAL 1:11811 VERTICAL 3.75IN/SEC

RECORDING POLARITY: COMPRESSION RECORDED AS NEG ON TAPE

PROCESSING POLARITY: POSITIVE NO. GIVES BLACK PEAK

Fig.1.2 Field recording and processing parameters.

SEFEL GEOPHYSICAL
SEISMIC DATA PROCESSING
LONDON ENGLAND

DATE PROCESSED JULY 1982
REEL NUMBER
CONTRACT NUMBER 840

FIELD RECORDING

RECORDED BY M.V. HANS EGEDE
DATE 13TH APRIL 1982 SYSTEM LITTON 888
FORMAT SEG C 1600 B.P.I. GAIN I.F.P.

ENERGY SOURCE

TYPE BOLT. PAR AIR GUN
ARRAY 1X8. 1X6 DEPTH 7M

STREAMER

LENGTH 1800M NO. TRACES 72
DEPTH 10M AVERAGE GROUP INTERVAL 25M
ARRAY 16 GEOPH/TR OVER 25M

PARAMETERS

RECORDING FOLD 36 S.P. SPACING 25M
SAMPLE INTERVAL 2MS RECORD LENGTH 4 SEC
RECORDING FILTER LO-6HZ. 18DB/OCT. HI-125HZ 72DB/OCT.

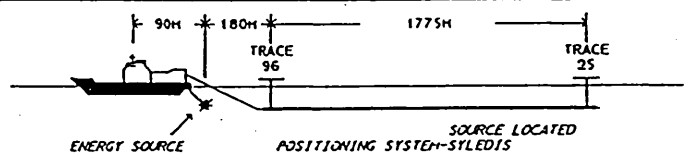

DIGITAL PROCESSING

SEQ	PROCESS	PARAMETERS
1	DEMULTIPLEX	SUB-SAMPLE 2TO4MS ANTI-ALIAS FILTER APPLIED
2	CDP SORT	36 FOLD
3	DEPHASE	INSTRUMENT FILTER RESPONSE COMPENSATION
4	GAIN RECOVERY	APPLING INVERSE AMPLITUDE DECAY CURVES
5	DECONVOLUTION	SEE BELOW
6	VELOCITY ANALYSIS	CVS EVERY 1.5 KM
7	NMO REMOVAL + MUTE	NMO CORRECTION AND STRETCH REMOVAL
8	HORIZONTAL STACK	
9	DECONVOLUTION	SEE BELOW
10	FILTER	BROAD PASS BAND FILTER (6-60HZ)
11	EQUALISATION	500MS WINDOWS 50% OVERLAP
12	MIGRATION	WAVE EQUATION MIGRATION
13	TV FILTER	SEE BELOW
14	EQUALISATION	WHOLE TRACE EQUALISATION
15	STATICS + DISPLAY	GUN AND CABLE DEPTH CORRECTIONS

ADDITIONAL PARAMETERS

DECON	* OPERATOR LENGTH	PREDICTIVE GAP	DERIVATION WINDOWS	APPLICATION WINDOWS
SEQ 5	200	24	N.T. 0-3000 MS	WHOLE TRACE
			F.T. 1700-4700 MS	WHOLE TRACE
SEQ 9	200	20	600-3600 MS	WHOLE TRACE

APPLICATION TIMES

FILTER	CUT OFF POINT	100% PASS POINT	100% PASS POINT	CUT OFF POINT	APPLICATION TIMES FOR SHOTPOINTS SPECIFIED		
					700MS OVERLAP		
SEQ13	7	10	55	65	1500MS		
	6	10	45	55	2800MS		
	5	10	35	45	3500MS		
	5	10	30	40	EOD		

ALL TIMES IN MILLISECONDS ALL FREQUENCIES IN HERTZ
FILTERS INTERPOLATED LINEARLY BETWEEN APPLICATION TIMES
APPLICATION TIMES INTERPOLATED LINEARLY BETWEEN SHOTPOINTS
*OPERATOR LENGTH GIVEN IS ACTIVE LENGTH ADD GAP FOR TOTAL LENGTH

SAMPLE RATE: 4MS: DATUM CORRECTION: 12MS TO MSL

SCALES: HORIZONTAL 1:11811 VERTICAL 3.75IN/SEC

RECORDING POLARITY: COMPRESSION RECORDED AS NEG ON TAPE

PROCESSING POLARITY: POSITIVE NO. GIVES BLACK PEAK

Fig.1.2 Field recording and processing parameters.

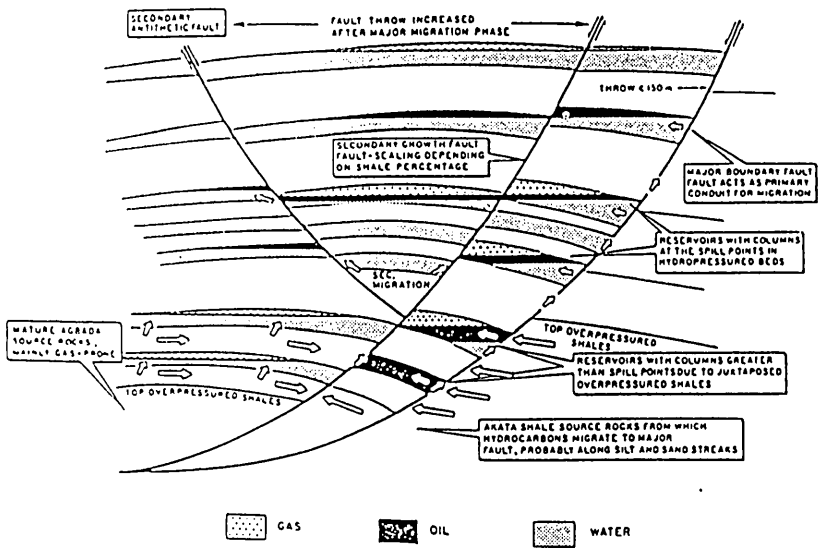

Fig.1.3a Typical roll-over structure.

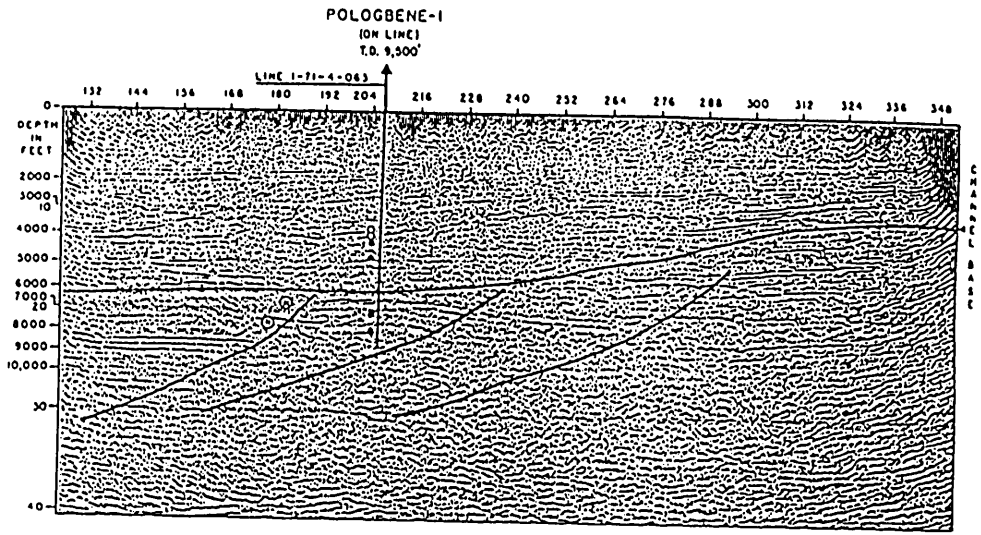

Fig.1.3b Stratigraphic play in slope channel fill.

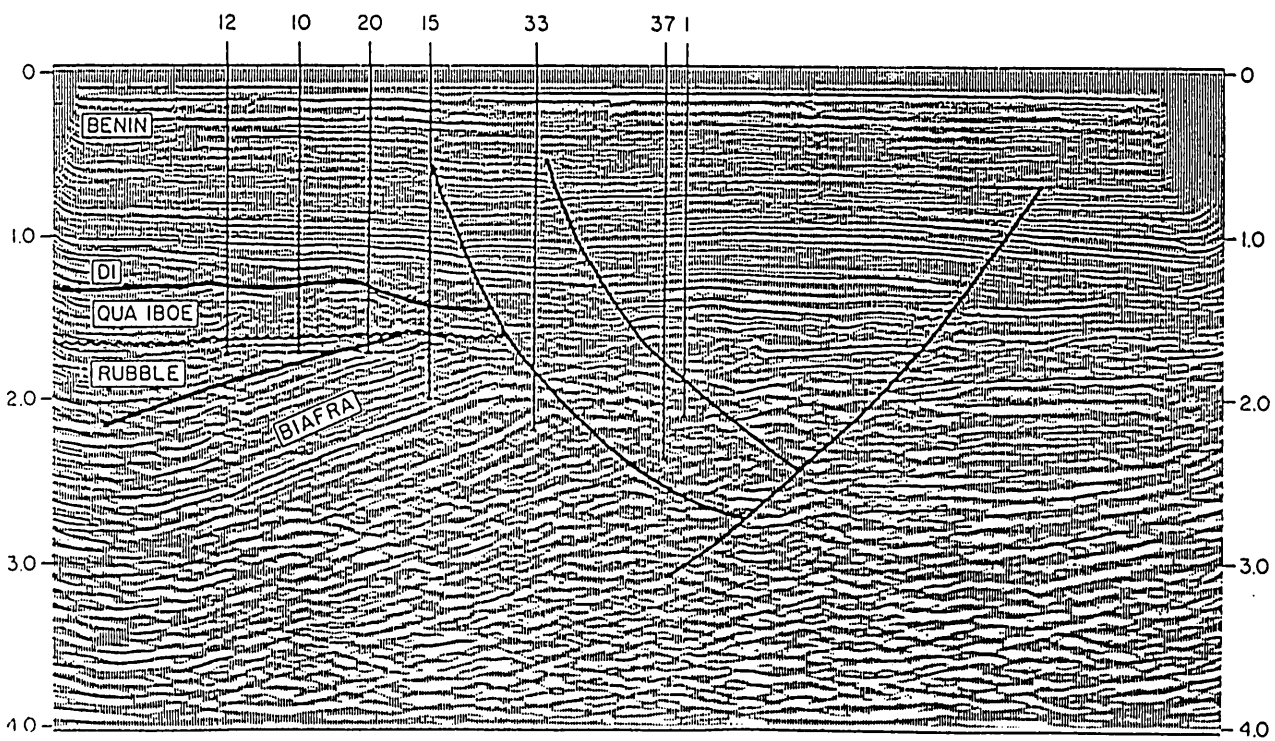

Fig.1.3c Truncation trap over paralic sequences.

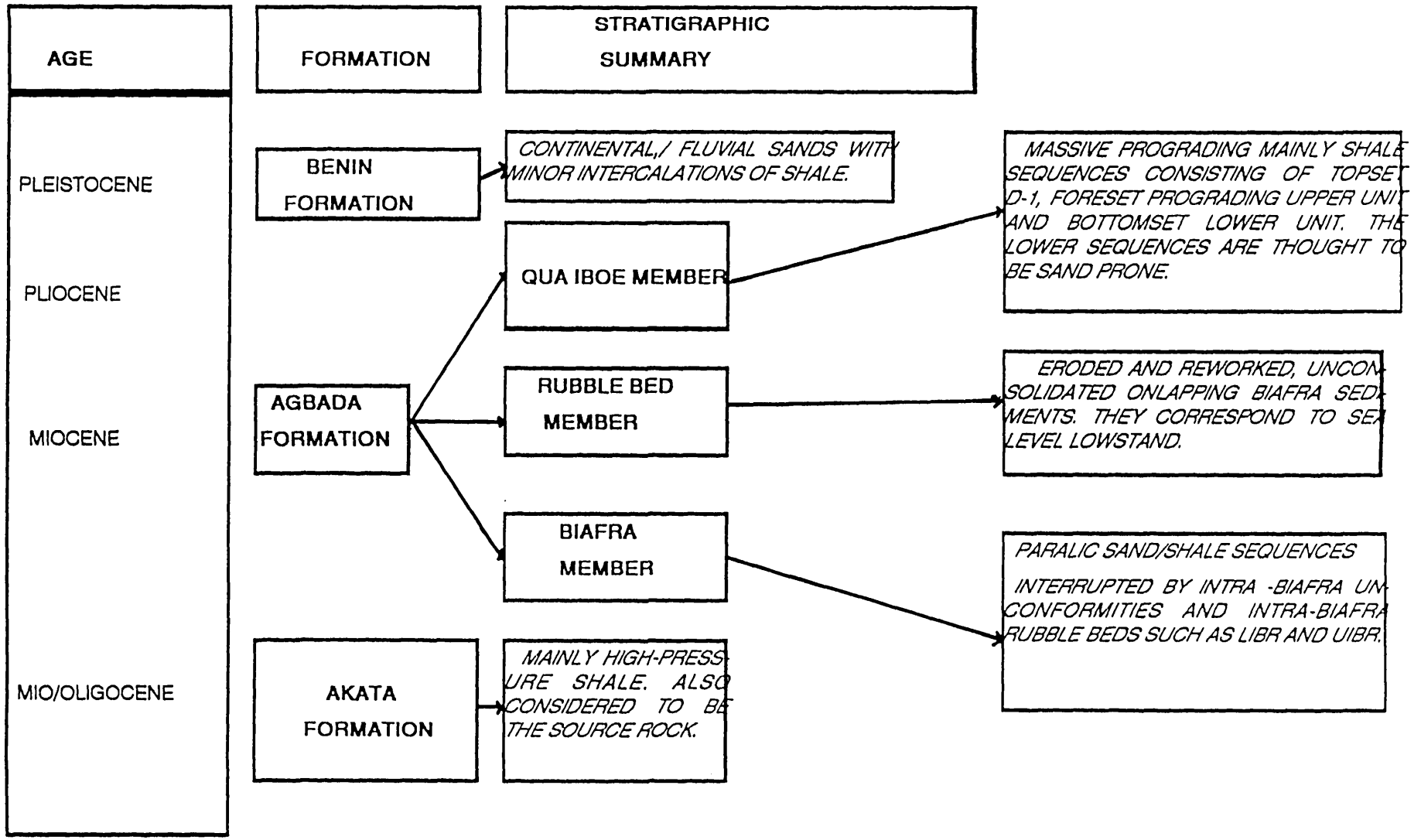

FIG.1.3d Litho-stratigraphic units of the study area.

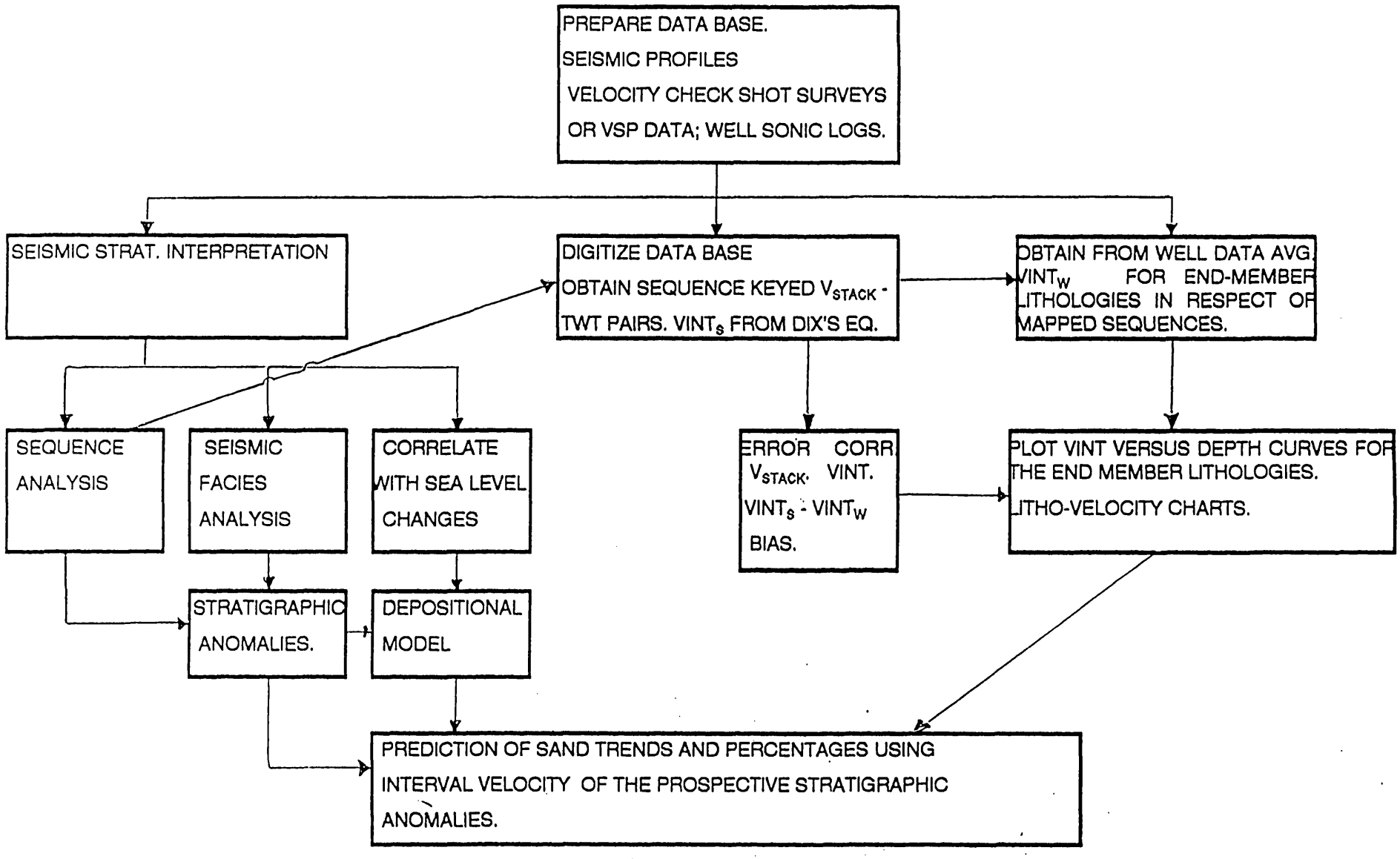

Fig.1.4a Flow diagram showing the methodology used.

SEISMIC SEQUENCE ANALYSIS. GLOSSARY OF TERMS (AFTER VAIL, 1988)

SEISMIC SEQUENCE

A seismic sequence corresponds to a depositional sequence seismically expressed by a gamut of seismic reflection patterns, formed as a result of the interaction between rates of eustacy, subsidence and sediment supply and is bounded by unconformities and their correlative conformities. They may be divided into TYPE 1 and TYPE 2 unconformities respectively.

TYPE 1 UNCONFORMITY:

Formed through subaerial exposure and concurrent subaerial erosion; and associated with basinward shift in coastal onlap and onlap over lying strata. i.e. R_F IS MORE THAN R_S AT DEP. SHORE LINE.

SYSTEM TRACTS: defined by their position within the sequence and are a linkage of contemporaneous depositional systems.

PARASEQUENCE: a relatively conformable succession of genetically related beds bounded by marine flooding surfaces (MFS).

TYPE 2 UNCONFORMITY:

is marked by subaerial exposure but shows no subaerial erosion associated with canyon cutting.

R_F IS LESS THAN R_S AT THE DEP. SHORE LINE.

SYSTEM TRACTS OF TYPE 1 SEQUENCES:

1. LOWSTAND S.T.
2. TRANSGRESSIVE S.T.
3. HIGHSTAND S.T.

Lowstand s.t. is the lowermost s.t. and in a basin with a shelf break may be subdivided into:

a. Basin-floor fan

b. Slope fan

c. Lowstand wedge.

Highstand s.t. is an upper s.t. occuring commonly on the shelf in both type 1 and type 2 sequences.

*****NOTE***

In the accompanying text, the terms LOWSTAND S.T. and HIGHSTAND S.T. have been substituted with LOWER S.T. & HIGHER S.T. respectively. This is because the terms lowstand and highstand by definition do not imply a unique period of time or position on a cycle of eustatic or relative sea level change. (Vail, 1988).

Figures overleaf show the schematic diagrams of the sequence types in this study.

SYSTEM TRACTS OF TYPE 2 SEQUENCES:

1. SHELF MARGIN S.T.
2. TRANSGRESSIVE S.T.
3. HIGHSTAND S.T.

Shelf margin s.t. is the lowermost s.t. associated with type 2 sequence boundary, commonly progradational and /or aggradational, the top of which is a transgressive surface.

Transgressive s.t. is considered the middle s.t. the top of which is a downlap surface.

Fig.1.4b Sequence boundary definitions and glossary of terms (after Vail, 1988).

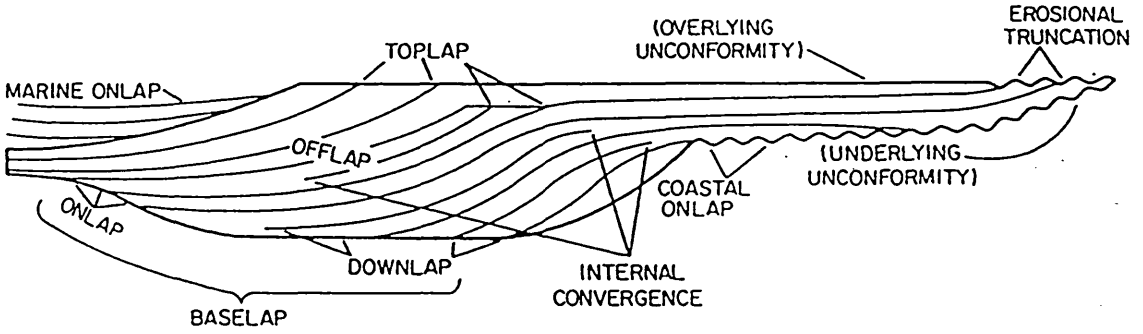

SEQUENCE STRATIGRAPHY
BLOCK DIAGRAM
SHOWING SEQUENCES, SYSTEMS TRACTS AND LITHOFACIES

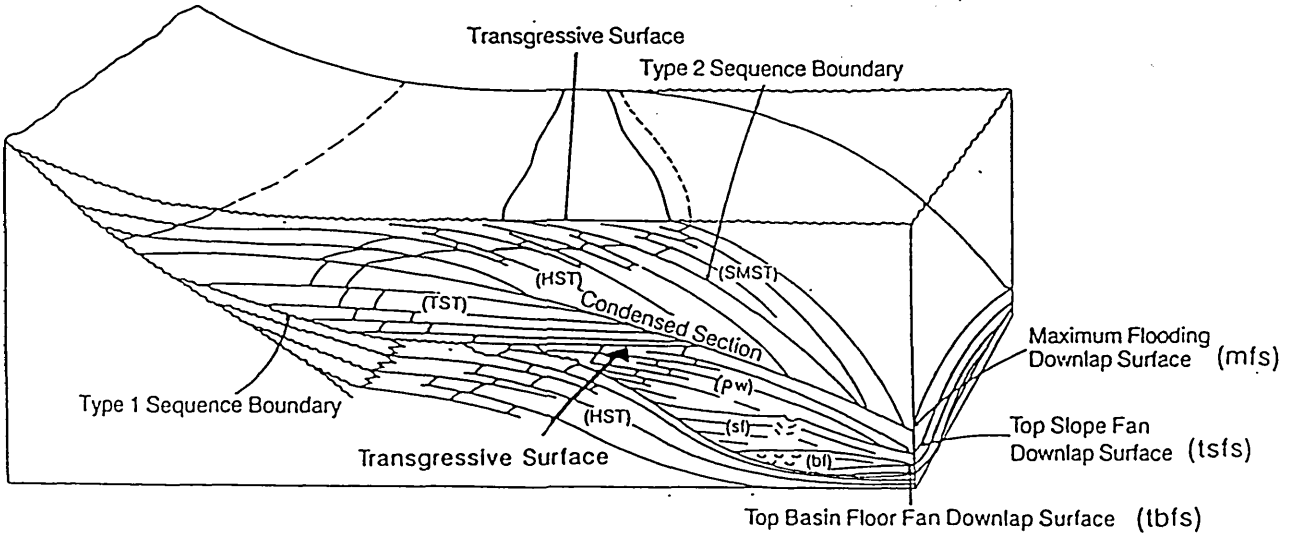

SILICICLASTIC LITHOFACIES

Fluvial	Coastal	Nearshore Sands	Marine Muds	Deep Marine Sands	Turbidite Mudstones
Alluvial Fans and Meandering Streams	or Delta Plain	Marine			
Braided Streams		Estuarine, Tidal			

Fig.1.4c Schematic diagram of sequence types.

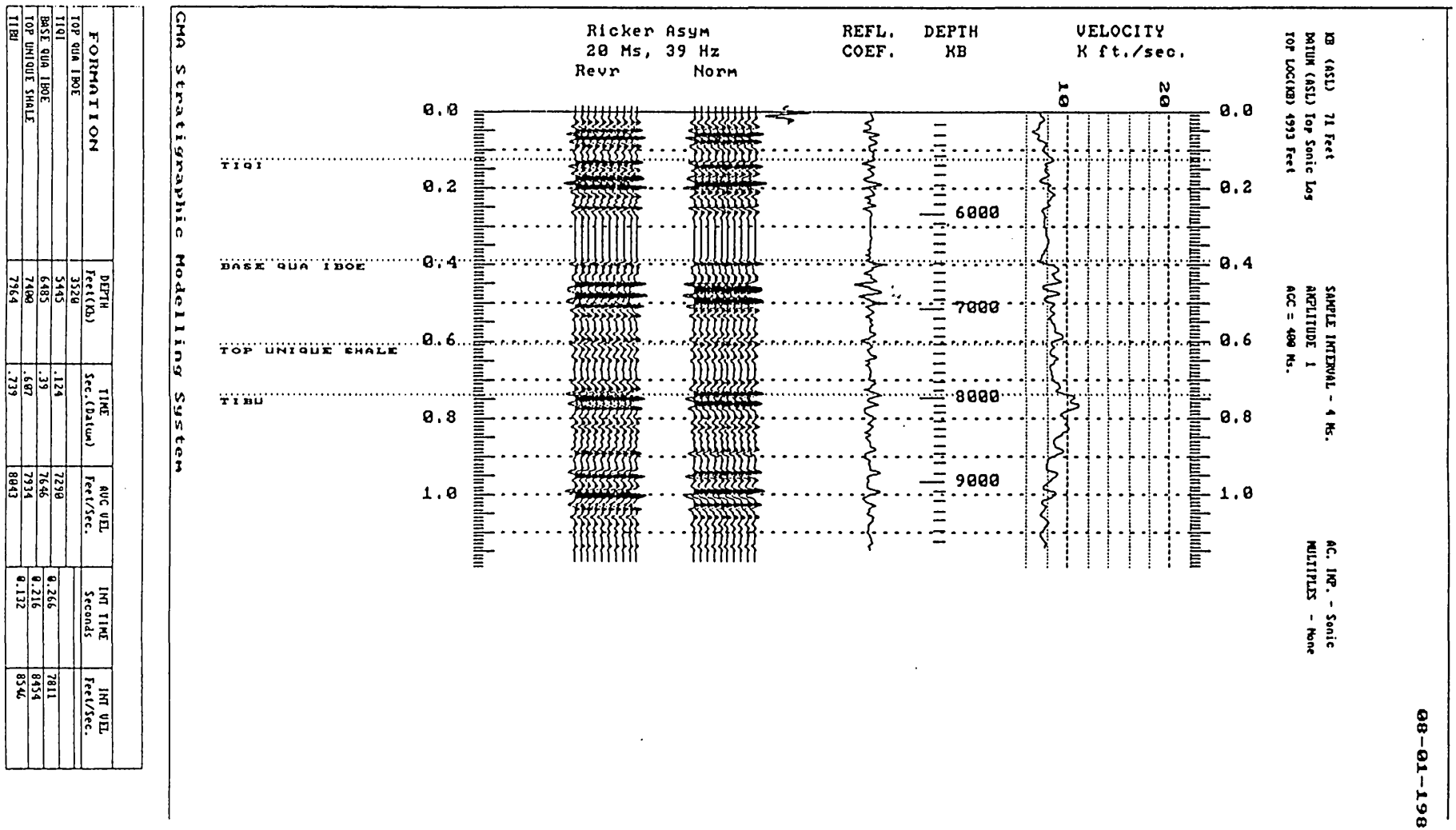

FORMATION	DEPTH Feet(Kb)	TIME Sec.(Datum)	AVG VEL Feet/Sec.	INT TIME Seconds	INT VEL Feet/Sec.
TOP QUA IBOE	3528				
TIQI	5445	.124	7298		
BASE QUA IBOE	6485	.39	7646	0.266	7811
TOP UNIQUE SHALE	7400	.687	7934	0.216	8454
TIBU	7964	.739	8043	0.132	8546

Fig.1.5 Typical GMA synthetic seismogram presentation.

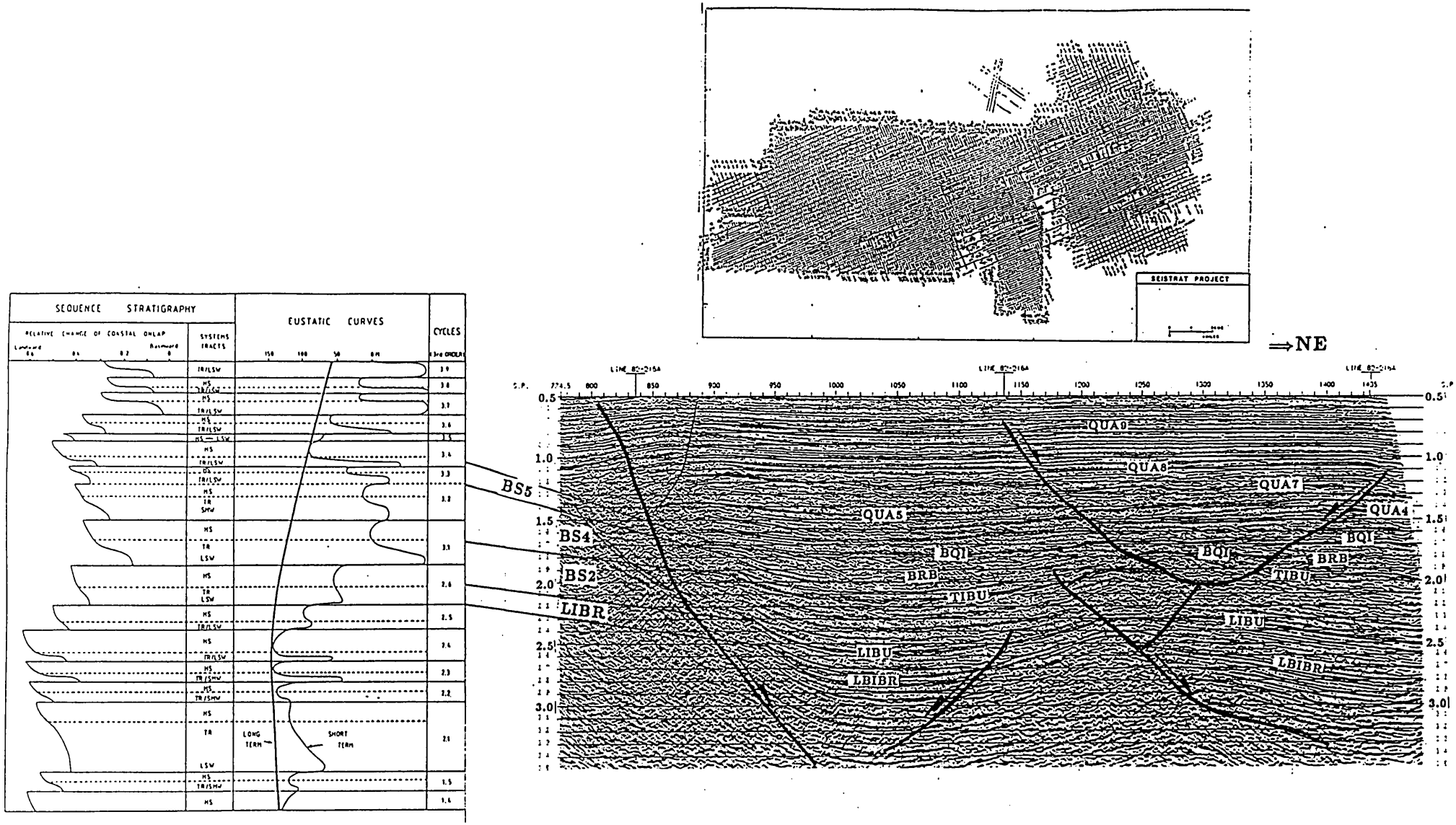

Fig.1.6 Seismic line 82-216a showing the correlation of stratigraphic sequences mapped with sea level change using the Haq *et al.*(1987) curve.

REFLECTION TERMINATIONS (AT SEQUENCE BOUNDARIES)

- LAPOUT
  - BASELAP
    - ONLAP
    - DOWNLAP
  - TOPLAP
- TRUNCATION
  - EROSIONAL
  - STRUCTURAL
- CONCORDANCE
  - (NO TERMINATION)

REFLECTION CONFIGURATIONS (WITHIN SEQUENCES)

- PRINCIPAL STRATAL CONFIGURATION
  - PARALLEL
  - SUBPARALLEL
  - DIVERGENT
  - PROGRADING CLINOFORMS
    - SIGMOID
    - OBLIQUE
    - COMPLEX SIGMOID-OBLIQUE
    - SHINGLED
    - HUMMOCKY CLINOFORM
  - CHAOTIC
  - REFLECTION-FREE
- MODIFYING TERMS

EVEN	HUMMOCKY
WAVY	LENTICULAR
REGULAR	DISRUPTED
IRREGULAR	CONTORTED
UNIFORM	
VARIABLE	

EXTERNAL FORMS (OF SEQUENCES AND SEISMIC FACIES UNITS)

- SHEET
- SHEET DRAPE
- WEDGE
- BANK
- LENS
- MOUND
- FILL

Fig.1.7a Reflection configurations and facies terminology.

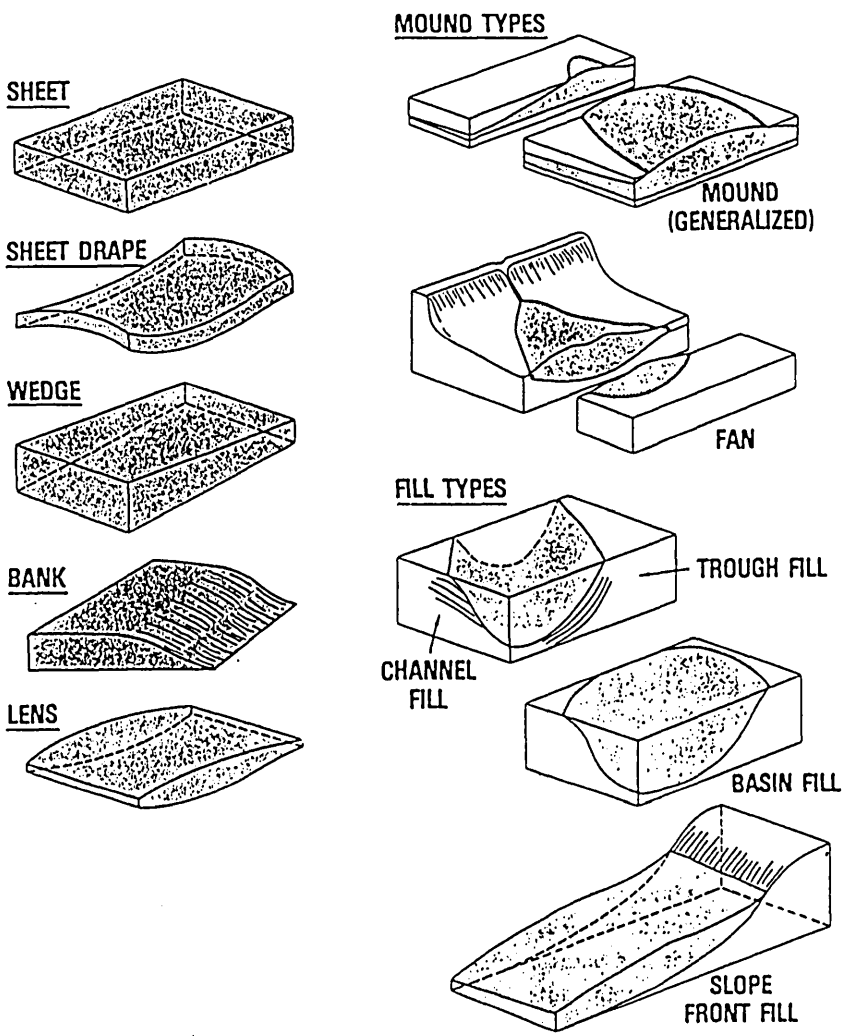

Fig.1.7b External geometry of some seismic facies.

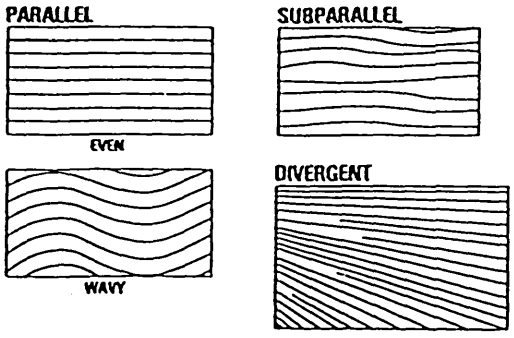

Parallel, subparallel and divergent seismic reflection configurations. From Mitchum et al. (1977).

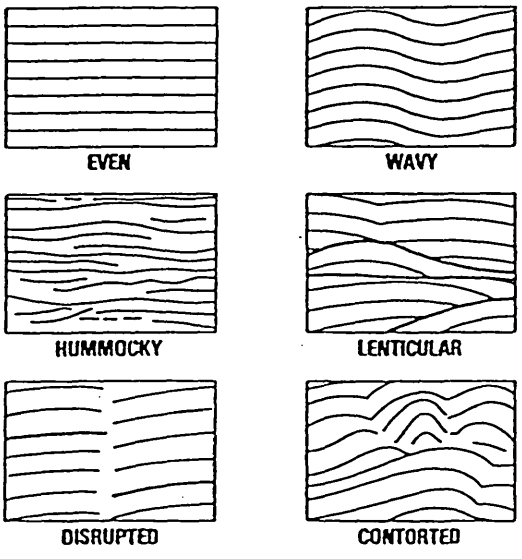

Some modifying seismic reflection configurations. From Mitchum et al. (1977).

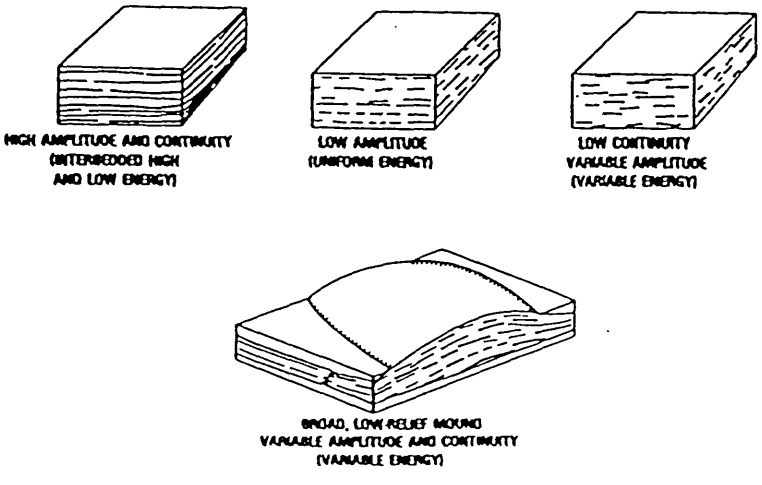

Fig.1.7c Parallel/divergent seismic seismic facies.

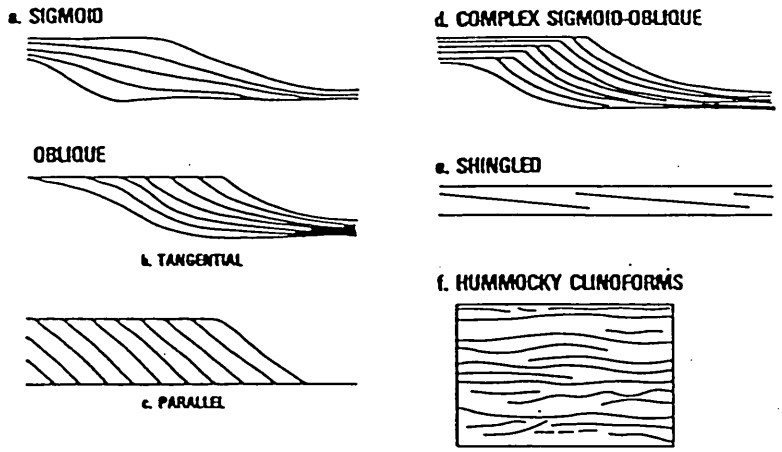

Progradational seismic reflection patterns. From Mit chum et al. (1977).

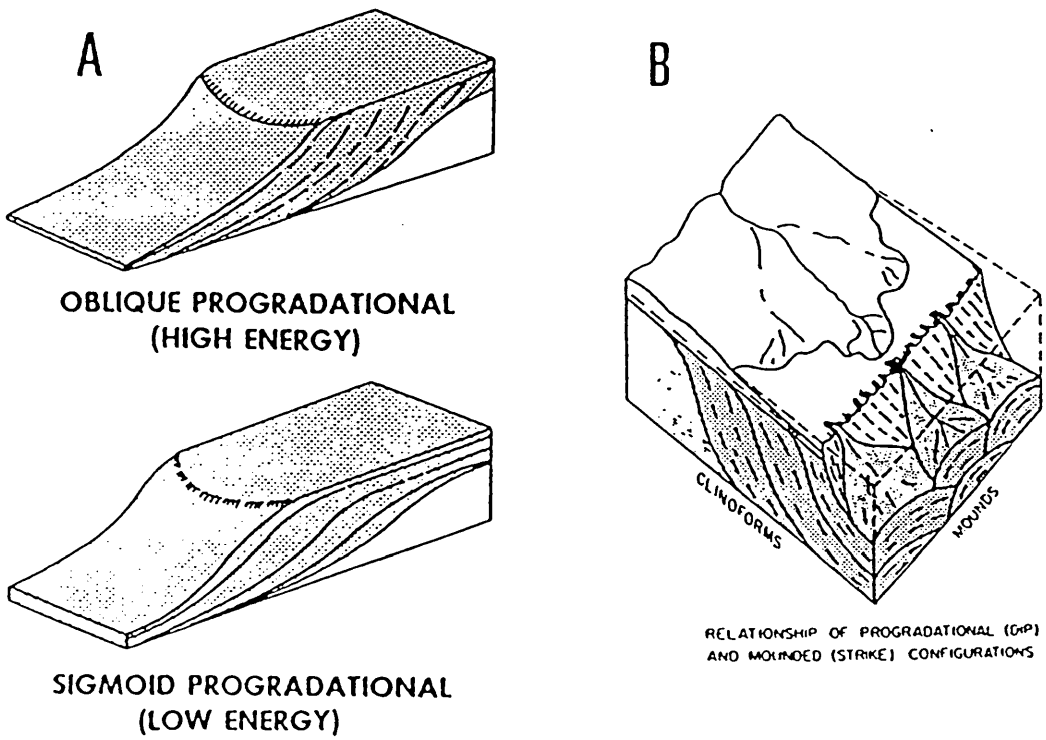

Fig.1.7d Progradational facies types.

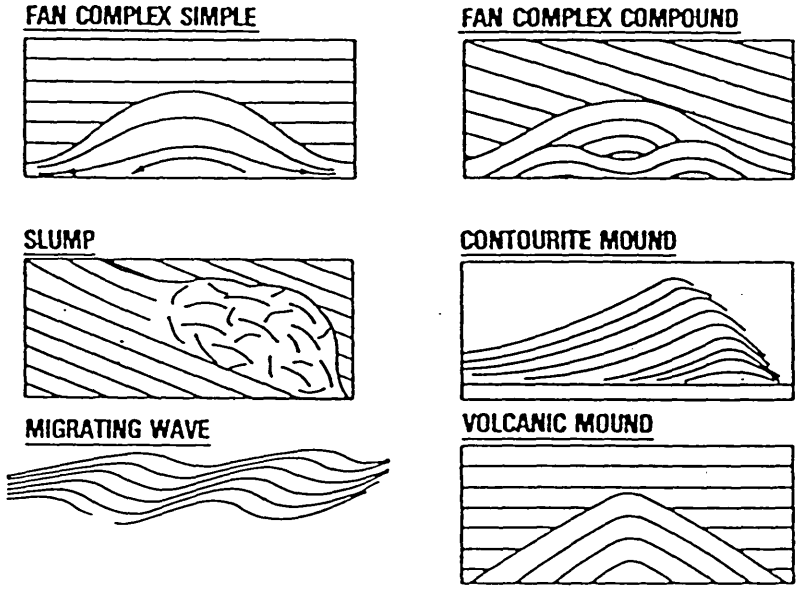

Clastic mounded seismic facies configurations. From Mitchum et al. (1977).

Fig.1.7e Mounded and drape facies types.

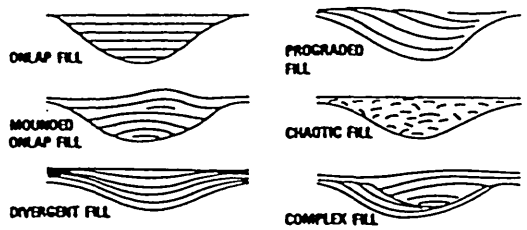

Figure 41. Fill seismic facies configurations. From Mitchum et al. (1977).

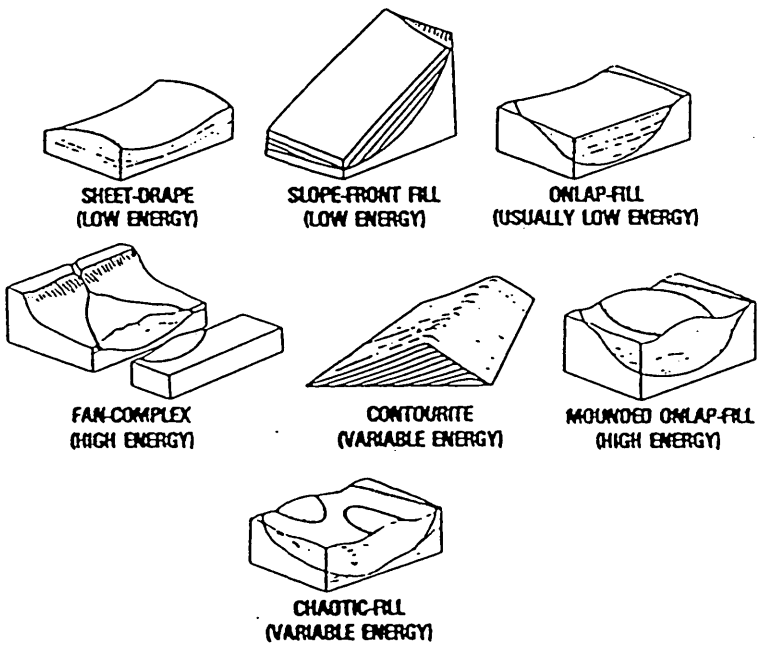

Fig.1.7f Onlap and fill seismic facies types.

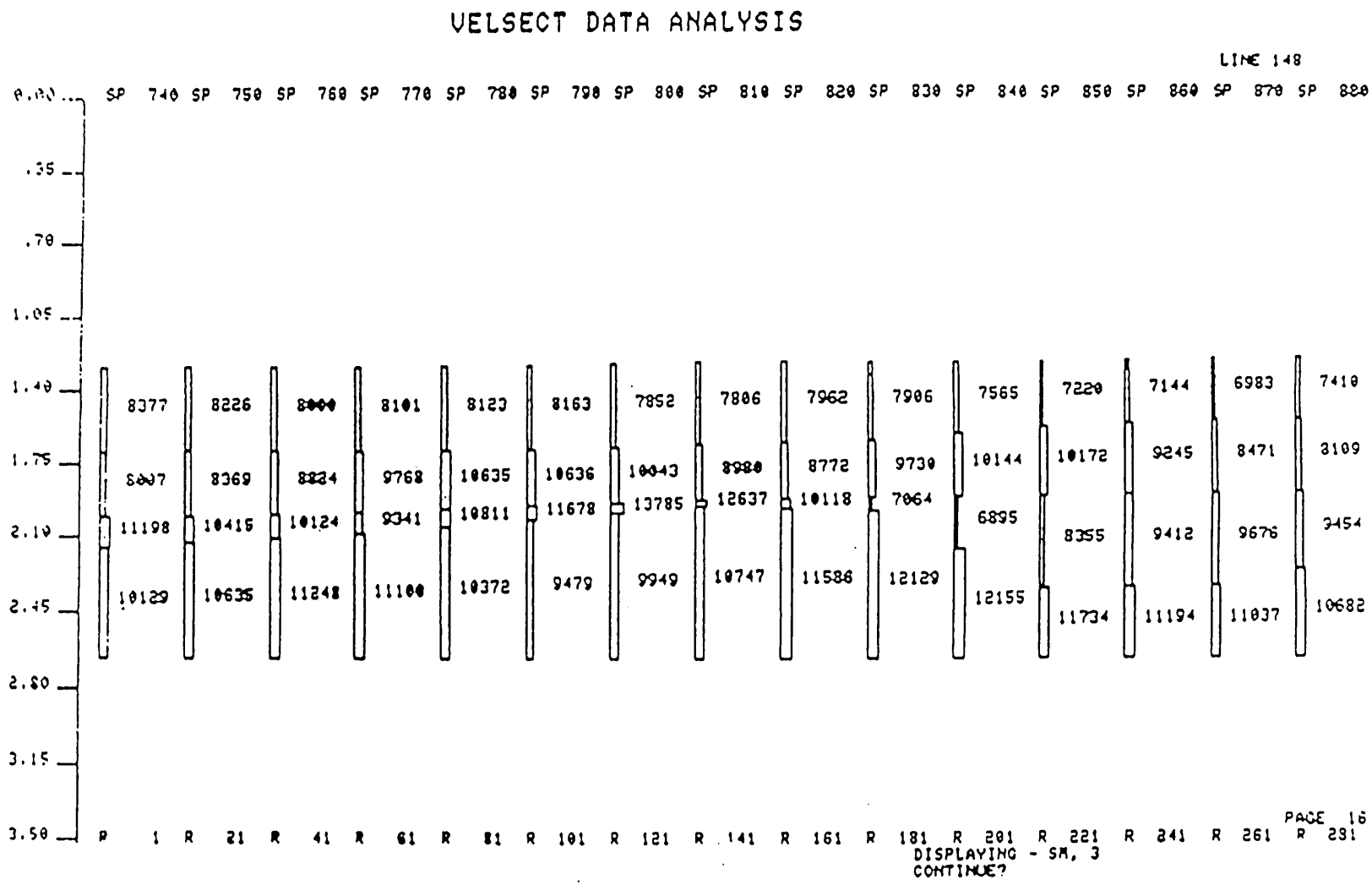

Fig.1.8a Velsect data analysis.

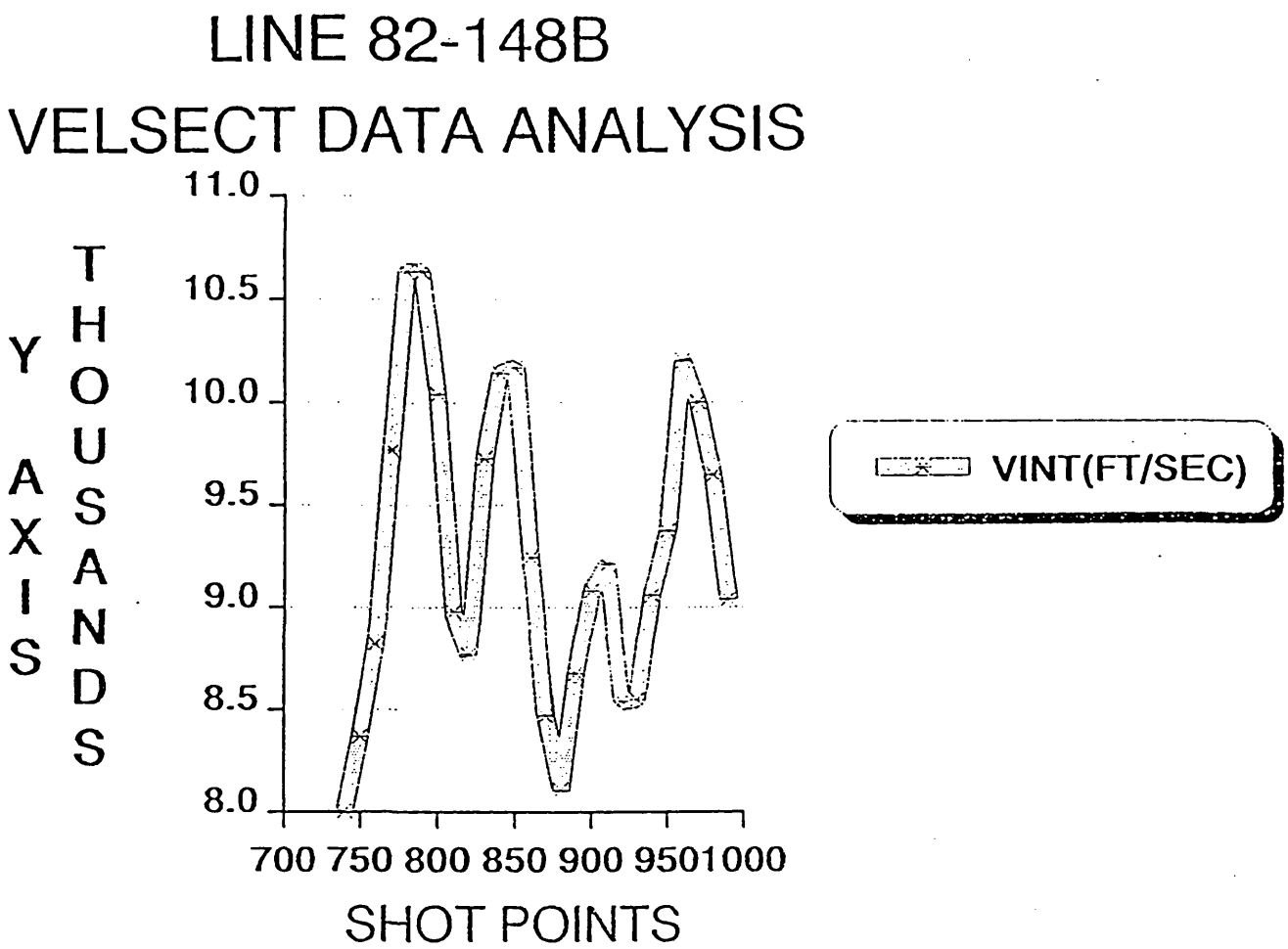

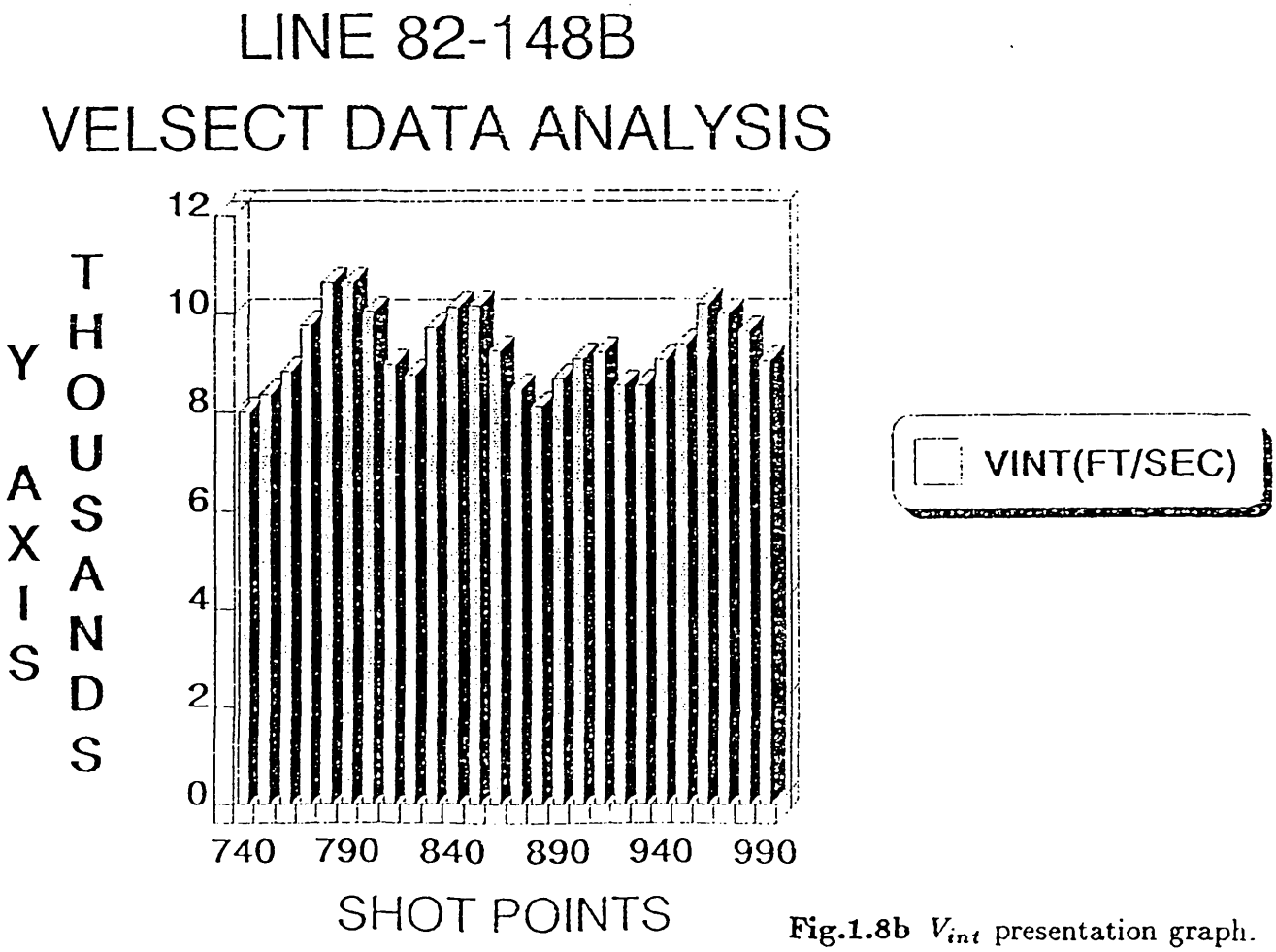

Fig.1.8b V_{int} presentation graph.

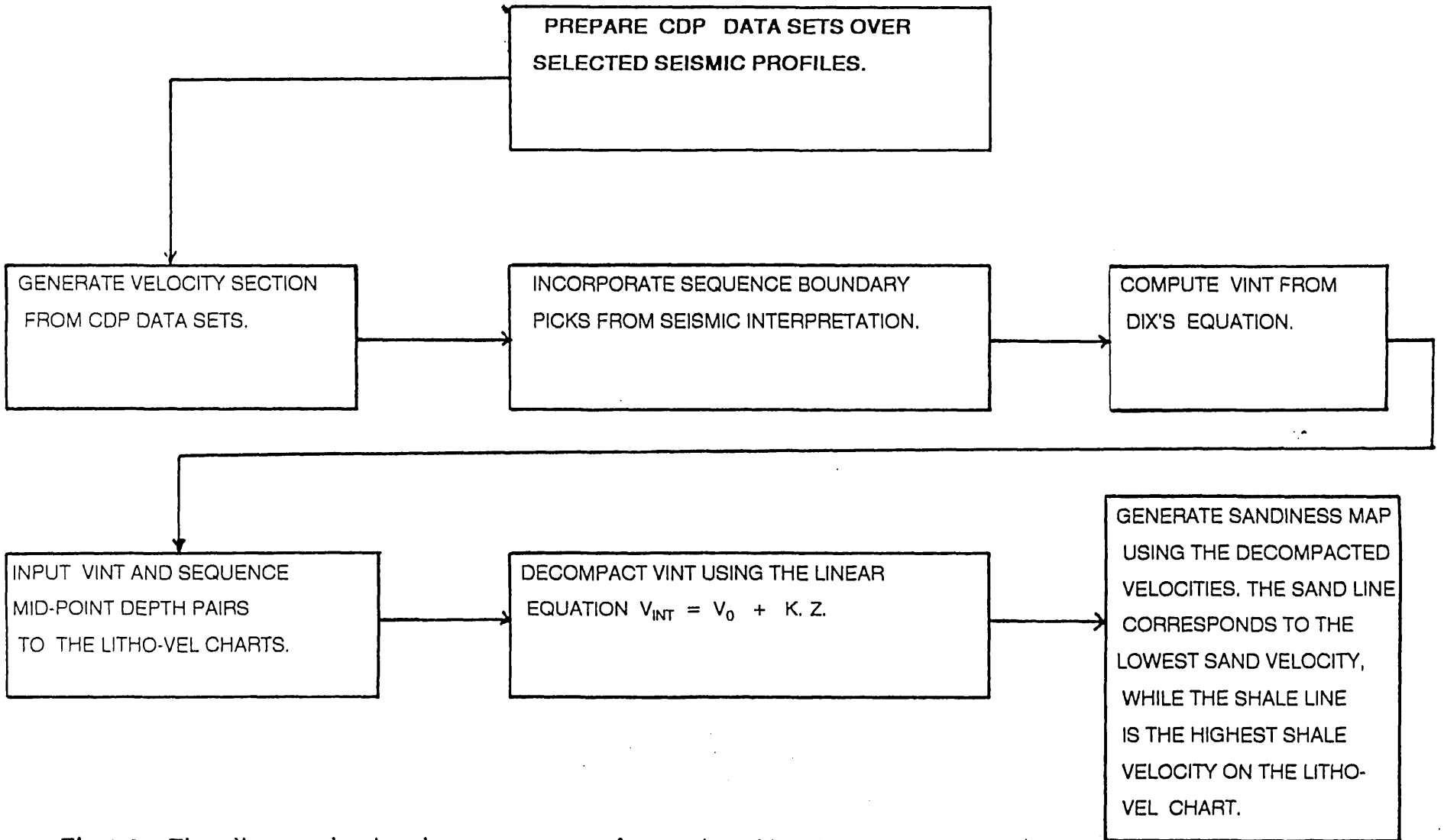

Fig.1.8c Flow diagram showing the sequence steps for stratigraphic velocity interpretation.

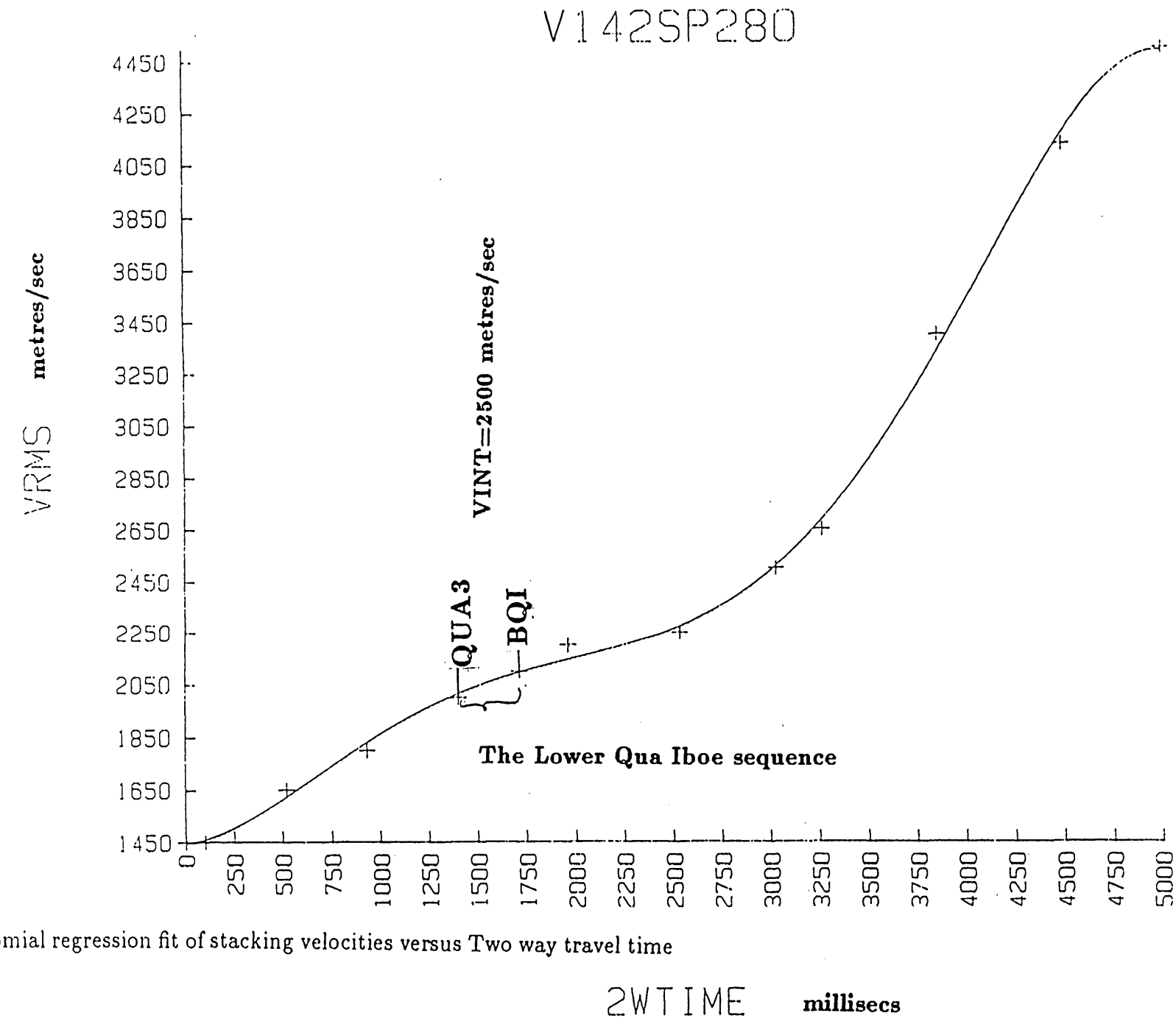

Fig.1.8d Polynomial regression fit of stacking velocities versus Two way travel time

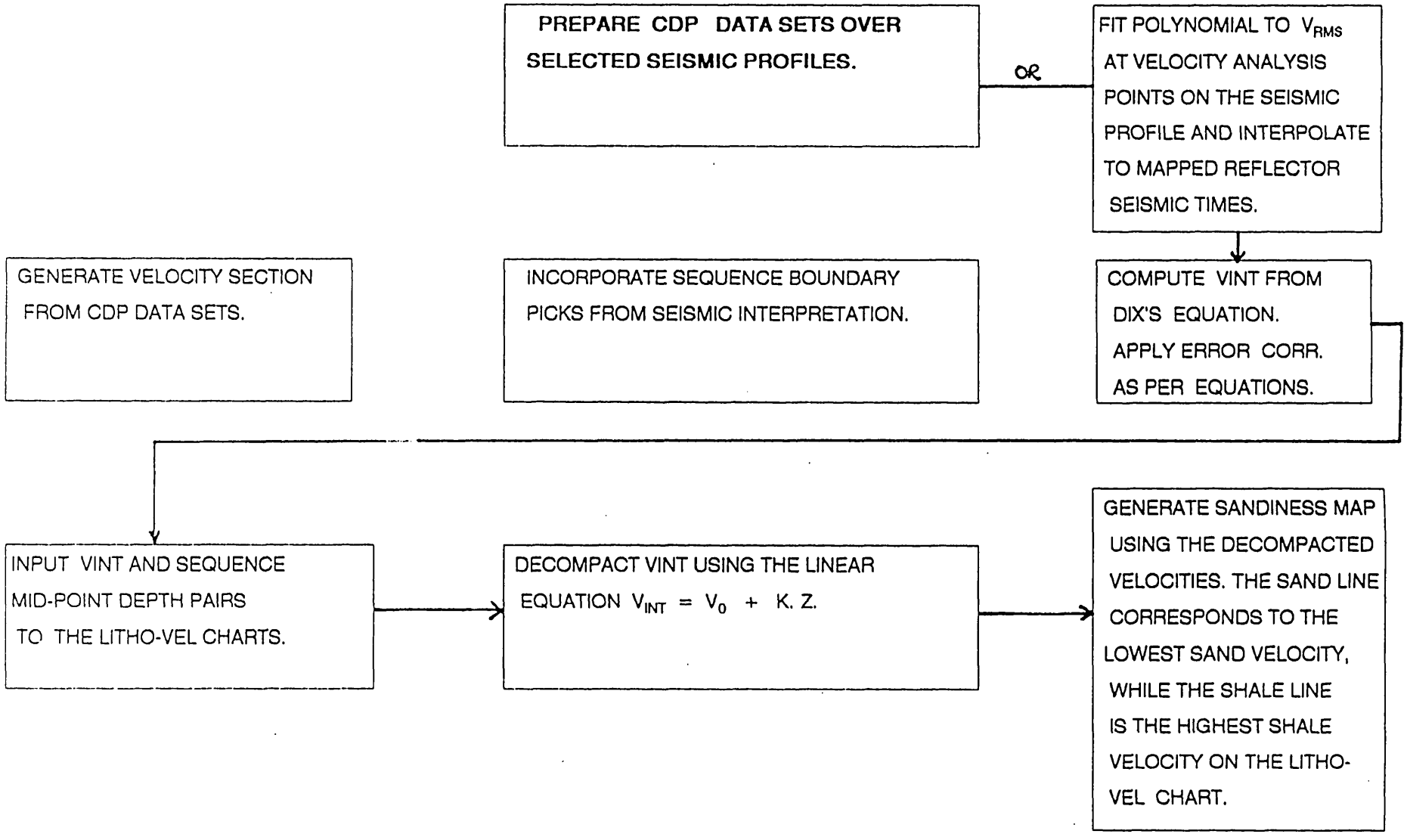

Fig.1.8e Modified flow diagram showing the sequence steps of stratigraphic velocity interpretation.

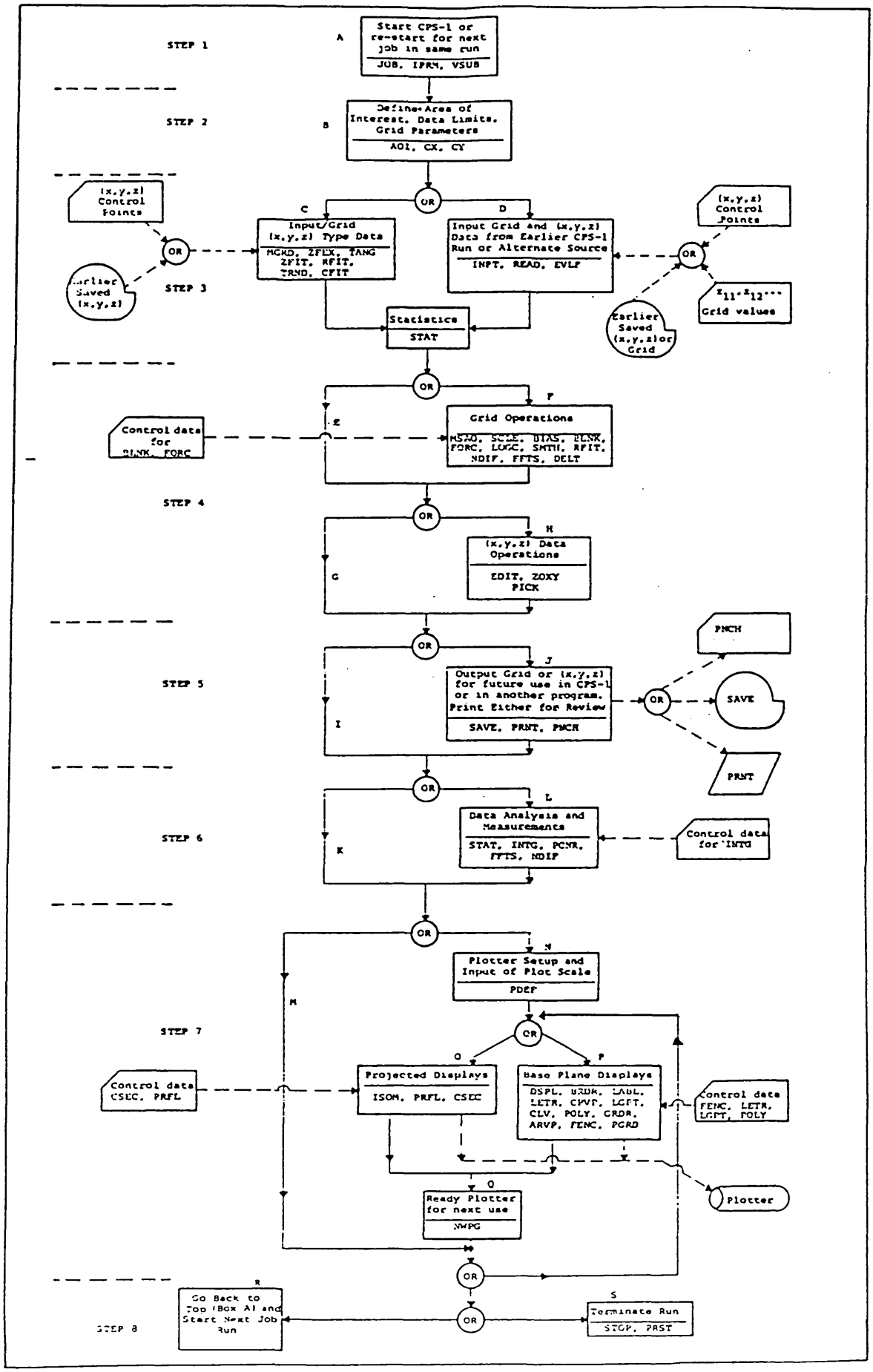

Logic Diagram for the Recommended CPS-1 Verb Program

Fig.1.9a Flow diagram showing the CPS-1 mapping software algorithm structure.

```
                                CPS-1 DIGITISING PACKAGE
                                ========================
Version PEH 1.02
                                          Options

1. Digitise map of seismic lines. ( DIGIMAP )

2. Digitise seismic events/horizons. ( DEVNT )

3. Digitise fault polygons from map. ( DIGIFLT )

4. Generate CPS-1 files from map and event files. ( MASH )

5. Digitise a contour map. ( DIGICONT )

6. Digitise a spot height map. ( DIGISPOT )

7. Help.

8. Exit.

                                        Option >
```

```
                MASH MAP AND SEISMIC HORIZON FILE GENERATOR

        1. Get a map file.

        2. Get one or more horizon/event files.

        3. Define the event to be used.

        4. Review the map file.

        5. Review a horizon/event file.

        6. Generate the output file.

        7. Help.

        8. Exit from the programme.

Option >
```

Fig.1.9b&c CPS-1 display listing.

CHAPTER TWO

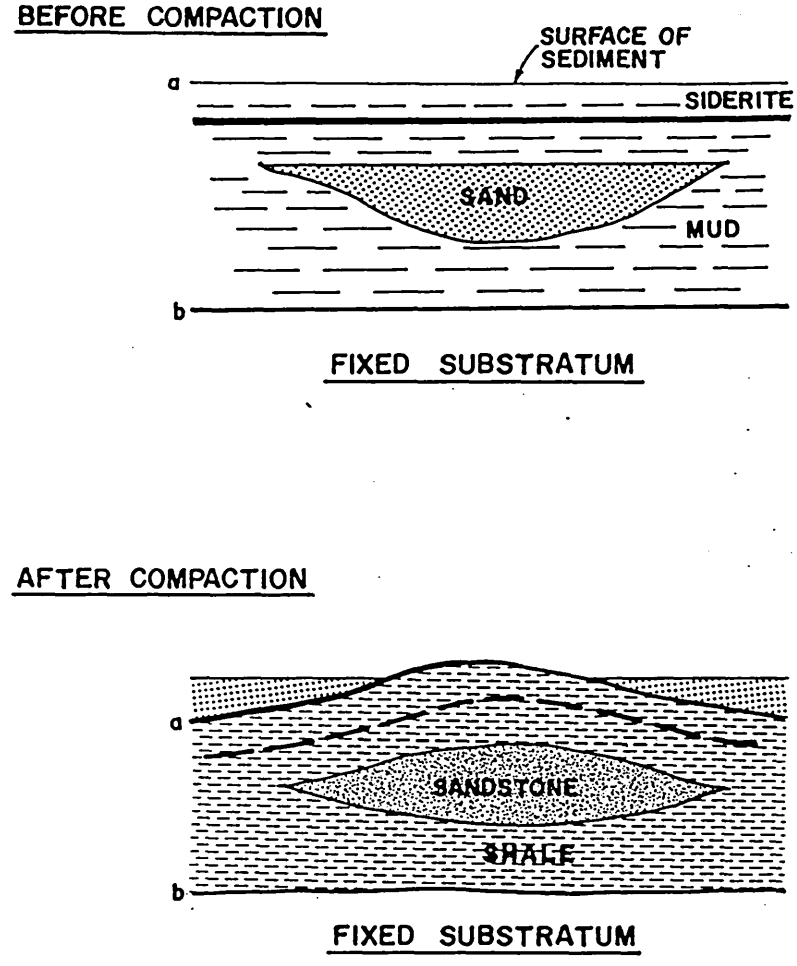

DISTORTION OF A CHANNEL SAND DUE TO COMPACTION (MODIFIED BY PETTIJOHN, POTTER AND SIEVER, 1972, AFTER DUPUY, OSWALDT AND SENS, 1963 AND COINED FROM GEOMORPHOLOGY OF SAND BODIES)

Fig.2.1 Distortion of a channel sand due to compaction (modified by Pettijohn, Potter and Siever(1972))

LBIBR- Lower Base Intra Biafra Rubble.

LIBU- Lower Intra Biafra Unconformity.

BIBR- Base Intra Biafra Rubble.

TIBU- Top Intra Biafra Unconformity.

BIBBEN- Base Intra Biafra Benin sands.

BRB- Base Rubble Beds

BQI- Base Qua Iboe.

TIQI- Top Intra Qua Iboe

QUA3 etc- Intra Qua Iboe horizon 3 etc

Pu- Pleistocene Unconformity

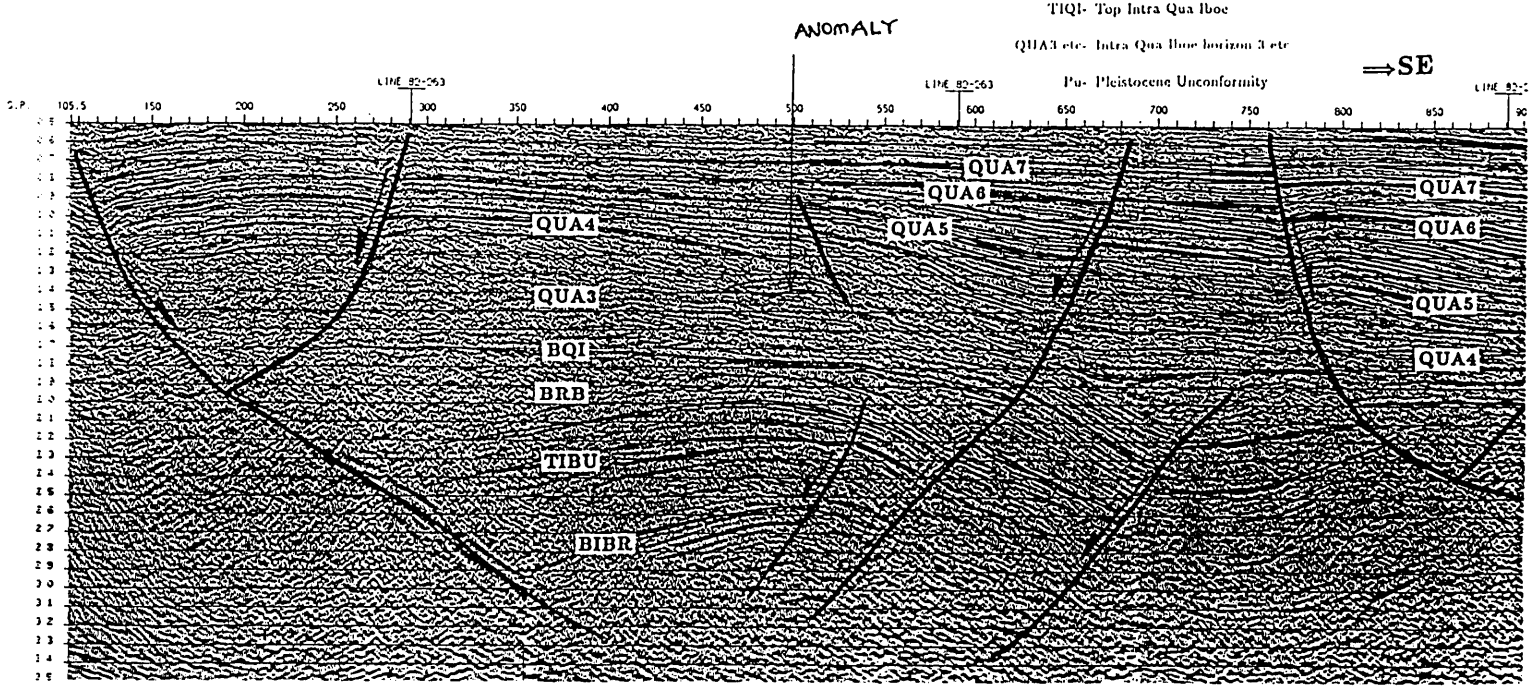

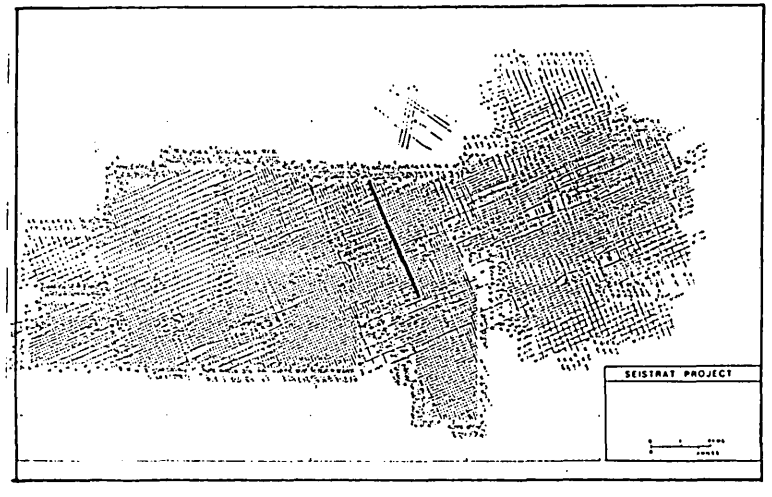

Fig.2.2a Seismic Line 82-263 showing an anomaly at the toe of progradation(shot points 450 to 530) at 1.4secs. Note that the stratigraphic anomaly occurs within QS3 bounded by Qua3 and Qua4 within the paleobasin defined by Fault-3.

LBIBR- Lower Base Intra Biafra Rubble.

LIBU- Lower Intra Biafra Unconformity.

BIBR- Base Intra Biafra Rubble.

TIBU- Top Intra Biafra Unconformity.

BIBBEN- Base Intra Biafra Benin sands.

BRB- Base Rubble Beds

BQI- Base Qua Iboe.

TIQI- Top Intra Qua Iboe

QUA3 etc- Intra Qua Iboe horizon 3 etc

Pu- Pleistocene Unconformity

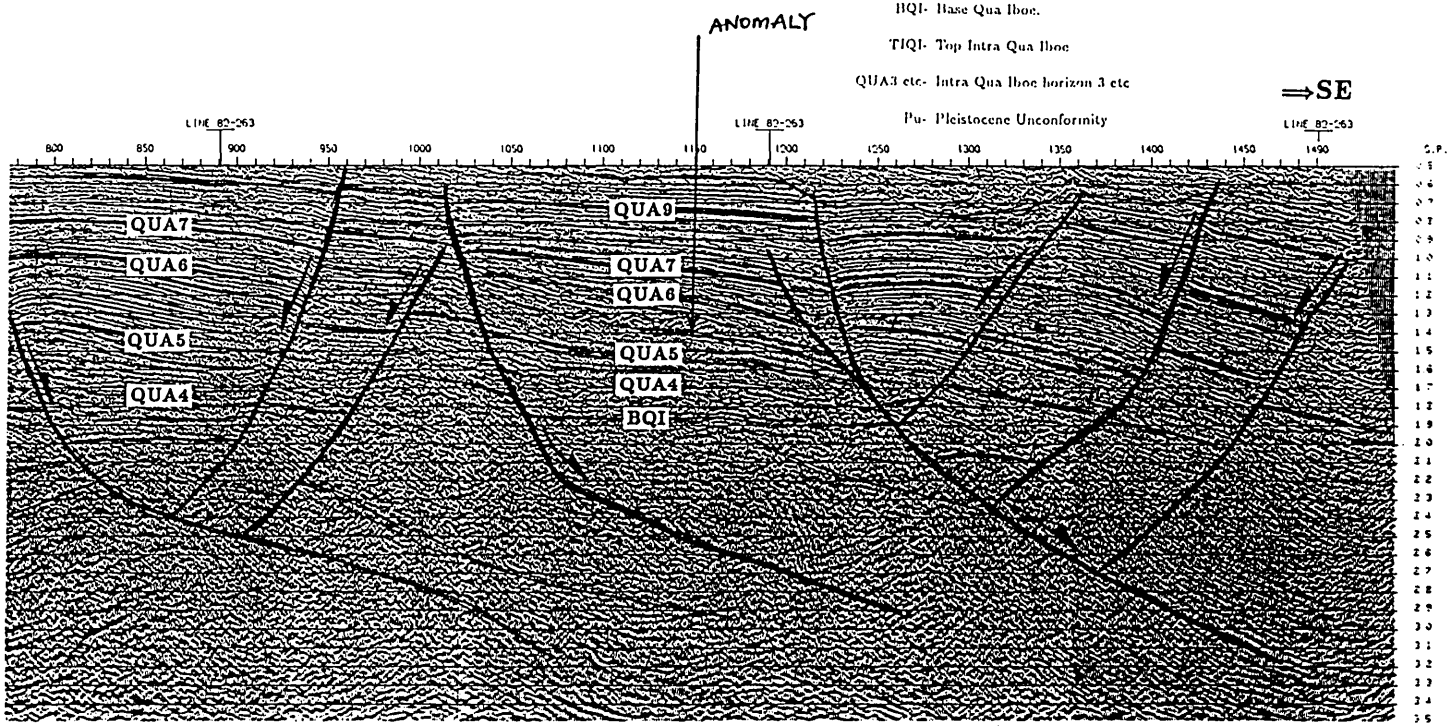

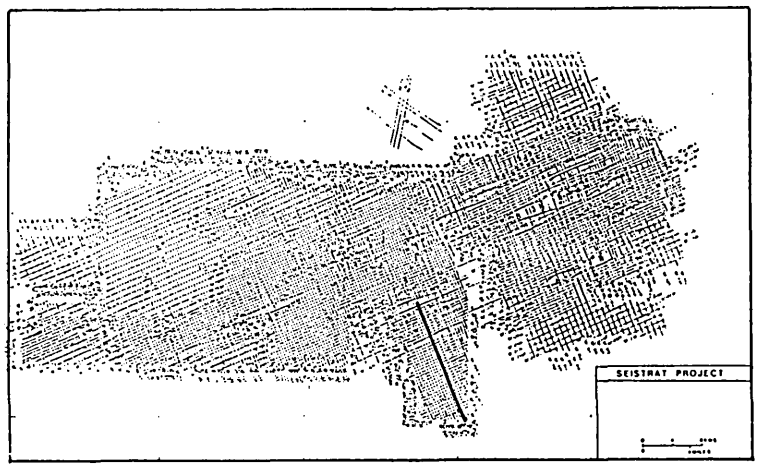

Fig.2.2b Seismic Line 82-263 showing a Stratigraphic anomaly formed by slumping off the progradational slope(shot points 1080 to 1170). Anomaly occurs between Qua5 and Qua6.

LIBBR- Lower Base Intra Biafra Rubble

LIBU- Lower Intra Biafra Unconformity.

BIBR- Base Intra Biafra Rubble.

TIBU- Top Intra Biafra Unconformity.

BIBBEN- Base Intra Biafra Benin sands.

BRB- Base Rubble Beds

BQI- Base Qua Iboe.

TIQI- Top Intra Qua Iboe

QUA3 etc- Intra Qua Iboe horizon 3 etc

Pu- Pleistocene Unconformity

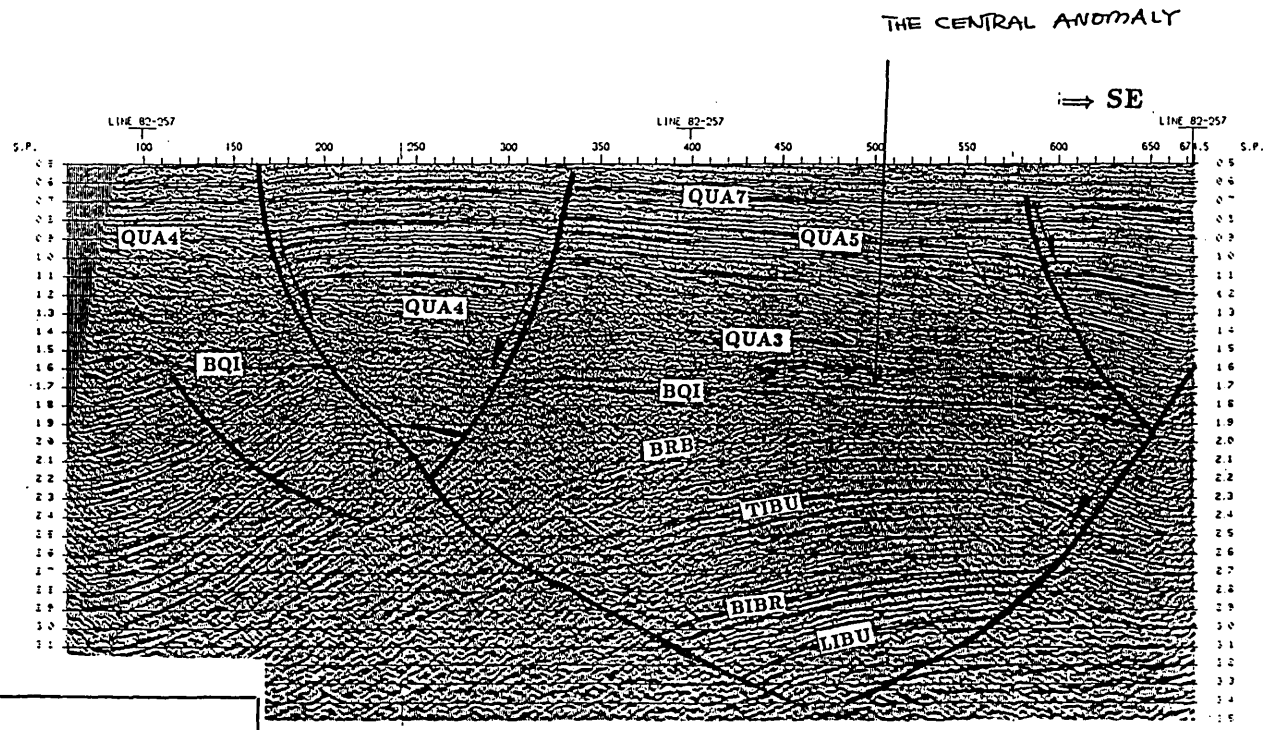

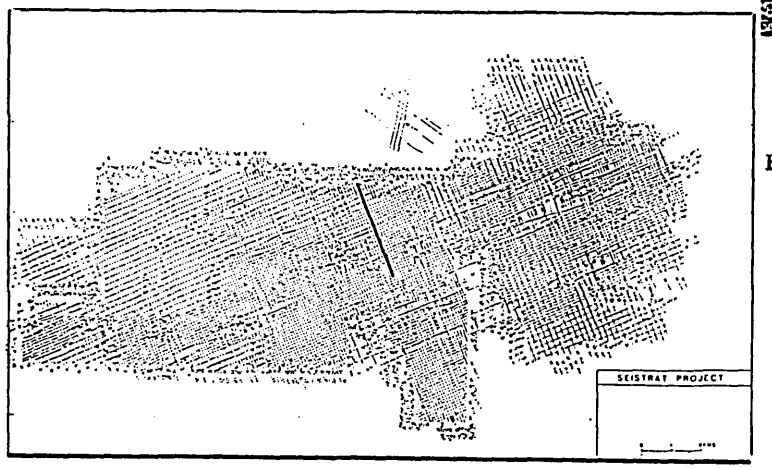

Fig.2.2c Line 82-257 showing the central stratigraphic anomaly with a predominant axis or trend occurring within the Lower Qua Iboe(between Qua3 and the BQI). Note the thickening into the paleobasin fault by both the Rubble Beds and the Upper Intra Biafra Rubble(UIBR) as indicated.

LIBRB: Lower Base Intra Biafra Rubble.

LIBU: Lower Intra Biafra Unconformity

BIBR: Base Intra Biafra Rubble

TIBU: Top Intra Biafra Unconformity

BIBBLN: Base Intra Biafra Bonn sands.

BRB: Base Rubble Beds

BQI: Base Qua Iboe.

TIQI: Top Intra Qua Iboe

QUA3 etc: Intra Qua Iboe horizon 3 etc

Pu: Pleistocene Unconformity

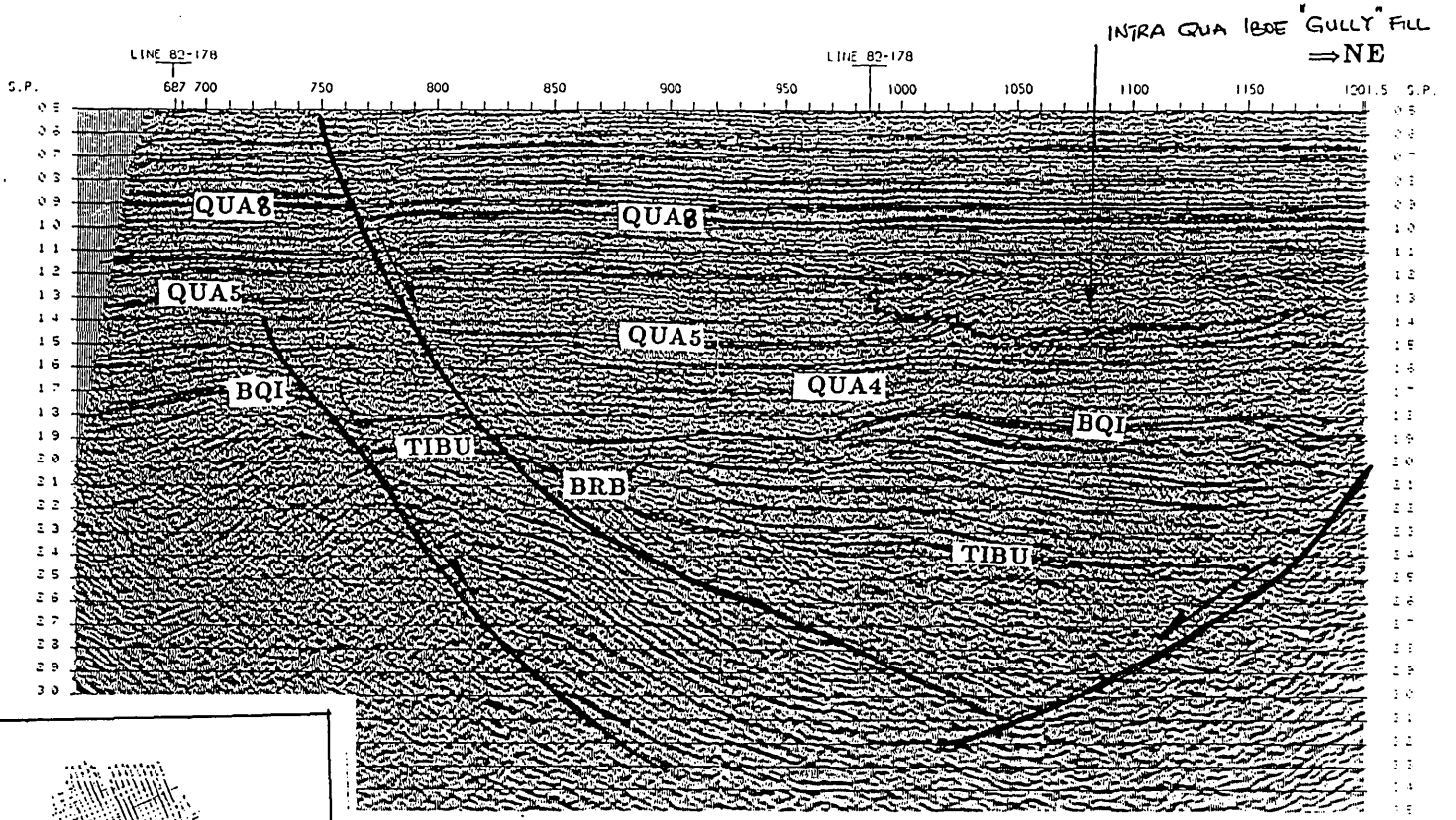

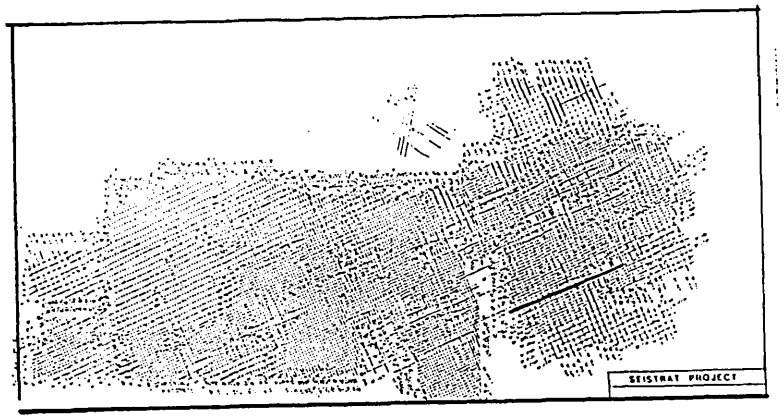

Fig.2.2d Seismic Line 82-178 showing an anomaly associated with chaotic and disrupted seismic facies(shot points 970 to 1201). The base of the anomaly is Qua5, and the top Qua7. This is the Intra Qua Iboe "gully" fill (discussed later under Upper Qua Iboe analysis) and it is a canyon fill formed by an Early Pleistocene Lowstand and subsequent infilling during highstand.

LIBU- Lower Intra Biafra Unconformity

BIBR- Base Intra Biafra Rubble

TIBU- Top Intra Biafra Unconformity.

BIBBEN- Base Intra Biafra Benin sands.

BRB- Base Rubble Beds

BQI- Base Qua Iboe.

TIQI- Top Intra Qua Iboe

QUA3 etc- Intra Qua Iboe horizon 3 etc

Pu- Pleistocene Unconformity

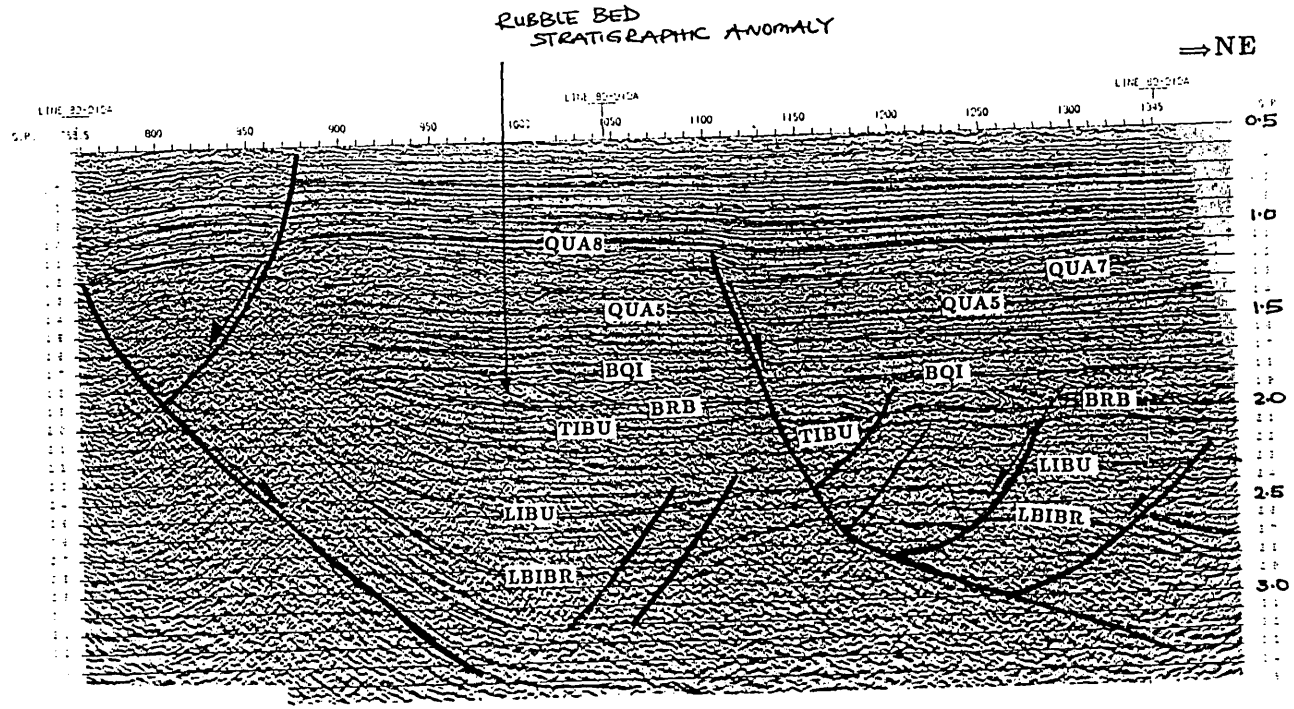

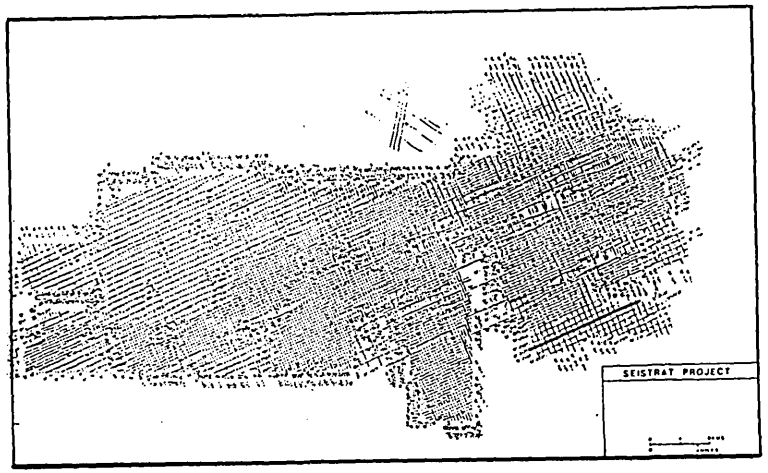

Fig.2.2e Seismic Line 82-212a over the southeastern anomaly of the Rubble Beds(between 1.7 and 2secs). Note the offlapping clinoform patterns characteristic of the seismic facies.

LIBU- Lower Intra Biafra Unconformity.

BIBR- Base Intra Biafra Rubble

TIBU- Top Intra Biafra Unconformity

BIBBEN- Base Intra Biafra Benin Shale

BRB- Base Rubble Beds

BQI- Base Qua Boe.

TIQI- Top Intra Qua Boe

QUA3 etc- Intra Qua Boe horizon 3 etc

Pu- Pleistocene Unconformity

THE CENTRAL ANOMALY

⟹NE

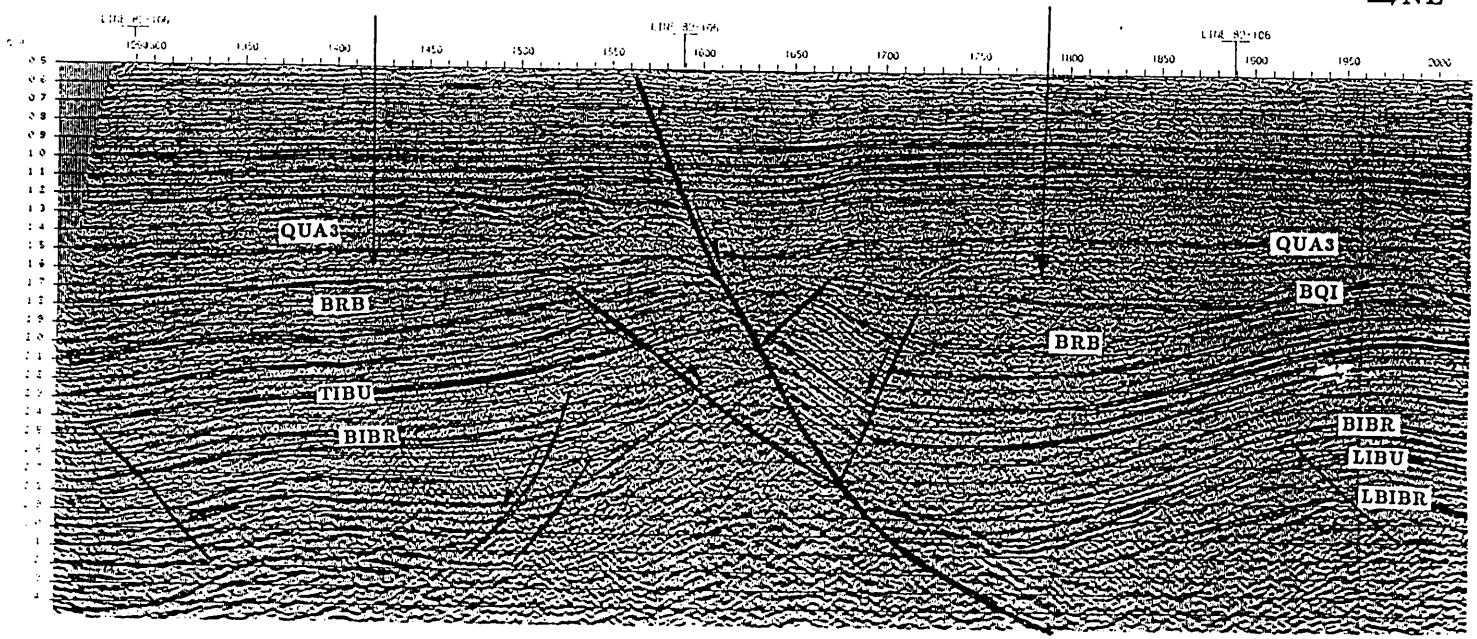

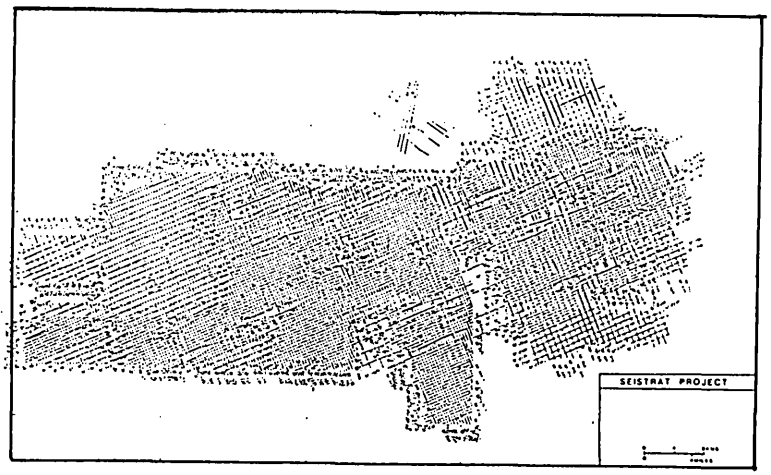

Fig.2.2f Seismic Line 82-106 showing parallel high amplitude reflectors within a generally subdued amplitude medium.

Fig.2.2g Distribution of stratigraphic anomalies within the Rubble Beds.

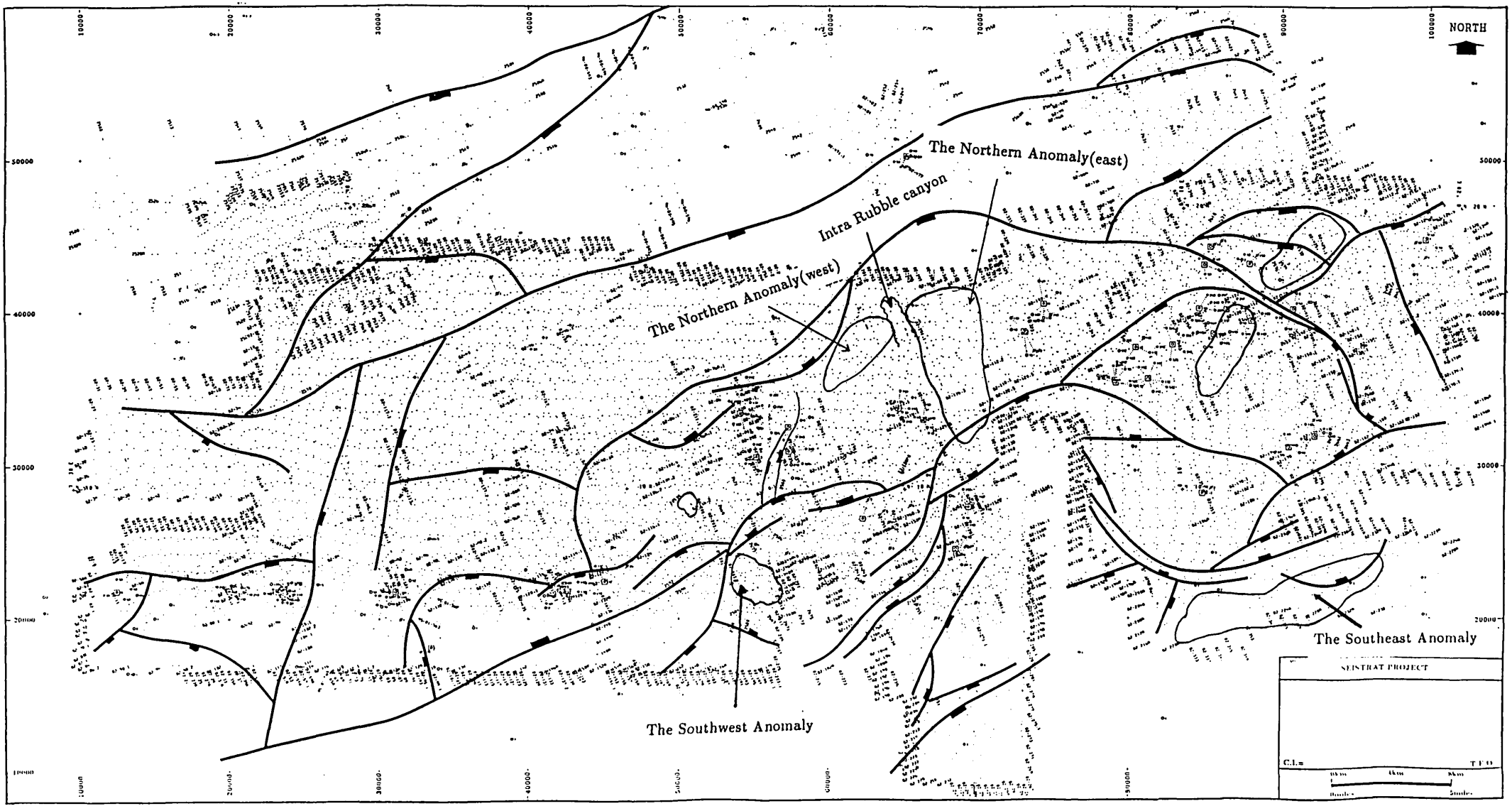

Fig.2.2h A composite of the distribution of stratigraphic anomalies within the various Qua Iboe sequences. Most of the anomalies occur within the Lower Sequences(QS1, QS2, & QS3).

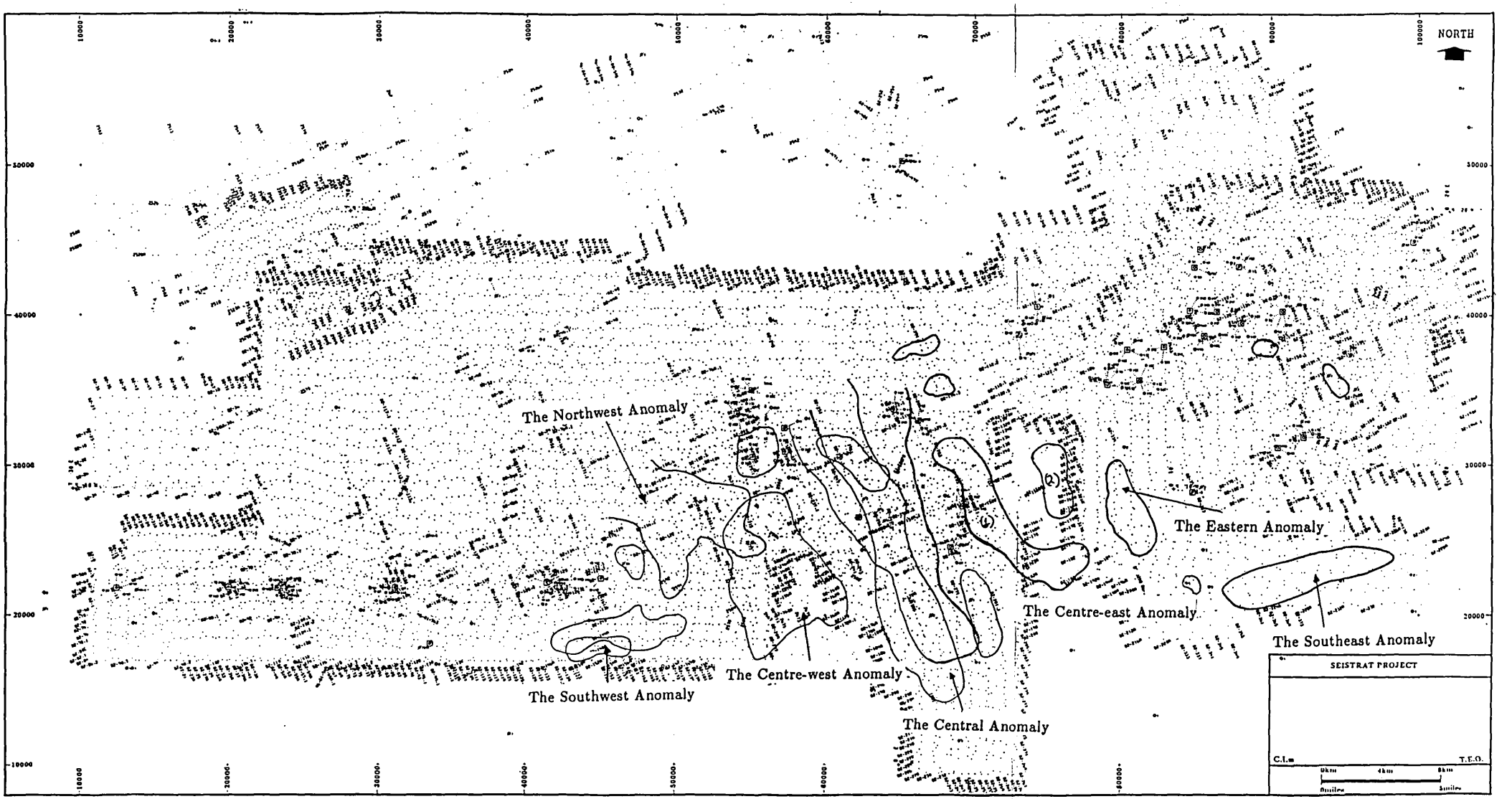

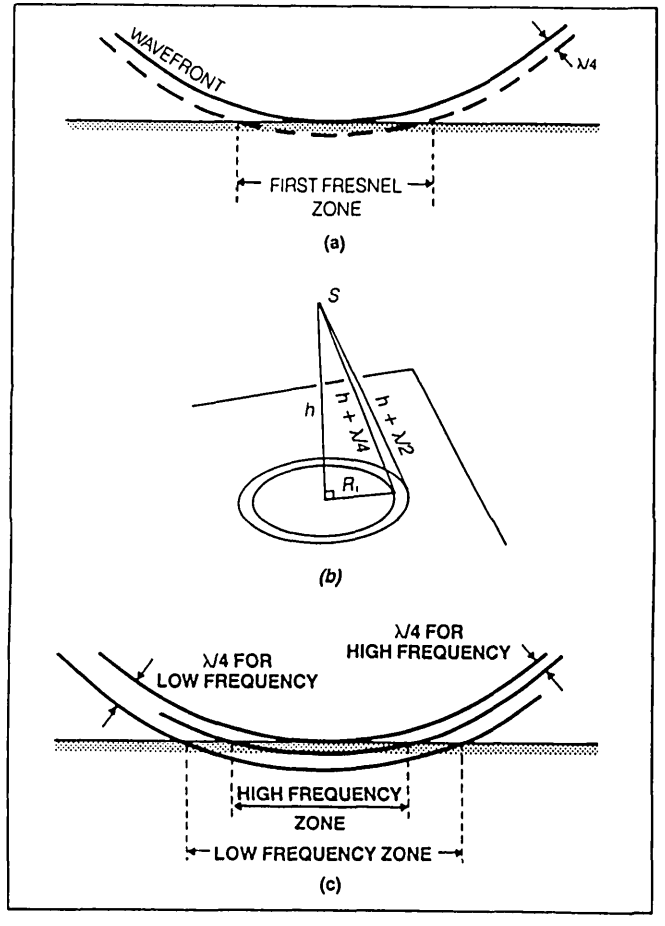

Fig.2.3a How to determine the diameter of the first *Fresnel Zone* (after Sheriff, 1980).

Fig.2.3b Monogram for determining the size of the Fresnel zone. (After Sheriff, 1980).

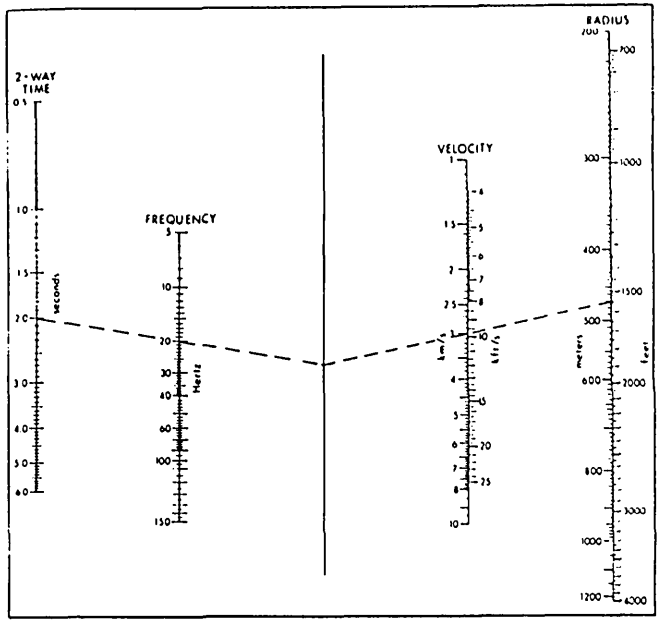

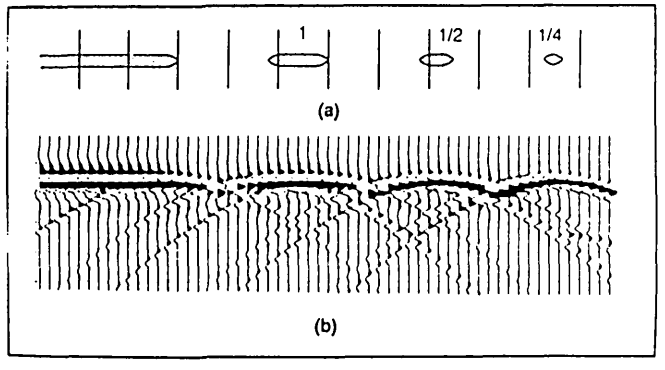

Fig.2.3c Reflections from strips of various widths measured in Fresnel zone units. (After Meckel and Nath, 1977).

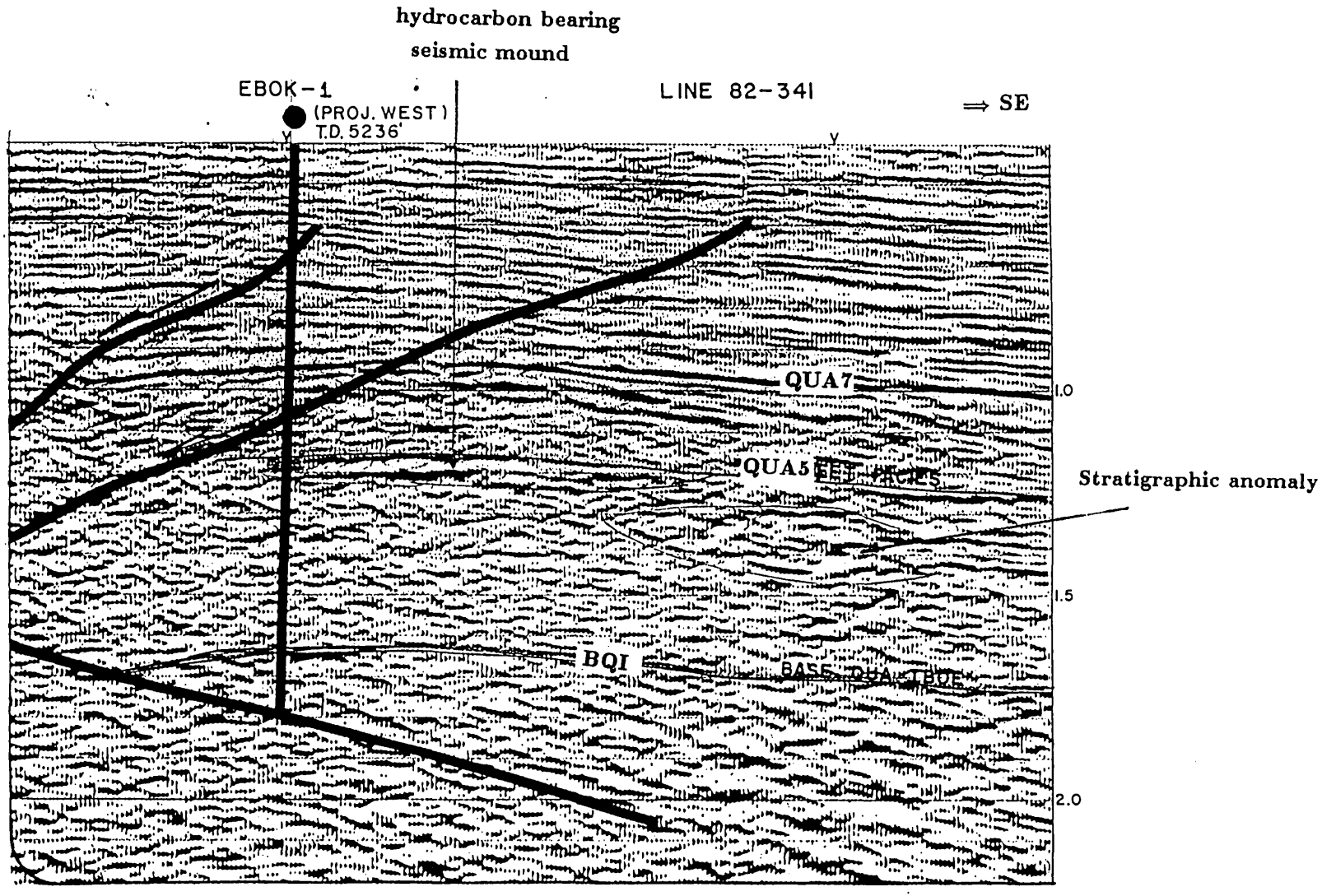

Fig.2.3d Seismic mound of the Upper Qua Iboe baselapping Qua5

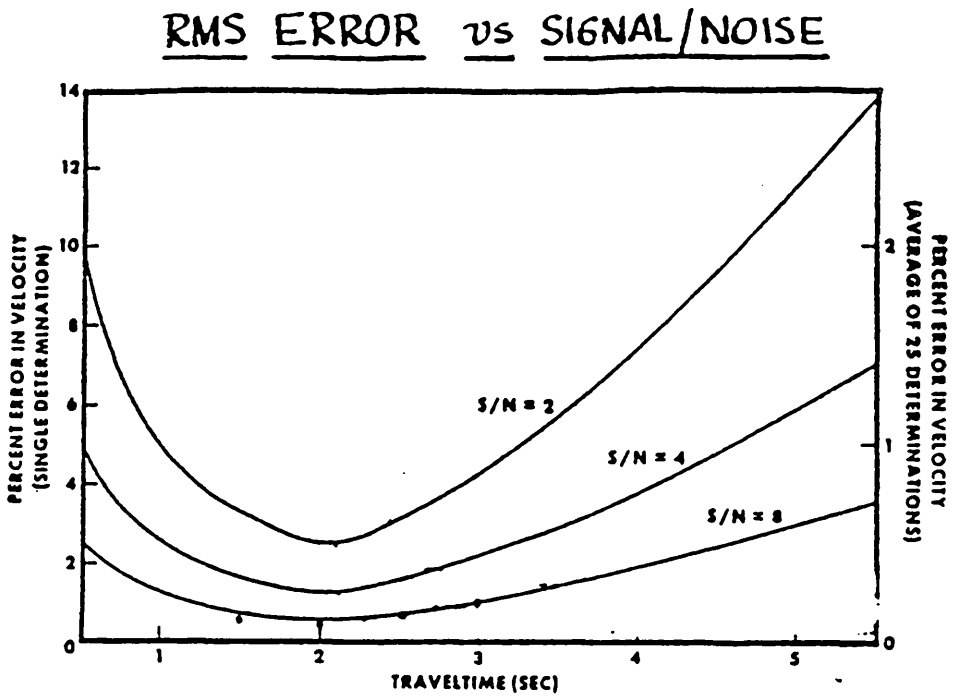

Fig.2.4a The CDP method as a focussing devise and the velocity accuracy with increased traveltime. Graph of percentage error versus traveltime shows that increased traveltime decreases past two seconds because the moveout is getting smaller. Shallower events have increased velocity error because the far traces are muted. (After Al-Chalabi, 1977).

Fig.2.4b Graph showing the logarithmic relationship between velocity error ratio $\frac{\Delta V_{I_n}}{\Delta v_{n-1}}$ and time thickness to depth ratio $\frac{T_n - T_{n-1}}{T_{n-1}}$ for the Lower Qua Iboe sequence.

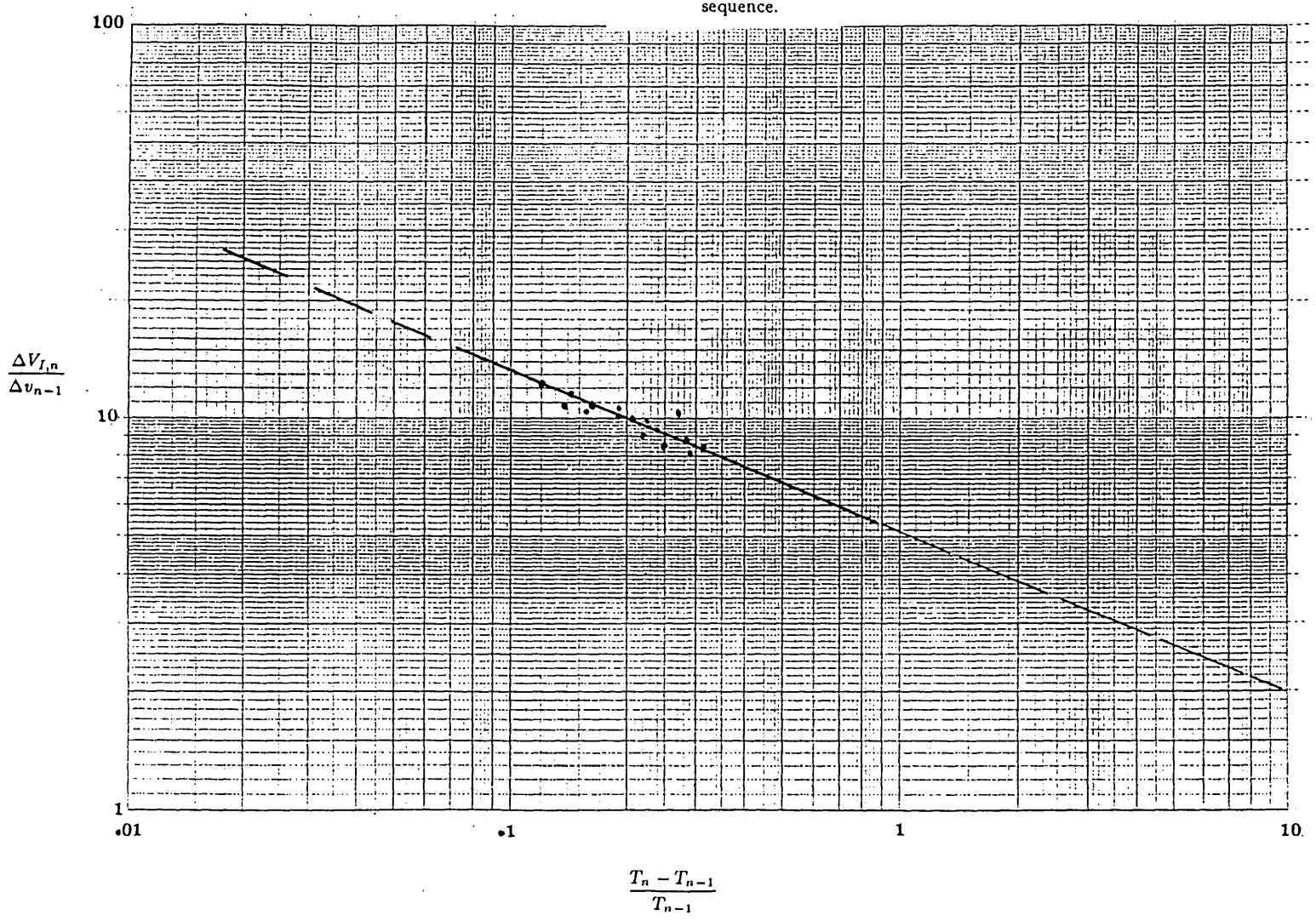

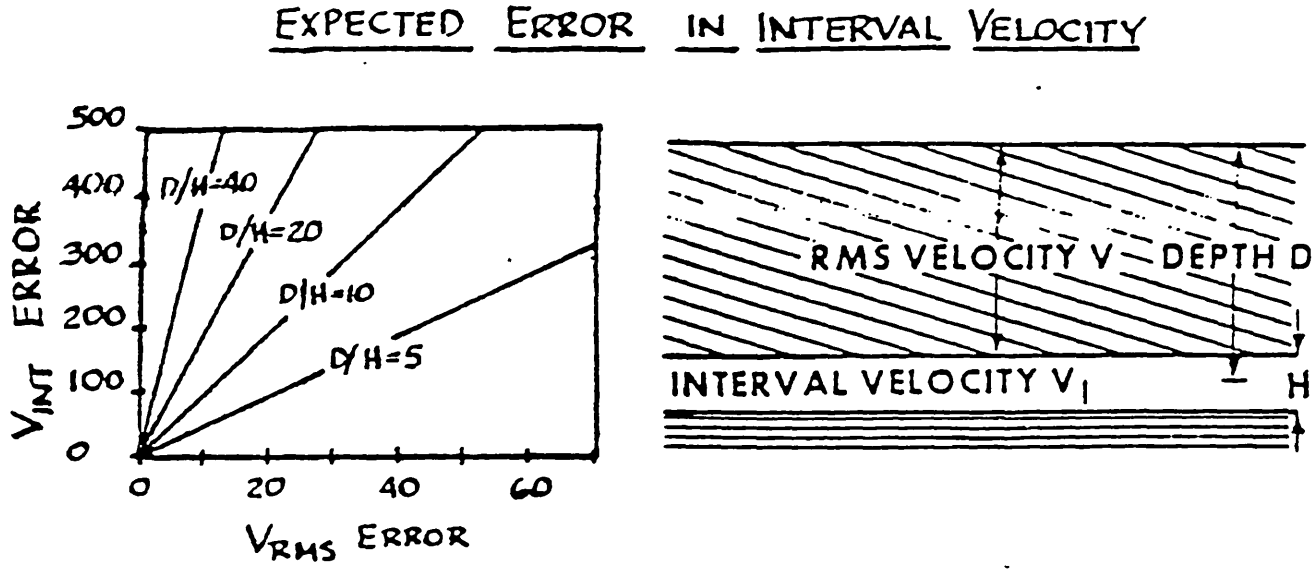

Fig.2.4c Amplification of the expected error in V_{int} *vis a vis* V_{rms}.

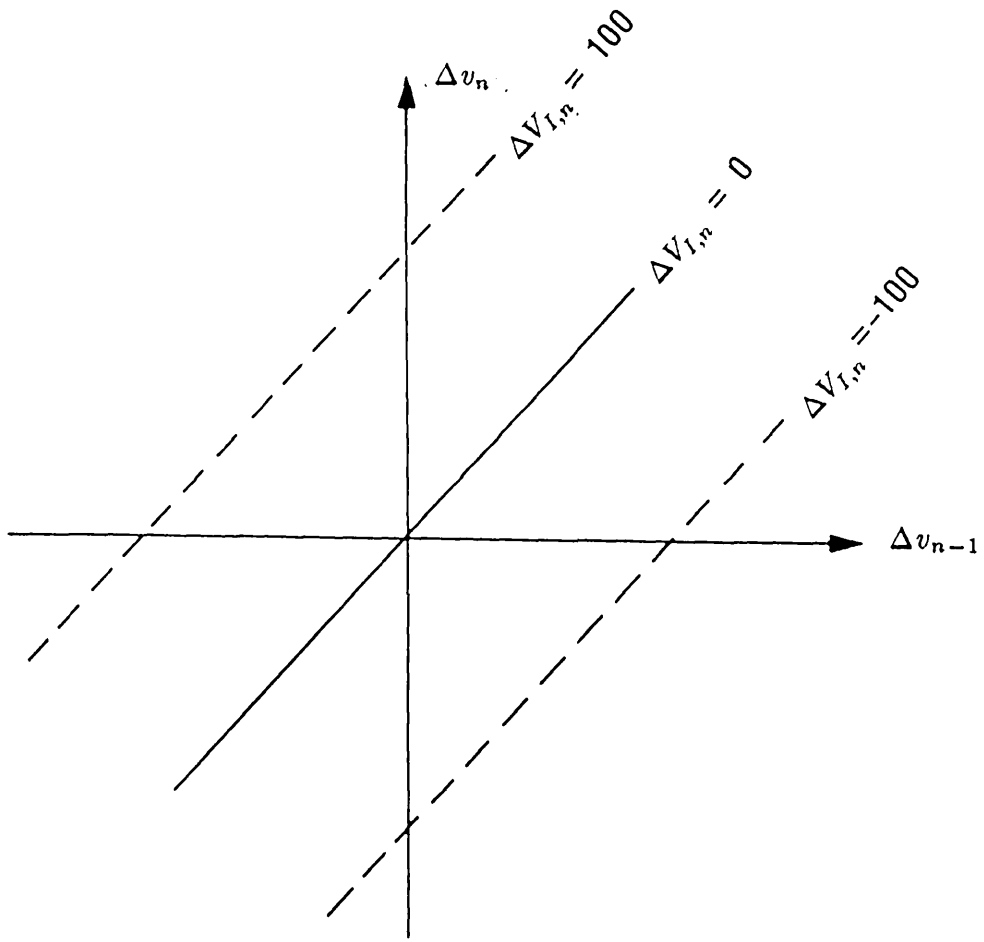

Fig.2.4d Schematic graph of interval velocity errors $\Delta V_{I,n}$ calculated by means of Dix's equation, as a function of errors in V_{rms} estimation. (After Cordier, 1985.)

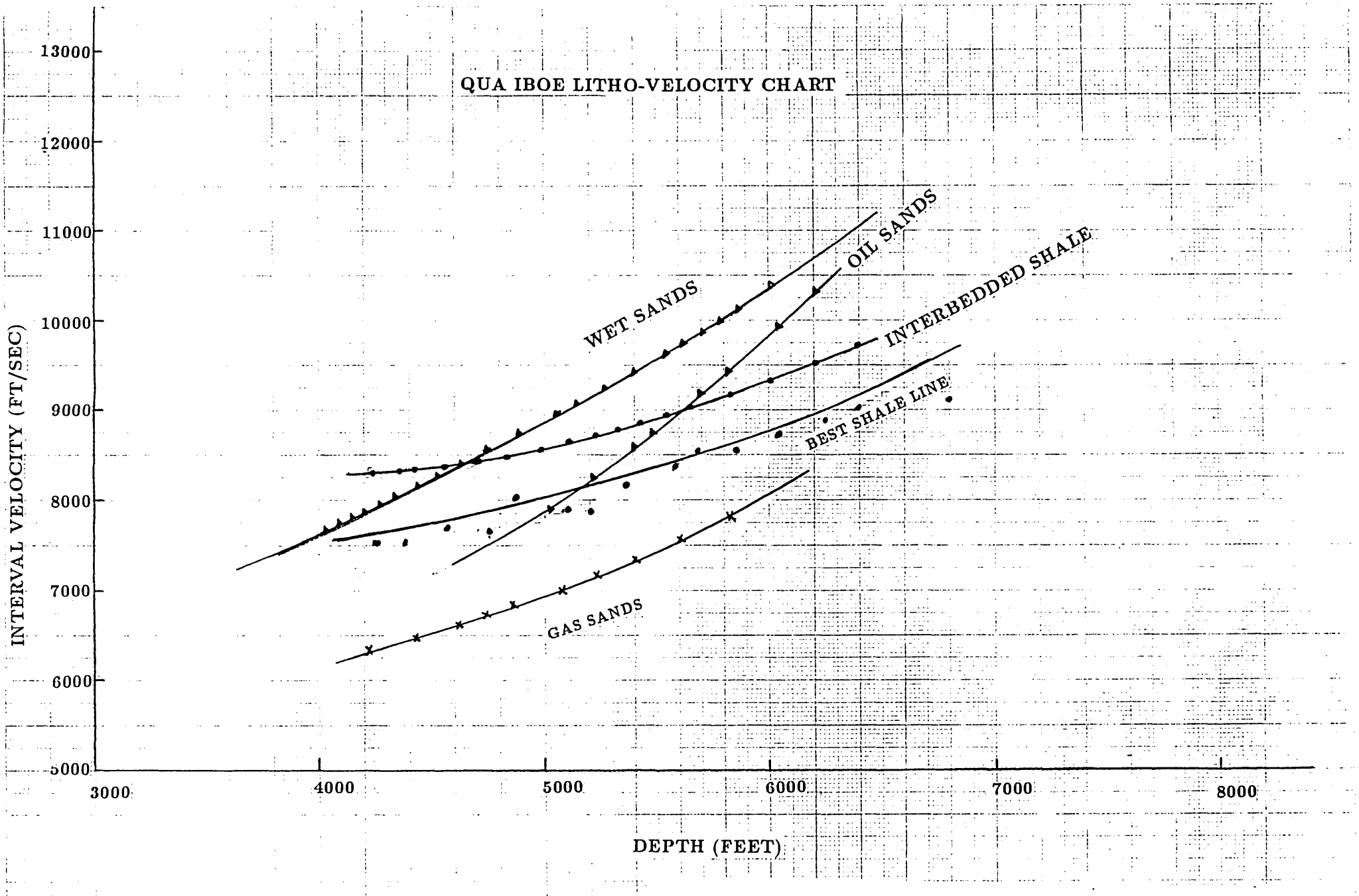

Fig.2.5a Qua Iboe litho-velocity chart.

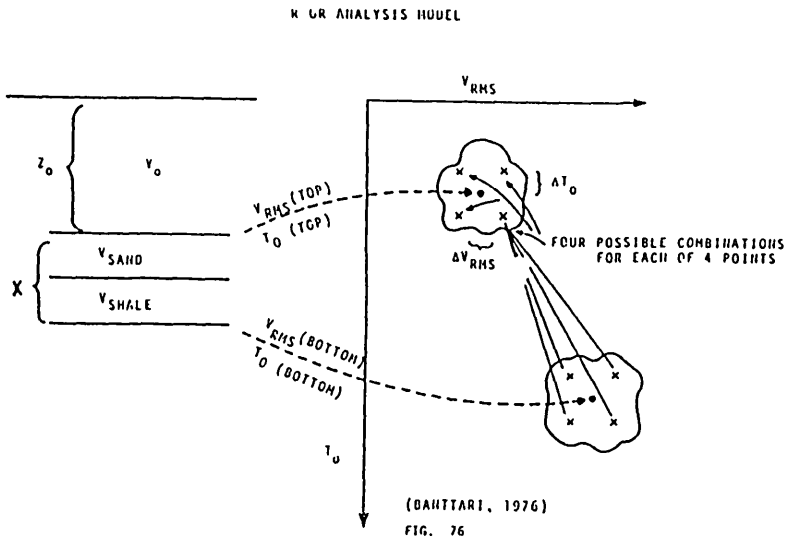

(BANTTARI, 1976)
FIG. 76

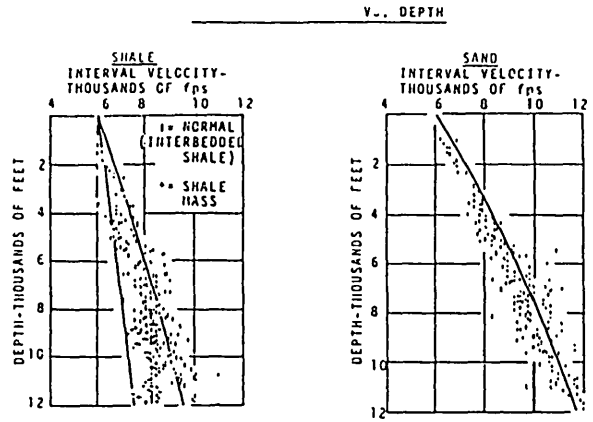

OFFSHORE LOUISIANA CVL DATA AFTER MUSGRAVE

DEPTH	$\bar{V}_{SAND}$	$\bar{V}_{SHALE}$
0	6000	6000
-4000'	8250	7400
-8000'	10000	8500
-12000'	11500	9250

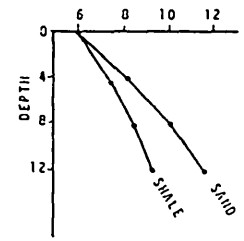

(AFTER BANTTARI, 1976)

A SIMPLIFIED ERROR ANALYSIS

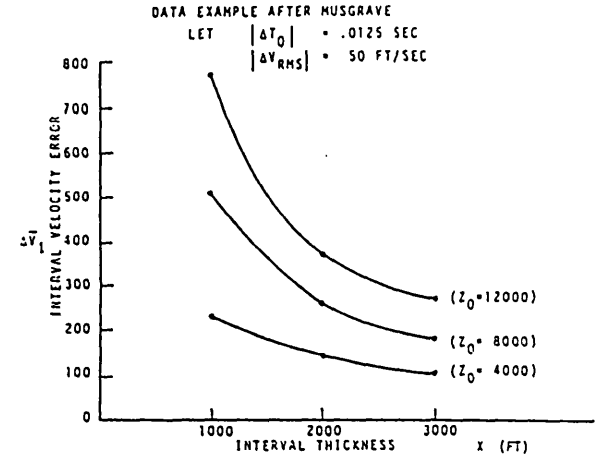

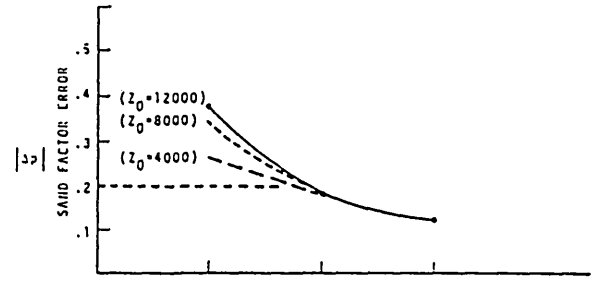

FIG. 7
(BANTTARI, 19..)

ERROR INTRODUCED BY COMPONENT VELOCITY VARIATION

(BANTTARI)

ASSUME $V_{SAND} = \bar{V}_{SAND} \mp \Delta_{SAND}$

$V_{SHALE} = \bar{V}_{SHALE} \mp \Delta_{SHALE}$

$$P+(\Delta) = \frac{(\bar{V}_{SAND} + \Delta)\,[V_I - (\bar{V}_{SHALE} + \Delta)]}{V_I(\bar{V}_{SAND} - \bar{V}_{SHALE})}$$

$$P-(\Delta) = \frac{(\bar{V}_{SAND} - \Delta)\,[V_I - (\bar{V}_{SHALE} - \Delta)]}{V_I(\bar{V}_{SAND} - \bar{V}_{SHALE})}$$

FOR ANY OBSERVATION OF V_I:
$P+(\Delta)$ AND $p-(\Delta)$ ARE THE EXTREME VALUES OF SAND FACTOR
$p(o)$ IS THE VALUE WHICH WOULD BE COMPUTED

DEFINE

$$E(\Delta) = \left\{\frac{|P(o) - P+(\Delta)| + |P(o) - PO(\Delta)|}{2}\right\} = \text{MAXIMUM ERROR INDUCED BY VARIATION}$$

EXAMPLE AFTER MUSGRAVE

Z = 6000' V_{SAND} = 10000 ± 500, V_{SHALE} = 8500 ± 500;
V_I = 9190 1/s $P(o)$ = .50, $P+(500)$=.15

$P-(500)$=.82 $E(\Delta)$=.33

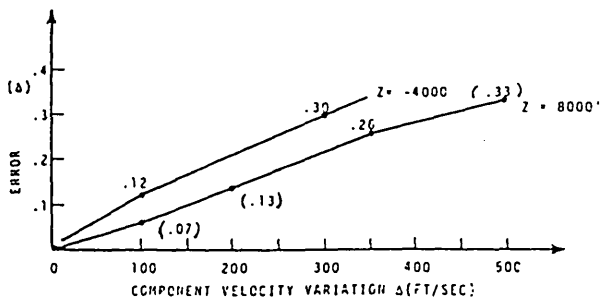

REQUIRED ACCURACY OF INTERVAL VELOCITIES

$V_{OBS} = V_I \mp \Delta V_I$

$\Delta p = P_{OBS} - P_I$

$$= \frac{V_{SAND}}{[V_I \pm \Delta V_I]}\,\frac{([V_I \pm \Delta V_I] - V_{SHALE})}{(V_{SAND} - V_{SHALE})} - \frac{V_{SAND}\,(V_I - V_{SHALE})}{V_I(V_{SAND} - V_{SHALE})}$$

SMALL COMPARED TO V_I

$$\boxed{\approx \pm \frac{V_{SAND}\;\Delta V_I}{V_I(V_{SAND} - V_{SHALE})}}$$

USE $V_I = V_I(p=.5)$

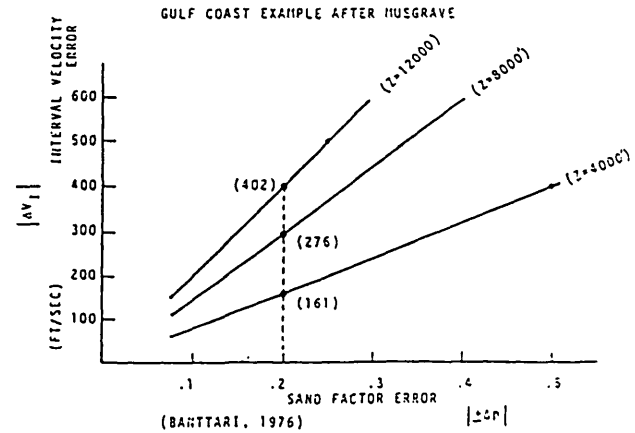

(BANTTARI, 1976)

Fig.2.5b A simplified error analysis model. (After Banttari, 1976 in Hilterman, 1981).

CHAPTER THREE

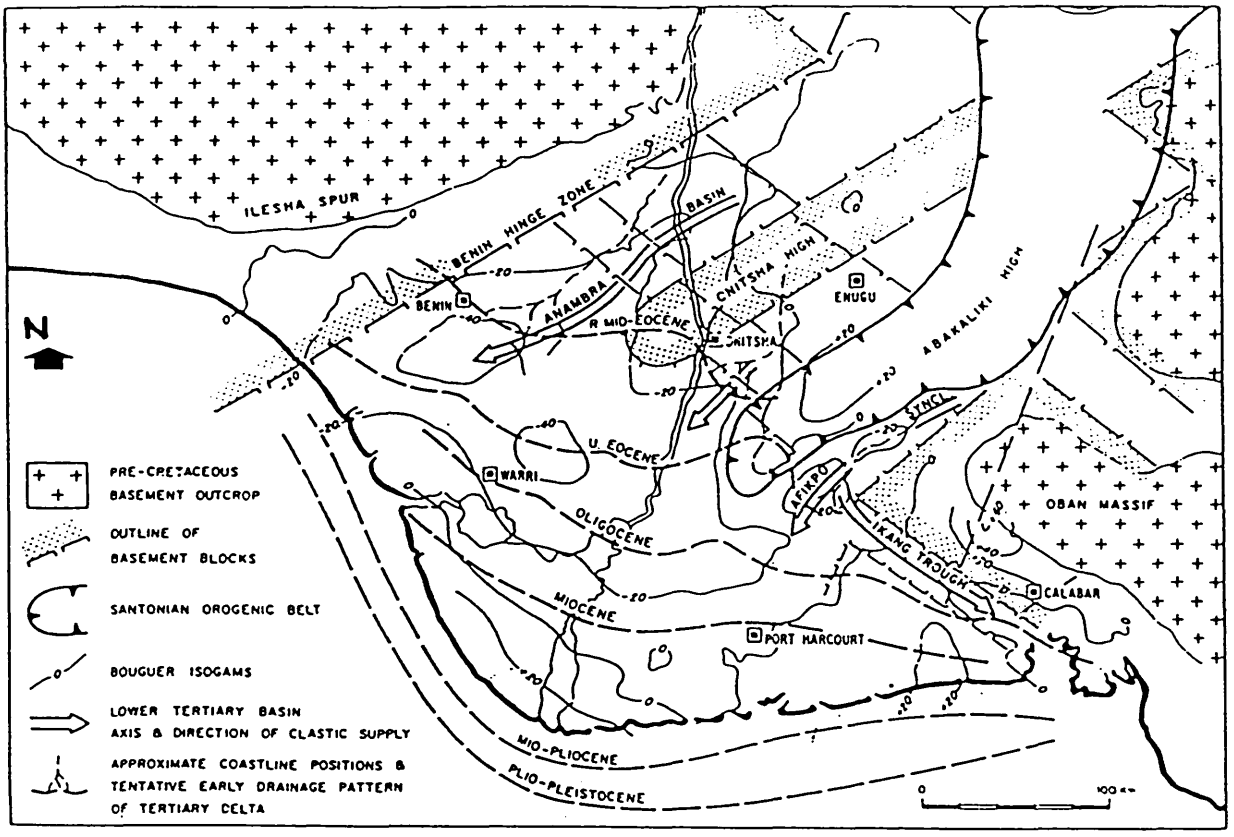

Fig.3.1 Structural composite of the regional tectonic frame work of the Niger Delta during the Cenozoic. (Based on various authors in Whiteman, 1982.)

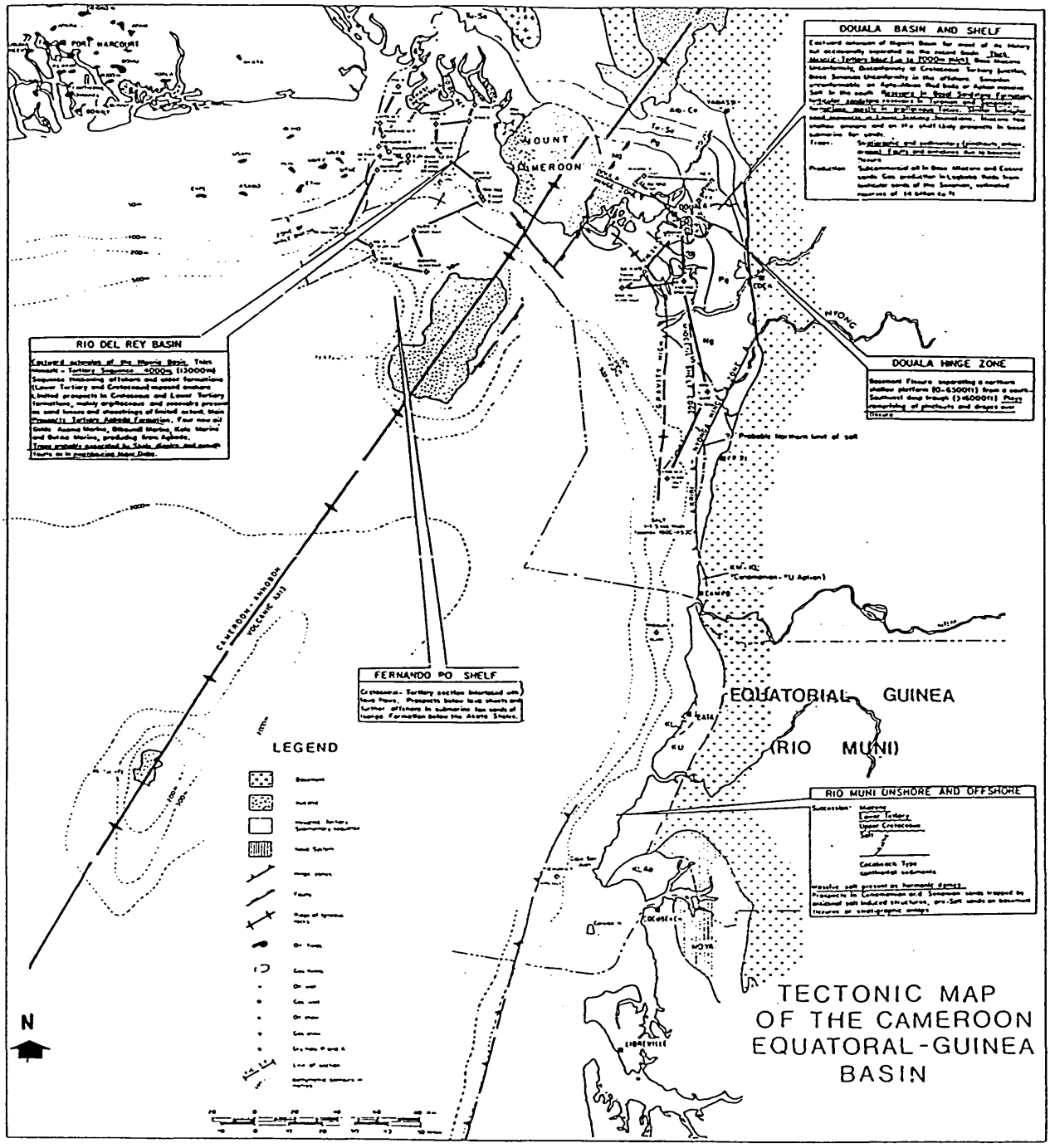

Fig.3.2 Tectonic setting of the eastward extension of the delta and its relationship with the Rio del Rey basin. (Based on Dike, 1975 in Whiteman, 1982).

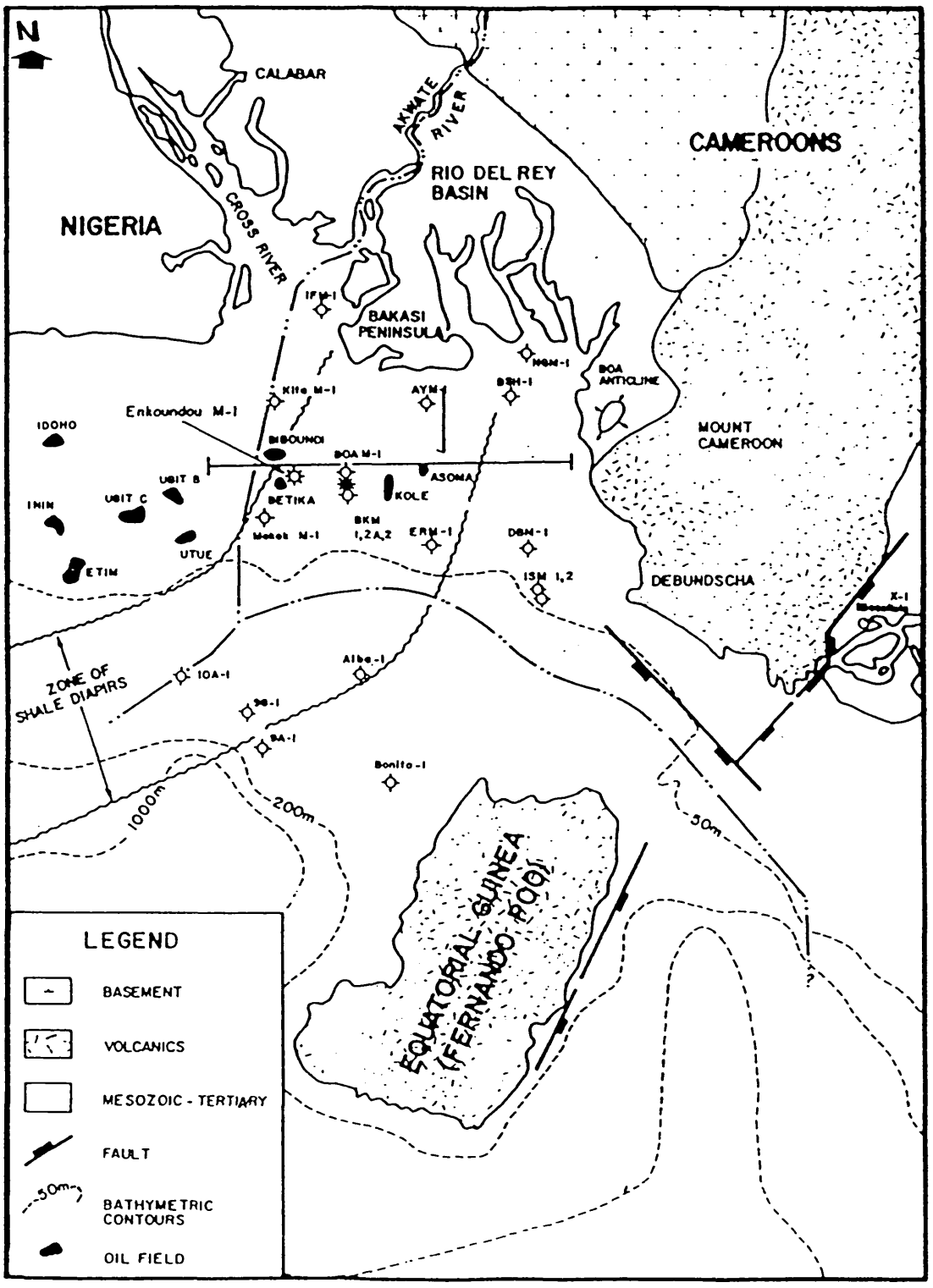

Fig.3.3a The zone of shale diapirs, SE Niger Delta. (After Dike, 1975).

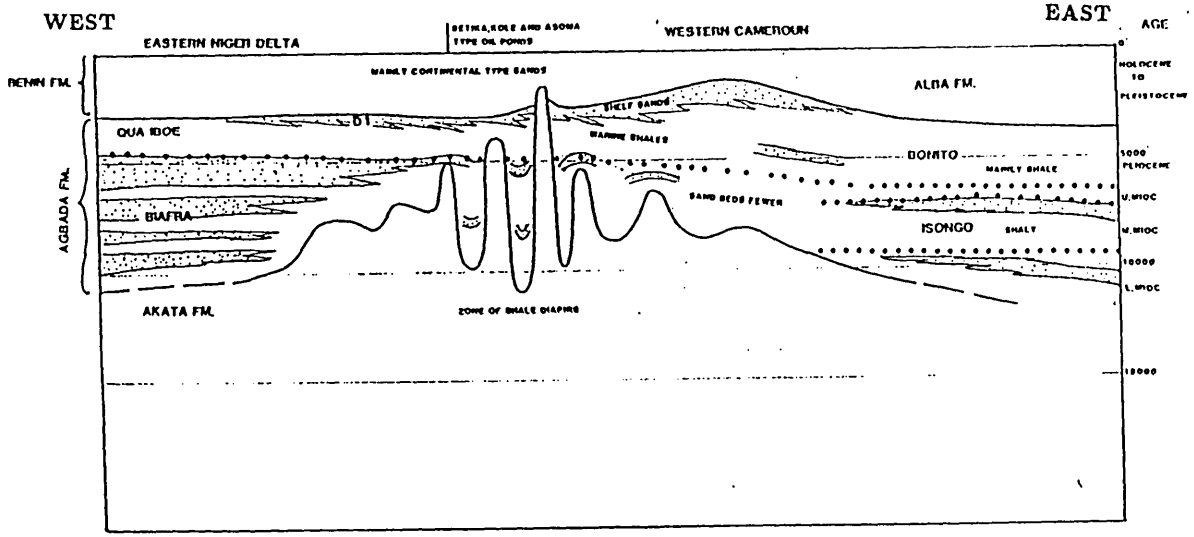

SCHEMATIC STRUCTURAL/STRATIGRAPHIC SECTION OFFSHORE EASTERN NIGER DELTA AND WESTERN CAMEROUN.

MODIFIED FROM DIKE(1975)

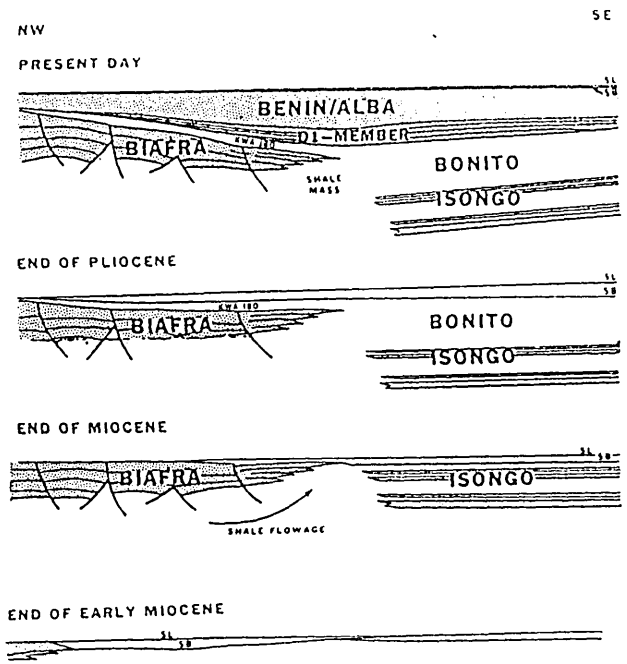

MODEL FOR THE DEPOSITIONAL HISTORY OF OFFSHORE EASTERN NIGER DELTA AND WESTERN CAMEROUN

Fig.3.3b Schematic cross-section across the zone of shale diapirs showing the relationship between the eastern delta and the Rio del rey basin. The equivalent Agbada formation in western Cameroun is called the Isongo formation made up of Lower and Middle Miocene Biafra type sediments compared to the Agbada formation which mainly Middle to Upper Miocene. A model for the depositional history is also shown. The Cameroun-Annobon volcanic axis (shown in Fig.3.2) is the most important tectonic feature and although it occurs to the east of the zone of shale diapirs was incidental to the shale diapirism and regional tectonism considered in the text.

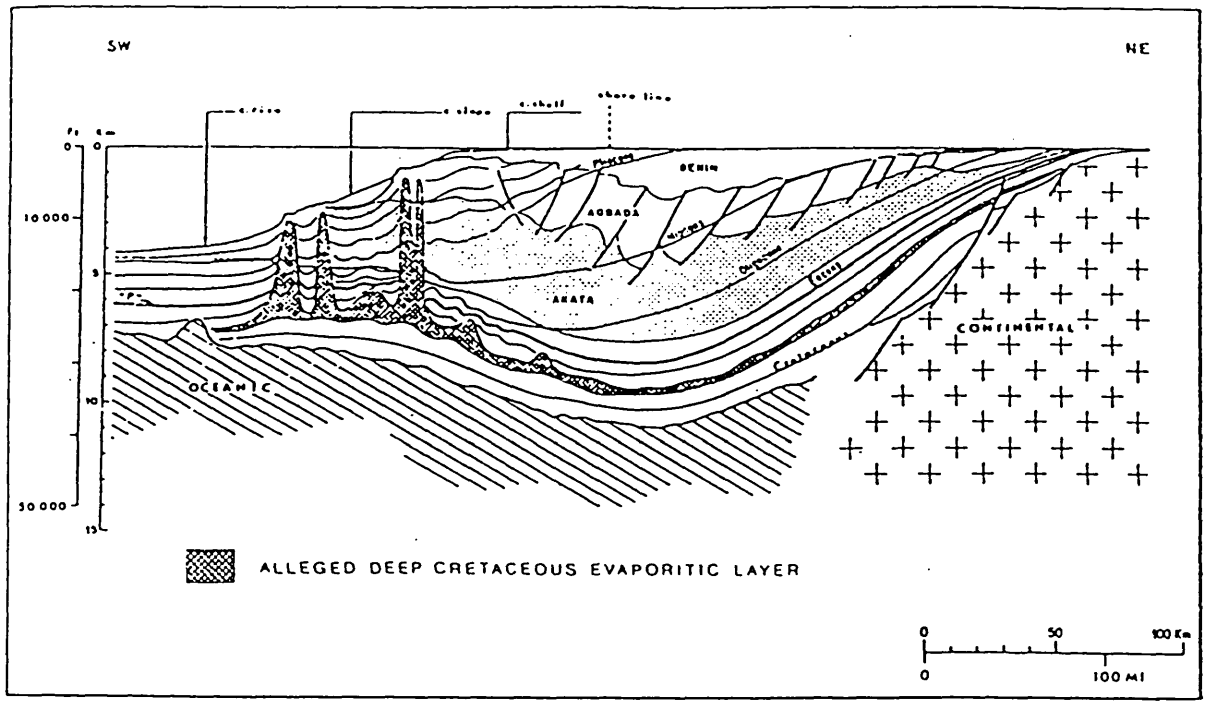

Fig.3.4a A hypothetical section showing the sedimentary bulge. (After Whiteman, 1982).

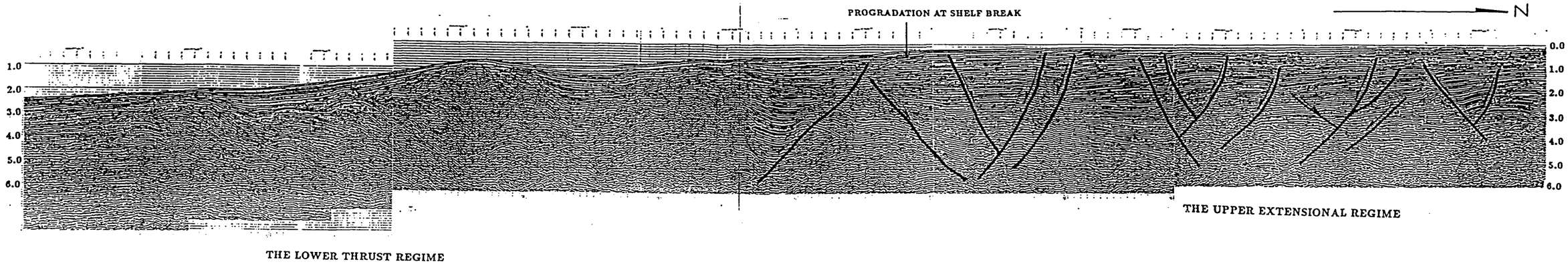

Fig.3.4b Regional seismic line showing the continental shelf and slope. The upper extensional regime of the Niger Delta characterized by growth faulting (in the northern parts of the profile) is shown. The lower thrust regime or toe occurs to the south.

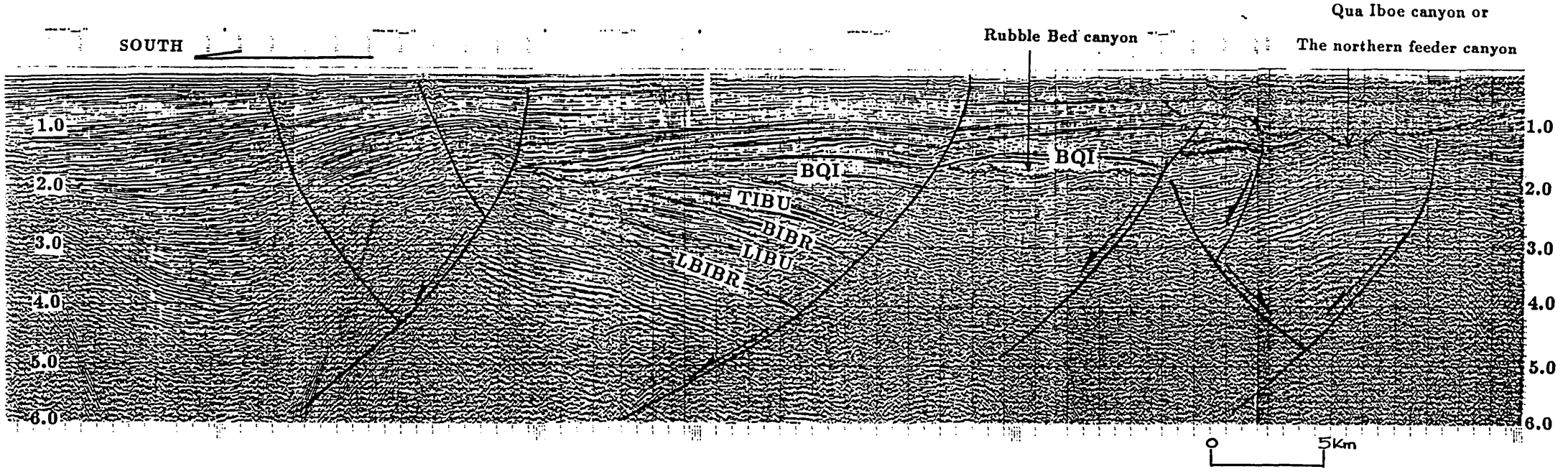

Fig.3.4c Regional seismic line showing canyon incision on the shelf.

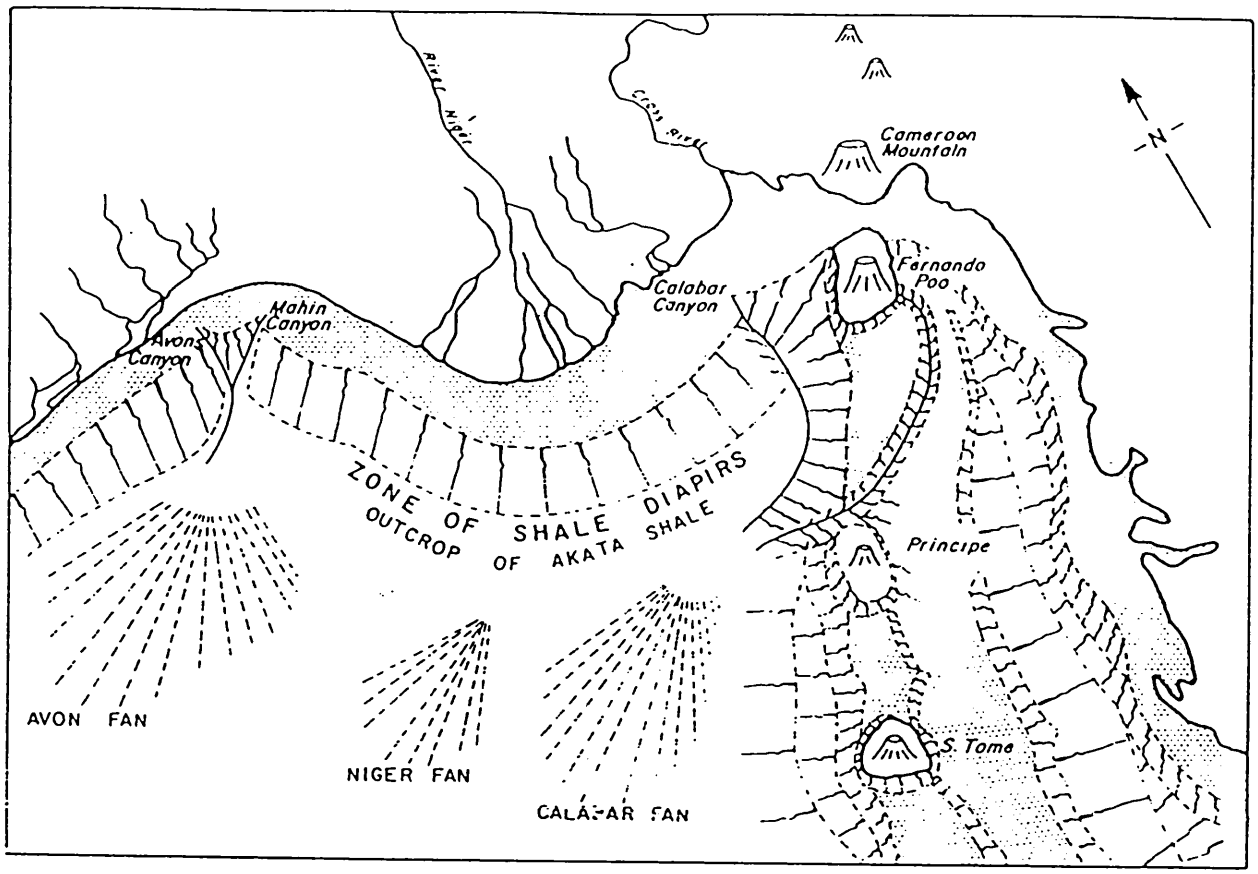

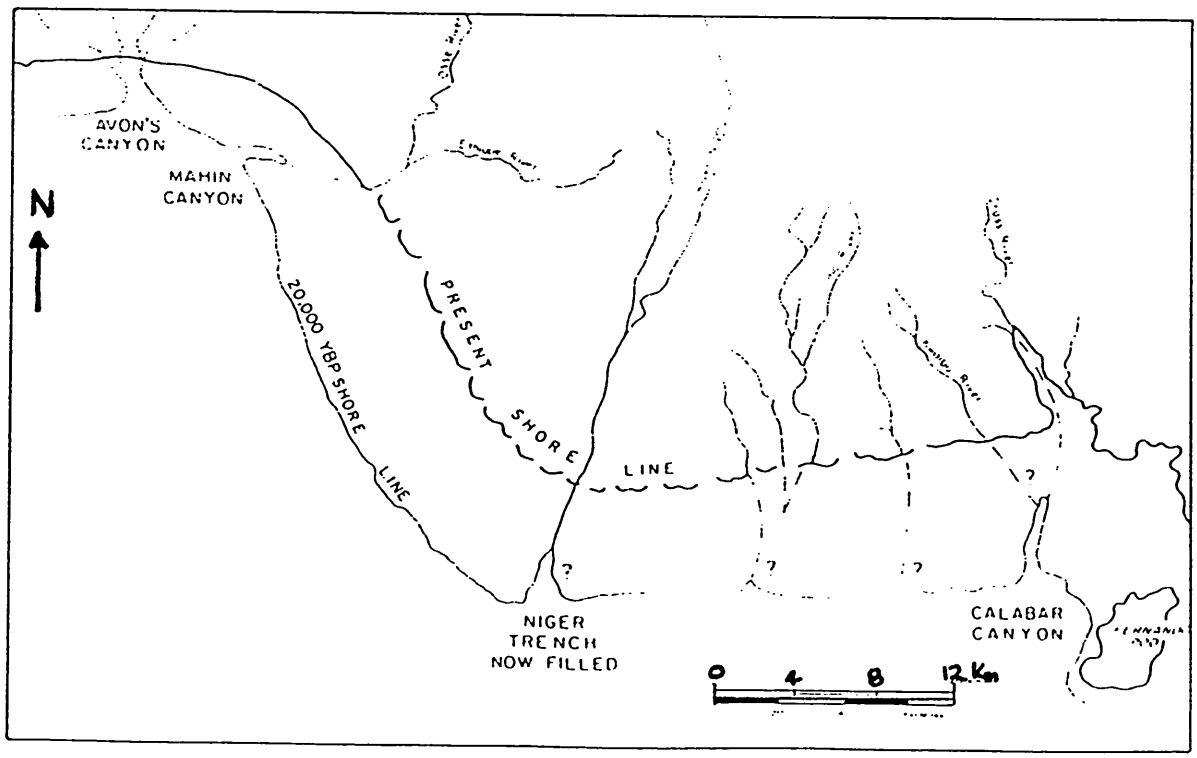

Fig.3.5 Canyon incisions of the Niger continental slope. (After Burke, 1972).

P(---) THESE ARE PALYNOLOGIC ZONES RECOGNIZED IN CONTINENTAL TO MARINE FACIES TYPES USED AS TIME MARKERS.

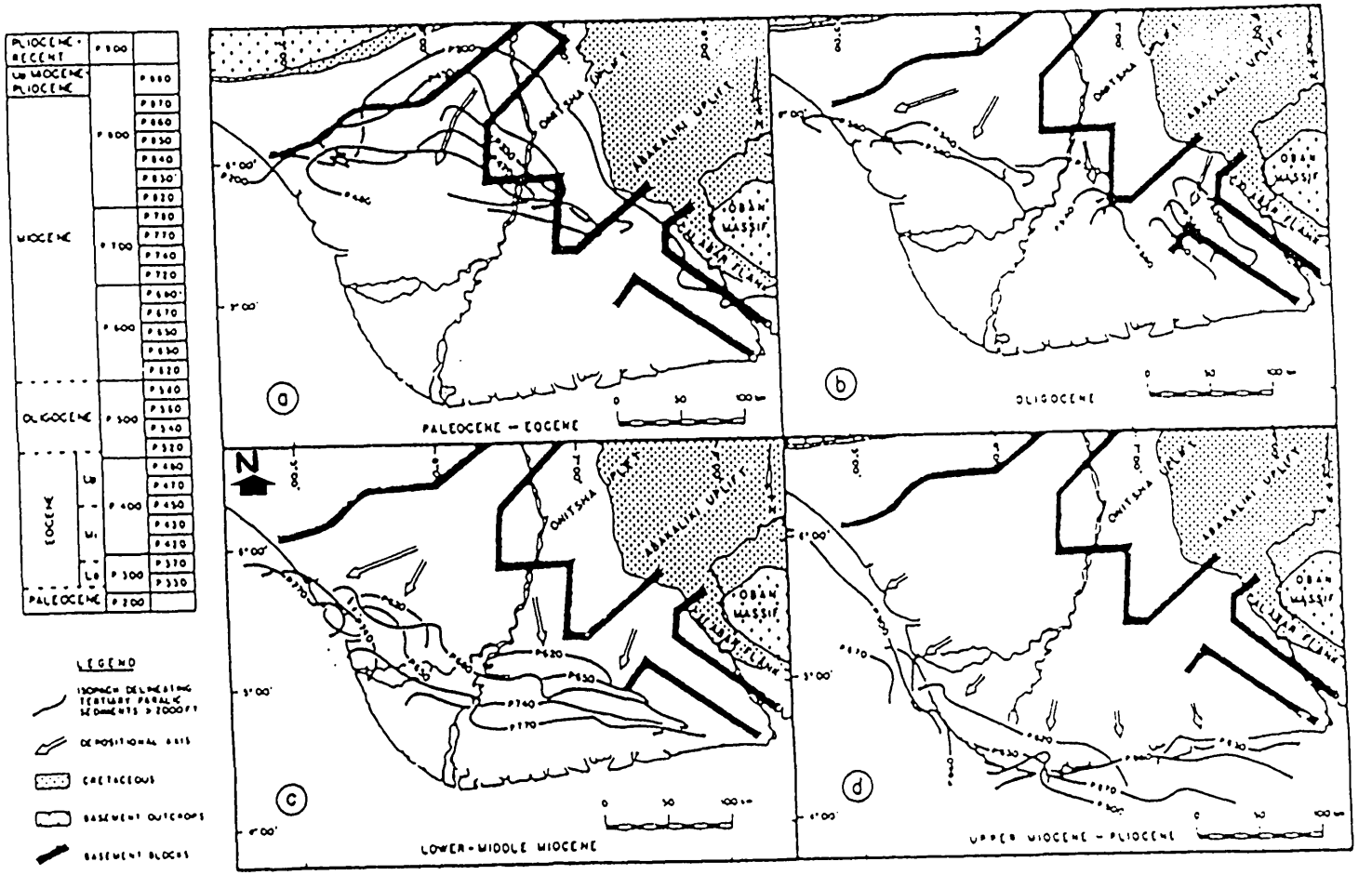

Fig.3.6a Stratigraphic evolution of the Niger Delta. (After Evamy *et al.* 1978).

STRATIGRAPHY

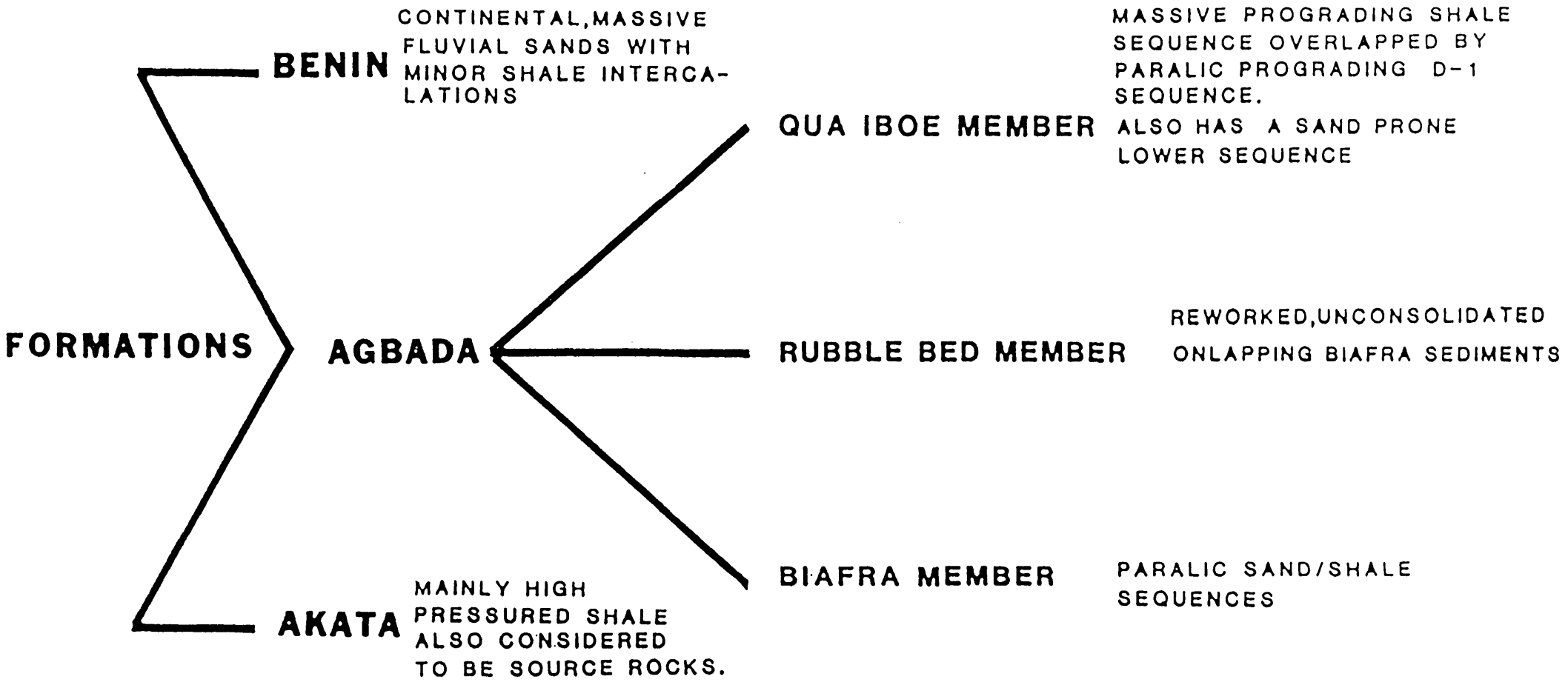

Fig.3.6b Major formation units of the study area.

BIBR- Base Intra Biafra Rubble.

TIBU- Top Intra Biafra Unconformity.

BIBBEN- Base Intra Biafra Benin sands.

BRB- Base Rubble Beds

BQI- Base Qua Iboe.

TIQI- Top Intra Qua Iboe

QUA3 etc- Intra Qua Iboe horizon 3 etc

Pu- Pleistocene Unconformity

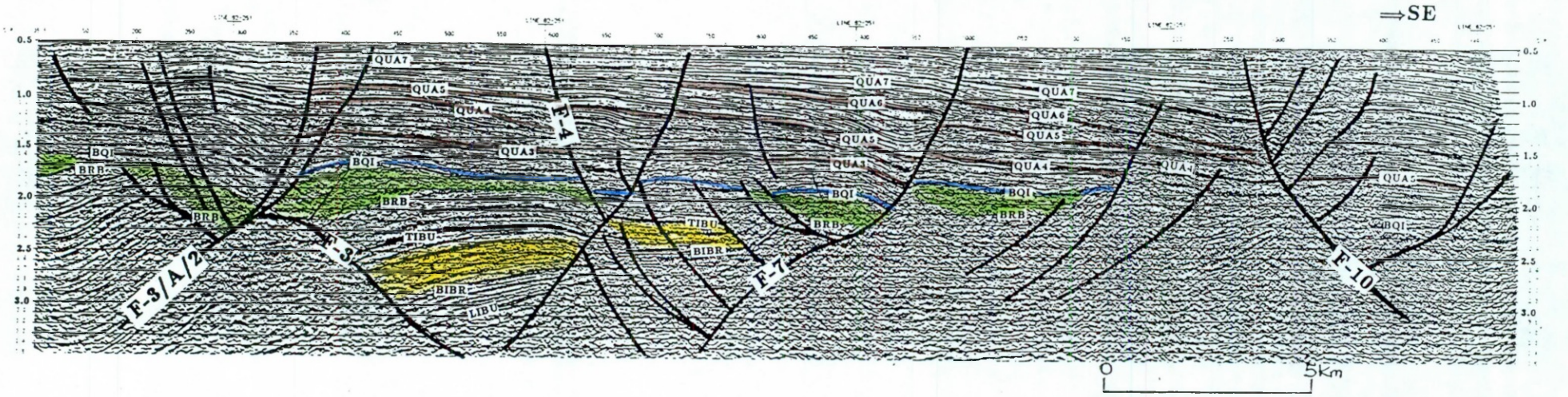

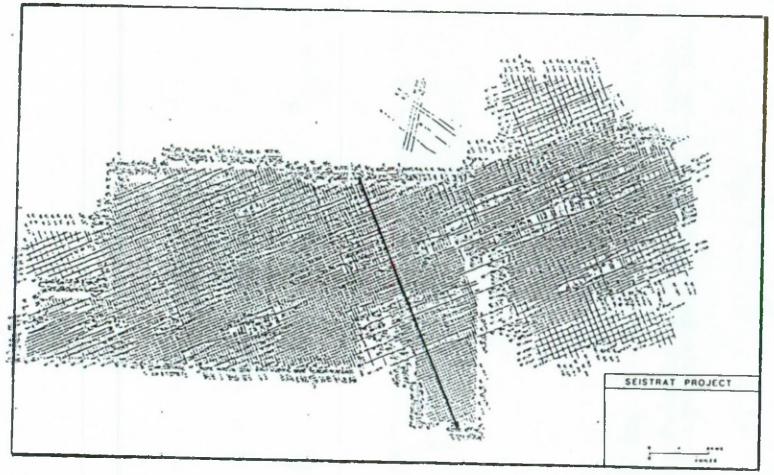

Fig.3.7 Seismic line 82-251. Major stratigraphic sequences mapped in the study area.

LBIBR- Lower Base Intra Biafra Rubble.

LIBU- Lower Intra Biafra Unconformity.

BIBR- Base Intra Biafra Rubble.

TIBU- Top Intra Biafra Unconformity.

BIBBEN- Base Intra Biafra Benin sands.

BRB- Base Rubble Beds

BQI- Base Qua Iboe.

TIQI- Top Intra Qua Iboe

QUA3 etc- Intra Qua Iboe horizon 3 etc

Pu- Pleistocene Unconformity

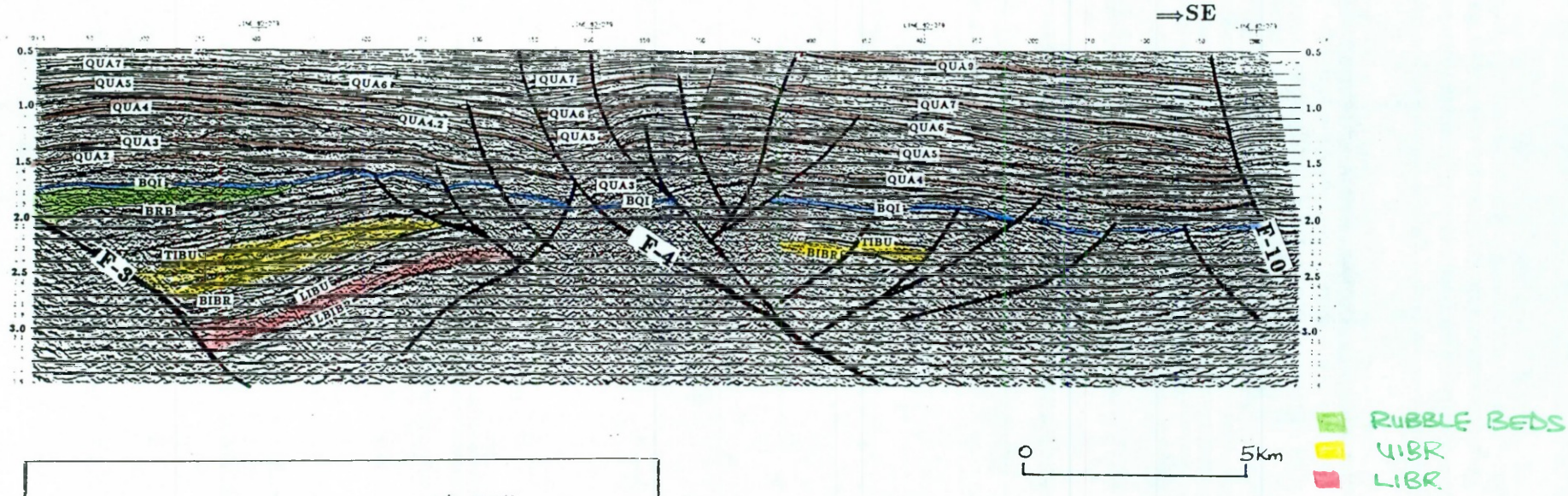

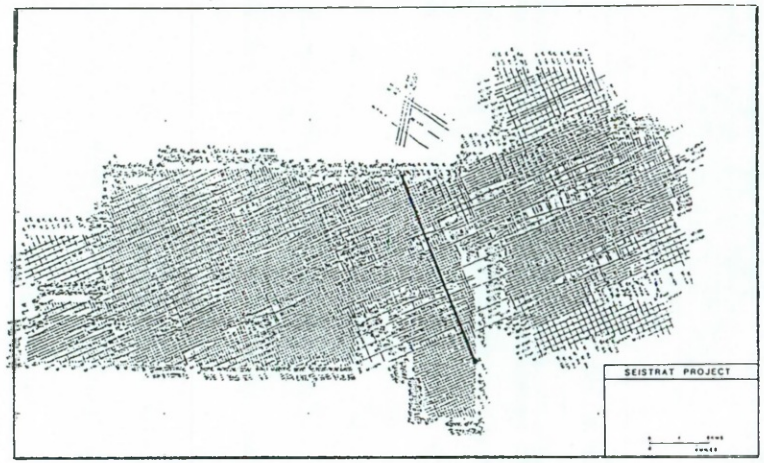

Fig.3.8 Seismic line 279. Pliocene stratigraphic sequence subdivisions.

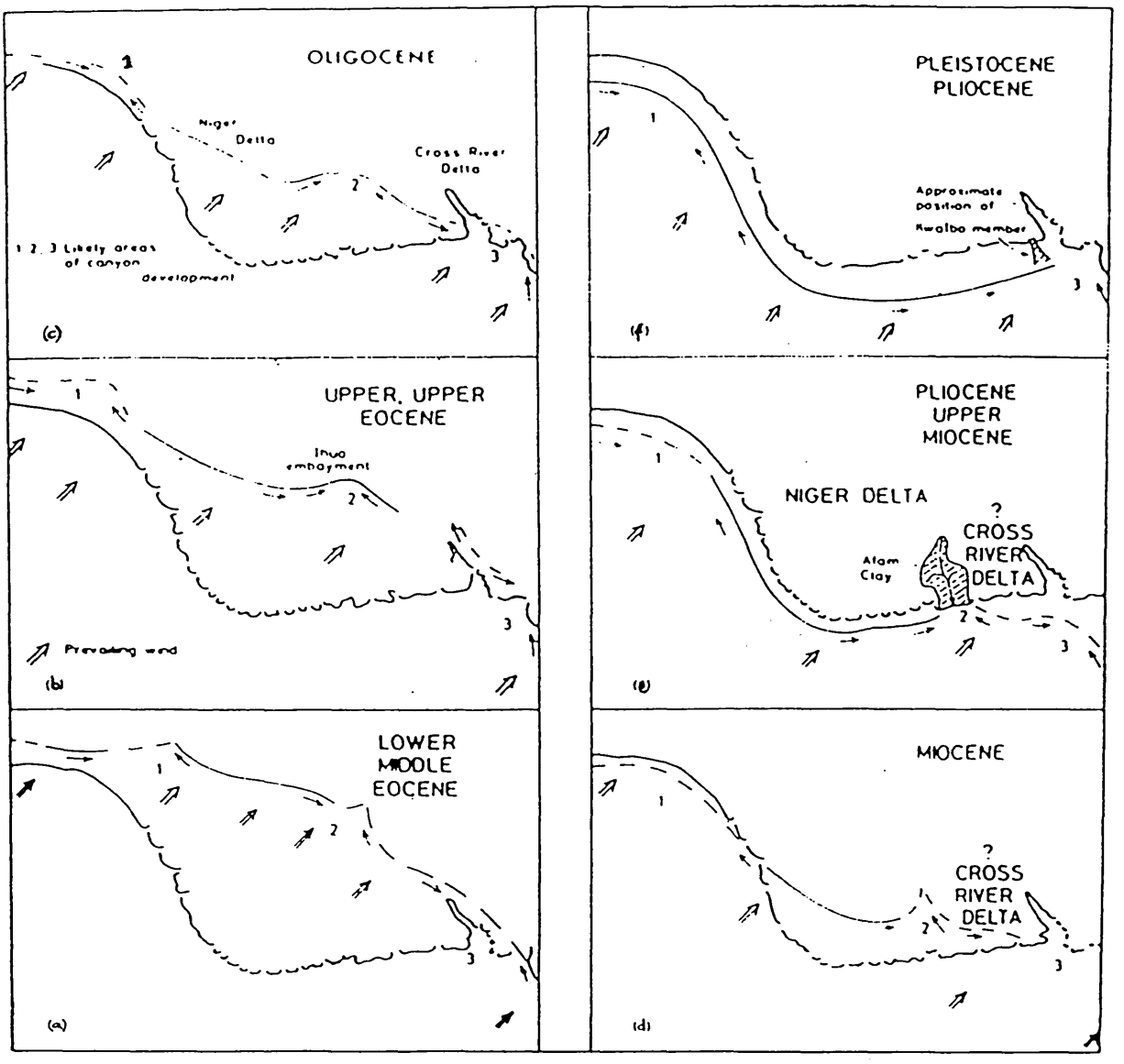

Fig.3.9 Development of the Eastern Delta from Oligocene to Pleistocene. (After Burke, 1972)

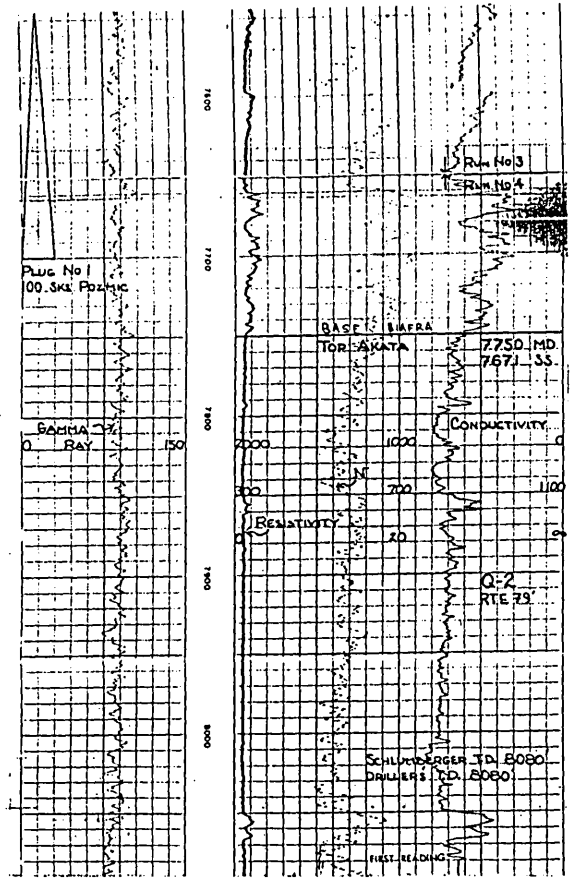

Fig.3.10a Petrophysical characteristics of the Akata formation. In this figure, the Top Akata pick is based on the drop in the shale resistivity and corresponding increase in conductivity. Although not shown this pick is often correlated with the sonic log where an increase in interval transit time indicates a drop in velocity due to over pressure.

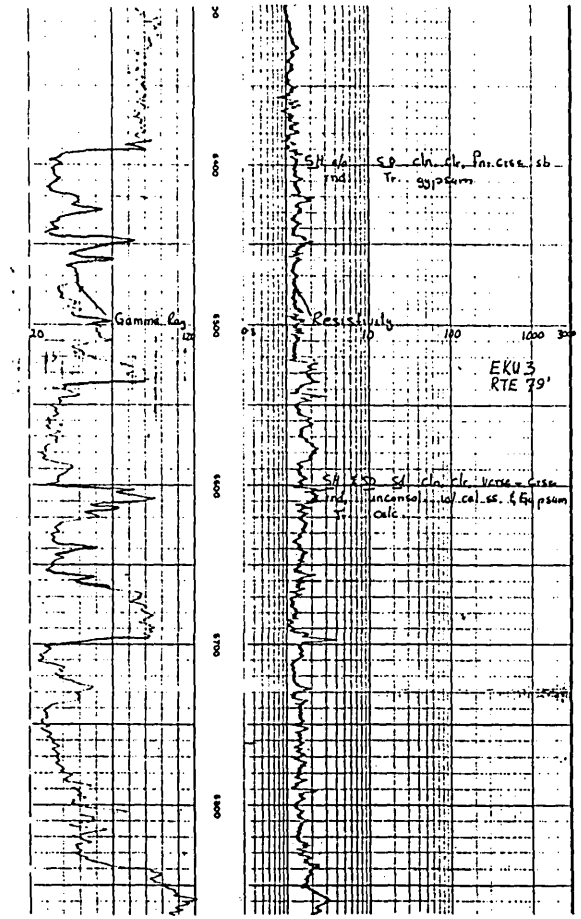

Fig.3.10b Petrophysical characteristics of the Biafra member. This is often characterized by the paralic sand-shale sequence depicted by the Gamma ray curve.

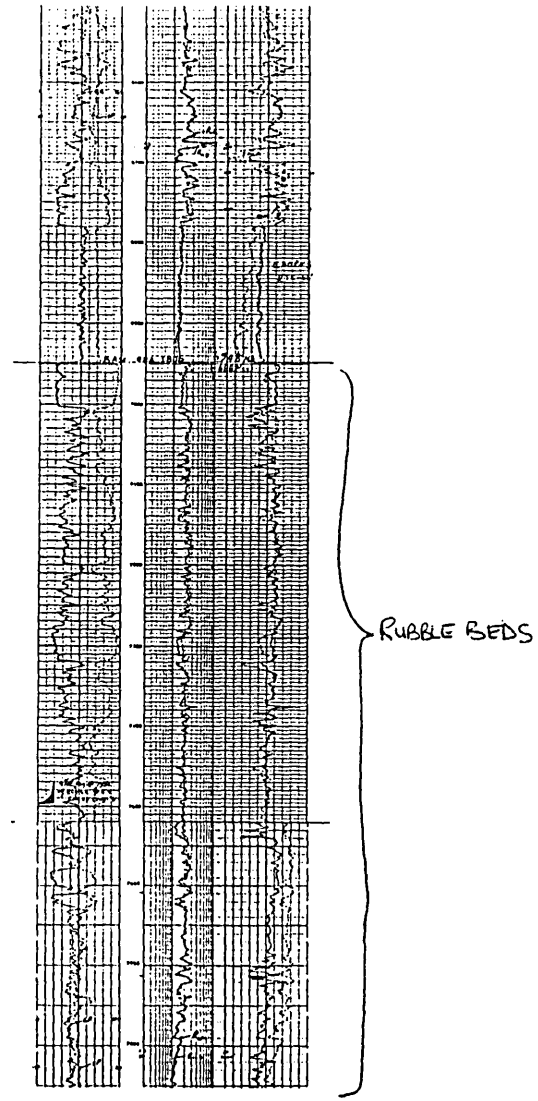

Fig.3.10c Petrophysical characteristics of the Rubble Bed member. As evident here, there is often little distinction in the log motif between the Biafra and Rubble Beds except that the Gamma ray curve is often highly serrated as shown. The Rubble Beds may also be a continuous shale column especially when canyon associated. Dipmeter plots show a scatter as against uniform dips characteristic of the Biafra.

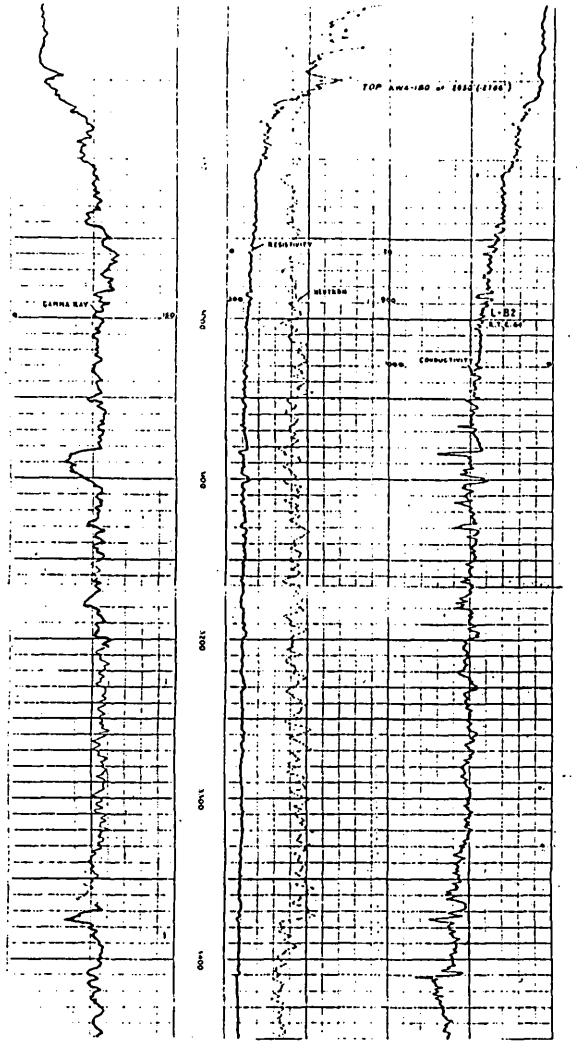

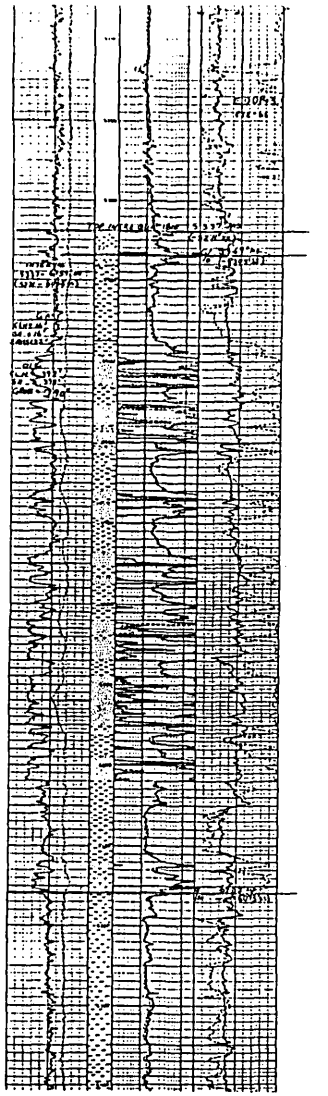

Fig.3.10d Petrophysical characteristics of the Qua Iboe member. To the left, the Qua Iboe is basically a massive shale sequence. When turbidites are present, the log to the left is more characteristic.

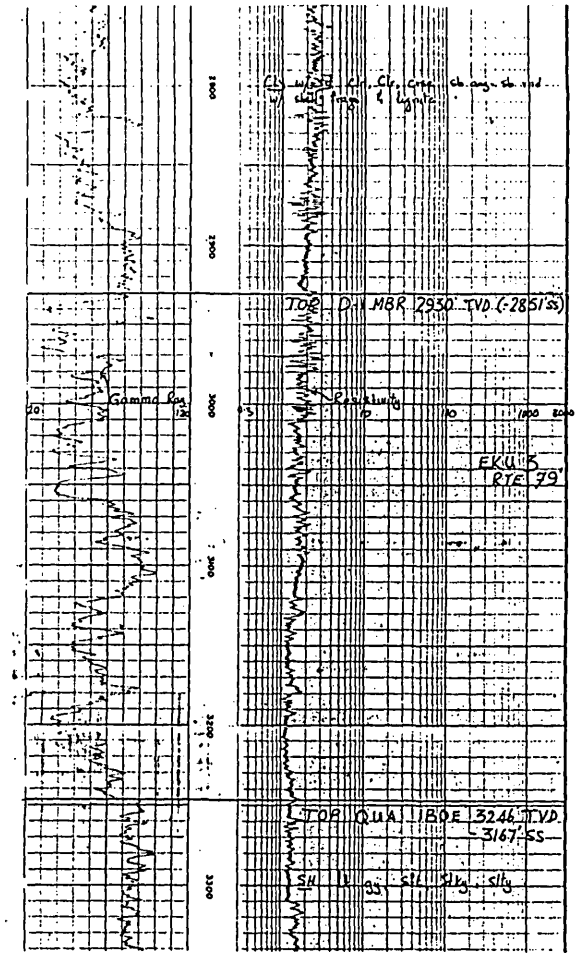

Fig.3.10e The D-1 is often characterized by upward coasening log motif as shown. It represents a transitional sequence between the Qua Iboe and the Benin formation.

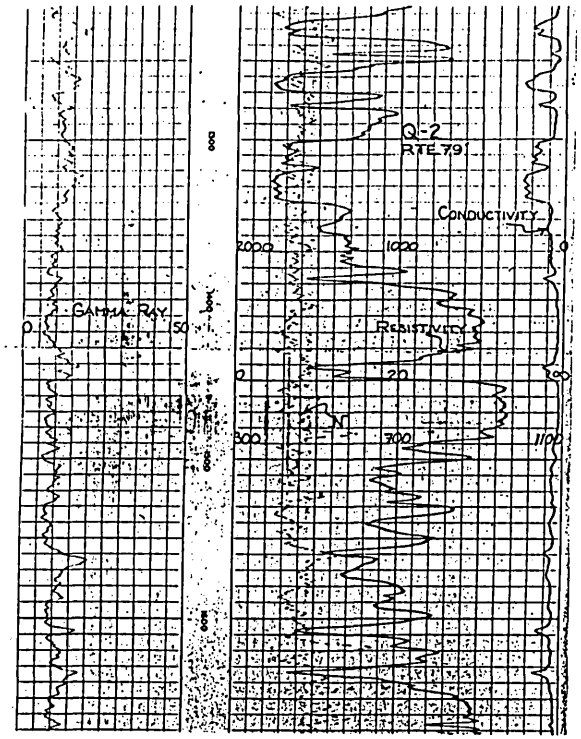

Fig.3.10f Petrophysical characteristics of the Benin formation. Note the massive sands characterized by low Gamma ray readings and the fresh water environment depicted by the resistivity curve.

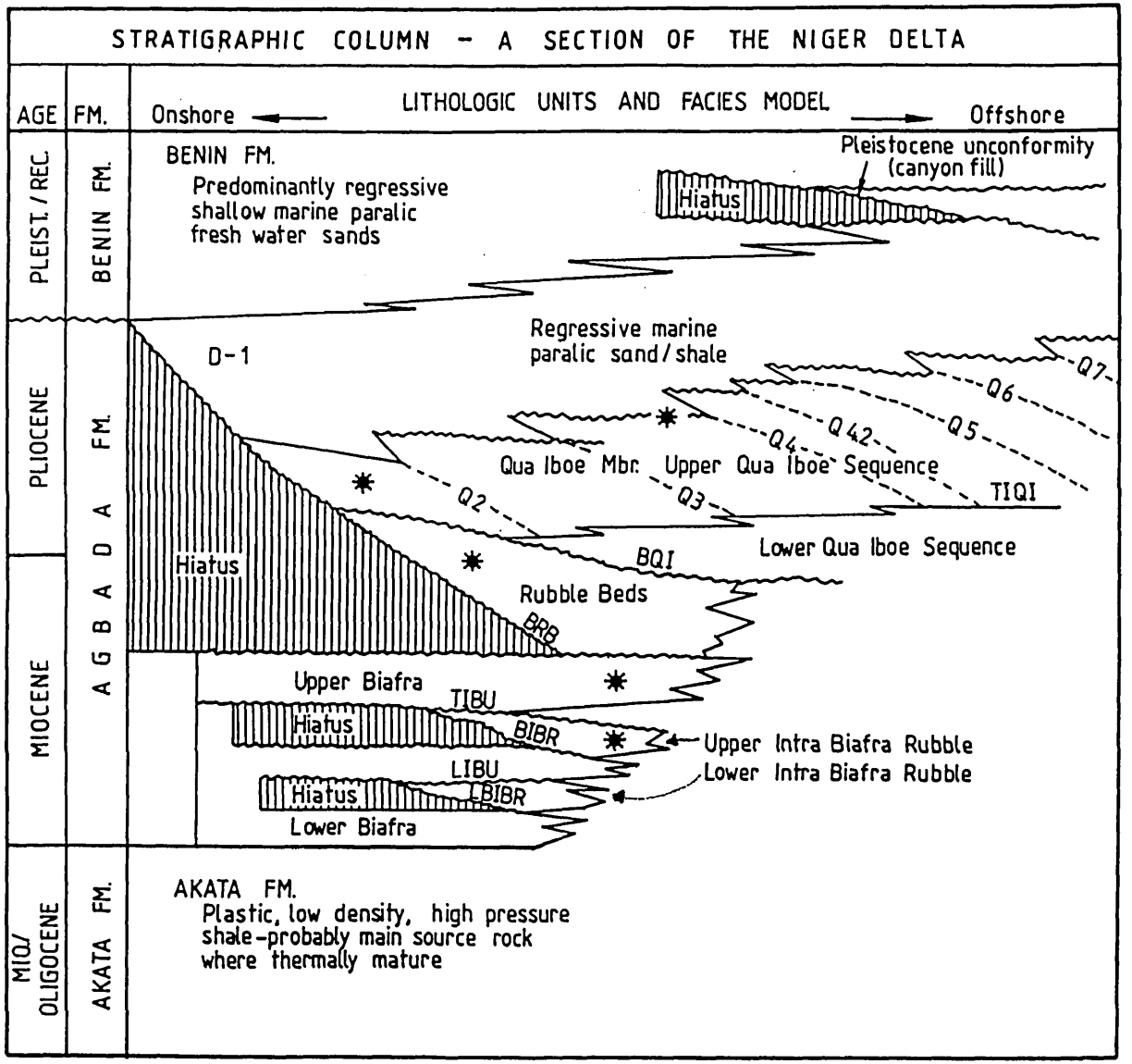

Fig.3.11a A generalized stratigraphic column showing the vertical succession of lithologies.

LBHBR- Lower Base Intra Biafra Rubble.

LHBU- Lower Intra Biafra Unconformity.

BHBR- Base Intra Biafra Rubble.

THBU- Top Intra Biafra Unconformity.

BHBBEN- Base Intra Biafra Benin sands.

BRB- Base Rubble Beds.

BQI- Base Qua Iboe.

TIQI- Top Intra Qua Iboe.

QUA3 etc- Intra Qua Iboe horizon 3 etc.

Pu- Pleistocene Unconformity.

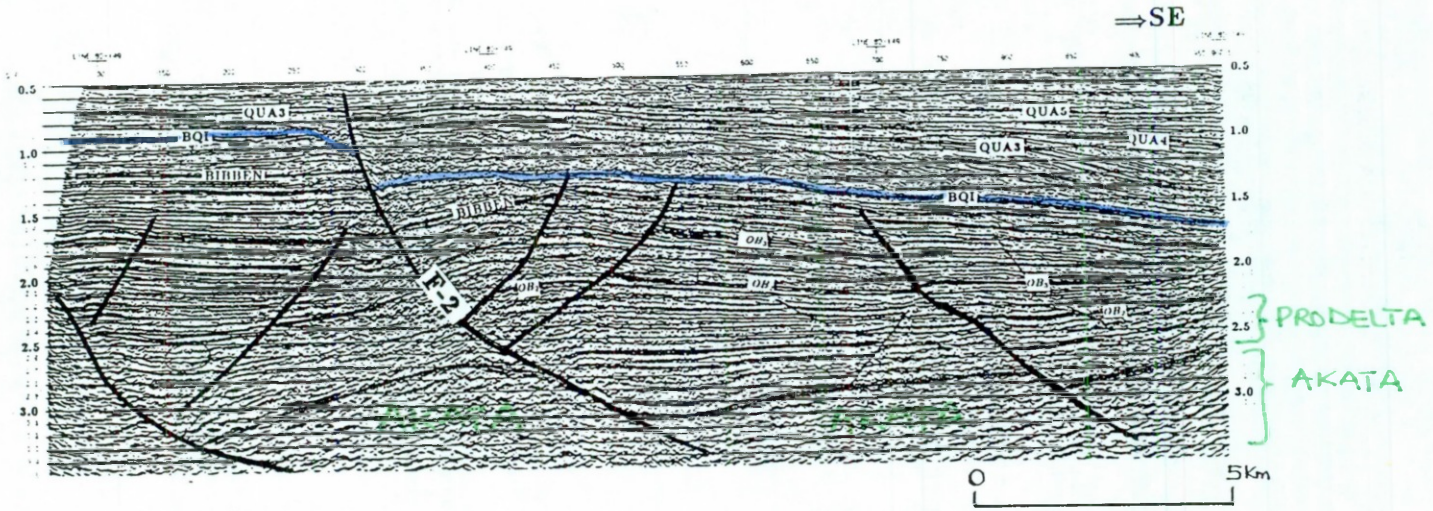

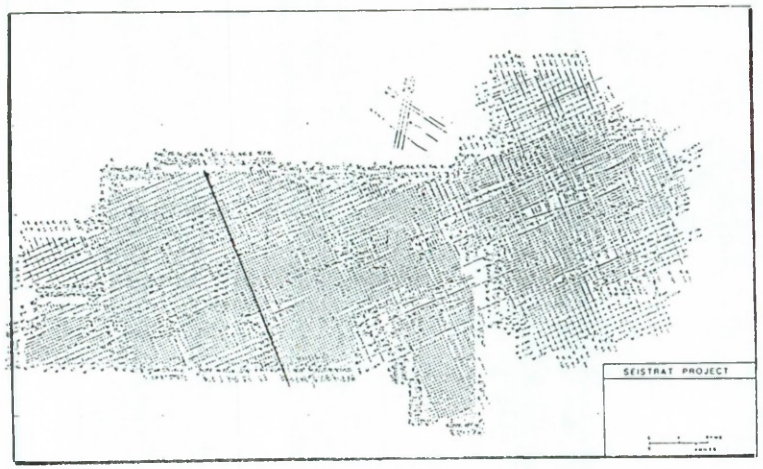

Fig.3.11b Seismic line 82-149 showing prodelta facies shaling out into Akata.

LBIBR- Lower Base Intra Biafra Rubble.

LIBU- Lower Intra Biafra Unconformity.

BIBR- Base Intra Biafra Rubble.

TIBU- Top Intra Biafra Unconformity.

BIBBEN- Base Intra Biafra Benin sands.

BRB- Base Rubble Beds

BQI- Base Qua Iboe.

TIQI- Top Intra Qua Iboe

QUA3 etc- Intra Qua Iboe horizon 3 etc

Pu- Pleistocene Unconformity

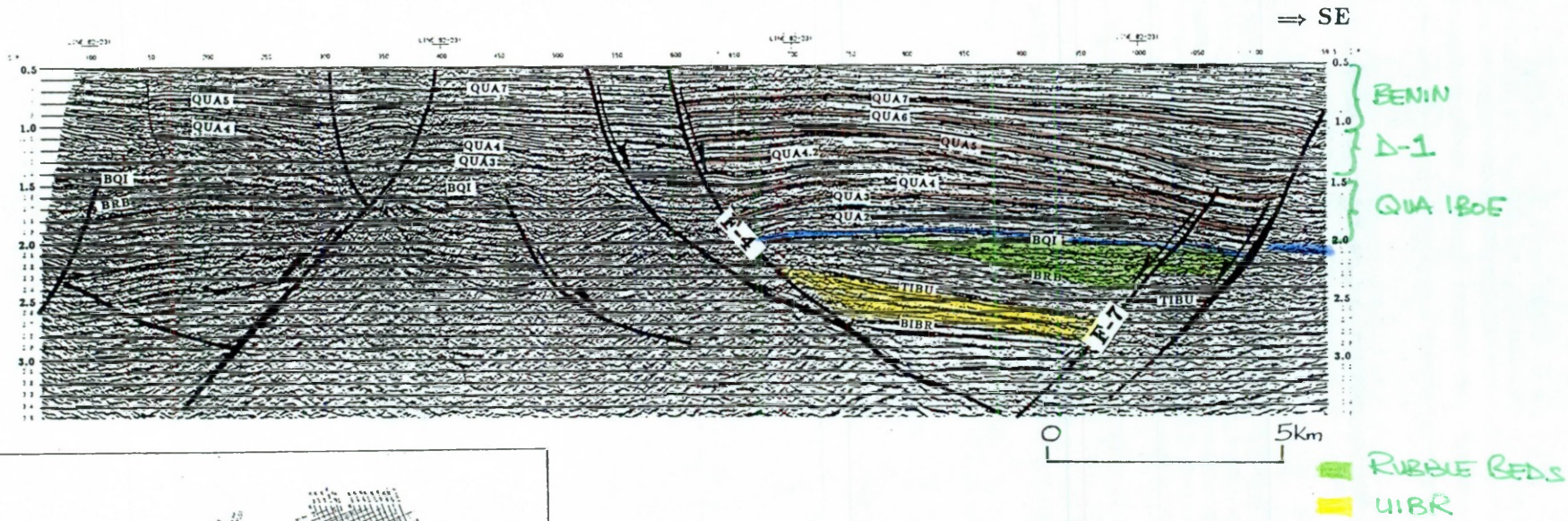

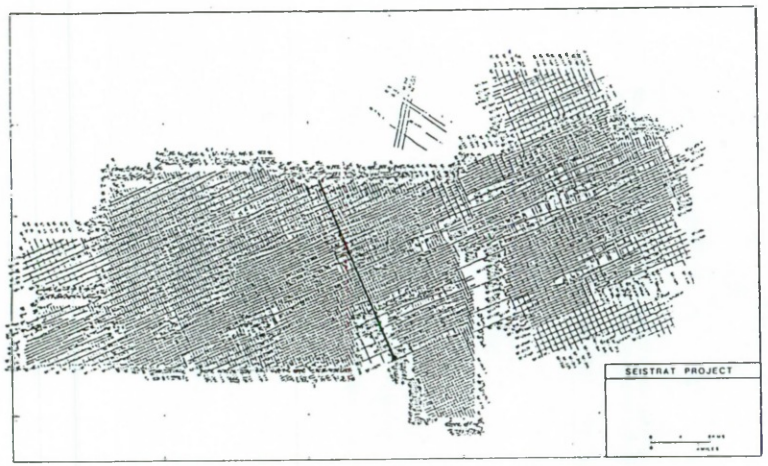

Fig.3.11c Seismic line 82-231 showing the major subdivisions of the Agbada formation to the west.

LBIBR- Lower Base Intra Biafra Rubble.

LIBU- Lower Intra Biafra Unconformity.

BIBR- Base Intra Biafra Rubble.

TIBU- Top Intra Biafra Unconformity.

BIBBEN- Base Intra Biafra Benin sands.

BRB- Base Rubble Beds

BQI- Base Qua Iboe.

TIQI- Top Intra Qua Iboe

QUA3 etc- Intra Qua Iboe horizon 3 etc

Pu- Pleistocene Unconformity

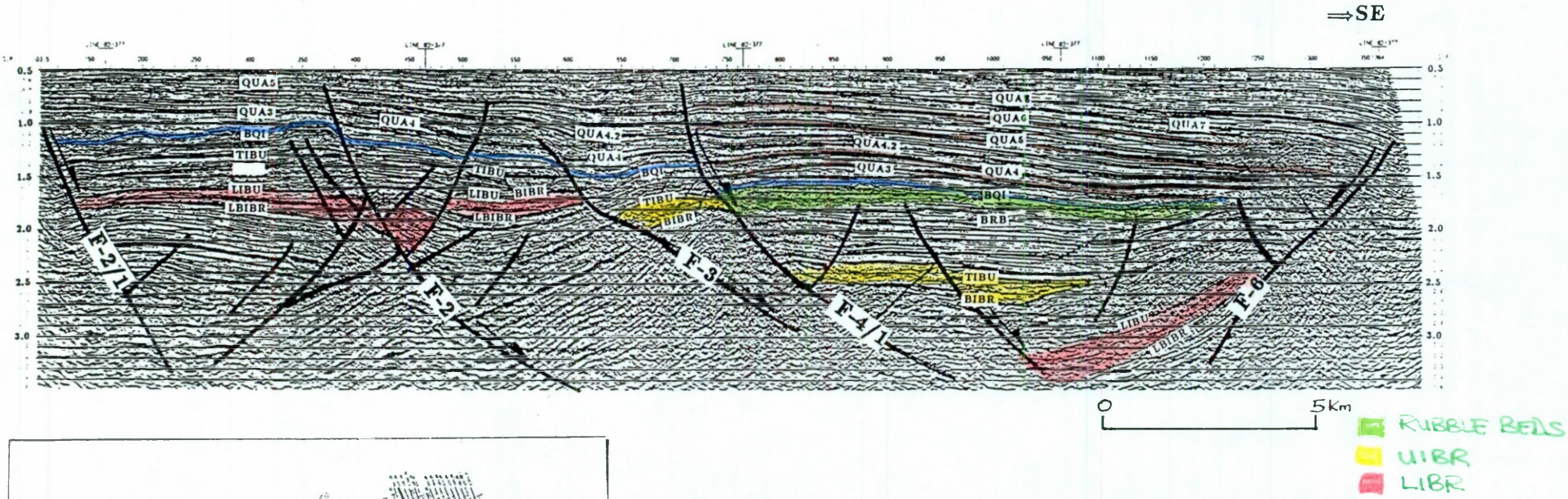

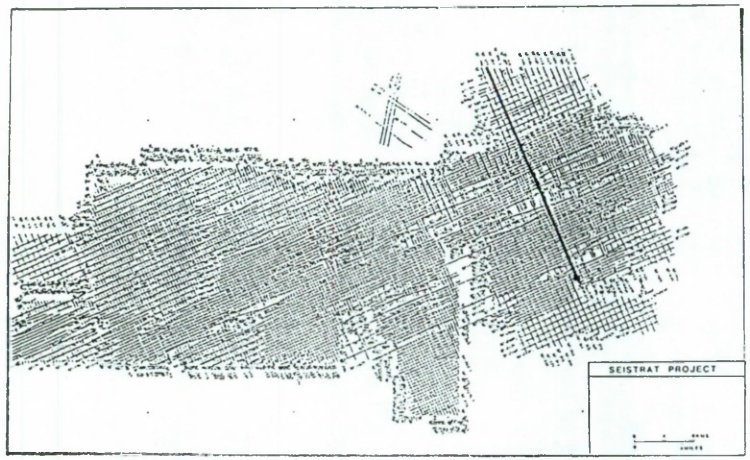

Fig.3.11d Seismic line 82-377 showing the major subdivisions of the Agbada formation to the east.

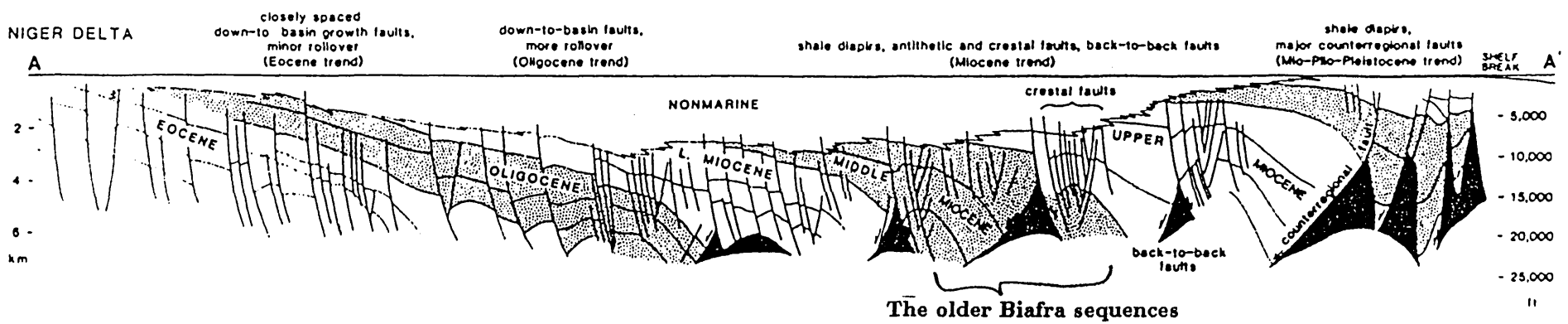

Fig.3.12 Regional cross-section. (After Evamy *et al.*, 1978).

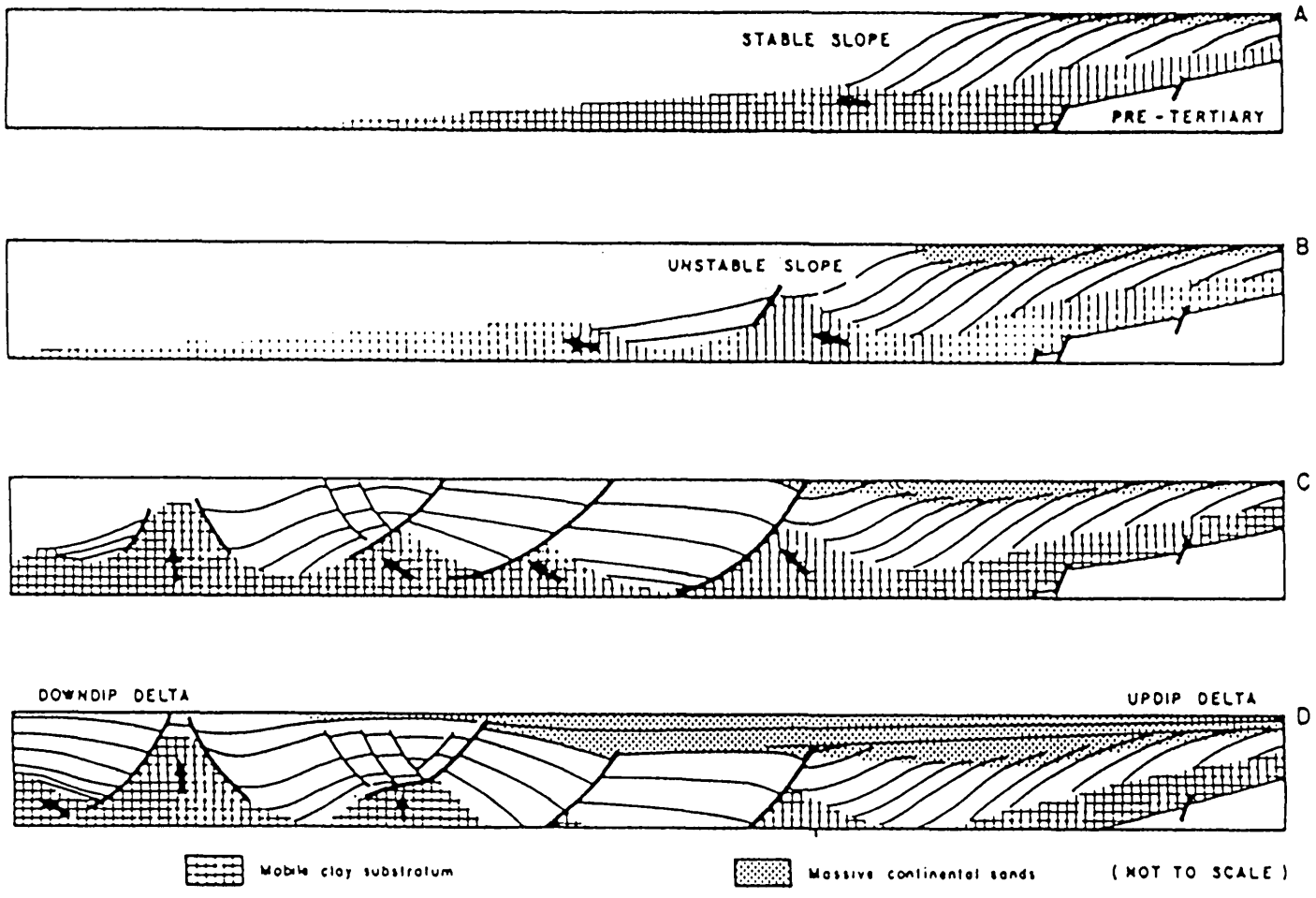

Prograding offlap sequence. No deformation on basin flanks with thin clay substratum. Initiation of clay ridge at toe of advancing slope.

As growth of clay ridge continues, a growth fault is initiated. Deposition of continental sands in depressions created by compaction of offlap sequence and clay flowage.

As delta builds basinward, younger clay ridges are formed. Clay upheaval structures in downdip parts of delta.

Late subsidence causes tilt and deposition of thick continental sands. Continued growth of shale upheaval structures induces expansion fault patterns and "back to back" faulting in downdip delta.

Fig.3.13b Development of simple and complex growth faults. (After Merki, 1972).

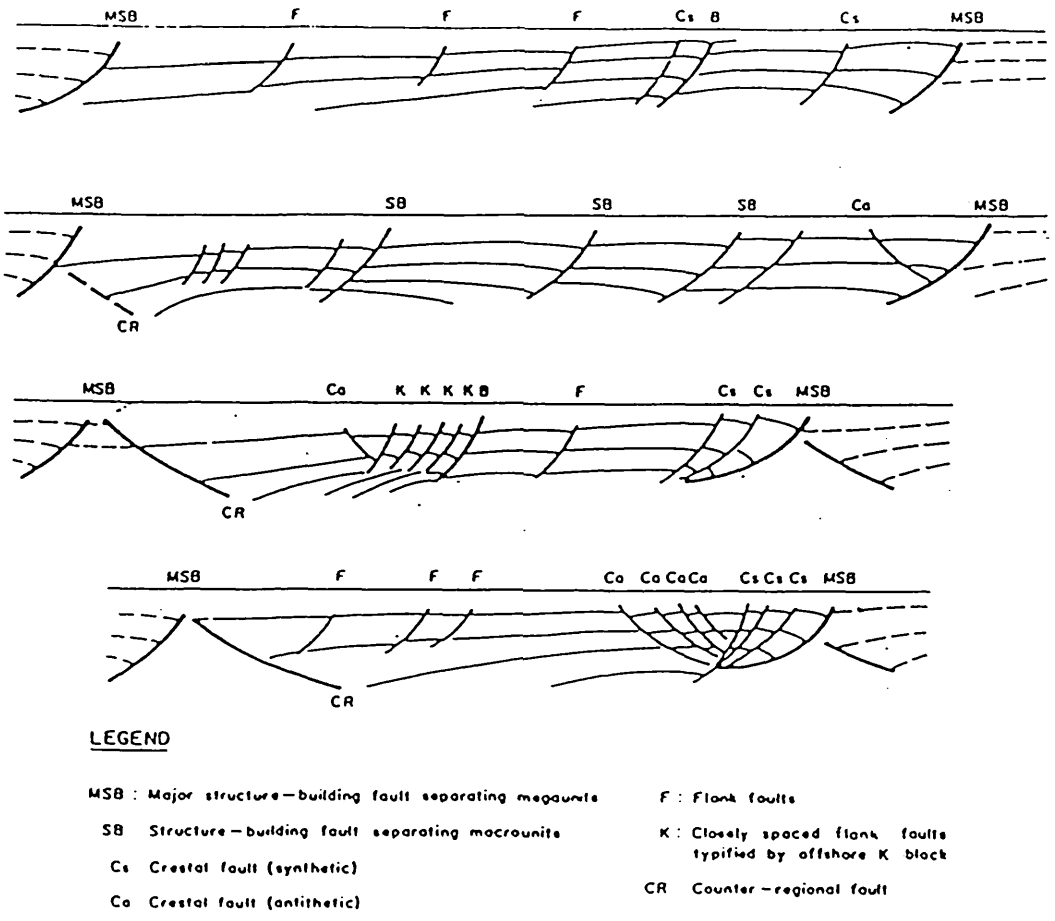

Fig.3.13a Megaunits and associated synsedimentary faults. (After Evamy *et al.*, 1978).

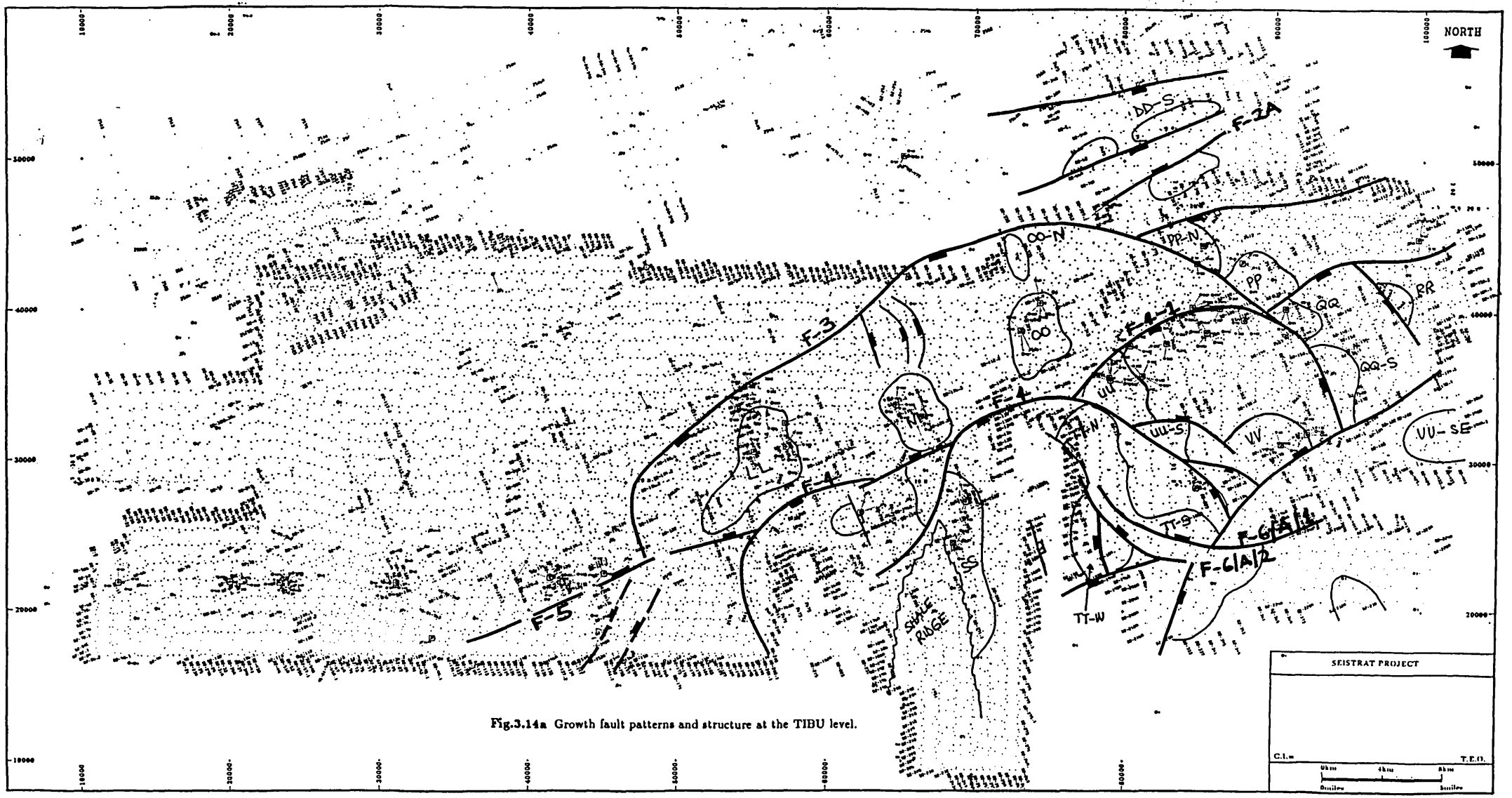

Fig.3.14a Growth fault patterns and structure at the TIBU level.

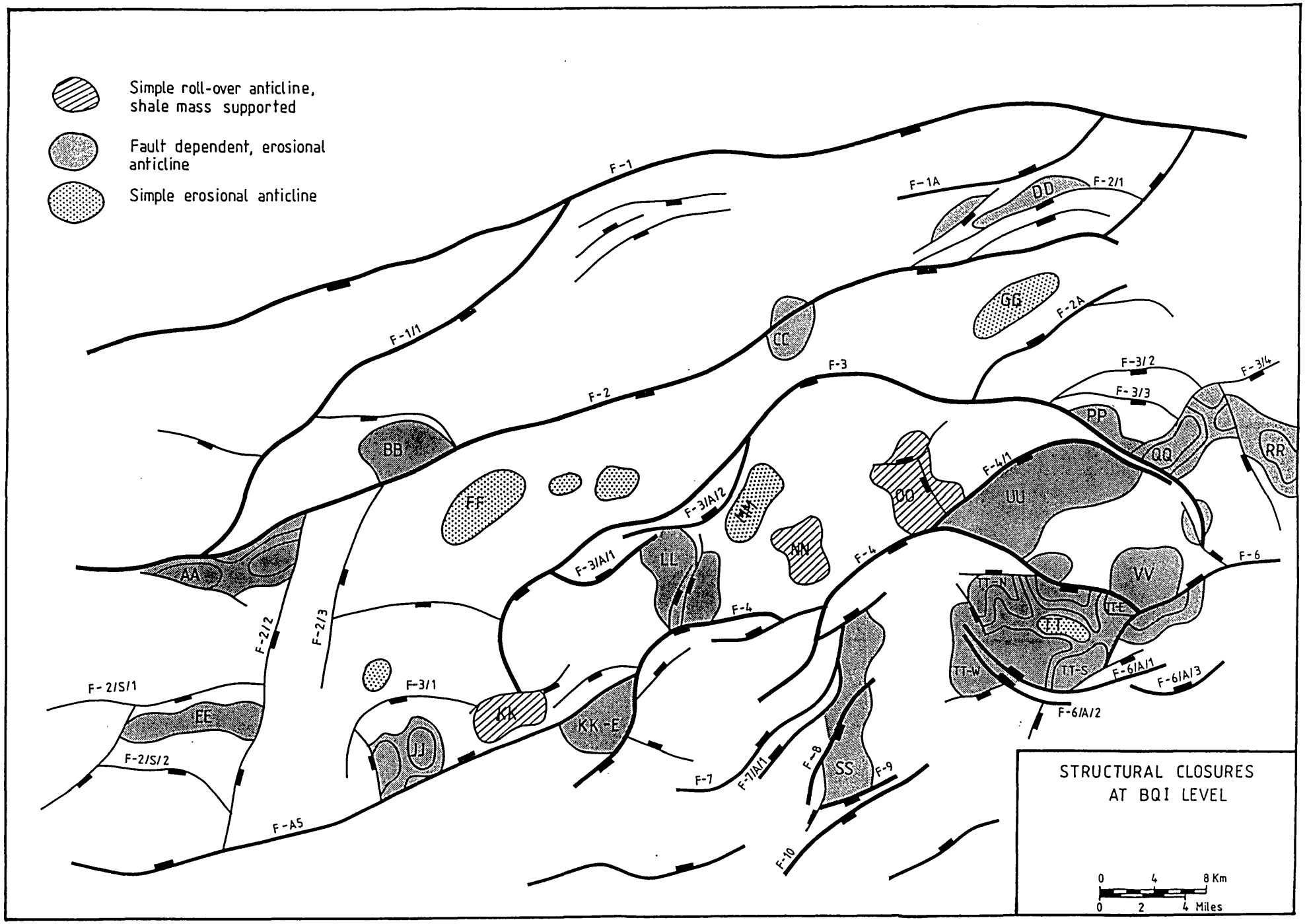

Fig.3.14b Growth fault patterns at the BQI level and associated structures.

Fig.3.14c Growth fault patterns at the QUA5 level and associated rollover structures.

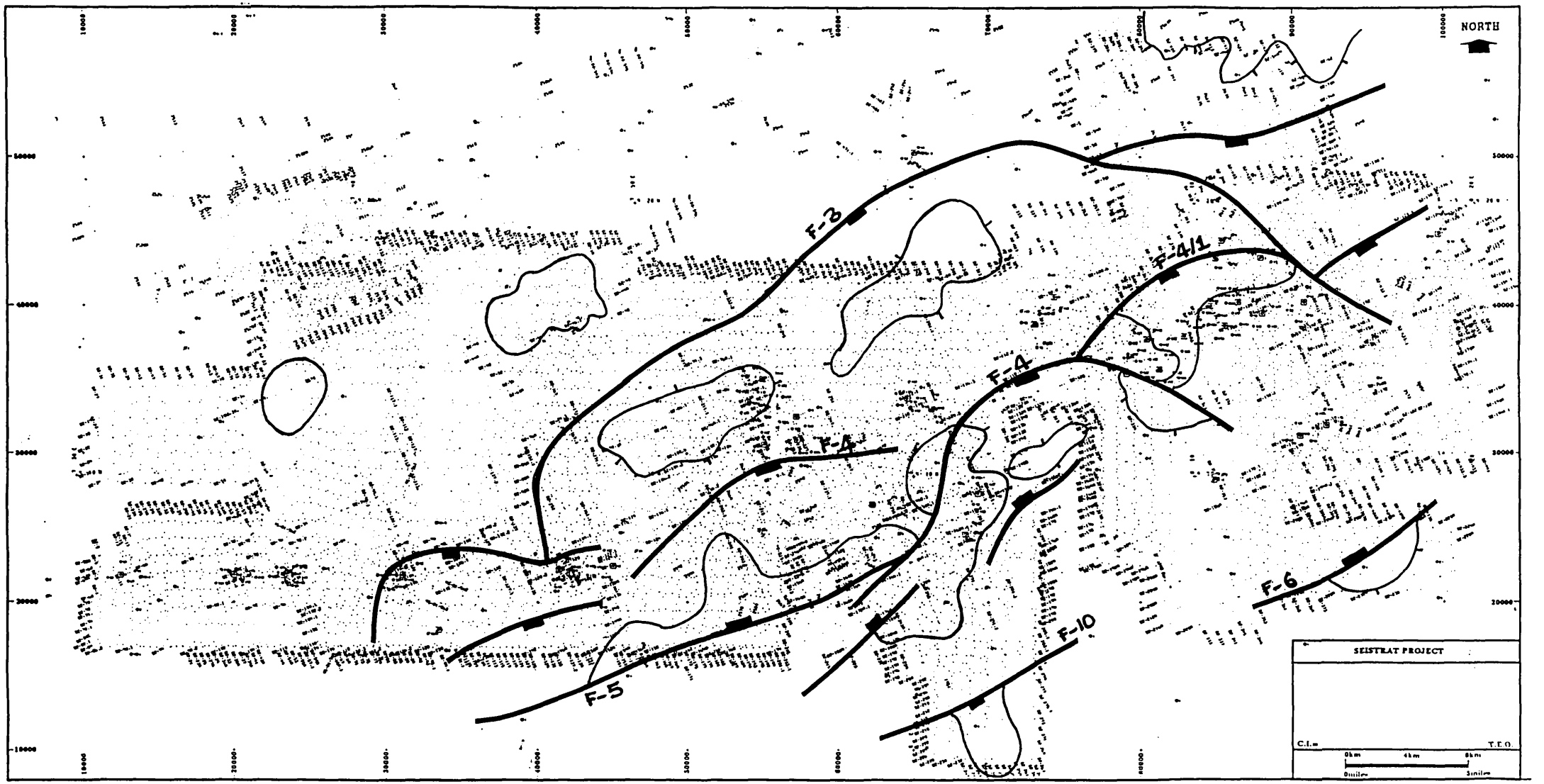

LBIBR- Lower Base Intra Biafra Rubble.

LIBU- Lower Intra Biafra Unconformity.

BIBR- Base Intra Biafra Rubble.

TIBU- Top Intra Biafra Unconformity.

BIBBEN- Base Intra Biafra Benin sands.

BRB- Base Rubble Beds

BQI- Base Qua Iboe.

TIQI- Top Intra Qua Iboe

QUA3 etc- Intra Qua Iboe horizon 3 etc

Pu- Pleistocene Unconformity

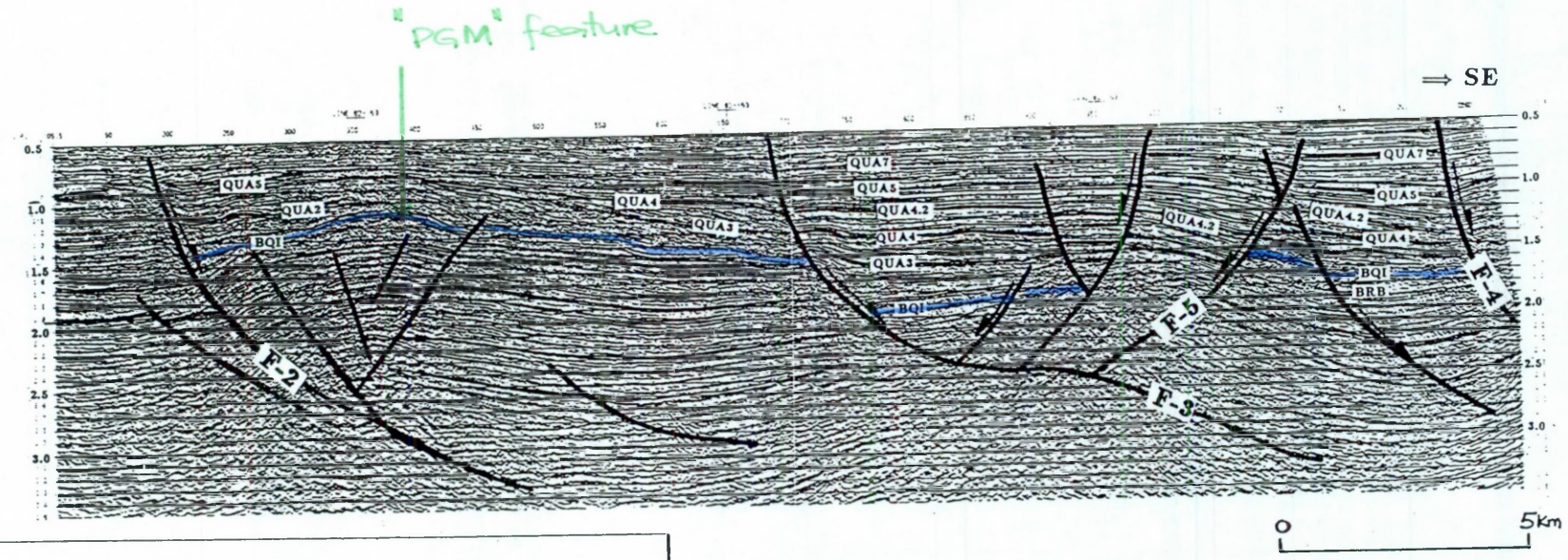

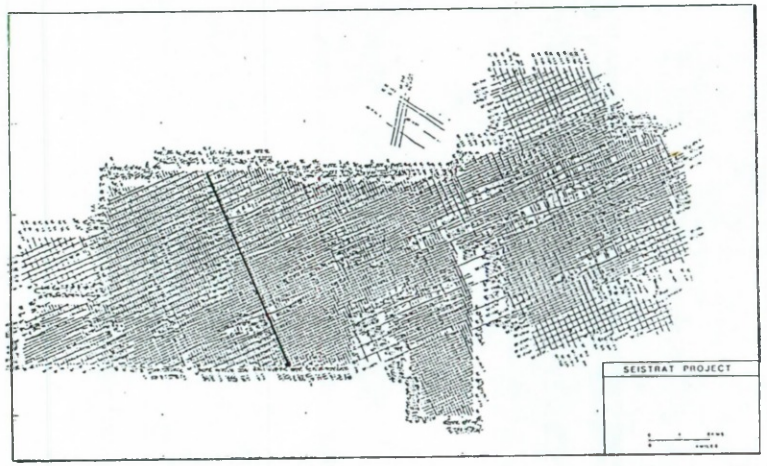

Fig.3.15a Seismic example of the PGM feature showing terracing at the BQI level. The associated simple erosional cuesta (structure FF in Fig.3.14b) is also shown(Line 82-163).

LIBBR- Lower Base Intra Biafra Rubble.

LIBU- Lower Intra Biafra Unconformity.

BIBR- Base Intra Biafra Rubble.

TIBU- Top Intra Biafra Unconformity.

BIBBEN- Base Intra Biafra Benin sands.

BRB- Base Rubble Beds

BQI- Base Qua Iboe.

TIQI- Top Intra Qua Iboe

QUA3 etc- Intra Qua Iboe horizon 3 etc

Pu- Pleistocene Unconformity

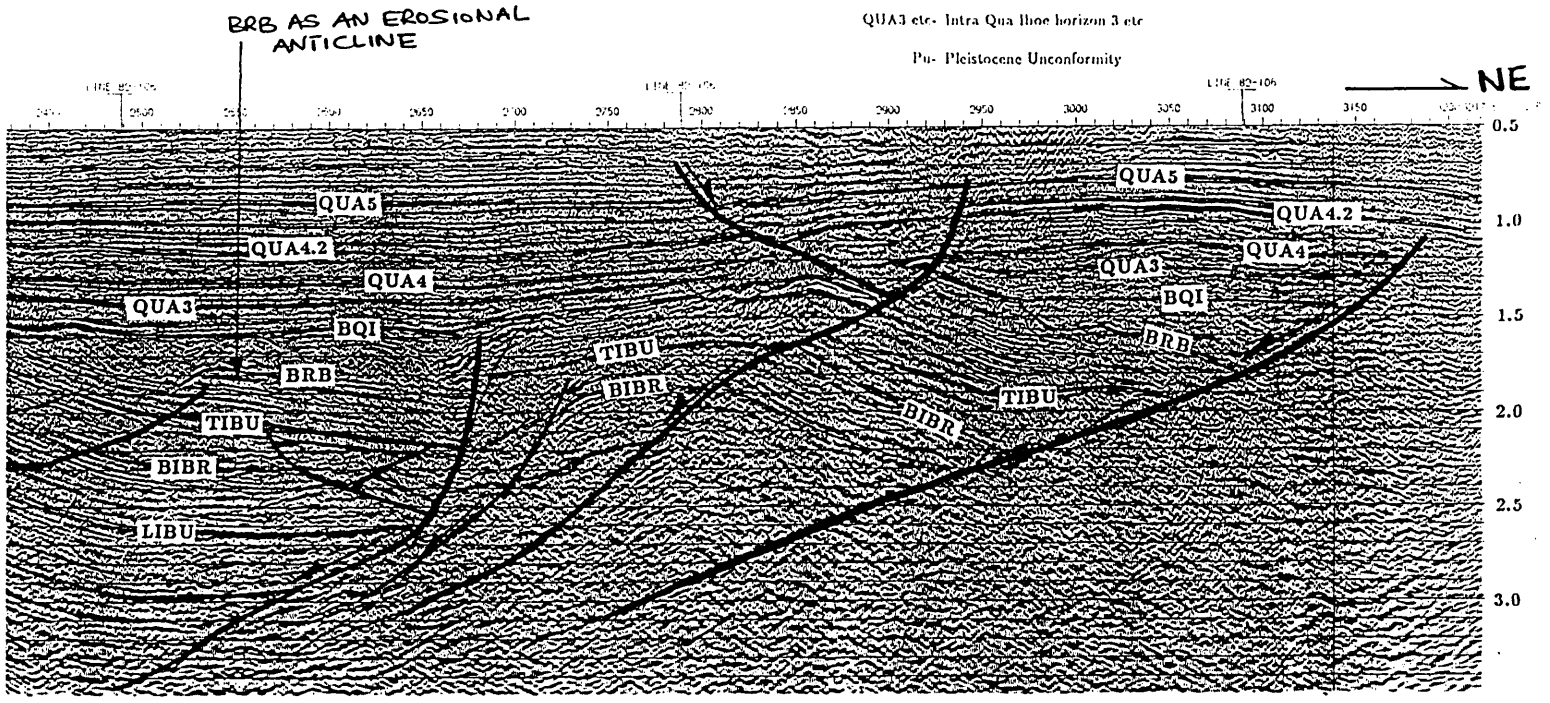

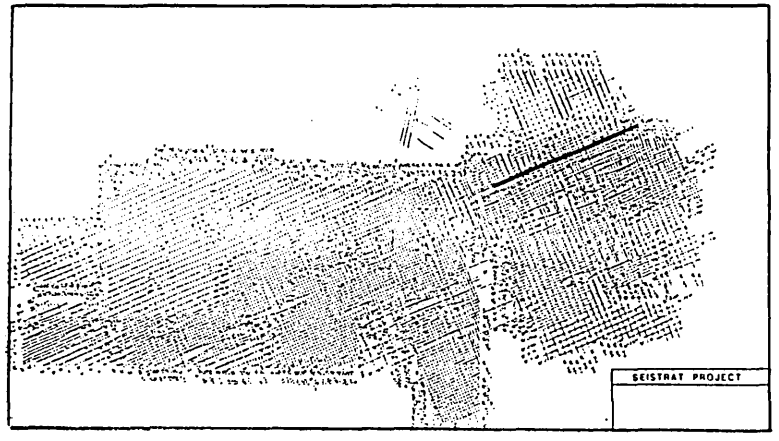

Fig.3.15b Seismic example of the PGM feature at the Base Rubble Bed level. (Line 82-106)

LIBBR- Lower Base Intra Biafra Rubble.

LIBU- Lower Intra Biafra Unconformity.

BIBR- Base Intra Biafra Rubble.

TIBU- Top Intra Biafra Unconformity.

BIBBEN- Base Intra Biafra Benin sands.

BRB- Base Rubble Beds

BQI- Base Qua Iboe.

TIQI- Top Intra Qua Iboe

QUA3 etc- Intra Qua Iboe horizon 3 etc

Pu- Pleistocene Unconformity

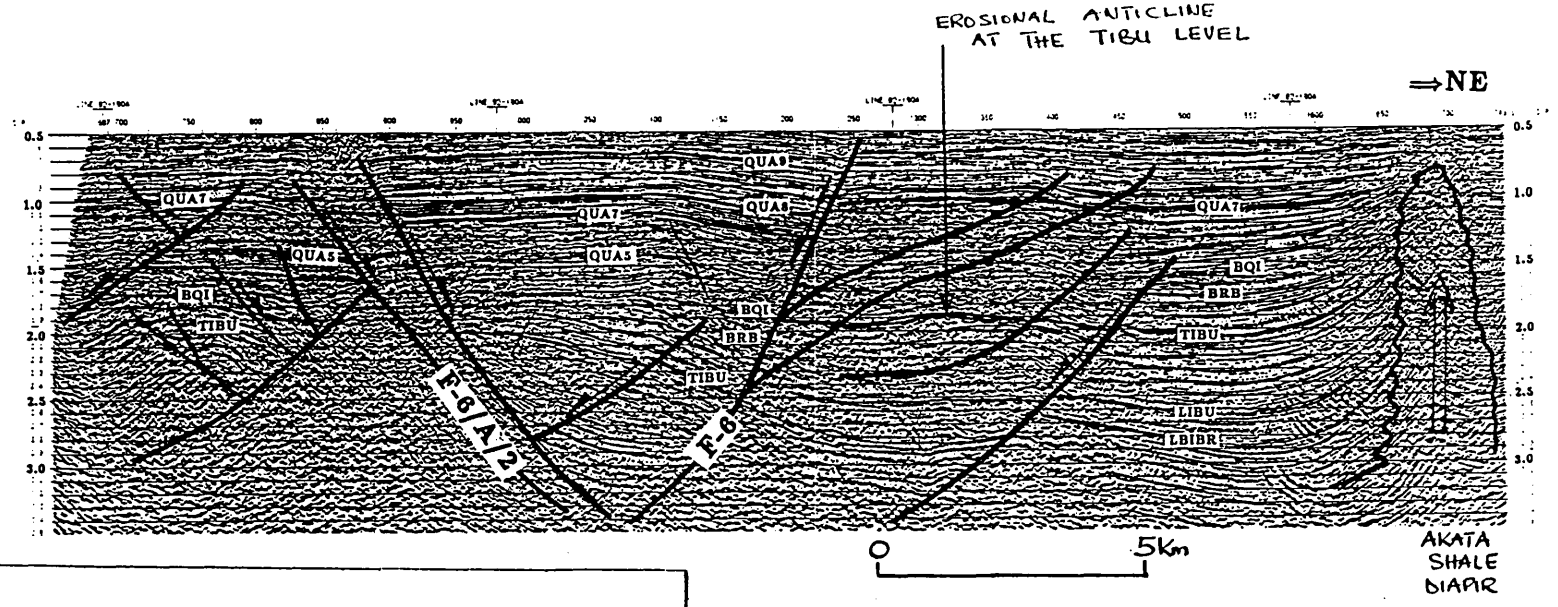

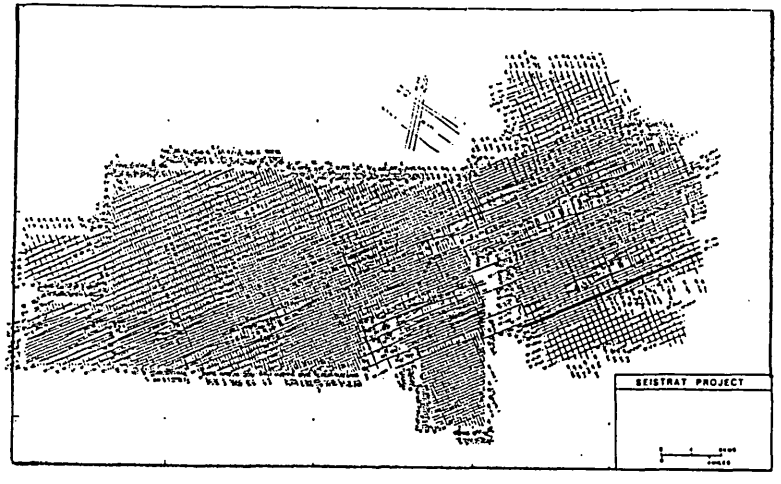

Fig.3.15c Simple erosional anticline at the TIBU level. (Line 82-190a)

LBIBR- Lower Base Intra Biafra Rubble.

LIBU- Lower Intra Biafra Unconformity.

BIBR- Base Intra Biafra Rubble.

TIBU- Top Intra Biafra Unconformity.

BIBBEN- Base Intra Biafra Benin sands.

BRB- Base Rubble Beds

BQI- Base Qua Iboe.

TIQI- Top Intra Qua Iboe

QUA3 etc- Intra Qua Iboe horizon 3 etc

Pu- Pleistocene Unconformity

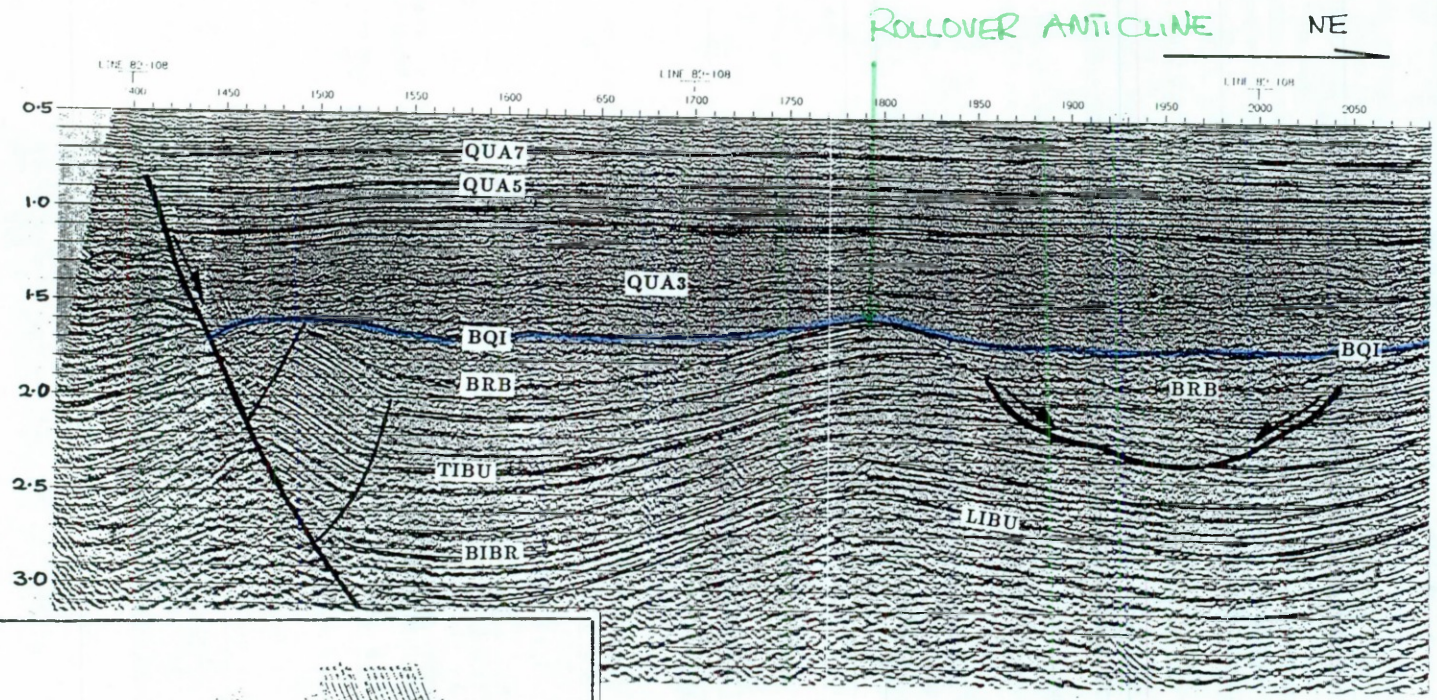

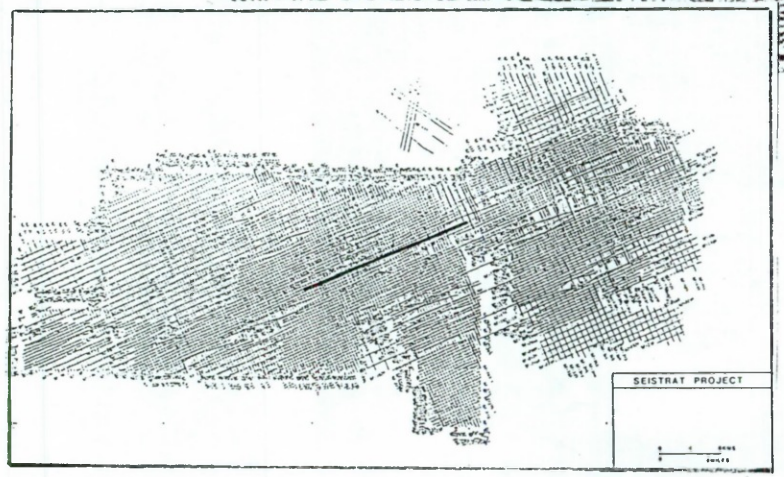

Fig.3.16 Seismic example of a simple rollover anticline (shale mass supported(Line 82-108)). This commonly occurs within the palaeobasin defined by Fault-3.

LBIBR- Lower Base Intra Biafra Rubble.

LIBU- Lower Intra Biafra Unconformity.

BIBR- Base Intra Biafra Rubble.

TIBU- Top Intra Biafra Unconformity.

BIBBEN- Base Intra Biafra Benin sands.

BRB- Base Rubble Beds

BQI- Base Qua Iboe.

TIQI- Top Intra Qua Iboe

QUA3 etc- Intra Qua Iboe horizon 3 etc

Pu- Pleistocene Unconformity

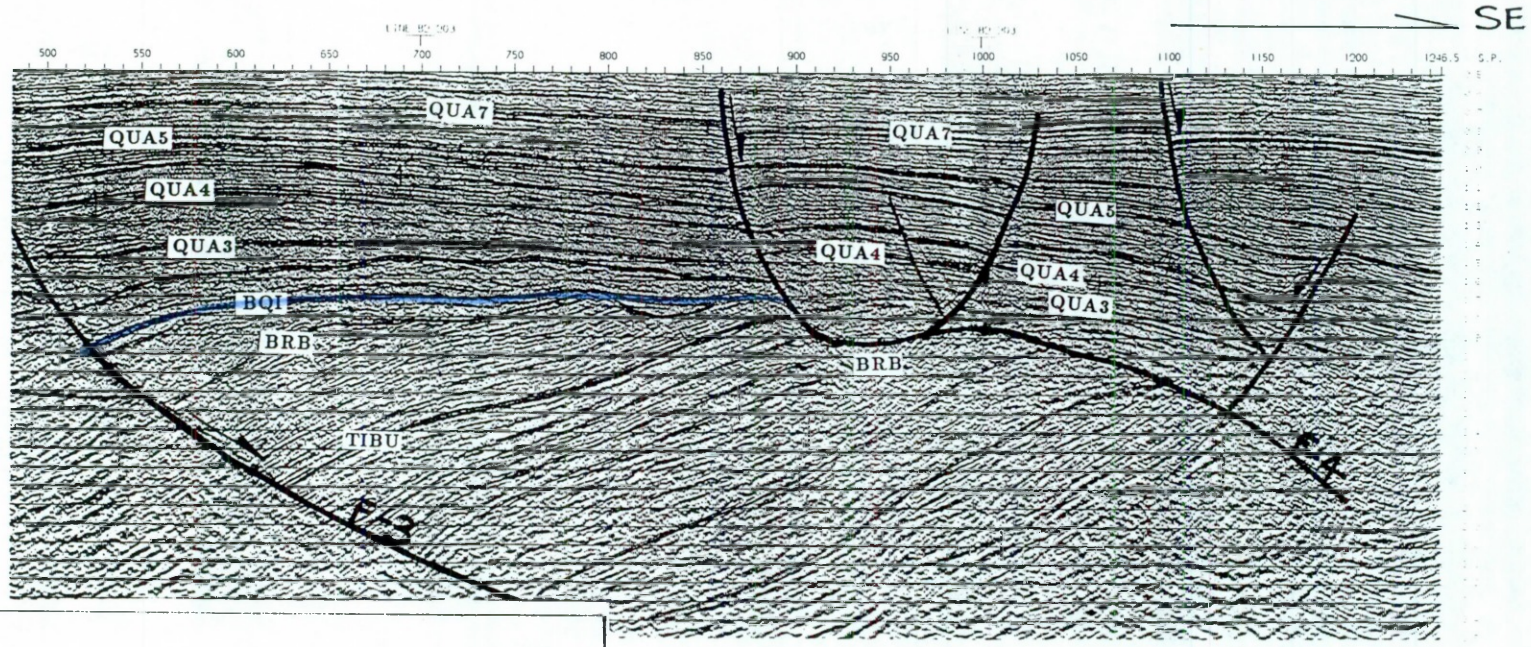

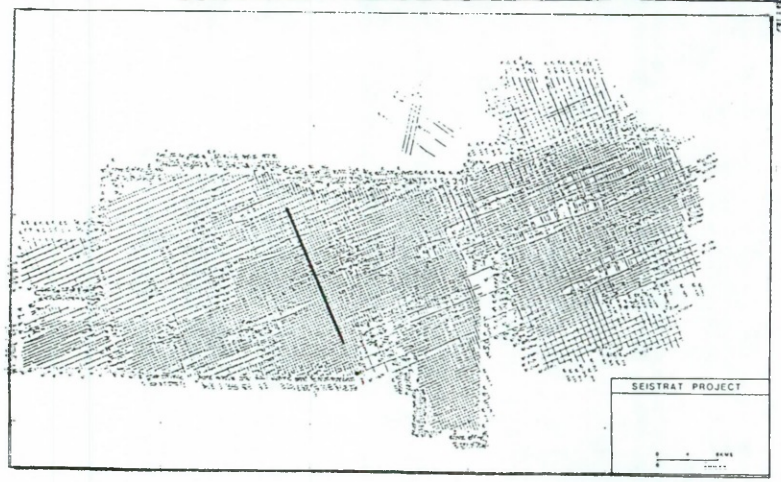

Fig.3.17 Rollover structure with landward dips and Rubble Bed onlap (line 82-203).

LIBR- Lower Intra Biafra Rubble.

LIBU- Lower Intra Biafra Unconformity.

BIBR- Base Intra Biafra Rubble.

TIBU- Top Intra Biafra Unconformity.

BIBBEN- Base Intra Biafra Benin sands.

BRB- Base Rubble Beds

BQI- Base Qua Iboe.

TIQI- Top Intra Qua Iboe

QUA3 etc- Intra Qua Iboe horizon 3 etc

Pu- Pleistocene Unconformity

SE

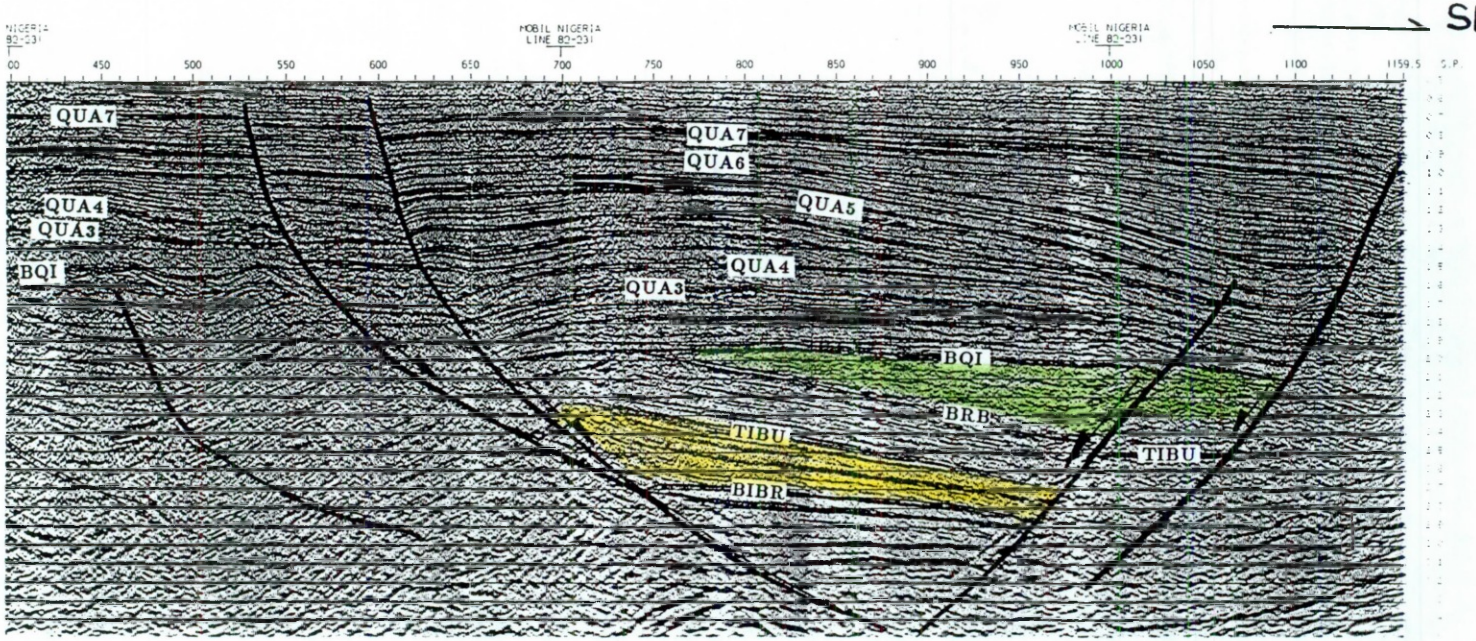

RUBBLE BEDS

LIBR

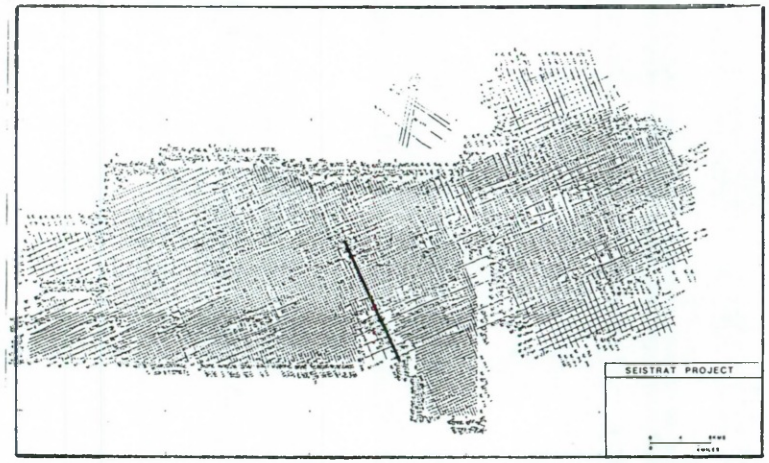

Fig.3.18 Rollover structure with seaward dips (line 82-231).

LBIBR- Lower Base Intra Biafra Rubble.

LIBU- Lower Intra Biafra Unconformity.

BIBR- Base Intra Biafra Rubble.

TIBU- Top Intra Biafra Unconformity.

BIBBEN- Base Intra Biafra Benin sands.

BRB- Base Rubble Beds

BQI- Base Qua Iboe.

TIQI- Top Intra Qua Iboe

QUA3 etc- Intra Qua Iboe horizon 3 etc

Pu- Pleistocene Unconformity

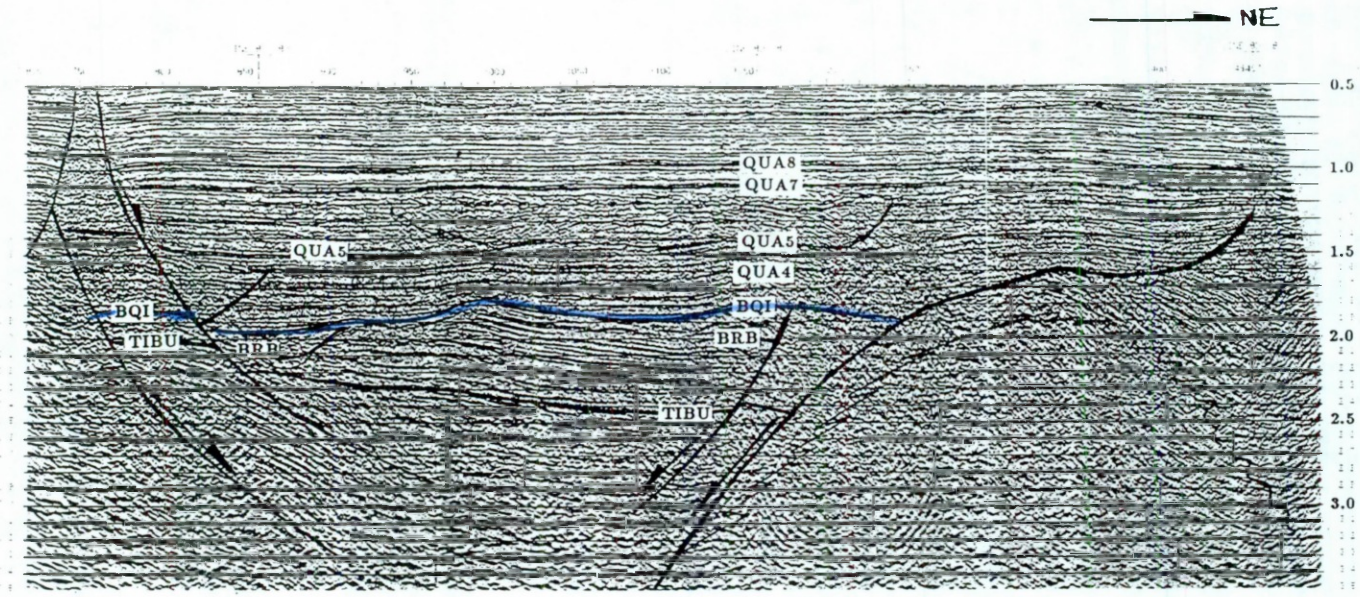

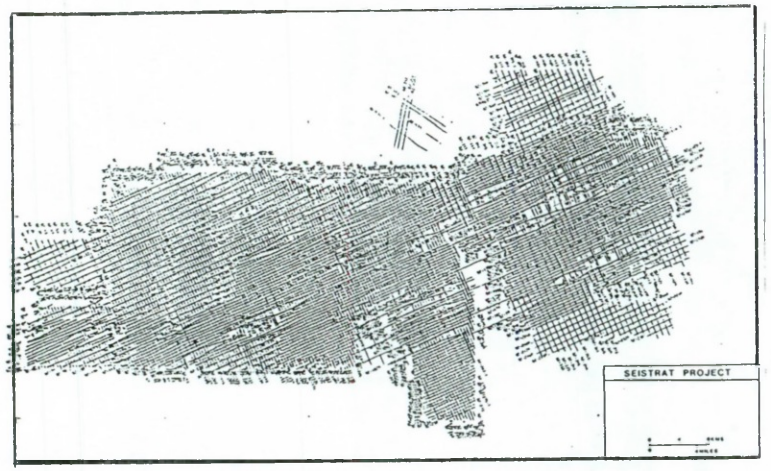

Fig.3.19a Shale mass structure flank. (Line 82-180).

LBIBR- Lower Base Intra Biafra Rubble.

LIBU- Lower Intra Biafra Unconformity.

BIBR- Base Intra Biafra Rubble.

TIBU- Top Intra Biafra Unconformity.

BIBBEN- Base Intra Biafra Benin sands.

BRB- Base Rubble Beds

BQI- Base Qua Iboe.

TIQI- Top Intra Qua Iboe

QUA3 etc- Intra Qua Iboe horizon 3 etc

Pu- Pleistocene Unconformity

N

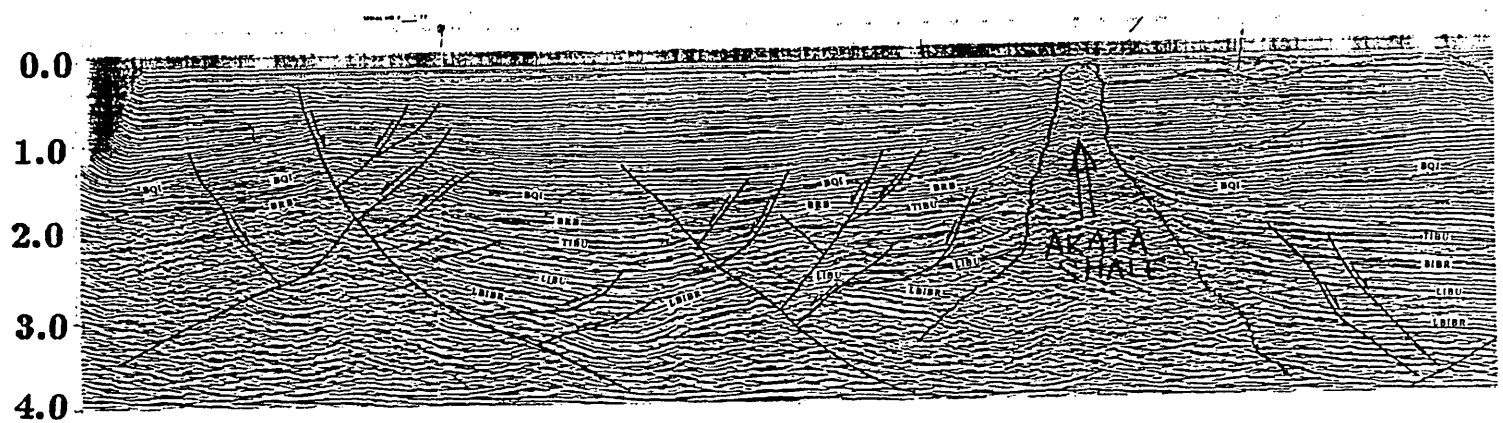

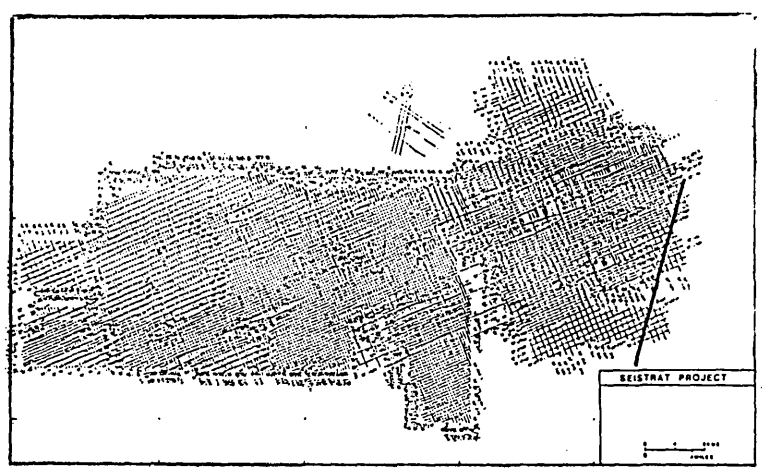

Fig.3.19b Shale diapir; line A-23).

LBIBR- Lower Base Intra Biafra Rubble.

LIBU- Lower Intra Biafra Unconformity.

BIBR- Base Intra Biafra Rubble.

TIBU- Top Intra Biafra Unconformity.

BIBBEN- Base Intra Biafra Benin sands.

BRB- Base Rubble Beds

BQI- Base Qua Iboe.

TIQI- Top Intra Qua Iboe

QUA3 etc- Intra Qua Iboe horizon 3 etc

Pu- Pleistocene Unconformity

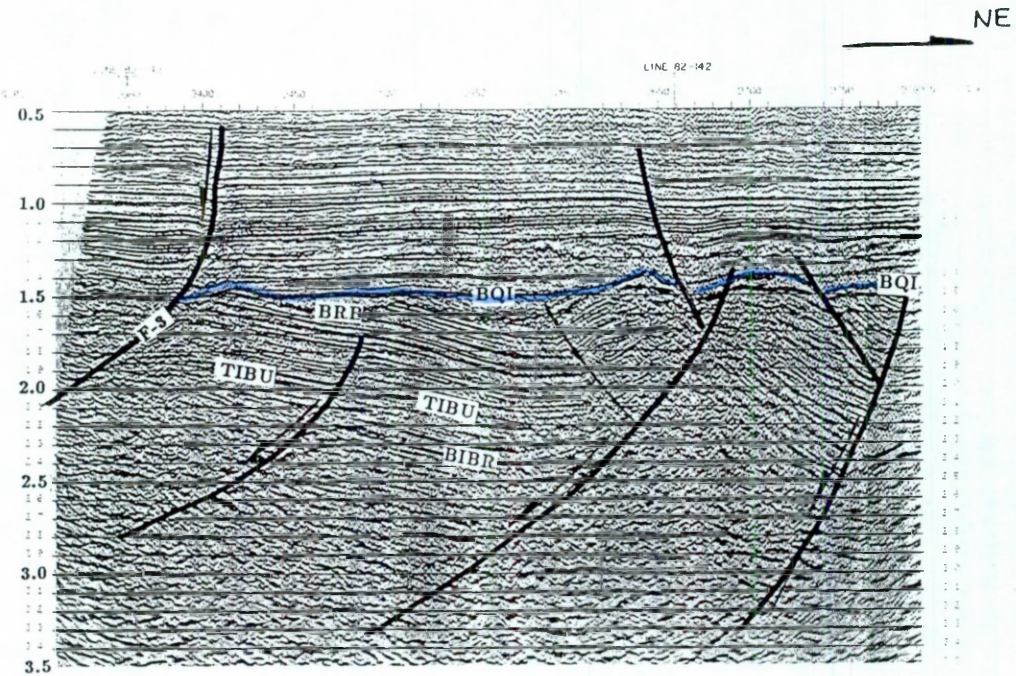

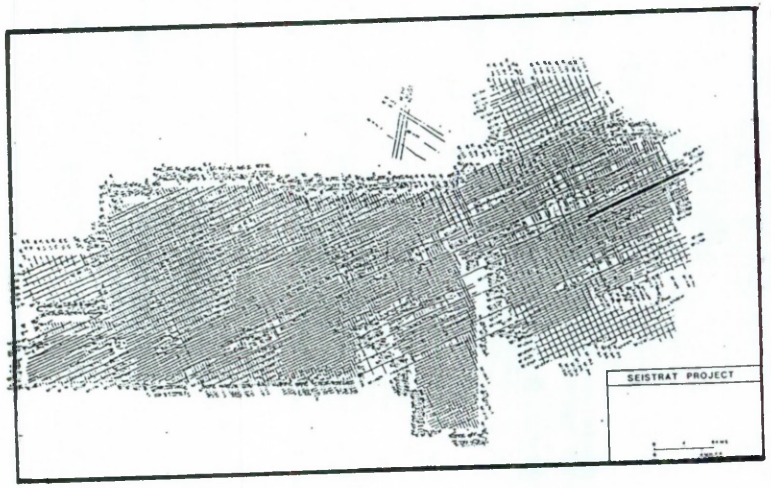

Fig.3.20 Shale mass structure crestal

Fig.3.21 TIBU structural map of the southeastern area. Tectonic activity was high in this area and this is represented by the many relict fault blocks evident.

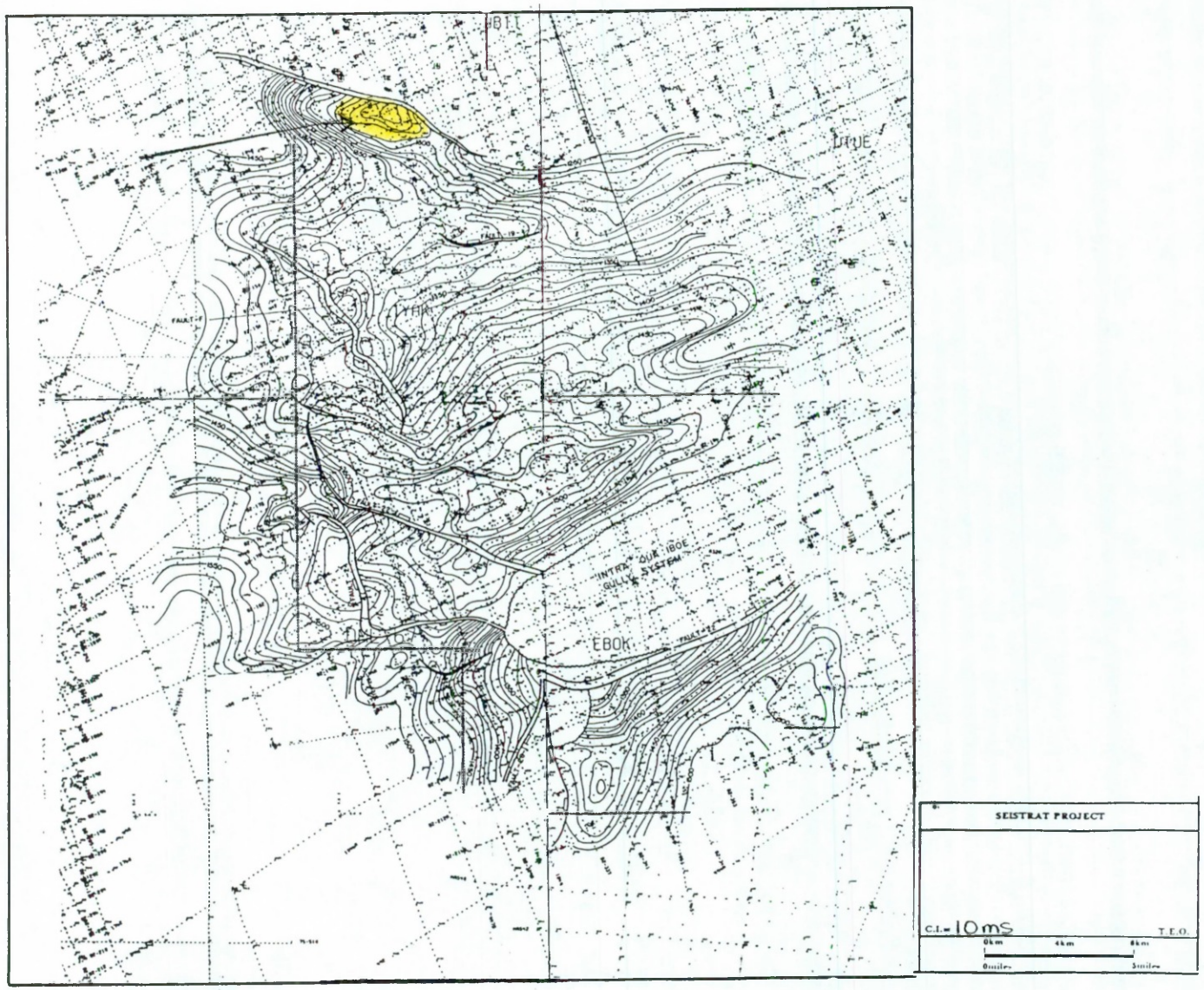

Fig.3.22 Structural time map of QUA5 level, southeastern area. Note the anneal-ment type structure(arrowed) associated with Fault-4. The structure was formed as a result of the renewal of fault dynamism in Mid. Pliocene.

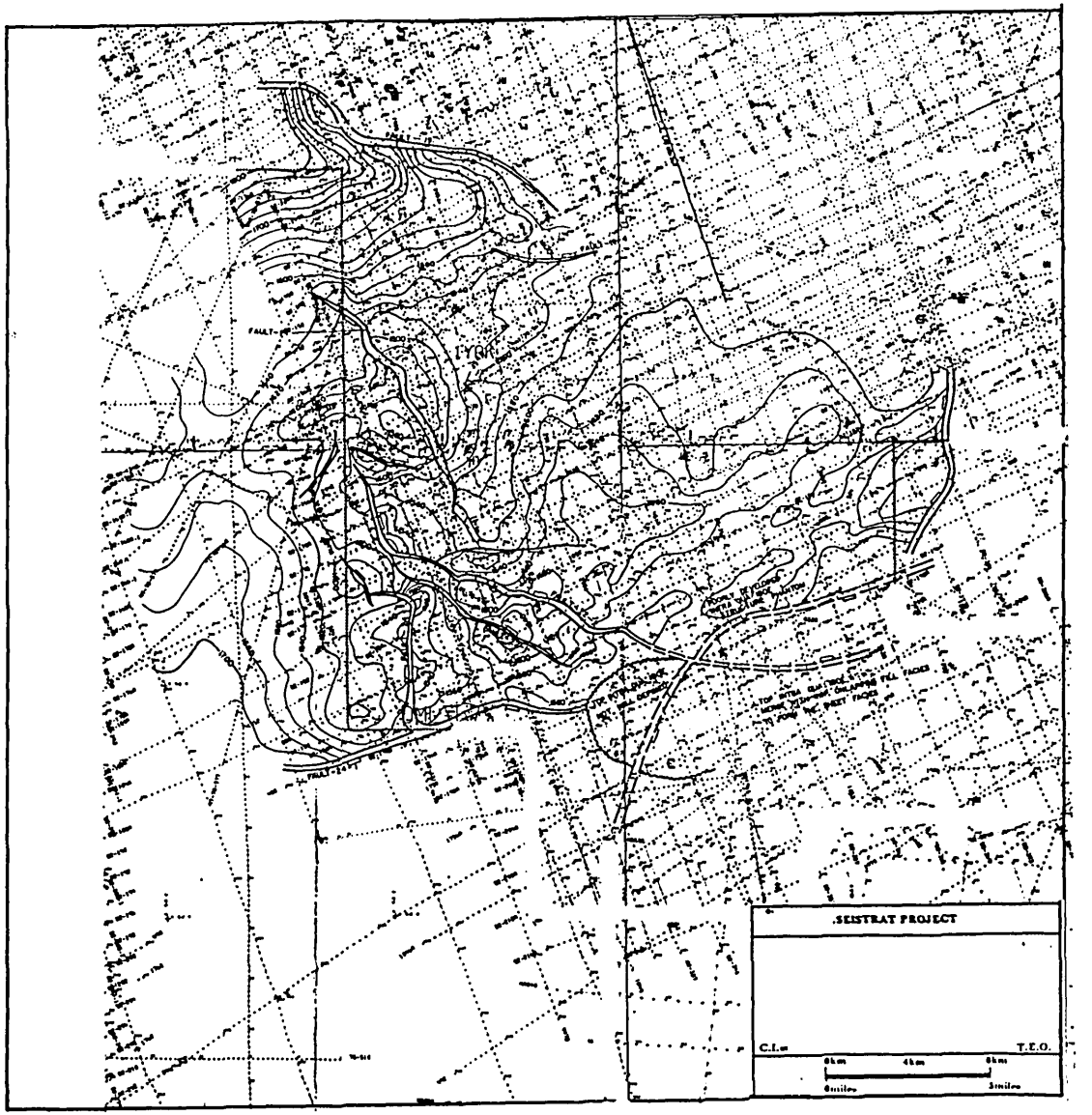

Fig.3.23 Structural map of the QUA4 level (SE block). Note the absence of the annealment type structure at this level which was prior to the fault dynamism.

CHAPTER FOUR

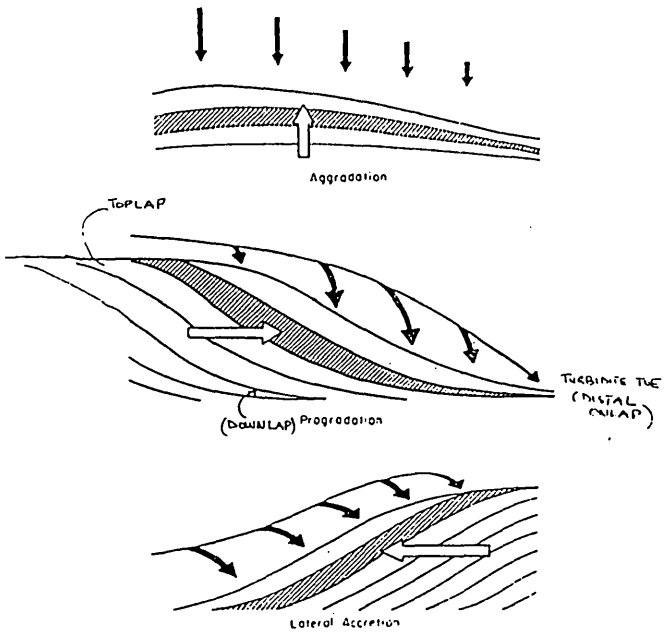

Progradation,lateral accretion,and aggradation sedimentary processes, and geometries of resultant depositional units. After Galloway and others(1979)

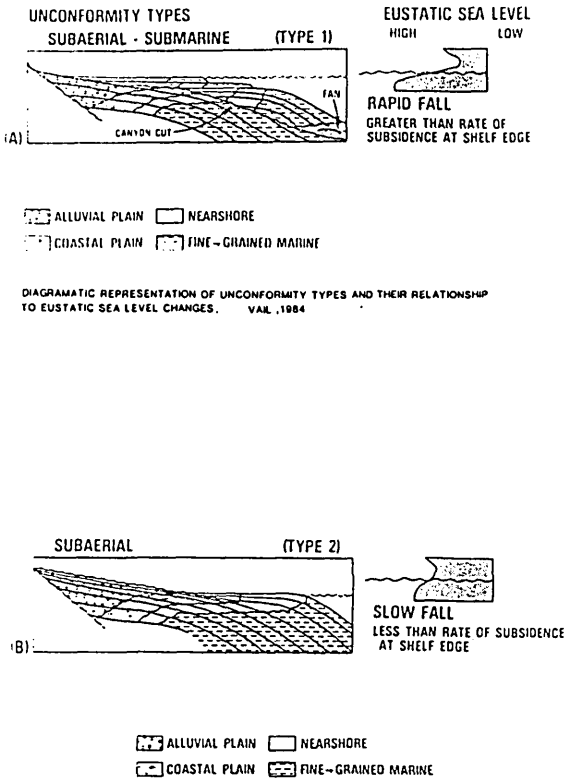

Fig.4.1a Seismic sequence analysis terminology and definition of unconformity types.

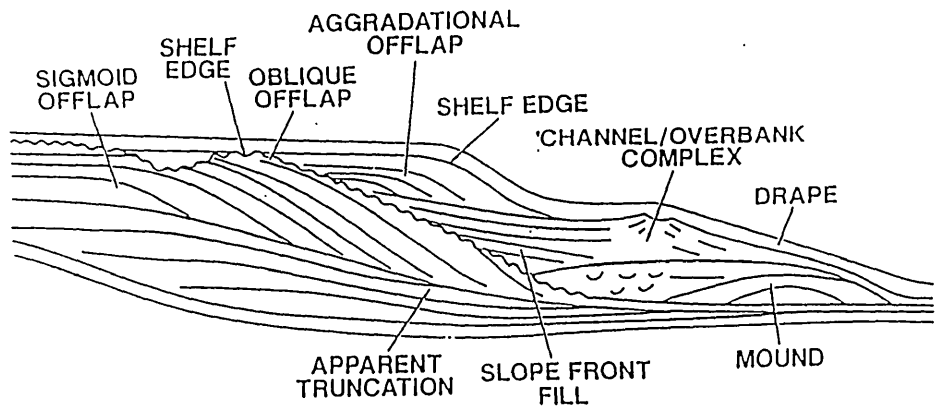

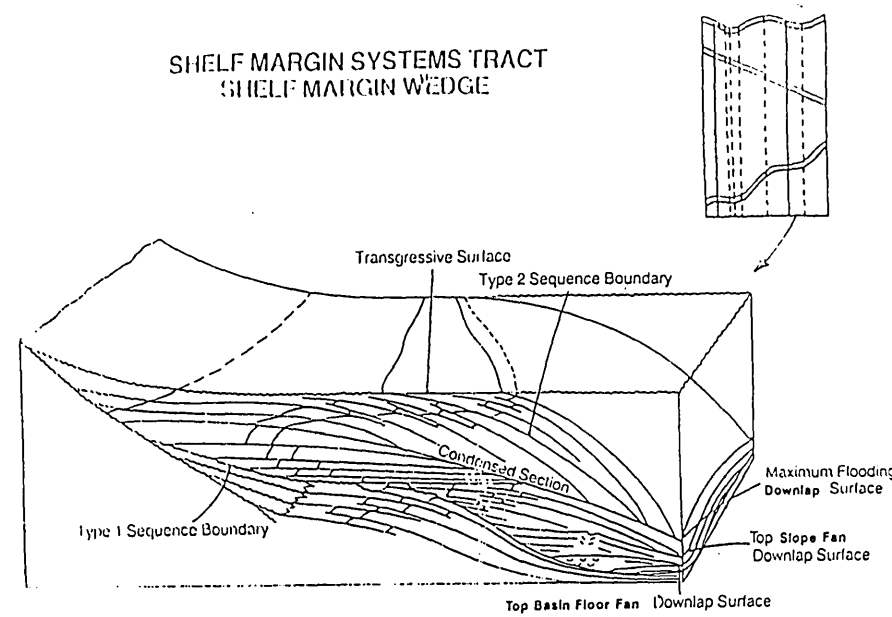

After Vail *et al.*, 1988

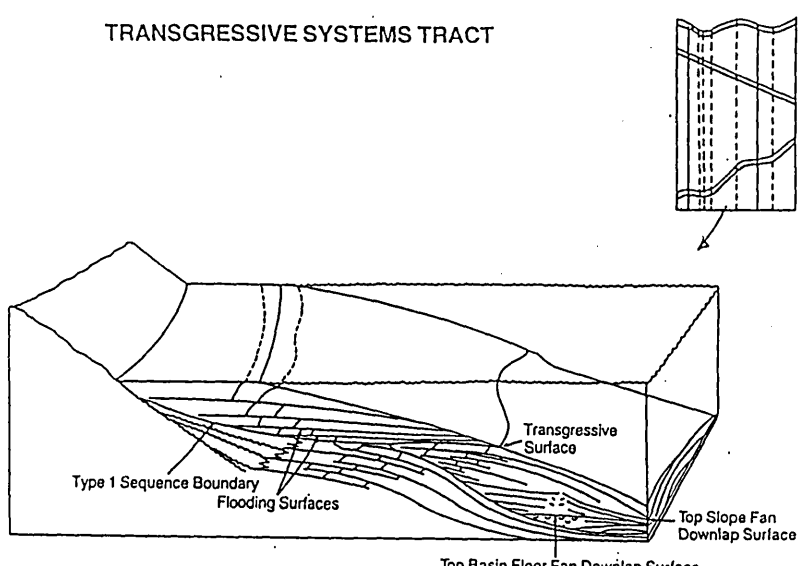

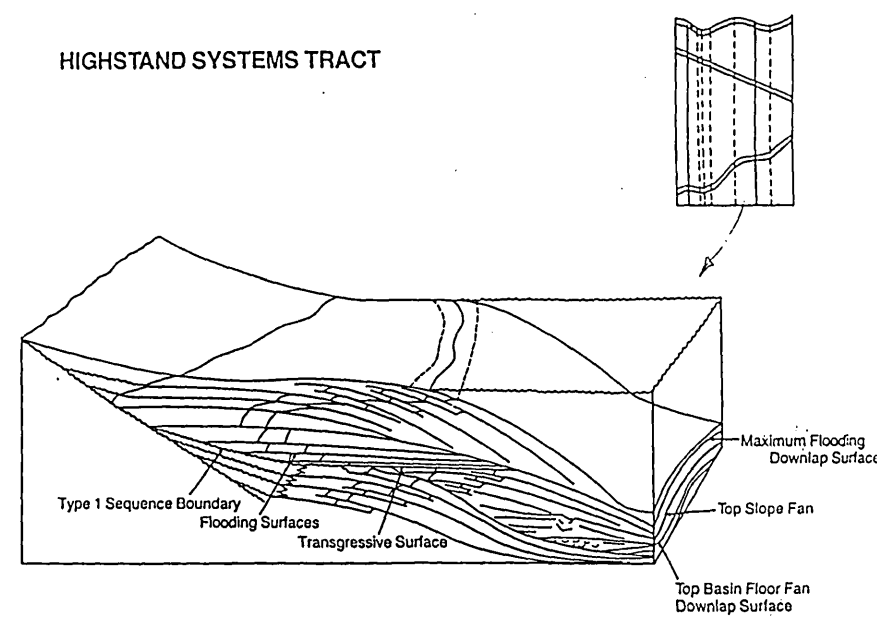

Fig.4.1b Schematic sections showing the diagrammmatic representation of boundary relationships and different system tracts.

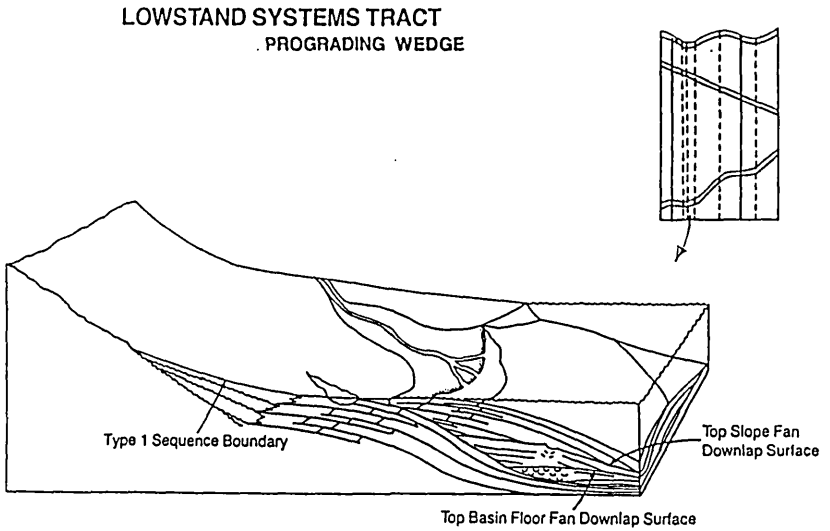

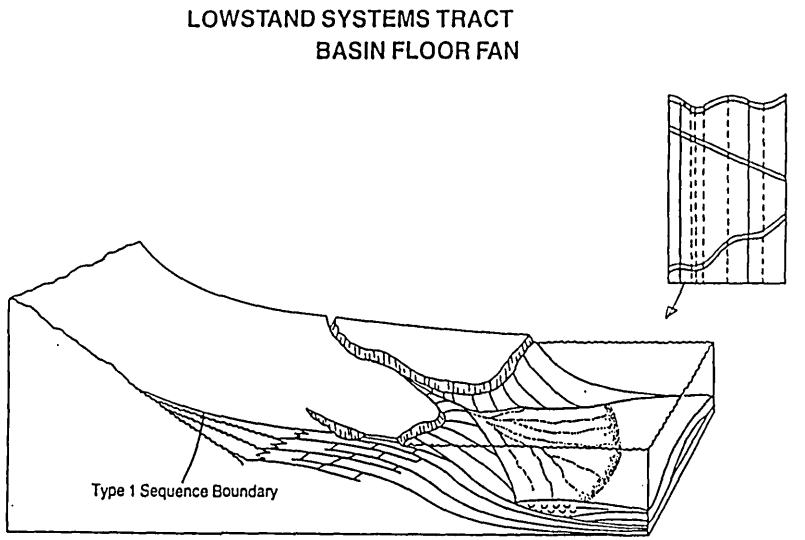

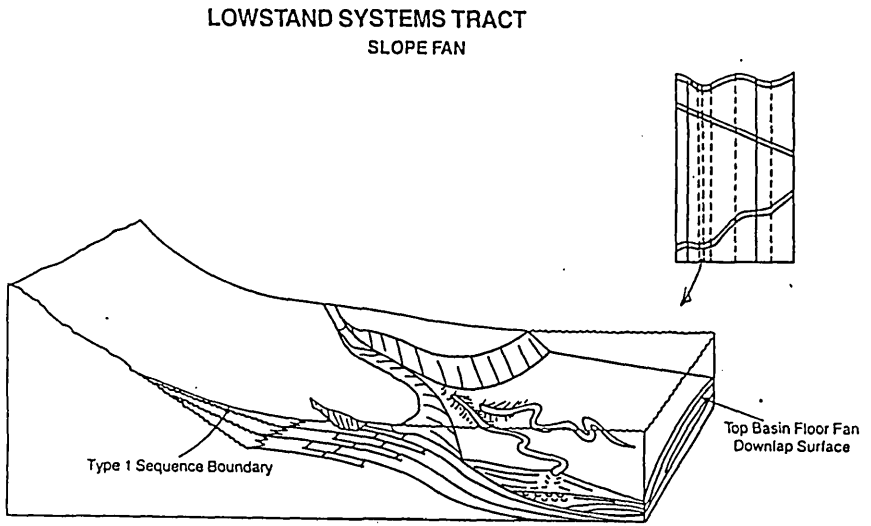

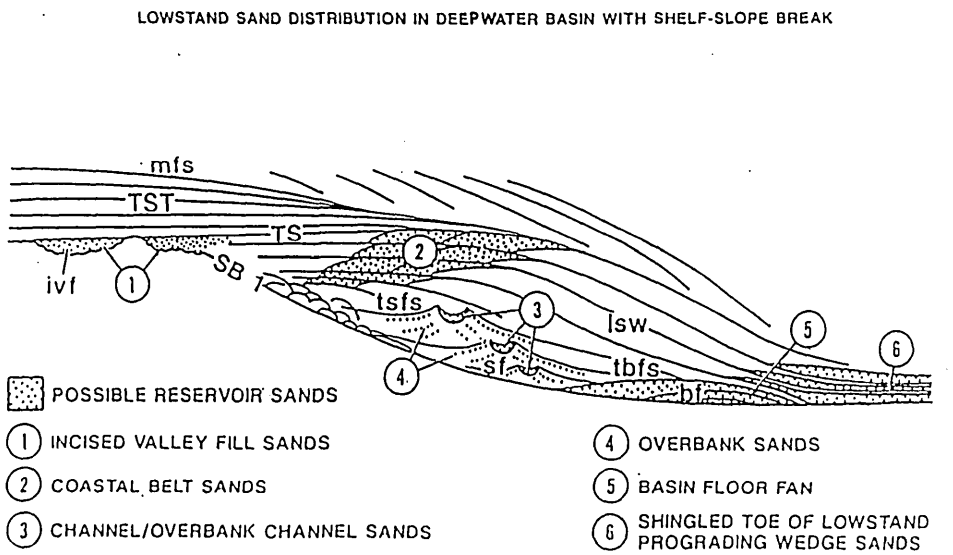

Fig.4.1c Schematic sections showing the Lower System Tract (Vail's Lowstand System Tract). The various types are discussed in the text.

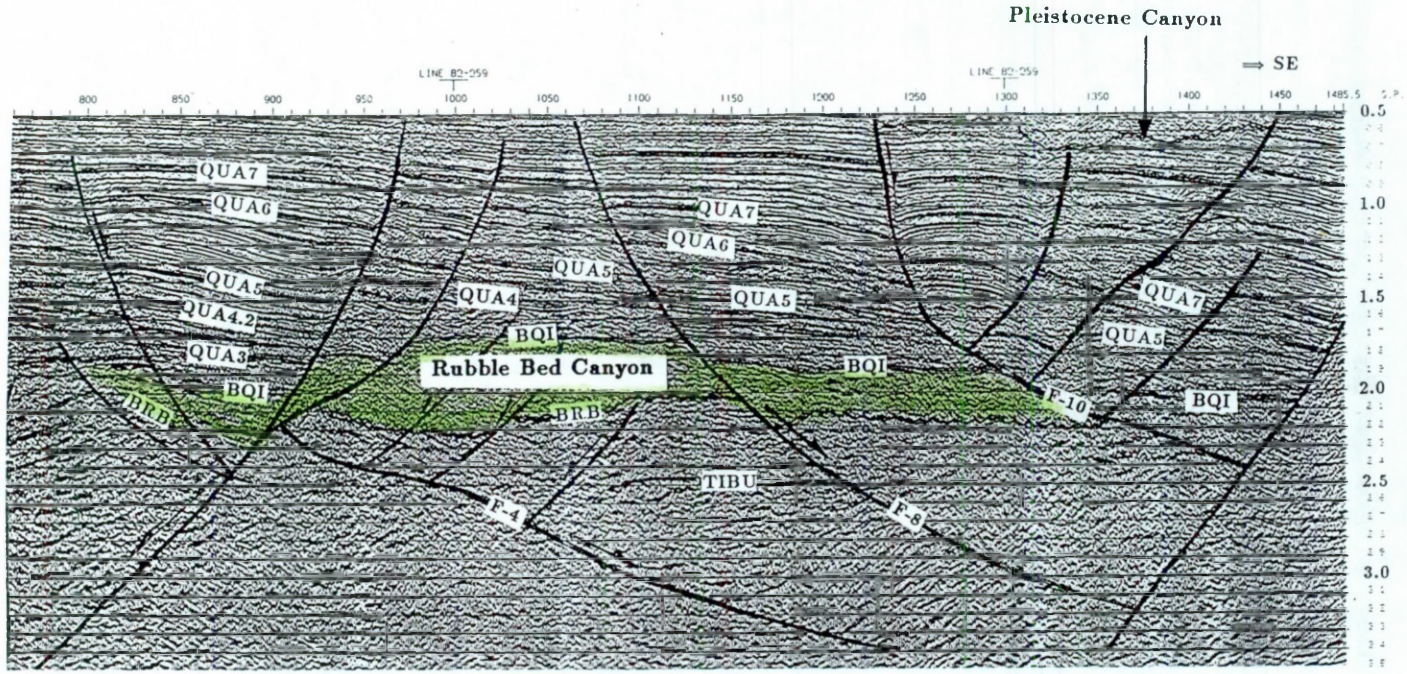

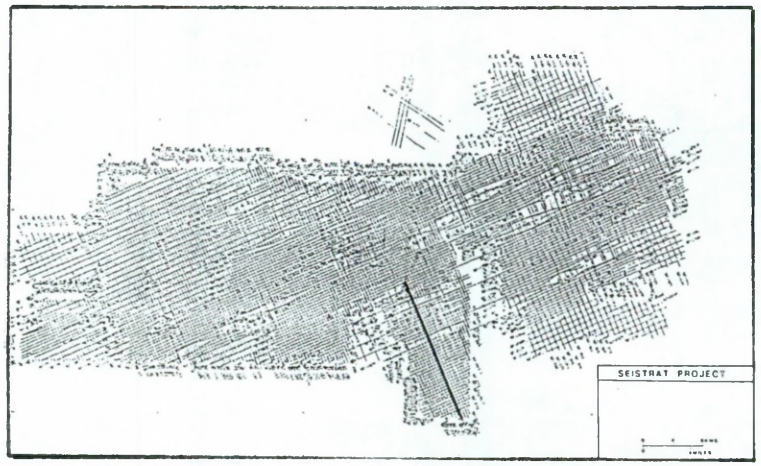

Fig.4.2 Canyons and their relationship to shelf(line 82-259). Note the Late Miocene Rubble Bed canyon obscured on the downthrown side of Fault-8 by shale tectonism. The Late Pleistocene canyon is apparent at 0.6secs between shot points 1250 and 1450. Both canyons trend NW-SE.

LBIBR- Lower Base Intra Biafra Rubble.

LIBU- Lower Intra Biafra Unconformity.

BIBR- Base Intra Biafra Rubble.

TIBU- Top Intra Biafra Unconformity.

BIBBEN- Base Intra Biafra Benin sands.

BRB- Base Rubble Beds

BQI- Base Qua Iboe.

TIQI- Top Intra Qua Iboe

QUA3 etc- Intra Qua Iboe horizon 3 etc

Pu- Pleistocene Unconformity

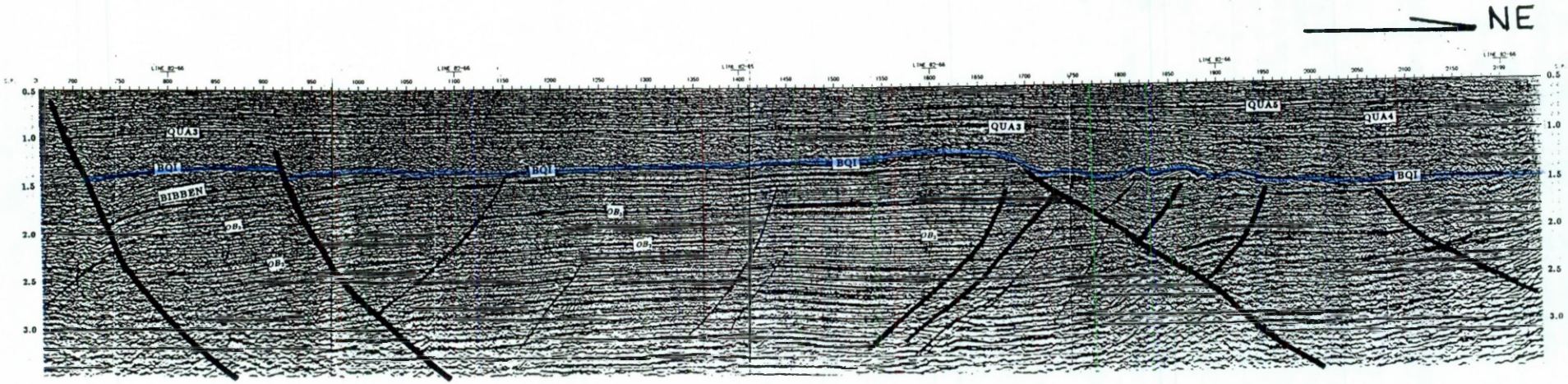

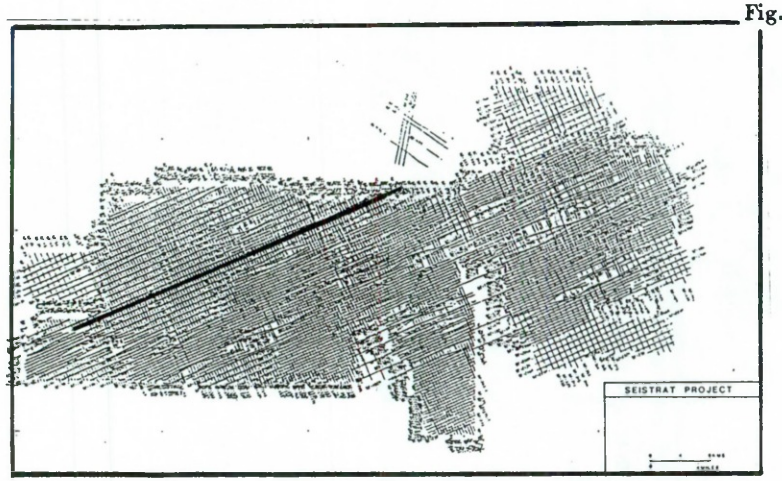

Fig.4.3a Seismic line 82-66 showing the 4 Older Biafra sequences mapped. Each sequence corresponds to a depositional cycle beginning with regression and topped by a paralic transgressive section. Also see Biafra Seismic facies analysis (pages 124 and 125).

LBIBR- Lower Base Intra Biafra Rubble.

LIBU- Lower Intra Biafra Unconformity.

BIBR- Base Intra Biafra Rubble.

TIBU- Top Intra Biafra Unconformity.

BIBBEN- Base Intra Biafra Benin sands.

BRB- Base Rubble Beds

BQI- Base Qua Iboe.

TIQI- Top Intra Qua Iboe

QUA3 etc- Intra Qua Iboe horizon 3 etc.

Pu- Pleistocene Unconformity

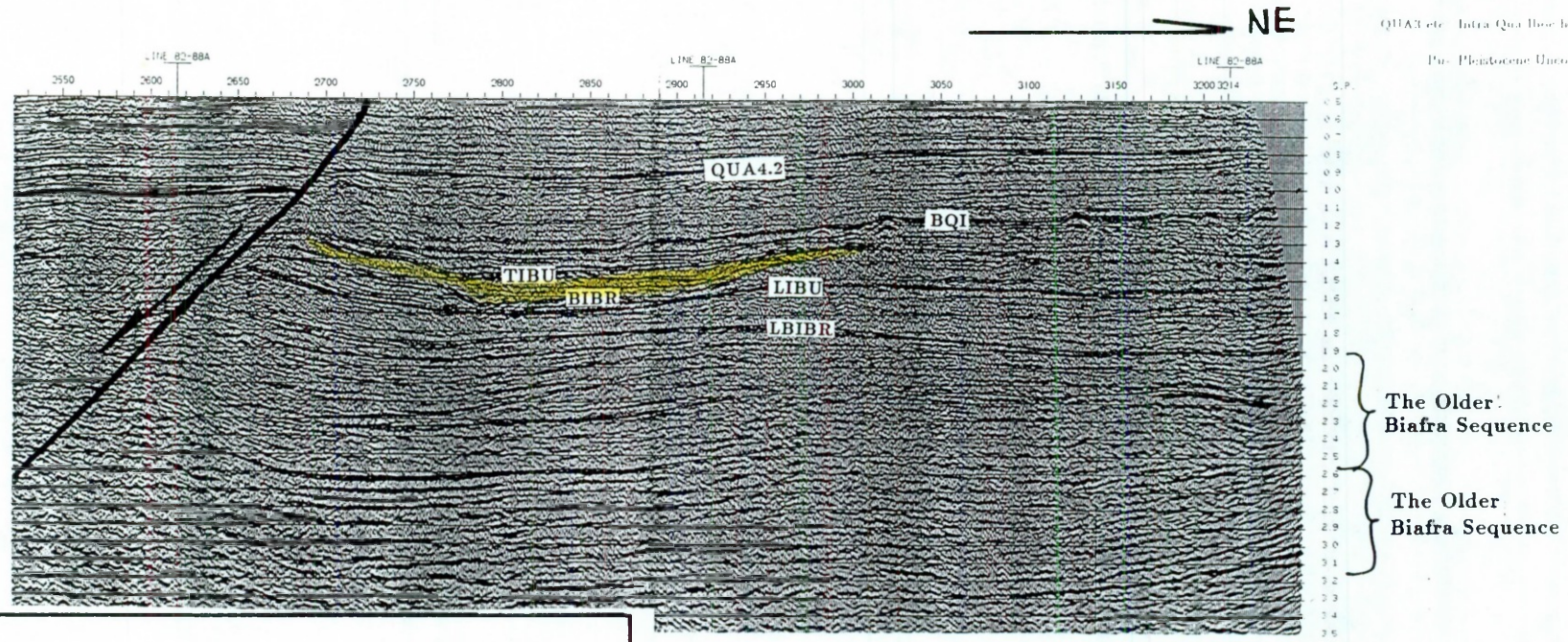

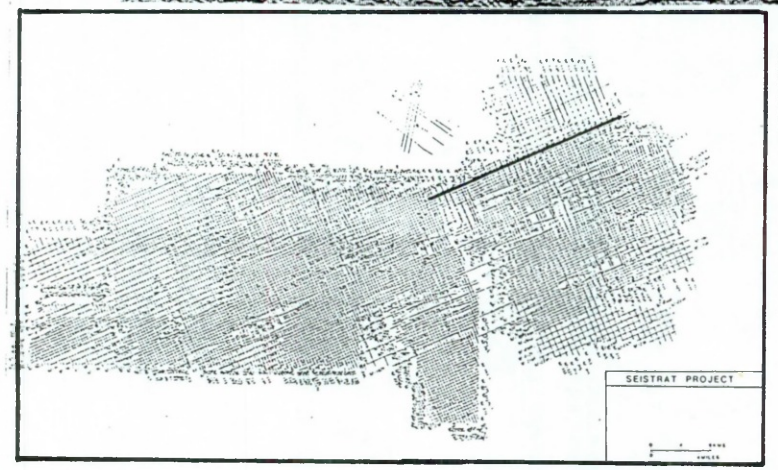

Fig.4.3b Seismic line 82-88a showing the two prograding cycles to the northeast of the study area, that constitute the Older Biafra. These are mainly Shelf-margin system tracts.

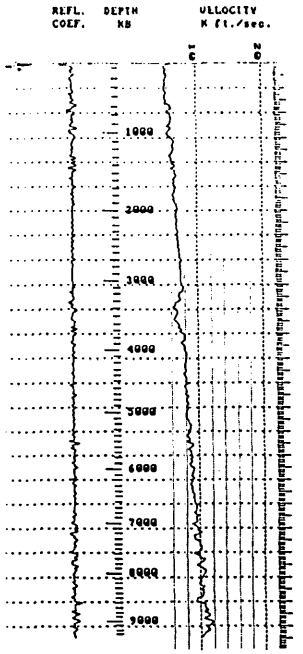

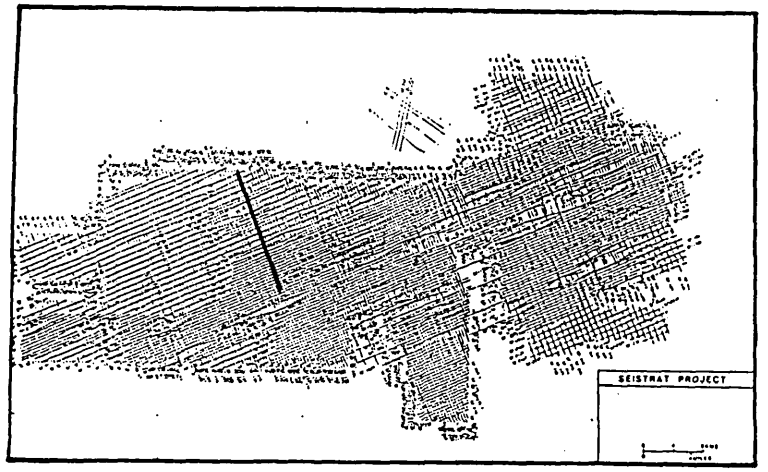

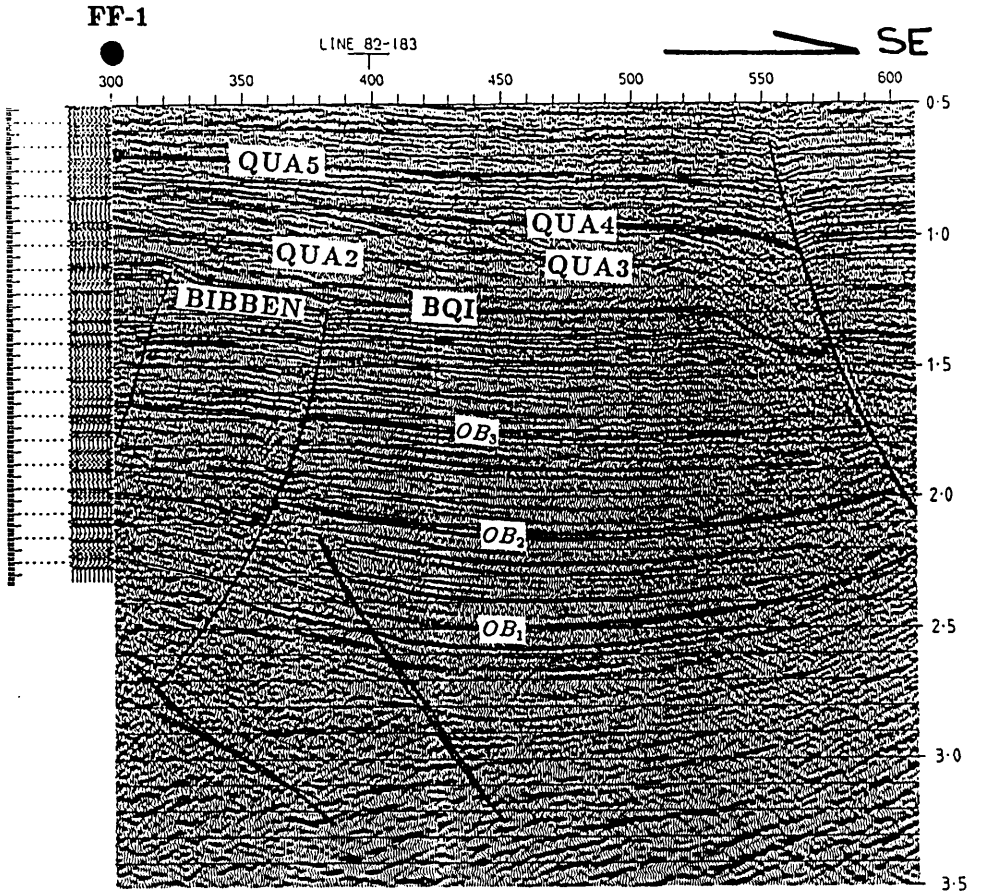

Fig.4.3c Synthetic seismogram fit of the Older Biafra horizons over line 82-183 (NW of the study area).

LIBU- Lower Intra Biafra Unconformity.

BIBR- Base Intra Biafra Rubble.

TIBU- Top Intra Biafra Unconformity.

BIBBEN- Base Intra Biafra Benin sands.

BRB- Base Rubble Beds

BQI- Base Qua Iboe.

TIQI- Top Intra Qua Iboe

QUA3 etc- Intra Qua Iboe horizon 3 etc

Pu- Pleistocene Unconformity

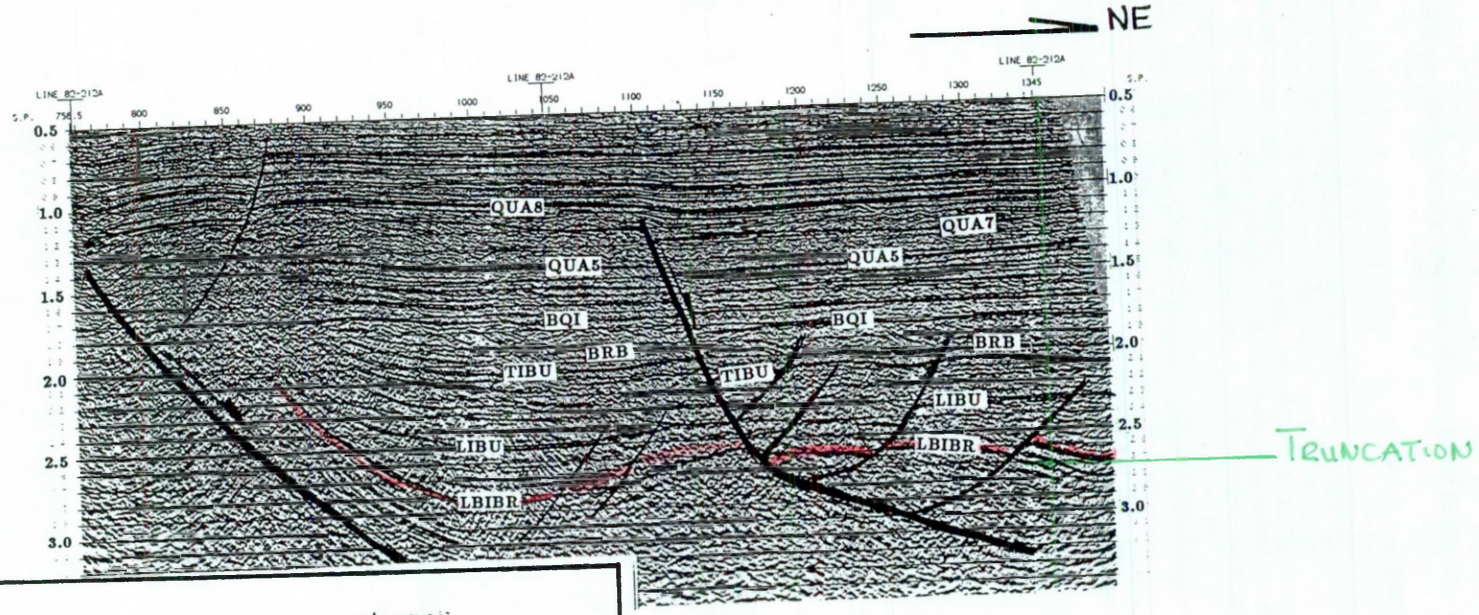

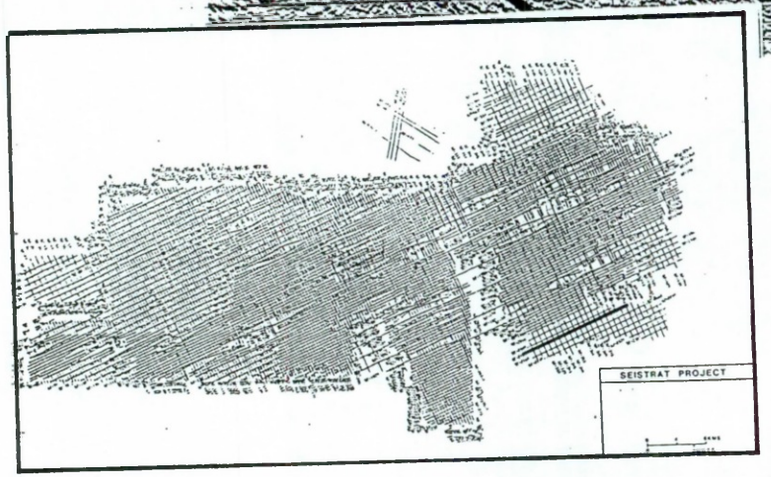

Fig.4.4a Line 82-212a showing the Lower Base Intra Biafra Rubble (LBIBR) as an erosional unconformity to the southeast.

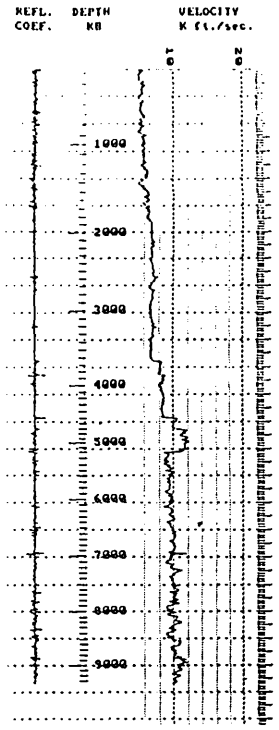

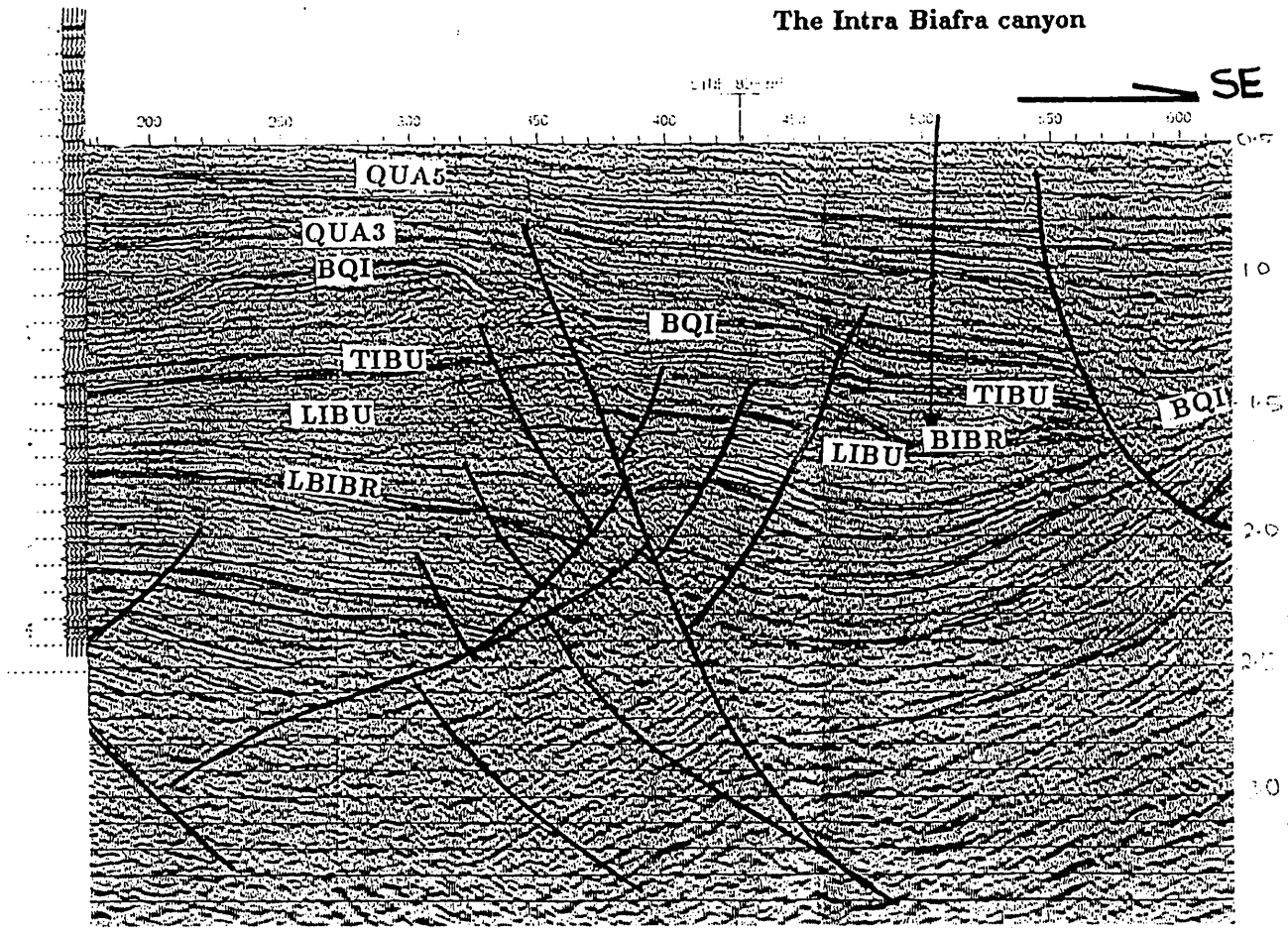

Fig.4.4b Synthetic seismogram fit for LBIBR and LIBU over line 82-385.

LBIBR- Lower Base Intra Biafra Rubble.

LIBU- Lower Intra Biafra Unconformity.

BIBR- Base Intra Biafra Rubble.

TIBU- Top Intra Biafra Unconformity.

BIBBEN- Base Intra Biafra Benin sands.

BRB- Base Rubble Beds

BQI- Base Qua Iboe.

TIQI- Top Intra Qua Iboe

QUA3 etc- Intra Qua Iboe horizon 3 etc

Pu- Pleistocene Unconformity

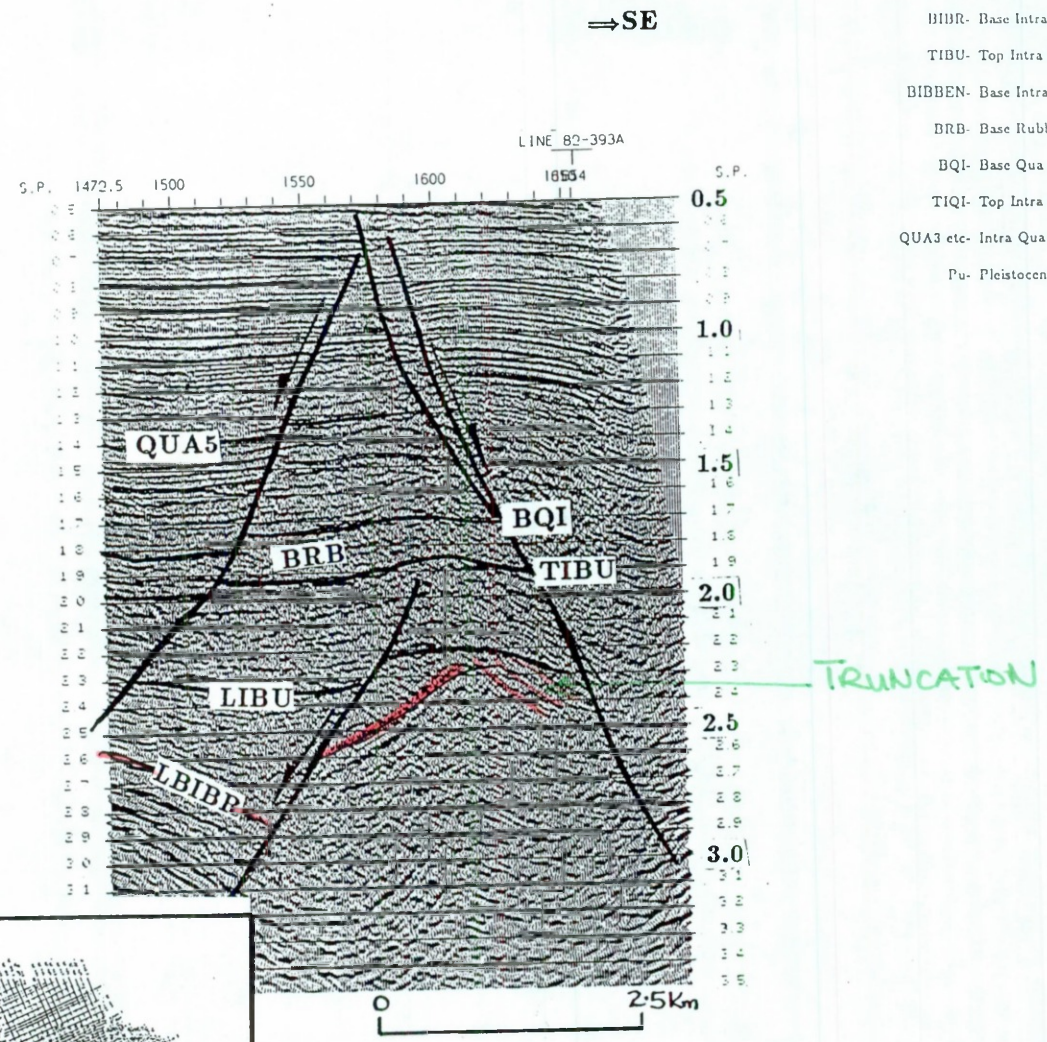

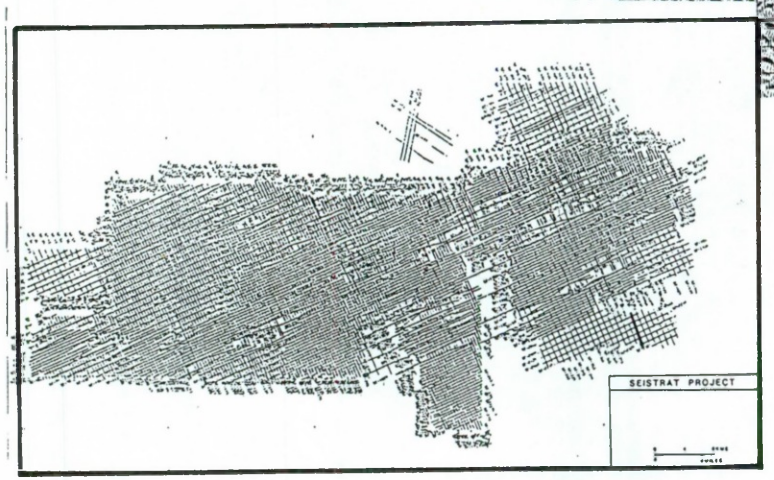

Fig.4.5a Line 82-393a showing the Lower Intra Biafra Unconformity (LIBU) showing truncation where the LIBR is absent and conformity when LIBR is present.

LIBBR- Lower Base Intra Biafra Rubble.

LIBU- Lower Intra Biafra Unconformity.

BIBR- Base Intra Biafra Rubble.

TIBU- Top Intra Biafra Unconformity.

BIBBEN- Base Intra Biafra Benin sands.

BRB- Base Rubble Beds

BQI- Base Qua Iboe.

TIQI- Top Intra Qua Iboe

QUA3 etc- Intra Qua Iboe horizon 3 etc

Pu- Pleistocene Unconformity

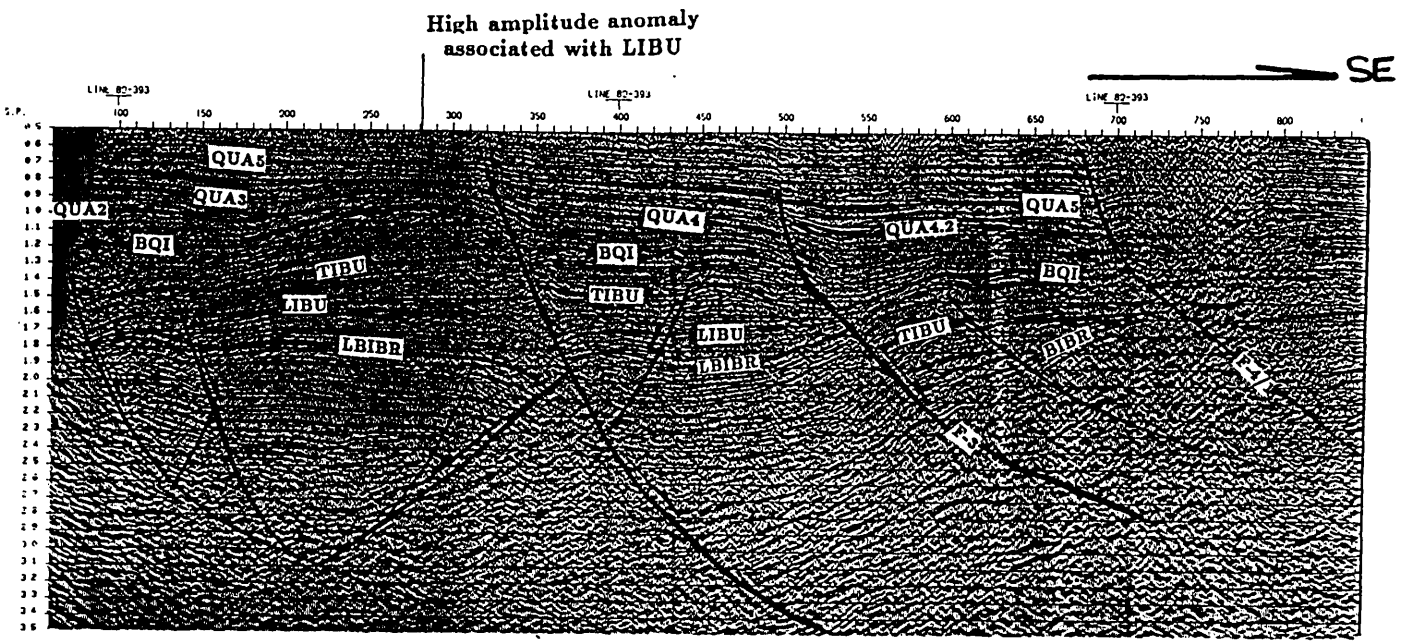

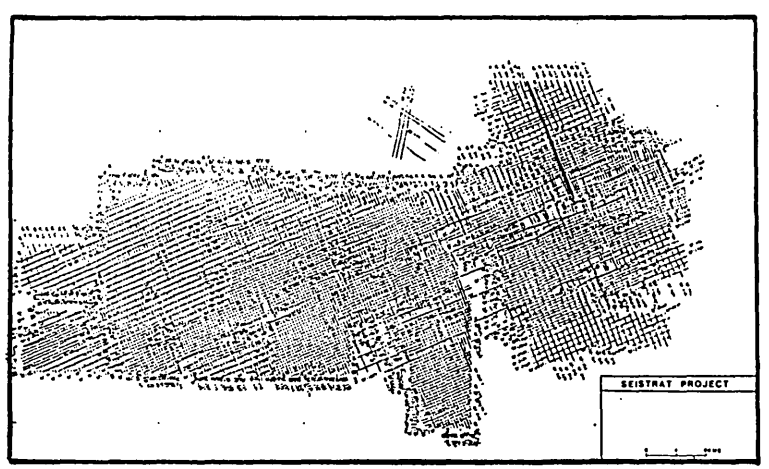

Fig.4.5b Line 82-393 showing high amplitude anomalies associated with the LIBU.

LBIBR- Lower Base Intra Biafra Rubble.

LIBU- Lower Intra Biafra Unconformity.

BIBR- Base Intra Biafra Rubble.

TIBU- Top Intra Biafra Unconformity.

BIBBEN- Base Intra Biafra Benin sands.

BRB- Base Rubble Beds

BQI- Base Qua Iboe.

TIQI- Top Intra Qua Iboe

QUA3 etc- Intra Qua Iboe horizon 3 etc

Pu- Pleistocene Unconformity

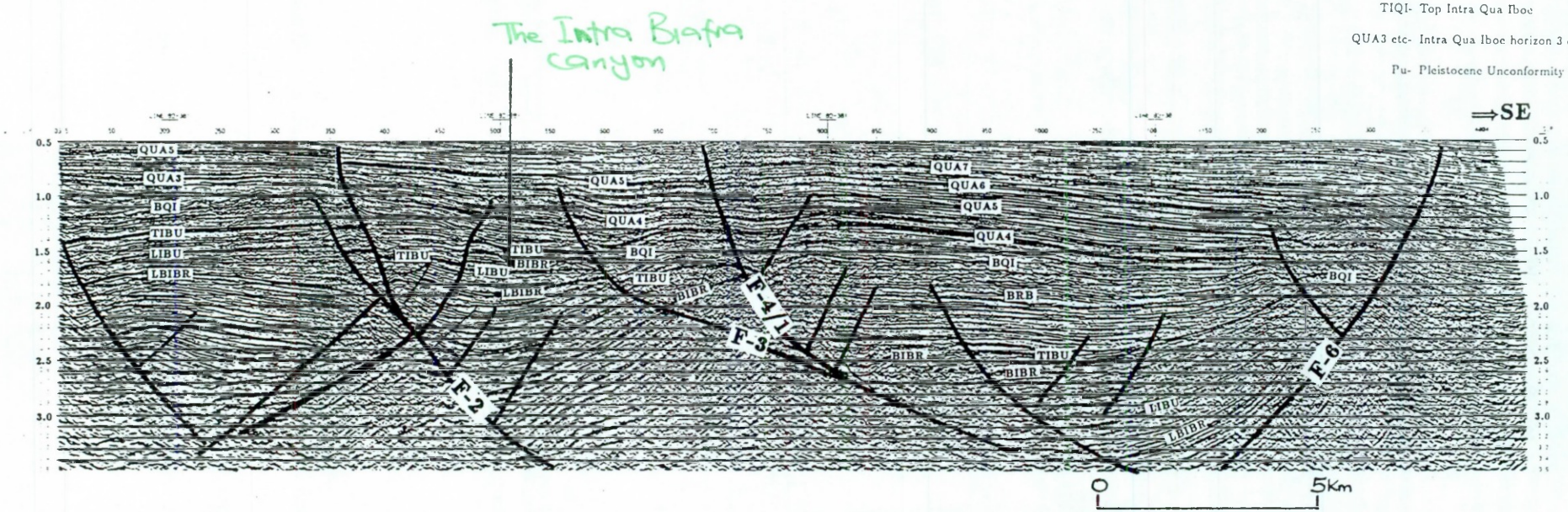

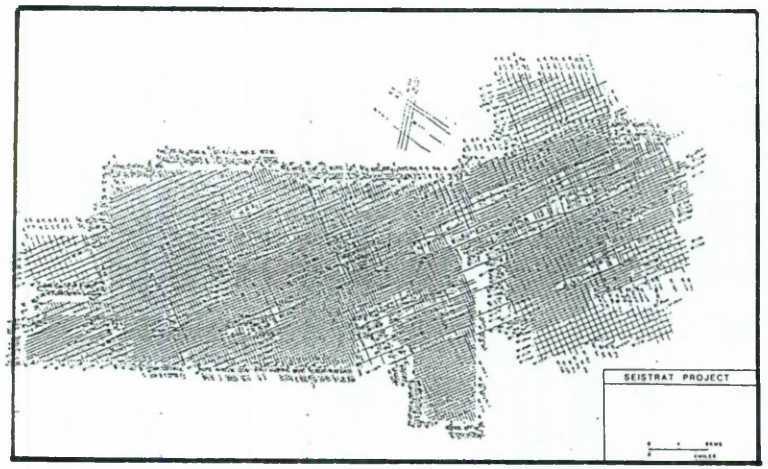

Fig.4.6a Line 82-381 showing the Base Intra Biafra Rubble (BIBR) as an erosional unconformity (northeast area) and a surface of onlap southwards.

LBIBR- Lower Base Intra Biafra Rubble.

LIBU- Lower Intra Biafra Unconformity.

BIBR- Base Intra Biafra Rubble.

TIBU- Top Intra Biafra Unconformity.

BIBBEN- Base Intra Biafra Benin sands.

BRB- Base Rubble Beds

BQI- Base Qua Iboe.

TIQI- Top Intra Qua Iboe

QUA3 etc- Intra Qua Iboe horizon 3 etc

Pu- Pleistocene Unconformity

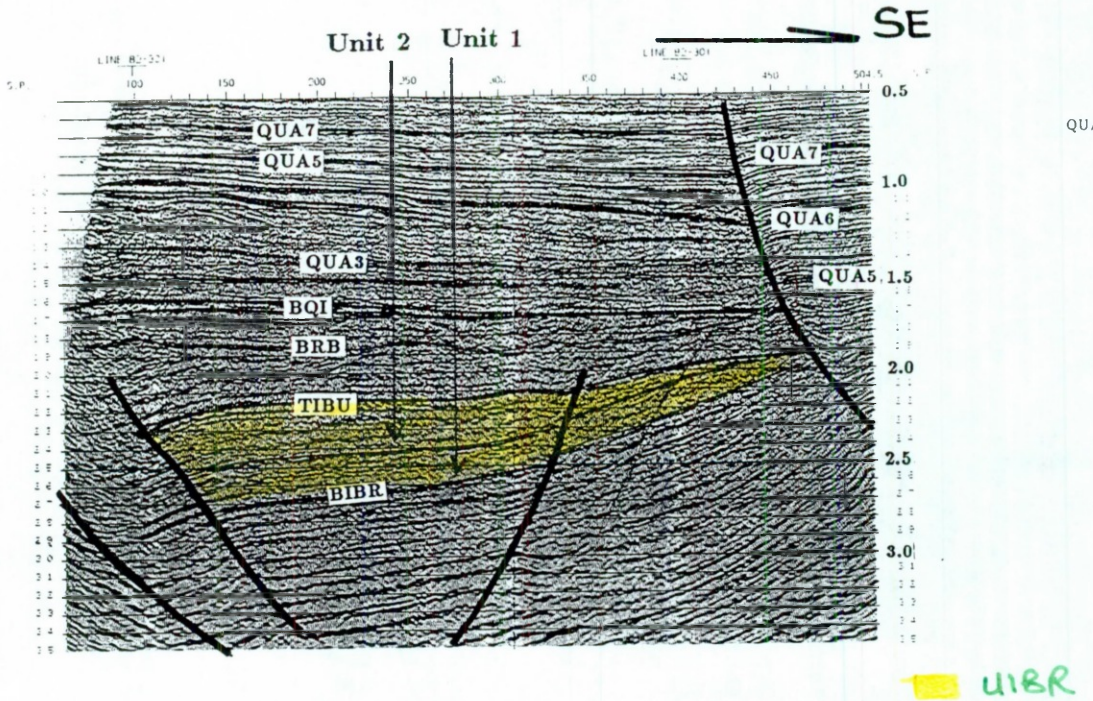

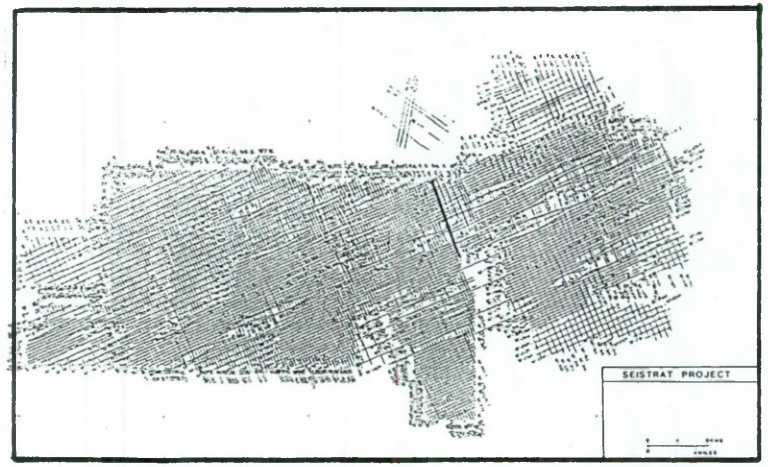

Fig.4.6b Line 82-301 showing a less erosional BIBR. Note the differentiation of the Upper Intra Biafra Rubble (UIBR) into 2 units. The lower unit appears to be the distal facies; the upper unit is slope front fill facies.

LBIBR- Lower Base Intra Biafra Rubble.

LIBU- Lower Intra Biafra Unconformity.

BIBR- Base Intra Biafra Rubble.

TIBU- Top Intra Biafra Unconformity.

BIBBEN- Base Intra Biafra Benin sands.

BRB- Base Rubble Beds

BQI- Base Qua Iboe.

TIQI- Top Intra Qua Iboe

QUA3 etc- Intra Qua Iboe horizon 3 etc

Pu- Pleistocene Unconformity

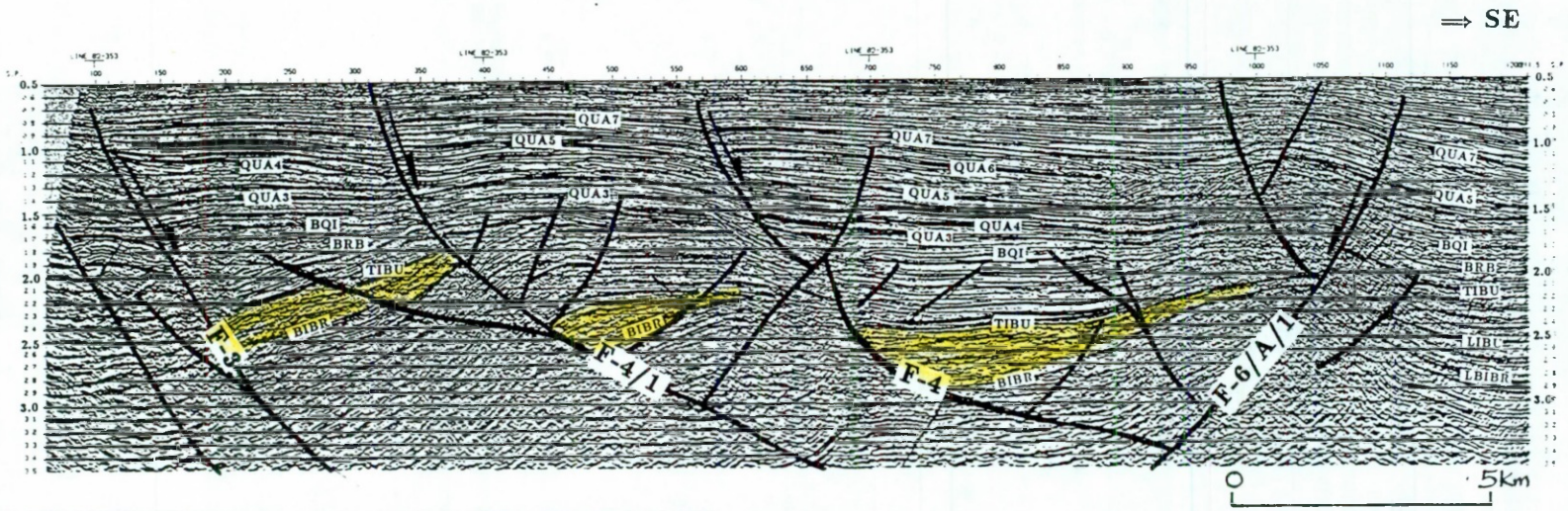

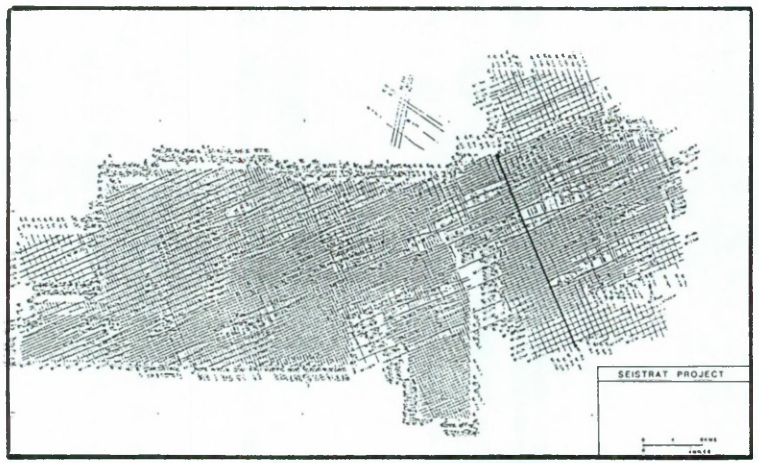

Fig.4.7a Line 82-353 showing the Top Intra Biafra Unconformity (TIBU) with associated truncation and Upper Intra Biafra Rubble onlap.

LBIBR- Lower Base Intra Biafra Rubble.

LIBU- Lower Intra Biafra Unconformity.

BIBR- Base Intra Biafra Rubble.

TIBU- Top Intra Biafra Unconformity.

BIBBEN- Base Intra Biafra Benin sands.

BRB- Base Rubble Beds

BQI- Base Qua Iboe.

TIQI- Top Intra Qua Iboe

QUA3 etc- Intra Qua Iboe horizon 3 etc

Pu- Pleistocene Unconformity

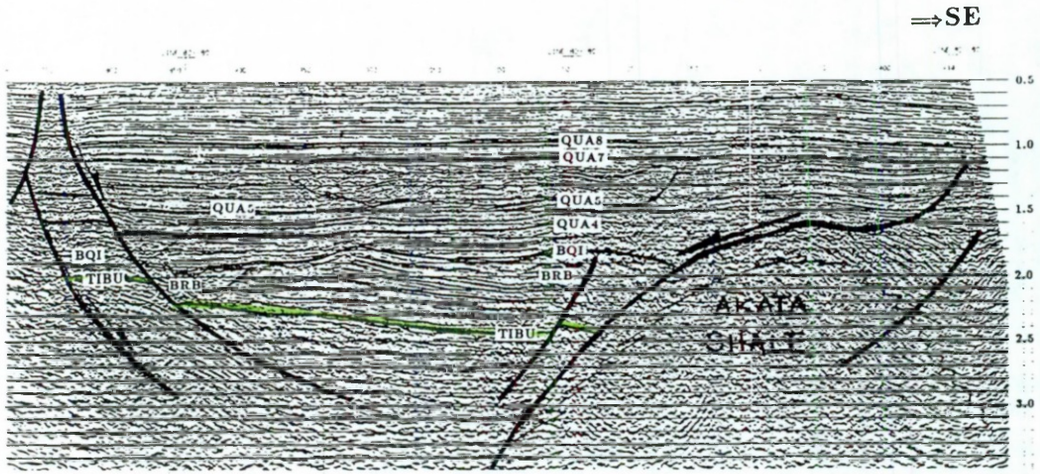

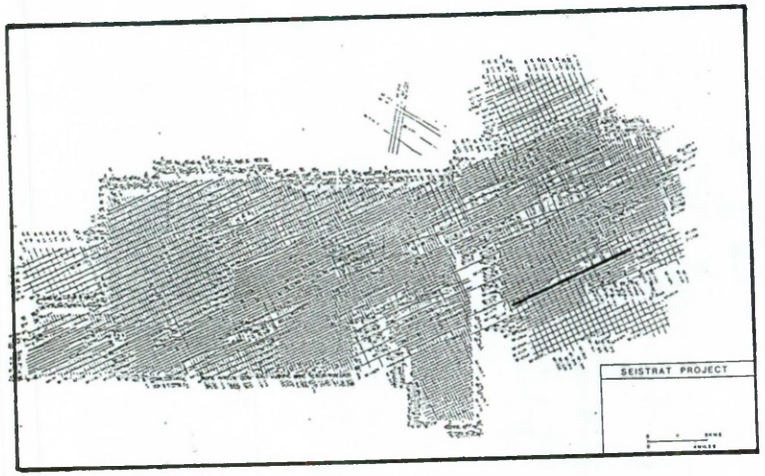

Fig.4.7b Angular unconformity at the TIBU level may also be caused by upwarping of a depositonal shale mass forming what was referred to in Chapter 3 as "shale mass structure - flank"(line 82-180).

LBIBR- Lower Base Intra Biafra Rubble.

LIBU- Lower Intra Biafra Unconformity.

BIBR- Base Intra Biafra Rubble.

TIBU- Top Intra Biafra Unconformity.

BIBBEN- Base Intra Biafra Benin sands.

BRB- Base Rubble Beds

BQI- Base Qua Iboe.

TIQI- Top Intra Qua Iboe

QUA3 etc- Intra Qua Iboe horizon 3 etc

Pu- Pleistocene Unconformity

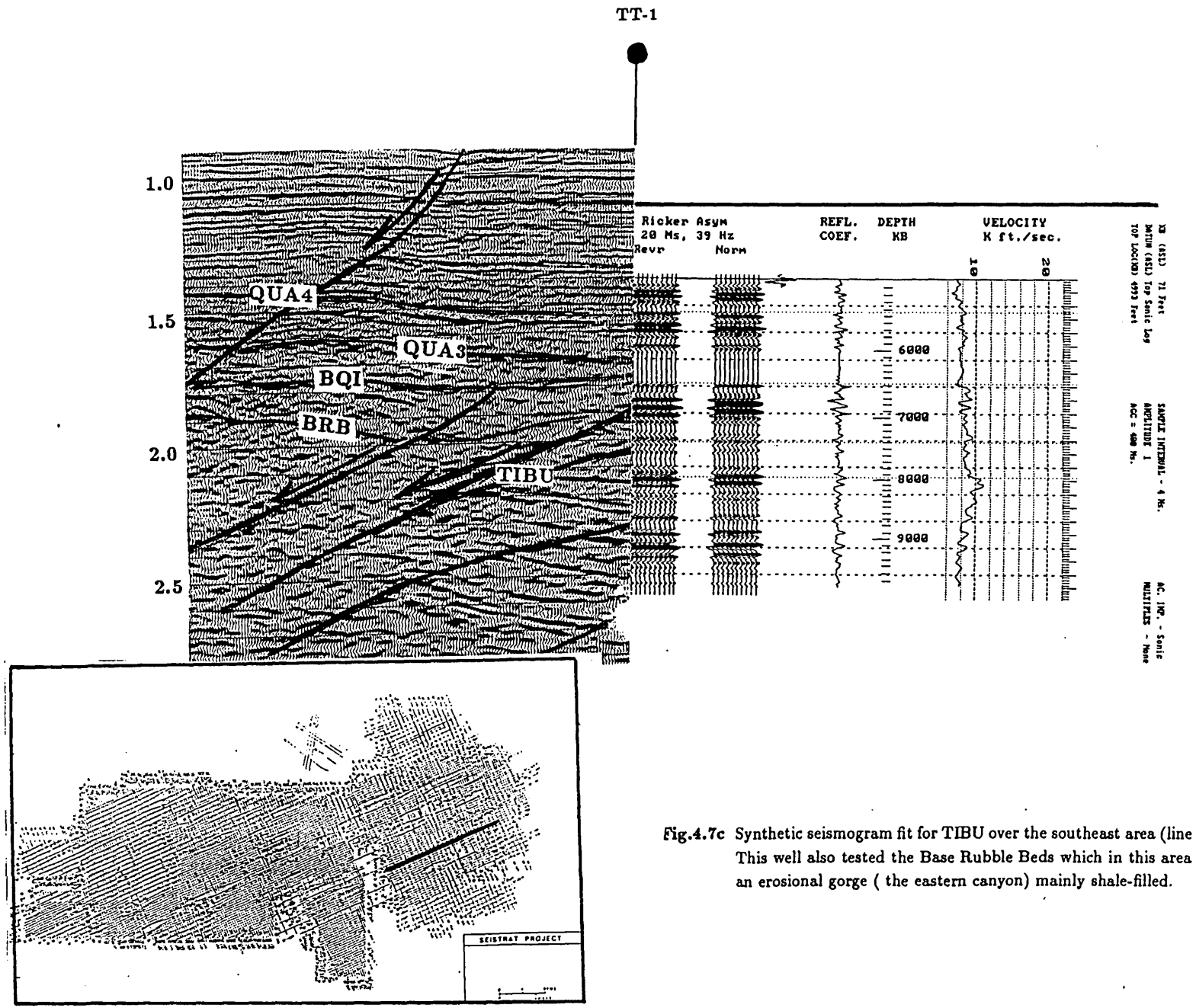

Fig.4.7c Synthetic seismogram fit for TIBU over the southeast area (line 82-162b). This well also tested the Base Rubble Beds which in this area occurs as an erosional gorge (the eastern canyon) mainly shale-filled.

LBIBR- Lower Base Intra Biafra Rubble.

LIBU- Lower Intra Biafra Unconformity.

BIBR- Base Intra Biafra Rubble.

TIBU- Top Intra Biafra Unconformity.

BIBBEN- Base Intra Biafra Benin sands.

BRB- Base Rubble Beds

BQI- Base Qua Iboe.

TIQI- Top Intra Qua Iboe

QUA3 etc- Intra Qua Iboe horizon 3 etc

Pu- Pleistocene Unconformity

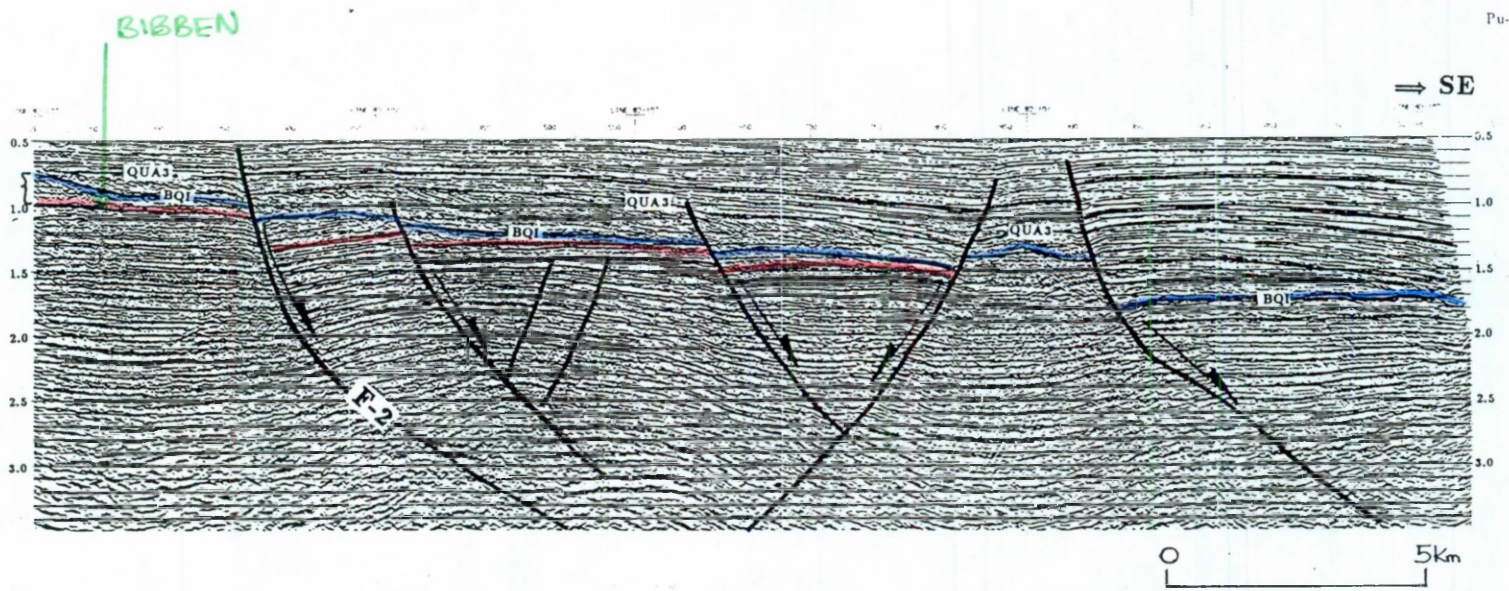

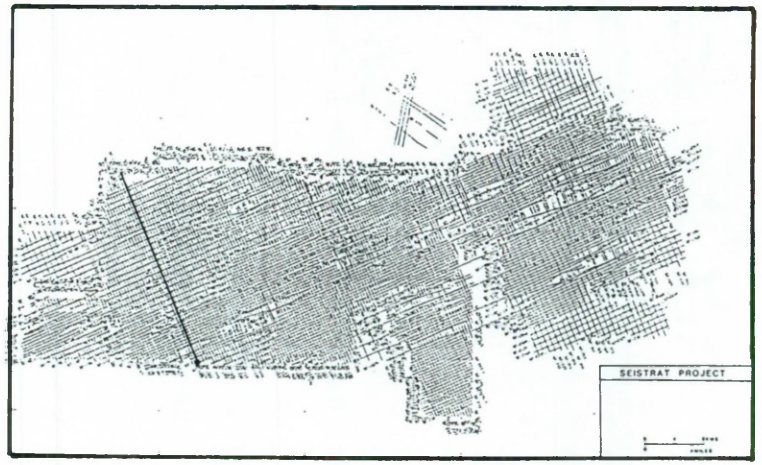

Fig.4.8a Seismic line 82-107 showing the horizon BIBBEN truncated against the BQI to the south of the profile. Also note the thinning of Qua Iboe shale northward as an onlap prograding wedge.

LBIBR- Lower Base Intra Biafra Rubble.

LIBU- Lower Intra Biafra Unconformity.

BIBR- Base Intra Biafra Rubble.

TIBU- Top Intra Biafra Unconformity.

BIBBEN- Base Intra Biafra Benin sands.

BRB- Base Rubble Beds

BQI- Base Qua Iboe.

TIQI- Top Intra Qua Iboe

QUA3 etc- Intra Qua Iboe horizon 3 etc

Pu- Pleistocene Unconformity

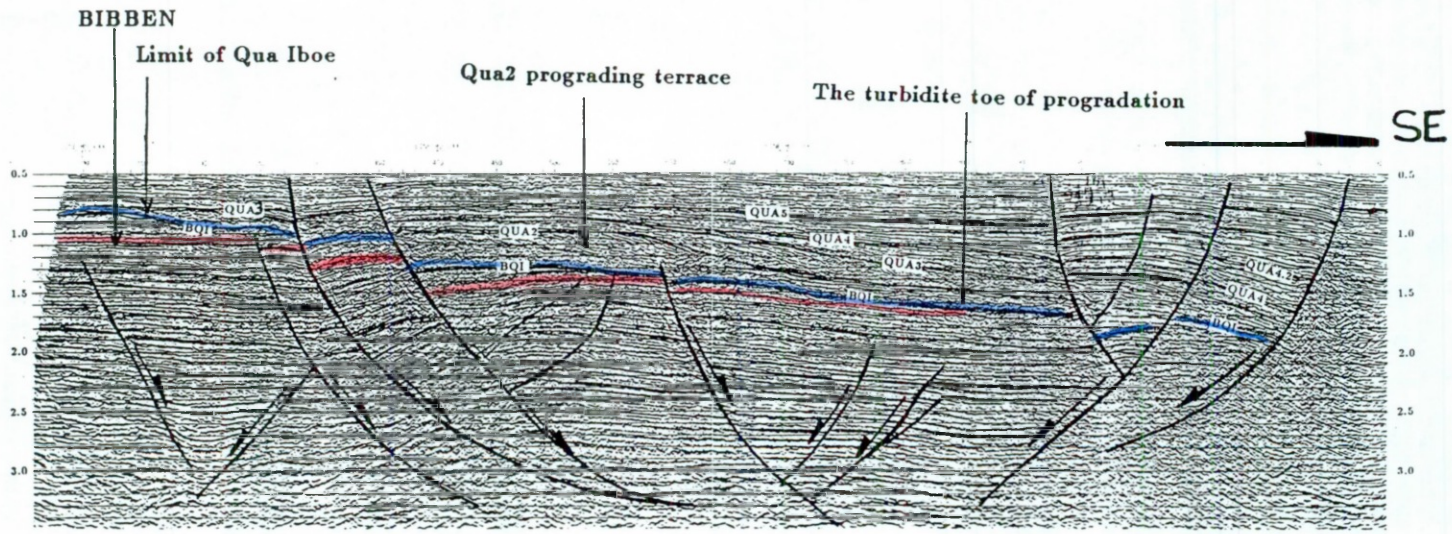

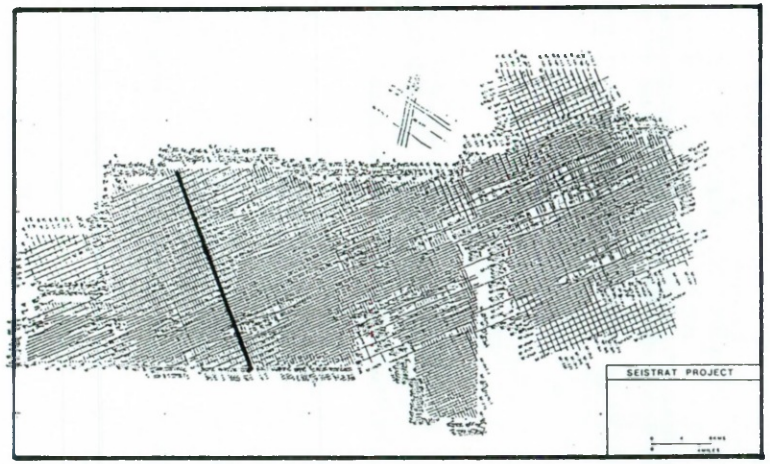

Fig.4.8b Seismic evidence of the limit of Qua Iboe shale which north of the paleobasin thins into a veneer overlain by the Benin sands(line 82-133). Also note the Qua2 prograding terrace and the turbidite toe of progradation further south.

LBIBR- Lower Base Intra Biafra Rubble.

LIBU- Lower Intra Biafra Unconformity.

BIBR- Base Intra Biafra Rubble.

TIBU- Top Intra Biafra Unconformity.

BIBBEN- Base Intra Biafra Benin sands.

BRB- Base Rubble Beds

BQI- Base Qua Iboe.

TIQI- Top Intra Qua Iboe

QUA3 etc- Intra Qua Iboe horizon 3 etc

Pu- Pleistocene Unconformity

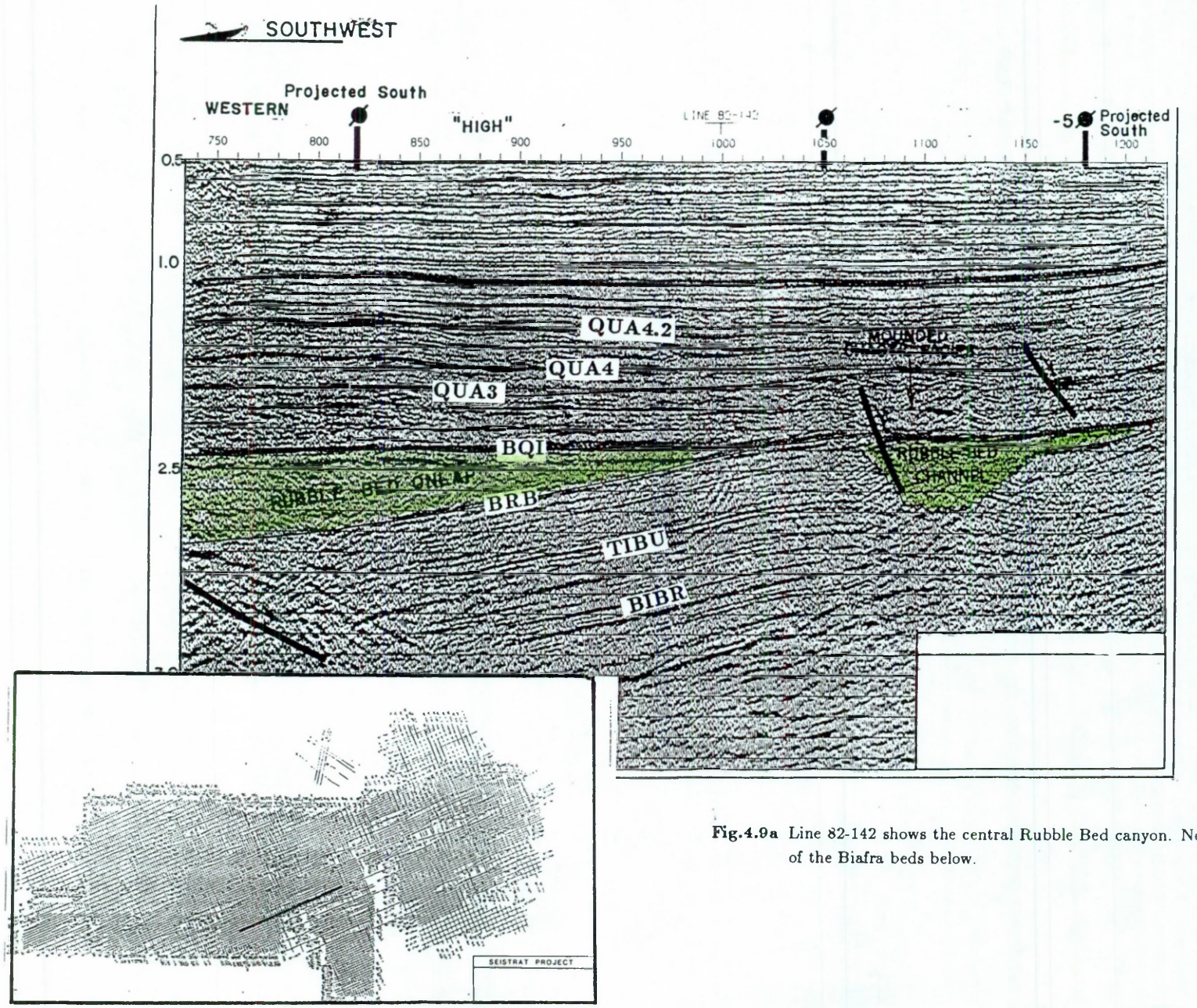

RUBBLE BEDS

Fig.4.9a Line 82-142 shows the central Rubble Bed canyon. Note the truncation of the Biafra beds below.

LIBBR- Lower Base Intra Biafra Rubble.

LIBU- Lower Intra Biafra Unconformity.

BIBR- Base Intra Biafra Rubble.

TIBU- Top Intra Biafra Unconformity.

BIBBEN- Base Intra Biafra Benin sands.

BRB- Base Rubble Beds

BQI- Base Qua Iboe.

TIQI- Top Intra Qua Iboe

QUA3 etc- Intra Qua Iboe horizon 3 etc

Pu- Pleistocene Unconformity

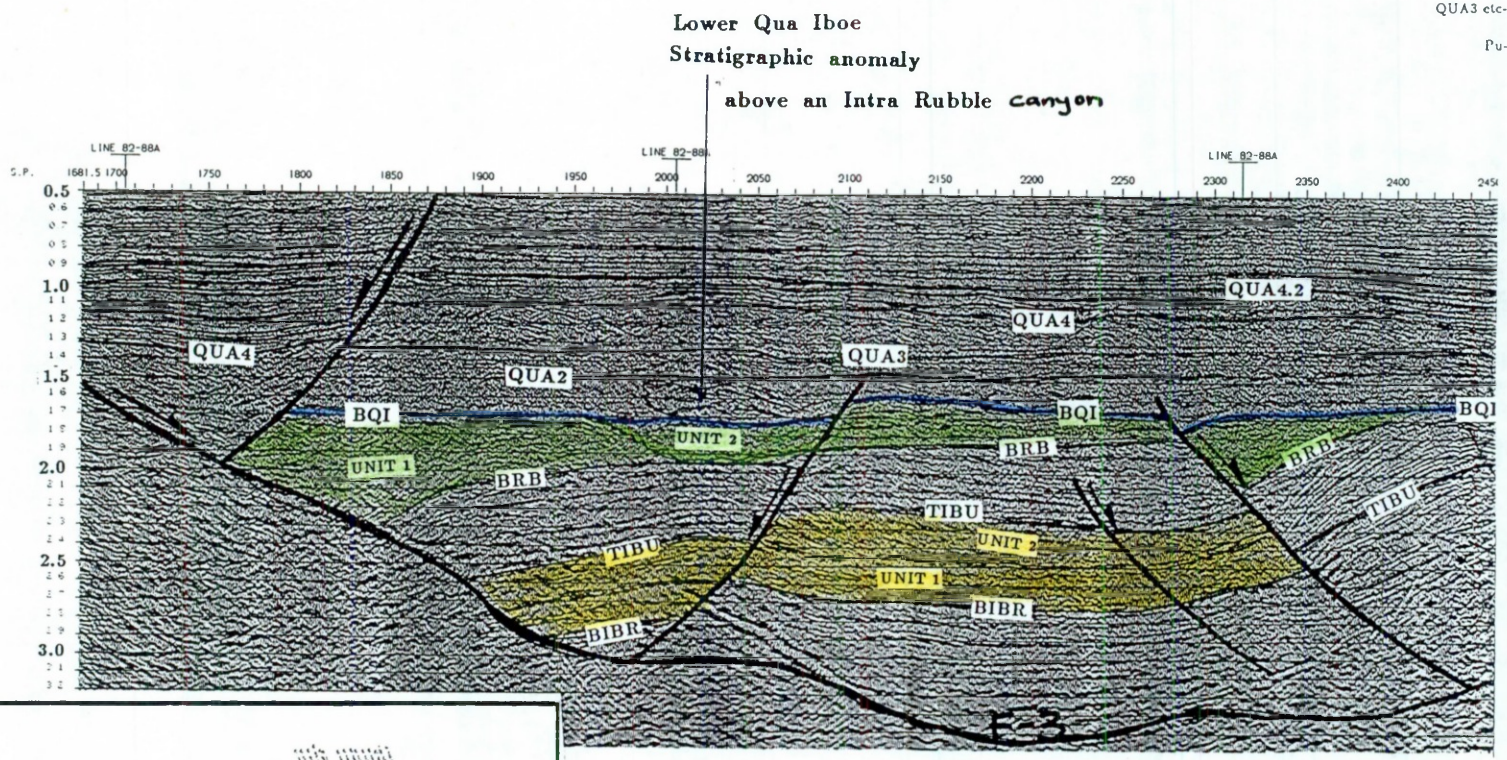

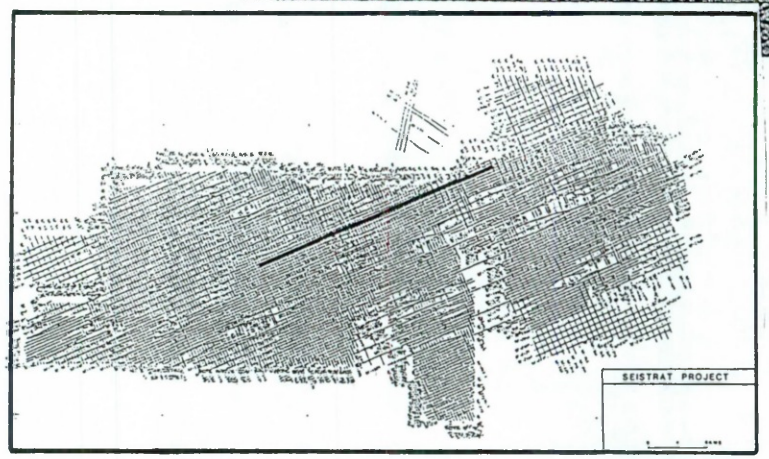

UIBR

RUBBLE BEDS

Fig.4.9b Line 82-88a shows seismic evidence of Intra Rubble unconformities. Rubble Bed subdivision is possible with Unit 1 forming the northern anomaly and Unit 2 the Intra Rubble channel shown. The mounded facies of the northern anomaly is also evident.

LBIBR- Lower Base Intra Biafra Rubble.

LIBU- Lower Intra Biafra Unconformity.

BIBR- Base Intra Biafra Rubble.

TIBU- Top Intra Biafra Unconformity.

BIBBEN- Base Intra Biafra Benin sands.

BRB- Base Rubble Beds

BQI- Base Qua Iboe.

TIQI- Top Intra Qua Iboe

QUA3 etc- Intra Qua Iboe horizon 3 etc

Pu- Pleistocene Unconformity

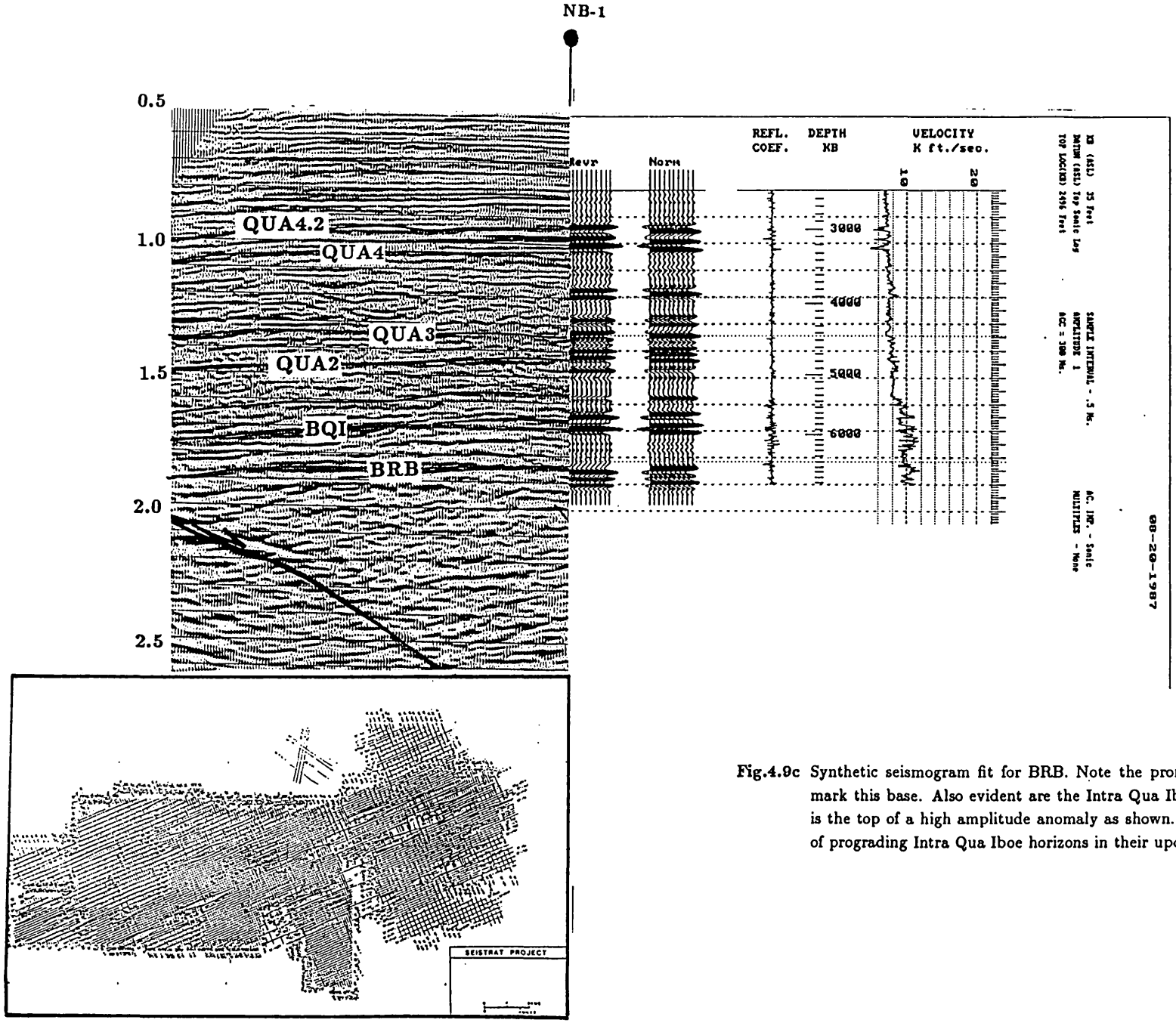

Fig.4.9c Synthetic seismogram fit for BRB. Note the prominent reflectors that mark this base. Also evident are the Intra Qua Iboe horizons. QUA4.2 is the top of a high amplitude anomaly as shown. This is characteristic of prograding Intra Qua Iboe horizons in their updip portions.

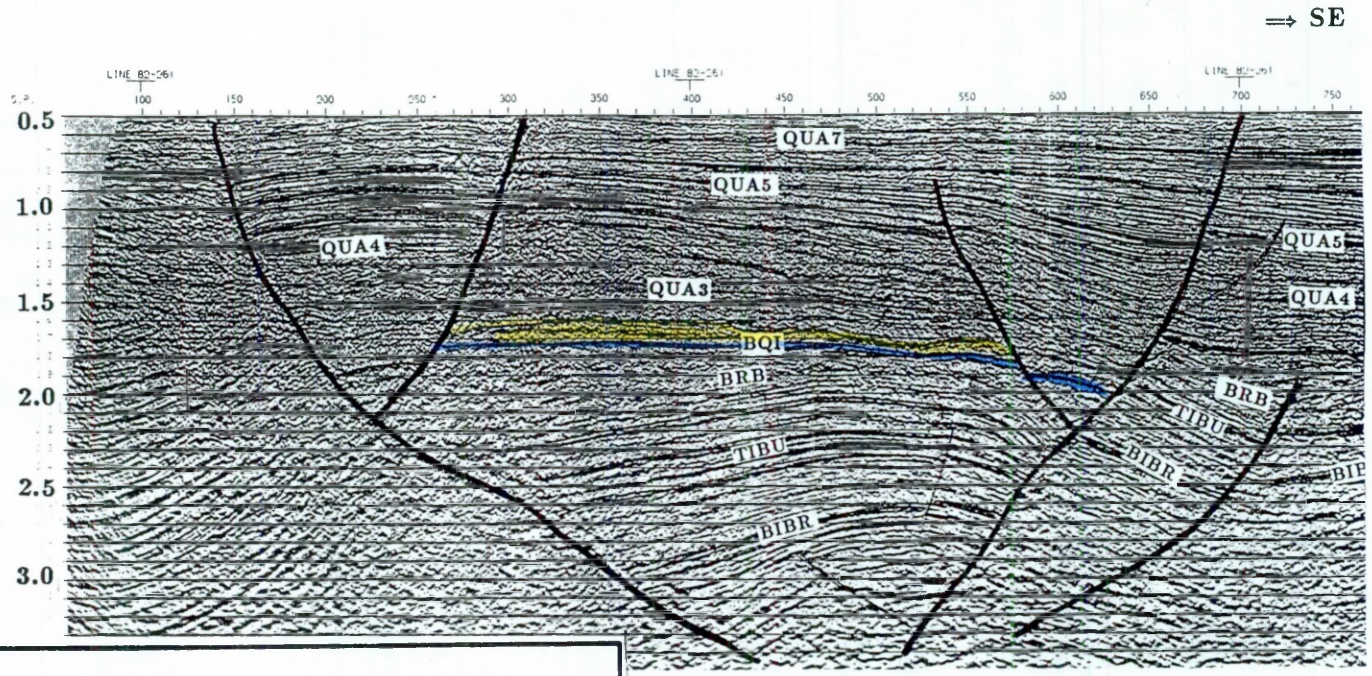

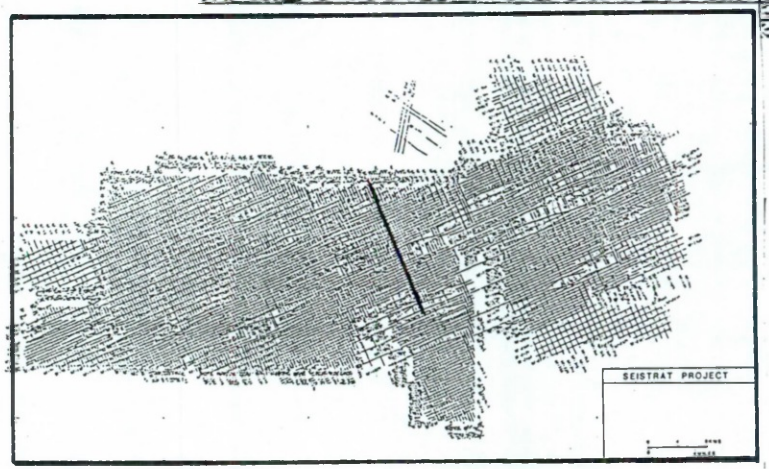

Fig.4.10a Line 82-261 shows the hummocky reflectors overlying the BQI unconformity. They are termed in the text basal transgressive sands, but also form part of the central Intra Qua Iboe anomaly (SEQ.QS1).

LBIBR- Lower Base Intra Biafra Rubble.

LIBU- Lower Intra Biafra Unconformity.

BIBR- Base Intra Biafra Rubble.

TIBU- Top Intra Biafra Unconformity.

BIBBEN- Base Intra Biafra Benin sands.

BRB- Base Rubble Beds

BQI- Base Qua Iboe.

TIQI- Top Intra Qua Iboe

QUA3 etc- Intra Qua Iboe horizon 3 etc

Pu- Pleistocene Unconformity

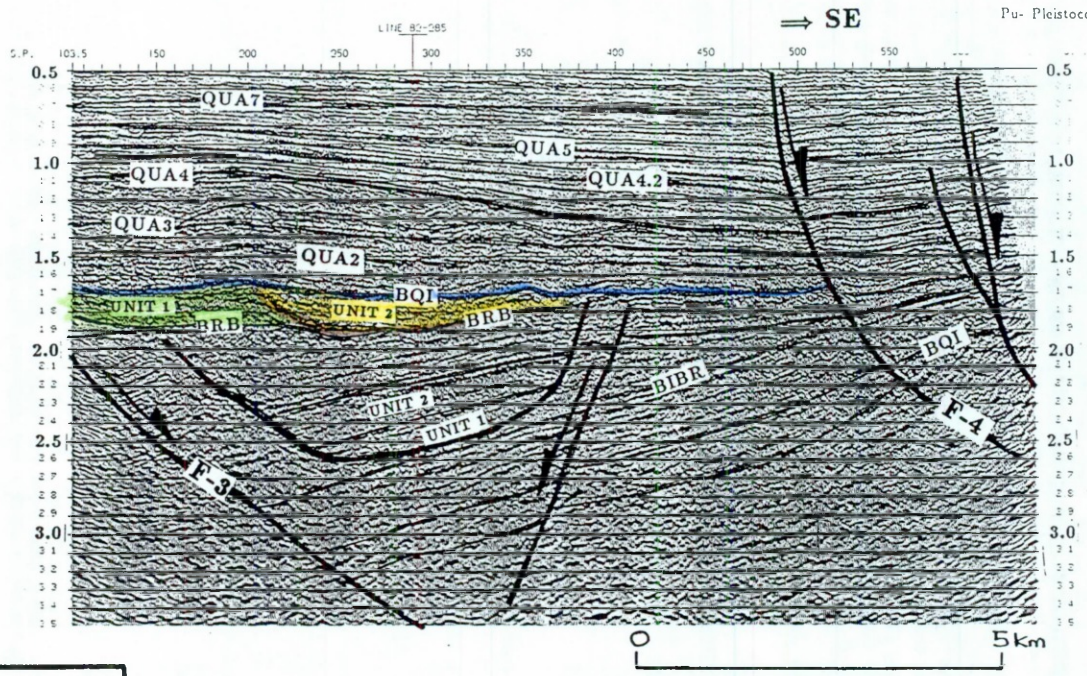

UNIT 2 RUBBLE
UNIT 1 RUBBLE

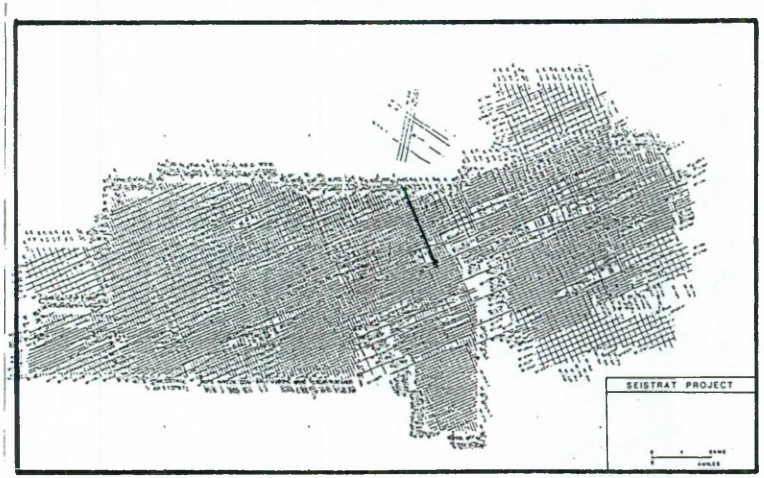

Fig.4.10b Line 82-285 shows the relationship between the two Rubble Bed regimes (Units 1 and 2) and the BQI. At shot point 300, the BQI pick becomes tenuous because of the erosional channel of 'Unit 2' Rubble. The pick becomes reliable again where Biafra beds truncate against the BQI.

LBIBR- Lower Base Intra Biafra Rubble.

LIBU- Lower Intra Biafra Unconformity.

BIBR- Base Intra Biafra Rubble.

TIBU- Top Intra Biafra Unconformity.

BIBBEN- Base Intra Biafra Benin sands.

BRB- Base Rubble Beds

BQI- Base Qua Iboe.

TIQI- Top Intra Qua Iboe

QUA3 etc- Intra Qua Iboe horizon 3 etc

Pu- Pleistocene Unconformity

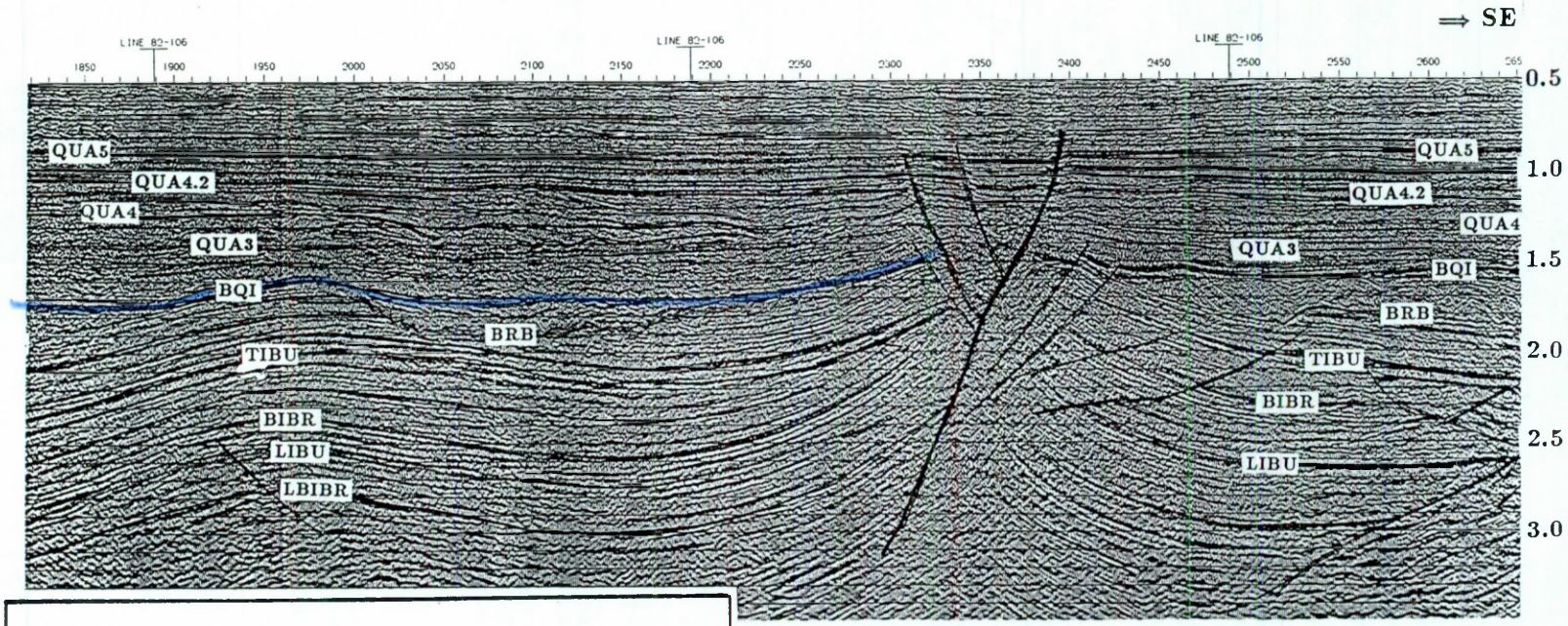

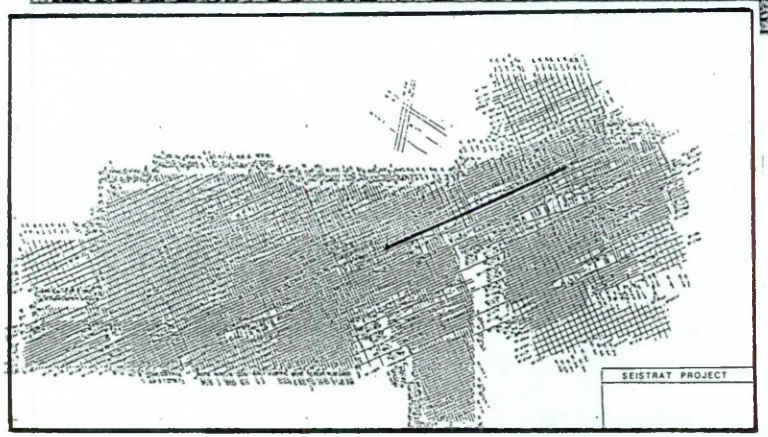

Fig.4.10c Seismic line 82-106, showing the lateral changes in the acoustic patterns from a weak reflector cycle at the crest of a BQI structure to several weak to strong cycles at the flank. (Shot point 2050 - 2250).

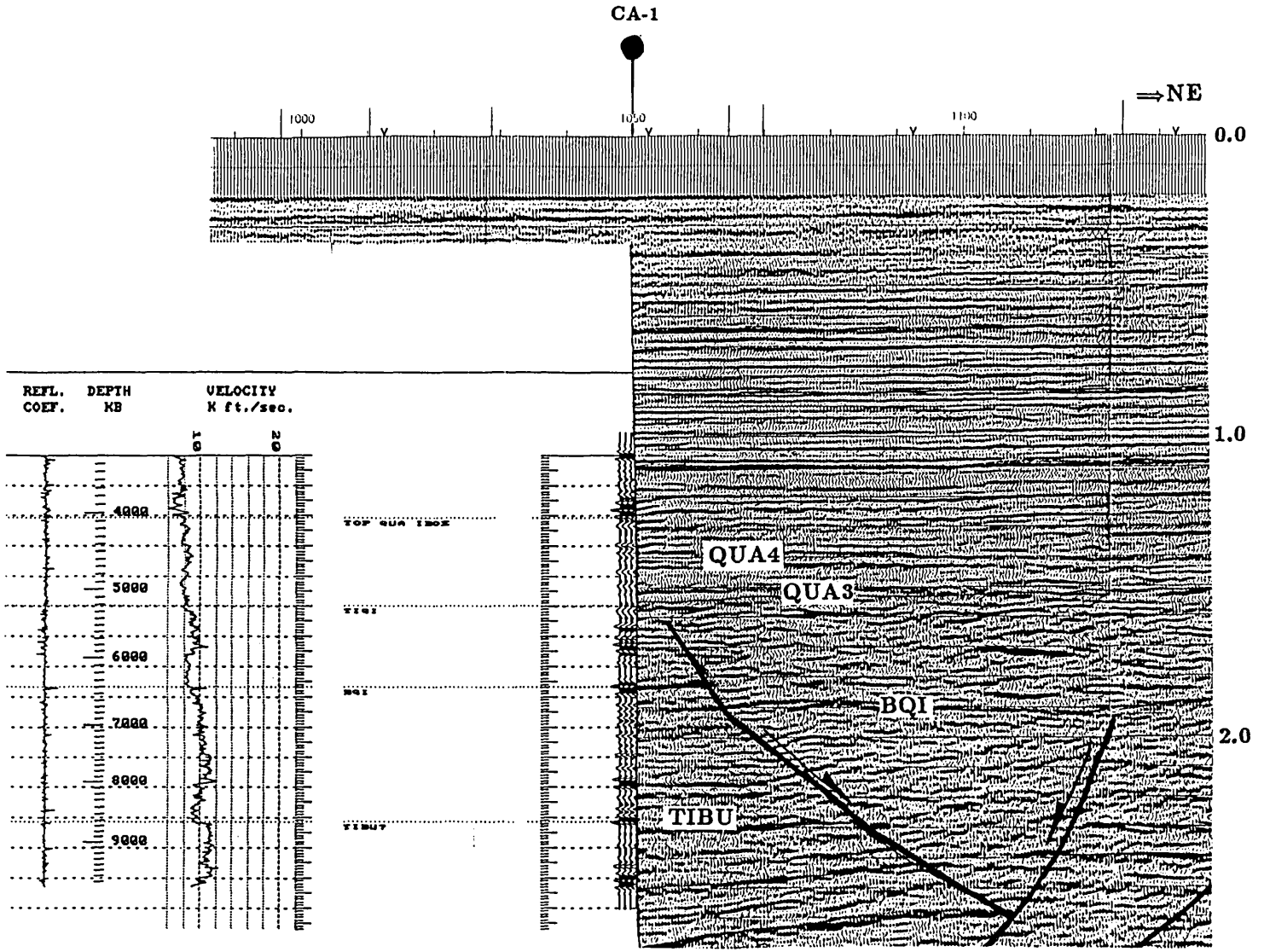

LBIBR- Lower Base Intra Biafra Rubble.

LIBU- Lower Intra Biafra Unconformity.

BIBR- Base Intra Biafra Rubble.

TIBU- Top Intra Biafra Unconformity.

BIBBEN- Base Intra Biafra Benin sands.

BRB- Base Rubble Beds

BQI- Base Qua Iboe.

TIQI- Top Intra Qua Iboe

QUA3 etc- Intra Qua Iboe horizon 3 etc

Pu- Pleistocene Unconformity

FORMATION	DEPTH Feet(Kb)	TIME Sec.(Datum)	AVG VEL Feet/Sec.	INT TIME Seconds	INT VEL Feet/Sec.
TOP B-I	2632				
TOP QUA IBOE	4060	.208	7325	0.252	7973
TIQI	5223	.459	7704	0.268	8769
BQI	6395	.767	8972	0.447	9981
TIBU?	8625	1.214	8775		

KB (ASL) 66 Feet
DATUM (ASL) Top Sonic Log
TOP LOG(KB) 2308 Feet

SAMPLE INTERVAL - .5 Ms.
AMPLITUDE 1
AGC = 400 Ms.

AC. INP. - Sonic
MULTIPLES - None

Fig.4.10d Synthetic seismogram fit for the BQI with Biafra Beds truncating. Intra Qua Iboe horizons are also shown (line 82-142).

LBIBR- Lower Base Intra Biafra Rubble.

LIBU- Lower Intra Biafra Unconformity.

BIBR- Base Intra Biafra Rubble.

TIBU- Top Intra Biafra Unconformity.

BIBBEN- Base Intra Biafra Benin sands.

BRB- Base Rubble Beds

BQI- Base Qua Iboe.

TIQI- Top Intra Qua Iboe

QUA3 etc- Intra Qua Iboe horizon 3 etc

Pu- Pleistocene Unconformity

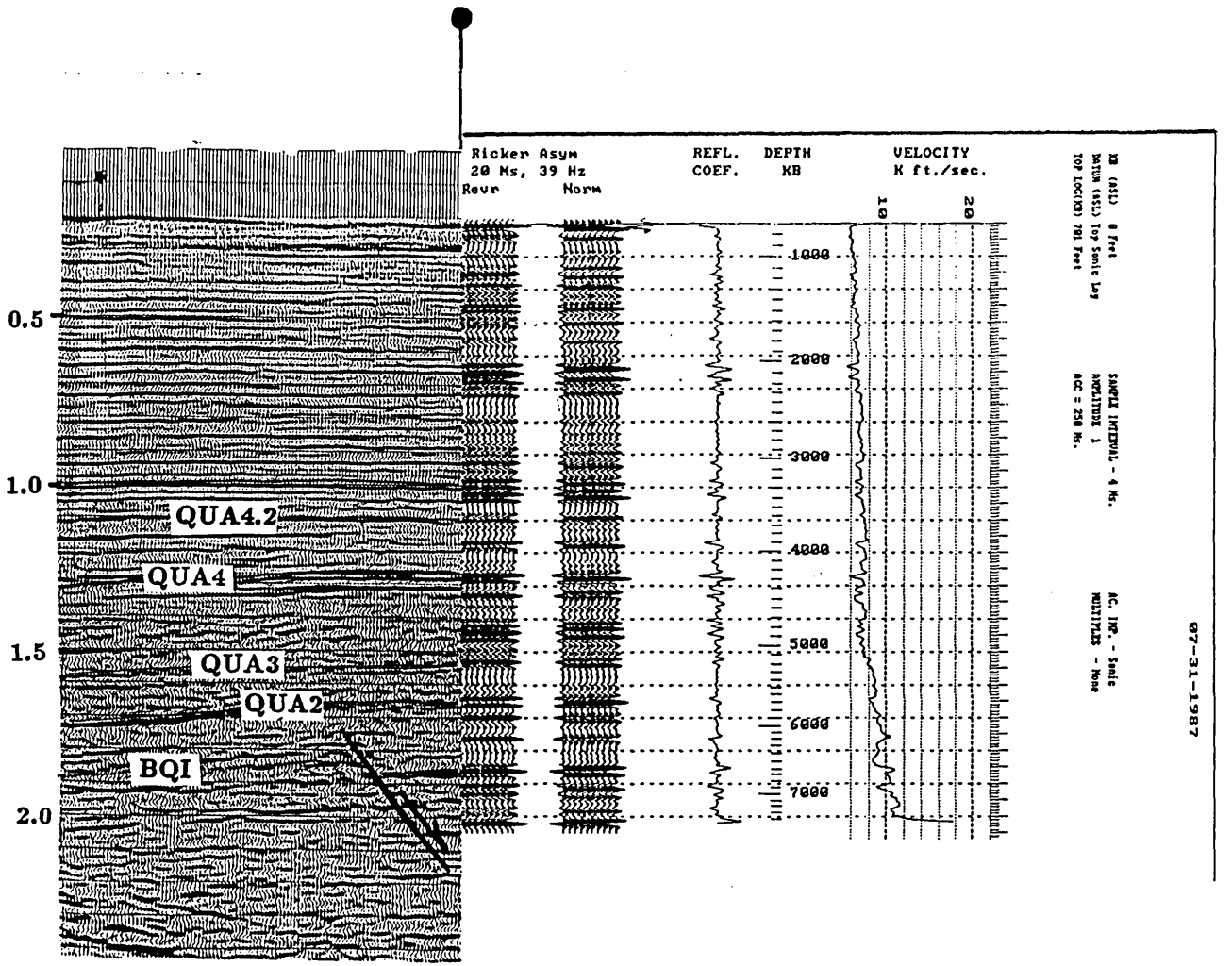

Fig.4.10e Synthetic seismogram fit for the BQI over Rubble Beds and the Intra Qua Iboe horizons. Note the high amplitude anomaly associated with QUA4 which may be compared to that evident in Fig.4.9c. The former occurs in the centre of the acreage, whlie the latter is to the west.

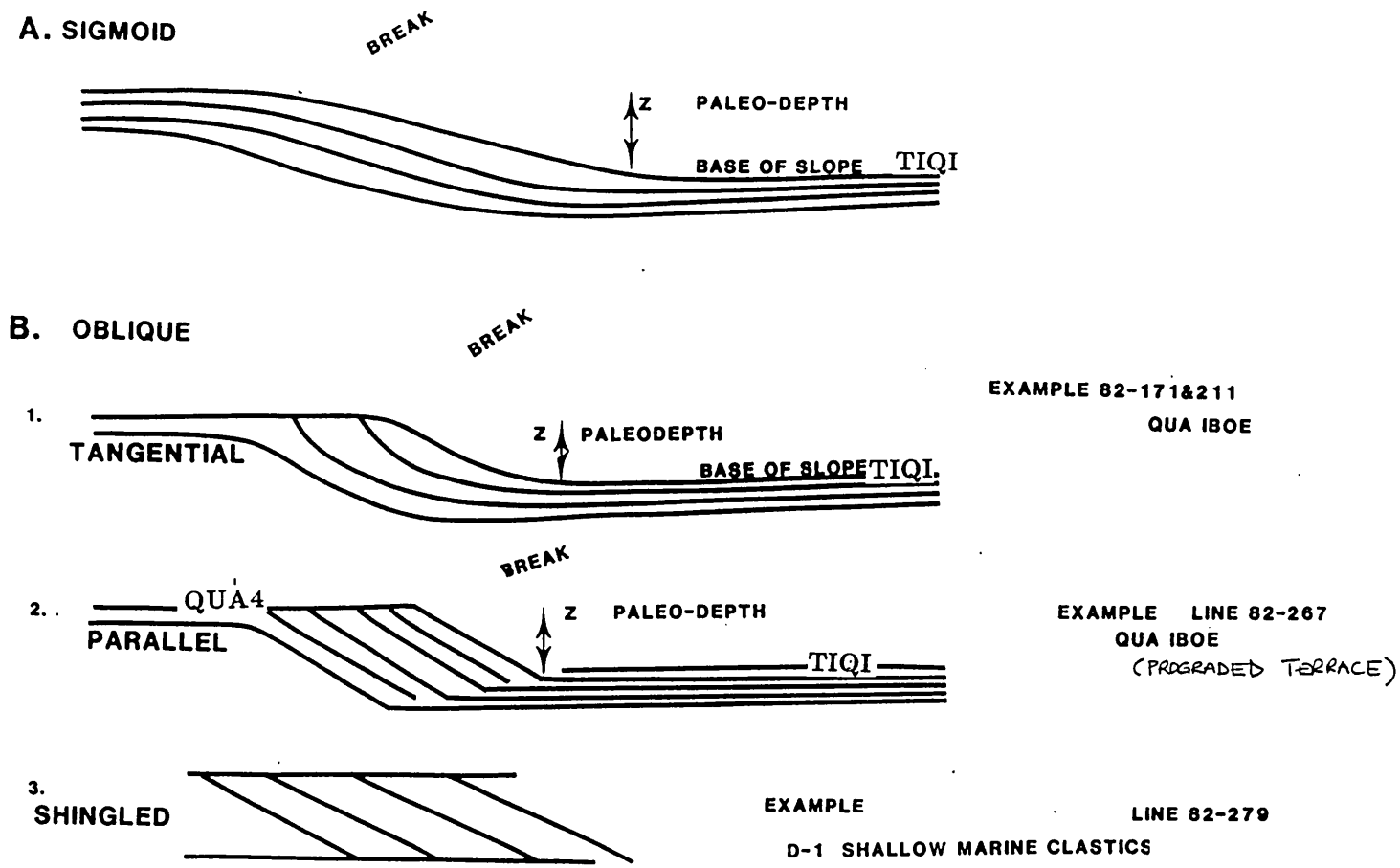

Fig.4.11a Schematic diagram showing how Intra Qua Horizons were defined and mapped.

LBIBR- Lower Base Intra Biafra Rubble.

LIBU- Lower Intra Biafra Unconformity.

BIBR- Base Intra Biafra Rubble.

TIBU- Top Intra Biafra Unconformity.

BIBBEN- Base Intra Biafra Benin sands.

BRB- Base Rubble Beds

BQI- Base Qua Iboe.

TIQI- Top Intra Qua Iboe

QUA3 etc- Intra Qua Iboe horizon 3 etc

Pu- Pleistocene Unconformity

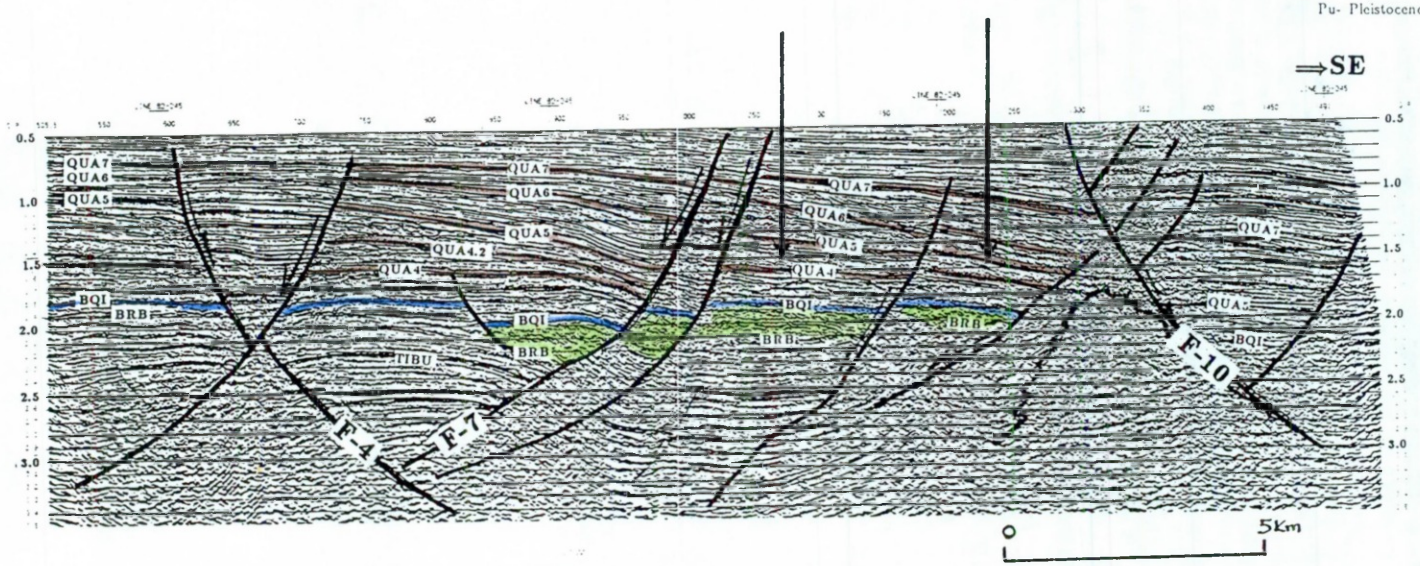

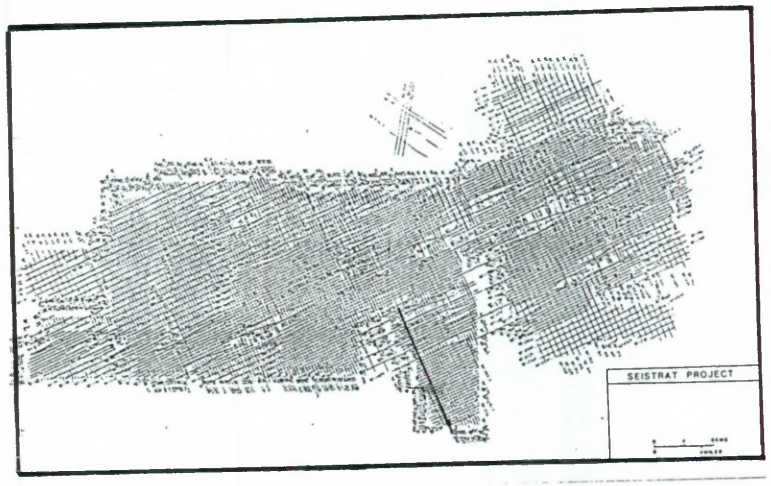

Fig.4.11b Seismic example (line 82-245) of Qua Iboe progradation and the turbidite toe.

LBIBR- Lower Base Intra Biafra Rubble.

LIBU- Lower Intra Biafra Unconformity.

BIBR- Base Intra Biafra Rubble.

TIBU- Top Intra Biafra Unconformity.

BIBBEN- Base Intra Biafra Benin sands.

BRB- Base Rubble Beds

BQI- Base Qua Iboe.

TIQI- Top Intra Qua Iboe

QUA3 etc- Intra Qua Iboe horizon 3 etc

Pu- Pleistocene Unconformity

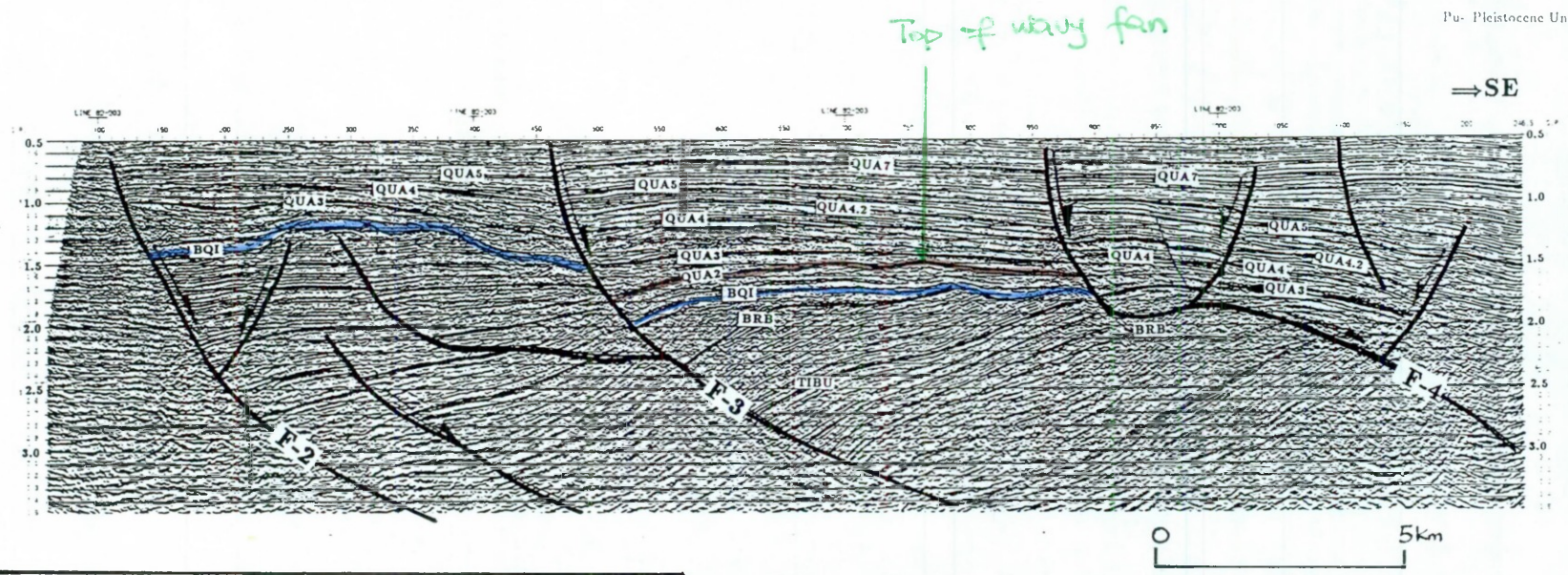

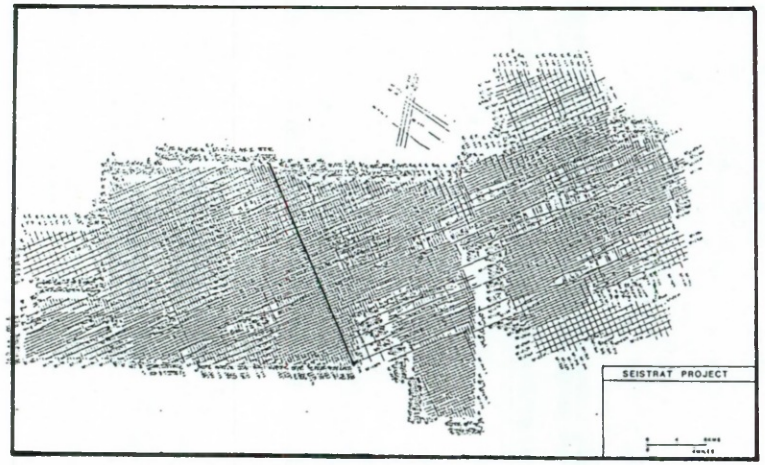

Fig.4.11c Line 82-203 shows the Qua2 which is the oldest Intra Qua Iboe horizon mapped. It is the top of a mounded, wavy fan - shaped feature that constitutes the western anomaly of the Lower Qua Iboe sequence.

LBIBR- Lower Base Intra Biafra Rubble.

LIBU- Lower Intra Biafra Unconformity.

BIBR- Base Intra Biafra Rubble.

TIBU- Top Intra Biafra Unconformity.

BIBBEN- Base Intra Biafra Benin sands.

BRB- Base Rubble Beds

BQI- Base Qua Iboe.

TIQI- Top Intra Qua Iboe

QUA3 etc- Intra Qua Iboe horizons etc

Pu- Pleistocene Unconformity

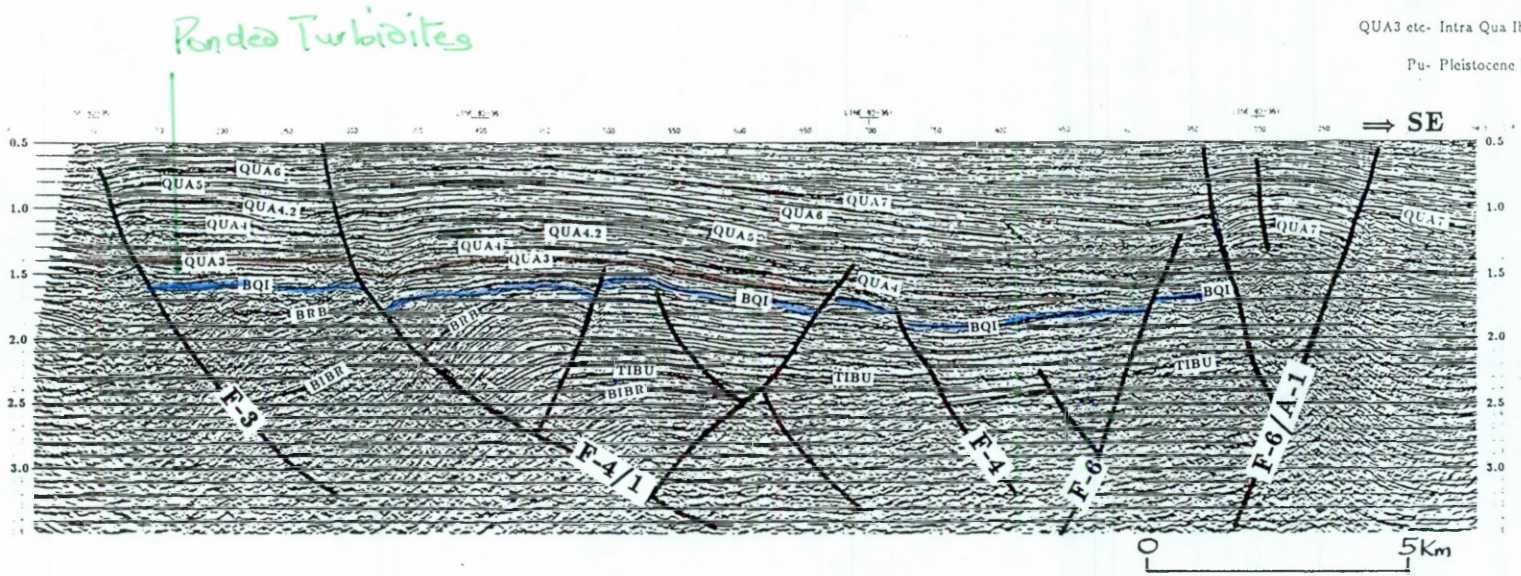

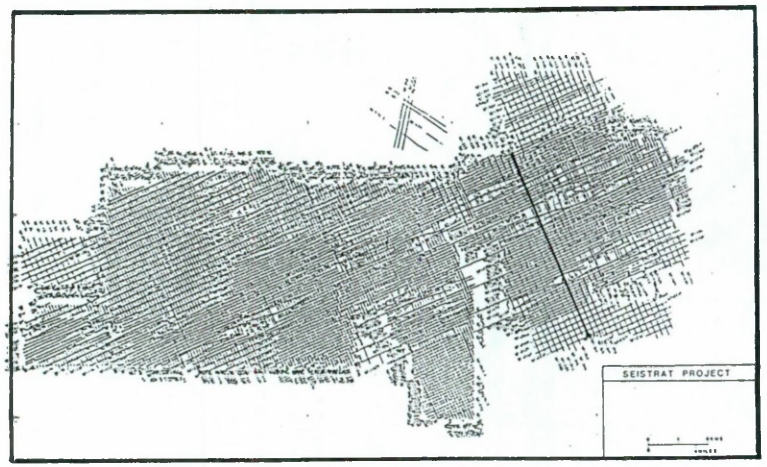

Fig.4.11d Line 82-361 shows Qua3 as the top of a ponded onlapping fill facies to the northeast which southward becomes top of a sheet drape facies.

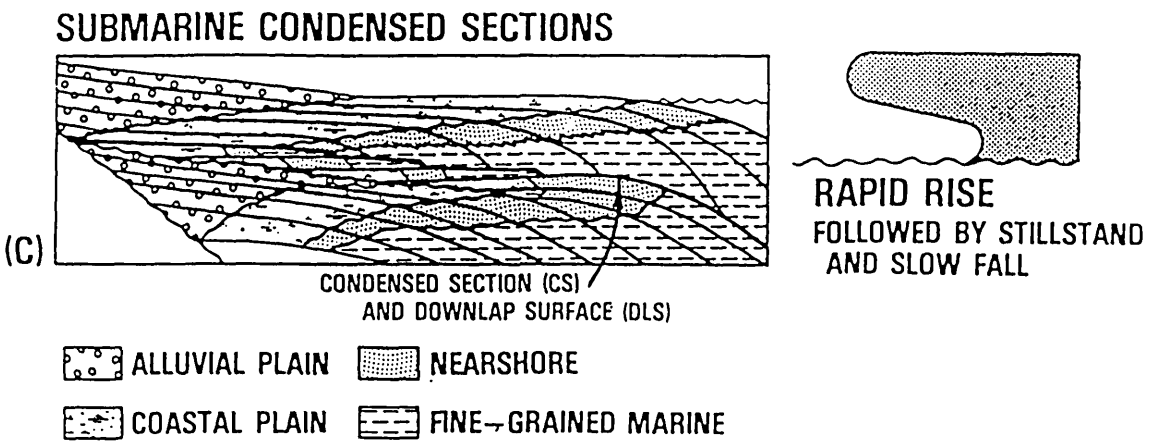

CONDENSED SECTIONS AND THEIR RELATIONSHIP TO EUSTATIC SEA LEVEL CHANGES

VAIL ,1984

Fig.4.11e Condensed sections.

LBIBR- Lower Base Intra Biafra Rubble.

LIBU- Lower Intra Biafra Unconformity.

BIBR- Base Intra Biafra Rubble.

TIBU- Top Intra Biafra Unconformity.

BIBBEN- Base Intra Biafra Benin sands.

BRB- Base Rubble Beds

BQI- Base Qua Iboe.

TIQI- Top Intra Qua Iboe

QUA3 etc- Intra Qua Iboe horizon 3 etc

Pu- Pleistocene Unconformity

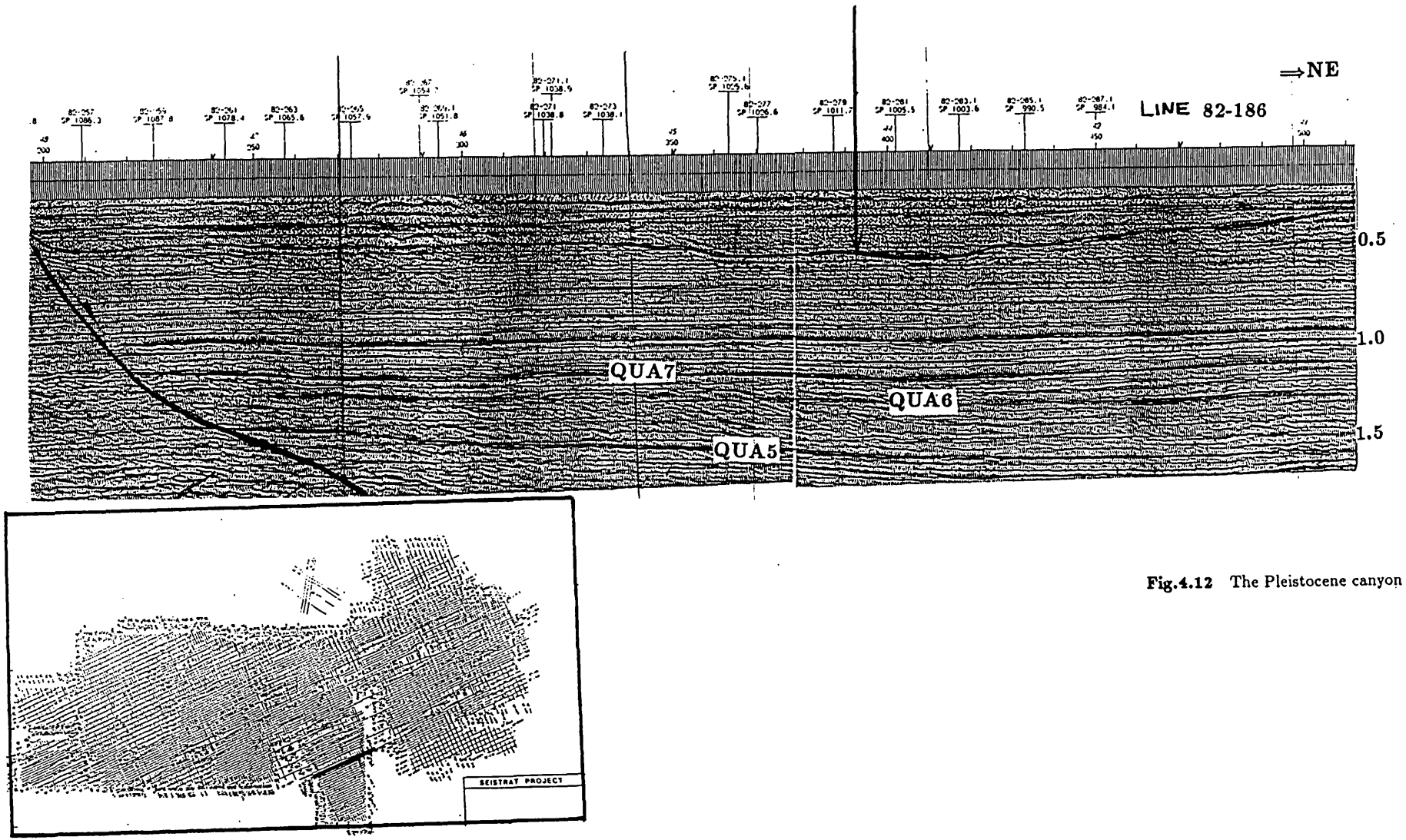

Fig.4.12 The Pleistocene canyon .

LBIBR- Lower Base Intra Biafra Rubble.
LIBU- Lower Intra Biafra Unconformity.
BIBR- Base Intra Biafra Rubble.
TIBU- Top Intra Biafra Unconformity.
BIBBEN- Base Intra Biafra Benin sands.
BRB- Base Rubble Beds
BQI- Base Qua Iboe.
TIQI- Top Intra Qua Iboe
QUA3 etc- Intra Qua Iboe horizon 3 etc
Pu- Pleistocene Unconformity

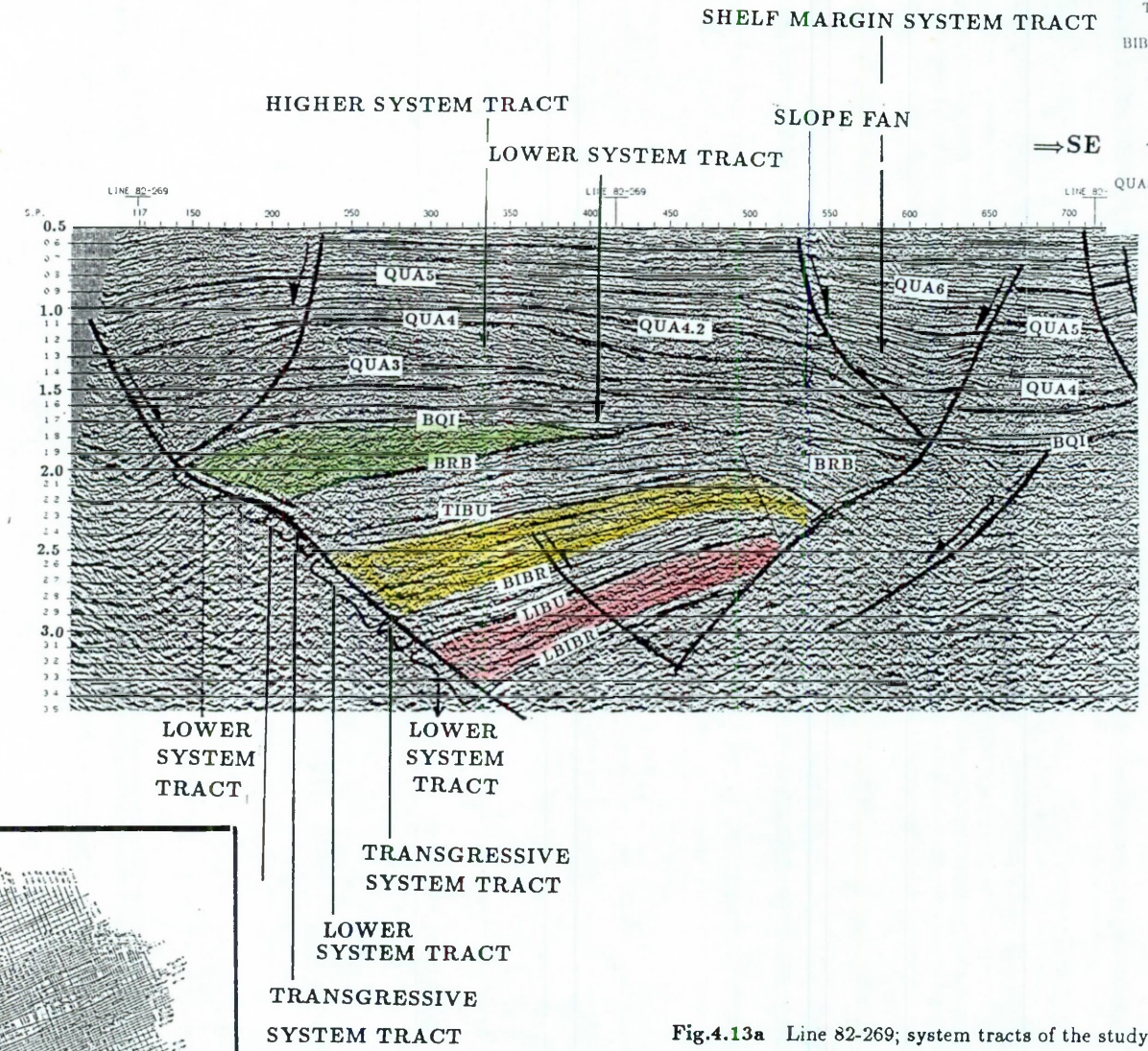

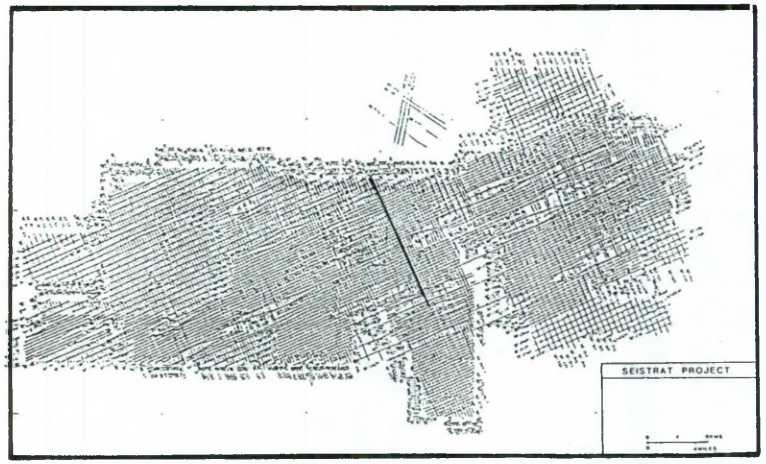

Fig.4.13a Line 82-269; system tracts of the study area .

LOWSTAND SYSTEM TRACTS IN DIFFERENT TECTONIC SETTINGS

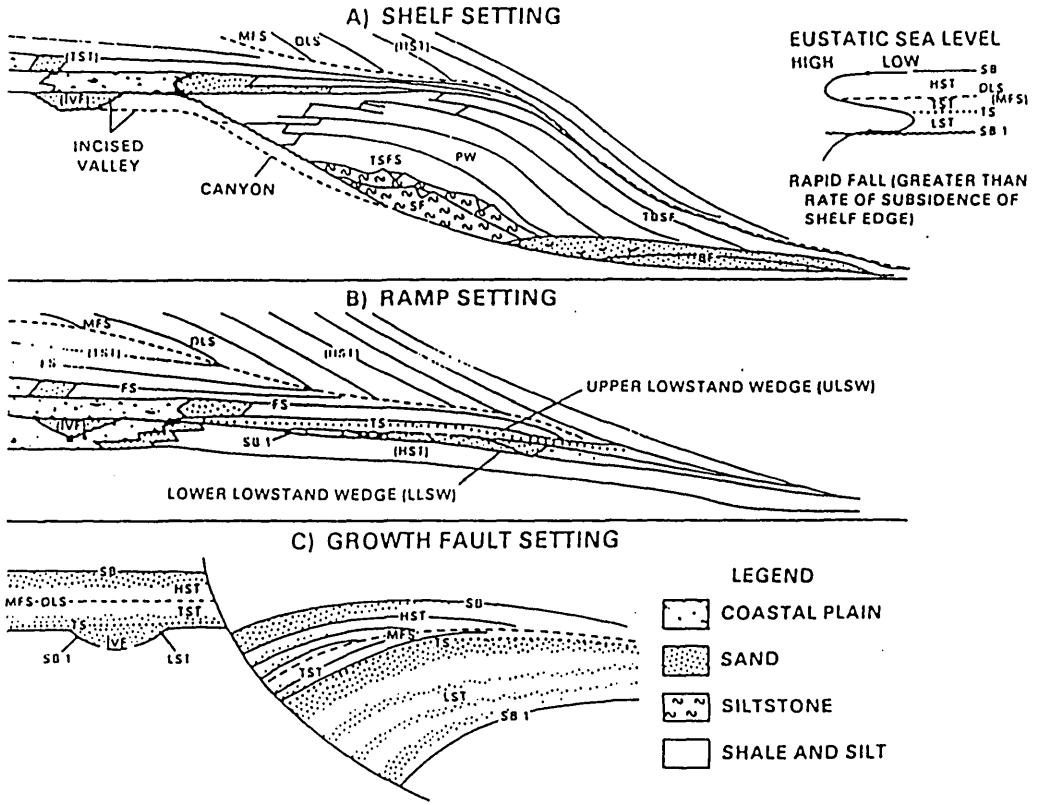

(Vail, 1988)

Fig.4.13b The Lower system tracts in different tectonic settings. This example line 82-127, is for a shelf setting.(see overleaf)

LBIBR- Lower Base Intra Biafra Rubble.
LIBU- Lower Intra Biafra Unconformity.
BIBR- Base Intra Biafra Rubble.
TIBU- Top Intra Biafra Unconformity.
BIBBEN- Base Intra Biafra Benin sands.
BRB- Base Rubble Beds
BQI- Base Qua Iboe.
TIQI- Top Intra Qua Iboe
QUA3 etc- Intra Qua Iboe horizon 3 etc
Pu- Pleistocene Unconformity

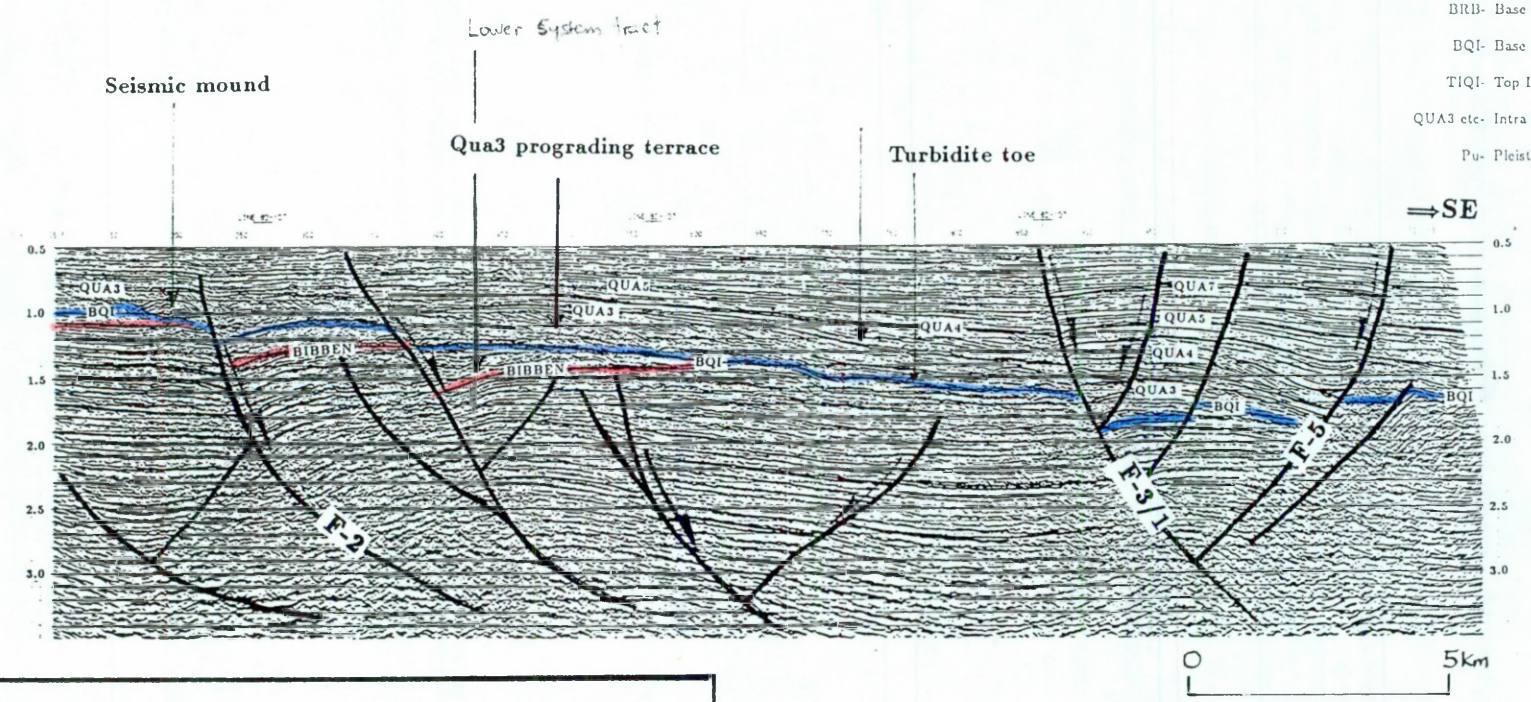

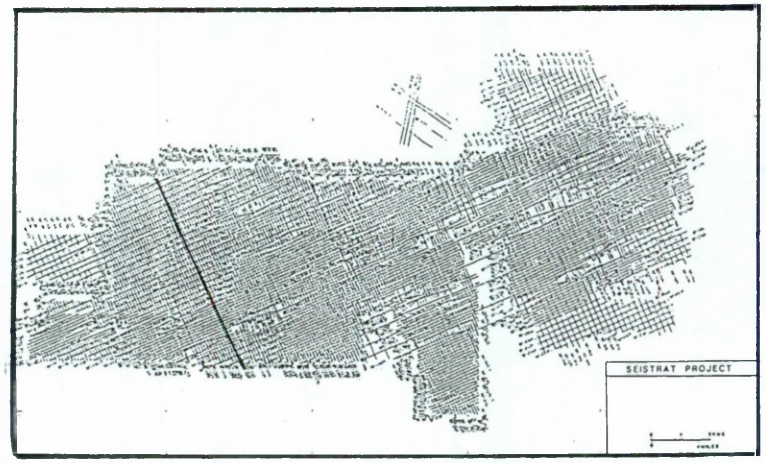

Fig.4.13b The Lower system tracts in different tectonic settings. This example line 82-127, is for a shelf setting.

LBIBR- Lower Base Intra Biafra Rubble.

LIBU- Lower Intra Biafra Unconformity.

BIBR- Base Intra Biafra Rubble.

TIBU- Top Intra Biafra Unconformity.

BIBBEN- Base Intra Biafra Benin sands.

BRB- Base Rubble Beds

BQI- Base Qua Iboe.

TIQI- Top Intra Qua Iboe

QUA3 etc- Intra Qua Iboe horizon 3 etc

Pu- Pleistocene Unconformity

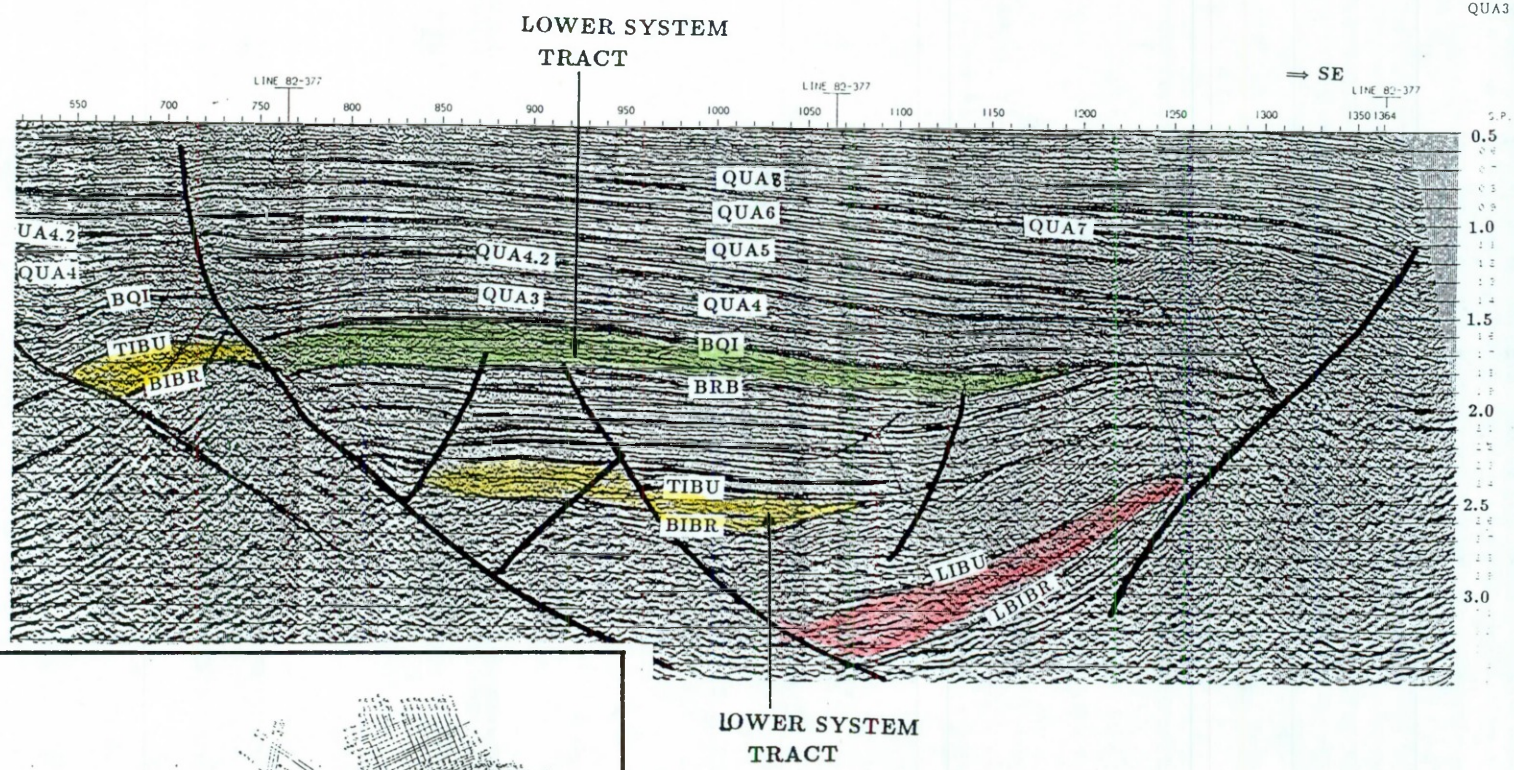

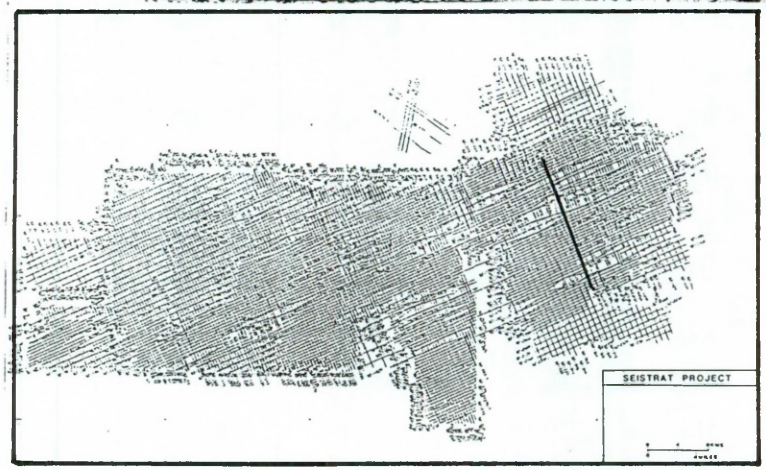

Fig.4.13c The Lower System tract in a growth fault setting. Seismic example comes from line 82-377.

LBIBR- Lower Base Intra Biafra Rubble.

LIBU- Lower Intra Biafra Unconformity.

BIBR- Base Intra Biafra Rubble.

TIBU- Top Intra Biafra Unconformity.

BIBBEN- Base Intra Biafra Benin sands.

BRB- Base Rubble Beds

BQI- Base Qua Iboe.

TIQI- Top Intra Qua Iboe

QUA3 etc- Intra Qua Iboe horizon 3 etc

Pu- Pleistocene Unconformity

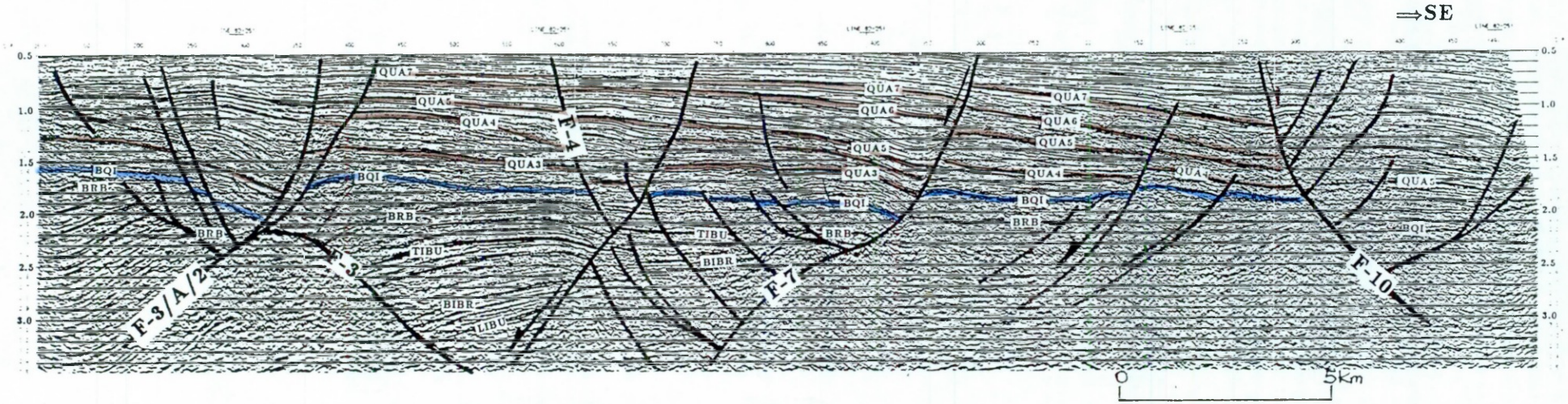

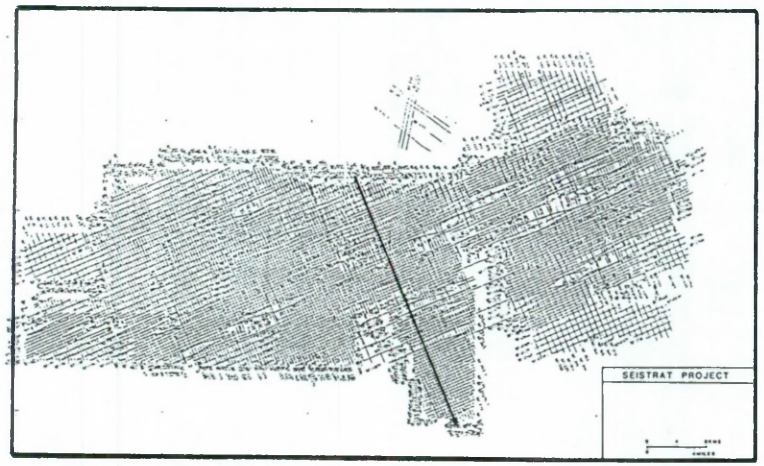

Fig.4.13d Line 82-251 shows the progradational sets mapped within the Qua Iboe and their relationship to Lowstand wedges. The lowstand wedge corresponds to the Lower Qua Iboe between BQI and Qua3 which is the $TIQI_3$. Each prograding arm subsequently becomes a TIQI (see Fig.4.11a) as shown by Qua4 and Qua5 to the south.

LBIBR- Lower Base Intra Biafra Rubble.

LIBU- Lower Intra Biafra Unconformity.

BIBR- Base Intra Biafra Rubble.

TIBU- Top Intra Biafra Unconformity.

BIBBEN- Base Intra Biafra Benin sands.

BRB- Base Rubble Beds

BQI- Base Qua Iboe.

TIQI- Top Intra Qua Iboe

QUA3 etc- Intra Qua Iboe horizon 3 etc

Pu- Pleistocene Unconformity

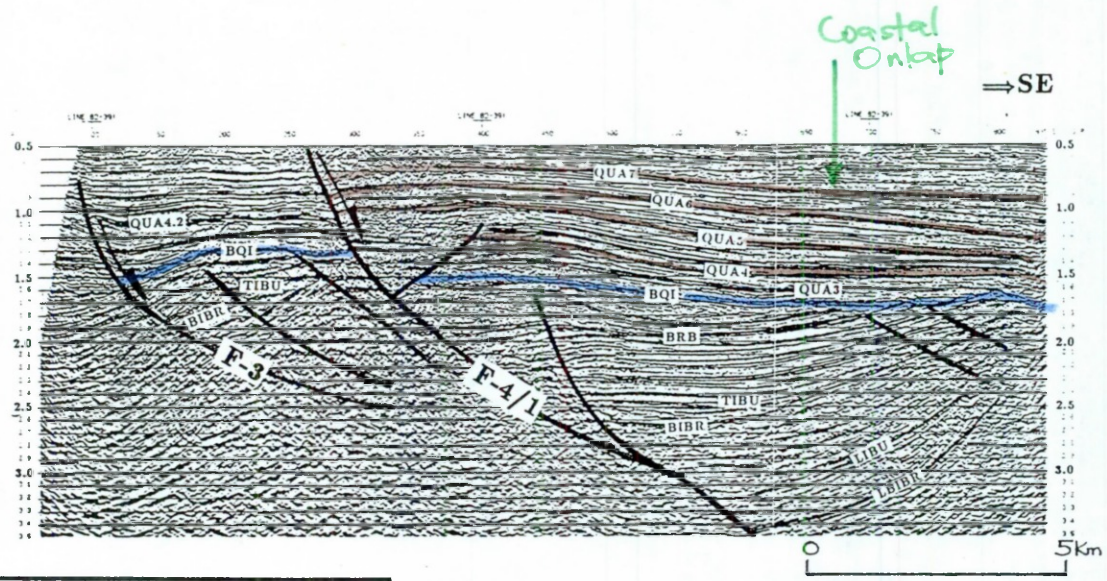

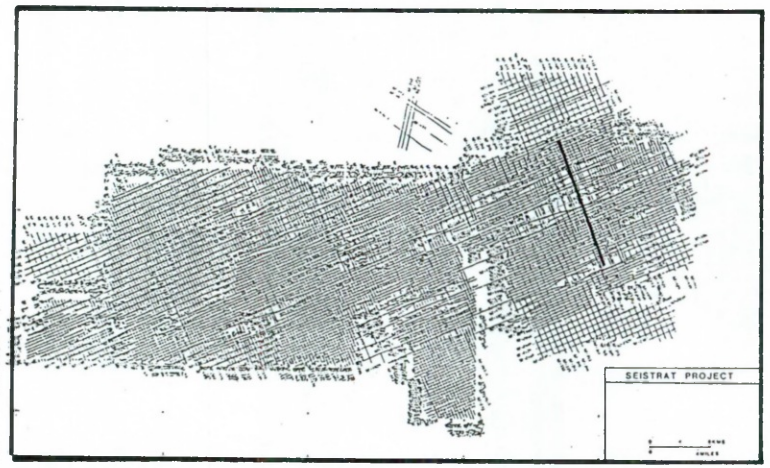

Fig.4.13e Line 82-391 illustrates the aggradational sets mapped(see Fig.4.1a) which is typical of the Qua Iboe to the east. From Qua4 to Qua7, a rising sea level is confirmed by the landward migration of high amplitude anomalies in the updip portions of the sequences. Qua7 defines the base of coastal onlap migrating downward due to falling sea level.

CHAPTER FIVE

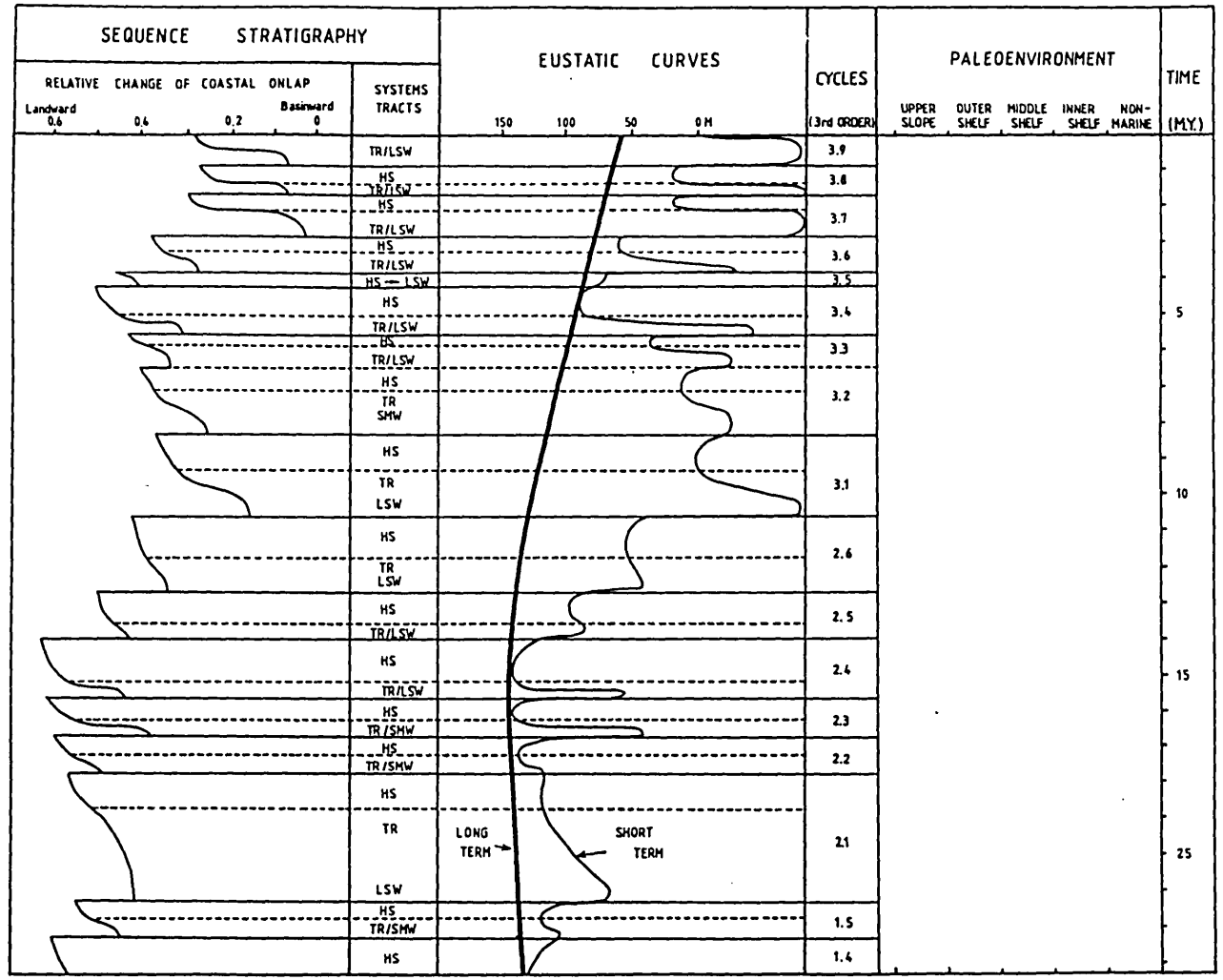

Fig.5.1a The relative change of coastal onlap and eustatic sea level curve from Haq *et al.*(1987).

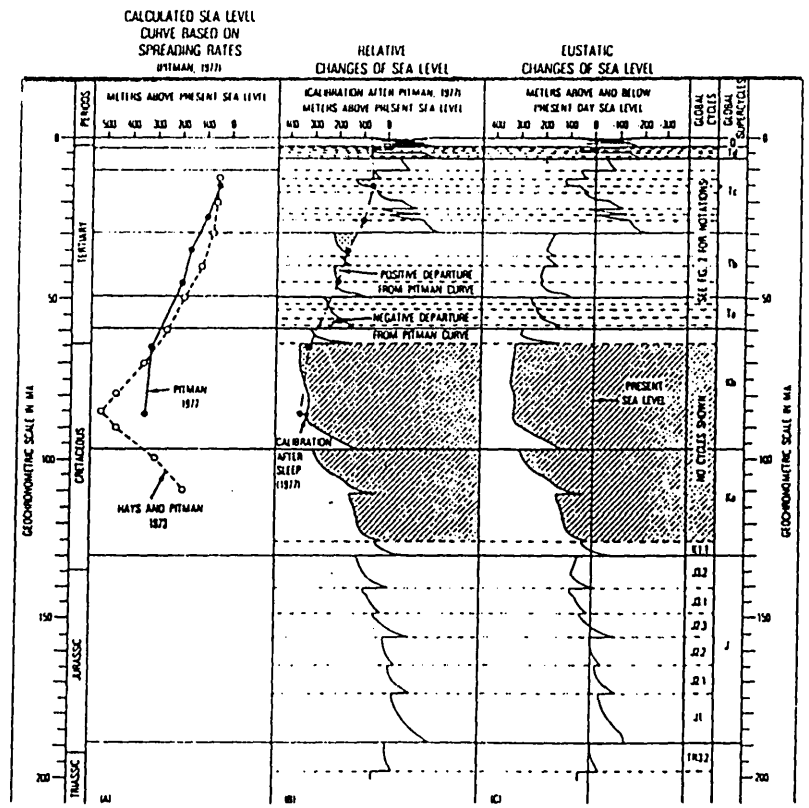

Fig.5.1b The 1977 reference curves from Vail *et al.*(1977).

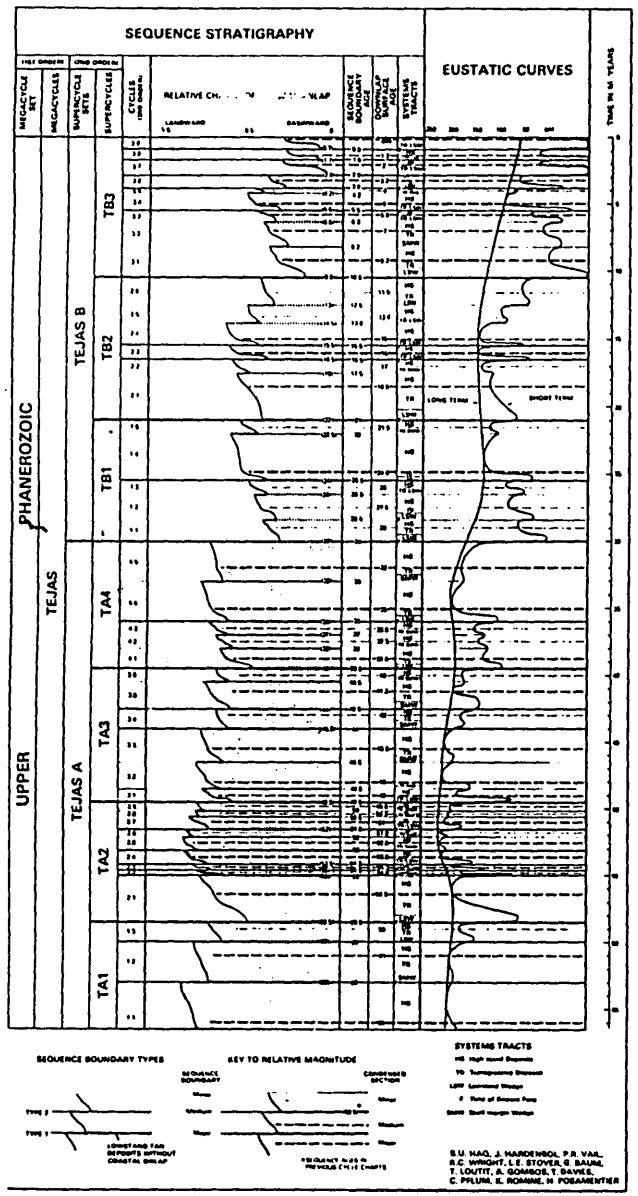

1987

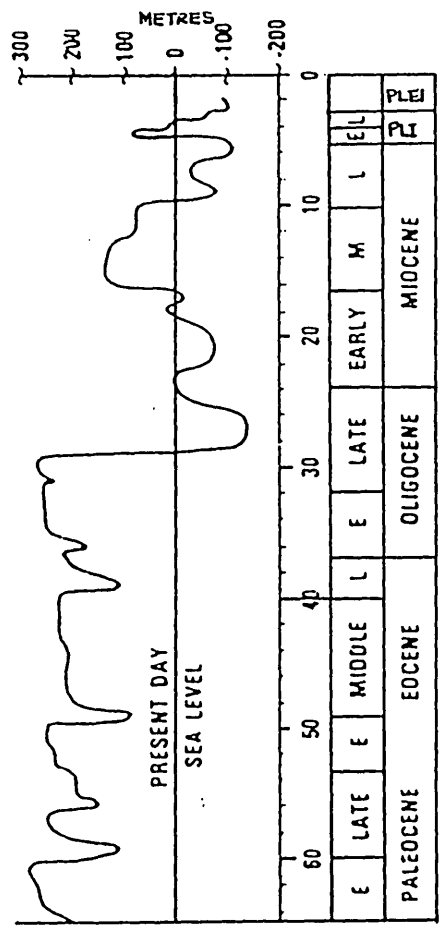

1979

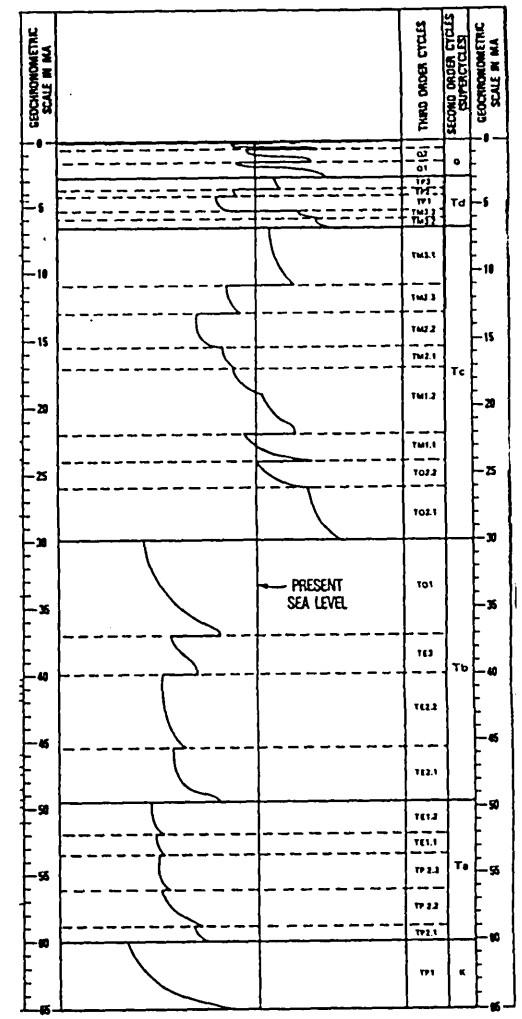

1977

Fig.5.2a,b,c Metamorphosis of the eustatic sea level curve estimates from 1977 to 1987. Comparisons drawn between these curves are discussed in the text.

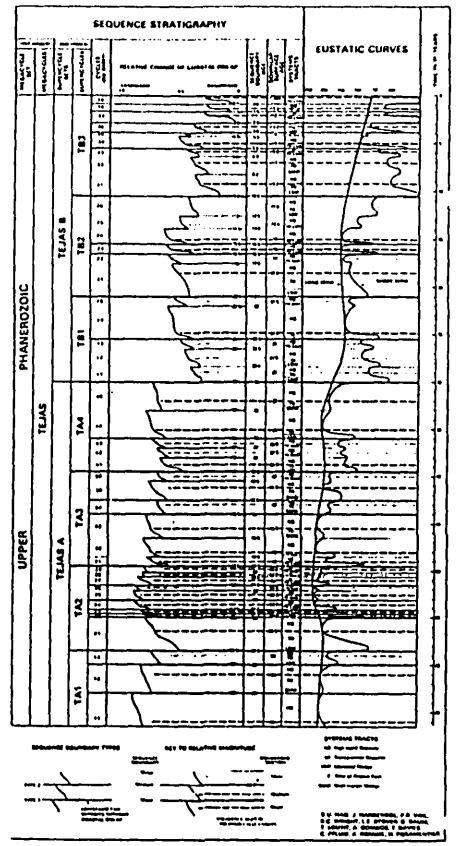

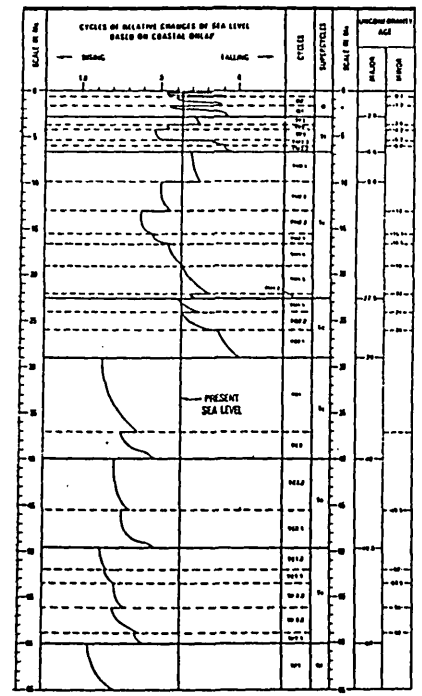

Fig.5.3a,b Correlation between the relative change of coastal onlap curve from Haq *et al.*(1987) and cycles of relative changes in sea level based on coastal onlap from Vail *et al*(1977).

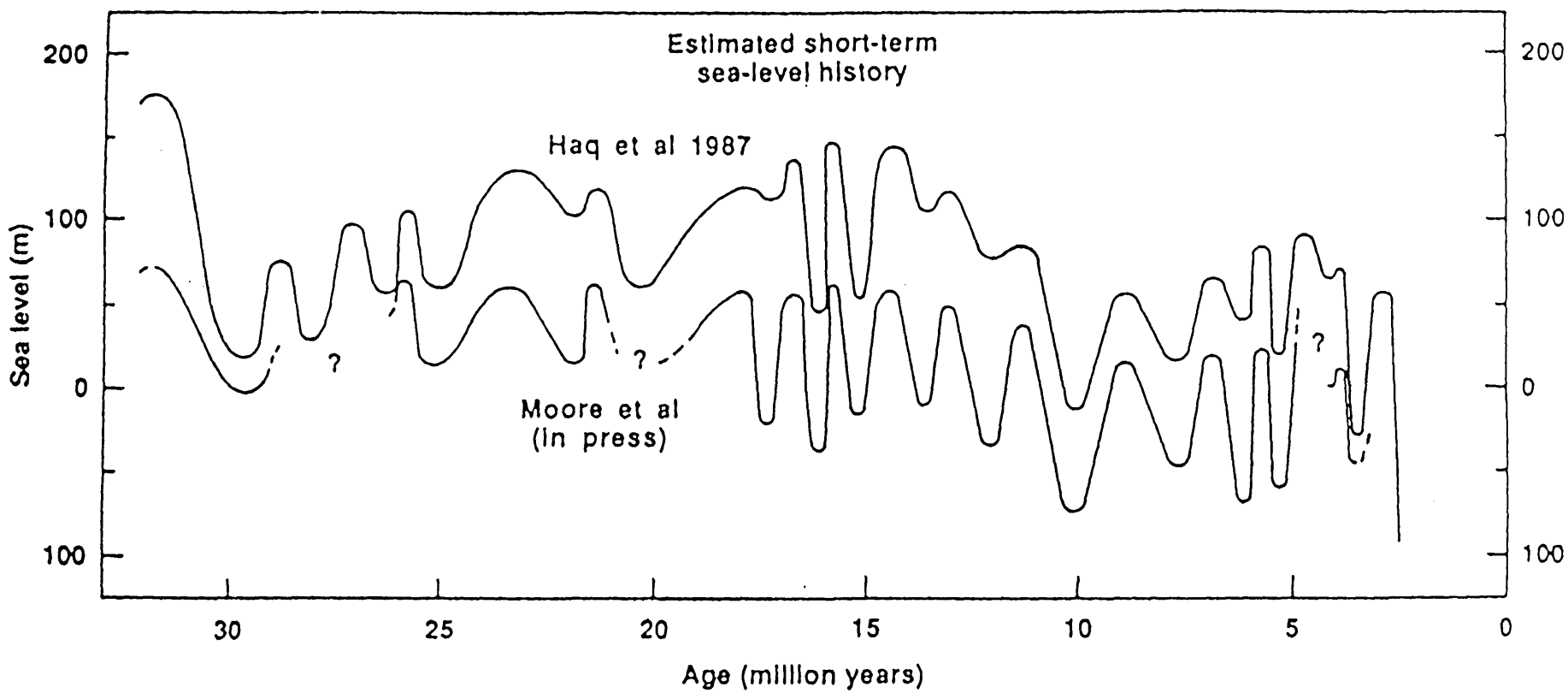

Fig.5.4 Correlation of the Moore *et al.* and Haq *et al.* curves.

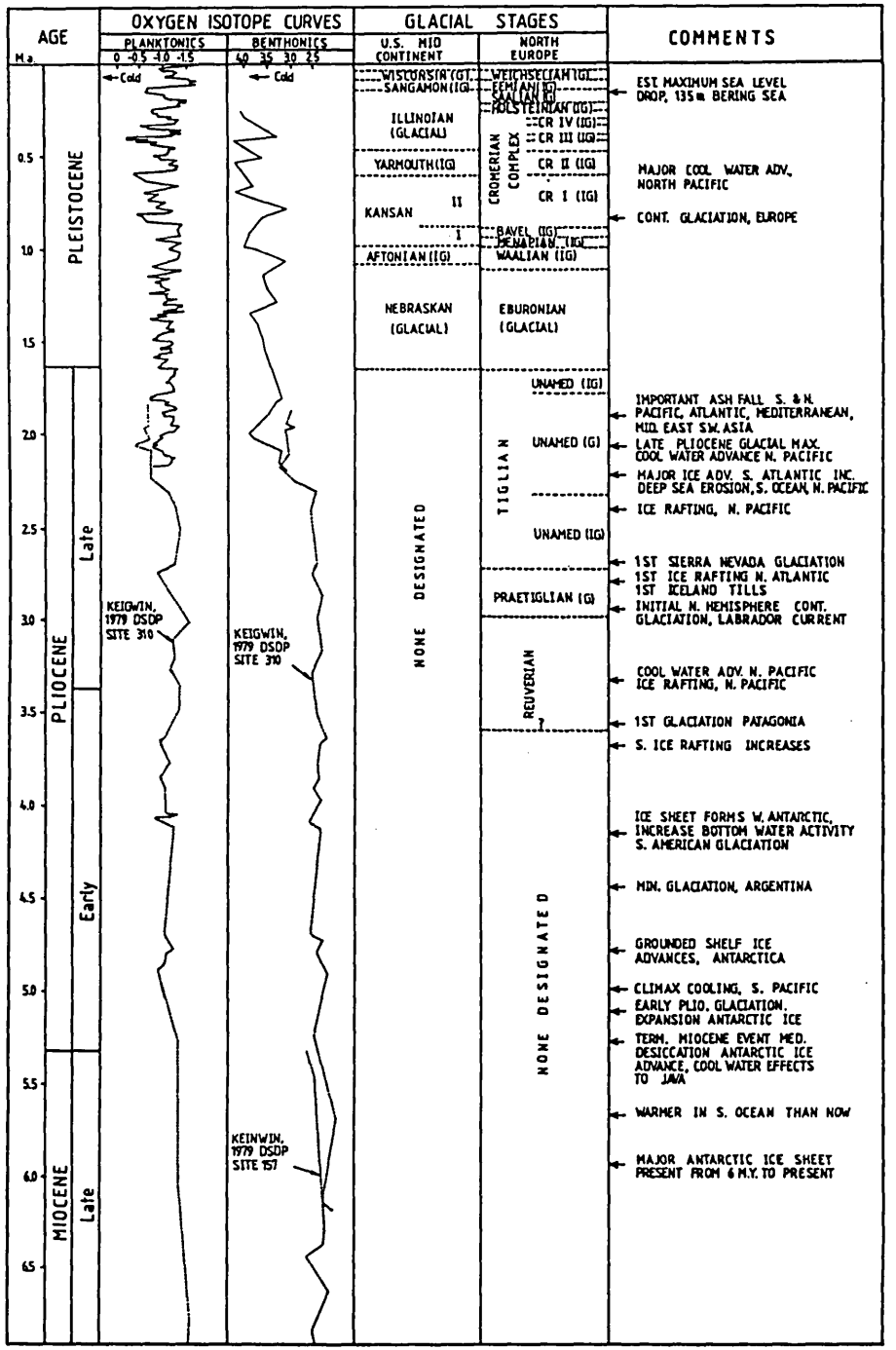

Fig.5.5 Late Neogene Oxygen-18 curves(compiled from various authors).

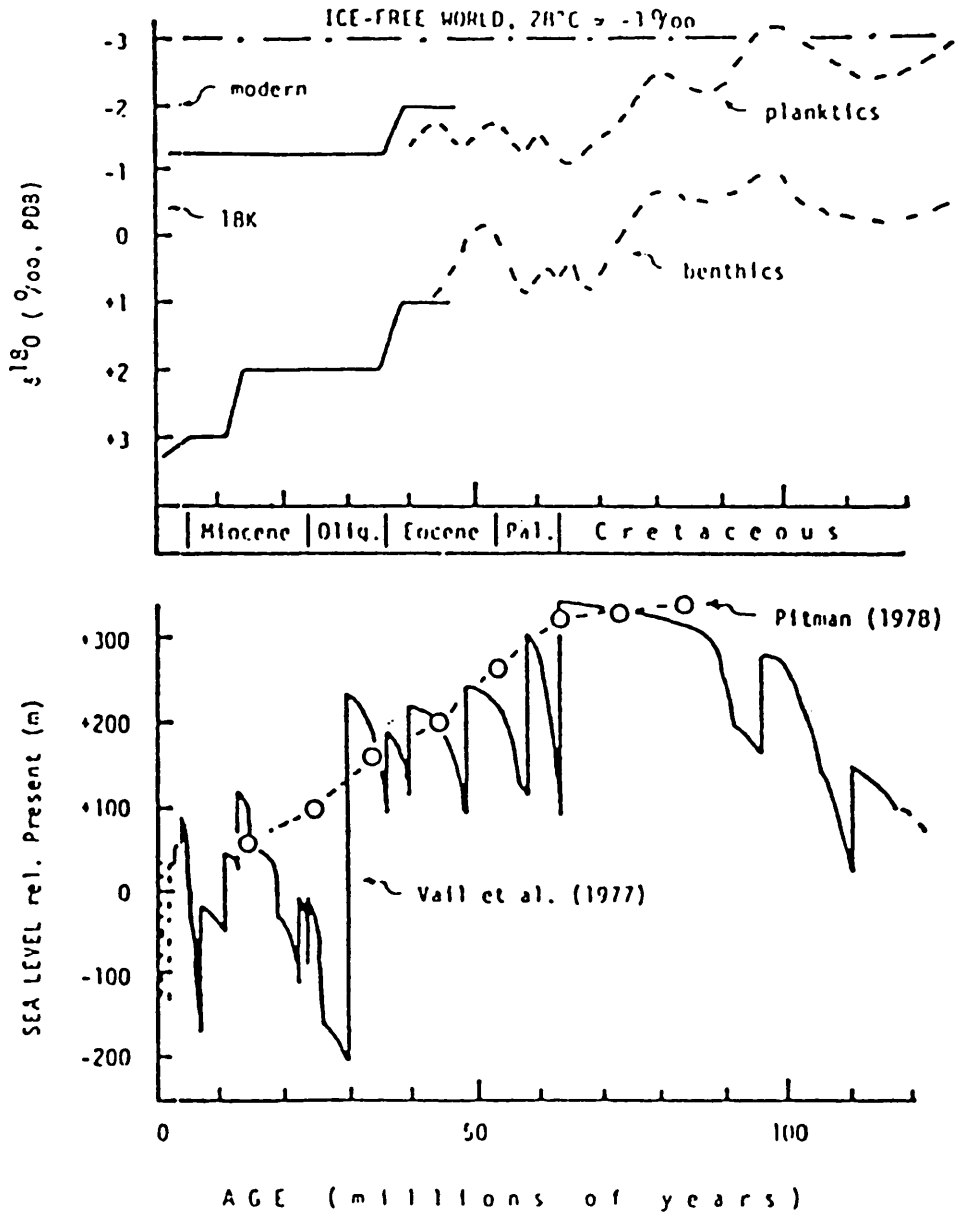

Comparison of the 100-m.y. oxygen-18 record to the seismic stratigraphy "relative sea level curve". ADAPTED FROM MATTTHEWS(1984).

Fig.5.6a Comparison of Vail's curve to the Oxygen-18 curve.

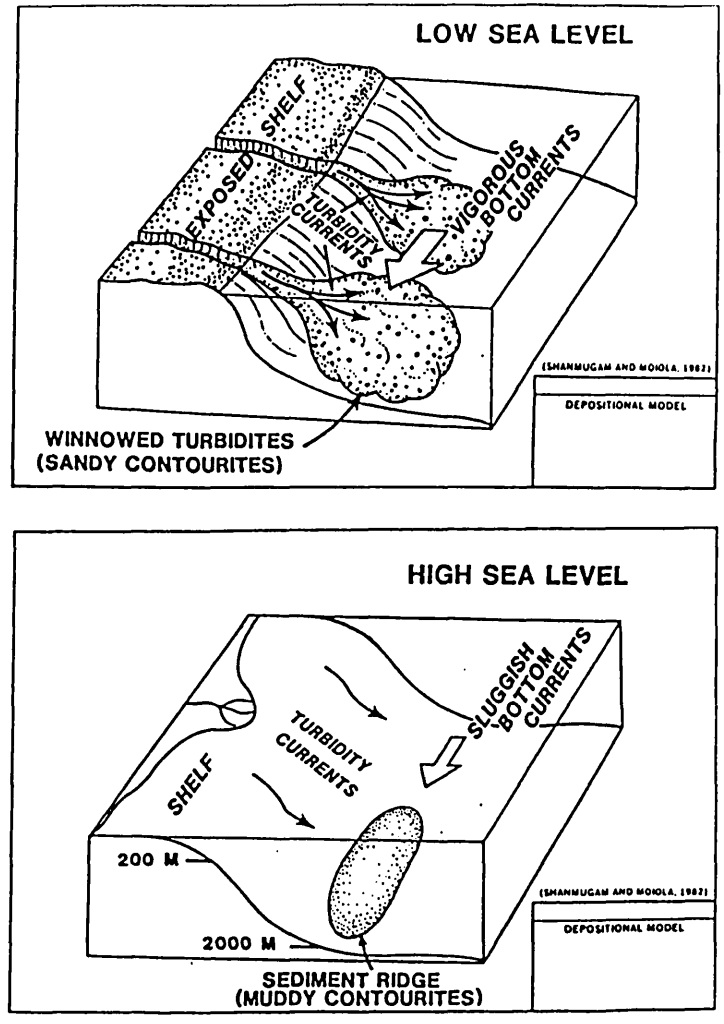

Fig.5.6b Model of deep sea turbidite deposition during changes in eustatic sea level (after Shanmugam and Moiola, 1982).

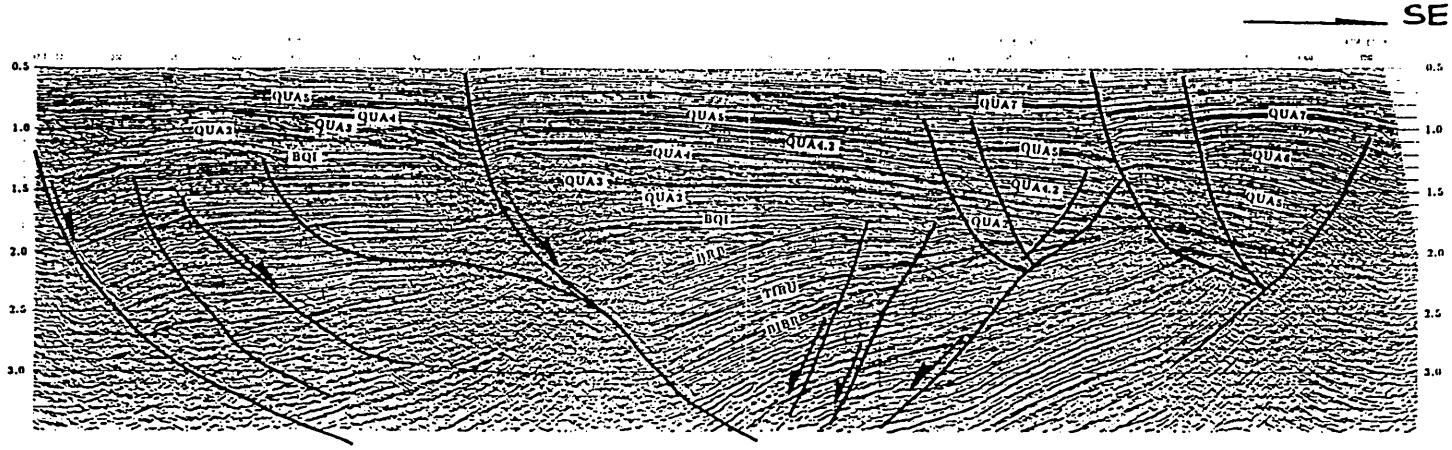

Fig.5.7a,b Chronostratigraphic chart line 82-197. The Older Biafra sequences occur north of the palaeobasin. Both the UIBR and the LIBR occur within the palaeobasin, the latter as a result of the shale uplift of Older Biafra truncated at the BQI. (Compare with Fig.5.8a,b).

CHRONOSTRATIGRAPHIC CHART LINE 82-197

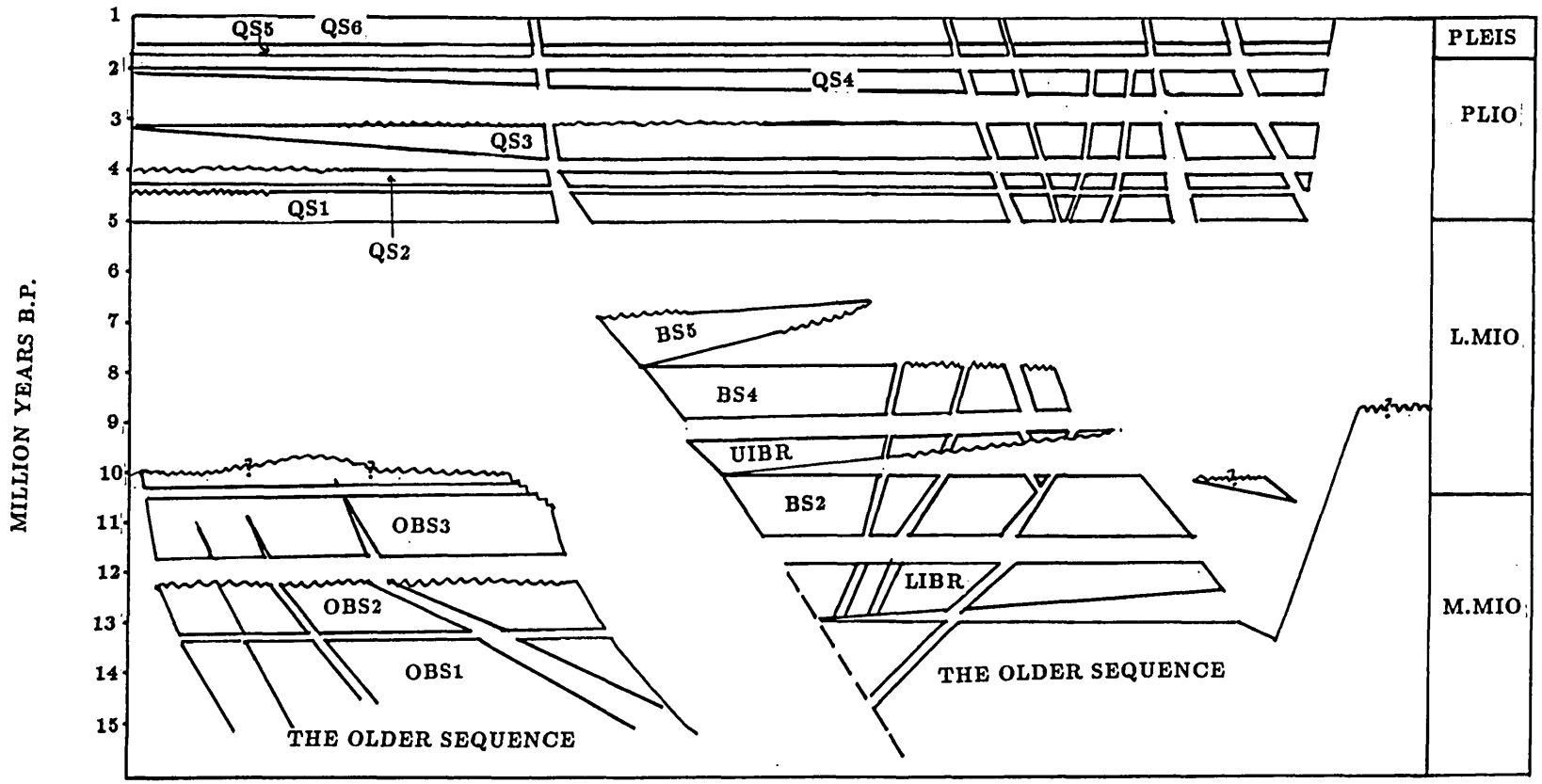

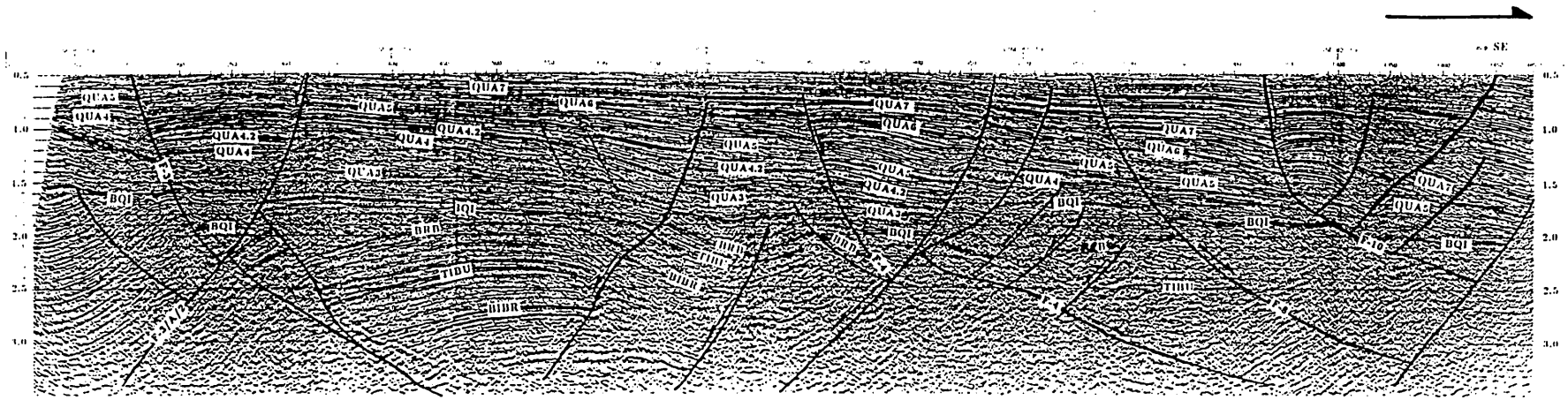

Fig.5.8a,b Chronostratigraphic chart line 82-259. The older Biafra sequences are poorly represented within the palaeobasin in the central area, largely due to shaling out of Biafra. The LIBR has not been identified along this profile.

CHRONOSTRATIGRAPHIC CHART LINE 82-259

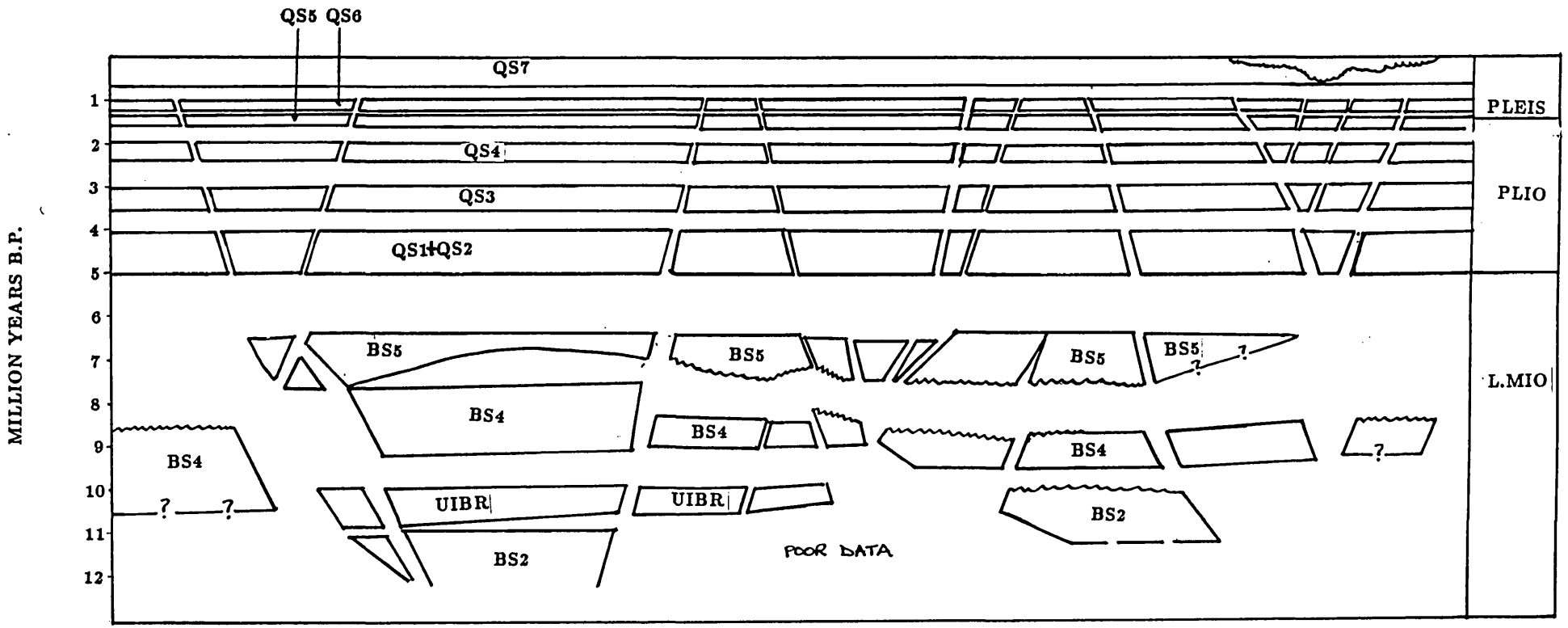

Fig.5.9a,b Chronostratigraphic chart line 82-373. The older sequences are evident to the north and south of this profile. The LIBR also appears to have been extensive. By inference, the proto-embayment was more extensive with the deposition of LIBR, but more restricted during UIBR and the Rubble Beds(BS5) deposition.

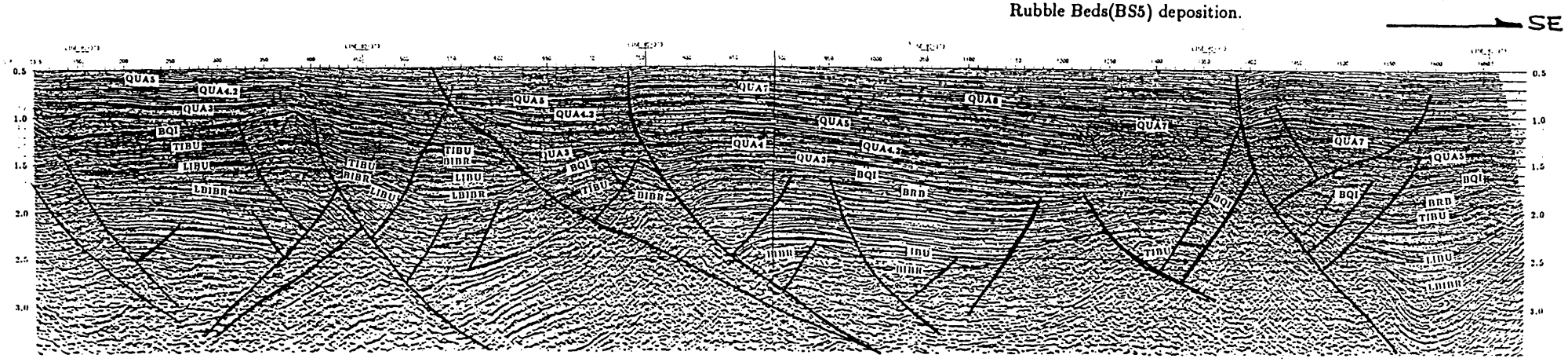

CHRONOSTRATIGRAPHIC CHART LINE 82-373

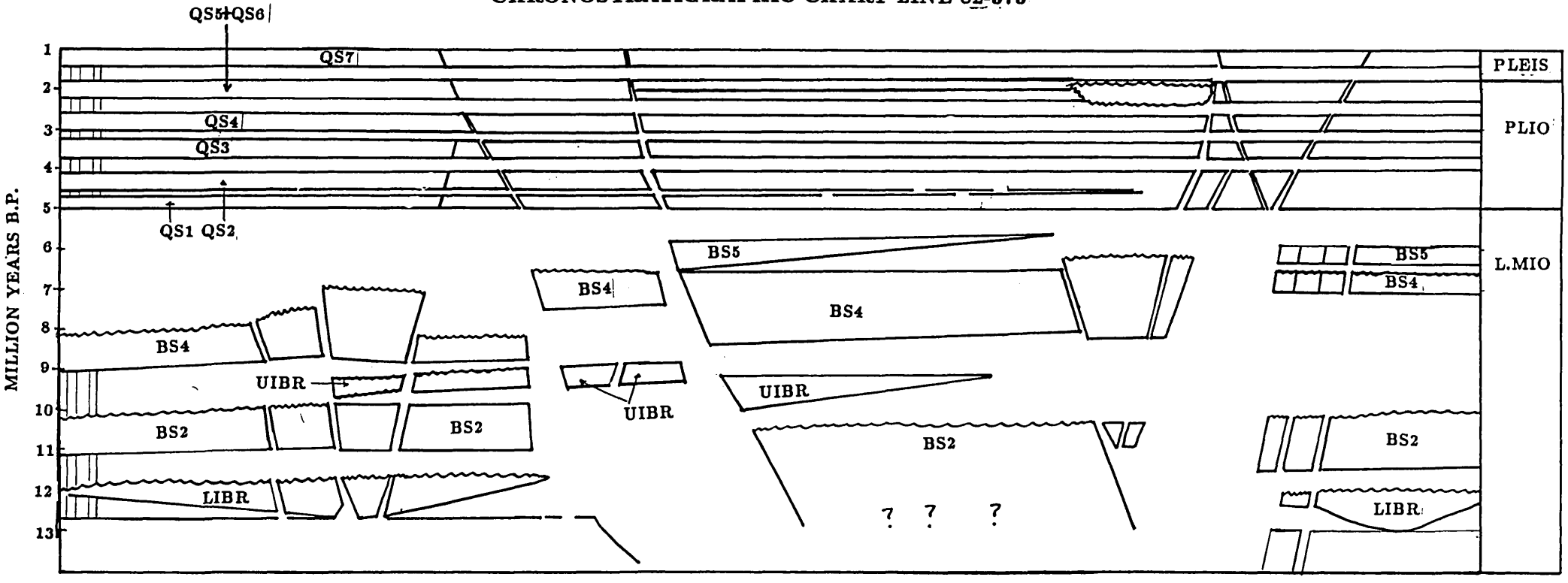

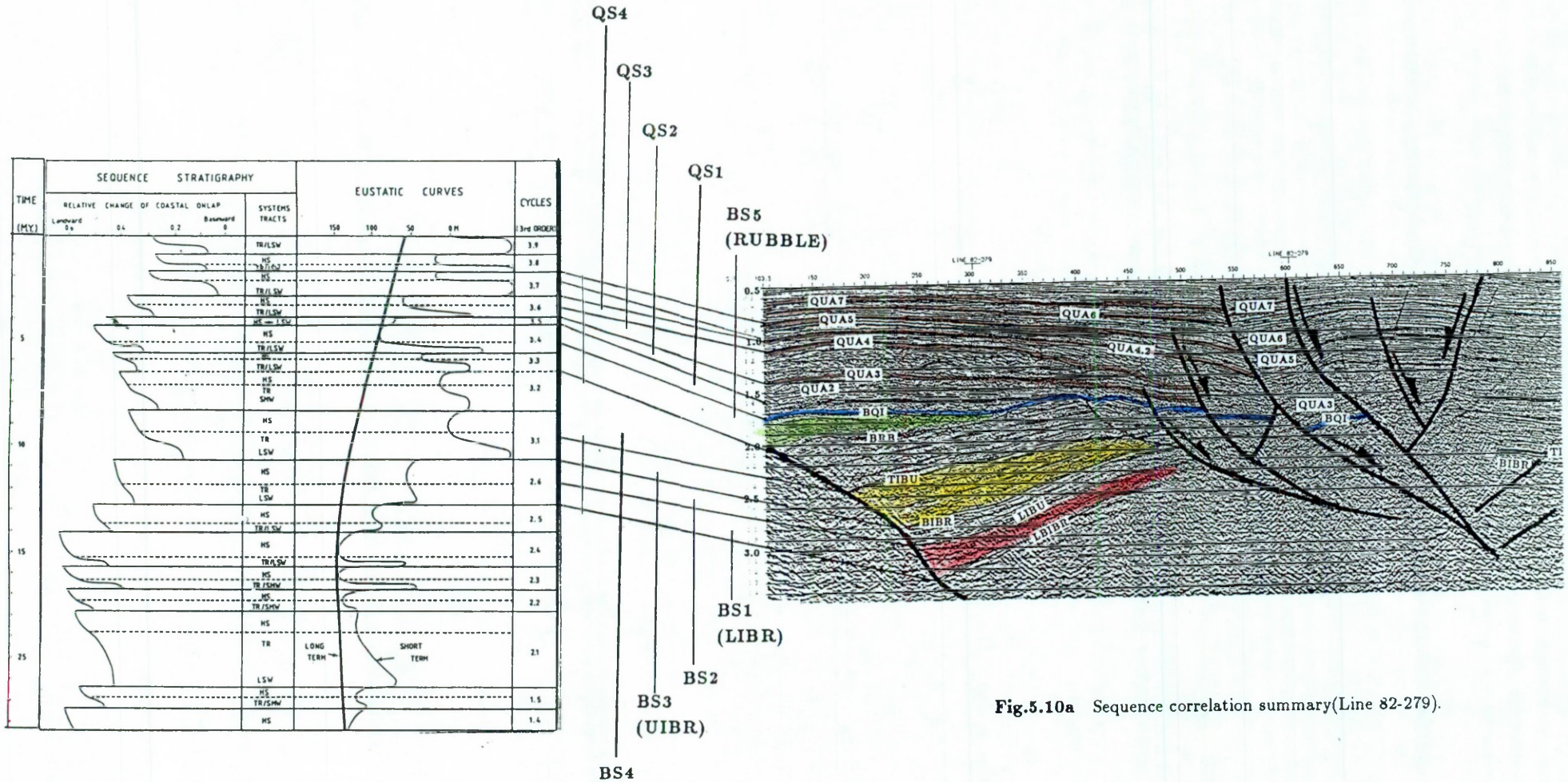

Fig.5.10a Sequence correlation summary(Line 82-279).

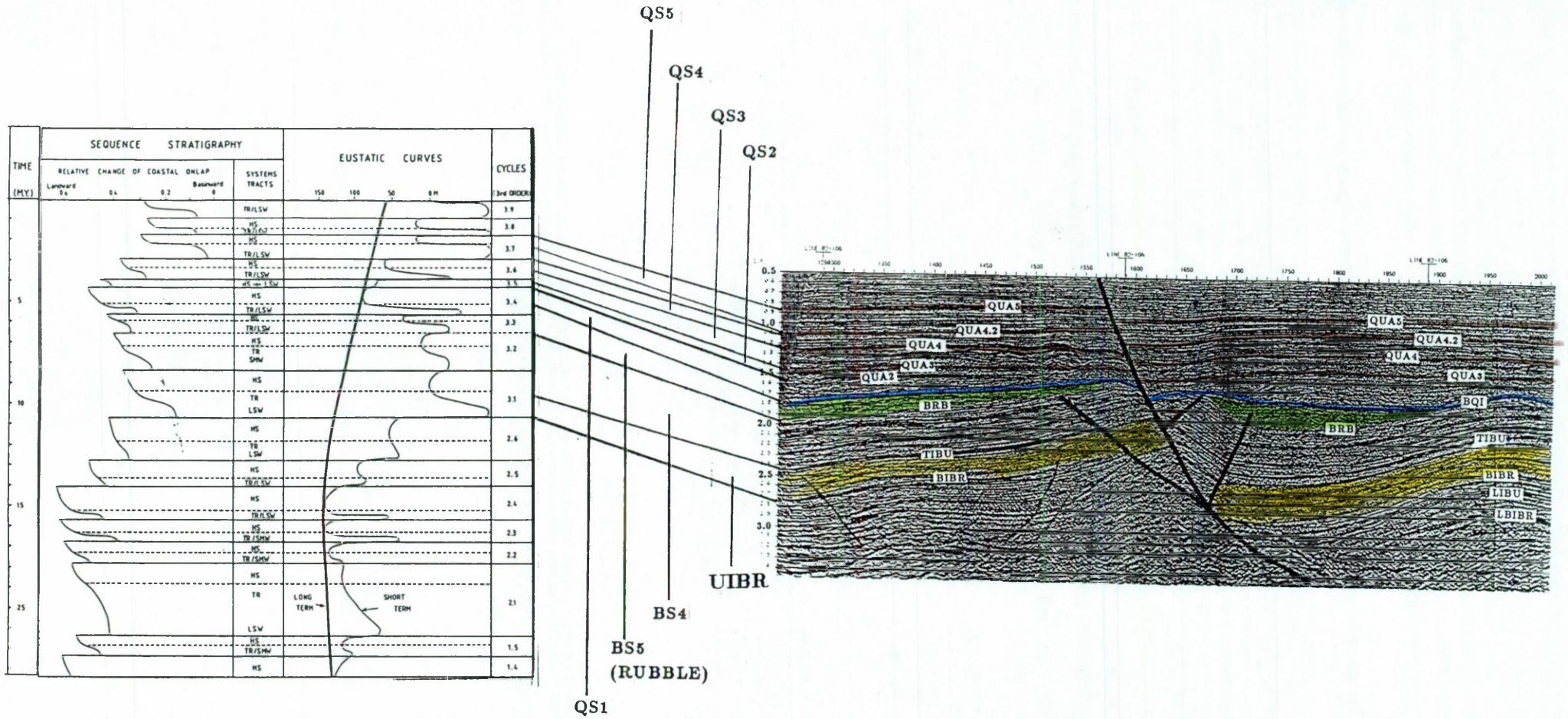

Fig.5.10b Sequence correlation summary(Line 82-106).

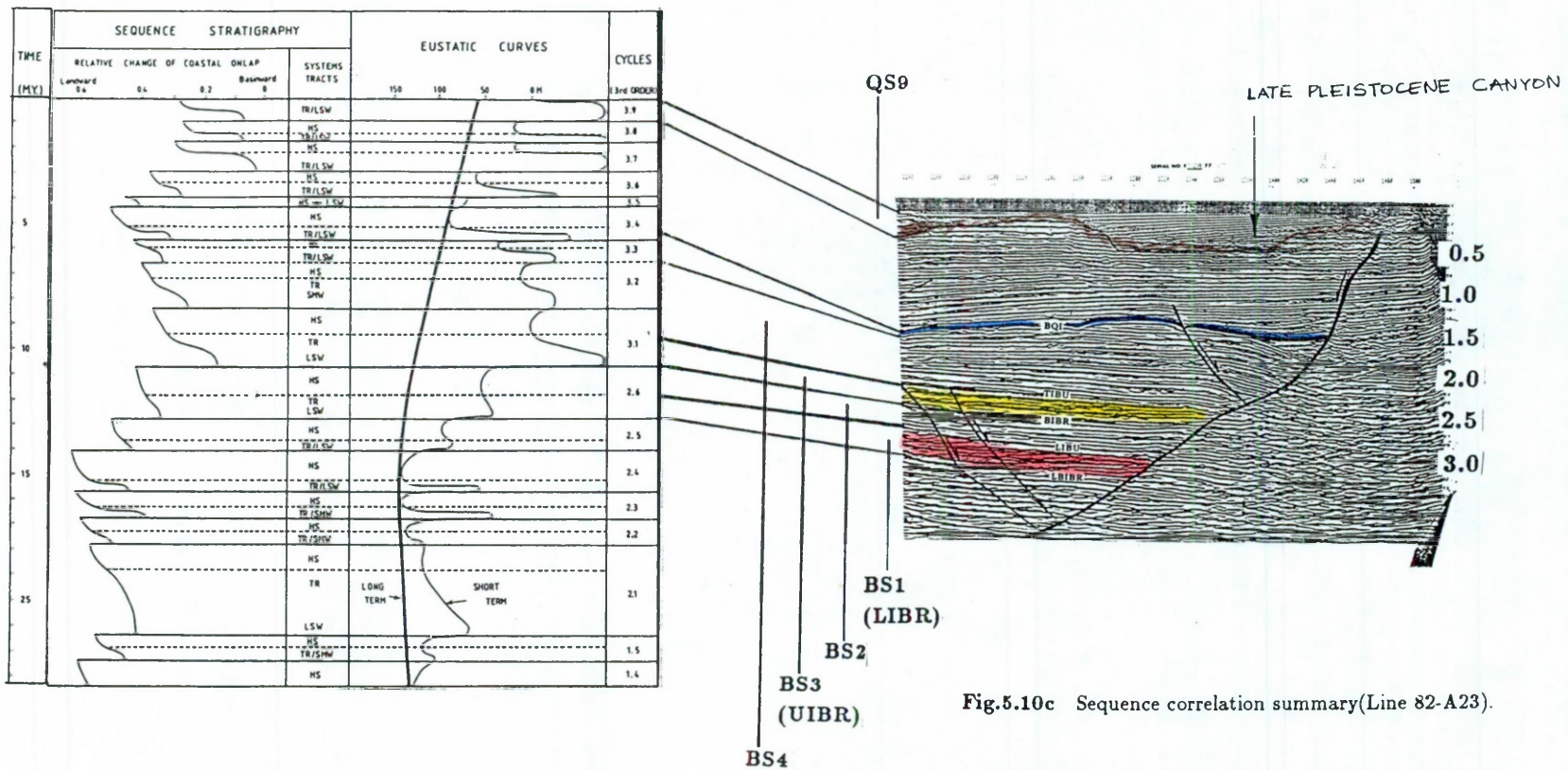

Fig.5.10c Sequence correlation summary(Line 82-A23).

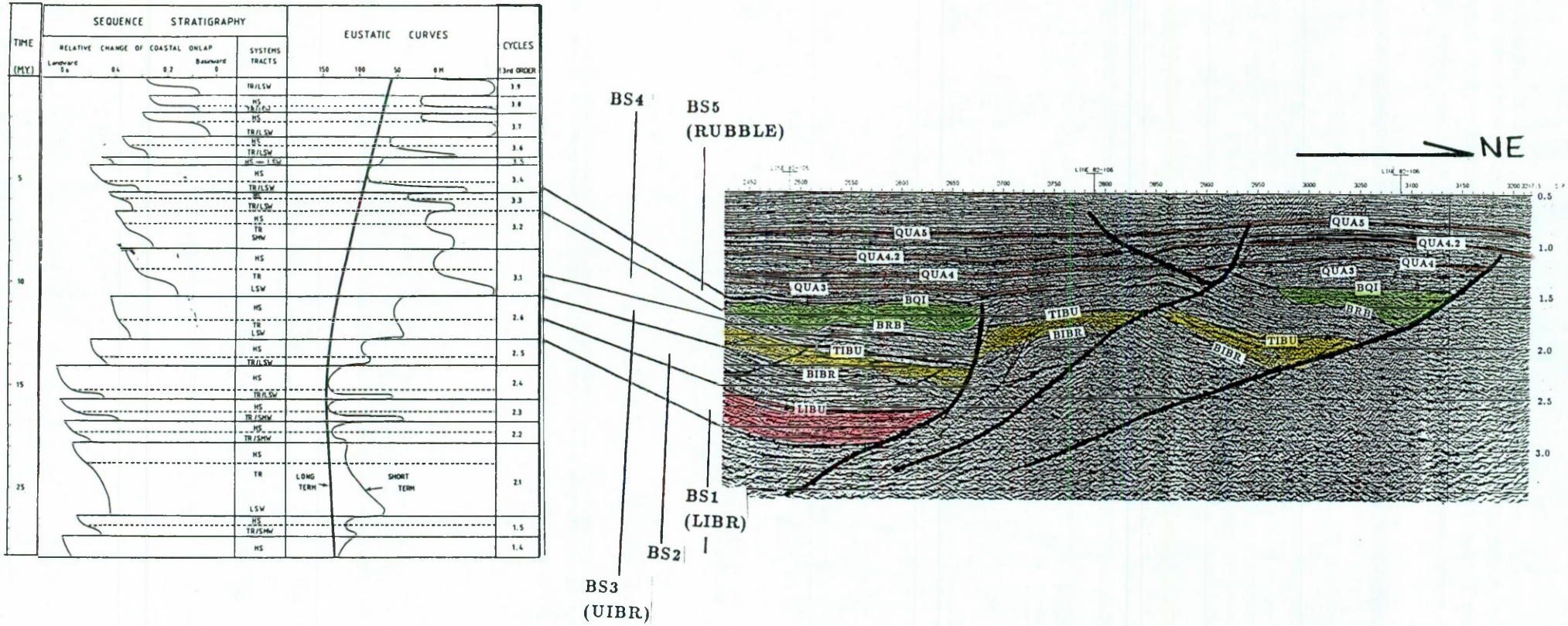

Fig.5.10d Sequence correlation summary(Line 82-106).

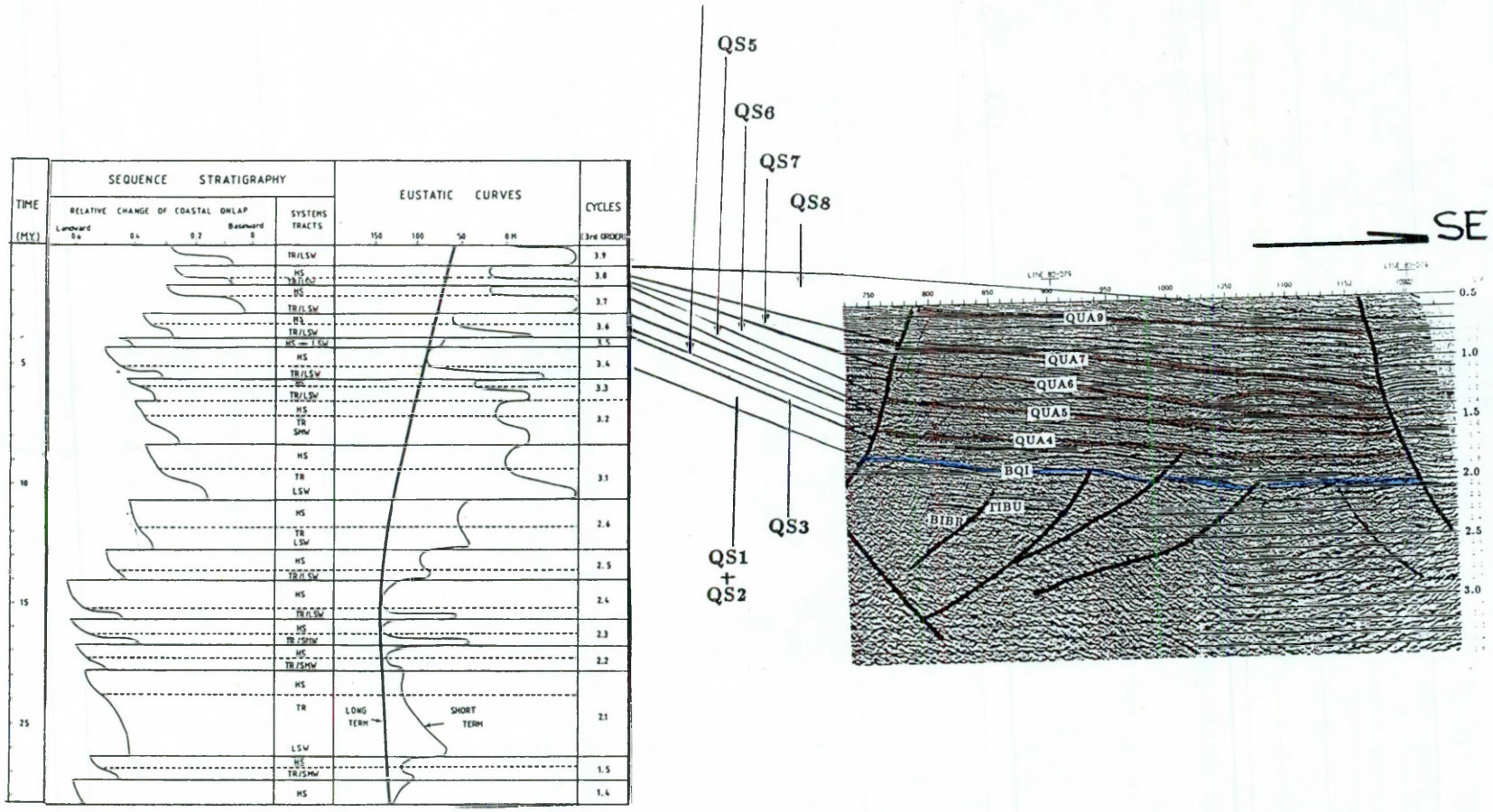

Fig.5.10e Sequence correlation summary(Line 82-279).

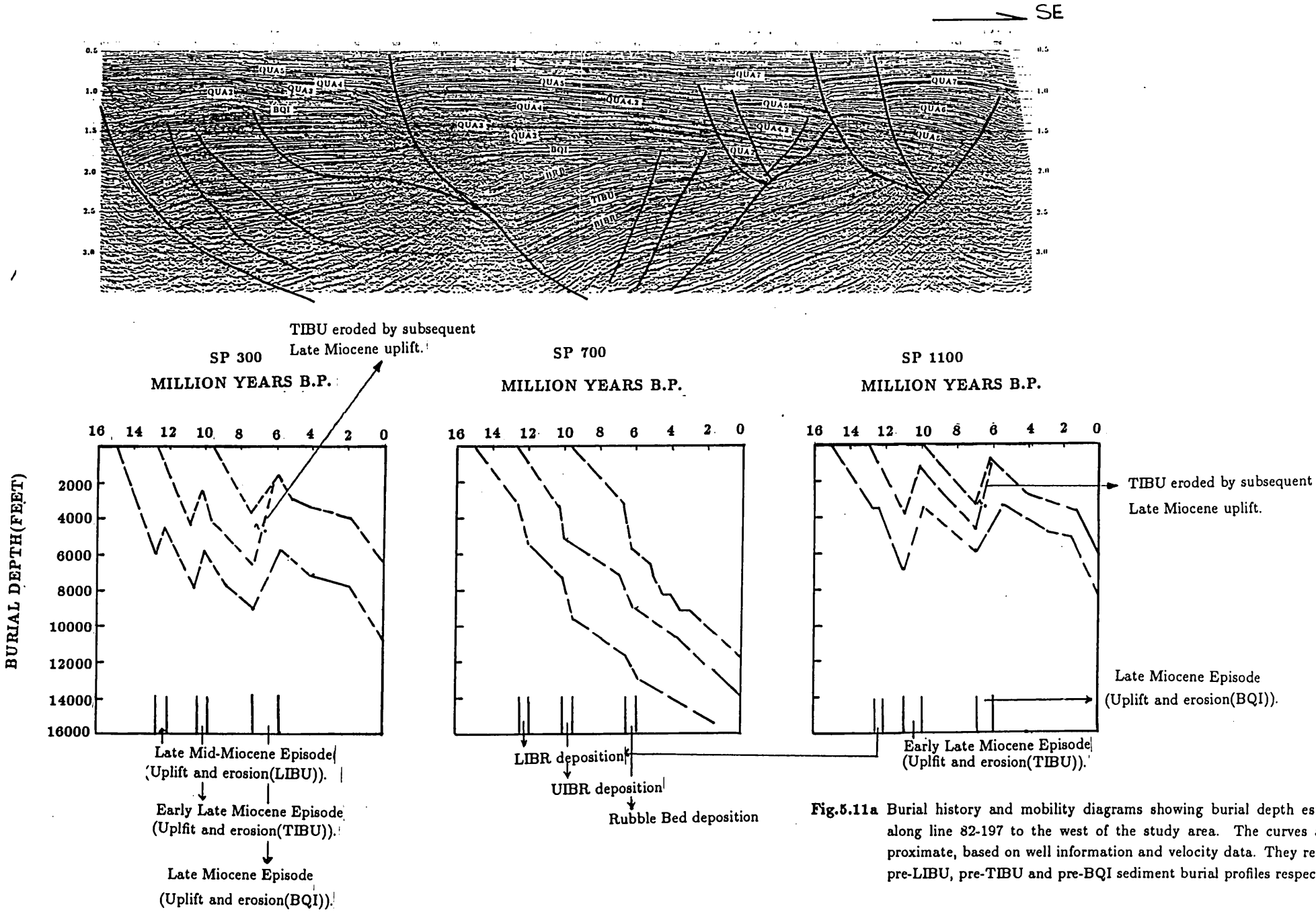

Fig.5.11a Burial history and mobility diagrams showing burial depth estimates along line 82-197 to the west of the study area. The curves are approximate, based on well information and velocity data. They represent pre-LIBU, pre-TIBU and pre-BQI sediment burial profiles respectively.

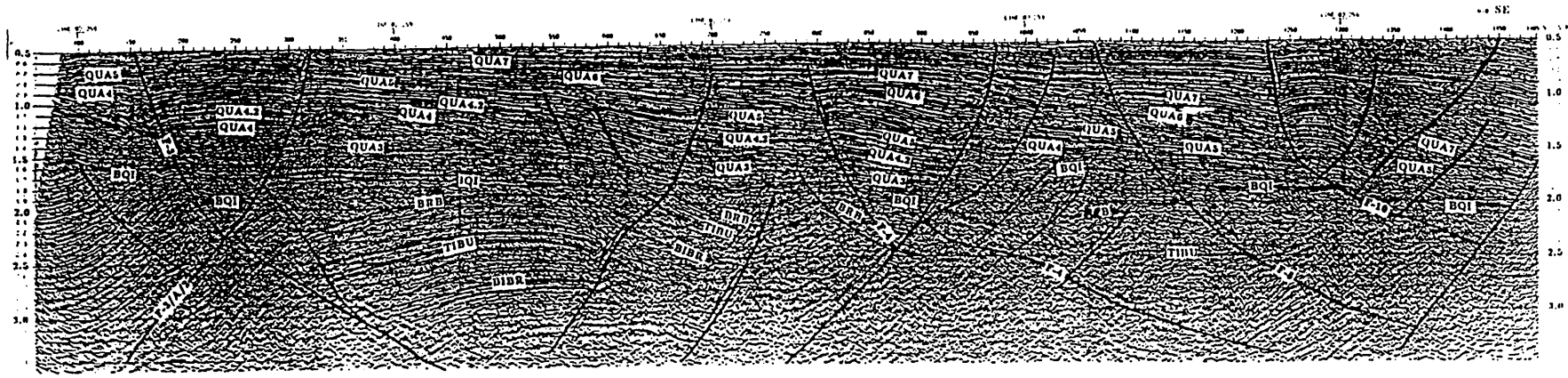

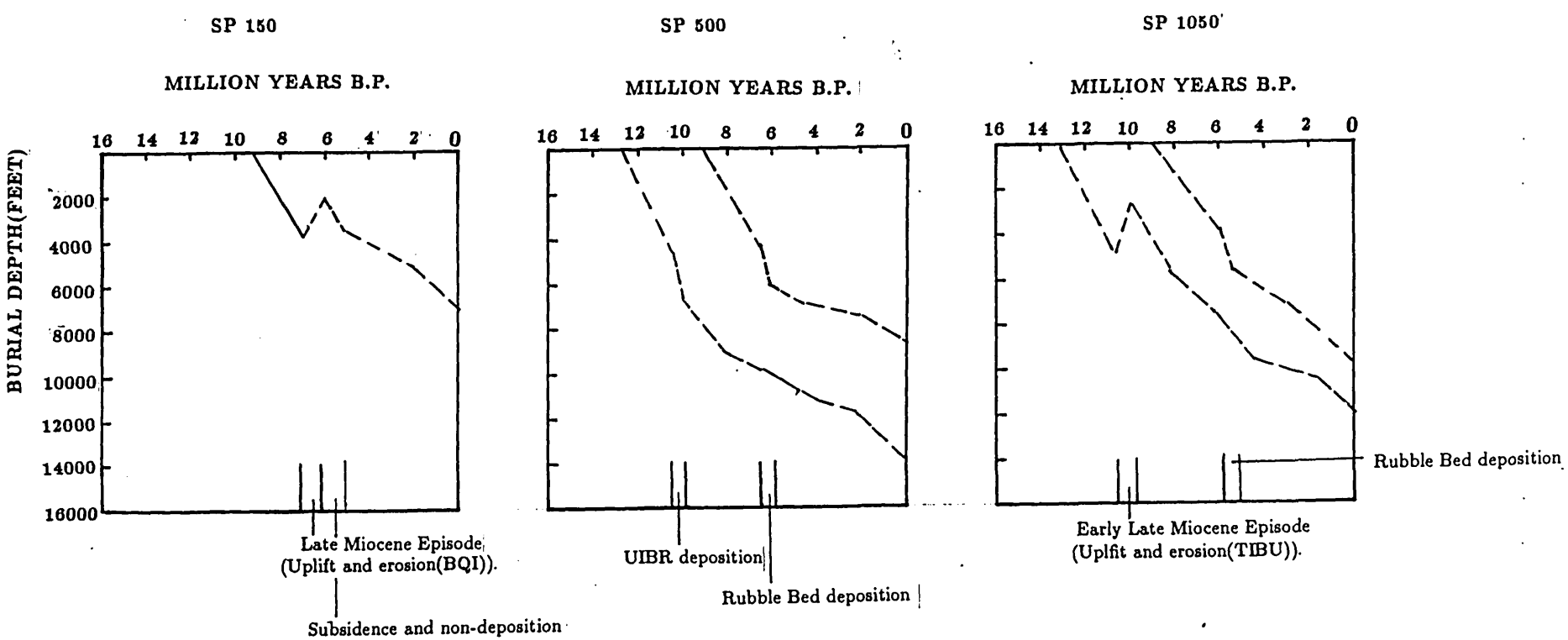

Fig.5.11b Burial history diagrams showing burial depth estimates for specific shot points on line 82-259 in the central part of the study area. The major episodes of tectonism are as indicated.

Fig.5.11c Burial history diagrams showing burial depth estimates along line 82-373 in the eastern part of the study area.

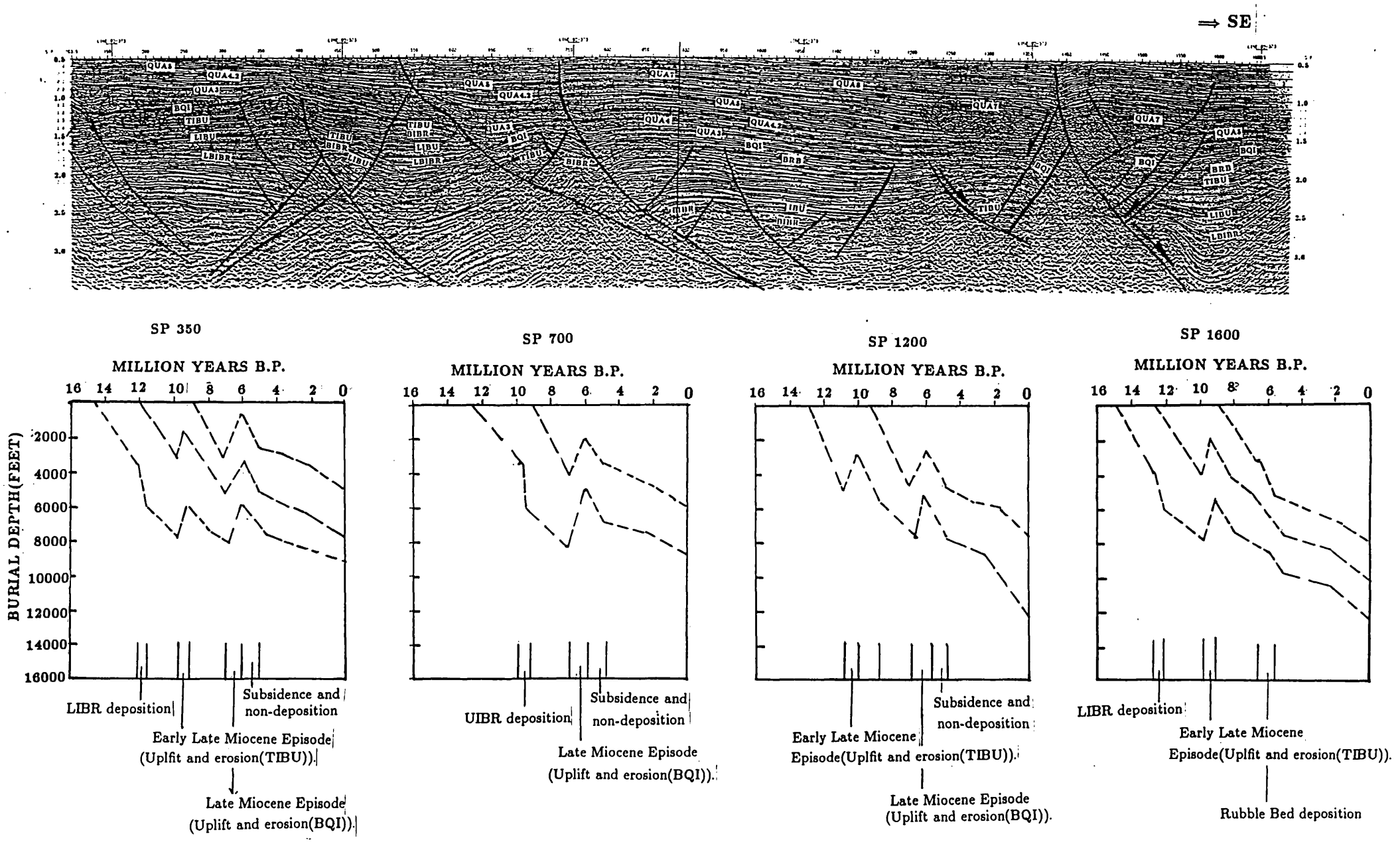

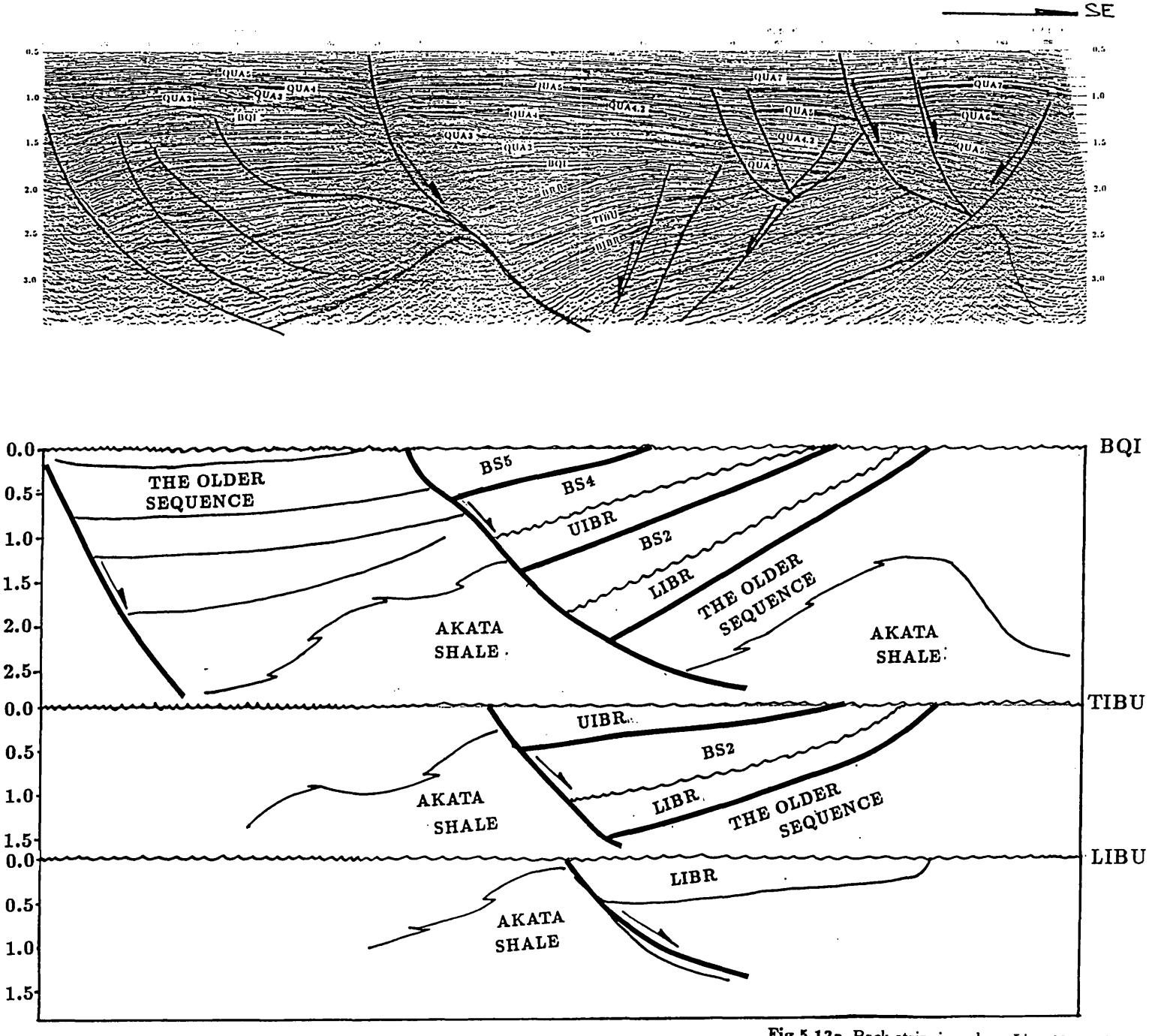

Fig.5.12a Back-stripping along Line 82-197 in TWT slices from the LIBU, TIBU, and BQI. The two Intra Biafra Rubble (LIBR and UIBR) and the Rubble Beds (BS5) are shown as developed within the palaeobasin.

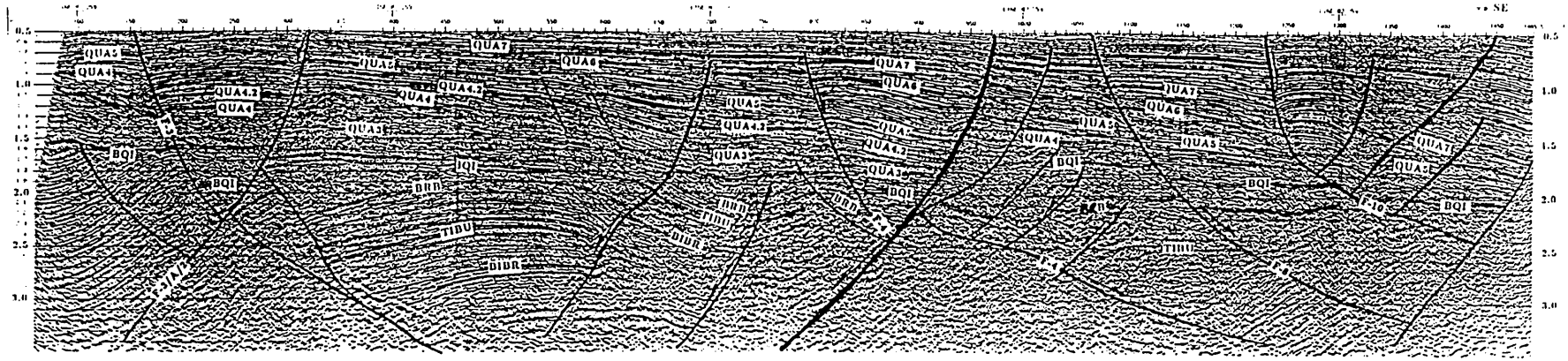

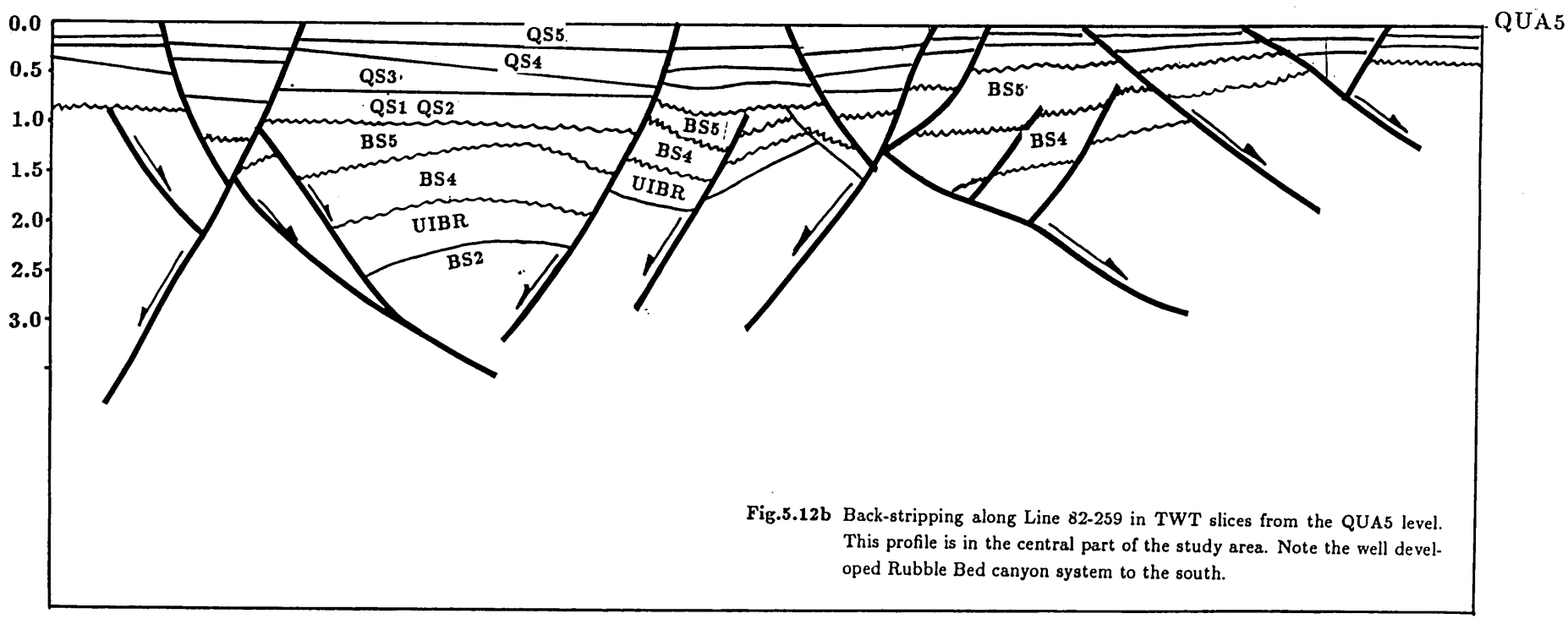

Fig.5.12b Back-stripping along Line 82-259 in TWT slices from the QUA5 level. This profile is in the central part of the study area. Note the well developed Rubble Bed canyon system to the south.

Fig.5.12c Back-stripping along line 82-373 in TWT slices from the LIBU and TIBU levels. Note the well developed Lower Intra Biafra Rubble (LIBR) onlap system to the north as well as within the palaeobasin.

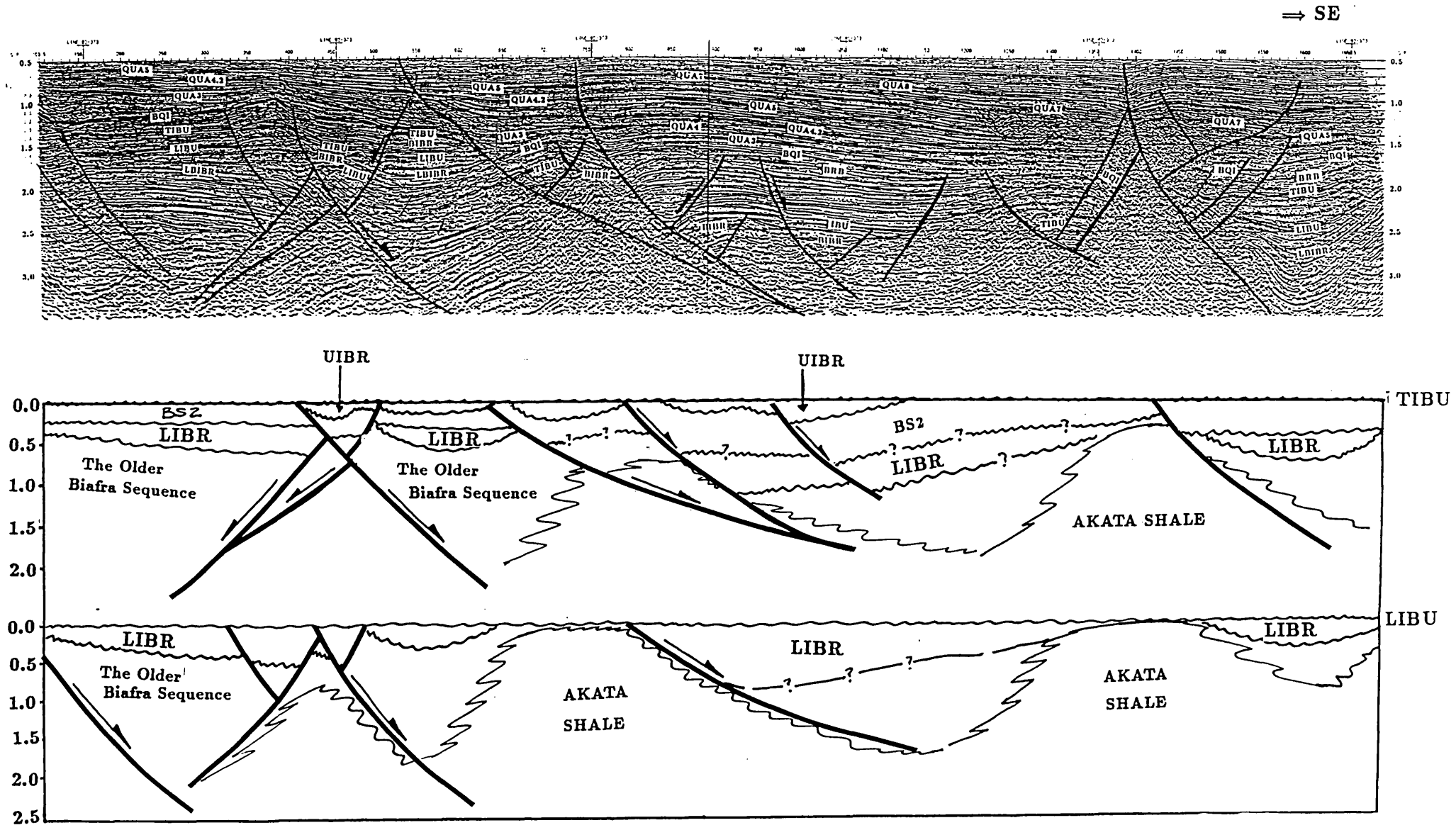

CHAPTER SIX

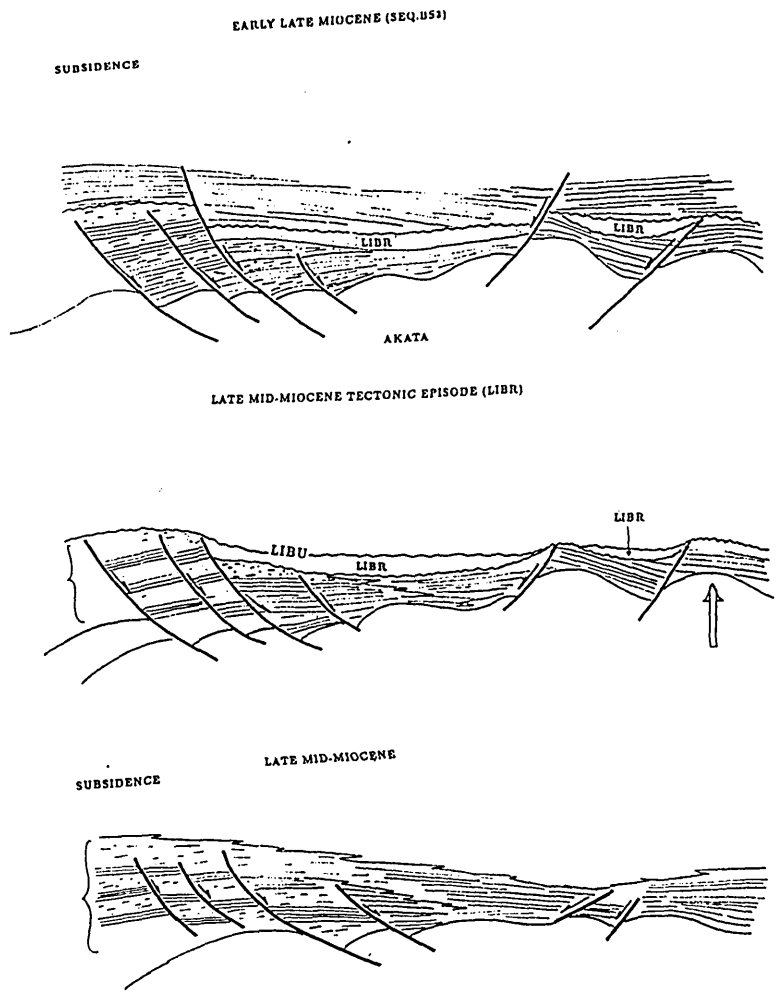

Fig.6.1a Biafra structural and stratigraphic evolution showing the development of sequences from Late Mid-Miocene to Early Late Miocene. The stages of structural deformation are as outlined in Chapter 3.

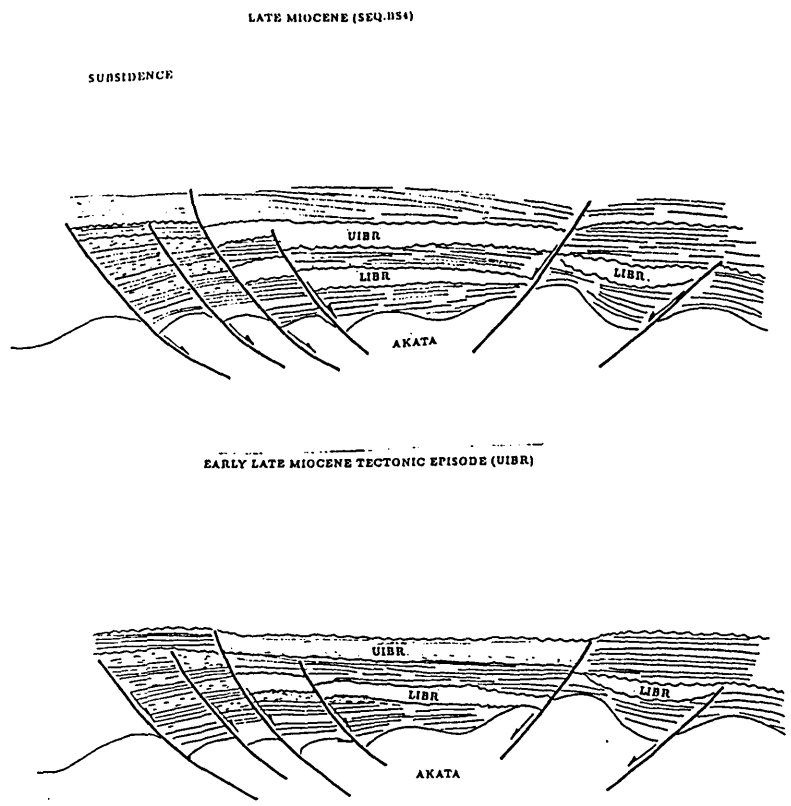

Fig.6.1b Biafra structural and stratigraphic evolution showing the of sequences UIBR and SEQ.BS4.

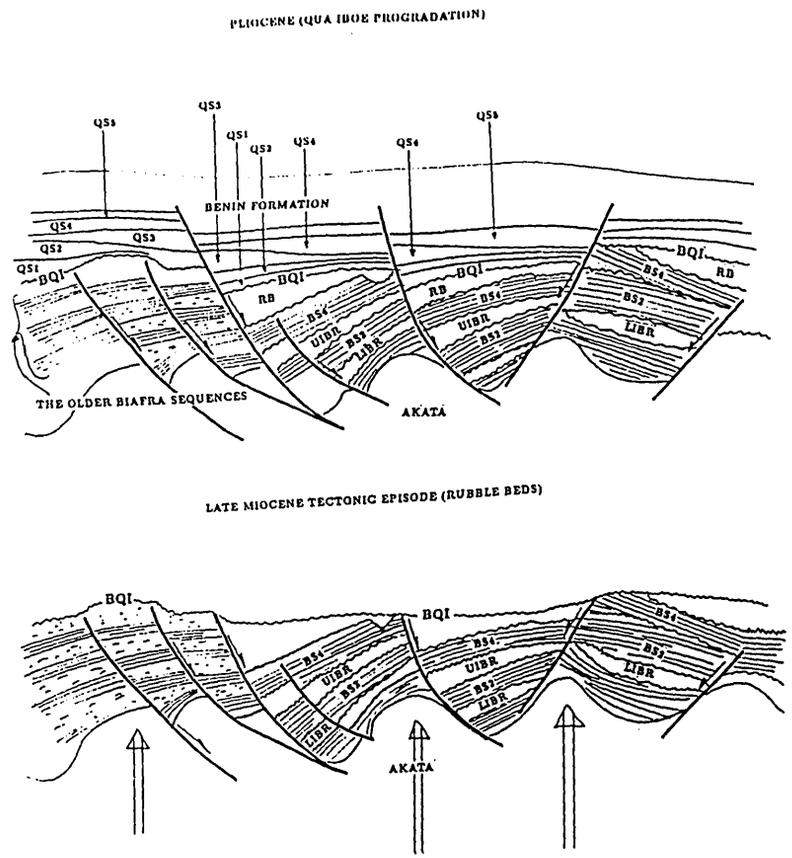

Fig.6.1c Biafra structural and stratigraphic evolution showing the formation of Rubble Beds (the Late Miocene tectonic episode) and Pliocene Progradation.

LDIBR- Lower Base Intra Biafra Rubble.

LIBU- Lower Intra Biafra Unconformity.

BIBR- Base Intra Biafra Rubble.

TIBU- Top Intra Biafra Unconformity.

BIBBEN- Base Intra Biafra Benin sands.

BRB- Base Rubble Beds

BQI- Base Qua Iboe.

TIQI- Top Intra Qua Iboe

QUA3 etc- Intra Qua Iboe horizon 3 etc

Pu- Pleistocene Unconformity

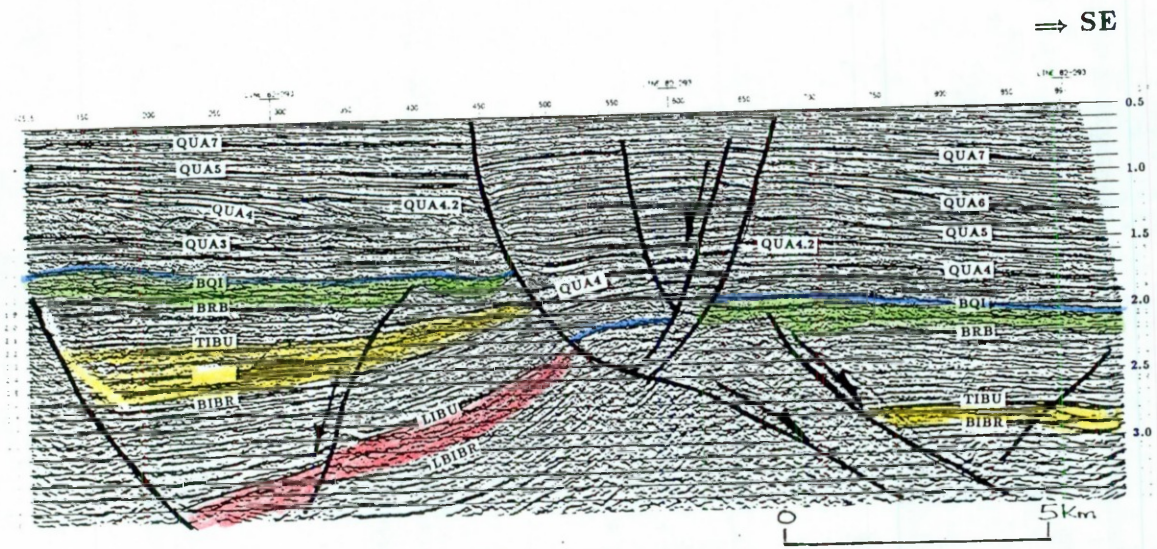

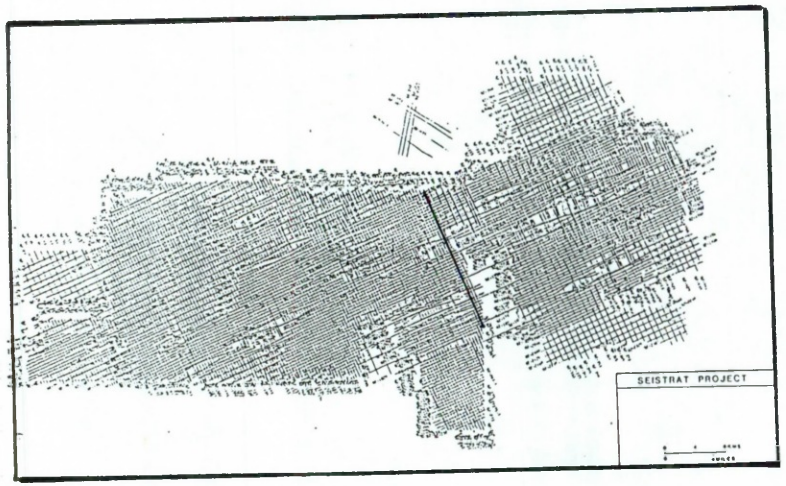

RUBBLE BEDS
UIBR
LIBR

Fig.6.1d Line 82-293 showing Intra Biafra faulting within the palaeobasin associated with uplift at the time of the Top Intra Biafra Unconformity.

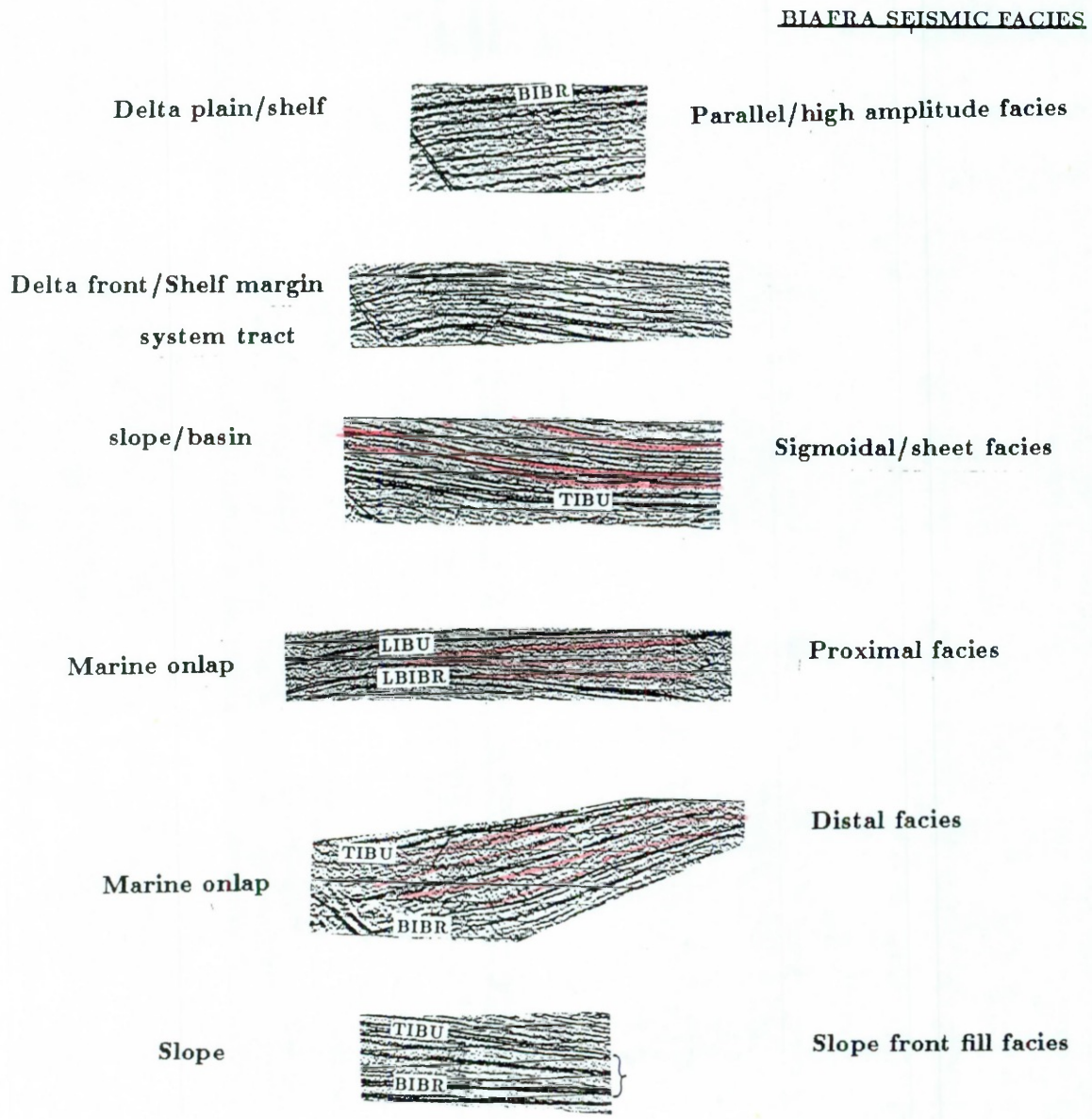

Fig.6.2 Representative seismic facies types of the Biafra. The figure shows the delta plain facies (parallel to divergent reflectors); the delta front (prograding high amplitude facies); prodelta to turbidites(variable amplitude sheet facies); and proximal onlap, distal onlap and slope front fill facies.

LBIBR- Lower Base Intra Biafra Rubble.

LIBU- Lower Intra Biafra Unconformity.

BIBR- Base Intra Biafra Rubble.

TIBU- Top Intra Biafra Unconformity.

BIBBEN- Base Intra Biafra Benin sands.

BRB- Base Rubble Beds

BQI- Base Qua Iboe.

TIQI- Top Intra Qua Iboe

QUA3 etc- Intra Qua Iboe horizon 3 etc

Pu- Pleistocene Unconformity

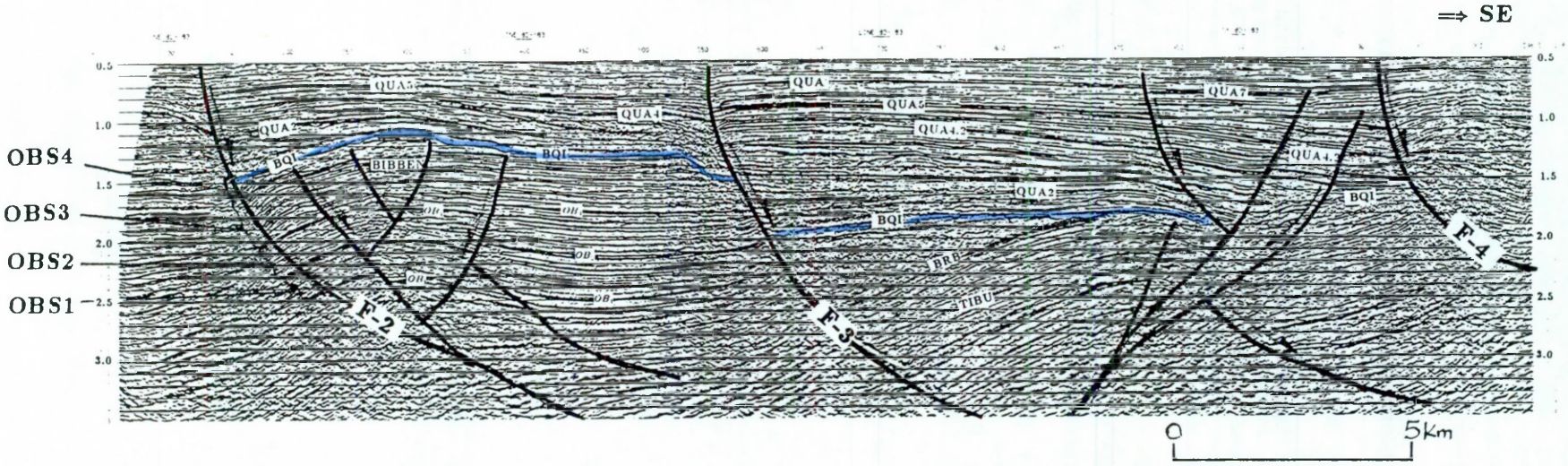

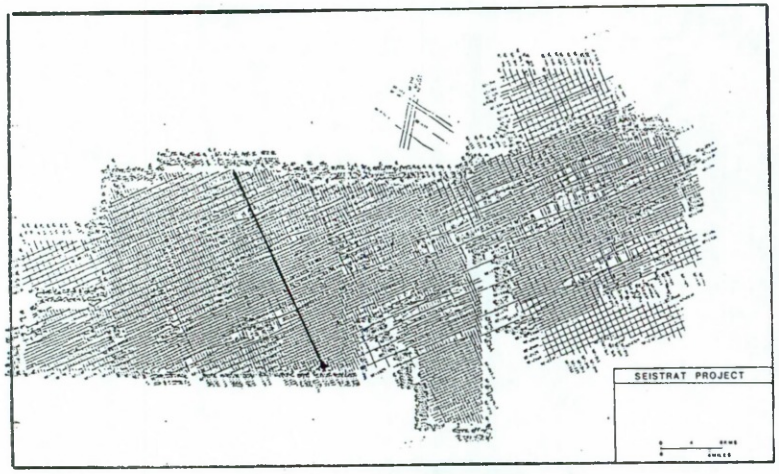

Fig.6.3a Line 82-183 showing the Older Biafra sequences in the northwest. Four distinct depositional cycles are evident.

LIBR- Lower Base Intra Biafra Rubble.

LIBU- Lower Intra Biafra Unconformity.

BIBR- Base Intra Biafra Rubble.

TIBU- Top Intra Biafra Unconformity.

BIBBEN- Base Intra Biafra Benin sands.

BRB- Base Rubble Beds

BQI- Base Qua Iboe.

TIQI- Top Intra Qua Iboe

QUA3 etc- Intra Qua Iboe horizon 3 etc

Pu- Pleistocene Unconformity

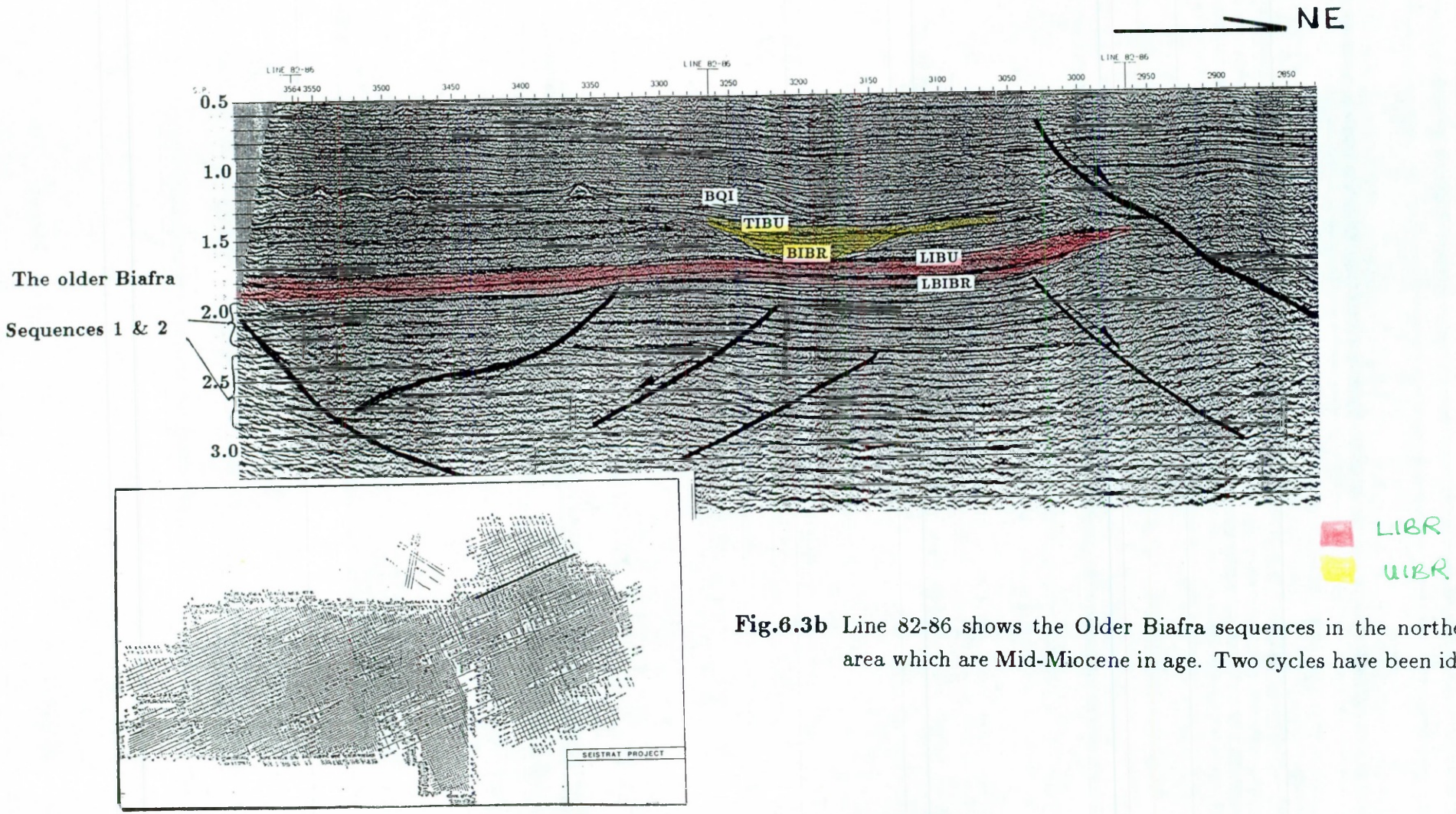

Fig.6.3b Line 82-86 shows the Older Biafra sequences in the northeast of study area which are Mid-Miocene in age. Two cycles have been identified here.

LBIBR- Lower Base Intra Biafra Rubble.

LIBU- Lower Intra Biafra Unconformity.

BIBR- Base Intra Biafra Rubble.

TIBU- Top Intra Biafra Unconformity.

BIBBEN- Base Intra Biafra Benin sands.

BRB- Base Rubble Beds

BQI- Base Qua Iboe.

TIQI- Top Intra Qua Iboe

QUA3 etc- Intra Qua Iboe horizon 3 etc

Pu- Pleistocene Unconformity

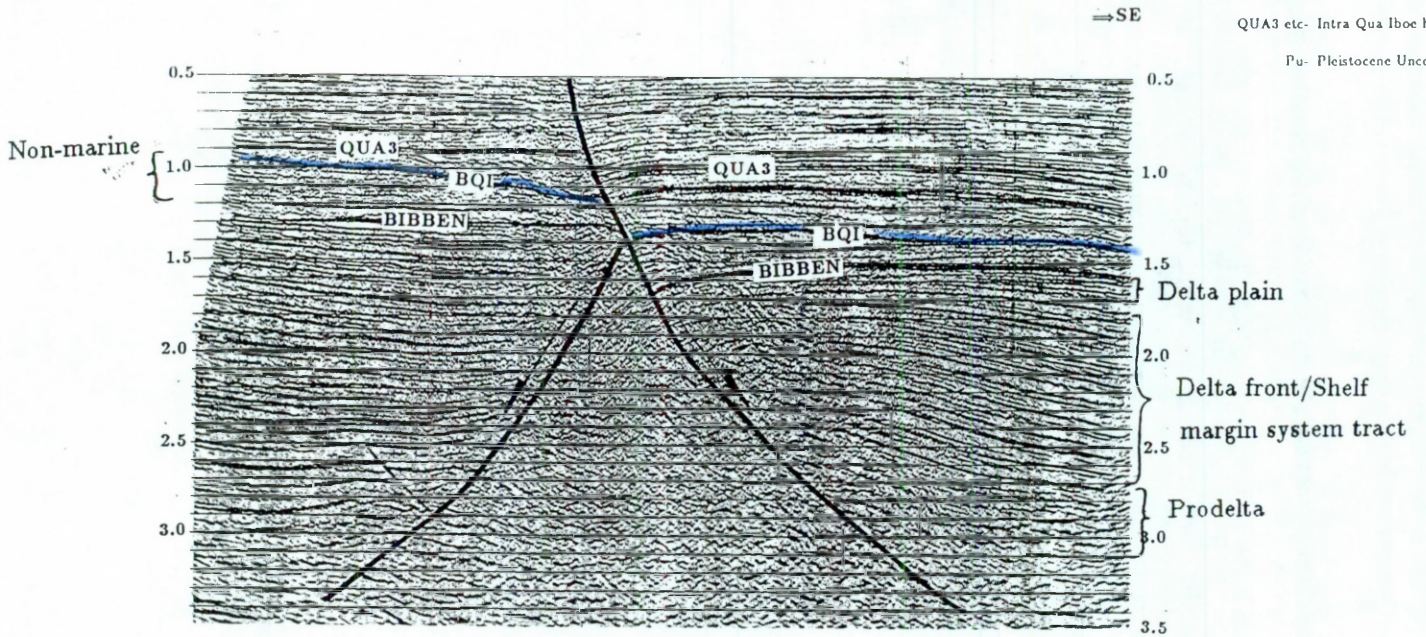

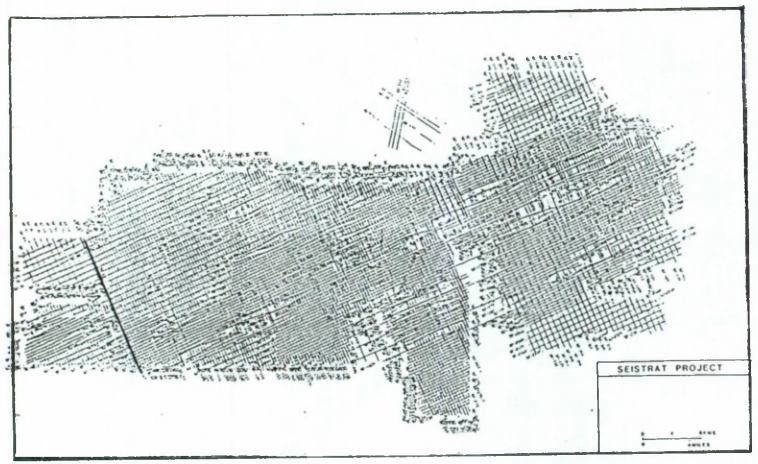

Fig.6.3c Line 82-69 illustrating the Older sequences thickening westwards.

Fig.6.4 Map showing the limit of truncation of BIBBEN in the northwest. This limit roughly parallels the palaeo-shelf edge in Miocene as well as Pliocene.

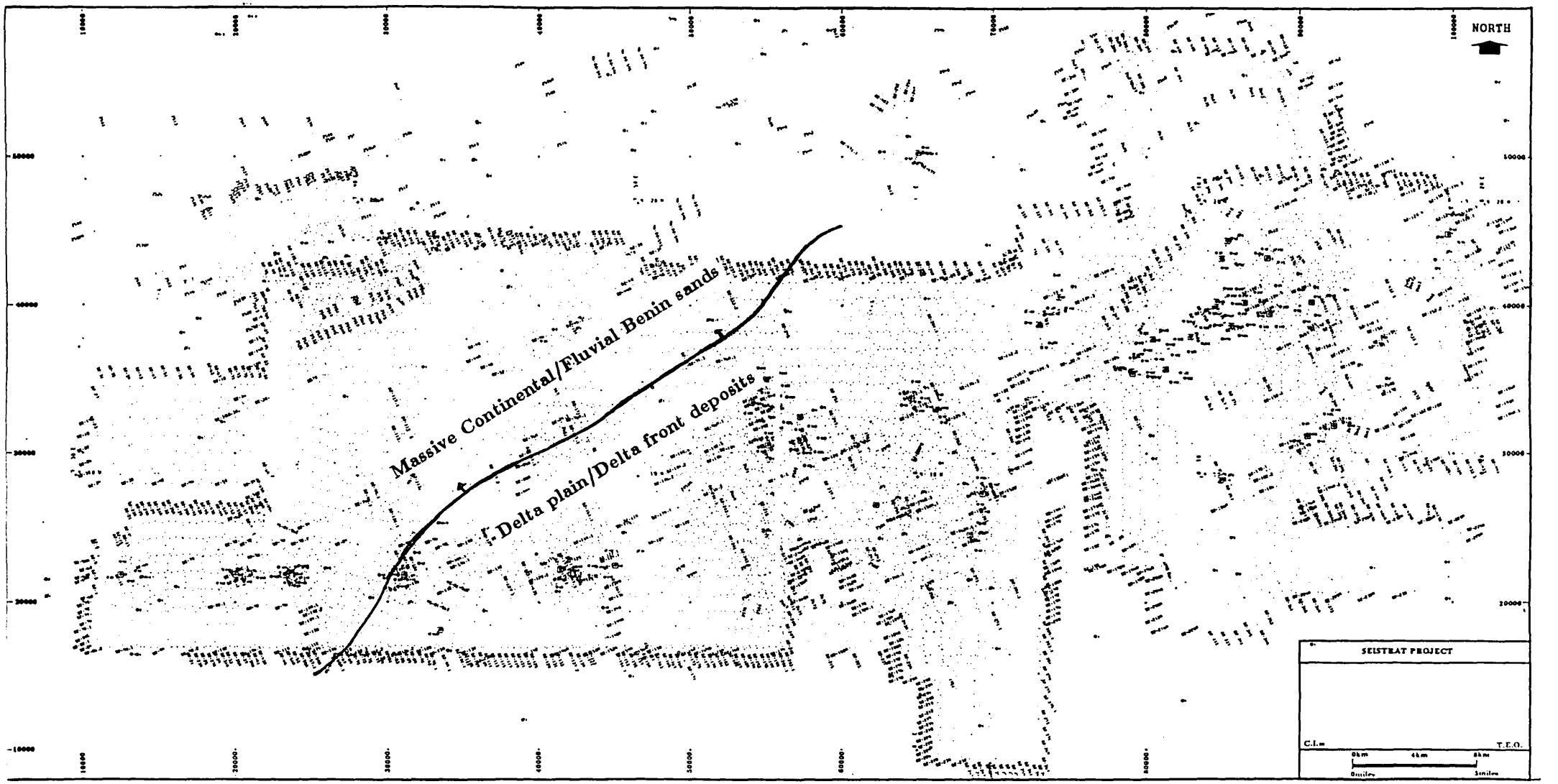

LBIBR- Lower Base Intra Biafra Rubble.

LIBU- Lower Intra Biafra Unconformity.

BIBR- Base Intra Biafra Rubble.

TIBU- Top Intra Biafra Unconformity.

BIBBEN- Base Intra Biafra Benin sands.

BRB- Base Rubble Beds

BQI- Base Qua Iboe.

TIQI- Top Intra Qua Iboe

QUA3 etc- Intra Qua Iboe horizon 3 etc

Pu- Pleistocene Unconformity

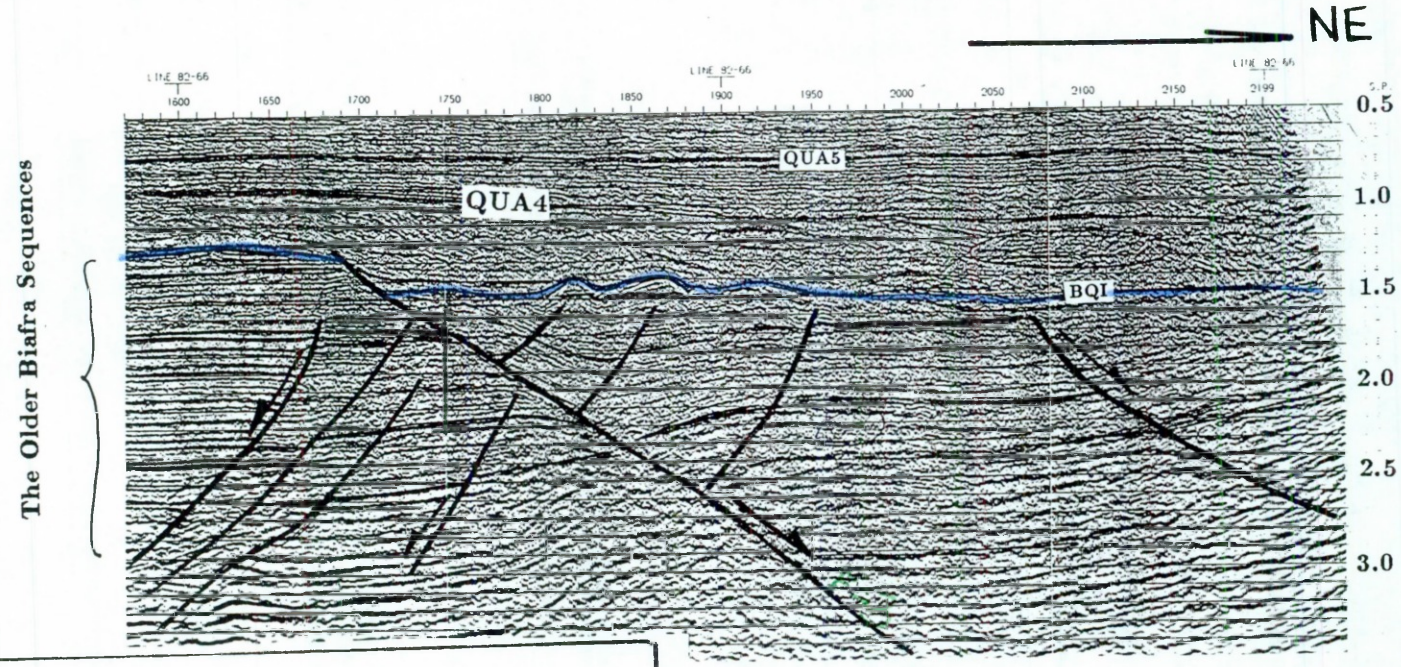

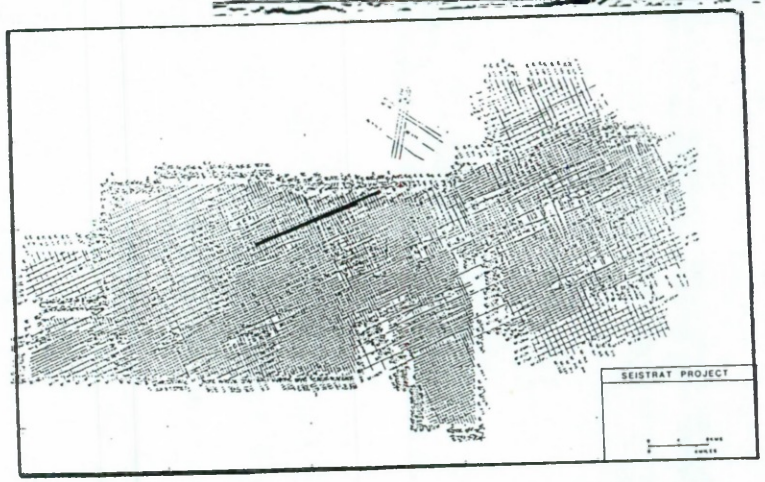

Fig.6.5 Line 82-66 illustrates the limit of the proto-embayment or palaeobasin with the Older Biafra sequences truncating against Fault-3 (the palaeobasin margin). Correlation across Fault-3 is tenuous. Also see Fig.3.12, the regional cross-section. The Older sequences corresponds to the Mid-Miocene as shown.

LBIBR- Lower Base Intra Biafra Rubble.

LIBU- Lower Intra Biafra Unconformity.

BIBR- Base Intra Biafra Rubble.

TIBU- Top Intra Biafra Unconformity.

BIBBEN- Base Intra Biafra Benin sands.

BRB- Base Rubble Beds

BQI- Base Qua Iboe.

TIQI- Top Intra Qua Iboe

QUA3 etc- Intra Qua Iboe horizon 3 etc

Pu- Pleistocene Unconformity

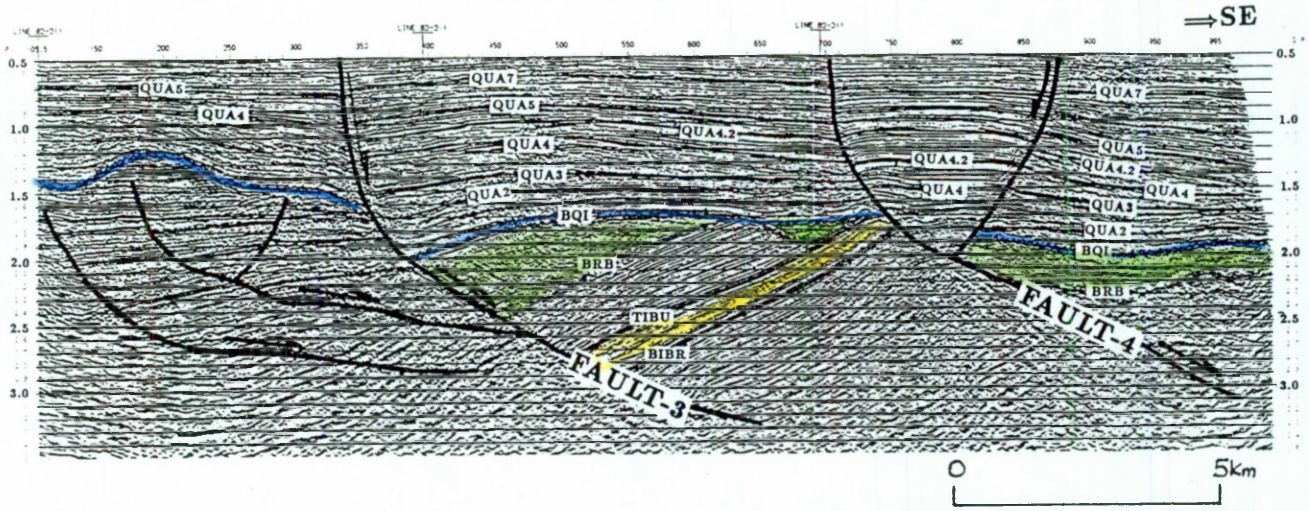

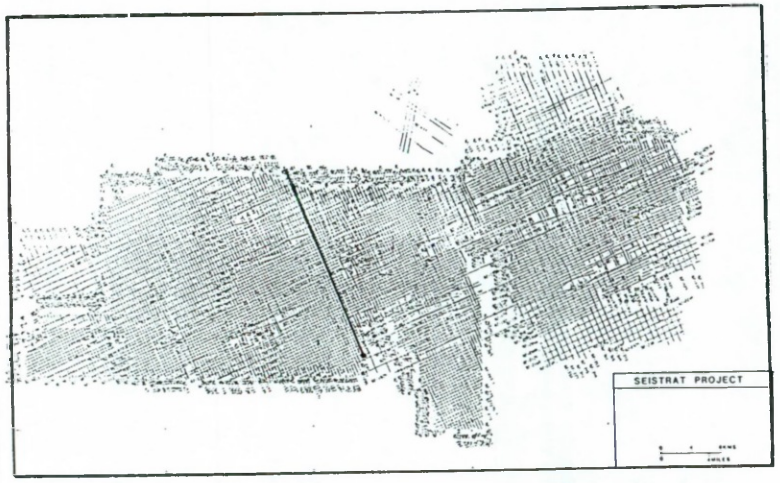

Fig.6.6 Line 82-211 (NW-SE) illustrates the relationship of the Older sequences with the sequences within the palaeobasin. The shaling out of the Older sequences within the basin is butressed in the structural evolution model presented in Figs.6.1a,b&c.

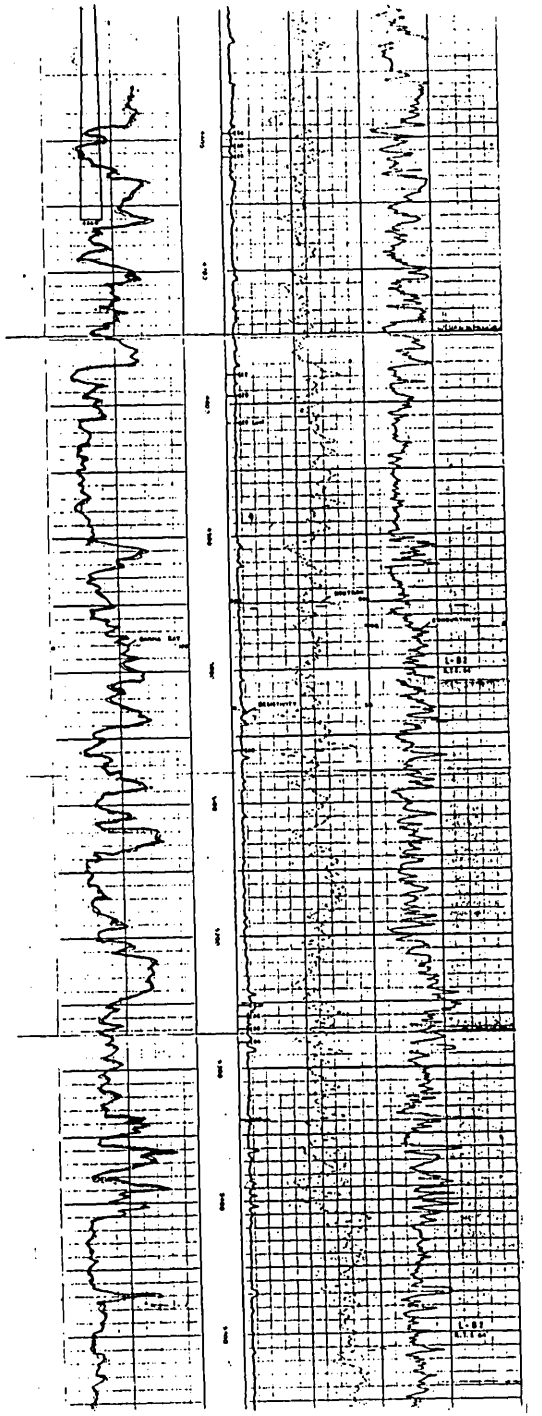

Fig.6.7a Characteristic log response of the subdued amplitude facies of the Older Biafra Sequence is typically massive sand with a block log motif. The parallel/divergent seismic character consists of intercalations of sands and shales (NW of the study area).

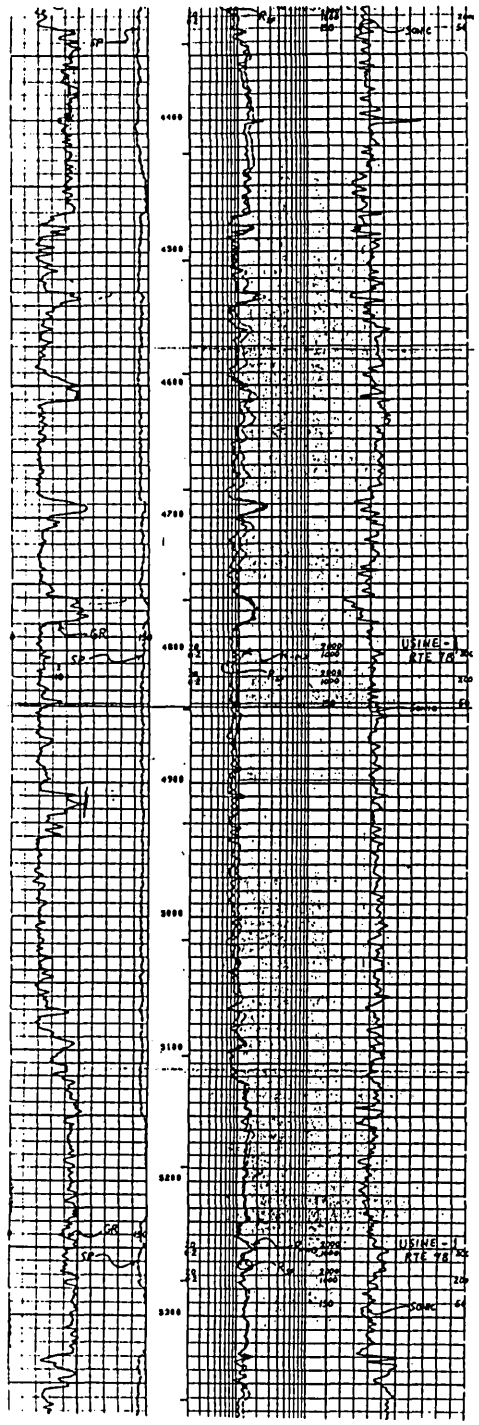

Fig.6.7b The massive sands in the NW thicken westwards as is evident from this log.

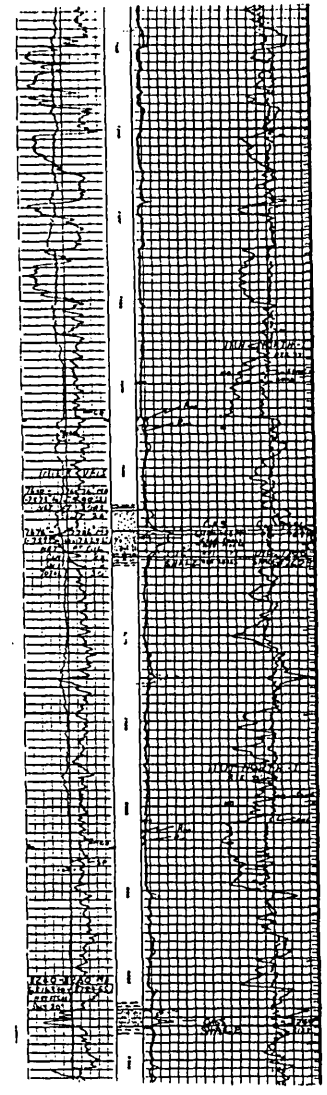

Fig.6.7c Characteristic log response of the Older Biafra sequences in the NE of the study area. Coarsening upward sequences typify the updip portions of the shelf margin system tract shaling at the toe into prodelta shales. High amplitude anomalies mark the beginning of each depositional cycle.

Fig.6.8a Composite facies distribution map of older sequences. This indicates that in Mid-Miocene, substantial deltaic build-up from the northwest extended furthest to the south into the present embayment as against progradation from the northeast which appears to have been less. This also echoes the present day shape of the Niger Delta.

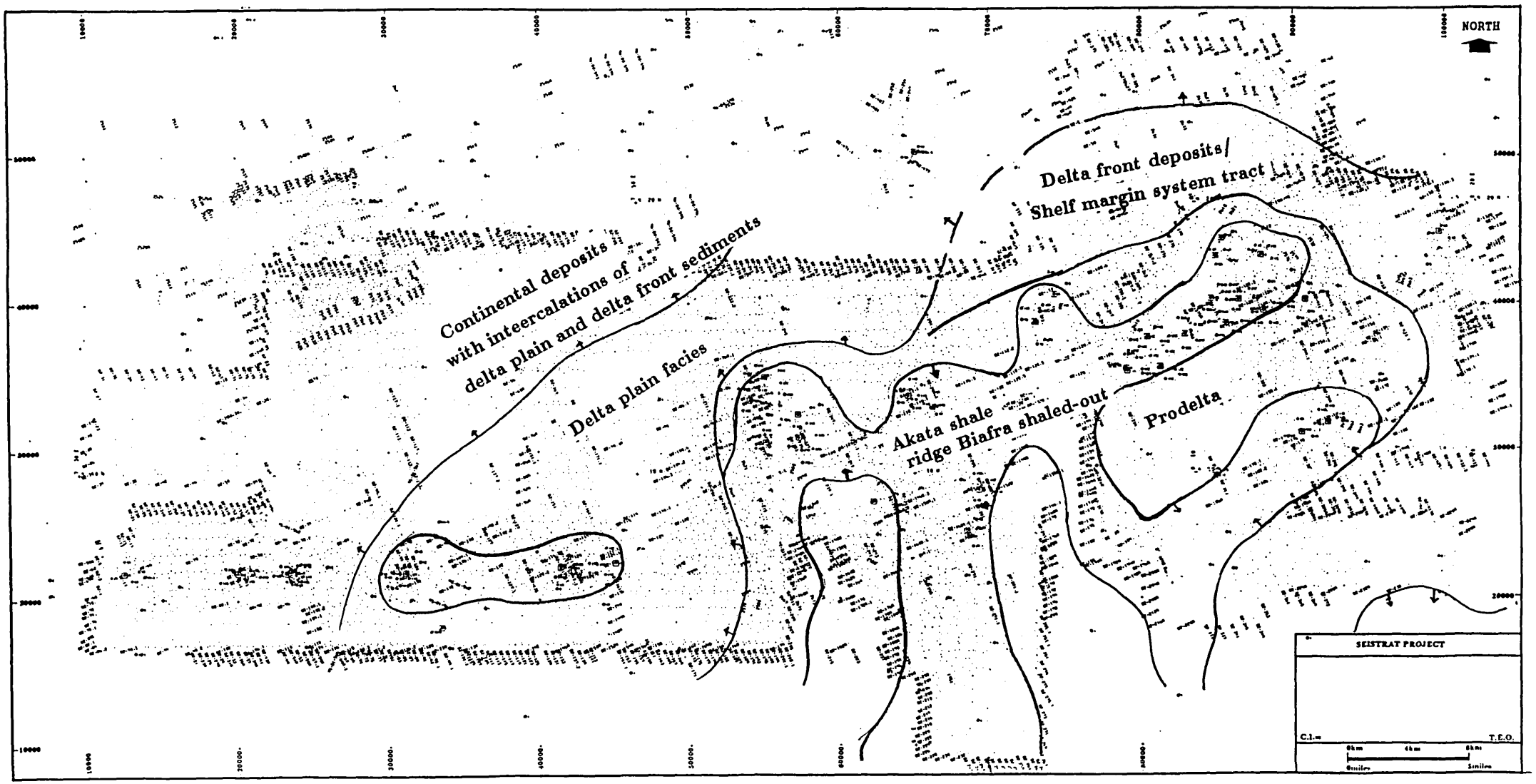

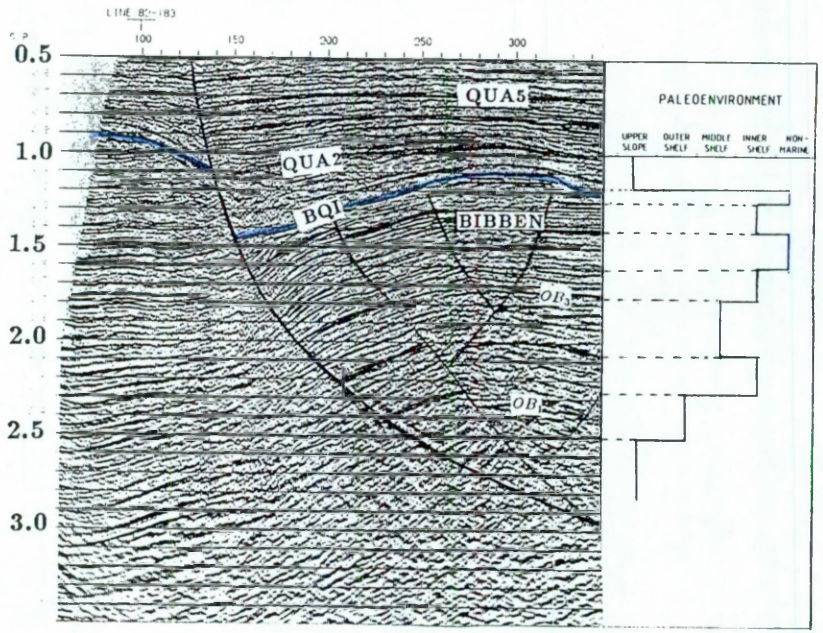

Fig.6.8b Paleoenvironment curve of the northwest area based on well data correlation showing the environment of deposition of the Older sequences in relation to other sequences.

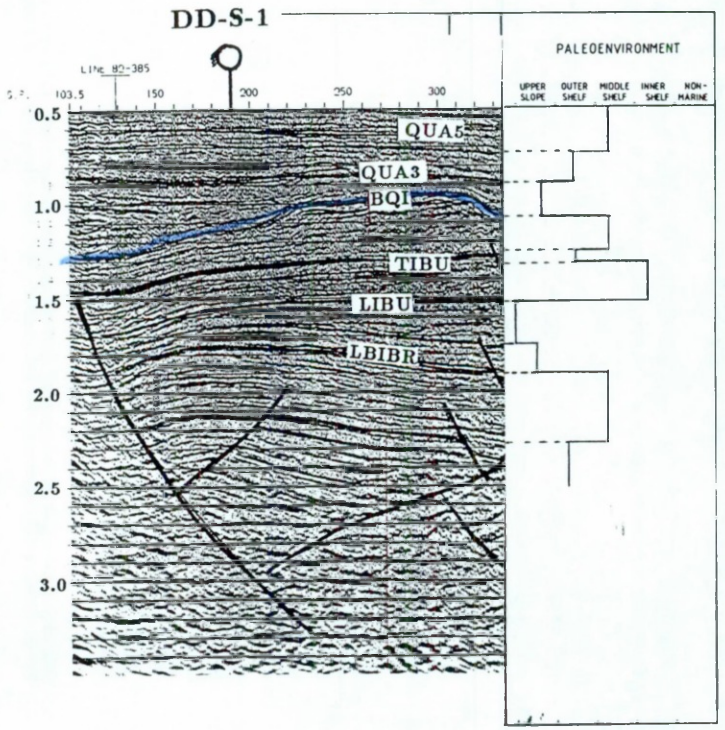

Fig.6.8c Paleoenvironment curve of the northeast area based on well data correlation showing the environment of deposition of the Older Biafra sequences *vis a vis* other mapped sequences.

Fig.6.9 Facies distribution map of LIBR. Note that in the east-central part of the study area, the presence or otherwise of LIBR is obscured by shale tectonism.

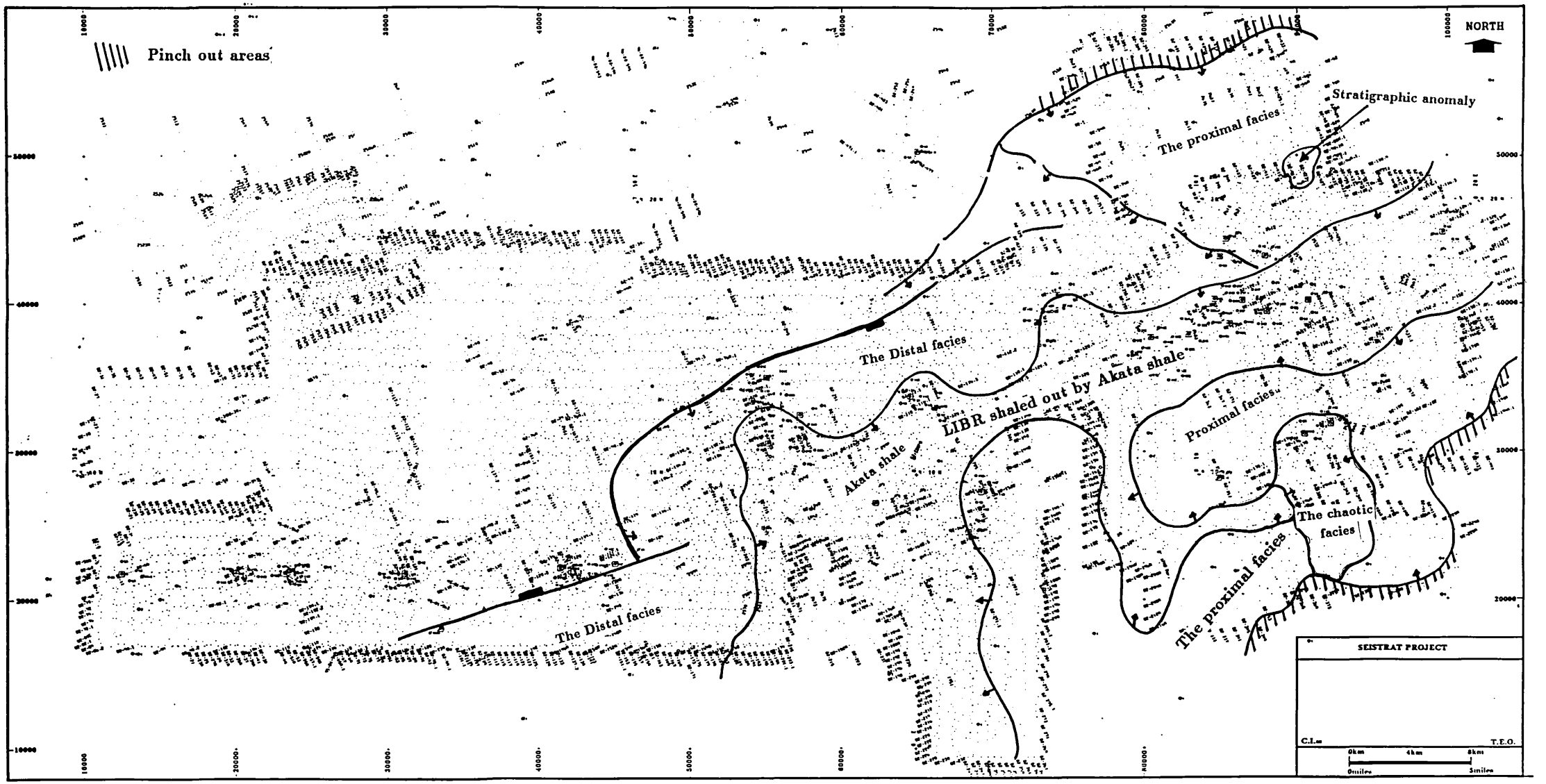

LBIBR- Lower Base Intra Biafra Rubble.

LIBU- Lower Intra Biafra Unconformity.

BIBR- Base Intra Biafra Rubble.

TIBU- Top Intra Biafra Unconformity.

BIBBEN- Base Intra Biafra Benin sands.

BRB- Base Rubble Beds

BQI- Base Qua Iboe.

TIQI- Top Intra Qua Iboe

QUA3 etc- Intra Qua Iboe horizon 3 etc

Pu- Pleistocene Unconformity

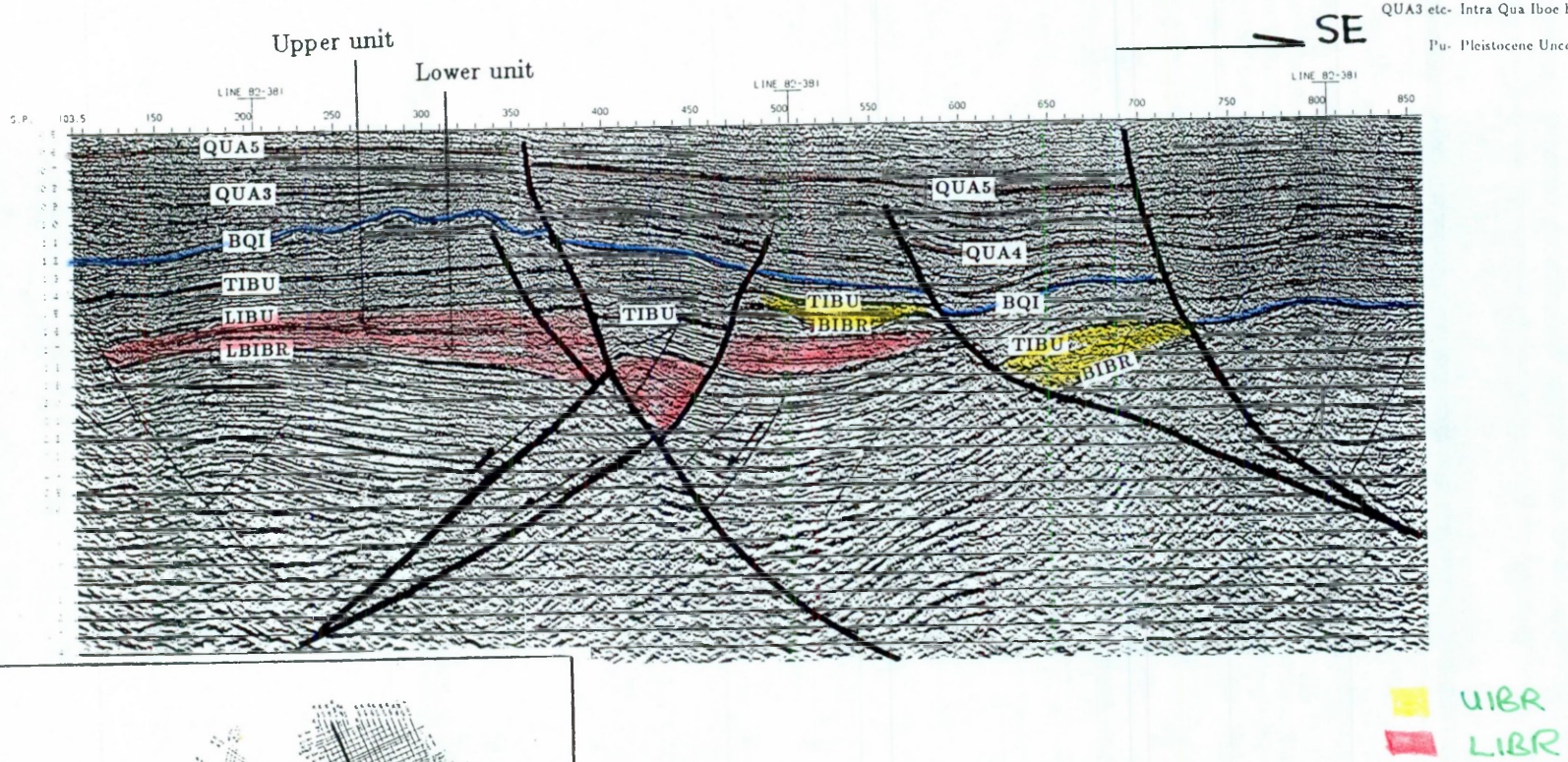

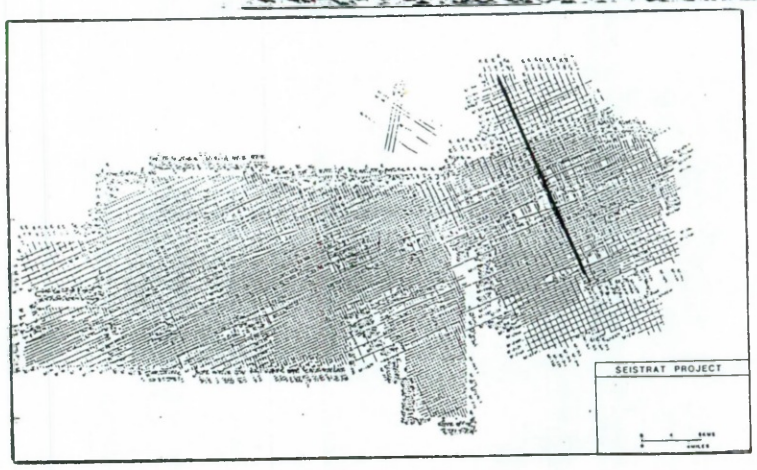

Fig.6.10a Line 82-381 shows the differentiation of the LIBR into two units: a lower onlapping and an upper offlapping unit.

LBIBR- Lower Base Intra Biafra Rubble.

LIBU- Lower Intra Biafra Unconformity.

BIBR- Base Intra Biafra Rubble.

TIBU- Top Intra Biafra Unconformity.

BIBBEN- Base Intra Biafra Benin sands.

BRB- Base Rubble Beds

BQI- Base Qua Iboe.

TIQI- Top Intra Qua Iboe

QUA3 etc- Intra Qua Iboe horizon 3 etc

Pu- Pleistocene Unconformity

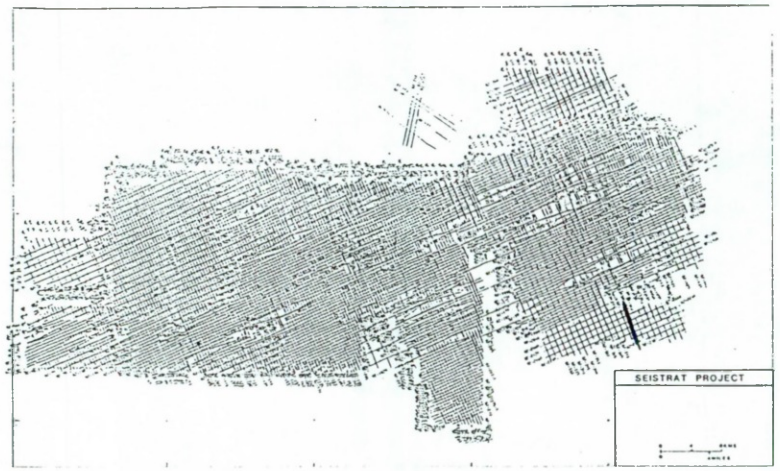

RUBBLE BEDS

LIBR

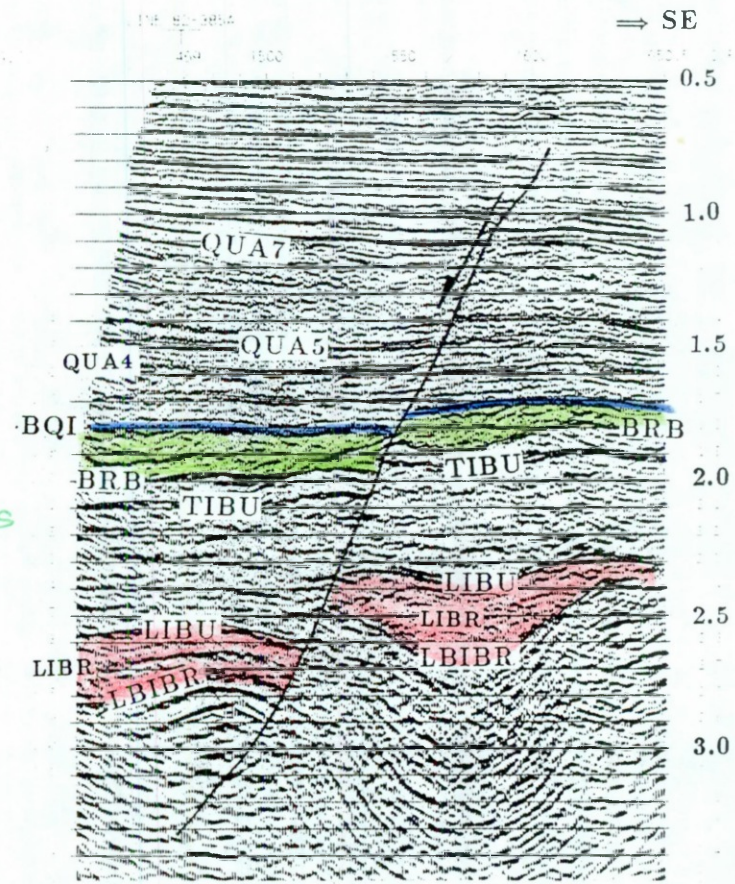

Fig.6.10b Typical LIBR facies type in the southeast of study area

LIBBR- Lower Base Intra Biafra Rubble
LIBU- Lower Intra Biafra Unconformity
BIBR- Base Intra Biafra Rubble.
TIBU- Top Intra Biafra Unconformity.
BIBBEN- Base Intra Biafra Benin sands.
BRB- Base Rubble Beds
BQI- Base Qua Iboe.
TIQI- Top Intra Qua Iboe
QUA3 etc- Intra Qua Iboe horizon 3 etc
Pu- Pleistocene Unconformity

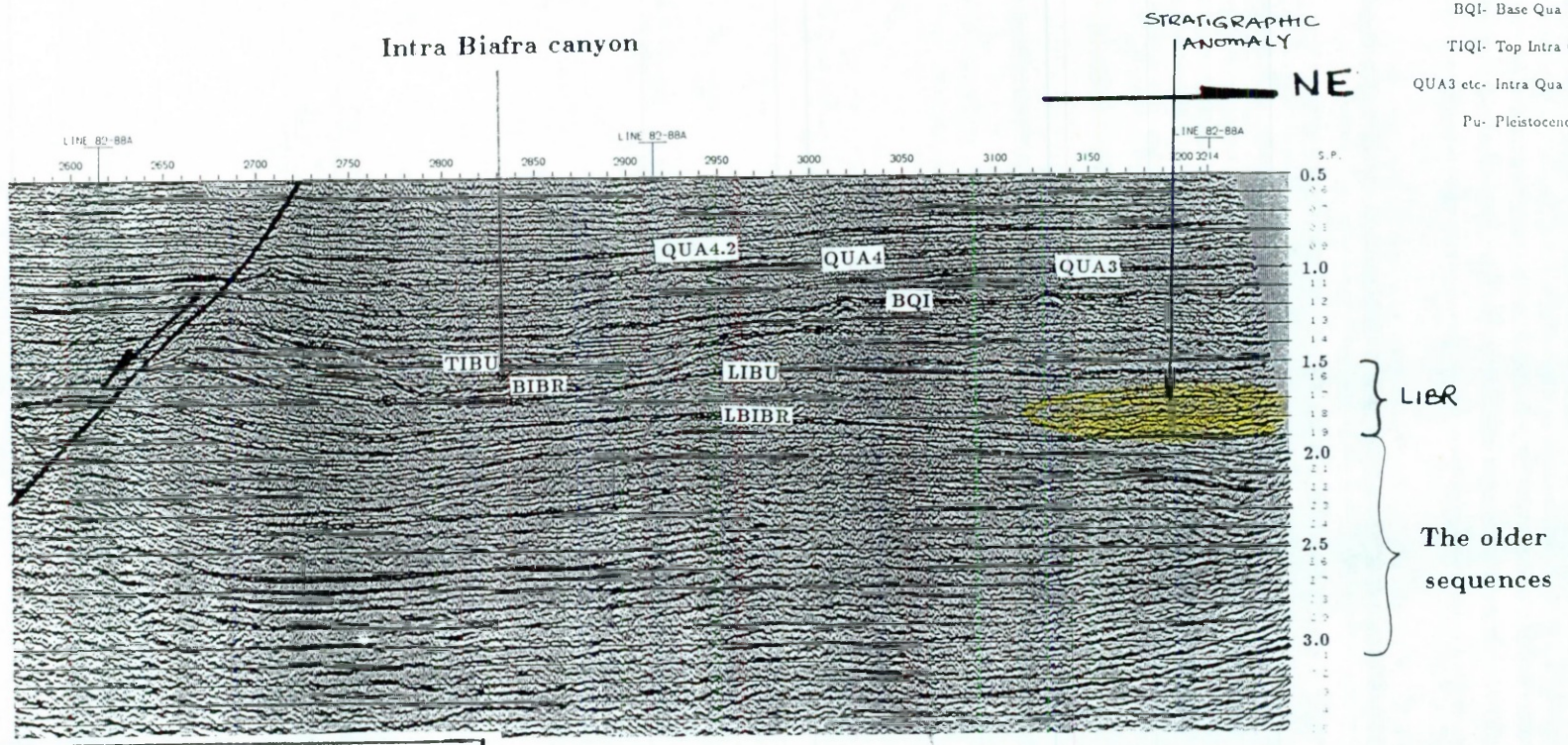

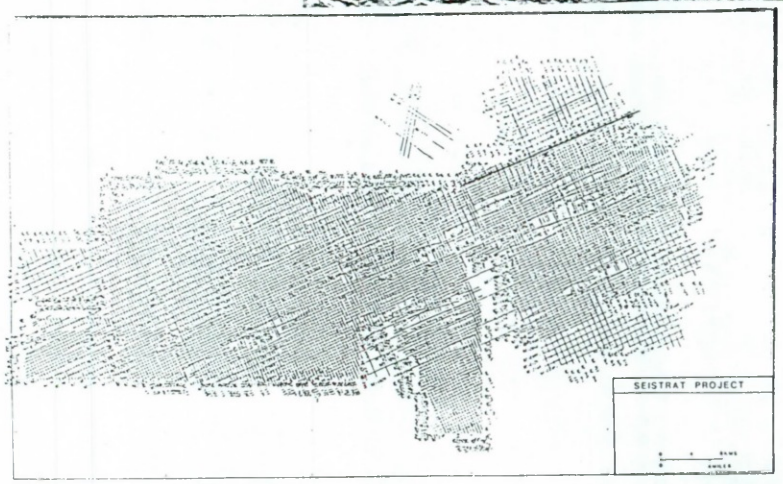

Fig.6.10c A stratigraphic anomaly within the LIBR showing the characteristic seismic mounding. Apart from high amplitude anomalies at the top of LIBR to the north, seismic mounds are not typical. This is a recommended play for exploratory drilling (line 82-88a).

Fig.6.11a Isochron of SEQ.BS2.

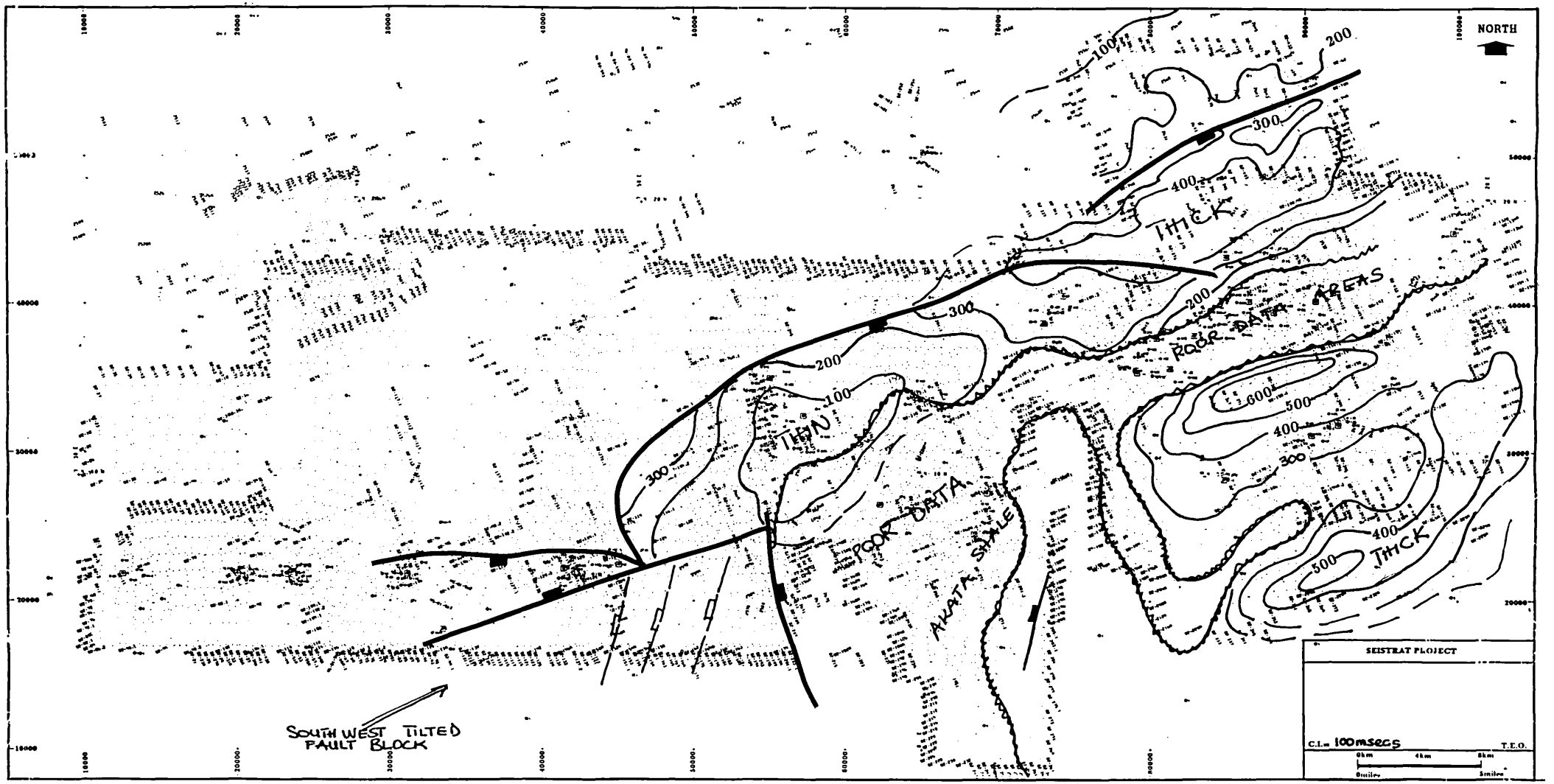

LBIBR- Lower Base Intra Biafra Rubbl.

LIBU- Lower Intra Biafra Unconformit

BIBR- Base Intra Biafra Rubble.

TIBU- Top Intra Biafra Unconformity.

BIBBEN- Base Intra Biafra Benin sands.

BRB- Base Rubble Beds

BQI- Base Qua Iboe.

TIQI- Top Intra Qua Iboe

QUA3 etc- Intra Qua Iboe horizon 3 etc

Pu- Pleistocene Unconformity

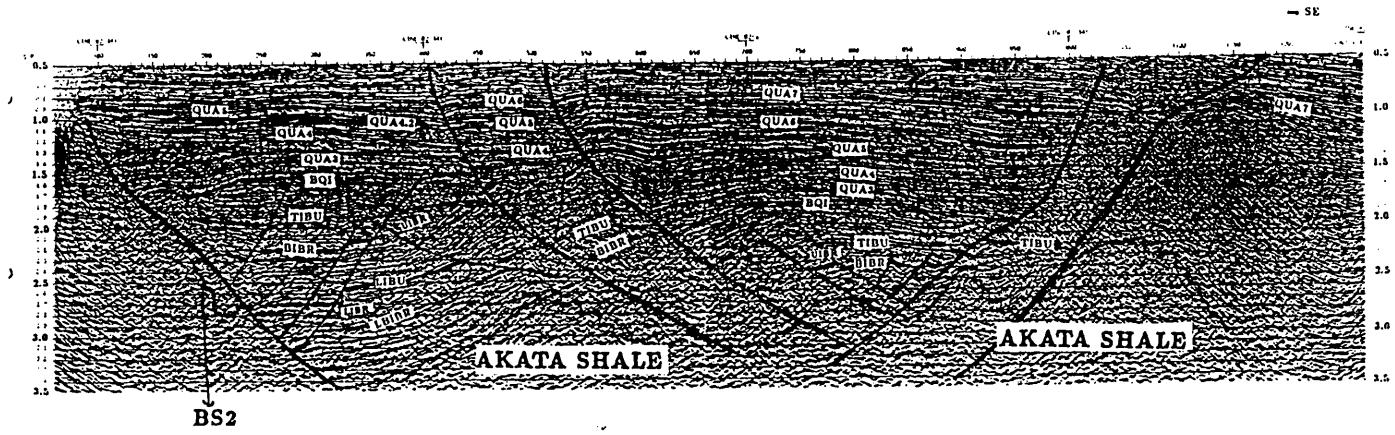

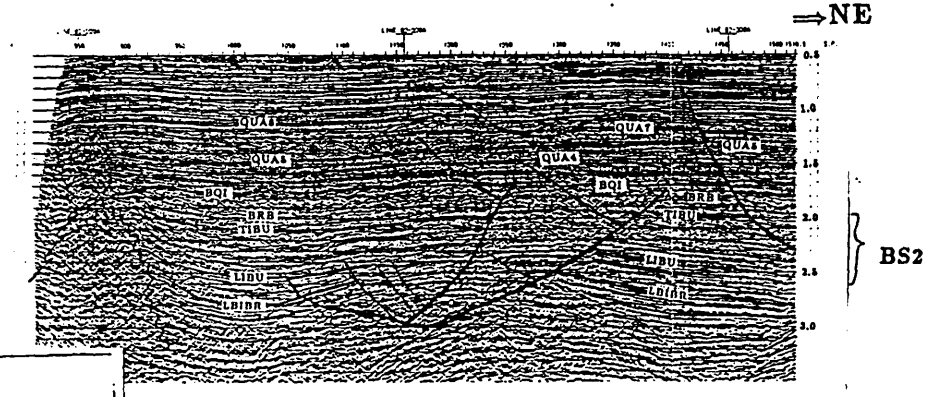

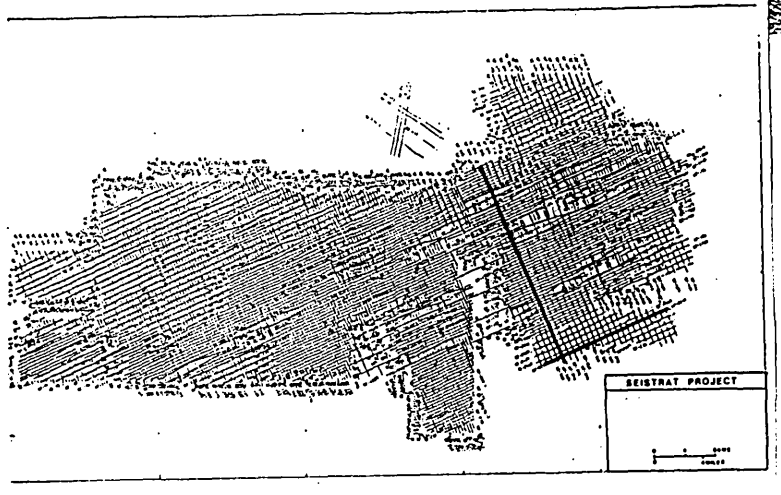

Fig.6.11b&c SEQ.BS2 is largely evident in the northeast and southeast. In the middle seqment of the study area, it appears to have been shaled out although to the southwest, the sequence is truncated against the BQI. (see line 82-197 Fig.5.7a,b.)

LBIBR- Lower Base Intra Biafra Rubble.

LIBU- Lower Intra Biafra Unconformity.

BIBR- Base Intra Biafra Rubble.

TIBU- Top Intra Biafra Unconformity.

BIBBEN- Base Intra Biafra Benin sands.

BRB- Base Rubble Beds

BQI- Base Qua Iboe.

TIQI- Top Intra Qua Iboe

QUA3 etc- Intra Qua Iboe horizon 3 etc

Pu- Pleistocene Unconformity

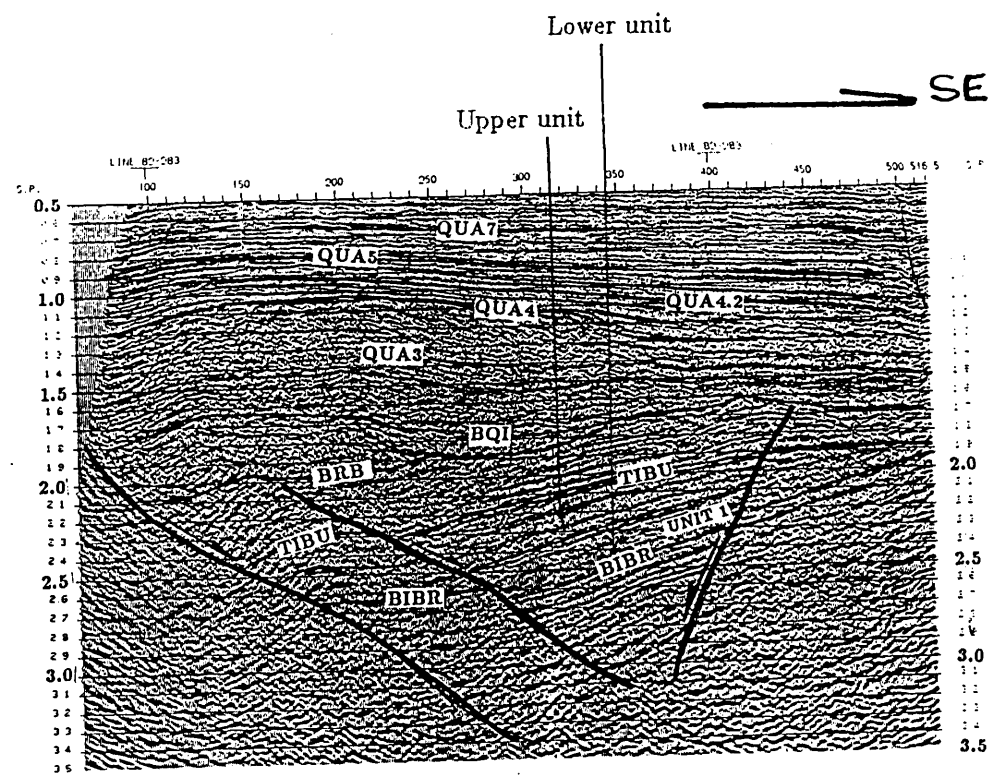

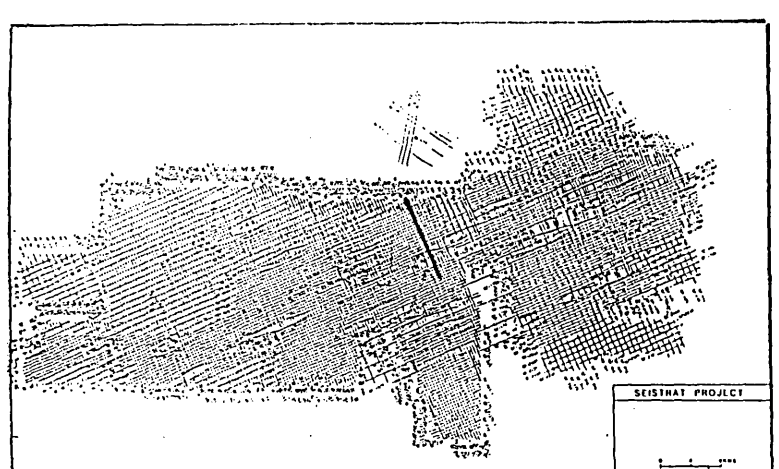

Fig.6.12a Line 82-283 illustrates the UIBR system including differentiation into lower and upper units.

LBIBR- Lower Base Intra Biafra Rubble.

LIBU- Lower Intra Biafra Unconformity.

BIBR- Base Intra Biafra Rubble.

TIBU- Top Intra Biafra Unconformity.

BIBBEN- Base Intra Biafra Benin sands.

BRB- Base Rubble Beds

BQI- Base Qua Iboe.

TIQI- Top Intra Qua Iboe

QUA3 etc- Intra Qua Iboe horizon 3 etc

Pu- Pleistocene Unconformity

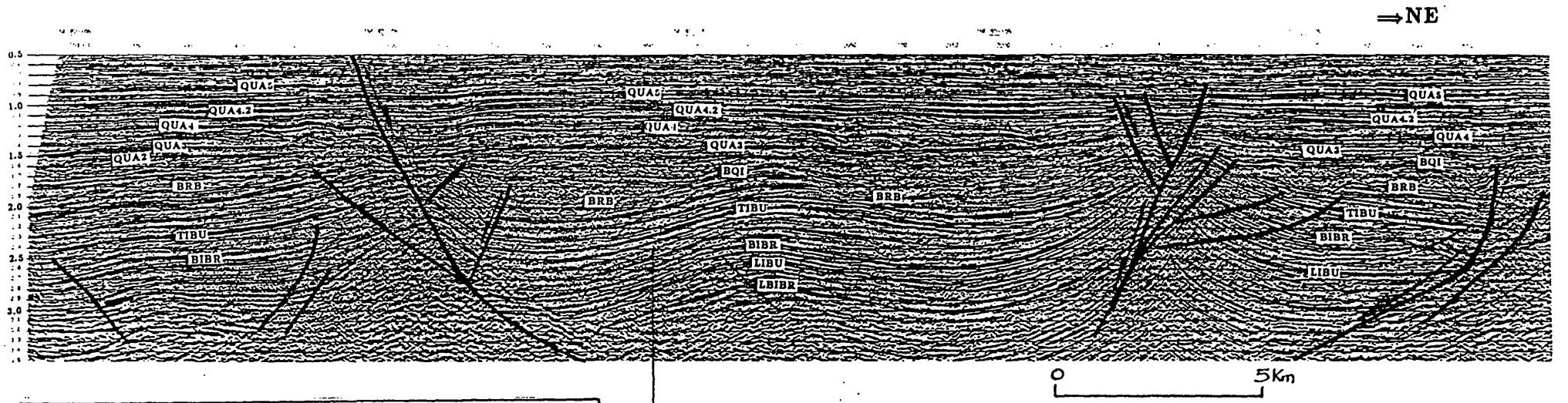

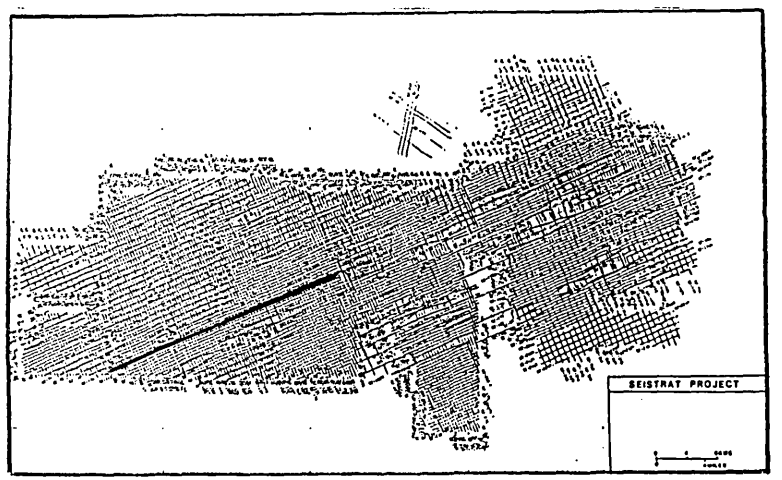

Fig.6.12b Line 82-106 shows the the UIBR prograding westwards. The dominant direction of sediment movement appears to have been from the NE-SW from the erosion of the NE block, and SE-NW, from the erosion of the southeast block

LBIBR- Lower Base Intra Biafra Rubble.

LIBU- Lower Intra Biafra Unconformity.

BIBR- Base Intra Biafra Rubble.

TIBU- Top Intra Biafra Unconformity.

BIBBEN- Base Intra Biafra Benin sands.

BRB- Base Rubble Beds

BQI- Base Qua Iboe.

TIQI- Top Intra Qua Iboe

QUA3 etc- Intra Qua Iboe horizon 3 etc

Pu- Pleistocene Unconformity

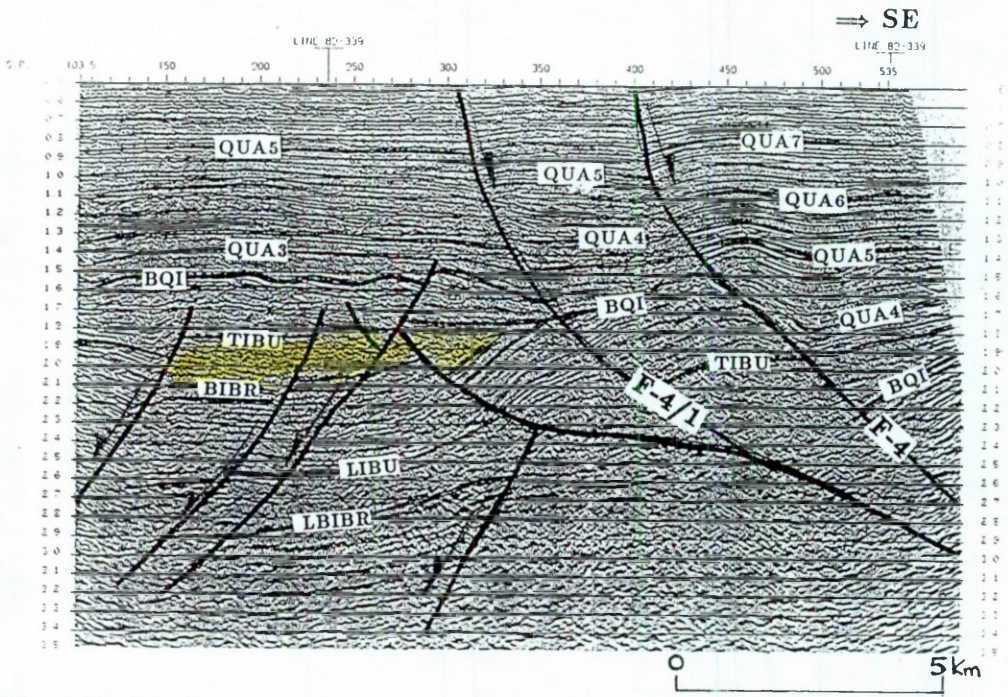

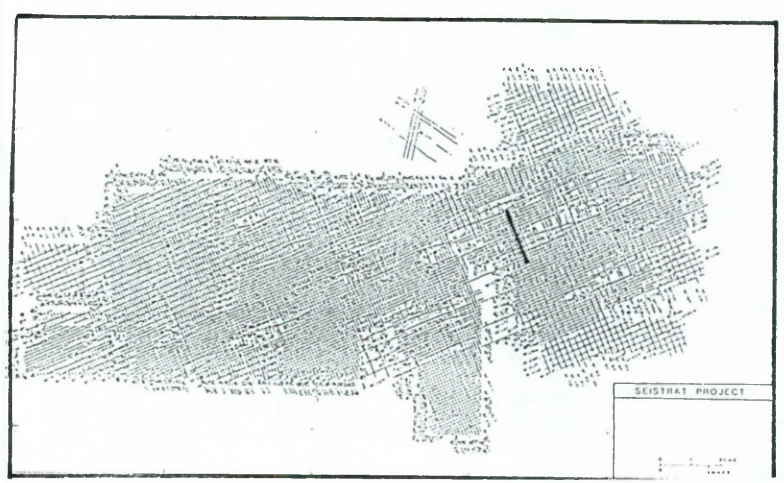

Fig.6.12c Line 82-339 shows the chaotic onlapping fill facies associated with an erosional gorge at the BIBR.

LBIBR- Lower Base Intra Biafra Rubble.

LIBU- Lower Intra Biafra Unconformity.

BIBR- Base Intra Biafra Rubble.

TIBU- Top Intra Biafra Unconformity.

BIBBEN- Base Intra Biafra Benin sands.

BRB- Base Rubble Beds

BQI- Base Qua Iboe.

TIQI- Top Intra Qua Iboe

QUA3 etc- Intra Qua Iboe horizon 3 etc

Pu- Pleistocene Unconformity

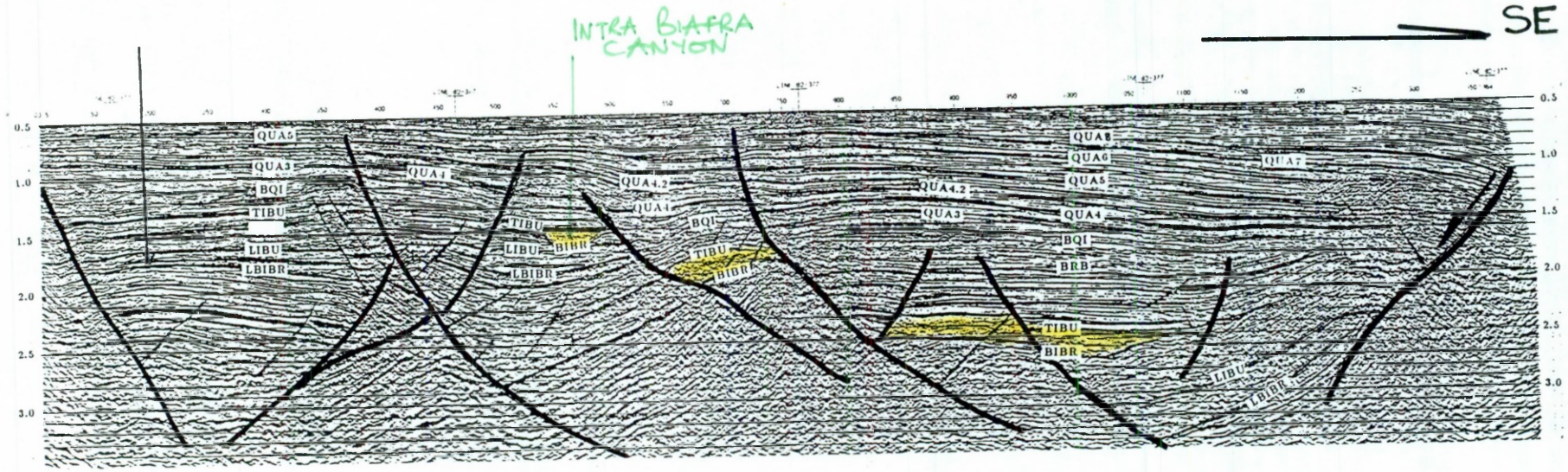

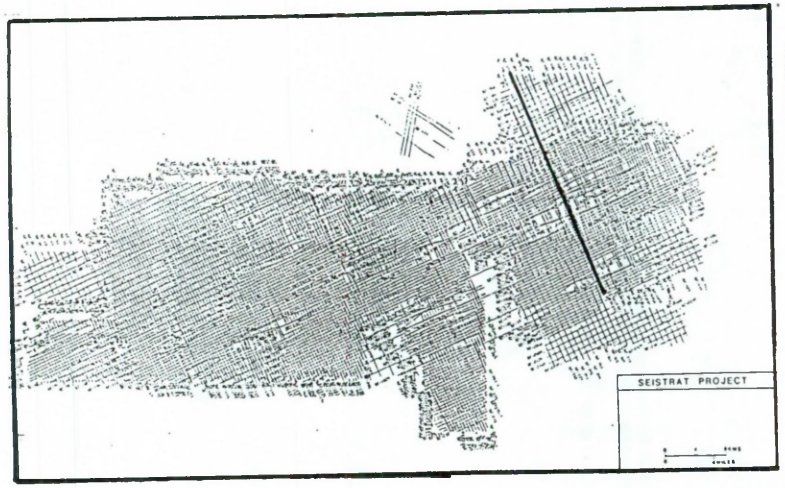

Fig.6.12d Line 82-377 shows truncation at the BIBR and the vertical stacking of high amplitude anomalies within LIBR.

Fig.6.13a Facies distribution of UIBR.

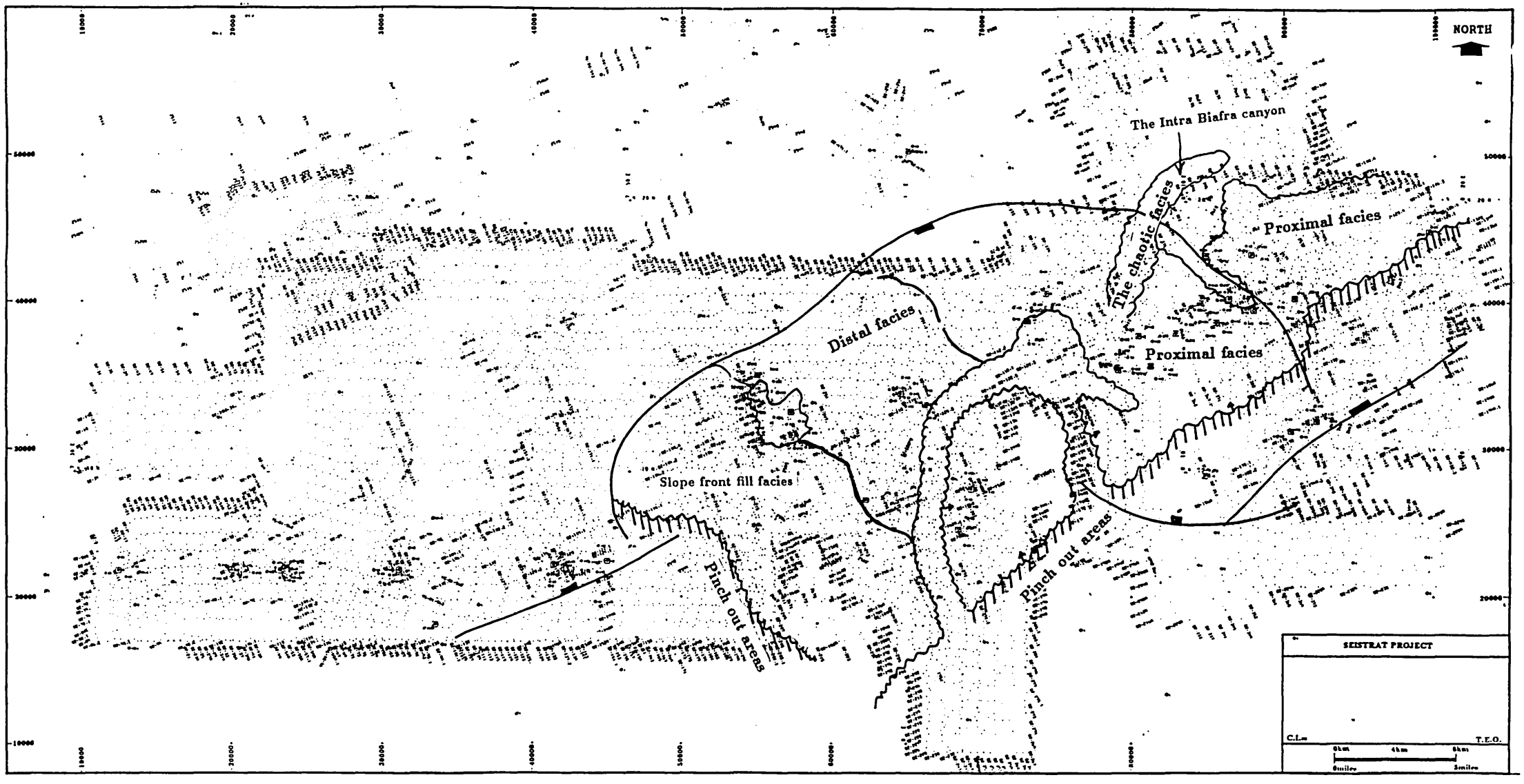

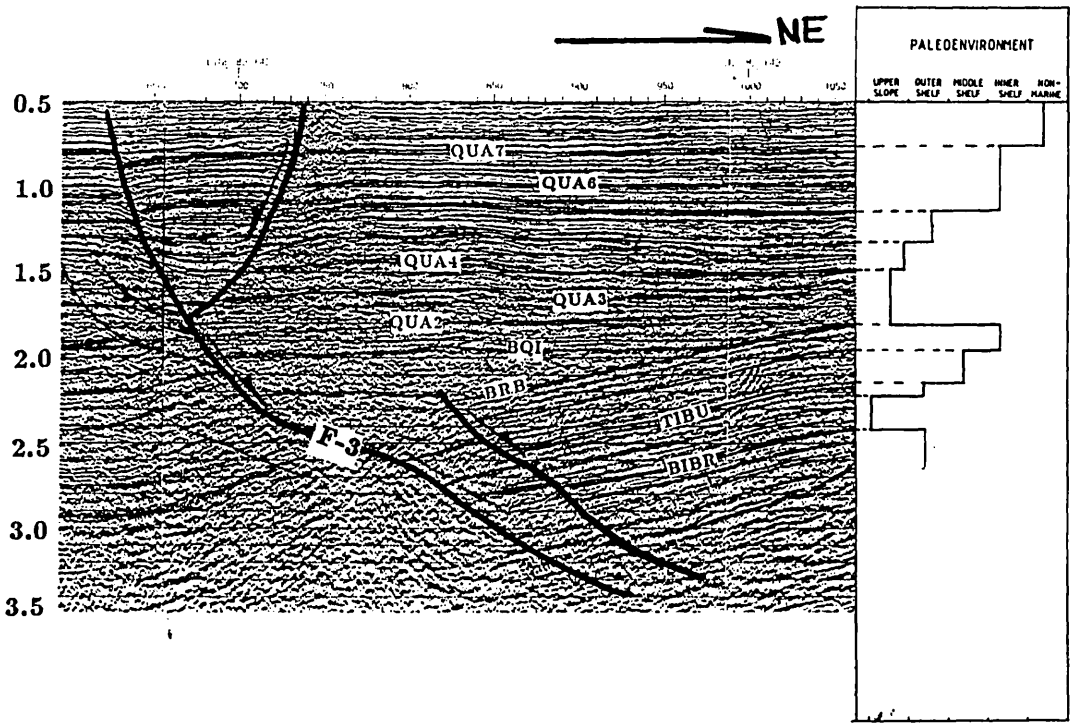

Fig.6.13b Paleoenvironment curve of the central study area showing the environment of deposition of the UIBR *vis a vis* other mapped sequences.

LBIBR- Lower Base Intra Biafra Rubble.

LIBU- Lower Intra Biafra Unconformity.

BIBR- Base Intra Biafra Rubble.

TIBU- Top Intra Biafra Unconformity.

BIBBEN- Base Intra Biafra Benin sands.

BRB- Base Rubble Beds

BQI- Base Qua Iboe.

TIQI- Top Intra Qua Iboe

QUA3 etc- Intra Qua Iboe horizon 3 etc

Pu- Pleistocene Unconformity

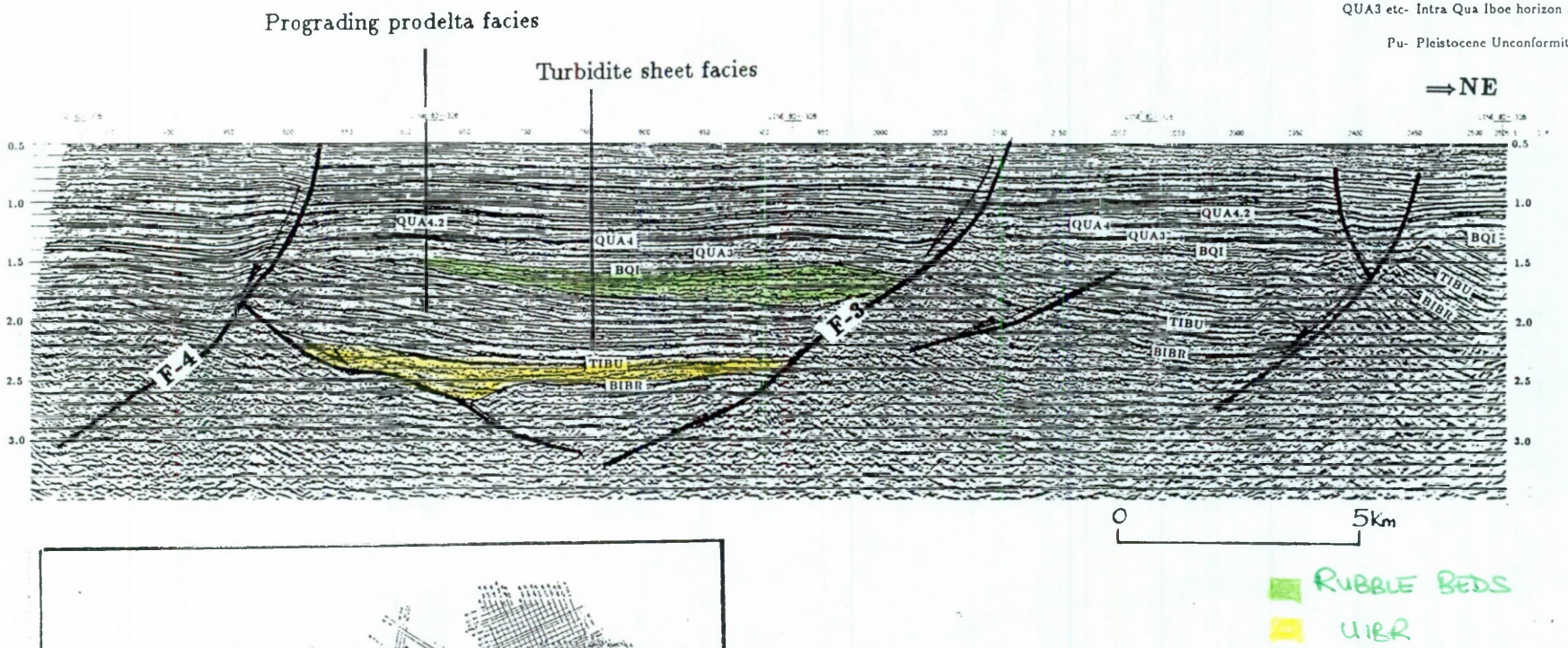

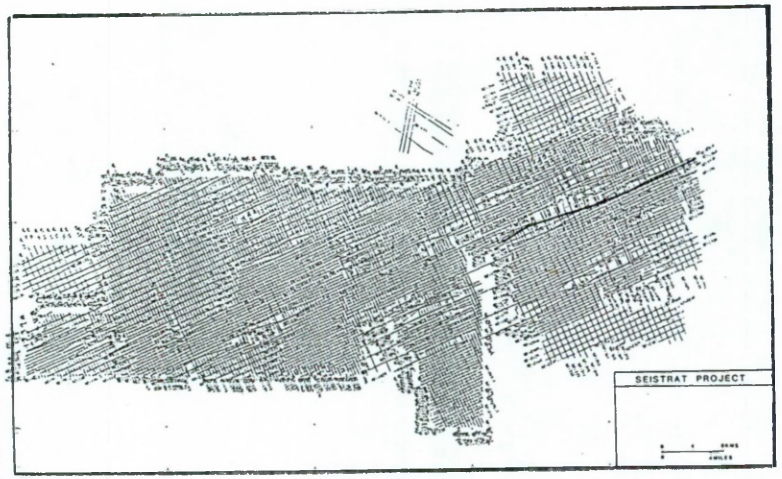

Fig.6.15 Line 82-132a illustrates the eastward progradation of SEQ.BS4. A prodelta facies forming turbidites with the characteristic sheet facies at the toe of progradation.

Fig.6.16a Facies distribution for SEQ.BS4. This sequence is largely truncated and eroded at the BQI level in the northwest and southwest of the study area (see line 82-197, fig.5.7a,b) and occurs as a thin veneer in the southeast(Fig.6.10b).

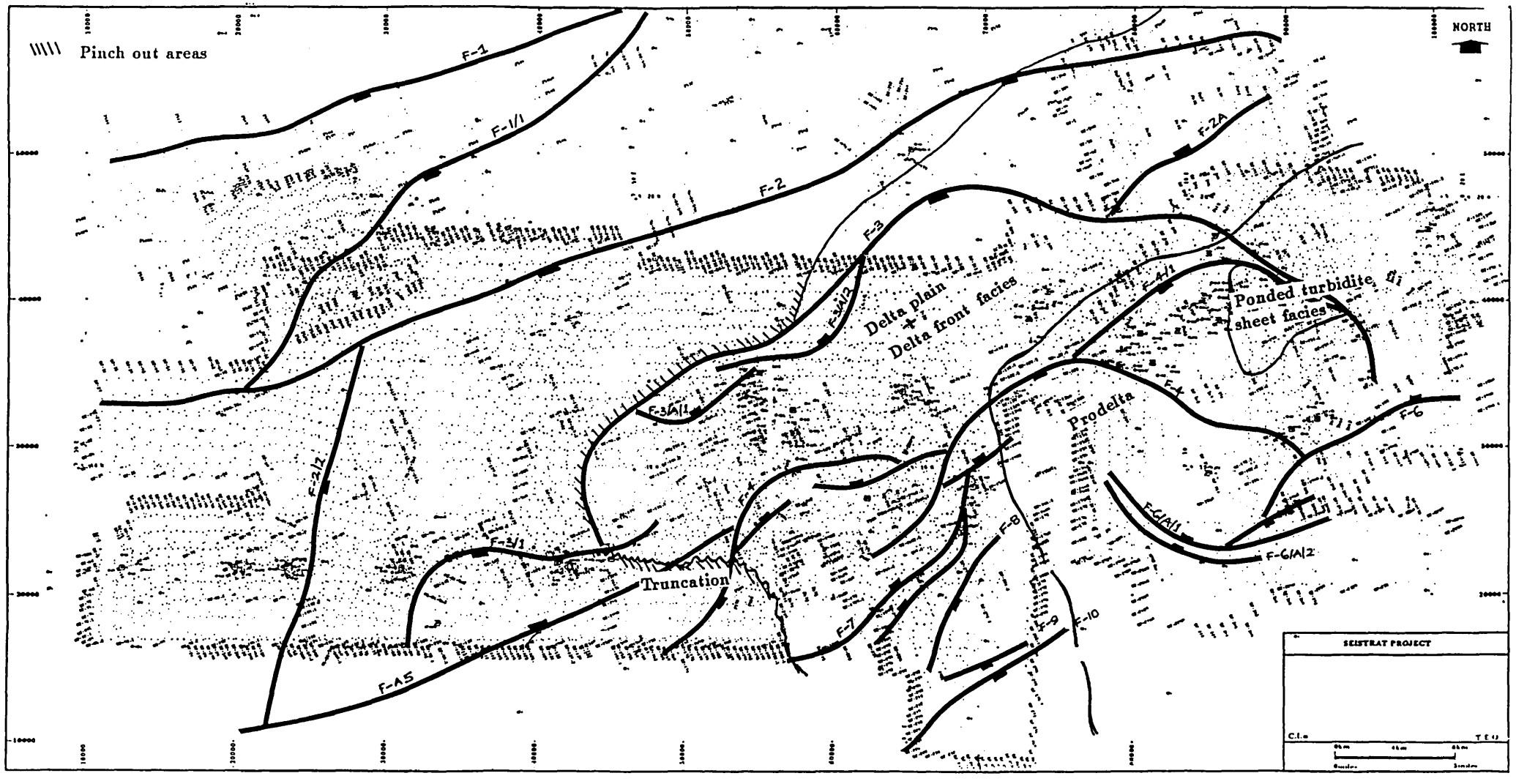

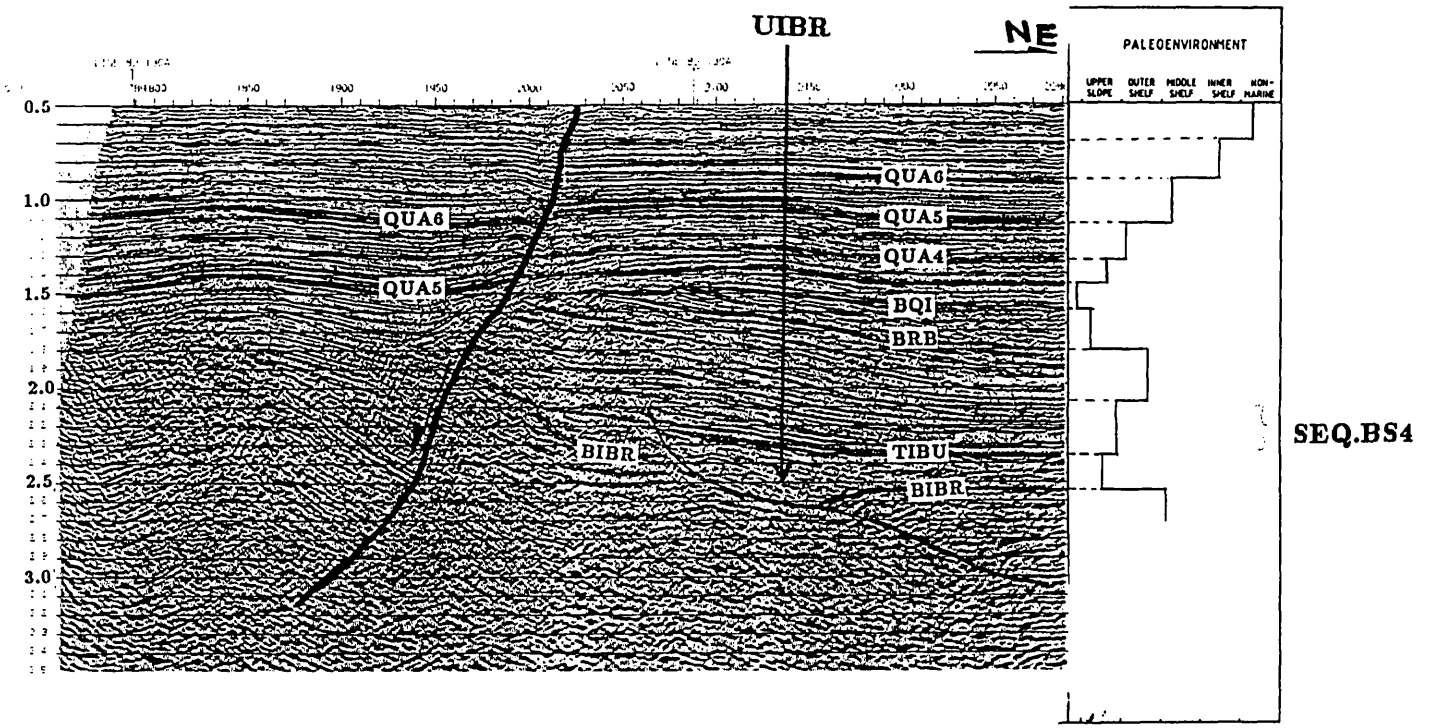

Fig.6.16b Paleoenvironment curve of the east central area showing the environment of deposition of SEQ.BS4 as compared to other mapped sequences.

Fig.6.17a Sand percentage map of the Biafra based on selected well data. Note that higher sand percentages apply in northern areas. Sand percentage calculations are however dependent on the depth reached by the various wells, which is often based on the hydrocarbon objectives.

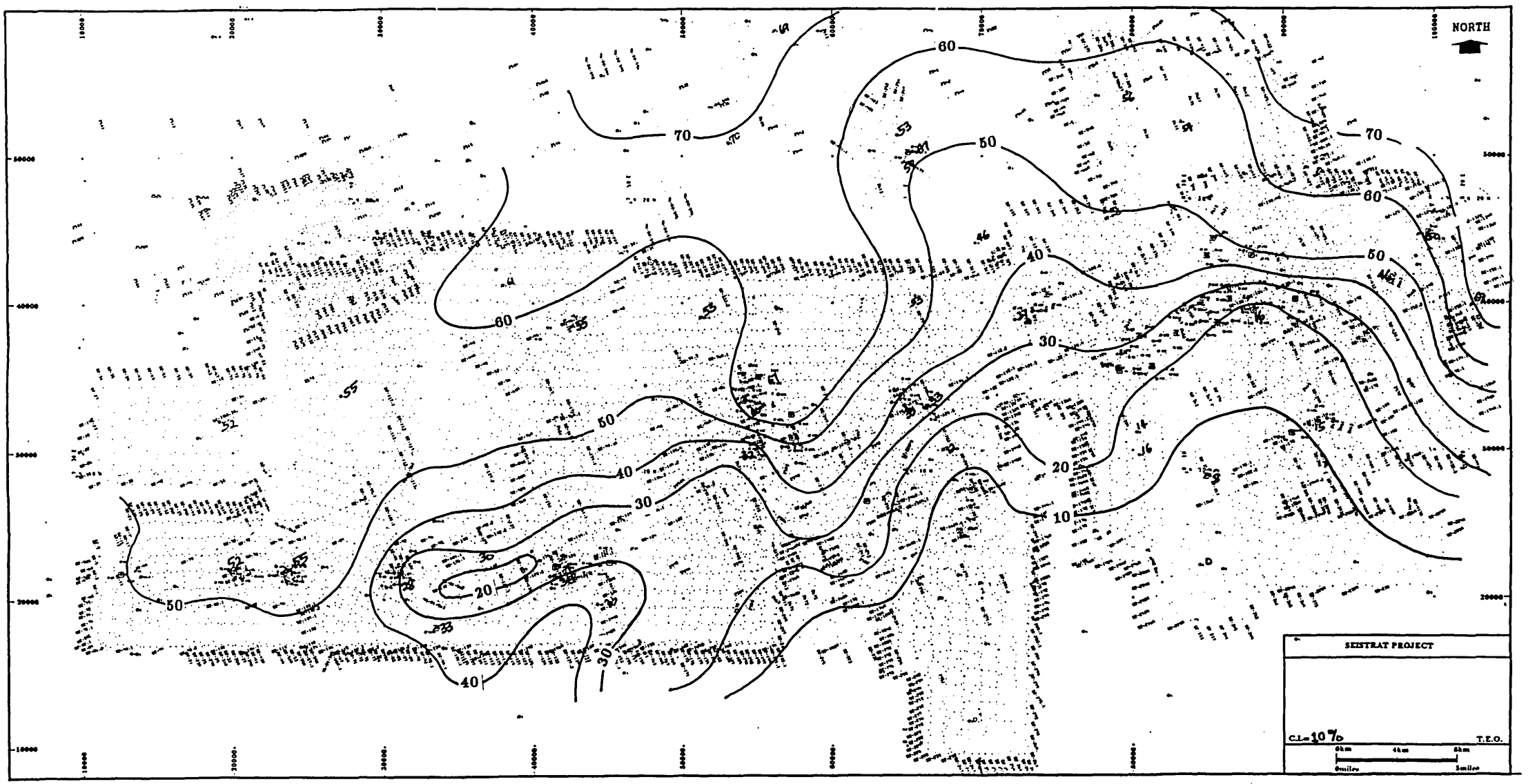

Fig.6.17b Average interval velocity map of the Biafra. Higher average interval velocities are evident to the west, north and east, corresponding to areas of either higher sand percentage and/or uplift. The eastern, northern and western parts of the acreage are known to have been tectonically active. See Structure at the TIBU and BQI levels (Fig.3.14a&b).

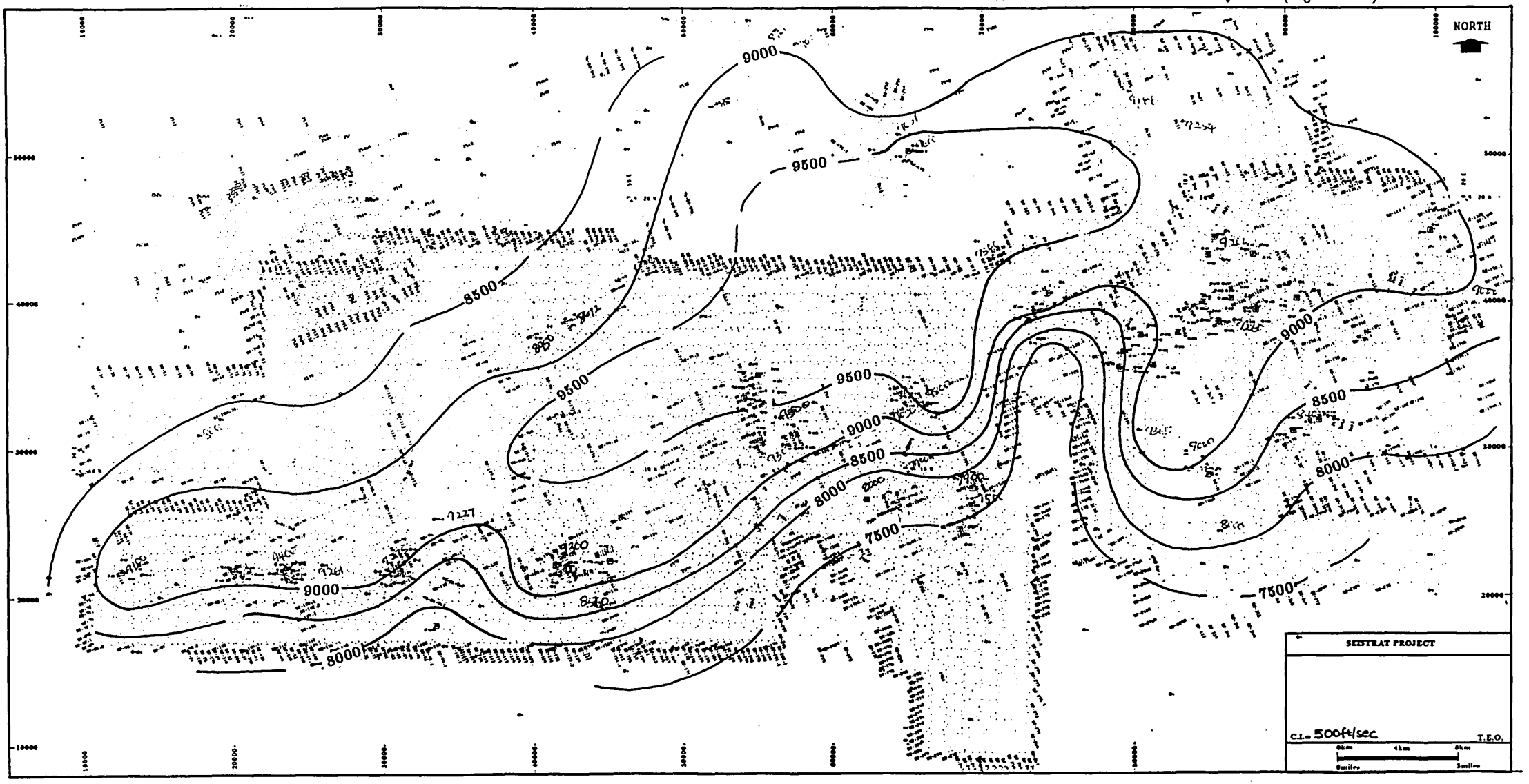

Fig.6.18 Superposition of the average velocity map and sand percentage map within the Biafra. The main sand trend falls within the zone of higher interval velocities. Within the palaeobasin, the UIBR system is the main contributor to sand development.

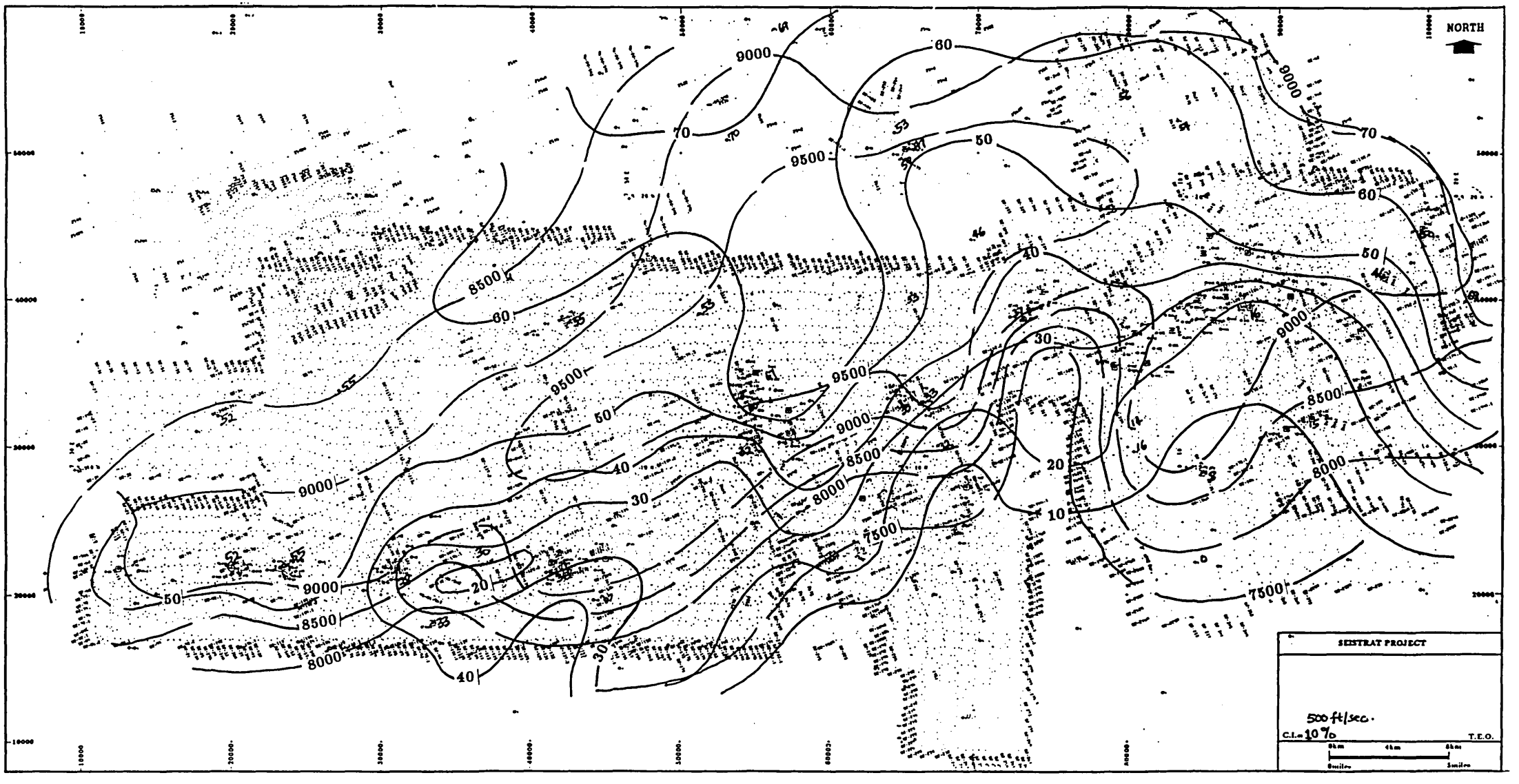

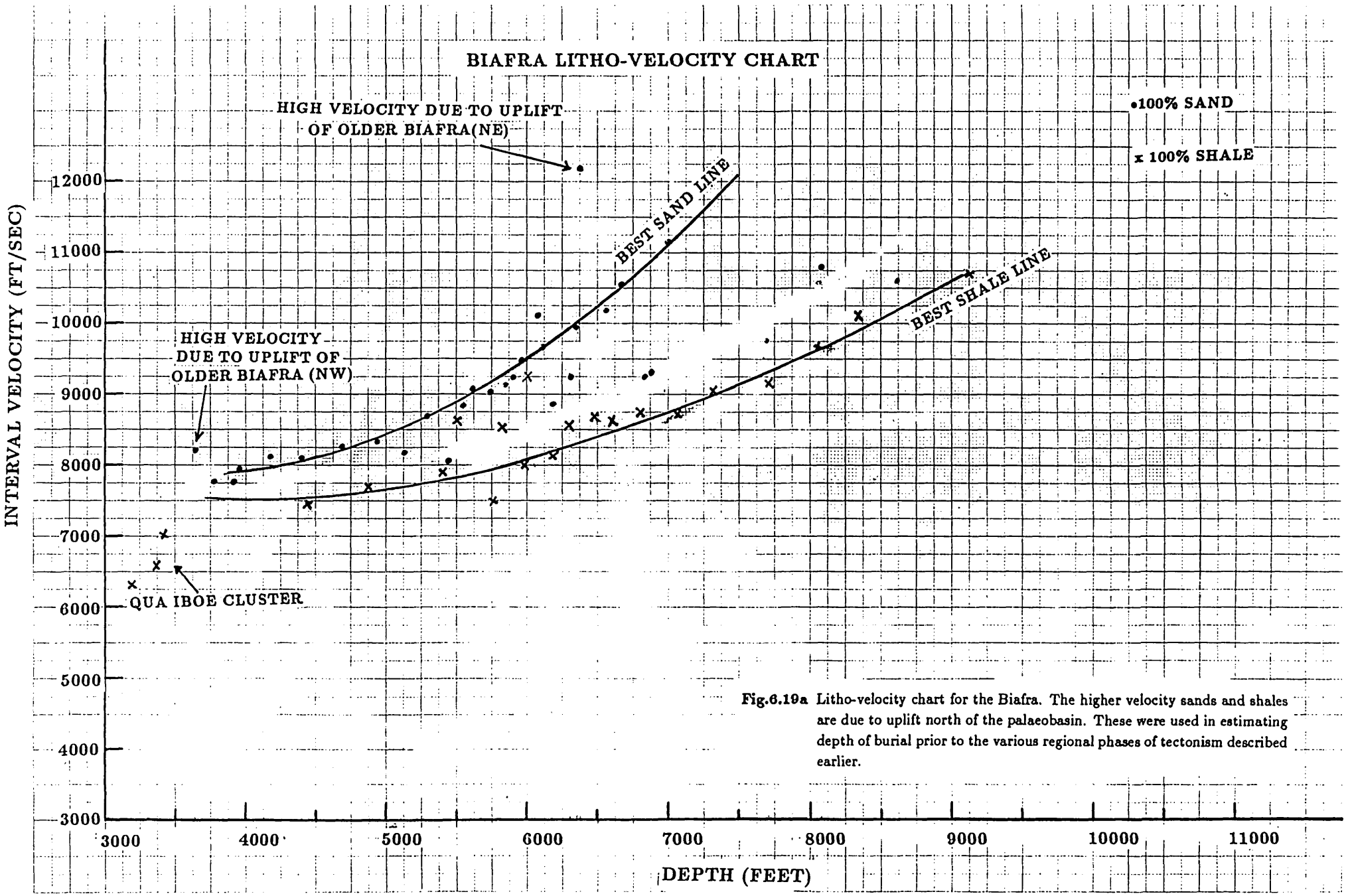

Fig.6.19a Litho-velocity chart for the Biafra. The higher velocity sands and shales are due to uplift north of the palaeobasin. These were used in estimating depth of burial prior to the various regional phases of tectonism described earlier.

Fig.6.19b Probable 'sand' distribution within the Intra Biafra Rubble regimes (UIBR and LIBR) based on seismic interval velocity analysis. This is superimposed on the seismic facies distribution map of UIBR.

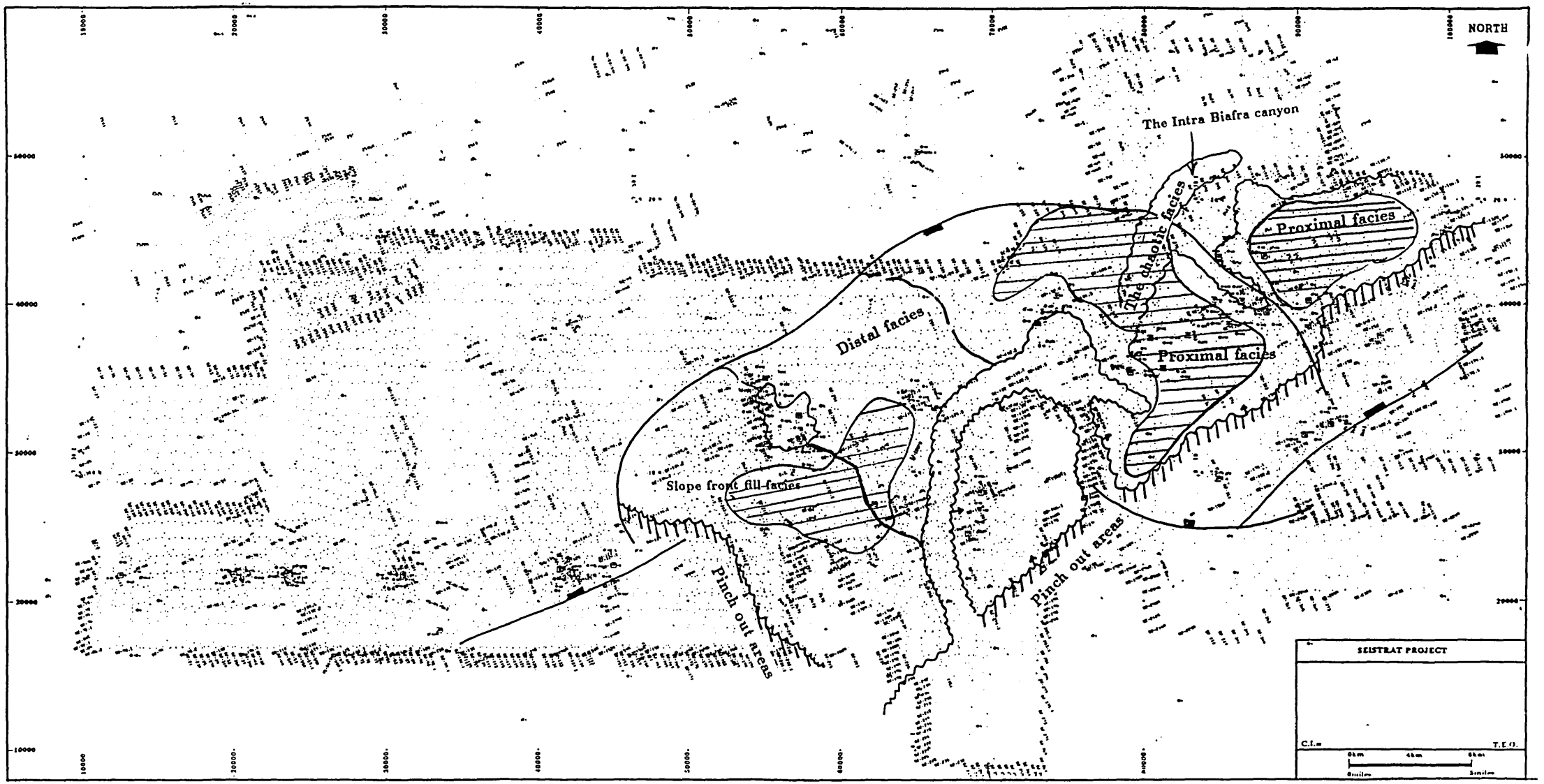

Fig.6.20 A composite map of the limit of delta front sediments for the various Biafra sequences.

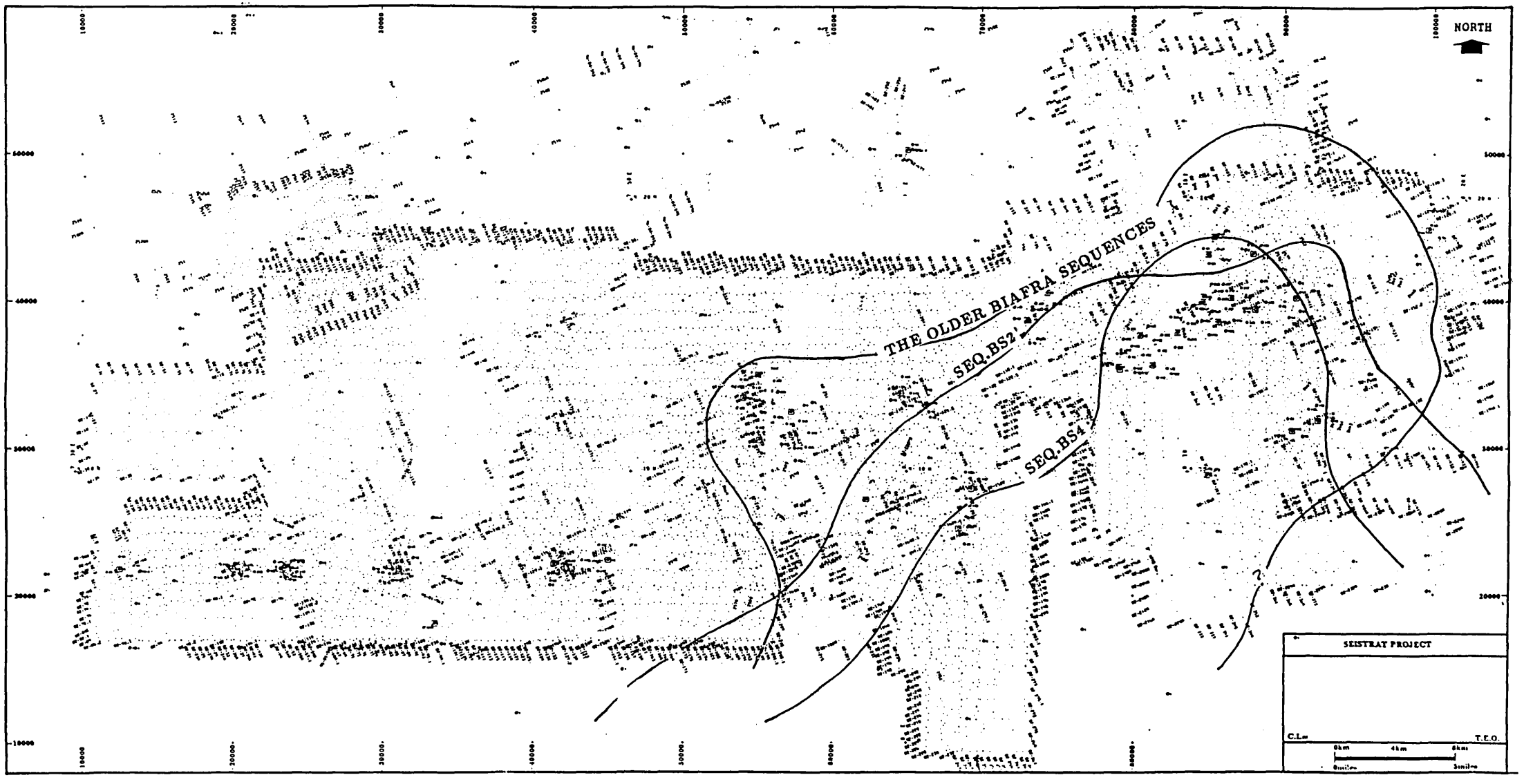

CHAPTER SEVEN

LBIBR- Lower Base Intra Biafra Rubble.

LIBU- Lower Intra Biafra Unconformity.

BIBR- Base Intra Biafra Rubble.

TIBU- Top Intra Biafra Unconformity.

BIBBEN- Base Intra Biafra Benin sands.

BRB- Base Rubble Beds

BQI- Base Qua Iboe.

TIQI- Top Intra Qua Iboe

QUA3 etc- Intra Qua Iboe horizon 3 etc

Pu- Pleistocene Unconformity

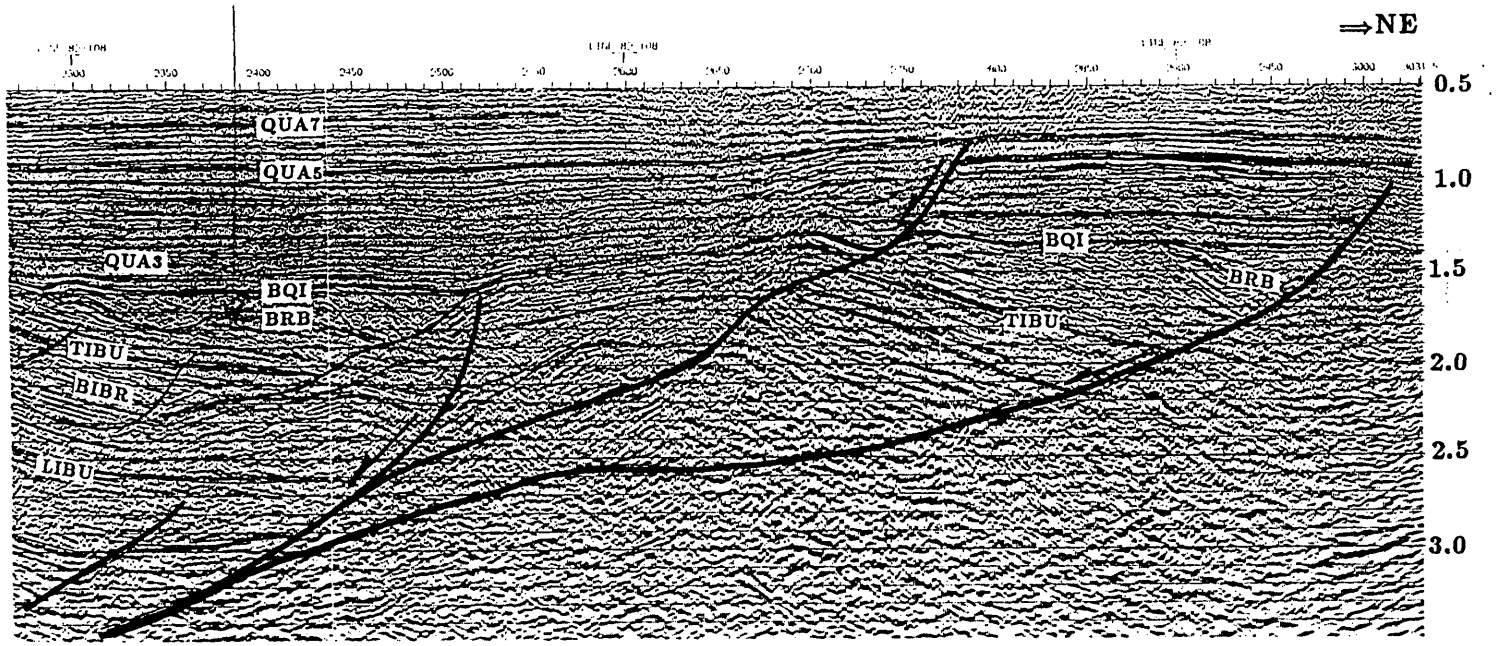

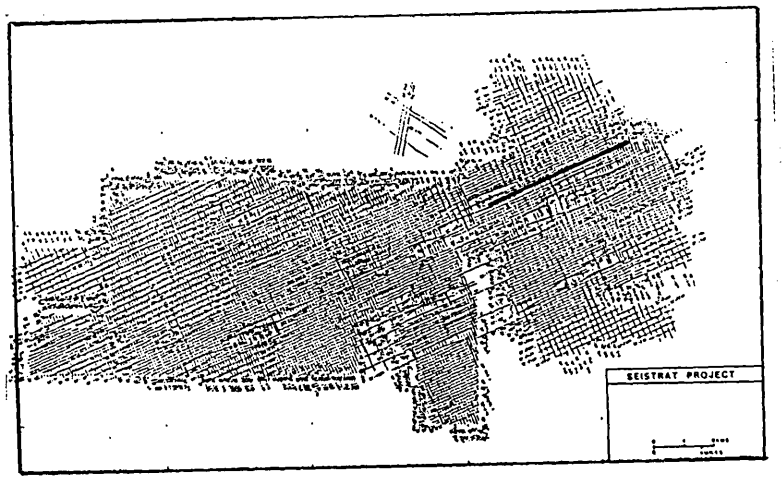

Fig.7.1 Line 82-108 shows the Base Rubble Beds(BRB) as a PGM feature. This feature occurs in the east-central part of the study area and the structure is associated with the east-central canyon system of the Rubble beds.

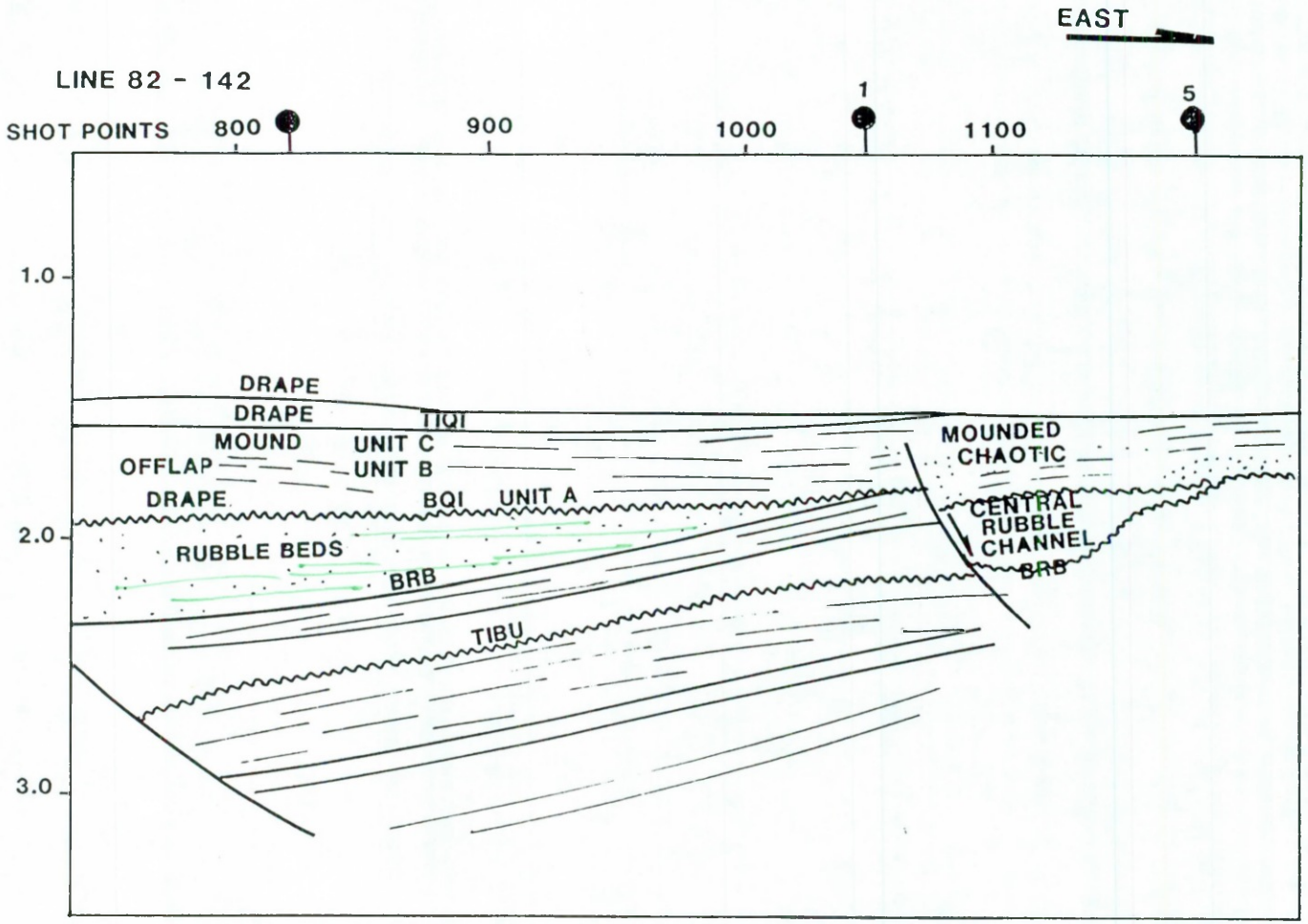

Fig.7.2 Line 82-142 shows a typical tilted fault-block with Rubble Bed onlap on both sides of the fault.

LIBBR- Lower Base Intra Biafra Rubble.

LIBU- Lower Intra Biafra Unconformity.

BIBR- Base Intra Biafra Rubble.

TIBU- Top Intra Biafra Unconformity.

BIBBEN- Base Intra Biafra Benin sands.

BRB- Base Rubble Beds

BQI- Base Qua Iboe.

TIQI- Top Intra Qua Iboe

QUA3 etc- Intra Qua Iboe horizon 3 etc

Pu- Pleistocene Unconformity

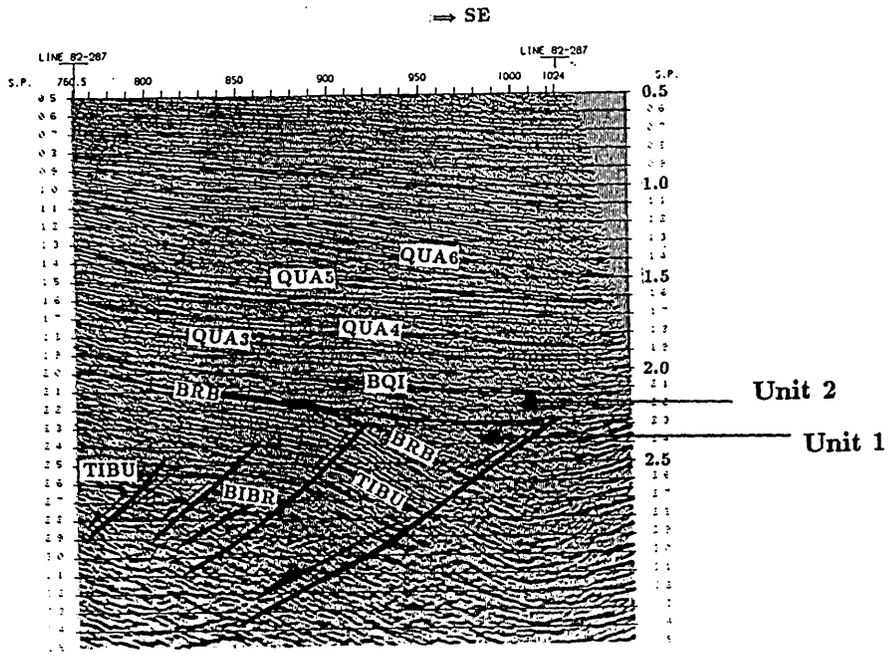

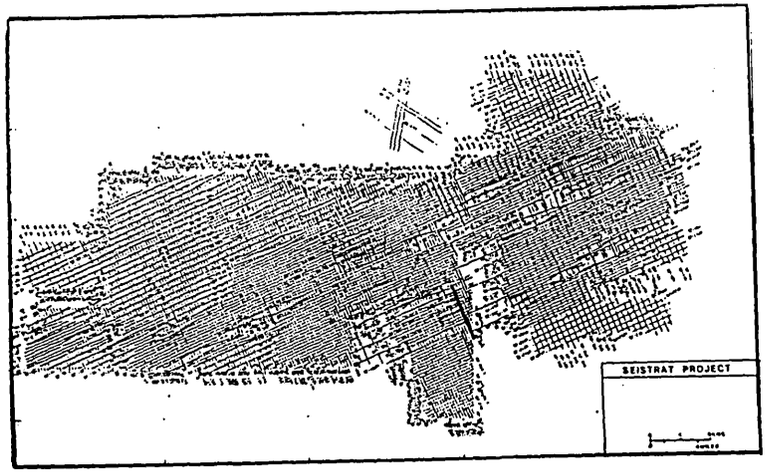

Fig.7.3a Unit 1 Rubble is shown on line 82-287 characterized by the distal facies. This sequence appears to have been formed mainly as in-filling sediments in low lying areas during sea level lowstand and are limited to the south-central embayment and east of study area.

LBIBR- Lower Base Intra Biafra Rubble.

LIBU- Lower Intra Biafra Unconformity.

BIBR- Base Intra Biafra Rubble.

TIBU- Top Intra Biafra Unconformity.

BIBBEN- Base Intra Biafra Benin sands.

BRB- Base Rubble Beds

BQI- Base Qua Iboe.

TIQI- Top Intra Qua Iboe

QUA3 etc- Intra Qua Iboe horizon 3 etc

Pu- Pleistocene Unconformity

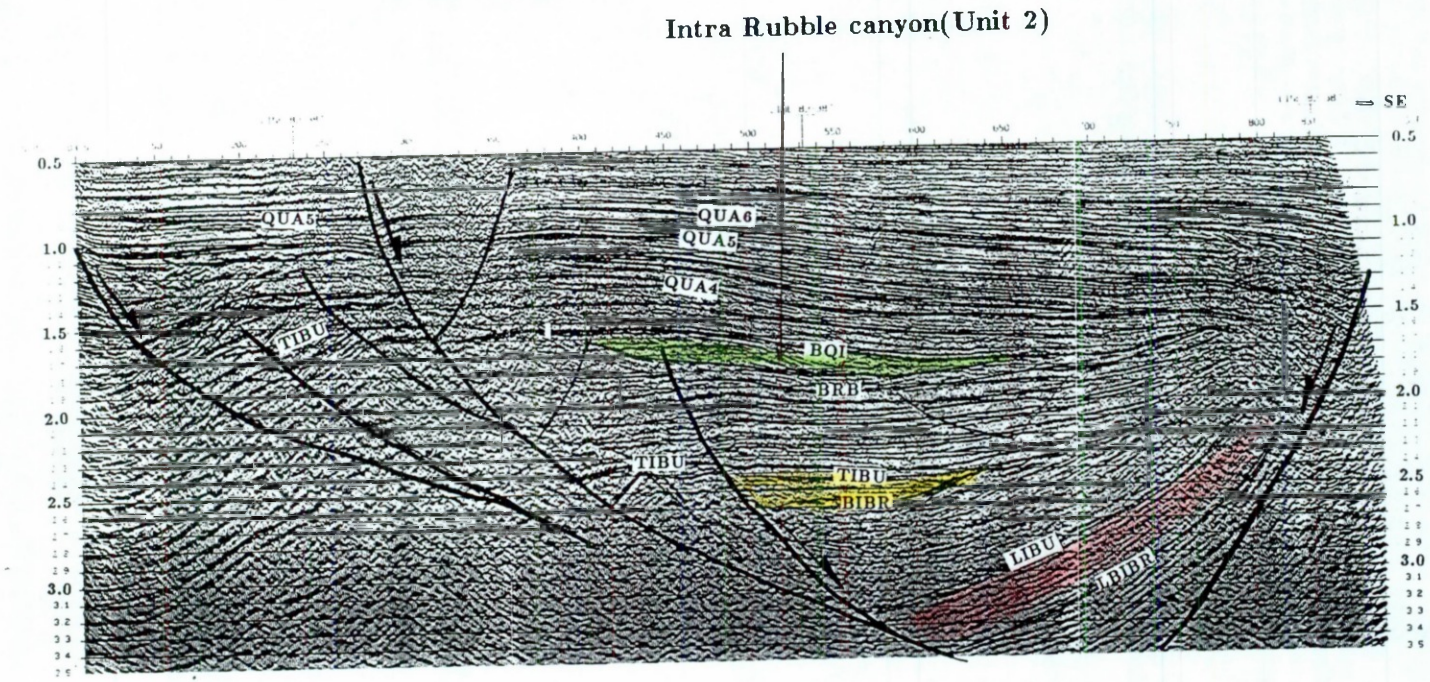

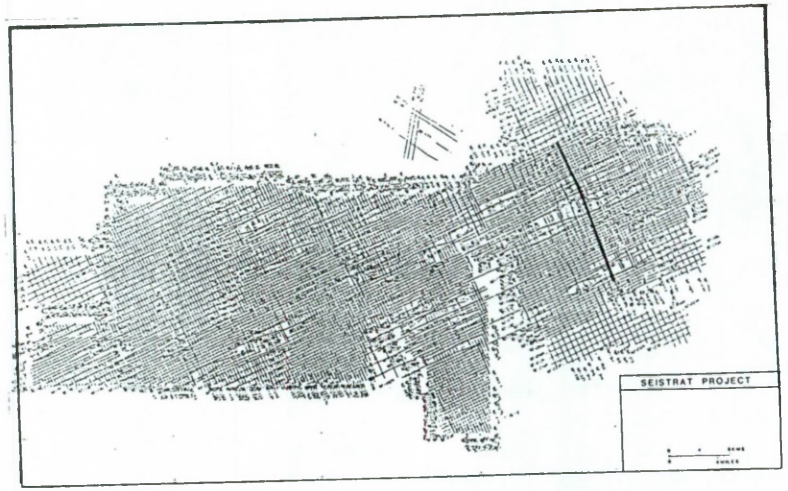

Fig.7.3b Unit 2 Rubble (82-387) is often characterized by canyon development, chaotic and offlapping fill facies.

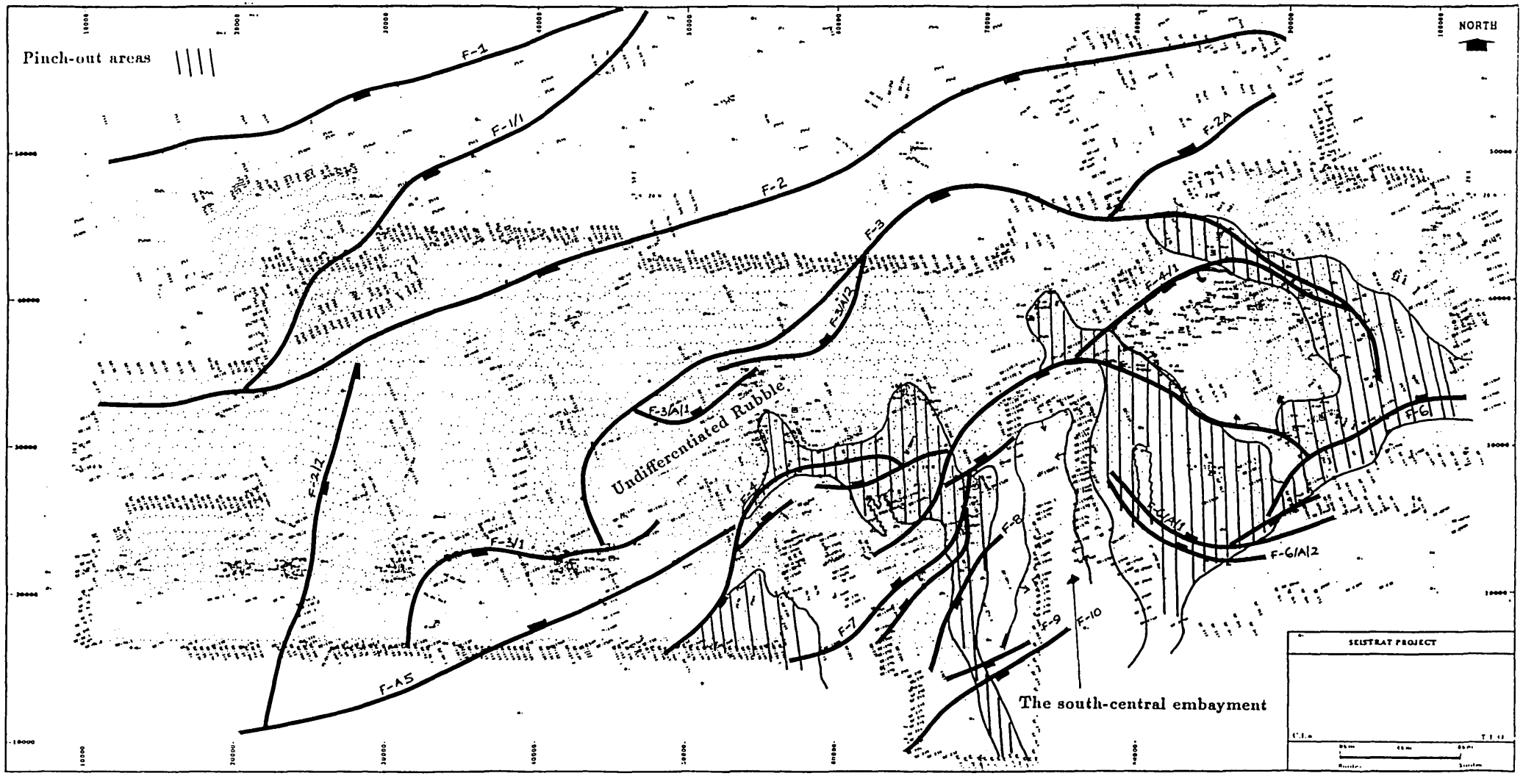

Fig.7.4 Limits of the distribution of Unit 1 Rubble Beds.

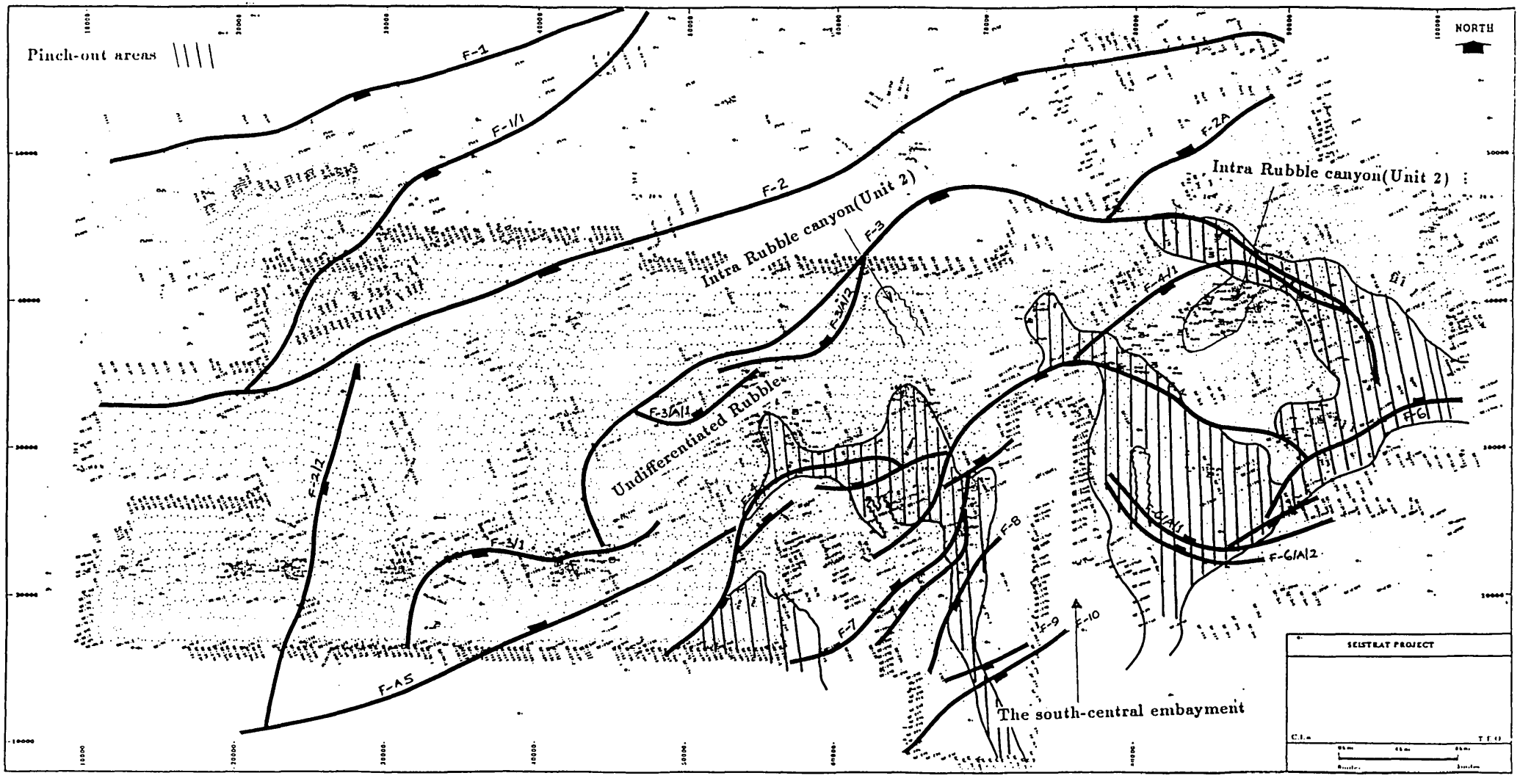

Fig.7.5 Limits of the distribution of Unit 2 Rubble Beds.

SEISMIC FACIES UNITS OF RUBBLE BEDS

	UNIT	ENVIRONMENTAL FACIES INTERPRETATION
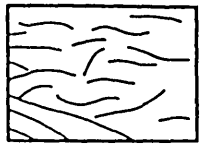	(1) CHAOTIC FILL - COMMONLY EROSIONAL GOUGE AT BASE.	GRAVITY, MASS TRANSPORT AND HIGH ENERGY. TURBIDITY CURRENT SEDIMENTS.
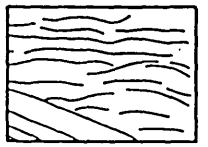	(2) MOUNDED ONLAPPING FILL - IRREGULARY MOUNDED, CONTINUOUS, WAVY TO PARALLEL.	RELATIVELY HIGH VELOCITY TURBIDITY CURRENT DEPOSITS.
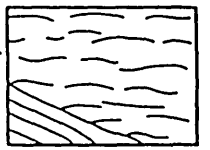	(3) PROXIMAL ONLAPPING FILL - PRIMARILY HUMMOCKY, GRADING UPWARD INTO MORE CONTINUOUS REFLECTION CONFIGURATION.	MODERATELY HIGH VELOCITY TURBIDITY CURRENT DEPOSITS COMMONLY GRADING TO CHAOTIC AND MOUNDED ONLAP FILL.
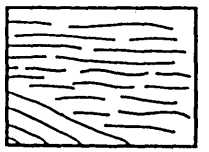	(4) DISTAL ONLAPPING FILL - MORE SUBDUED HUMMOCKY CONFIGURATION AND HIGHER CONTINUITY THAN (3).	RELATIVELY LOW VELOCITY TURBIDITY DEPOSITS, LOWER ENERGY ENVIRONMENT LOCATED FURTHER FROM SOURCE AREA THAN PROXIMAL ONLAPPING FILL.
	(5) PROGRADING FILL CHARACTERIZED BY PROGRADING CLINOFORMS WITH PROMINENT REFLECTORS, OFTEN HUMMOCKY AT THE BASE.	HIGH TO MODERATE VELOCITY TURBIDITY DEPOSITS COMMONLY GRADING TO MOUNDED ONLAP

Fig.7.6 Seismic facies types of the Rubble Beds.

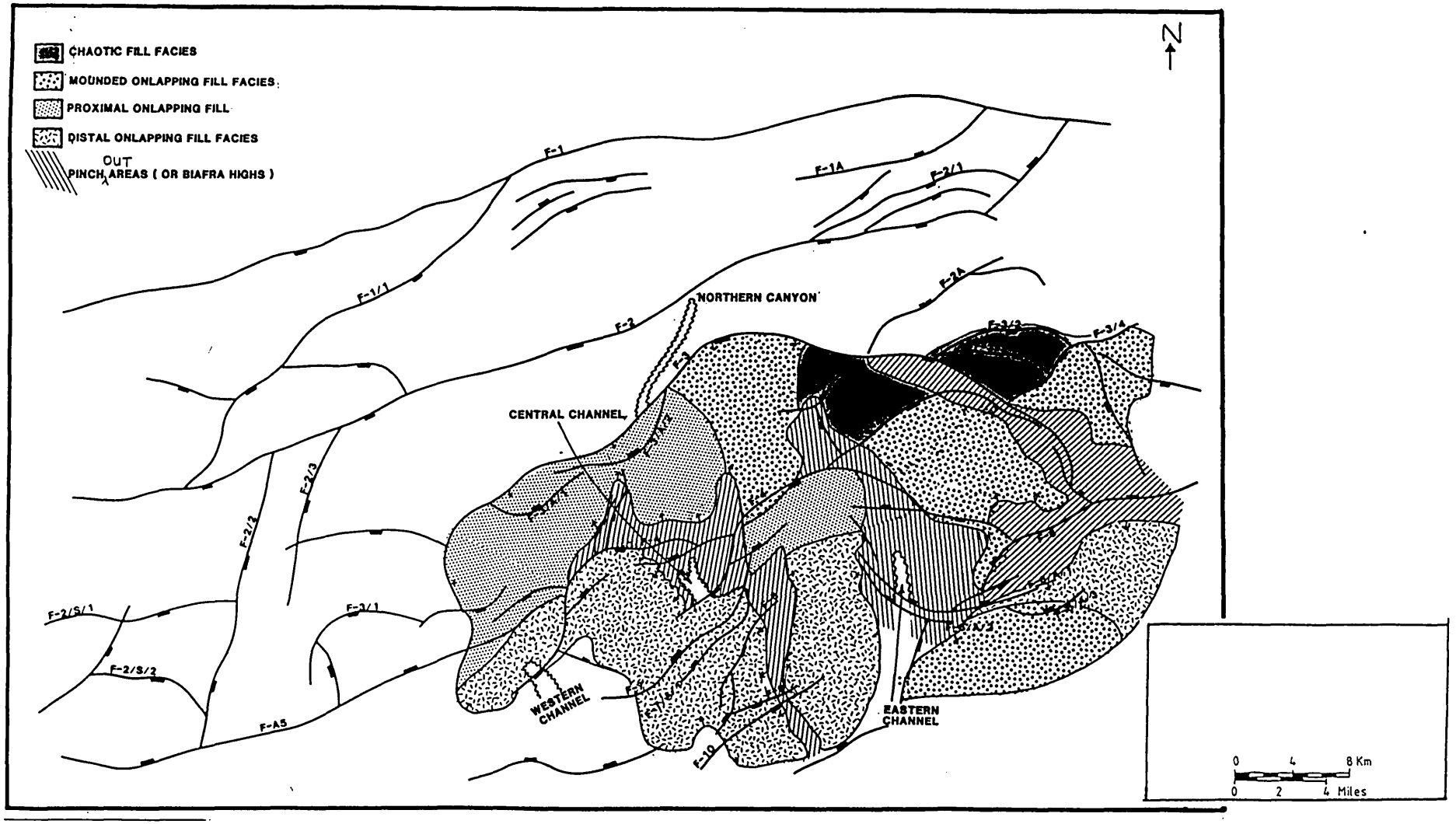

Fig.7.7 Facies distribution of the Rubble Beds.

LBIBR- Lower Base Intra Biafra Rubble.

LIBU- Lower Intra Biafra Unconformity.

BIBR- Base Intra Biafra Rubble.

TIBU- Top Intra Biafra Unconformity.

BIBBEN- Base Intra Biafra Benin sands.

BRB- Base Rubble Beds

BQI- Base Qua Iboe.

TIQI- Top Intra Qua Iboe

QUA3 etc- Intra Qua Iboe horizon 3 etc

Pu- Pleistocene Unconformity

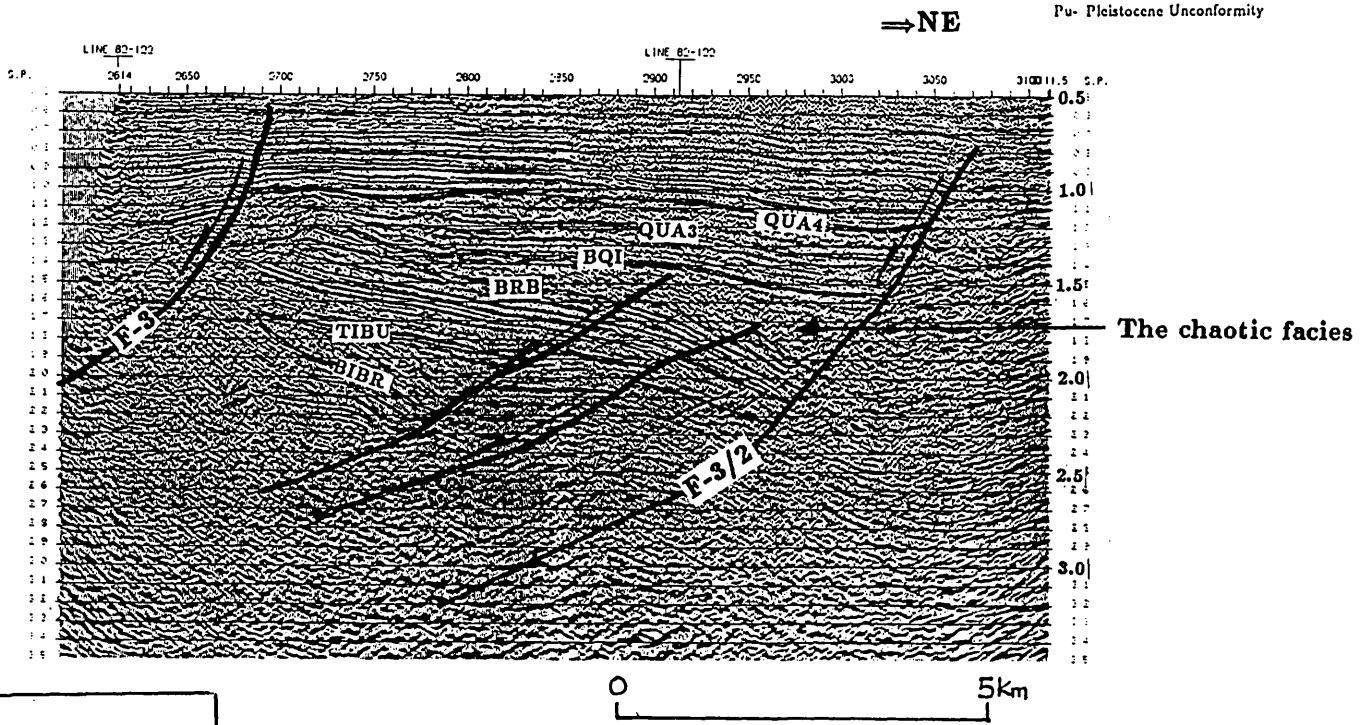

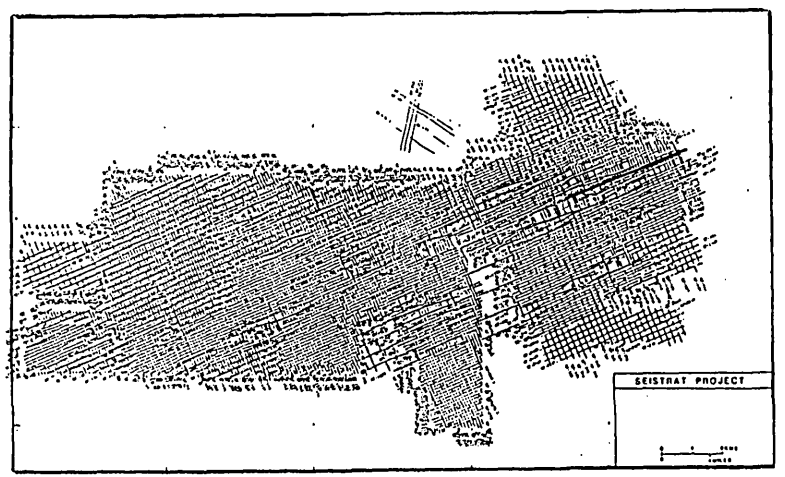

Fig.7.8a Line 82-122, The chaotic facies.

LBIBR- Lower Base Intra Biafra Rubble.

LIBU- Lower Intra Biafra Unconformity.

BIBR- Base Intra Biafra Rubble.

TIBU- Top Intra Biafra Unconformity.

BIBBEN- Base Intra Biafra Benin sands.

BRB- Base Rubble Beds

BQI- Base Qua Iboe.

TIQI- Top Intra Qua Iboe

QUA3 etc- Intra Qua Iboe horizon 3 etc

Pu- Pleistocene Unconformity

The proximal facies

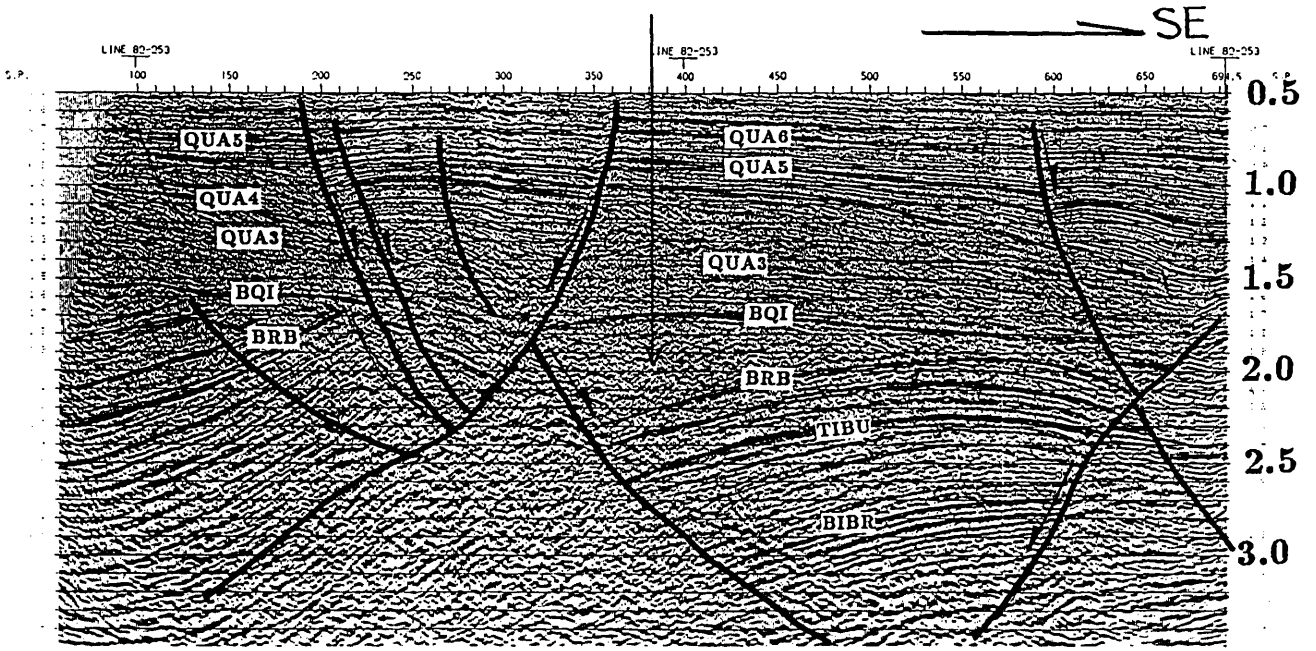

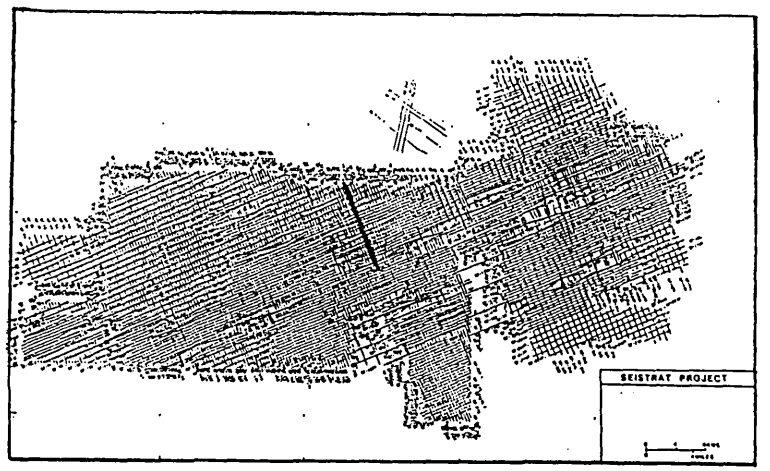

Fig.7.8b Line 82-253, the proximal facies.

LBIBR- Lower Base Intra Biafra Rubble.

LIBU- Lower Intra Biafra Unconformity.

BIBR- Base Intra Biafra Rubble.

TIBU- Top Intra Biafra Unconformity.

BIBBEN- Base Intra Biafra Benin sands.

BRB- Base Rubble Beds

BQI- Base Qua Iboe.

TIQI- Top Intra Qua Iboe

QUA3 etc- Intra Qua Iboe horizon 3 etc

Pu- Pleistocene Unconformity

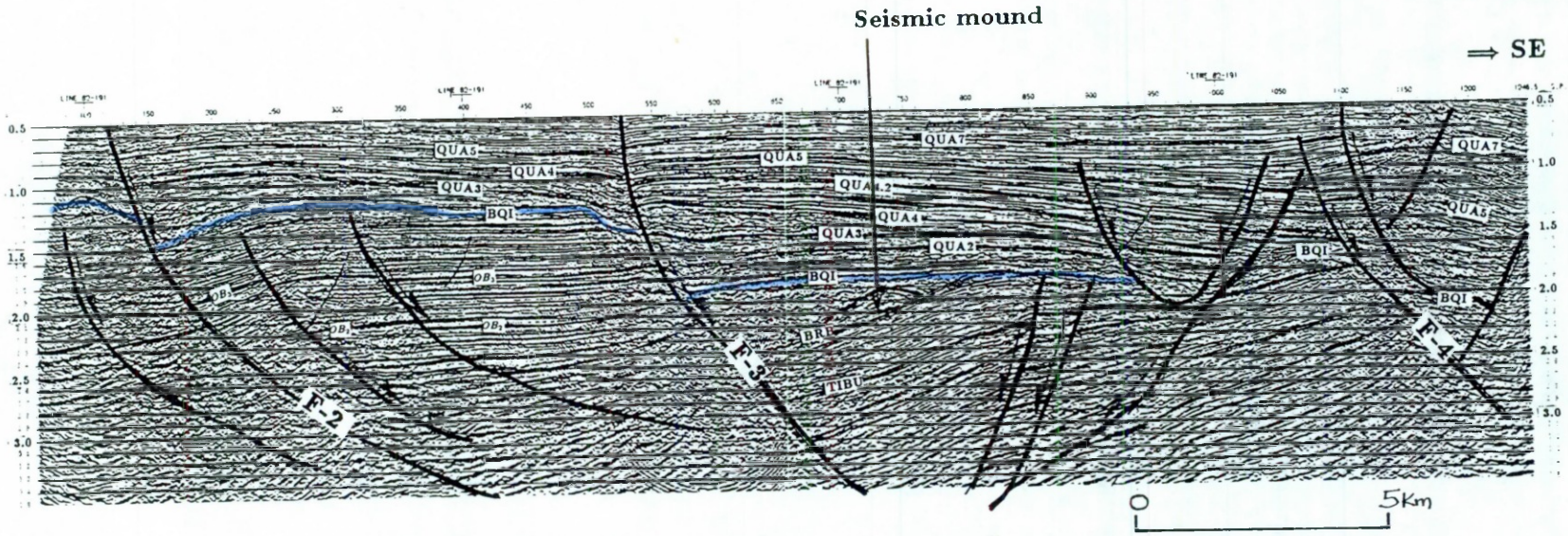

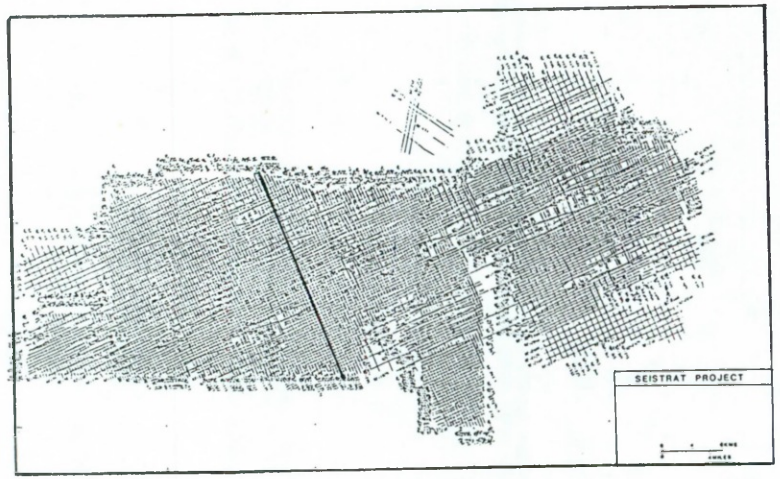

Fig.7.8c Line 82-191, the proximal facies showing seismic mounding at the base.

LIBR- Lower Base Intra Biafra Rubble.

LIBU- Lower Intra Biafra Unconformity.

BIBR- Base Intra Biafra Rubble.

TIBU- Top Intra Biafra Unconformity.

BIBBEN- Base Intra Biafra Benin sands.

BRB- Base Rubble Beds

BQI- Base Qua Iboe.

TIQI- Top Intra Qua Iboe

QUA3 etc- Intra Qua Iboe horizon 3 etc

Pu- Pleistocene Unconformity

The mounded onlap facies

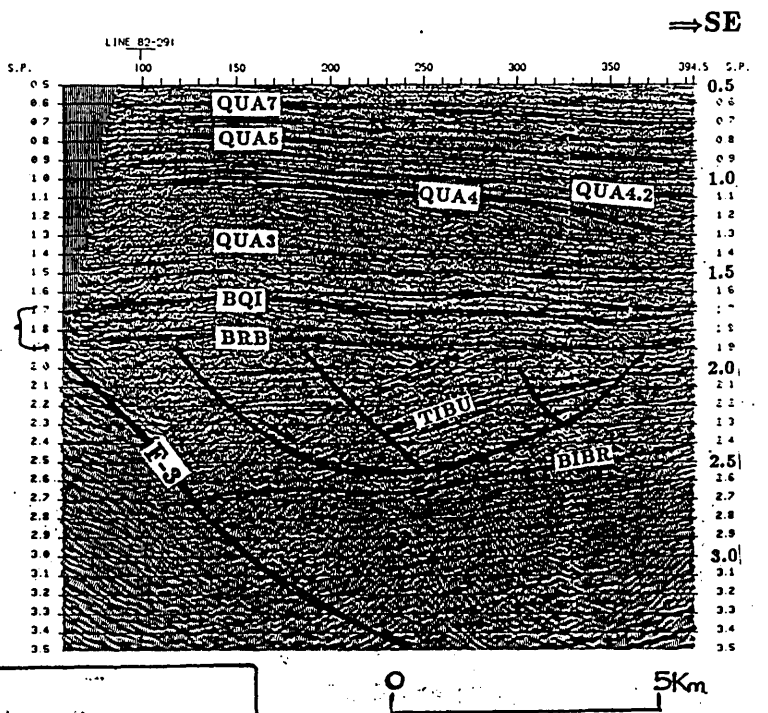

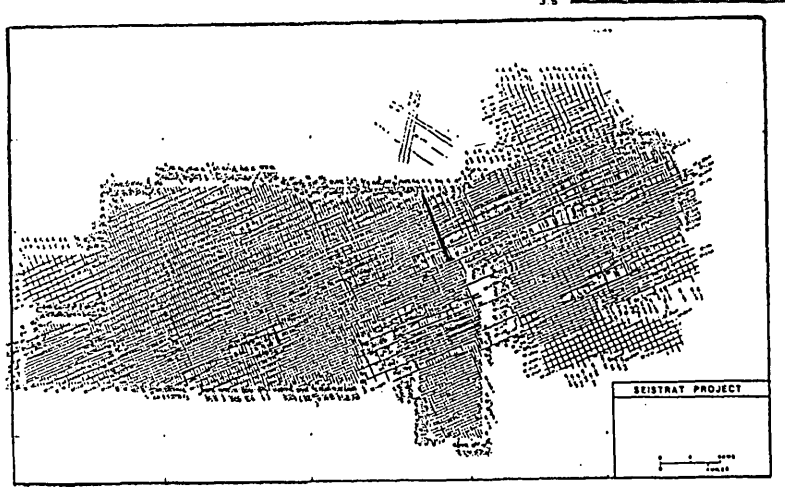

Fig.7.8d Line 82-291, the mounded onlap facies.

LBIBR- Lower Base Intra Biafra Rubble.

LIBU- Lower Intra Biafra Unconformity.

BIBR- Base Intra Biafra Rubble.

TIBU- Top Intra Biafra Unconformity.

BIBBEN- Base Intra Biafra Benin sands.

BRB- Base Rubble Beds

BQI- Base Qua Iboe.

TIQI- Top Intra Qua Iboe

QUA3 etc- Intra Qua Iboe horizon 3 etc

Pu- Pleistocene Unconformity

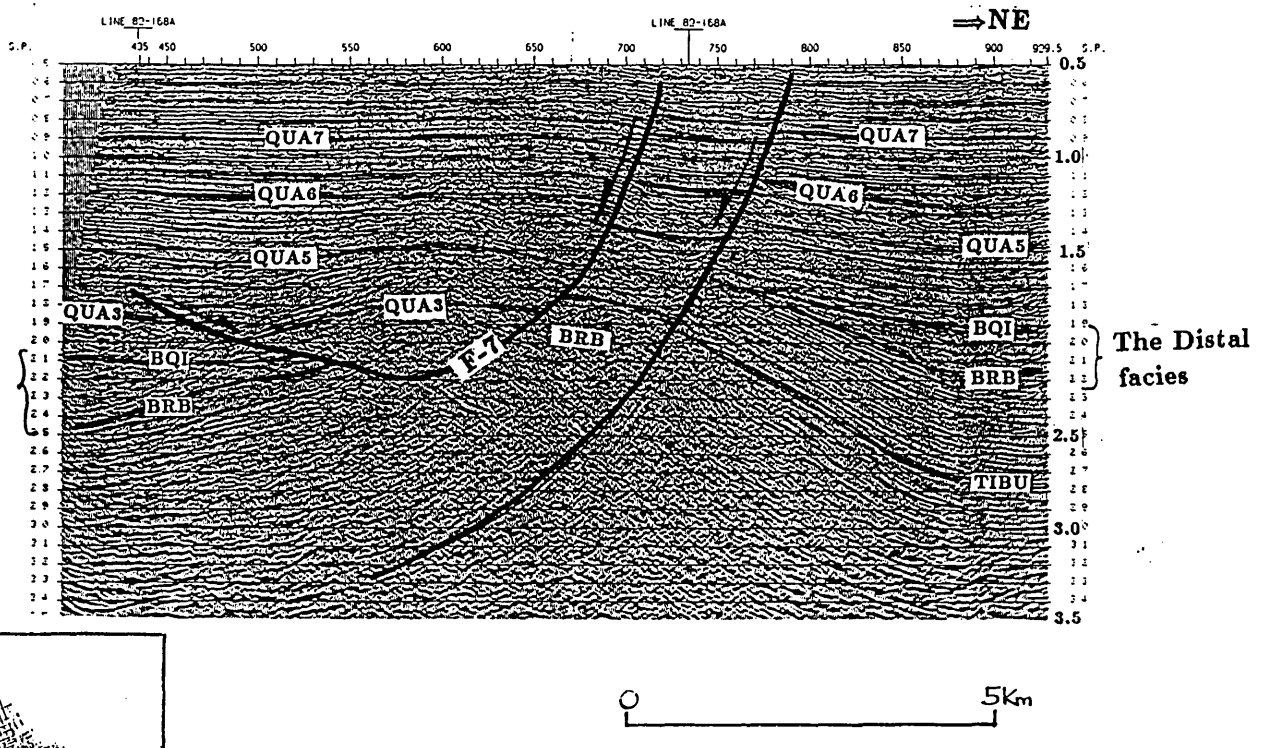

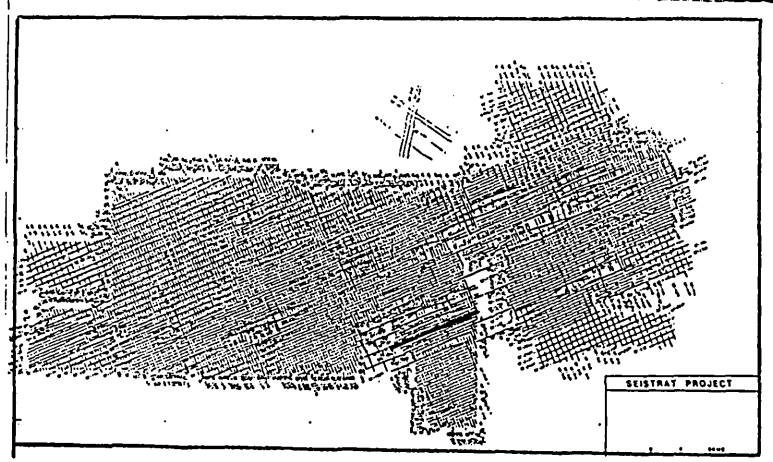

Fig.7.8e Line 82-168a, the distal onlap facies.

LBIBR- Lower Base Intra Biafra Rubble.

LIBU- Lower Intra Biafra Unconformity.

BIBR- Base Intra Biafra Rubble.

TIBU- Top Intra Biafra Unconformity.

BIBBEN- Base Intra Biafra Benin sands.

BRB- Base Rubble Beds

BQI- Base Qua Iboe.

TIQI- Top Intra Qua Iboe

QUA3 etc- Intra Qua Iboe horizon 3 etc

Pu- Pleistocene Unconformity

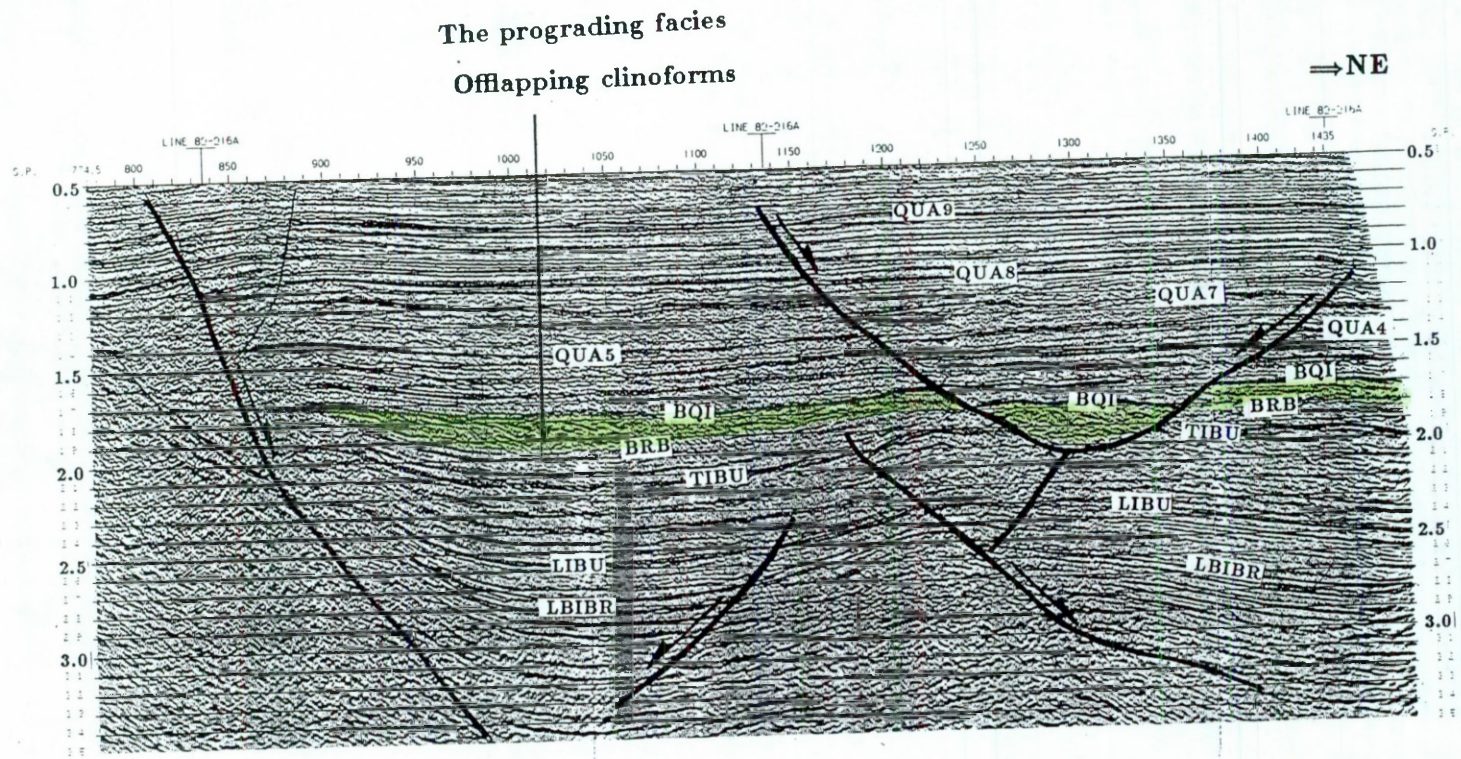

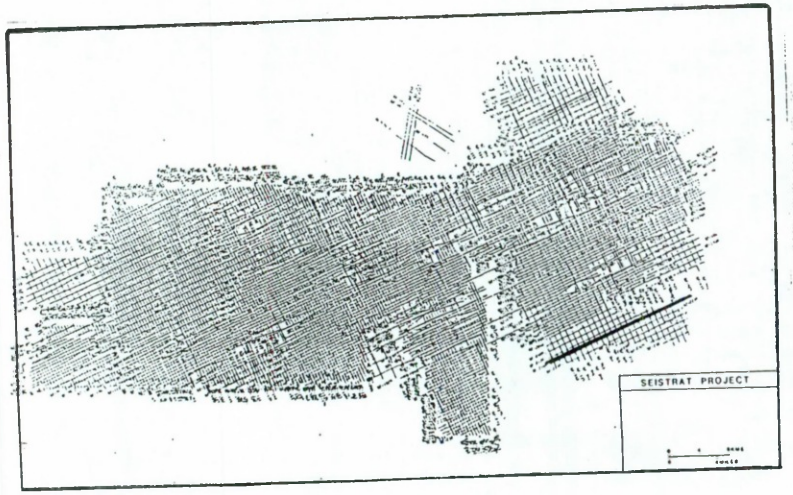

Fig.7.8f Line 82-216a, the prograding facies.

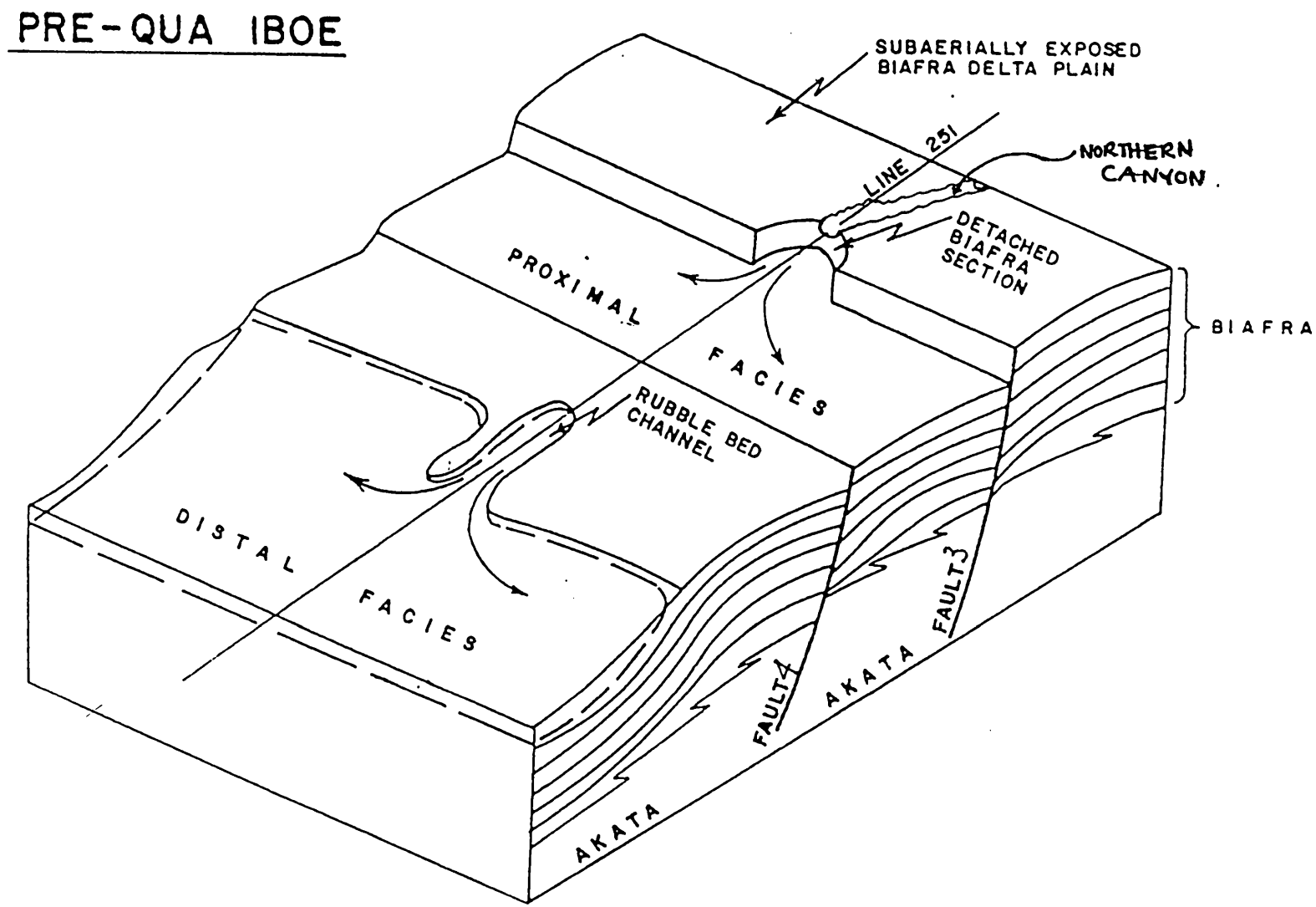

Fig.7.9a Rubble Bed depositional model.

TEO

PROPOSED MECHANISMS FOR BIAFRA MEMBER EROSION

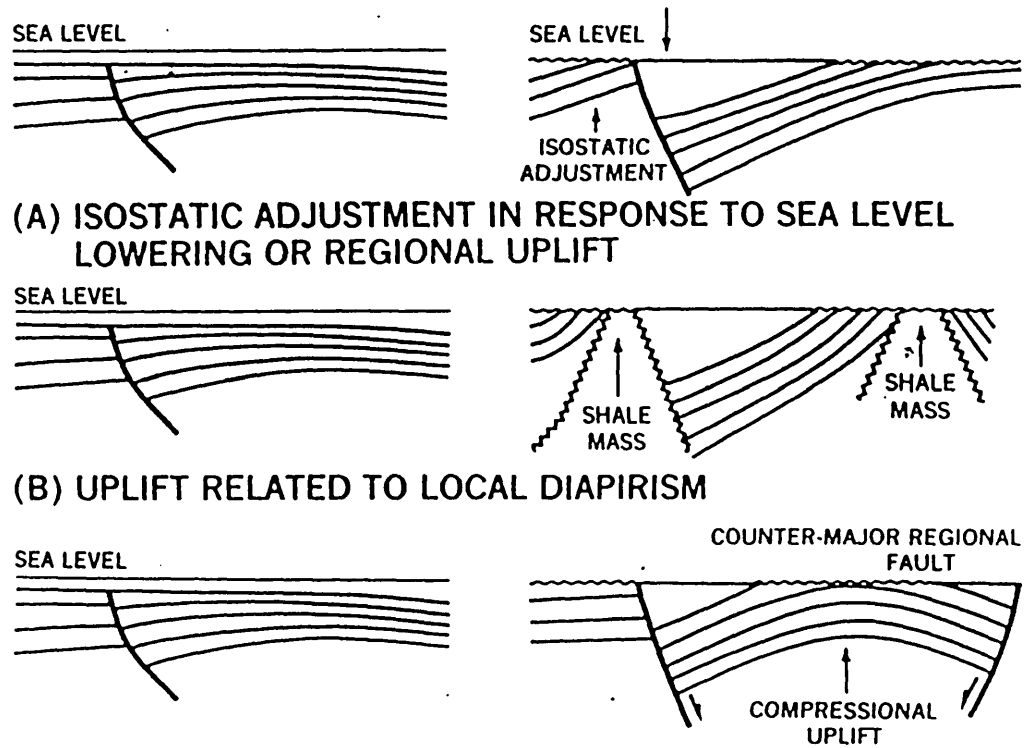

Fig.7.9b An illustration showing the various likely mechanisms for Rubble Bed formation.

THE MASS GRAVITY TRANSPORT PROCESS
(APPLICATION TO THE STUDY AREA)

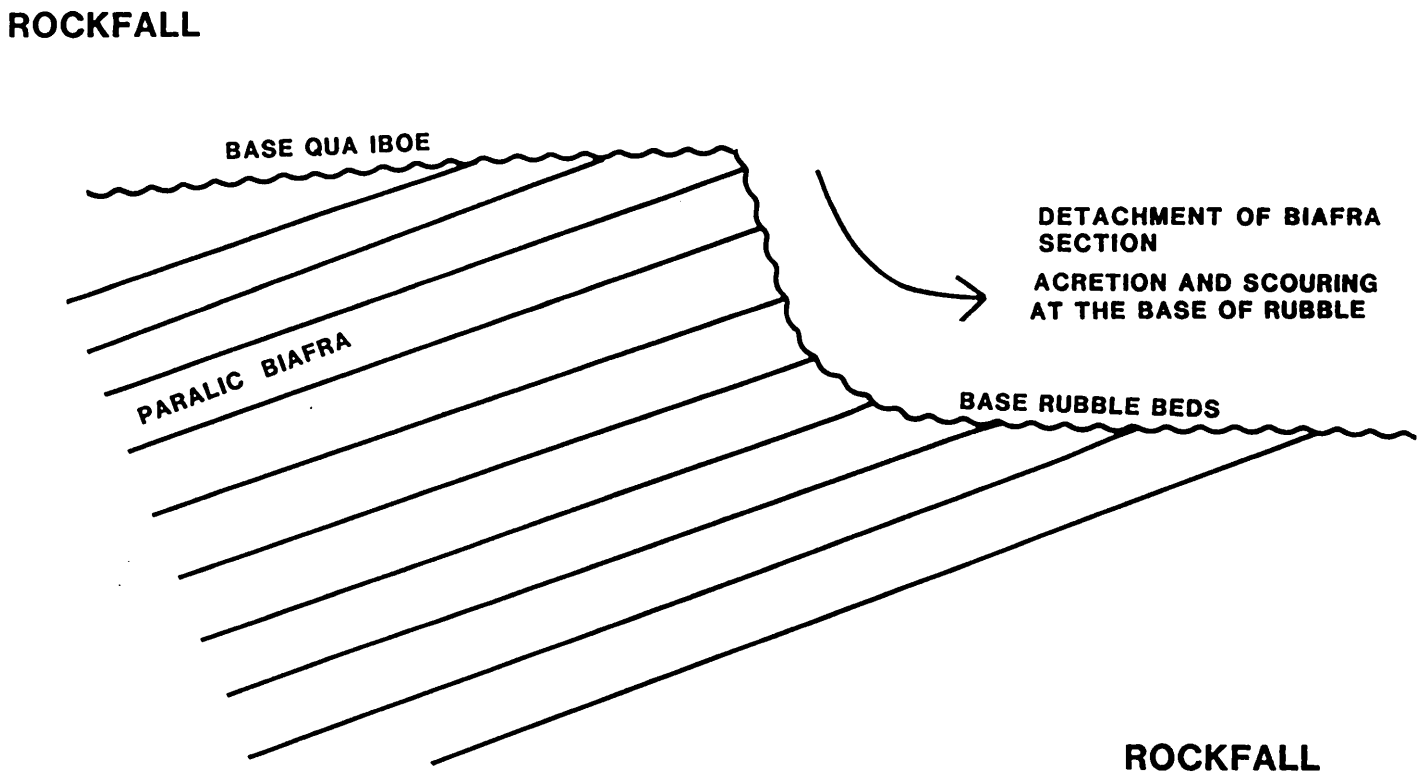

MODIFIED FROM KRUIT ET AL 1975

Fig.7.10a Rockfall.

LBIBR- Lower Base Intra Biafra Rubble.

LIBU- Lower Intra Biafra Unconformity.

BIBR- Base Intra Biafra Rubble.

TIBU- Top Intra Biafra Unconformity.

BIBBEN- Base Intra Biafra Benin sands.

BRB- Base Rubble Beds

BQI- Base Qua Iboe.

TIQI- Top Intra Qua Iboe

QUA3 etc- Intra Qua Iboe horizon 3 etc

Pu- Pleistocene Unconformity

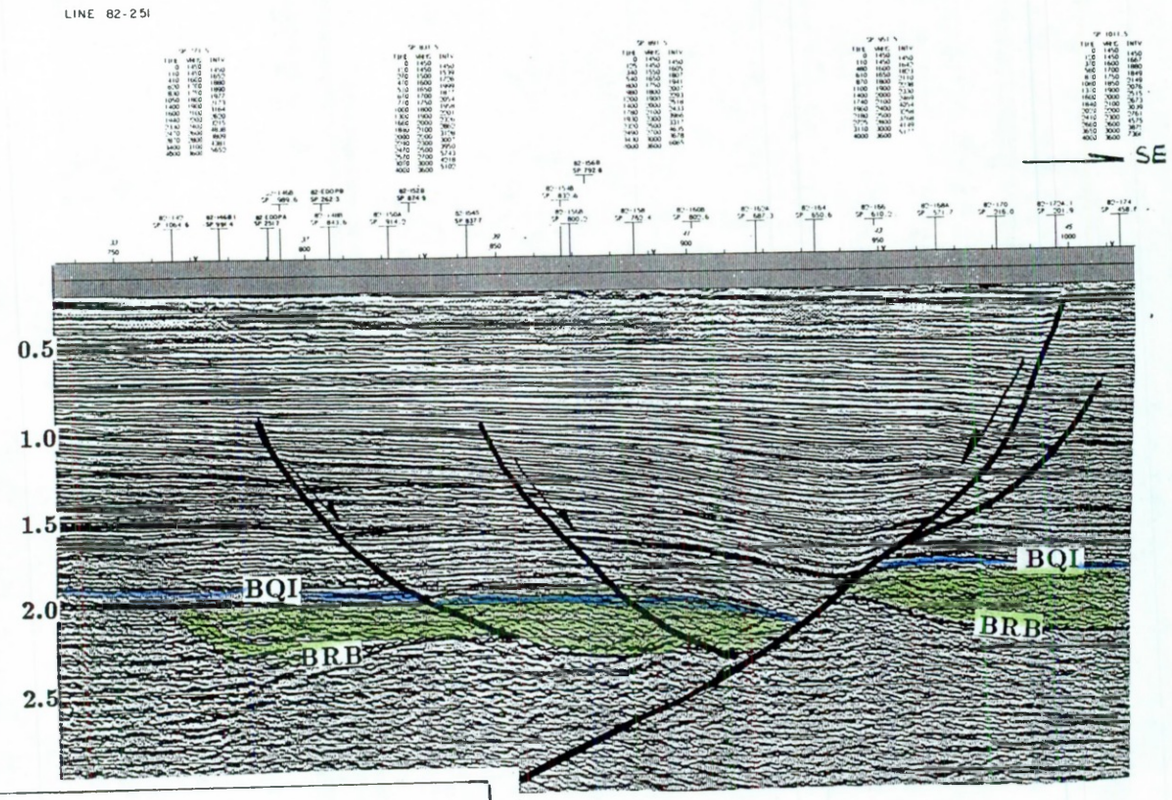

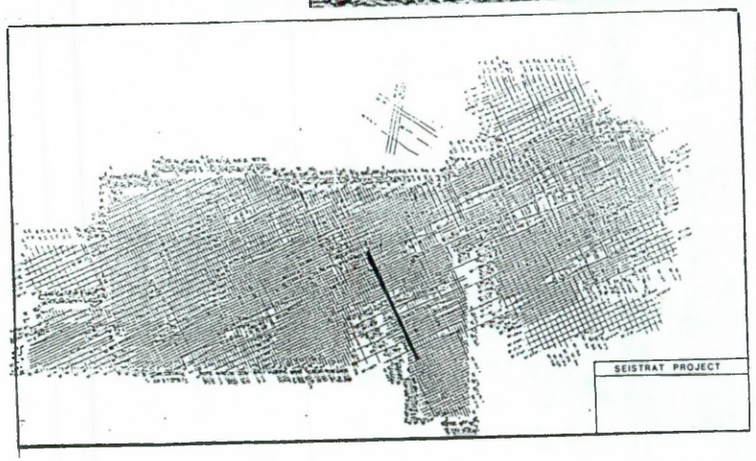

Fig.7.10b Development of channel system(82-251) .

LBIBR- Lower Base Intra Biafra Rubble.

LIBU- Lower Intra Biafra Unconformity.

BIBR- Base Intra Biafra Rubble.

TIBU- Top Intra Biafra Unconformity.

BIBBEN- Base Intra Biafra Benin sands.

BRB- Base Rubble Beds

BQI- Base Qua Iboe.

TIQI- Top Intra Qua Iboe

QUA3 etc- Intra Qua Iboe horizon 3 etc

Pu- Pleistocene Unconformity

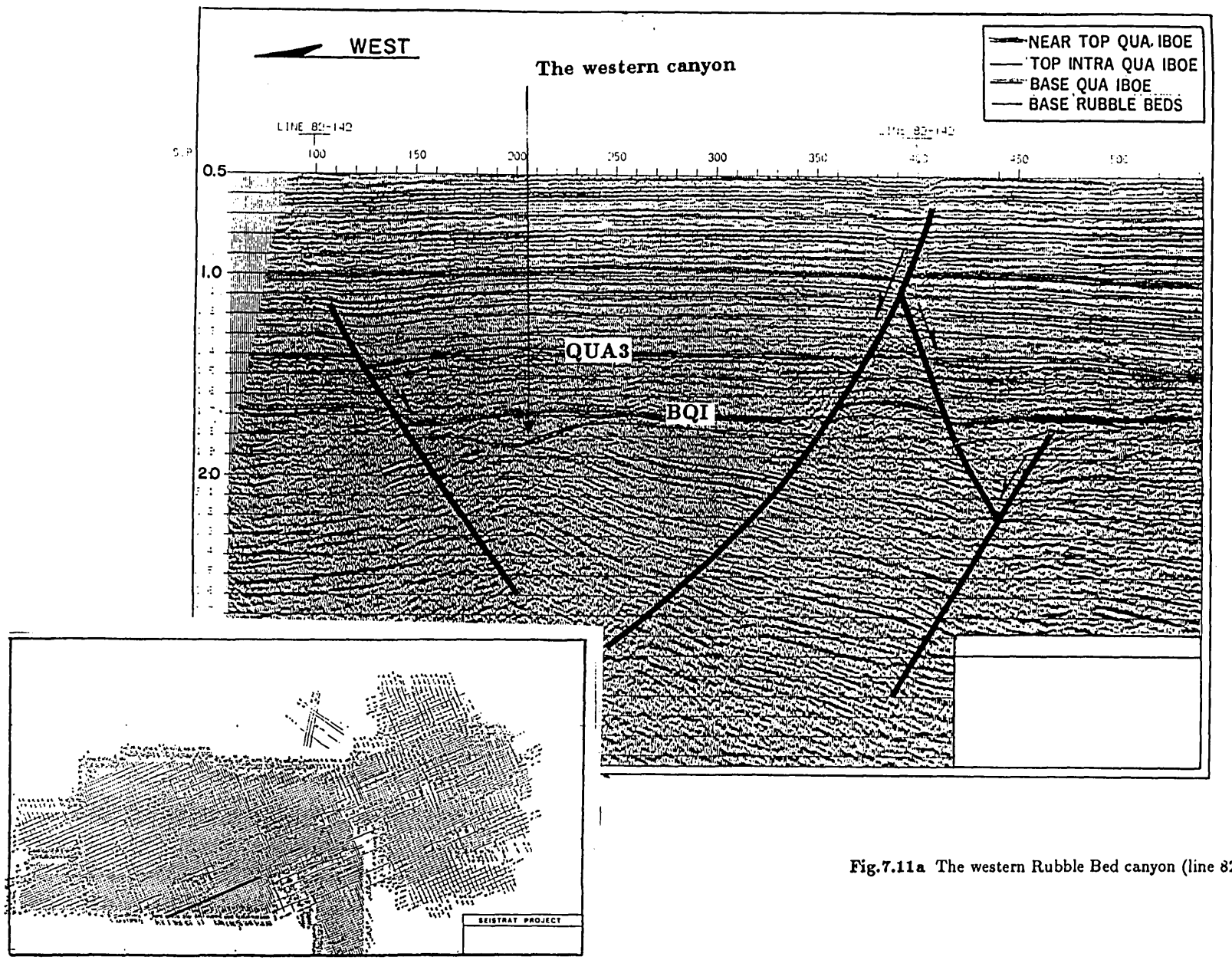

Fig.7.11a The western Rubble Bed canyon (line 82-142).

LBIBR- Lower Base Intra Biafra Rubble.

LIBU- Lower Intra Biafra Unconformity.

BIBR- Base Intra Biafra Rubble.

TIBU- Top Intra Biafra Unconformity.

BIBBEN- Base Intra Biafra Benin sands.

BRB- Base Rubble Beds

BQI- Base Qua Iboe.

TIQI- Top Intra Qua Iboe

QUA3 etc- Intra Qua Iboe horizon 3 etc

Pu- Pleistocene Unconformity

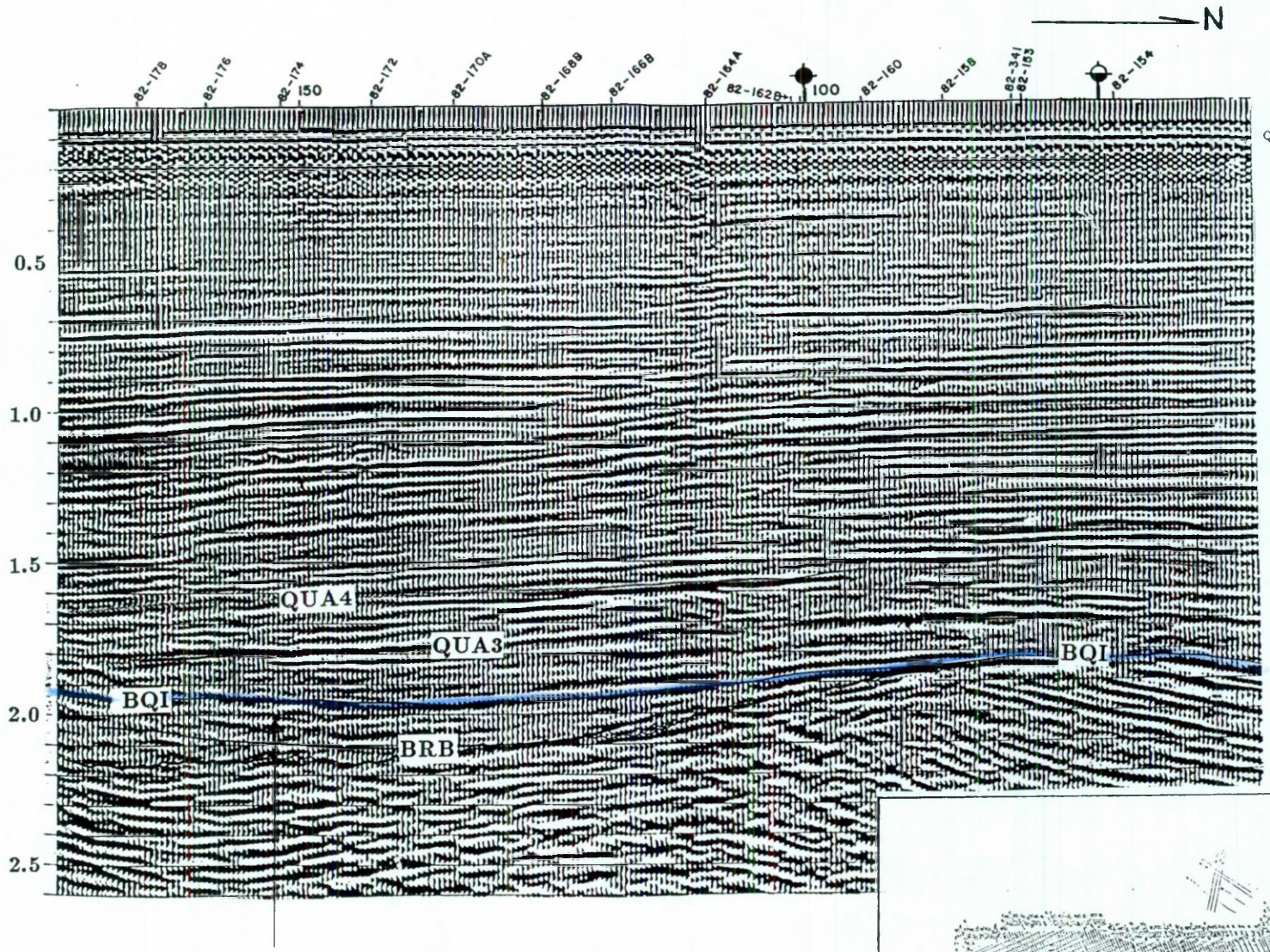

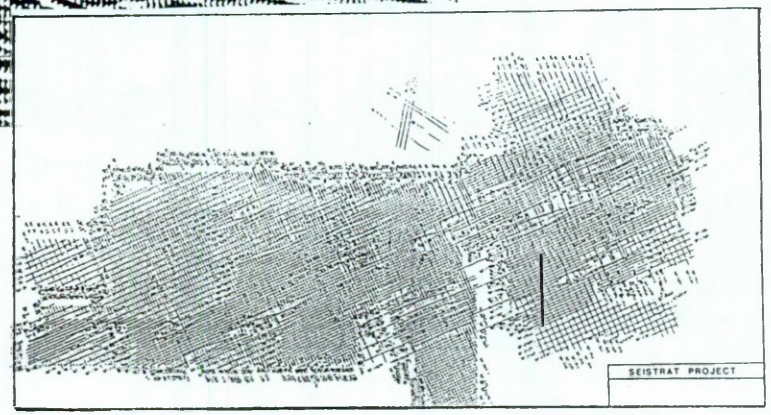

Fig.7.11b The eastern canyon (line 1656). Note the subdued amplitude seismic facies and the eroded base. The seismic line is along the strike of the canyon.

Fig.7.12 Distribution of Stratigraphic anomalies within the Rubble Beds. Note the two northern anomalies, a minor western anomaly and the southeastern anomaly. The most prospective are the northern and southeastern anomalies.

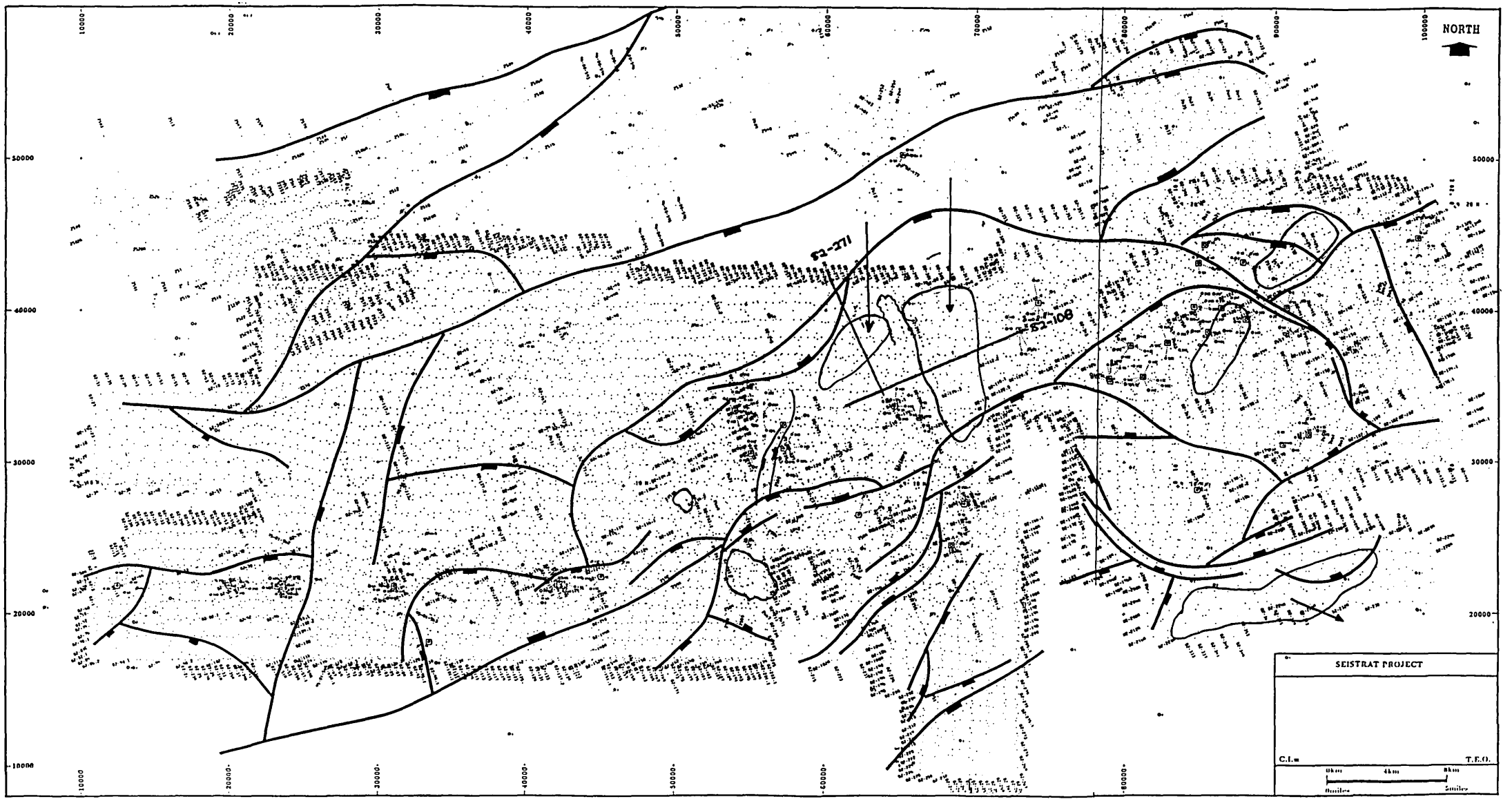

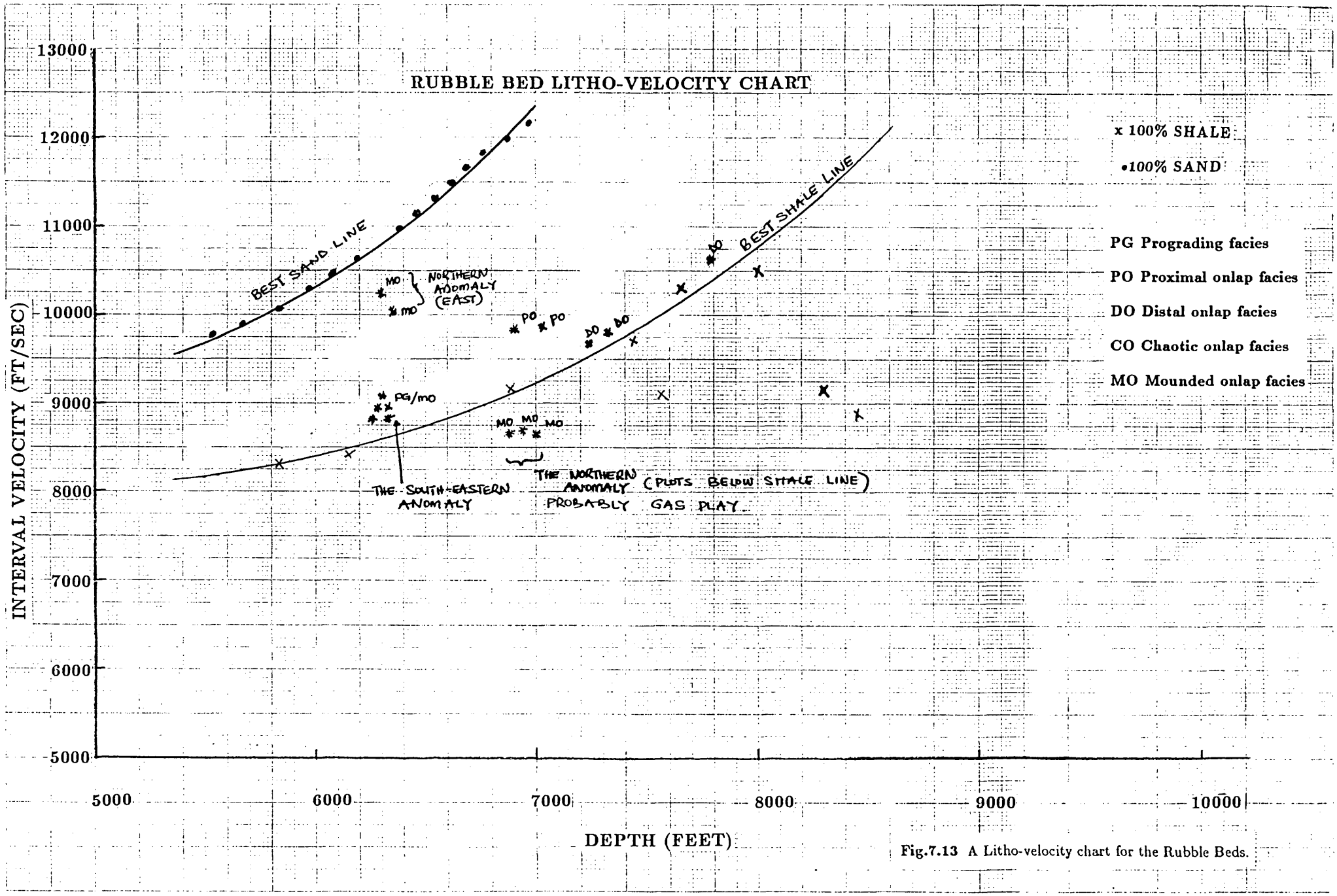

Fig.7.13 A Litho-velocity chart for the Rubble Beds.

47 1242
K+E 20 x 20 TO THE INCH x 10 x 15 INCHES KEUFFEL & ESSER CO. MADE IN U.S.A.

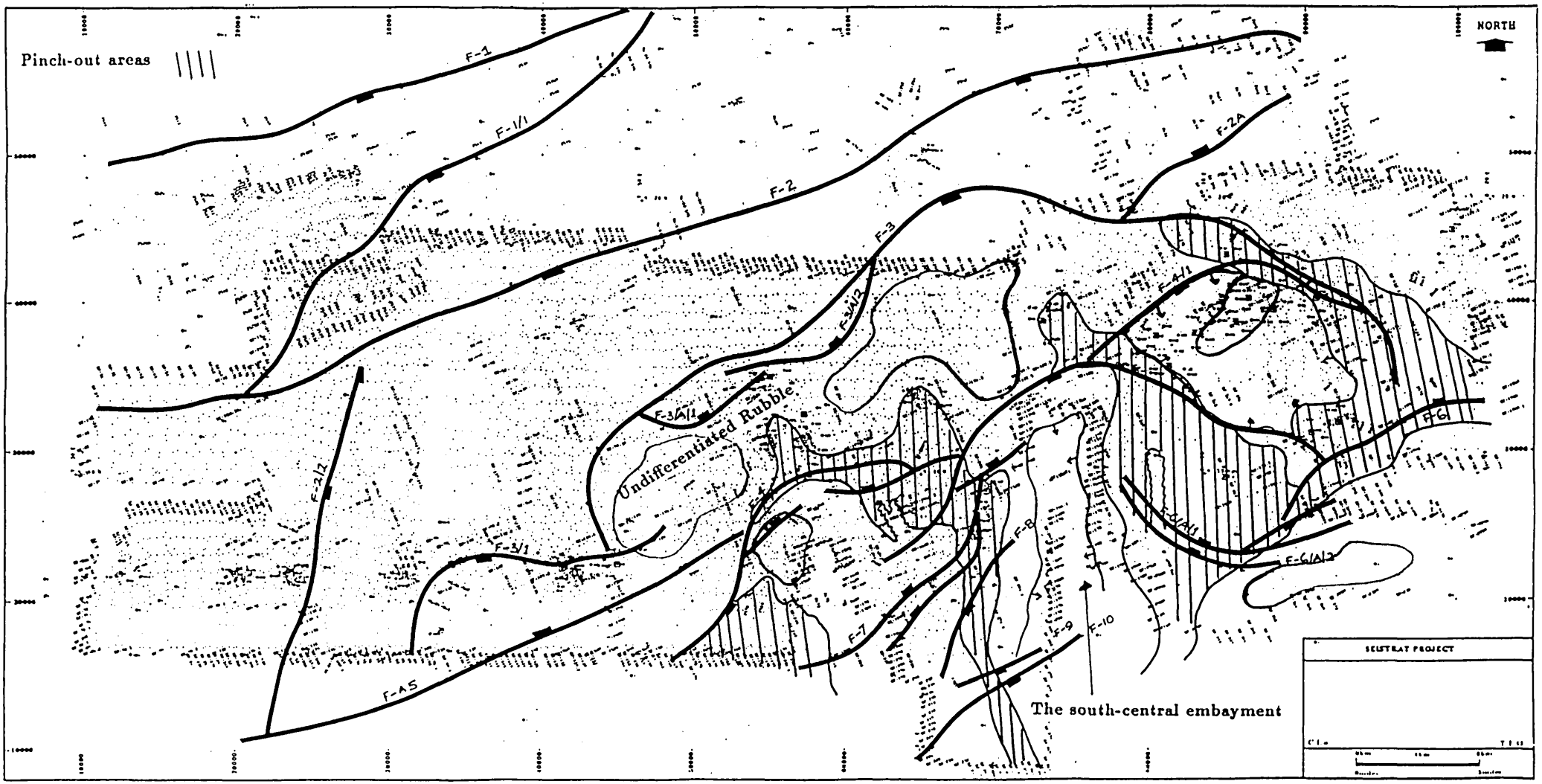

Fig.7.14 Probable distribution of 'sand' build-ups based on seismic interval velocity analysis.

LBIBR- Lower Base Intra Biafra Rubble.

LIBU- Lower Intra Biafra Unconformity.

BIBR- Base Intra Biafra Rubble.

TIBU- Top Intra Biafra Unconformity.

BIBBEN- Base Intra Biafra Benin sands.

BRB- Base Rubble Beds

BQI- Base Qua Iboe.

TIQI- Top Intra Qua Iboe

QUA3 etc- Intra Qua Iboe horizon 3 etc

Pu- Pleistocene Unconformity

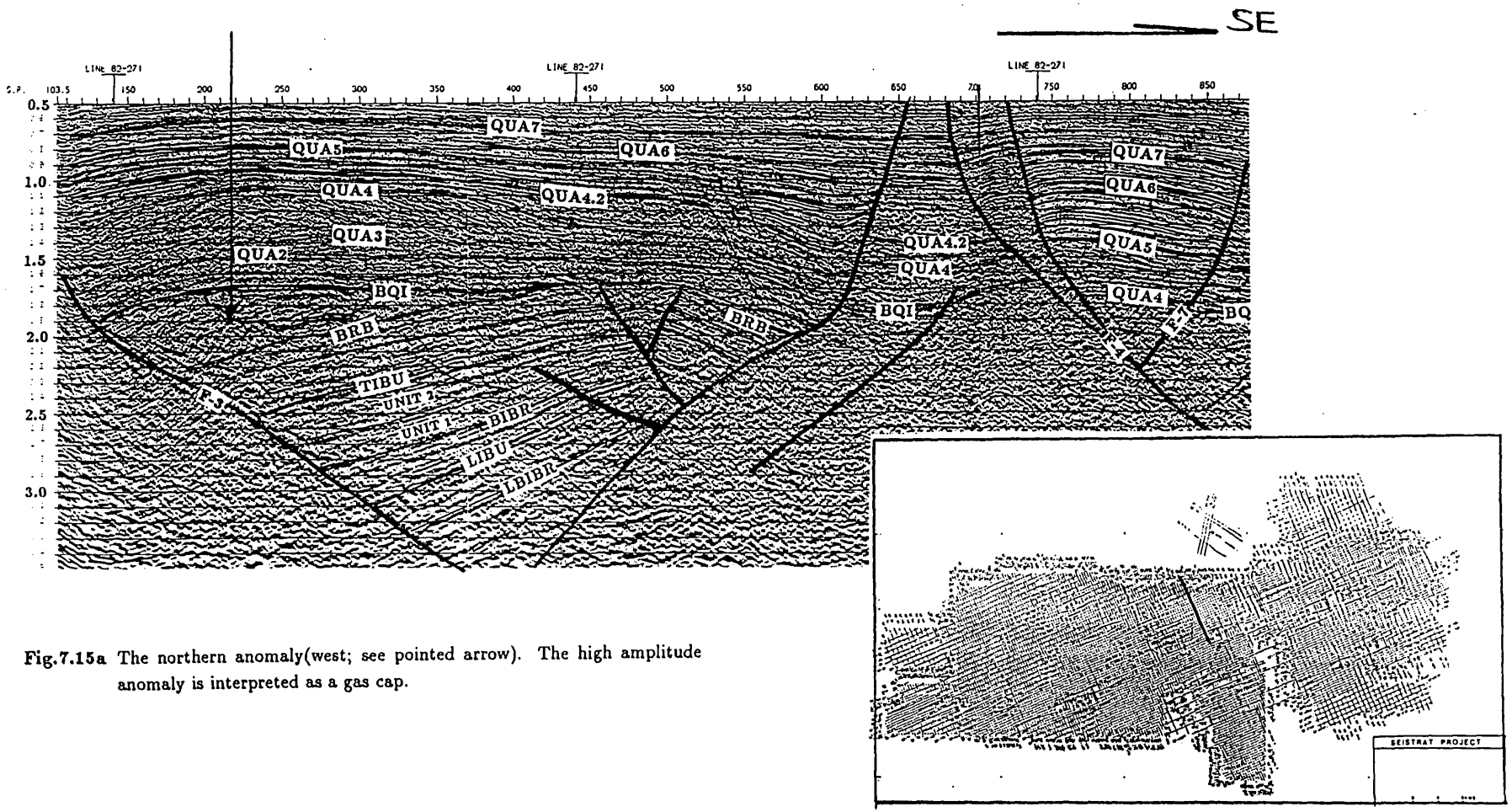

Fig.7.15a The northern anomaly(west; see pointed arrow). The high amplitude anomaly is interpreted as a gas cap.

LIBBR- Lower Base Intra Biafra Rubble.

LIBU- Lower Intra Biafra Unconformity.

BIBR- Base Intra Biafra Rubble.

TIBU- Top Intra Biafra Unconformity.

BIBBEN- Base Intra Biafra Benin sands.

BRB- Base Rubble Beds

BQI- Base Qua Iboe.

TIQI- Top Intra Qua Iboe

QUA3 etc- Intra Qua Iboe horizon 3 etc

Pu- Pleistocene Unconformity

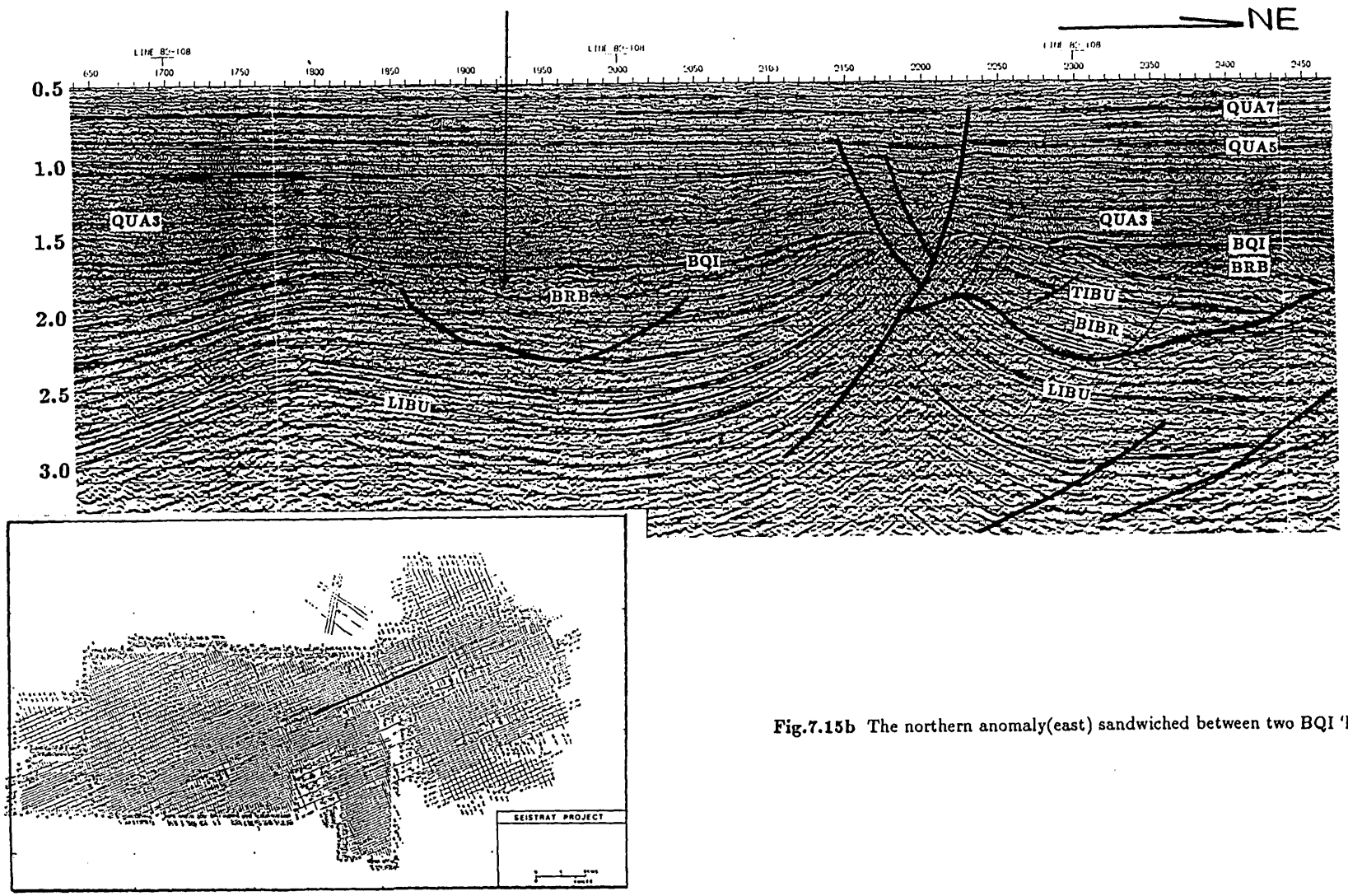

Fig.7.15b The northern anomaly(east) sandwiched between two BQI 'highs'.

LBIBR- Lower Base Intra Biafra Rubble.

LIBU- Lower Intra Biafra Unconformity.

BIBR- Base Intra Biafra Rubble.

TIBU- Top Intra Biafra Unconformity.

BIBBEN- Base Intra Biafra Benin sands.

BRB- Base Rubble Beds

BQI- Base Qua Iboe.

TIQI- Top Intra Qua Iboe

QUA3 etc- Intra Qua Iboe horizon 3 etc

Pu- Pleistocene Unconformity

The southeastern anomaly

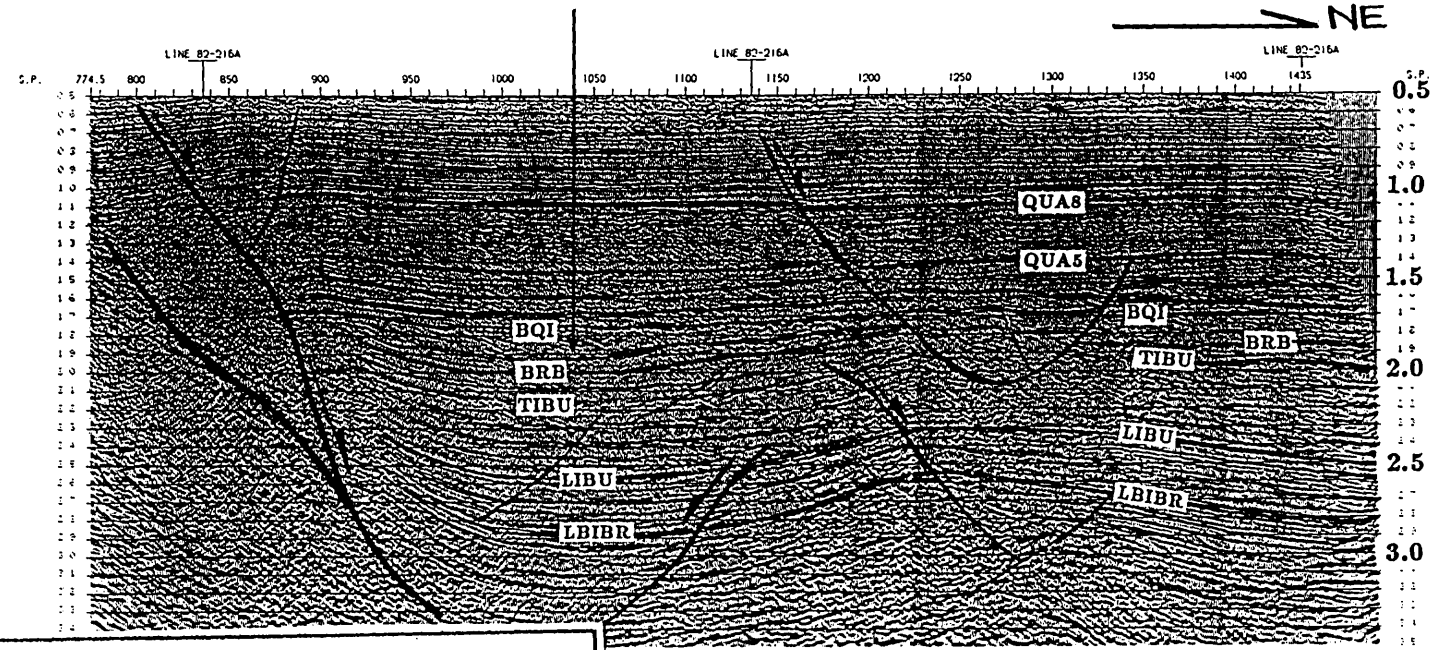

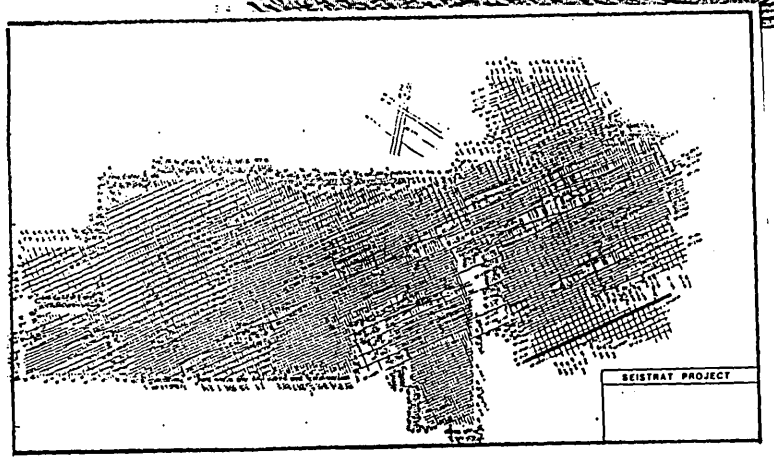

Fig.7.15c The southeastern anomaly

CHAPTER EIGHT

Fig.8.1 The limit of the Qua Iboe shale in the study area is shown. This SW-NE trending limit appears to parallel the present day coast line and is consistent with the trend of the paleobasin hinge line to the west. The eastern limit exceeds the area of study. This limit also constitutes the limit of the Qua Iboe embayment referred to in Chapter 9. Qua Iboe build-up to the south occurs in progradational sets.

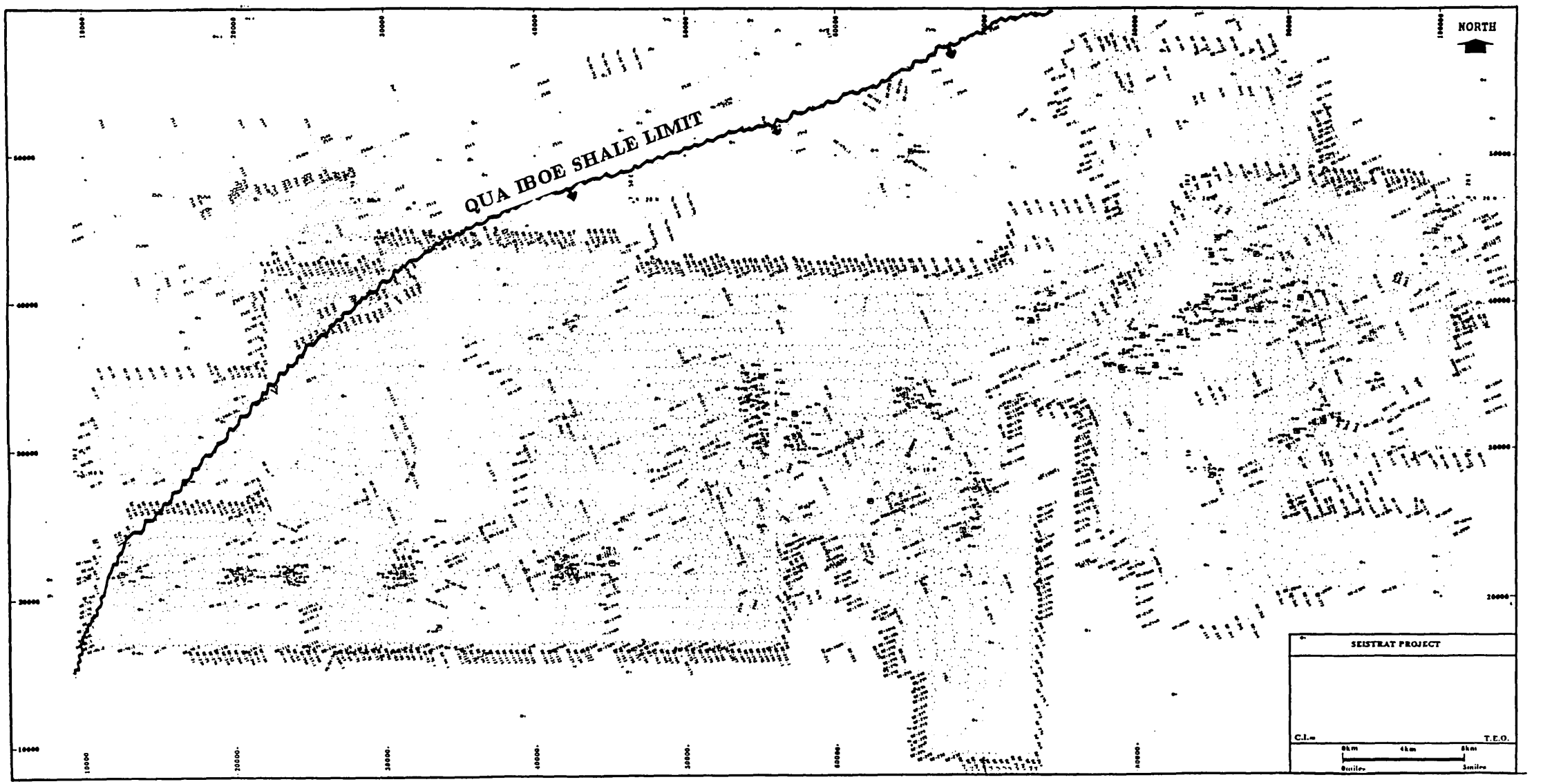

LBIBR- Lower Base Intra Biafra Rubble.

LIBU- Lower Intra Biafra Unconformity.

BIBR- Base Intra Biafra Rubble.

TIBU- Top Intra Biafra Unconformity.

BIBBEN- Base Intra Biafra Benin sands.

BRB- Base Rubble Beds

BQI- Base Qua Iboe.

TIQI- Top Intra Qua Iboe

QUA3 etc- Intra Qua Iboe horizon 3 etc

Pu- Pleistocene Unconformity

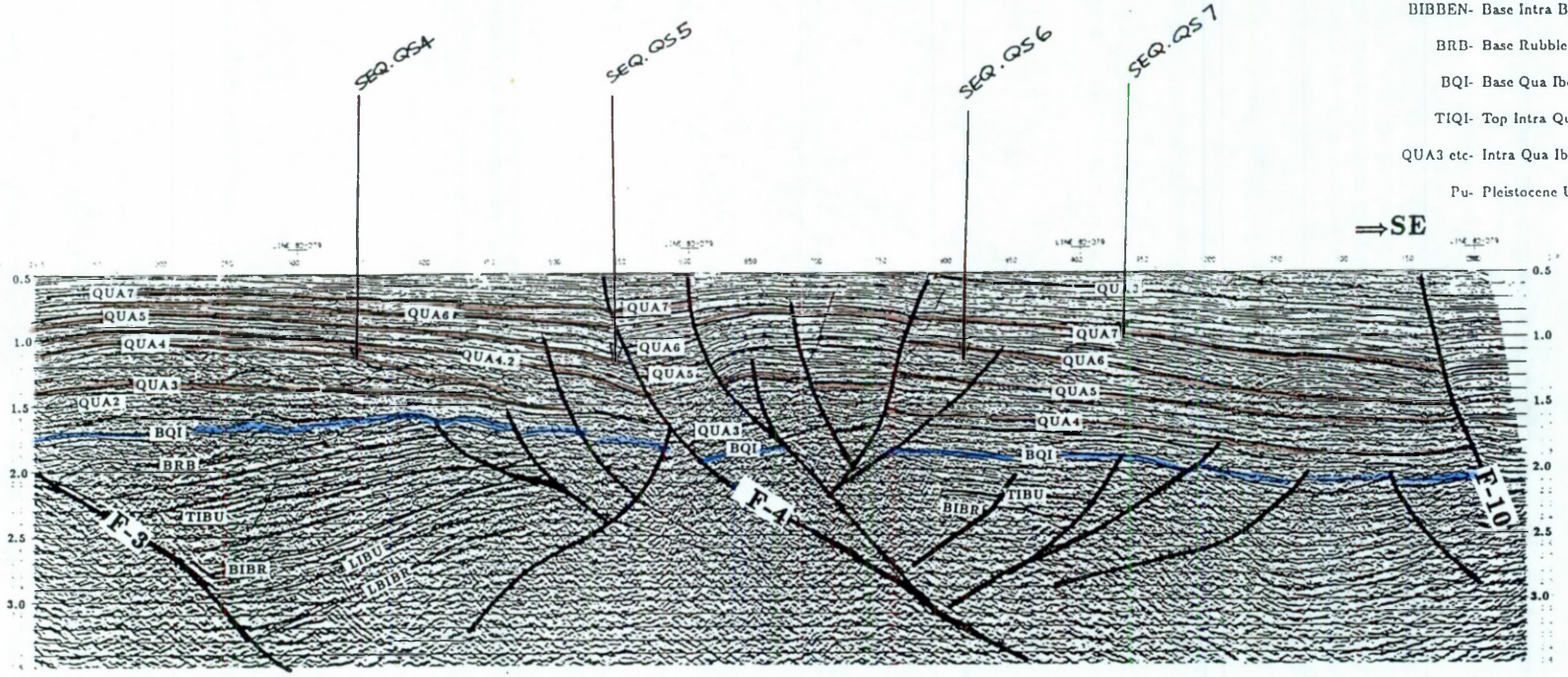

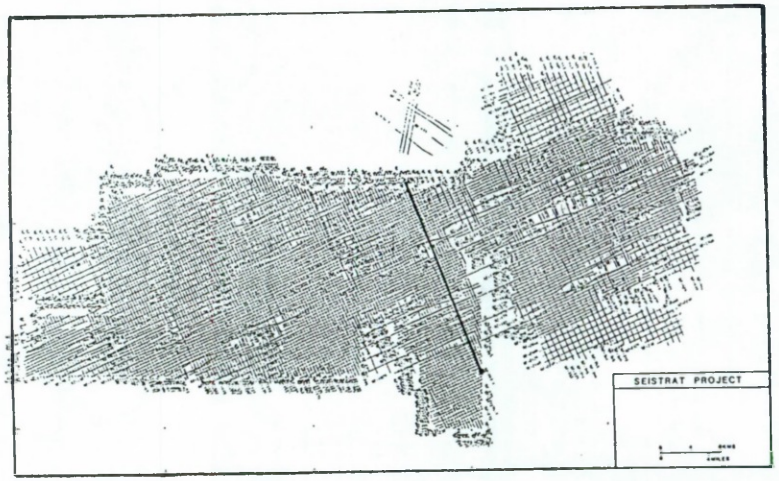

Fig.8.2a Qua Iboe classification is illustrated in line 82-279. Qua3 is a downlap surface upon which seismic mounds may be observed. The lower Qua Iboe sequence consists of the interval between horizon Qua4 and BQI. The Intra Qua Iboe 'sand' package is the interval between Qua3 and BQI. Shelf edges may be picked at the point of commencement of slope progradation as illustrated in the figure. The shelf edge for Qua5 is obscured by growth faulting and is picked at the boundary of the structure controlling growth fault.(Winker and Edwards, 1983, assert that most growth faults occur at the shelf edge.) Note the slump feature above Qua6 between shot points 1050 and 1150.

LBIBR- Lower Base Intra Biafra Rubble.

LIBU- Lower Intra Biafra Unconformity.

BIBR- Base Intra Biafra Rubble.

TIBU- Top Intra Biafra Unconformity.

BIBBEN- Base Intra Biafra Benin sands.

BRB- Base Rubble Beds

BQI- Base Qua Iboe.

TIQI- Top Intra Qua Iboe

QUA3 etc- Intra Qua Iboe horizon 3 etc

Pu- Pleistocene Unconformity

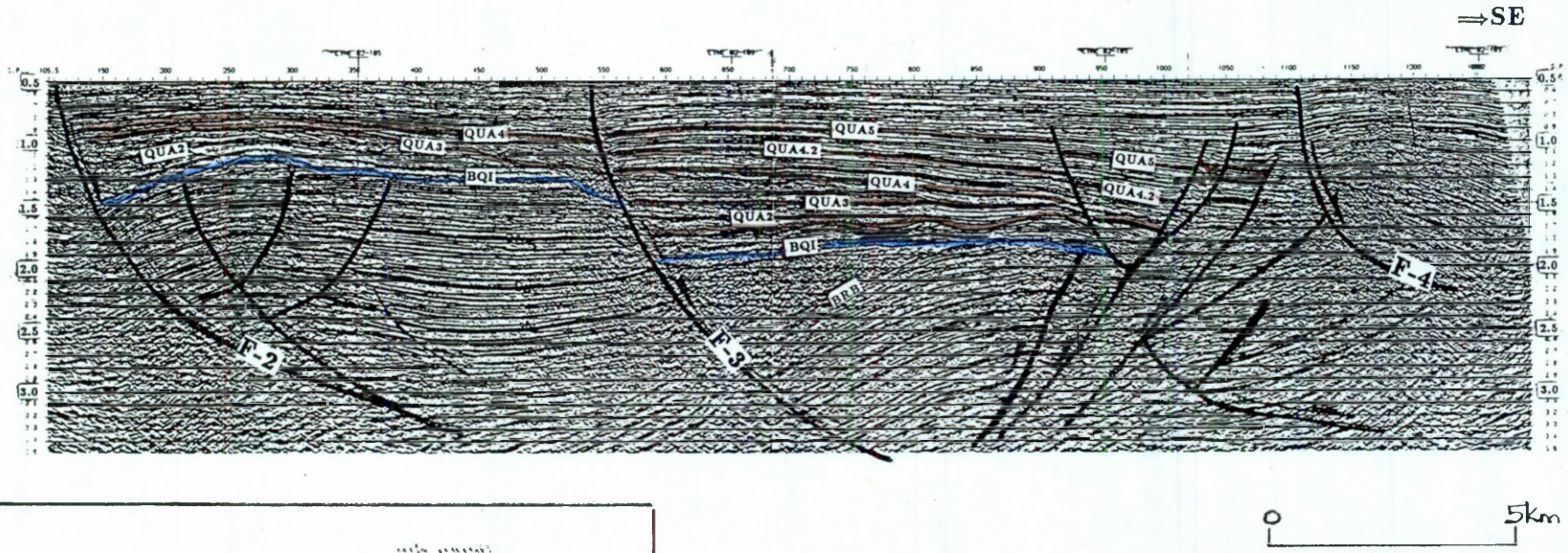

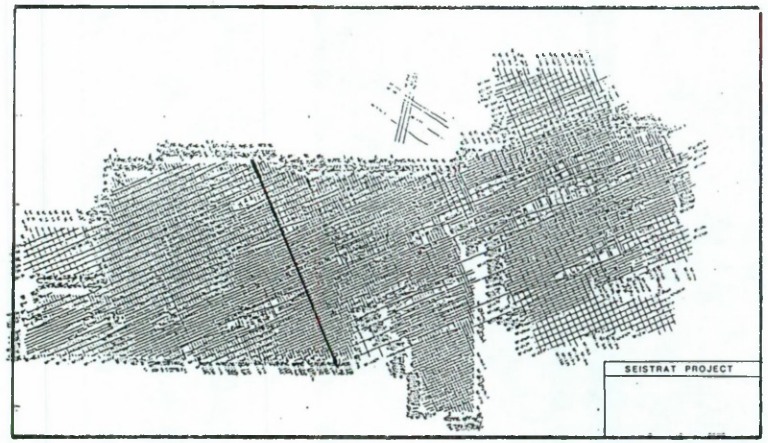

Fig.8.2b Line 82-185 illustrates the progradational sets mapped north and south of the palaeobasin hinge(Fault-3). Qua2 encloses a sheet drape facies north of the palaeobasin and the mounded hummocky facies of the centre- west stratigraphic anomaly within the palaeobasin. Qua3 on the other hand is a surface of truncation to the north and a downlap surface to the south. Qua4 is a truncated surface north and within the palaeobasin.

Fig.8.3 Composite map of shelf breaks for the respective sequences mapped. The shelf breaks appear to parallel the palaeobasin boundary.

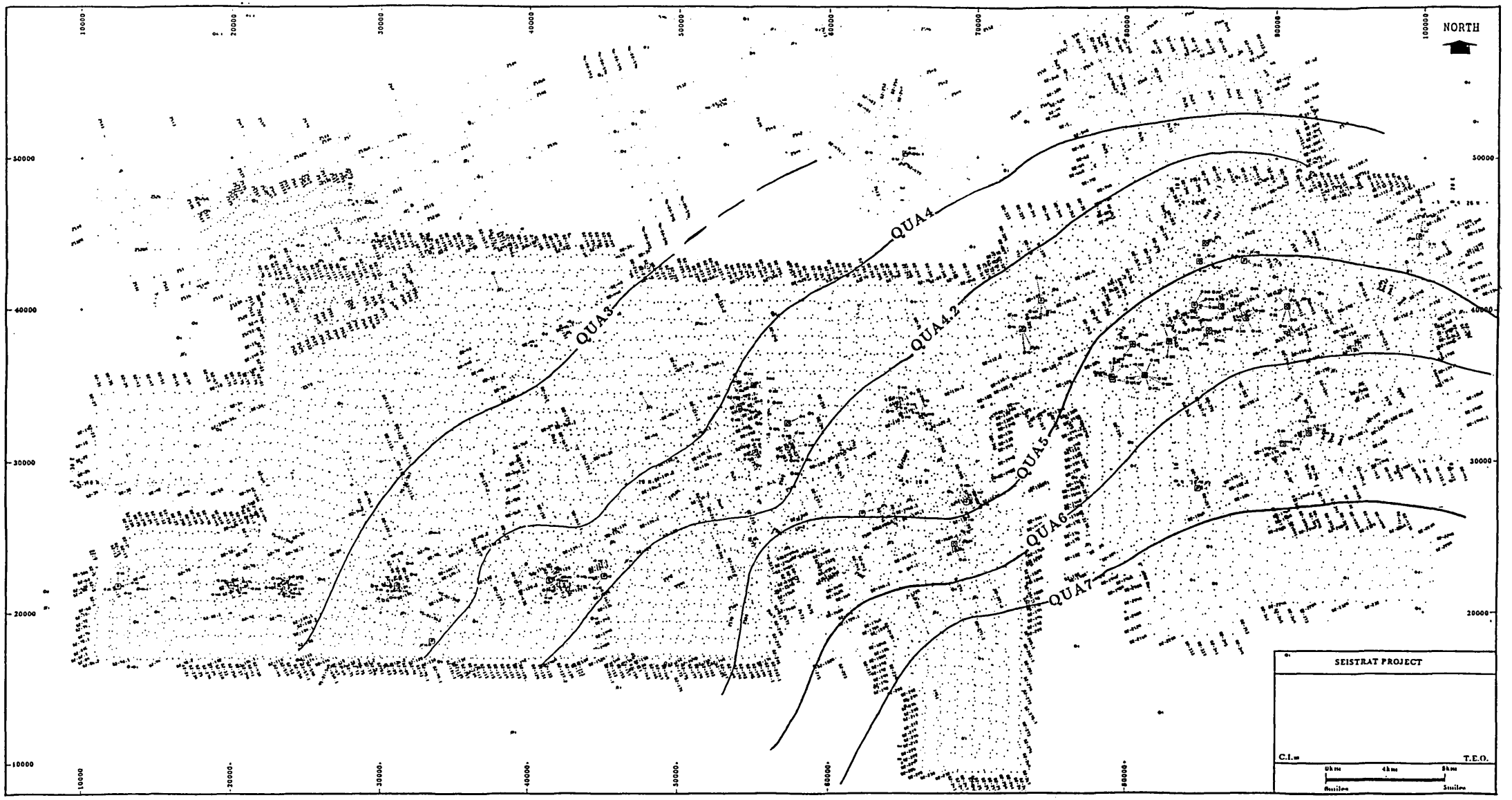

Shelf/delta plain

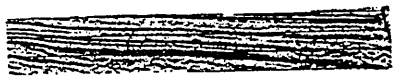

parallel/divergent variable amplitude

Slope facies

Oblique progradation

Slope facies

Sigmoidal progradation

Slope facies

Subdued amplitude drape

Basinal facies

sheet facies

Fig.8.4 Representative seismic facies types of the Qua Iboe.

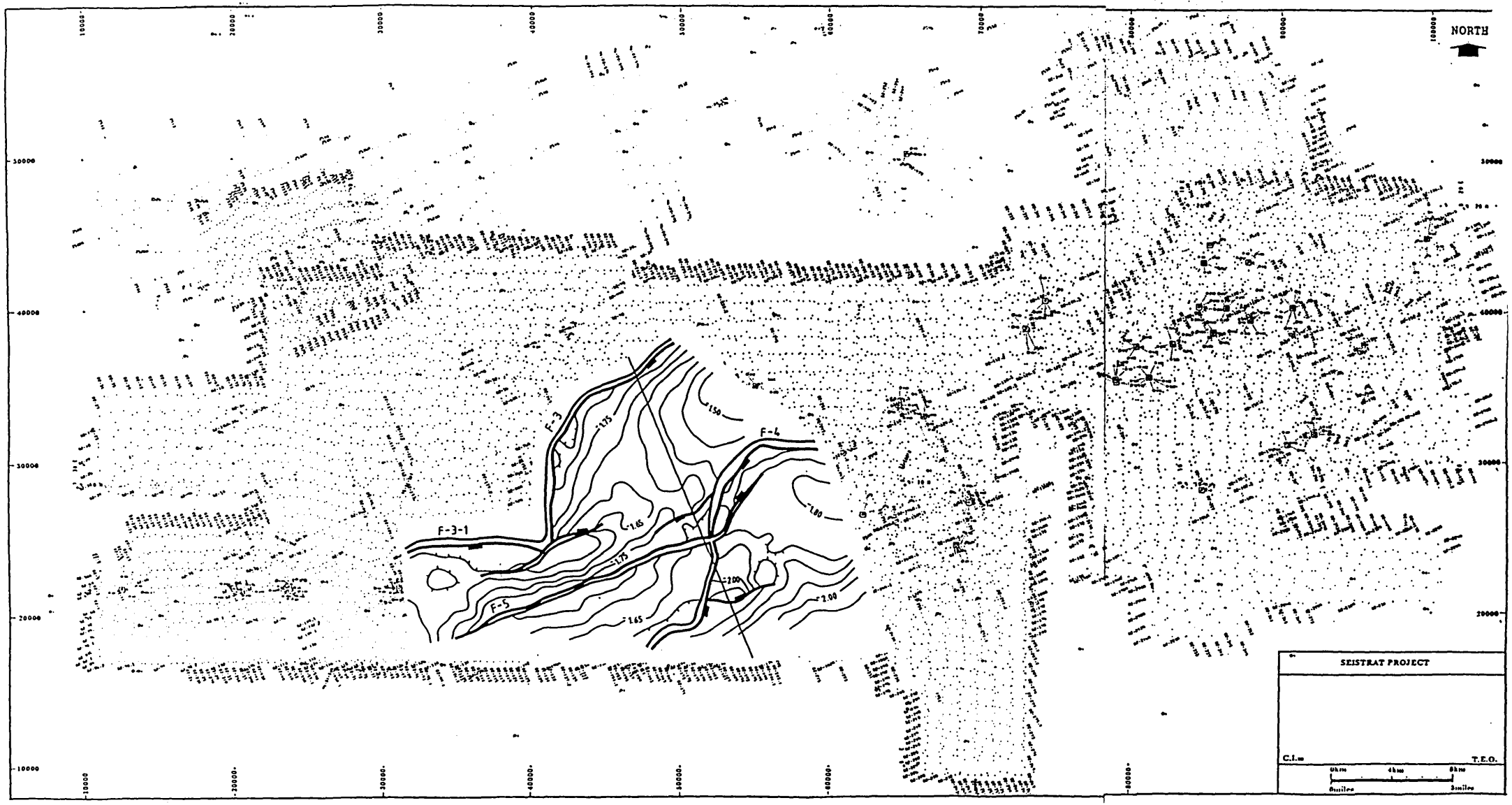

Fig.8.5a Structural map of Horizon QUA2. The Qua2 unconformity appears to be limited to the east by the central anomaly. However, the equivalent Qua2 to the northeast is the top of a ponded turbidite sequence(see Line 82-409, Fig.8.6b).

Fig.8.5b Isochron map of SEQ.QS1. Note the thickening and thinning associated with the northwest anomaly.

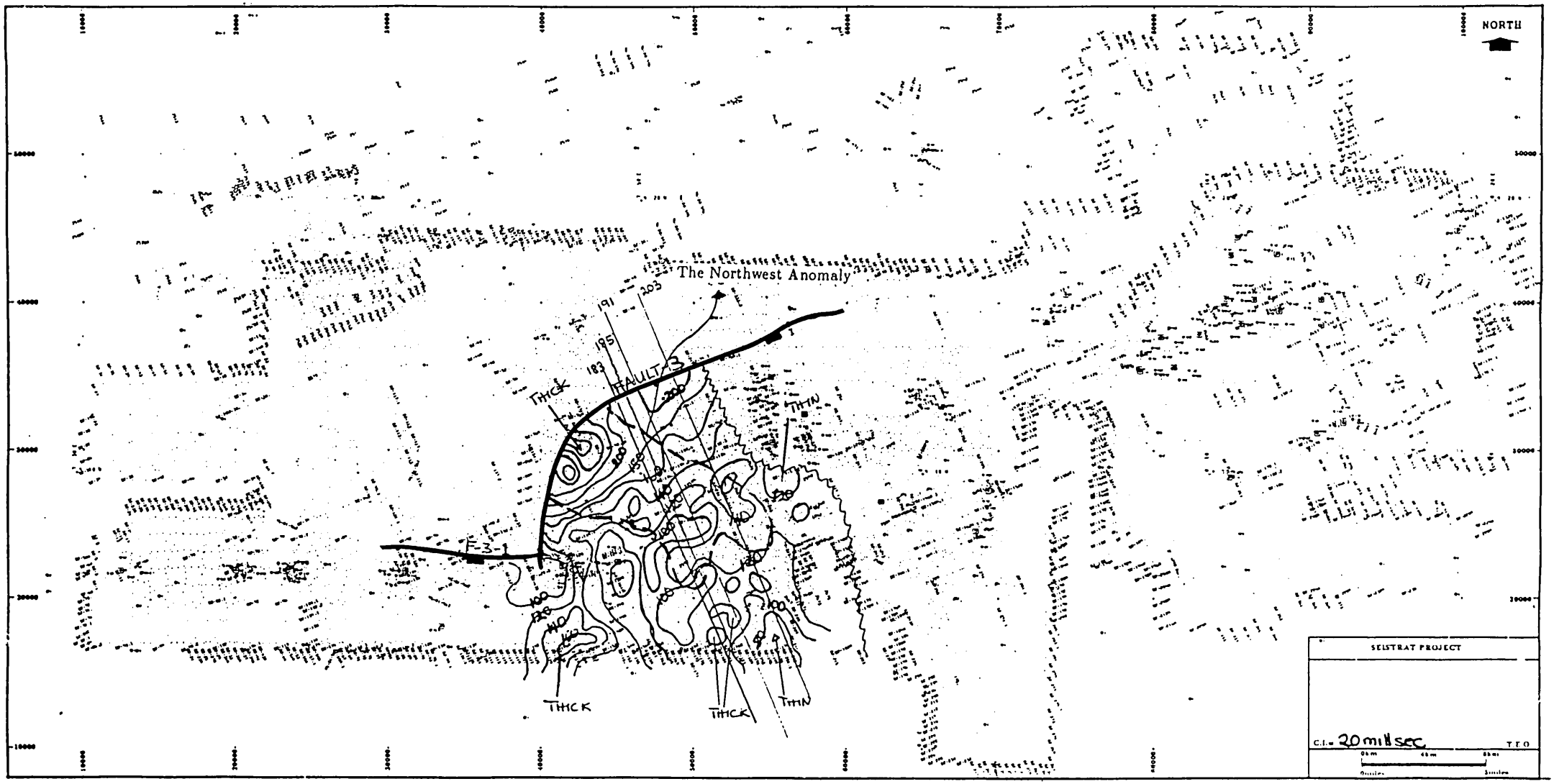

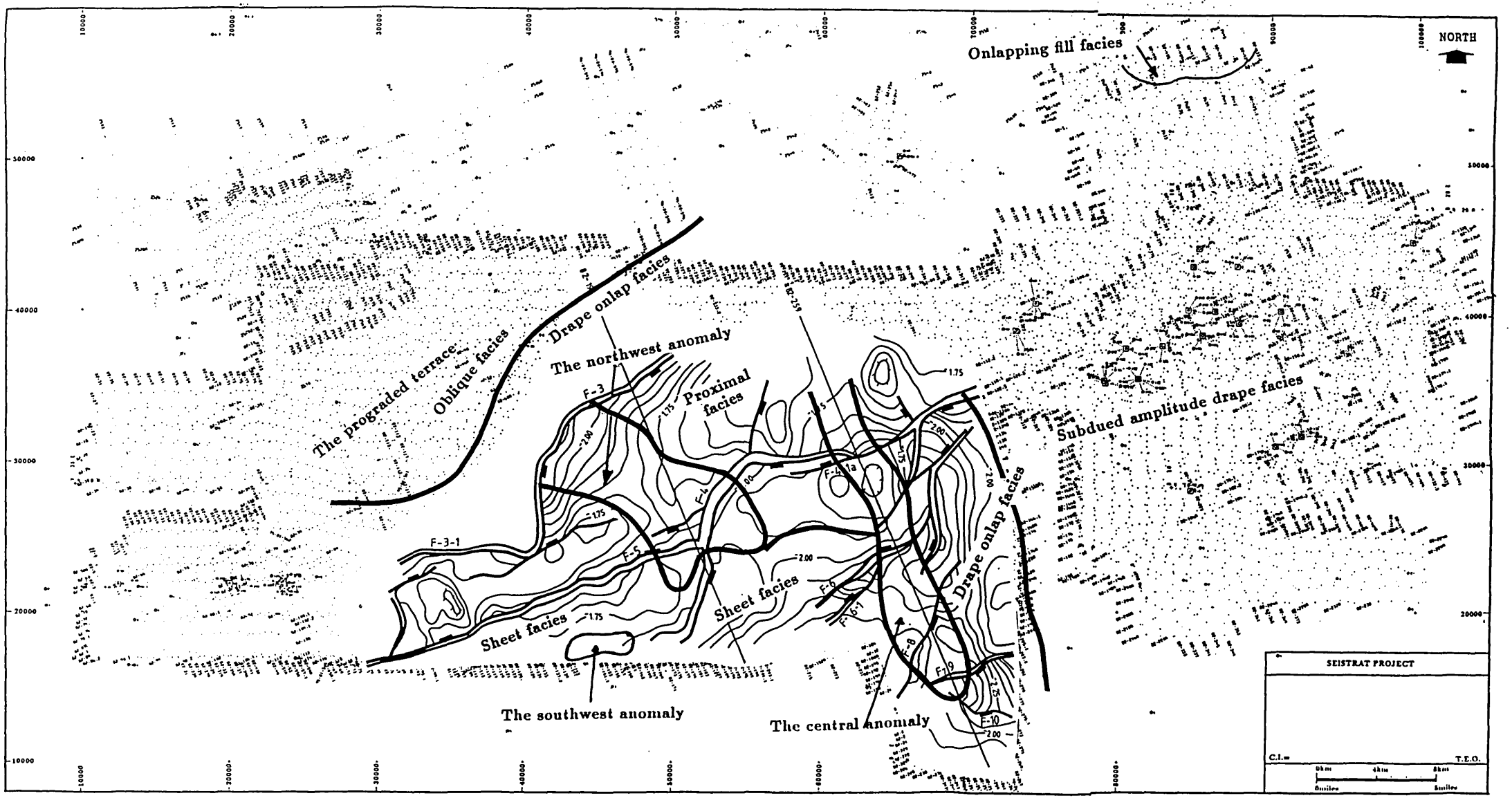

Fig.8.5c Facies distribution map of SEQ.QS1 superimposed over the structural time map of the BQ1 which this sequence overlies. The relationship between the seismic stratigraphic anomalies and bathymetric lows is obvious.

LBIBR- Lower Base Intra Biafra Rubble.

LIBU- Lower Intra Biafra Unconformity.

BIBR- Base Intra Biafra Rubble.

TIBU- Top Intra Biafra Unconformity.

BIBBEN- Base Intra Biafra Benin sands.

BRB- Base Rubble Beds

BQI- Base Qua Iboe.

TIQI- Top Intra Qua Iboe

QUA3 etc- Intra Qua Iboe horizon 3 etc

Pu- Pleistocene Unconformity

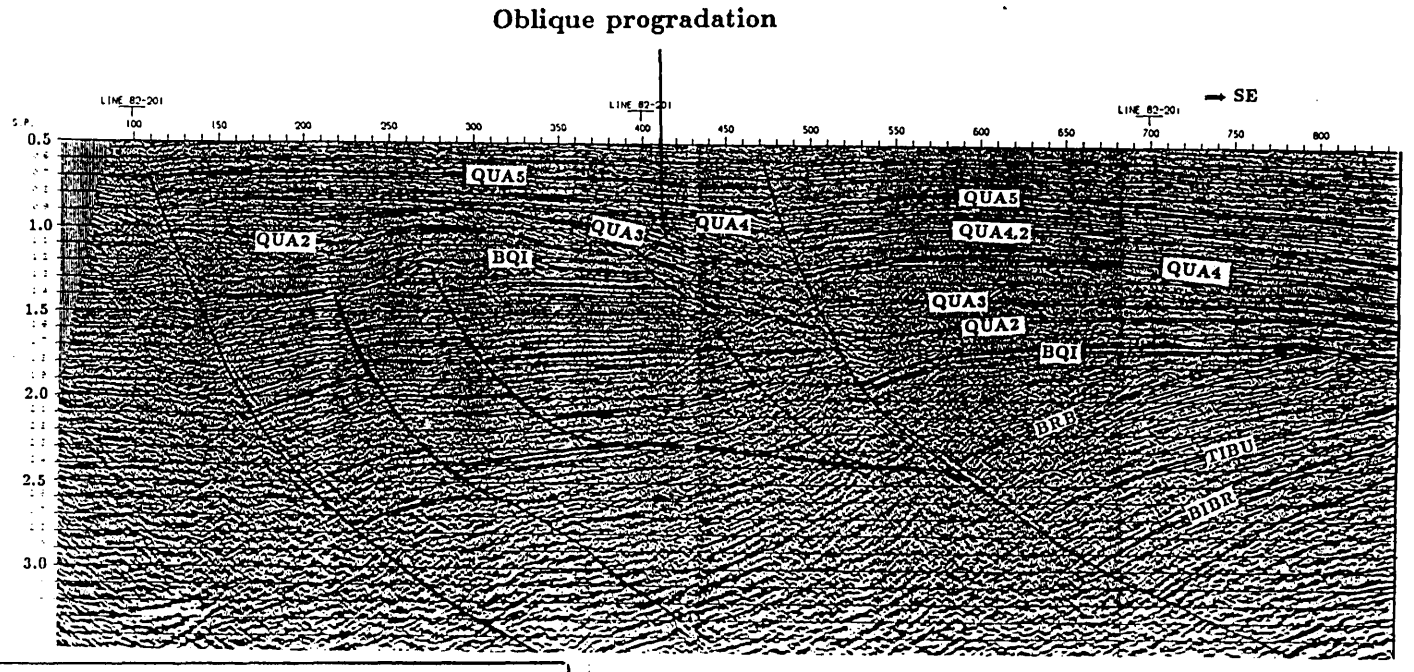

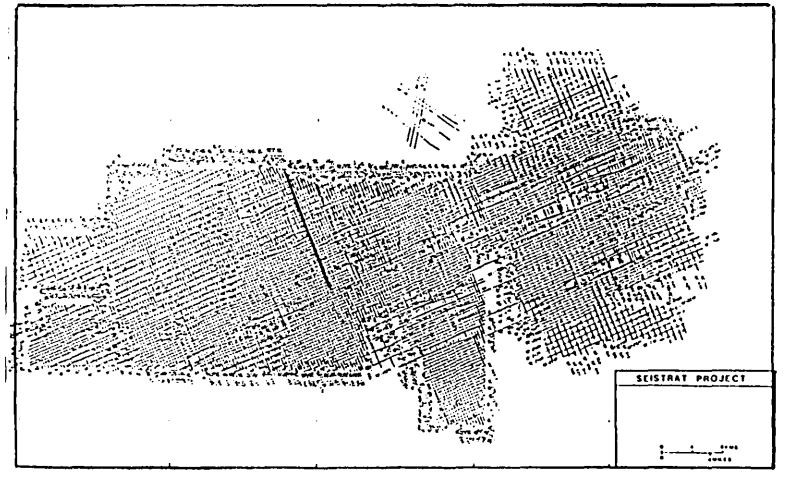

Fig.8.6a Line 82-201 to the west of the study area showing increasing prominence of oblique progradation to the north.

LBIBR- Lower Base Intra Biafra Rubble.

LIBU- Lower Intra Biafra Unconformity.

BIBR- Base Intra Biafra Rubble.

TIBU- Top Intra Biafra Unconformity.

BIBBEN- Base Intra Biafra Benin sands.

BRB- Base Rubble Beds

BQI- Base Qua Iboe.

TIQI- Top Intra Qua Iboe

QUA3 etc- Intra Qua Iboe horizon 3 etc

Pu- Pleistocene Unconformity

Ponded turbidites onlapping a PGM feature

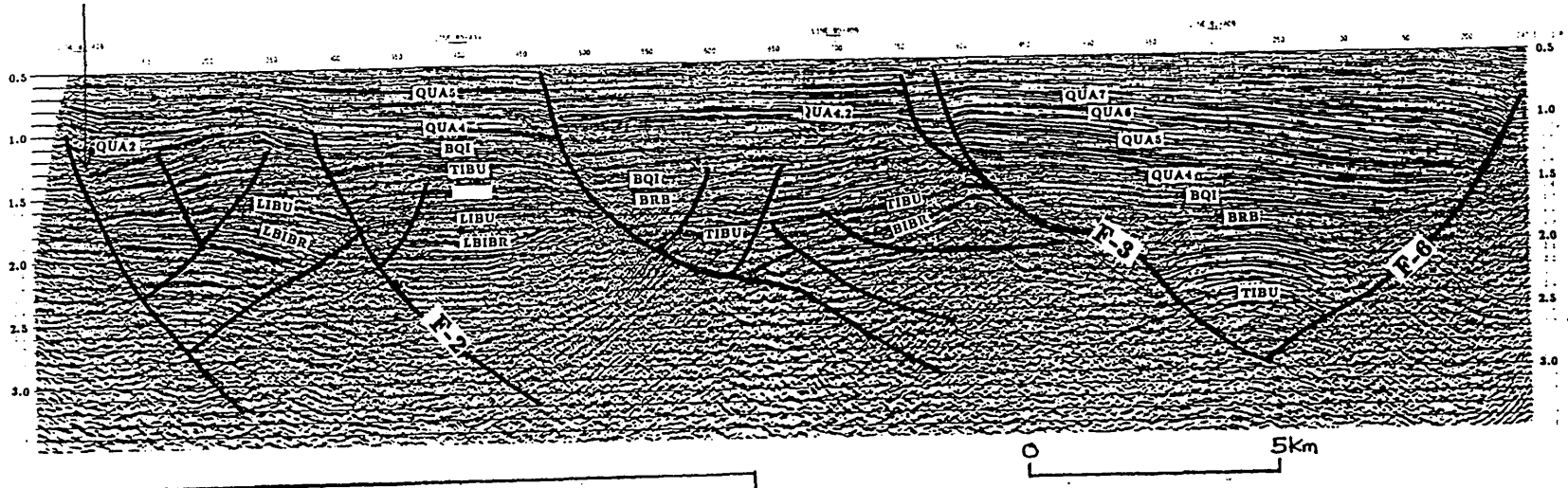

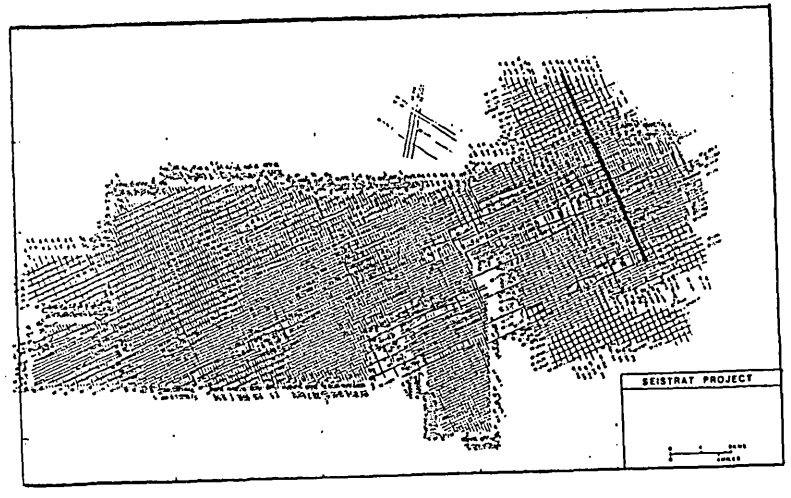

Fig.8.6b Seismic line 82-409 east of the study area showing the ponded sequence QS1 to the north. Southward, sigmoidal progradation is dominant.

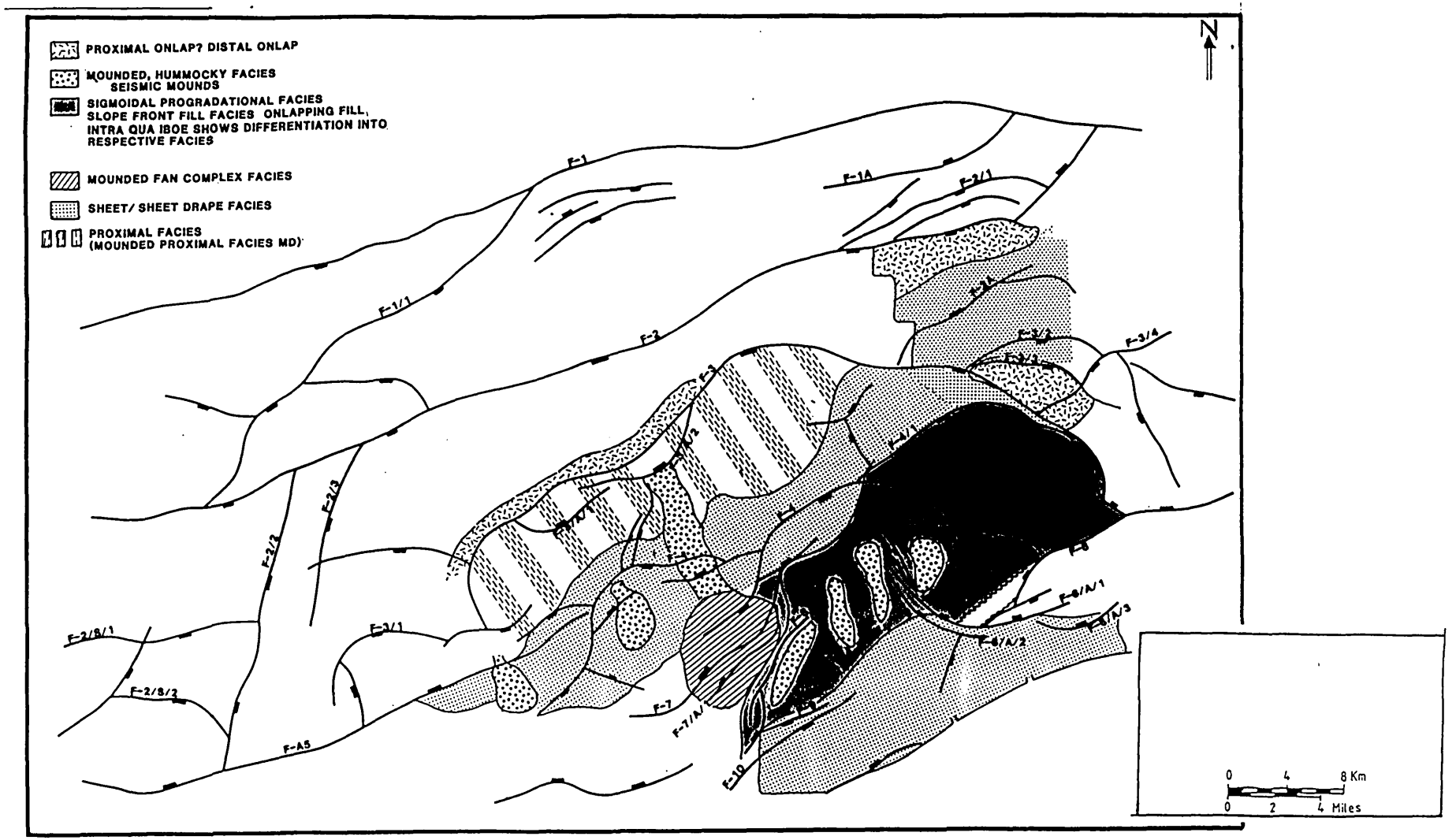

Fig.8.6c Facies distribution map of SEQ.QS1 and SEQ.QS2 combined. These sequences combine to make up the Intra Qua Iboe 'sand' package.

Fig.8.6d Composite map of the distribution of seismic stratigraphic anomalies within SEQ.QS1 and QS2.

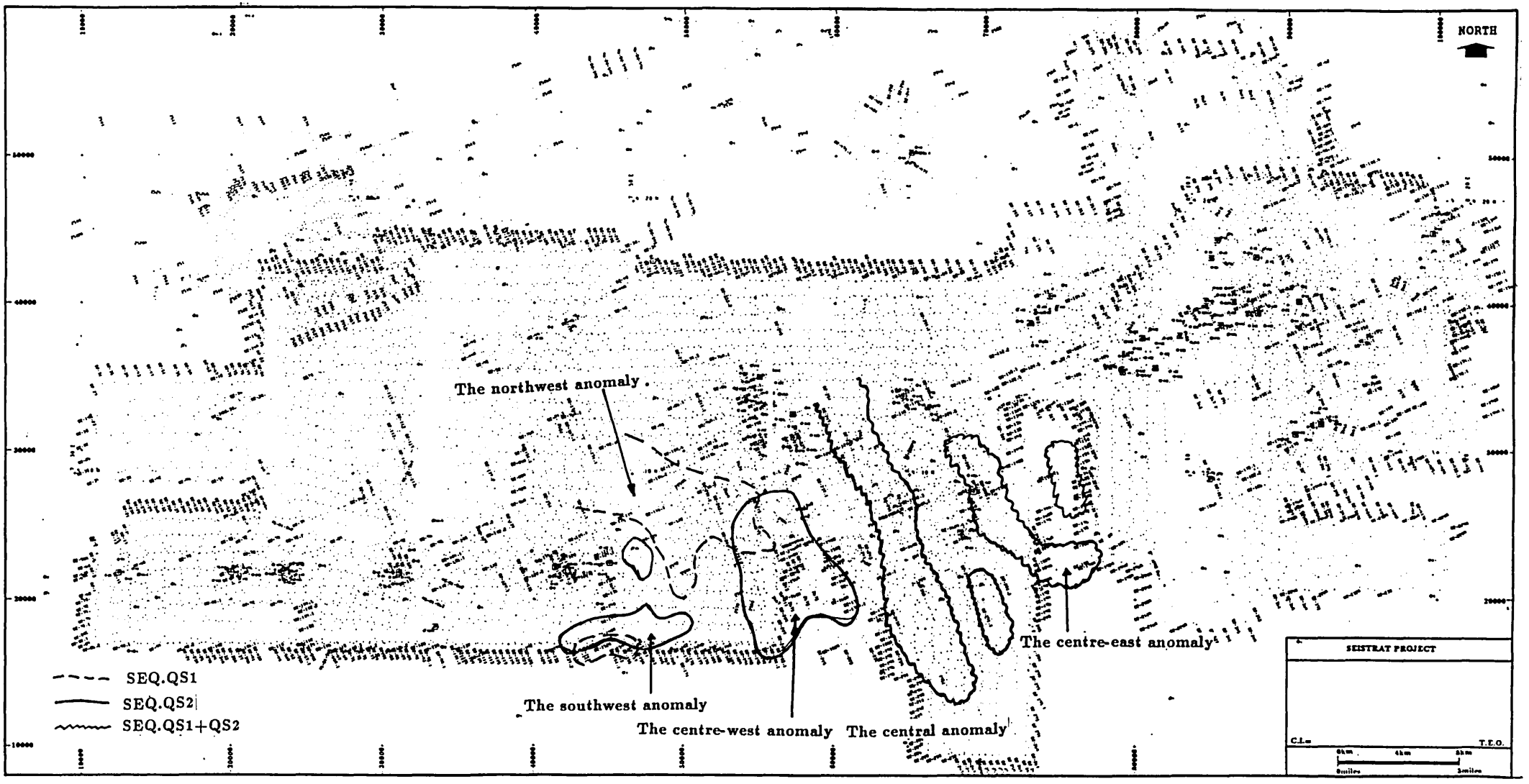

LBIBR- Lower Base Intra Biafra Rubble.

LIBU- Lower Intra Biafra Unconformity.

BIBR- Base Intra Biafra Rubble.

TIBU- Top Intra Biafra Unconformity.

BIBBEN- Base Intra Biafra Benin sands.

BRB- Base Rubble Beds

BQI- Base Qua Iboe.

TIQI- Top Intra Qua Iboe

QUA3 etc- Intra Qua Iboe horizon 3 etc

Pu- Pleistocene Unconformity

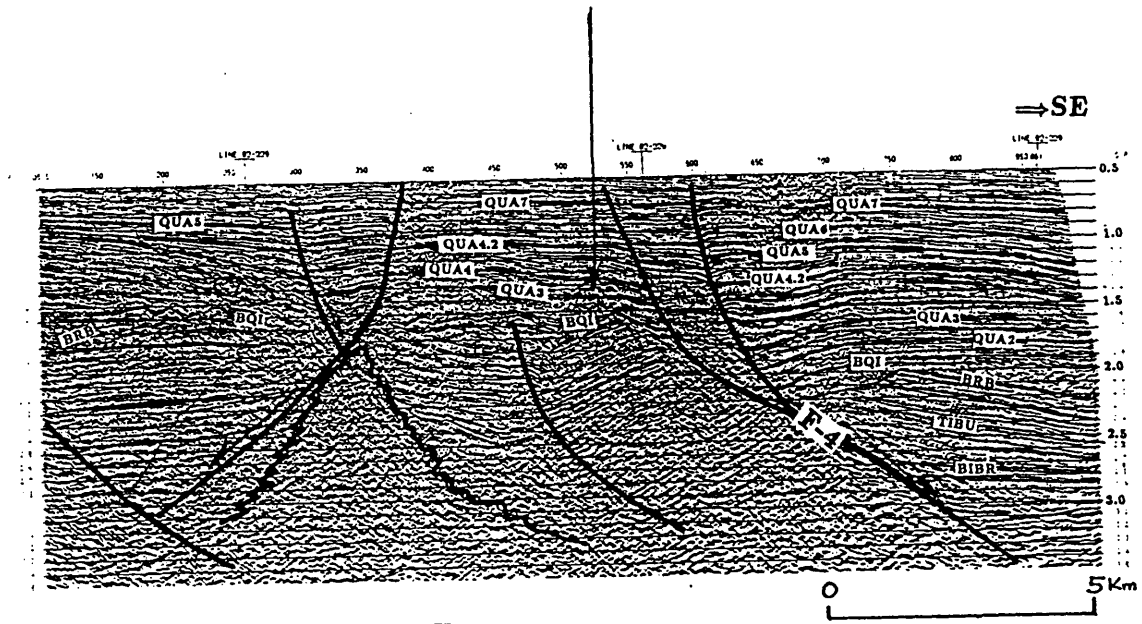

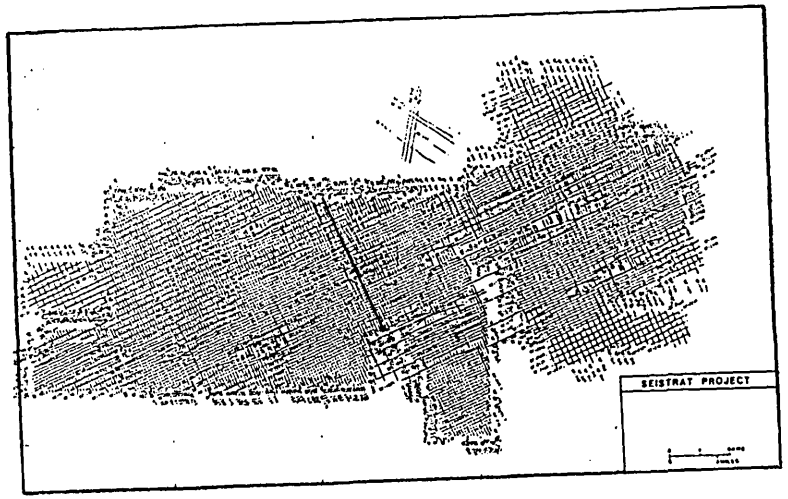

Fig.8.7a Line 82-229 shows a stratigraphic anomaly at the toe of progradation. This occurs between Qua3 and Qua4(see arrow).

Fig.8.7b Distribution of seismic mounds associated with the 'turbidite' toe of progradation.

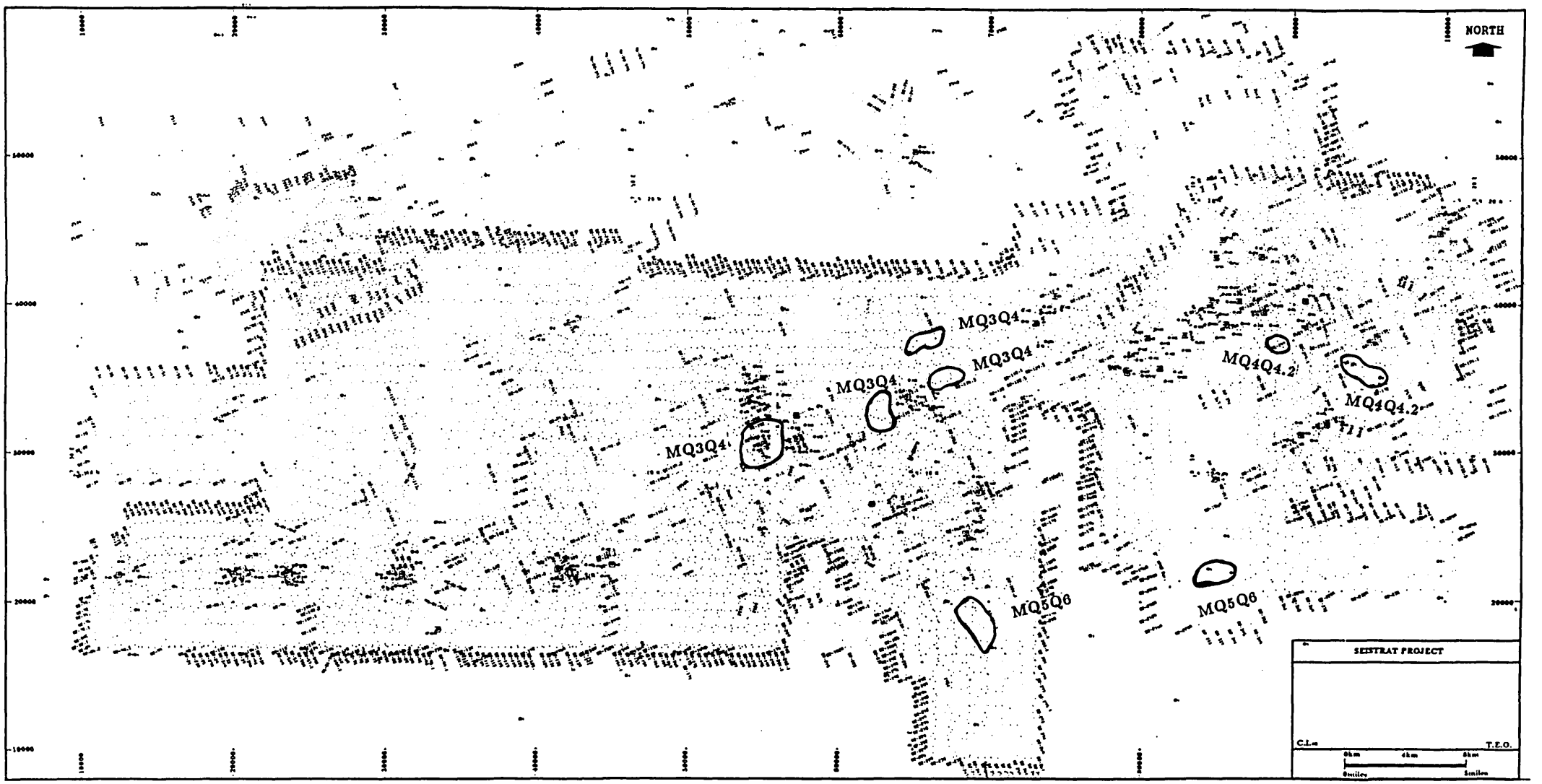

LBIBR- Lower Base Intra Biafra Rubble.

LIBU- Lower Intra Biafra Unconformity.

BIBR- Base Intra Biafra Rubble.

TIBU- Top Intra Biafra Unconformity.

BIBBEN- Base Intra Biafra Benin sands.

BRB- Base Rubble Beds

BQI- Base Qua Iboe.

TIQI- Top Intra Qua Iboe

QUA3 etc- Intra Qua Iboe horizon 3 etc

Pu- Pleistocene Unconformity

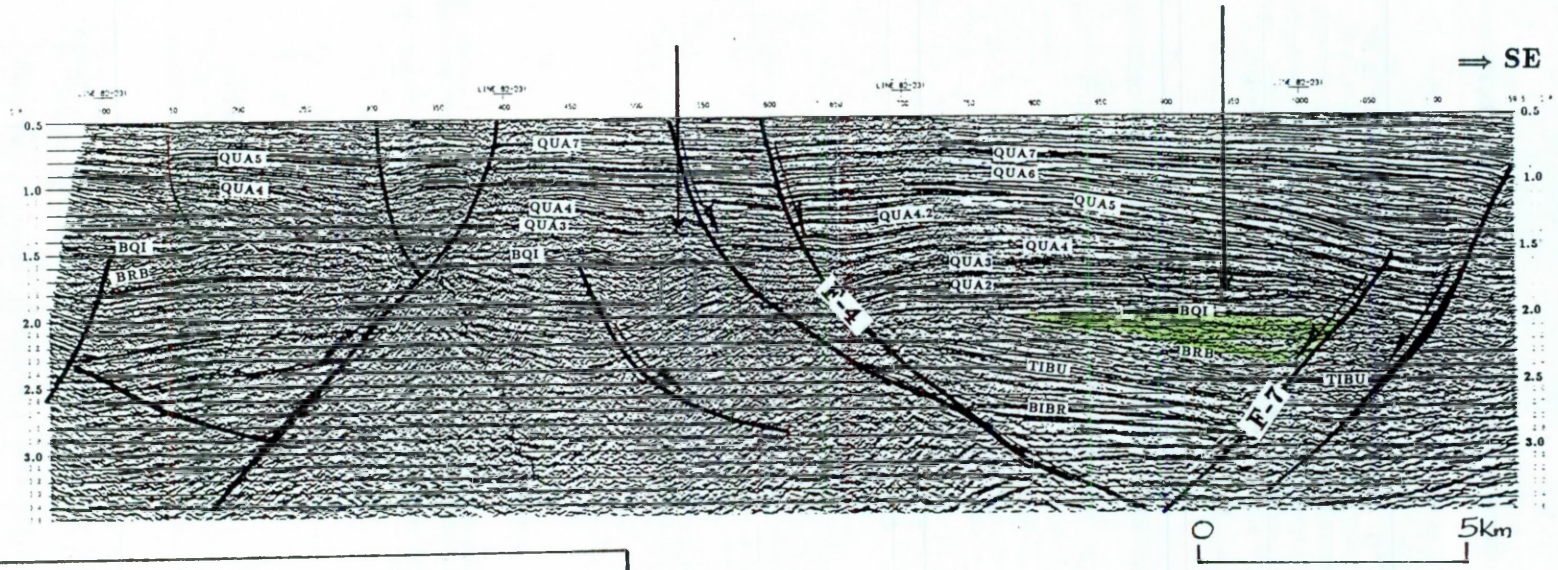

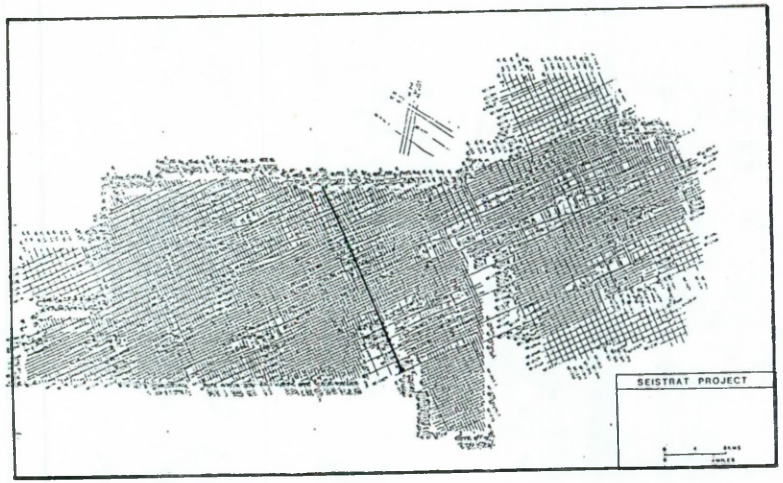

Fig.8.7c Line 82-231 showing the seismic mound on the upthrown side of a fault forming a trap and a seismic mound on the downthrown side of Fault-4(see arrows).

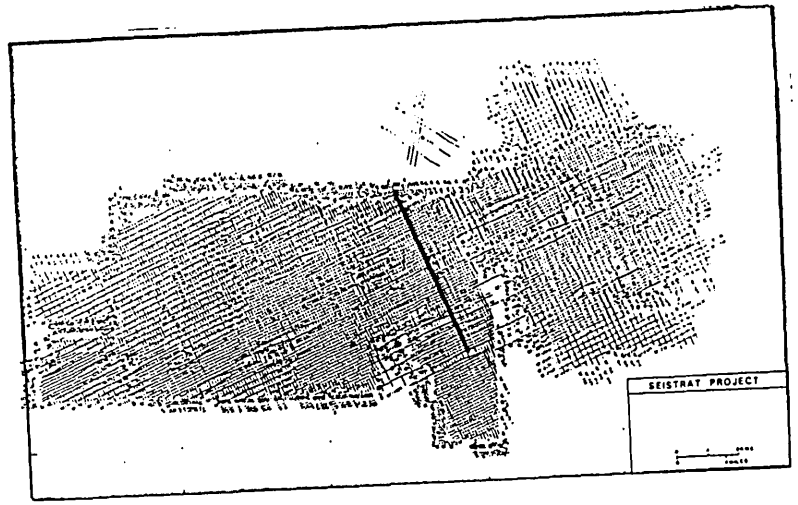

LBIBR- Lower Base Intra Biafra Rubble.

LIBU- Lower Intra Biafra Unconformity.

BIBR- Base Intra Biafra Rubble.

TIBU- Top Intra Biafra Unconformity.

BIBBEN- Base Intra Biafra Benin sands.

BRB- Base Rubble Beds

BQI- Base Qua Iboe.

TIQI- Top Intra Qua Iboe

QUA3 etc- Intra Qua Iboe horizon 3 etc

Pu- Pleistocene Unconformity

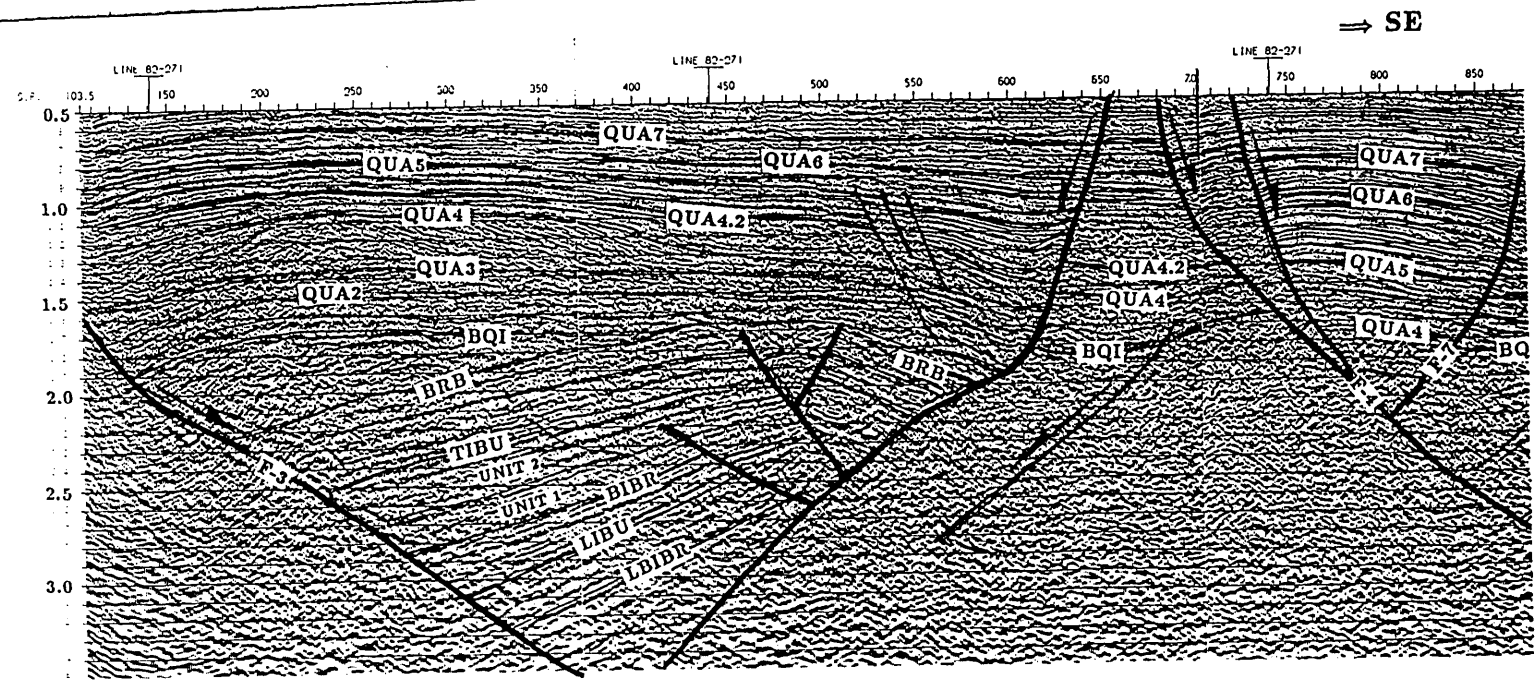

Fig.8.7d The prograding terrace, showing the build-up of oblique clinoforms between Qua3 and Qua4 (line 82-271).

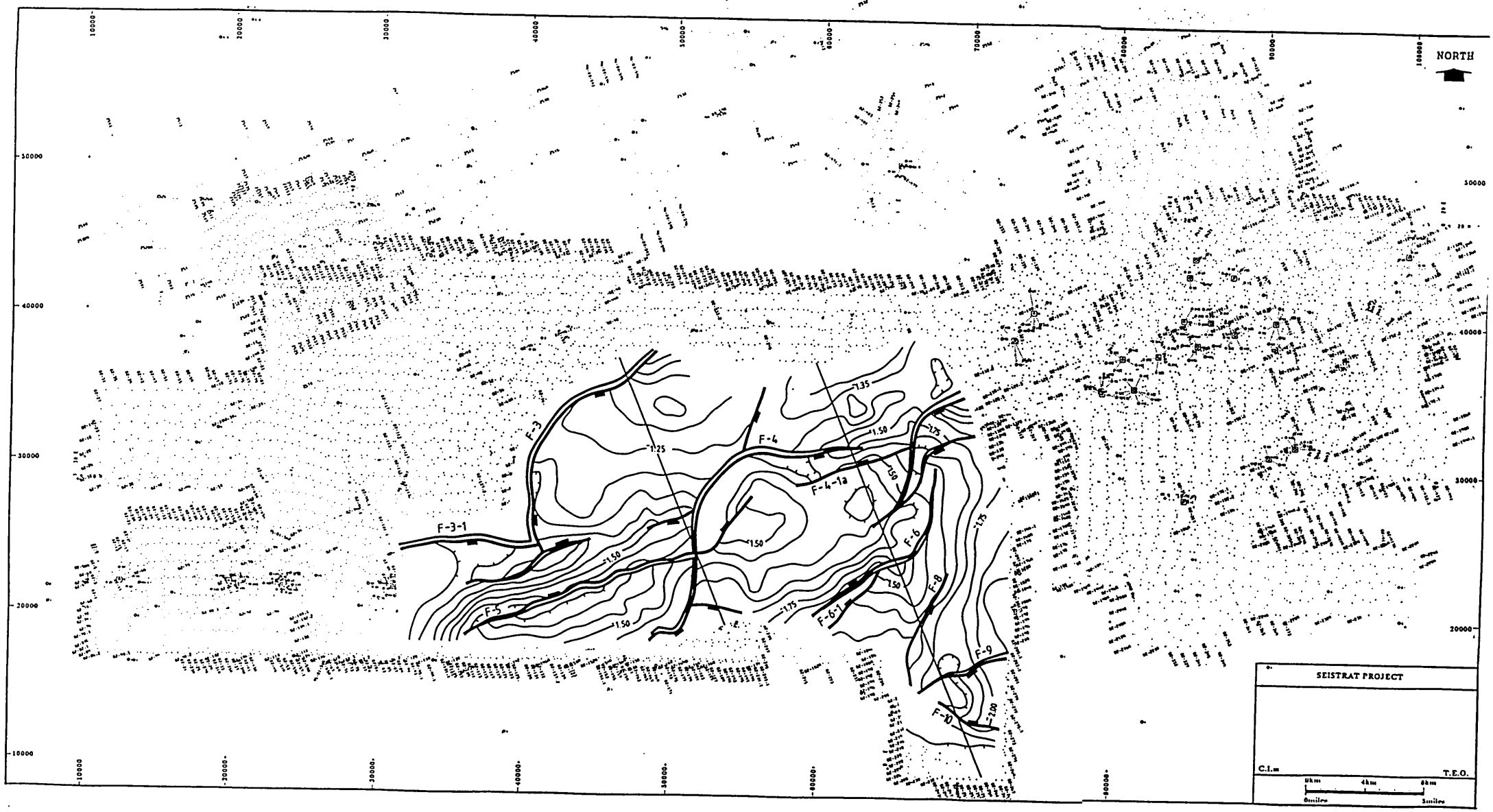

Fig.8.8a Structural map of Horizon QUA4 showing the prograded terrace close to the margins of the palaeobasin.

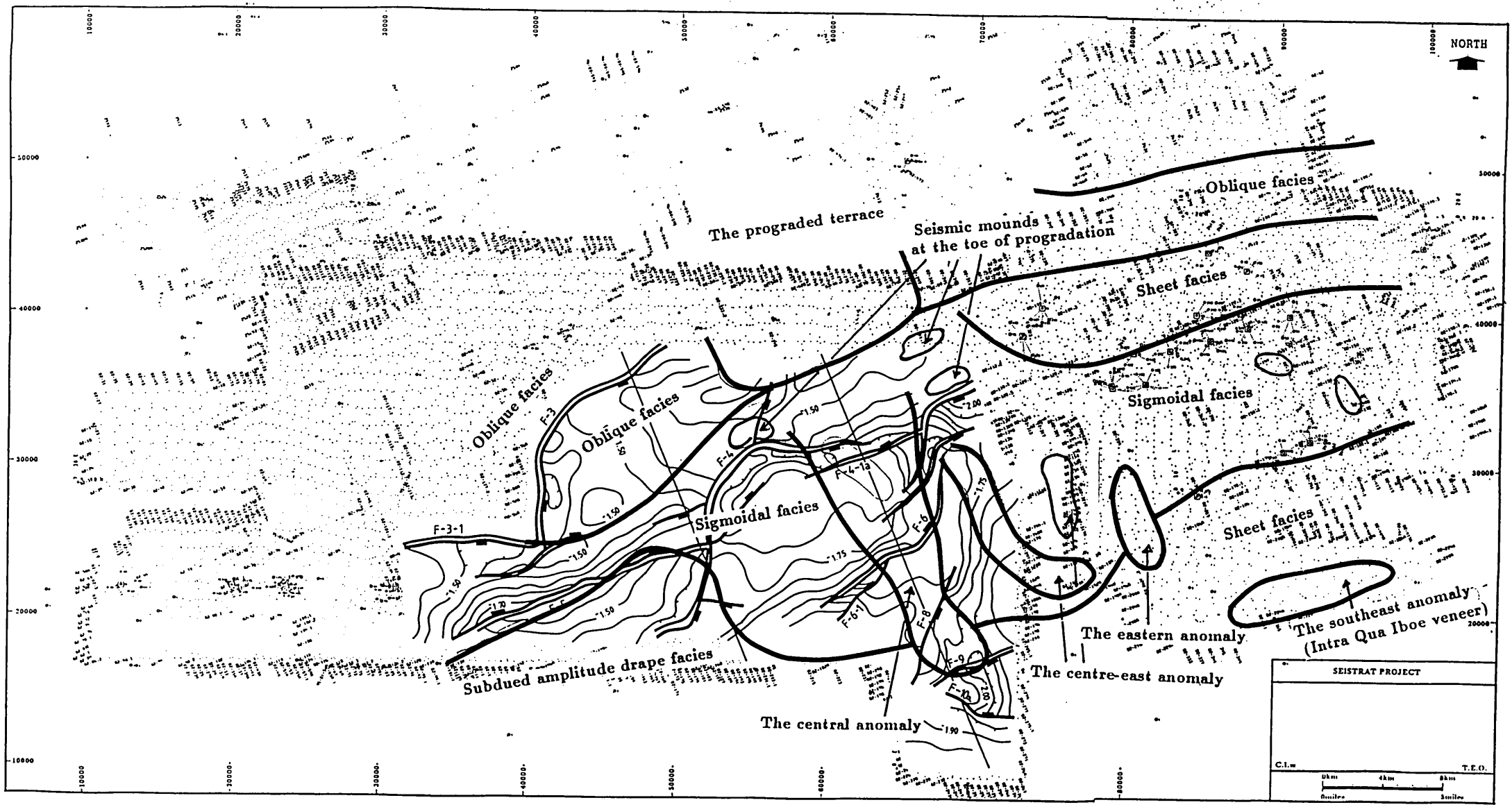

Fig.8.8b Facies distribution within SEQ.QS3 superimposed over the structural time map of Horizon QUA3.

LBIBR- Lower Base Intra Biafra Rubble.

LIBU- Lower Intra Biafra Unconformity.

BIBR- Base Intra Biafra Rubble.

TIBU- Top Intra Biafra Unconformity.

BIBBEN- Base Intra Biafra Benin sands.

BRB- Base Rubble Beds

BQI- Base Qua Iboe.

TIQI- Top Intra Qua Iboe

QUA3 etc- Intra Qua Iboe horizon 3 etc

Pu- Pleistocene Unconformity

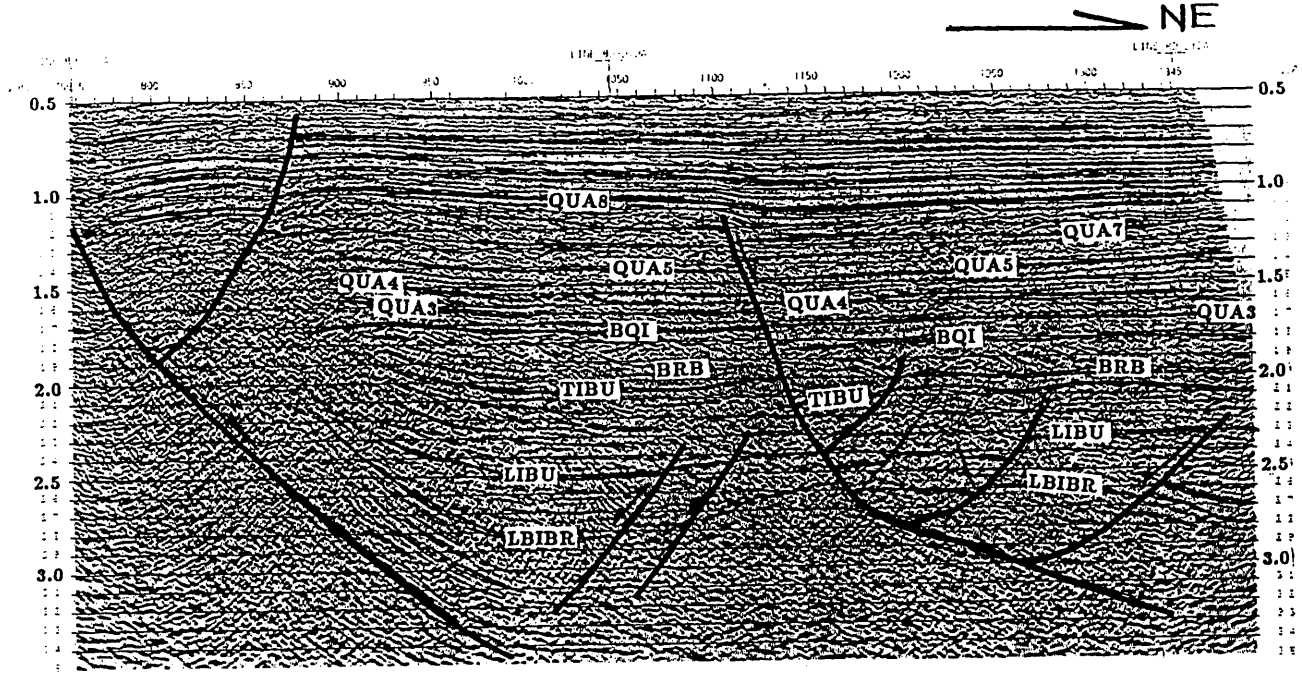

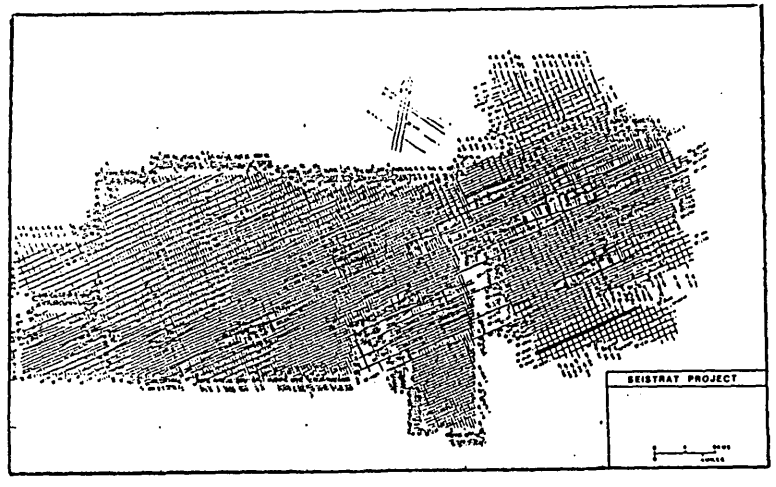

Fig.8.8c Line 82-212a shows oblique clinoforms occurring within QS3. Note the vertical succession of seismic facies within the Intra Qua Iboe: from the subdued amplitude drape facies between BQI and QUA3, the Oblique facies between QUA3 and QUA4, and the Sheet facies between QUA4 and QUA5.

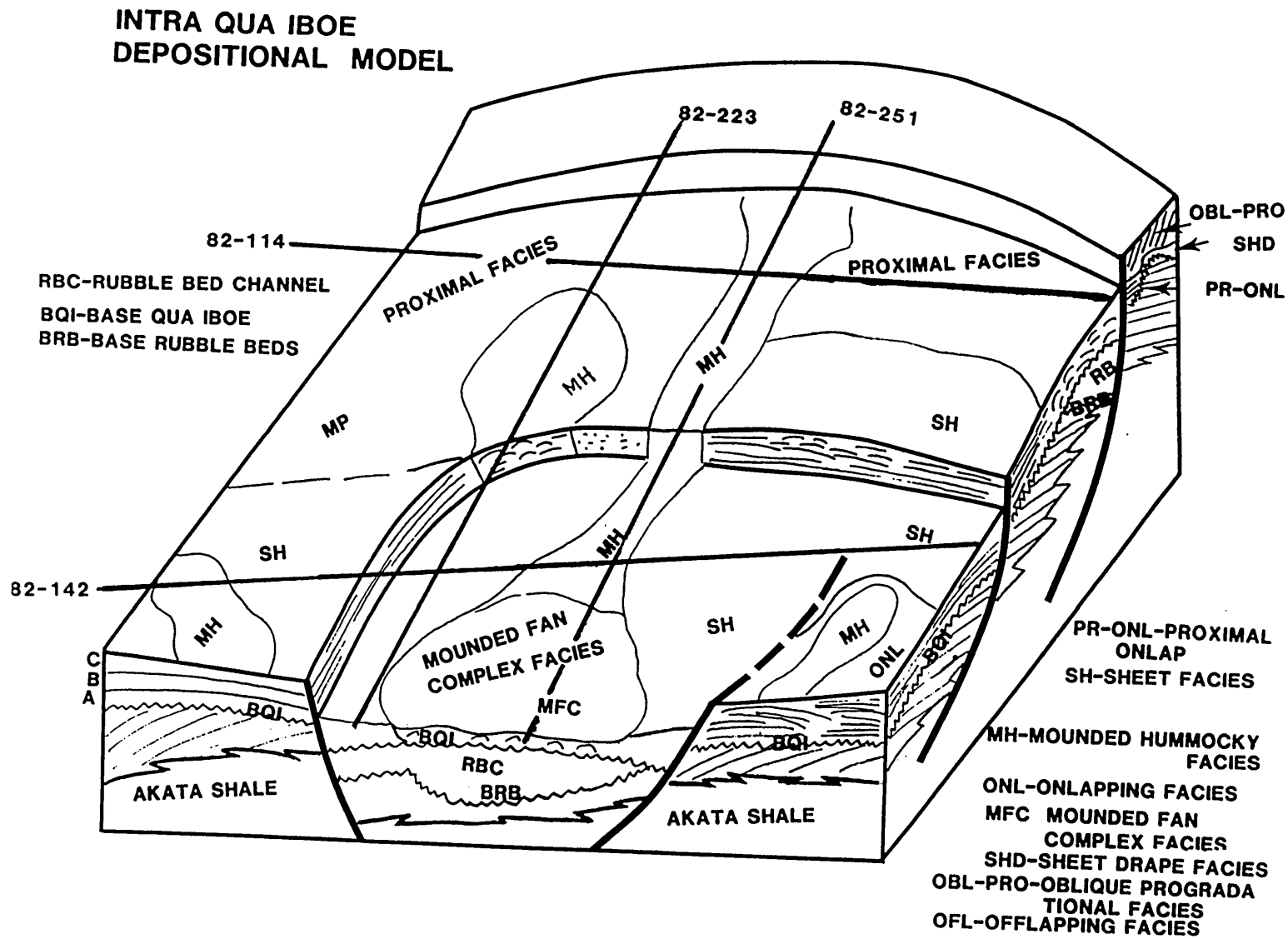

Fig.8.9a The Lower Qua Iboe depositional model.

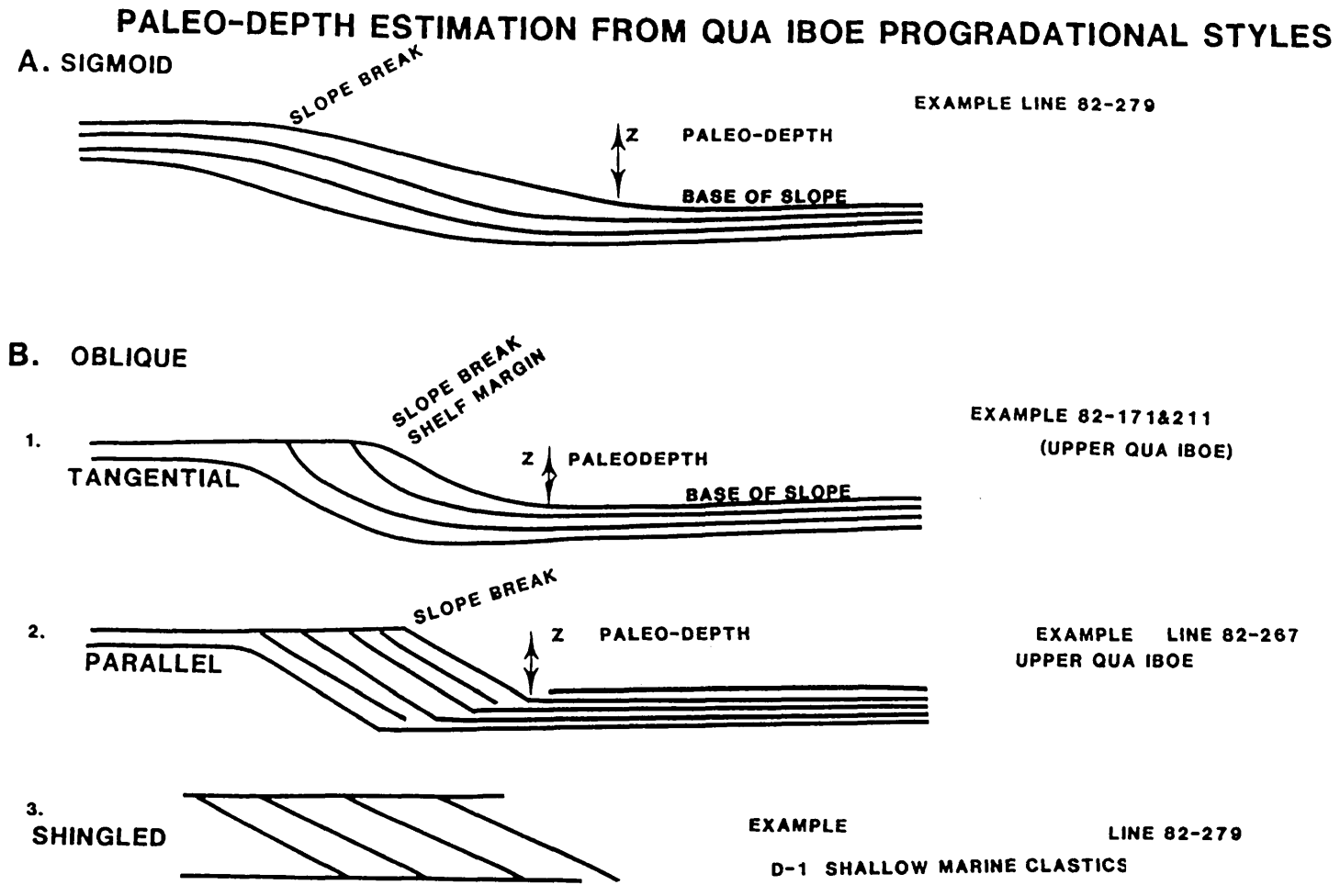

Fig.8.10a Paleodepth estimation from progradation.

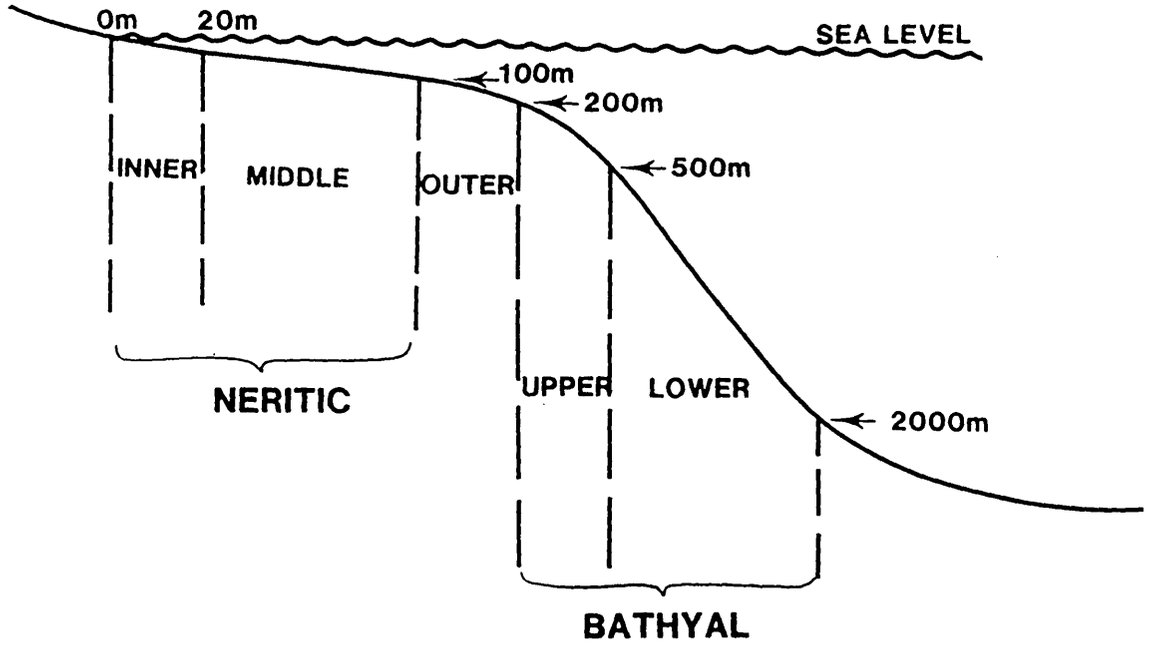

ENVIRONMENTAL DEPTH ZONES

Fig.8.10b Environmental depth zones.

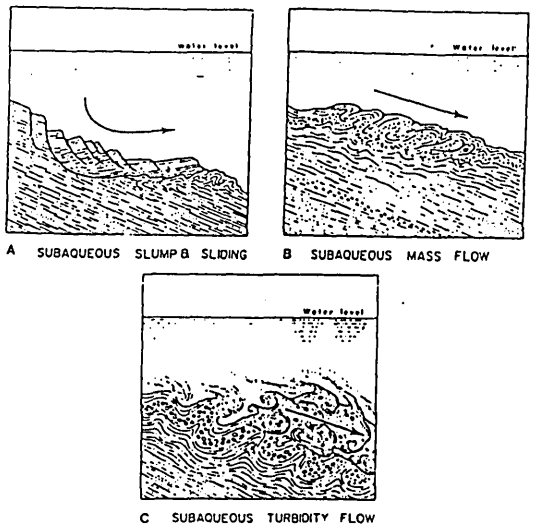

SUBAQUEOUS GRAVITY MOVEMENT OF SEDIMENT: SLUMPING, MASS FLOW, AND TURBIDITY FLOW. (From Dott, 1963)

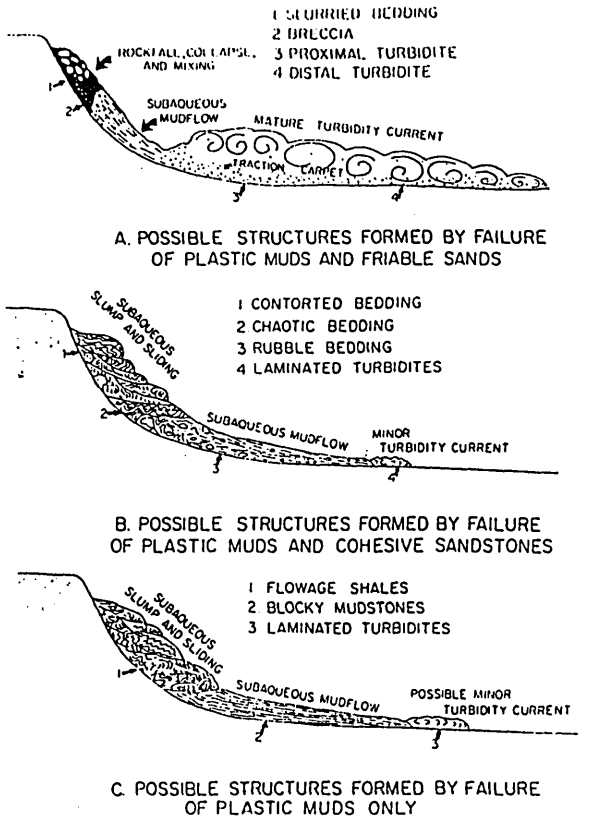

SLOPE FACIES DEVELOPED BY SUBMARINE SLUMP, SLIDES, AND ROCK FALLS. BASED ON MISSISSIPIAN JACKFORK FLYSCH FACIES, OKLAHOMA. FROM MORRIS (1971)

Fig.8.10c Process continuum in deep sea sedimentation.

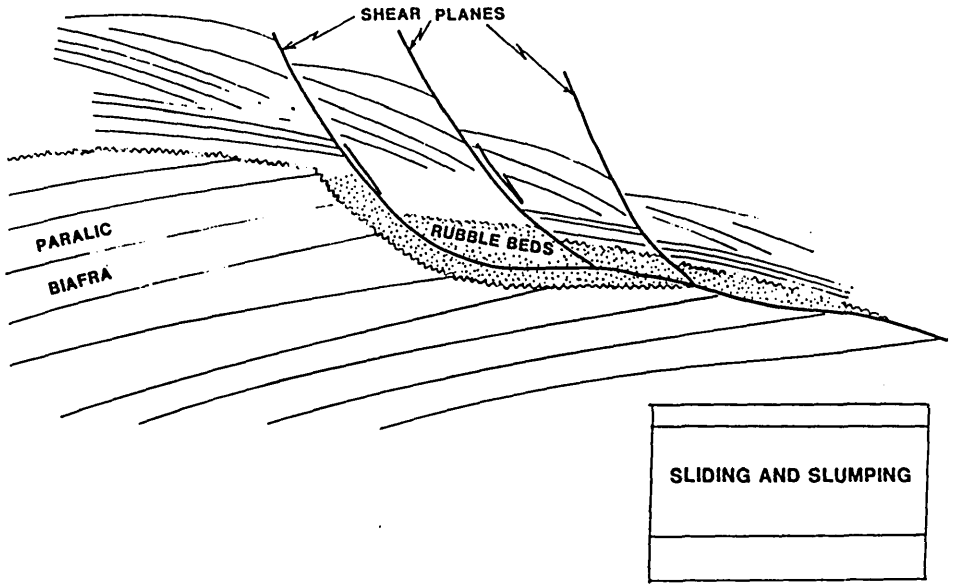

Fig.8.10d Seismic evidence of slumping (line 82-251).

A. TROUGH OR CANYON

B. MOUNDING

1. Dip oriented section

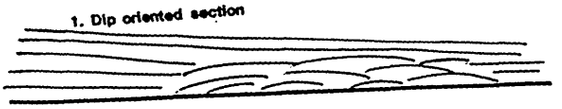

2. Strike oriented section

C. CLINOFORM REFLECTION PATTERNS

1. Thinning clinoform reflection interval

2. Underlying seismic facies interval onlapping and offlapping a depositional slope

Fig.8.11

SEISMIC INDICATORS OF TURBIDITE SEQUENCES.
AFTER BERG (1982)

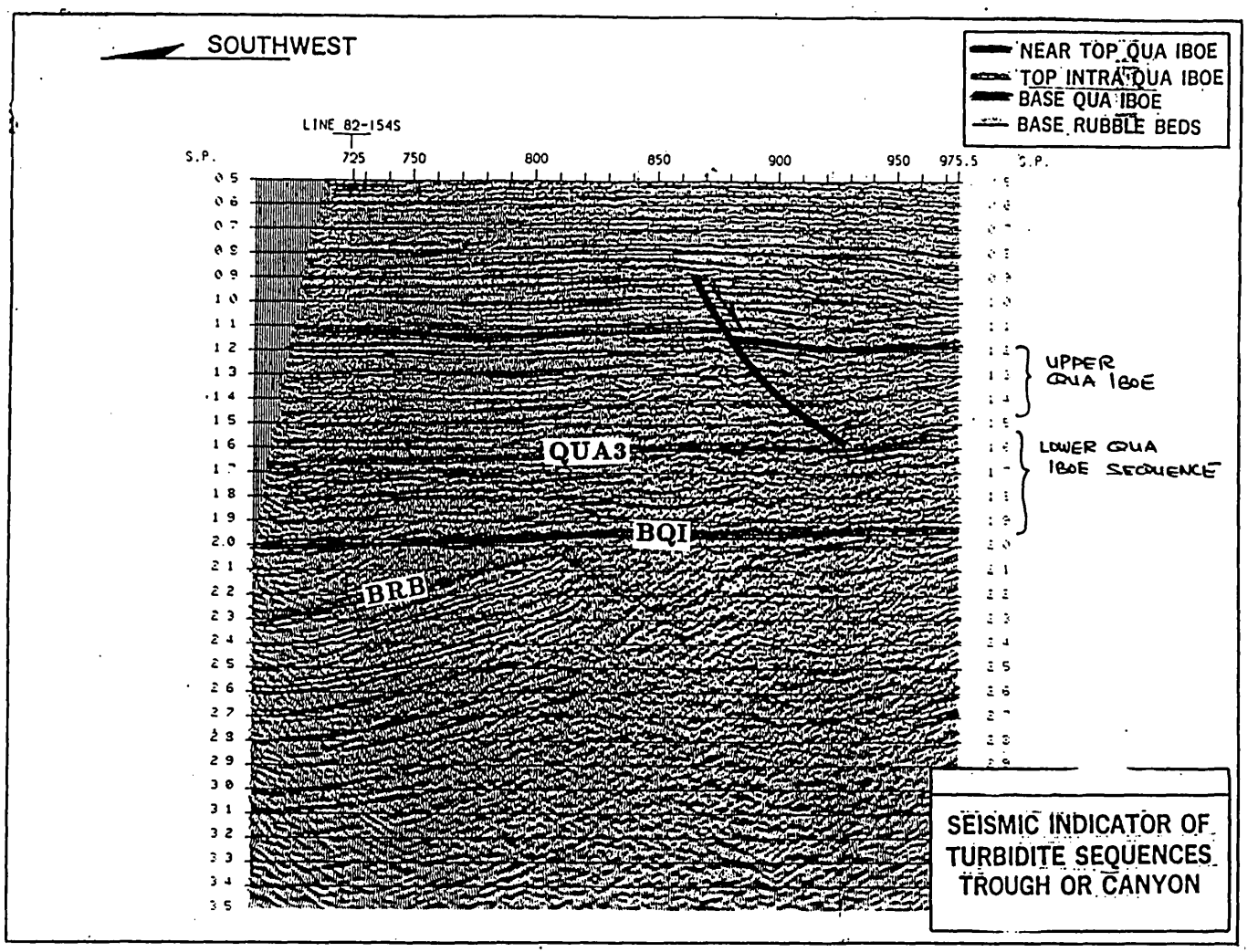

Fig.8.12a Seismic indicator of turbidite sequences(Trough or Canyon). (Line 82-154s).

LBIBR- Lower Base Intra Biafra Rubble.

LIBU- Lower Intra Biafra Unconformity.

BIBR- Base Intra Biafra Rubble.

TIBU- Top Intra Biafra Unconformity.

BIBBEN- Base Intra Biafra Benin sands.

BRB- Base Rubble Beds

BQI- Base Qua Iboe.

TIQI- Top Intra Qua Iboe

QUA3 etc- Intra Qua Iboe horizon 3 etc

Pu- Pleistocene Unconformity

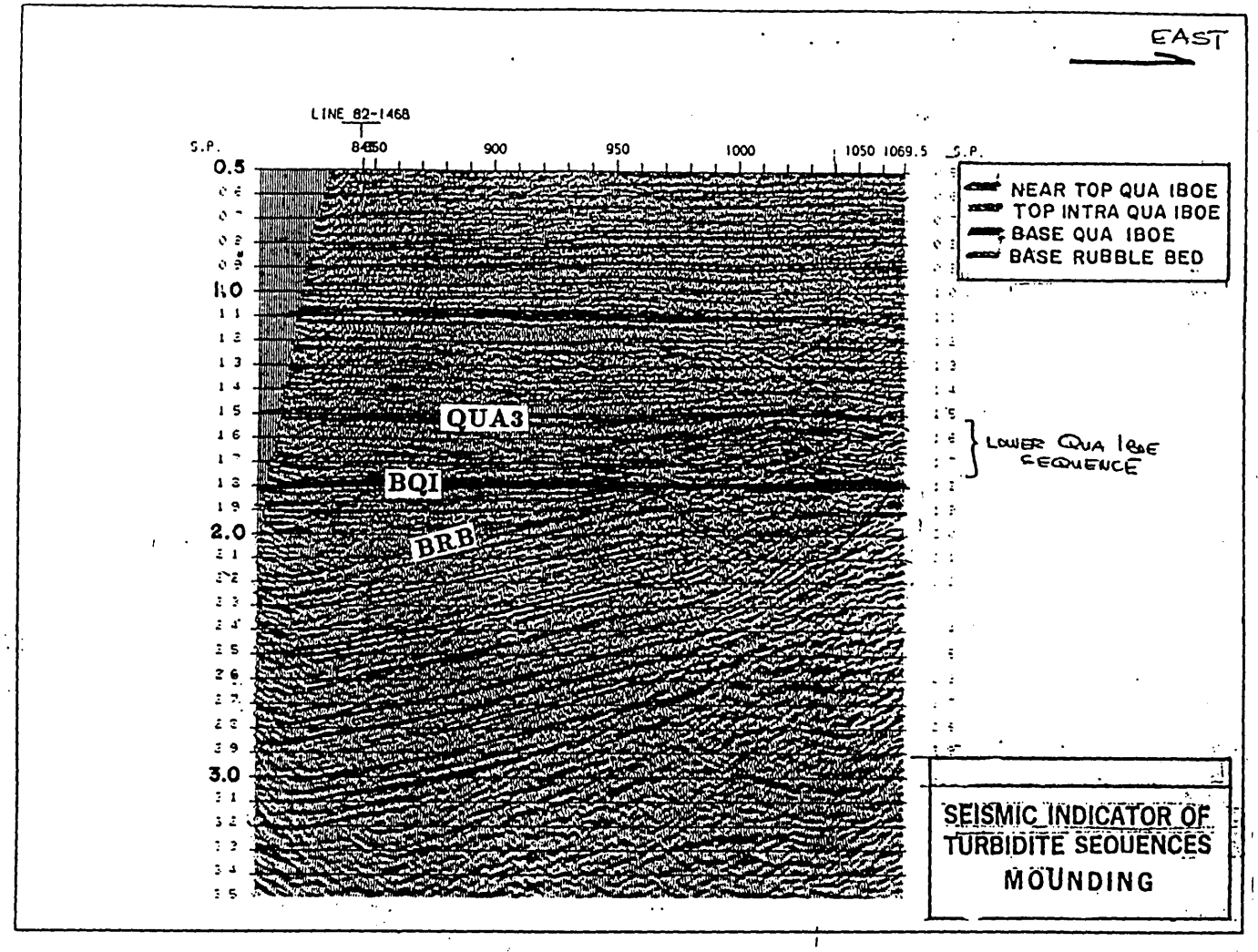

Fig.8.12b Seismic indicator of turbidite sequences(mounding). (Line 82-146b).

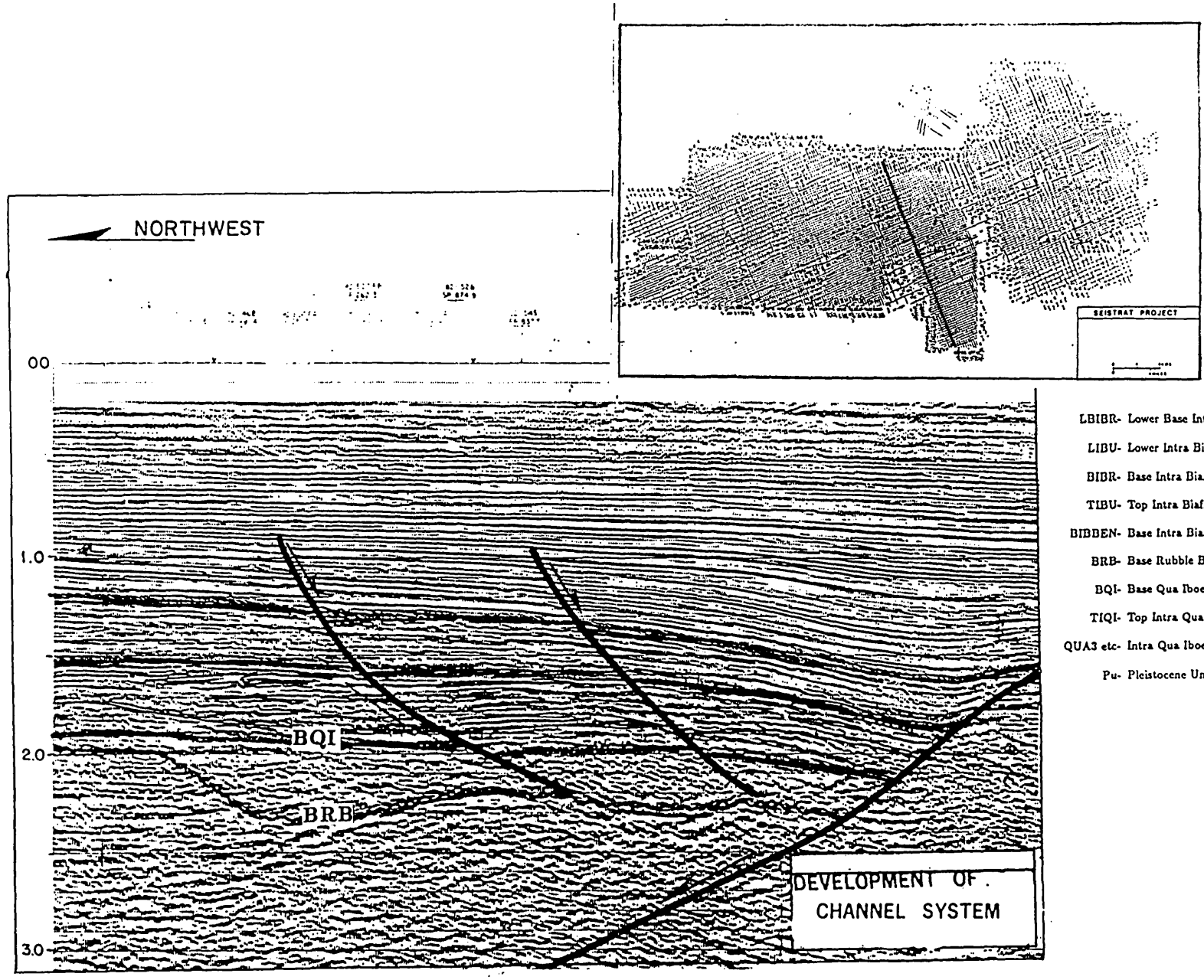

LBIBR- Lower Base Intra Biafra Rubble.

LIBU- Lower Intra Biafra Unconformity.

BIBR- Base Intra Biafra Rubble.

TIBU- Top Intra Biafra Unconformity.

BIBBEN- Base Intra Biafra Benin sands.

BRB- Base Rubble Beds

BQI- Base Qua Iboe.

TIQI- Top Intra Qua Iboe

QUA3 etc- Intra Qua Iboe horizon 3 etc

Pu- Pleistocene Unconformity

Fig.8.12c Line 82-251 showing seismic mounding along the central anomaly. Note also, the Rubble Bed canyon beneath.

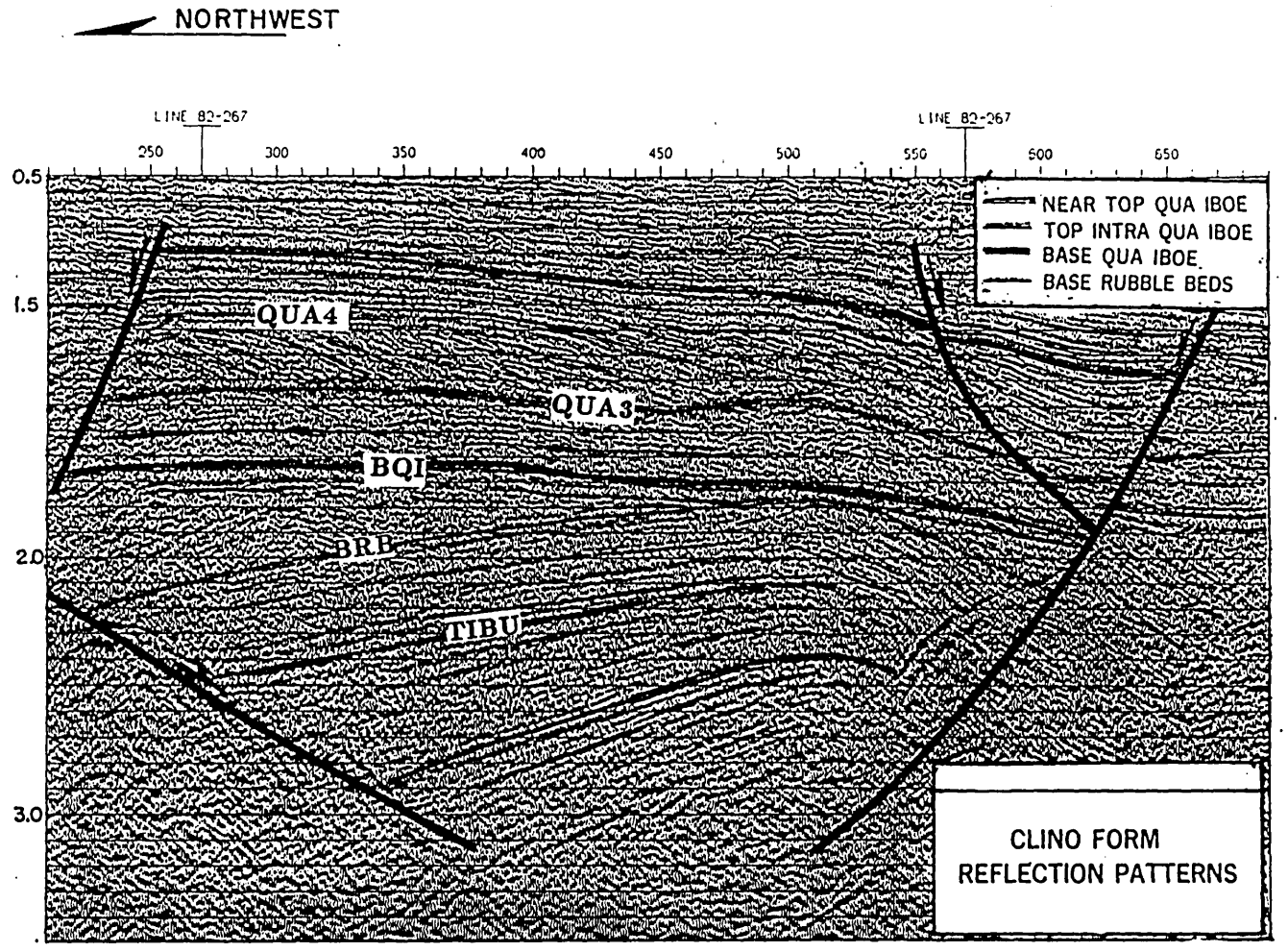

Fig.8.12d Line 82-267 showing a thinning clinoform reflection pattern. This profile is over the prograded 'terrace'.

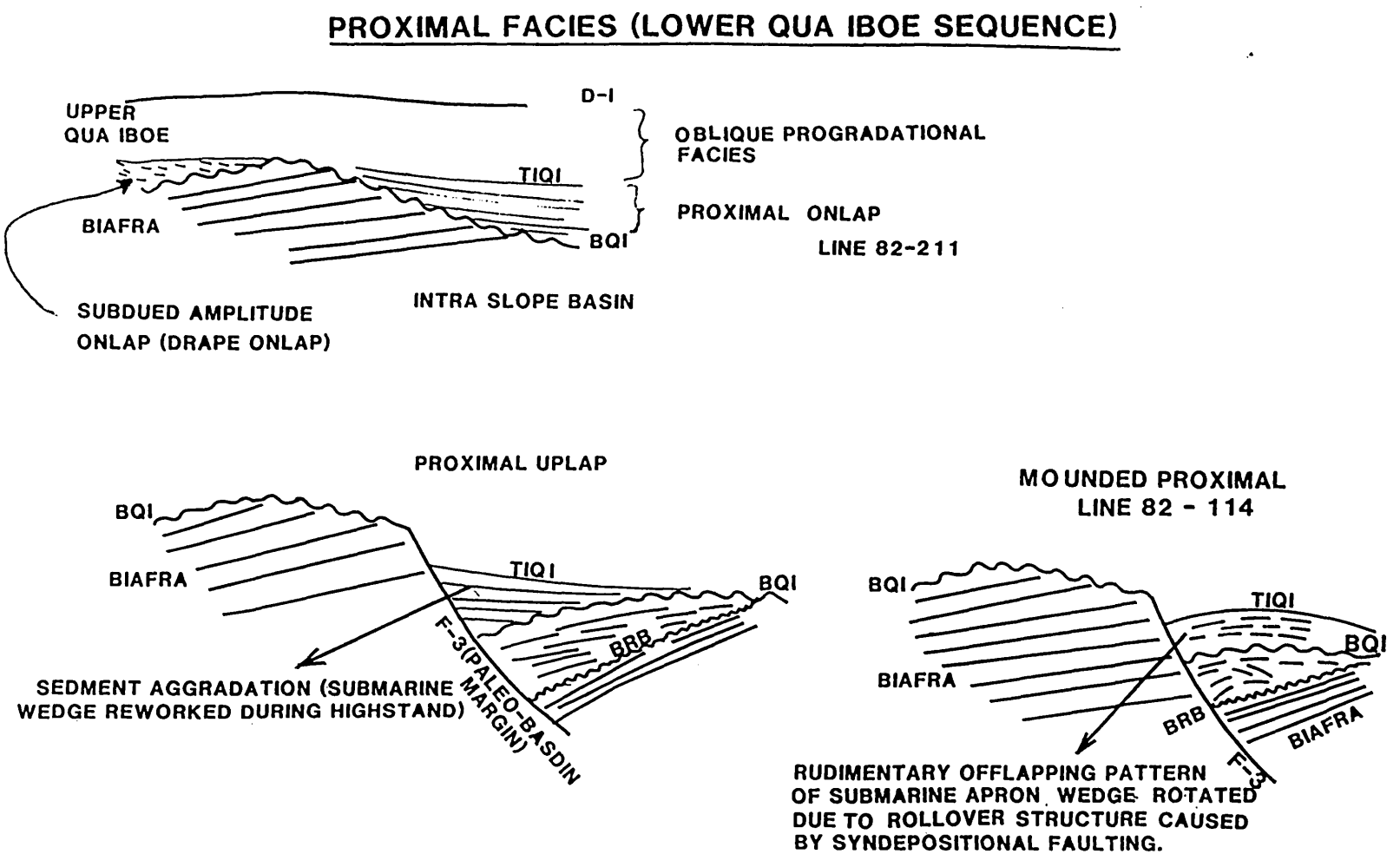

Fig.8.13a An illustration of the variations prevalent with the Proximal facies.

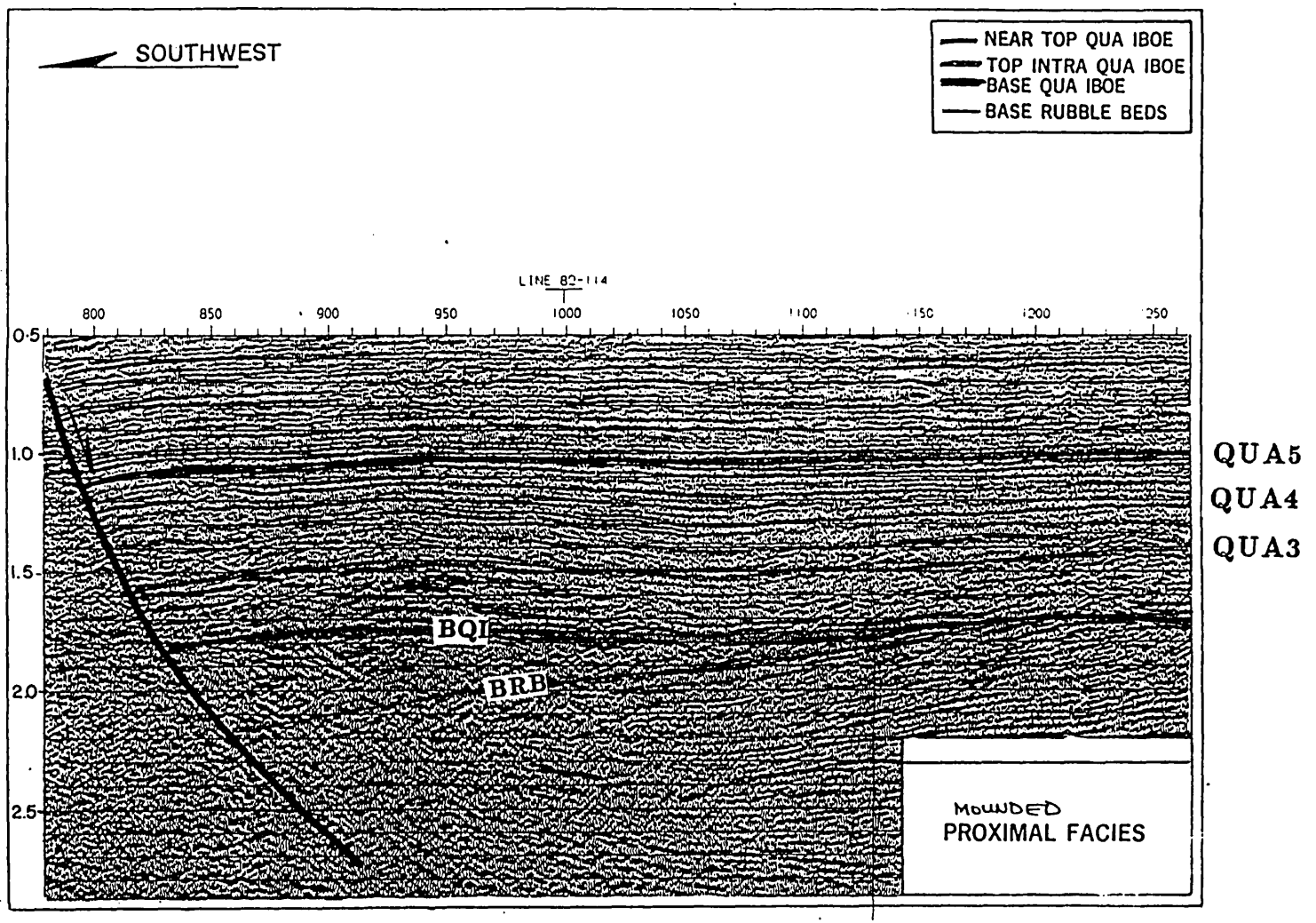

Fig.8.13b Mounded proximal facies.

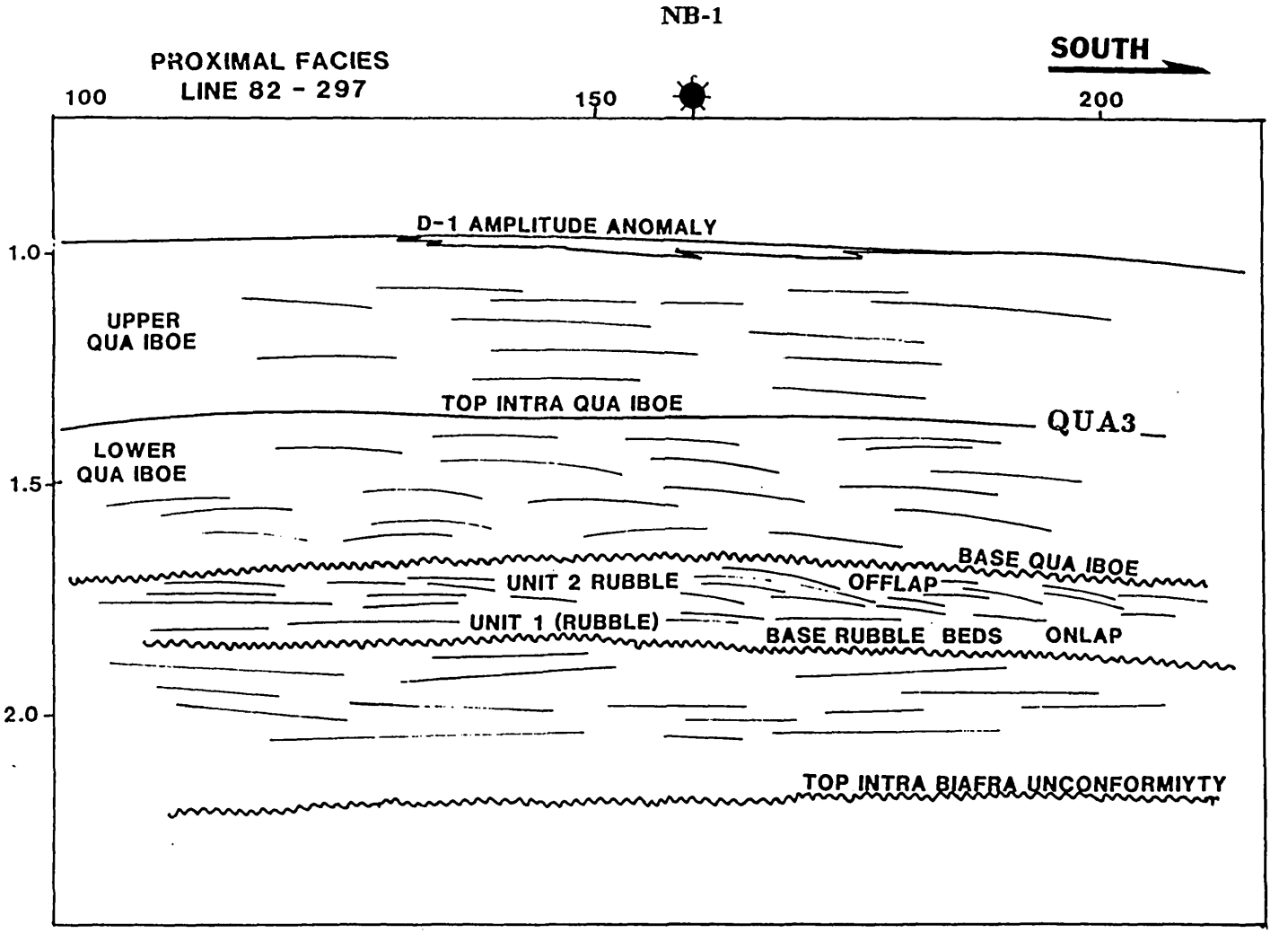

Fig.8.13c Line 82-297 showing the relationship between the proximal facies of the Rubble Beds and the Lower Qua Iboe.

LBIBR- Lower Base Intra Biafra Rubble.

LIBU- Lower Intra Biafra Unconformity.

BIBR- Base Intra Biafra Rubble.

TIBU- Top Intra Biafra Unconformity.

BIBBEN- Base Intra Biafra Benin sands.

BRB- Base Rubble Beds

BQI- Base Qua Iboe.

TIQI- Top Intra Qua Iboe

QUA3 etc- Intra Qua Iboe horizon 3 etc

Pu- Pleistocene Unconformity

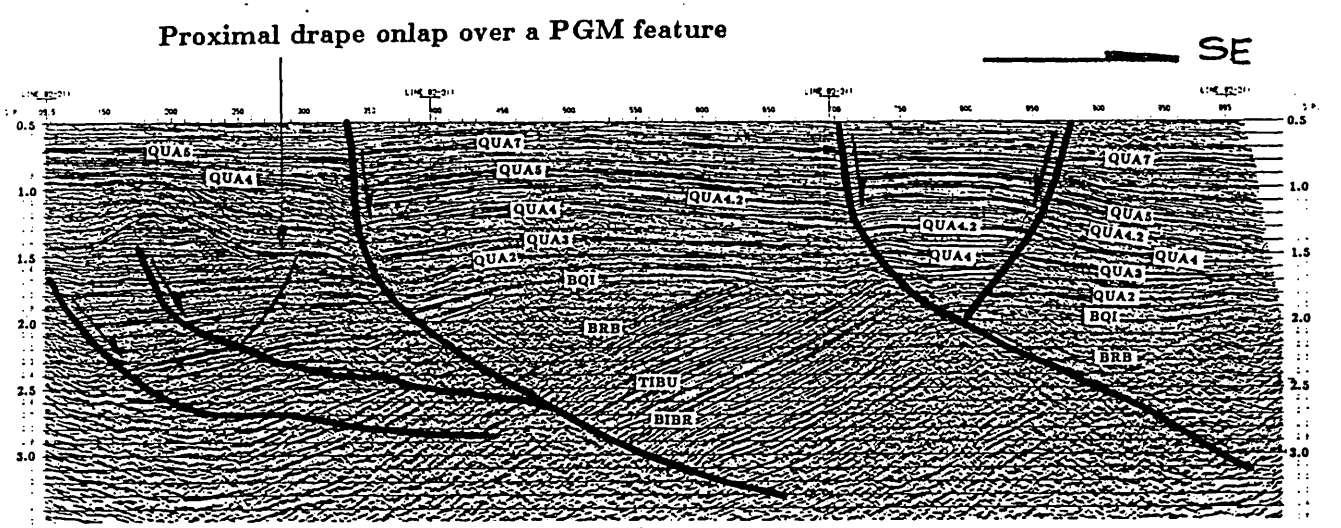

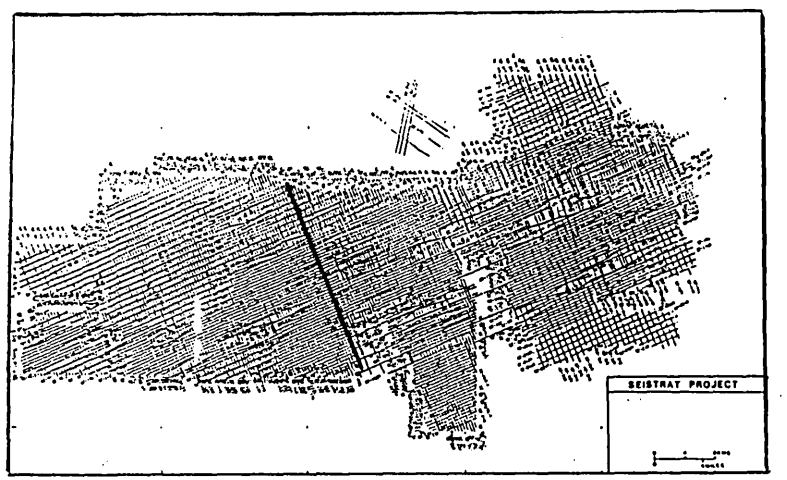

Fig.8.13d Proximal onlap(line 82-211).

LIBBR Lower Base Intra Biafra Rubble.

LIBU Lower Intra Biafra Unconformity.

BIBR Base Intra Biafra Rubble.

TIBU- Top Intra Biafra Unconformity.

BIBBEN- Base Intra Biafra Benin sands.

BRB- Base Rubble Beds

BQI- Base Qua Iboe.

TIQI- Top Intra Qua Iboe

QUA3 etc- Intra Qua Iboe horizon 3 etc

Pu- Pleistocene Unconformity

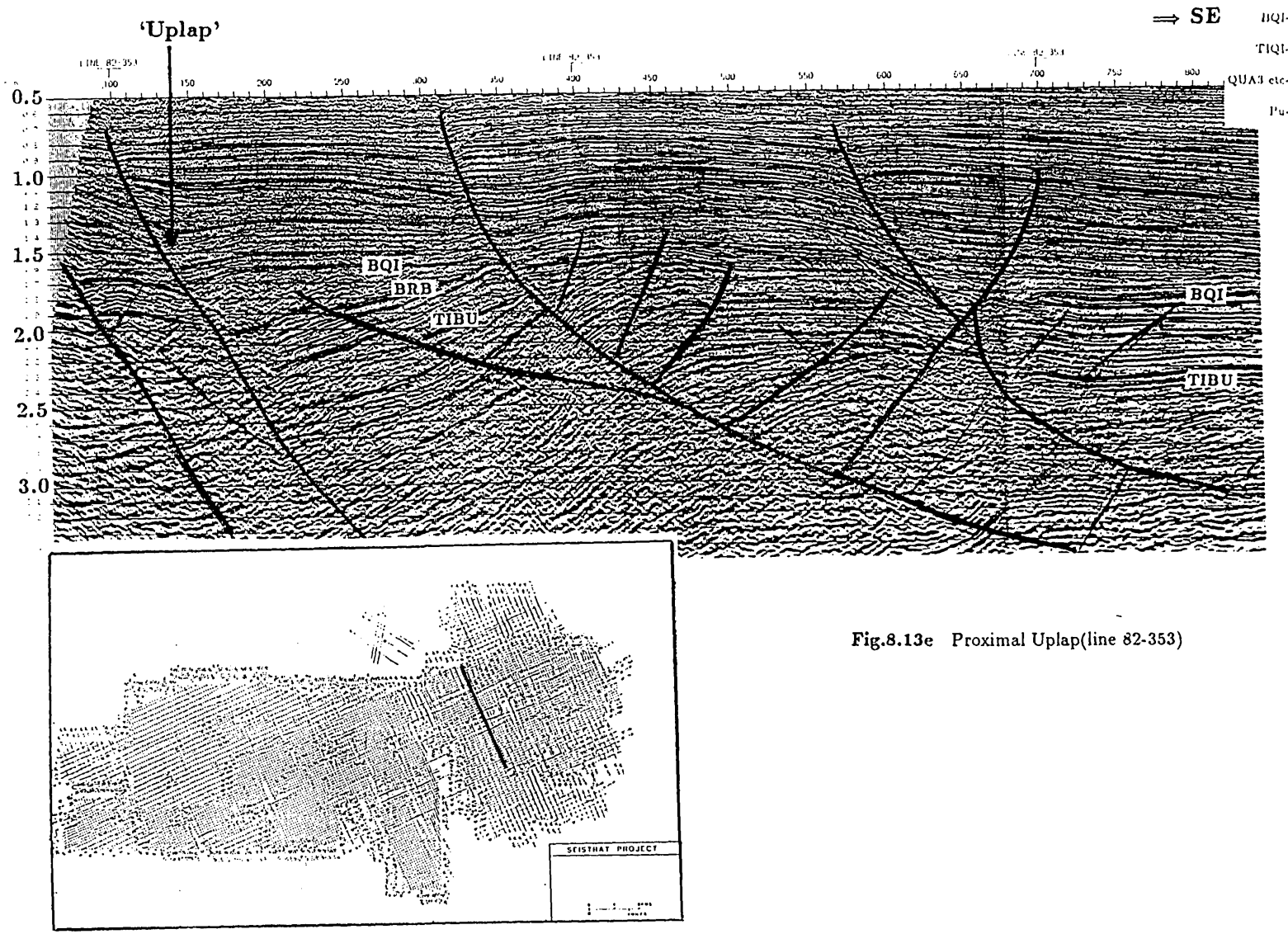

Fig.8.13e Proximal Uplap(line 82-353)

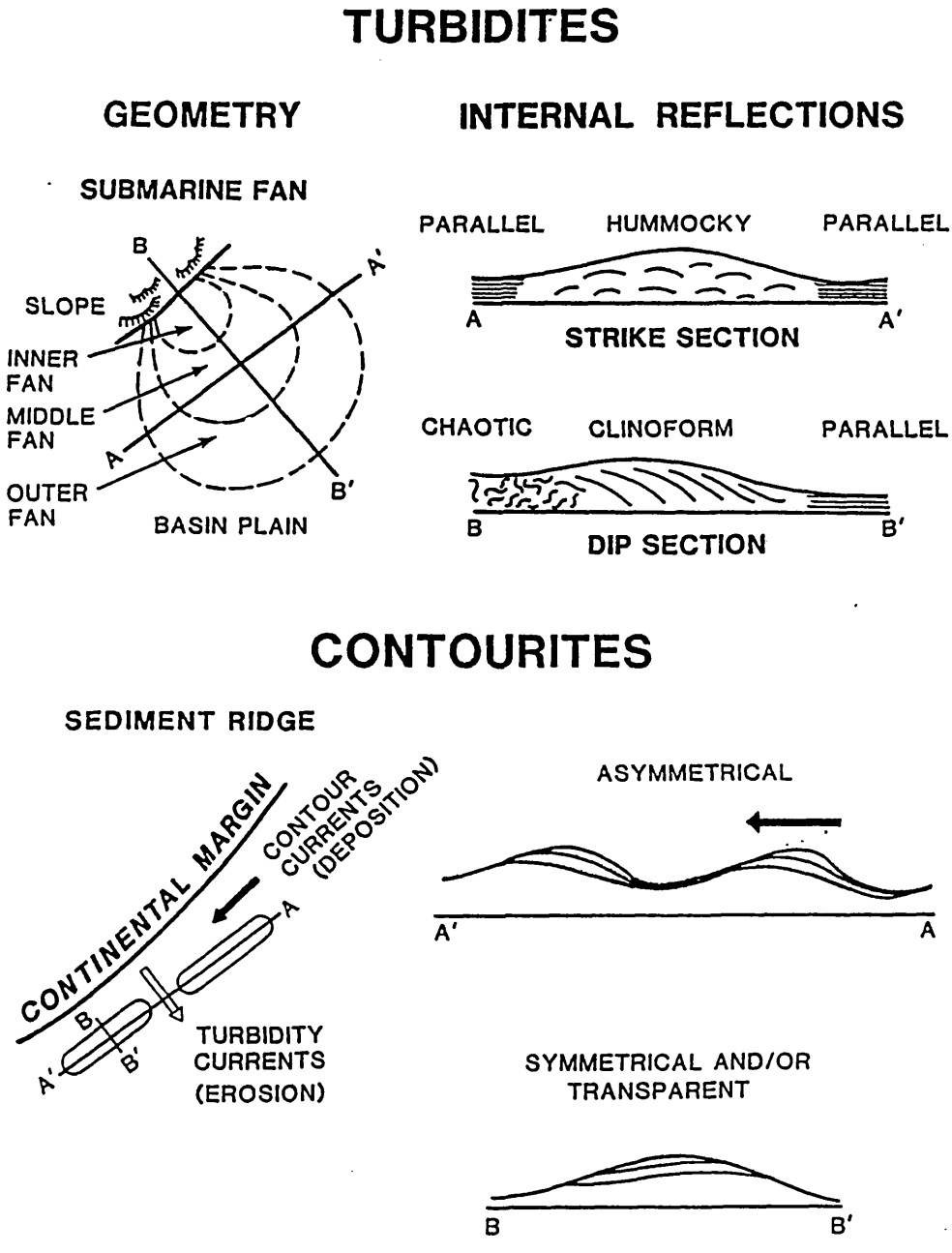

Fig.8.14a Seismic models showing the possible internal reflection patterns of turbidites in contrast to contourite packages. Also see Pettijohn *et al.*(1972), Fig.2.1.

Fig.8.15 Composite of the distribution of seimic mounds.

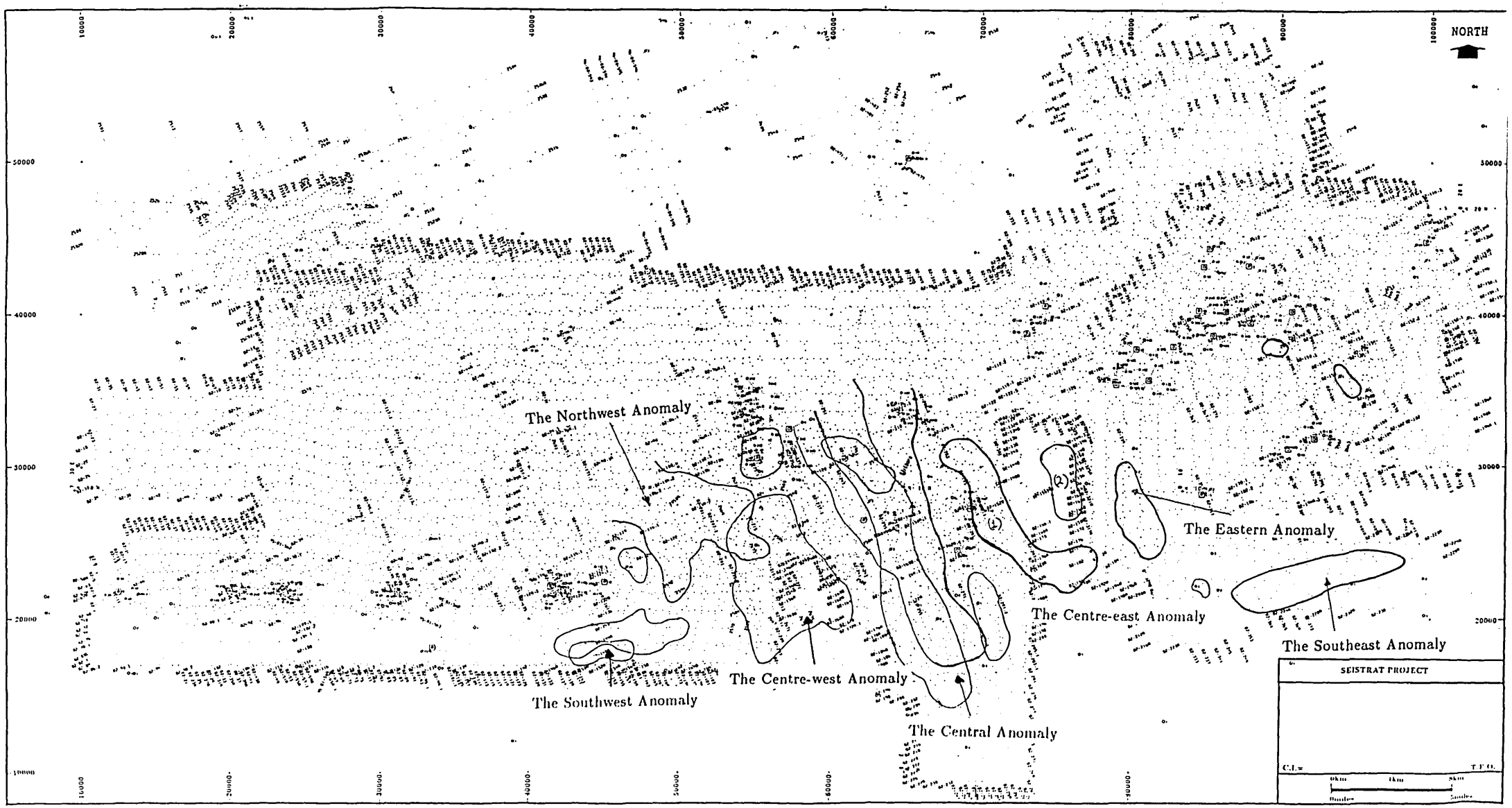

82-88a

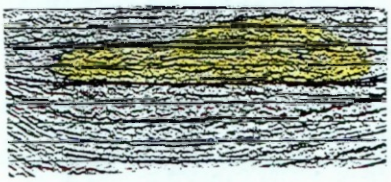

82-110

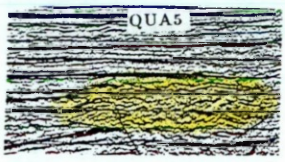

82-142

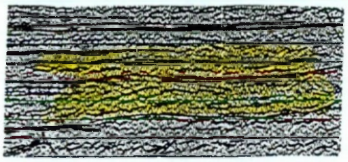

82-150a

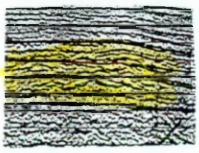

82-158

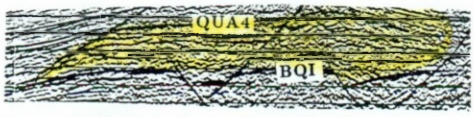

82-174

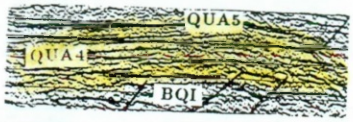

82-186

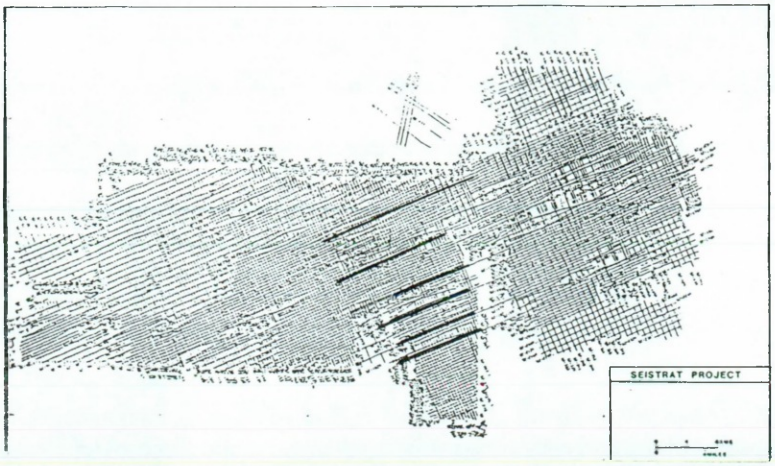

Fig.8.16a Build-up of the central anomaly.

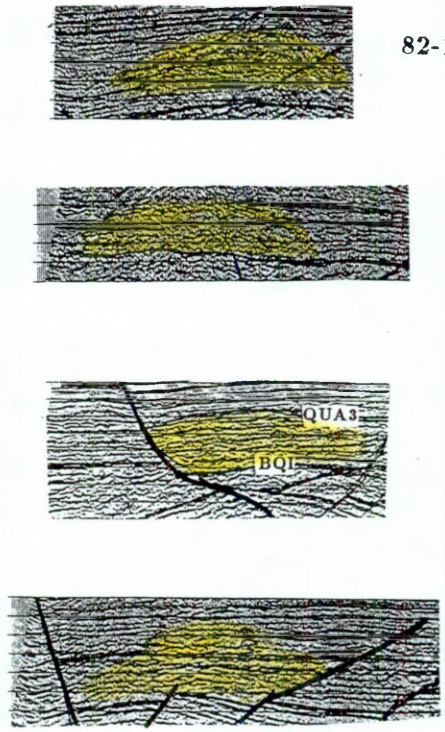

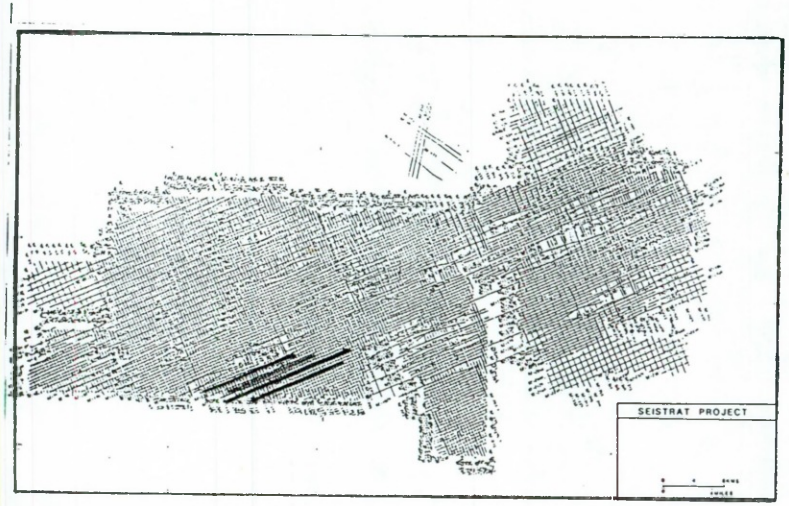

Fig.8.16b Build-up of the southwest anomaly.

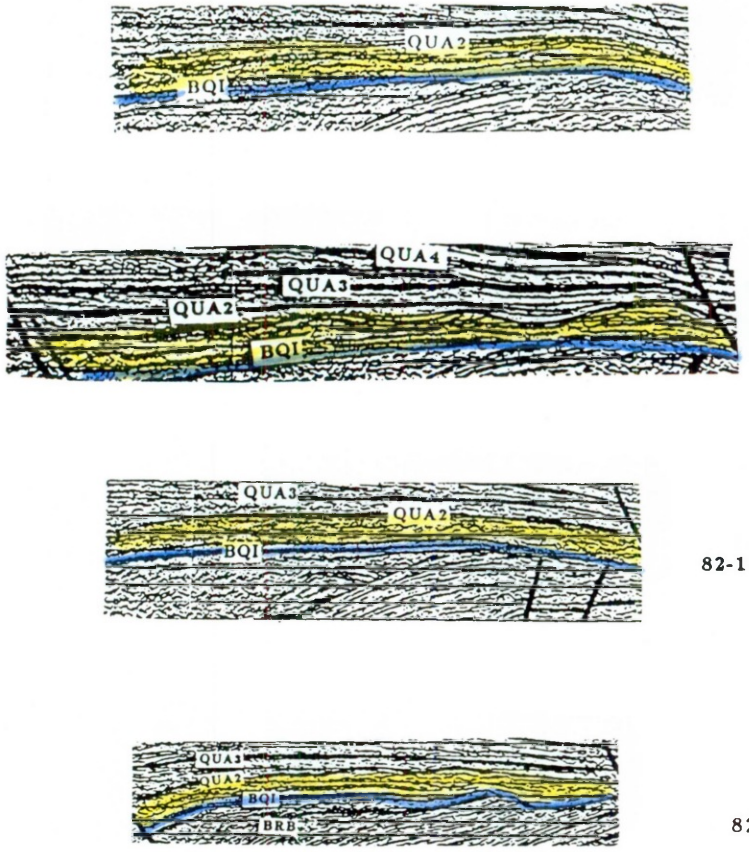

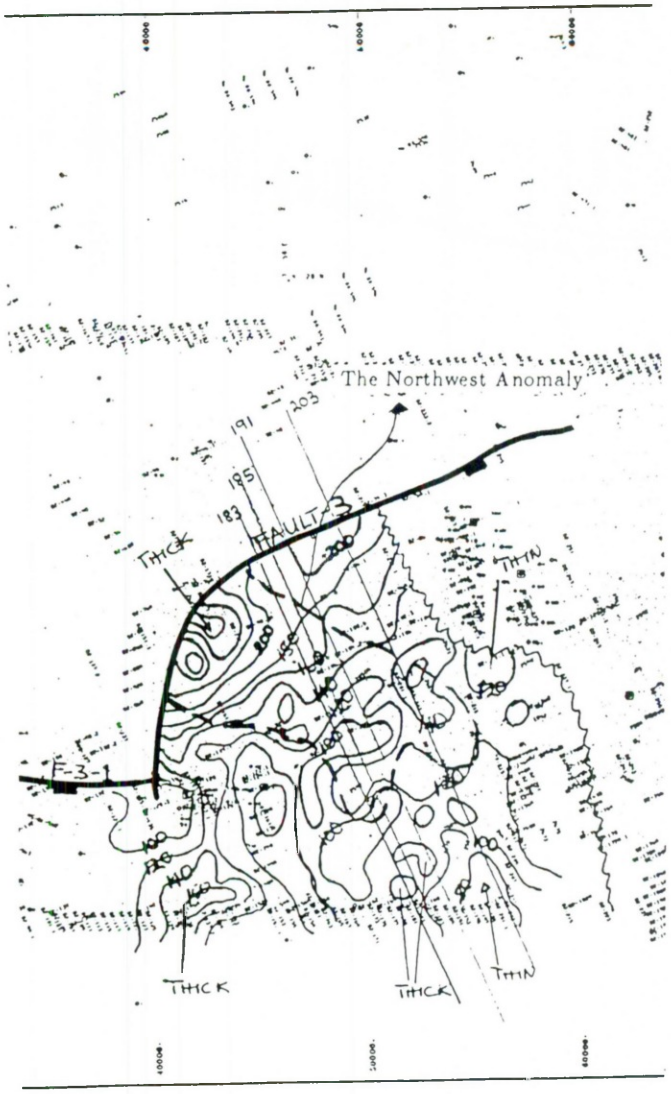

Fig.8.16c Build up of the northwest anomaly and Isochron of SEQ.QS1 over the anomaly.

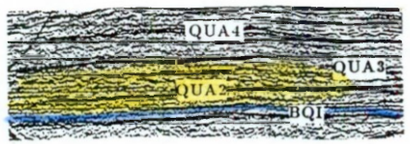

82-142

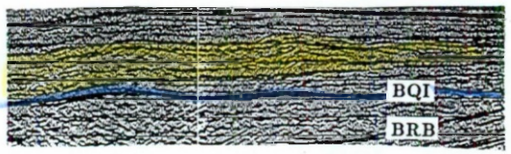

82-150a

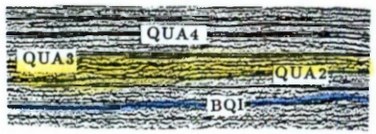

82-158

Fig.8.16d Build-up of the centre-west anomaly southward.

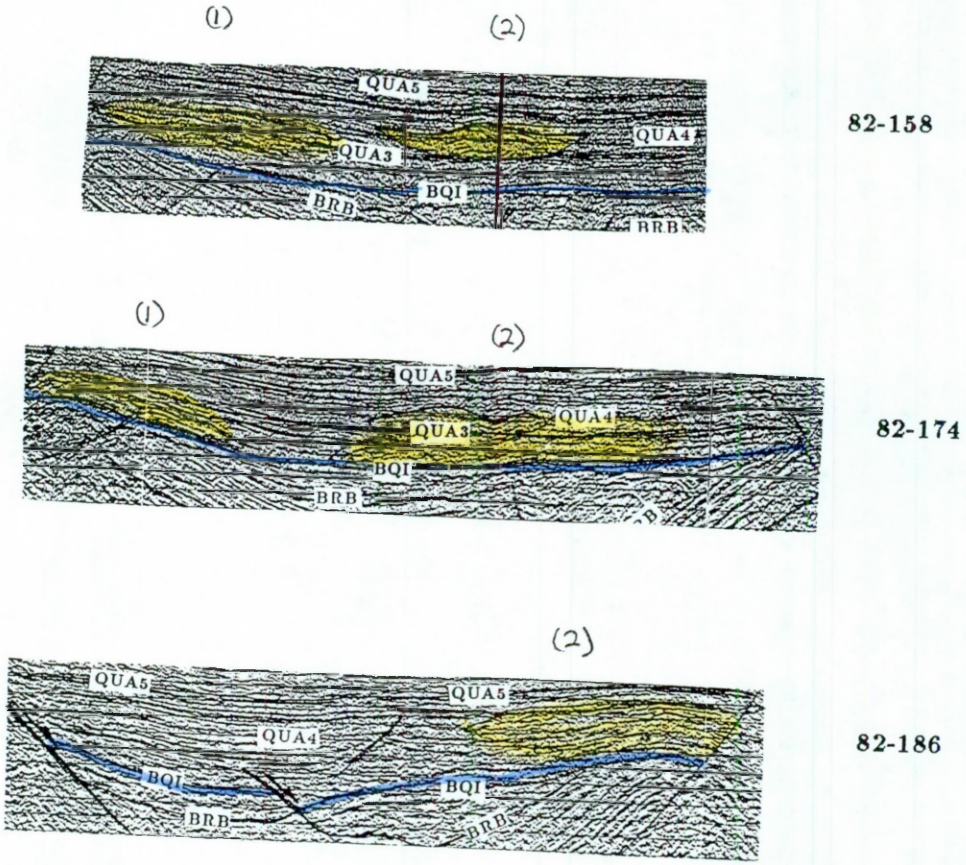

Fig.8.16e The centre-east(1&2) anomaly.

82-158

82-162b

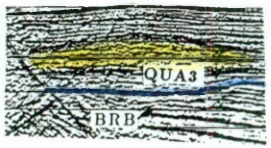

82-174

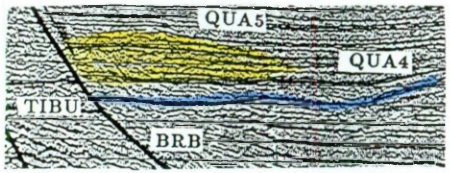

82-178

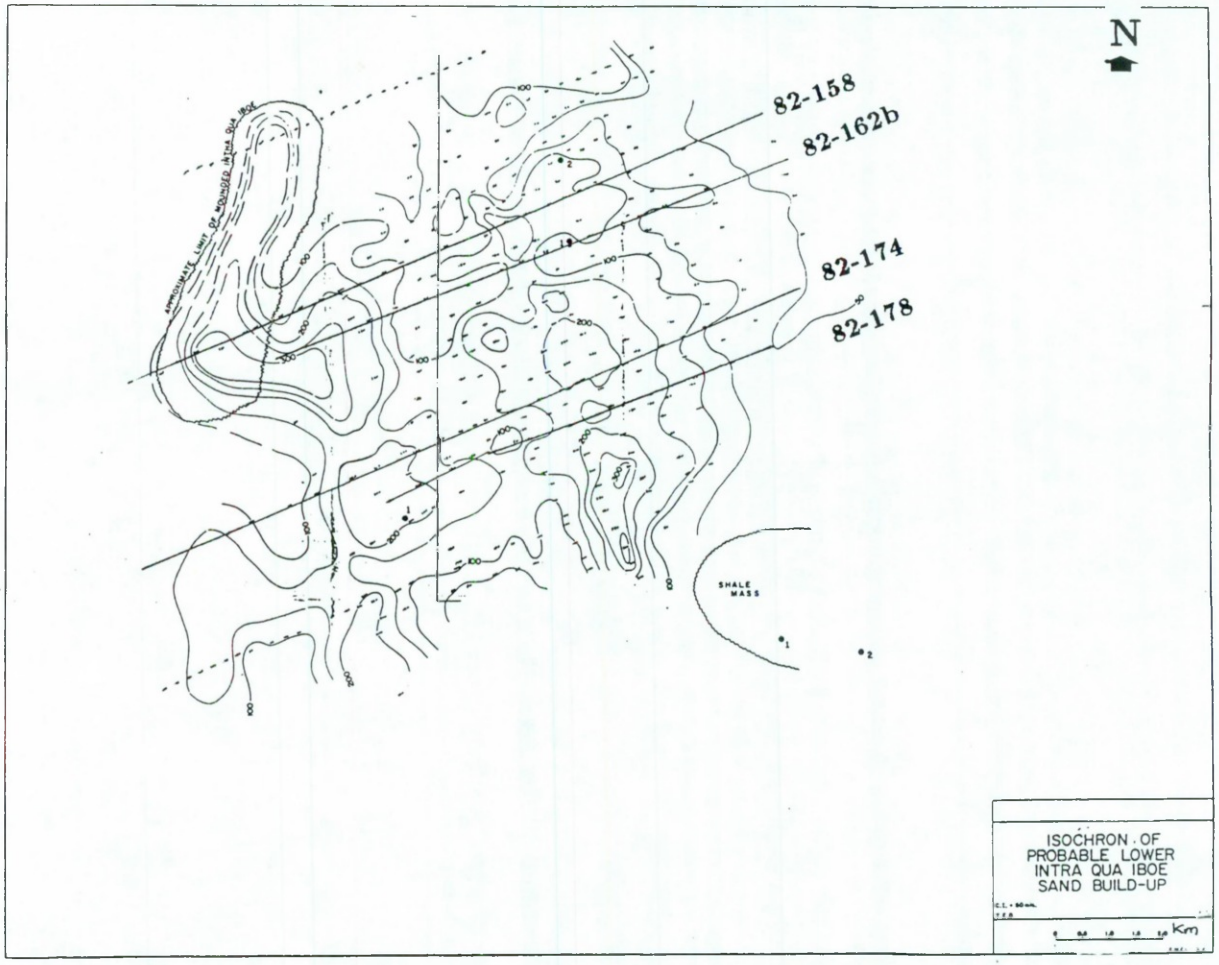

Fig.8.16f The eastern anomaly

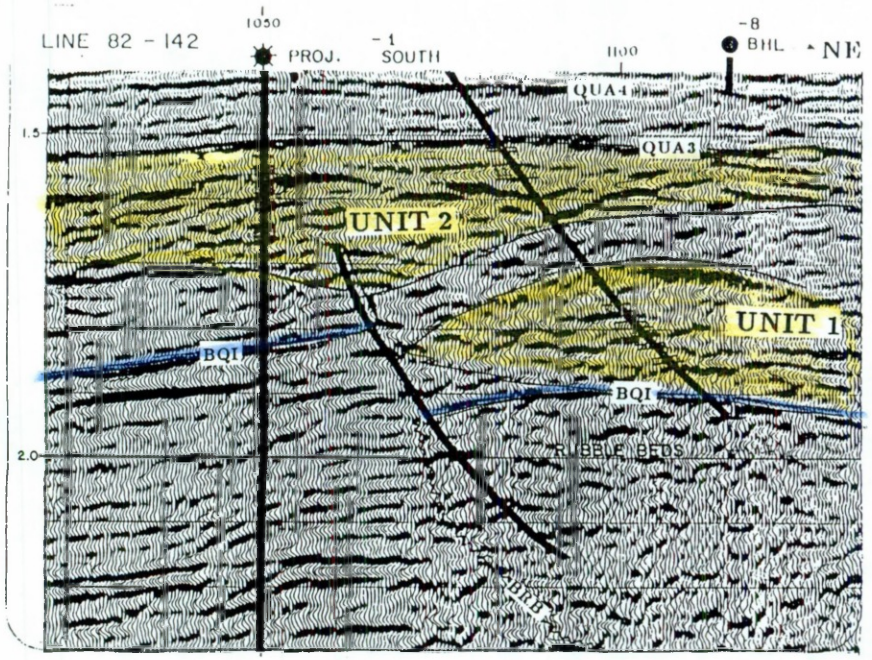

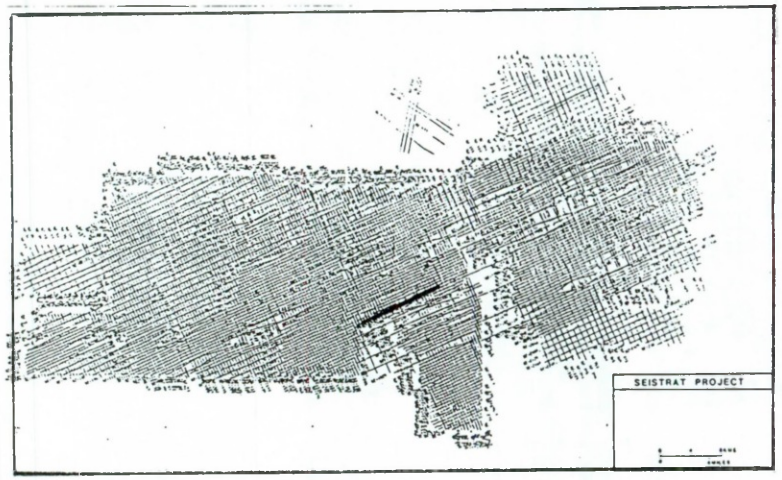

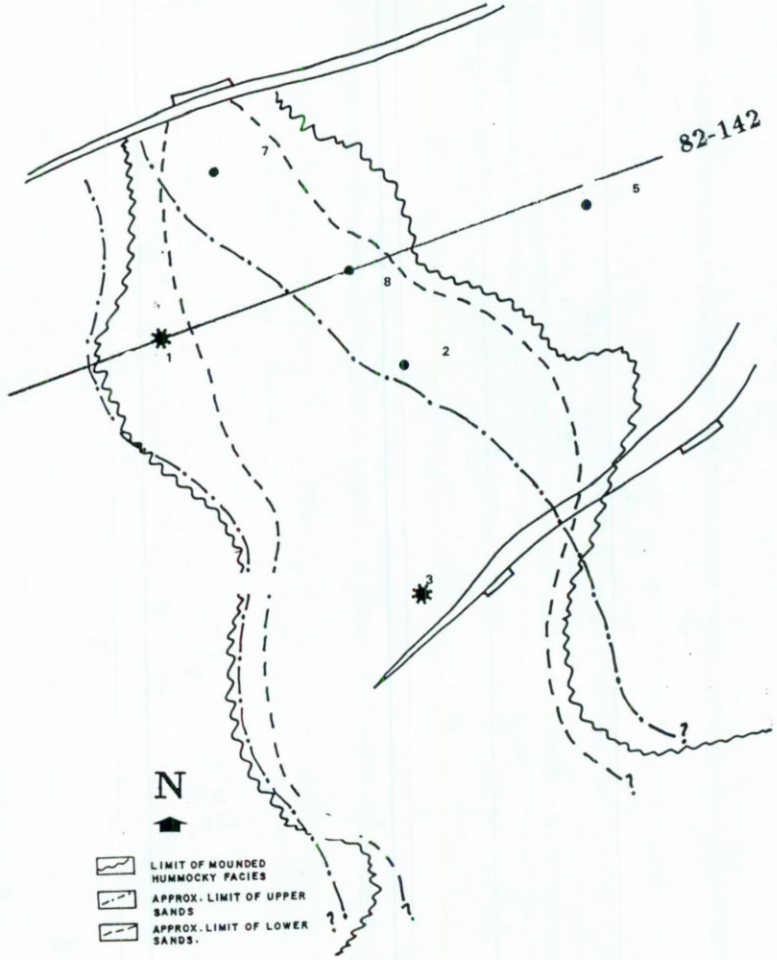

Fig.8.17 Line 82-142, showing the two main sand bodies that make up the central anomaly. Also shown is the detailed extent of the anomaly close to well CA-1.

LBIBR- Lower Base Intra Biafra Rubble.

LIBU- Lower Intra Biafra Unconformity.

BIBR- Base Intra Biafra Rubble.

TIBU- Top Intra Biafra Unconformity.

BIBBEN- Base Intra Biafra Benin sands.

BRB- Base Rubble Beds

BQI- Base Qua Iboe.

TIQI- Top Intra Qua Iboe

QUA3 etc- Intra Qua Iboe horizon 3 etc

Pu- Pleistocene Unconformity

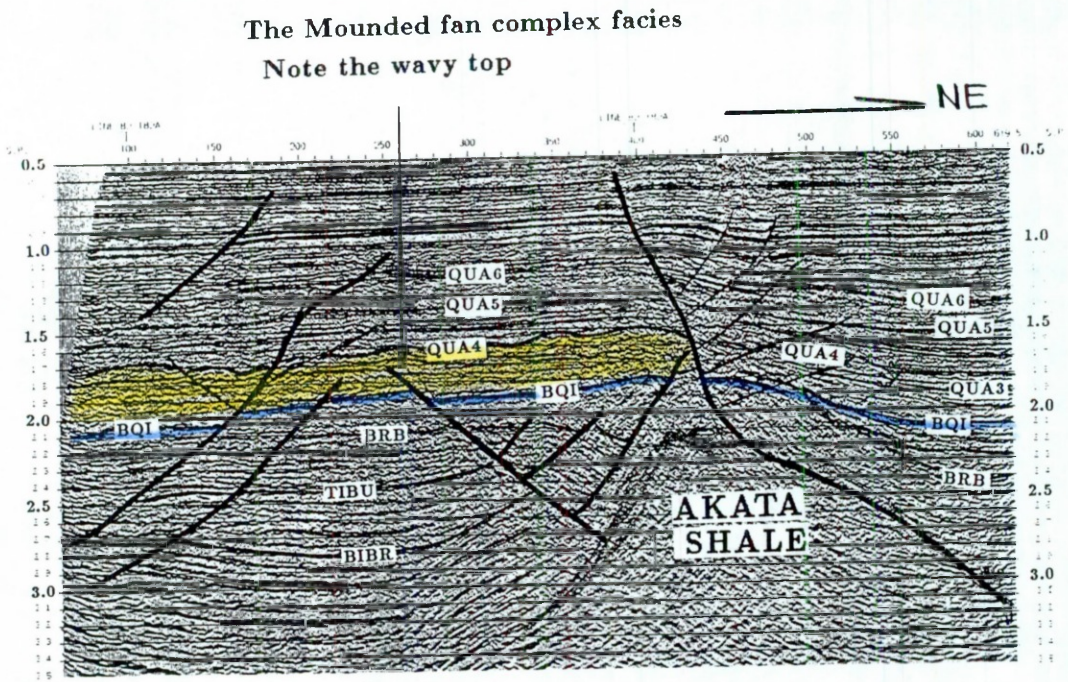

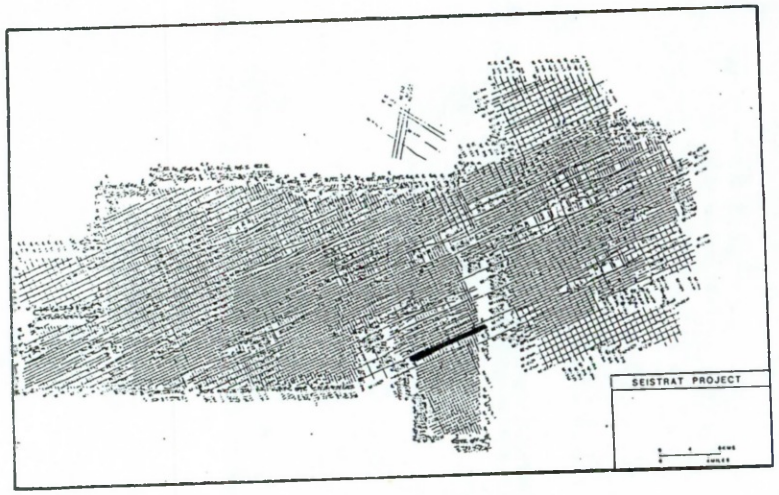

Fig.8.18a Mounded fan complex facies(line 82-182a).

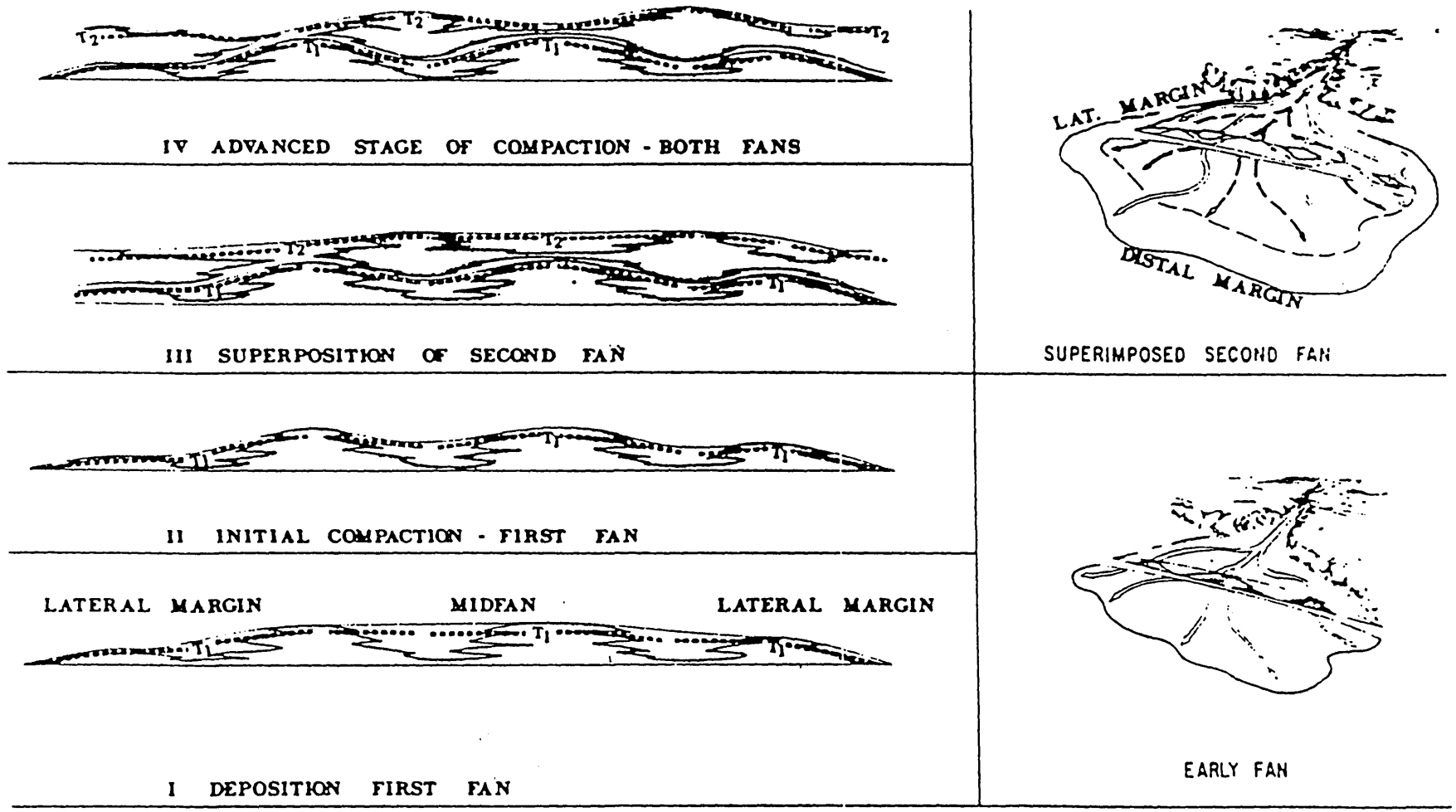

DEPOSITIONAL MODEL SHOWING SEDIMENTARY ACCOMODATION AND ALTERNATE STACKING WITH VERTICAL OFFSET OF DISTRIBUTARY CHANNELS. (AFTER MACPHERSON, 1978.)

Fig.8.18b Depositional model of stacked channels.

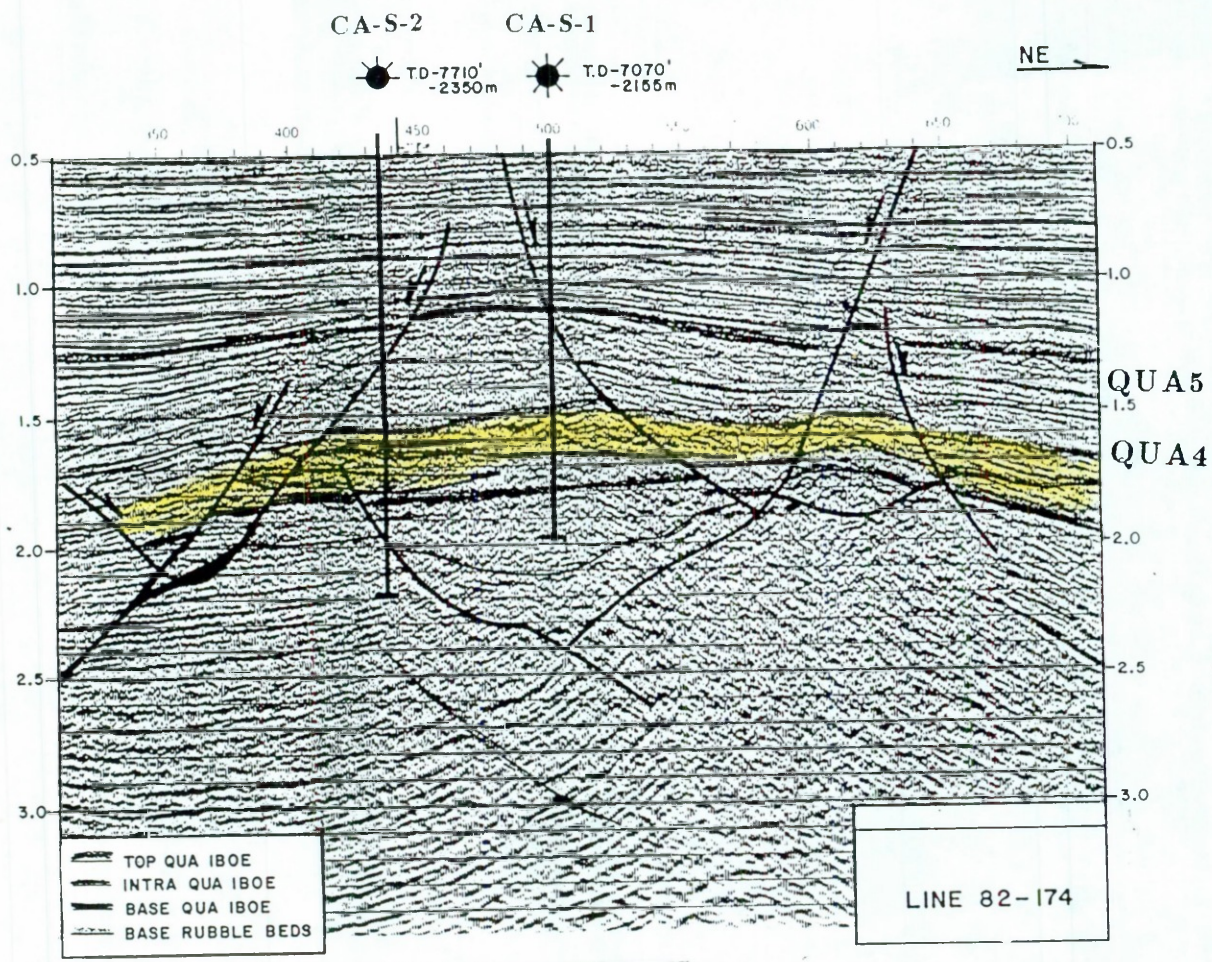

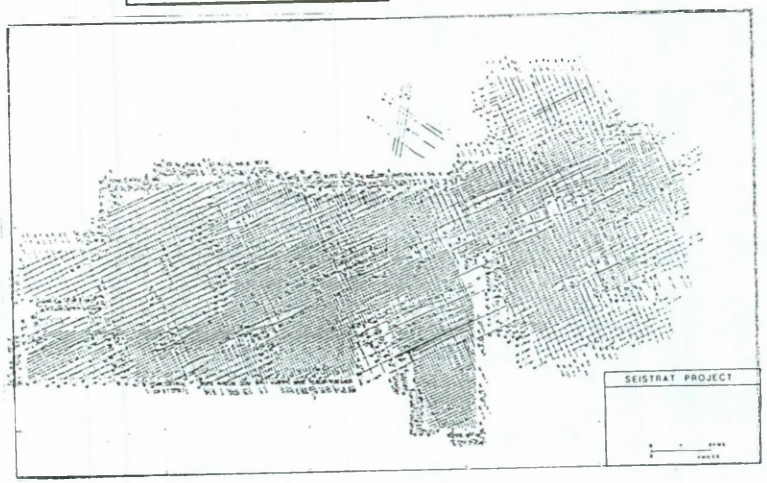

Fig.8.19a Line 82-174 showing the typical wavy top morphology of the mounded fan complex facies. The lateral margins are ponded and extent beyond the seismic profile.

LBIBR- Lower Base Intra Biafra Rubble.

LIBU- Lower Intra Biafra Unconformity.

BIBR- Base Intra Biafra Rubble.

TIBU- Top Intra Biafra Unconformity.

BIBBEN- Base Intra Biafra Benin sands.

BRB- Base Rubble Beds

BQI- Base Qua Iboe.

TIQI- Top Intra Qua Iboe

QUA3 etc- Intra Qua Iboe horizon 3 etc

Pu- Pleistocene Unconformity

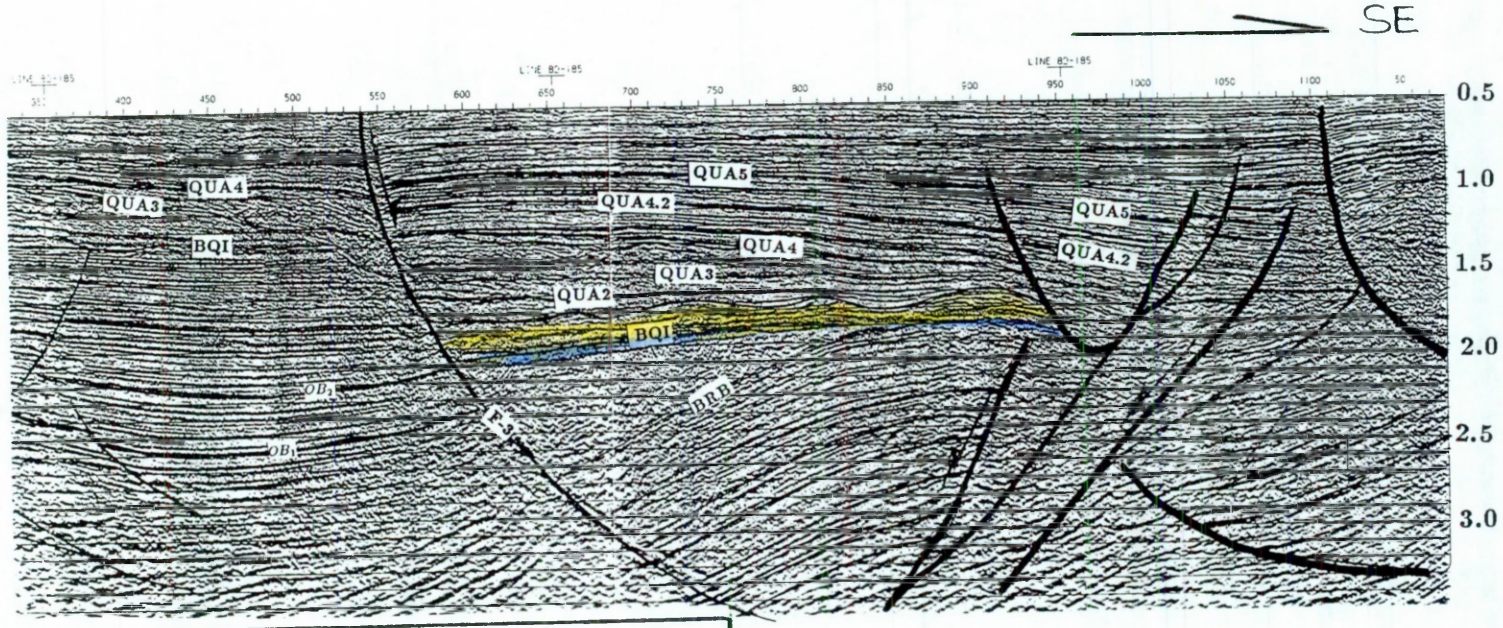

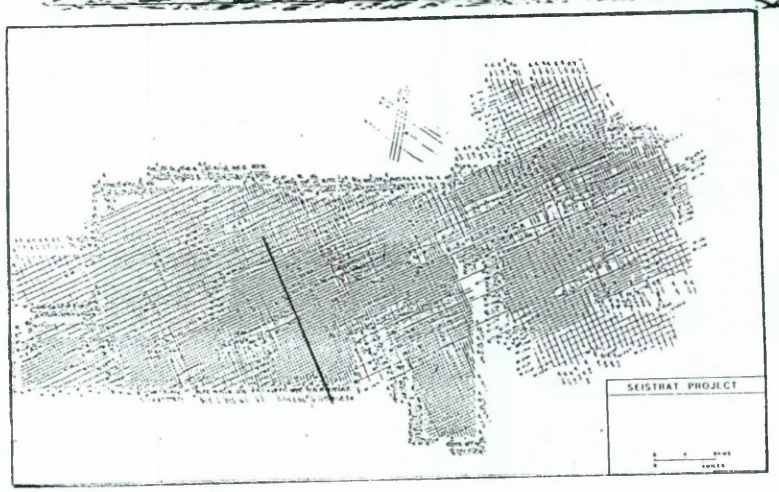

Fig.8.19b Line 82-185 showing the wavy top morphology of the northwest anomaly.

LBIBR- Lower Base Intra Biafra Rubble.

LIBU- Lower Intra Biafra Unconformity.

BIBR- Base Intra Biafra Rubble.

TIBU- Top Intra Biafra Unconformity.

BIBBEN- Base Intra Biafra Benin sands.

BRB- Base Rubble Beds

BQI- Base Qua Iboe.

TIQI- Top Intra Qua Iboe

QUA3 etc- Intra Qua Iboe horizon 3 etc

Pu- Pleistocene Unconformity

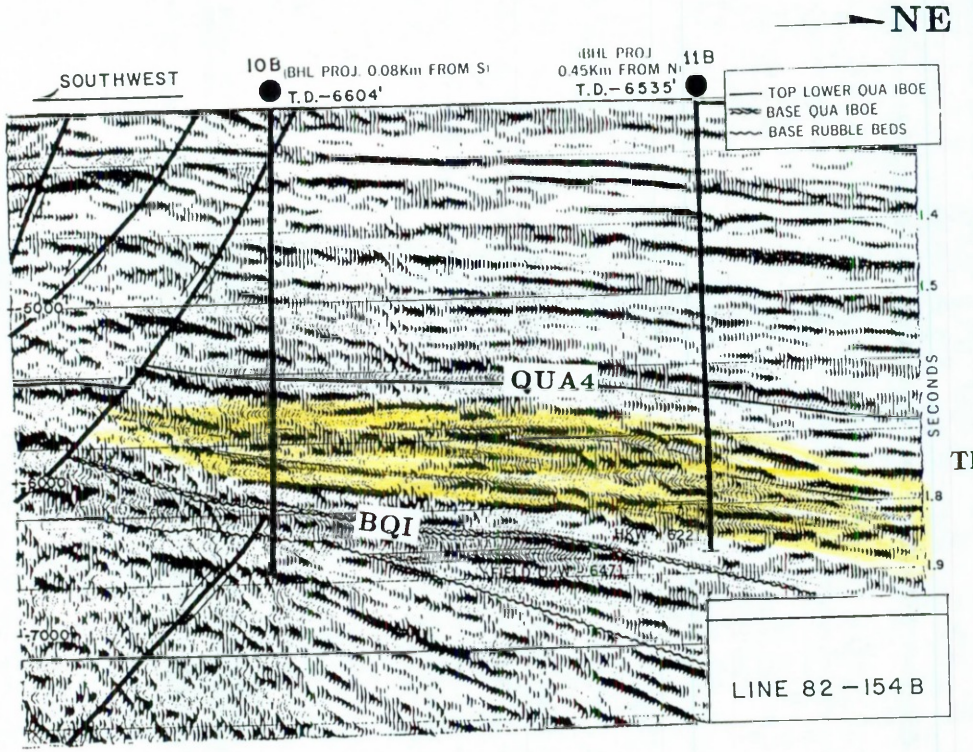

The Mounded onlap facies

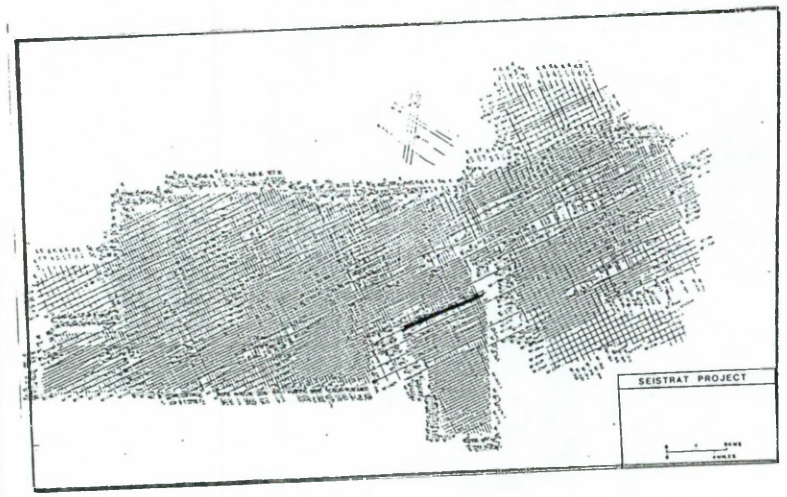

Fig.8.20 Line 82-154b showing mounded onlap facies.

LIBBR- Lower Base Intra Biafra Rubble.
LIBU- Lower Intra Biafra Unconformity
BIBR- Base Intra Biafra Rubble.
TIBU- Top Intra Biafra Unconformity.
BIBBEN- Base Intra Biafra Benin sands.
BRB- Base Rubble Beds
BQI- Base Qua Iboe.
TIQI- Top Intra Qua Iboe
QUA3 etc- Intra Qua Iboe horizon 3 etc
Pu- Pleistocene Unconformity

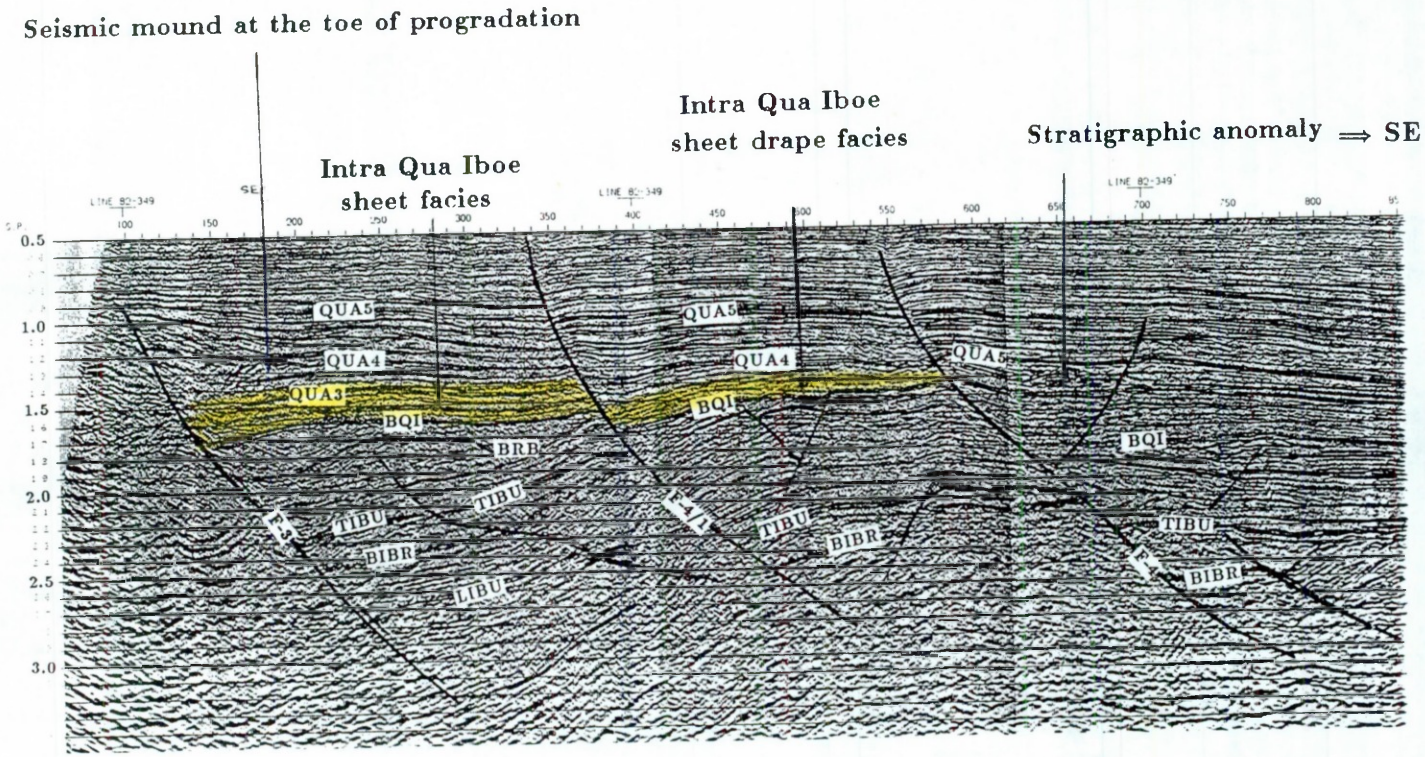

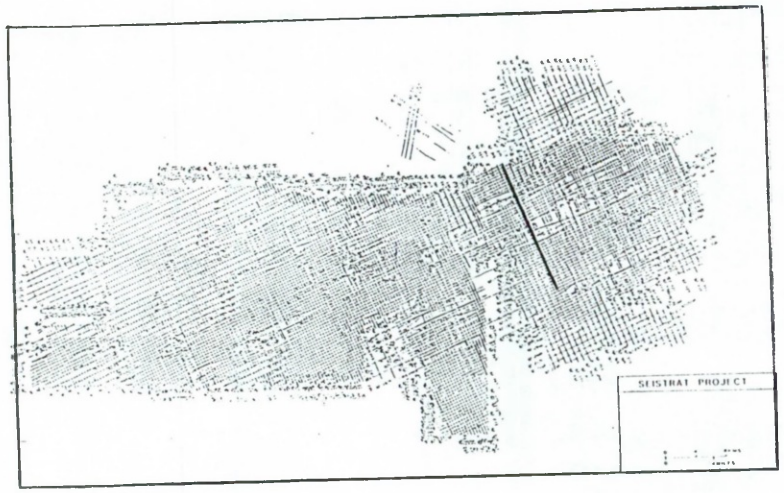

Fig.8.21a Sheet facies: line 82-349 shows the sheet facies shaling out southward into the sheet drape and blanket facies.

LBIBR: Lower Base Intra Biafra Rubble

LIBU: Lower Intra Biafra Unconformity.

BIBR: Base Intra Biafra Rubble.

TIBU: Top Intra Biafra Unconformity.

BIBBEN- Base Intra Biafra Benin sands.

BRB- Base Rubble Beds

BQI- Base Qua Iboe.

TIQI- Top Intra Qua Iboe

QUA3 etc- Intra Qua Iboe horizon 3 etc

Pu- Pleistocene Unconformity

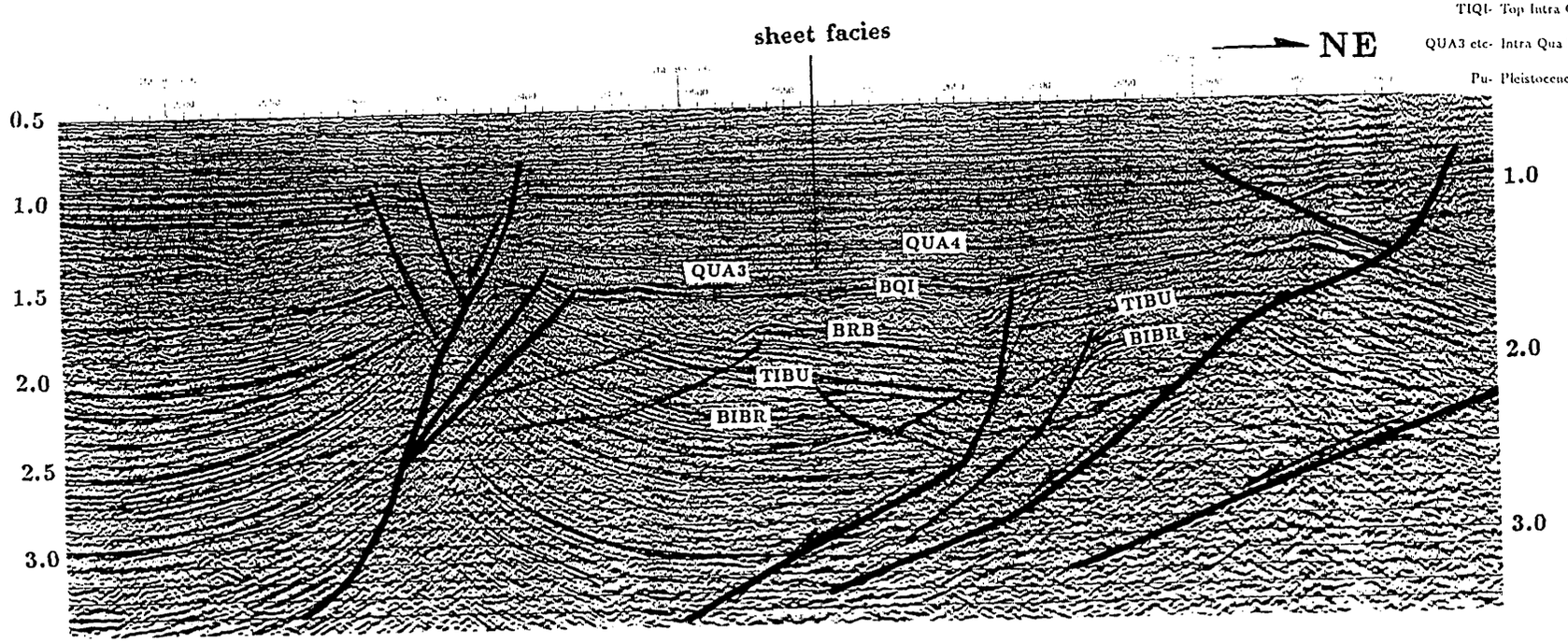

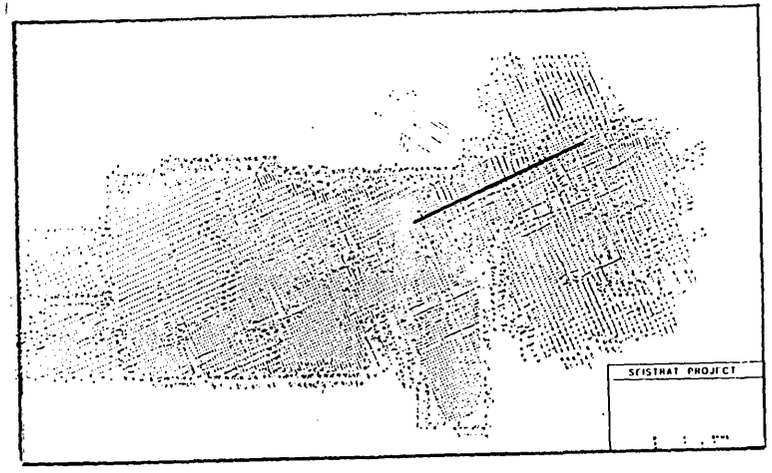

Fig.8.21b Typical sheet facies to the east of the study area.

LBIBR- Lower Base Intra Biafra Rubble.

LIBU- Lower Intra Biafra Unconformity.

BIBR- Base Intra Biafra Rubble.

TIBU- Top Intra Biafra Unconformity.

BIBBEN- Base Intra Biafra Benin sands.

BRB- Base Rubble Beds

BQI- Base Qua Iboe.

TIQI- Top Intra Qua Iboe

QUA3 etc- Intra Qua Iboe horizon 3 etc

Pu- Pleistocene Unconformity

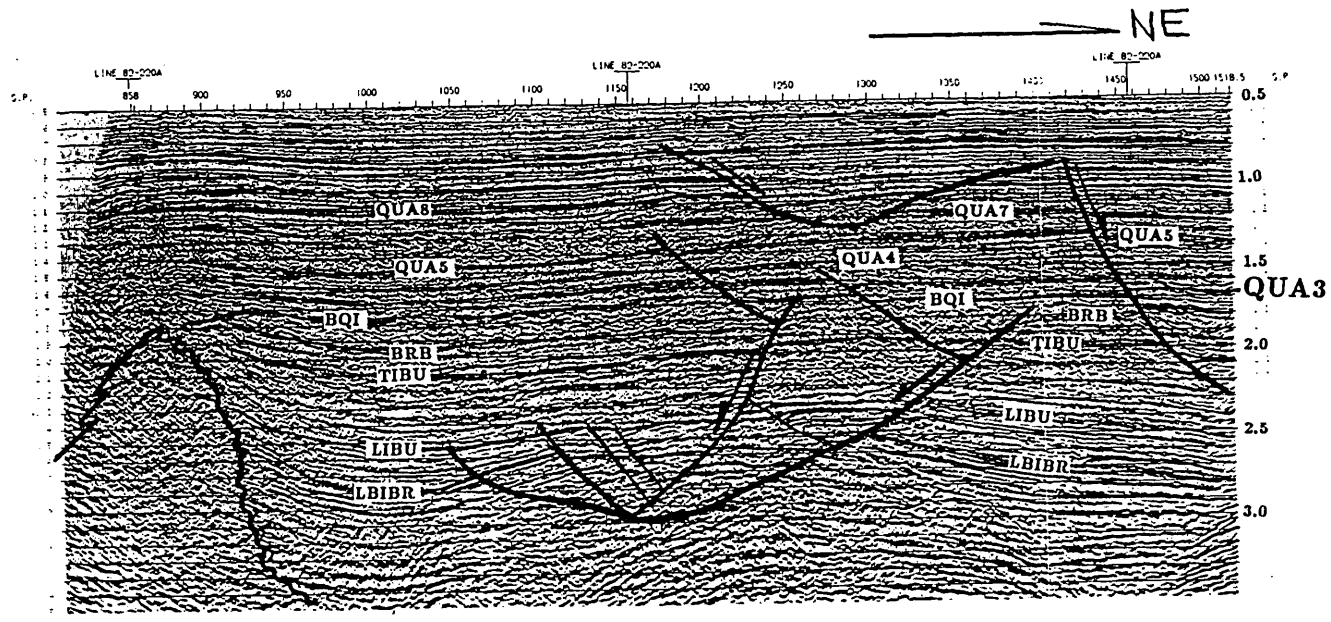

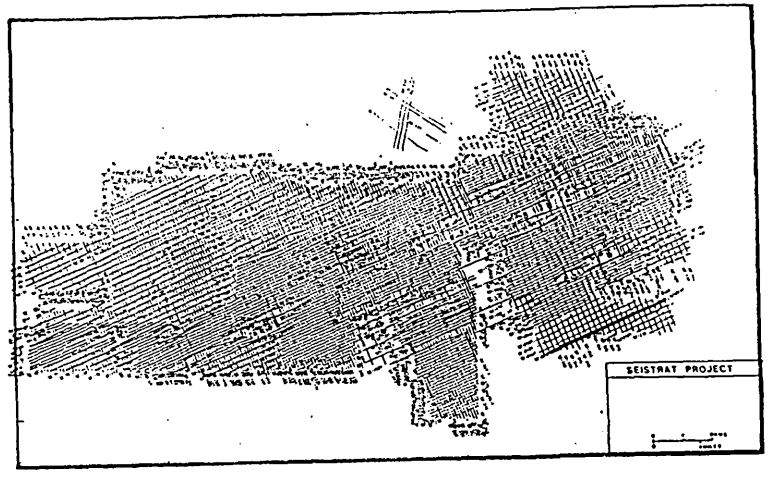

Fig.8.22 Line 82-220a shows the tripartite subdivision of the Lower Qua Iboe sequences.

LBIBR- Lower Base Intra Biafra Rubble.

LIBU- Lower Intra Biafra Unconformity.

BIBR- Base Intra Biafra Rubble.

TIBU- Top Intra Biafra Unconformity.

BIBBEN- Base Intra Biafra Benin sands.

BRB- Base Rubble Beds

BQI- Base Qua Iboe.

TIQI- Top Intra Qua Iboe

QUA3 etc- Intra Qua Iboe horizon 3 etc

Pu- Pleistocene Unconformity

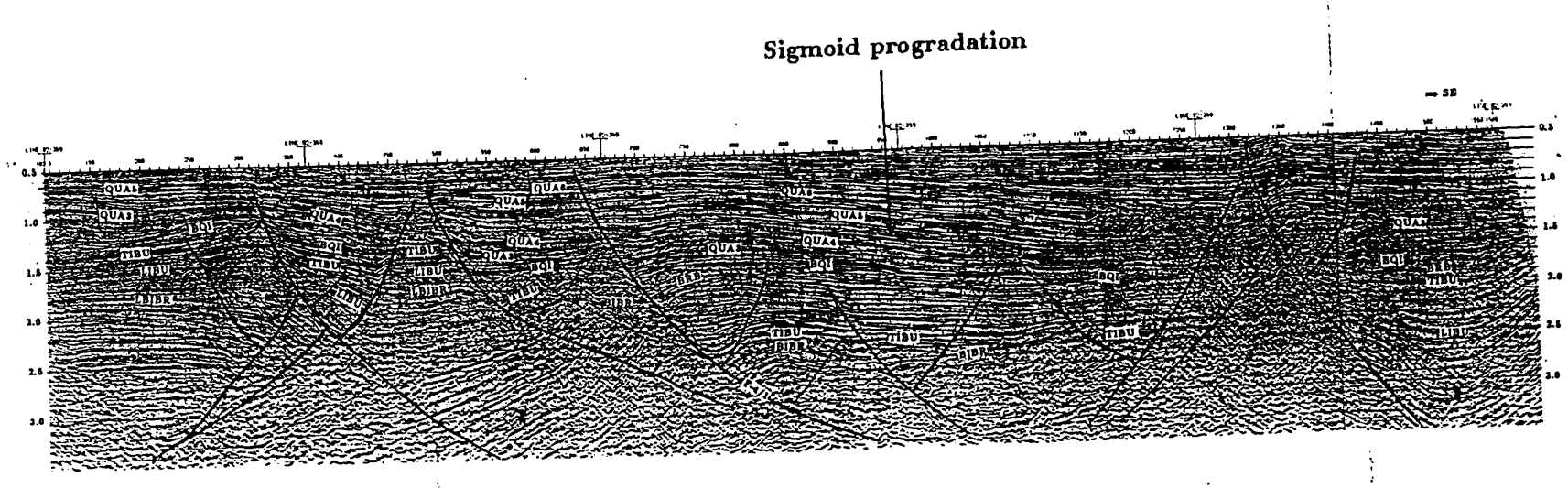

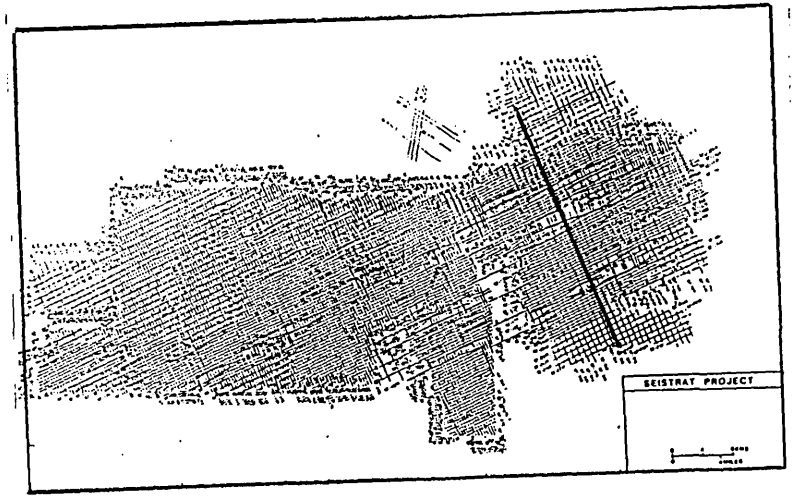

Fig.8.23 Sigmoidal facies: line 82-369 .

LBIBR- Lower Base Intra Biafra Rubble.

LIBU- Lower Intra Biafra Unconformity.

BIBR- Base Intra Biafra Rubble.

TIBU- Top Intra Biafra Unconformity.

BIBBEN- Base Intra Biafra Benin sands.

BRB- Base Rubble Beds

BQI- Base Qua Iboe.

TIQI- Top Intra Qua Iboe

QUA3 etc- Intra Qua Iboe horizon 3 etc

Pu- Pleistocene Unconformity

Oblique progradation

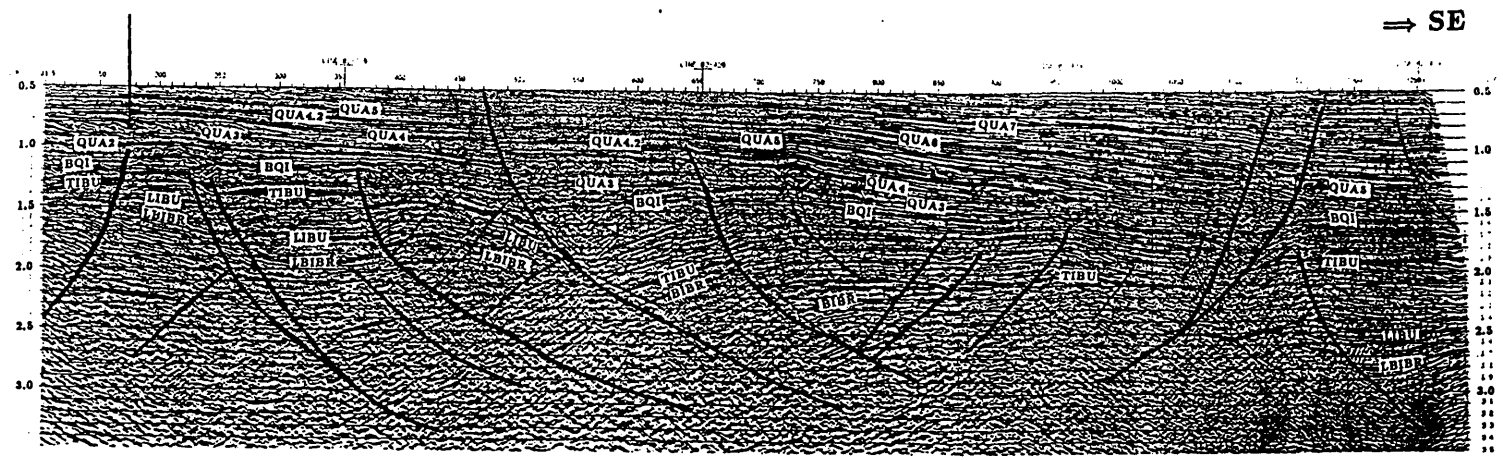

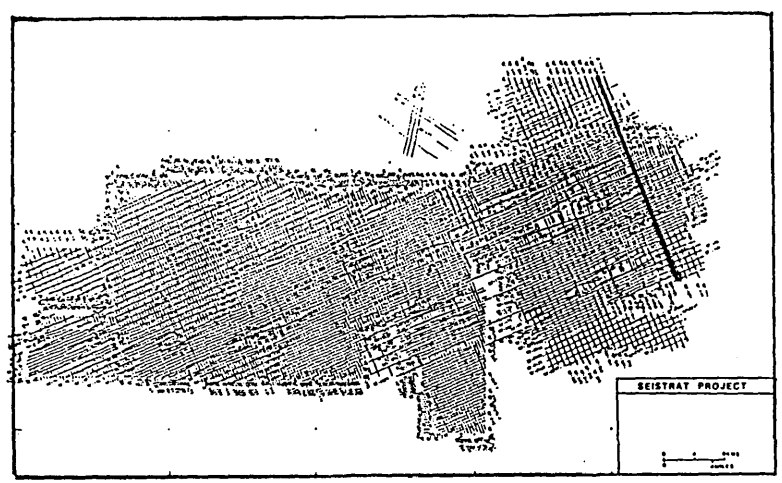

Fig.8.24 Oblique facies tending southwards towards sigmoidal facies, line 82-429.

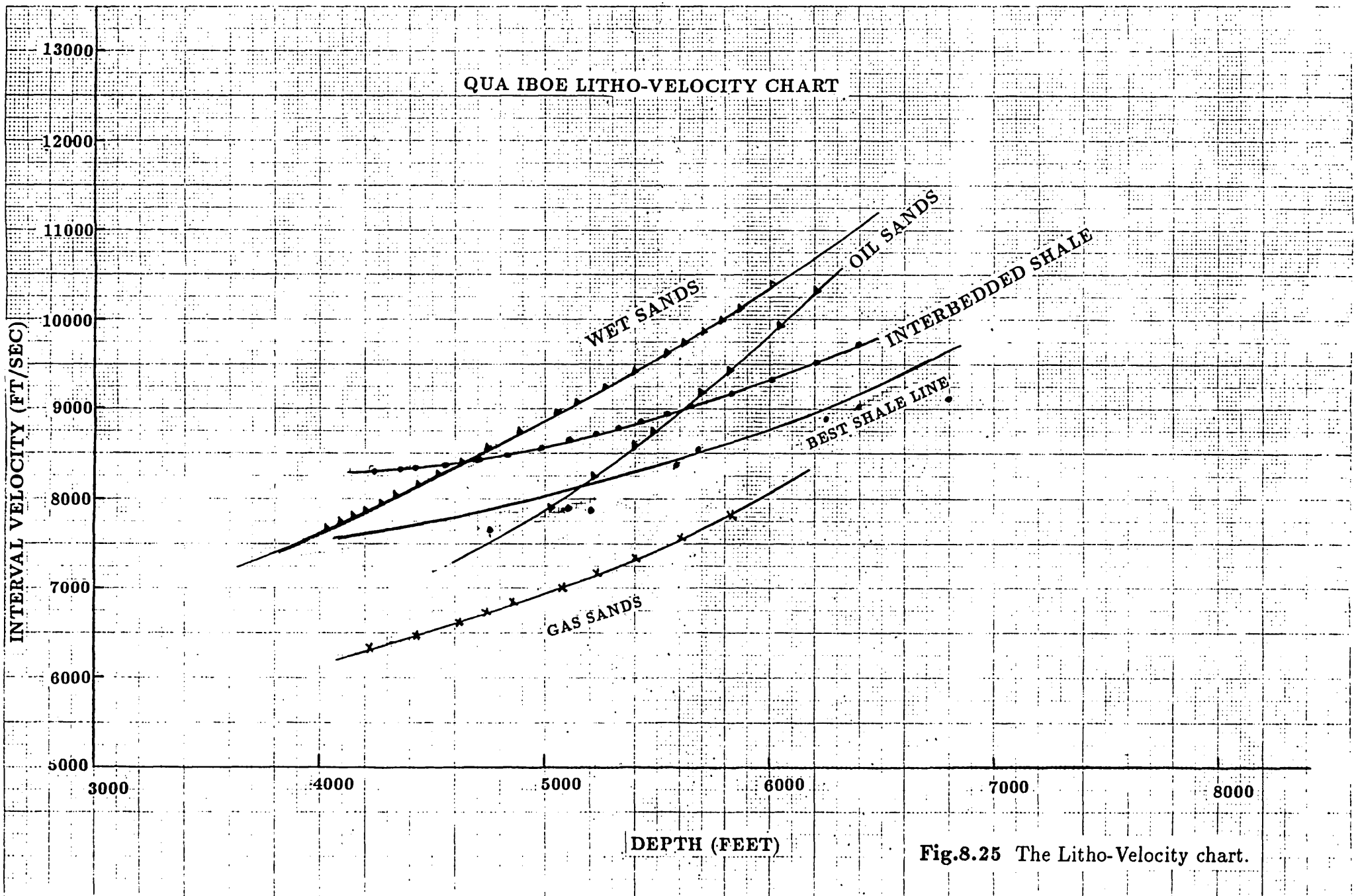

Fig.8.25 The Litho-Velocity chart.

47 1242
K+E 20 x 20 TO THE INCH • 10 x 15 INCHES KEUFFEL & ESSER CO. MADE IN U.S.A.

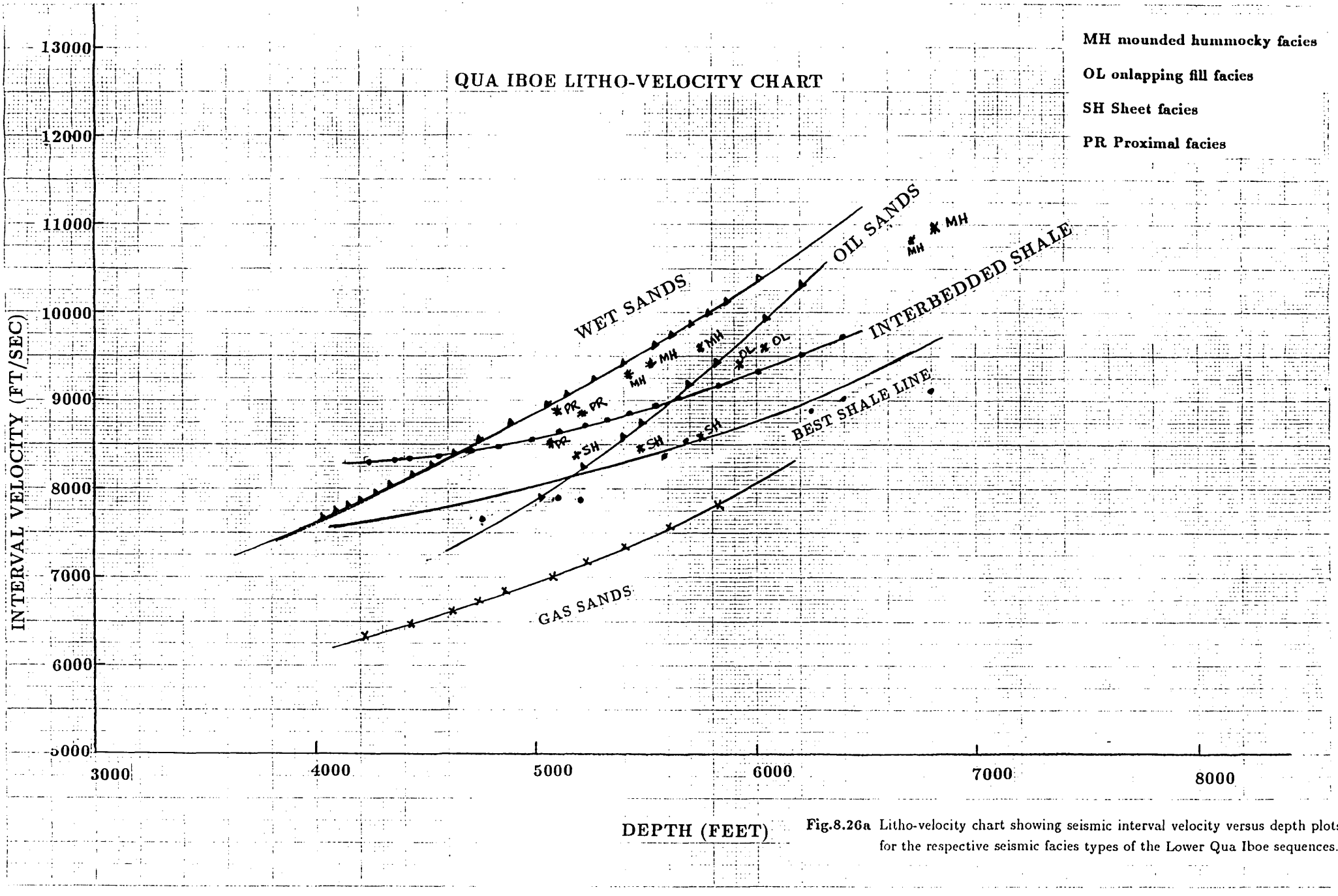

Fig.8.26a Litho-velocity chart showing seismic interval velocity versus depth plots for the respective seismic facies types of the Lower Qua Iboe sequences.

47 1242
20 x 20 TO THE INCH • 10 x 15 INCHES
KEUFFEL & ESSER CO. MADE IN U.S.A.

Fig.8.26b Map showing 'sand' trends within the Lower Qua Iboe sequences based on seismic interval velocity data. This when compared with the composite map of seismic anomalies(Fig.8.15) shows broad correspondence.

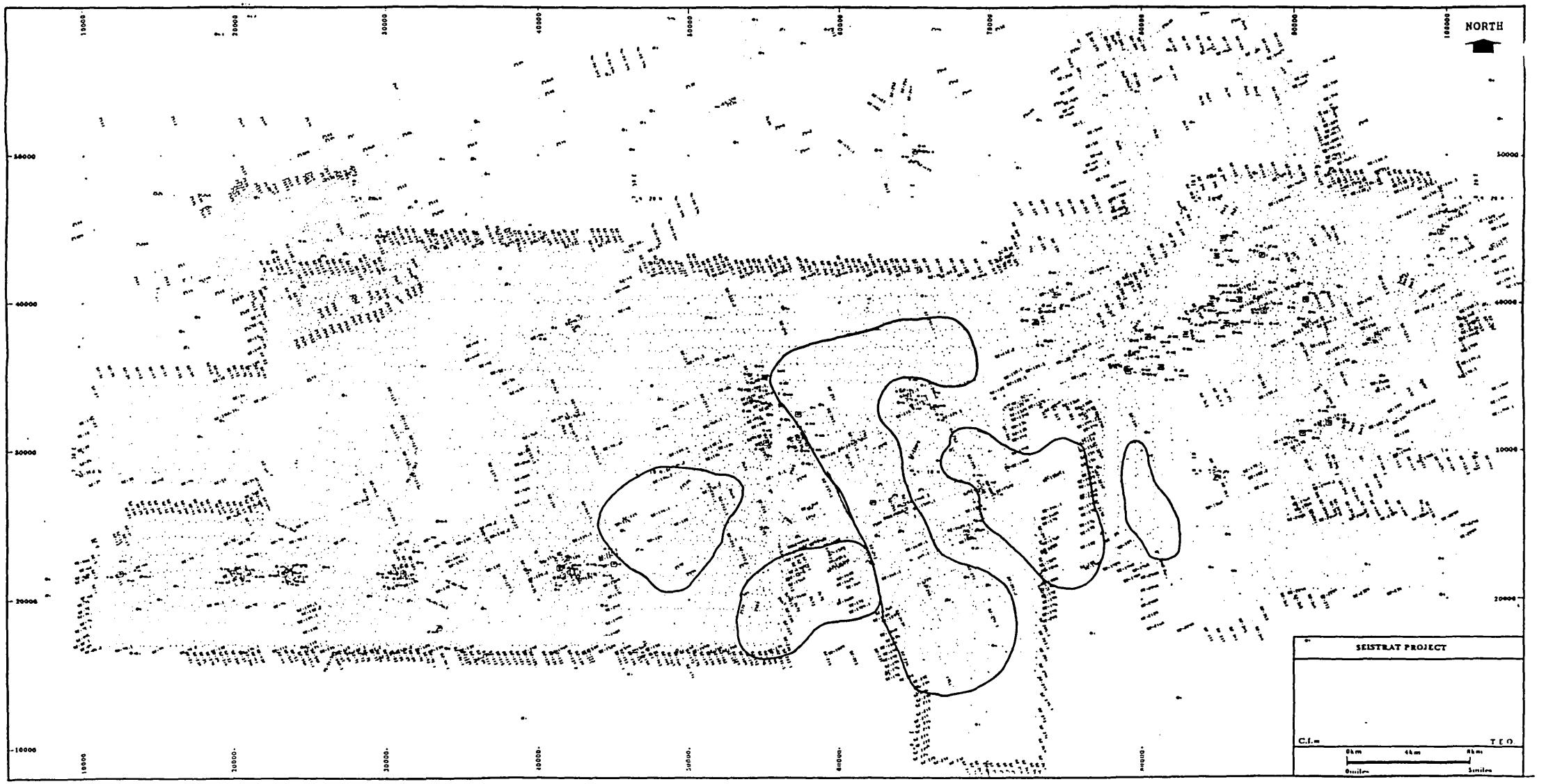

Fig.8.26c Map of the 'Coefficient of Heterogeneity', g at the BQ1 level in the central part of the study area.

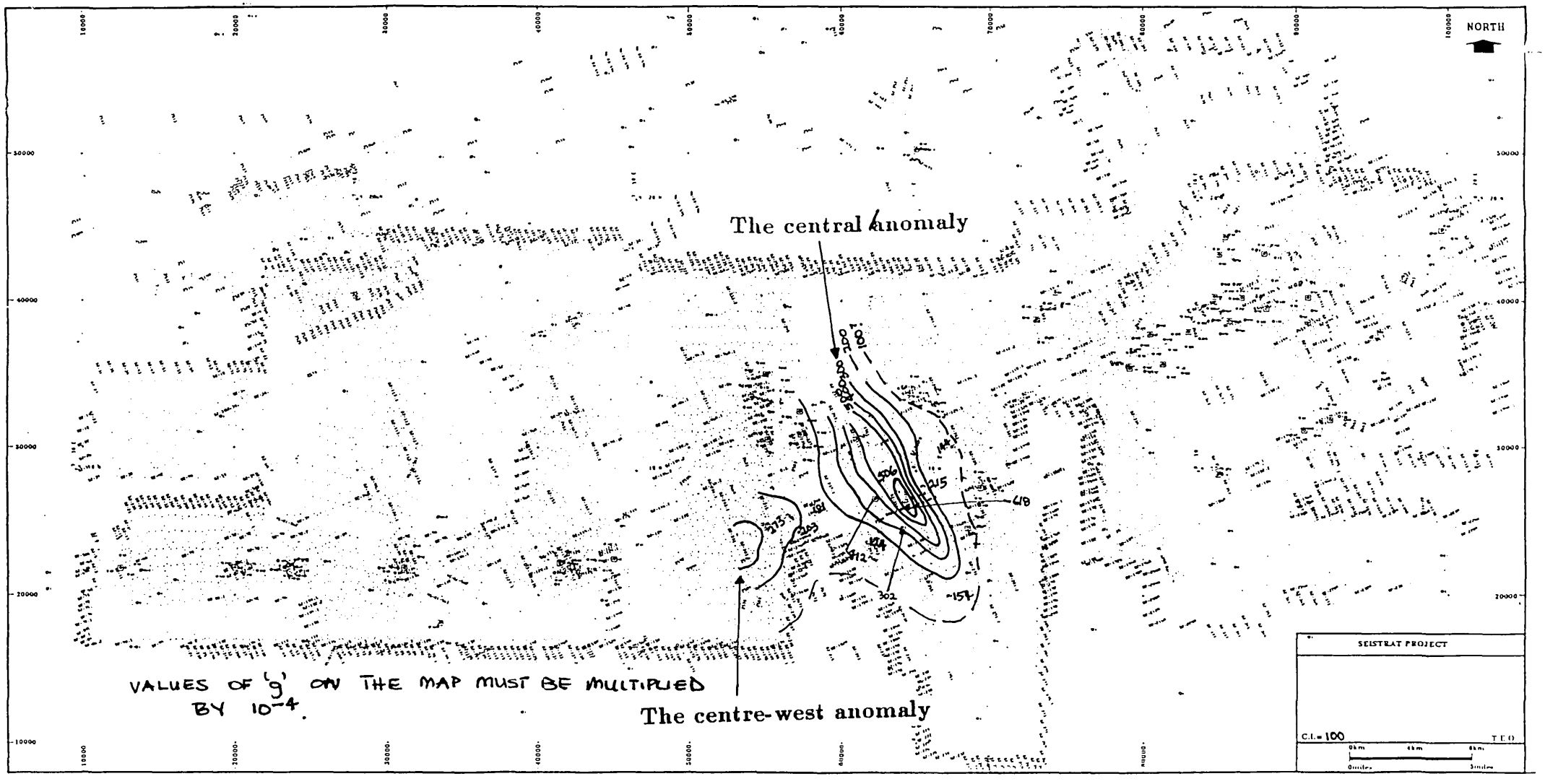

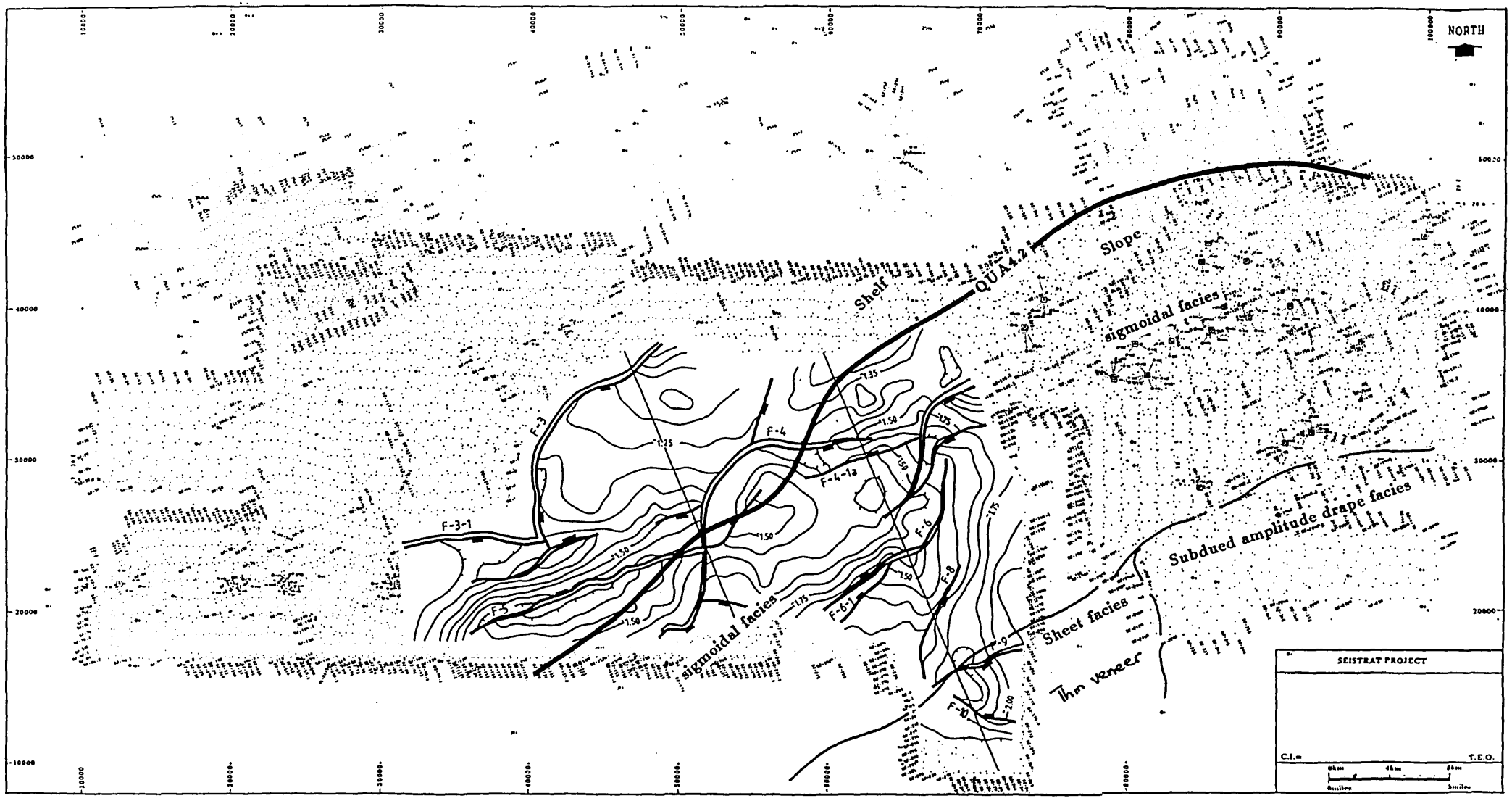

Fig.8.27a Facies distribution map of SEQ.QS4 superimposed on the structural time map of Horizon QUA4.

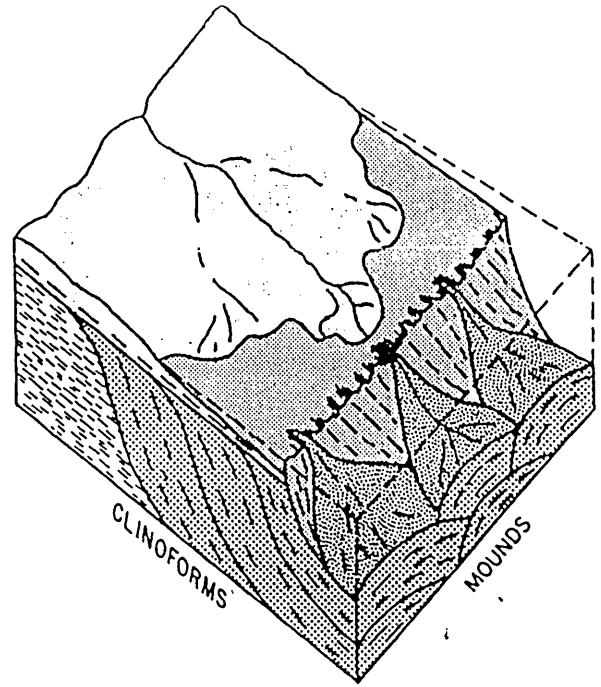

LBIBR- Lower Base Intra Biafra Rubble.

LIBU- Lower Intra Biafra Unconformity.

BIBR- Base Intra Biafra Rubble.

TIBU- Top Intra Biafra Unconformity.

BIBBEN- Base Intra Biafra Benin sands.

BRB- Base Rubble Beds

BQI- Base Qua Iboe.

TIQI- Top Intra Qua Iboe

QUA3 etc- Intra Qua Iboe horizon 3 etc

Pu- Pleistocene Unconformity

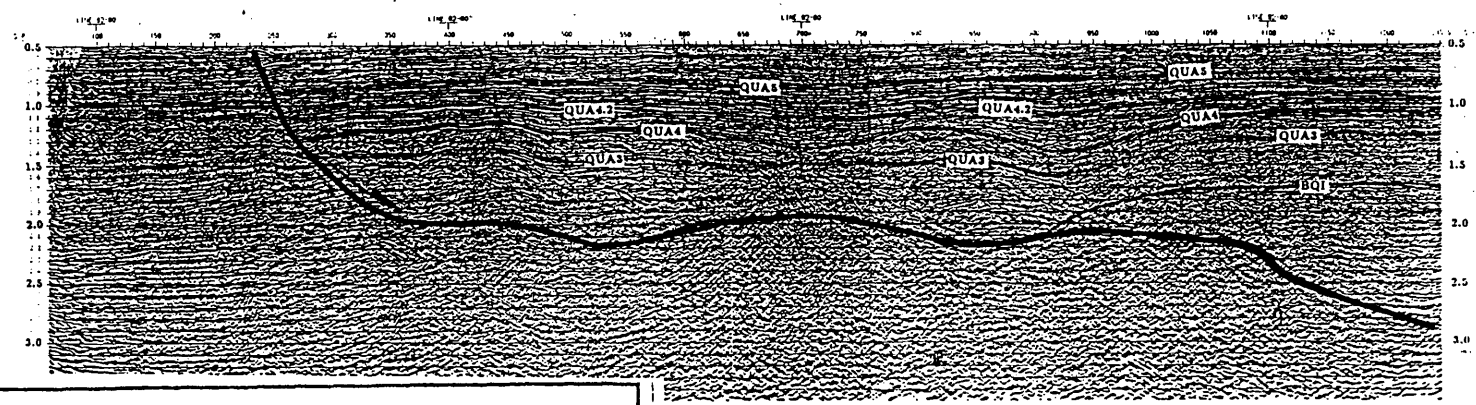

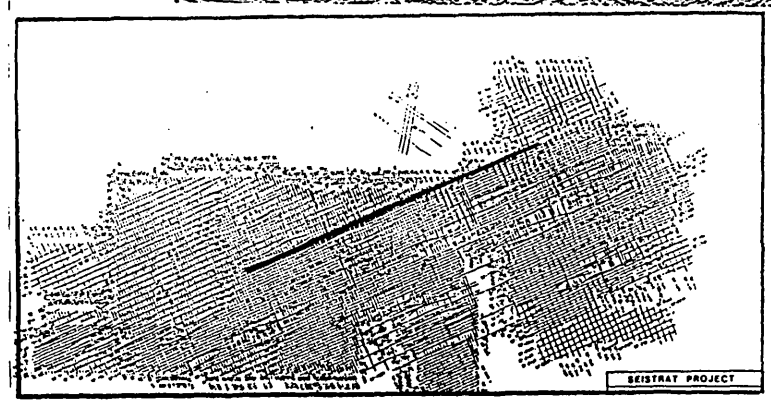

Fig.8.27b Line 82-86 showing the slope lobes typical of seismic sections along strike or transverse of a prograding set of clinoforms. These are distinct from the seismic mounds defined as seismic stratigraphic anomalies. Also attached is a schematic diagram of these features.

LBIBR- Lower Base Intra Biafra Rubble.

LIBU- Lower Intra Biafra Unconformity.

BIBR- Base Intra Biafra Rubble.

TIBU- Top Intra Biafra Unconformity.

BIBBEN- Base Intra Biafra Benin sands.

BRB- Base Rubble Beds

BQI- Base Qua Iboe.

TIQI- Top Intra Qua Iboe

QUA3 etc- Intra Qua Iboe horizon 3 etc

Pu- Pleistocene Unconformity

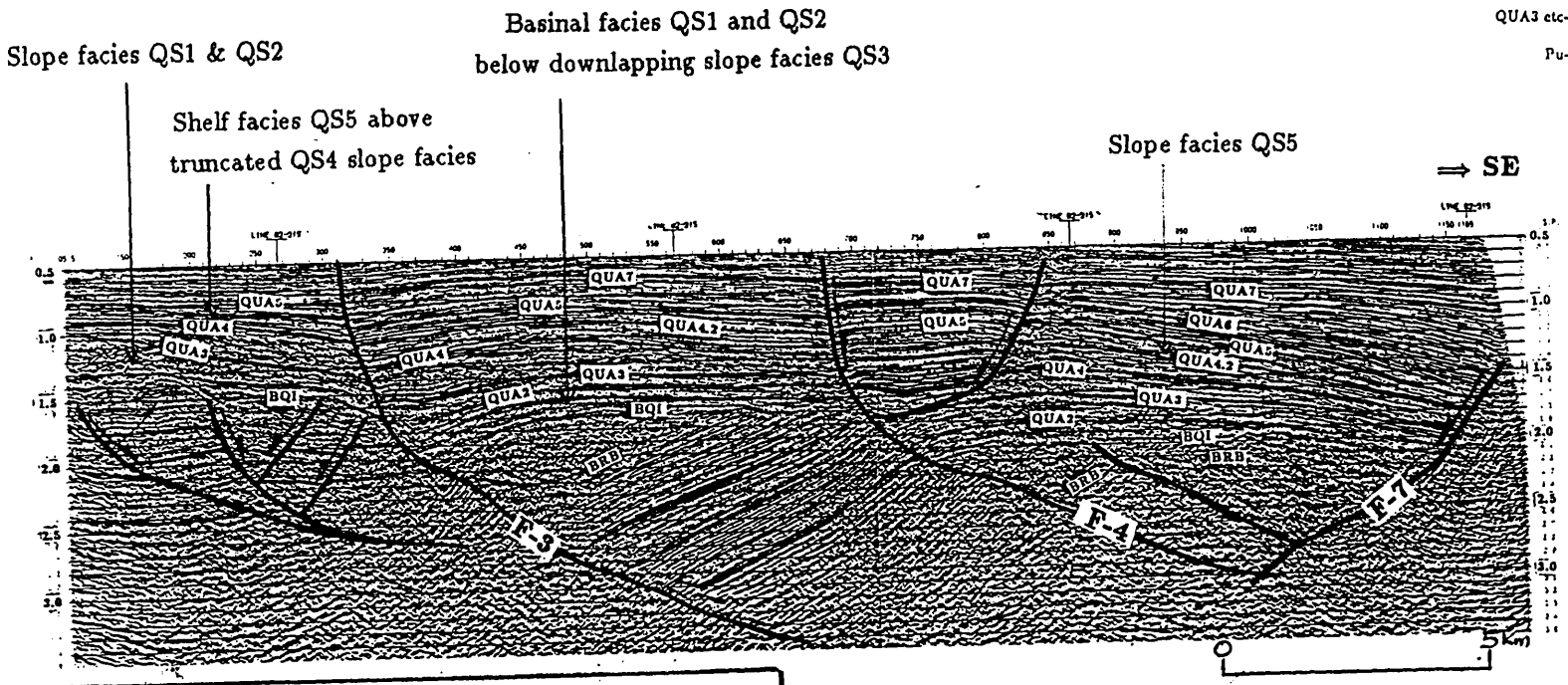

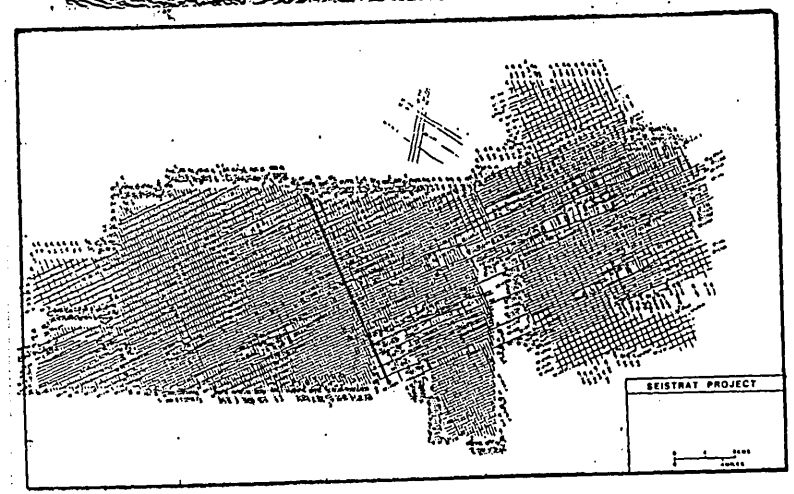

Fig.8.28a Line 82-215 illustrates the interplay between shelf and slope as a consequence of sea level changes.

LBIBR- Lower Base Intra Biafra Rubble.

LIBU- Lower Intra Biafra Unconformity.

BIBR- Base Intra Biafra Rubble.

TIBU- Top Intra Biafra Unconformity.

BIBBEN- Base Intra Biafra Benin sands.

BRB- Base Rubble Beds

BQI- Base Qua Iboe.

TIQI- Top Intra Qua Iboe

QUA3 etc- Intra Qua Iboe horizon 3 etc

Pu- Pleistocene Unconformity

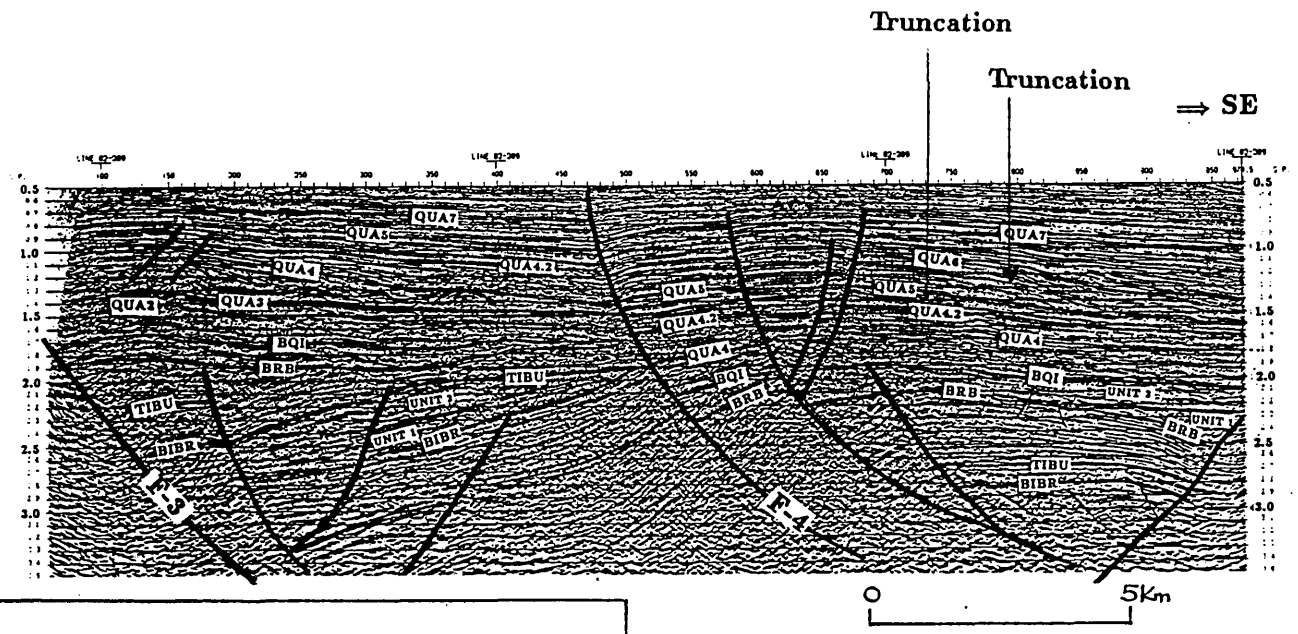

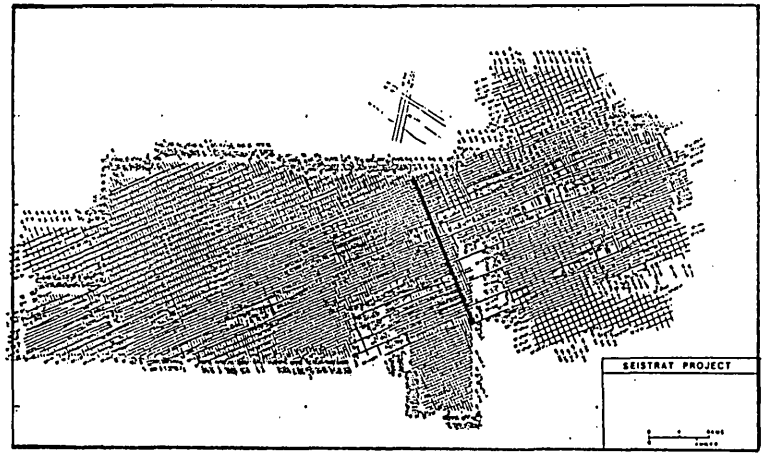

Fig.8.28b Line 82-289 shows the erosional truncation associated with the top of SEQ.QS5(Qua5) at the commencement of SEQ.QS5 slope progradation.

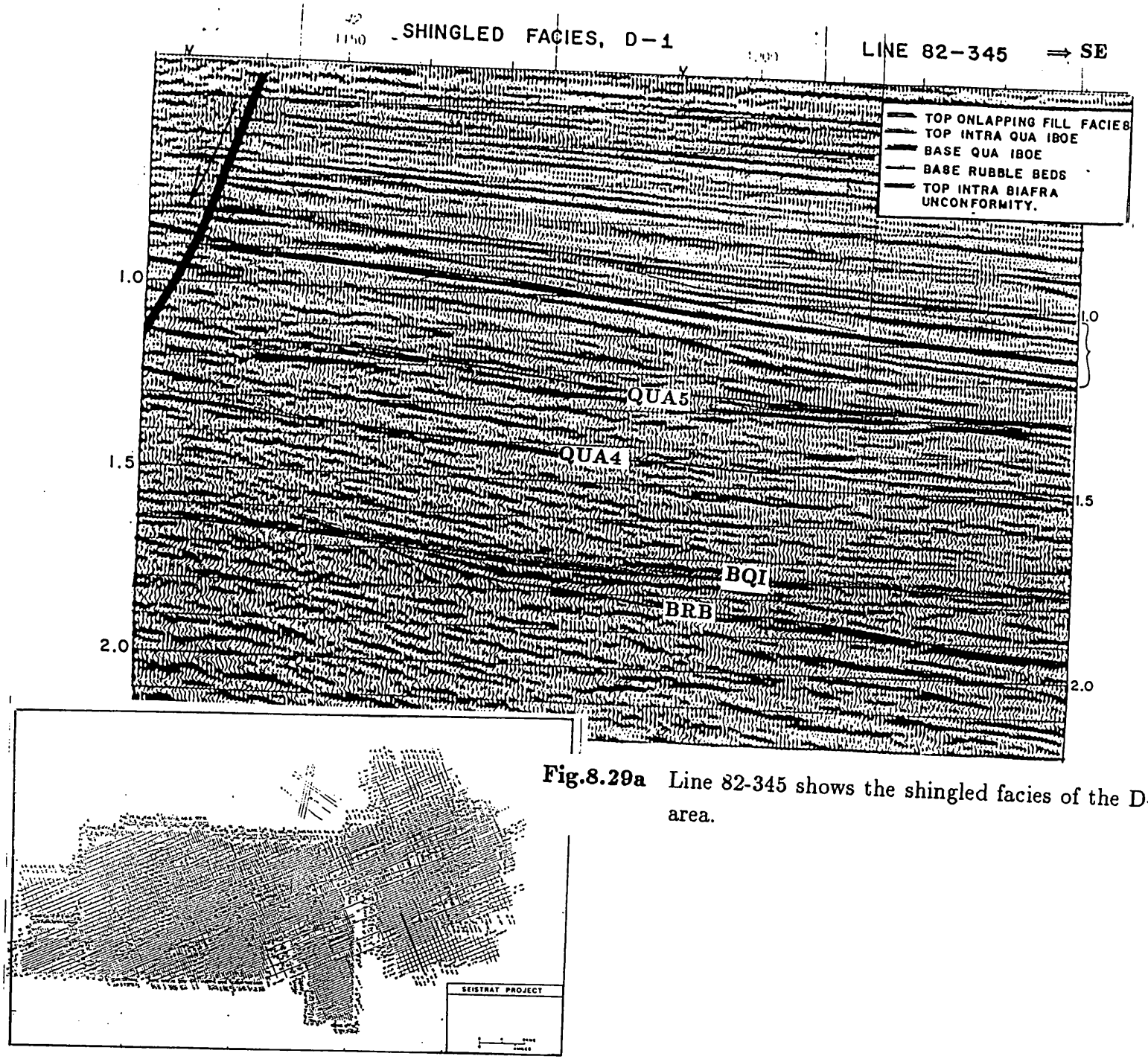

Fig.8.29a Line 82-345 shows the shingled facies of the D-1 southeast of the study area.

LBIBR- Lower Base Intra Biafra Rubble.
LIBU- Lower Intra Biafra Unconformity.
BIBR- Base Intra Biafra Rubble.
TIBU- Top Intra Biafra Unconformity.
BIBBEN- Base Intra Biafra Benin sands.
BRB- Base Rubble Beds
BQI- Base Qua Iboe.
TIQI- Top Intra Qua Iboe
QUA3 etc- Intra Qua Iboe horizon 3 etc
Pu- Pleistocene Unconformity

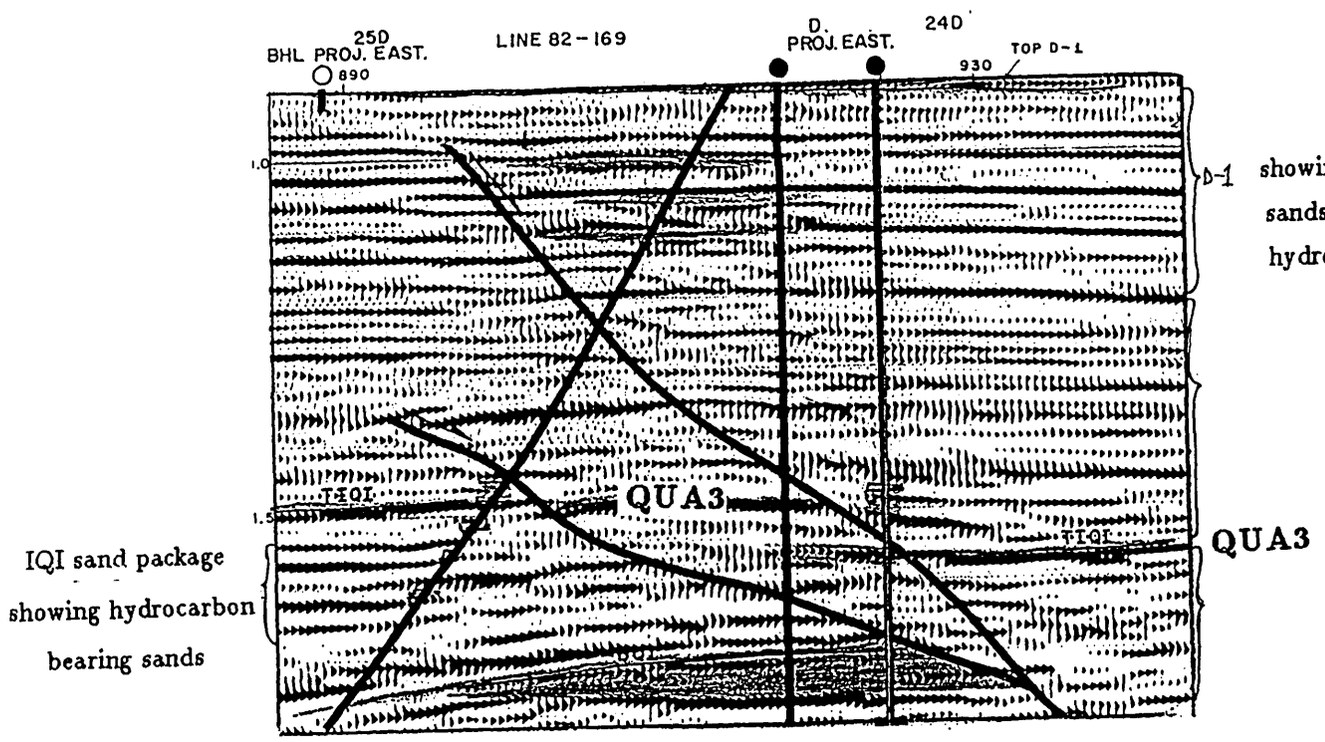

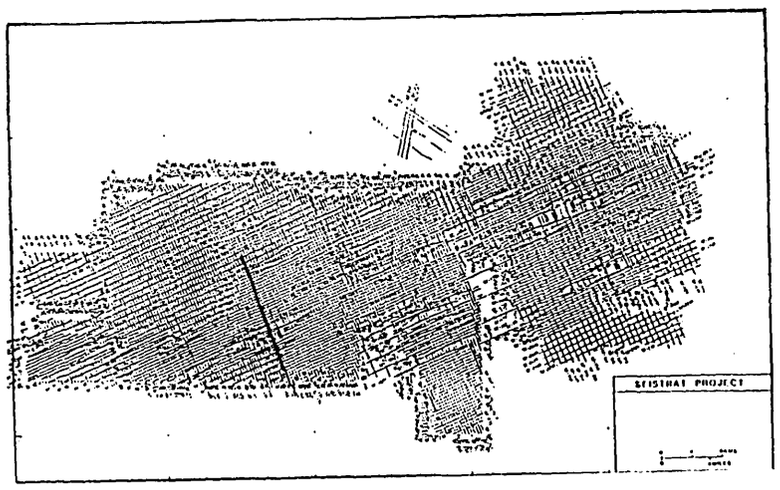

Fig.8.29b Line 82-169 illustrates the shingled configuration of most D-1 type sequences in the northwestern part of the study area.

Fig.8.29c Facies distribution map of SEQ.QS5 superimposed on the structural time map of Horizon QUA4.2.

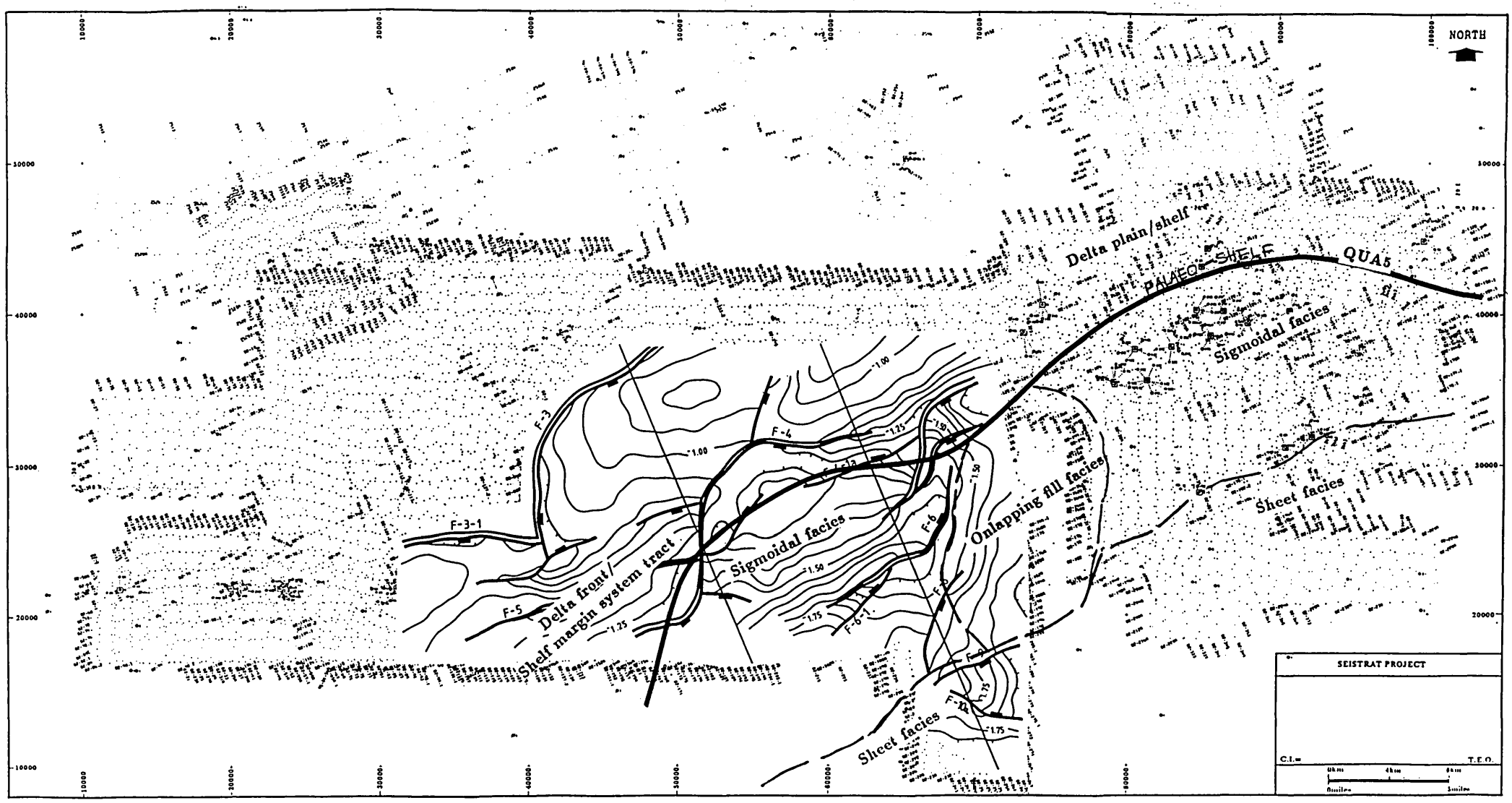

LBIBR- Lower Base Intra Biafra Rubble.

LIBU- Lower Intra Biafra Unconformity.

BIBR- Base Intra Biafra Rubble.

TIBU- Top Intra Biafra Unconformity.

BIBBEN- Base Intra Biafra Benin sands.

BRB- Base Rubble Beds

BQI- Base Qua Iboe.

TIQI- Top Intra Qua Iboe

QUA3 etc- Intra Qua Iboe horizon 3 etc

Pu- Pleistocene Unconformity

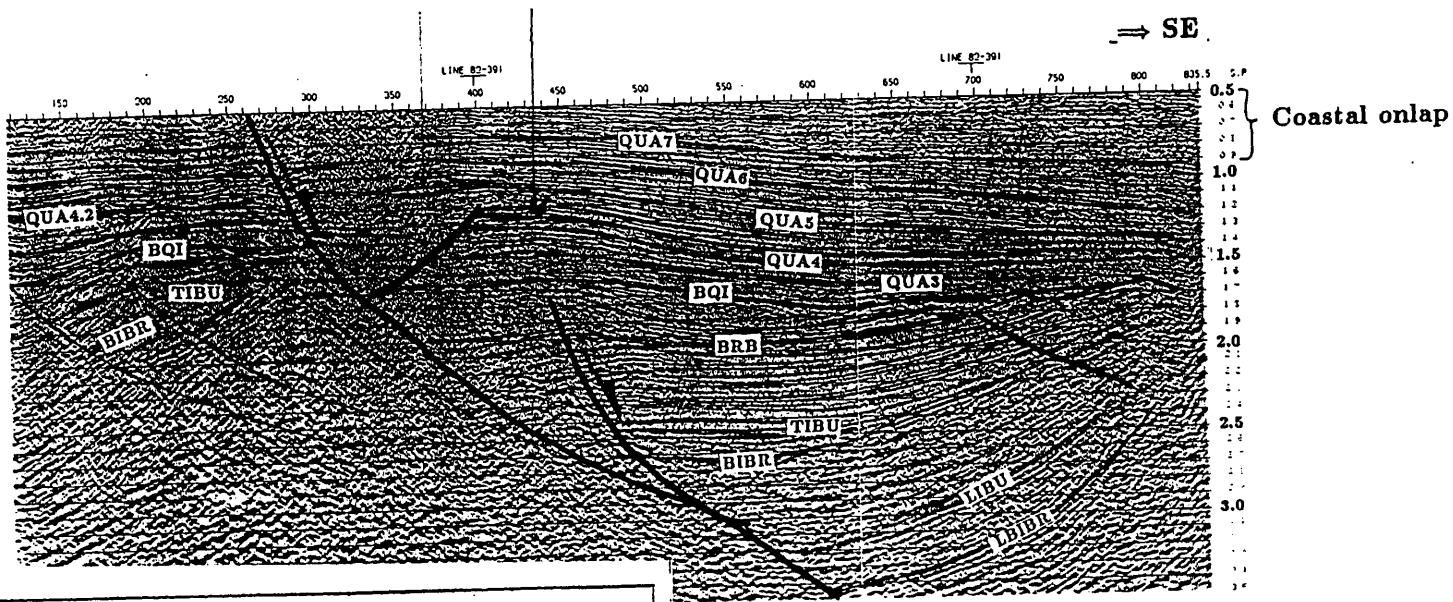

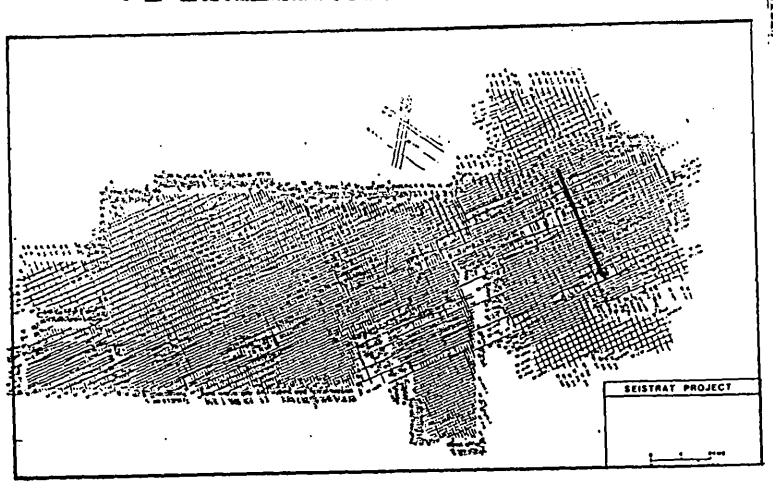

Fig.8.29d Line 82-385 illustrates the high amplitude anomalies prevalent in the updip portions of progradation. With sigmoidal progradation, seismic mounds at the turbidite toe is uncommon because of the lower energy environment of deposition compared to oblique progradation.

Fig.8.30 Facies distribution map of SEQ.QS7.

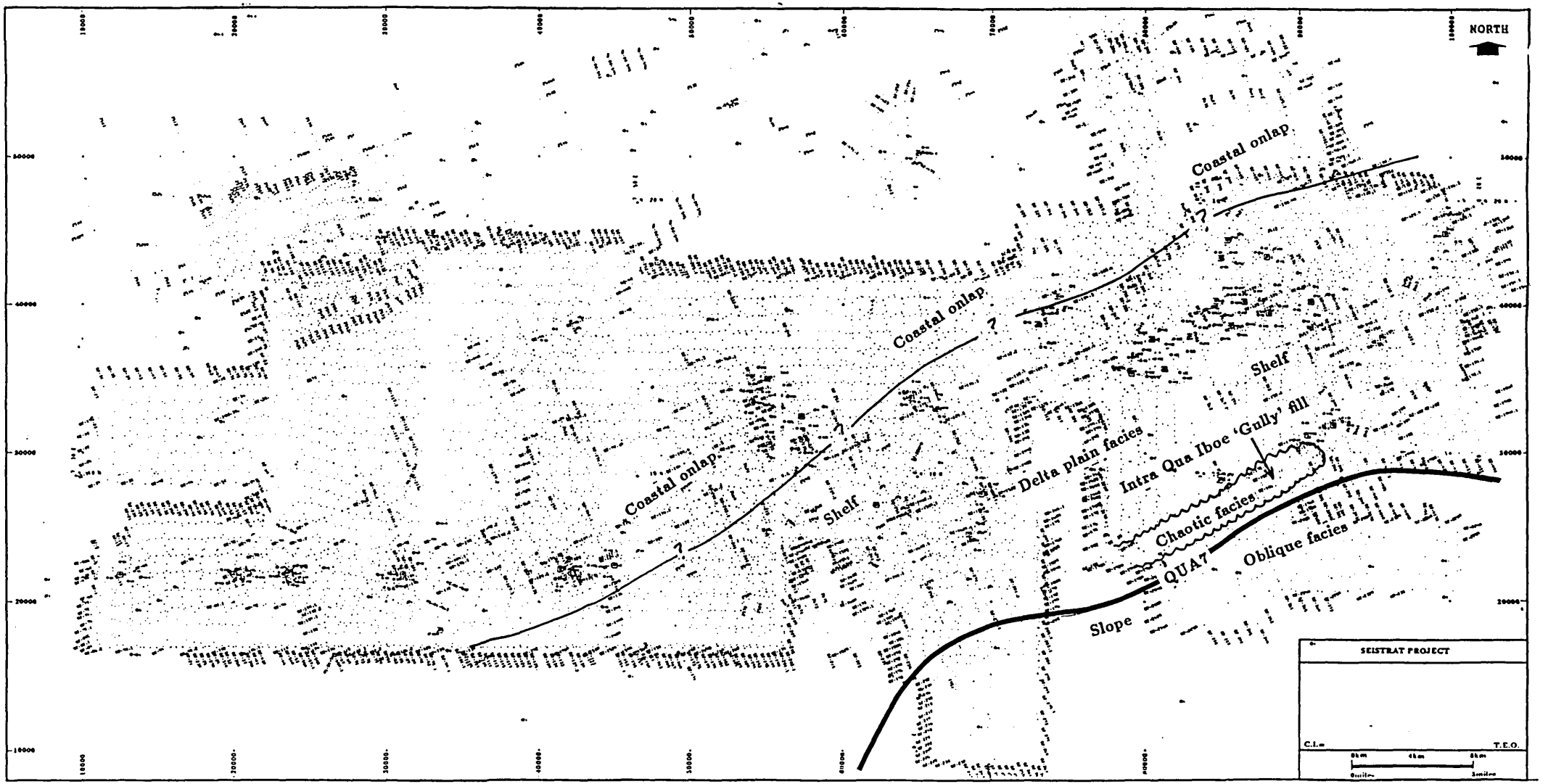

LBIBR- Lower Base Intra Biafra Rubble.

LIBU- Lower Intra Biafra Unconformity.

BIBR- Base Intra Biafra Rubble.

TIBU- Top Intra Biafra Unconformity.

BIBBEN- Base Intra Biafra Benin sands.

BRB- Base Rubble Beds

BQI- Base Qua Iboe.

TIQI- Top Intra Qua Iboe

QUA3 etc- Intra Qua Iboe horizon 3 etc

Pu- Pleistocene Unconformity

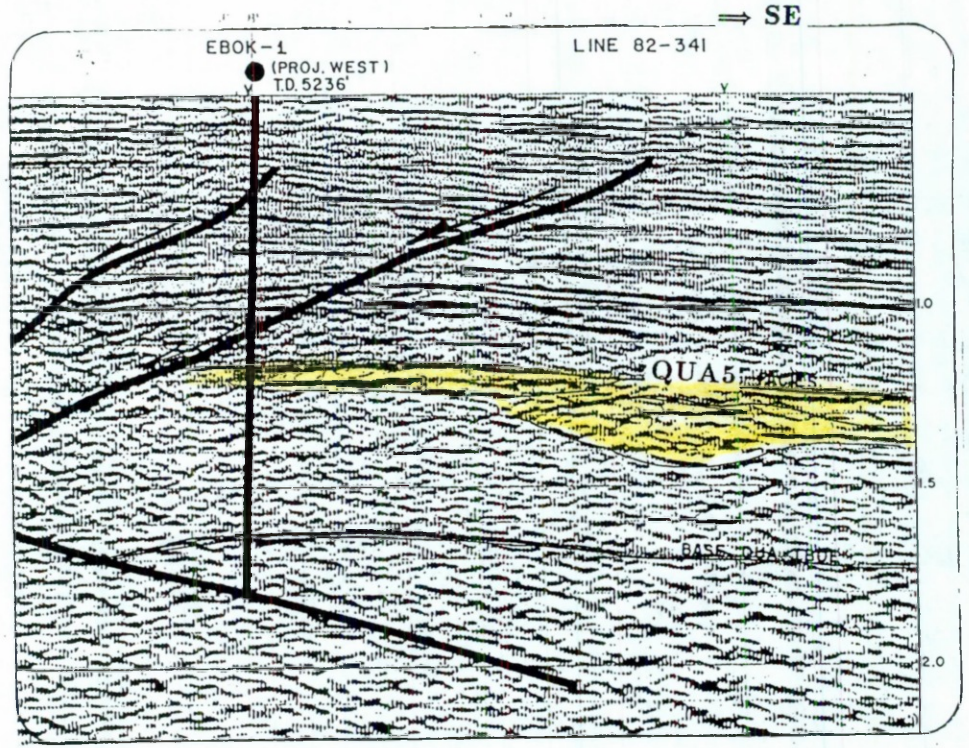

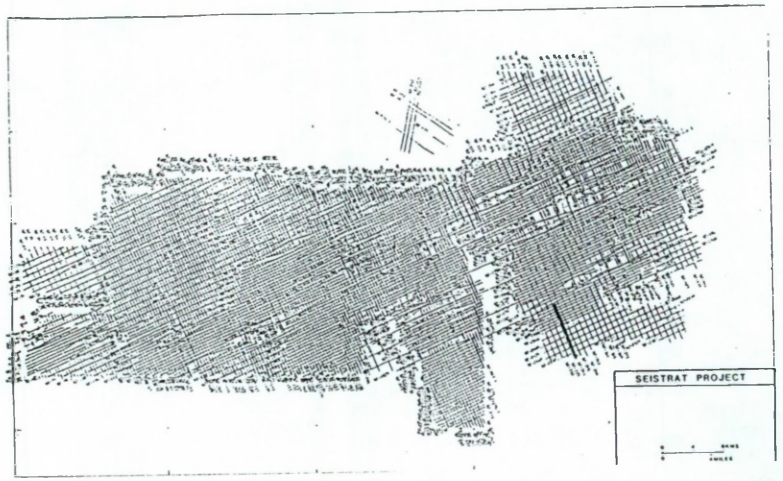

Fig.8.31 Line 82-341 shows mounding at the toe of oblique progradation in the southeast of study area. Like similar features fed from oblique progradation updip(such as evident with SEQ.QS3), they are often characterized by coarse clastics.

LBIBR- Lower Base Intra Biafra Rubble.

LIBU- Lower Intra Biafra Unconformity.

BIBR- Base Intra Biafra Rubble.

TIBU- Top Intra Biafra Unconformity.

BIBBEN- Base Intra Biafra Benin sands.

BRB- Base Rubble Beds

BQI- Base Qua Iboe.

TIQI- Top Intra Qua Iboe

QUA3 etc- Intra Qua Iboe horizon 3 etc

Pu- Pleistocene Unconformity

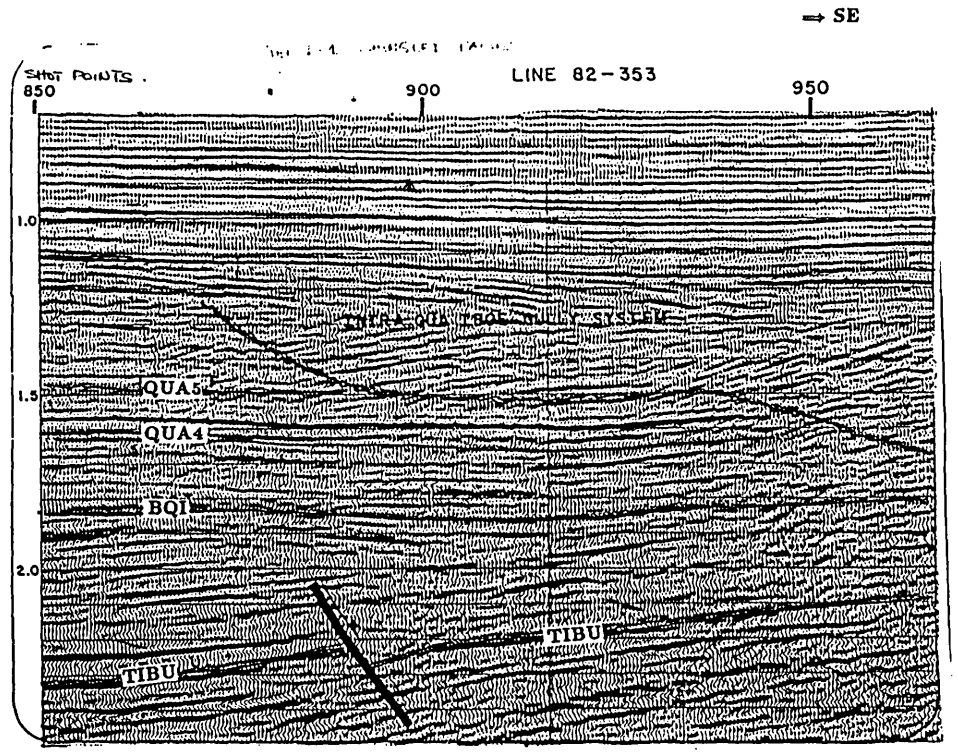

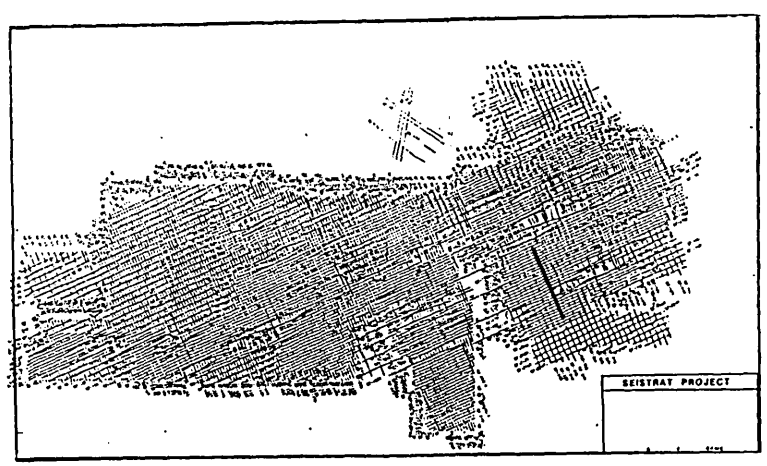

LBIBR- Lower Base Intra Biafra Rubble.

LIBU- Lower Intra Biafra Unconformity.

BIBR- Base Intra Biafra Rubble.

TIBU- Top Intra Biafra Unconformity.

BIBBEN- Base Intra Biafra Benin sands.

BRB- Base Rubble Beds

BQI- Base Qua Iboe.

TIQI- Top Intra Qua Iboe

QUA3 etc- Intra Qua Iboe horizon 3 etc

Pu- Pleistocene Unconformity

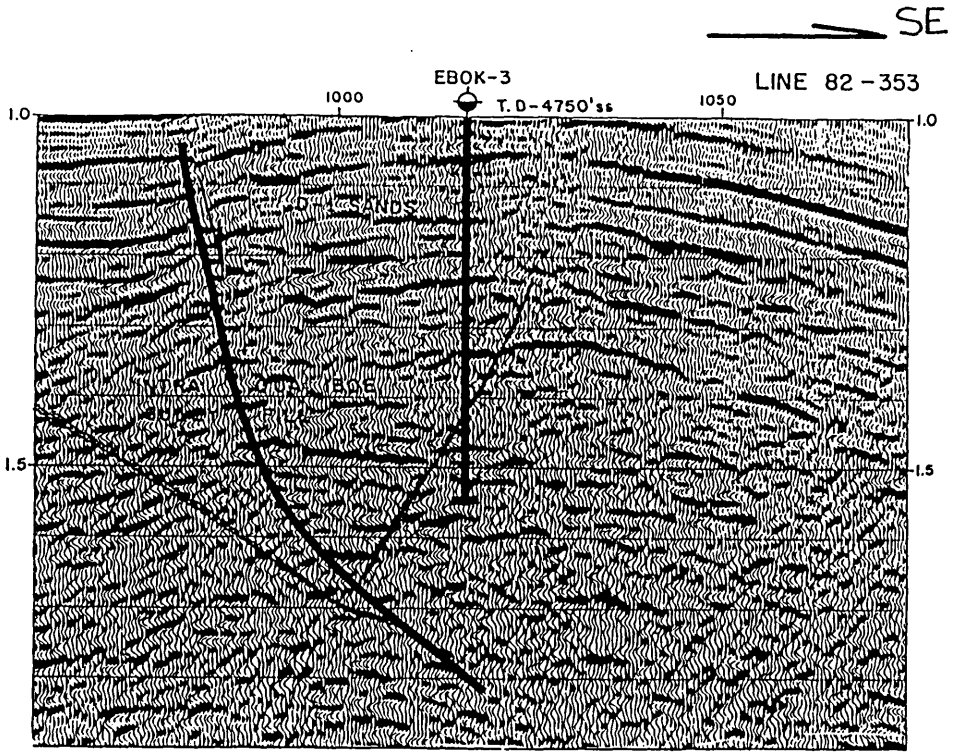

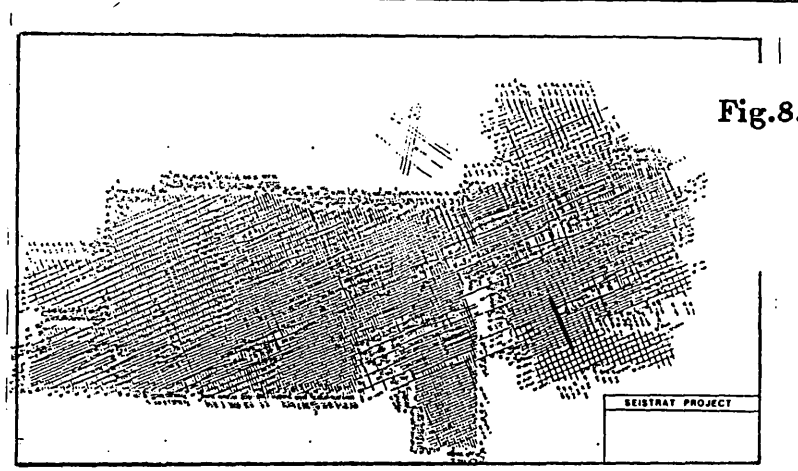

Fig.8.32a&b The chaotic facies of the Intra Qua Iboe gully system. This is an Early Pleistocene canyon trending NE-SW and obscured due to shale tectonics to the south. This trend is at variance with the established trends so far noted in the study area.

LBIBR- Lower Base Intra Biafra Rubble.

LIBU- Lower Intra Biafra Unconformity.

BIBR- Base Intra Biafra Rubble.

TIBU- Top Intra Biafra Unconformity.

BIBBEN- Base Intra Biafra Benin sands.

BRB- Base Rubble Beds

BQI- Base Qua Iboe.

TIQI- Top Intra Qua Iboe

QUA3 etc- Intra Qua Iboe horizon 3 etc

Pu- Pleistocene Unconformity

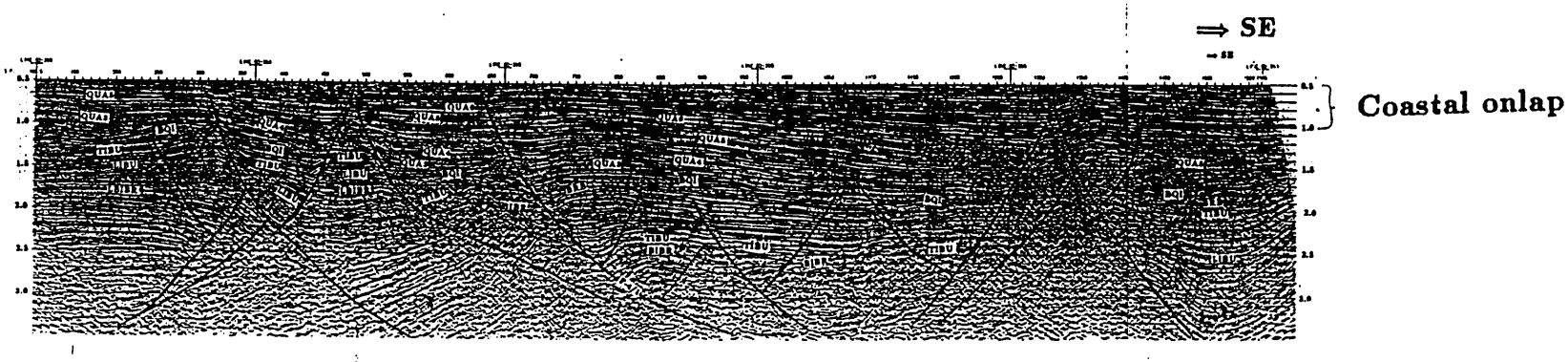

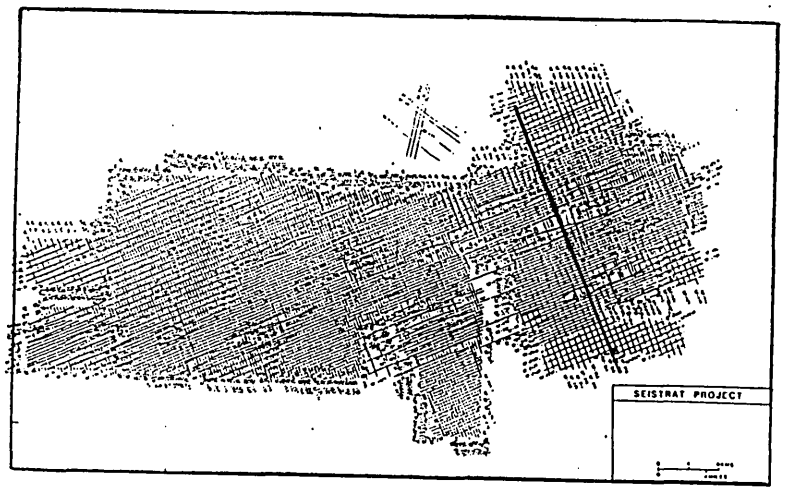

Fig.8.33 Seismic line 82-369, illustrates the coastal onlap associated with SEQ.QS8. The coastal onlap consists mainly of Benin formation sediments and the surface of onlap is Qua8 which is also top D-1 in this area.

LBIBR- Lower Base Intra Biafra Rubble.

LIBU- Lower Intra Biafra Unconformity.

BIBR- Base Intra Biafra Rubble.

TIBU- Top Intra Biafra Unconformity.

BIBBEN- Base Intra Biafra Benin sands.

BRB- Base Rubble Beds

BQI- Base Qua Iboe.

TIQI- Top Intra Qua Iboe

QUA3 etc- Intra Qua Iboe horizon 3 etc

Pu- Pleistocene Unconformity

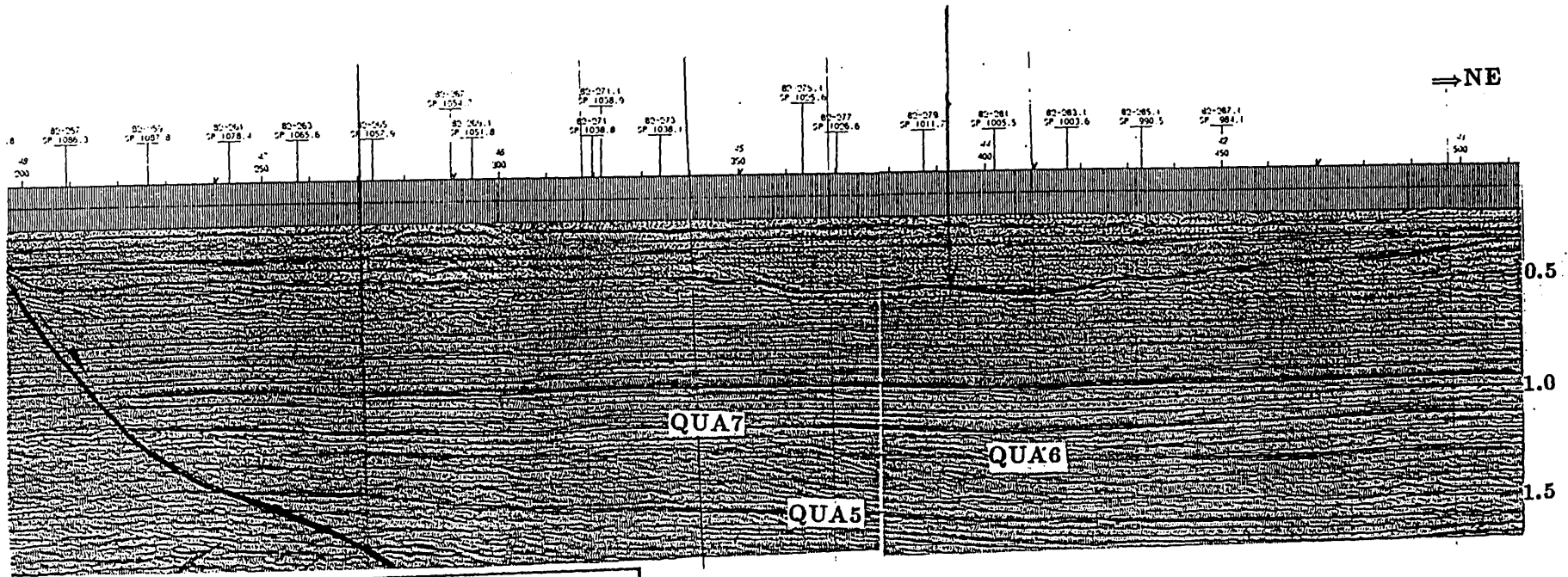

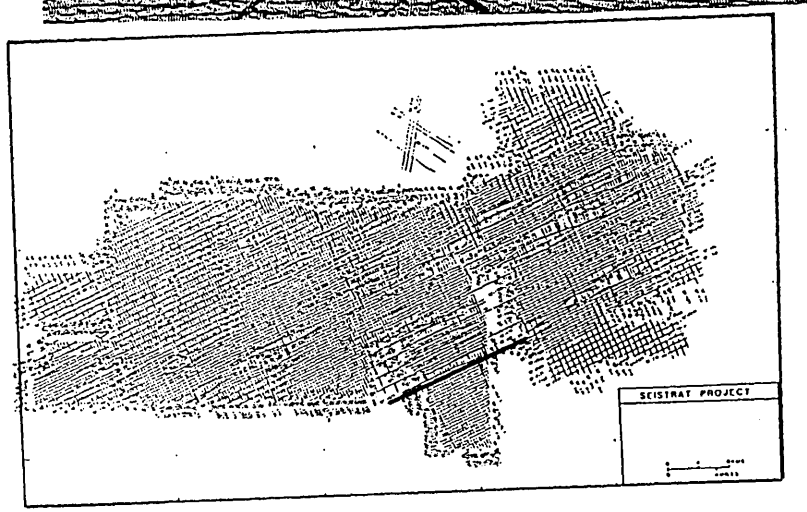

Fig.8.34a The south-central Late Pleistocene canyon(line 82-186).

LBIBR- Lower Base Intra Biafra Rubble.

LIBU- Lower Intra Biafra Unconformity.

BIBR- Base Intra Biafra Rubble.

TIBU- Top Intra Biafra Unconformity.

BIBBEN- Base Intra Biafra Benin sands.

BRB- Base Rubble Beds

BQI- Base Qua Iboe.

TIQI- Top Intra Qua Iboe

QUA3 etc- Intra Qua Iboe horizon 3 etc

Pu- Pleistocene Unconformity

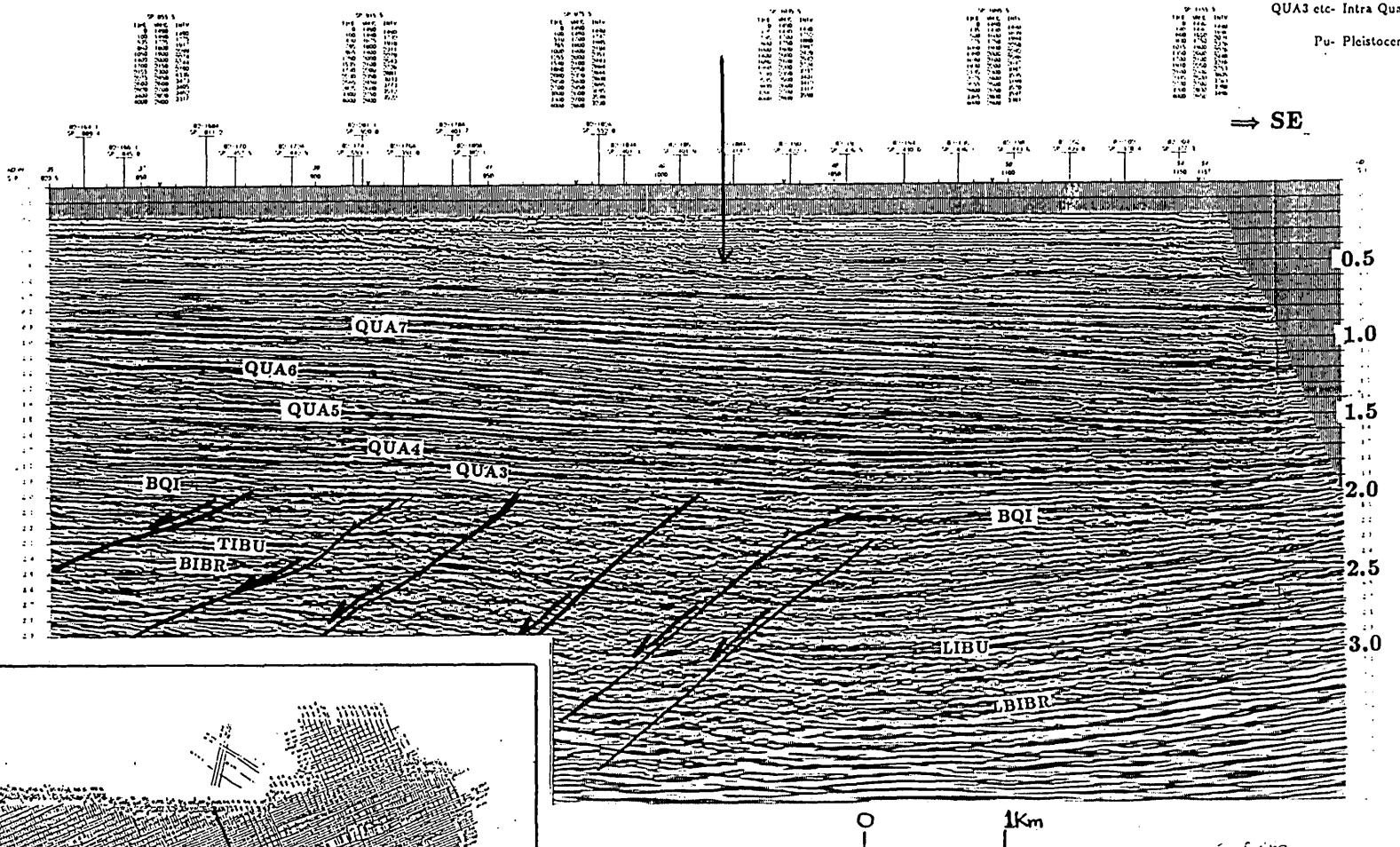

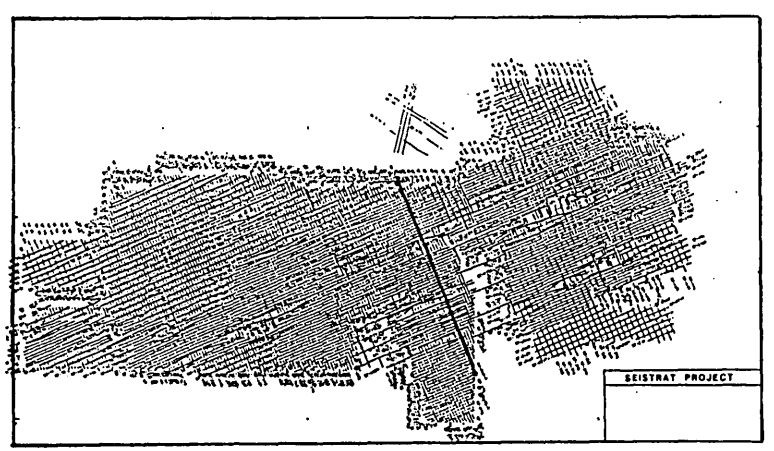

Fig.8.34b The south-central Late Pleistocene canyon (line 82-281).

LBIBR- Lower Base Intra Biafra Rubble.

LIBU- Lower Intra Biafra Unconformity.

BIBR- Base Intra Biafra Rubble.

TIBU- Top Intra Biafra Unconformity.

BIBBEN- Base Intra Biafra Benin sands.

BRB- Base Rubble Beds

BQI- Base Qua Iboe.

TIQI- Top Intra Qua Iboe

QUA3 etc- Intra Qua Iboe horizon 3 etc

Pu- Pleistocene Unconformity

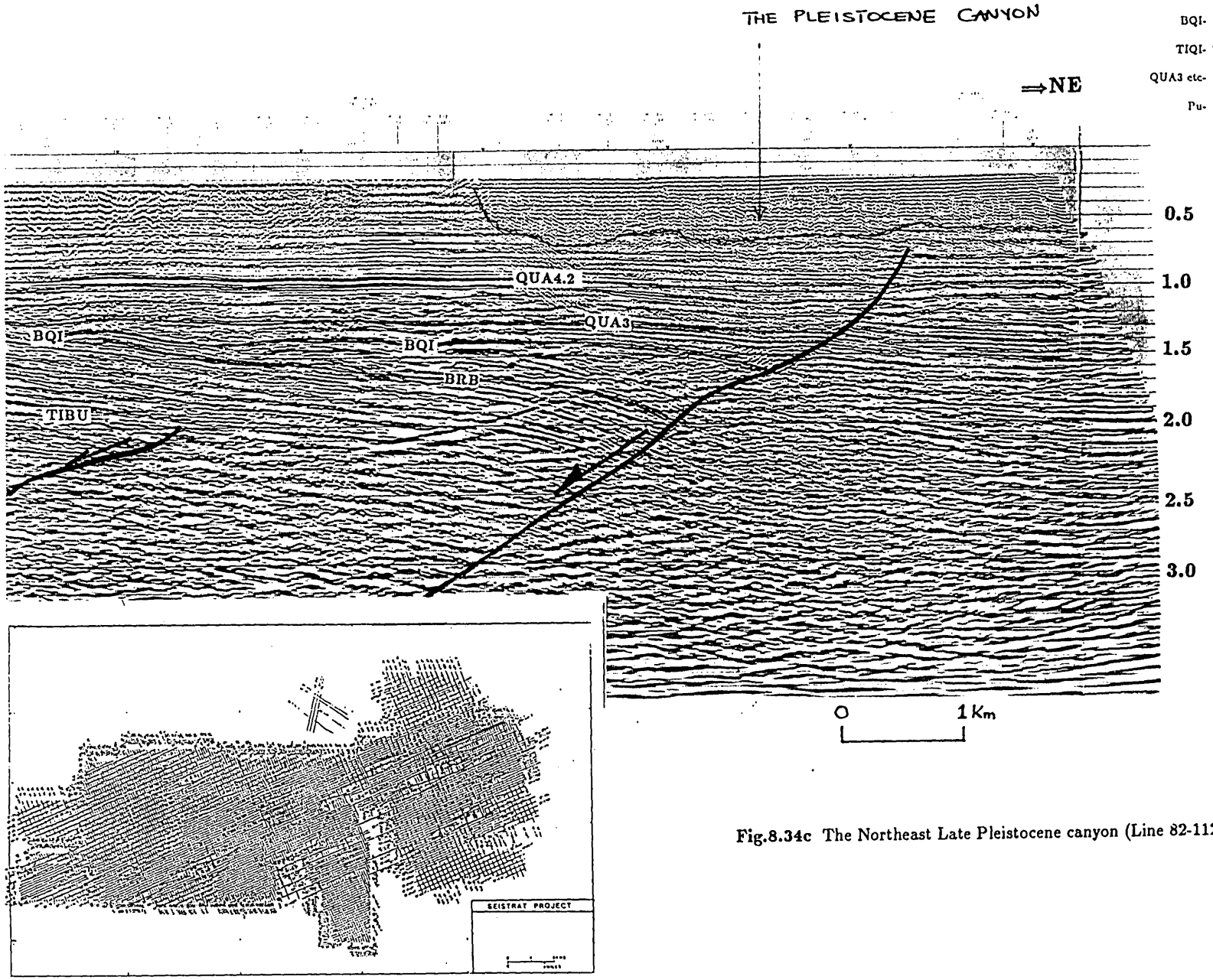

Fig.8.34c The Northeast Late Pleistocene canyon (Line 82-112).

LBIBR- Lower Base Intra Biafra Rubble.

LIBU- Lower Intra Biafra Unconformity.

BIBR- Base Intra Biafra Rubble.

TIBU- Top Intra Biafra Unconformity.

BIBBEN- Base Intra Biafra Benin sands.

BRB- Base Rubble Beds

BQI- Base Qua Iboe.

TIQI- Top Intra Qua Iboe

QUA3 etc- Intra Qua Iboe horizon 3 etc

Pu- Pleistocene Unconformity

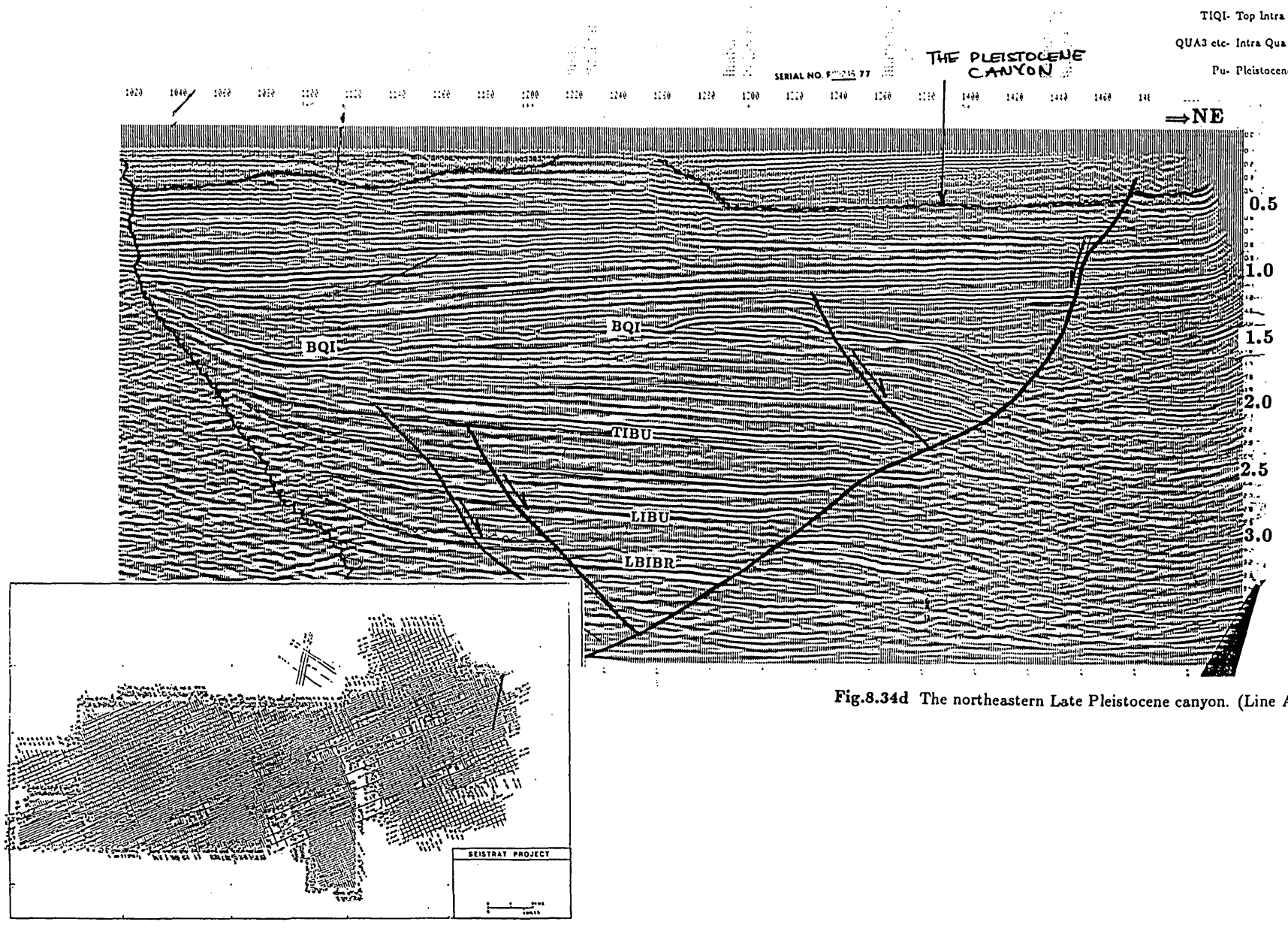

Fig.8.34d The northeastern Late Pleistocene canyon. (Line A-23).

Fig.8.35 Map showing the distribution of the Pleistocene canyons in the study area. The NW-SE trending canyon to the south follows the axis established by the central canyon of the Rubble Beds, and the northern canyon of the Rubble and Qua Iboe. The northeastern pleistocene canyon also trends NW-SE.

LBIBR- Lower Base Intra Biafra Rubble.

LIBU- Lower Intra Biafra Unconformity.

BIBR- Base Intra Biafra Rubble.

TIBU- Top Intra Biafra Unconformity.

BIBBEN- Base Intra Biafra Benin sands.

BRB- Base Rubble Beds

BQI- Base Qua Iboe.

TIQI- Top Intra Qua Iboe

QUA3 etc- Intra Qua Iboe horizon 3 etc

Pu- Pleistocene Unconformity

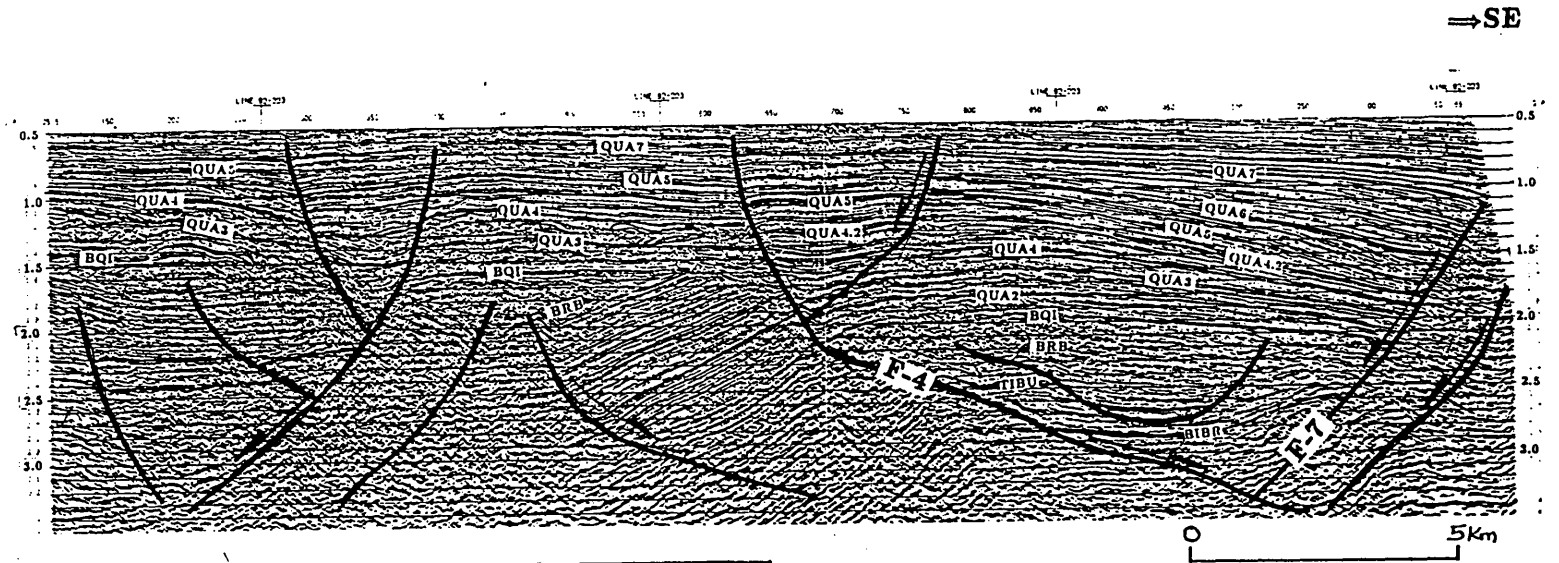

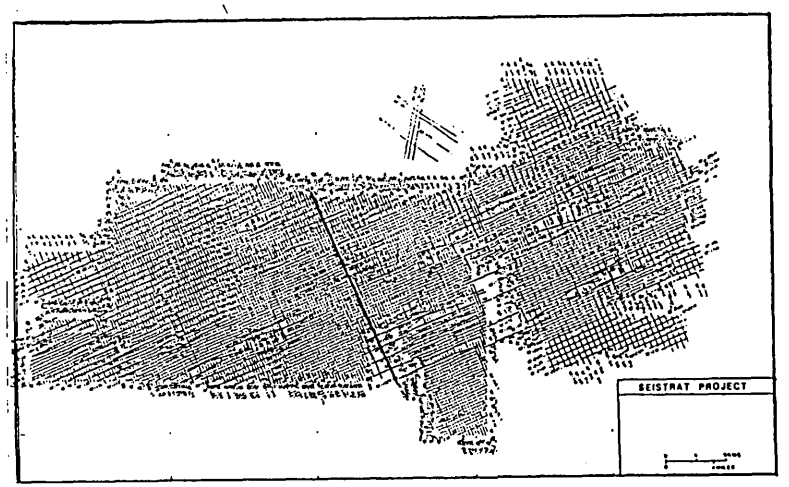

Fig.8.36 Line 82-223 illustrates the lateral facies changes within Qua Iboe progradational sequences from non-marine facies up-slope to a basinal marine facies downdip. The Qua Iboe is thus, the distal marine shale equivalent of the Benin formation. Qua Iboe origin cannot therefore be attributed to canyon or gully fill.

CHAPTER NINE

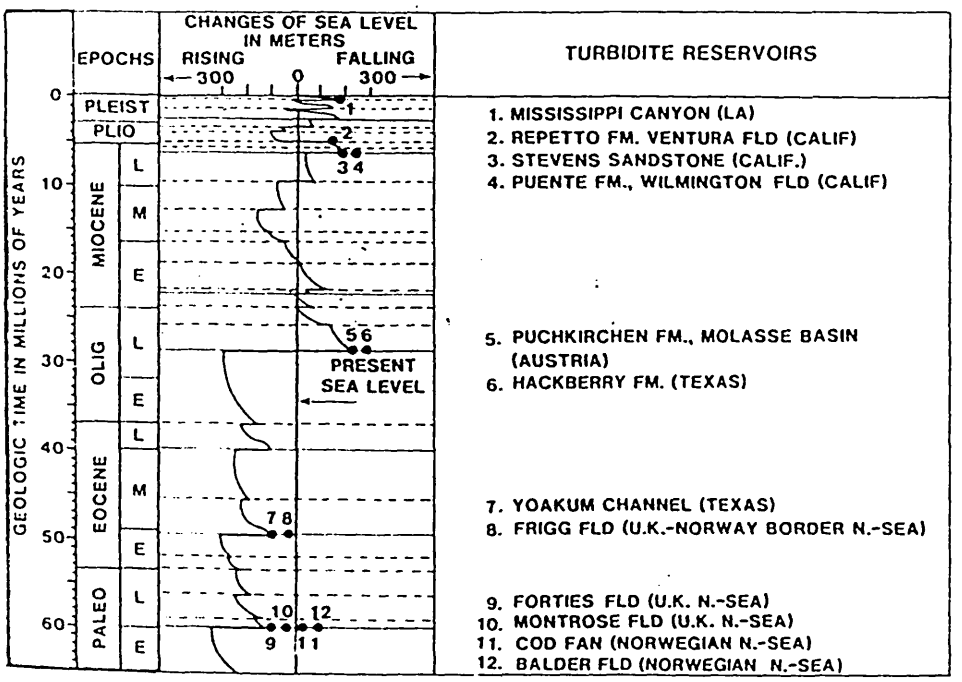

Fig.9.1 Hydrocarbon bearing submarine canyon and fan deposits that closely correspond with Vail and Hardenbol's(1979) lowstands of sea level. (After Shanmugam and Moiola, 1982).

DEEP-WATER MARINE ENVIRONMENTS

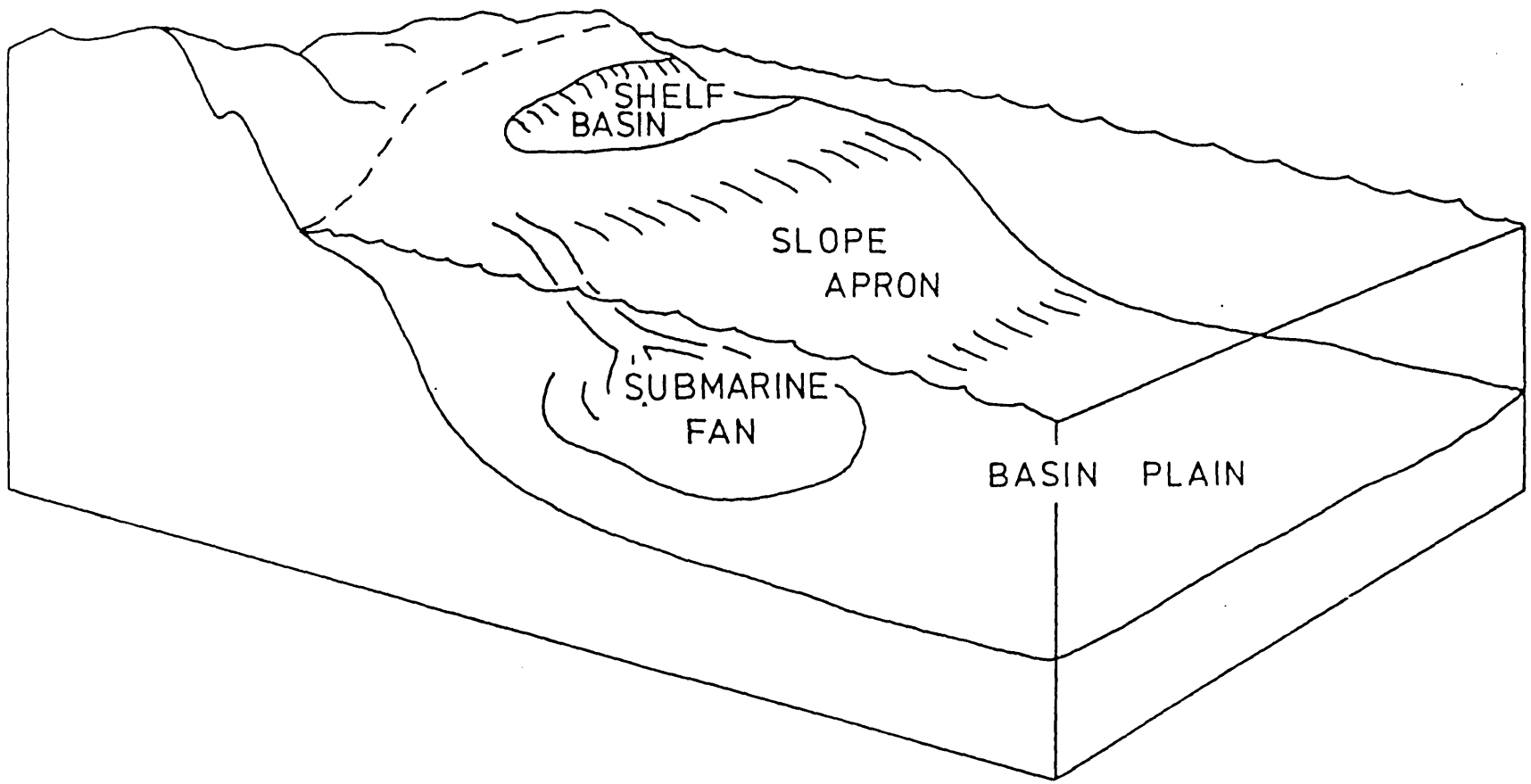

Fig.9.2b Slope apron model. (After Bouma, 1988).

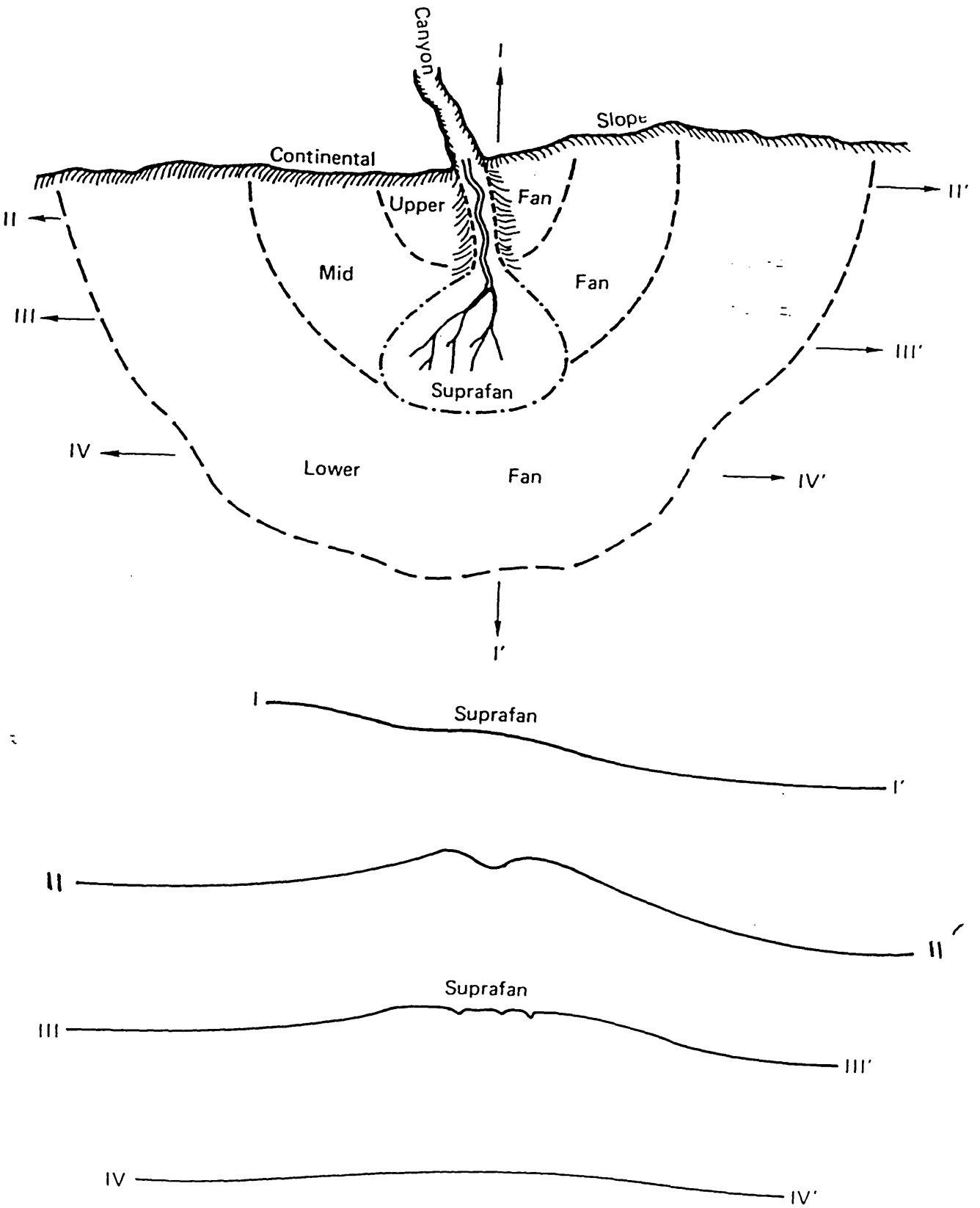

Fig.9.3a Schematic presentation of a model for submarine fan growth emphasizing active and abandoned depositional lobes, termed suprafan. (After Normark, 1978)

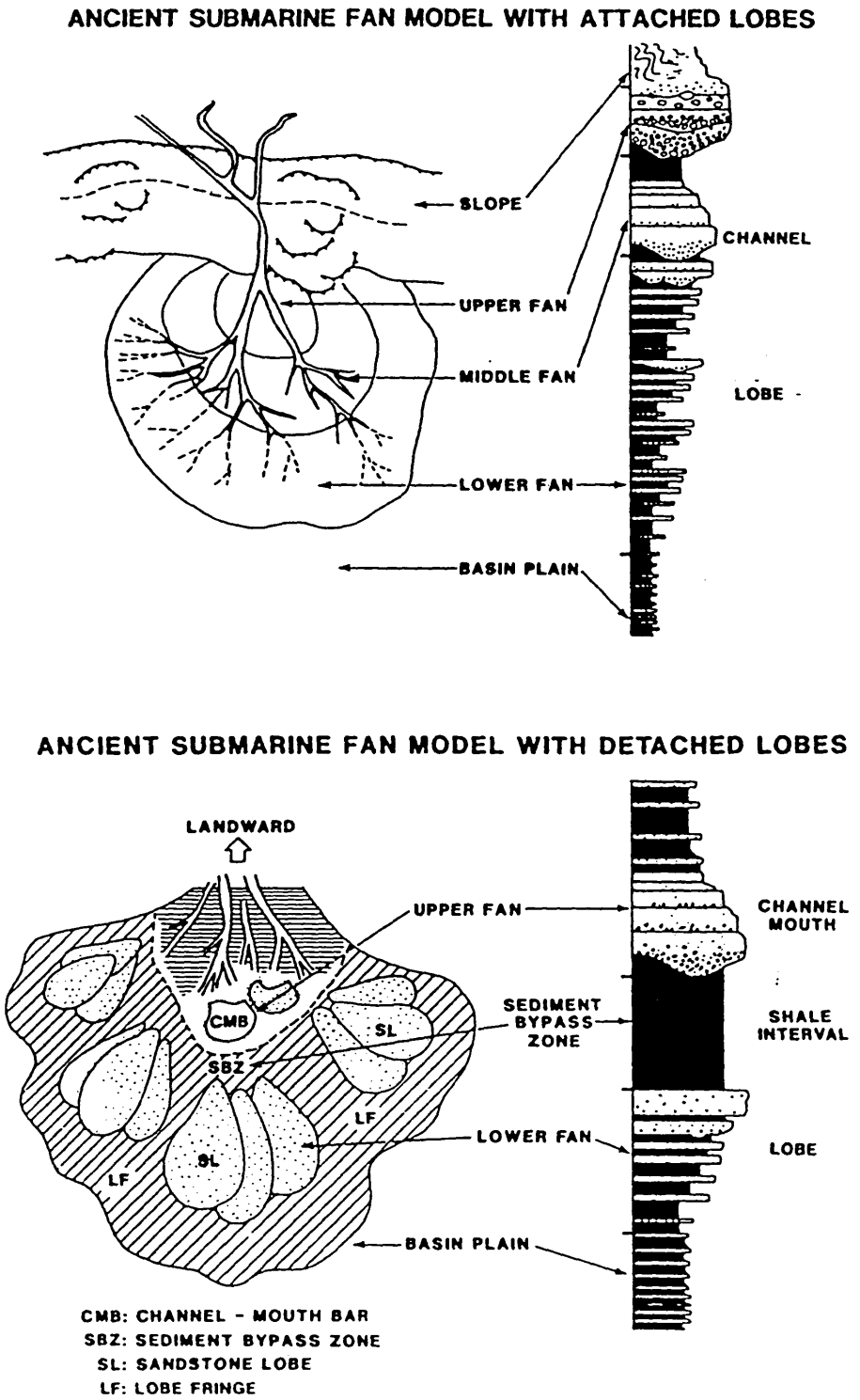

Fig.9.3b Models for ancient submarine fans. Top: Submarine fan with attached depositional lobes. The vertical progradational sequence shows thinning-upward channel fills, and thickening-upward depositional lobe cycles. (After Mutti and Ricci Lucchi, 1975).

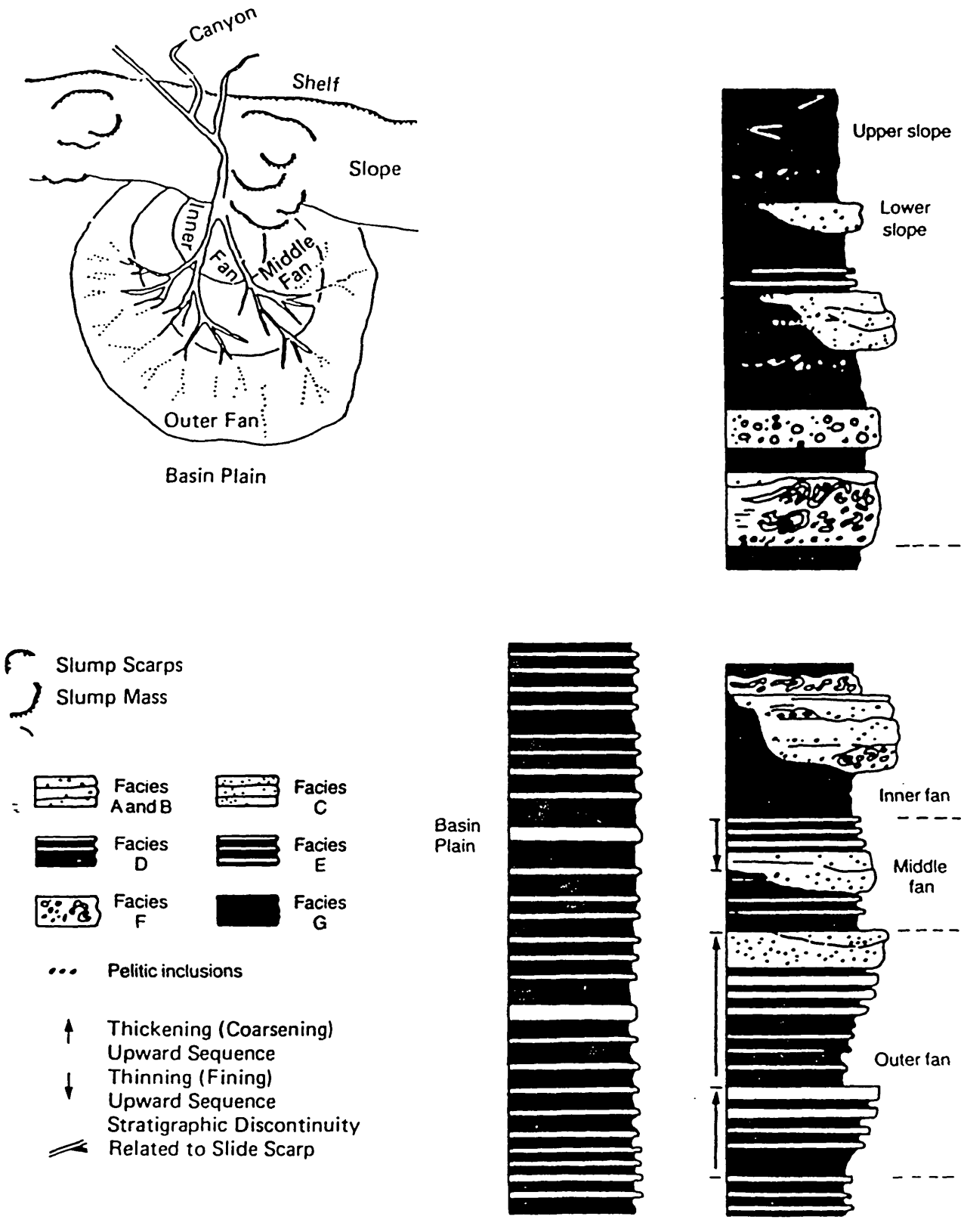

Fig.9.3c Depositional framework of turbidite lithofacies and representative stratigraphic sections of turbidite facies associations. (After Mutti and Ricci Lucchi, 1972).

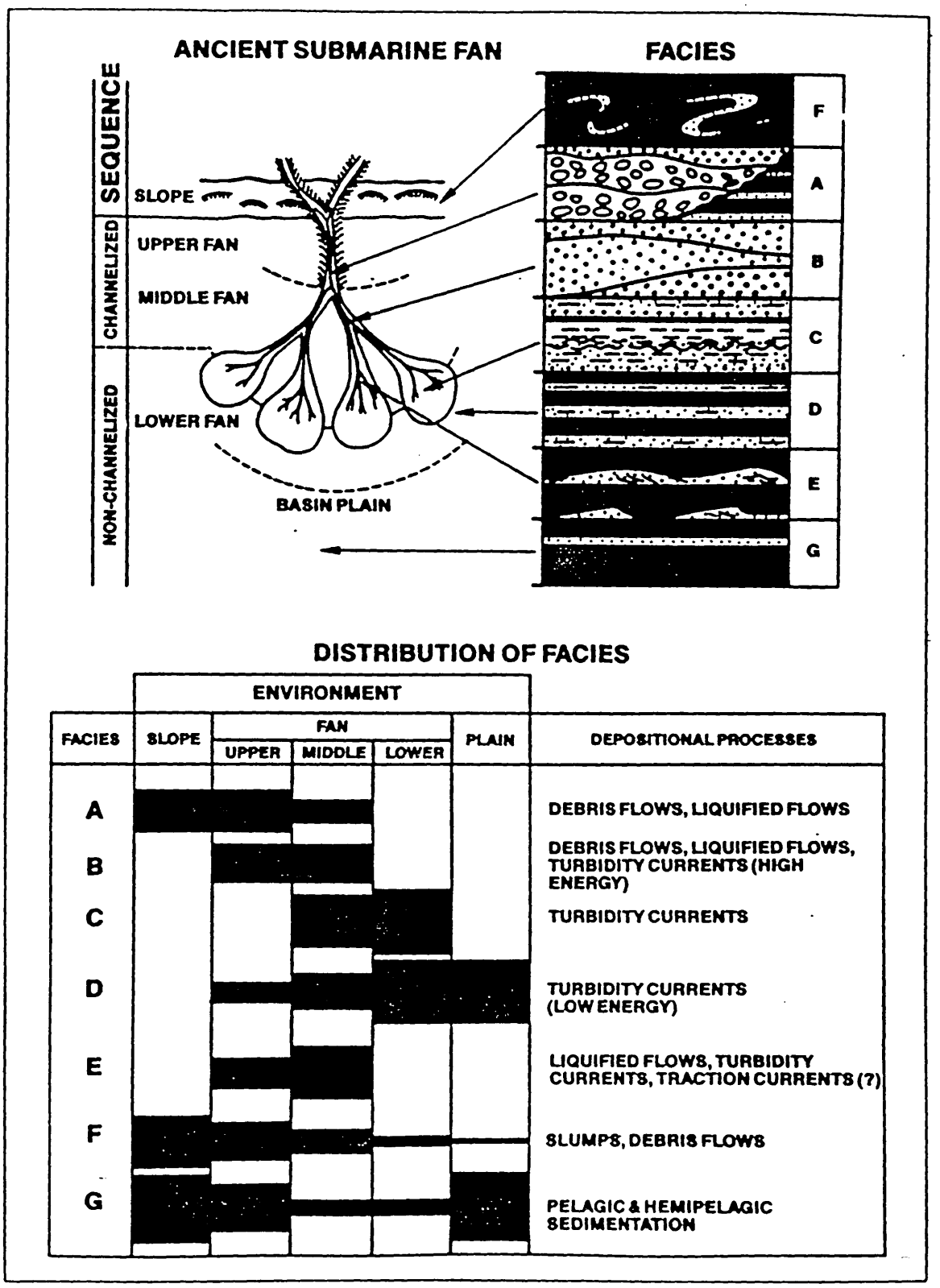

Fig.9.3d The Mutti-Ricci Lucchi submarine fan model showing lithofacies associations for channelized and non-channelized sequences. (After Shanmugam and Moiola, 1985).

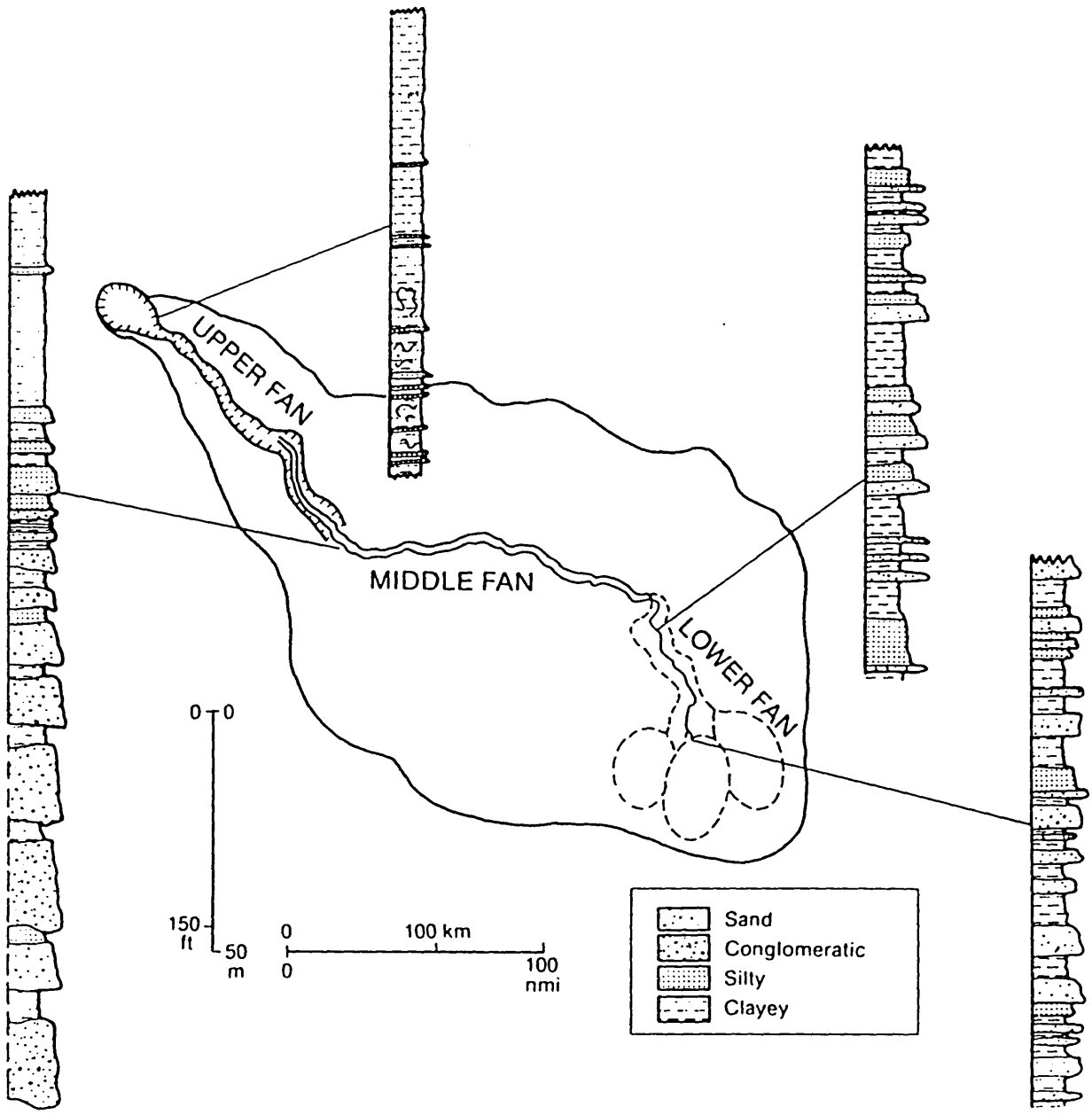

Fig.9.4a The Mississippi submarine fan model. (After Bouma, 1988).

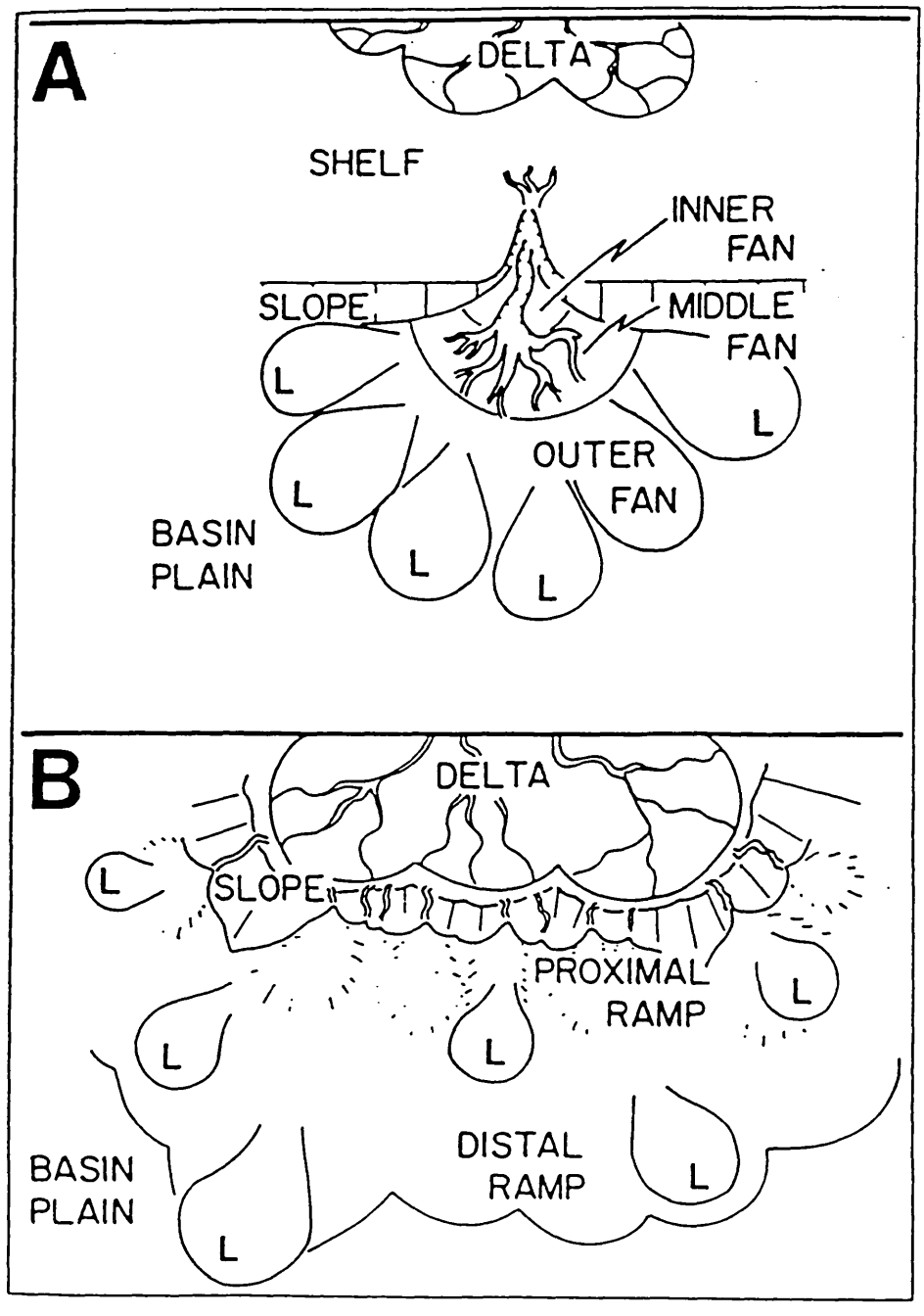

Fig.9.4b The Submarine ramp model by Heller and Dickinson (B) compared to the Mutti and Ricci Lucchi canyon-fed submarine fan model (A). In B the delta margin has prograded to the shelf break, and deposition lobes (L) occur locally in both proximal and distal ramp areas. (From Heller and Dickinson, 1985).

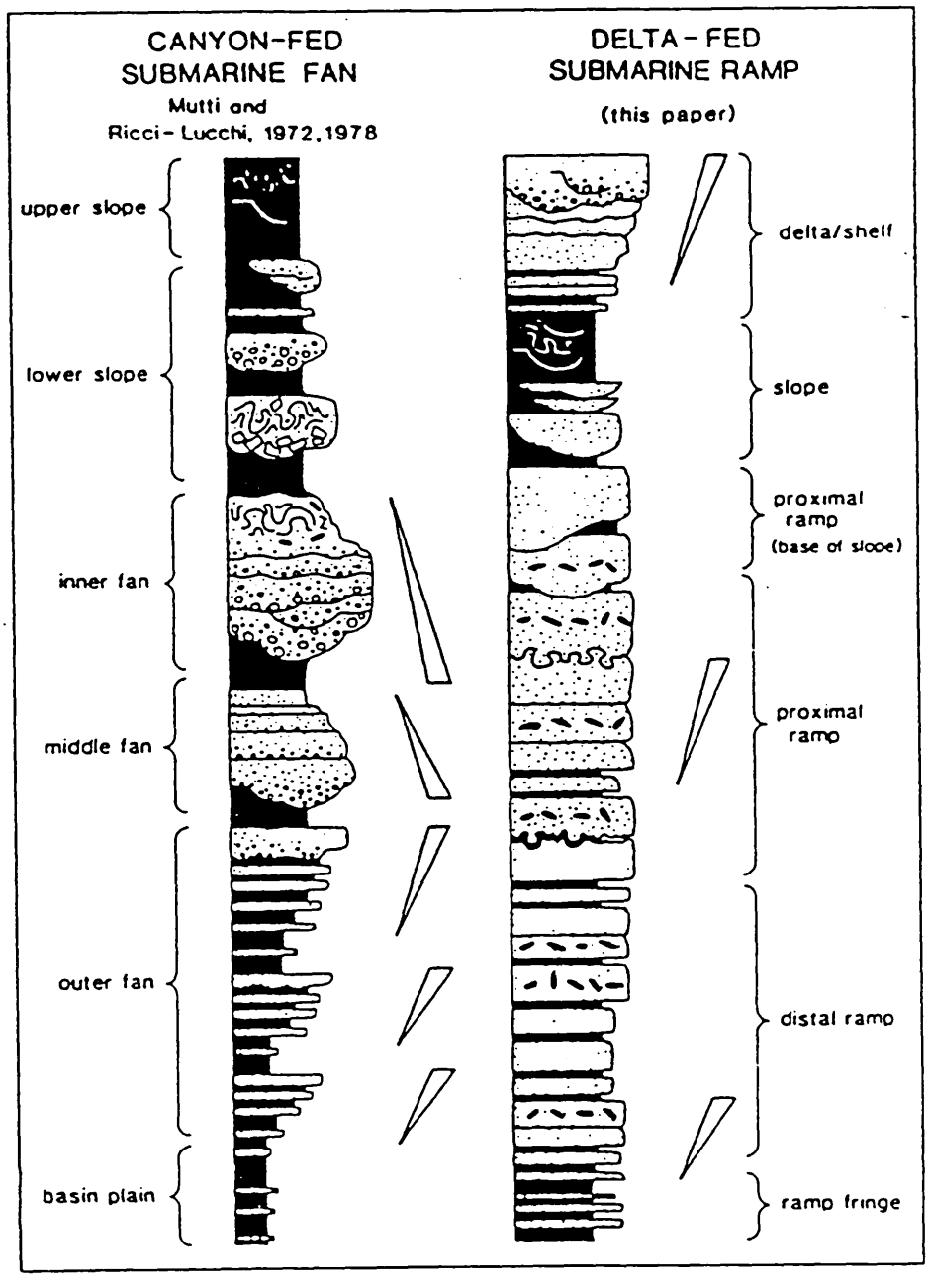

Fig.9.4c Schematic stratigraphic successions that can be produced by prograding turbidite systems. On the left is the canyon-fed (point source) submarine fan system from Mutti and Ricci Lucchi. To the right is the submarine ramp facies model by Heller and Dickinson. (After Heller and Dickinson, 1985).

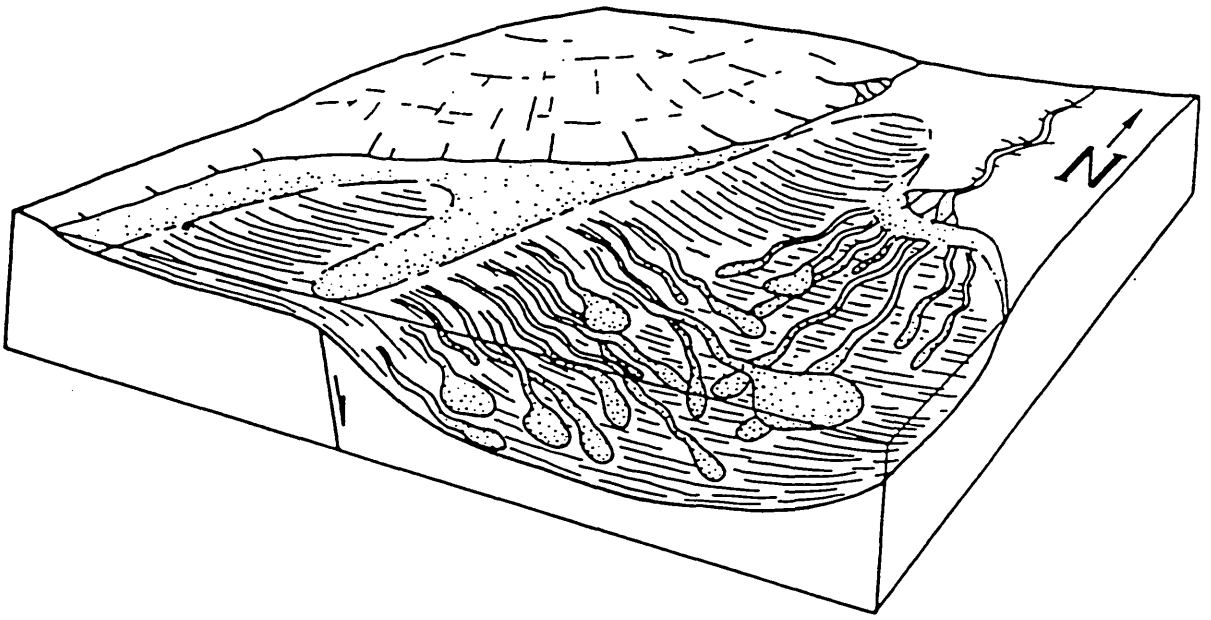

Fig.9.4d Palaeogeographic reconstruction of the setting in Greenland based on the model by Surlyk. Size of the sandstone bodies is greatly exaggerated. The north-eastern delta was fairly short lived. (After Surlyk, 1987).

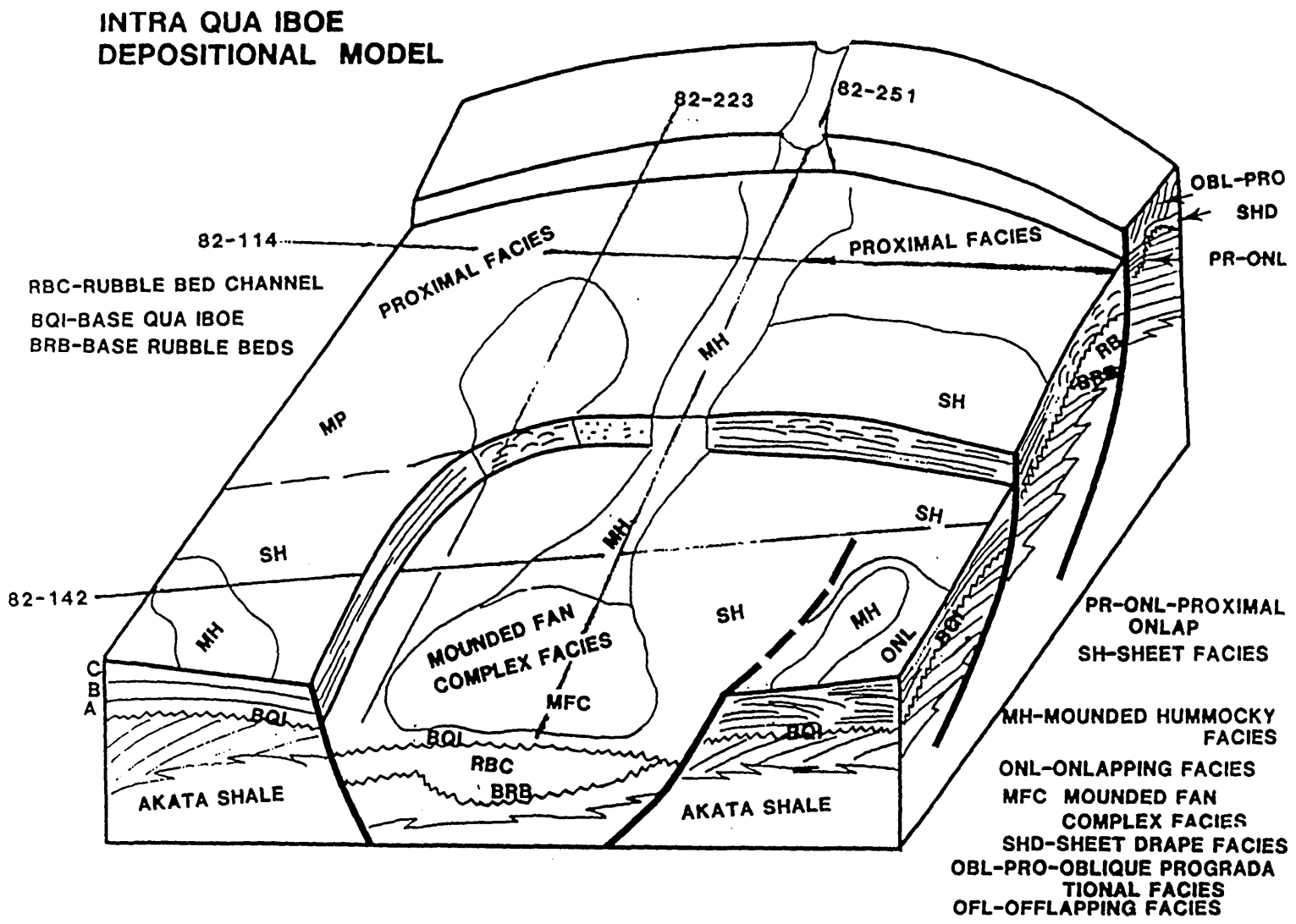

Fig.9.5a The Lower Qua Iboe submarine fan model

Fig.9.5b Map showing the distribution of seismic mounds within the Lower Qua Iboe sequences.

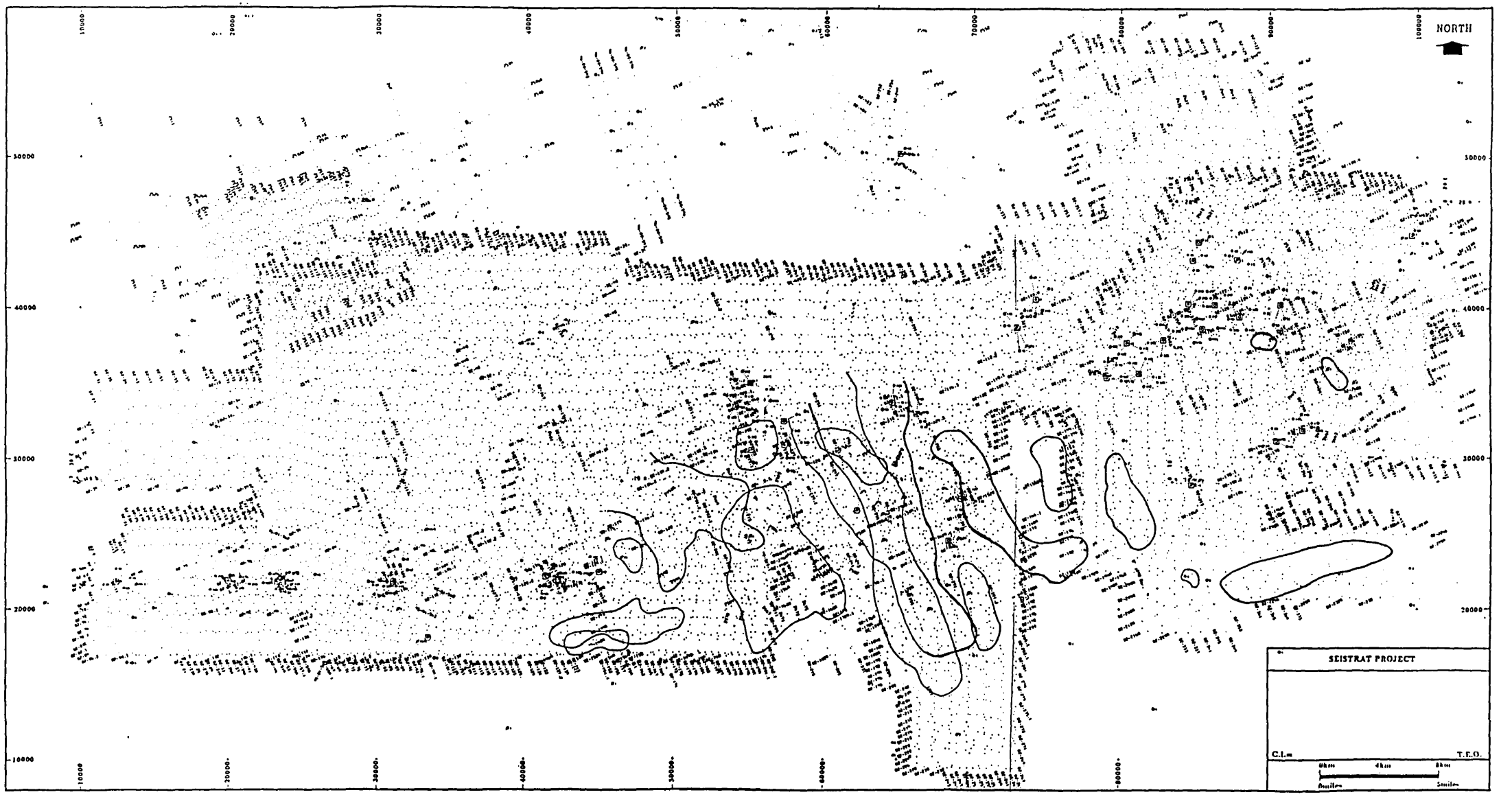

Summary of Direct Seismic Criteria for Recognition of Submarine Fans

	LOWER FAN	UPPER FAN	CANYON FILL
UPPER SURFACE	Commonly high-amplitude, continuous reflection; overall mound shape, convex-upward, no pronounced levees; overlying units onlap or downlap; can be flat in center	High central channel; concave-upward levees sloping to flanks, becoming smaller downdip; leveed channel complex is irregular moundy	Transverse section flat to concave upward; filled with upper fan and later canyon fill
LOWER SURFACE	Fills depositional lows, commonly between older lobes	Depressed in center, rising to flanks to flanks	"V" or "U" shaped notch or structural low, common erosional truncation of slope and underlying slope and shelf units
INTERNAL REFLECTION PATTERN			
-Configuration	Bidirectional opposing downlap away from one or more depositional axes or lobes, convex-upward; may be chaotic; may be irregular moundy in upper part	Bidirectional opposing downlap, dipping to flanks from central channel; concave-upward levee configuration; stacked or a slumped leveed channel complex may be irregular moundy	Shale-prone onlap fill to prograding; transverse profile concave upward
-Amplitude	Commonly high, can be low	Variable, commonly low	Commonly low, lenses of high high
-Continuity	Commonly discontinuous; lower part more continuous	Levees fairly continuous; levee complex may give discontinuous pattern	Commonly fairly continuous; some discontinuous lenses
-Other	Commonly broad cycle breadth	"Bow-tie" differactions from central channel	
AGE RELATIONSHIPS	Commonly older than much of upper fan; deposited at canyon mouth or on slope or basin plain	Commonly younger than most of lower fan; may form much of canyon fill	Lower surface of canyon is older than lower fan; canyon is filled mostly by upper fan and later units

Fig.9.6 Seismic criteria for fan recognition. (After Mitchum, 1985).

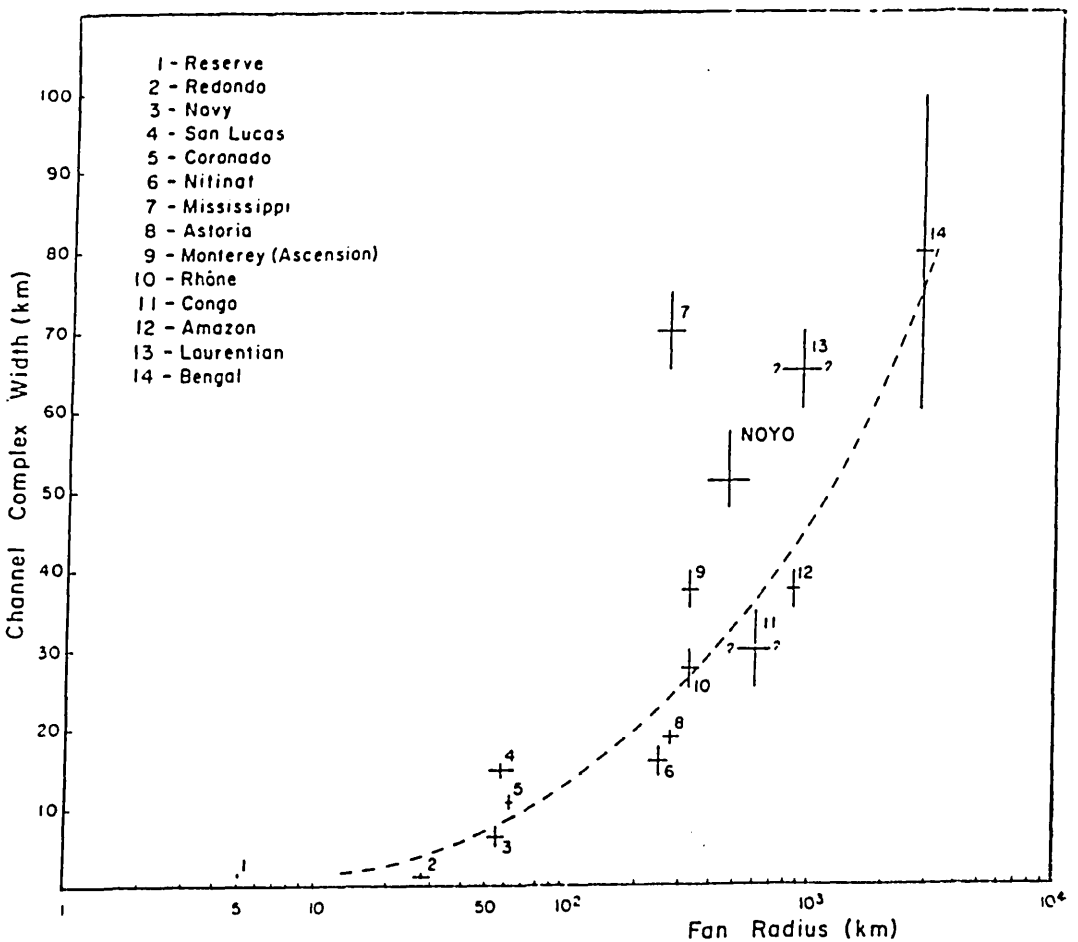

Fig.9.7 Relationship between width of fan-valley levee complex and fan radius. Modified from Normark(1978), with addition of Noyo Valley of Delgada fan. Values plotted are for fan-valley crossing on uppermost fan.

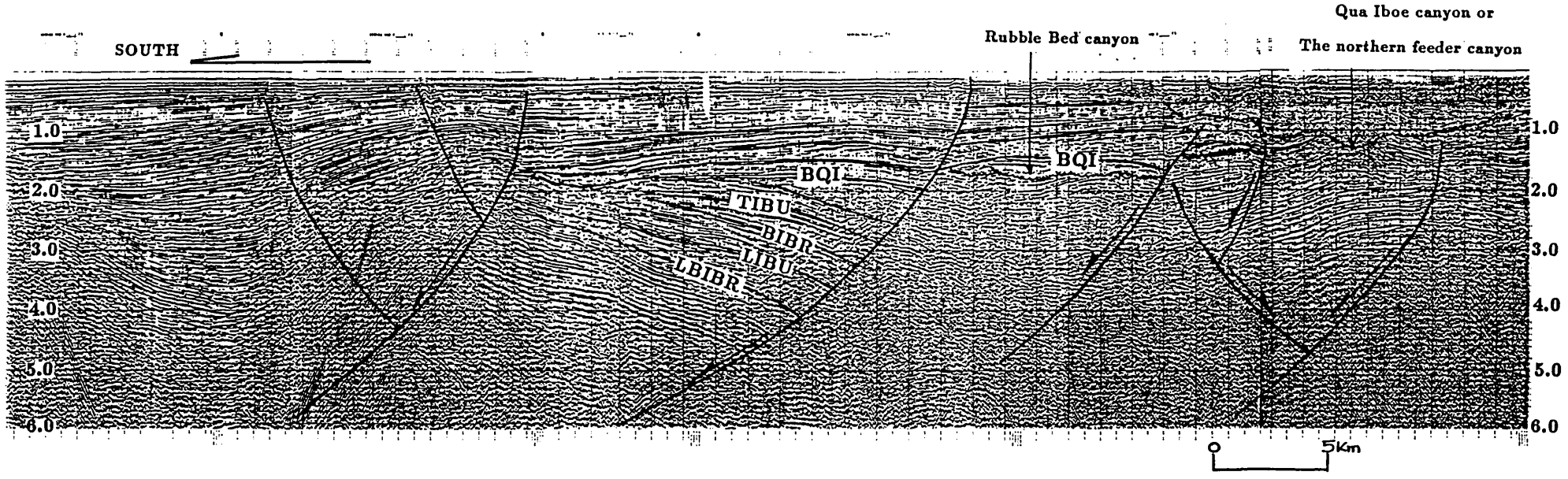

Fig.9.8a Regional seismic profile showing both the Rubble Bed and Qua Iboe canyons. The Qua Iboe canyon is called the northern feeder canyon. (Note the seismic line is unmigrated).

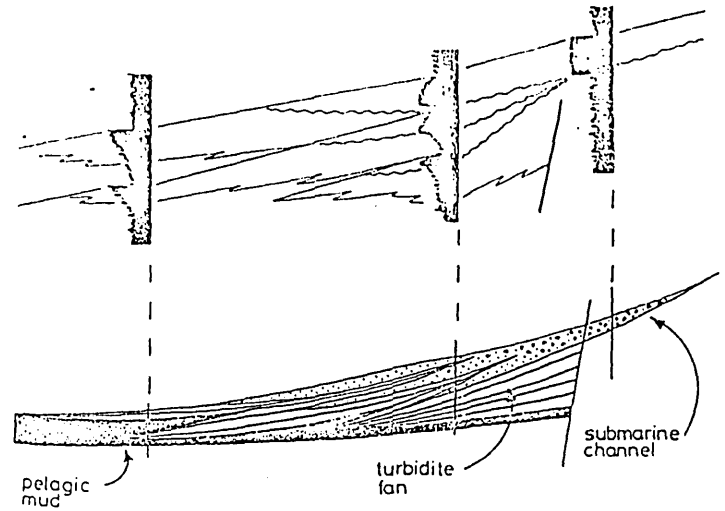

Cross-sectional diagram through a submarine channel fan complex showing the lateral arrangement of gamma log motifs (Selley, 1977).

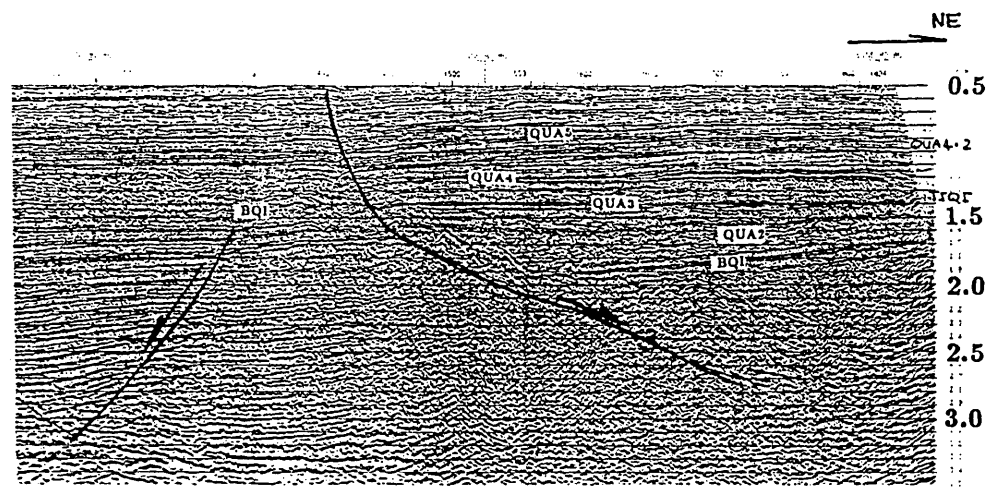

Fig.9.8b Cross - sectional diagram through a submarine channel fan complex shows the lateral arrangement of gamma log motifs (Selley, 1977). Seismic example of a proximal turbidite fan of the Lower Qua Iboe sequences. Note the 'uplap' of proximal facies at the palaeobasin margin (Fault-3).

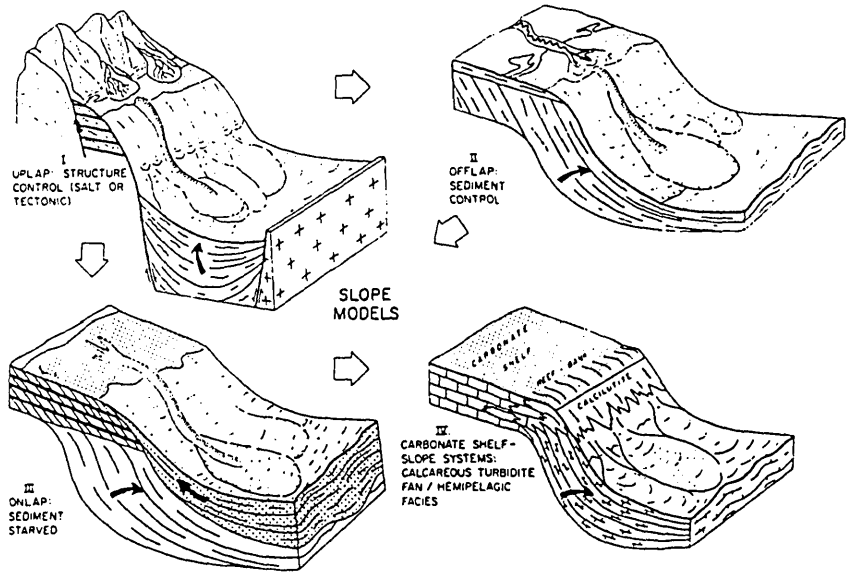

Conceptual slope depositional models. Modified from Brown and Fisher (1977).

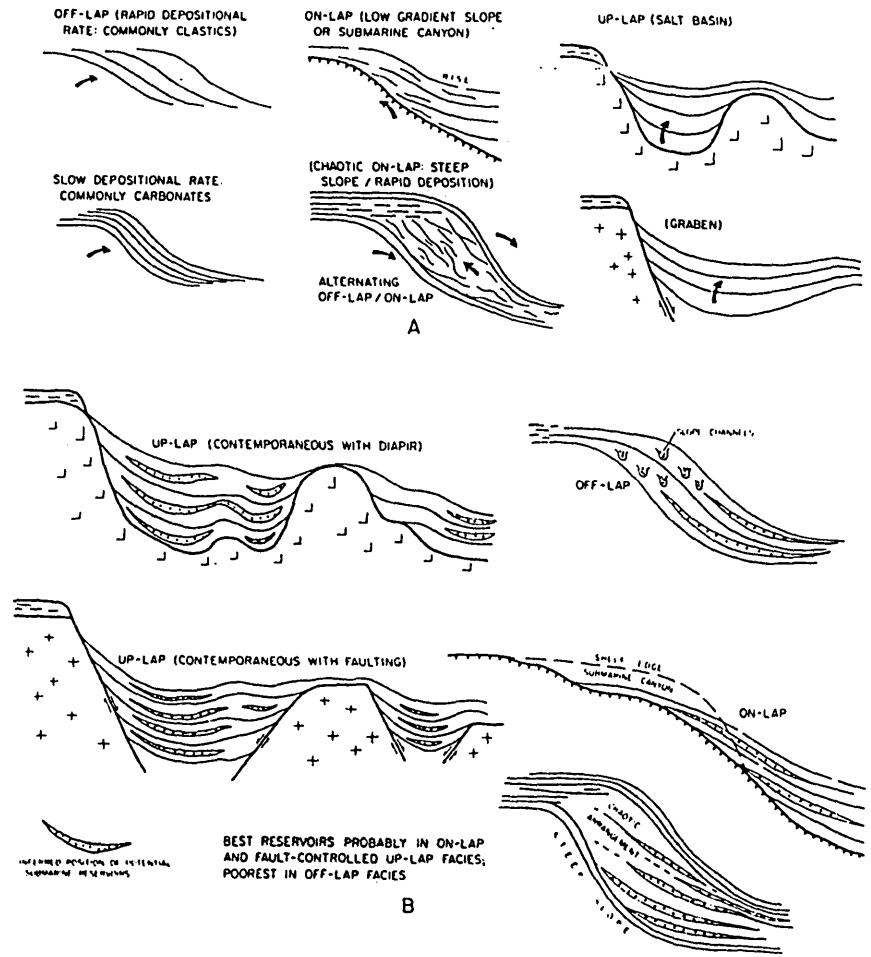

Fig.9.9a&b Seismic stratigraphic slope reflection configurations and inferred distribution of submarine fan reservoirs. (A) Characreistic configurations and (B) Inferred sand distribution. (After Brown and Fisher, 1977).

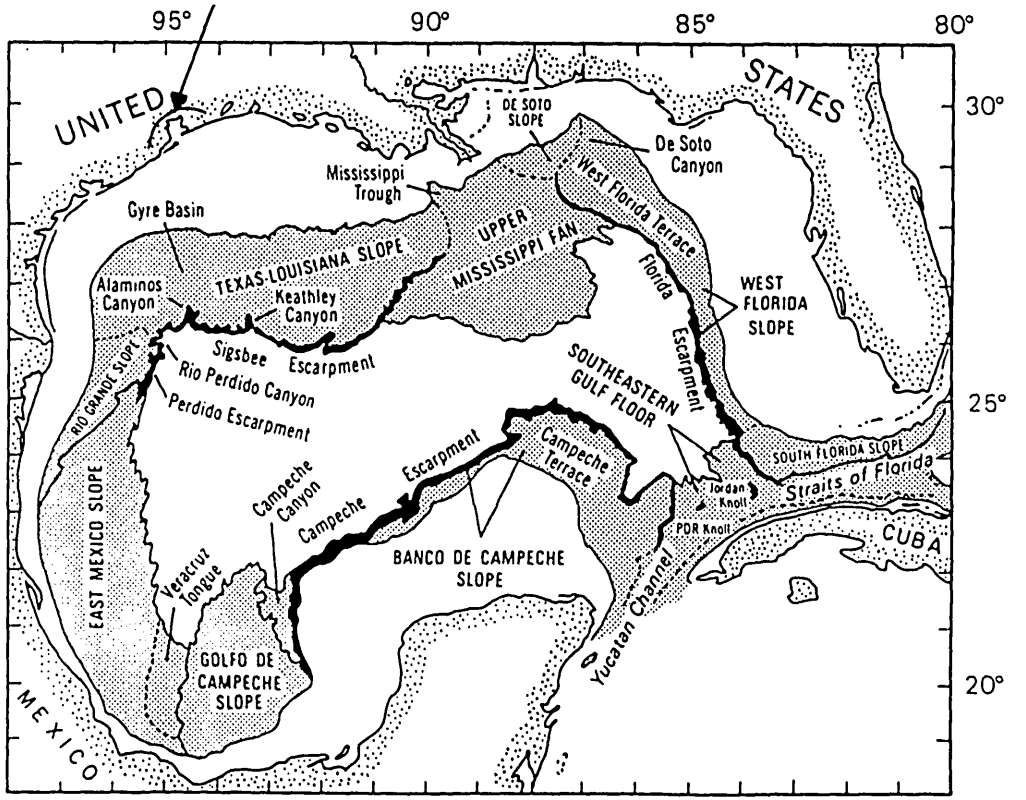

Fig.9.10 Index map of the Gulf of Mexico showing the Texas-Louisiana slope. The present day Texas-Louisiana shelf is to the north, and the locality of the Hackberry is shown (see arrow).

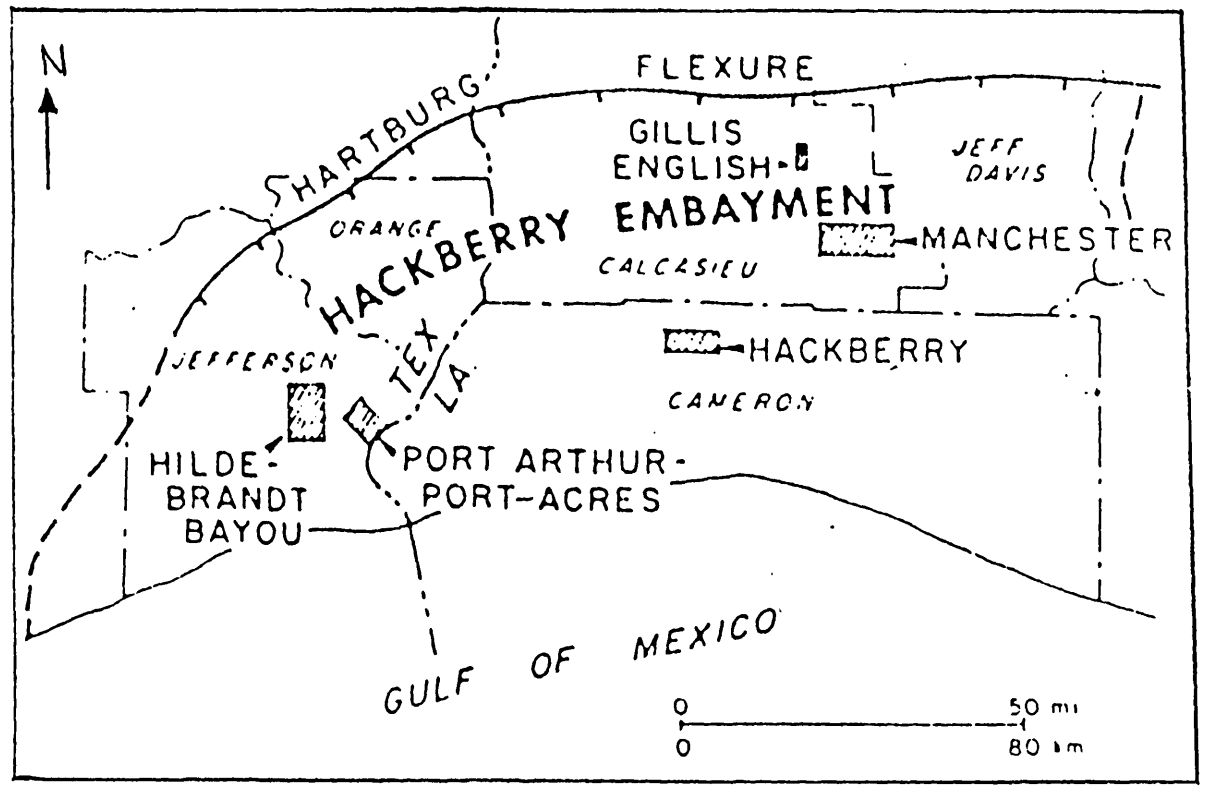

Fig.9.11 Extent of the Hackberry Embayment in southeast Texas and southwest Louisiana.

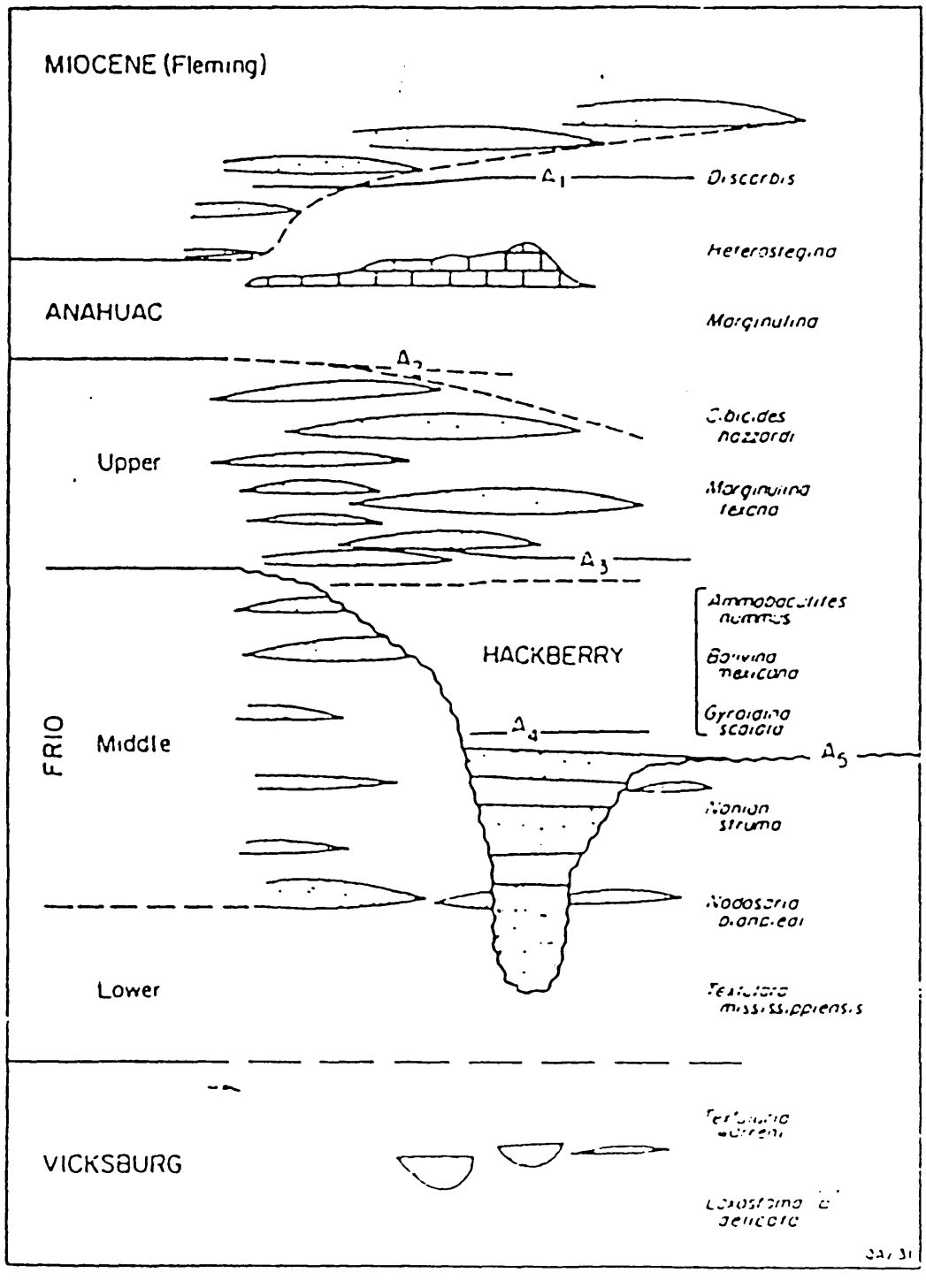

Fig.9.12a Stratigraphic setting of Hackberry onlap slope system.

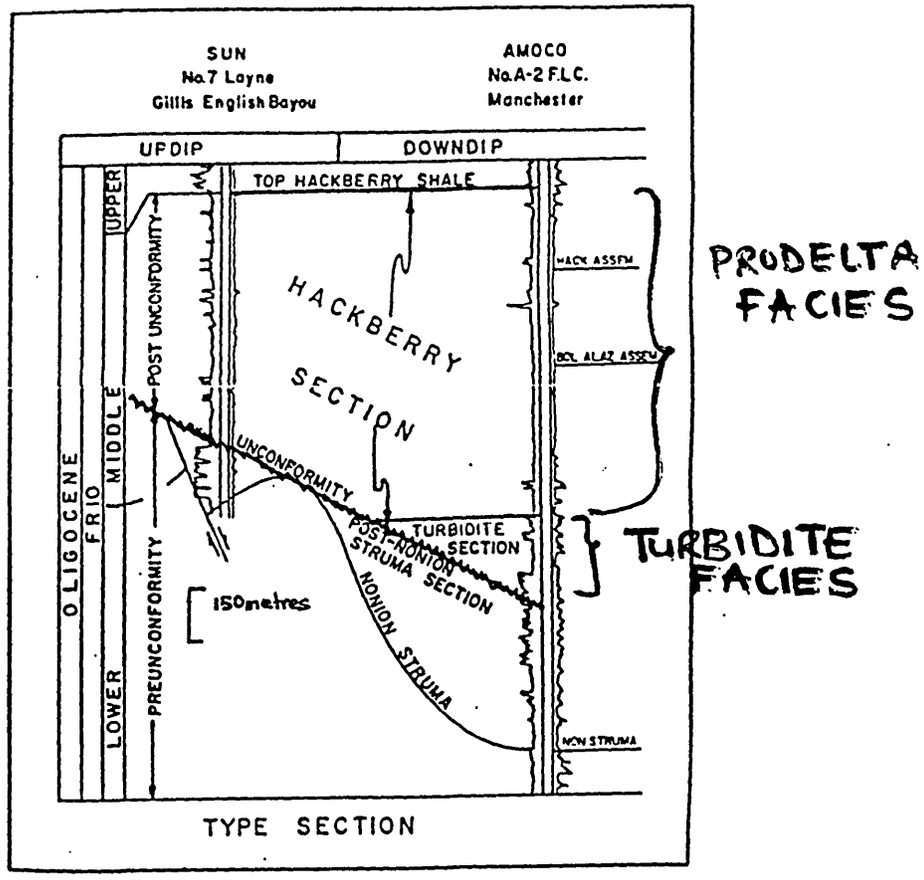

Fig.9.12b Stratigraphic setting of the Hackberry onlap slope system.

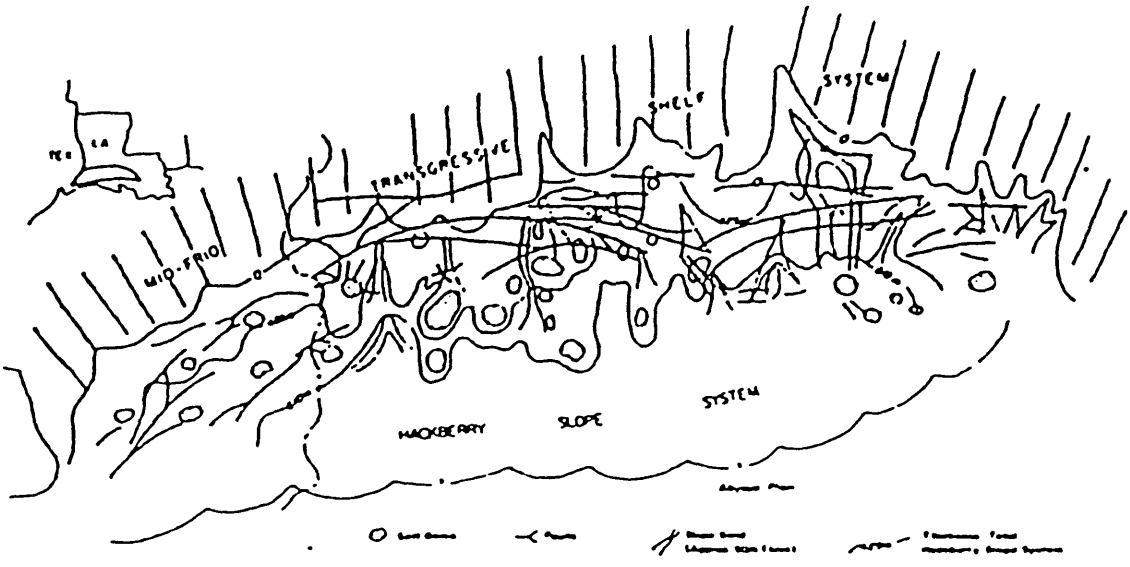

Depositional overview of the Hackberry slope system. From Brown and Fisher (1977).

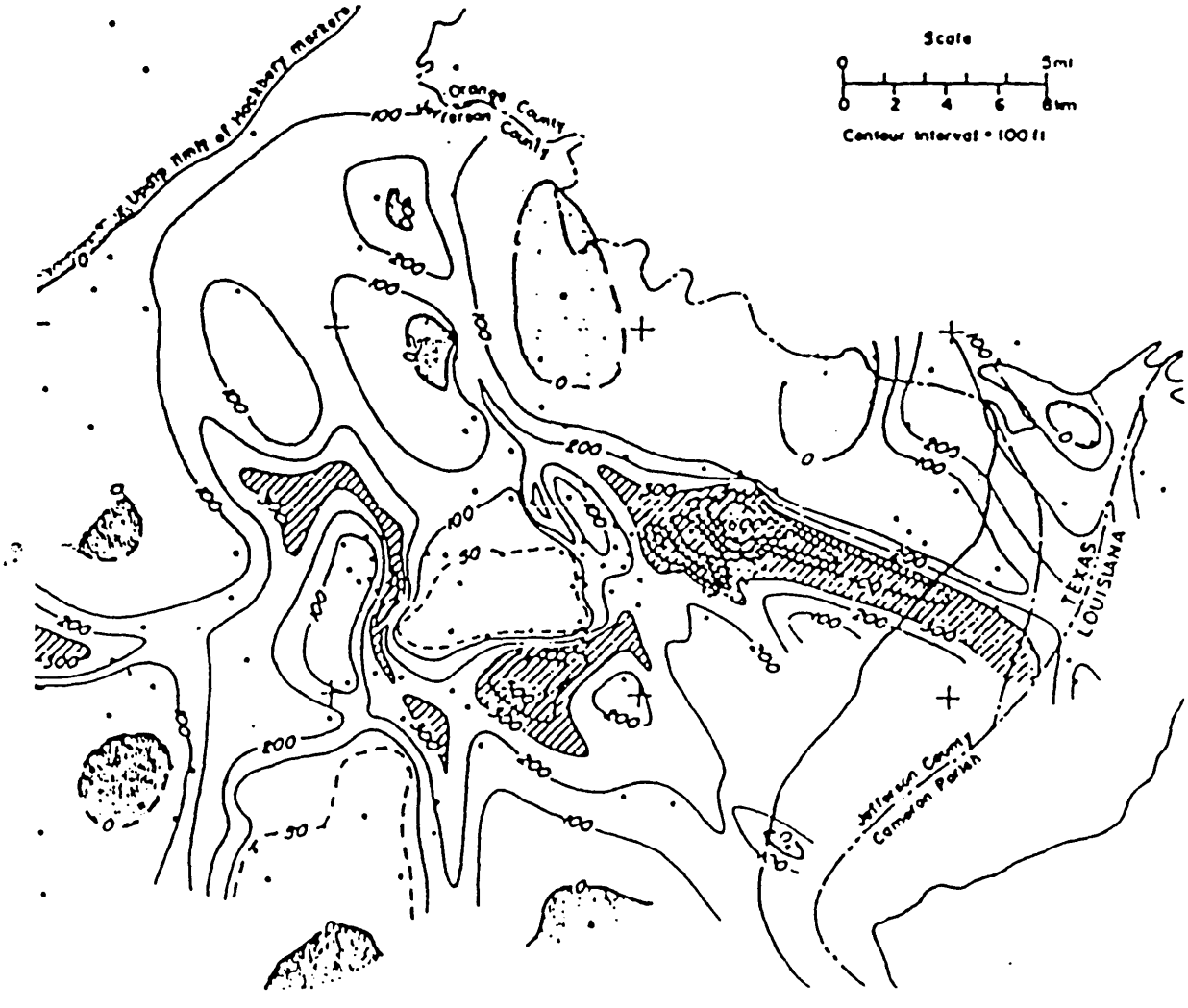

Fig.9.13 Depositional overview of the Hackberry slope system and net-sand isopach map of the western submarine channel complex, Hacknerry slope system. (After Brown and Fisher, 1977 and Ewing and Reed, 1985).

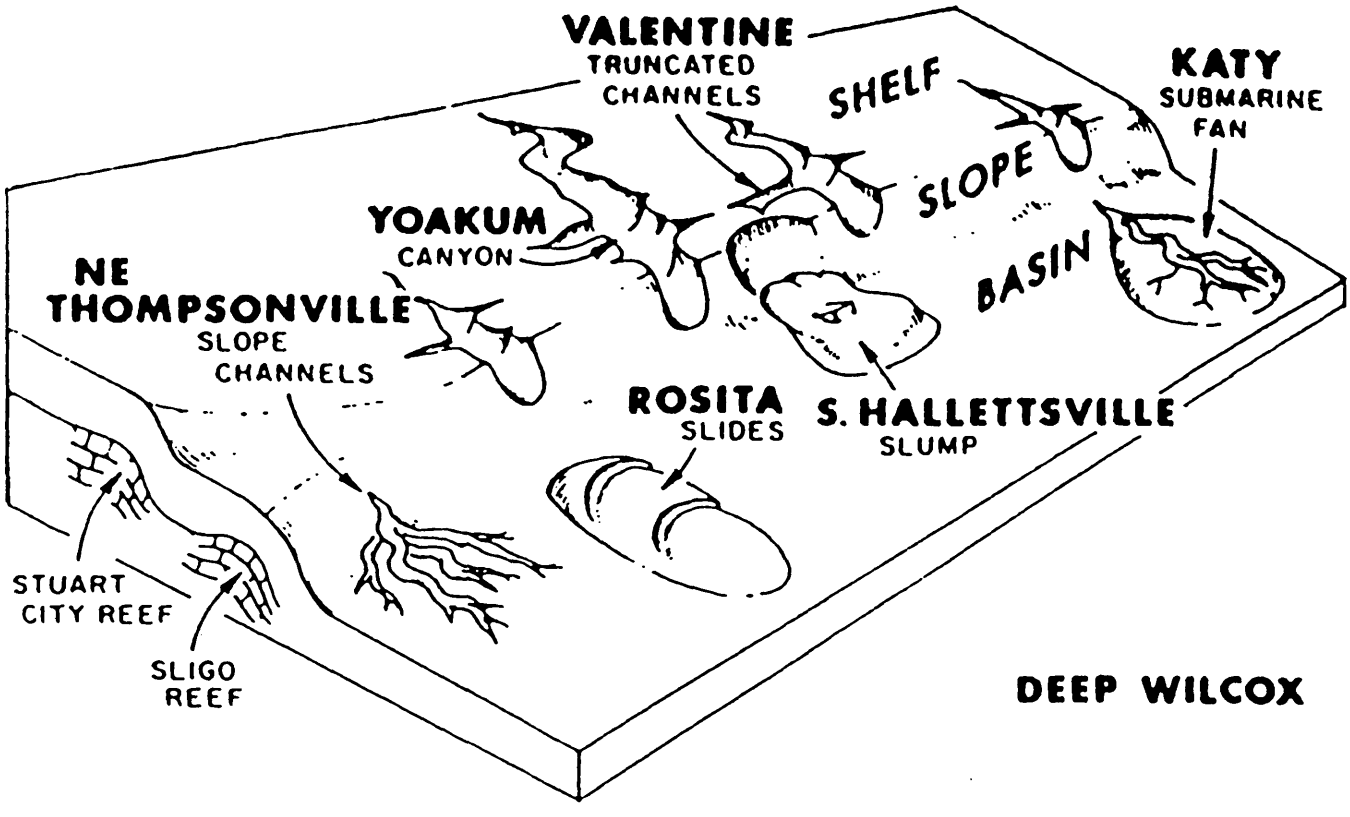

Fig.9.14 A diagram showing the deeper water topograpghy that developed during the Palaeocene and early Eocene. Location of the slope was controlled by the Lower Cretaceous shelf margin. Field areas (bold letters) illustrate local occurrence of reservoir sandstones of different ages, but it may be assumed that similar processes and deposits were contemporaneous throughout the early Tertiary.(After Berg and Powers, 1980).

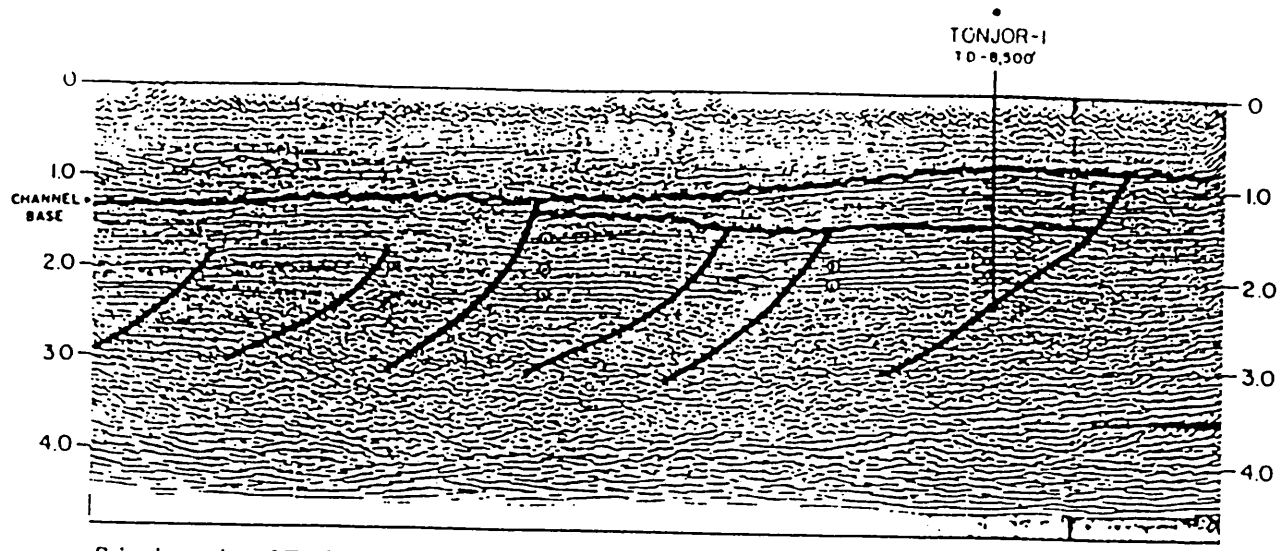

–Seismic section of Tonjor field, western Niger delta.

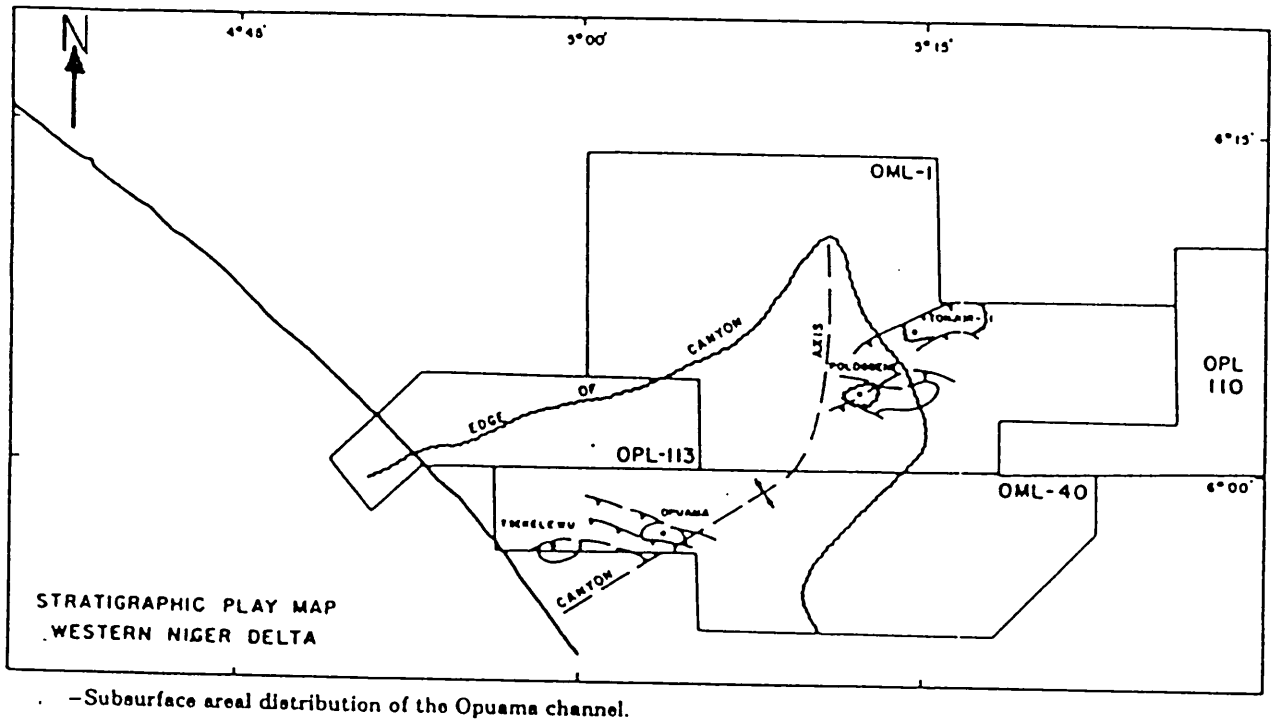

–Subsurface areal distribution of the Opuama channel.

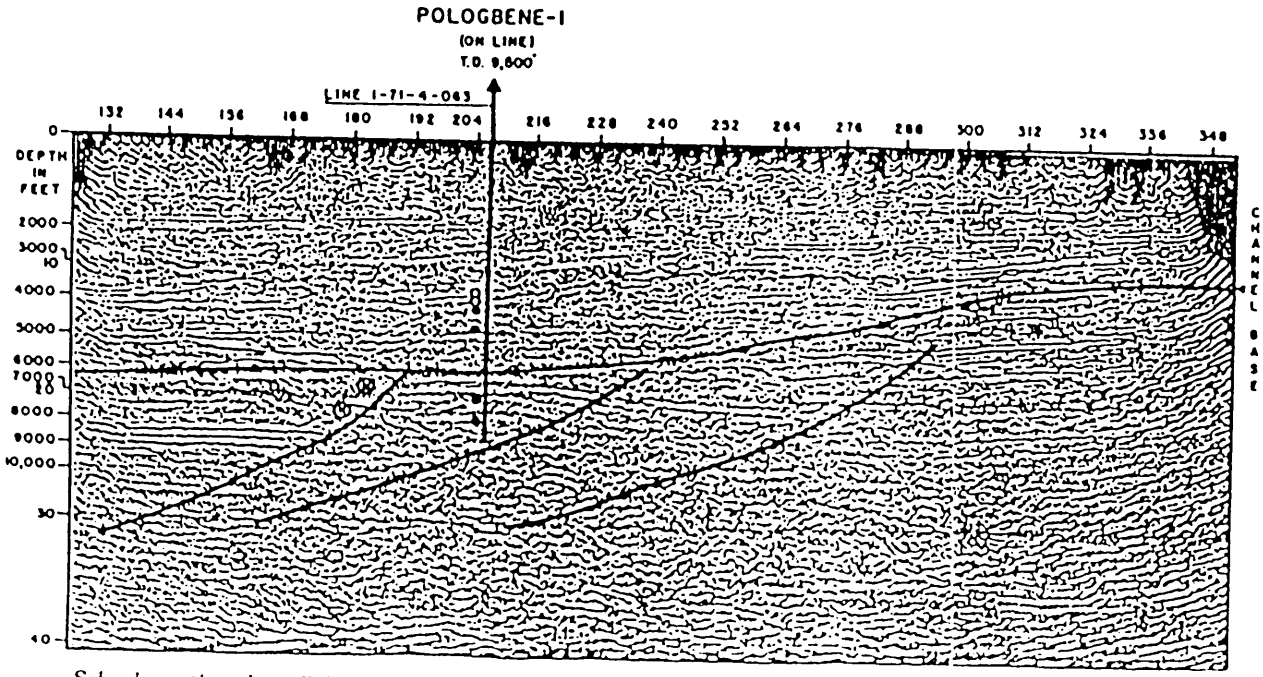

–Seismic section along Pologbene 1, western Niger delta.

Fig.9.15 Canyon fills of the Niger Delta. (After Orife & Avbovbo, 1982).

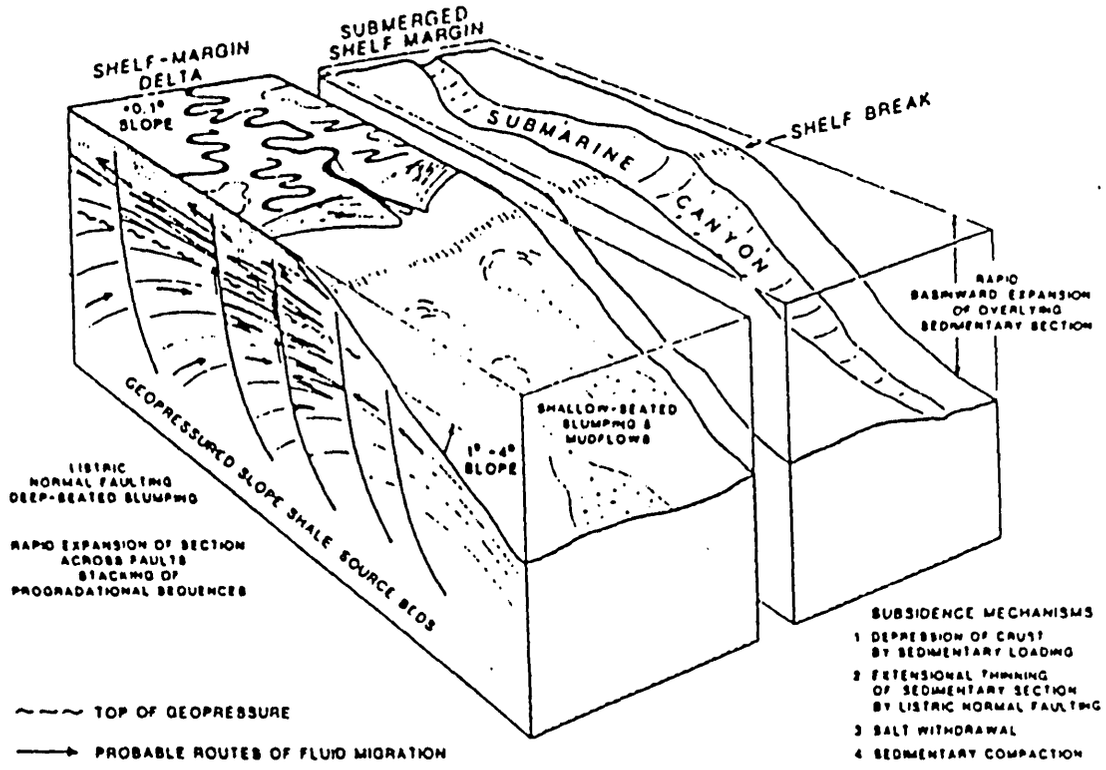

Figure 2. Reservoir settings and structural framework of unstable clastic continental margins. From Winker and Edwards (1983).

Fig.9.17 Reservoir settings and structural framework of unstable clastic continental margins. (After Winker and Edwards, 1983). Note, in a submerged shelf margin (e.g. the eastern part of the study area), slumping characterized by mounds are less common incomparison to areas of active delta development (central part of the study area).

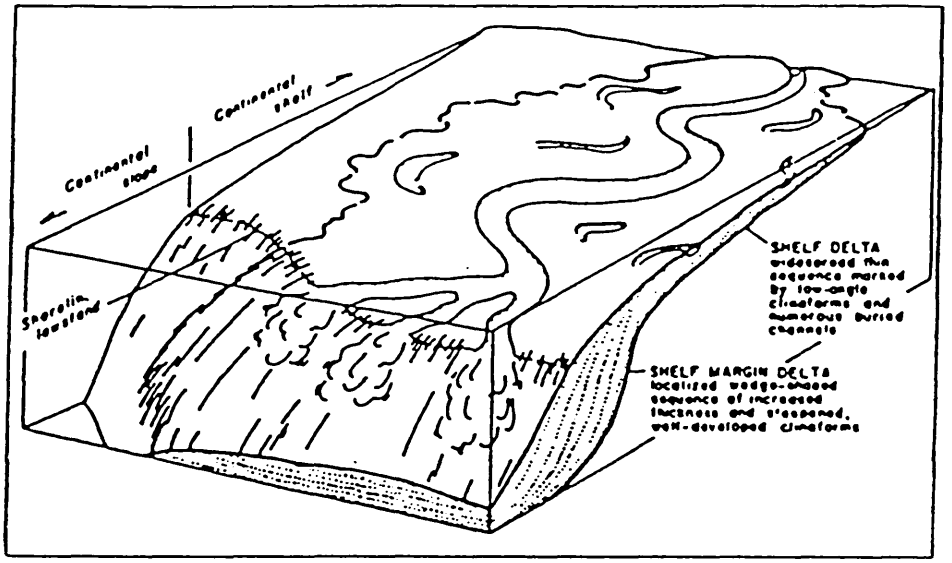

Fig.9.18 Shelf margin deltas during lowstand of sea level (generalized model).

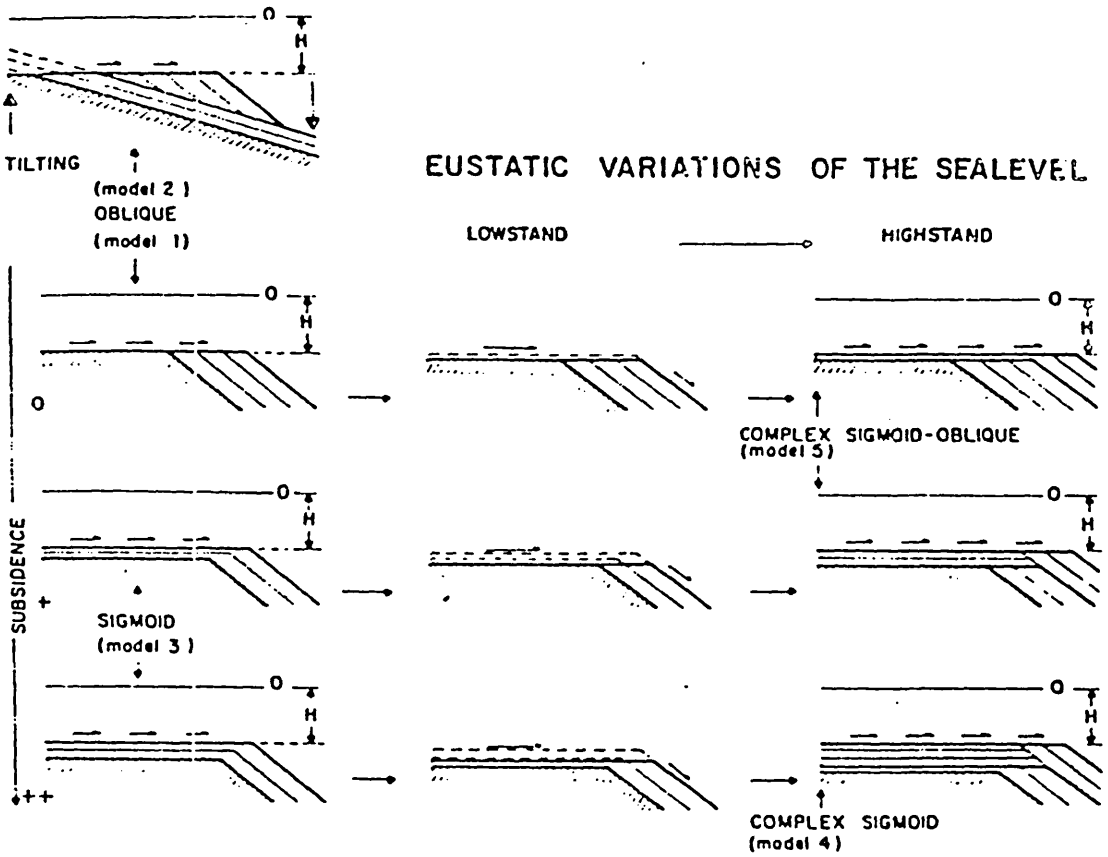

Fig.9.19 Progradation models and variants discussed in text. H is the shelfbreak depth below sea level. H is also the assumed equilibrium level at which most sedimentary particles come to rest. The strata which have accumulated are stippled. Arrows indicate direction of sedimentary by-passing and dashed lines show eroded layers. (After Mougenot *et al.* , 1983).

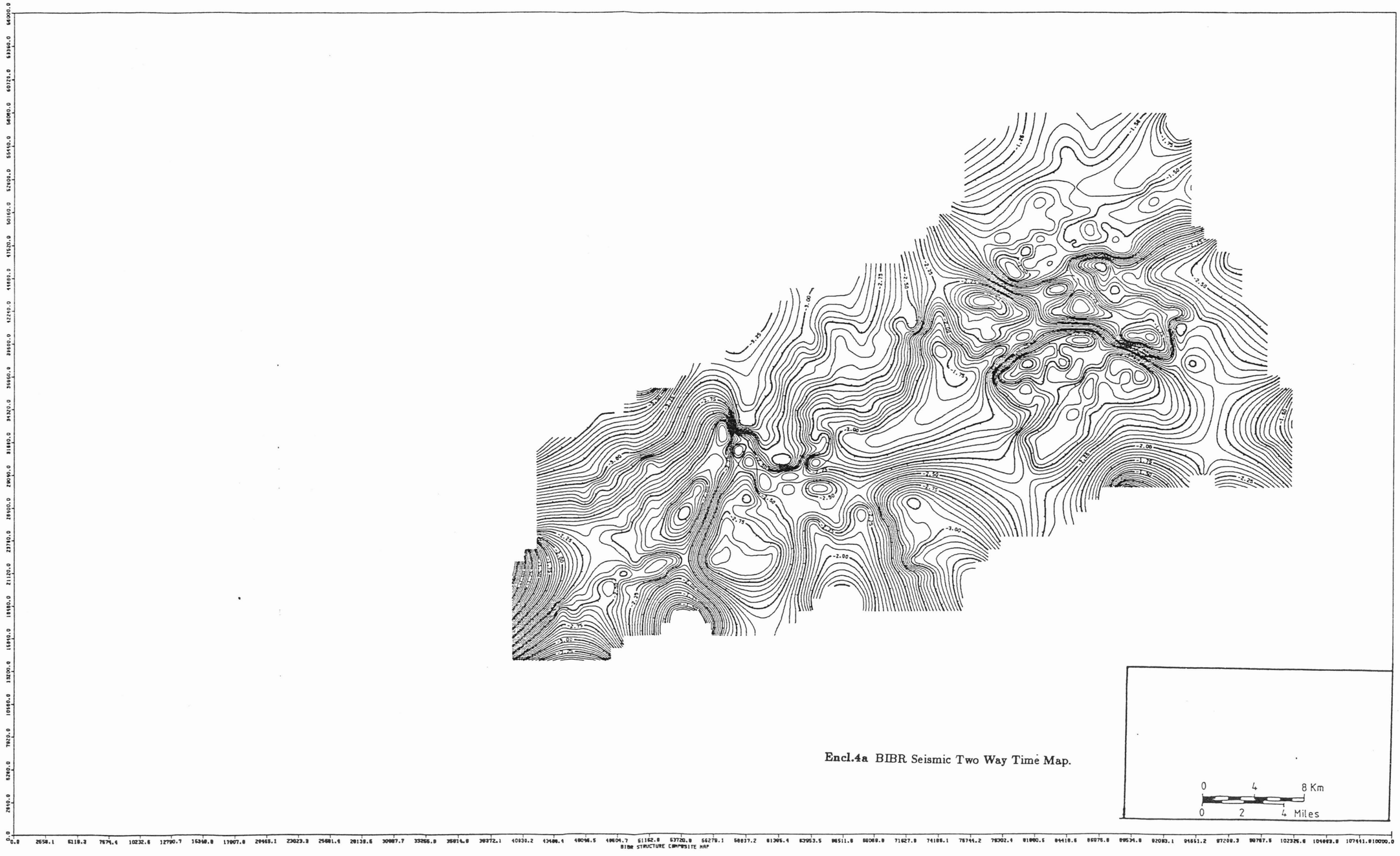

Encl.4a BIBR Seismic Two Way Time Map.

Encl.1 LBIBR Seismic Two Way Time Map.

Encl.3 Isochron of the Lower Intra Biafra Rubble(LIBR).

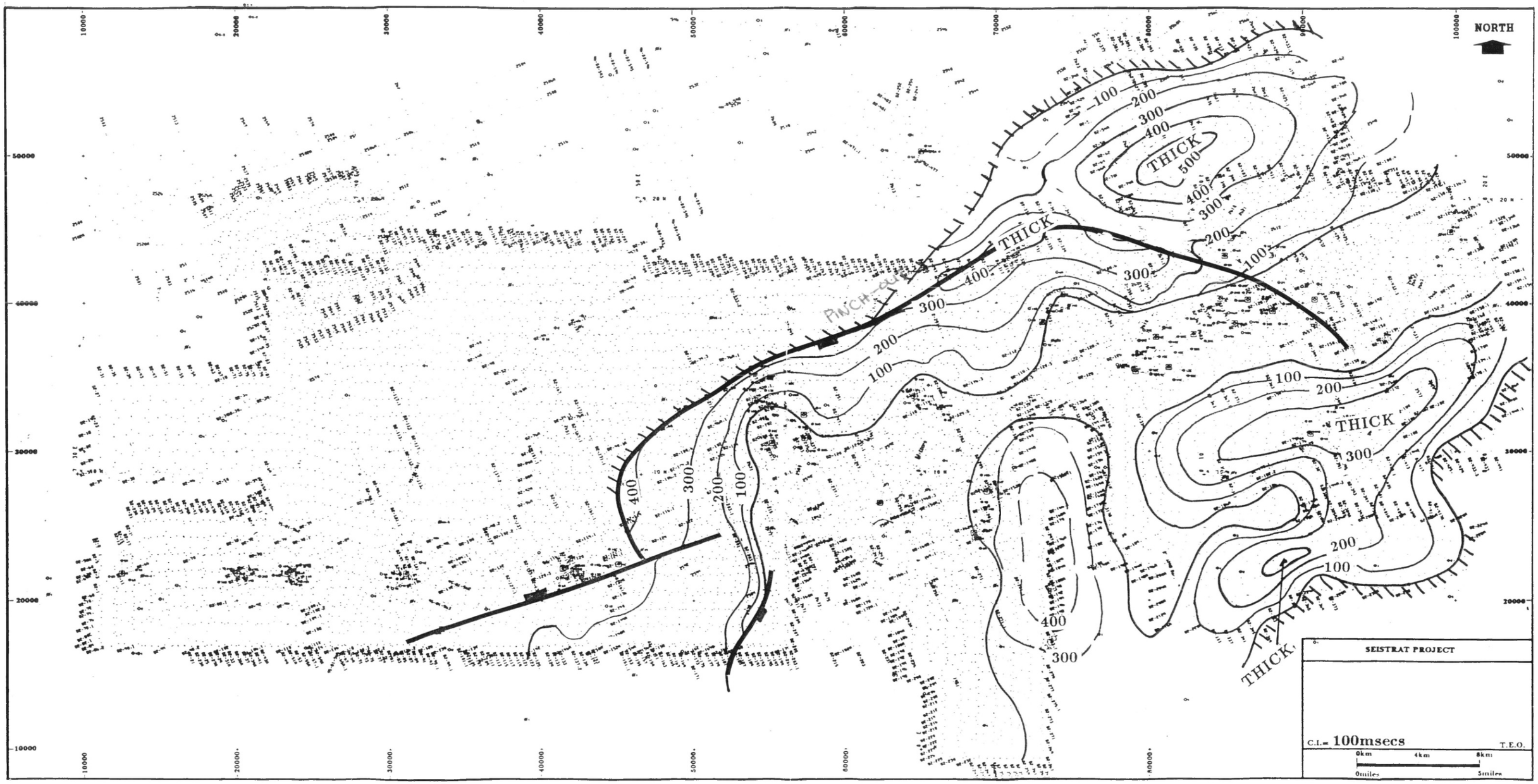

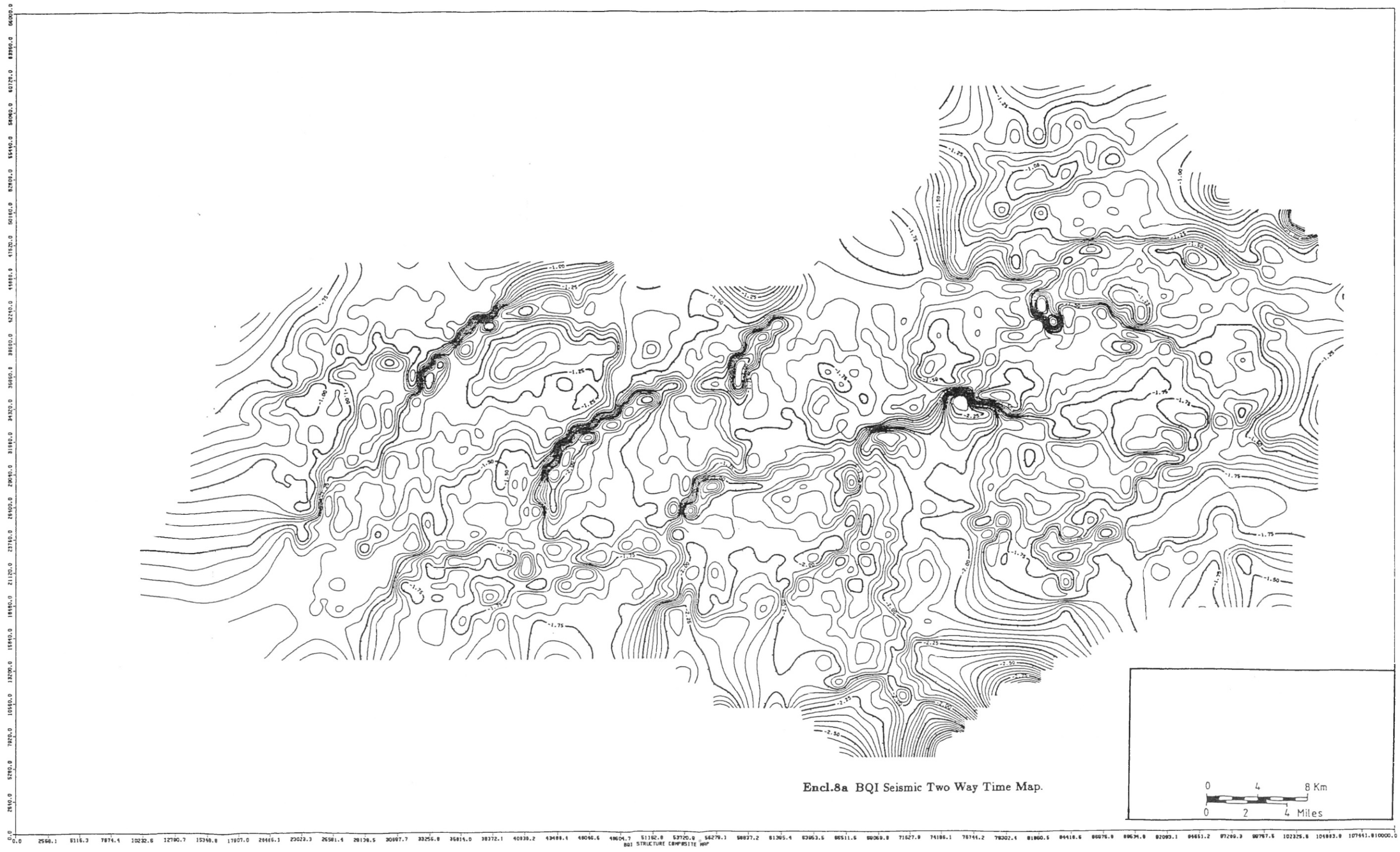

Encl.8a BQI Seismic Two Way Time Map.

USERNAME: PETTE PLOT JOBID: 1 G: 1 C: 1 DATE: 25-OCT-88 15:31

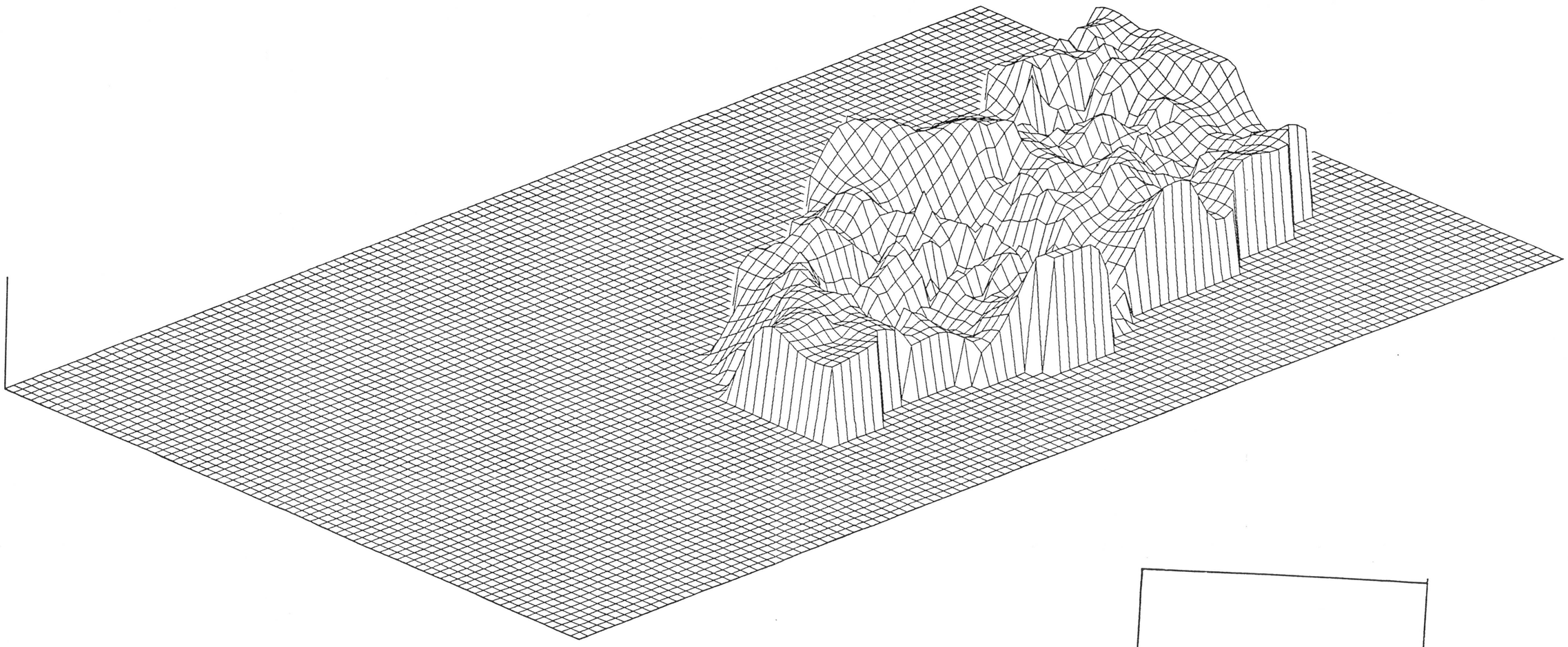

Encl.7b BRB Isometric Projection Map.

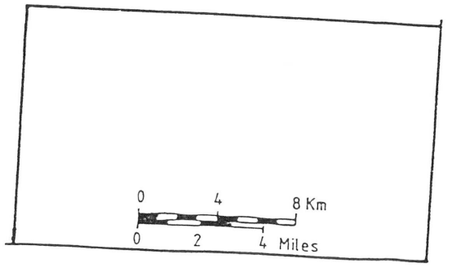

USERNAME: PETTE PLOT JOBID: 1 G: 1 C: 1 DATE: 25-OCT-88 15:31

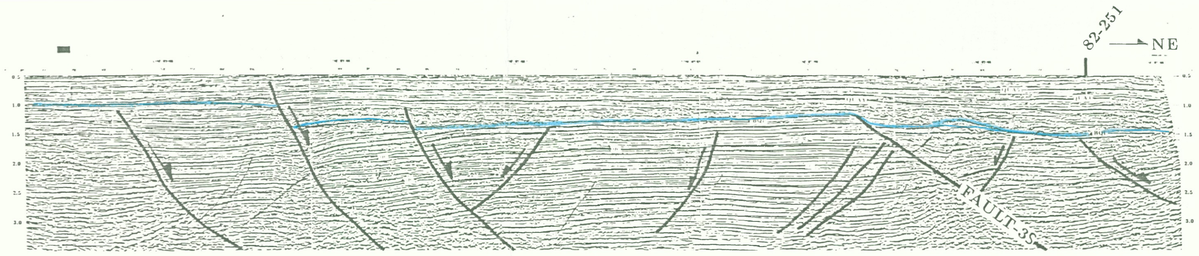

82-66 This profile shows the northern limit of the palaeobasin. East of Fault-3S is the excavated BQI. The Qua Iboe progrades into the proto-palaeobasin.

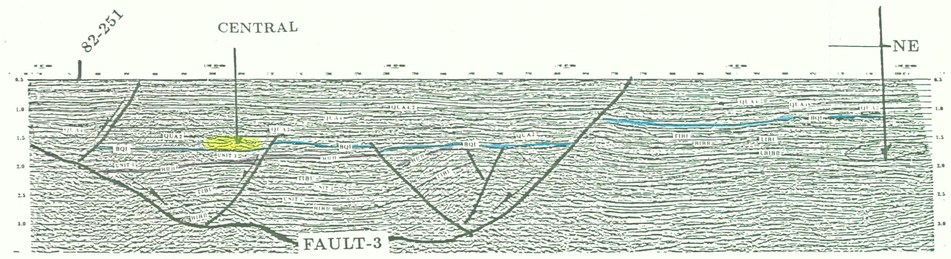

82-88A The palaeobasin as defined by Fault-3 shows the Upper Intra Biafra Rubble (UIBR) differentiated into two units and similarly, the Rubble Beds. The various Rubble identified, are formed on a destructive onlap slope system. The Lower Qua Iboe sequence also becomes well developed forming a constructive onlap slope system. Note the central anomaly above the Intra Rubble canyon(Unit 2; see arrow). To the east the Lower Intra Biafra Rubble shows a stratigraphic anomaly(see arrow).

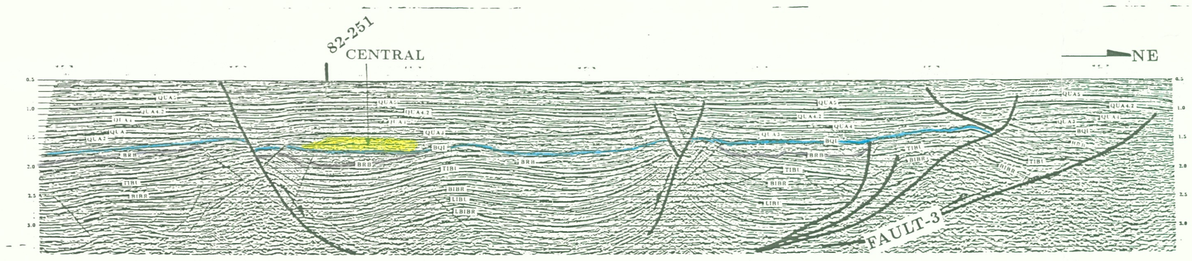

82-106 The palaeobasin is dominanted by shale mass controlled BQI structures. The central and northwest anomalies are as shown.

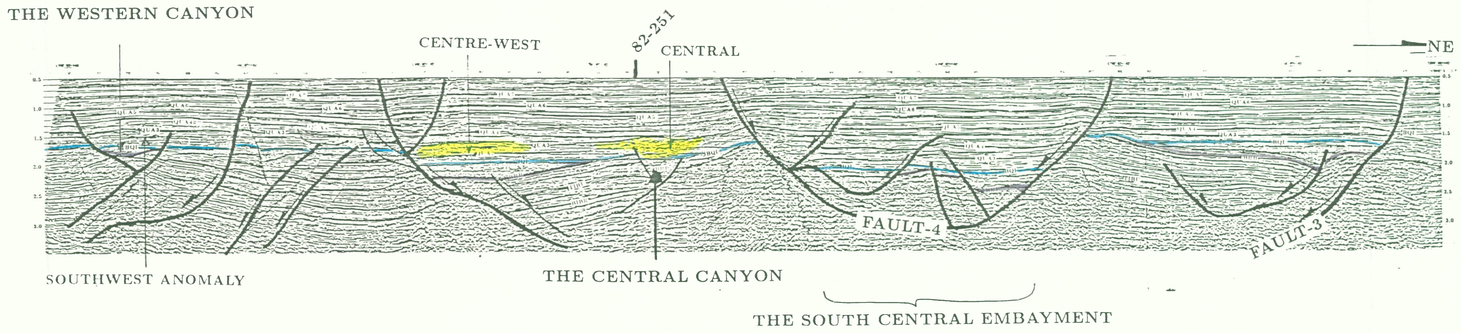

82-142 The Palaeobasin as a mega-turbidite slope basin shows the western and central canyons of the Rubble Beds and the central, centre-west, southwest and centre-east(2) anomalies.

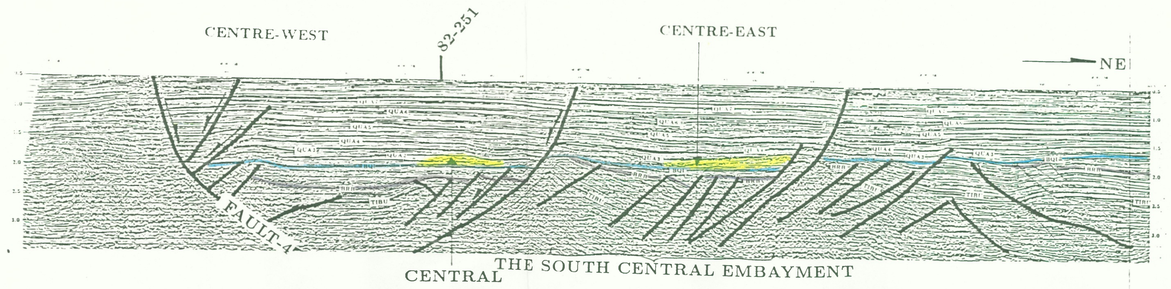

82-158 Tilted Intra Biafra fault blocks typify the palaeobasin to the south. Important features are the south-central Rubble Bed embayment. The centre-west, central and centre-east anomalies are as shown.

0 10km

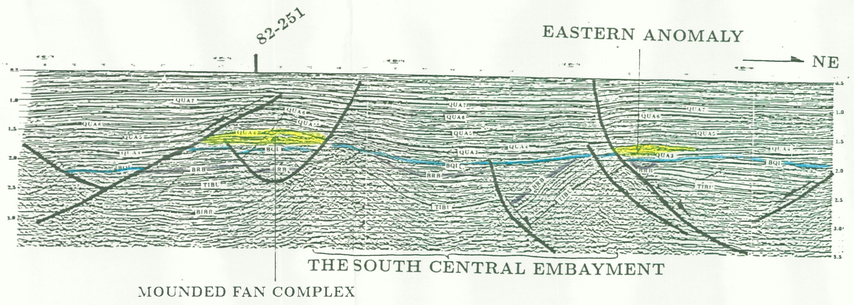

82-174 The central anomaly becomes the mounded fan complex facies although on this profile, it is faulted. The eastern anomaly is as shown.

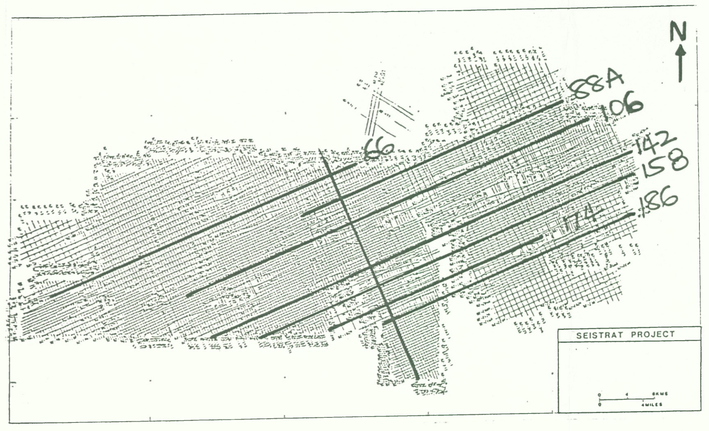

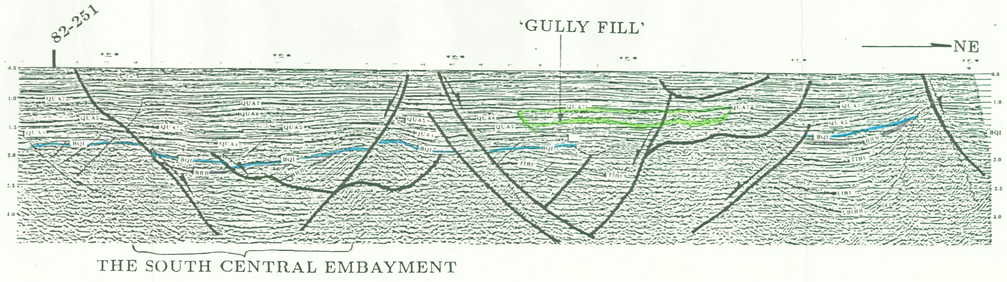

82-186 The dominant features of the palaeobasin remain shale mass induced structures and the Qua Iboe embayment is incised by a canyon system (the Intra Qua Iboe 'Gully' fill).

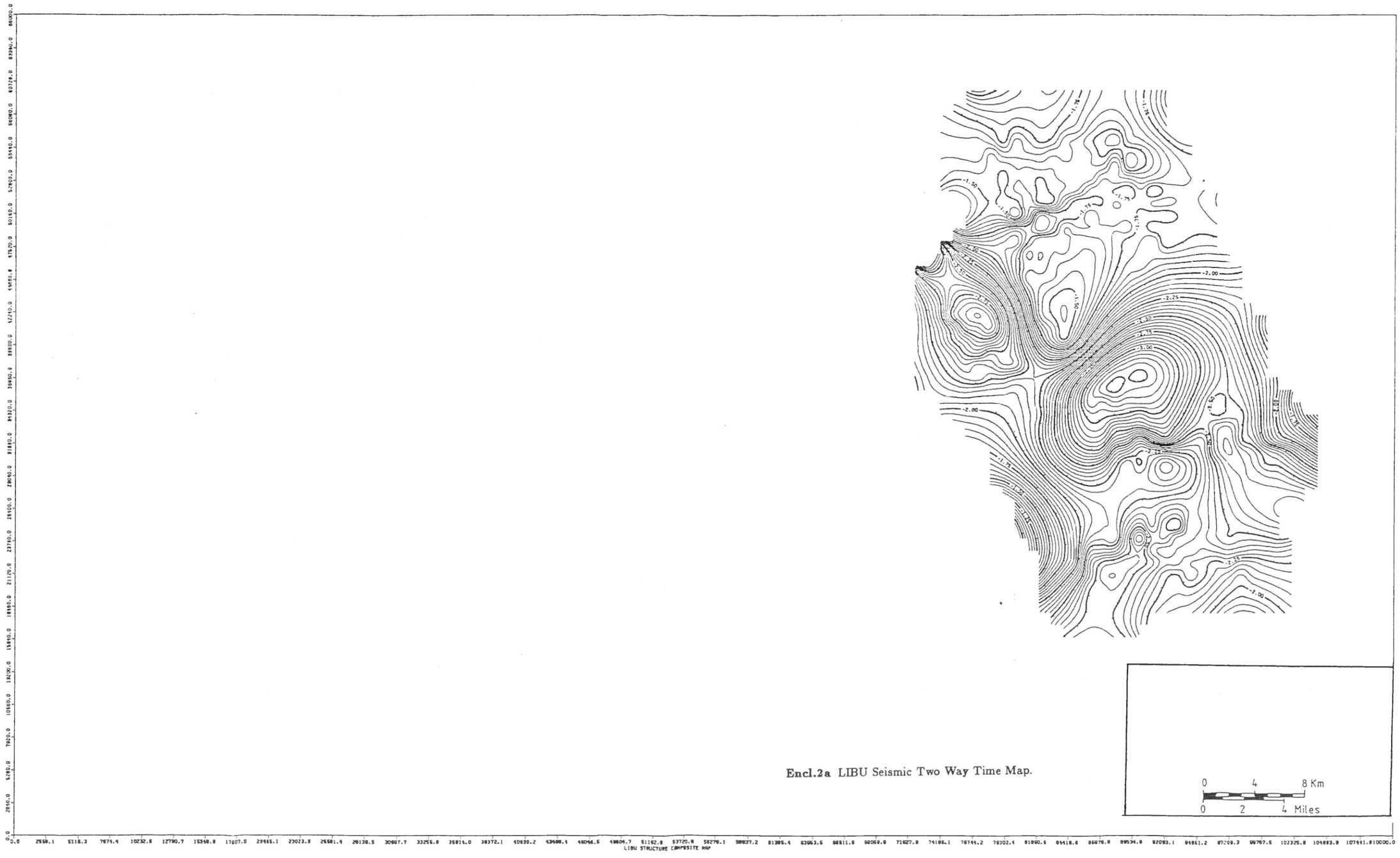

Encl.2a LIBU Seismic Two Way Time Map.

USERNAME: PETTE PLOT JOBID: 1 G: 1 C: 1 DATE: 25-OCT-88 14:46

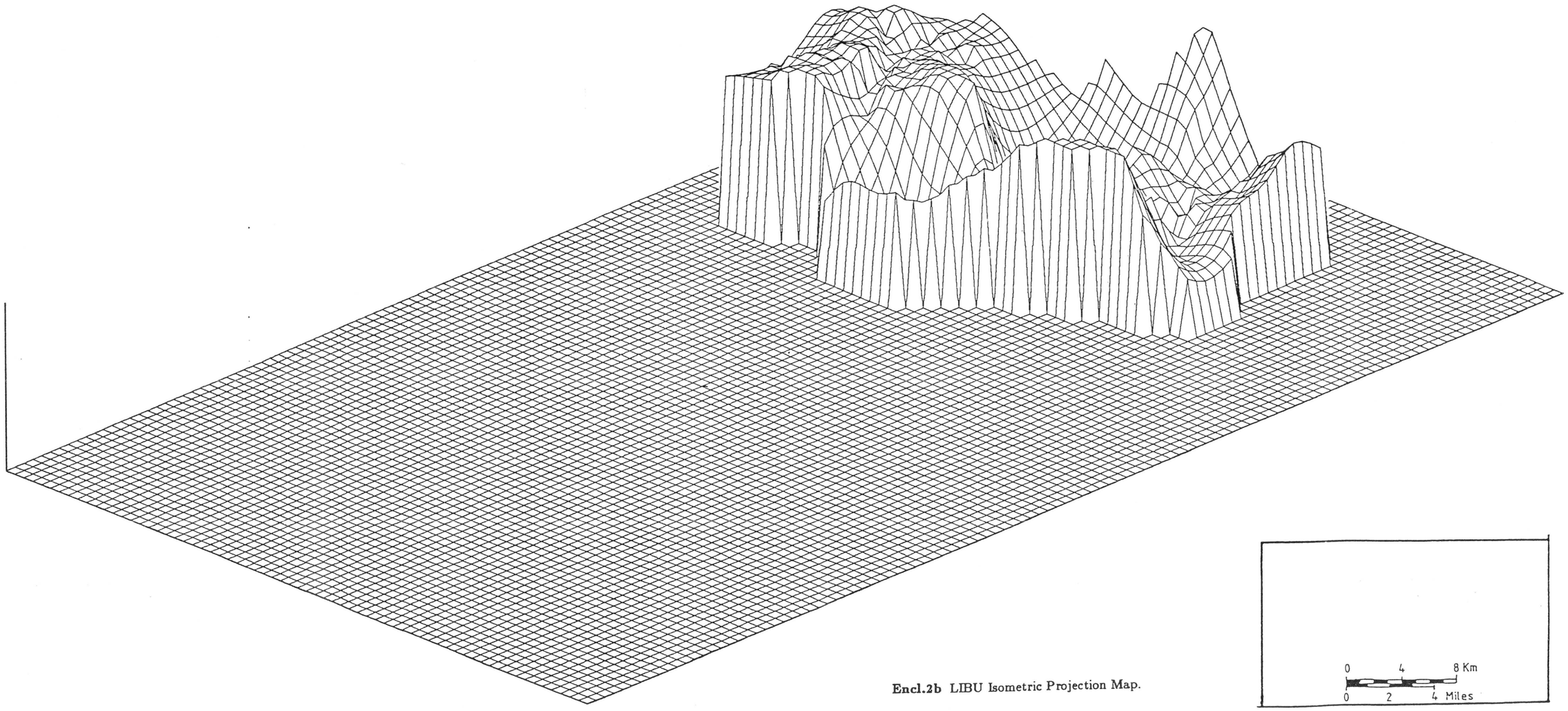

Encl.2b LIBU Isometric Projection Map.

USERNAME: PETTE PLOT JOBID: 1 G: 1 C: 1 DATE: 25-OCT-88 14:46

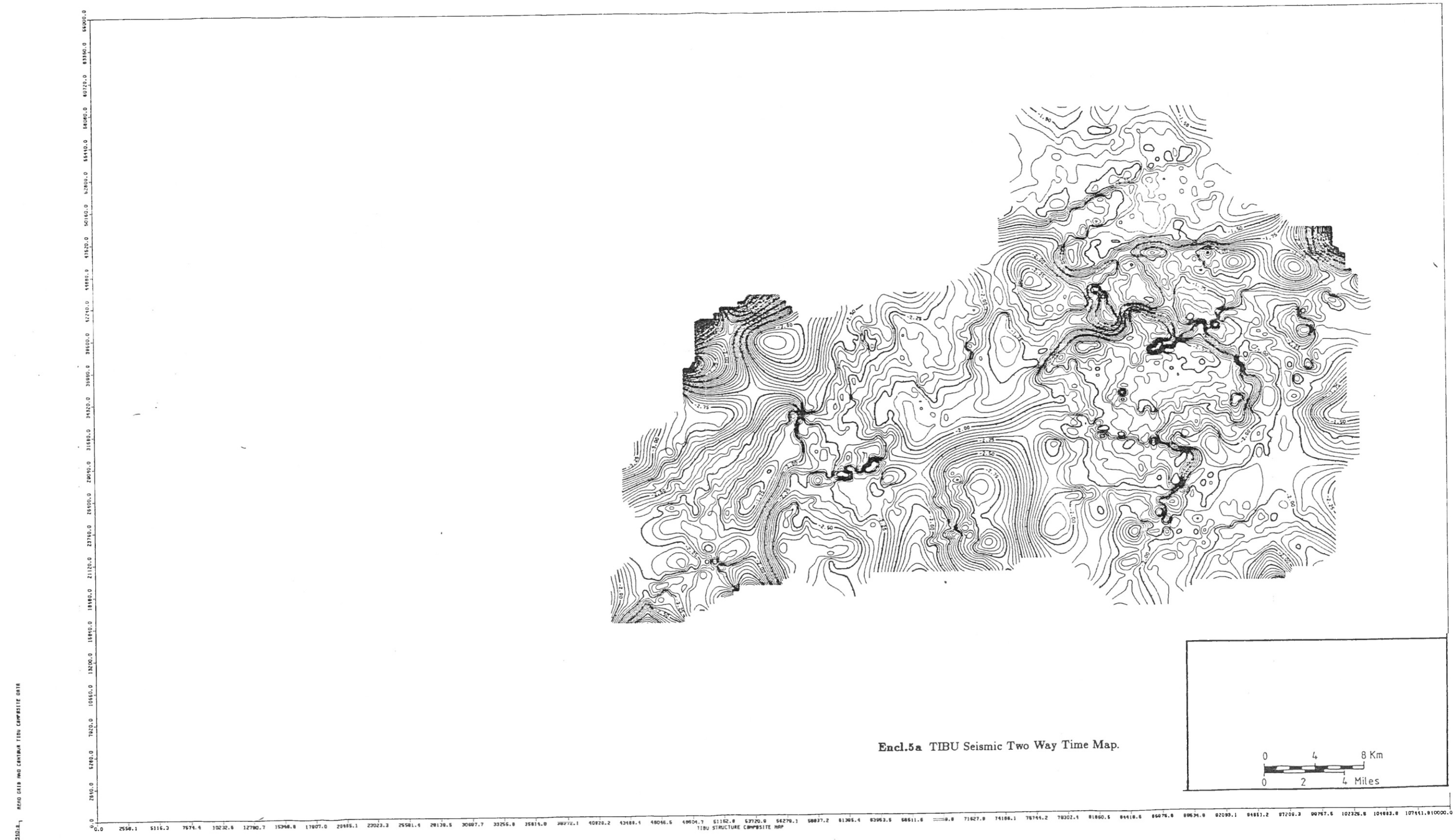

Encl.5a TIBU Seismic Two Way Time Map.

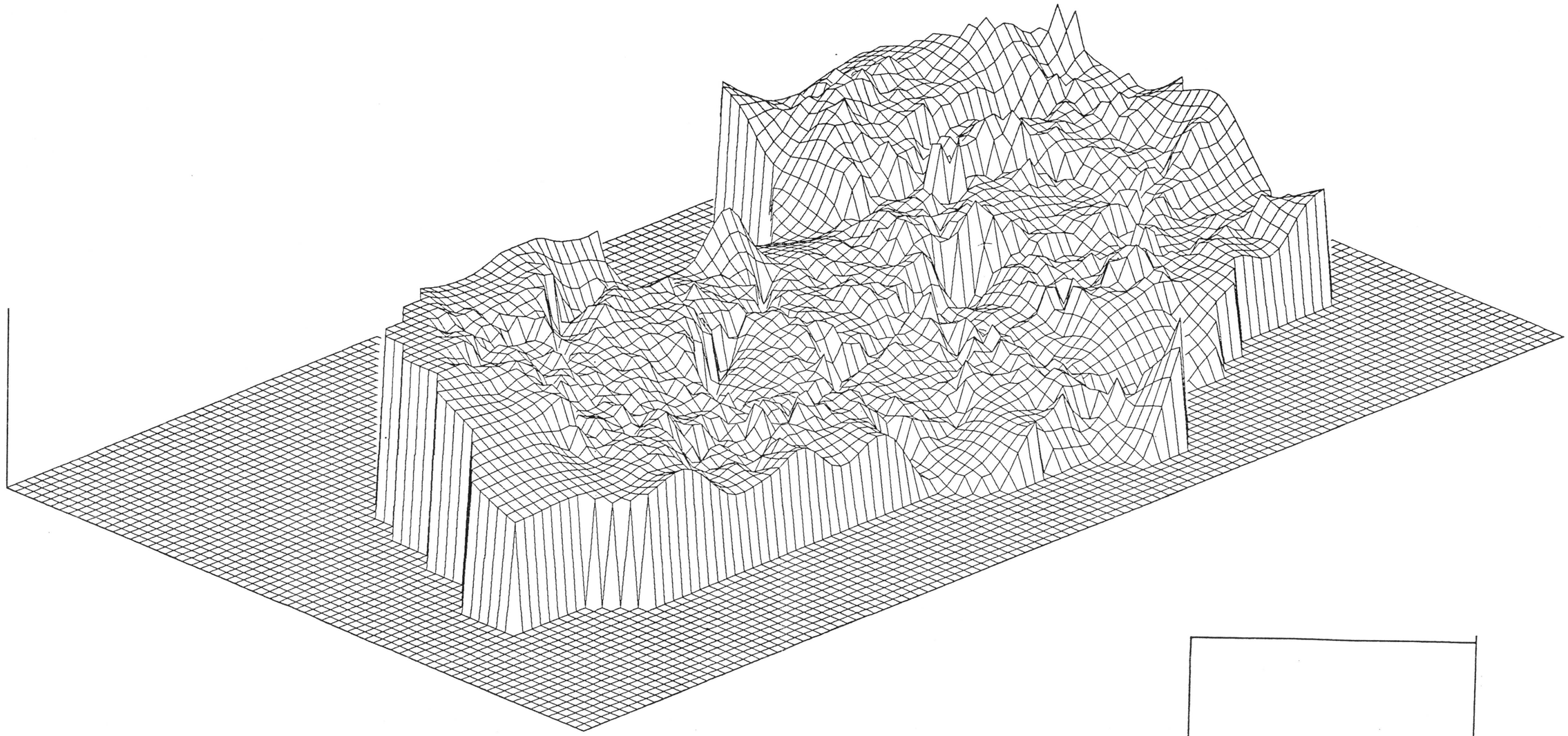

Encl.8b BQI Isometric Projection Map.

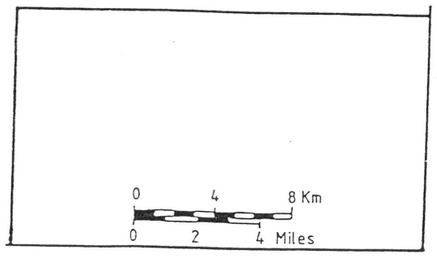

USERNAME: PETTE PLOT JOBID: 1 G: 1 C: 1 DATE: 26-OCT-88 13:59

Encl.6 Isochron of the Upper Intra Biafra Rubble(UIBR).

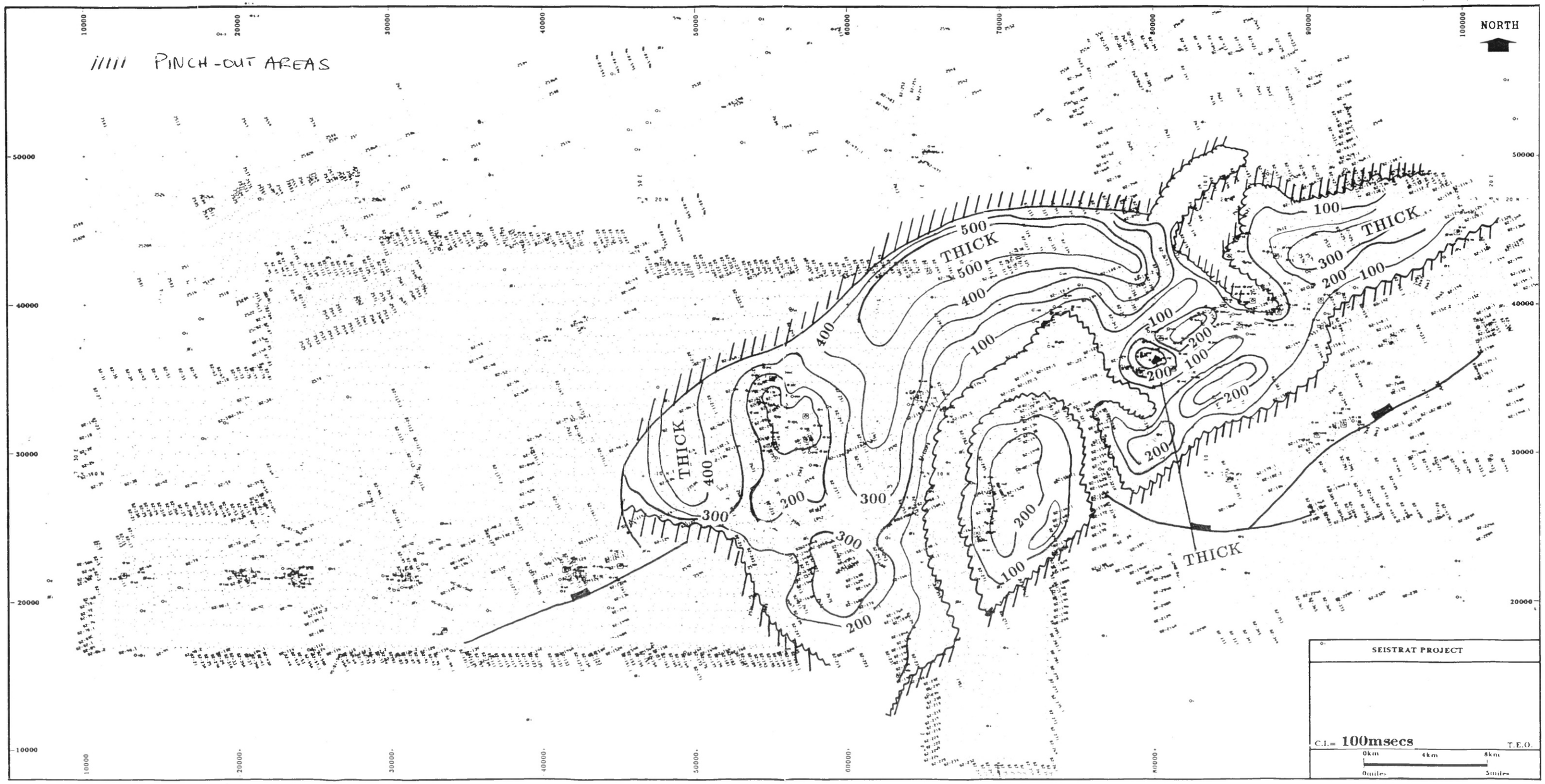

Encl.9 Isochron of the Rubble Beds.

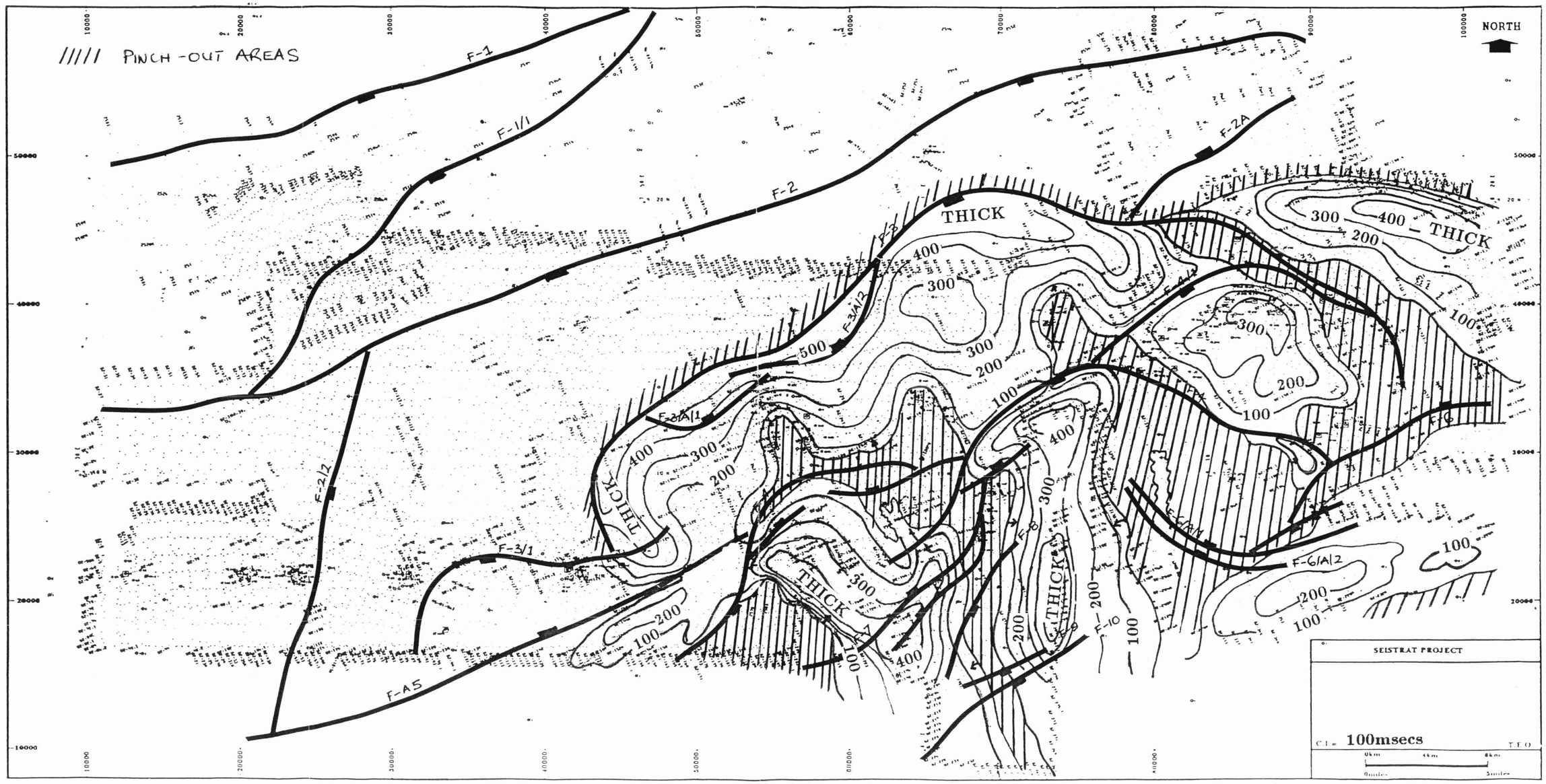

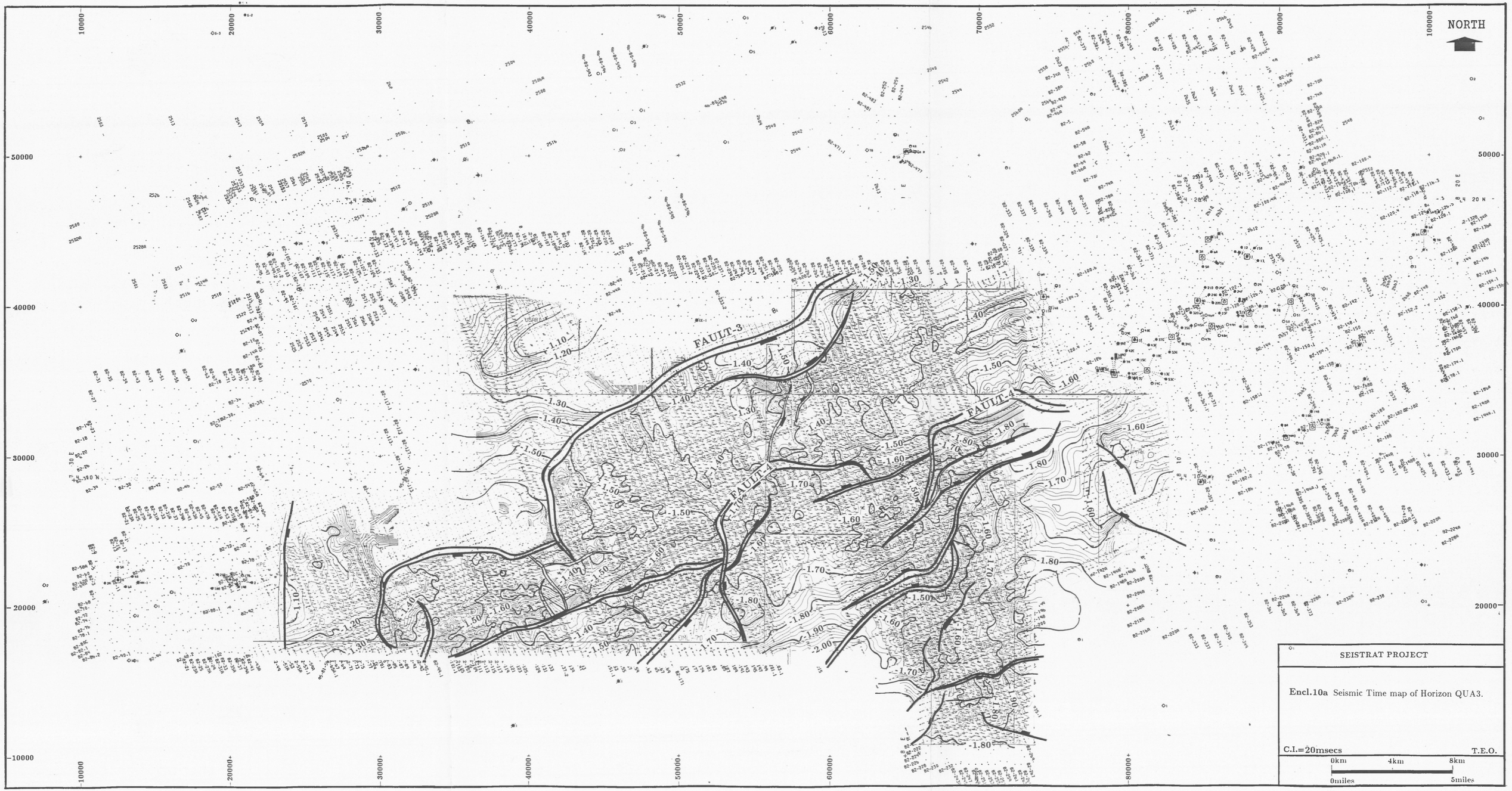
NORTH
FAULT-3
FAULT-4
FAULT-4
SEISTRAT PROJECT
Encl.10a Seismic Time map of Horizon QUA3.
C.I.=20msecs
T.E.O.
0km
4km
8km
0miles
5miles

SEISTRAT PROJECT

Encl.10b Isochron of the Intra Qua Iboe "sand" package. The thickening section in the central part of the study area corresponds to the central and centre-west anomalies respectively. Similarly, the eastern anomaly is shown.

C.I.= 20msecs T.E.O.

0km 4km 8km

0miles 5miles

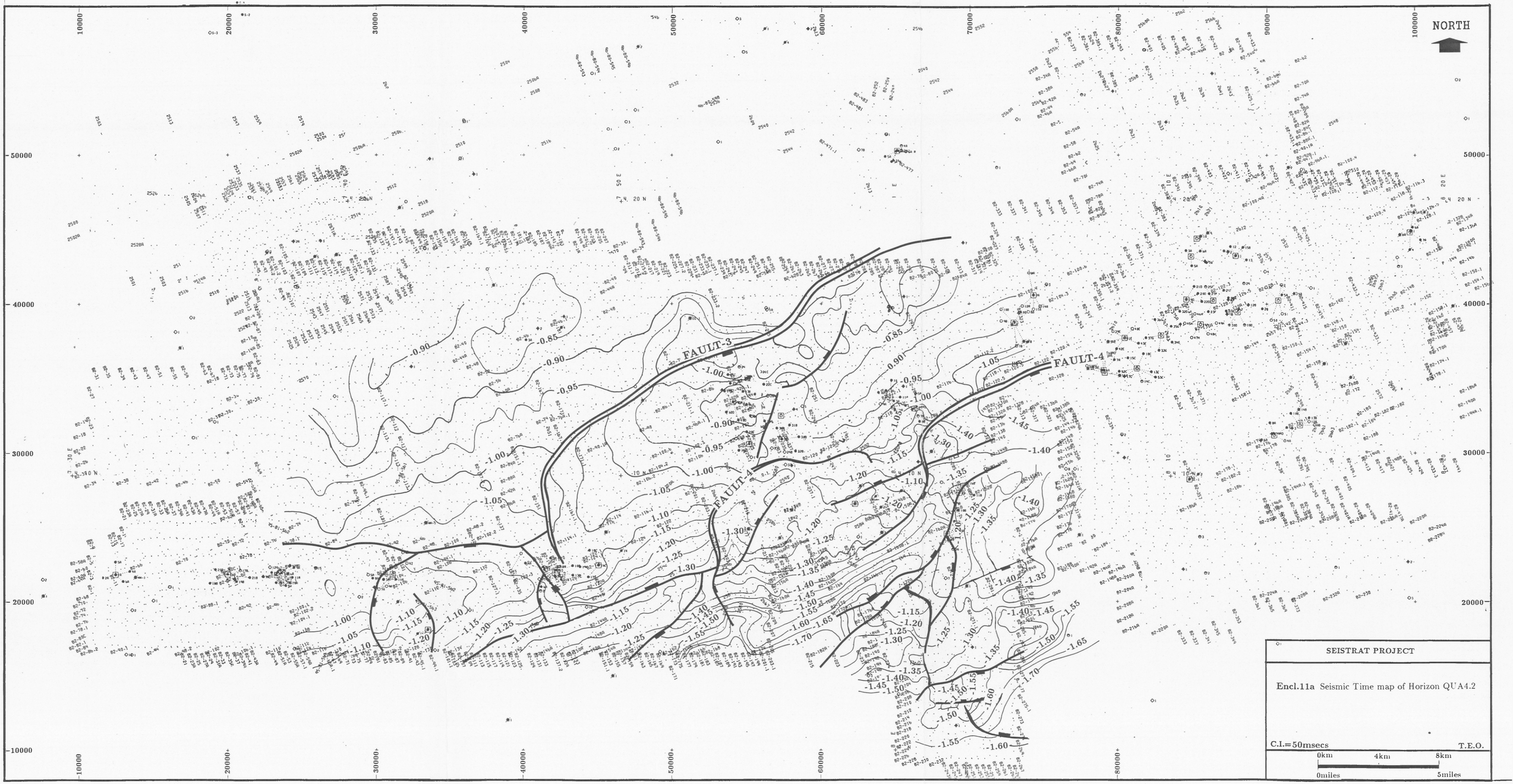
NORTH
FAULT-3
FAULT-4
FAULT-4
SEISTRAT PROJECT
Encl.11a Seismic Time map of Horizon QUA4.2
C.I.=50msecs
T.E.O.
0km
4km
8km
0miles
5miles

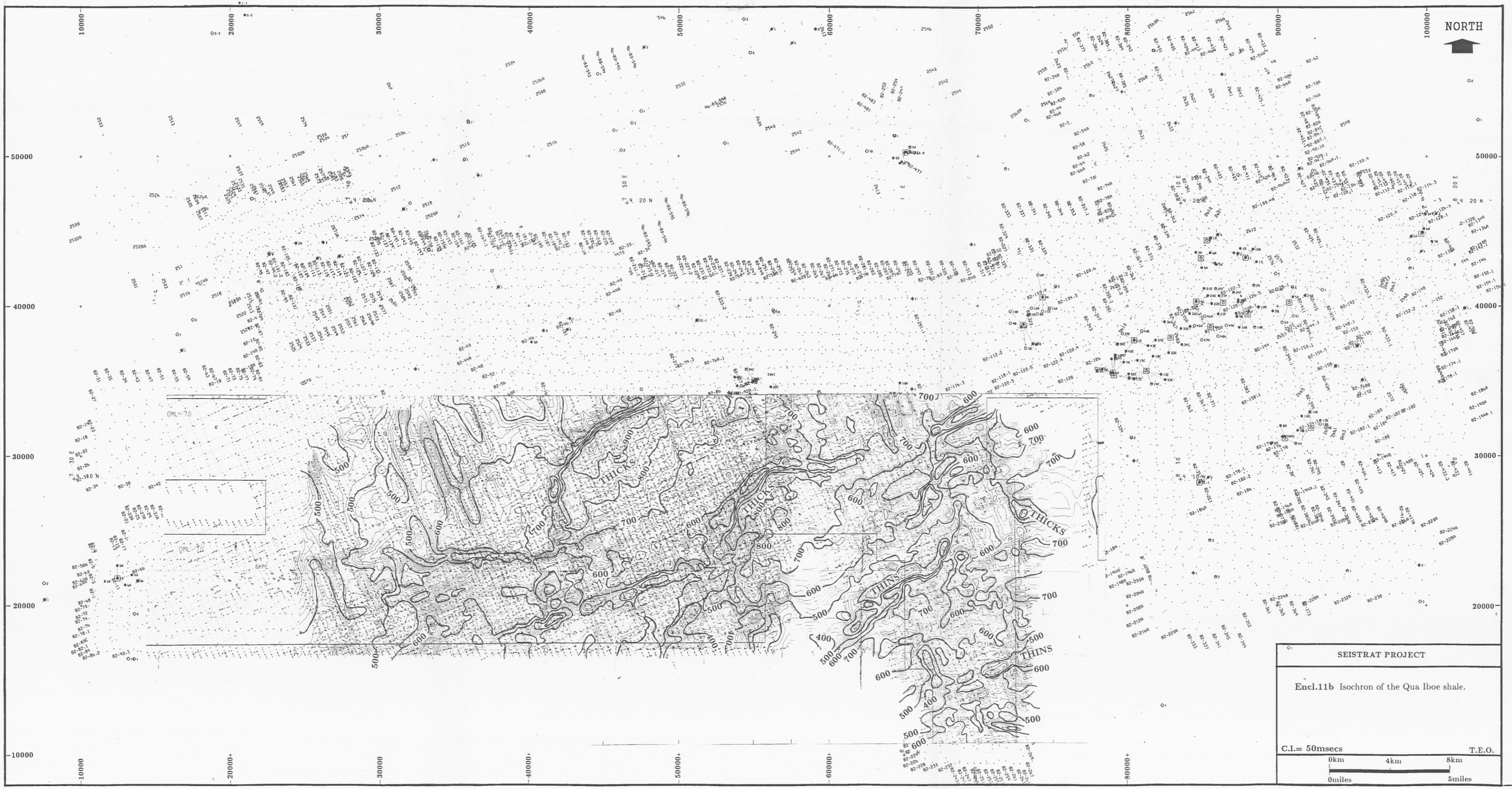
NORTH
THICKS
THINS
OML-70
EXPE
SEISTRAT PROJECT
Encl.11b Isochron of the Qua Iboe shale.
C.I.= 50msecs
T.E.O.
0km
4km
8km
0miles
5miles

LINE 82-197

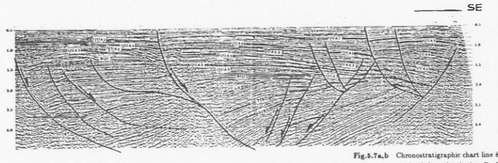

Fig.5.7a,b Chronostratigraphic chart line 82-197. The Older Biafra sequences occur north of the palaeobasin. Both the UIBR and the LIBR occur within the palaeobasin, the latter as a result of the shale uplift of Older Biafra truncated at the BQI. (Compare with Fig.5.8a,b).

CHRONOSTRATIGRAPHIC CHART LINE 82-197

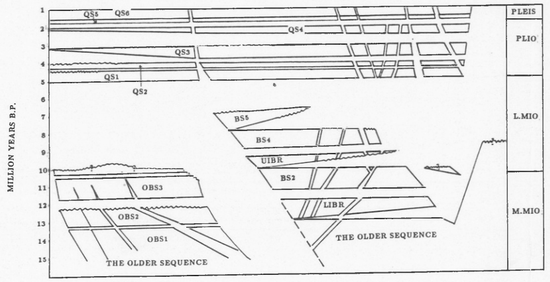

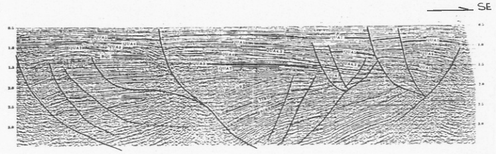

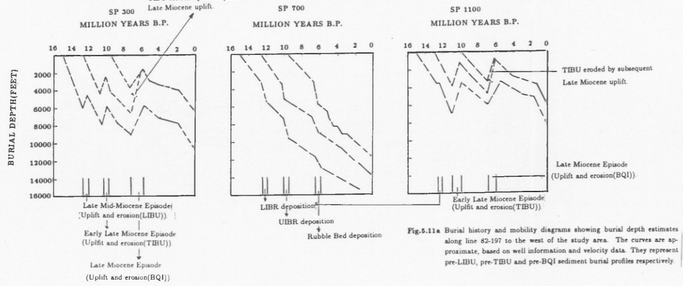

Fig.5.11a Burial history and mobility diagrams showing burial depth estimates along line 82-197 to the west of the study area. The curves are approximate, based on well information and velocity data. They represent pre-LIBU, pre-TIBU and pre-BQI sediment burial profiles respectively.

LINE 82-259

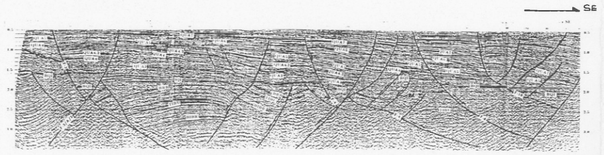

Fig.5.8a,b Chronostratigraphic chart line 82-259. The older Biafra sequences are poorly represented within the palaeobasin in the central area, largely due to shaling out of Biafra. The LIBR has not been identified along this profile.

CHRONOSTRATIGRAPHIC CHART LINE 82-259

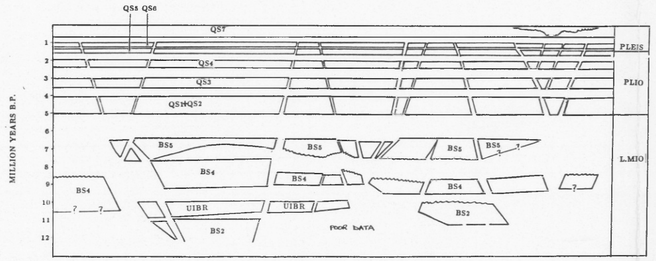

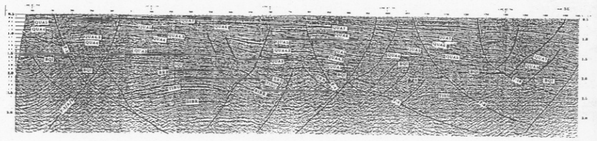

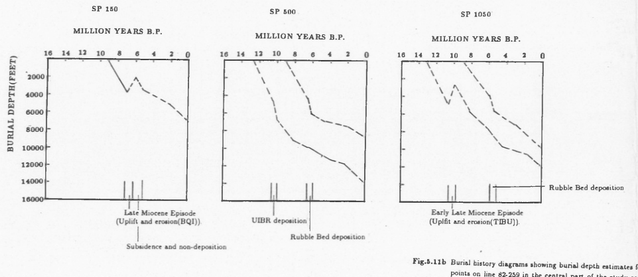

Fig.5.11b Burial history diagrams showing burial depth estimates for specific shot points on line 82-259 in the central part of the study area. The major episodes of tectonism are as indicated.

LINE 82-373

Fig.5.9a,b Chronostratigraphic chart line 82-373. The older sequences are evident to the north and south of this profile. The LIBR also appears to have been extensive. By inference, the proto-embayment was more extensive with the deposition of LIBR, but more restricted during UIBR and the Rubble Beds(BS5) deposition.

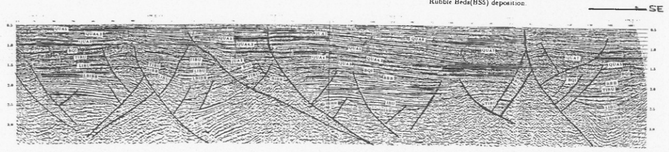

CHRONOSTRATIGRAPHIC CHART LINE 82-373

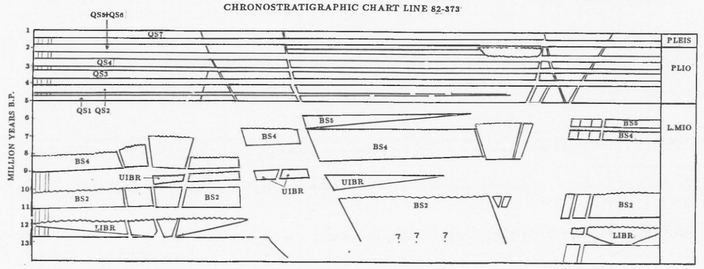

Fig.5.11c Burial history diagrams showing burial depth estimates along line 82-373 in the eastern part of the study area.

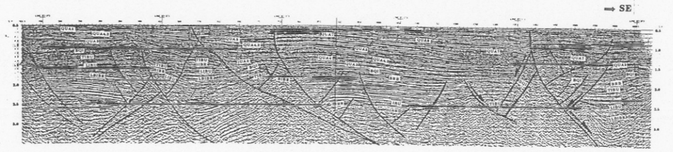

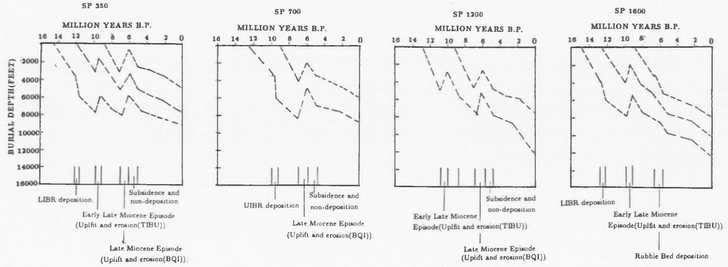

Encl.12 A composite of chronostratigraphic sections and burial history profiles across the study area(from west to east).

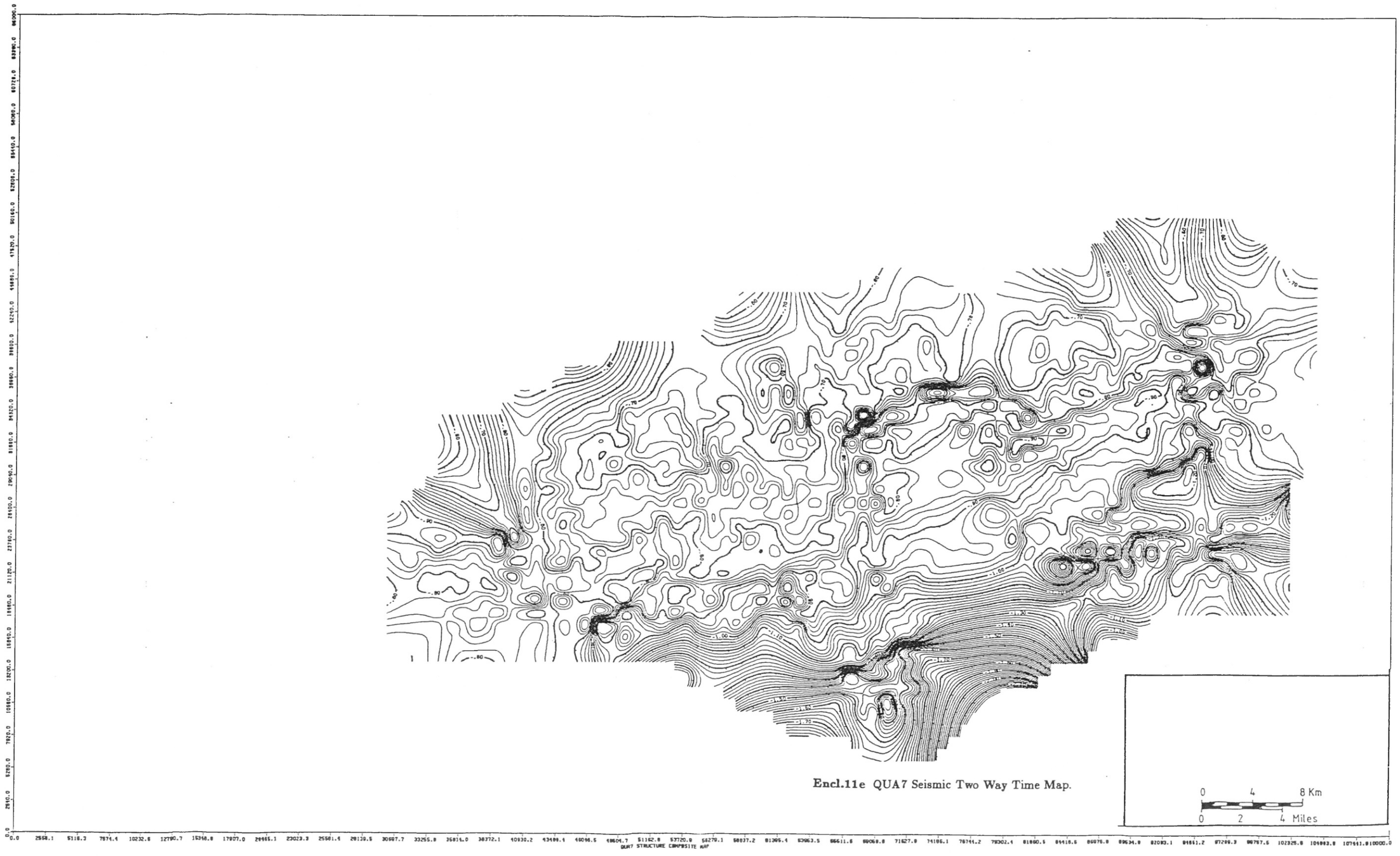

Encl.11e QUA7 Seismic Two Way Time Map.

Encl.11d QUA6 Seismic Two Way Time Map.

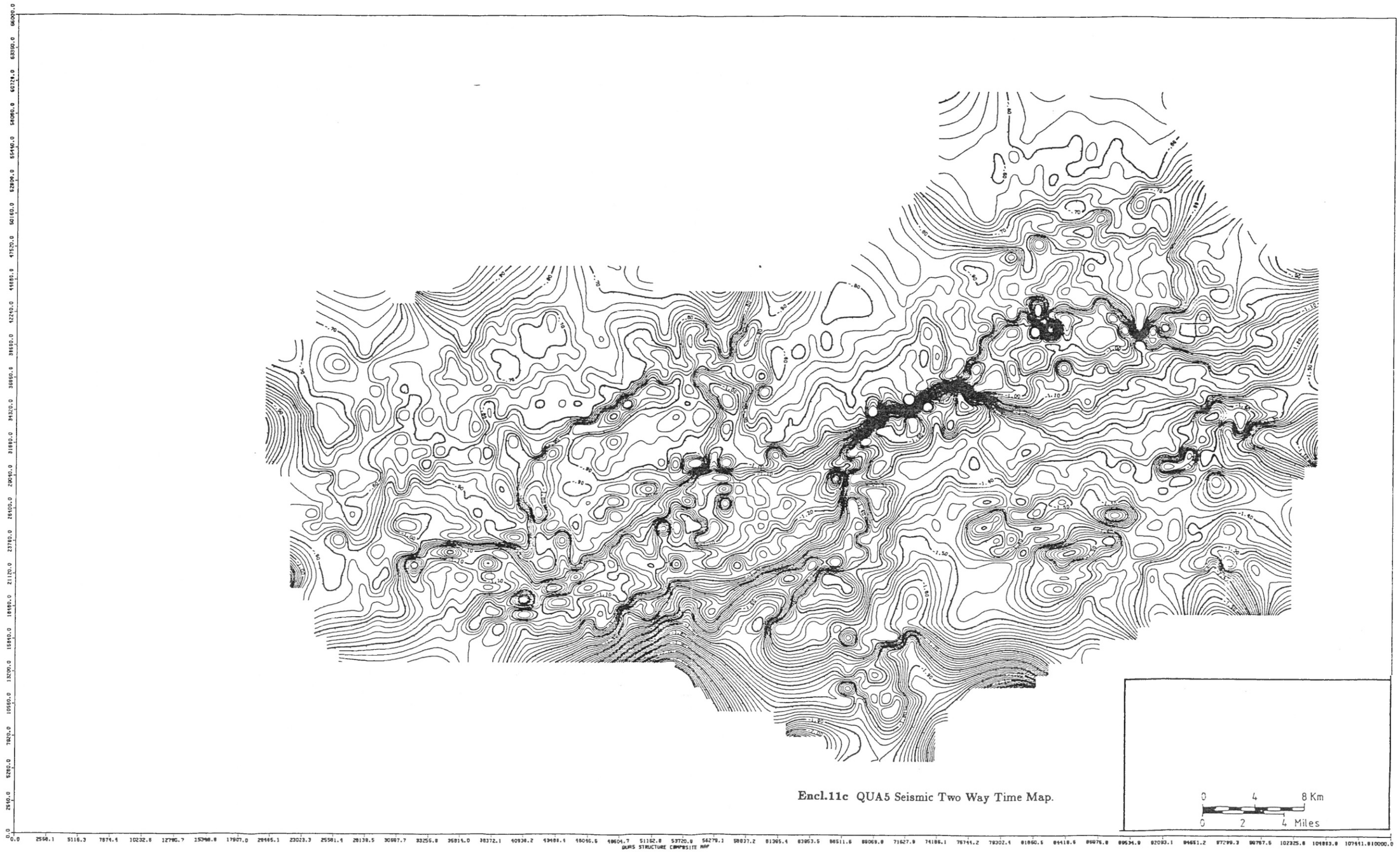

Encl.11c QUA5 Seismic Two Way Time Map.

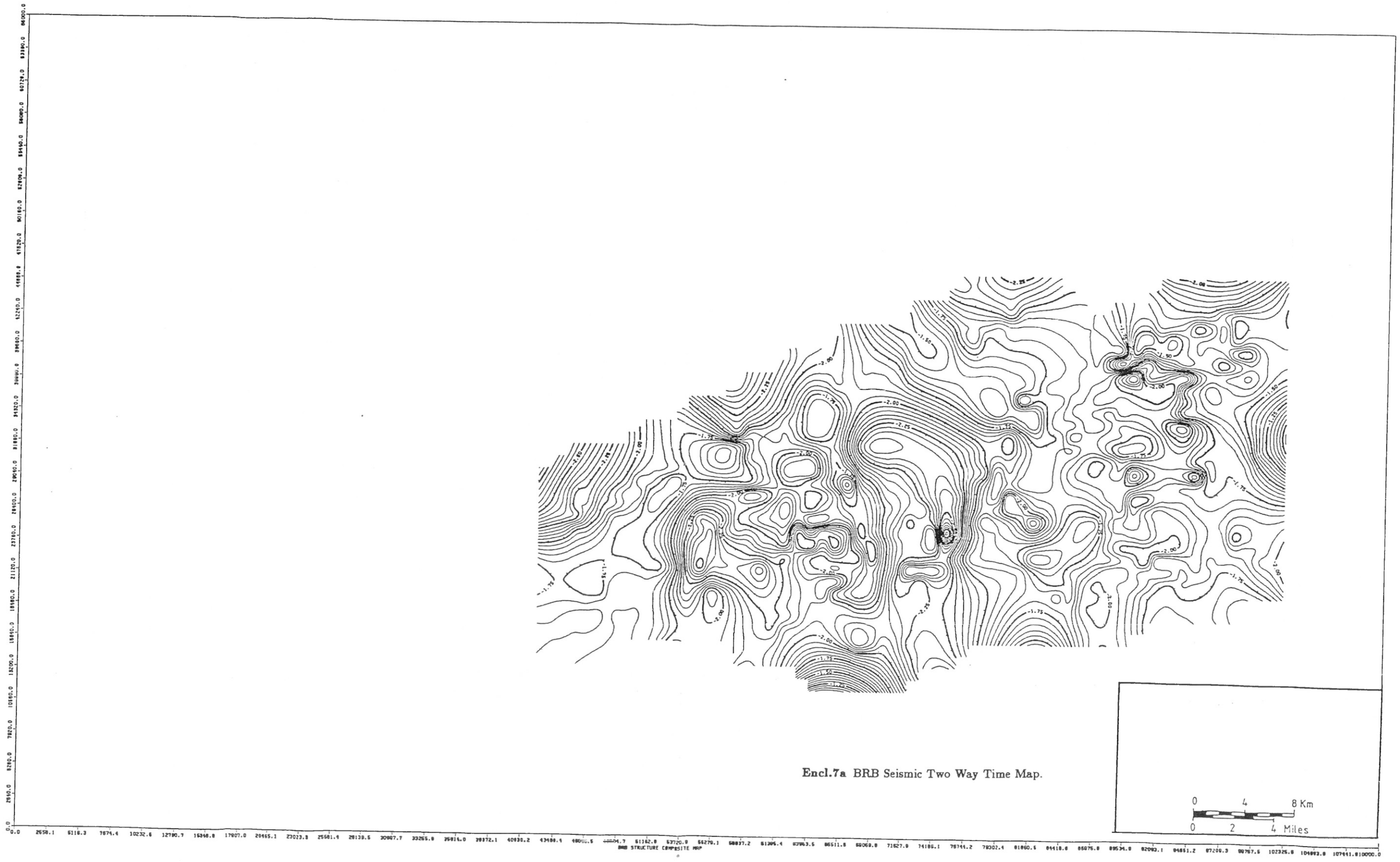

Encl.7a BRB Seismic Two Way Time Map.